



IMPERIAL INSTITUTE
OF
AGRICULTURAL RESEARCH, PUSA

THE
LONDON, EDINBURGH, AND DUBLIN
PHILOSOPHICAL MAGAZINE
AND
JOURNAL OF SCIENCE.

CONDUCTED BY

SIR OLIVER JOSEPH LODGE, D.Sc., LL.D., F.R.S.
SIR JOSEPH JOHN THOMSON, O.M., M.A., Sc.D., LL.D., F.R.S.
JOHN JOLY, M.A., D.Sc., F.R.S., F.G.S.
RICHARD TAUNTON FRANCIS, F.R.S.E.

AND

WILLIAM FRANCIS, F.I.S.

"Nec aranearum sane textus ideo melior quia ex se fila gignunt, nec noster
vilior quia ex alienis libamus ut apes." *Just. Lips. Polit. lib. i. cap. 1. Not.*

VOL. VI.—SEVENTH SERIES.

JULY—DECEMBER 1928.

LONDON:

TAYLOR AND FRANCIS, RED LION COURT, FLEET STREET.

SOLD BY SMITH AND SON, GLASGOW;—HODGES, FIGGIS, AND CO., DUBLIN;—
AND MME J. BOYVEAU, PARIS.

“Meditationis est perscrutari occulta; contemplationis est admirari
perspicua Admiratio generat questionem, questio investigationem,
investigatio inventionem.”—*Hugo de S. Victore.*

—“Cur spirent venti, cur terra dehiscat,
Cur mare turgescat, pelago cur tantus amaror,
Cur caput obscura Phœbus ferrugine condât,
Quid toties diros cogat flagrare cometas,
Quid pariat nubes, veniant cur fulmina cœlo,
Quo micet igne Iris, superos quis conciat orbes
Tam vario motu.”

J. B. Pinelli ad Mazonium.



CONTENTS OF VOL. VI.

(SEVENTH SERIES).

NUMBER XXXIV.—JULY 1928.

	Page
Miss Jessie Butterworth on the Complete Photo-electric Emission from Potassium	1
Prof. L. Wertenstein on a New Method of Determination of the Volume of 1 Curie Radon	17
Prof. A. Press on the Classical Reasonableness of the Quantum Theory and Simple Operative Solutions of Schrödinger's Equation.	33
Prof. T. Martin Lowry on the Electronic Theory of Valency.—Part VI. The Molecular Structure of Strong and Weak Electrolytes. (b) Reversible Ionization	50
Prof. F. K. Richtmyer on Multiple Ionization and the Absorption of X-Rays	64
Dr. A. M. Taylor on Polarization of Infra-red Radiation by Calcite.	88
Dr. T. J. I'a. Bromwich on a Method of Calculation suitable in certain Physical Problems	98
Messrs. R. T. Coe and H. W. Taylor on some Problems in Electrical Machine Design involving Elliptic Functions	100
Mr. H. A. Wheeler and Prof. F. D. Murnaghan on the Theory of Wave Filters containing a finite number of Sections	146
Mr. W. Ogawa on the Analogy between the Crystal Detector and a Vacuum Tube	175
Dr. J. Brentano on the Determination of the Atomic Scattering Power for X-Rays from Powders of Gold, Silver, and Aluminium for Cu K α Radiation. (Plate I.)	178
Mr. H. V. Lowry on the Magnetic Energy of Permanent Magnets and of Linear Currents	192
Prof. R. D. Kleeman on Chemical Interactions corresponding to the Constant of Mass Action, being a Function of the Volume and Masses of the Constituents, as well as of the Temperature and Catalytic Action.—I.	195
Dr. Y. Rocard on the Theory of Light-scattering in Liquids	204
Mr. J. A. Tomkins: A Note on the Magnetic Field of a Rectilinear Circuit and the Attraction of a Straight Wire	205
Mr. R. J. Van de Graaff on a new Method of determining the Mobility of Ions or Electrons in Gases	210
Prof. S. S. Bhatnagar and Mr. R. N. Mathur on the Magnetic Susceptibilities of Electronic Isomers.—Part II.	217
Mr. D. F. Martyn on the Frequency Variations of the Triode Oscillator. A Reply to Lieut.-Col. Edgeworth	223

	Page
Mr. A. J. Carr on Hamilton-Jacobi's Differential Equation in Dynamics	229
Prof. R. W. Wood and Prof. F. W. Loomis on Optically Excited Iodine Bands with Alternate Missing Lines. (Plate II.)	231
Notices respecting New Books :—	
Mr. K. K. Darrow's Introduction to Contemporary Physics ..	239
Prof. H. A. Lorentz's Lectures on Theoretical Physics	239
Messrs. G. H. Hardy, P. V. Seshu Aiyar, and B. M. Wilson's Collected Papers of Spinivasa Ramanujan	240
Prof. A. Findlay's The Phase Rule and its Applications	240

NUMBER XXXV.—AUGUST.

Mr. A. J. Carr on the General Solution of the Equation $\nabla^2\psi = \omega$ in n -dimensional Euclidean Space	241
Mr. R. T. Lattey on the Influence of the Solvent on the Mobility of Electrolytic Ions	258
Prof. R. W. Wood and Dr. E. Gaviola on the Factors governing the Appearance of the "Forbidden Line" 2656 in the Optical Excitation of Mercury. (Plate III.)	271
Dr. K. C. Kar on the Theory of the Pianoforte String	276
Prof. A. F. Westgren and Dr. A. J. Bradley on X-Ray Analysis of Silver Aluminium Alloys. (Plate IV.)	280
Dr. G. W. Kenrick on Radio Transmission Formulae	289
Mr. E. W. Chivers on the Steady Flow of Heat in a Rectangular Parallelepiped	305
Prof. R. W. Wood on Anti-Stokes Radiation of Fluorescent Liquids. (Plate V.)	310
Dr. W. Clarkson on the Measuring of Lags in Discharge	312
Mr. J. R. Cotter on a Method of Determining the Absolute Zero of Temperature	318
Mr. G. S. Mahajani on Hamilton-Jacobi's Differential Equation in Dynamics	320
Mr. C. E. Wynn-Williams on the Application of a Valve Amplifier to the Measurement of X-ray and Photo-Electric Effects	324
Dr. A. E. Ruark: Notes on Active Nitrogen	335
Prof. F. Allen and Mr. A. J. Fleming on the Graphical Representation of the Stimulation of the Retina by Colours	337
Miss Jessie Butterworth on the Photo-electric Thresholds of Potassium	352
Prof. R. W. Wood and Dr. E. Gaviola on the Power Relation of the Intensities of the Lines in the Optical Excitation of Mercury.	352
Mr. E. H. Synge on a Suggested Method for extending Microscopic Resolution into the Ultra-Microscopic Region	356
Notices respecting New Books :—	
Dr. K. Jellinek's Lehrbuch der Physikalischen Chemie	363
Dr. A. E. Everest's The Higher Coal-Tar Hydrocarbons	364
Prof. E. C. O. Baly's Spectroscopy	364
Prof. E. T. Whittaker's A Treatise on the Analytical Dynamics of Particles and Rigid Bodies with an Introduction to the Problem of Three Bodies	365
Dr. V. F. Hess's The Electrical Conductivity of the Atmosphere and its Causes	365
Messrs. V. E. Pullin and W. J. Wiltshire's X-Rays: Past and Present	366

Dr. E. W. Hobson's The Theory of Functions of a Real Variable and the Theory of Fourier's Series	366
Mr. L. J. Hudleston's Chemical Affinity	367
Dr. H. Jeffreys's Operational Methods in Mathematical Physics.	368
Prof. O. Veblen's Invariants of Quadratic Differential Forms ..	368

NUMBER XXXVI.—SEPTEMBER.

Dr. D. H. Black on the Direct Current Conductivity of Insulating Oils	369
Mr. J. A. V. Fairbrother on the Action of X-Rays on Colloidal Ceric Hydroxide	385
Prof. J. A. Crowther and Dr. W. N. Bond on the Thermal Measurement of X-Ray Energy	401
Mr. M. L. Oliphant on Selective Adsorption from Gaseous Mixtures by a Mercury Surface formed in the Mixture	422
Mrs. K. Lonsdale on the Evidence of the Anisotropy of the Carbon Atom	433
Mr. H. Buckley on the Radiation from the Inside of a Circular Cylinder.—Part II.	447
Mr. D. R. Barber on a Quartz Fibre Electrometer	458
Dr. D. B. Deodhar on New Bands in the Secondary Spectrum of Hydrogen.....	466
Messrs. P. Das and S. K. Datta on the Acoustics of Strings struck by a Hard Hammer	479
Mr. L. A. Welo: Magnetic Studies on Salts, with Particular reference to those with Complex Ions.....	481
Mr. L. L. Bircumshaw on the Surface Tension of Liquid Metals.—Part III.	510
Mr. J. Thomson on the Ultra-Violet Radiations emitted by Point Discharges	526
Dr. E. L. Ince on the Mathieu Functions of Stable Type	547
Prof. J. C. McLennan, Mr. J. H. McLeod, and Dr. R. Ruedy on the Zeeman Resolution of the Oxygen Spectral Line at $\lambda 5577 \text{ \AA}$, Auroral Green Line. (Plate VI.)	558
Mr. F. H. Schofield on the Effect on the Heat-flow through an Insulating Wall of Certain Modifications of Shape of its Isothermal Boundaries	567
Dr. L. F. Bates: Experiments on a Ferromagnetic Compound of Manganese and Arsenic.....	593
Notices respecting New Books:—	
Dr. Hilda P. Hudson's Cremona Transformations.....	598
Dr. I. B. Crandall's Theory of Vibrating Systems and Sound ..	598
Drs. A. H. Davis and G. W. C. Kaye's The Acoustics of Buildings	599
Mr. H. G. Forder's Foundations of Euclidean Geometry	599
Mr. T. G. Bedford's Practical Physics.....	600
Prof. A. Güntherschulze's Electric Rectifiers and Valves.....	600

NUMBER XXXVII.—OCTOBER.

Prof. W. D. Harkins and Dr. B. Mortimer on the Separation of Isotopes and a Further Separation of Mercury by Evaporative-Diffusion	601
Dr. W. J. Walker on the Relation between Kinematic Pairs and Links in a Mechanism	631

	Page
Dr. N. R. Campbell on the Photoelectric Properties of Thin Films of the Alkali Metals	633
Prof. R. D. Kleeman on Chemical Interactions corresponding to the Constant of Mass Action being a Function of the Volume and Masses of the Constituents as well as of the Temperature, and Catalytic Action.—II.	648
Mr. H. F. Biggs on Covalency, the Paramagnetism of Oxygen and Stereochemistry	659
Mr. C. D. Niven on the Crystal Structure of Calcium	665
Prof. J. C. McLennan, Messrs. C. D. Niven and J. O. Wilhelm on the Electrical Conductivity of Arsenic and Antimony at Low Temperatures	666
Prof. J. C. McLennan, Messrs. C. D. Niven and J. O. Wilhelm on the Resistance of Cæsium, Cobalt, and Chromium at Low Temperatures	672
Prof. J. C. McLennan, Messrs. C. D. Niven and J. O. Wilhelm on the Effect of Cadmium as an Impurity in Lead on the Conductivity of Lead	678
Prof. E. L. Harrington on the Experimental Evidence of the Aggregates of Active Deposit Atoms in Gases containing Radon. (Plate VII.)	685
Mr. G. A. Tomlinson on Molecular Cohesion. (Plate VIII.)	695
Dr. D. C. Rose on the Reflexion of Electrons from an Aluminium Crystal	712
Prof. R. W. Wood on the Raman Spectra of Scattered Radiation. (Plate IX.)	729
Prof. R. D. Kleeman on the Equation of State of a Perfect Gas	743

NUMBER XXXVIII.—NOVEMBER (SUPPLEMENT).

Mr. J. A. Chalmers on the Ionization Measurements of γ -Rays.	745
Dr. B. v. d. Pol and Mr. J. v. d. Mark on the Heartbeat considered as a Relaxation Oscillation, and an Electrical Model of the Heart. (Plates X.—XII.)	763
Mr. R. S. Bradley on the Adsorption of the Alkali Metals on a Mercury-Vacuum Interface	775
Prof. F. D. Murnaghan on the Application of Tensor Analysis to Physical Problems	779
Mr. R. M. Wilmotte on a General Theorem on Screened Impedances	788
Prof. W. B. Morton on the Penetration of an Electric Field through Wire-gauze	795
Mr. F. J. Selby on the Quantum Theory and the Analysis of Observations	801
Prof. F. H. Newman on the Continuous Spectrum of Hydrogen. (Plate XIII.)	807
Prof. F. H. Newman on the Electric Arc in Gases at Low Pressures	811
Mr. J. Bannon and Dr. H. L. Brose on the Motions of Electrons in Ethylene	817
Mr. A. Eagle on the Best Correction Factors for Harmonic Coefficients	824
Mr. F. E. Hoare on a Determination of the Stefan-Boltzmann Radiation Constant using a Callendar Radio Balance	828
Mr. R. C. J. Howland: Note on a Type of Determinantal Equation.	839

	Page
Dr. T. J. I'a. Bromwich on Heaviside's Formulæ for Alternating Currents in Cylindrical Wires.....	842
Dr. F. Trey on the Investigation of Predischarges. (Plate XIV.)..	854
Prof. J. S. Townsend and Mr. S. P. MacCallum on the Electrical Properties of Neon	857
Dr. A. J. Bradley on the Crystal Structure of Cu ₃ Al. (δ Copper-Aluminium.) (Plate XV.).....	878
Mr. H. Jones and Prof. R. Whiddington on the Energy Losses of Electrons in Hydrogen.....	889
Messrs. G. A. Lindsay and H. R. Voorhees on the K X-Ray Radiation. (Plate XVI.)	910
Dr. W. G. Shilling and Prof. J. R. Partington on the Measurements of the Velocity of Sound in Air, Nitrogen, and Oxygen, with special reference to the Temperature Coefficients of the Molecular Heats	920
Prof. G. P. Thomson on the Effect of Refraction on Electron Diffraction	939
Notices respecting New Books:—	
Handbuch der Radiologie	942
Dr. W. Burnside's The Theory of Probability.....	943
Proceedings of the Geological Society:—	
Mr. G. W. Tyrrell on the Analcite-Syenites and Associated Rocks of Ayrshire	943

NUMBER XXXIX.—NOVEMBER.

Mr. R. S. Maxwell on the Escape of Heat from a Harmonically Oscillating Hot Wire	945
Prof. A. T. Waterman on the Electrical Conductivity of Metals as a Function of Pressure according to the Sommerfeld Electron Theory	965
Drs. N. A. V. Piercy and E. G. Richardson on the Variation of Velocity Amplitude close to the Surface of a Cylinder moving through a Viscous Fluid	970
Mr. D. Meksyn on the Dynamics of an Electron	977
Dr. T. J. I'a. Bromwich on an Example of Operational Methods..	992
Dr. C. Fox on the Potential Function due to certain Plane Boundary Distributions	994
Mr. L. R. G. Trelor on the Intensity Distribution of the General and Characteristic X-Radiation from Molybdenum	1008
Dr. L. F. Richardson on the Amount of Uniformly-diffused Light that will go in Series through Two Apertures Forming Opposite Faces of a Cube.....	1019
Mr. O. V. Lossev on the Luminous Carborundum Detector and Detection Effect and Oscillations with Crystals. (Plates XVII.-XX.)	1024
Mr. R. C. Brown on Jaeger's Method as Applied to the Determination of the Surface Tension of Mercury	1044
Messrs. H. Terrey and C. M. Wright on the Crystal Structure of Mercury, Copper, and Copper Amalgam	1055
Proceedings of the Geological Society:—	
Dr. G. H. Mitchell on the Succession and Structure of the Borrowdale Volcanic Series in Troutbeck, Kentmere, and the Western Part of Long Sleddale (Westmorland)	1069

	Page
Mr. L. J. Chubb on the Geology of the Marquesas Islands (Central Pacific)	1070
Prof. P. G. H. Boswell's Lecture on the Geological Features of the New Mersey Tunnel	1071
Prof. G. B. Barbour on a Re-Excavated Cretaceous Valley on the Mongolian Border; and Mr. S. I. Tomkeieff on the Volcanic Complex of Calton Hill (Derbyshire)	1072

NUMBER XL.—DECEMBER.

Prof. V. A. Bailey and Mr. J. D. McGee on the Capture of Electrons by Molecules	1073
Prof. E. T. Jones on Spark Ignition. (Plates XXI. & XXII.) ..	1080
Messrs. A. C. Bailey and J. W. Woodrow on the Phosphorescence of Fused Quartz. (Plate XXIII.)	1104
Messrs. J. D. McGee and J. C. Jaeger on the Motion of Electrons in Pentane	1107
Dr. D. M. Wrinch on Spheroidal Harmonics as Hypergeometric Functions	1117
Messrs. A. E. Gillam and R. A. Morton on the Deterioration of Quartz Mercury Vapour Lamps and the Luminescence of Transparent Fused Quartz. (Plate XXIV.)	1123
Miss A. W. McDiarmid on the Electrification of Air by Friction..	1132
Mr. P. Vigoureux on the Development of Formulæ for the Constants of the Equivalent Electrical Circuit of a Quartz Resonator in Terms of the Elastic and Piezo-Electric Constants	1140
Dr. E. Gaviola on the Power Relation of the Intensities of the Lines in the Optical Excitation of Mercury.—Theory I.	1154
Dr. E. Gaviola on the Influence of Foreign Gases on the Optical Excitation of Mercury.—Theory II. (Plates XXV. & XXVI.) ..	1167
Dr. E. Gaviola and Prof. R. W. Wood on the Photosensitized Band Fluorescence of OH, HgH, NH, H ₂ O, and NH ₃ Molecules. (Plates XXVII. & XXVIII.)	1191
Prof. A. C. Menzies on Reversals in the Arc-Spectrum of Nickel..	1210
Mr. A. J. Carr on the General Solution of $\nabla^2\psi=\omega$	1216
Mr. F. E. Relton on the Buckling of a Thin Circular Plate by Heat	1217
Mr. T. C. Williams and Prof. E. J. Evans on the Electrical Conductivity of Dilute Liquid Amalgams of Gold and Copper at Various Temperatures	1231
Sir J. J. Thomson on Electronic Waves and the Electron.	1254
Prof. R. W. Wood: Note on Raman Lines under High Dispersion. (Plate XXIX.)	1282
Prof. C. W. Heaps on the Hall Effect in Galena and Molybdenite. Notice respecting New Book:—	1283
Dr. J. W. Mellor's A Comprehensive Treatise on Inorganic and Theoretical Chemistry	1287
Editorial Note	1287
Index	1288

P L A T E S.

- I. Illustrative of Dr. J. Brentano's Paper on the Determination of the Atomic Scattering Power for X-Rays from Powders of Gold, Silver, and Aluminium for Cu K α Radiation.
- II. Illustrative of Prof. R. W. Wood and Prof. F. W. Loomis's Paper on Optically Excited Iodine Bands with Alternate Missing Lines.
- III. Illustrative of Prof. R. W. Wood and Dr. E. Gaviola's Paper on the Factors governing the Appearance of the "Forbidden Line" 2656 in the Optical Excitation of Mercury.
- IV. Illustrative of Prof. A. F. Westgren and Dr. A. J. Bradley's Paper on X-Ray Analysis of Silver Aluminium Alloys.
- V. Illustrative of Prof. R. W. Wood's Paper on Anti-Stokes Radiation and Fluorescent Liquids.
- VI. Illustrative of Prof. J. C. McLennan, Mr. J. H. McLeod, and Dr. Richard Ruedi's Paper on the Zeeman Resolution of the Oxygen Spectral Line at λ 5577 Å.
- VII. Illustrative of Prof. E. L. Harrington's Paper on Experimental Evidence of the Existence of Aggregates of Active Deposit Atoms in Gases containing Radon.
- VIII. Illustrative of Mr. G. A. Tomlinson's Paper on Molecular Cohesion.
- IX. Illustrative of Prof. R. W. Wood's Paper on the Raman Spectra of Scattered Radiation.
- X-XII. Illustrative of Dr. B. van der Pol and Mr. J. van der Mark's Paper on the Heartbeat considered as a Relaxation Oscillation, and an Electrical Model of the Heart.
- XIII. Illustrative of Prof. F. H. Newman's Paper on the Continuous Spectrum of Hydrogen.
- XIV. Illustrative of Dr. F. Trey's Paper on the Investigation of Predischarges.
- XV. Illustrative of Dr. A. J. Bradley's Paper on the Crystal Structure of Cu₃Al.
- XVI. Illustrative of Messrs. G. A. Lindsay and H. R. Voorhees's Paper on the K X-Ray Absorption Edge of Iron.
- XVII-XX. Illustrative of Mr. O. V. Lossev's Paper on Luminous Carborundum Detector Effect and Oscillations with Crystals.
- XXI. & XXII. Illustrative of Prof. E. Taylor Jones's Paper on Spark Ignition.
- XXIII. Illustrative of Messrs. A. C. Bailey and J. W. Woodrow's Paper on the Phosphorescence of Fused Quartz.

- XXIV. Illustrative of Messrs. A. E. Gillam and R. A. Morton's Paper on the Deterioration of Quartz Mercury Vapour Lamps and the Luminescence of Transparent Fused Quartz.
- XXV. & XXVI. Illustrative of Dr. E. Gaviola's Paper on the Influence of Foreign Gases on the Optical Excitation of Mercury.—Theory II.
- XXVII. & XXVIII. Illustrative of Dr. E. Gaviola and Prof. R. W. Wood's Paper on the Photosensitized Band Fluorescence of OH, HgH, NH, H₂O, and NH Molecules.
- XXIX. Illustrative of Prof. R. W. Wood's Paper: A Note on Raman Lines under High Dispersion.

THE
LONDON, EDINBURGH, AND DUBLIN
PHILOSOPHICAL MAGAZINE
AND
JOURNAL OF SCIENCE.

[SEVENTH SERIES.]

JULY 1928.

- I. *The Complete Photo-electric Emission from Potassium.*
By Miss JESSIE BUTTERWORTH, B.Sc.*

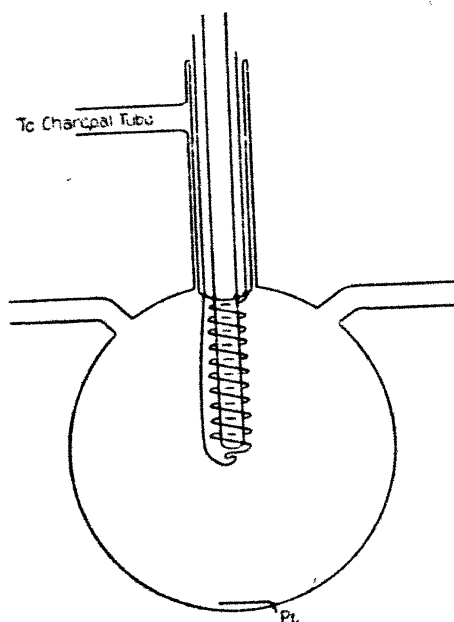
THIS paper is concerned mainly with the negative emission from potassium, but some account of experiments designed to investigate the possibility of a positive photo-electric emission from the metal will be given at the outset. Since Dember (*Ann. d. Phys.* xxx. p. 142, 1910) found that a cylinder surrounding a metal plate acquired a positive charge, when the plate was illuminated with ultra-violet light, a suitable field being applied, many experimenters have endeavoured to justify Dember's assumption that the phenomenon is due to the emission of positive photo-electric particles. Most of the later work seems to show that the effect is the result of the emission of electrons by metal parts of the apparatus which are not adequately screened from stray ultra-violet light. Du Bridge (*Phys. Rev.* p. 201, Feb. 1925) and E. J. Lorentz (*Phil. Mag.* vol. i. p. 499, 1926) in particular were unable to obtain a positive charging up when precautions against defective screening were taken. No observer, however, appears to have worked with the alkali metals, though, if the positive photo-electric effect does exist, it seems, *a priori*, probable that these metals would exhibit the effect to a greater degree than other metals known to be much less active as regards the normal effect.

* Communicated by Prof. William Wilson, F.R.S.

Experiments on the Positive Photo-electric Effect.

A glass bulb (fig. 1) 10 cm. in diameter, with two inlet tubes which terminated in a bottle-neck, was used. Sealed through the inverted end of the neck, as shown, was a filament of platinum wire, so that the loop of the wire was at the centre of the spherical bulb. Round the filament, but not touching it, was a spiral of platinum wire. Thus the filament was surrounded at the sides and bottom by a grid, and both grid and filament could be electrically heated. A fine

Fig. 1.



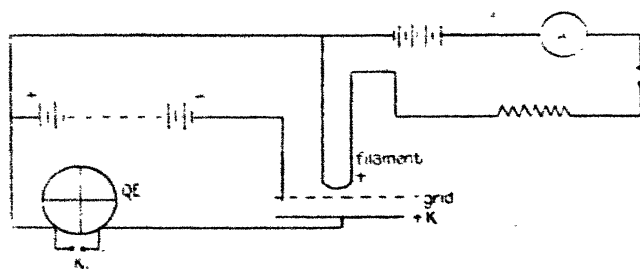
platinum wire was sealed through the bottom of the bulb to make contact with the potassium, which was to act as the third electrode.

A glass bottle containing clean potassium was allowed to slide down one of the side-tubes until stopped by a constriction. By means of the other side-tube the bulb was connected to liquid-air traps and a mercury-diffusion pump, backed by a "Hyvac" pump. After baking and pumping out, with the grid and filament glowing and the charcoal tube heated, the potassium was run over the constriction, which was then sealed off. This was done while the pumps were

working and the liquid-air traps were being cooled. After further pumping, the tube was sealed off and left overnight. Then the potassium was heated slightly once more, and run down to the bottom of the bulb to make contact with the platinum wire.

The glowing filament acted as a source of light, and in so doing gave off thermions, both negative and positive. The latter emission would, of course, almost disappear with constant glowing and a field helping the emission. If a positive photo-electric effect did exist, there would be positive and negative photo-electric currents from both the platinum grid and the potassium. When the connexions are made, as shown in fig. 2, the negative current from the grid and the positive one from the potassium alone can affect the quadrant electrometer.

Fig. 2.



The grid is negative with respect to the potassium, so that any electrons from the potassium are turned back, while any positive particles are attracted across to the grid, leaving a negative charge on the potassium, which, when the key K_1 is open, causes a deflexion of the needle of the electrometer. The field between the filament and grid will turn back any electrons emitted by the filament, while any positive particles from the same source will be turned back once they have passed through the grid. Hence the emission from the filament cannot affect the electrometer. There may be a negative photo-electric current from the grid, however, which will reach the potassium and charge it in the same manner as the positive current leaving it would do. Any positive photo-electric current from the grid will be turned back. The highest threshold frequency of potassium is known to be well in the infra-red portion of the spectrum, while that of platinum is in the ultra-violet. Consequently,

if no effect is produced upon the electrometer, using light whose wave-length is between the two threshold frequencies, it will mean that no positive photo-electric current is emitted from the potassium—at any rate, when those particular wave-lengths are employed.

The sensitivity of the electrometer was such that with 120 volts on the needle and a potential difference of one volt between the quadrants the deflexion produced would be 140 cm. on the lamp scale. The capacity of the system, the electrometer, and the bulb in series was very nearly 100 cm.

Owing to a slight charging up of the sealing-wax key and also to a small leak across the inside of the glass bulb, even when the filament was unheated, the image moved in the direction indicating a positive charging up of the potassium. Fortunately it was not too fast to be timed, and was constant over a short range of time—long enough for measurements to be taken. The effect looked for would mean a still slower rate of charging.

No change in the rate was noticed until the filament current rose to a value of 1.8 amps., corresponding to a temperature of over 800°C ., and it seemed reasonable to suppose that the negative platinum current was causing the change at this temperature. However, at this temperature the negative current was quite large (nearly 10^{-6} amp.). A stop-clock reading to .2 sec. was used, and it would have been easy to detect a change in the rate of 1 cm. in 10 secs. The difference of potential between the potassium and the grid was 96 volts: sufficient to saturate the negative currents at the temperatures employed.

TABLE I.

Filament current.	Time for image to travel 22 cm.
0	10.2 secs.
1.5 amps.	10.2 "
0	10.4 "
1.6 "	10.2 "
0	10.2 "
1.7 "	10.4 "
0	10.2 "
1.8 "	11.2 "

A change in the rate of charging up of 1 cm. in 10 secs. would mean a photo-electric current of 10^{-13} amp. For the potential difference

$$= \frac{\text{current} \times \text{time}}{\text{capacity}}$$

$$= \frac{1}{140 \times 300} \text{ E.S.U.}$$

$$\therefore \text{current} = \frac{1}{1.26} \times 10^{-13} \text{ amp.}$$

Hence a current of little over 1×10^{-14} amp. could have been detected.

Dember found the ratio of his negative to positive photo-electric currents to be $\frac{10^{-9}}{10^{-13}}$, i. e. 10^4 , whereas these experiments give the ratio as more than $\frac{10^{-6}}{10^{-13}}$, i. e. 10^7 . Hence, if the positive photo-electric effect does occur, it is at least a thousand times smaller than the current which Dember attributed to the emission of positive ions by photo-electric action.

The Threshold Frequencies of Potassium.

Richardson and Young (Proc. Roy. Soc. ser. A, vol. cvii. p. 377, 1925) found for a normal potassium surface a threshold frequency corresponding to a wave-length of 7000 A.U. After sensitizing the potassium surface by passing a glow-discharge through an atmosphere of hydrogen, the critical wave-length appeared to be somewhere between 9000 A.U. and 10,000 A.U. A usual thermionic threshold at a temperature of 200°C . is 10,000 A.U., and another occurs at about 30,000 A.U. No trace of a photo-electric threshold of this magnitude, however, was to be found, even for the sensitized surface. The following account gives details of the production, by vaporizing the metal, of a sensitized surface, for which two threshold frequencies were found.

Experiments on the Threshold Frequencies of Potassium.

The apparatus used to investigate the existence of the positive photo-electric effect was also used to measure the threshold frequency or frequencies of potassium, by measuring the complete photo-electric effect when in equilibrium with black-body radiation of known temperature. By heating the potassium at the bottom of the bulb with a small electric heater, it was vaporized and deposited in a thin film over the cool part of the spherical surface. To prevent the vapour condensing on or near the filament and grid, both

were heated throughout the operation, and also another electric heater was wound round the outside of the bottle-neck. By repeated heating and cooling of the potassium it was possible to obtain a comparatively thick and quite opaque mirror over the whole spherical surface. The gap on the glass in contact with the heater was covered by tipping the tube while the metal was still in the liquid state. At the first attempt the mirror of potassium evidently was not of sufficient thickness to make good electrical contact over the whole surface, for inconsistent readings of the photo-electric currents were obtained, doubtless due to certain portions of the surface becoming charged up after subjection to radiation for a few minutes. At the second attempt the film of potassium was made thicker, and this difficulty disappeared. Owing to repeated reflexions of the light emitted by the filament at the bright potassium surface, the system should give approximately black-body radiation, and at the same time a fresh metal surface could easily be obtained by heating and vaporizing the potassium. Also each heating would improve the conditions until all the substances, which had been left in the bulb and were capable of reacting with potassium, had been used up.

The law governing the relation between the saturated current and the temperature in the case of the complete

photo-electric effect is expressed by $C = AT^{\lambda} e^{-\frac{b}{T}}$ (see Richardson, *Phil. Mag.* vol. i. 1912), where C is the saturated photo-electric current, T is the temperature of the radiator, λ a constant which can take the values 2 or $\frac{1}{2}$, and b is the work function (ϕ) divided by the gas constant for one molecule (k). A is a constant depending on the area of the

surface. Therefore plotting values of $\log_{10} \frac{C}{T^{\lambda}}$ against $\frac{1}{T}$ should give a straight line, the slope giving the value of b .

The saturated currents C were comparatively large, and a sensitive galvanometer G_1 was used to measure them. The connexions were as shown in fig. 3. The two grid connexions and one side of the filament were connected to the positive side of a lamp-board in which the ten lamps were arranged in series and connected to the 240 volt-mains. The galvanometer G_1 was connected between two of the lamps, the other galvanometer terminal being connected straight to the potassium mirror. The resistance of the filament was measured at the various temperatures by means of a Wheatstone bridge arrangement. R_1 and R_2 were two

arms of a Post Office box, and Y was a coil of eureka wire 2 metres long, immersed in a flask filled with paraffin-oil, which in turn was surrounded by a water-bath. The resistance of the coil was 2.056 ohms. Its resistance was previously measured at 20° C. and at 100° C., no difference being detectable, and when surrounded by a water-bath the

Fig. 3.

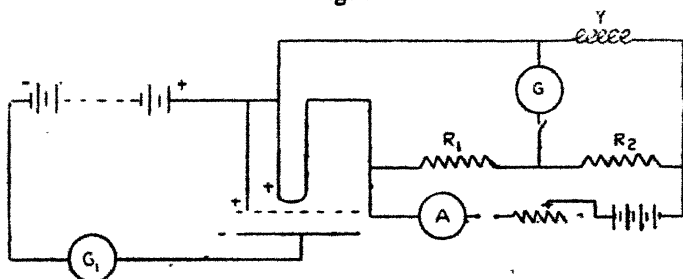
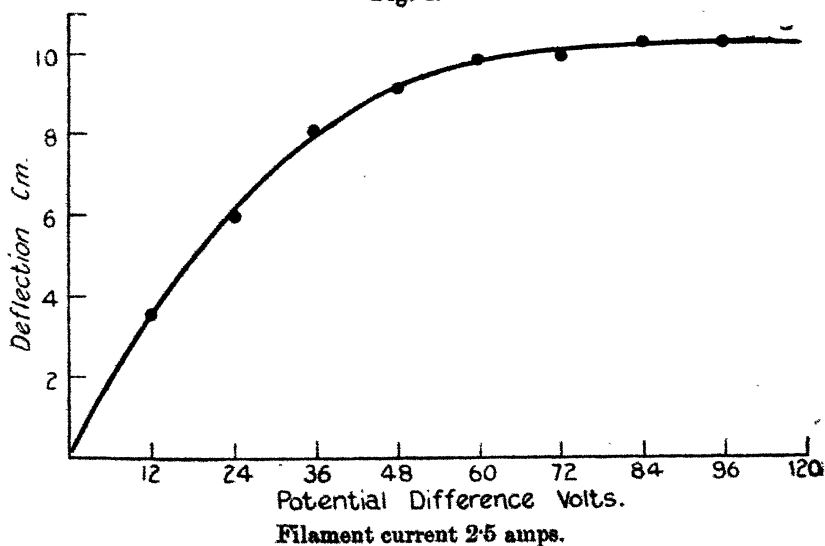


Fig. 4.



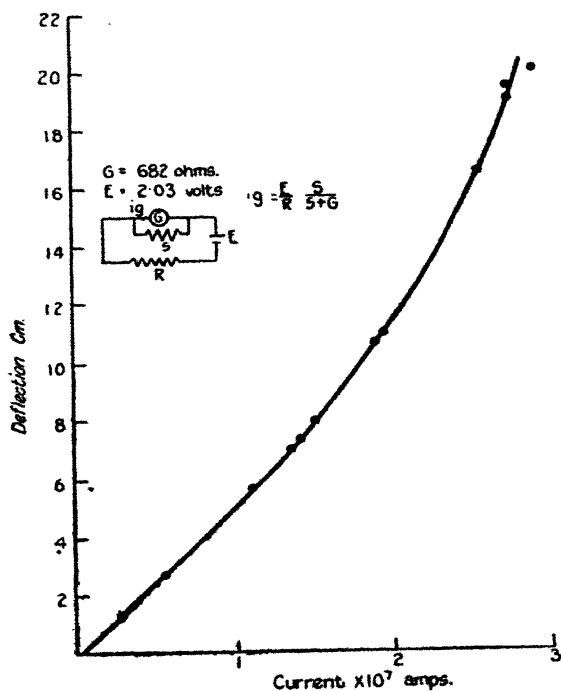
Potential Difference. Volts.	Deflexion. cm.	Potential Difference. Volts.	Deflexion. cm.
12	3.6	60	9.8
24	6.0	72	9.9
36	8.0	84	10.2
48	9.1	96	10.2

temperature varied over a range of less than 10° C., when the largest filament currents were used. Consequently under the conditions of experiment it was an invariable

resistance. The filament was heated by a battery of accumulators and the steady balance in the bridge found, using a dead-beat Onwood galvanometer G, which gave a deflexion of about 10 cm. on the scale for a change of resistance of 1 ohm in the variable arm of the box.

The photo-electric currents were well saturated, as is shown by fig. 4, the current-potential difference curve corresponding to a filament current of 2.5 amps. With the

Fig. 5.

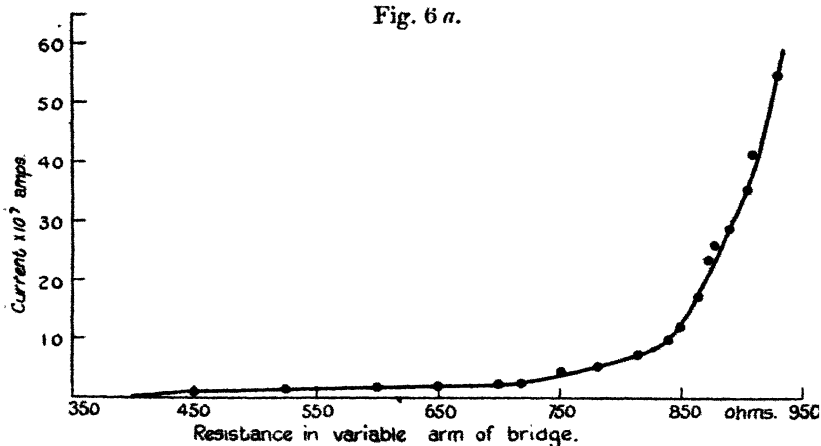


R ohms.	S ohms.	Current $\times 10^7$ amps.	Deflexion cm.
10^6	10	.29	1.3
10^6	20	.57	2.7
5×10^5	20	1.14	5.6
10^6	50	1.39	6.9
4×10^5	20	1.45	7.3
9×10^5	50	1.54	7.9
3×10^5	20	1.93	10.6
7×10^5	50	1.98	10.9
10^6	100	2.59	16.5
5×10^5	50	2.78	19.0
5×10^5	50	2.78	19.4
10^6	10	2.93	20.0

largest filament current used (3.5 amps.), saturation was secured by having 108 volts potential difference between the potassium and the filament, so this value was used throughout.

The graph plotted between current and resistance in the variable arm of the box, *i.e.* between current and filament temperature in arbitrary units, was of the form shown in figs. 6 *a* and 6 *b*. The initial rise and following flat portion was assumed to be due to a second and lower threshold frequency, for at this stage the filament was not glowing.

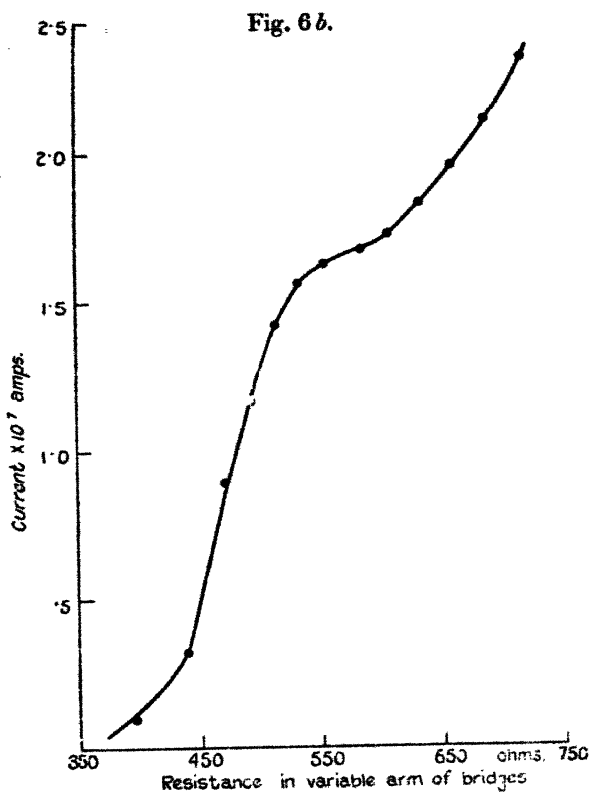
In order to ensure the best possible conditions, the potassium was then melted off the walls of the bulb and a completely fresh film deposited. As soon as this film was

Fig. 6 *a*.

sufficiently thick the charcoal tube was immersed in liquid air. A set of deflexion and resistance readings was taken about half an hour after the mirror had been deposited, and another set taken after the lapse of two and a half hours. Neither at this time nor next morning was any fatigue noticed; in fact, as will be mentioned later, the current over a certain range increased with time. The curves obtained with this fresh film agreed with those previously obtained.

Hysteresis effects were considerable. Readings were taken when the filament current was gradually increased, but if taken in the reverse order the difference between corresponding current readings was so great that for the lowest temperatures used the descending reading would be as much as twice the ascending reading. The effect disappeared quite rapidly with time; in the case of the high

temperatures so rapidly that the effect was not noticeable. Though the decay at lower temperatures was slower, the original ascending reading would be reached by leaving the apparatus for 10 to 15 minutes. The descending readings are inconsistent, for they depend on the time that lapses between altering the filament current and taking the reading of the deflexion and the corresponding filament resistance.



Resistance.	Deflexion.	Current $\times 10^7$.	Resistance.	Deflexion.	Current $\times 10^7$.
ohms.	cm.	amps.	ohms.	cm.	amps.
395	·45	·10	584	8·8	1·68
440	1·45	·32	607	9·1	1·73
472	4·3	·89	632	9·9	1·84
513	7·2	1·42	659	11·0	1·97
534	8·0	1·56	688	1·8 *	2·12
555	8·5	1·63	717	2·0 *	2·33

* Shunt 150 ohms.

The effect appeared to be in no way altered in the second case, when a presumably higher vacuum was contained in the bulb.

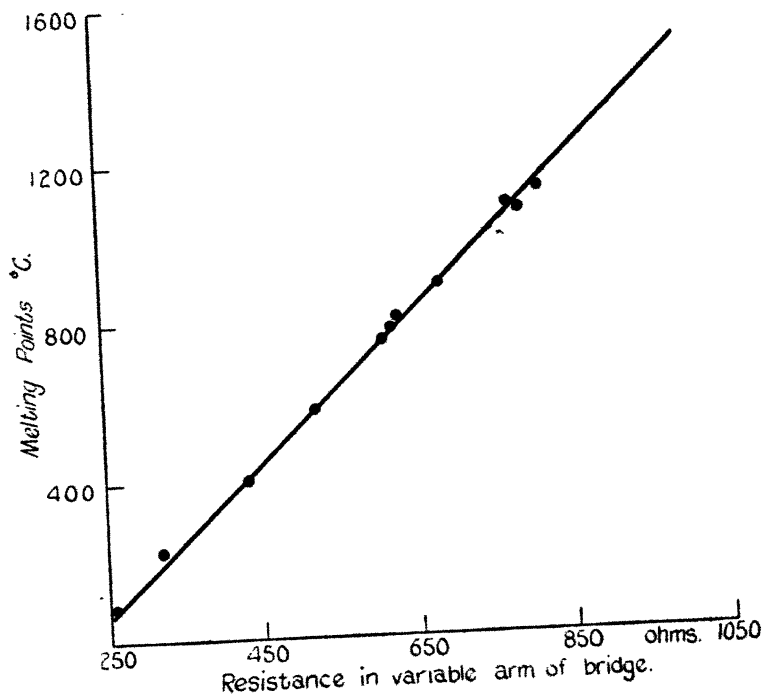
TABLE II.

Shunt ohms.	Resistance in variable arm of box ohms.	Deflexion. cm.	Temperature. ° C.	$\frac{1}{T} \times 10^4$.	Current $\times 10^7$ amps.	$\log_{10} \frac{C}{T^2} + 13$.	$\log_{10} \frac{C}{T} + 10$.
∞	400	.50	340	29.4	.12	.016	.813
	425	1.05	380	26.3	.23	.202	1.072
	437	1.60	405	24.7	.35	.323	1.240
	450	2.35	425	23.5	.49	.433	1.376
	462	3.35	445	22.5	.70	.547	1.507
	475	4.40	470	21.3	.90	.610	1.618
	487	5.30	485	20.5	1.08	.662	1.691
	500	6.75	505	19.8	1.35	.724	1.779
	525	7.60	553	18.1	1.50	.691	1.805
	550	8.25	605	16.5	1.60	.641	1.813
	575	8.60	657	15.2	1.65	.582	1.809
	600	9.25	712	14.0	1.75	.538	1.817
	625	9.65	777	12.9	1.80	.475	1.810
	650	10.40	830	12.1	1.90	.441	1.819
	675	1.75	890	11.2	2.05	.413	1.837
	700	1.95	920	10.9	2.25	.470	1.916
	717	2.00	945	10.6	2.33	.417	1.877
150	753	3.6	1005	9.95	4.16	.615	2.118
	782	4.6	1070	9.35	5.21	.658	2.202
	815	6.6	1135	8.80	7.32	.760	2.337
	839	9.4	1180	8.48	9.82	.848	2.456
	850	5.2	1200	8.33	12.00	.921	2.540
	867	5.8	1230	8.13	17.13	1.054	2.689
	876	8.2	1248	8.00	23.28	1.176	2.819
	882	10.4	1260	7.94	25.72	1.209	2.860
	890	10.8	1275	7.85	28.65	1.245	2.904
	905	16.6	1302	7.69	35.33	1.319	2.991
50	911	5.8	1338	7.60	41.10	1.381	3.056
	935	8.85	1360	7.35	59.30	1.506	3.206
After lapse of three days.							
∞ 150	542	9.3	600	16.7	1.75	.687	1.854
	579	1.9	675	14.8	2.22	.688	1.932
	607	2.1	725	13.8	2.44	.667	1.957
	649	2.4	810	12.4	2.79	.639	1.991
	654	2.5	820	12.2	2.88	.632	2.003
	706	2.8	915	10.9	3.33	.540	2.042
	715	3.1	935	10.7	3.60	.615	2.071
	751	3.9	1000	10.0	4.44	.647	2.147

The relation between filament temperature and resistance was found by opening the bulb and withdrawing the filament and grid, and then finding the resistances of the filament at the melting-points of certain crystals. The bridge arrangement was exactly the same as when taking readings of the photo-electric current, and minute crystals of substances

having well-defined melting-points were placed on the filament at its hottest part. The current passing through the filament was gradually increased, the Wheatstone balance being readjusted continually until the crystal, which was viewed through a microscope, melted. The graph obtained by plotting the melting-point temperature against the resistance in the variable arm of the box was a straight line (fig. 7).

Fig. 7.



Crystal.	Melting- Point °C.	Resistance. ohms.
Naphthalene.....	79	256
Silver nitrate	218	325
Potassium bichromate	400	435
Barium nitrate.....	575	525
Potassium bromide...	750	625
Sodium chloride	801	635
Sodium sulphate	884	683
Potassium sulphate...	1070	780
Stannic oxide	1180	815

Having determined the temperatures and the corresponding currents, graphs were plotted between $\log_{10} \frac{C}{T^3}$ and $\frac{1}{T}$, and

also between $\log_{10} \frac{C}{T^{\frac{1}{2}}}$ and $\frac{1}{T}$ (figs. 8 and 9). In both cases

Fig. 8.

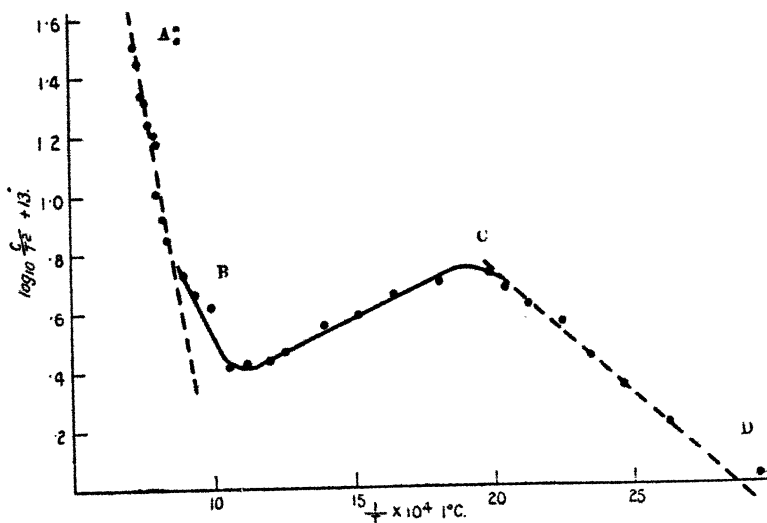
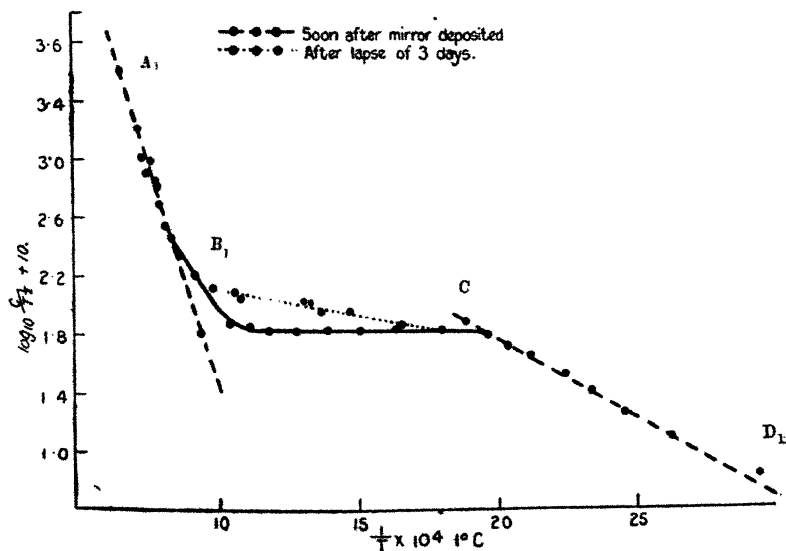


Fig. 9.



nearly all the points lie on three straight lines, and the slopes of the portions AB and CD are nearly the same in

both graphs. The intermediate portion BC, however, is quite different. When taking $\log_{10} \frac{C}{T^{\frac{1}{2}}}$ we have a line sloping in the positive direction, apparently indicating a value for b that is negative. In the other case the central line B_1C_1 is very nearly horizontal, but has a slight slope in the negative direction. This central portion corresponds to the almost horizontal part of the current-temperature curve in fig. 5, and this part does not appear to be very stable. The currents in this region gradually increased with time, not becoming absolutely constant until about three days after the potassium mirror had been deposited. Using readings obtained after this lapse of time, the general characteristics of this part of the two curves are unaltered, but the slope is different. The slope in the negative direction when plotting $\log_{10} \frac{C}{T^{\frac{1}{2}}}$ is increased and equal to $\cdot 026$. This is smaller than the others, namely $\cdot 64$ and $\cdot 11$. Apparently this would mean that for potassium there are three threshold frequencies for the sensitized surface. On the other hand, the intermediate portion may be represented by the sum of terms such as

$$C = A_1 T^k e^{-\frac{b}{T}} + A_2 T^k e^{-\frac{b_1}{T}},$$

where both terms are of about the same magnitude. The instability would then be due to some small portions, taking some time to decide which work-function to assume.

The results obtained show that potassium has at least two work-functions, corresponding to two critical wave-lengths, one at 9700 A.U. and the other at 57,000 A.U.

Since

$$C = A_1 T^k e^{-\frac{b_1}{T}},$$

of br

$$\log_e \frac{C}{T^{\frac{1}{2}}} = \log_e A_1 - \frac{b_1}{T},$$

Rate

so
$$b_1 = \frac{\text{slope} \times 10^4}{\log_{10} e} ^\circ \text{C.};$$

and since $k = 1.37 \times 10^{-16} \text{ ergs}/^\circ \text{C.},$

$$\phi = \frac{\text{slope} \times 10^4}{\log_{10} e} \times 1.37 \times 10^{-16} \text{ ergs};$$

and since $h = 6.547 \times 10^{-27} \text{ ergs/sec.},$

it follows that

$$\lambda_e = \frac{3 \times 10^{10} \times 6.547 \times 10^{-27} \times \log_{10} e}{\text{slope} \times 10^4 \times 1.37 \times 10^{-18}}.$$

$$\text{Also } \log_{10} A_1 = \log_{10} \frac{C}{T^{\frac{1}{4}}} + \frac{b_1}{T} \log_{10} e.$$

To determine the multiplying constants A_1 and A_2 , points are selected on the portions AB and CD respectively, where only one term is of importance in determining the value of the photo-electric current.

To determine A_1 :

$$T = 1248^\circ \text{ C.}$$

$$C = 23.28 \times 10^{-7} \text{ amp.}$$

To determine A_2 :

$$T = 405^\circ \text{ C.}$$

$$C = .35 \times 10^{-7} \text{ amp.}$$

TABLE III.

	AB.	$A_1 B_1$.	CD.	$C_1 D_1$.
Slope64	.64	.086	.11
$b^\circ \text{ C.}$	1.46×10^4	1.46×10^4	1.98×10^3	2.53×10^3
ϕ ergs	2.02×10^{-12}	2.02×10^{-12}	2.71×10^{-13}	3.47×10^{-13}
λ_e A.U.	9700	9700	50,000	57,000
Constant0089	.0089	2.3×10^{-7}	5.11×10^{-7}

Thus the relation governing the photo-electric current can be represented by

$$C = .0089 T^{\frac{1}{4}} e^{-\frac{1.46 \times 10^4}{T}} + 5.11 \times 10^{-7} T^{\frac{1}{4}} e^{-\frac{2.53 \times 10^3}{T}}.$$

The constant A_2 , multiplying the larger work-function is 1.8×10^4 times as great as the second. This supports the theory of "patches" put forward by Richardson and Young (Proc. Roy. Soc. Ser. A, 1925), indicating, as it does, that only a small portion of the surface responds to the lower frequency, while a much larger part, if not the whole surface, is excited by the higher frequency. If the whole of

16 *The Complete Photo-electric Emission from Potassium.*

the surface could respond to any of two or more threshold frequencies depending on the condition of the surface and illumination, the hysteresis effects could be explained. After being subjected for a few minutes to the illumination from the filament when at a high temperature, the "patch" of lower value ϕ might gradually acquire the larger value of the work-function, and so the current would increase, since at high temperatures, at any rate, the term containing the greater b predominates. When the filament temperature is reduced, this part of the surface does not revert to its former state directly, and while so reverting the current is larger than the corresponding one when ascending the scale of temperature. If this change does occur, it would also account for a creeping up of current noticed at high temperatures, the galvanometer mirror taking some time to come to a steady position. Consequently it seems probable that the whole of a sensitized potassium surface has one characteristic work-function, while certain small portions, distributed over the whole surface or collected together in patches, can possess one or more lower work-functions. When illuminated with light of long wave-length, only the smaller portion will contribute to the photo-electric current, and at shorter wave-lengths the rest of the surface plays its part, the smaller portion gradually changing until all the surface has acquired the greater work-function. This implies that the second constant A_2 is itself a function of the temperature. However, if the function is a low power of the temperature, it will have a negligible effect on the $\log_{10} \frac{C}{T^{\frac{1}{2}}}$ against $\frac{1}{T}$ graph and on the value of ϕ determined.

Summary.

No evidence has been found for the existence of a positive photo-electric emission, and it has been shown that, if such an effect does exist, it is less than 10^{-7} times the negative emission, from the same surface, measured in these experiments.

It is shown that potassium has at least two work-functions corresponding to the wave-length 9700 A.U. and 60,000 A.U. The results indicate that the "patches" of lower work-function form a very small part of the whole surface, and can acquire the greater work-function under the influence of prolonged illumination.

II. *A New Method of Determination of the Volume of 1 Curie Radon.* By L. WERTENSTEIN, *Professor of the Free University, Warsaw* *.

I. *Principle of the Method.*

THE first determinations of the volume of 1 curie of radon were made by Rutherford †, Debierne ‡, and Ramsay §. Their results were concordant; the volume of 1 curie of radon at 0° and normal pressure (called in this paper V_0) was found equal to .6 c.c. This value was in an excellent agreement with expectations from the theory of radioactive transformations based on the values of the fundamental radioactive and atomic constants as known at that period. The agreement is, however, not so good if one uses for calculations the values of those constants which are generally accepted at the present time. Adopting for Z the number of α -particles emitted in 1 sec. by 1 gm. Ra, $3.72 \cdot 10^{10}$, for N , the number of molecules of a perfect gas in 1 c.c. at N.T.P. $2.705 \cdot 10^{10}$, and for λ_r , the radioactive constant of radon, $2.1 \cdot 10^{-5}$, we get for V_0 .652 c.c. a value about 10 per cent. higher than the values obtained by Rutherford, Debierne, and Ramsay.

The methods used by those physicists were similar in principle; they consisted essentially in compressing carefully purified radon into a calibrated fine capillary.

The disadvantage of this method is that it is very difficult to prove that the final product is pure. Moreover, concentrated radon undergoes considerable changes of volume during the first hours after its preparation, and it is generally assumed that it is the final volume which is the right one.

It seemed to me interesting to attack this problem by a method which would permit the analysis of the purified radon. Owing to the extremely small quantities of gas involved, the only methods suitable for a quantitative analysis seemed to be methods based on the properties of highly rarefied gases. If we consider that the pressure of .1 curie of radon in a volume of 100 c.c. is equal to about .65 bar, we arrive at the conclusion that we are dealing in this problem with the range of pressure to which the laws of highly rarefied gases are fully applicable.

* Communicated by Sir E. Rutherford, O.M., P.R.S.

† E. Rutherford, *Phil. Mag.* p. 300 (1908).

‡ A. Debierne, *C. R.* p. 1264 (1909).

§ Gray and W. Ramsay, *Trans. Chem. Soc.* vol. iv. pp. 95, 1073 (1900).

The method described in this paper consists in measuring simultaneously the pressure and the coefficient of (external) friction of the gas. This coefficient is proportional in a highly rarefied chemically pure gas to its pressure and to the square root of its molecular weight, in a mixture of gases to the sum of the products of the pressure and the square root of the molecular weight of each constituent. The pressure was determined by means of a calibrated Knudsen gauge and the coefficient of friction by means of a quartz-fibre gauge. The "damping," indicated by this gauge as the inverse of the time during which the amplitude of the oscillations of the quartz fibre diminishes in a given ratio, is proportional to the coefficient of friction. Let p be the total pressure, $p_r, p_x, p_y \dots$ partial pressures of radon and other gases mixed with it, $M_r, M_x, M_y \dots$ molecular weights of these gases, d the damping. We shall have

$$p = p_r + p_x + p_y + \dots$$

$$d = a_r p_r + a_x p_x + a_y p_y + \dots \quad (1)$$

where

$$a_r = c \sqrt{M_r}, a_x = c \sqrt{M_x} \dots$$

The constant c can be determined experimentally, and so we see that equations (1) enable us to calculate the partial pressure of radon if there is only *one* gas of known molecular weight mixed with the radon.

In a previous paper * I have shown that purified radon contains always, apart from water and mercury vapour, traces of all gases initially present with the radon. Of these gases, however, CO_2 is by far the most important, and it is the only one which condenses with radon at the temperature of liquid air.

It is obvious that we can apply the above method for determining the pressure of radon if we can analyse the mixture of radon and CO_2 . This analysis can be made under good conditions if (1) it is possible to get rid of H_2O and Hg vapours, (2) the total pressure of the mixture is of the order of 1 bar, (3) the partial pressure of all impurities is small compared with that of radon.

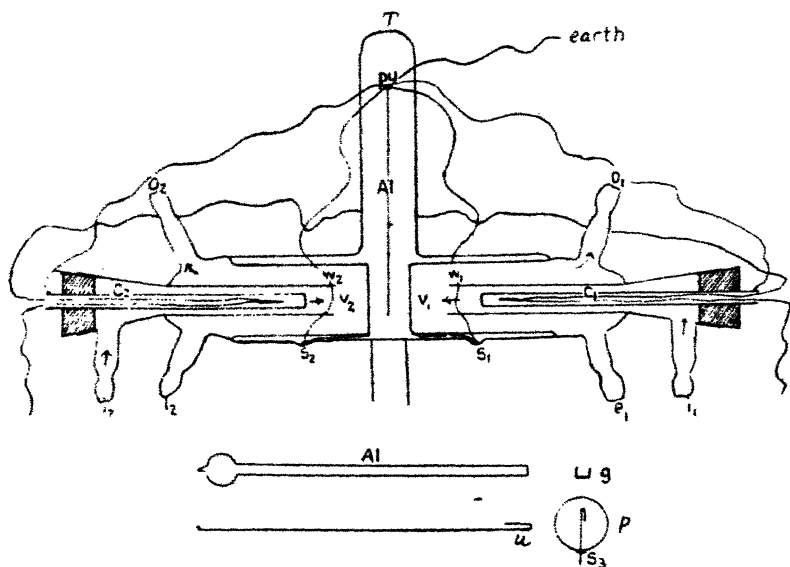
Condition (1) is easily fulfilled. The only precaution is that the radon must be introduced into the apparatus through a trap cooled to -120° , at which temperature the saturated vapour pressure of water and mercury is smaller than 10^{-3} bar, while radon and CO_2 remain in the gaseous state. A suitable thermostat for this temperature consists in a

* L. Wertenstein, "On the Purification of Radon," *Phil. Mag.* vol. v. p. 1017 (1928).

pentane bath heated electrically, and contained in a moderately exhausted non-silvered Dewar tube, surrounded by liquid air.

If conditions (2) and (3) are satisfied, which we shall see to be the case in the present work, we determine (a) the total pressure, p_1 , and damping, d_1 , of the mixture, (b) the pressure, p_a , and damping, d_a , found when a small part of the apparatus is cooled to the temperature of liquid air. The differences $p_1 - p_a = \Delta p$ and $d_1 - d_a = \Delta d$ are the pressure and damping due to radon and carbon dioxide. In order to calculate the partial pressure p_r of the radon and the degree

Fig. 1.



of its purity we have only to substitute in equations (1) Δp and Δd for p and d .

Knowing p_r we deduce V_0 , the volume of 1 curie of radon at N.T.P., from the equation

$$V_0 = \frac{p_r \cdot V \cdot 273}{(273 + t) \gamma \cdot 0.13 \cdot 10^6},$$

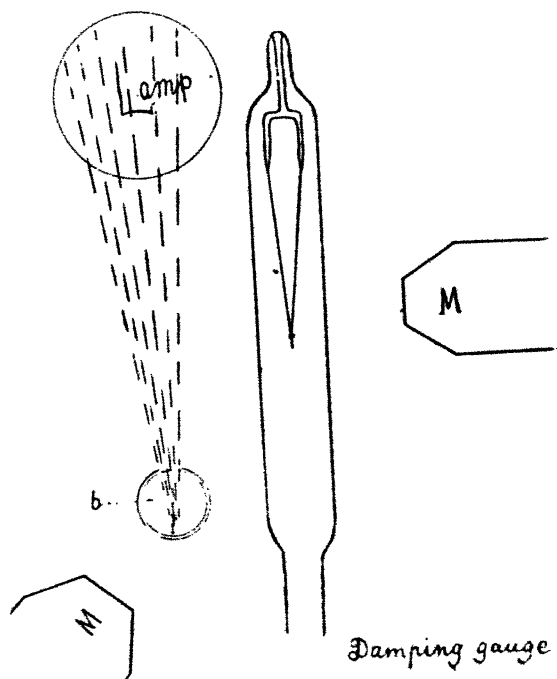
where V is the volume of the apparatus, t the temperature, and γ the quantity of radon expressed in curies.

II. Gauges and their Calibration.

The Knudsen^{*} gauge used in this work is shown in fig. 1. An aluminium leaf, about 6μ thick, cut off in the form

shown in A1 (fig. 1), hangs between flat and parallel faces the temperature of which can be changed by circulating water in vessels V_1 and V_2 . $l_1, l_2, i_1, i_2, o_1, o_2$ is the system of inlet and outlet tubes used for this circulation. The difference of temperature of the vessels is measured by means of thermocouples b_1, b_2 , and the deflexion of the leaf by means of a microscope provided with an eyepiece scale. We shall call "indication" π of the gauge the ratio of the deflexion

Fig. 2.



expressed in divisions of the microscope scale to the difference of temperatures expressed in divisions of the galvanometer scale.

The quartz-fibre gauge is represented in fig. 2. Its essential part is a system of two quartz fibres, about .03 mm. thick, sealed at the lower end at a sharp angle, while the upper ends are sealed into a lead glass fork fixed in the top of an ordinary glass tube. The lower end bears a short piece of a .1 mm. thick iron wire, by means of which the vibrations of the quartz system can be excited magnetically.

A microscope with an eyepiece scale is used for measuring the amplitude; if the illumination (shown on the left side of fig. 2) is convenient, the vibrating systems appear as a bright band with sharp ends. The band is seen to diminish slowly in width. The damping d is inversely proportional to the time during which the amplitude decreases in a given ratio.

For calculation purposes it was found convenient in this paper to use for this ratio the value 1.2 and to express the time in 10^5 sec.

For calibration, the gauges were joined to a McLeod gauge through a trap cooled to -120° in order to freeze out vapours. By means of a mercury fork the apparatus could be put into communication with a diffusion pump or with auxiliary arrangements for preparing and transferring small quantities of chemically pure gases. Hydrogen, oxygen, carbon dioxide, and xenon were used for calibration.

The whole apparatus must be thoroughly evacuated, after which we read the pressure p_0 at the McLeod gauge and the indications π_0 and d_0 of the Knudsen and damping gauges. p_0 is generally negligibly small. π_0 and d_0 correspond, under good experimental conditions, to a residual pressure of the order of .01 bar. This pressure is due to traces of water and mercury vapours, to which the McLeod gauge is insensitive.

We introduce into the apparatus one of the above-mentioned gases under a pressure of 2-3 bars, and we read the indications p_1 , π_1 , d_1 , of all instruments. We pump some gas off and obtain a new set of values p_2 , π_2 , d_2 .

These operations are repeated until the pressure drops to about .5 bar.

For each of the gases (k) used in this calibration we draw curves $\pi_k = f(p)$ and $d_k = \phi(p)$.

The functions are linear, and we have $\pi_k = b_k p + \pi_0$, and $d_k = a_k p + d_0$.

It is generally assumed that the Knudsen gauge is an absolute manometer, i.e., that its indications are independent of the nature of the gas. If this were true b_k ought to have for all gases the same value.

If, however, we examine this question more closely, we find that the force exerted on the leaf must depend on the kinetic energies of the molecules falling on it and reflected from it. If the temperatures of the faces between which the leaf hangs are given, these energies are functions of the accommodation coefficient of the gas filling the gauge. The accommodation coefficient increases in general with the

molecular weight; it has for hydrogen the value .28, for oxygen .8, for carbon dioxide .87. The highest value, .93, has been found for mercury vapour. Its upper theoretical limit is unity.

General considerations show that the indications of a Knudsen gauge, i. e., the constant b_k , must increase with the accommodation coefficient. In accordance with these considerations I have found for the four mentioned gases

$$b_{H_2} : b_{O_2} : b_{CO_2} : b_{Xe} = 79 : 100 : 104 : 105.$$

For our problem it is necessary to know the radon constant b_r . We cannot determine it directly. We see, however, that the values of b for the last three gases show only small variations. Assuming for b a value 1 per cent. higher than that of Xe, we are probably very close to the true value, for it must be expected that radon and xenon will behave in a very similar way.

During the course of the experiments the leaf had once to be changed and recalibrated. Before the change the sensitivity b_r of the gauge for radon was .0707 division of microscope per 1 bar and 1 division of the galvanometer scale. After the change b_r was .096 division of microscope per 1 bar and 1 division of the galvanometer scale. The deflexion of the galvanometer in actual experiments corresponded generally to 50 to 100 divisions and the deflexion of the leaf could be determined within 1/10 of a division, so that for pressures of the order of 1 bar the accuracy of measurement was about 1 per cent.

In the case of the damping gauge the problem of finding the constant a_r for radon is much easier as we have only to apply the formula

$$a_r/a_k = \sqrt{\frac{M_r}{M_k}}.$$

being the expression of Knudsen's law.

We can get a check of this formula by comparing the values a_r calculated from experimental values a_k for each of the gases used in the calibration. The comparison is represented on Table I.

The agreement is very good. I have used for calculations the value $a_r = 1164$, being the arithmetic average of values extrapolated from the oxygen and xenon data, which were obtained under the best conditions.

For CO, I have assumed the value $a_c = 517$ calculated from the same data. It seemed to me more reliable than the measured value 506, because the adsorption properties

of this gas described in a previous paper* obviously introduce some uncertainty in determinations of its pressure.

In equation (1) it was assumed implicitly that the indications of a Knudsen gauge do not depend on the nature of

TABLE I.

Gas.	Mol. weight.	a_k .	a_r .
Hydrogen	2.015	111.5	1175
Oxygen	32	442	1168
Carbon dioxide	44	506	1137
Xenon	130	890	1160

the gas. In reality, however, the experiment does not give us Δp , but

$$\Delta\pi = b_c p_c + b_r p_r.$$

Putting $b_c = .98b_r$, we can write these equations :

$$\left. \begin{aligned} \Delta p' &= \frac{\Delta\pi}{b_r} = p_r + .98p_c \\ \Delta d &= 1164p_r + 517p_c \end{aligned} \right\} \dots \dots (1a)$$

$\Delta p'$ is an apparent change of pressure, i.e., a change of pressure to which a change $\Delta\pi$ of indications of the gauge would correspond if the gas was pure radon.

From equations (1a) we get, writing for simplicity Δp instead of $\Delta p'$,

$$p_r = \frac{.98\Delta d - 517\Delta p}{623} \quad p_c = \frac{1164\Delta p - \Delta d}{623}.$$

III. Experimental arrangement.

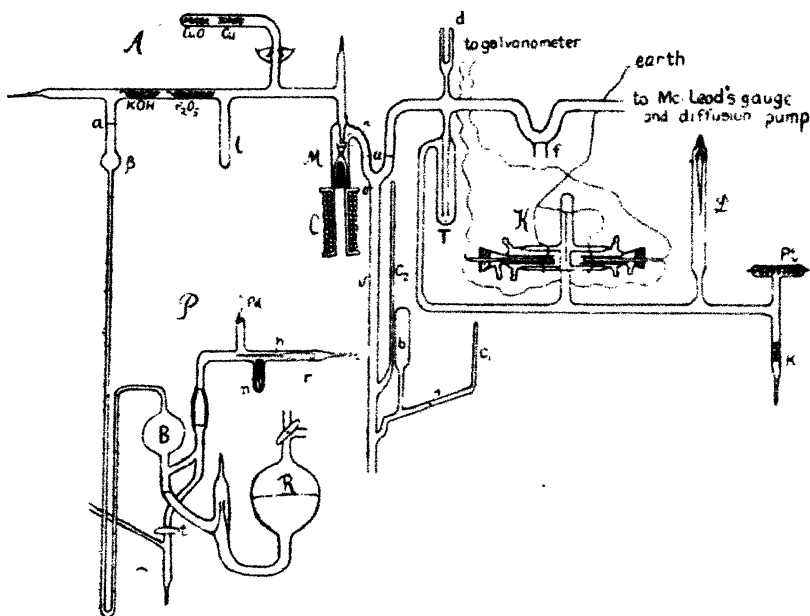
The apparatus has been constructed in such a way that purified radon could be introduced without having to open the apparatus to the atmosphere.

This precaution is essential, for since the pressure of the admitted gases is of the order of 1 bar, the apparatus must be exhausted beforehand to a "high vacuum." As is well known, such a state is destroyed if atmospheric air is admitted even for a short time.

* L. Wertenstein, *l. c.*

The general arrangement can be seen from fig. 3. It comprises three parts: (1) the manometric part with the Knudsen gauge *K* and damping gauge *D* and the trap *T*; (2) the purification apparatus *A* containing KOH and P_2O_5 in glass boats, CuO and Cu in a pyrex tube, and the tube *l* used for condensing radon in liquid air; and (3) the volumetric part, the use of which will be explained later. All parts can be evacuated by way of the mercury fork *f*. Part *A* can be put into communication with remaining parts by means of the mercury "tap" *M* operated electro-magnetically.

Fig. 3.



Before the experiment the whole apparatus has to be very carefully exhausted. The first operation consists in introducing partially purified radon into Part *A* by means of the transfer pump *P*, which has the advantage of avoiding the use of greased taps. The left branch of the capillary U-shaped tube has more than the barometric length, and, owing to this fact, it is possible to introduce air into the bulb *B*, while vacuum remains in *A* and other parts.

While the transfer pump is open to air we place in the horizontal tube *p* a thin-walled tube *r* containing partly purified radon (about .2 c.c. of gas), after which the tube *p* is sealed.

The bulb B is evacuated by means of a separate pump through the tap *t*, which is afterwards closed and covered with a column of mercury. The tube *r* is then broken by means of a simple magnetic device *m* and the radon is transferred to the purification part by operating the transfer pump, in which the movements of mercury are controlled by varying the pressure over the reservoir R. The radon is then left for 15–18 hours in contact with the KOH and P_2O_5 .

At the beginning and at the end of that period the pyrex tube containing CuO is heated for 30 minutes to about 600° .

After that time the radon contains only a small quantity of CO_2 , but an appreciable amount of gases which do not condense at the temperature of the liquid air. In order to pump out these gases, we surround the tube *l* with liquid air and open several times for 10 seconds the "tap" M, the mercury fork establishing the communication with the diffusion pump. When the evacuation is finished, the communication with the diffusion pump is cut off, the tube *l* allowed to warm up, and radon is distilled into the manometric apparatus by introducing a few drops of liquid air in the small Dewar tube *d*. After that we raise the mercury in the tube V, enclosing radon in the manometric part.

We can now proceed to determinations of pressure and damping. While the radon and CO_2 are still condensed in the small Dewar tube *d* we measure the residual pressure p_a and damping d_a of uncondensable gases. The liquid air is then evaporated quickly by introducing a copper wire into the small Dewar tube, and when this tube is at room temperature we determine the total pressure p_1 and damping d_1 .

We get in this way the values Δp and Δd defined on page 23. Liquid air can be used again in the same way as described above in order to obtain another set of values of Δp and Δd .

IV. Results.

I have executed in all four series of experiments. The first two series were of a preliminary character; they enabled me to work out the technique of the measurements, and also revealed some unforeseen experimental difficulties.

It was found that after introduction of radon the pressure and damping increased steadily, so that after some 30 minutes the pressure was twice as great as in the beginning. This increase is due to the evolution of gases from glass bombarded by α -rays. The increase of damping was, however, very small, and by measuring simultaneously the rate of increase of

pressure and damping, I found that the evolving gas was nearly pure hydrogen, so that the relative amount of CO_2 remains unchanged. This observation enabled me to calculate Δp and Δd in the following way:—

Curves $p_1 = f(t)$, $d_1 = p(t)$ were drawn for the total gas and similar curves for uncondensable gases. By taking the difference of ordinates of curves interpolated for the same time t , we get the values of Δp and Δd . Owing to the small number of experimental points [each determination takes a long time] the interpolations were a little uncertain. The results were, however, better than could be expected.

In the first experiments .0718 curie of radon was introduced into the apparatus. Its volume V was 157 c.c., the temperature of the room was 19° .

Three sets of measurements were taken. After the first set the radon was distilled back into the purification part, the evolved gases were pumped out and redistilled into the manometric part. During these operations .0018 curie radon was lost.

The results are represented in Table II. The first column of this table contains the value of Δp ; the second and third give the partial pressures p_r and p_c of radon and CO_2 , in the fourth we find the relative amount (or degree of purity) of the radon, in the fifth the quantity of radon in curies, in the sixth the value V_0 of the volume of 1 curie of radon deduced from the experimental data.

TABLE II.

Δp bar.	p_r bar.	p_c bar.	$\frac{p_r}{\Delta p}$	γ curie.	10^{-4} c.c.
.55	.289	.261	.528	.0718	5.83
.537	.323	.114	.749	.070	6.68
.465	.285	.180	.63	.070	5.9

The average value of V_0 is $6.14 \cdot 10^{-4}$ c.c., showing that the method gives results very near to the truth even under unfavourable conditions.

In order to improve these conditions it was necessary to eliminate the effect of the gases evolved from the glass walls by the bombardment of the α -particles.

The measurements of damping indicating that the evolving gases consisted chiefly of hydrogen, I added to the apparatus

a device for oxidizing the hydrogen. The water-vapour formed on oxidation ought to be condensed in the trap cooled to -120° .

For this purpose I used a small tube, Pt (fig. 3), containing a thin platinum wire through which a current could be sent. The platinum wire was covered by electrolysis with copper oxidized afterwards by glowing the wire.

It was found that this simple device enabled me to realise the steady conditions necessary for taking reliable measurements. The next experiment performed with this arrangement was, however, not quite satisfactory owing to some imperfections of the technique. The temperature of the glowing wire was not adjusted to the right value; during the experiment the temperature of the trap went up to -105° . The result was that the evolution of gas was still half as much as in the first experiment, and the water-vapour formed was not completely removed by the trap, as was shown by the fact that the pressure of *condensable* gases increased steadily, while in the previous experiment it remained constant.

It was, however, found possible to deduce from the measurement the partial pressure of radon. Δp and Δd being in this case due to three gases, radon, CO_2 , and H_2O , it was necessary to calculate the amount of water-vapour. This was done in the following way. By measuring simultaneously the increase of total pressure and damping, we can analyse the evolving gas consisting of hydrogen and water-vapour and determine the partial pressure of water-vapour. The additional damping due to that vapour can be calculated from its molecular weight. Subtracting from Δp and Δd the partial pressure and damping due to water-vapour, we have again the case of two constituents only, to which equations (1a) are applicable.

In this experiment .1386 curie radon was used.

The volume of the apparatus was 180 c.c. The results of two sets of measurements are shown on Table III.

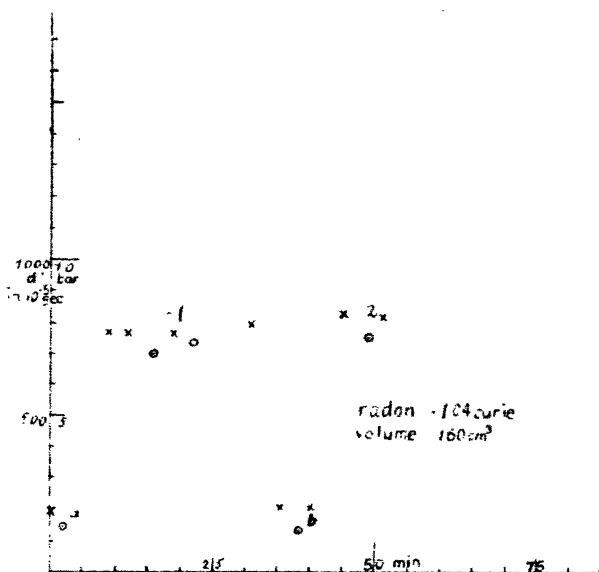
TABLE III.

Δp bar.	p_r bar.	p_c bar.	$\frac{p_r}{\Delta p}$	γ curies.	$\frac{V}{10^{-4}}$ c.c.
.817	.519	.298	.635	.1386	6.2
.961	.527	.434	.55	.1386	6.29

The larger amount of CO_2 in the second set is probably to be explained by the fact that in the interval between the two sets radon was kept condensed during about 15 minutes in order to pump off evolved gases. As was shown in my previous paper, glass contains always traces of absorbed CO_2 , which distil on to the radon during its condensation in liquid air.

The agreement of values of V_0 obtained in the two sets is satisfactory. The method of calculating the results is, however, complicated, so that these experiments cannot be considered as conclusive.

Fig. 4.

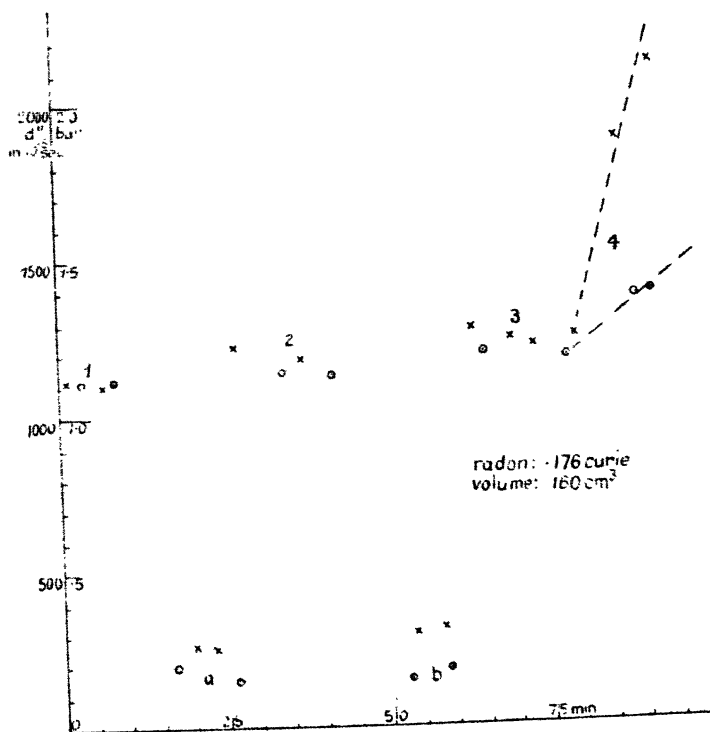


In the third and fourth experiments, which will be described now, I succeeded in surmounting the experimental difficulties of the problem. In these experiments (1) the whole apparatus was baked out to 350° before the introduction of radon, (2) a tube containing a few pieces of KOH was added in order to reduce the amount of CO_2 , (3) the temperatures of the glowing wire and of the trap were carefully adjusted. The volume of the apparatus was 160 c.c., .104 curie radon was used in the third, and .176 curie in the fourth experiment.

The results are represented graphically in figs. 4 and 5. In these figures the values of pressures are represented by

crosses, the values of damping by circles. Groups of points and circles marked by figures 1, 2, etc., were obtained with total gas, those marked by letters *a*, *b*, etc., with uncondensable gas only. The group marked 4 on fig. 5 was obtained after the current through the Pt wire was cut off. This group shows that hydrogen is still evolved but disappears nearly completely when the CuO is heated, as may be seen from the approximate constancy of the pressure of the total

Fig. 5.



gas during the first period of the experiment. The oscillation of individual values of total pressure and damping are relatively small, those corresponding to uncondensed gases are more important, which is probably due to the smallness of effects observed. There was still a slow general increase of pressure, about 8 per cent. during a whole experiment. In order to eliminate the error due to this residual evolution of gas, the results have been calculated in the following way

For each group an arithmetic average p_1, d_1, p_a, d_a , etc., was calculated. From these values $\Delta p, \Delta d$ were calculated as

$$\frac{p_1 + p_2}{2} - p_a \dots, \quad d_2 - \frac{d_a + d_b}{2}, \text{ etc.}$$

The final results are collected in Table IV.

TABLE IV.

Experiment.	Δp bar.	p_r bar.	p_c bar.	$\frac{p_r}{\Delta p}$.	γ curie.	V_0 10^{-4} c.c.
3	·586	·433	·143	·75	·104	6·15
	·597	·454	·143	·77		6·41
4	·896	·743	·153	·825	...	6·26
	·909	·753	·153	·825	·176	6·33
	·908	·808	·1	·89	...	6·8

It will be noticed that the degree of purity of radon was in these experiments higher than in the first experiments.

The average value of V_0 is $6·39 \cdot 10^{-4}$ c.c., and is probably correct within 5 per cent.

The average of the values obtained in the first two experiments is $6·19 \cdot 10^{-4}$ c.c., differing by about 3 per cent. from the final value. This small disagreement shows that with this method even in very imperfect conditions relatively good results can be obtained.

The constant V_0 is connected directly with the number of α -particles emitted in one second by 1 g. Ra. From $V_0 = 6·39 \cdot 10^{-4}$ c.c., we get $Z = 3·62 \cdot 10^{10}$.

The method described in this paper could be further improved by constructing more sensitive gauges. The main difficulties arise from the violent effects taking place in presence of radon. It would therefore seem desirable to find a material which does not give off gases when bombarded by α -rays*. On the other hand, it seems that the method could be applied successfully to another similar problem, viz., the determination of the volume of He produced in one second by 1 g. Ra.

* Since this paper was written I have found that glass baked out to a temperature of 450° does not give out any appreciable amount of gas under the action of α -rays.

V. Determination of V_0 by use of Capillary Tubes.

The results of this work show that I was unable to obtain pure radon; the relative amount of CO_2 varied in different experiments from 15 per cent. to 45 per cent. of the total quantity of gas. It will be remembered that in the method of compressing the purified radon into a capillary tube the initial volume undergoes generally a marked diminution ranging from 30 per cent. to 50 per cent. of its final value. It seems clear that in this method also pure radon was not obtained by use of chemical processes only. It is highly probable that the final purification takes place in the capillary, the impurities being absorbed by glass under the action of α -rays.

In order to throw some light on this question, I have executed some experiments by the method of the capillary tube using an apparatus described in a previous paper*, and also the arrangement shown on fig 3. To the vertical tube V a sloped tube S, ending in a calibrated capillary C_1 , was sealed. Another capillary C_2 of the same bore as C_1 sealed to V, allowed the pressure of compressed gas to be determined by means of a cathetometer. The use of the bulb b will be explained later.

The first experiment was performed with the apparatus described in my previous paper. The results were very similar to those obtained by Rutherford. 40.5 millieuries radon were introduced into a capillary. The contraction amounted to 30 per cent. of the final value, which corresponded to $V_0 = 6.4 \cdot 10^{-4}$ c.c.

It would seem surprising that in presence of rarefied radon gas is evolved, while the concentrated radon acts as a "clean-up" agent. This apparent contradiction is easily explained if we consider that the first effect is due to collisions between α -particles and the walls of the apparatus, while the second one is a consequence of collisions between molecules and α -particles. It is probable that, in analogy with the clean-up effects observed in a triode valve, ionized or excited molecules are readily absorbed by the material of walls. If the pressure is very low the number of collisions with free molecules is negligibly small, and therefore under these conditions the evolution of gas is more important than its absorption.

In a concentrated state radon atoms as well as molecules of impurities are struck by α -particles, and it seemed there-

* L. Wertenstein, *loc. cit.*

fore probable that radon itself may be partly absorbed in the capillary tubes.

In order to verify this hypothesis I have tried to repeat the experiment with radon as pure as possible; if radon was absorbed, the final volume ought to be smaller than its theoretical value.

I have used for this experiment radon the degree of purity of which has been tested by the "damping" method. This radon was distilled into the tube S (wrapped for this purpose, as usual, with cotton wool, soaked in liquid air). This tube contained some fused KOH in order to diminish further the amount of CO_2 . Before compressing the radon into the capillary, it was submitted to another kind of purification based on laws of flow of highly rarefied gases. For that purpose the bulb *b*, connected to S through a 5 mm. wide capillary, was used. After the radon had been condensed, mercury was brought into such a position that the communication with *b* was shut off. When the radon was set free after removal of liquid air, the mercury was lowered for a few seconds below the opening of the capillary.

During that short time a part of the radon passed into the bulb *b*, but, according to the laws of flow of gases, the relative amount of CO_2 which went to this bulb must have been much larger. The remaining gas was introduced into the capillary C_1 .

The results of the experiment confirmed my hypothesis. The initial volume of the radon corresponded to $V_0 = 5.9 \cdot 10^{-4}$ c.c., the final volume (determined on the next day and corrected for radioactive decay) to $V_0 = 4.34 \cdot 10^{-4}$ c.c.

We see that nearly 30 per cent. of the radon was absorbed.

In order to ascertain the nature of this absorption the radon was pumped out and the tube heated during exhaustion to 200° . Subsequent measurements of the γ -ray activity showed that the tube retained about 20 per cent. of the initial quantity of radon (taking account of the radioactive decay).

The amount of concentrated radon absorbed on glass seems to increase with the time during which the radon is kept in the capillary. In another experiment performed with less pure radon the initial volume corresponded to $V_0 = 7.91 \cdot 10^{-4}$ c.c., the final value, measured on the next day, to $6.2 \cdot 10^{-4}$ c.c. After four days the radon was pumped off as in the previous experiments. It was found that the glass retained strongly 40 per cent. of the initial quantity of radon absorbed.

It is probable that the "clean-up" effect of α -rays is selective. It is obviously much smaller for radon than for other gases, and this explains probably why the method of the capillary tube gives in general results very close to truth.

The work described in this paper was performed during the years 1925/1926 and 1926/1927 in the Cavendish Laboratory.

It is a great pleasure for me to express my best thanks to Sir Ernest Rutherford for his kindness in receiving me in the Cavendish Laboratory, in placing at my disposal the large quantities of radon and other experimental resources, and in showing a permanent interest in the progress of my work.

I am grateful to Dr. J. Chadwick for his help and interest.

My stay in England was made possible by a fellowship granted by the International Education Board.

I wish to express my thanks to this Board.

III. *The Classical Reasonableness of the Quantum Theory and Simple Operative Solutions of Schrödinger's Equation.* By Prof. A. PRESS*.

PART I.

The Differential Equation of an Excitation Field.

IN a paper appearing in the *Philosophical Magazine* for Dec. 1927, the writer likened the action of a radiating harmonic oscillator to that of a reed or organ-pipe fed by a source of air under pressure. As the pressure was increased the organ-pipe responded but slightly to an increase in intensity of the note emitted, for a point was soon reached when the dominant note suddenly changed to a higher harmonic. It was later shown by strictly classical analysis that the amplitude of the radiation wave always bore a definite ratio to the amplitude of the normal non-radiating component. In the following, therefore, reference to the normal non-radiating component will be sufficient.

For the pipe above referred to, the excitation field contemplated would be that due to the blowing stream causing it to emit a note. It will be on the basis of the above analogy with the radiating harmonic oscillator that the following analysis will be developed. In general there will be a

* Communicated by the Author.

variable velocity potential P in such an exciting stream because of the action of the organ-pipe wall of the slit or the reed, which, due to the vibrations, affects the distribution of pressure head in the stream contiguous thereto. As the slit wall or reed vibrates outwardly and inwardly the stream becomes blocked and more open alternately. The wave-front of pressure intensity (and therefore of velocity potential) will travel backwards along the stream toward the source as long as the slit wall in its alternations gives freer egress to the excitation stream. With the return of the slit wall or reed and the blocking of the stream, the wave-front of pressure intensity (and therefore of velocity potential) returns in the direction of the stream-flow. There is thus an alternation of the wave-front position along the stream depending on the frequency of the note emitted. The equation of the velocity potential therefore becomes

$$\frac{\partial^2 P}{\partial x^2} = \frac{1}{u^2} \frac{d^2 P}{dt^2}, \quad \dots \dots \dots (1)$$

with u as the velocity with which a disturbance can travel along the stream for a given mean velocity w of the stream itself.

Relationship between the various Velocities concerned.

As the momentary velocity w of the stream is increased relative to x , the momentary velocity u at x , with which any disturbance in the velocity potential can proceed, will diminish in value, but correspondingly the momentum at any moment of the slit wall or reed (mv), and therefore the velocity v , will increase. That is to say, although there is phase correspondence between the v of the alternating slit wall or reed and u with which the phase of the potential disturbance travels with respect to the excitation stream velocity w at x , the one velocity v increases, whereas the u at any x diminishes inversely with increasing w . The above complies with one of Schrödinger's * conditions, in which u represents the velocity of his ψ -function, and v the momentary velocity occurring in the kinetic energy expression of Hamilton's function E_0 .

Postulates of the Mechanical Constraints

If, now, in the hypothetical case of a "Radiating Harmonic Oscillator" the maximum kinetic energy of the alternating member due to its extreme position (analogous to that of

* See Schrödinger, "Undulatory Mechanics," *Phys. Rev.*, Dec. 1926.

the slit wall or reed above) is so limited that we have a connecting equation of the type

$$\nu = \frac{E_0}{\frac{1}{2}h_0'} = \frac{E_0}{h_0} = \frac{1}{\frac{1}{2}h_0} (\frac{1}{2}mv_{\max}^2)^*, \dots (2)$$

then the function solving equation (1) must be of the form

$$P = P(x) \cdot \sin \left(\frac{2\pi E_0}{h_0} t \right). \dots (3)$$

This will enable a considerable simplification to be performed in solving symbolically equation (1).

It has already been stated that u , at any moment pertaining to the instantaneous velocity of the P wave-front, is inversely proportional to the mean stream velocity w . Similarly the v of the kinetic energy term, having reference to the radiator (the wall of the slit or reed, as it were), is for the same moment directly proportional to the mean stream velocity w . It would be therefore reasonable to write that

$$u = h_1 \frac{E_0}{mv} = h_1 \frac{(\frac{1}{2}mv_{\max}^2)}{mv}, \dots (4)$$

and the Fourier law of dimensions will be satisfied.

Schrödinger's Differential Equation. Split Form of Planck's Constant.

By virtue of equation (2), the solution of equation (1) being of the form

$$P = P(x) \cdot \sin \frac{2\pi E_0}{h_0} t, \dots (5)$$

this enables us to write symbolically that

$$\frac{d^2}{dt^2} = - \frac{4\pi^2 E_0^2}{h_0^2} = - \frac{4\pi^2}{h_0^2} (\frac{1}{2}mv_{\max}^2)^2. \dots (6)$$

Making use of the latter, (1) transforms to

$$\frac{\partial^2 P}{\partial x^2} + \frac{4\pi^2 E_0^2}{u^2 h_0^2} P = 0. \dots (7)$$

There then remains to express u in terms of E_0 by virtue of (4). Introducing the latter, we have that

$$\Delta P + \frac{8\pi^2 m}{(\frac{1}{2}h_0'/h_1)^2} (\frac{1}{2}mv^2) P = 0, \dots (8)$$

* The justification of this type of Quantum Formula will be gone into later. See end Part I.

indicating that what Schrödinger calls Planck's constant h is in the above analogy really given by the following split form, namely

$$h = \frac{2}{3} h_0' h_1 = \text{Planck's constant} \\ = (\text{proportionality factor for the frequency with respect to the normal energy content}) \times (\text{proportionality factor of the phase velocity in the stream with respect to the inverse of the velocity of the radiator}^* \dots \dots \dots (9)$$

To throw equation (8) into the form used by Schrödinger with such telling effect, we note that the kinetic energy $\frac{1}{2}mv^2$ is really given by

$$E_0 - V = \frac{1}{2}mv^2, \dots \dots \dots (10)$$

where V is the potential (elastic energy content analogously of the flexed slit wall or reed), and E_0 is the maximum energy content, kinetic plus potential, which for any given frequency is conservatively a constant. Thus we have that

$$\Delta P + \frac{8\pi^2m(E_0 - V)}{h^2}P = 0, \dots \dots \dots (11)$$

where the P above corresponds to Schrödinger's ψ -function.

If, now, the excitation stream is considered expressible by means of the radius coordinate r instead of the x , then V can also be expressed in the form

$$V = \frac{-e^2}{r}, \dots \dots \dots (12)$$

where e is the electronic charge. Then, as Schrödinger has shown, E_0 must conform to the requirement

$$E_0 = \frac{-2\pi^2me^4}{h^2n^2}; \quad n = 1, 2, 3, 4, \dots \dots (13)$$

in order that finite single-valued solutions shall follow. The whole quantum theory therefore hinges on the above apparently classical type of development. A simple derivation of (13) by Operator Methods will be given herewith.

The Hamiltonian Mechanics of the Radiating Harmonic Oscillator.

It is well to bear in mind that, if e in electrical theory is the applied force and q is the displacement, the work equation is

$$\partial H = e \partial q, \dots \dots \dots (14)$$

* See footnote with reference to (2).

and for hysteresis as well as radiation the e is not in time-phase with the displacement q . Thus, if

$$\left. \begin{aligned} q &= q_1 \sin vt + q_2 \cos vt = (q_1 + q_2 j) \sin vt, \\ e &= e_1 \sin vt + e_2 \cos vt = (e_1 + e_2 j) \sin vt, \end{aligned} \right\}^* \quad (15)$$

then with

$$q = k e$$

the k is complex, time operationally, and is of the form

$$\left. \begin{aligned} k &= k_1 - k_2 j, \\ \text{with } \nu j &= \frac{d}{dt}. \end{aligned} \right\} \dots \dots \dots (15 a)$$

Adopting, now, Maxwell's definition of momentum p , we can write

$$\frac{\partial p}{\partial t} = e, \dots \dots \dots (15 b)$$

which leads to the equation

$$\dot{q} = -\nu^2 (k_1 - k_2 j) p_0 \dagger \dots \dots \dots (16)$$

That is to say, whenever radiation occurs the momentum p is not to be taken in time-phase with the velocity \dot{q} of the displacement. The out-of-phase component corresponds to the radiation requirement.

The Modified Hamiltonian Equations of motion for radiation can now be written as

$$d\mathbb{H} = \frac{\partial \mathbb{H}}{\partial q} dq + \frac{\partial \mathbb{H}}{\partial p} dp,$$

where it would follow, if \mathbb{H} diminishes with q , that then, by virtue of (14) and (15), we should adopt the minus sign and write

$$\frac{\partial \mathbb{H}}{\partial q} = -\dot{p}; \quad \frac{\partial \mathbb{H}}{\partial p} = \dot{q}. \dots \dots \dots (17)$$

Note that the first of (17) is of potential type and the second of (17) kinetic or motional. Now, solving equations (17) in the light of (16), and adopting the form provisionally that

$$p = p_0 \sin vt, \dots \dots \dots (18)$$

* See paper by writer in Phil. Mag. (Dec. 1927) for this type of analysis in radiation theory.

† For the interpretation of this formula in terms of mechanical momentum and the reaction equivalence for radiation, see further.

it follows, after integration, that

$$\underline{H} = -\frac{\nu^2 k_1}{2} p^2 + k_2 \nu p \dot{p} - \dot{p} q. \quad (19)$$

The latter leads to the equations :

$$\left. \begin{aligned} \underline{H} &= \underline{E}_0 + \underline{H}_r, \\ \text{where } \underline{H}_r &= \frac{1}{2} \nu^2 p_0^2 k_1 \cos 2\nu t, \\ \underline{E}_0 &= \frac{3}{2} \nu^2 p_0^2 k_1. \end{aligned} \right\} \quad (20)$$

The last of (20), since it is independent of time, applies to the conservative part of the system, whereas the second or \underline{H}_r represents the radiation term of energy. The conclusion is then forced upon us, that whenever *simply sinoidal* radiation takes place from an harmonic oscillator, then the condition is *ipso facto* imposed, with regard to amplitudes, that

$$\frac{\underline{E}_0}{\underline{H}_r} = 3. \quad (21)$$

In other words, a pure radiative harmonic action of an oscillator cannot exist classically save under the condition that the radiation system regularly absorbs and radiates energy equal to one-third of its normal non-radiating content. The above therefore explains why \underline{E}_0 alone can be used in the Schrödinger equation.

Relationship of Momentum to Velocity.

Turning to the justification of equation (2), which is fundamental in Quantum Theory, by the aid of (15) and (15 a) we have for the velocity the expression

$$\begin{aligned} \dot{q} &= \frac{d}{dt} q = q_1 \frac{d}{dt} \sin \nu t + \frac{1}{\nu} q_2 \frac{d^2}{dt^2} \sin \nu t \\ &= -q_2 \nu \cdot \sin \nu t + q_1 \cdot \frac{d}{dt} \sin \nu t. \end{aligned} \quad (23)$$

With respect to a true mechanical momentum p (of non-radiative character therefore), it follows, postulating as before

$$p = p_0 \sin \nu t, \quad (18)$$

that by virtue of (16) we have

$$\dot{q} = -\nu^2 k_1 p_0 \sin \nu t + \nu k_2 p_0 \frac{d}{dt} \sin \nu t. \quad (24)$$

It is the first term that corresponds to the mechanical momentum component sought, since (18) itself involves the

sine function of the time. The second term of (24), which is radiatively necessary, then complies with the second of (23). That is to say, with regard to the "velocity complex" \dot{q} , the first or real part gives the true velocity component growing out of an actual bodily displacement of the slit wall or reed. *The second or imaginary component of \dot{q} in (16), which really depends on the rate with which the bodily displacement takes place, has reference to the radiation reaction.*

Equating coefficients for the first terms of (23) and (24), we have

$$\begin{aligned} \nu^2 k_1 p_0 &= -q_2 \nu \\ \text{or} \quad \nu k_1 p_0 &= q_2. \end{aligned} \quad (25)$$

Yet for a reed flexing merely to produce a fundamental the bodily velocity will be relatively small, but the maximum displacement q_2 will be large. On the other hand, for an overtone the displacement q_2 will be relatively small (whether due to a note produced because of the progressive flattening of the reed or not*), but the momentum p_0 , and therefore the velocity ν , will be large. We are therefore justified in assuming the possible proportionality

$$q_2 = \frac{h_0'}{p_0}. \quad (26)$$

If, then, this is equated to (25), to find the value of k_1 we have that

$$h_0' = \nu k_1 p_0^2. \quad (27)$$

Substituting in the classical requirement of (20), we have that

$$E_0 = \frac{3}{4} h_0' \nu = h_0 \nu \quad (28)$$

which clearly suggests Planck's Quantum formula.

PART II.

The Differential Equation for the Balmer Series.

Given the equation (1), namely

$$\frac{d^2 P}{dt^2} = u^2 \Delta P, \quad (1)$$

* In the case of the Harmonica or "mouth-organ" a visible flattening of the reed takes place. In fact, with too much air-pressure the slot becomes closed and no note is emitted.

the symbolical solution leading to (5) above would be of the form

$$P = A(r, \theta, \phi) \cdot e^{(u \cdot \Delta^{1/2})t} \dots \quad (27')$$

The latter will lead to a sinoidal time function such as (5), provided it can be shown that $u\Delta^{1/2}$ as an operator really can be made equal in succession to a series of constants (Eigenwerthe) which are imaginary and not real.

Consider, then, preferably the argument P of the type

$$\left. \begin{array}{l} \text{where} \quad \left\{ \begin{array}{l} P = RYT, \\ T = f(t), \\ Y = F(\theta, \phi), \\ R = F(r). \end{array} \right\} \dots \dots \dots (27a) \end{array} \right\}$$

Introducing the latter into ΔP and noting that

$$\Delta = \frac{\partial^2}{\partial r^2} + \frac{2}{r} \frac{\partial}{\partial r} + \frac{1}{r^2} \left\{ \frac{1}{\sin^2 \theta} \cdot \frac{\partial^2}{\partial \phi^2} + \frac{\partial^2}{\partial \theta^2} + \cot \theta \cdot \frac{\partial}{\partial \theta} \right\}, \dots \dots (28a)$$

it is quickly seen that

$$\Delta P = TY(\Delta R) + TR(\Delta Y),$$

and Y can preferably be taken as a surface zonal harmonic. Since on substituting $r^l Y_l$ in (28a), we find

$$\Delta Y = -\frac{l(l+1)}{r^2} \cdot Y \dots \dots \dots (29)$$

Therefore

$$\begin{aligned} \Delta P &= YT \left\{ \Delta R - R \frac{l(l+1)}{r^2} \right\} P \\ &= \left\{ \frac{\Delta R}{R} - \frac{l(l+1)}{r^2} \right\} P, \dots \dots \dots (30) \end{aligned}$$

and symbolically as a multiplying operator coefficient,

$$\Delta = \frac{\Delta R}{R} - \frac{l(l+1)}{r^2} \dots \dots \dots (31)$$

If, then, in (1) we can set (with n instead of l)

$$u^2 \Delta = u^2 \left\{ \frac{\Delta R}{R} - \frac{n(n+1)}{r^2} \right\} = -c^2, \dots \dots (32)$$

* This sort of value practically applies where the A-function is given arbitrarily for some moment ($t=0$). Subsequent values of P follow from developing the exponential and applying it to A.

where c is one of a possible set of whole numbers, equation (27') will give the needed sinoidal time function.

Cross multiplying (32) and reducing, we have

$$\Delta R = \left\{ \frac{c^2}{u^2} - \frac{n(n+1)}{r^2} \right\} R = 0.$$

Substituting now the value of u^2 from (4), it follows that

$$\frac{c^2}{u^2} = c^2 \cdot \frac{m^2 v^2}{h_1^2 (\frac{1}{2} m v_{\max}^2)^2} = \frac{2c^2 m (E_0 + e^2/r)}{h_1^2 E_0^2}.$$

The equation then becomes

$$\Delta R + \left\{ \frac{2c^2 m}{h_1^2 E_0^2} \left(E_0 + \frac{e^2}{r} \right) - \frac{n(n+1)}{r^2} \right\} R = 0. \quad (33)$$

On the other hand, starting with equation (11), in which we set $V = -e^2/r$ and $K = h/2\pi$, we have that

$$\Delta P + \frac{2m}{K^2} \left\{ E_0 + \frac{e^2}{r} \right\} P = 0.$$

Making use of (30) and (27 a), it then follows that

$$TY \left\{ \Delta R - R \frac{n(n+1)}{r^2} \right\} + \frac{2m}{K^2} \left\{ E_0 + \frac{e^2}{r} \right\} TYR = 0,$$

which, on reduction and rearrangement, gives

$$\Delta R + \left\{ \frac{2m}{K^2} \left(E_0 + \frac{e^2}{r} \right) - \frac{n(n+1)}{r^2} \right\} R = 0. \quad (34)$$

On comparison with (33) it is at once seen that we need to equate

$$\frac{2c^2}{h_1^2 E_0^2} = \frac{8\pi^2}{h^2}; \quad \text{with } c^2 = \left(\frac{2\pi h_1}{h} E_0 \right)^2 = \left(\frac{2\pi}{\frac{h}{h_0}} \right)^2 E_0^2 = (2\pi\nu)^2. \quad (35)$$

It is from (34) that the possible values of n are to be obtained to produce the Balmer series of energy levels.

The Schrödinger Equation and the Bohr's Levels.

Equation (34) can also be written symbolically in the form $\left(\frac{d}{dr} = r_1 \right)$,

$$\left\{ r_1^2 + \frac{2}{r} r_1 + \left(A + \frac{B}{r} - \frac{C}{r^2} \right) \right\} y = 0. \quad (37)$$

The writer has already shown (see Trans. Roy. Soc. Canada, 1927) that the above can be factored operationally into the form

$$\begin{aligned} & \{(r_1 + \rho)r_1 M\} y \\ &= M \left[r_1^2 + \left(\rho + \frac{2}{M} \frac{dM}{dr} \right) r_1 + \frac{1}{M} \left\{ \rho \frac{dM}{dr} + \frac{d^2 M}{dr^2} \right\} \right] y \\ &= (r_1^2 + P_0 r_1 + Q_0) y = 0^*, \dots \dots \dots (38) \end{aligned}$$

provided we set

$$\begin{aligned} P_0 &= \rho + \frac{2}{M} \frac{dM}{dr}, \\ Q_0 &= \frac{1}{M} \left\{ \rho \frac{dM}{dr} + \frac{d^2 M}{dr^2} \right\}. \end{aligned}$$

On eliminating M from the two equations, it follows that we need to satisfy the relation

$$P_0^2 + 2 \frac{dP_0}{dr} - 4Q_0 = \rho^2 + 2 \frac{d\rho}{dr}. \dots \dots (39)$$

Clearly, from (37) and (38), we have

$$P_0^2 = \frac{4}{r^2}; \quad 2 \frac{dP_0}{dr} = -\frac{4}{r^2},$$

so that (39) reduces to

$$\rho^2 + 2 \frac{d\rho}{dr} + 4 \left(A + \frac{B}{r} - \frac{C}{r^2} \right) = 0. \dots \dots (39')$$

Now, a solution of (39') is obviously of the form

$$\rho = a - \frac{b}{r}, \dots \dots \dots (40)$$

for we then have that

$$a^2 - 2 \frac{ab}{r} + \frac{b^2}{r^2} + 4 \left(A + \frac{B}{r} - \frac{C}{r^2} \right) = 0. \dots (41)$$

This can be satisfied by equating coefficients separately to zero, as we have

$$\left. \begin{aligned} a^2 + 4A &= 0, \\ -2ba + 4B &= 0, \\ b^2 + 2b - 4C &= 0, \end{aligned} \right\} \dots \dots \dots (42)$$

* The algebra of these operators is non-commutative because of the variable coefficients.

with

$$A = \frac{2mE}{K^2}; \quad B = \frac{2me}{K^2}; \quad C = n(n+1). \quad (43)$$

Evaluating the unknown parameters in terms of the known, the first of (42) gives

$$a = 2\sqrt{-A} = 2\sqrt{\frac{-2mE}{K^2}}. \quad (44)$$

On the other hand, introducing (44) into the second of (42) results in

$$4B = 4\sqrt{-A} \cdot b; \quad b = B/\sqrt{-A}. \quad (45)$$

Again, the last of (42) gives

$$\left(\frac{b}{2}\right)^2 + \frac{b}{2} = n^2 + n,$$

and the solution of (46) is clearly of the form

$$n = \frac{b}{2} = \frac{B}{2\sqrt{-A}} = \frac{me^2}{K^2} \sqrt{-2mE/K^2}, \quad (47)$$

which agrees with Schrödinger's formula (15¹), p. 368 of his 'Wellenmechanik.'

If, then, n is to be taken as a whole number to ensure single-valued solutions, it follows that E_0 must be taken negatively to avoid imaginaries in (47). It thus follows, on squaring, that we have the condition from (47) that

$$-E = \frac{me^4}{2K^2} \cdot \frac{1}{n^2}.$$

Substituting, therefore, the value of K in terms of the Planck constant $h/2\pi$, we have, finally, that

$$-E = \frac{2\pi^2 me^4}{h^2 n^2} \Big|_{n=1, 2, 3, 4, \dots} \quad (48)$$

which is identical with Bohr's requirement for the energy levels as referred to by Schrödinger, p. 371, *l. c.*

* $n=b/2$ is not the only type of solution. Solving for n in terms of b , we can take $b/2=n+1$ because of the square-root sign in (45).

PART III.

The Linear Oscillator Problem.

Taking the case of a single coordinate q , we have for the kinetic energy the expression

$$T = \frac{1}{2}\dot{q}^2,$$

wherein the mass m is properly included in q . Then for the potential energy we have

$$V = 2\pi^2\nu_0^2 q^2.$$

Schrödinger's equation then becomes, as he has shown ('Wellenmechanik'), p. 514,

$$\frac{d^2P}{dq^2} + \frac{8\pi^2}{h^2} (E_0 - 2\pi^2\nu_0^2 q^2)P = 0. \quad (49)$$

If, then, we set

$$a = \frac{8\pi^2 E_0}{h^2}; \quad b = \frac{16\pi^4 \nu_0^2}{h^2},$$

the equation becomes

$$\frac{d^2P}{dq^2} + (a - bq^2)P = 0 = \frac{d^2y}{dq^2} + (a - bq^2)y. \quad (50)$$

To solve the latter, again the method just indicated can be employed.

In this case operationally the differential equation becomes

$$\begin{aligned} \{q_1^2 + (a - bq^2)\} y = 0 &= \{q_1^2 + P_1 q_1 + Q_1\} y \\ &= \{(q_1 + \rho)q_1 M\} y, \end{aligned}$$

wherein the new P_1 is really zero and Q_1 stands for

$$Q_1 = (a - bq^2).$$

The subsidiary equation takes the form, therefore,

$$\begin{aligned} P_1^2 + 2 \frac{dP_1}{dq} - 4Q_1 &= \rho^2 + 2 \frac{d\rho}{dq}, \\ \rho^2 + 2 \frac{d\rho}{dq} + 4(a - bq^2) &= 0. \quad (51) \end{aligned}$$

Now, the solution of this type of equation is either

$$\text{or} \quad \left. \begin{aligned} \rho &= Aq \\ \rho &= Aq + \frac{B}{q} \end{aligned} \right\}. \quad (52)$$

Taking the first solution, it follows, on introduction, that

$$A^2q^2 + 2A + 4(a - bq^2) = 0. \quad . \quad . \quad . \quad (53)$$

This will be satisfied if we set

$$\left. \begin{aligned} 2A + 4a &= 0 & ; & & A^2 &= 4b, \\ A &= -2a & ; & & 4a^2 &= 4b, \\ \frac{a}{\sqrt{b}} &= -1, \end{aligned} \right\} \quad . \quad . \quad . \quad (54)$$

which corresponds to one of the "Eigenwerthe" or better parametral values, or "parametrals," quoted by Schrödinger (see *l. c.* Eq. (25), p. 515).

Turning now to the second type of solution, viz.

$$\rho = Aq + \frac{B}{q},$$

we have to satisfy the relation

$$A^2q^2 + B^2/q^2 + 2AB + 2A - \frac{2B}{q^2} + 4(a - bq^2) = 0. \quad (55)$$

This will be met if we equate

$$\left. \begin{aligned} 2AB + 2A + 4a &= 0, \\ A^2 - 4b &= 0, \\ B^2 - 2B &= 0. \end{aligned} \right\} \quad . \quad . \quad . \quad (56)$$

The last gives

$$B = 2;$$

so that, introduced into the first of the set, we have

$$6A + 4a = 0,$$

$$A = -\frac{2}{3}a.$$

Thus, on substitution into the second, it results that

$$\frac{4}{9}q^2 = 4b$$

$$\text{or} \quad \frac{a}{\sqrt{b}} = 3, \quad . \quad . \quad . \quad . \quad . \quad . \quad (57)$$

which is the second of the Eigenwerthe enumerated by Schrödinger.

To obtain further values the solution of (51) needs to be generalized. This will permit the introduction of a general parametral expression N similar to the $n(n+1)$ term

occurring in the solution for the Bohr energy levels. Thus for the term Aq in (52) we can set

$$\chi = f(q),$$

whereas for the B/q term we can preferably take

$$\frac{1}{Y} \cdot \frac{dY}{dq} = F(q).$$

In this way we have

$$\rho = A\chi + \frac{B}{Y} \cdot \frac{dq}{dY} \dots \dots \dots (57')$$

Introducing the latter into (51) gives

$$\begin{aligned} \rho^2 &= A^2\chi^2 + \left(\frac{B}{Y} \cdot \frac{dY}{dq}\right)^2 + 2AB \frac{\chi}{Y} \cdot \frac{dY}{dq}, \\ 2 \frac{d\rho}{dq} &= 2A \frac{d\chi}{dq} + 2 \frac{B}{Y} \left\{ \frac{d^2Y}{dq^2} - \frac{1}{Y} \cdot \left(\frac{dY}{dq}\right)^2 \right\}, \end{aligned}$$

and we have, instead of (51),

$$\begin{aligned} A^2\chi^2 + 2A \frac{d\chi}{dq} + 4(a - bq^2) \\ = \frac{1}{Y^2} \left(\frac{dY}{dq}\right)^2 (2B - B^2) + \frac{2B}{Y} \left\{ \frac{d^2Y}{dq^2} + A\chi \frac{dY}{dq} \right\}. \end{aligned} \quad (58)$$

The first term on the right-hand side can easily be avoided by setting

$$B = 2.$$

On the other hand, no harm will be done by placing

$$A = 1.$$

If, then, in addition, we set

$$\frac{4}{Y} \left\{ \frac{d^2Y}{dq^2} + \chi \frac{dY}{dq} \right\} = -4N,$$

or, what is the same thing,

$$\frac{d^2Y}{dq^2} + \chi \frac{dY}{dq} + NY = 0, \dots \dots \dots (59)$$

the resulting equation will be of the form

$$\chi^2 + 2 \frac{d\chi}{dq} + 4\{(a - N) - bq^2\} = 0 \dots \dots (60)$$

Whether N can be introduced into (60) will depend on what values are possible for N in the equation (59) *.

The new solution ρ of (51) thus becomes

$$\rho = \chi + \frac{d}{dq} (\log Y).$$

Dealing, then, with (60) instead of (51), we know that

$$\chi = Aq \quad . \quad . \quad . \quad . \quad . \quad (62)$$

is a solution. This should at least lead to the result (54) as well as (57). Introducing (62) in (60) gives

$$A^2 q^2 + 2A + 4 \{ (a - N) - bq^2 \} = 0. \quad . \quad . \quad (63)$$

Equating coefficients separately to zero gives

$$A^2 = 4b; \quad A = -2\sqrt{b}; \quad A = 2(N - a) = -2\sqrt{b},$$

whence

$$\frac{a - N}{\sqrt{b}} = 1. \quad . \quad . \quad . \quad . \quad . \quad (64)$$

If, now, we make

$$N = 0, \quad . \quad . \quad . \quad . \quad . \quad (65)$$

$$\frac{a}{\sqrt{b}} = 1; \quad . \quad . \quad . \quad . \quad . \quad (54)$$

but with

$$\frac{N}{\sqrt{b}} = 2 \quad . \quad . \quad . \quad . \quad . \quad (66)$$

we shall have

$$\frac{a}{\sqrt{b}} = 1 + \frac{N}{\sqrt{b}} = 3, \quad . \quad . \quad . \quad . \quad (57)$$

which is the second Eigenwerthe magnitude required.

* In reality equation (59) can be written as

$$\frac{d^2 Y}{dq^2} + P_1 \frac{dY}{dq} + Q_1 Y = 0,$$

where

$$P_1 = \chi; \quad Q_1 = N.$$

Under these conditions a solution can then be made to depend, as already shown, on the subsidiary equation of the type

$$\chi^2 + 2 \frac{d\chi}{dq} + 4N = \rho^2 + 2 \frac{d\rho}{dq},$$

which, of course, is identical with (60). Whatever N 's are solutionally possible in (51) are equally possible in (59). Thus it remains to determine what discrete values N needs to have in order to be able to build up a set of parametral values and functions.

However, if we take the more general type of solution, viz.

$$\chi = Aq + \frac{B}{q},$$

then we have, by the steps leading to (54), on substituting there $a-N$ for a , that

$$\left. \begin{aligned} \frac{a-N}{\sqrt{b}} &= 3, \\ \frac{a}{\sqrt{b}} &= 3 + \frac{N}{\sqrt{b}}. \end{aligned} \right\} \dots \dots (67)$$

This will surely give (57) by taking condition (65), namely

$$N = 0. \dots \dots (65)$$

On the other hand, introducing condition (66) would give

$$\frac{a}{\sqrt{b}} = 3 + \frac{N}{\sqrt{b}} = 5 \dots \dots (68)$$

$$\text{or} \quad \frac{a-N}{\sqrt{b}} = 5. \dots \dots (69)$$

For the further parametral values of the series an additional parametral expression M' can be introduced into (57) in exactly the same way as N was introduced into (51), and then we have to consider an equation of the type

$$Z^2 + 2 \frac{dZ}{dq} + 4 \{ (a-N-M') - bq^2 \} = 0, \dots (70)$$

with an equation of condition to suit, namely

$$\frac{d^2Y}{dq^2} + Z \frac{dY}{dq} + M'Y = 0, \dots (71)$$

etc.

The parametral values (Eigenwerthe) are evidently now of the form

$$\frac{a}{\sqrt{b}} = 2n+1 \Big|_{n=0, 1, 2, 3 \text{ etc.}} \dots (72)$$

Substituting values of a and b as indicated above, we finally have for the energy-level values

$$E_0 = \frac{2n+1}{2} h\nu_0 \Big|_{n=1, 2, 3 \text{ etc.}}, \dots (73)$$

showing that half quanta are needed for their designation.

SUMMARY.

On the bases of a mechanical analogy Schrödinger's Wave Equation is obtained by employing the idea of an excitation stream of air to a reed or organ-pipe. The above equation of wave-motion then applies to the varying velocity potential of the stream. It is found that the reed or organ-pipe when excited gives a relationship between the velocity of the vibrating reed or slit wall and the mean velocity of the stream. In this way, also, a relationship is found between the speed of the pulsating wave-front of the velocity potential and the mean stream velocity. By combining the two a proportionality factor h_1 results, which latter needs to be combined with the constant h_0 derived from assuming a proportionality law between the normal energy content of the oscillator wall and the frequency set up. It is shown that the latter really follows because, as the pressure goes up, the maximum displacement of the reed or slit wall actually diminishes with the increase in momentum. This is in conformity with the fact that in the harmonica or "mouth-organ" the reed-opening becomes more and more closed as one blows harder and harder. That is, the Planck constant h is split up according to the formula $h = h_0 h_1$.

Introducing the above factors into the differential equation of wave-motion results in the final form of Schrödinger without the use of the Hamilton Varying Action principle or the Hamilton-Jacobi equation.

It had already been shown by the writer that on purely classical grounds there must always be a fixed relationship between the amplitude of the pure harmonic radiated energy and the normal non-radiated content of the oscillator. This explains why, in solving Schrödinger's Equation for the Balmer series, we need only consider the conservative system of the radiator.

By means of a general operational method analogous to the factoring method employed by Heaviside, the writer has shown that equations of the type used by Schrödinger can be solved in an effectively simple way. The "Eigenwerthe" are first deduced, and later only are the Eigenfunktionen developed automatically, without having to resort to a previous study of Laguerre polynomials or Hermitian functions.

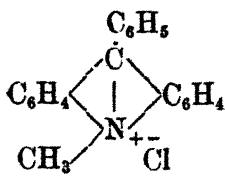
1314 18th St., N.W.,
Washington, D.C., U.S.A.,
Jan. 1. 1928.

IV. *The Electronic Theory of Valency.*—Part VI. *The Molecular Structure of Strong and Weak Electrolytes.*
 (b) *Reversible Ionization.* By T. MARTIN LOWRY*.

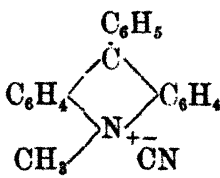
THE theory of complete ionization has met with such marked success that it might easily be supposed that it could be applied to all electrolytes. The present paper therefore contains a review of some cases in which the ionization of an electrolyte is reversible instead of complete.

True Electrolytes and Pseudo-electrolytes.

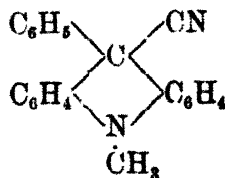
The most obvious examples of reversible ionization are provided by those compounds in which neutralization of the opposite charges of the ions is rendered possible by a change of molecular structure. Thus, according to the electronic theory of valency, a quaternary ammonium chloride must remain permanently ionized, since both the ammonium ions and the chloride ions carry complete shells of electrons and cannot share electrons without creating a surplus. There are, however, a number of cases in which this surplus can be disposed of by a rearrangement of bonds within the molecule, giving rise to a wholly covalent compound. This change takes place with greater readiness when the chlorine is replaced by an anion of a less strongly negative character, *i. e.*, by a radicle which is less hungry for electrons, and therefore more ready to share them with another atom. Thus methylphenylacridinium chloride is a true electrolyte, which remains permanently ionized in aqueous solutions: but, when sodium cyanide is added, a progressive fixation of cyanogen ions takes place, until after about a day at 25°, the conductivity is found to have fallen almost to the value for sodium chloride, as a result of the complete conversion of the ionized "true salt" into an insoluble "pseudo-salt" †.



Methylphenylacridinium chloride.



Methylphenylacridinium cyanide.

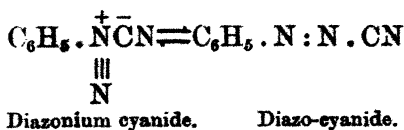


Methylphenylcyanoacridine.

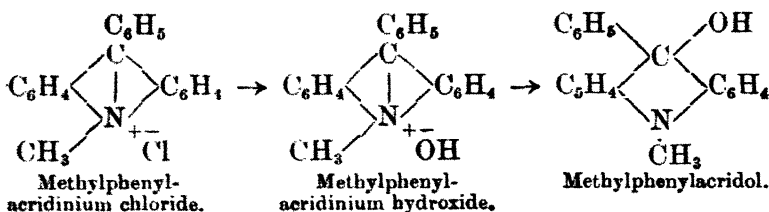
* Communicated by the Faraday Society.

† Hantzsch and Kalb, *Ber.* xxxii. p. 3109 (1899).

A similar change of structure can be effected in the diazocyanides by separating the "salt" from aqueous solutions and dissolving it in a non-ionizing solvent, when it behaves as a typical non-electrolyte, whereas in water it behaves just like the chloride



Precisely similar considerations apply to the fixation of a hydroxyl-ion. Thus a solution of methylphenylacridinium chloride, when mixed with an equivalent quantity of sodium hydroxide, shows at first the normal conductivity of such a mixture; but this conductivity diminishes progressively to that of sodium chloride as the hydroxyl is "fixed" by the anion.



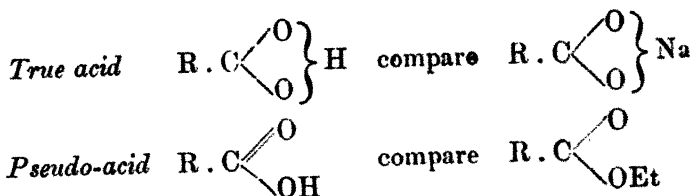
The acridol, which is formed as a product, is a tertiary amine-alcohol, compare $(\text{C}_6\text{H}_5)_2\text{NMe}$ and $(\text{C}_6\text{H}_5)_3\text{C} \cdot \text{OH}$. It is therefore just as true a base as trimethylamine, but differs from other tertiary bases in that one of the alkyl-radicles carries a hydroxyl-group, which is eliminated in the form of water as soon as the base has performed its characteristic function of accepting a proton from an acid. Although, therefore, it is commonly referred to as a "pseudo-base," it would perhaps be described more accurately as a "pseudo-alkali," i. e., as a non-electrolytic isomer of a quaternary ammonium hydroxide.

Strong and Weak Acids.

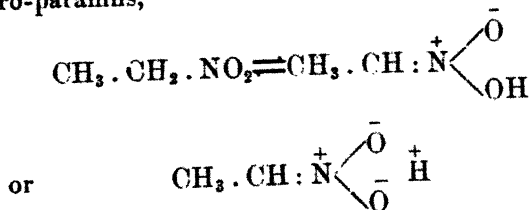
Whilst the conception of a "strong electrolyte" is a very modern one, the existence of strong and weak acids has been familiar for 1000 years or more, and had already been interpreted in many other ways before the strength of an acid was finally correlated with its electrical conductivity in

dilute solutions. The theory of complete ionization therefore receives its most serious challenge from the existence of weak acids, which obey Ostwald's dilution law ($\alpha \propto c^{-1/2}$, where α is small), and cannot therefore also obey the dilution formula for strong electrolytes ($1 - \alpha \propto c^{1/2}$, where α is large).

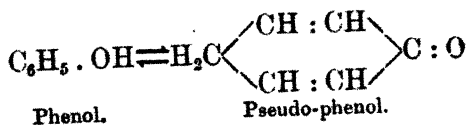
In order to account for the existence of these weak acids, Hantzsch has suggested* that carboxylic acids can exist in two interconvertible isomeric forms; thus :



A dynamic isomerism of this type is actually observed in the nitro-paraffins,



and is an obvious factor in reducing the acidity of the compound, which must be diminished in direct proportion to the extent to which the true acid is converted into the isomeric pseudo-acid. It is, however, by no means certain that the contrast between strong and weak acids depends in other cases on so definite a phenomenon. For instance, we need not suppose that phenol owes its weak acidity to conversion into an isomeric pseudo-phenol,



since it is sufficient to postulate that, whilst the $-\bar{\text{O}}\text{Na}^+$ radicle of sodium phenate is permanently ionized, the $-\text{OH}$ radicle of phenol is held together by a real bond, just

* Ber. l. p. 1438 (1917).

as in the case of the alcohols. Dissolution of the sodium compound in water would then give rise to a direct dissociation of ready-made ions as indicated by the equation,



whereas, in the case of phenol itself, ions could only be produced as the result of a destruction of neutral molecules, by the rupture of the hydrogen-oxygen bond, as in the equation :



Some care is needed in order to formulate these views in accordance with modern theories of atomic structure, since, as I pointed out in an article on "The Uniqueness of Hydrogen"*, exceptional difficulty is experienced in deciding whether an atom of hydrogen is linked to the rest of the molecule by a real bond or by a mere electrovalence. This difficulty arises from the fact that, since the hydrogen "shell" contains 0 or 2 instead of 8 electrons, the ordinary static symbolism makes no distinction between these two

forms of union. Thus, in the case of $\text{H}:\ddot{\text{Cl}}:$, the same electronic formula serves equally well to represent a pair of

ions, $\text{H}^+\bar{\text{Cl}}^-$, with 0 and $2+8+8$ electrons, or a covalent compound, $\text{H}-\text{Cl}$, in which 2 of the 18 electrons are shared by the two atoms. When, however, a dynamic model is used, and shared electrons are regarded as moving in binuclear orbits, a clear distinction between the two types of union again becomes possible, according as the orbits of the electrons in question surround two nuclei or only one. If this distinction is admitted, it appears probable that hydrogen is covalent in all its compounds, and that the free hydrogen

ion or naked proton represented by the symbol H^+ does not exist except as a transient product in a vacuum-tube or the like. This conclusion follows, on the one hand, from the fact that there are no electrostatic forces to prevent such a nucleus from falling inside the electronic orbits of any other atom with which it may collide, and, on the other hand, from numerical data which show that the union of a proton with water to form a hydrated hydrogen ion would liberate not less than 260,000 calories†. The ionization of an acid

* Lowry, 'Chemistry and Industry,' xlii. p. 43 (1923).

† Fajans, *Ber. deut. physik. Ges.* xxi. p. 709 (1919).

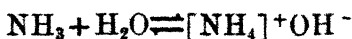
(which does not take place when the pure compound is merely melted) must then be formulated as depending on an interaction of the acidic hydride with water, or the like, giving rise to an oxonium ion, as in the equation,



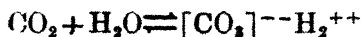
It will be seen, however, that this scheme still possesses the characteristic which is now put forward as a typical property of "weak" electrolytes, that the opposite electric charges of the ions can be neutralized without any violation of the "octet" rule, giving rise to products in which the electrovalence of the ions is replaced by a real bond.

Strong and Weak Bases.

Bases resemble acids in exhibiting a very wide range of strengths. Thus the soluble metallic hydroxides (which include the alkalis) are all strong bases, and their strength is shared by the quaternary ammonium hydroxides, where the formation of a covalent bond between nitrogen and oxygen is prevented by the fact that the nitrogen is unable to attach itself by real bonds to five atoms simultaneously. Weak bases appear to be of two main types, since covalent compounds can be formed, either by fixing the hydroxyl-group by a real bond to an isomeric form of the kation, as in the acridinium compounds cited above, or by eliminating it in the form of a covalent molecule of water. The latter case is extremely common. Thus the amines generally behave as weak bases, since the concentration of hydroxyl-ions in their solutions depends on an interaction with water : *e. g.*,



compare

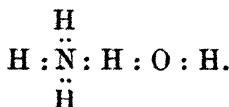


the ready reversibility of which is shown by the complete removal of ammonia from its aqueous solutions by boiling, or of aniline by steam-distillation. Since, however, this dehydration has the effect of eliminating the unbalanced electric charges from the system, giving rise exclusively to covalent compounds, this explanation is in close agreement with the general proposition set out above as regards the essential characteristics of a weak electrolyte.

The problem of weak bases has, however, been carried one stage further by Moore and Winmill*, who have shown by

* Journ. Chem. Soc. ci. p. 1675 (1912).

distribution experiments that the weakness of the primary, secondary, and tertiary amines can only be partially attributed to dehydration of the hydroxide, and by Latimer and Rodebush*, who have suggested that the hydrate $\text{NH}_3, \text{H}_2\text{O}$ may be formulated as

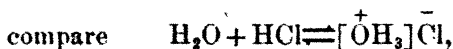
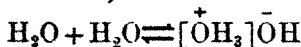


This formula represents the monohydrate as a covalent isomer of ammonium hydroxide,

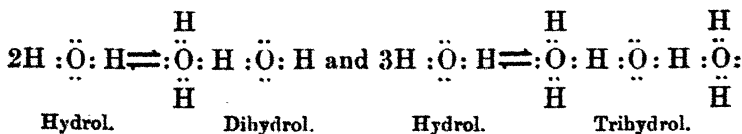


in which the hydroxyl radicle is united to the ammonium radicle by a real bond, as required by our definition of a weak electrolyte. The fulfilment of this condition is not vitiated by the fact that, since quadrivalent nitrogen is positively-charged, and bivalent hydrogen is negatively charged, the resulting molecule would exhibit the phenomenon which J. J. Thomson has described as "intramolecular ionization"†.

The bivalency of hydrogen is also of value in accounting for the fact that the polymerization of liquid water is not accompanied by ionization. Thus, if hydrogen were always univalent, the formation of a double-molecule would be represented by the scheme,



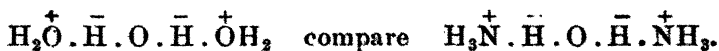
and the product would be an oxonium hydroxide, just like ammonium hydroxide; but, if the hydrogen is bivalent, the formation of double and triple molecules can be represented, without any formation of free ions, by the schemes,



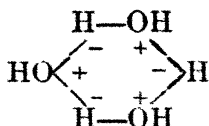
* Journ. Amer. Chem. Soc. xlii. p. 1431 (1920); cf. G. N. Lewis, 'Valence,' p. 110 (1923).

† Phil. Mag. (6) xxvii. p. 757 (1914); cf. Lowry, Trans. Faraday Soc. xviii. p. 285 (1923), and Phil. Mag. (6) xlv. p. 1105 (1923).

Here again the polymerized molecules must exhibit "intramolecular ionization," since the tervalent oxonium oxygen is positively-charged, and the bivalent hydrogen negatively-charged, as in the formula,



Alternatively the trihydrol can be represented by a ring structure dissected from the crystal-lattice of ice, thus



Strong and Weak Salts.

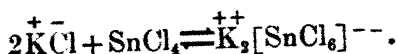
The number of metallic salts which are obviously "strong electrolytes" is so large that it is not always easy to realize that a salt, like an acid or base, may be a "weak electrolyte." In the following paragraphs, therefore, a number of examples have been brought together of salts which behave as weak electrolytes; and evidence is again cited to show that these compounds owe their peculiar inertness to the possibility of forming covalent bonds between the ions.

(a) *Stannic Chloride*.—An ionic aggregate, in which each ion is surrounded by a number of ions of opposite sign (*e. g.*, 6 in the NaCl lattice or 8 in the CsCl lattice), provides ideal conditions for utilizing the residual affinity of the ions to produce a rigid crystal structure. When therefore a substance, which has the formula of a salt, exhibits the fusibility and volatility of an organic compound, the view at once suggests itself that we are probably dealing with integral molecules, rather than with a continuous network of ions. We are therefore not surprised when stannic chloride (b.p. 114°, f.p. -33°) fails to show the electrolytic properties of a typical fused salt, since its obvious properties are those of a collection of individual molecules and not of an aggregate of ions. This general conclusion has received specific confirmation from the X-ray analysis of crystals of stannic iodide, where it has been shown that each atom of tin is surrounded tetrahedrally by four atoms of iodine, just as in the case of a covalent carbon-compound.

No data are given in the tables for the conductivity of pure stannic chloride, which appears to behave as an

insulator, like pure hydrogen chloride or pure water. In aqueous solution it is hydrolyzed to colloidal stannic acid, $\text{SnCl}_4 + 4\text{H}_2\text{O} \rightleftharpoons \text{Sn}(\text{OH})_4 + 4\text{HCl}$, which appears to contribute nothing to the conductivity of the acid solution*. In liquid sulphur dioxide, however, it behaves as a weak electrolyte, giving $\Lambda_0 = 0.068$, $\Lambda_{14} = 0.04$, $\Lambda_{262} = 0.262$. Although, therefore, the metal and the halogen in stannic chloride carry complete octets of electrons, it is still possible to ionize one of the bonds; but, as the tin is then left with an outer shell of only 6 electrons, this condition is too unstable to persist except as a minor feature of the final equilibrium.

Stannic chloride can, however, be converted in a strong electrolyte by combination with potassium chloride to form potassium stannic chloride,



The crystals of this compound have been shown by X-ray analysis to be an ionic aggregate of the same type as fluorspar; but, in forming this aggregate, the tin has not been separated from the chlorine, since (if we accept Langmuir's theory of coordination†) it now forms part of a complex anion in which *six* atoms of chlorine, instead of only *four*, are united by real bonds to the central atom of metal. This change is obviously accompanied by conversion of a tetrahedral into an octahedral configuration. The view that an octahedral 6-coordination compound gives rise to a square configuration when converted into a 4-coordination compound, cannot therefore be maintained in this case, although it appears to have been established in the case of platinum.

(b) *Mercury Salts*.—Special interest attaches to the behaviour of the salts of mercury, since this element resembles hydrogen in the readiness with which it gives rise to "weak electrolytes," both in the molten state and in solution. This peculiar behaviour can, however, be attributed to the fact that this element, in complete defiance of the simple octet rule of the electronic theory, is equally ready to form covalent and electrovalent compounds. Evidence in support of this statement is set out in Tables I. and II. and in the paragraphs which follow.

* Foster, Phys. Rev. ix. p. 41 (1899).

† Journ. Amer. Chem. Soc. xli. p. 868 (1919).

TABLE I.

Specific Conductivity of Fused Salts.

(a) *Strong Electrolytes.*

$\left\{ \begin{array}{l} \text{NaCl } 3.34 \text{ at } 800^\circ \\ \text{NaBr } 3.06 \text{ } \\ \text{NaI } 2.70 \text{ } \end{array} \right.$	$\left\{ \begin{array}{l} \text{AgCl } 4.98 \text{ at } 800^\circ \\ \text{AgBr } 3.50 \text{ } \\ \text{AgI } 2.52 \text{ } \end{array} \right.$	$\left\{ \begin{array}{l} 4.48 \text{ at } 600^\circ \\ 3.18 \text{ } \\ 2.52 \text{ } \end{array} \right.$
$\left\{ \begin{array}{l} \text{KCl } 2.19 \text{ at } 800^\circ \\ \text{KBr } 1.75 \text{ } \\ \text{KI } 1.64 \text{ } \end{array} \right.$	$\left\{ \begin{array}{l} \text{TlCl } 1.700 \text{ at } 800^\circ \\ \text{TlBr } 1.127 \text{ } \\ \text{TlI } 0.840 \text{ } \end{array} \right.$	$\left\{ \begin{array}{l} 1.082 \text{ at } 427^\circ \text{ (m.p.)} \\ 0.803 \text{ } 457^\circ \\ 0.523 \text{ } 436^\circ \end{array} \right.$

(b) *Weak Electrolytes.*

HgI_2 0.0066 at 320°	HgCl_2 0.0078 at 276° (m.p.)
0.0071 " 288°	
0.0085 " 260°	
0.0118 " 253° (m.p.)	

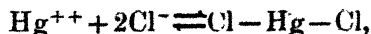
Data for aqueous solutions of mercury-salts are as follows :—

TABLE II.

Equivalent Conductivities of Mercury Salts.

<i>Mercurous Salts.</i>	<i>Mercuric Salts.</i>
$\text{HgClO}_4 \Lambda_{10}^{25} = 110 \quad \alpha = 0.76$	$\frac{1}{2} \text{Hg}(\text{ClO}_4)_2 \Lambda_{10}^{25} = 105 \quad \alpha = 0.77$
$\text{HgNO}_3 \Lambda_{32}^{18} = 59 \quad \alpha = 0.56$	$\frac{1}{2} \text{Hg}(\text{NO}_3)_2 \Lambda_{32}^{25} = 6.3 \quad \alpha = 0.04$
(in $N/10 \text{ HNO}_3$)	$\frac{1}{2} \text{HgCl}_2 \Lambda_{32}^{25} = 1.77 \quad \alpha = 0.013$
	$\frac{1}{2} \text{Hg}(\text{CN})_2 \Lambda_{15}^{25} = 0.10 \quad \alpha = 0.0007$

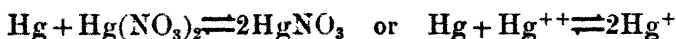
The weak and variable electrolytic conductivities of the mercury salts are just what one might expect if the positively-charged mercury ions were able to unite with the negatively-charged anions to form covalent compounds, *e. g.*,



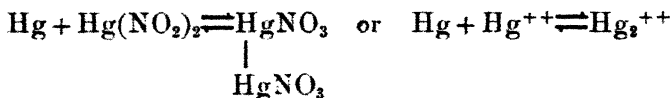
but it would be merely arguing in a circle to use these low conductivities as evidence of the formation of covalent compounds. It should be noted, however, that the conductivity of mercuric chloride is much lower than that of the nitrate, and that, whilst the coefficient of ionization of mercuric chloride is only about 1 per cent. at $N/32$, the two perchlorates, in which the halogen is completely enveloped by four tetrahedrally disposed atoms of oxygen, have actually passed over into the group of strong electrolytes (compare barium perchlorate) with coefficients of 76 per cent. and 77 per cent. respectively at a concentration of $N/10$.

On the other hand, mercuric cyanide, which was described by Prussia in 1898* as a non-conductor, behaves exactly like an organic compound in which ionization is just beginning to be possible (compare CMe_3I in liquid SO_2).

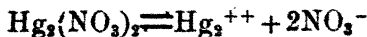
Fortunately, however, direct evidence is available to prove that mercury does actually form covalent compounds of the type that has been postulated as characteristic of "weak electrolytes." Thus, as long ago as 1898, Ogg showed† that the ratio between the two nitrates of mercury, when in equilibrium with metallic mercury and a given concentration of nitric acid, is constant. This result cannot be reconciled with the equation,



but is in close agreement with the requirements of the equation,



The mercurous ion is, therefore, not a simple charged atom Hg^+ but a covalent complex $\text{Hg}^+ - \text{Hg}^+$. This conclusion was confirmed by determinations of the electromotive force of concentration-cells, as well as by other methods of investigation. The later measurements by Schilow‡ of the transport-number and conductivity of mercurous nitrate, in aqueous solutions and in presence of dilute nitric acid, also support Ogg's conclusion that mercurous nitrate is a *ternary* electrolyte, the ionization of which must be represented by the scheme,



and not by the simple scheme for a *binary* electrolyte,



Even more conclusive are the recent observations of Mauguin§ and of Havighurst|| on the X-ray analysis of crystals of mercurous chloride, bromide, and iodide. Nearly

* Gazz. xxviii. p. 117.

† Zeit. phys. Chem. xxvii. pp. 285-311 (1898).

‡ Zeit. anorg. Chem. cxxxiii. p. 55 (1924).

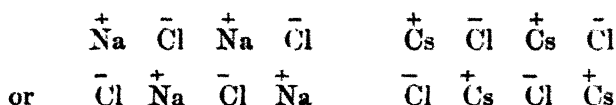
§ Compt. Rend. clxxviii. p. 1913 (1924).

|| Am. Journ. Sci. x. p. 15 (1925).

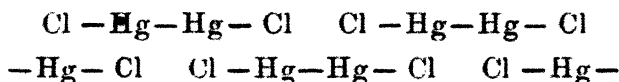
all of the binary haloid salts crystallize in the cubic lattice, *e. g.*,

NaCl, KCl, AgCl, AgBr, on a face-centred cubic lattice,
CsCl, CsI, TlCl, TlBr, on a body-centred cubic lattice,
CuCl, CuBr, CuI, AgI, on the diamond or zinc sulphide
type of cubic lattice.

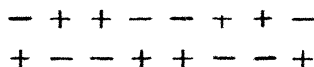
The mercurous haloids, however, all crystallize in the tetragonal system; and X-ray analysis has shown that the arrangement of the atoms of metal and halogen is not a simple alternation, as in rock-salt or caesium chloride,



but an alternation of *pairs* of atoms as in the scheme,

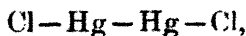


Since the scheme,

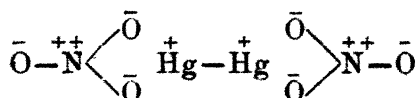


is impossible as a stable arrangement of positive and negative ions, Havighurst concludes that "The structure of these crystals indicates the existence of the chain-molecule Cl—Hg—Hg—Cl. The strong double refraction which has been observed is to be expected from a crystal having this structure"*. The unusual cleavage of the compound is also in agreement with this structure.

From this evidence it is clear that mercury can exhibit either a covalence of 2 as in calomel,

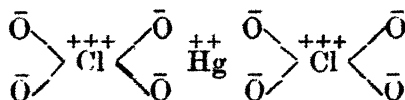


or a covalence of 1 and a positive electrovalence of 1 as in mercurous nitrate,

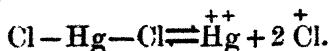


* Am. Journ. Sci. x. p. 15 (1925).

or a positive electrovalence of 2 as in mercuric perchlorate,



The way is therefore open for a reversible equilibrium between free ions and real molecules, of precisely the same type as has been postulated in the case of other weak electrolytes, *e.g.*,



(c) *Coordinated Salts*.—In the category of weak electrolytes we must also include a large number of coordination compounds, since it is clear that, as the firmness with which a metal is coordinated to the negative radicle is increased, its coefficient of ionization must be diminished, or, in other words, that its efficiency as an electrolyte must decay *pari passu* with the increase of the efficiency of the coordination. Since, however, Sidgwick considers that the act of coordination consists in the formation of a bond by the transfer of an electron from one atom to another, these cases can obviously be included within the limits of our specification of the principal condition for the production of weak electrolytes.

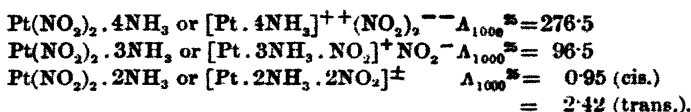
Unfortunately, data in reference to the ionization of compounds of this type are scanty, since most of them, in losing their character as strong electrolytes, become insoluble in water, and therefore pass right over to the category of non-electrolytes. Intermediate cases are, however, provided by the salts of organic hydroxy-acids. Thus Calame has shown by determinations of freezing-point that, whilst calcium *lactate* is ionized to the extent of 40 per cent. at a concentration of 0.257 *N*, the copper salt is ionized only to the extent of 17 per cent. at 0.271 *N**. In the same way, Tower has reported † that, whilst the molecular conductivities of the *succinates* of Ni, Co, and Mg are very similar at all concentrations, the molecular conductivities of the *tartrate* and *malate* of cobalt and nickel are very much smaller than those either of the magnesium salts or of the corresponding succinates. Again, Calame has shown that the coefficient of ionization of copper *malate* is only 4 per cent. in *N*/4.628 solution, 10 per cent. in *N*/74 solution, and 19 per cent. in *N*/592 solution, whereas zinc *maleate* (where coordination is

* *Zeit. phys. Chem.* xxvii. p. 401 (1898).

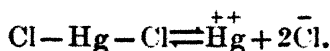
† *Journ. Amer. Chem. Soc.* xxii. p. 501 (1900); xxiv. p. 1012 (1902).

prevented by the elimination of the hydroxyl group) is dissociated to the extent of 22 per cent., 44 per cent., and 69 per cent. in solutions of similar concentrations. All these results are in accord with the view that the coordination of the ions of a metallic salt tends to convert it into a "weak electrolyte."

Other examples of weak electrolytes are afforded by the so-called "non-valent" coordination-complexes. Thus the following values are recorded for the conductivities of the amines of platinous nitrite* :—



It is commonly stated that substances such as $[\text{Pt} \cdot 2\text{NH}_3 \cdot 2\text{NO}_2]^{\pm}$, $[\text{Pt} \cdot 2\text{NH}_3 \cdot 4\text{Cl}]^{\pm}$ and $[\text{Co} \cdot 3\text{NH}_3 \cdot 3\text{NO}_2]^{\pm}$ are "non-electrolytes," but this statement is not in harmony with a summary of the experimental data in which it is said that "the compound is a very poor conductor of the electric current in aqueous solutions." If this description is correct, *i. e.*, if the feeble conductivity which is observed even in freshly-prepared solutions of these compounds cannot be explained away by the hydrolysis of the complex, these "non-valent" amines must be classed with the "weak electrolytes," which exhibit a small electrolytic conductivity as a result of the reversible ionization of a covalent complex, compare



(d) *Carbonium Salts*.—These salts are characterized by very wide range of conductivities. Thus Walden† found the following values for the equivalent conductivities of a series of halogen salts dissolved in liquid sulphur dioxide at 0° :—

KI	$\Lambda_{96} = 59.5$	$\Lambda_{2000} = 142.3$
$(\text{C}_6\text{H}_5)_3\text{CBr}$	$\Lambda_{96} = 108.5$	$\Lambda_{2001} = 152$
$(\text{C}_6\text{H}_5)_3\text{CCl}$	$\Lambda_{105} = 15.0$	
$(\text{CH}_3)_3\text{CI}$	$\Lambda_{17} = 0.7$	

The tertiary halides therefore cover the whole of the available range of conductivities, some of them being better conductors than a typical "strong electrolyte" like potassium iodide, whilst others have no conductivity at all. The same

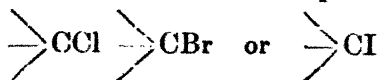
* Tschugaeff and Wladimiroff, *Journ. Russ. phys. Chem. Ges.* lii. p. 135 (1920).

† *Ber.* xxxv. p. 2023 (1902).

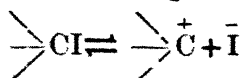
conclusion follows from the observations of Gomborg*, who gives the following values for the degree of dissociation of some carbonium salts at -8° and $v=100$, in comparison with the value for tetramethylammonium bromide,

$(C_6H_5)_3CCl$ 12 per cent. $(C_6H_5 \cdot C_6H_4)_2CCl$ 45 per cent.
 $(C_6H_5)_3CBr$ 61 per cent. $(CH_3)_4NBr$ 56 per cent.

In all these carbonium salts the rules of valency permit the formation of a covalent bond between the carbon of the kation and the halogen of the anion, giving rise to a true molecule instead of an ionic doublet. Since the carbon-halogen bond is usually too strong to be ionized by mere dissolution in a solvent, most of the compounds of the type



are non-conductors; but when the bond is weakened †, *e. g.*, by substitution and by replacing chlorine or bromine by iodine, so that ionization according to the scheme



becomes possible, the compounds pass into the group of "weak electrolytes," although they do not usually exhibit this property in aqueous solutions; and, finally, when the formation of a bond is rendered even more difficult † by the introduction of bulky aromatic substituents the salts are actually better conductors than many "strong electrolytes."

Summary.

(a) Although most electrolytes are ionized completely, even in the solid state, there are many compounds in which ionization is incomplete and reversible.

(c) Compounds of this type, in which neutralization of the ionic charges is not prevented by the laws of valency, behave as "weak electrolytes," unless the bond between the radicles is too weak to hinder the ionization of the molecule.

(d) "Weak electrolytes" of this class are found amongst acids and bases, pseudo-electrolytes, coordinated salts, and a few simple metallic salts such as mercuric chloride, where covalent molecules can be formed from the ions.

University Chemical Laboratory,
Cambridge.

* Journ. Amer. Chem. Soc. xlv. p. 1818 (1922); xlv. p. 206 (1923).

† Flürscheim, *loc. cit.* and Journ. Chem. Soc. xcv. p. 718 (1909).

V. *Multiple Ionization and the Absorption of X-Rays.* By F. K. RICHTMYER, *Professor of Physics, Cornell University* *.

1. A VERY large majority of the lines in the X-ray spectra of the elements are produced by transitions between ionized states in which one electron is missing from one or the other of the several levels—K, L, M. . . . These lines, frequently called “diagram lines,” belong to the so-called “X-ray spectra of the first kind.”

As is well known, there are, in addition to these “diagram” lines, numerous faint lines which cannot be explained by transitions between the levels which give rise to the spectra of the first kind. These faint lines are variously known as: (1) “satellites,” since they accompany a prominent line of the first kind, usually on the short wave-length side of the latter, although satellites on the long wave-length side are also known; (2) “non-diagram” lines, since they cannot be represented on the energy-level diagram usually adopted for lines of the first kind; (3) “spark” lines, since Wentzel proposed a theory of the origin of these lines which involved multiple ionization in the inner electron shells in the same way that the optical spark lines originate in multiple ionization, or excitation, in optical levels; or (4) “X-ray spectra of the second, third . . . kind,” according as the excited states giving rise to the lines are due, according to Wentzel’s theory, to double, triple . . . ionization of the respective electron shells.

The intimate relation which is known to exist between the X-ray spectra of the first kind and the directly-observed absorption discontinuities (K, L. . .), suggest the query: Are there in X-ray absorption spectra discontinuities or other peculiarities corresponding to these spectra of the second, third . . . kind? Before discussing this question it is pertinent to review briefly the evidence pro and con regarding Wentzel’s theory of the origin of these lines.

2. In Table I. are given some typical examples of non-diagram lines, together with the initial and final states corresponding to each line according to Wentzel’s† scheme

* Communicated by the Author. The Author acknowledges with many thanks assistance from the Heckscher Research Fund of Cornell University.

† *Ann. der Phys.* lvi. p. 437 (1921). *Zeits. f. Phys.* xxxi. p. 445 (1925).

of multiple ionization. In Wentzel's terminology K^2 stands for an atom which has lost both K-electrons; KL^2 for an atom which has lost one K- and two L-electrons; etc. The lines $K\alpha_3$ and $K\alpha_4$ form a close doublet, which has been measured over the range of elements Na(11) to Zn(30), but

TABLE I.

Some typical Non-diagram Lines and their origin.

Line.	Origin.		Kind.	Reference.
	Initial state.	Final state.		
Satellites of the $K\alpha$ doublet. ($K \longrightarrow L$)				
$K\alpha_3$	KL	L^2	Second	1
$K\alpha_4$	K^2	KL	Second	1
$K\alpha'$	KM	LM	Second	1
$K\alpha_5$	KL^2	L^3	Third	1
$K\alpha_6$	K^2L	KL^2	Third	1
Satellite of $K\beta$. ($K \longrightarrow M$.)				
$K\beta'$	KL	LM	Second	2
Satellites of $L\beta_1$. ($L_{III} \longrightarrow N_{IV, V}$)				
$L\beta_1'$	$L_{III}M_V$	$M_VN_{IV, V}$	Second	2
$L\beta_1''$	$L_{III}M_{IV}$	$M_{III}N_{IV, V}$	Second	2

¹ Quoted in Siegbahn's 'The Spectroscopy of X-Rays,' p. 106, from the measurements of Hjalmer, Dolejsk, and Dolejsk & Siegbahn. Wetterblad (*Zeits. f. Phys.* xlii. p. 611, 1927) gives the results of some careful measurements of the wave-lengths of these lines for Na, Mg, and Al.

² Druyvesteyn, *Zeits. f. Phys.* xliii. p. 707 (1927). Druyvesteyn gives also measurements of satellites of Ly_1 and $Ly_{2,3}$. Some of the data used by Druyvesteyn are from the previous measurements of Coster (*Phil. Mag.* xliii. p. 1070, 1922), who also reports satellites of $L\alpha_1$.

the components of the doublet have not been separated for elements of higher atomic number than Ca(20). The pair $K\alpha_5$ and $K\alpha_6$ has been measured for only four elements Na(11) to Si(14). Druyvesteyn's measurements of $K\beta''$

extend from K(19) to Fe(26) ; and of $L\beta_2'$ and $L\beta_2''$ from Nd(41) to Sb(51). For elements heavier than Sb(51) these latter lines are not resolved, and are listed by Siegbahn and by Coster as β_{11} and β_{12} .

The evidence in favour of Wentzel's scheme of multiple ionization as an explanation of the origin of satellites falls under several heads :—

(a) According to the theory, the difference in frequency ($K\alpha_5 - K\alpha_2$) for a given element should equal the difference ($K\alpha_3 - K\alpha_1$) for the same element. Data are available for only four elements, Na(11) to Si(14), to check this predicted equality.

According to the recent measurements of Wetterblad*, the frequency difference ($K\alpha_3 - K\alpha_1$) is some 8 per cent. higher than the difference ($K\alpha_5 - K\alpha_2$)—which is, perhaps, as good a check as could be expected, considering the difficulties of the measurements.

(b) The frequency difference ($K\alpha_6 - K\alpha_4$) for one element should equal the difference ($K\alpha_3 - K\alpha_1$) for the element of next higher atomic number. Wetterblad's measurements confirm this within 1 or 2 per cent. This is, perhaps, the strongest support for Wentzel's theory.

(c) Druyvesteyn† shows that the difference in frequency between a satellite and its "parent" line is for a given element computable from certain of the energy levels of that element and of the element of next higher atomic number. For example, the frequency difference $(K\beta'' - K\beta)_Z$ for an element of atomic number Z should, subject to certain very close approximations, be given by

$$(K\beta'' - K\beta)_Z = (L - M)_{(Z+1)} - (L - M)_Z,$$

where L and M are the frequencies of the L and M levels. Druyvesteyn applies this general principle to the satellites of $K\beta_2$, $L\beta_2$, $L\gamma_1$, and $L\gamma_{2,3}$, and obtains experimental verification of the predicted equality, which, again considering the difficulties of the wave-length measurements and the small wave-length differences involved, is perhaps within the limits of error of measurement for the satellite $K\beta'''$ (parent line : $K\beta_1$). The agreement is much less satisfactory for the L satellites.

(d) Wentzel originally assumed that double ionization of an atom might be brought about by successive collisions with two cathode-ray electrons. For example, an atom which

* *Zeits. f. Phys.* xlii. p. 611 (1927).

† *Loc. cit.* xliii. p. 707 (1927).

had already lost an electron in a collision might, before making a capture to fill the vacant place, collide with a second cathode-ray electron and become doubly ionized. But it was later shown that the life of the atoms in the excited states is so short that the probability of double ionization by this method is far too small to account for the observed intensities of the satellites. Accordingly, doubly-ionized atoms, if present in the target of an X-ray tube in sufficient numbers to produce spark lines as observed, must be produced as a result of a *single* collision with a cathode-ray electron which, then, must have sufficient energy to remove *both* electrons from the atom. Thus, to remove both K-electrons from an atom should require a cathode-ray electron *the energy of which is a little more than twice as great as the energy required to remove only one K-electron*. In other words, the critical exciting voltage for $K\alpha_1$ should be a little more than twice as great as that for $K\alpha_{1,2}$. Coster* showed that only one of the satellites of the $L\alpha$ line of silver, namely $L\alpha_3$, was produced at an excitation voltage of 4700, the other satellites appearing only at a voltage in excess of *twice* the excitation voltage (3350) of $L\alpha$ —as was to be expected from the theory.

3. However, the above experimental evidence in favour of the double ionization theory is neither so extensive nor so exact as to be altogether convincing. Further, there is some evidence, both direct and indirect, against the theory:—

(a) Of the direct evidence, the most significant is the observation of Bäcklin†, who studied the critical excitation voltage for the satellites of $K\alpha_{1,2}$ of aluminium, and showed that the lines $K\alpha_3$ and $K\alpha_4$ could be produced at an exciting voltage somewhat *less* than twice the exciting voltage of the $K\alpha_{1,2}$ lines. Bäcklin concluded that, on the theory of double ionization, the lines $K\alpha_{3,4}$ should be produced only at voltages *above* 3100; whereas actually Bäcklin found that these lines were produced at 2900 ± 50 volts. Taken at face value, this result is at variance with the observations of Coster, mentioned in the preceding paragraph, regarding the critical excitation voltage of the satellites of $L\alpha$. But in comparing these two observations account must be taken of two circumstances: (1) Bäcklin was working very close to the critical voltage, and it is quite possible that his maximum

* Phil. Mag. xliv. p. 569 (1922).

† Zeits. f. Phys. xxvii. p. 30 (1924).

voltages may have been sufficiently above the estimated values to exceed the critical value, 3100 volts. Coster's voltages were not adjusted to as narrow limits as were Bäcklin's. (2) Bäcklin found the lines $K\alpha_2$ and $K\alpha_1$ were produced by an exciting voltage some 5 per cent. below the estimated maximum; while Coster showed that the $L\alpha$ satellites were *not* produced by an exciting voltage 30 per cent. below the estimated minimum. Perhaps if these limits had been narrower the two experiments would have been in agreement.

(b) Siegbahn and Larson* report that a number of the satellites of the $L\alpha$ lines of Mo(42) are found at an exciting voltage only 30 per cent. above the critical excitation for $L\alpha$; and that *no new satellites appear when the voltage passes twice the exciting voltage for $L\alpha$* , indicating that, even when the energy of a cathode-ray electron is sufficient to remove two L-electrons by "a single act," such doubly-ionized atoms, if present in the target, do not contribute to the production of the *observed* satellites.

(c) The satellites appear to have certain physical characteristics which differentiate them from the "diagram" lines, and which indicate that the method of production must be somewhat more complex than that suggested by Wentzel's original scheme. Many writers report that some, at least, of the satellites are much broader than the corresponding diagram lines, and probably have a complex structure. Thus Coster† reports that the lines $L\beta_2'$ and $L\beta_2$ for Ag(47), satellites of $L\beta_1$, are "very broad and diffuse; that they are symmetrical at low exciting voltages, but that at higher voltages they become "much more intense on their long wave-length side," suggesting that the lines are made up of (unresolved) components which behave differently with increasing voltage.

4. The well-known relation which exists between the absorption of X-rays and the *fluorescent* spectra of the first kind suggests that, if it can be shown that the *spark* lines can be produced by fluorescence, then one might, *perhaps*, expect that the evidence concerning the spark lines should be found in X-ray absorption spectra: for example, absorption discontinuities, very small, of course, since the spark lines are weak, might appear at the wave-lengths corresponding to the critical excitation frequencies of the several groups of

* 'Spectroscopy of X-Rays,' p. 194.

† Phil. Mag. xlv. p. 569 (1922). Coster calls these lines $L\beta_{11}$ and $L\beta_{12}$.

spark lines, just as similar discontinuities are observed in connexion with the spectra of the first kind. Early attempts to produce spark lines by fluorescence were either negative or inconclusive. But recently Coster and Druyvesteyn* have shown that it is possible to produce satellites in the X-ray spectrum of Fe(26) by using the radiation from a copper target excited by 30,000 volts. However (and, from the standpoint of the absorption of X-rays, this is a matter of greatest importance), according to the estimates of Coster and Druyvesteyn, the intensity of the satellites was certainly not over 2 per cent., and probably less than 1 per cent., of the intensity of the fluorescent lines of the first kind. Therefore, absorption discontinuities, corresponding to these spark lines, *if present at all* in absorption spectra, are probably less than 1 per cent. as large as the discontinuities corresponding to lines of the first kind. It is quite obvious that to detect such small discontinuities with certainty would require that the measurements of absorption coefficients be made with the highest precision—indeed, with a precision higher than any which, in the writer's opinion, have been reported up to the present.

However, it does not necessarily follow that the hypothesis of multiple ionization, as an explanation of the origin of spark lines, requires that there should be corresponding absorption discontinuities in X-ray absorption spectra. In order that there should be such discontinuities it would be necessary that the energy, $h\nu$, of an incident quantum should, by a "primary act," cause the expulsion of *two* electrons either from the same or from different levels. The preponderance of evidence, however, seems to be opposed to this possibility, and Coster and Druyvesteyn are of opinion that double ionization comes about as a *secondary* process: an absorbed quantum causes the expulsion of a *single* electron (call it the primary photoelectron) from a given level; if this primary electron possesses sufficient energy, it may, on its way out of the atom, collide with an electron of the same or of another level, and cause the expulsion of the latter electron, the process resulting in a doubly-ionized atom. It should be pointed out, however, that if this latter be the correct sequence of events which produces multiply ionized states, *no increase in absorption of the primary X-ray beam should be observed as, with increasing frequency, the frequency of the primary beam passes the frequency ν_m corresponding to the energy $h\nu_m$ necessary for multiple ionization.* Rather, on

* *Zeits. f. Phys.* xl. p. 265 (1927).

this view, the *energy* for producing the spark lines comes from the kinetic energy initially given to the *primary* photoelectron, which, as it leaves the atom after having knocked out another electron, must therefore possess less energy than it would have had if no secondary process had occurred, by at *least* the energy necessary to remove the second electron. There is no reason to expect that these *secondary* events in *any way* modify the absorption probability of the primary quantum. No discontinuity in the absorption spectrum should be observed at a frequency corresponding to the energy required for double ionization. Rather, as Robinson* points out, evidence concerning spark lines is to be expected in the magnetic spectrum of the photoelectrons ejected by a monochromatic beam of incident X-rays.

5. In this connexion mention may be made of a recent important paper by Alexander † which touches on the subject of multiple ionization. Alexander concludes, from a careful study of certain data on the variation of (X-ray) mass absorption coefficients $\frac{\mu}{\rho}$ as a function of wave-length, that at a wave-length λ_K' , approximately $\frac{\lambda_K}{2}$, where λ_K is the wave-length of the K absorption discontinuity, the coefficient k in the well-known empirical equation

$$\frac{\mu}{\rho} = k\lambda^3 + \frac{\sigma}{\rho}$$

undergoes a sudden change, the value of k for $\lambda < \lambda_K'$ being some 30 per cent. greater than the value of k for $\lambda > \lambda_K'$. Alexander interprets this "break" in the absorption curve, shown diagrammatically by the full line in fig. 1, as marking the frequency ν_K' at which the energy of the quantum $h\nu$ becomes just sufficient "to remove both K-electrons as a single act. At this point twice as many electrons should be produced, although their speed at the periphery of the atom is zero." ‡

This *empirical* description of the relation between $\frac{\mu}{\rho}$ and λ^3 , as shown graphically in fig. 1, is perhaps justified by the experimental data. It has been long known that the λ^3

* Phil. Mag. iv. p. 763 (1927).

† Loc. cit. iv. p. 670 (1927).

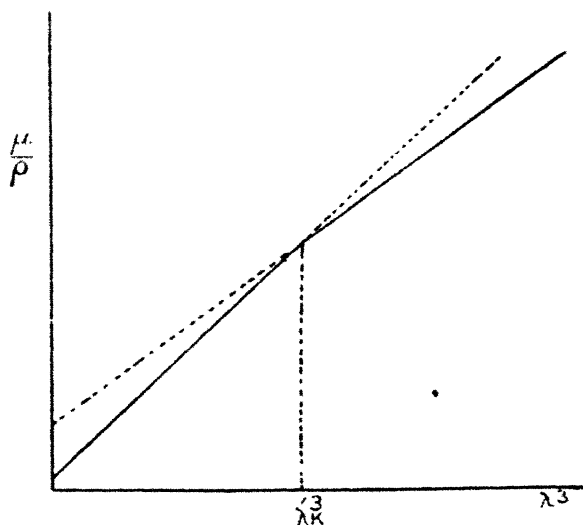
‡ Alexander, loc. cit. p. 679.

law of absorption gives only a close approximation to the experimental facts, and that if the equation

$$\frac{\mu}{\rho} = k\lambda^3 + \frac{\sigma}{\rho}$$

be established empirically for frequencies considerably in excess of the K limit, the values of $\frac{\mu}{\rho}$ determined by extrapolation toward the K limit are higher than the observed values. The present writer pointed this out some years ago *, and indeed, in the graph of the data on the absorption

Fig. 1.



of molybdenum as a function of λ^3 (see fig. 6 of article cited), two straight lines, slightly inclined to each other, were drawn †. Further, in connexion with a precision study of the λ^3 law in the neighbourhood of the K limit ‡,

the writer has observed that, although the graph of $\frac{\mu}{\rho}$ as a function of λ^3 on the short wave-length side of, but near to, the K limit is *rigorously* a straight line with no suggestion of deviation therefrom as the limit is approached, the slope

* Phys. Rev. xviii. p. 13 (1921). See p. 26 of article cited.

† These data on molybdenum are included by Alexander in his discussion above cited.

‡ Phys. Rev. xxvii. p. 794 (1926).

of this line is somewhat less than that of the *similar* straight line observed at much shorter wave-lengths. This point is brought out by the writer's data on Sn(50)*, from which two slopes k' and k (in the above terminology) are respectively 755 and 592, in substantial agreement with Alexander's values (data by Allen) of 750 and 583.

In any event the observational data do not seem to *preclude* the possibility that there may be a "break" in the $\frac{\mu}{\rho} - \lambda^3$ curve as suggested by Alexander, although the deviations from the λ^3 law may be represented empirically in different ways. For example, Allen† concludes, from a study of observed data on absorption coefficients of several substances over a wide range of wave-lengths, that absorption-coefficients as a function of λ can be given by a formula (derived on theoretical grounds by Wentzel) of the type

$$\frac{\mu}{\rho} = k_1 \lambda^3 + k_2 \lambda^{3.5} + k_3 \lambda^{3.5} + \frac{\sigma}{\rho}.$$

Previously Allen was of the opinion that the empirical relation was

$$\frac{\mu}{\rho} = k \lambda^{2.92} + \frac{\sigma}{\rho}.$$

These various empirical formulæ illustrate the fact that more precise experimental data on absorption-coefficients are needed to establish, unambiguously, the exact *empirical* law of X-ray absorption. (See, for example, section 7, p. 84.)

However, granted for the moment that the data on X-ray absorption are such as to warrant the conclusion that a

"break" in the $\frac{\mu}{\rho} - \lambda^3$ curve occurs at λ_K' as suggested by Alexander, the interpretation of this break as indicating the beginning of double ionization of the K shell seems by no means justified by the present experimental facts. There are several very weighty arguments against such an interpretation:—

(a) If the wave-length λ_K' of the "break," corresponding to frequency ν_K' , represents the beginning of double ionization of the K shell as a result of the photoelectric expulsion of both K-electrons by the absorption of the *single* quantum $h\nu_K'$ or greater, then the energy $h\nu_K'$ must be at least a little greater than *twice* the energy $h\nu_K$ required to remove a *single*

* National Academy of Sciences, Washington Meeting, April 1927. Phys. Rev. Dec. 1927.

† Phys. Rev. xxix. p. 918 (1927).

K-electron, since, because of the effective increase in nuclear charge, the energy required to remove the *second* electron should be a little greater than the energy required for the removal of the first. However, of the thirteen values of ν_K' determined by Alexander, *only four occur at frequencies more than twice the frequency of the K limit*, as is shown in Table II., in which columns 1 and 2 are taken from Alexander's paper, column 3 from Siegbahn's 'Spectroscopy of X-Rays,' and column 4 is the ratio of column 2 to column 3. Alexander's interpretation would require, in the case of Ag(47) for example, that the energy required to remove the *second* K-electron should be only 75 per cent. as great as that required to remove the

TABLE II.

Element.	$\left(\frac{\nu}{R}\right)_K = A.$	$\left(\frac{\nu}{R}\right)_K = B.$	Ratio A/B.
Fe 26.....	1235	524	2.36
Ni 28.....	1311	612	2.14
Cu 29.....	1451	661	2.20
"	1235	"	1.87
"	1078	"	1.63
Zn 30.....	1715	703	2.44
Mo 42.....	2745	1474	1.86
Ag 47.....	3350.	1879	1.78
"	3290	"	1.75
Sn 50.....	3781	2148	1.76
W 74.....	8064	5117	1.57
Pt 78.....	9027	5764	1.56
Au 79.....	9214	5941	1.56

first K-electron—a conclusion quite at variance with our fundamental concepts of multiple ionization.

On the basis of Wentzel's theory of the origin of spark lines, it is possible to compute the energy required for double ionization of the K shell, by the method used by Turner*, for the elements Na(11) to Zn(30), and by an extrapolation (of course only approximately justifiable) as far as Sn(50). Turner showed that the energy K_Z^2 (in $\frac{\nu}{R}$ units) necessary to remove *both* K-electrons from an atom of atomic number Z is given, to a very close approximation, by the expression

$$K_Z^2 = K_Z + L_{(Z+1)} + (\alpha_4)_Z, \quad \dots \quad (1)$$

* Phys. Rev. xxvi. p. 143 (1925). Turner's computations, based on the only data then available, are for the elements Na(11) to S(16).

where K_Z is the value of $\frac{\nu}{R}$ for the K limit of the atom in question, $(\alpha_1)_Z$ is the value of $\frac{\nu}{R}$ of the satellite $K\alpha_1$, and $L_{(Z+1)}$ is the value of $\frac{\nu}{R}$ for the L limit of an atom of atomic number $(Z+1)$. Siegbahn* gives the measurements of Hjalmer, of Dolejšek, and of Dolejšek and Siegbahn for the wave-lengths of the spark lines $K\alpha_3$ and $K\alpha_4$ from Na(11) to Zn(30). (These lines are not separated for elements of higher atomic number than Ca(20).) The wave-lengths of these are given in columns 2 and 3 of Table III. For purposes of computation and extrapolation we may write equation (1) in the form (by adding and subtracting $K\alpha_2$)

$$K_Z^2 = 2K_Z + (L_{II,(Z+1)} - L_{II,Z}) + (K\alpha_4 - K\alpha_2)_Z, \quad (2)$$

in which, for reasons which will appear presently, we identify the L limit of equation (1) with L_{II} . The sum of the two brackets on the right represents the amount by which the energy required for the double ionization of the K shell is in excess of that required for single ionization. Both brackets are always positive. A very interesting, and perhaps suggestive, relation may be shown to exist between the satellites $K\alpha_3, 4$ and the diagram line $K\alpha_2$. If the *square root* of the *difference* in frequency between $K\alpha_4$ and $K\alpha_2$ be plotted as a function of atomic number, the upper *straight line* shown in fig. 2 results. A similar plot for the difference $(K\alpha_3 - K\alpha_2)$ gives the *lower* straight line. Since the satellites $K\alpha_3$ and $K\alpha_4$ are not separated for elements above Ca(20), the observed wave-lengths for elements of atomic number greater than 20 are therefore the centre of gravity of the two lines, and are seen to fall between the two straight lines extended. These two differences, $(K\alpha_4 - K\alpha_2)$ and $(K\alpha_3 - K\alpha_2)$, have the characteristic of a screening doublet, with a *difference* in screening constant of (almost) unity. From this graph one finds that over the range Na(11) to Cu(29) the difference in $\frac{\nu}{R}$ between $K\alpha_4$ and $K\alpha_2$ is given empirically by

$$\left(\frac{\Delta\nu}{R}\right)_{(K\alpha_4 - K\alpha_2)} = 49 \times 10^{-4} (Z + 0.4)^2. \quad (3)$$

An extension of equation (3) as far as Sn(50) is approximately justified. The values of $\frac{\Delta\nu}{R}$ computed from this equation are given under "B" in column 10 of Table III.

* 'Spectroscopy of X-Rays,' p. 106.

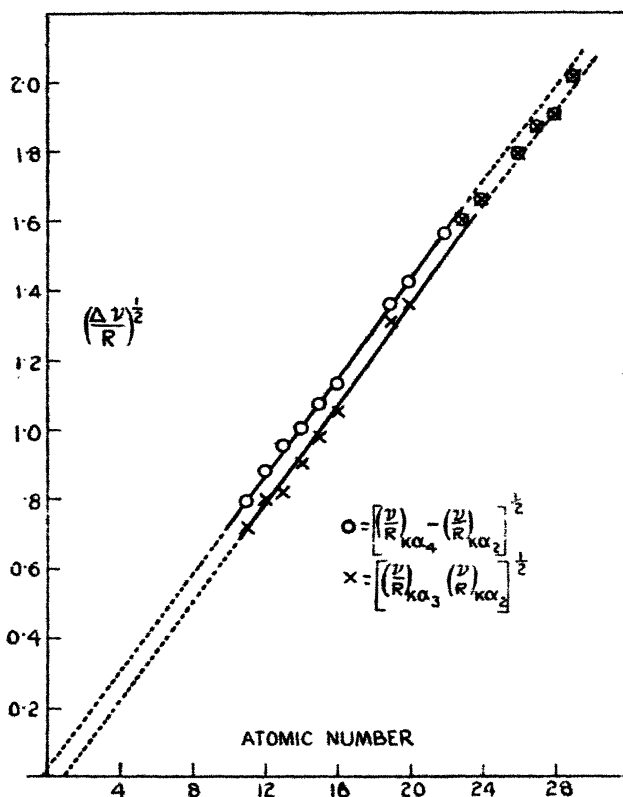
TABLE III.—Computation of the Energy required for Double Ionization of the K-level.
Data from Siegbahn's 'Spectroscopy of X-Rays,' except where indicated.

Element.	Wave-length (Ångströms).		$(\Delta\nu/R)$.			$\sqrt{\Delta\nu/R}$.		$\left(\frac{\nu}{R}\right)_{\text{II}}$.	$\left(\frac{\nu}{R}\right)_K = K.$	B.	K^2 .	$K^2/K.$
	$K\alpha_3$.	$K\alpha_1$.	$\alpha_1 - \alpha_2$.	$\alpha_2 - \alpha_3$.	$\alpha_3 - \alpha_4$.	$\alpha_4 - \alpha_5$.	$\alpha_5 - \alpha_6$.					
Na 11	118039 ¹	117869 ¹	0.63	0.32	0.79	0.72	—	2.16	78.64 ³	0.64	159.63	2.0248
Mg 12	98000 ¹	97842 ¹	0.70	0.64	0.80	0.80	—	3.47	95.81	0.75	194.04	2.0.46
Al 13	82658 ¹	82501 ¹	0.92	0.71	0.96	0.84	—	5.14	114.07	0.88	232.09	2.0240
Si 14	70638	70537	1.01	0.83	1.01	0.91	—	7.01	135.16 ³	1.02	274.28	2.0389
P 15	61022	60950	1.16	0.96	1.08	0.98	—	9.89	158.26	1.16	319.71	2.0302
S 16	53294	53233	1.29	1.10	1.14	1.05	—	11.92	181.81	1.32	367.85	2.0232
K 19	37110	37068	1.86	1.72	1.36	1.31	—	21.49	265.33	1.85	546.89	2.0236
Ca 20	33323	33300	2.04	1.84	1.42	1.36	—	25.87	297.48	2.04	601.40	2.0216
Sc 21	—	—	—	—	1.50	1.50	—	30.27	331.17	2.25	668.00	2.0171
Ti 22	27269	—	2.42	—	1.56	1.56	—	33.68	363.43	2.45	737.71	2.0188
Va 23	24846	—	2.56	—	1.60	1.60	—	38.08	402.27	2.60	812.27	2.0192
Cr 24	22733	—	2.75	—	1.66	1.66	—	43.12 ²	441.23 ²	2.92	890.44	2.0181
Mn 25	—	—	—	—	—	—	—	48.18 ²	481.83 ²	3.16	972.08	2.0175
Fe 26	19233	—	3.22	—	1.70	1.70	—	53.44 ²	524.70 ²	3.42	1057.02	2.0172
Co 27	17774	—	3.49	—	1.80	1.80	—	59.04 ²	568.24 ²	3.68	1145.82	2.0165
Ni 28	16476	—	3.63	—	1.91	1.91	—	64.70 ²	614.12 ²	3.95	1237.81	2.0156
Cu 29	15307	—	4.05	—	2.02	2.02	—	70.32 ²	661.59 ²	4.25	1334.21	2.0167
Zn 30	—	—	—	—	—	—	—	77.10 ²	—	—	—	—
Zr 40	—	—	—	—	—	—	—	169.6	1325.8	8.0	2671.4	2.0149
Nb 41	—	—	—	—	—	—	—	181.4	—	—	—	—
Sb 51	—	—	—	—	—	—	—	323.6	2241.7	12.9	4517.9	2.0132
Te 52	—	—	—	—	—	—	—	340.3	—	—	—	—

¹ Wetterblad, *Zeits. f. Phys.* xlii. p. 611 (1927). ² Thoreus, *Phil. Mag.* ii. p. 1107 (1926). ³ Estimated by Turner (*loc. cit.*).

The value of K^2 is then readily computed by use of equation (2). Column 12 of Table III. shows the ratio $\frac{K^2}{K}$, which is seen to decrease very slowly with increasing atomic number, but of course remains in excess of 2.000. In fig. 3 is shown

Fig. 2.

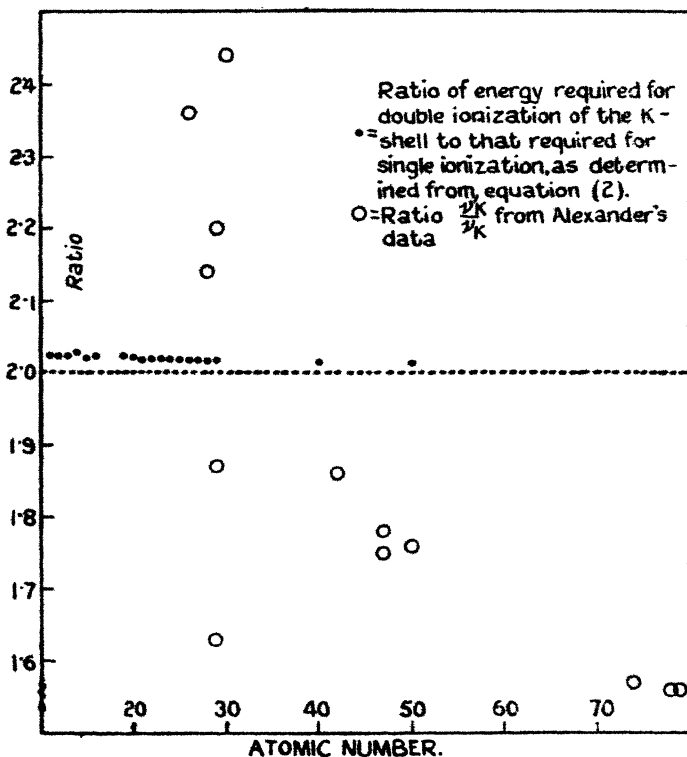


the ratio $\frac{K^2}{K}$ for double K-ionization as computed from equation (2) and, for comparison, the ratio $\frac{\nu_{K'}}{\nu_K}$ from Table I., as determined by Alexander. It is quite apparent that, *so far as existing data go*, one is not justified in concluding that there is any obvious relation between Alexander's ν_K break and the double ionization of the K level.

(b) As pointed out above, the intensity of the spark lines is so weak that, granted Wentzel's theory, one would not

expect to find a change of shape in the $\frac{\mu}{\rho} - \lambda^3$ curve as great as that reported by Alexander. Further, if λ_K' marks the beginning of double ionization, one should find a "jump" or discontinuity in the curve similar to the K, L_I , L_{II} , discontinuities, instead of simply a bend *. But Alexander's curves show no such "jump."

Fig. 3.



* Alexander's suggestion that, beginning with the wave-length λ_K' , "both K-electrons are removed by a single act" and that "twice as many electrons are produced" implies that, beyond this critical wave-length, all K absorption results in double ionization of the K shell and that no single ionization occurs. Were this the case, and were the values of λ_K' those given by Alexander, the fluorescent K series lines produced by absorption of radiation of wave-length $\lambda < \lambda_K'$ should be quite different from those wave-lengths when produced by radiation $\lambda > \lambda_K'$. In other words, the fluorescent spectra of the first kind, when produced by absorption of radiation extending on both sides of λ_K' , as, for example, in the experiments of Coster and Druyvesteyn (*loc. cit.*) should be double. No such duplicity in fluorescent spectra has been reported.

(c) Wentzel's theory attributes the line $K\alpha_3$ to the transition $KL \rightarrow L^2$. One should expect, therefore, a break in the $\frac{\mu}{\rho} - \lambda^3$ curve at the frequency corresponding to simultaneous ionization of the K and the L shells. This "break" should occur for an element of atomic number Z at a frequency ν_{KL} , given to a close approximation, by

$$h\nu_{KL} = h\nu_K + h\nu_{L(Z+1)}.$$

The writer's data on Sn(50)* show that no such break is observed in the predicted region.

(d) As pointed out above (Sect. 4), the existing data seem to indicate that double ionization occurs as a *secondary* process, rather than as a *primary* act in which two electrons are simultaneously expelled by the absorption of a single quantum. We should not therefore expect to find in the X-ray absorption spectra evidence concerning the processes which give rise to the (fluorescent) spark spectra.

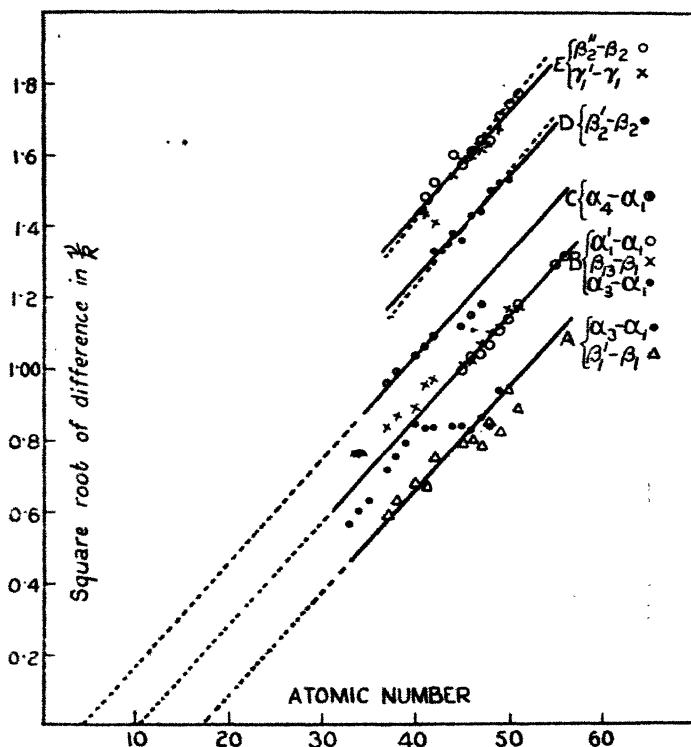
In short, the conclusion seems justified that the "break" represented in fig. 1, *if real*, must be explained on some other grounds than multiple ionization.

6. The two straight lines in fig. 2 resemble a Moseley diagram, and perhaps warrant a few brief suggestions, admittedly highly speculative, concerning a possible alternative theory of the origin of X-ray satellites. The lines $K\alpha_4$ and $K\alpha_3$ are usually considered satellites of $K\alpha_1$. But if the square root of the difference in frequency between either of these lines and $K\alpha_1$ be plotted against atomic number, one does not obtain a straight line. The straight lines of fig. 2 suggest the possibility that $K\alpha_4$ and $K\alpha_3$ are satellites of $K\alpha_2$ instead of $K\alpha_1$. One inquires whether satellites of other lines, when plotted as in fig. 2, yield similar straight lines. Unfortunately, data bearing on this question are exceedingly limited, partly because measurements of many of the satellites have been made for only a few elements, and partly because the diffuse nature of some of the satellites and their closeness to the parent line make it difficult to obtain wave-length measurements with high precision—a matter of considerable importance in consideration of the fact that the differences in frequency between satellites and the "parent" lines are, in general, only a fraction of 1 per cent. In Table IV. are given the square roots of the frequency differences between some of the more prominent satellites and the respective parent lines. A Moseley plot of these data is shown in figs. 2

* *Loc. cit.* Phys. Rev., Dec. 1927.

and 4. Fig. 4 contains data on *eight* satellites: three of $L\alpha_1$, two of $L\beta_1$, two of $L\beta_2$, and one of $L\gamma_1$. The points seem to fall into *five* groups, through which *parallel** straight lines, A, B, C, D, and E, have been drawn. Although there is considerable scattering, the points seem to fit these straight lines reasonably well. Further, in several cases, points from different satellites fall upon, or near, the same line. For example, from atomic number 45

Fig. 4.



to 51, the difference $(L\alpha_1' - L\alpha_1)$ coincides very nearly with $(L\beta_{13} - L\beta_1)$. The difference $(L\beta_2'' - L\beta_2)$ is almost the same as $(L\gamma_1' - L\gamma_1)$.

One is now tempted to suggest the hypothesis that these satellites are produced by *two-electron* transfers, similar to the primed lines (terms) in optical spectra. Or, for example, that the line $K\alpha_4$ is the result of the *simultaneous* jump of

* Perhaps the dotted lines at D and E are better

one electron from the L_{II} level to a vacancy in the K shell, and of another electron from an optical level into a vacancy in the M shell, *both transfers cooperating to emit a single quantum*. The fact that the graphs of figs. 2 and 4 are, at least approximately, similar to the Moseley diagram for X-ray lines is itself strongly suggestive of the possibility that the graphs represent X-ray lines (perhaps semi-optical lines) such as might be produced by *single-electron transfers*.

If so, we might picture the production of $K\alpha_4$ as follows:—An atom becomes, by one of several possible processes, doubly ionized; i. e., it lacks one K-electron and one M-electron. First, let us say, the vacant M shell is filled by an electron dropping from an optical orbit for which transfer the atom behaves (since it lacks a K-electron) very nearly like an atom of the next higher atomic number; and an amount of energy, call it $(M-O)_{(Z+1)}$, is released. The transfer L_{II} to K then occurs and energy $(K-L_{II})_Z$ is released, which gives the first-order line $K\alpha_2$. If these two events occur simultaneously, a single quantum, corresponding to $K\alpha_4$, might be emitted, and we should have

$$K\alpha_4 = (K-L_{II})_Z + (M-O)_{(Z+1)}$$

$$\text{or} \quad K\alpha_4 - K\alpha_2 = (M-O)_{(Z+1)}.$$

It might, perhaps, be expected that a Moseley plot of the "line" $(M-O)_{(Z+1)}$ would yield (approximately) a Moseley graph.

In support of this hypothesis one may introduce the following evidence:—

(a) The lines of figs. 2 and 4, particularly of fig. 2, are Moseley graphs.

(b) The order of magnitude of the quantity $(K\alpha_4 - K\alpha_2)_Z$ is what one might expect for the quantity $(M-O)_{(Z+1)}$. Unfortunately, only a qualitative check of this predicted equality is possible. Taking Na(11), for example, we do not know what *optical* frequencies would be emitted by an atom which has lost a K-electron. But the work required to remove the valence electron from such a K-ionized Na atom should be of the order of magnitude of, or a little greater than, the work to remove the *second* valence electron from a Mg(12) atom. The latter is*, in terms of $\frac{\nu}{R}$, 1.105. The term $(M-O)_{(Z+1)}$ should be somewhat smaller than this. Actually $(K\alpha_4 - K\alpha_2)$ for Na is

* Paschen and Götze, 'Serien Gesetze der Linien Spektren.' Berlin, 1922.

0.64. Going to the other end of the series of elements for which we have data on $K\alpha_4$, namely Cu(29), we should expect that $(K\alpha_4 - K\alpha_3)$ should be somewhat smaller than the energy of the M levels of Cu. Siegbahn gives for $M_{III,IV}$ for Cu, $5.2 \frac{\nu}{R}$. From Table II. one observes that $(K\alpha_4 - K\alpha_3)$ for Cu is $4.05 \frac{\nu}{R}$. Further, the order of magnitude of the corresponding differences for the L satellites is the same as that of the energy of the outermost electron levels of the respective atoms.

(c) On this hypothesis we should expect that there might be several different semi-optical transfers of the “(M—O)” type which could co-operate with a given parent line in producing the observed satellite, which, then, should have a “fine structure.” As previously mentioned, many of the satellites are broader and more diffuse than the diagram lines.

Opposed to this hypothesis of two-electron transfers as an explanation of satellites are the following arguments:—

(1) Wetterblad’s* recent measurements confirm with reasonable precision the equality of the differences $(K\alpha_2 - K\alpha_1)_Z$ and $(K\alpha_3 - K\alpha_1)_{(Z+1)}$, predicted by Wentzel’s theory of multiple ionization. This confirmation, however, has been made only for the four elements Na(11) to Si(14), and only for the satellites of $K\alpha_{1,2}$.

(2) Druyvesteyn’s† computation of the frequency of the satellite $K\beta'''$ from that of the parent line $K\beta_1$, for the elements K(19) and Fe(26) on the basis of Wentzel’s theory agrees within experimental error with observations.

(3) Coster’s measurements seem to indicate that the critical excitation potentials for satellites are considerably higher than would be expected if they were produced by the two-electron transfers herein suggested. On the contrary, Bäcklin’s measurements‡ appear to invalidate the measurements of Wetterblad referred to in (1) above, since the latter, on the one hand, confirm Wentzel’s postulate that the line $K\alpha_4$ arises from double ionization of the K shell, while the former, on the other hand, show that $K\alpha_4$ is produced under conditions where double ionization seems impossible.

In short, the only categorical statement concerning X-ray satellites which at present seems entirely justified is that the theory of their origin is as yet an unsolved problem!

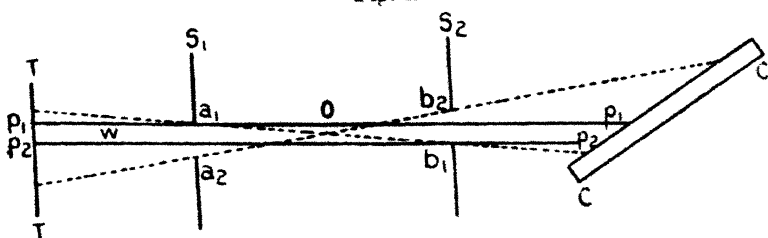
* *Loc. cit.*

† *Loc. cit.*

‡ *Loc. cit.*

7. In making measurements of X-ray absorption-coefficients with a precision sufficient to detect such small discontinuities as might correspond to the spectra of the second kind as discussed above, it is necessary to be meticulous in the elimination of, or correction for, the various experimental errors. Among these is the error introduced by the fact that the slit system used in the X-ray spectrometer is of finite width. With sufficiently narrow slits the error is negligible. But with slit-widths as great as have been used in some of the measurements of absorption-coefficients reported in the literature of the subject, the error may amount to several per cent. The magnitude of the error depends on the slit-width, the material under investigation, the wave-length at which the measurement is made, and the voltage applied to the X-ray tube. By making certain justifiable simplifications, one can compute the order of magnitude of the error in any particular case.

Fig. 5.



In fig. 5, let S_1 and S_2 be the two slits of the X-ray spectrometer; TT the target of the X-ray tube; and CC the crystal. Let the slit-widths be equal and be represented by a_1a_2 and b_1b_2 *. Let the X-ray "brightness" of the target be uniform, and assume that we have a perfect crystal. Then X-rays will be incident onto the crystal at all angles from that corresponding to the incident direction a_1b_1 , reflected wave-length λ_1 , to that corresponding to a_2b_2 , reflected wave-length λ_2 . Let the angle † $a_1Oa_2 = \Delta\theta$. Then the wave-length range, $\lambda_1 - \lambda_2 = \Delta\lambda$, included in the bundle of X-rays reflected from the crystal, is, from Bragg's equation,

$$\Delta\lambda = 2d \cos \theta_0 \Delta\theta,$$

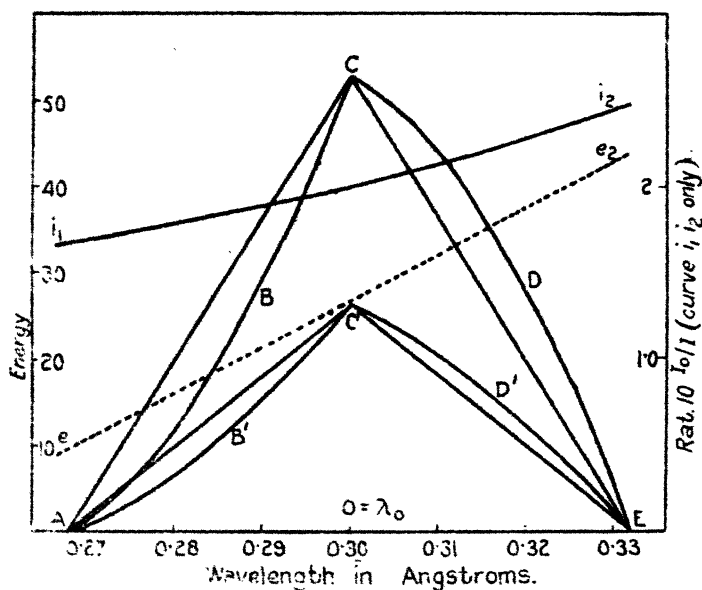
where d is the grating space of the crystal and θ_0 is the

* The slit-widths are grossly exaggerated in the figure in comparison with the distance between slits.

† In any actual case very small.

angle which the axis of the slit system makes with the crystal. The X-ray energy corresponding to a wave-length λ within this range $\Delta\lambda$ and entering the ionization chamber after reflexion from the crystal, is limited by the edges of the slit system and varies from zero at λ_1 to a maximum at angle θ_0 , and back to zero at λ_2 . For example, the intensity of radiation of wave-length λ_p corresponding to the incident direction p_1p_1 is determined, as is readily seen from the figure, by the distance W between the parallel lines p_1p_1 and p_2p_2 .

Fig. 6.



If we assume that the X-ray spectral energy distribution from the target is constant over the range $\lambda_1 - \lambda_2$, then it follows, since in any actual case the angle a_1oa_2 is very small, that the energy distribution reflected from the crystal into the ionization chamber is given, in this ideal case, by the triangle ACE of fig. 6. If, now, there be inserted in the path of the beam an absorber which transmits, at each wave-length between λ_1 and λ_2 , exactly 50 per cent. of this incident radiation, the energy distribution of the reflected radiation will be given by the triangle AC'E, each ordinate of which is exactly half of the corresponding ordinate of

ACE. The ratio I/I_0 (ratio of transmitted to incident radiation in the equation $I = I_0 e^{-\mu x}$) will be given by

$$\frac{I}{I_0} = \frac{\text{area } AC'B}{\text{area } ACB} = \frac{OC'}{OC} = \frac{1}{2}.$$

It is obvious that the finite width of the slit has in this case introduced no error in the observed ratio I/I_0 . If, however, (1) the spectral energy distribution in the incident radiation is not uniform, and (2) the absorber, because of variation of absorption-coefficient with wave-length, transmits different amounts at each wave-length, the result is somewhat different.

To take a concrete case:—Certain measurements of absorption-coefficients have been reported in which the slit-widths were such that the angle $a_1 o a_2$ of fig. 5 was about 30 minutes of arc. Let us consider the error introduced in measuring the absorption-coefficient of copper at a wave-length 0.3 \AA ., when the spectral energy distribution in this region is that corresponding to the continuous spectrum excited by some 50,000 volts. In this case the spectral range λ_1 to λ_2 of fig. 5 corresponds to, roughly, 0.06 \AA . (calcite crystal). The spectral energy distribution over this range is represented by the line $* e_1 e_2$ of fig. 6, the ordinate at λ_0 being arbitrarily taken as unity. Let the copper absorber be chosen of such thickness that at $\lambda = 0.3 \text{ \AA}$. it transmits 0.50 of the incident energy. Then, assuming the approximate linear relation between λ^3 and the mass absorption-coefficient in this region, the ratio I_0/I of the incident to the transmitted radiation at each wave-length λ in the region $0.27 < \lambda < 0.33$ is given by the line $i_1 i_2$ of fig. 6. Multiplying each ordinate of the triangle ACE by the corresponding ordinate of the spectral energy distribution curve of the incident radiation ($e_1 e_2$) gives ABCDE, which is the spectral energy distribution of the radiation I_0 as reflected into the ionization chamber. Dividing the ordinates of this latter curve by the ratio I_0/I at each wave-length gives AB'C'D'E, which is the energy distribution in the radiation I (*i. e.*, the radiation entering the ionization chamber after passing through the absorber). The *observed* ratio I/I_0 is given by

$$\frac{I}{I_0} = \frac{\text{area } AB'C'D'E}{\text{area } ABCDE}.$$

* A linear relation is assumed for the energy distribution between λ_1 and λ_2 for simplicity in computation. The final result is not materially changed by this assumption.

This ratio is not quite equal to the ratio $OC'/OC=0.500$, which is the ratio to be expected if an infinitely narrow slit system were used. By measuring the two areas, and observing how much the observed ratio I/I_0 differs from 0.500, one can obtain the error in the resulting value of the mass absorption-coefficient.

As an illustration of order of magnitude, there are given in Table V. the errors, computed as above, for copper of three thicknesses such as to transmit, respectively, $1/10$, $1/2$, and $4/5$ of the incident beam, and for spectral energy distributions corresponding roughly to 50,000 and to 60,000 volts.

TABLE V.

Errors, in per cent., in measuring mass absorption-coefficients of copper at $\lambda=0.3 \text{ \AA.}$ with a slit system 0.06 \AA. wide, at two voltages. A positive error means that the observed value is too large.

Transmission at $\lambda=0.3 \text{ \AA.}$	Error in per cent.	
	$V=60,000.$	$V=50,000.$
0.100	-0.8	+1.7
0.500	0.0	+1.8
0.800	+0.4	+3.8

Of course, the values are only approximate because of the simplifying assumptions which have been made. For elements of higher atomic number than copper the error becomes greater (so long as $\lambda=0.3$ is in the K-absorption region). The error becomes greater at shorter wave-lengths and *vice versa*. The error becomes rapidly smaller the smaller the slit-width (rather, the smaller the ratio $\Delta\lambda/\lambda$).

While these errors are not large, they must be taken into account when attempting to measure absorption-coefficients with a precision of the order of $1/10$ per cent. Either a correction for the finite width of the slit must be made, or one must use a slit system sufficiently narrow so that the error is less than the desired precision. This latter is made somewhat difficult by the fact that the energy transmitted by a slit system of the type shown in fig. 5 decreases as the square of the slit-width.

Summary.

1. The question has been raised: Are there in X-ray absorption spectra discontinuities corresponding to the so-called "spark" lines analogous to the K, L, K . . . discontinuities corresponding to the diagram lines? The present evidence seems to indicate that the processes which give rise to the spark lines are secondary processes, and we should not therefore expect to find evidence concerning their origin in absorption spectra. But in any event the spark lines are so weak compared with the diagram lines that existing data on X-ray absorption-coefficients are not sufficiently precise to detect such discontinuities as might occur.

2. It is shown that a straight line (Moseley graph) results when one plots the square root of the difference in frequency between a spark line and its "parent" line as a function of atomic number. This suggests the possibility that spark lines may originate in two-electron transfers.

3. In making precise measurements of X-ray absorption-coefficients, it is necessary to use slits sufficiently narrow to eliminate the "slit-width" error. The magnitude of this error is computed for one special case, and it is shown that with slit-widths as wide as some which have been used, errors as large as several per cent. may occur in the neighbourhood of 0.3 \AA .

Göttingen,
January 14, 1928.

VI. *Polarization of Infra-red Radiation by Calcite.* By
A. M. TAYLOR, M.A., Ph.D., Ramsay Memorial Research
Fellow*.

Introduction.

IN a recent communication⁽¹⁾ it was shown by examination between wave-lengths 8μ and 14μ that interference effects are to be observed in the absorption spectrum of a thin slice of calcite, and it was further suggested that a great many absorption bands which were found by Schaefer, Bormuth, and Matossi⁽²⁾ in their work on various carbonates, and which they attributed to "combination tones" formed from the several fundamental frequencies of vibration, were spurious and in reality owed their origin to

* Communicated by Dr. E. K. Rideal.

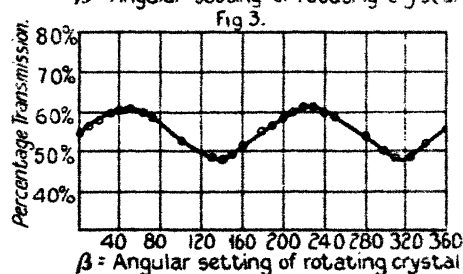
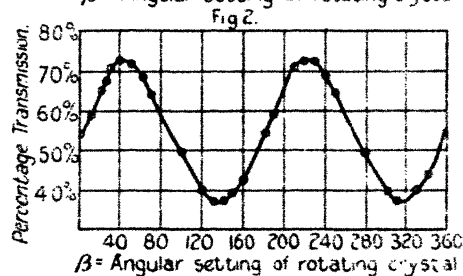
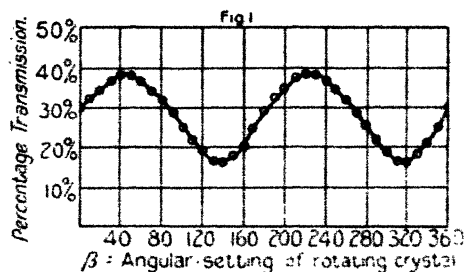
interference within the crystal film. That these bands are not, however, all due to such a cause is shown by the fact that, while the wave-lengths of successive maxima or minima when substituted in an interference formula $(1/\lambda_1 - 1/\lambda_2) = 1/2nz$, where z is the thickness of the crystal film, give a series of values for n , the refractive index of the material, which indicate the general course of the λ, n curve, the experimental points lie very raggedly about the mean, having divergencies considerably greater than would be expected solely from error in observation. This must imply that the bands found are due to the superposition of interference fringes upon a real variation in intensity caused by selective absorption at particular wave-lengths. It may be remarked that the greatest raggedness occurs about $\lambda = 11.3\mu$, where there is known to be an intense absorption band for waves having any component of their electric vector along the axis of the crystal, and it is reasonable to suppose that other gross divergencies from the mean line are similarly due to the presence of real absorption.

Accordingly some method was sought by which the true absorption could be differentiated from interference effects. The immediately obvious one of using thicker slices of the absorbing material, thereby causing the interference bands to become finer and less pronounced and the absorption bands to be intensified, did not appear practicable owing to the fact that general absorption usually masked the whole when thicker slices were employed, the more particularly because in the most debatable region from 8μ to 14μ the spectral energy is very weak. In the following pages is described a method, based on polarization of the infra-red radiation by the absorbing crystal itself, by which the desired analysis has been effected.

Method.

The three fundamental frequencies of vibration in carbonates, which are active in absorbing radiation⁽³⁾ (*i. e.* which involve a periodic variation of the electric moment of the CO_3 group), lie at wave-lengths of about 7μ , 11μ , and 14μ ⁽⁴⁾, and are polarized with the electric vector of the first and last perpendicular to, that of the other parallel to, the optic axis. If, therefore, a thin slice of crystal be cut parallel to the optic axis, radiation of wave-length approximating to any of these fundamentals will, on transmission normally to the slice, suffer partial absorption, and the transmitted beam will be more or less polarized with the electric vector at right angles to that of the particular

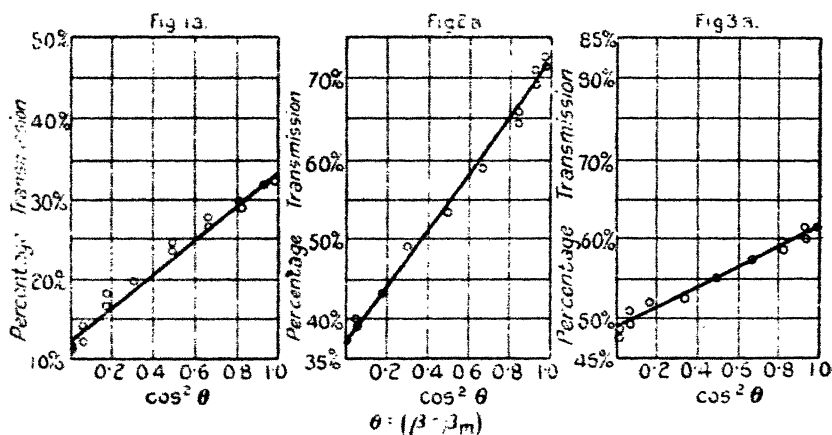
vibration concerned in the absorption. Clearly, if such radiation be now allowed to fall upon a second crystal similarly cut, the final intensity of the transmitted beam will depend upon the angle θ at which the optic axis of the second crystal is disposed relatively to that of the first, being a maximum when the axes are parallel and a minimum when they are perpendicular. In short, the two crystals will behave in the infra-red region at the appropriate wave-



lengths, just as two crystals of tourmaline do in the visible, the first acting as a polarizer, the second as an analyser.

To test this the author examined the behaviour of two pieces of calcite 0.1 mm. and 0.05 mm. thick respectively, which were cut parallel to the optic axis. Observed under crossed nicols in sodium light the orientation of the crystals appeared to be perfectly accurate, so far as could be judged by eye from the character of the interference brushes.

The crystals were mounted in brass holders, and one was arranged so as to rotate* with great precision some 1 mm. or so in front of the second crystal, of which the setting was fixed. Both crystals were then mounted in the sliding crystal holder of a spectrometric apparatus already described in previous papers⁽⁶⁾, and the ratio of the intensity I_t of the transmitted beam to I_0 , that of the incident beam, was measured for different values of θ , using only radiation of one particular wave-length. It should be mentioned that each crystal was provided with a circular stop to limit the width of the beam, and the stop of the fixed crystal was smaller than that of the rotating crystal, both stops, however, being carefully centred about the axis of rotation. This axis was normal to both crystal slices, and coincided with



the central ray of the cone of radiation passing through them. The slices were ground accurately plane-parallel, and therefore, with the above precautions, any observed variation with θ of the intensity of the transmitted beam must of necessity be ascribed to polarization effects.

The experimental values of the ratio I_t/I_0 for three different values of λ , each in the neighbourhood of an absorption band, are plotted in figs. 1 to 3, against β , the reading of the pointer on the divided circle bearing the rotating crystal. The angle β_m , at which I_t/I_0 becomes a maximum, is the same in each case, and I_t/I_0 goes through a complete cycle in 180° of arc. If I_t/I_0 be plotted against $\cos^2(\beta - \beta_m)$ a straight line is obtained (figs. 1 a to 3 a),

* For the loan of a suitably divided circle I am indebted to Dr. W. A. Wooster of the Mineralogical Department here.

indicating the character of the relation which exists between I_t and θ , where $\theta = (\beta - \beta_m)$. As will be shown, this relationship is demanded by theory, and is a proof that the effect is due to polarization of the radiation by the crystals, and, moreover, it will be seen that the effect may be used for obtaining a solution of the problem in hand.

Consider the passage of a beam of monochromatic radiation of incident intensity $2I_0$ through the crystals along the axis of rotation of the movable specimen. The beam is supposed to be unpolarized, and the direction of the electric vector is therefore a random one. There must then be an even distribution of the components of the electric vectors resolved parallel and perpendicular to the optic axis of the first crystal, so that the intensities of the radiation polarized in these two directions must be equal, and given by I_0 . The absorption and reflexion coefficients of the crystal for these two portions of the incident beam are not, however, the same; they may be written as α_1 and R_1 parallel to, and α_2 and R_2 perpendicular to, the optic axis. Treating each part separately, and taking into account only the first two terms of the series of multiply reflected beams which are produced, and which can reinforce or interfere with each other, the intensity I of each part after transmission is, following the method of a previous paper⁽¹⁾, given by an expression

$$I = I_1 + I_2 + 2 \cos \phi \sqrt{I_1 I_2},$$

where I_1 is the direct and I_2 the intensity of the twice reflected beam, and ϕ is the angle of the phase difference between them. As before⁽¹⁾

$$I_1 = I_0(1 - R)^2 e^{-\alpha z},$$

$$I_2 = I_0(1 - R)^2 R^2 e^{-3\alpha z},$$

where z is the thickness of the crystal slice, whence

$$I = I_0(1 - R)^2(e^{-\alpha z} + R^2 e^{-3\alpha z} + 2R \cos \phi e^{-2\alpha z}),$$

which, as R is dependent upon α and upon n the refractive index, which is itself an implicit function of α , may for brevity be written (ϕ also being a function of n),

$$I = I_0 \cdot F(\alpha_1, z) \text{ parallel to the optic axis,}$$

and

$$I = I_0 \cdot F(\alpha_2, z) \text{ perpendicular to the optic axis.}$$

Now consider these two portions of the transmitted beam, when incident upon the second crystal, of which the optic axis is inclined at an angle θ to that of the first. As there is a random distribution of phase between the two portions of the beam transmitted through the first crystal, the equivalent intensities of the components obtained by resolving the electric vectors parallel to and perpendicular to the optic axis of the second, may be expressed by squaring and adding the amplitudes resolved in the appropriate directions, so that

$$I = I_0 \cdot F(\alpha_1, z_1) \cos^2 \theta + I_0 \cdot F(\alpha_2, z_1) \sin^2 \theta$$

parallel to the optic axis,

and

$$I_y = I_0 \cdot F(\alpha_1, z_1) \sin^2 \theta + I_0 \cdot F(\alpha_2, z_1) \cos^2 \theta$$

perpendicular to the axis.

After transmission through the second crystal these parts have intensities given by $I_x \cdot F(\alpha_1, z_2)$ and $I_y \cdot F(\alpha_2, z_2)$ respectively, and since the random distribution of phase is still preserved the total intensity of the transmitted beam of radiation is given by

$$I_t = I_0 [\{ F(\alpha_1, z_1) \cdot F(\alpha_1, z_2) + F(\alpha_2, z_1) \cdot F(\alpha_2, z_2) \} \cos^2 \theta + \{ F(\alpha_2, z_1) \cdot F(\alpha_1, z_2) + F(\alpha_1, z_1) \cdot F(\alpha_2, z_2) \} \sin^2 \theta].$$

If $\alpha_1 = \alpha_2$ this reduces to

$$I_t = 2I_0 \cdot F(\alpha, z_1) \cdot F(\alpha, z_2),$$

so that the intensity is therefore independent of θ .

If, however, $\alpha_1 \neq \alpha_2$, this becomes, on making the substitution $\sin^2 \theta = 1 - \cos^2 \theta$,

$$I_t = 2I_0(A + B \cos^2 \theta),$$

where A and B are functions of the α 's and z 's. That is to say, the intensity varies as $\cos^2 \theta$, which is, in fact, the relation that was found experimentally (*cf.* figs. 1 a-3 a), and this is a definite proof that the effect observed is indeed due to partial polarization of the radiation on transmission through a plate of calcite cut parallel to the optic axis. Having verified this, the expression for I_t may be used to discover the presence of true absorption as distinct from decrease in intensity due to interference fringes. The importance of the expression is that it gives a value for I_t , which is independent of θ so long as $\alpha_1 = \alpha_2$, but if

this condition be not fulfilled, I_t passes through maximum and minimum values as θ varies from 0 to 2. The expression is cumbersome, and must be simplified by neglecting the terms due to multiply reflected beams. $F(\alpha, z)$ is then replaced by the approximation $e^{-\alpha z}$, and if the further simplification be made that the two crystals are of equal thickness, so that $z_1 = z_2$,

$$I_t = I_0 \{ (e^{-2\alpha_1 z} + e^{-2\alpha_2 z}) \cos^2 \theta + 2e^{-(\alpha_1 + \alpha_2)z} \sin^2 \theta \}.$$

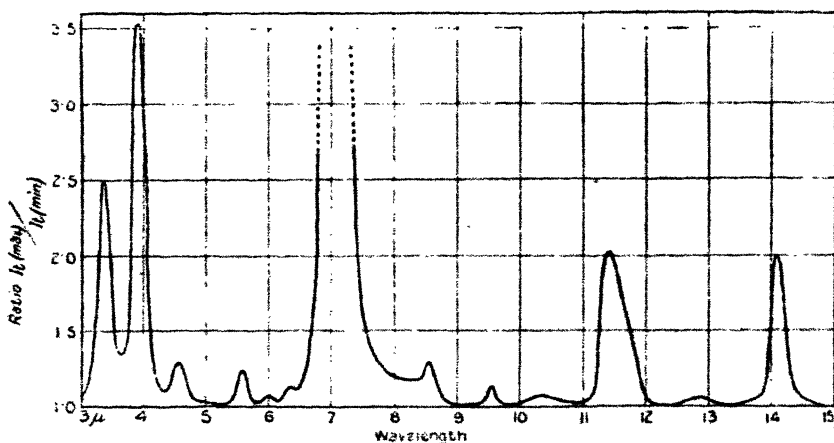
The maximum value of I_t occurs when $\theta = 0$, the minimum when $\theta = \pi/2$, so that

$$I_t(\text{max.})/I_t(\text{min.}) = (e^{-2\alpha_1 z} + e^{-2\alpha_2 z})/2e^{-(\alpha_1 + \alpha_2)z}$$

or

$$I_t(\text{max.})/I_t(\text{min.}) = \frac{1}{2} \{ e^{-(\alpha_1 - \alpha_2)z} + e^{(\alpha_1 - \alpha_2)z} \} . . .$$

Fig. 4.



This ratio is a maximum when $(\alpha_1 - \alpha_2)$ is either a maximum or a minimum, and is unity so long as $\alpha_1 = \alpha_2$. If experimental curves be constructed to show the variation of this ratio for different wave-lengths throughout the spectrum, they will indicate clearly the absorption bands by maxima of $I_t(\text{max.})/I_t(\text{min.})$, and by this means true absorption may be differentiated from the spurious variation in the intensity of the transmitted beam produced by interference within each crystal slice.

Using the two pieces of calcite already examined, such a curve was obtained experimentally, and it shows the three

fundamentals at 7μ , 11μ , and 14μ , together with some other bands (fig. 4). In order to try to amplify the effect at the less pronounced maxima, two thicker pieces of calcite 0.65 mm. thick were ground and polished* and the curve re-determined by their aid. At wave-lengths greater than 6μ this was not possible, however, as the opacity of the material became too great to allow of making accurate measurements of the transmitted intensity.

On comparison of fig. 4, with the results given by Schaefer, Bormuth, and Matossi⁽²⁾ for the bands found in the absorption spectrum of calcite, it will be seen that a number of lines which they attributed to combination tones, but which Taylor and Rideal⁽¹⁾ showed were really due to interference, are eliminated, and the number of bands which remain to be explained in terms of combination tones is much smaller than before. Previously, Schaefer assumed that the inactive frequency predicted from mathematical analysis⁽³⁾, *i. e.* the frequency of symmetrical expansion and contraction of the CO_2 group, which involves no alteration in electric moment, is, nevertheless, active when combined with other frequencies; in other words, though itself it is not connected with any variation of electric moment, merely referring to a mechanical vibration of frequency ν_0 , yet it develops an effective variation of electric moment of the same frequency when combined with other active vibrations. Schaefer states that without this assumption it is impossible to account for the whole of the observed spectrum. Even so, his observed and calculated wave-lengths do not agree to any very high order of accuracy, and, as the following table shows, equally good correspondence may be obtained without making use of the inactive frequency ν_0 . Only those frequencies are shown in this table which are verified by the method described (*cf.* fig. 4).

Table of Frequencies.

Nature of band.	Observed λ .	Observed $1/\lambda$.	Origin.	Calculated $1/\lambda$.
Fundamental	94μ	0.0106	ν'''	—
Fundamental	55μ	0.0182	ν''	—
Fundamental	30μ	0.0333	ν'	—

* For which I am indebted to the Department of Mineralogy in Cambridge.

Table of Frequencies (*continued*).

Nature of band.	Observed λ .	Observed $1/\lambda$.	Origin.	Calculated $1/\lambda$.
Fundamental	14.16 μ	0.0706	ν_1	—
	12.9 μ	0.077	$\nu_1 - \nu_2$	0.078
Fundamental	11.38 μ	0.088	ν_3	—
	10.4 μ	0.096	$\nu_3 + \nu'''$	0.098
	9.5 μ	0.105	$\nu_3 + \nu''$	0.106
	8.47 μ	0.118	$\nu_2 + \nu' + \nu''$	0.122
Fundamental	6.7 μ	0.143	ν_1	—
	7.0 μ	0.149		
	6.3 μ	0.159	$\nu_2 + \nu_3$	0.159
	6.0 μ	0.167	$\nu_1 + \nu''$	{ 0.161
				{ 0.167
	5.54 μ	0.181	$\nu_1 + \nu'$	{ 0.176
				{ 0.182
	{ 4.64 μ	0.216	$\nu_1 + \nu_2$	{ 0.213
	{ 4.50 μ	0.222		{ 0.220
	{ 3.93 μ	0.255	$2\nu_1 - \nu'$	{ 0.255
	{ 3.87 μ	0.259		{ 0.265
First Harmonic	{ 3.47 μ	0.289	$2\nu_1$	{ 0.286
	{ 3.35 μ	0.298		{ 0.298
	{ 3.10 μ	0.323	$2\nu_1 + \nu'$	{ 0.319
	{ 3.04 μ	0.329		{ 0.331
	{ 2.78 μ	0.360	$2\nu_1 + \nu_2$	{ 0.357
	{ 2.74 μ	0.365		{ 0.367
	{ 2.53 μ	0.395	$2\nu_1 + \nu_2 + \nu'$	{ 0.390
	{ 2.50 μ	0.400		{ 0.402
Second Harmonic	{ 2.33 μ	0.430	$3\nu_1$	{ 0.429
	{ 2.30 μ	0.435		{ 0.447

The criticisms which may be made of the table are sufficiently obvious, but it may be noted that a great many possible combinations would fall about the region 6 to 7 μ and are therefore not separately observable; but it may be that their presence contributes to the great depth and breadth of the absorption band at this point, which is exceptionally intense for a single "line," even though a fundamental lies within the limits of the band. One other point of interest is concerned with the band at 3.9 μ , which Schaefer explains as being due to the combination $\nu_1 + \nu_0$, and which should therefore have the same structure as $2\nu_1$ which falls at 3.4 μ . In the above table it is suggested that it is formed by $2\nu_1 - \nu'$, but it is also possible that $\nu_1 + \nu_2 + \nu'$ contributes to the production of the band. Such a superposition would

mask the sharpness of the doublet structure associated with ν_1 , and this is in agreement with observation, for throughout the series of carbonates the band at 3.9μ is unresolved, only the merest suggestion of a doublet being given by Schaefer's curves⁽²⁾, in contrast to that at 3.4μ , which is a very clearly defined doublet.

At the same time a very awkward detail is that of the relative intensities of the bands at 3.9μ and 3.1μ , that which in the above table is supposed to be due to $2\nu_1 - \nu'$ being very strong, whereas that due to $2\nu_1 + \nu'$ is comparatively weak. It is not claimed that the suggestions embodied in the above table are in any sense final, because it is impossible to expect exact numerical agreement between calculated and observed values, so long as a correction analogous to that found by Kratzer⁽⁶⁾ in the overtones of gaseous molecules is neglected, as has perforce been the case in this paper.

Summary.

The experiments have shown that infra-red rays are partially polarized by transmission through thin plates of calcite cut parallel to the optic axis, and such polarization effects have been used to determine which of the bands observed in the absorption spectrum of calcite really correspond to maxima of absorption, and which are merely spurious and due to interference effects. It is also suggested that the spectrum can be explained without assuming the inactive frequency to be active in combination.

The apparatus used was that described in previous papers⁽³⁾. My thanks are specially due to Dr. E. K. Rideal for his continued interest and encouragement.

The Laboratory of Physical Chemistry,
The University of Cambridge.
March 1928.

References.

- (1) Taylor & Rideal, *Phil. Mag.* iv. p. 682 (1927).
- (2) Schaefer, Bormuth, & Matossi, *Zeit. für Phys.* xxxix. p. 648 (1927).
- (3) Kornfeld, *Zeit. für Phys.* xxvi. p. 205 (1924).
- (4) Schaefer & Schubert, *Ann. der Phys.* l. p. 283 (1916).
- (5) Taylor & Rideal, *Proc. Roy. Soc. A*, cxv. p. 589 (1925); Rawlins, Taylor, & Rideal, *Zeit. für Phys.* xxxix. p. 660 (1926).
- (6) Kratzer, *Zeit. für Phys.* iii. p. 289 (1920).

VII. *A Method of Calculation suitable in certain Physical Problems.* By T. J. I'A. BROMWICH*.

IN certain physical problems, there are many examples of pairs of quantities (say x, y) which are connected by a relation of the type

$$y = Ax^n, \quad . \quad . \quad . \quad . \quad . \quad . \quad (1)$$

A and n being constants (independent of x, y).

Naturally one would usually reduce such a formula as (1) to the logarithmic form

$$\log y = \log A + n \log x \quad . \quad . \quad . \quad . \quad . \quad (2)$$

for the purposes of numerical work.

But, during 1918, I was placed in the position of having to make many calculations of this kind; and the conditions were such that x and y could not differ greatly from certain standard values x_0 and y_0 . After some experience in the actual work of the calculations, I convinced myself that a more accurate (as well as a more rapid) method was to calculate the value of the difference $(y - y_0)$ in terms of $(x - x_0)$.

Having recently learned that this transformation could be used with great advantage (in a totally different problem), it has seemed worth while to write out a short account of my method, with the hope that it may prove as useful to other calculators as it has been to myself.

Write, for brevity,

$$(x - x_0)/x_0 = t, \quad (y - y_0)/y_0 = v. \quad . \quad . \quad . \quad (3)$$

Then the equation (1) leads to

$$y/y_0 = (x/x_0)^n \quad . \quad . \quad . \quad . \quad . \quad (4)$$

$$\text{or} \quad 1 + v = (1 + t)^n. \quad . \quad . \quad . \quad . \quad (5)$$

Thus, using the binominal theorem, we have, from (5),

$$v = nt + \frac{1}{2}n(n-1)t^2 + \dots \quad . \quad . \quad . \quad (6)$$

For such problems as can be handled conveniently by this method, t is so small that t^3 may safely be neglected (and in many cases t^2 is also negligible).

* Communicated by the Author.

Thus we can write

$$v = nt\{1 + \frac{1}{2}(n-1)t\} \quad . \quad . \quad . \quad (7)$$

or

$$y - y_0 = k(x - x_0)\{1 - (x - x_0)/x_1\} \quad . \quad . \quad . \quad (8)$$

where we have written

$$k = ny_0/x_0, \quad x_1 = 2x_0/(1-n), \quad . \quad . \quad . \quad (9)$$

these values being independent of x, y .

To illustrate the actual working of the method, let us take an idealised example of the actual problem with which I was concerned in 1918: that is, the "adjustment" of cordite charges. Without giving exact values, the naval 15-inch guns (in 1914-1918) may be represented by taking y_0 to be a charge of 420 lb. and x_0 to be a velocity of 2400 f./s. For M.D. cordite the index n may be taken to be $-10/7$ (with four-figure accuracy).

Thus from (9) we find that

$$k = -\frac{1}{4} \frac{\text{lb.}}{\text{f./s.}}, \quad x_1 = 2000 \text{ f./s. (roughly)} \quad . \quad . \quad (10)$$

To complete the illustration, let us consider the adjustments necessary for differences of velocity $x - x_0 = \pm 50$ f./s.

Then (8) gives on substitution from (10)

$$x - x_0 = +50 \text{ f./s.}, \quad y - y_0 = -12.2 \text{ lb.}$$

$$\text{and} \quad x - x_0 = -50 \text{ f./s.}, \quad y - y_0 = +12.8 \text{ lb.}$$

That is, in the practical forms,

$$x = 2450 \text{ f./s.}, \quad y = 407 \text{ lb. 12 oz.}$$

$$x = 2350 \text{ f./s.}, \quad y = 432 \text{ lb. 12 oz.}^*$$

Again, if $x - x_0 = \pm 20$ f./s., the second-order terms are negligible and the adjustment is simply ∓ 5 lb.

* With large charges the results are only worked out to the nearest $\frac{1}{4}$ lb (=4 oz.). The meaning of the last line (for example) is that, if a charge of 420 lb. gives a velocity of 2350 f./s., then 432 lb. 12 oz. should give 2400 f./s. But so large a correction as 50 f./s. would not usually be made without further firing-proofs.

VIII. *Some Problems in Electrical Machine Design involving Elliptic Functions.* By R. T. COE, M.A., M.Sc.Tech., A.M.I.E.E., and H. W. TAYLOR, M.I.E.E.*

SUMMARY.

IN this paper the authors investigate four problems, three concerning the air-gap flux-distribution of a machine for various conditions of slotting and grooving on one side of the gap, and the other concerning the temperature distribution in the insulation between two conductors and the sides of a slot. The former have special reference to the subject of pole-face losses, and experimental results available for one of the cases considered are found to be in satisfactory agreement with the theoretical results obtained.

These four problems, which can all be treated as two-dimensional, are dealt with by the method of conformal transformation, and, by considering symmetrical figures, the results are obtained in the form of equations involving elliptic functions.

By a systematic treatment the authors show how numerical results may be calculated from such expressions without the difficulties usually associated with elliptic functions.

The results are collected together in the form of curves ready for immediate application to any particular problem.

SYNOPSIS.

I. Introduction.

II. The Variation of Flux-Density on a smooth Pole-face opposite a Succession of Open Slots.

(a) Analysis of Problem.

(b) Practical Deductions.

(i.) Maximum, Minimum, and Mean Flux-densities on smooth Pole-face.

(ii.) The Gap Coefficient K_g .

(iii.) Calculation of Flux-density Variation along smooth Pole-face.

* Communicated by Sir Richard T. Glazebrook, K.C.B., F.R.S.

III. The Flux-Distribution associated with a Slot of Finite Depth.

- (a) Analysis of Problem.
- (b) Practical Deductions.
 - (i.) Flux-Density at Centre of Slot Bottom.
 - (ii.) Effective Width of Slot.
 - (iii.) Gap Coefficient K_g for Repeated Slots.

IV. The Temperature indicated by an Embedded Temperature Detector placed between the two Layers of Conductors in a large Stator Winding.

V. The Flux-Distribution associated with a Grooved Pole-face.

- (a) Analysis of Problem.
- (b) Practical Deductions.
 - (i.) Flux Density on Grooved Surface.
 - (ii.) The Additional Gap Length equivalent to the Grooves.
 - (iii.) Gap Coefficient K_g for Air-gap of finite length.

I. INTRODUCTION.

The writing of this paper arose, in the first place, out of a consideration of the flux-distribution in the air-gap between a smooth pole-face and a succession of open slots. The mathematical analysis of this problem has already been given by F. W. Carter in a recent paper *, and he shows that the solution involves elliptic functions having two parameters which depend on the relative dimensions of the slot, tooth, and gap. He also indicates the difficulty that arises in choosing suitable values of these parameters to correspond to any given dimensions.

By a systematic treatment the authors of the present paper show how numerical results can be obtained. Values of two parameters which fix the relative dimensions of the slot, tooth, and gap are determined for a large number of particular cases, and hence the values of quantities required are calculated over the whole practical range.

In addition to the above problem, three other problems in electrical machine design are investigated by the methods developed.

* F. W. Carter, "The Magnetic Field of the Dynamo Electric Machine," *Journal I. E. E.* lxiv. p. 1117 (1926).

II. THE VARIATION OF FLUX-DENSITY ON A SMOOTH POLE-FACE OPPOSITE A SUCCESSION OF OPEN SLOTS.

(a) *Analysis of Problem.*

A knowledge of the manner in which the flux-density varies on a smooth pole-face opposite a succession of open slots is of interest in connexion with a study of pole-face losses. In some cases large fluctuations are possible in this flux-density, and the resulting eddy currents set up in the surface skin of the pole-face may cause considerable heating. A particular case in point is that of the solid pole-face of turbo-alternator rotors.

It will be shown later that for practical purposes the variation in pole-face flux-density can be taken as sinusoidal between a maximum value B_1 under the centre of a tooth and a minimum value B_2 under the centre of a slot. ~~the~~

To give some useful information as to the way in which the magnitude of this flux ripple depends on the ratio of slot opening to gap length, and also on the ratio of slot opening to tooth width, the authors have made calculations over a range of values of $\frac{s}{g}$ from 0 to 3 and $\frac{s}{t}$ from 0 to 5,

where g = gap length,

s = slot width,

and t = tooth width.

Most practical cases will be within the above range.

The problem can be considered as two-dimensional and is solved by the method of conformal transformation.

The most convenient transformation for the first part of the problem is that used by F. W. Carter, since by making suitable changes in the form of the resulting equations the calculations can be made almost entirely from existing tables of Elliptic Functions. Since this same transformation is modified for use in several other problems dealt with later in the present paper, it is developed briefly below in a form particularly suited for calculation purposes.

The method of conformal transformation as applied to the solution of such a problem in two dimensions may be regarded as a means of relating the field in a simplified figure representing the problem in a plane called the z plane to a portion of a uniform rectangular field in a plane called the χ plane.

If x and y are the coordinates of a point in the z plane, z is taken as the complex quantity $x+jy$, and if ϕ and ψ are the amounts of magnetic potential and flux associated with the given point, then χ is taken either as $\psi+j\phi$ or $\phi+j\psi$ according to whether the flux lines in the uniform field are to be vertical or horizontal.

The flux-density at any point is given by the differential coefficient $\frac{d\chi}{dz}$ at that point.

The transformation between z and χ is made through one or more intermediate variables ζ , ζ_1 , etc., each of which represents a flux-distribution in a plane. Points in the various planes are represented by the complex quantities $\zeta=\xi+j\eta$, $\zeta_1=\xi_1+j\eta_1$, etc.

Since the only figures considered have straight line boundaries, the Schwarz transformation theorem can be employed to obtain the relation between successive variables. The Schwarz transformation theorem gives the values of the differential coefficients $\frac{dz}{d\zeta}$, $\frac{d\zeta}{d\zeta_1}$, etc., while the constants of

integration that arise are evaluated from the various boundary conditions of the problem. It is generally best to express both z and χ in terms of ζ rather than consider the very complicated direct relation between them.

Since the process of integration is considerably simplified by considering a symmetrical figure in the z plane, the figure considered in the given problem is taken as the smallest repeating section of the air-gap field together with its image relative to the smooth pole-face, as indicated by OAB CDC₁B₁A₁ in fig. 1.

The point O is taken as the origin of the z plane and made to correspond to the origin of the ζ plane, while the pairs of points A and A₁, B and B₁, C and C₁, D and D₁ are made to correspond to the values of $\zeta = \pm 1, \pm \frac{1}{k}, \pm \frac{1}{k_1}$ and $\pm \infty$ respectively.

By the Schwarz theorem the transformation from the z plane to the ζ plane is given by

$$\frac{dz}{d\zeta} = A \frac{(1-k^2\zeta^2)^{\frac{1}{2}}}{(1-k_1^2\zeta^2)(1-\zeta^2)^{\frac{1}{2}}}, \quad \dots \dots (1)$$

whence

$$z = A \int_0^{\zeta} \frac{(1-k^2\zeta^2)^{\frac{1}{2}} d\zeta}{(1-k_1^2\zeta^2)(1-\zeta^2)^{\frac{1}{2}}} \dots \dots (2)$$

whence equating real and imaginary parts and substituting for A from equation (4),

$$\frac{g}{s} = \frac{K}{\pi} \left(\frac{\operatorname{sn} \alpha \operatorname{dn} \alpha}{\operatorname{cn} \alpha} - Z(\alpha) \right), \quad \dots \quad (5)$$

and

$$\frac{t}{s} = \frac{2K'}{\pi} \left(\frac{\operatorname{sn} \alpha \operatorname{dn} \alpha}{\operatorname{cn} \alpha} - Z(\alpha) \right) - \frac{\alpha}{K}. \quad \dots \quad (6)$$

The elliptic functions in the above expressions are all to modulus k .

Equations (5) and (6) determine the relation between $\frac{g}{s}$ and $\frac{t}{s}$ on the one hand and k and α or their equivalents on the other.

For the purpose of numerical calculation, it is preferable to deal with the modular angle θ and the amplitude angle ϕ of the first elliptic integral involved in the above equations. These are defined by the relations

$$k = \sin \theta$$

and

$$k_1 = k \operatorname{sn} \alpha = k \sin \phi,$$

so that equations (5) and (6) become

$$\frac{g}{s} = \frac{K}{\pi} (\tan \phi \cos \theta_1 - Z(\alpha)) \quad \dots \quad (7)$$

and

$$\frac{t}{s} = \frac{2K'}{\pi} (\tan \phi \cos \theta_1 - Z(\alpha)) - \frac{r^0}{90}, \quad \dots \quad (8)$$

where

$$\theta_1 = \arcsin k_1 = \arcsin (\sin \theta \sin \phi)$$

and

$$\frac{r^0}{90} = \frac{\alpha}{K} = \frac{F(\phi, \theta)}{K}.$$

The chief difficulty in using the above results lies in the fact that we usually wish to investigate a problem for which the values of $\frac{s}{g}$ and $\frac{s}{t}$ are specified, and this requires recourse to the method of cross plotting in order to determine corresponding values of θ and ϕ .

By the method outlined below, the authors have found the values of θ and ϕ as given in Table I. for a large number of cases in the range of $\frac{s}{g}$ from 0 to 3 and $\frac{s}{t}$ from 0 to 5.

Values $\frac{s}{g}$ and $\frac{s}{t}$ were calculated from equations (7) and (8) for a number of values θ and r° , the intermediate

TABLE I.

Values of θ and ϕ in degrees for Problem of Slots opposite smooth Pole-face.

$\frac{s}{g}$		0.5.	0.75.	1.0.	1.5.	2.0.	2.5.	3.0.
$\frac{s}{t}=0$	$\left\{ \begin{array}{l} \theta \dots\dots 0 \\ \phi \dots\dots 76.0 \end{array} \right.$	0	69.5	63.4	53.1	45.0	38.6	33.7
$\frac{s}{t}=0.25$	$\left\{ \begin{array}{l} \theta \dots\dots 33.2 \\ \phi \dots\dots 77.0 \end{array} \right.$	13.7	69.7	63.6	53.13	45.0	—	—
$\frac{s}{t}=0.5$	$\left\{ \begin{array}{l} \theta \dots\dots 65.1 \\ \phi \dots\dots 81.1 \end{array} \right.$	42.1	72.2	64.7	53.3	45.0	38.6	33.7
$\frac{s}{t}=0.75$	$\left\{ \begin{array}{l} \theta \dots\dots 77.3 \\ \phi \dots\dots 84.0 \end{array} \right.$	59.5	72.5	67.1	54.3	45.4	38.8	33.7
$\frac{s}{t}=1.0$	$\left\{ \begin{array}{l} \theta \dots\dots 82.7 \\ \phi \dots\dots 85.8 \end{array} \right.$	68.7	77.8	69.3	55.6	46.0	39.1	33.9
$\frac{s}{t}=1.25$	$\left\{ \begin{array}{l} \theta \dots\dots 85.0 \\ \phi \dots\dots 88.6 \end{array} \right.$	74.3	79.5	71.4	57.1	46.9	39.6	34.1
$\frac{s}{t}=1.5$	$\left\{ \begin{array}{l} \theta \dots\dots 86.2 \\ \phi \dots\dots 87.3 \end{array} \right.$	77.8	81.0	72.9	58.6	47.9	40.1	34.7
$\frac{s}{t}=2.0$	$\left\{ \begin{array}{l} \theta \dots\dots 87.9 \\ \phi \dots\dots 88.1 \end{array} \right.$	81.9	83.0	75.3	60.9	49.7	41.4	35.5
$\frac{s}{t}=3.0$	$\left\{ \begin{array}{l} \theta \dots\dots — \\ \phi \dots\dots — \end{array} \right.$	85.4	84.8	78.1	64.5	52.7	44.0	37.5
$\frac{s}{t}=5.0$	$\left\{ \begin{array}{l} \theta \dots\dots — \\ \phi \dots\dots — \end{array} \right.$	87.5	86.1	80.7	68.2	56.7	47.6	40.6

quantities ϕ and $Z(\alpha)$, being obtained directly by reference to the "Smithsonian" Tables of Elliptic Functions*.

Curves were drawn giving θ , ϕ , and $\frac{s}{g}$ plotted against $\frac{s}{t}$ for a number of values of r° and from values obtained from

* "Smithsonian" Mathematical Formulæ and Tables of Elliptic Functions. Smithsonian Publication 2672.

these curves further curves were drawn giving θ and ϕ against $\frac{s}{g}$ for a number of values of $\frac{s}{t}$.

Having determined the relation between the z and ζ planes we now turn to that between the ζ plane and χ plane, the latter representing a uniform field.

Since both the potential difference and amount of flux associated with the problem figure are finite, the upper half of the ζ plane is transformed into a finite portion of the uniform χ plane as indicated in fig. 1.

To preserve similarity between the figures in the various planes, the flux lines in the χ plane are made horizontal so that

$$\chi = \phi + j\psi.$$

The transformation from the ζ to the χ plane is given by

$$\frac{d\chi}{d\zeta} = \frac{B}{(1-\zeta^2)^{\frac{1}{2}}(1-k_1^2\zeta^2)^{\frac{1}{2}}}. \quad \dots \quad (9)$$

Making the origins of the two planes correspond

$$\chi = B \int_0^{\zeta} \frac{d\zeta}{(1-\zeta^2)^{\frac{1}{2}}(1-k_1^2\zeta^2)^{\frac{1}{2}}} = BF(\zeta, k_1). \quad \dots \quad (10)$$

Using the fact that when $\zeta=1$, $\chi=\phi_0$ the potential difference across the gap, we obtain

$$B = \frac{\phi_0}{K_1}. \quad \dots \quad (11)$$

From equations (1), (4), (9), and (11) the flux-density at any point is given by

$$\begin{aligned} \frac{d\chi}{dz} &= \frac{d\chi}{d\zeta} \cdot \frac{d\zeta}{dz} = \frac{\phi_0 \pi}{K_1 g} \frac{\operatorname{cn} \alpha}{\operatorname{sn} \alpha \operatorname{dn} \alpha} \frac{(1-k^2 \operatorname{sn}^2 \alpha \cdot \zeta^2)^{\frac{1}{2}}}{(1-k^2 \zeta^2)^{\frac{1}{2}}} \\ &= \frac{\phi_0}{g} \times \frac{K}{K_1} \left(1 - \frac{\operatorname{cn} \alpha Z(\alpha)}{\operatorname{sn} \alpha \operatorname{dn} \alpha} \right) \frac{(1-k^2 \operatorname{sn}^2 \alpha \cdot \zeta^2)^{\frac{1}{2}}}{(1-k^2 \zeta^2)^{\frac{1}{2}}}, \quad \dots \quad (12) \end{aligned}$$

where $\frac{\phi_0}{g}$ is the flux-density that would exist in a uniform gap of the given length and with the given potential difference across it.

In the form best suited for calculation

$$\frac{d\chi}{dz} = \frac{\phi_0}{g} \times \frac{K}{K_1} \left(1 - \frac{Z(\alpha)}{\tan \phi \cos \theta_1} \right) \frac{(1-\sin^2 \theta_1 \cdot \zeta^2)^{\frac{1}{2}}}{(1-\sin^2 \theta \cdot \zeta^2)^{\frac{1}{2}}}. \quad (13)$$

(b) *Practical Deductions.*(i.) *Maximum, Minimum, and Mean Flux-densities on smooth Pole-face.*

The maximum flux-density B_1 on the smooth pole-face occurs opposite the middle of a tooth where $\zeta=0$. From equation (13)

$$B_1 = \frac{\phi_0}{g} \times \frac{K}{K_1} \left(1 - \frac{Z(\alpha)}{\tan \phi \cos \theta_1} \right). \quad (14)$$

The minimum flux-density, B_2 , occurs opposite the middle of a slot where $\zeta=1$ and is given by

$$\left. \begin{aligned} B_2 &= \frac{\phi_0}{g} \times \frac{K}{K_1} \left(1 - \frac{Z(\alpha)}{\tan \phi \cos \theta_1} \right) \sin \phi \\ &= B_1 \sin \phi \end{aligned} \right\} \dots (15)$$

From equations (10) and (11) the increase in χ as ζ increases from 1 to $\frac{1}{k_1}$ is $j \frac{\phi_0 K_1'}{K_1}$. This gives the flux per half-tooth pitch, so that

$$\text{Mean flux-density } B_m = \frac{\phi_0 \frac{K_1'}{K_1}}{\frac{s+t}{2}} = \frac{\phi_0}{g} \times \frac{\frac{2g}{s+t} K_1'}{1 + \frac{t}{s}}. \quad (16)$$

The values of B_1 , B_2 , and B_m are given in Table II., these having been calculated at the same time as the values of θ and ϕ for Table I. The variation of maximum and minimum flux-densities with $\frac{s}{g}$ are shown in fig. 2 for the three cases where $\frac{s}{t} = 0, 1.0$, and 2.0 respectively. For the sake of completeness, values have been included in Table II. for the limiting case where $\frac{s}{t} = \infty$, i. e., where the tooth has zero width. In this case

$$B_1 = \frac{\phi_0}{g} \times \frac{\frac{g\pi}{s}}{K_1 \tanh \frac{g\pi}{s}},$$

$$B_2 = \frac{\phi_0}{g} \times \frac{\frac{g\pi}{s}}{K_1},$$

TABLE II.

Values of maximum flux-density B_1 , minimum flux-density B_2 , and mean flux-density B_m , on smooth pole-face as percentages of flux-density in uniform gap.

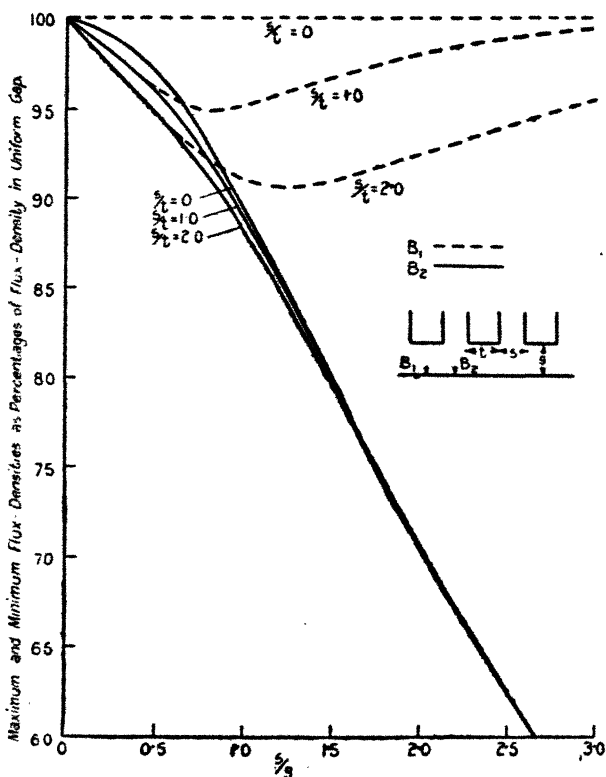
$\frac{s}{g}$		0.25.	0.5.	0.75.	1.0.	1.5.	2.0.	2.5.	3.0.
$\frac{s}{t}=0$	B_1	100.0	100.0	100.0	100.0	100.0	100.0	100.0	100.0
	B_2	99.2	97.0	93.7	89.5	80.0	70.7	62.5	55.5
	B_m	100.0	100.0	100.0	100.0	100.0	100.0	100.0	100.0
$\frac{s}{t}=0.25$	B_1	99.2	99.5	99.7	99.9	100.0	100.0	100.0	100.0
	B_2	99.1	97.0	93.5	89.5	80.0	70.7	62.5	55.5
	B_m	99.2	98.4	97.7	97.0	95.6	94.4	93.4	92.5
$\frac{s}{t}=0.5$	B_1	98.8	98.1	98.1	98.9	99.5	99.9	100.0	100.0
	B_2	"	96.8	93.4	89.4	80.0	70.7	62.5	55.5
	B_m	"	97.6	96.1	94.9	92.6	90.6	89.0	87.8
$\frac{s}{t}=0.75$	B_1	98.4	97.0	96.4	97.1	98.5	99.2	99.7	99.9
	B_2	"	96.5	93.2	89.3	80.0	70.7	62.5	55.5
	B_m	"	96.8	95.1	93.5	90.5	87.9	85.7	83.9
$\frac{s}{t}=1.0$	B_1	98.1	96.3	95.0	95.3	96.8	98.3	99.1	99.7
	B_2	"	96.0	93.0	89.2	79.8	70.7	62.5	55.5
	B_m	"	96.2	94.3	92.3	89.1	86.0	83.3	81.4
$\frac{s}{t}=1.25$	B_1	97.8	95.7	94.2	93.9	95.2	96.6	98.0	98.9
	B_2	"	95.5	92.7	89.1	79.8	70.6	62.5	55.5
	B_m	"	95.6	93.4	91.4	87.7	84.5	81.5	79.1
$\frac{s}{t}=1.5$	B_1	97.5	95.1	93.5	92.6	93.6	95.2	96.9	98.1
	B_2	"	"	92.4	88.7	79.8	70.6	62.5	55.5
	B_m	"	"	92.7	90.4	86.5	83.1	80.0	77.3
$\frac{s}{t}=2.0$	B_1	97.2	94.5	92.5	91.1	91.1	92.7	94.3	95.7
	B_2	"	"	91.7	88.4	79.7	70.5	62.5	55.5
	B_m	"	"	91.9	89.5	85.1	81.2	77.8	74.7
$\frac{s}{t}=3.0$	B_1	96.8	93.8	91.2	89.1	87.7	88.4	89.9	91.2
	B_2	"	"	90.7	87.2	79.0	70.2	62.4	55.5
	B_m	"	"	90.9	88.2	83.3	78.9	75.0	71.8
$\frac{s}{t}=5.0$	B_1	96.4	93.0	89.7	87.1	84.2	83.5	84.1	85.4
	B_2	"	"	89.5	85.7	77.5	69.6	62.1	55.4
	B_m	"	"	89.6	86.5	81.1	76.3	72.3	69.2
$\frac{s}{t}=\infty$	B_1	94.7	89.9	85.8	82.0	76.3	72.5	70.0	69.1
	B_2	"	"	"	81.7	74.0	66.5	59.6	53.9
	B_m	"	"	"	81.9	75.2	69.3	64.5	60.8

$$B_m = \frac{\phi_0}{g} \times \frac{2g}{s} \frac{K_1'}{K_1},$$

where K_1 is the complete first elliptic integral to modulus

$$k_1 = \sin \alpha = \tanh \frac{\sigma \pi}{s}.$$

Fig. 2.



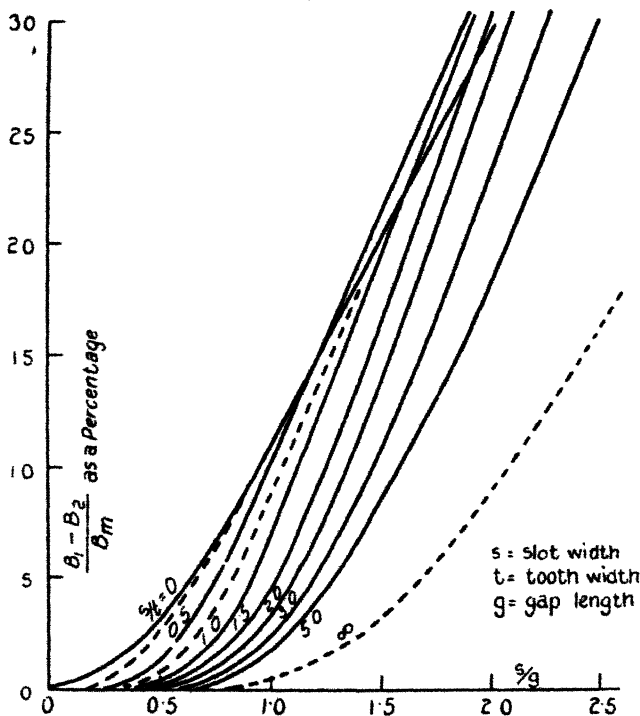
Curves giving maximum and minimum flux-densities on smooth pole-face opposite a succession of open slots.

In practice it is the mean flux-density in the air-gap that is known, and so it is desirable to give the total variation of flux-density on the smooth pole-face due to the opposing slots as a factor or percentage of the mean flux-density. The curves of fig. 3 have therefore been calculated from

Table II. and show the way in which $\frac{B_1 - B_2}{B_m}$ expressed as a percentage varies with the ratio $\frac{s}{g}$ for a number of values of $\frac{s}{t}$.

Assuming the flux variation to be sinusoidal, the pole-face eddy-current loss will be proportional to the square of the total variation between the maximum and minimum values.

Fig. 3.

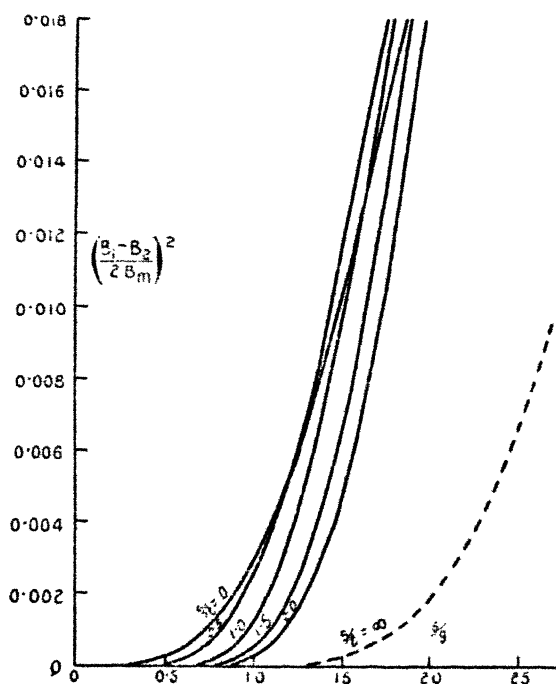


Curves giving total variation of flux-density on smooth pole-face as percentage of mean flux-density.

The curves of fig. 4 show the way in which the pole-face eddy-current loss varies with the ratio $\frac{s}{g}$ for various values of $\frac{s}{t}$, the mean gap flux-density, the slot pitch, and the relative velocity between the slots and pole-face being assumed to be constant. It is seen that for any given value of $\frac{s}{t}$ the pole-face loss is negligible up to a certain value of

$\frac{s}{g}$ and then increases very rapidly. Thus, for instance, if the ratio $\frac{s}{g}$ is increased from 0.8 to 1.2 by shortening the air-gap of a machine the eddy-current pole-face loss will be increased by an average of eight times for values of $\frac{s}{t}$ between 0.5 and 1.0. It is therefore important to keep down the value of the ratio $\frac{s}{g}$ if a small pole-face loss is required.

Fig. 4.

Curves showing variation of pole-face eddy-current loss with $\frac{s}{g}$.

There is usually a limit to the extent by which the ratio $\frac{s}{g}$ can be reduced either by decreasing the slot width or by increasing the length of the gap, and so a knowledge of the critical value of $\frac{s}{g}$ shown by the above results is of some importance to electrical machine designers.

Experimental confirmation of the above theoretical results for a particular ratio of slot to tooth width is obtained from tests carried out by T. F. Wall and S. P. Smith * with the particular object of investigating pole-face losses due to armature teeth. The particular machine on which tests were made had open slots, the ratio of slot width to tooth width being 0.72. The pole-face loss was measured with the machine on no load for various lengths of air-gap, the mean gap flux-density being maintained at the same value in each case. From results obtained over a range of values of $\frac{s}{g}$ from 1.2 to 4.8 it was deduced that the losses were proportional to $\left(\frac{s}{g}\right)^{3.5}$.

This result may be compared with that for the theoretical case considered where $\frac{s}{t} = 0.75$. The amplitude of the flux ripple, as given by the appropriate curve of fig. 3, is found to be proportional to $\left(\frac{s}{g}\right)^{1.66}$ over the range of $\frac{s}{g}$ from 1.2 to 3. The eddy-current pole-face loss, which is proportional to the square of this variation in flux-density, is, therefore, proportional to $\left(\frac{s}{g}\right)^{3.3}$. The hysteresis loss will only be a small fraction of the eddy-current loss, and so the agreement must be regarded as very satisfactory.

In an actual machine there is considerable difficulty in the way of separating the pole-face loss from the other losses. General experience, however, supports the above conclusions that, beyond a certain value of $\frac{s}{g}$, the pole-face losses may become excessive.

(ii.) *The Gap Coefficient K_g .*

By the gap coefficient is meant the ratio of the length of the equivalent unslotted gap to the length of the actual gap, the equivalent gap being such that for a flux-density equal to the mean flux-density in the actual gap the same potential difference is required across it.

* T. F. Wall & S. P. Smith, "Experimental Determination of the Losses in Pole Shoes due to Armature Teeth," *Journal I. E. E.* xl. p. 577 (1908).

If g' is the length of the equivalent unslotted gap

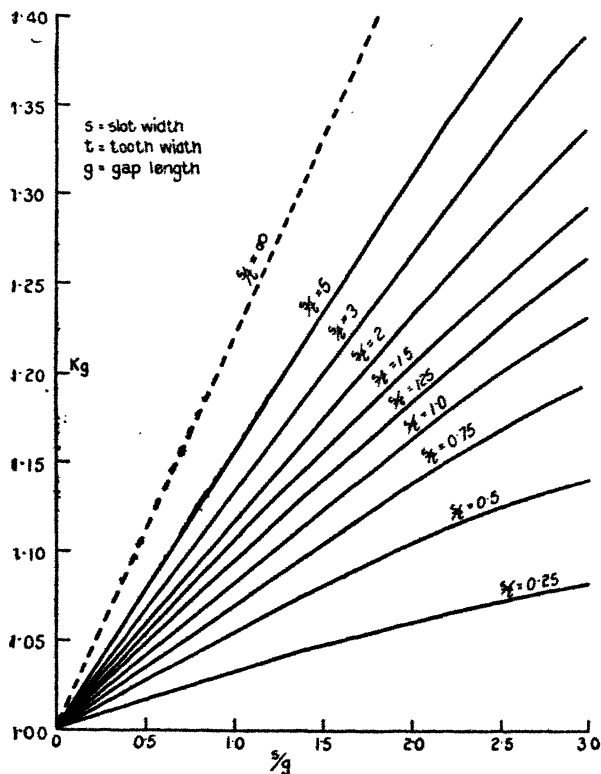
$$\phi_0 = B_m g',$$

therefore

$$K_g = \frac{g'}{g} = \frac{\phi_0}{g} \times \frac{1}{B_m} \dots \dots \dots (17)$$

Curves calculated from the above expression are shown in fig. 5.

Fig. 5.



Curves giving the gap coefficient K_g for an air-gap uniformly slotted on one side.

An approximate method of calculating the gap coefficient for the case considered was first worked out by F. W. Carter* on the assumption that the effective width of each slot was the same as that of a single slot with the gap extending to infinity on either side.

* F. W. Carter, "Air-Gap Induction," 'Electrical World and Engineer,' xxxviii. p. 884 (1901).

The formula given reduces to

$$K_s = \frac{1 + \frac{t}{s}}{1 + \frac{t}{s} - \frac{2}{\pi} \left\{ \arctan \frac{s}{2g} - \frac{g}{s} \log \left(1 + \frac{s^2}{4g^2} \right) \right\}} \quad (18)$$

Comparing values given by this formula with those calculated from equation (17) for the more exact case, the agreement is found to be surprisingly good, the error being less than 0.5 per cent. (negative), for values of $\frac{s}{t}$ less than 3, and $\frac{s}{g}$ less than 2.5. The error increases somewhat for larger values of $\frac{s}{t}$ and $\frac{s}{g}$, but the approximation is sufficiently good for practical calculations involving the total air-gap flux.

It must not be concluded from the above that the influence of a slot does not extend beyond the middle of the adjacent teeth, for, as Table II. clearly shows, for most practical cases the flux-density on the smooth pole-face opposite the middle of a tooth has by no means reached the limiting value for the uniform field. The method used in this paper has therefore been essential for the complete study of the flux-density variation on the smooth pole-face.

(iii.) *Calculation of Flux-density Variation along smooth Pole-face.*

Although, as already shown, the values of the maximum and minimum flux-densities on the smooth pole-face can readily be determined, the calculation of the flux-density at intermediate points is much more involved, as it requires a knowledge of the relation between z and ζ in the range where ζ has purely imaginary values between 0 and $j\infty$.

From equations (3) and (4),

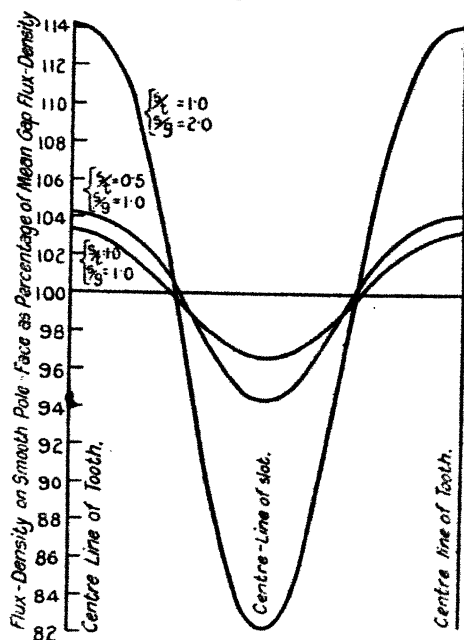
$$z = \frac{s}{\pi} \left\{ \frac{\operatorname{sn} \alpha \operatorname{dn} \alpha}{\operatorname{cn} \alpha} p - \Pi(p, \alpha, k) \right\} \quad (19)$$

Along the smooth pole-face,

$$\left. \begin{aligned} p &= F(j\eta, k), \\ &= jF\left(\frac{\eta}{(1+\eta^2)^{\frac{1}{2}}}, k'\right), \\ &= j\beta \text{ say, where } \beta \text{ is a quantity} \\ &\quad \text{lying between 0 and } K' \end{aligned} \right\}; \quad (20)$$

$$z = \frac{s}{\pi} \left\{ j\beta \frac{\operatorname{sn} \alpha \operatorname{dn} \alpha}{\operatorname{cn} \alpha} - \Pi(j\beta, \alpha, k) \right\} \\ = \frac{s}{\pi} \left\{ j\beta \left(\frac{\operatorname{sn} \alpha \operatorname{dn} \alpha}{\operatorname{cn} \alpha} - Z(\alpha) \right) + \frac{1}{2} \log \frac{\Theta(\alpha + j\beta)}{\Theta(\alpha - j\beta)} \right\} \quad (21)$$

[Fig. 6.]



Curves showing variation of flux-density on smooth pole-face opposite uniformly slotted pole-face.

Jacobi's Θ function, which occurs in the above expression, is defined for modulus k by the series

$$\Theta(t) = 1 - 2q \cos \frac{\pi t}{K} + 2q^4 \cos \frac{2\pi t}{K} - 2q^9 \cos \frac{3\pi t}{K} + \dots \quad (22)$$

in which $q = e^{-\frac{K'}{K}\pi}$.

Expanding the Θ functions of equation (21) in series form, and separating their real and imaginary parts, and also using the relation from equation (6) that

$$\frac{\operatorname{sn} \alpha \operatorname{dn} \alpha}{\operatorname{cn} \alpha} - Z(\alpha) = \frac{\pi}{2K'} \left(\frac{t}{s} + \frac{\alpha}{K} \right),$$

the expression for z in a form convenient for calculation reduces to

$$z = j \frac{s}{2} \left\{ \left(\frac{t}{s} + \frac{r^0}{90} \right) \frac{\beta}{K'} + \frac{\mu^0}{90} \right\}, \quad (23)$$

where

$$\frac{r^0}{90} = \frac{\alpha}{K},$$

and

$$\mu^0 = \arctan \frac{2q \sinh \frac{\pi\beta}{K} \sin 2r^0 - 2q^4 \sinh \frac{2\pi\beta}{K} \sin 4r^0 + \dots}{1 - 2q \cosh \frac{\pi\beta}{K} \cos 2r^0 + 2q^4 \cosh \frac{2\pi\beta}{K} \cos 4r^0 + \dots}$$

expressed in degrees.

In the above expression for μ^0 the quantities q , K , and r^0 depend on the dimensions of the problem and so are fixed for any particular case. Thus β is the only quantity in the expression for z which varies as one moves along the smooth pole-face, and so it is best to make the numerical calculations by taking a number of values of $\frac{\beta}{K}$ between 0 and 1.

The flux-density is obtained by putting $\zeta = j\eta$ in equation (13), giving

$$\frac{d\chi}{dz} = \frac{\phi_0}{g} \times \frac{K}{K'} \left(1 - \frac{Z(\alpha)}{\tan \phi \cos \theta_1} \right) \frac{(1 + \sin^2 \theta_1 \cdot \eta^2)^{\frac{1}{2}}}{(1 + \sin^2 \theta \cdot \eta^2)^{\frac{1}{2}}}, \quad (24)$$

where as before

$$\sin \theta = k,$$

$$\sin \phi = \operatorname{sn} \alpha,$$

and

$$\sin \theta_1 = \sin \theta \cdot \sin \phi.$$

For given dimensions of the slot, tooth, and gap, the only quantity that varies in the above expression for the flux-density on the pole-face is η , and this is related to β by the equation

$$\beta = F \left(\frac{\eta}{(1 + \eta^2)^{\frac{1}{2}}}, k' \right),$$

so that the value of η corresponding to any chosen value of $\frac{\beta}{K'}$ can be found by the use of tables of the first elliptic integral.

The variation of flux-density along the smooth pole-face has been calculated for three typical cases, as below.

Case 1. $\frac{s}{t} = 1.0$, $\frac{s}{g} = 1.0$.

Corresponding to $\theta = 54.9^\circ$ and $\phi = 69.3^\circ$ as given by Table I., the value of r° is 63.31° , so that equation (23) reduces to

$$z = j \frac{s}{2} \left(1.7035 \frac{\beta}{K'} + \frac{\mu^\circ}{90} \right),$$

where

$\mu^\circ = \arctan$

$$\frac{0.11042 \sinh 2.676 \frac{\beta}{K'} + 0.000429 \sinh 5.352 \frac{\beta}{K'}}{1.0 + 0.08204 \cosh 2.676 \frac{\beta}{K'} - 0.0000129 \cosh 5.352 \frac{\beta}{K'}}.$$

Equation (24) giving the flux-density reduces to

$$\frac{d\chi}{dz} = \frac{\phi_0}{g} \times 0.9533 \frac{(1 + 0.58572 \eta^2)^{\frac{1}{2}}}{(1 + 0.66936 \eta^2)^{\frac{1}{2}}}.$$

The wave-form of the flux-density variation over one slot pitch as calculated from the above expressions is shown in fig. 6. On analysis its equation as represented by the first five harmonics is given by

$$B = B_m + \frac{B_1 - B_2}{2} (1.012 \cos \theta - 0.012 \cos 2\theta - 0.002 \cos 3\theta + 0.004 \cos 4\theta - 0.002 \cos 5\theta),$$

the amplitudes of the harmonics being expressed as fractions of half the total variation between the maximum and minimum flux-densities. From the smoothness of the wave-form it is expected that all higher harmonics will be negligible.

Assuming the effective permeability of the surface skin of the pole-face to be the same for all the harmonics, the loss per unit area due to each harmonic is proportional to $\frac{A^2}{n^4}$ *, where A = amplitude and n = order of harmonic.

On this basis, the loss factor which gives the ratio of the actual loss to the loss calculated for a single sine wave of amplitude $\frac{B_1 - B_2}{2}$ is found to be 1.024.

* See F. W. Carter, "Pole-face Eddy-current Loss," *Journal I. E. E.* liv. p. 170. (1916).

Case 2. $\frac{s}{t} = 1.0$, $\frac{s}{g} = 2.0$.

From Table I., $\theta = 21.4^\circ$ and $\phi = 46.0^\circ$, giving $r^\circ = 44.98^\circ$,

$$z = j\frac{s}{2} \left(1.4998 \frac{\beta}{K'} + \frac{\mu^\circ}{90} \right),$$

where

$$\mu^\circ = \arctan \frac{0.01786 \sinh 4.719 \frac{\beta}{K'}}{1.0 - 0.0000104 \cosh 4.719 \frac{\beta}{K'}}$$

and

$$\frac{d\chi}{dz} = \frac{\phi_0}{g} \times 0.9827 \frac{(1 + 0.06889 \eta^2)^{\frac{1}{2}}}{(1 + 0.13314 \eta^2)^{\frac{1}{2}}}.$$

The flux-density is represented by the equation

$$B = B_m + \frac{B_1 - B_2}{2} (1.019 \cos \theta - 0.117 \cos 2\theta - 0.017 \cos 3\theta + 0.005 \cos 4\theta + 0.005 \cos 5\theta),$$

giving a loss factor of 1.049.

Case 3. $\frac{s}{t} = 0.5$, $\frac{s}{g} = 1.0$.

From Table I., $\theta = 26.9^\circ$ and $\phi = 64.7^\circ$, giving $r^\circ = 63.38^\circ$,

$$z = j\frac{s}{2} \left(2.7043 \frac{\beta}{K'} + \frac{\mu^\circ}{90} \right),$$

where

$$\mu^\circ = \arctan \frac{0.02294 \sinh 4.247 \frac{\beta}{K'}}{1.0 + 0.01714 \cosh 4.247 \frac{\beta}{K'}}$$

and

$$\frac{d\chi}{dz} = \frac{\phi_0}{g} \times 0.9889 \frac{(1 + 0.16732 \eta^2)^{\frac{1}{2}}}{(1 + 0.20470 \eta^2)^{\frac{1}{2}}}.$$

The flux-density is represented by the equation

$$B = B_m + \frac{B_1 - B_2}{2} (0.990 \cos \theta - 0.143 \cos 2\theta + 0.002 \cos 3\theta + 0.013 \cos 4\theta + 0.007 \cos 5\theta),$$

giving a loss factor of 0.995.

It will be apparent that the calculation of the exact wave-form of the flux-density variation on the smooth pole-face is too tedious to be performed except in special cases. The results obtained for the three cases worked out above

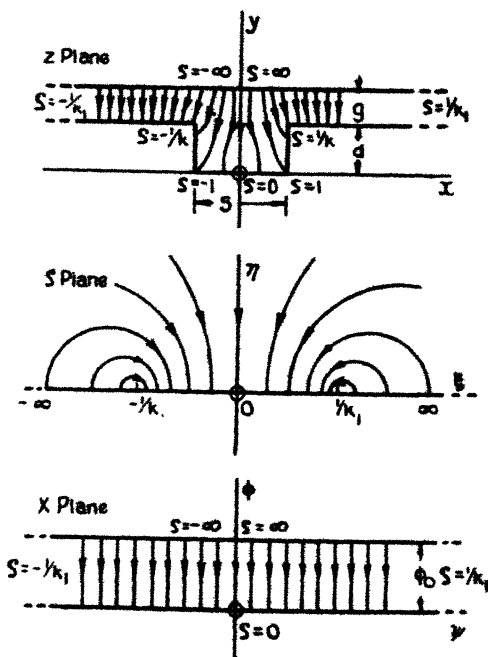
indicate that, as regards the eddy-current loss in the pole-face, sufficiently close approximation can be obtained by treating the variation of flux-density as sinusoidal between the limits indicated by the curves of fig. 3.

III. THE FLUX-DISTRIBUTION ASSOCIATED WITH A SLOT OF FINITE DEPTH.

(a) *Analysis of Problem.*

In cases where slots of comparatively small depth form part of the air-gap boundary, it is sometimes desirable to

Fig. 7.



The flux-distribution due to a slot of finite depth.

have means of estimating the effective slot width as affected by the finite depth.

Considering a single slot with the air-gap extending to infinity on either side as shown in fig. 7, the same transformation as in the previous problem can be employed between the z and ζ planes, so that it is fairly simple to

calculate results over a range of values of $\frac{d}{s}$ and $\frac{s}{g}$, where

d = depth of slot,

s = width of slot,

and

g = length of gap.

Taking $\frac{d}{s}$ and $\frac{s}{g}$ as variables and identifying d , s , and g with $\frac{t}{2}$, $2g$, and $\frac{s}{2}$ in the results for the previous problem as given by equations (1), (4), (5), and (6) the transformation from the z plane to the ζ plane is seen to be given by

$$\frac{dz}{d\zeta} = \frac{2g}{\pi} \frac{\operatorname{sn} \alpha \operatorname{dn} \alpha}{\operatorname{cn} \alpha} \frac{(1-k^2\zeta^2)^{\frac{1}{2}}}{(1-k^2 \operatorname{sn}^2 \alpha \cdot \zeta^2)(1-\zeta^2)^{\frac{1}{2}}}, \quad (25)$$

or

$$z = \frac{2g}{\pi} \left\{ \frac{\operatorname{sn} \alpha \operatorname{dn} \alpha}{\operatorname{cn} \alpha} p - \Pi(p, \alpha) \right\}, \quad (26)$$

where $p = F(\zeta \cdot k)$.

The parameters α and k are determined by the equations

$$\frac{s}{g} = \frac{4K}{\pi} \left(\frac{\operatorname{sn} \alpha \operatorname{dn} \alpha}{\operatorname{cn} \alpha} - Z(\alpha) \right), \quad (27)$$

and

$$\frac{d}{g} = \frac{2K'}{\pi} \left(\frac{\operatorname{sn} \alpha \operatorname{dn} \alpha}{\operatorname{cn} \alpha} - Z(\alpha) \right) - \frac{\alpha}{K}, \quad (28)$$

or in form best suited for calculation, the equivalent parameters θ and ϕ are determined by

$$\frac{s}{g} = \frac{4K}{\pi} (\tan \phi \cos \theta_1 - Z(\alpha)) \quad (29)$$

and

$$\frac{d}{g} = \frac{2K'}{\pi} (\tan \phi \cos \theta_1 - Z(\alpha)) - \frac{r^0}{90}, \quad (30)$$

where

$$\sin \theta = k, \quad \sin \phi = \operatorname{sn} \alpha, \quad \sin \theta_1 = k \operatorname{sn} \alpha,$$

and

$$\frac{r^0}{90} = \frac{\alpha}{K} = \frac{F(\phi, \theta)}{K}.$$

In Table III. are given the associated values of θ and ϕ required for a number of particular cases for $\frac{d}{s}$ between 0 and 2.0 and $\frac{s}{g}$ between 0 and 5.

The Schwarz transformation between the ζ and χ planes is given by

$$\frac{d\chi}{d\zeta} = \frac{B}{1 - k^2 \operatorname{sn}^2 \alpha \cdot \zeta^2}, \quad \dots \quad (31)$$

TABLE III.

Values of θ and ϕ in Degrees for Problem of Single Slot of Finite Depth.

$\frac{s}{g}$		0.25	0.5	1.0	2.0	3.0	5.0
$\frac{d}{s} = 0.1$	θ	58.4	59.1	61.5	67.4	72.9	80.5
	ϕ	9.2	18.0	33.9	56.7	69.8	81.4
$\frac{d}{s} = 0.2$	θ	43.6	44.1	46.1	51.7	57.7	65.8
	ϕ	8.2	16.1	30.5	51.4	63.8	75.9
$\frac{d}{s} = 0.3$	θ	32.2	32.7	34.4	39.2	44.1	51.3
	ϕ	7.8	15.2	28.7	48.5	60.3	72.5
$\frac{d}{s} = 0.4$	θ	23.8	24.1	25.5	29.3	32.7	38.1
	ϕ	7.5	14.7	27.7	47.0	58.7	70.5
$\frac{d}{s} = 0.5$	θ	17.5	17.7	18.7	21.5	24.4	28.9
	ϕ	7.25	14.4	27.2	46.0	57.2	69.5
$\frac{d}{s} = 0.75$	θ	8.01	8.13	8.58	9.88	11.23	13.87
	ϕ	7.15	14.13	26.70	45.22	56.58	68.48
$\frac{d}{s} = 1.0$	θ	3.67	3.70	3.92	4.52	5.13	6.13
	ϕ	7.12	14.07	26.60	45.07	56.37	68.20
$\frac{d}{s} = 2.0$	θ	0.16	0.16	0.17	0.20	0.22	0.27
	ϕ	7.12	14.05	26.57	45.0	56.32	68.20

whence, on making the origins of the two planes correspond

$$\begin{aligned} \chi &= B \int_0^\zeta \frac{d\zeta}{1 - k^2 \operatorname{sn}^2 \alpha \cdot \zeta^2} \\ &= \frac{B}{k \operatorname{sn} \alpha} \operatorname{arc} \tanh (k \operatorname{sn} \alpha \cdot \zeta) \quad \dots \quad (32) \end{aligned}$$

By considering the point $\zeta = \frac{1}{k \operatorname{sn} \alpha}$ where χ takes on a sudden increment $j\phi_0$ where ϕ_0 is the potential difference between the two sides of the gap, we obtain

$$B = \frac{2\phi_0 k \operatorname{sn} \alpha}{\pi}, \quad \dots \quad (33)$$

so that in calculation form

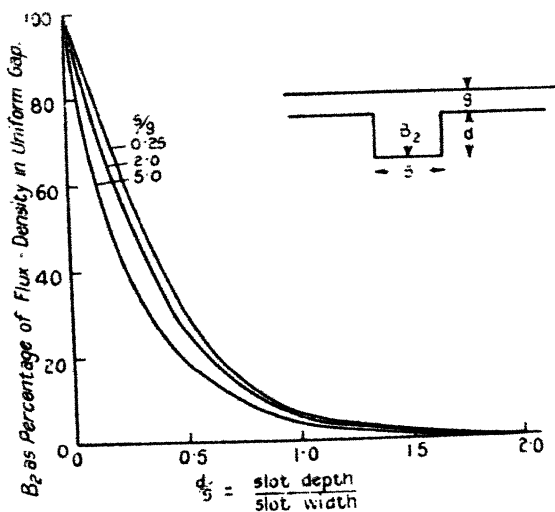
$$\chi = \frac{2\phi_0}{\pi} \operatorname{arc} \tanh (\sin \theta_1 \cdot \zeta). \quad \dots (34)$$

The flux-density at any point is given by

$$\frac{d\chi}{dz} = \frac{d\chi}{d\zeta} \cdot \frac{d\zeta}{dz} = \frac{\phi_0}{g} \times \frac{\sin \theta \cos \phi}{\cos \theta_1} \frac{(1-\zeta^2)^{\frac{1}{2}}}{(1-\sin^2 \theta \cdot \zeta^2)^{\frac{1}{2}}}, \quad (35)$$

$\frac{\phi_0}{g}$ being the flux-density in the given gap where it has become uniform.

Fig. 8.



Curves giving flux-density of centre of slot bottom.

(b) *Practical Deductions.*

(i.) *Flux-Density at Centre of Slot Bottom.*

This is obtained by putting $\zeta = 0$ in equation (35) giving

$$B_2 = \frac{\phi_0}{g} \times \frac{\sin \theta \cos \phi}{\cos \theta_1} \quad \dots (36)$$

The variation of the flux-density at the middle of the slot bottom with the ratio $\frac{d}{s}$ is shown in fig. 8 for a number of values of $\frac{s}{g}$.

From the curves it is seen that the flux-density at the bottom of the slot depends chiefly on the ratio $\frac{d}{s}$ and becomes almost negligible (less than 1 per cent.) when the depth of the slot exceeds 1.6 times its width. Slots deeper than this can obviously be considered as of infinite depth as far as concerns their effect on the magnetic field of the air-gap.

(ii.) *Effective Width of Slot.*

By the effective width of the slot is meant a width that can be used for calculation purposes on the basis that the flux in the air-gap is uniform on either side of the effective slot but is zero across it. The effective width slot is obviously less than the actual width slot by an amount which allows for the reduced density across the actual slot and the fringing at the corners.

Considering any point on the slotted side of the air-gap but outside the slot, the "lost flux" on the side due to the presence of the slot is given by the real part of $\left(\frac{\phi_0}{g}z - \chi\right)$ where z and χ correspond to the point considered. Although the value of this expression becomes constant as the flux-density in the gap becomes uniform, it is best calculated as the mathematical limit corresponding to the point of the gap which is at an infinite distance from the slot. Thus the lost flux for the whole slot is given by the real part of

$$2 \lim_{\zeta \rightarrow \frac{1}{k \sin \alpha}} \left(\frac{\phi_0}{g} z - \chi \right).$$

Let

$$\zeta = \frac{1}{k \sin(\alpha + t)},$$

so that

$$t \rightarrow 0 \quad \text{as} \quad \zeta \rightarrow \frac{1}{k \sin \alpha}.$$

Then

$$p = F(\zeta, k) = \alpha + t + jK',$$

and substituting this value in equation (26)

$$\begin{aligned} z &= \frac{2g}{\pi} \left\{ \frac{\sin \alpha \operatorname{dn} \alpha}{\operatorname{cn} \alpha} (\alpha + t + jK') - \Pi(\alpha + t + jK', \alpha) \right\} \\ &= \frac{g}{\pi} \left\{ \frac{\pi}{2gK} (\alpha + t + jK') + \log \frac{\Theta(2\alpha + t + jK')}{\Theta(t + jK')} \right\} \end{aligned}$$

$$= \frac{q}{\pi} \left\{ \frac{s\pi}{2gK} (\alpha + t + jK') - j \frac{\alpha\pi}{K} \right. \\ \left. + \log \frac{\sin \frac{\pi(2\alpha+t)}{2K} - q^2 \sin \frac{3\pi(2\alpha+t)}{2K} + q^6 \sin \frac{5\pi(2\alpha+t)}{2K} \dots}{\sin \frac{\pi t}{2K} - q^2 \sin \frac{3\pi t}{2K} + q^6 \sin \frac{5\pi t}{2K} \dots} \right\} \dots \dots \dots (37)$$

where $q = e^{-\frac{\pi K'}{K}}$.

Also from equations (32) and (33)

$$\chi = \frac{2\phi_0}{\pi} \operatorname{arc} \tanh \frac{\operatorname{sn} \alpha}{\operatorname{sn}(\alpha+t)} \\ = \frac{\phi_0}{\pi} \log \frac{\operatorname{sn}(\alpha+t) + \operatorname{sn} \alpha}{\operatorname{sn}(\alpha+t) - \operatorname{sn} \alpha} \dots \dots \dots (38)$$

Using equations (37) and (38) the "lost flux" for the whole slot is given by the real part of

$$2 \lim_{t \rightarrow 0} \left(\frac{\phi_0}{g} z - \chi \right) = \frac{\phi_0}{\pi} \left\{ \frac{s\pi\alpha}{gK} \right. \\ \left. + 2 \log \left\{ \frac{K \operatorname{cn} \alpha \operatorname{dn} \alpha}{\pi \operatorname{sn} \alpha} \frac{\left(\sin \frac{\pi\alpha}{K} - q^2 \sin \frac{3\pi\alpha}{K} + q^6 \sin \frac{5\pi\alpha}{K} \dots \right)}{(1 - 3q^2 + 5q^6 \dots)} \right\} \right\} \dots \dots \dots (39)$$

The effective width of the slot s_e is the width which would be occupied by the above quantity of flux in a uniform gap of length g and with a potential difference ϕ_0 and is therefore obtained by dividing the above expression by $\frac{\phi_0}{g}$;

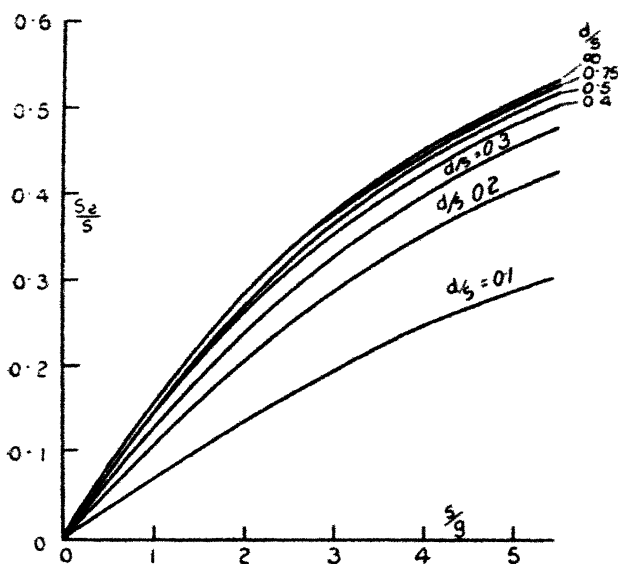
$$\therefore s_e = \frac{s\alpha}{K} \\ + \frac{2g}{\pi} \log \left\{ \frac{K \operatorname{cn} \alpha \operatorname{dn} \alpha}{\pi \operatorname{sn} \alpha} \frac{\left(\sin \frac{\pi\alpha}{K} - q^2 \sin \frac{3\pi\alpha}{K} + q^6 \sin \frac{5\pi\alpha}{K} \dots \right)}{(1 - 3q^2 + 5q^6 \dots)} \right\} \dots \dots \dots (40)$$

In a form better suited for calculation purposes

$$\frac{s_e}{s} = \frac{r^0}{90} + \frac{2g}{\pi s} \log_e \left\{ \frac{K \cos \theta_1}{\pi \tan \phi} \frac{(\sin 2r^0 - q^2 \sin 6r^0 + q^4 \sin 10r^0 \dots)}{(1 - 3q^2 + 5q^4 \dots)} \right\} \quad (41)$$

The values of K , q , θ_1 , and r^0 are derived directly from the parameters θ and ϕ by the relations

Fig. 9.



Curves giving effective width of a slot of finite depth.

K = complete first elliptic integral to modular angle θ .

$$q = e^{-\frac{K}{K'}}.$$

$$\theta_1 = \arcsin (\sin \theta \sin \phi),$$

and

$$\frac{r^0}{90} = \frac{F(\phi, \theta)}{K}.$$

The numerical value of q is usually so small that only two or three terms need be taken in the series of equation (41) to give 4-figure accuracy.

The final results are given in the form of curves in fig. 9.

(iii.) *Gap Coefficient K_g for repeated Slots.*

For the case of repeated slots of infinite depth it was shown that the gap coefficient could be obtained with sufficient accuracy for practical purposes by taking the effective width of the slot the same as for a single slot with the gap extending to infinity on either side.

In the same way it is expected that a similar approximation can be made in the case of slots of finite depth, so that the gap coefficient is given approximately by

$$K_g = \frac{s+t}{s+t-s_e} = 1 + \frac{\frac{s_e}{s}}{1 + \frac{t}{s} - \frac{s_e}{s}} \quad \dots \quad (42)$$

IV. THE TEMPERATURE INDICATED BY AN EMBEDDED TEMPERATURE-DETECTOR PLACED BETWEEN THE TWO LAYERS OF CONDUCTORS IN A LARGE STATOR WINDING.

Since the heat generated in the conductors of a machine by the load current has to pass through the surrounding layer of insulation before it is finally conducted away to the ventilating channels by the iron of the core, a considerable temperature difference exists across this insulation in virtue of its bad thermal conductivity.

In representative present-day designs the temperature drop in the insulation round the conductor is of the order of 40° C. for a total temperature rise of 80° C. above the ambient air, as indicated by an embedded temperature detector generally placed at a point on the centre line of the slot and midway between the two conductors or groups of conductors.

The highest temperature in the insulation occurs at the surface of the conductor, so that an embedded temperature detector located midway between two adjacent layers of conductors will indicate a temperature somewhat lower than this maximum value.

The present investigation was made to determine the extent to which the actual conductor temperature exceeds the indicated temperature over a wide range of practical cases.

For the problem considered it assumed that there is a constant temperature difference between the conductors and the iron of the core and also that the material of the

128 Messrs. R. T. Coe and H. W. Taylor : *Some Problems in*
insulation is isotropic, that is, has the same conductivity in
all directions.

The former assumption is justified since, owing to the
much greater conductivity of the copper and iron compared
with the insulation, any temperature variations existing in
the conductor itself or in the iron adjacent to the slot
must be very small compared with the total temperature
drop across the insulation. The latter assumption must also
be reasonably true, since all processes of insulating the
conductors of large stator windings aim at excluding air
films or pockets from the body of the insulation.

With the above assumptions the flow of heat through the
insulation is subject to the same laws as magnetic flux in
air, and so the isothermals or lines of constant temperature,
and the lines of heat flow, can be obtained by methods
similar to those already employed in the magnetic problems.

In general, the height of the conductor or layer of
conductors will be several times the thickness of the insulation
between the conductors, so that a close approximation to the
actual problem can be preserved by considering only the
region between two conductors of infinite depth. This
enables use to be made of the same primary transformation
between the z and ζ planes as employed in the two previous
problems.

The result obtained by considering two conductors will
also apply with a reasonable degree of approximation to the
case of laminated conductors, as the thickness of insulation
between individual laminations is small compared with the
thickness of their common wrapping.

The problem under consideration is represented by the
top diagram of fig. 10. The portion of the figure indicated
by OABCD($C_1B_1A_1O$) is of the same shape as that considered
in the previous magnetic problems and therefore leads to the
same transformation from the z plane to the ζ plane.

In the present problem the most convenient variables to
employ are the two ratios $\frac{d_1}{W}$ and $\frac{d_2}{d_1}$, where

d_1 = thickness of side insulation,

d_2 = half thickness of insulation between conductors,

and

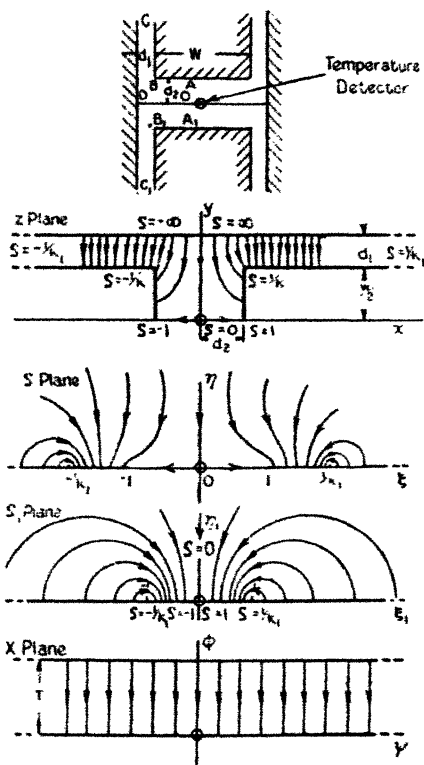
W = width of conductors.

By identifying d_1 , d_2 , and W with $\frac{d}{2}$, g , and t respectively
in equations (1), (4), (5), and (6) of the first magnetic

problem, the transformation from the z plane to the ζ plane is seen to be given by

$$\frac{dz}{d\zeta} = \frac{2d_1 \operatorname{sn} \alpha \operatorname{dn} \alpha}{\pi \operatorname{cn} \alpha} \frac{(1 - k^2 \zeta^2)^{\frac{1}{2}}}{(1 - \zeta^2)^{\frac{1}{2}} (1 - k^2 \operatorname{sn}^2 \alpha \cdot \zeta^2)^{\frac{1}{2}}}, \quad (43)$$

Fig. 10.



Flow of heat through insulation between conductors and iron.

where
$$\frac{d_2}{d_1} = \frac{2K}{\pi} \left\{ \frac{\operatorname{sn} \alpha \operatorname{dn} \alpha}{\operatorname{cn} \alpha} - Z(\alpha) \right\}, \quad \dots \quad (44)$$

and
$$\frac{W}{d_1} = \frac{4K'}{\pi} \left\{ \frac{\operatorname{sn} \alpha \operatorname{dn} \alpha}{\operatorname{cn} \alpha} - Z(\alpha) \right\} - \frac{2\alpha}{K} \dots \quad (45)$$

The ranges of values of the two variables likely to be met with in practice are

$$\frac{d_1}{W} \text{ from } 0 \text{ to } 0.5 \quad \text{and} \quad \frac{d_2}{d_1} \text{ from } 1.0 \text{ to } 2.0.$$

Table IV. has been drawn up showing the associated values of θ and ϕ required to give various values of $\frac{d_1}{W}$ and $\frac{d_2}{d_1}$ in this range. ($k = \sin \theta$ and $\sin \alpha = \sin \phi$.)

For the mathematical treatment it is immaterial whether the heat flows upwards or downwards in the z plane figure and so to preserve similarity with the other problems it is taken as flowing downwards. The portions of the lower

TABLE IV.
Values of θ and ϕ in Degrees for Temperature-Detector Problem.

	$\frac{d_2}{d_1}$	1.0	1.2	1.4	1.6	1.8	2.0
$\frac{d_1}{W} = 0$	$\begin{cases} \theta & \dots\dots 0 \\ \phi & \dots\dots 45.0 \end{cases}$	0 45.0	0 50.2	0 54.4	0 58.0	0 60.9	0 63.4
$\frac{d_1}{W} = 0.1$	$\begin{cases} \theta & \dots\dots 0.03 \\ \phi & \dots\dots 45.0 \end{cases}$	0.03 45.0	0.14 50.2	0.43 54.4	0.89 58.0	1.60 60.9	2.60 63.4
$\frac{d_1}{W} = 0.2$	$\begin{cases} \theta & \dots\dots 2.06 \\ \phi & \dots\dots 45.0 \end{cases}$	2.06 45.0	4.18 50.2	7.06 54.4	10.4 58.2	14.2 61.3	18.4 63.4
$\frac{d_1}{W} = 0.3$	$\begin{cases} \theta & \dots\dots 7.55 \\ \phi & \dots\dots 45.1 \end{cases}$	7.55 45.1	12.25 50.5	17.75 55.1	23.35 59.1	28.75 62.5	34.25 65.6
$\frac{d_1}{W} = 0.4$	$\begin{cases} \theta & \dots\dots 14.55 \\ \phi & \dots\dots 45.5 \end{cases}$	14.55 45.5	21.4 50.7	28.2 56.0	34.5 60.4	40.8 64.2	46.7 67.6
$\frac{d_1}{W} = 0.5$	$\begin{cases} \theta & \dots\dots 21.4 \\ \phi & \dots\dots 46.0 \end{cases}$	21.4 46.0	29.1 52.0	36.6 57.3	43.4 62.0	49.5 65.9	54.9 69.3

boundary between $\zeta = 1$ and $\frac{1}{k}$ and between $\zeta = -1$ and $-\frac{1}{k}$ are assumed to be at zero temperature and the whole upper boundary from $\zeta = \frac{1}{k}$ to ∞ and from $\zeta = -\frac{1}{k}$ to $-\infty$ at a temperature T .

Owing to the fact that there are two disconnected portions of the ζ plane real axis which are at zero temperature, the transformation from the ζ plane to a portion of the uniform x plane cannot be completed in one operation. We therefore use an additional plane which will be called the ζ_1 plane and

in which these two disconnected portions of isothermal are brought together. In doing this, the intermediate part of the ζ real axis, representing the two halves of a portion of the middle stream line of the figure, becomes transformed into the two sides of a finite portion of the imaginary axis of the ζ_1 plane.

By the Schwarz transformation theorem

$$\frac{d\zeta_1}{d\zeta} = \frac{B\zeta}{(\zeta^2-1)^{\frac{1}{2}}}, \quad \dots \dots \dots (46)$$

whence, making the origins of the two planes correspond,

$$\zeta_1 = B \int_0^\zeta \frac{\zeta d\zeta}{(\zeta^2-1)^{\frac{1}{2}}} = B(\zeta^2-1)^{\frac{1}{2}}. \quad \dots \dots (47)$$

Since the constant B only occurs in an intermediate transformation, its value may be chosen in any convenient way.

The final transformation from the ζ_1 plane to the χ plane can be simplified somewhat by choosing B so that

$$\zeta_1 = 1 \text{ when } \zeta = \frac{1}{k_1}.$$

Then from equation (47)

$$B = \frac{k_1}{k_1'}, \quad \dots \dots \dots (48)$$

so that

$$\zeta_1 = \frac{k_1}{k_1'} (\zeta^2-1)^{\frac{1}{2}}. \quad \dots \dots \dots (49)$$

The transformation from the ζ_1 plane to the uniform χ plane is given by

$$\frac{d\chi}{d\zeta_1} = \frac{C}{1-\zeta_1^2}, \quad \dots \dots \dots (50)$$

and on making the origins of the two planes correspond

$$\begin{aligned} \chi = \psi + j\phi &= C \int_0^{\zeta_1} \frac{d\zeta_1}{1-\zeta_1^2} \\ &= C \operatorname{arc} \tanh \zeta_1. \quad \dots \dots (51) \end{aligned}$$

To evaluate the constant C we use the fact that when ζ_1 increases through the value unity, χ increases by jT . Therefore from the above equation

$$jT = \frac{C}{2} \times j\pi,$$

giving

$$C = \frac{2}{\pi} T,$$

so that

$$\begin{aligned}\chi &= \frac{2}{\pi} T \operatorname{arc} \tanh \zeta_1 \\ &= \frac{2}{\pi} T \operatorname{arc} \tanh \left\{ \frac{k_1}{k_1'} (\zeta^2 - 1)^{\frac{1}{2}} \right\}. \quad (52)\end{aligned}$$

At the point where the detector is placed, $\zeta = 0$, so that

$$\begin{aligned}\chi_d &= \frac{2}{\pi} T \operatorname{arc} \tanh j \frac{k_1}{k_1'} \\ &= j \frac{2}{\pi} T \operatorname{arc} \tan \frac{k_1}{k_1'} \\ &= j \frac{2}{\pi} T \operatorname{arc} \sin k_1. \quad \dots \dots \dots (53)\end{aligned}$$

The temperature difference between the detector and conductors as a fraction of the total temperature difference between the iron core and the conductors is therefore given by

$$\frac{2}{\pi} \operatorname{arc} \sin k_1.$$

In calculation form, $\operatorname{arc} \sin k_1 = \theta_1$ and is found in degrees, so that the fraction of the total temperature is given by the simple expression

$$\frac{\theta_1^\circ}{90^\circ}.$$

The curves of fig. 11 show the temperature difference between the detector and core as a percentage of the total temperature drop across the insulation. These curves were calculated from Table IV. using the relation that

$$\theta_1 = \operatorname{arc} \sin (\sin \theta \sin \phi).$$

If the two layers of insulated conductors were assembled together in the slot so as to touch one another the value of $\frac{d_2}{d_1}$ would be unity. Actually, however, it is necessary to separate them by say a wooden strip, and in this case if we assume the detector to be embedded in the middle of the strip, the value of $\frac{d_2}{d_1}$ will be greater than unity, depending on the relative thicknesses of the coil insulation and separator.

The following figures are typical of an 11,000 volt turbo-alternator winding :—

Width of slot = 1.0 inch.

Depth of conductors ... = 2.5 inches.

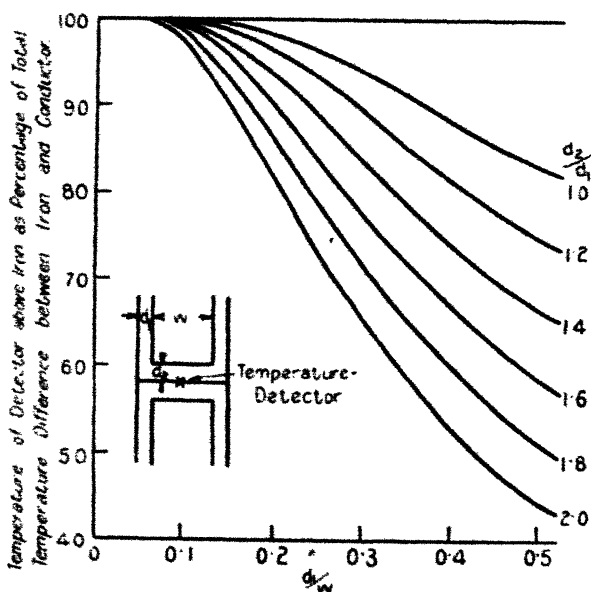
Width of conductors... = 0.6 inch.

Thickness of insulation = 0.2 inch.

Thickness of separator . = 0.2 inch.

From the above values $\frac{d_1}{W} = 0.333$.

Fig. 11.



Curves giving the temperature indicated by an embedded temperature-detector between the two layers of a stator winding.

If the separator were absent the detector would indicate 92.5 per cent. of the total temperature difference between the conductors and the core. If the detector were inserted in the middle of the separator we should have a value of

1.5 for $\frac{d_2}{d_1}$ giving an observed temperature difference of 77 per cent. of the actual value. The detector, however, would probably be placed on one side of the separator, and

134 Messrs. R. T. Coe and H. W. Taylor : *Some Problems in*
in this case would indicate about 83 per cent. of the total
temperature drop in the insulation.

If this machine were designed to give an indicated
temperature rise of 80° C. above ambient by the embedded
temperature detector and if the temperature rise of the core
iron were 40° C. then the temperature of the conductor
would exceed the recorded temperature by

$$40 \times \frac{17}{83} = 8^{\circ} \text{ C. approx.}$$

The insulation in contact with the copper is therefore
subjected to a temperature 88° C. above the ambient air.

V. THE FLUX-DISTRIBUTION ASSOCIATED WITH A GROOVED POLE-FACE.

(a) *Analysis of Problem.*

For some time past it has been a common practice to turn
circumferential grooves in pole-faces, particularly of turbo-
alternator rotors in cases where these seemed liable to over-
heat due to the effect of eddy-current losses caused by flux-
tufting from opposing teeth. The cooler running which is
known to result from this procedure seems to be due partly
to the better cooling caused by the increased turbulence of
the stream of ventilating air, and partly to an actual reduction
in the pole-face losses caused by the change in the configura-
tion of the pole-face and the flux-distribution along it.

In this latter connexion a knowledge of the flux-distrib-
ution round these grooves along a longitudinal section of
the rotor is of interest as providing a step towards a
complete understanding of the nature of the pole-face losses
in this case.

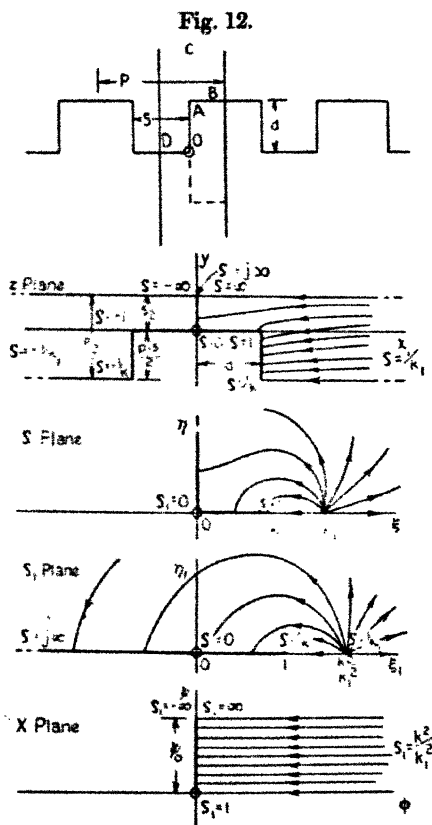
If the length of the air-gap were small compared with the
width of the projection between adjacent grooves the flux-
distribution could be obtained from that due to a single slot
of finite depth as considered in section III. of this paper.

However, with the turbo-alternator the air-gap will
usually be several times the width of either the grooves or
projections, and in this case a better approximation can be
obtained by taking the flux-distribution round the grooves as
due to flux streaming to the rotor surface from infinity.
The flux-distribution is expected to have become sensibly
uniform at a distance from the rotor surface equal to the
length of the actual air-gap.

The variation of flux-density round the rotor due to the

main poles, together with superimposed ripples due to the stator slots, will be comparatively gradual, so that as a first approximation the flux-distribution at any section may be treated as two-dimensional.

A symmetrical z plane figure is obtained by taking a parallel strip of the field corresponding to half a groove



The flux-distribution round the circumferential grooves of a turbo-alternator rotor.

pitch as shown by OABCD in fig. 12, together with its image relative to the line OD. It is interesting to compare this figure with the z plane figure of the previous problems (see fig. 1).

Making the points O, A, B, C, D correspond to values for of 0, 1, $\frac{1}{k}$, $\frac{1}{k_1}$, and ∞ respectively with negative values for

136 Messrs. R. T. Coe and H. W. Taylor: *Some Problems in*
the image points, the transformation from the z plane to the
upper half of the ζ plane is given by the Schwarz theorem as

$$\frac{dz}{d\zeta} = A \frac{(1-\zeta^2)}{(1-k_1^2\zeta^2)(1-k^2\zeta^2)^{\frac{1}{2}}}, \quad \dots \quad (54)$$

whence, on making the origins of the two planes correspond,

$$z = A \int_0^\zeta \frac{(1-\zeta^2)d\zeta}{(1-k_1^2\zeta^2)(1-k^2\zeta^2)^{\frac{1}{2}}}. \quad \dots \quad (55)$$

This integral is best calculated in terms of elliptic functions
by making the same change of variable as in the first
problem.

Thus let $\zeta = \operatorname{sn} q$ to modulus k ,

also let $k_1 = k \operatorname{sn} \alpha$ to modulus k .

With these substitutions the above integral reduces to

$$z = A \left\{ q - \frac{\operatorname{dn} \alpha}{k^2 \operatorname{sn} \alpha \operatorname{cn} \alpha} \Pi(q, \alpha) \right\}. \quad \dots \quad (56)$$

The constant A can be determined by using the fact that
as ζ increases through the value $\frac{1}{k_1} = \frac{1}{k \operatorname{sn} \alpha}$, z takes on a
sudden increment $j \frac{p}{2}$ where $p =$ pitch of groove.

Thus from equation (55),

$$A = \frac{p}{\pi} \frac{k^2 \operatorname{sn} \alpha \operatorname{cn} \alpha}{\operatorname{dn} \alpha}. \quad \dots \quad (57)$$

The constants k and α are obtained in terms of the
dimensions of the problem by considering the point for which

$$z = d - j \frac{p-s}{2},$$

where $d =$ depth of groove,

and $s =$ width of groove.

At this point

$$\zeta = \frac{1}{k},$$

therefore $q = F\left(\frac{1}{k}, k\right) = K + jK'.$

Since $\Pi(K + jK', \alpha) = (K + jK')Z(\alpha) + j \frac{\pi \alpha}{2K},$

we have from equations (56) and (57),

$$d - j\frac{p-s}{2} = \frac{p}{\pi} \left\{ (K + jK') \left(\frac{k^2 \operatorname{sn} \alpha \operatorname{cn} \alpha}{\operatorname{dn} \alpha} - Z(\alpha) \right) - j\frac{\pi \alpha}{2K} \right\},$$

from which, on equating real and imaginary parts,

$$\frac{d}{p} = \frac{K}{\pi} \left(\frac{k^2 \operatorname{sn} \alpha \operatorname{cn} \alpha}{\operatorname{dn} \alpha} - Z(\alpha) \right), \quad \dots \quad (58)$$

and

$$\frac{s}{p} = \frac{2K'}{\pi} \left(\frac{k^2 \operatorname{sn} \alpha \operatorname{cn} \alpha}{\operatorname{dn} \alpha} - Z(\alpha) \right) + 1 - \frac{\alpha}{K}. \quad (59)$$

In forms more suited for calculation purposes, the above equations become

$$\frac{d}{v} = \frac{K}{\pi} \left(\frac{\sin^2 \theta \sin \phi \cos \phi}{\cos \theta_1} - Z(\alpha) \right), \quad \dots \quad (60)$$

and

$$\frac{s}{p} = \frac{2K'}{\pi} \left(\frac{\sin^2 \theta \sin \phi \cos \phi}{\cos \theta_1} - Z(\alpha) \right) + 1 - \frac{r^0}{90}, \quad (61)$$

where

$$\sin \theta = k, \quad \sin \phi = \operatorname{sn} \alpha, \quad \sin \theta_1 = k \operatorname{sn} \alpha,$$

and

$$\frac{r^0}{90} = \frac{F(\phi, \theta)}{K}.$$

The most convenient variables in this problem are $\frac{d}{s}$ and $\frac{s}{p}$.

As in the previous problems, it is desirable to know the associated values of the parameters θ and ϕ that correspond to particular values of $\frac{d}{s}$ and $\frac{s}{p}$, and so Table V. has been prepared as a result of calculations and cross-plotting from equations (60) and (61) and covers a range of values of $\frac{d}{s}$ up to unity and $\frac{s}{p}$ between 0.1 and 0.9.

In considering the further transformation from the ζ plane to the uniform χ plane we note that, in addition to fixing the nature of the boundaries of the complete symmetrical figure that have been transformed into the real axis of the ζ plane, we have to arrange that the line OD which has been transformed into the imaginary axis of the ζ plane shall be at the same potential as the portion OAB of the original figure.

The first step is to simplify the problem so that all the boundaries we wish to fix are represented by the real axis of a plane, and we do this by transforming the first quadrant of the ζ plane into the top half of an auxiliary plane which will be called the ζ_1 plane.

By the Schwarz theorem the necessary transformation is

$$\frac{d\zeta}{d\zeta_1} = B \zeta_1^{\frac{1}{2}} \quad (62)$$

and on making the origins of the two planes correspond

$$\zeta = B \int_0^{\zeta_1} \frac{d\zeta_1}{\zeta_1^{\frac{1}{2}}} = 2B\zeta_1^{\frac{1}{2}} \quad (63)$$

Table V.

Values of θ and ϕ in Degrees for Grooved Rotor Problem.

$\frac{s}{p}$		0.1	0.3	0.5	0.7	0.9
$\frac{d}{s} = 0.1$	θ	32.0	33.1	36.0	41.5	55.0
	ϕ	83.8	71.1	58.3	44.5	28.7
$\frac{d}{s} = 0.25$	θ	52.5	54.0	56.1	60.1	70.0
	ϕ	86.1	78.4	70.0	60.9	50.1
$\frac{d}{s} = 0.5$	θ	72.6	73.2	74.3	76.3	81.1
	ϕ	88.7	84.6	80.9	76.7	71.1
$\frac{d}{s} = 0.75$	θ	81.9	82.4	82.95	83.7	85.85
	ϕ	89.2	87.55	85.9	83.9	81.3
$\frac{d}{s} = 1.0$	θ	86.3	86.5	86.75	87.15	88.2
	ϕ	89.65	88.85	88.0	87.2	86.0

Since this is only an intermediate transformation it is convenient to choose the constant B so that $\zeta_1 = 1$, when

$\zeta = \frac{1}{k}$. Thus from equation (63),

$$B = \frac{1}{2k}, \quad (64)$$

$$\text{and} \quad \zeta_1 = k^2 \zeta^2. \quad (65)$$

Noting that the flux concerned is finite, we now transform the top half of the ζ_1 plane into a strip of the uniform χ plane. To preserve the similarity between the figures in

the various planes the strip in the χ plane is taken parallel to the real axis, and as the flux lines go in this direction we take $\chi = \phi + j\psi$ where ϕ represents potential.

The point for which $\zeta = \frac{1}{k_1}$ and therefore $\zeta_1 = \frac{k^2}{k_1^2} = \frac{1}{\text{sn}^2 \alpha}$ has now been taken back to infinity as in the original z plane figure.

By the Schwarz theorem the necessary transformation is

$$\frac{d\chi}{d\zeta_1} = \frac{C}{(1-\zeta_1)^{\frac{1}{2}}(1-\text{sn}^2 \alpha \cdot \zeta_1)^{\frac{1}{2}}} \dots \dots (66)$$

Making the origin in the χ plane correspond to the point $\zeta_1 = 1$, we have

$$\chi = C \int_1^{\zeta_1} \frac{d\zeta_1}{(1-\zeta_1)^{\frac{1}{2}}(1-\text{sn}^2 \alpha \cdot \zeta_1)^{\frac{1}{2}}} \dots \dots (67)$$

$$= -\frac{2C}{\text{sn} \alpha \text{cn} \alpha} \text{arc sin} \left\{ \text{sn} \alpha \frac{(1-k^2 \zeta^2)^{\frac{1}{2}}}{(1-k^2 \text{sn}^2 \alpha \cdot \zeta^2)^{\frac{1}{2}}} \right\}. \quad (68)$$

To evaluate the constant C we use the fact that as ζ increases through the value $\frac{1}{k_1}$, that is, as ζ_1 increases through the value $\frac{1}{\text{sn}^2 \alpha}$, there is a sudden increase in χ of amount $j\psi_0$ where ψ_0 is the amount of flux entering the rotor surface per half groove pitch.

Using equation (67) this gives

$$C = -j \frac{\text{sn} \alpha \text{cn} \alpha}{\pi} \psi_0, \dots \dots (69)$$

and substituting this value in equation (68),

$$\chi = j\psi_0 \frac{2}{\pi} \text{arc sin} \left\{ \text{sn} \alpha \frac{(1-k^2 \zeta^2)^{\frac{1}{2}}}{(1-k^2 \text{sn}^2 \alpha \cdot \zeta^2)^{\frac{1}{2}}} \right\}. \dots (70)$$

The flux-density at any point is given by

$$\frac{d\chi}{dz} = \frac{d\chi}{d\zeta_1} \cdot \frac{d\zeta_1}{d\zeta} \cdot \frac{d\zeta}{dz}.$$

On using equations (66), (62), and (54) after inserting the values of the constants given by equations (69), (64), and (57), the final expression for the flux-density becomes

$$\frac{d\chi}{dz} = \frac{2\psi_0}{p} \text{dn} \alpha \frac{\zeta}{(\zeta^2 - 1)^{\frac{1}{2}}}. \dots \dots (71)$$

The mean flux-density in the air-gap is given by

$$B_m = \frac{2\psi_0}{\pi},$$

and so

$$\frac{d\chi}{dz} = B_m \times \operatorname{dn} \alpha \frac{\zeta}{(\zeta^2 - 1)^{\frac{1}{2}}}. \quad \dots \quad (72)$$

(b) *Practical Deductions.*

(i.) *Flux-Density on Grooved Surface.*

Along the top of the projection between two grooves the minimum flux-density B_1 occurs at the middle point where

$\zeta = \frac{1}{k}$; therefore

$$\begin{aligned} B_1 &= B_m \times \operatorname{dn} \alpha \frac{1}{(1 - k^2)^{\frac{1}{2}}} \\ &= B_m \times \frac{\cos \theta_1}{\cos \theta}, \quad \dots \quad (73) \end{aligned}$$

where $\theta_1 = \arcsin(\sin \theta \sin \phi)$.

Along the bottom of the rotor groove the maximum flux-density B_2 occurs at the mid-point where $\zeta = \infty$; therefore

$$\begin{aligned} B_2 &= B_m \times \operatorname{dn} \alpha \\ &= B_m \times \cos \theta, \quad \dots \quad (74) \end{aligned}$$

Fig. 13 shows B_1 and B_2 plotted against $\frac{d}{s}$ for a number of values of $\frac{s}{p}$ and obtained from the values of θ and ϕ given in Table V.

Should it be desired to obtain the variation of flux-density round the complete groove, this can be done by a method similar to that employed in the problem of flux distribution due to consecutive slots.

Along the bottom of the groove in going from the corner O to the centre point D, ζ varies from 0 to ∞ and the value of z in terms of ζ is obtained by using the Θ function series when evaluating the third elliptic integral in equation (56). Along the side of the groove where ζ varies from 0 to 1 the third elliptic integral may be evaluated either from its Θ function series or directly from suitable tables. Along the top of the projection between the grooves ζ is greater than unity, and here, again, the third elliptic integral can only be evaluated from its series.

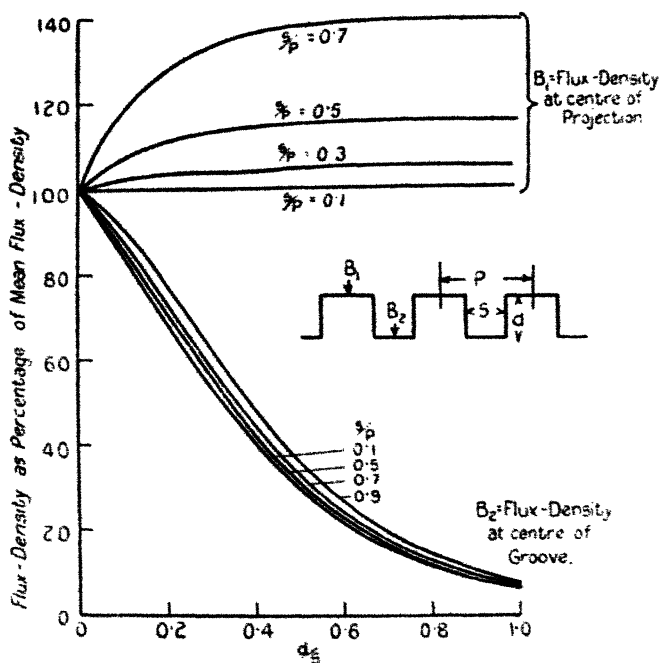
In each of these three regions, the flux-density in terms of ζ can be calculated directly from the simple expression of equation (72).

(ii.) *The Additional Gap-Length Equivalent to the Grooves.*

An expression for this additional gap-length is obtained by considering the extra potential required to send the flux across the infinite gap due to the grooving. This extra potential is given by the real part of

$$\lim_{\zeta \rightarrow \frac{1}{k \tan \alpha}} \{ \chi - B_m(z-d) \}.$$

Fig. 13.



Curves giving flux-densities at middles of projection and groove on grooved rotor.

From equations (56) and (57),

$$\begin{aligned} z &= \frac{p}{\pi} \left\{ \frac{k^2 \operatorname{sn} \alpha \operatorname{cn} \alpha}{\operatorname{dn} \alpha} q - \Pi(q, \alpha) \right\} \\ &= \frac{p}{\pi} \left\{ \left(\frac{k^2 \operatorname{sn} \alpha \operatorname{cn} \alpha}{\operatorname{dn} \alpha} - Z(\alpha) \right) + \frac{1}{2} \log \frac{\Theta(q+\alpha)}{\Theta(q-\alpha)} \right\}. \end{aligned}$$

Using equation (58) this simplifies to

$$z = \frac{p}{\pi} \left\{ \frac{d\pi}{pK} q + \frac{1}{2} \log \frac{\Theta(q+\alpha)}{\Theta(q-\alpha)} \right\} \dots \dots (75)$$

To evaluate the limit which gives the extra amount of potential required, let

$$\zeta = \frac{1}{k \operatorname{sn}(\alpha+t)}$$

so that

$$t \rightarrow 0 \text{ as } \zeta \rightarrow \frac{1}{k \operatorname{sn} \alpha}.$$

Now

$$q = F(\zeta, k) = \alpha + t + jK',$$

so that substituting in equation (75),

$$\begin{aligned} z &= \frac{p}{\pi} \left\{ \frac{d\pi}{pK} (\alpha + t + jK') + \frac{1}{2} \log \frac{\Theta(2\alpha + t + jK')}{\Theta(t + jK')} \right\} \\ &= \frac{p}{\pi} \left\{ \frac{d\pi}{pK} (\alpha + t + jK') + j \frac{\alpha\pi}{2K} \right. \\ &\quad \left. + \frac{1}{2} \log \frac{\sin \frac{\pi(2\alpha+t)}{2K} - q^2 \sin \frac{3\pi(2\alpha+t)}{2K} + \dots}{\sin \frac{\pi t}{2K} - q^2 \sin \frac{3\pi t}{2K} + q^4 \sin \frac{5\pi t}{2K} - \dots} \right\} \dots \dots (76) \end{aligned}$$

From equation (70)

$$\chi = j\psi_0 \frac{2}{\pi} \operatorname{arcsin} \left\{ \operatorname{sn} \alpha \frac{(1 - k^2 \zeta^2)^{\frac{1}{2}}}{(1 - k^2 \operatorname{sn}^2 \alpha \cdot \zeta^2)^{\frac{1}{2}}} \right\},$$

whence on substituting

$$\zeta = \frac{1}{k \operatorname{sn}(\alpha+t)}$$

and noting that

$$2\psi_0 = B_m p,$$

we have

$$\chi = j \frac{p B_m}{\pi} \operatorname{arcsin} \left\{ -j \frac{\operatorname{sn} \alpha \operatorname{cn}(\alpha+t)}{(\operatorname{sn}^2(\alpha+t) - \operatorname{sn}^2 \alpha)^{\frac{1}{2}}} \right\}.$$

Turning this into the logarithmic form by the relation

$$\begin{aligned} \arcsin ju &= j \log \{u + (u^2 + 1)^{\frac{1}{2}}\}, \\ \chi &= \frac{pB_m}{\pi} \log \frac{\operatorname{sn} \alpha \operatorname{cn} (\alpha + t) + \operatorname{cn} \alpha \operatorname{sn} (\alpha + t)}{(\operatorname{sn}^2 (\alpha + t) - \operatorname{sn}^2 \alpha)^{\frac{1}{2}}}. \quad (77) \end{aligned}$$

Using equations (76) and (77), the extra potential required, due to the grooves, is given by:—

$$\begin{aligned} &\text{Real part of } \lim_{t \rightarrow 0} \{\chi - B_m(z - d)\} \\ &= \frac{pB_m}{\pi} \left\{ \frac{1}{2} \log \frac{2 \operatorname{sn} \alpha \operatorname{cn}^2 \alpha}{\sin \frac{\pi \alpha}{K} - q^2 \sin \frac{3\pi \alpha}{K} + \dots} + \frac{d\pi}{p} \left(1 - \frac{\alpha}{K}\right) \right. \\ &\quad \left. + \lim_{t \rightarrow 0} \frac{1}{2} \log \frac{\sin \frac{\pi t}{2K} - q^2 \sin \frac{3\pi t}{2K} + q^6 \sin \frac{5\pi t}{2K} - \dots}{\operatorname{sn} (\alpha + t) - \operatorname{sn} \alpha} \right\} \\ &= \frac{pB_m}{\pi} \left\{ \frac{1}{2} \log \frac{\pi}{K} \frac{\operatorname{sn} \alpha \operatorname{cn} \alpha}{\operatorname{dn} \alpha} \frac{(1 - 3q^2 + 5q^6 - \dots)}{\left(\sin \frac{\pi \alpha}{K} - q^2 \sin \frac{3\pi \alpha}{K} + \dots\right)} \right. \\ &\quad \left. + \frac{d\pi}{p} \left(1 - \frac{\alpha}{K}\right) \right\}. \end{aligned}$$

The increase in the effective gap-length corresponding to the above amount of extra potential is obtained by dividing the latter by the potential gradient or flux-density in the uniform field at a great distance from the grooved surface. This potential gradient is given by B_m , so that the additional gap-length is

$$\begin{aligned} \delta g &= \frac{p}{2\pi} \log \left\{ \frac{\pi}{K} \frac{\operatorname{sn} \alpha \operatorname{cn} \alpha}{\operatorname{dn} \alpha} \frac{(1 - 3q^2 + 5q^6 - \dots)}{\left(\sin \frac{\pi \alpha}{K} - q^2 \sin \frac{3\pi \alpha}{K} + \dots\right)} \right\} \\ &\quad + d \left(1 - \frac{\alpha}{K}\right). \quad (78) \end{aligned}$$

Putting this in a form more suitable for calculation purposes, we have

$$\begin{aligned} \frac{\delta g}{s} &= \frac{1}{2\pi s} \log_e \left\{ \frac{\pi}{K} \frac{\sin \phi \cos \phi}{\cos \theta_1} \frac{(1 - 3q^2 + 5q^6 - \dots)}{(\sin 2r^\circ - q^2 \sin 6r^\circ + \dots)} \right\} \\ &\quad + \frac{d}{s} \left(1 - \frac{r^\circ}{90}\right). \quad (79) \end{aligned}$$

The notation employed is the same as in the previous problems, so that the various quantities involved in the above formula are obtained directly from the two parameters θ and ϕ by the following relations:—

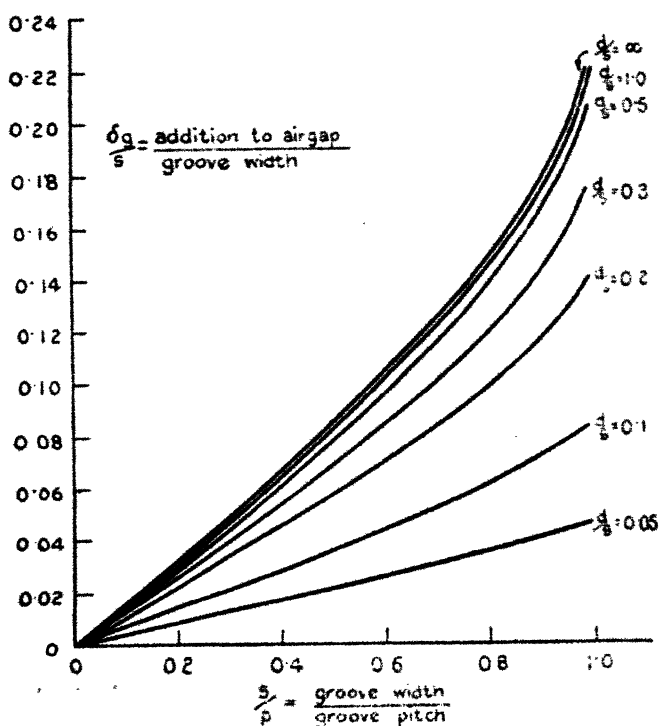
$$q = e^{-\frac{K'}{K}\pi}$$

K and $K' =$ complete first elliptic integrals to modular angle θ ,

$$\theta_1 = \arcsin(\sin \theta \sin \phi),$$

$$\frac{r^0}{90} = \frac{F(\phi, \theta)}{K}$$

Fig. 14.



Curves giving increase in effective gap-length due to presence of grooves.

Using the values of θ and ϕ given in Table V., the curves of fig. 14 have been calculated from equation (79). These curves show the value of $\frac{\delta g}{s}$ plotted against $\frac{s}{p}$ for a

number of values of $\frac{d}{s}$. Over the whole range of cases covered the numerical value of q is so small that only the first two or three terms are required in evaluating the two series involved.

The values of $\frac{\delta q}{s}$ for the limiting case where $\frac{s}{p} = 1$ and the projections between adjacent grooves have zero width, were calculated by considering the simplified transformations holding in this case. The required limit reduces to

$$\lim_{\frac{s}{p} \rightarrow 1} \left(\frac{\delta q}{s} \right) = \frac{1}{\pi} \left\{ \log_e 2 - \log_e \left(1 + e^{-\frac{2\pi p}{d}} \right) \right\}. \quad (80)$$

The limiting case where the grooves are of infinite depth was dealt with in a similar manner, the additional gap-length in this case being given by

$$\lim_{\frac{d}{s} \rightarrow \infty} \left(\frac{\delta q}{s} \right) = \frac{1}{2\pi} \frac{p}{s} \left\{ \left(1 + \frac{s}{p} \right) \log_e \left(1 + \frac{s}{p} \right) + \left(1 - \frac{s}{p} \right) \log_e \left(1 - \frac{s}{p} \right) \right\}. \quad (81)$$

From fig. 14, it will be seen that when the depth of the groove is greater than its width it has no appreciable effect on the additional gap-length.

(iii.) Gap Coefficient K_g for Air-gap of Finite Length.

Owing to the fact that the flux distribution in the case of an infinite gap rapidly becomes uniform away from the grooved surface, a reasonable approximation to the value of the gap coefficient for cases where the gap-length is not less than several times the groove width can be obtained by taking

$$\text{Gap coefficient } K_g = \frac{g + \delta q}{g} = 1 + \frac{s}{g} \left(\frac{\delta q}{s} \right), \quad (82)$$

where $\frac{\delta q}{s}$ is obtained from the curves of fig. 14.

Engineering Department,
British Thomson-Houston Co. Ltd., Rugby.
March 1928.

IX. *The Theory of Wave Filters containing a finite number of Sections.* By HAROLD A. WHEELER, B.S. in Phys., and FRANCIS D. MURNAGHAN, M.A., Ph.D., Associate Professor of Applied Mathematics, Johns Hopkins University*.

I. INTRODUCTION.

THE simple electric wave filter is built up of a number of recurrent sections connected in succession as shown in fig. 1. When a steady alternating voltage E_0 is impressed at one end of the filter, the resulting voltage E_n at the other end bears a ratio to the impressed voltage which is a function of the frequency of alternation. In the present uses to which filters are put, it is desirable that this response ratio be constant in certain predetermined frequency bands—the transmission (pass) bands—and as small as possible in the remaining suppression (stop) bands. The degree to which this condition can be realized determines the merit of any given filter. The location of the frequency bands depends on the structure of the recurrent sections.

The response-ratio functions of the frequency can be expressed in terms of determinants. The simplest determinant of this type— D_n in Part V. of this paper—was evaluated fifty years ago by Rayleigh† in connexion with the problem of determining natural frequencies of vibration of a loaded string. The complete determinant, $D_n(a, b)$, was given by Pupin‡, and was evaluated by a different method. The most extensive study of the wave filter has been made in connexion with loaded telephone lines, and is based on Campbell's solution of the infinite line§, i. e., the filter with an infinite number of sections. The real distinction between the infinite line and the finite line is the presence of reflexions at the terminations of the latter. The behaviour of a finite line is similar to that of the same number of sections in an infinite line, when the terminating impedances are so chosen as nearly to avoid reflexions, so that the infinite line solution has been found very useful.

In the present paper response formulæ are developed for finite Campbell filters, so that reflexions are taken account of without having to make special adjustment of the end conditions, automatically taking account of reflexions.

* Communicated by the Authors.

† 'Theory of Sound,' vol. i. p. 120 (1877).

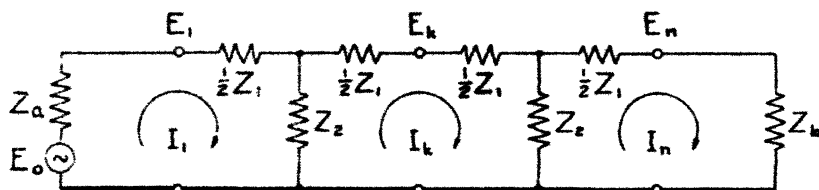
‡ Proc. A. I. E. E. xvi. p. 93 (1899).

§ Bell System Tech. Jour. p. 1 (Nov. 1922).

Particular attention is given to the non-dissipative constant-K type filter, terminated by any values of resistance. The M-derived type, due to Zobel *, is also treated, and its advantages over the former type are shown. These response formulæ are useful in that they show the deviations from the ideal performance and from the approximate solution based on the infinite line. The solution for the latter ideal case is then obtained as a limiting case of the solution for the actual finite line, and the expressions for the iterative impedance and propagation exponent are derived.

The natural frequencies of finite, conservative lines of recurrent structure are of theoretical interest, and bear a close relationship to the filter properties of the same lines. On applying our method to this problem, a convenient graphical solution, which is applicable to lines of any recurrent structure, however complex, is obtained. In this

Fig. 1.

Wave filter with mid-series terminations, $(n-1)$ sections.

connexion two variations from the recurrent line will be described. The first may be called an exponential line, and is built up of sections whose impedances change in geometric progression from section to section. The second is an alternating line with two recurrent sections in alternating succession.

Throughout our paper the terminology and notation generally used in papers dealing with the electric wave filter are adhered to. The term "frequency" denotes the number f of cycles per second; the "angular frequency" is the number ω of radians per second, so that $\omega = 2\pi f$.

II. WAVE-FILTER CIRCUITS, MID-SERIES TERMINATION.

1. *The Solution for a Finite Line.*—Fig. 1 shows a Campbell (*loc. cit.*) filter circuit built up of recurrent

* Bell System Tech. Jour. ii. p. 16 (1923).

for a filter of $(n-1)$ sections. The corresponding ratio with no filter sections interposed ($n-1=0$) is

$$G_1 = \frac{E_{n=1}}{E_0} = \frac{Z_b}{Z_a + Z_b} = \frac{w_b}{w_a + w_b}.$$

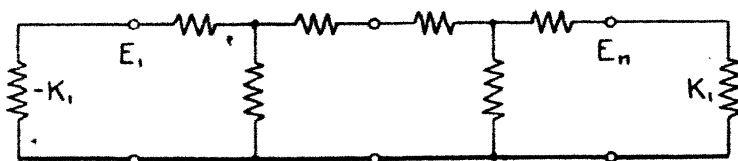
In the response solutions to be developed, it is most convenient to solve for the relative response ratio

$$\frac{G_n}{G_1} = \frac{w_a + w_b}{D_n(a, b)},$$

which shows immediately the result of interposing the $(n-1)$ filter sections between the terminating impedances. The reciprocal of this ratio is given by Eqs. (14) and (15) for the general case.

2. *Iterative Impedance of Infinite Line.*—Fig. 2 shows a segment of $(n-1)$ sections removed from an infinite line.

Fig. 2.



Wave filter with mid-series terminations, arranged to assimilate a segment of an infinite line.

The remainder of the line on the left (input) side has been replaced by its equivalent impedance $-K_1^*$, and the remainder of the line on the right (output) side is replaced by its impedance K_1 . This equivalent impedance is known as the iterative impedance of the infinite line. In applying the analysis of the preceding paragraph to the present case, we note that $E_0=0$ (absent), so that $D_n(a, b)$ must vanish if the other voltages are to exist in the line. Since we desire a solution independent of n , we note in Eq. (13) for $D_n(a, b)$ that the even powers of $(n-1)\Gamma$ are concentrated in $\cosh(n-1)\Gamma$ and the odd powers in $\sinh(n-1)\Gamma$. The

* Any generator circuit connected to an impedance, $Z=E/I$, may be represented as the negative impedance, $-Z=-E/I$, since the terminal voltage E of the generator circuit is equal to that of the impedance, and the current into the former is $-I$, the reverse of the current into the latter.

150 Mr. Wheeler and Prof. Murnaghan on the Theory of
expression vanishes for all values of n when the two re-
spective coefficients are equated to zero :

$$w_a + w_b = 0, \quad w_a w_b + \sinh^2 \Gamma = 0.$$

It is convenient to substitute for this case

$$w_k = \frac{K_1}{Z_2}, \quad w_a = -w_k, \quad w_b = w_k.$$

Then the two coefficients vanish when $w_k = \sinh \Gamma$. Since

$$\cosh \Gamma = 1 + \frac{Z_1}{2Z_2} : \sinh \Gamma = \sqrt{\frac{Z_1}{Z_2}} \sqrt{1 + \frac{Z_1}{4Z_2}},$$

$$\cosh \frac{1}{2} \Gamma = \sqrt{1 + \frac{Z_1}{4Z_2}},$$

and therefore

$$K_1 = \sqrt{Z_1 Z_2} \sqrt{1 + \frac{Z_1}{4Z_2}} = \sqrt{Z_1 Z_2} \cdot \cosh \frac{1}{2} \Gamma$$

is the required impedance.

3. *Propagation Exponent* of Infinite Line.*—The finite line behaves as the same number of sections in an infinite line when either or both of the terminating impedances are made equal to the iterative impedance, thereby avoiding repeated terminal reflexions. We have

$Z_a = K_1$, $w_a = w_k = \sinh \Gamma$; and (or) $Z_b = K_1$, $w_b = w_k = \sinh \Gamma$,
so that Eq. (15) reduces to the simple form

$$\frac{G_n}{G_1} = \frac{w_a + w_b}{D_n(a, b)} = \exp - (n-1)\Gamma, \quad \frac{G_2}{G_1} = \exp - \Gamma. \quad (1)$$

The latter equation defines the propagation exponent Γ in terms of the voltage ratio across a single section, while the former equation gives the voltage ratio across $(n-1)$ sections, in an infinite line.

The propagation exponent is complex in general, and we write $\Gamma = A + iB$, where the attenuation exponent A accounts for changes in magnitude of the voltage from section to section, and the phase angle B accounts for the corresponding phase displacements.

* The usual term "propagation constant" is misleading, since the quantity is not constant but a function of the frequency. In such cases the terms "coefficient," "factor," etc., are to be preferred, since they are descriptive, and do not imply constancy.

The "velocity of propagation" may be defined as

$$V = \frac{\omega}{B} \text{ (sections per second).}$$

If an irregular wave is to be transmitted without distortion, the velocity must be independent of the frequency, which requires that the phase angle vary in proportion to the frequency.

The ideal wave-filter is non-dissipative. By this we mean that there is no power dissipation in the filter sections, but only the unavoidable or required dissipation in the terminating circuits. In this case Z_1 and Z_2 are imaginary, as explained in Part VI., making w real. The field of w is then logically divided into three parts, in which Γ is real, imaginary, and complex respectively. The frequency bands of the filter may be classified in this way, since each value of w corresponds to one or more frequencies. Such a classification follows.

Direct-suppression (stop) bands :

$$\begin{aligned} +\infty \geq w \geq +1, \quad +\infty \geq A \geq 0, \quad B = 0, \\ w = \cosh \Gamma = \cosh A, \quad \sinh \Gamma = \sinh A, \\ \cosh \frac{1}{2}\Gamma = \cosh \frac{1}{2}A, \quad \sinh \frac{1}{2}\Gamma = \sinh \frac{1}{2}A. \end{aligned}$$

Transmission (pass) bands :

$$\begin{aligned} +1 \geq w \geq -1, \quad A = 0, \quad 0 \leq B \leq \pi, \\ w = \cosh \Gamma = \cos B, \quad \sinh \Gamma = i \cdot \sin B, \\ \cosh \frac{1}{2}\Gamma = \cos \frac{1}{2}B, \quad \sinh \frac{1}{2}\Gamma = i \cdot \sin \frac{1}{2}B. \end{aligned}$$

Reverse-suppression (stop) bands :

$$\begin{aligned} -1 \geq w \geq -\infty, \quad 0 \leq A \leq +\infty, \quad B = \pi, \\ w = \cosh \Gamma = -\cosh A, \quad \sinh \Gamma = -\sinh A, \\ \cosh \frac{1}{2}\Gamma = i \cdot \sinh \frac{1}{2}A, \quad \sinh \frac{1}{2}\Gamma = i \cdot \cosh \frac{1}{2}A. \end{aligned}$$

In the transmission bands the attenuation is zero ; in the direct- and reverse-suppression bands, respectively, there is attenuation without or with reversal of polarity across each section. The boundary between a transmission and an adjacent suppression band, $w = \pm 1$, corresponds to a cut-off frequency f_c . The boundary between adjacent direct- and reverse-suppression bands, $w = \pm \infty$, corresponds to a frequency f_∞ of infinite attenuation.

4. *Response of Non-Dissipative Finite Lines with Resistance Terminations.*—In the absence of the theory of the present paper, Eq. (1) has been used as an approximate solution for the finite line, nearly correct when the terminating impedances are approximately equal to the iterative impedance. The errors in the approximate solution will appear in the following discussion.

We will proceed to derive the response formulæ for non-dissipative filters with a finite number of sections and with resistance terminations. The non-dissipative condition can be nearly realized in practice, so these formulæ will represent very nearly the actual performance of such filters. In these cases Z_1 and Z_2 are imaginary, while $Z_a = R_a$ and $Z_b = R_b$ are real, so that we have w real, w_a and w_b imaginary. The response formula is then given by Eq. (16), since

$$\left| \frac{G_1}{G_n} \right|^2 = \left| \frac{D_n(a, b)}{w_a + w_b} \right|^2.$$

On substituting

$$w_a = \frac{R_a}{Z_2}, \quad w_b = \frac{R_b}{Z_2}, \quad \text{and} \quad \sinh \Gamma = w_k = \frac{K_1}{Z_2},$$

we have

$$\left| \frac{G_1}{G_n} \right|^2 = 1 - \frac{(R_a^2 - K_1^2)(R_b^2 - K_1^2)}{(R_a + R_b)^2 K_1^2} \sinh^2 (n-1) \Gamma. \quad (2)$$

In transmission bands this becomes

$$\left| \frac{G_1}{G_n} \right|^2 = 1 + \frac{(R_a^2 - K_1^2)(R_b^2 - K_1^2)}{(R_a + R_b)^2 K_1^2} \sin^2 (n-1) B. \quad (3)$$

When $R_a = R_{ab} = R_b$, these formulæ simplify to

$$\left| \frac{G_1}{G_n} \right|^2 = 1 - \frac{1}{4} \left(\frac{R_{ab}}{K_1} - \frac{K_1}{R_{ab}} \right)^2 \sinh^2 (n-1) \Gamma, \quad \dots \quad (4)$$

and, in transmission bands,

$$\left| \frac{G_1}{G_n} \right|^2 = 1 + \frac{1}{4} \left(\frac{R_{ab}}{K_1} - \frac{K_1}{R_{ab}} \right)^2 \sin^2 (n-1) B. \quad \dots \quad (5)$$

These formulæ will be applied to examples of two classes of filter designs, the constant-K class and the M-derived class.

The constant-K class of filter structures, due to Campbell, is characterized by the condition

$$\sqrt{Z_1 Z_2} = K_c \text{ (constant, real).}$$

Fig. 3 shows a filter of this class:

$$Z_1 = i\omega L_2, \quad Z_2 = \frac{1}{i\omega C_2}, \quad K_c = \frac{L_1}{C_2}.$$

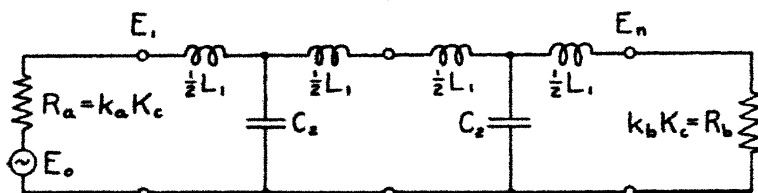
The cut-off frequencies are determined by

$$w = 1 - \frac{1}{2}\omega^2 L_1 C_2 = \pm 1 : \omega_c = 0, \quad \frac{2}{\sqrt{L_1 C_2}}.$$

Since one cut-off frequency is zero, this design is called a low-pass filter. Because of its simplicity, it will be used as an example in the succeeding developments. Formulæ derived in terms of Γ are readily translated to ω by noting that

$$\frac{\omega}{\omega_c} = \frac{1 - \cosh \Gamma}{2}, \quad \frac{\omega}{\omega_c} = \pm i \cdot \sinh \frac{1}{2} \Gamma.$$

Fig. 3.



Low-pass filter, constant-K class, mid-series terminations.

In transmission band, $\frac{\omega}{\omega_c} = \sin \frac{1}{2} B$; in reverse-suppression band $\frac{\omega}{\omega_c} = \cosh \frac{1}{2} A$.

Having defined the constant-K class, and given a low-pass filter as an example, we proceed to develop response formulæ applying to all filters in this class. Since K_c is constant and real, the iterative impedance and the terminating impedances are conveniently expressed in terms of K_c :

$$K_1 = K_c \cosh \frac{1}{2} \Gamma, \quad Z_a = R_a = k_a K_c, \quad Z_b = R_b = k_b K_c.$$

Substituting in Eq. (2), we find

$$\left| \frac{G_1}{G_n} \right|^2 = 1 - \frac{(k_a^2 - \cosh^2 \frac{1}{2} \Gamma)(k_b^2 - \cosh^2 \frac{1}{2} \Gamma)}{(k_a + k_b)^2 \cosh^2 \frac{1}{2} \Gamma} \sinh^2 (n-1) \Gamma. \quad (6)$$

This simplifies for $k_a = k_b = 1$ to

$$\left| \frac{G_1}{G_n} \right|^2 = 1 - \frac{\sinh^4 \frac{1}{2} \Gamma}{4 \cosh^2 \frac{1}{2} \Gamma} \sinh^2 (n-1) \Gamma. \quad (7)$$

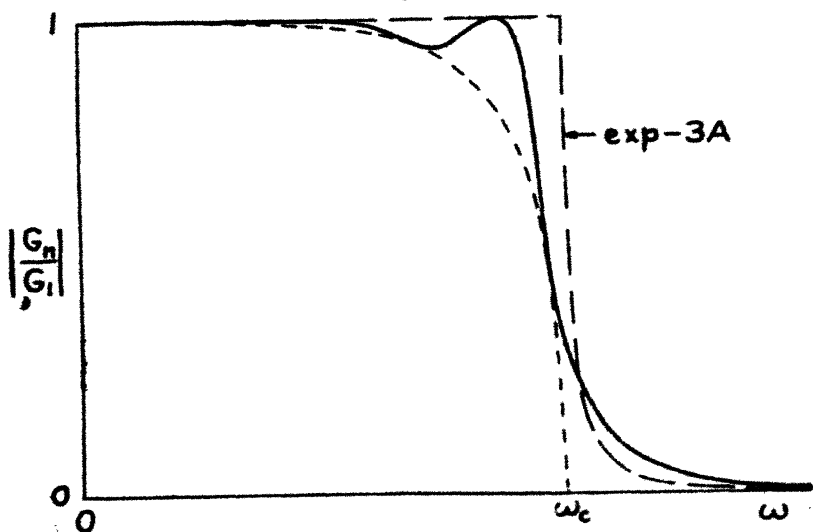
While the above expressions are real, they involve imaginary quantities, so that for computations it is desirable to write an individual formula in terms of the variable component of Γ in each class of frequency bands. Making the necessary substitutions in Eq. (7), for example, we have the following expressions for the several frequency bands.

Direct-suppression bands: This case is impossible in the constant-K class of filters because Z_1 and Z_2 are imaginary and $Z_1 Z_2$ is real, making Z_1/Z_2 negative and $w \leq 1$.

Transmission bands: ($K_1 = K_c \cos \frac{1}{2}B$).

$$\left| \frac{G_1}{G_n} \right|^2 = 1 + \frac{\sin^4 \frac{1}{2}B}{4 \cdot \cos^2 \frac{1}{2}B} \cdot \sin^2 (n-1)B. \quad (8)$$

Fig. 4.



Response curve of three-section low-pass filter, constant-K class,
 $R_a = R_b = K_c$.

Reverse-suppression bands: ($K_1 = iK_c \sinh \frac{1}{2}A$).

$$\left| \frac{G_1}{G_n} \right|^2 = 1 + \frac{\cosh^4 \frac{1}{2}A}{4 \cdot \sinh^2 \frac{1}{2}A} \cdot \sinh^2 (n-1)A. \quad (9)$$

Indeterminate value:

$$A=0: \frac{\sinh^2 (n-1)A}{4 \cdot \sinh^2 \frac{1}{2}A} = (n-1)^2; \quad \left| \frac{G_1}{G_n} \right|^2 = 1 + (n-1)^2. \quad (10)$$

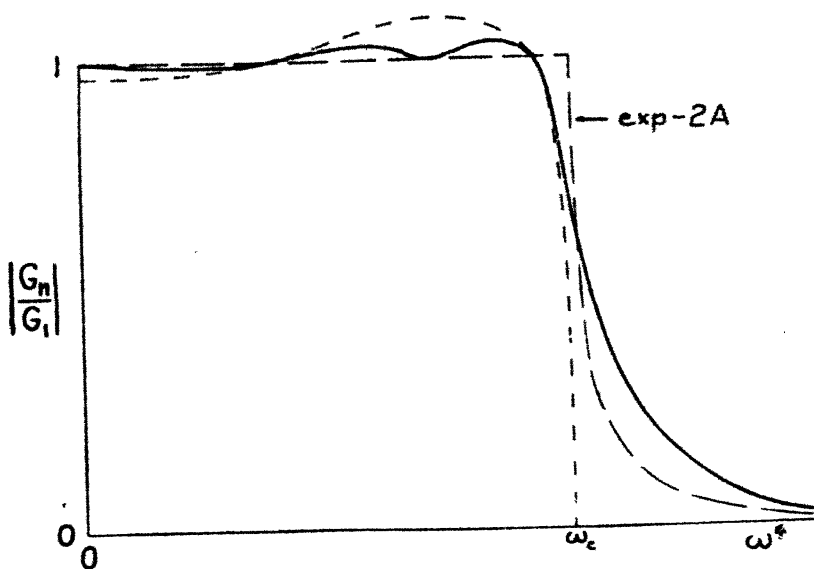
Fig. 4 is the response curve of a three-section, low-pass filter with $R_a = R_b = K_c$, computed by formulæ (8), (9),

and (10). The dashed line ($\exp -3A$) is the approximate curve based on the voltage ratio across the same number of sections in an infinite line, Eq. (1). The dotted line shows the maximum deviation from unity of the response curve for any number of sections. The computed response curve, within the transmission band, oscillates $(n-1)$ times between the dotted curve and unity.

From Eq. (6) it is apparent that the coefficient of $\sin^2(n-1)B$ can be made to vanish at two values of B , within the transmission bands, by making

$$k_a = \cos \frac{1}{2}B_a, \quad k_b = \cos \frac{1}{2}B_b.$$

Fig. 5.



Response curve of two-section low-pass filter, constant-K class,
 $k_a = \cos \frac{3}{4}\pi$, $k_b = \cos \frac{1}{4}\pi$.

The departure from unity of the response curve can be reduced to a minimum by making this coefficient vanish at two values of B for which $\sin^2(n-1)B$ has its maximum value unity. Fig. 5 is a response curve of a two-section, low-pass filter following this plan, computed by Eq. (6). The value of $\sin^2 2B$ is unity when $2B = \frac{1}{2}\pi$ or $\frac{3}{2}\pi$; we take $B_a = \frac{3}{4}\pi$ and $B_b = \frac{1}{4}\pi$, so that $\cos \frac{1}{2}B_a = k_a = 0.38$, $\cos \frac{1}{2}B_b = k_b = 0.92$.

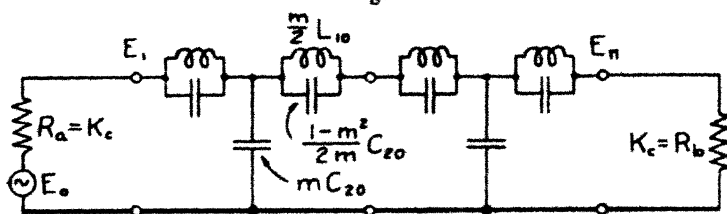
The second term in the response formulæ is the result of repeated terminal reflexions when neither terminating impedance is equal to the iterative impedance. In the foregoing example such reflexions were reduced to a minimum by the choice of terminating resistance values.

The M-derived class of filter structure, due to Zobel (*loc. cit.*), more closely approximates a constant iterative impedance. Any structure (Z_1, Z_2) in this class is derived from the corresponding constant-K structure (Z_{10}, Z_{20}) by the following substitutions :

$$\frac{1}{Z_1} = \frac{1}{mZ_{10}} + \frac{1-m^2}{4mZ_{20}}, \quad Z_2 = \frac{Z_{20}}{m}, \quad 0 \leq m \leq 1.$$

The derived Z_1 comprises the two impedances, mZ_{10} and $\frac{4mZ_{20}}{1-m^2}$, connected in parallel. Fig. 6 shows the low-pass filter derived from the constant-K structure of fig. 3.

Fig. 6.



Low-pass filter, M-derived class, mid-series terminations.

— We will proceed to derive the response formulæ for the M-derived class of filters having

$$R_a = R_b = R^{ab} = K_c = \sqrt{Z_{10}Z_{20}} \text{ (constant, real).}$$

It is required to know the iterative impedance K_1 , expressed in terms of K_c and Γ , for substitution in Eq. (4). Since

$$K_1 = \sqrt{Z_1 Z_2} \cdot \cosh \frac{1}{2} \Gamma,$$

$$\frac{K_1}{R^{ab}} = \cosh \frac{1}{2} \Gamma \sqrt{\frac{Z_1}{Z_{10}} \cdot \frac{Z_2}{Z_{20}}} = \frac{\cosh \frac{1}{2} \Gamma}{\sqrt{1 + (1-m^2) \frac{Z_{10}}{4Z_{20}}}}.$$

Recalling that

$$\cosh \Gamma = 1 + \frac{Z_1}{2Z_2},$$

we have

$$\sinh^2 \frac{1}{2} \Gamma = \frac{\cosh \Gamma - 1}{2} = \frac{Z_1}{4Z_2} = \frac{Z_{10}}{4Z_{20}} \cdot \frac{m^2}{1 + (1-m^2) \frac{Z_{10}}{4Z_{20}}},$$

from which

$$1 + (1-m^2) \frac{Z_{10}}{4Z_{20}} = \frac{1}{1 - \frac{1-m^2}{m^2} \sinh^2 \frac{1}{2} \Gamma}.$$

This gives

$$\frac{K_1}{R_{ab}} = \cosh \frac{1}{2} \Gamma \sqrt{1-c} \sinh^2 \frac{1}{2} \Gamma,$$

$$\text{where} \quad c = \frac{1-m^2}{m^2}.$$

Then

$$\frac{R_{ab}}{K_1} - \frac{K_1}{R_{ab}} = \frac{1 - \left(\frac{K_1}{R_{ab}}\right)^2}{\frac{K_1}{R_{ab}}} = - \frac{\sinh^2 \frac{1}{2} \Gamma (1-c \cosh^2 \frac{1}{2} \Gamma)}{\cosh \frac{1}{2} \Gamma \sqrt{1-c} \sinh^2 \frac{1}{2} \Gamma}.$$

Substituting in Eq. (4),

$$\left| \frac{G_1}{G_n} \right|^2 = 1 - \frac{\sinh^2 \frac{1}{2} \Gamma (1-c \cosh^2 \frac{1}{2} \Gamma)^2}{4 \cosh^2 \frac{1}{2} \Gamma (1-c \sinh^2 \frac{1}{2} \Gamma)} \cdot \sinh^2 (n-1) \Gamma. \quad (11)$$

The M-derived and constant-K classes merge when $k_a = k_b = 1$ and $m = 1$, $c = 0$, making Eqs. (7) and (11) identical.

This last formula simplifies somewhat when

$$m = \frac{1}{\sqrt{3}} = 0.58, \quad c = \frac{1-m^2}{m^2} = 2,$$

and this value is in accord with design practice. Making this substitution in Eq. (11),

$$\left| \frac{G_1}{G_n} \right|^2 = 1 - \frac{\sinh^4 \frac{1}{2} \Gamma \cosh^2 \Gamma}{4 \cosh^2 \frac{1}{2} \Gamma (1-2 \sinh^2 \frac{1}{2} \Gamma)} \cdot \sinh^2 (n-1) \Gamma. \quad (12)$$

Fig. 7 is a response curve of a three-section, low-pass filter of this design, showing a close approximation between the actual curve given by Eq. (12) and the dashed curve ($\exp - 3A$). This response curve very closely approaches the ideal condition of uniform response within the transmission band and immediate cut-off at the edge of the band.

With Γ as the independent variable, it is necessary, before plotting the curve, to express the abscissas in terms of frequency. The cut-off frequencies of the M-derived

158 Mr. Wheeler and Prof. Murnaghan on the Theory of structures are equal to those of the corresponding constant-K structures. For the filter (L_{10} , C_{20}) of figs. 6 and 7,

$$w = 1 + \frac{Z_1}{2Z_2} = 1 + \frac{Z_{10}}{2Z_{20}} \frac{m^2}{1 + (1-m^2) \frac{Z_{10}}{4Z_{20}}} = \pm 1$$

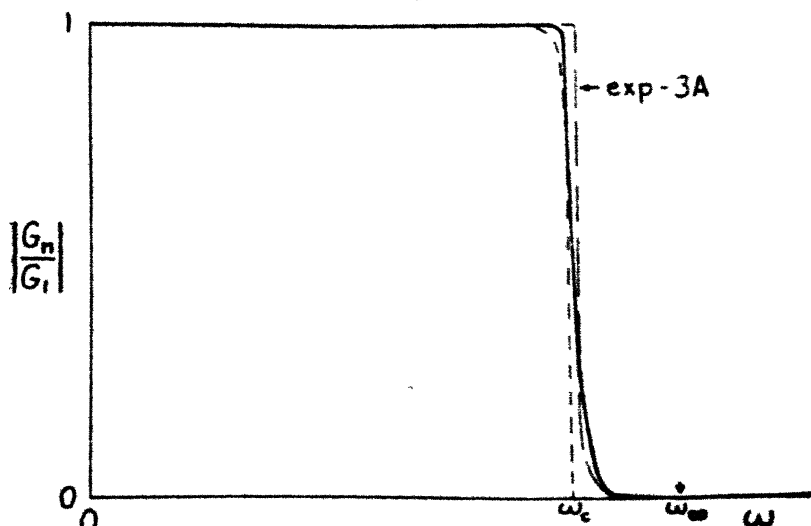
gives

$$-\frac{Z_{10}}{4Z_{20}} = \frac{\omega^2 L_{10} C_{20}}{4} = 0, 1 \text{ and } \omega_c = 0, \frac{2}{\sqrt{L_{10} C_{20}}}.$$

Then, from the preceding results,

$$\frac{\omega^2}{\omega_c^2} = -\frac{Z_{10}}{4Z_{20}} = \frac{-\sinh^2 \frac{1}{2} \Gamma}{m^2 - (1-m^2) \sinh^2 \frac{1}{2} \Gamma}$$

Fig. 7.



Response curve of three-section low-pass filter, M-derived class,
 $m = 1/\sqrt{3}$.

gives the variation of frequency with F . In the transmission band,

$$\frac{\omega^2}{\omega_c^2} = \frac{\sin^2 \frac{1}{2} B}{m^2 + (1-m^2) \sin^2 \frac{1}{2} B};$$

in the reverse-suppression band,

$$\frac{\omega^2}{\omega_c^2} = \frac{\cosh^2 \frac{1}{2} A}{m^2 + (1-m^2) \cosh^2 \frac{1}{2} A};$$

160 Mr. Wheeler and Prof. Murnaghan on the Theory of these equations take the form

$$\begin{aligned}(w + w_a)E_1 - E_2 &= w_a E_0 \\ &\dots \dots \dots \\ -E_{k-1} + 2wE_k - E_{k+1} &= 0 \\ &\dots \dots \dots \\ -E_{n-1} + (w + w_b)E_n &= 0.\end{aligned}$$

The determinant of the coefficients is $D_n(a, b)$, as before, and the cofactor of the element in the first row and last column being unity, we have

$$E_n = \frac{w_a E_0}{D_n(a, b)}.$$

The response ratio is found as before; thus

$$\begin{aligned}G_n = \frac{E_n}{E_0} &= \frac{w_a}{D_n(a, b)}, \quad G_1 = \frac{E_{n-1}}{E_0} = \frac{Z_b}{Z_a + Z_b} = \frac{w_a}{w_a + w_b}, \\ \frac{G_n}{G_1} &= \frac{w_a + w_b}{D_n(a, b)}.\end{aligned}$$

This relative response ratio is equal to that of Part II., and its reciprocal is given by Eqs. (14) and (15).

The only real difference between the analysis of the mid-shunt structure and that of the mid-series structure is the difference in the substitutions w_a and w_b ; the necessary modifications of the solutions in Part II. will be described briefly.

2. *Iterative Impedance.*—The mid-shunt iterative impedance is denoted by K_2 . Corresponding to the mid-series solution,

$$\frac{Z_1}{K_2} = w_k = \sinh \Gamma, \quad K_2 = \frac{\sqrt{Z_1 Z_2}}{\sqrt{1 + \frac{Z_1}{4Z_2}}} = \frac{\sqrt{Z_1 Z_2}}{\cosh \frac{1}{2} \Gamma}.$$

3. *Propagation Exponent.*—Since w is the same for both structures, there is no change in the propagation exponent Γ , determined by

$$\cosh \Gamma = w = 1 + \frac{Z_1}{2Z_2}.$$

4. *Response of Finite Lines.*—The general response formulæ given by Eqs. (2) to (5), in terms of K_1 , are also

correct for the mid-shunt case, substituting K_2 for K_1 . The formulæ given for the constant-K class of filters are correct for the latter case, after substituting the following definitions of k_a and k_b :

$$Z_a = R_a = \frac{K_c}{k_a}, \quad Z_b = R_b = \frac{K_c}{k_b}.$$

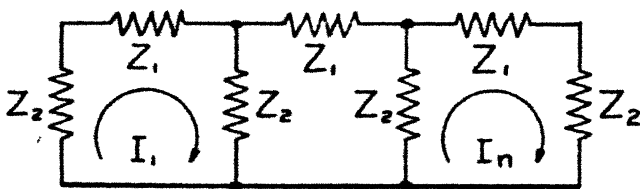
Therefore figs. 4 and 5 apply interchangeably to both structures.

The M-derived class of filters requires a different recurrent structure for mid-shunt termination, which will not be described here; but, with this modification, the same formulæ and the curve of fig. 7 are applicable.

IV. FREE OSCILLATIONS IN CONSERVATIVE LINES.

1. *The Solution for a Recurrent Line.*—The problem of free oscillations in conservative lines is generally familiar,

Fig. 9.



Simple recurrent line with open ends, $(2n+1)$ elements.

and it was in the solution of this problem that the elementary wave-filter determinant had its origin. After describing the simple case, two further cases will be treated, each of which has an element of novelty. The determinants referred to are treated in Part V.

The classical example of the recurrent line is the periodically loaded string; in solving this problem, Lord Rayleigh evaluated the determinant D_n . The electric line shown in fig. 9 presents the same problem; we shall solve for its natural frequencies of oscillation. Proceeding as in Part II., we have a system of n linear equations in terms of the currents, I_1, I_2, \dots, I_n , in the successive meshes of the line. On substituting

$$\cosh \Gamma = w = 1 + \frac{Z_1}{2Z_2},$$

162 Mr. Wheeler and Prof. Murnaghan on the Theory of
as before, the equations take the form

$$\begin{aligned} 0 &= 2wI_1 - I_2 \\ &\dots \dots \dots \\ 0 &= -I_{k-1} + 2wI_k - I_{k+1} \\ &\dots \dots \dots \\ 0 &= -I_{n-1} + 2wI_n. \end{aligned}$$

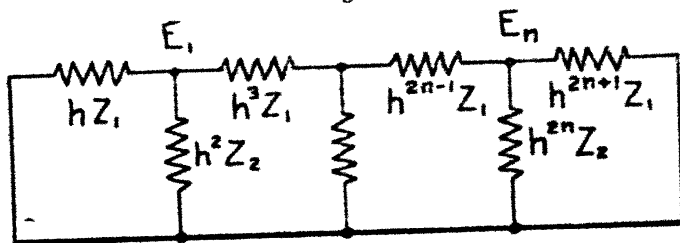
The determinant of the coefficients is D_n , and the condition for solutions other than zero is that

$$0 = D_n = \frac{\sinh(n+1)\Gamma}{\sinh \Gamma},$$

which is satisfied only when $\Gamma = iB$, $A = 0$; hence

$$\frac{\sin(n+1)B}{\sin B} = 0,$$

Fig. 10.



Exponential line with closed ends, $(2n+1)$ elements.

so that

$$B = \frac{k\pi}{n+1}, \quad k = 1, 2, \dots n.$$

For any given structure (Z_1, Z_2) there are one or more natural frequencies corresponding to each of the n solutions for B .

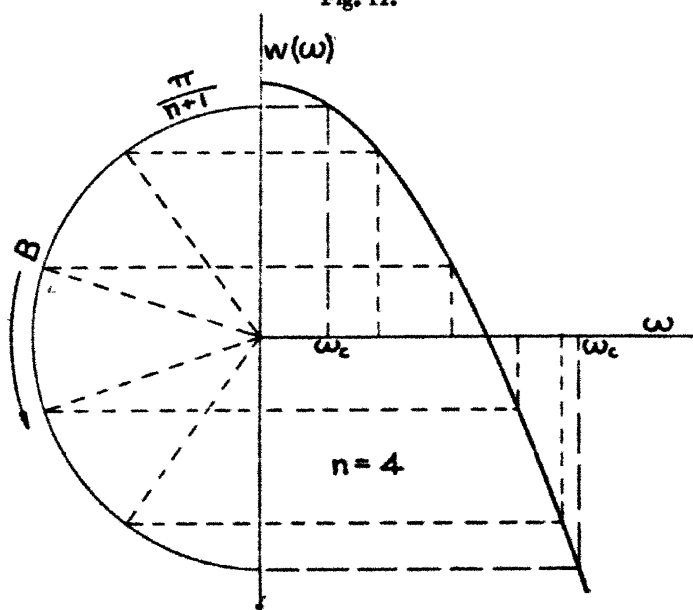
Graphical solutions for the natural frequencies will be given for the two succeeding cases, which are more novel and interesting. It is important to note that the natural frequencies depend on the number of elements in the line, but lie within bands bounded by the cut-off frequencies ω_c , which are independent of the number of sections, depending only on the properties of the recurrent structure.

2. *Exponential Line with Closed Ends.*—Fig. 10 shows an exponential line similar to the simple recurrent line, but

164 Mr. Wheeler and Prof. Murnaghan on the Theory of
in the line, the solutions all lie between the cut-off
frequencies ω_c corresponding to $w = \pm 1$.

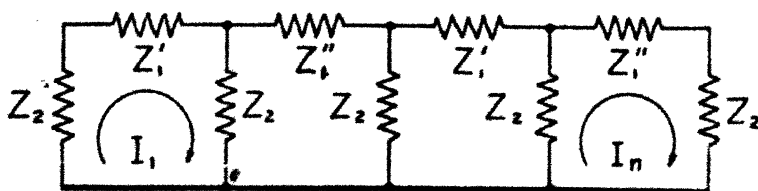
These free oscillations may be regarded as standing waves
resulting from terminal reflexions, which are avoided, as far
possible, in the design of wave filters. From this explanation

Fig. 11.



Graphical solution for natural frequencies of exponential line (L_1, C_2).

Fig. 12.



Alternating line with open ends, $(2n+1)$ elements.

it is an immediate consequence that the natural frequencies
lie within the transmission bands of the line.

3. *Alternating Line with Open Ends.*—Fig. 12 shows an
alternating line, similar to the simple recurrent line, but
built up of two different sections recurring in alternating

succession along the line. This type of line is suggested by a doubly loaded string described by Born and von Kármán*. The procedure in this case is the same as before. Upon introduction of the notation

$$w' = 1 + \frac{Z_1'}{2Z_2}, \quad w'' = 1 + \frac{Z_1''}{2Z_2},$$

the n linear equations for the currents in the various meshes of the network take the form

$$\begin{aligned} 0 &= 2w'I_1 - I_2 \\ 0 &= -I_1 + 2w''I_2 - I_3 \\ 0 &= -I_2 + 2w'I_3 - I_4 \\ &\dots \dots \dots \\ 0 &= -I_{n-1} + 2w''I_n. \end{aligned}$$

The determinant of the coefficients is ' D_n ', so that the natural frequencies are determined by

$$0 = 'D_n'' = \frac{\sinh(n+1)\Gamma}{\sinh \Gamma}, \quad \cosh \Gamma = \sqrt{w'w''}.$$

This condition is satisfied when $\Gamma = iB$, $A = 0$:

$$0 = \frac{\sin(n+1)B}{\sin B}, \quad B = \frac{k\pi}{n+1}, \quad k=1, 2, \dots n.$$

The graphical solution, based on these values of B , is shown in fig. 13 for the structure $Z_1 = i\omega L_1$, $Z_2 = \frac{1}{i\omega C_2}$. The natural frequencies lie in two bands bounded by the cut-off frequencies ω_c .

V. WAVE-FILTER DETERMINANTS.

1. *Elementary Form.*—The simplest form of wave-filter determinant arises from the analysis of the type of line shown in fig. 9, described in Part IV. Denoting it by D_n , we have

$$D_n = \begin{vmatrix} 2w & -1 & 0 & \dots & 0 \\ -1 & 2w & -1 & \dots & 0 \\ 0 & -1 & 2w & \dots & 0 \\ \dots & \dots & \dots & \dots & \dots \\ 0 & 0 & 0 & \dots & 2w \end{vmatrix} \quad (n \geq 1).$$

nth
order

* *Phys. Zeit.* xiii. p. 303 (1912).

It is important to note that the cofactor of the element in the first row and last column of D_n is unity :

$$(-1)^{n-1} \begin{vmatrix} -1 & 2w & -1 & \dots & 0 \\ 0 & -1 & 2w & \dots & 0 \\ 0 & 0 & -1 & \dots & 0 \\ \vdots & \vdots & \vdots & \ddots & \vdots \\ 0 & 0 & 0 & \dots & -1 \end{vmatrix} = (-1)^{2n-2} = 1.$$

(n-1)th
order

2. *Mid-Termination Form.*—The most useful wave-filter determinant is that which arises from the filters shown in figs. 1 and 8, Parts II. and III. This determinant is

$$D_n(a, b) = \begin{vmatrix} w+w_a & -1 & 0 & \dots & 0 \\ -1 & 2w & -1 & \dots & 0 \\ 0 & -1 & 2w & \dots & 0 \\ \vdots & \vdots & \vdots & \ddots & \vdots \\ 0 & 0 & 0 & \dots & w+w_b \end{vmatrix} \quad (n \geq 2),$$

nth
order

which is similar to one evaluated by Pupin (*loc. cit.*) by a method of infinite series. $D_n(a, b)$ is readily expressed in terms of D_n . Writing the terminal elements of the principal diagonal in the forms $2w + (w_a - w)$ and $2w + (w_b - w)$, it appears that $D_n(a, b)$ is the sum of four determinants:

$$D_n(a, b) = D_n + (w_a - w)D_{n-1} + (w_b - w)D_{n-1} + (w_a - w)(w_b - w)D_{n-2}.$$

But

$$D_n - 2wD_{n-1} = -D_{n-2}, \quad w = \cosh \Gamma, \quad D_n = \frac{\sinh(n+1)\Gamma}{\sinh \Gamma}, \text{ etc.}$$

Hence

$$\begin{aligned} D_n(a, b) &= (w_a + w_b)(D_{n-1} - wD_{n-2}) + (w_a w_b + w^2 - 1)D_{n-2} \\ &= (w_a + w_b) \frac{\sinh n\Gamma - \cosh \Gamma \sinh(n-1)\Gamma}{\sinh \Gamma} \\ &\quad + (w_a w_b + \sinh^2 \Gamma) \frac{\sinh(n-1)\Gamma}{\sinh \Gamma}. \end{aligned}$$

Also

$$\begin{aligned} \sinh n\Gamma - \cosh \Gamma \cdot \sinh(n-1)\Gamma &= \frac{1}{2} \cdot \sinh n\Gamma - \frac{1}{2} \cdot \sinh(n-2)\Gamma \\ &= \sinh \Gamma \cdot \cosh(n-1)\Gamma, \end{aligned}$$

so that

$$\begin{aligned} D_n(a, b) &= (w_a + w_b) \cosh(n-1)\Gamma \\ &\quad + \frac{w_a w_b + \sinh^2 \Gamma}{\sinh \Gamma} \sinh(n-1)\Gamma. \quad (13) \end{aligned}$$

The most convenient and useful expressions of this result are

$$\frac{D_n(a, b)}{w_a + w_b}$$

$$= \cosh(n-1)\Gamma + \frac{w_a w_b + \sinh^2 \Gamma}{(w_a + w_b) \sinh \Gamma} \sinh(n-1)\Gamma \quad (14)$$

$$= \exp(n-1)\Gamma + \frac{(w_a - \sinh \Gamma)(w_b - \sinh \Gamma)}{(w_a + w_b) \sinh \Gamma} \sinh(n-1)\Gamma, \quad (15)$$

since $\cosh(n-1)\Gamma + \sinh(n-1)\Gamma = \exp(n-1)\Gamma$.

For use in the analysis of non-dissipative filters, Parts II. and III., the modulus of this complex expression is required in the case of

w real, w_a and w_b imaginary.

This makes $\cosh(n-1)\Gamma$, $w_a w_b$, $\sinh^2 \Gamma$, and $\frac{\sinh(n-1)\Gamma}{\sinh \Gamma}$ all real, so that in (14) the first term is real and the second term is imaginary. Multiplying (14) by its conjugate imaginary, the square of the modulus is

$$\begin{aligned} & \left| \frac{D_n(a, b)}{w_a + w_b} \right|^2 \\ &= \cosh^2(n-1)\Gamma - \left[\frac{w_a w_b + \sinh^2 \Gamma}{(w_a + w_b) \sinh \Gamma} \right]^2 \sinh^2(n-1)\Gamma \\ &= \cosh^2(n-1)\Gamma \\ & \quad - \left[\frac{(w_a - \sinh \Gamma)(w_b - \sinh \Gamma)}{(w_a + w_b) \sinh \Gamma} + 1 \right]^2 \sinh^2(n-1)\Gamma \\ &= 1 - \frac{(w_a - \sinh \Gamma)(w_b - \sinh \Gamma)}{(w_a + w_b) \sinh \Gamma} \\ & \quad \times \left[\frac{w_a - \sinh \Gamma}{(w_a + w_b) \sinh \Gamma} (w_b - \sinh \Gamma) + 2 \right] \sinh^2(n-1)\Gamma \\ &= 1 - \frac{(w_a^2 - \sinh^2 \Gamma)(w_b^2 - \sinh^2 \Gamma)}{(w_a + w)^2 \sinh^2 \Gamma} \sinh^2(n-1)\Gamma. \quad (16) \end{aligned}$$

When $\sinh \Gamma = 0$, the indeterminate forms are evaluated by making

$$\frac{\sinh^2(n-1)\Gamma}{\sinh^2 \Gamma} = (n-1)^2.$$

3. *Exponential Line Form.*—This determinant arises from the exponential type of line shown in fig. 10, Part IV.:

$$D_n(\text{exp}) = \begin{vmatrix} 2w & -1/h & 0 & \dots & 0 \\ -h & 2w & -1/h & \dots & 0 \\ 0 & -h & 2w & \dots & 0 \\ \cdot & \cdot & \cdot & \cdot & \cdot \\ \text{nth} & & & & \\ \text{order} & 0 & 0 & 0 & \dots & 2w \end{vmatrix} \quad (n \geq 1).$$

Expanding in terms of the first row, we have

$$D_n(\text{exp}) = 2wD_{n-1}(\text{exp}) - D_{n-2}(\text{exp}).$$

Also we note that $D_1(\text{exp}) = D_1$, $D_2(\text{exp}) = D_2$, etc., so we conclude that

$$D_n(\text{exp}) = D_n.$$

The cofactors in $D_n(\text{exp})$, however, are different in general from those in D_n .

4. *Alternating Line Forms.*—The alternating line of the type shown in fig. 12, Part IV., gives rise to determinants similar to D_n , but with two elements in alternating succession along the principal diagonal. These forms are indispensable to some problems, and are capable of manipulation similar to the foregoing treatment of the elementary form. There are four distinct forms under this heading, differentiated by the different pairs of elements in the terminal positions of the principal diagonals:

$$'D_n'' = \begin{vmatrix} 2w' & -1 & 0 & \dots & 0 \\ -1 & 2w'' & -1 & \dots & 0 \\ 0 & -1 & 2w' & \dots & 0 \\ \cdot & \cdot & \cdot & \cdot & \cdot \\ \text{nth} & & & & \\ \text{order} & 0 & 0 & 0 & \dots & 2w'' \end{vmatrix} \quad (n \text{ even}, \geq 2),$$

$$'D_n' = \begin{vmatrix} 2w' & -1 & 0 & \dots & 0 \\ -1 & 2w'' & -1 & \dots & 0 \\ 0 & -1 & 2w' & \dots & 0 \\ \cdot & \cdot & \cdot & \cdot & \cdot \\ \text{nth} & & & & \\ \text{order} & 0 & 0 & 0 & \dots & 2w' \end{vmatrix} \quad (n \text{ odd}, \geq 1).$$

Then $'D_n'$ and $'D_n''$ are the same as $'D_n''$ and $'D_n'$ respectively, except that w' and w'' are interchanged.

Expanding as in the case of D_n , we have the equations

$$\begin{aligned} 'D_n'' &= 2w' \cdot ''D_{n-1}'' - 'D_{n-2}'', \\ ''D_{n-1}'' &= 2w'' \cdot 'D_{n-2}' - ''D_{n-3}'', \\ 'D_{n-2}' &= 2w' \cdot ''D_{n-3}'' - 'D_{n-4}'. \end{aligned}$$

Multiplying the second equation by $2w'$, and adding all three, we have $'D_n'' = 2(2w'w'' - 1)'D_{n-2}'' - 'D_{n-4}''$, a difference equation in $'D_n''$. Proceeding as before, taking the trial solution $'D_n'' = cx^n$ (c any constant), we have for x the biquadratic equation $x^4 - 2(2w'w'' - 1)x^2 + 1 = 0$, giving

$$x^2 = (2w'w'' - 1) \pm \sqrt{(2w'w'' - 1)^2 - 1}.$$

Making the substitution

$$2w'w'' - 1 = \cosh 2\Gamma, \quad \sqrt{w'w''} = \cosh \Gamma,$$

we have

$$x^2 = \cosh 2\Gamma \pm \sinh 2\Gamma = \exp \pm 2\Gamma, \quad x = \exp \pm \Gamma.$$

Then $'D_n''$ is a linear combination of $\exp n\Gamma$ and $\exp -n\Gamma$, or of $\cosh n\Gamma$ and $\sinh n\Gamma$: $'D_n'' = c_1 \cosh n\Gamma + c_2 \sinh n\Gamma$. c_1 and c_2 are determined by the "initial conditions," as before, $c_1 = 1$ and $c_2 = \coth \Gamma$, so that

$$'D_n'' = \frac{\sinh(n+1)\Gamma}{\sinh \Gamma}.$$

Interchanging w' and w'' makes no difference, so that also

$$''D_n' = \frac{\sinh(n+1)\Gamma}{\sinh \Gamma}.$$

Following a similar procedure, we have

$$'D_n' = c_1 \cosh n\Gamma + c_2 \sinh n\Gamma,$$

$$c_1 = \sqrt{w'/w''}, \quad c_2 = \sqrt{w'/w''} \cdot \coth \Gamma:$$

$$'D_n' = \sqrt{w'/w''} \frac{\sinh(n+1)\Gamma}{\sinh \Gamma}.$$

Interchanging w' and w'' ,

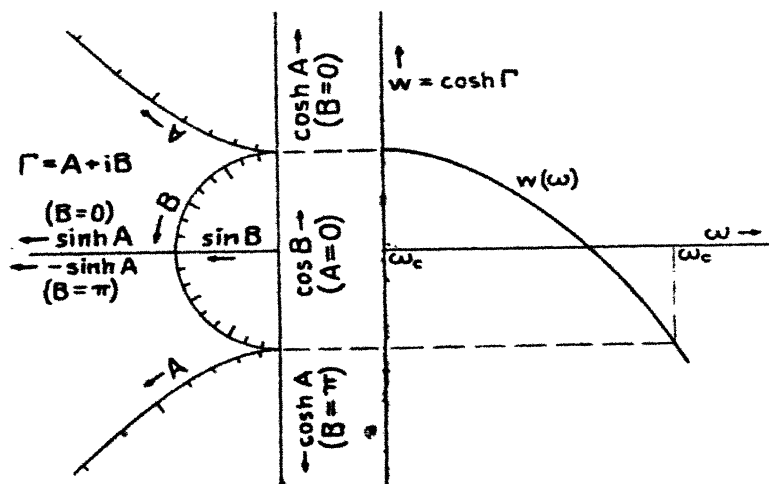
$$''D_n'' = \sqrt{w''/w'} \frac{\sinh(n+1)\Gamma}{\sinh \Gamma}.$$

5. *Graphical Charts.*—In the application of the above determinants to wave-filter problems, we note that w and Γ are functions of the frequency of alternation, $w(\omega) = \cosh F(\omega)$,

the functions depending on the structure (Z_1, Z_2). The solutions in terms of F are, however, independent of the nature of the function $\Gamma(\omega)$ as long as it complies with the conditions imposed, and this fact makes these solutions particularly valuable. Several charts will be described, which can be used to show in a convenient manner the relationships between the various quantities involved.

The solutions in Parts II. and III., for non-dissipative filters, require that w be real, and the field of w is logically divided into three parts, as described. With this restriction, fig. 14 gives a convenient arrangement for showing the

Fig. 14.

Functions of $\Gamma(\omega)$ for any function $w(\omega)$.

relationship between Γ and ω with the aid of a curve of $w(\omega)$. Corresponding to any abscissa ω , the ordinate of the curve determines the value of Γ . The partitioning of the w axis corresponds to the three kinds of frequency bands.

In fig. 14 the F functions shown on the left may be replaced by a curve of any solution in terms of F , plotted in the left-horizontal direction. This solution is then easily applied to any desired filter structures by drawing in the curves of $w(\omega)$.

If desired, the infinite plane (ω, w) may be represented in a square chart, as shown in fig. 15. The part of the curve which lies outside of $w = \pm 1$ in fig. 14 is folded over by

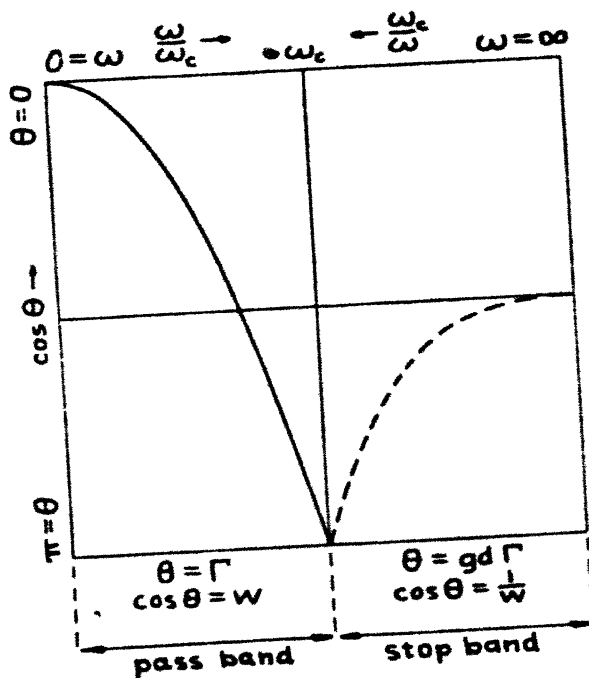
172 Mr. Wheeler and Prof. Murnaghan on the Theory of substitution in terms of the Gudermannian angle, $\text{gd } \Gamma$, as follows:—

Transmission band :

$$+1 \geq w \geq -1, \quad A = 0, \quad 0 \leq B \leq \pi,$$

$$w = \cosh \Gamma = \cos B = \cos \theta \text{ (solid curve).}$$

Fig. 15.



Square chart of functions shown in fig. 14.

Suppression bands :

$$+1 \geq \frac{1}{w} \geq -1, \quad +\infty \geq A \geq 0, \quad B = 0 \text{ or } \pi,$$

$$\theta = \text{gd } \Gamma : w = \cosh \Gamma = \pm \cosh A = \sec \theta$$

$$\sinh \Gamma = \pm \sinh A = \tan \theta,$$

$$\frac{1}{w} = \cos \theta \text{ (dotted curve).}$$

In general, both w and F are complex numbers, though this paper is largely restricted to w real. When w is complex, we denote its real and imaginary parts by u and v respectively :

$$w = u + iv = \cosh (A + iB) = \cosh A \cos B + i \sinh A \sin B.$$

Equating real and imaginary terms respectively,

$$u = \cosh A \cdot \cos B, \quad v = \sinh A \cdot \sin B.$$

Charts for reading A and B in terms of u and v can readily be prepared by drawing the level curves for A and B on the (u, v) plane, which are orthogonal families of ellipses and hyperbolas, respectively, determined by the following equations :—

$$A \text{ constant : } \frac{u^2}{\cosh^2 A} + \frac{v^2}{\sinh^2 A} = \cos^2 B + \sin^2 B = 1.$$

$$B \text{ constant : } \frac{u^2}{\cos^2 B} - \frac{v^2}{\sin^2 B} = \cosh^2 A - \sinh^2 A = 1.$$

VI. DIFFERENTIAL EQUATIONS UNDERLYING ELECTRIC IMPEDANCE.

The problems treated in this paper are in reality solutions of second-order differential equations involved in the definition of the complex electric impedance. Appreciation of this situation makes it possible to apply the same solutions to other systems, such as mechanical or molecular structures, which may lead to the same differential equations.

In a simple series circuit including resistance R , inductance L , and capacitance C , the instantaneous values of current I_i and applied voltage E_i are related by the equation

$$RI_i + L \frac{dI_i}{dt} + \frac{1}{C} \int I_i dt = E_i.$$

In the case of steady, sinusoidal, alternating current, and applied voltage,

$$E_i = E_m \cos \omega t, \quad I_i = I_m \cos (\omega t - \phi),$$

we may choose to express these quantities in terms of the unit rotating vector, $\exp i\theta$, with the understanding that we refer to the real projection, $\cos \theta$. Then we write

$$E_i = E_m \exp i\omega t, \quad I_i = I_m \exp i\omega t,$$

174 *Wave Filters containing a finite number of Sections.*

in which I_m is complex, including the phase rotation, $\exp -i\phi$, as a factor. We substitute

$$\frac{dI_i}{dt} = i\omega I_i, \quad \int I_i dt = \frac{I_i}{i\omega}$$

in the first equation :

$$I_i \left(R + i\omega L + \frac{1}{i\omega C} \right) = E_i.$$

It is customary to use, instead of the peak values (E_m, I_m), the effective (root-mean-square) values of voltage and current :

$$E = \frac{E_m}{\sqrt{2}}, \quad I = \frac{I_m}{\sqrt{2}}.$$

We define the impedance Z as the ratio of voltage to current, which is, in this case,

$$Z = \frac{E_i}{I_i} = \frac{E_m}{I_m} = \frac{E}{I} = R + i\omega L + \frac{1}{i\omega C}.$$

An impedance is, in general, a complex function of ω , of which the real and imaginary parts are, respectively, the resistance R and the reactance X :

$$Z(\omega) = R(\omega) + iX(\omega) = |Z| \exp i\phi(\omega),$$

$$|Z| = \sqrt{R^2 + X^2} = \left| \frac{E}{I} \right|, \quad \tan \phi = \frac{X}{R}.$$

The phase angle ϕ defined by the above equations is the angle by which the current alternations lag behind the voltage alternations. This phase displacement is implicitly included in the complex impedance, in the complex factor $\exp i\phi$.

The power in any impedance is

$$(E_i I_i)_{\text{mean}} = |I|^2 \cdot Z = R |I|^2 + iX |I|^2,$$

of which the actual power dissipation in heat (or work) is represented by the real part :

$$P = R |I|^2 = |E| \cdot |I| \cdot \cos \phi.$$

When this term is zero, the impedance is non-dissipative.

Johns Hopkins University,
Baltimore, Md.

May 31, 1927.

X. Analogy between the Crystal Detector and a Vacuum Tube.
By WAKASABRO OGAWA.*

MANY theories of the crystal detector have been published, but none of them has been accepted as satisfactory. According to the writer's theory, the rectification by a crystal detector is brought about by the difference of electrons emitted from each electrode.

An investigation of the electron emission from crystals in the cold state was carried out to prove the theory positively. A crystal detector couple, consisting of a copper rod and a galena crystal, was sealed in a glass tube, a small space being left free without contact between the metal and the crystal. The tube was evacuated from a side tube. An electrolytic bath of Na_2SO_4 solution containing phenolphthalein was connected in series with the tube to show the polarity of the current if rectified. When A.C. potential was applied to the tube a glow discharge started between copper and galena when the voltage attained a certain value, and the colour of the phenolphthalein solution near an electrode corresponding to copper turned red. By this experiment it was known that the current is rectified by a cold vacuum tube with two electrodes of copper and galena and the rectified current flows in the same direction as the contact rectifier consisting of the same materials. In this case the only cause to which the rectifying action can be ascribed is the difference of electron emissions from the electrodes, such others as thermoelectrical or electrolytic effect having nothing to do with it. Then two electrodes of different metals or crystals of which the electron emissions were to be compared were sealed in a glass tube. As the emission is influenced by the physical state and dimension of the surface, care was taken to make the conditions of these two electrodes as equal as possible. As in the former case, the electrode which has stronger electron emission than the other was ascertained from the direction of the rectified current. Many couples of different metals and crystals were tested by this method, and as the result the following order of electron emission was obtained, magnesium having the strongest electron emission in the series : natural galena with the best sensitivity ; synthetic galena with 5 per cent. Ag ; silicon ; Pt ; Ag ; Cu ; german silver ; brass ; Pb ; Fe ; iron pyrites ; simple synthetic galena ; carborundum :

* Communicated by the Author.

zincite ; Al ; Mg. These results all well correspond with those obtained by the writer's experiments with crystal detectors and also with the order arranged after the electron affinities of metals determined by many previous investigators. By these experiments the following facts are now established ; (1) rectification is possible by two separate electrodes of different electron emissions in the cold state ; (2) the direction of rectified current in this case is quite the same with that rectified by the contact rectifier composed of the same electrode materials. The essential differences between these two rectifiers are the distance between the electrodes and the surface area from which electron emissions occur. In the vacuum tube there is always a layer of air between the two electrodes and ionization of gas molecules necessarily occurs. In the crystal rectifier, it will be natural to think of the distance between the electrodes as varying from the real contact to the wide space involving the ordinary atmosphere. As the lattice constant for metals and crystals has a value of $3.2\text{--}5.8 \times 10^{-8}$ cm. and the mean distance between gas molecules under normal pressure is 3.33×10^{-7} cm., the free space of nearly from 6×10^{-8} to 60×10^{-8} cm. will not allow the existence of gas molecules, and at least free electronic emissions may be possible in the space of this dimension. But as the free mean path of electrons in the atmosphere at normal pressure is nearly 9×10^{-5} cm., the electrons are able to reach the opposite electrode without collision with gas molecules in the wider space far beyond 60×10^{-8} . It may be, therefore, possible to say that the emission at the free space of a contact rectifier occurs in the highest vacuum, and no ionization of gas molecules is involved in an ordinary case of the wireless detector.

But in the case of the battery charger, which is another type of contact rectifiers consisting of two plate electrodes of metal and metallic oxide or sulphide and which is thought by the present writer to act on the same principle as ordinary crystal detectors, the electron emissions seem to occur even in a wider space involving an ordinary atmosphere in virtue of a higher potential.

Another difference between the crystal detector and the vacuum tube used in the preceding experiments is the surface from which electrons are emitted. In the vacuum tube the electrode surface works as a whole including any heterogeneous parts if present, while in a crystal detector only a special portion is brought to work and heterogeneous parts will work as such. For example, in an argentiferous synthetic galena, silver grains between PbS crystals will always

exert their influence upon the electron emissions in a vacuum tube, but in a crystal detector their effects will be quite different according to the position of the needle point. But there will be no difference in a homogeneous substance. At the first sight the surface area emitting electrons appears to be very different in a needle point and in a crystal. But this is not true, because the emissions only occur in the limited portion of the electrodes which come face to face within a certain limited distance and other parts will remain idle. In short, there is no substantial difference between a crystal detector and the vacuum tube except the metallic conduction at the real contact points in the former. This analogy is illustrated by figs. 1 and 2. Suppose A and B

Fig. 1.

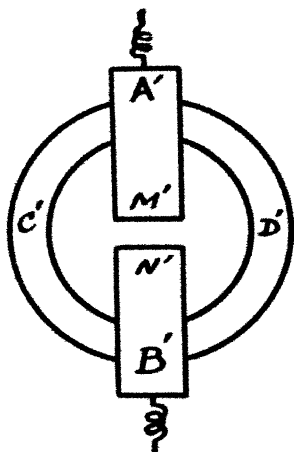
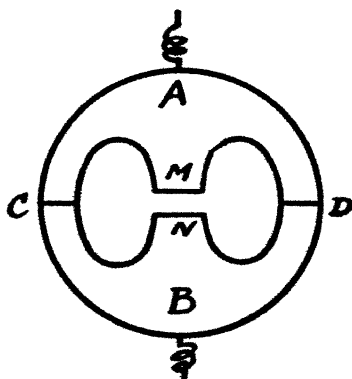


Fig. 2.



in fig. 1 to be two components of a crystal detector which are in contact really at C and D. The distance between M and N is thought to be so small that any molecules of gases are not admitted to enter between this space, that is to say, the space is vacuum. In fig. 2, A' and B' are the electrodes and C'-D' denotes a glass bulb of a vacuum tube. The real contact portions denoted by C and D will serve as the supports of the electrodes and correspond to the glass bulb C'-D' of the vacuum tube. C-D and C'-D' will equally make a route of leakage current if they are not good insulators and if this leakage attains to a certain value the potential difference between M and N as well as M' and N' will drop to such a value that electron emissions between

the electrodes will become impossible. As C and D in the crystal detector are composed of the same materials as the electrodes, it is impossible to ensure an insulation of high degree, more or less leakage as metallic conduction being inevitable. Thus it will be clear that the proper electrical resistance is of the prime importance in a crystal to be used as a detector.

In conclusion, a crystal detector is nothing else than a cold vacuum tube which works as a rectifier by the difference of electron emissions from two electrodes badly insulated.

Electrotechnical Laboratory,
Tokyo, Japan.

XI. *The Determination of the Atomic Scattering Power for X-Rays from Powders of Gold, Silver, and Aluminium for Cu K α Radiation. By J. BRENTANO, D.Sc., Lecturer in Physics, Manchester University*.*

[Plate I.]

Summary.

IN the present paper experiments are described intended to obtain comparative values for the scattering power of gold, silver, and aluminium.

The measurements are made with small powder particles, and a method is employed in which the intensities are measured from composite layers. Some points concerning this method, which makes it possible to overcome certain difficulties encountered in measuring the intensities of X-ray reflexions from powders, are discussed, and the procedure is indicated for evaluating the photographic records.

The results of the experiments indicate that, for the elements of high atomic weight examined in the state of very fine powders, the scattered intensities increase considerably less rapidly than F^2 and that better agreement is obtained by assuming the scattered intensity proportional to F . These results are discussed.

-
1. **I**N a previous paper † a discussion was given of some intensity measurements of X-ray reflexions obtained from extremely fine powders of rock-salt.

* Communicated by the Author.

† J. Brentano, Phil. Mag. iv. p. 620 (1927).

The object of these measurements, which were recorded with a photographic method, was not to obtain data of a higher degree of accuracy than had been obtained from measurements on large crystal faces, but to verify whether the measurements made on large crystals were not affected to any considerable extent by extinction.

It resulted that in the particular case of rock-salt extinction effects played a very small part, but it was found that in other cases where these effects were large, the breaking up of a crystal into a powder could, in general, not be considered a reliable means for eliminating extinction, unless the particles are of the order of 10^{-6} or 10^{-5} cm. in diameter, so that only a limited advantage is obtained by using coarser powders in preference to large crystals.

2. In the present paper some measurements are described, directed to verify the general assumptions on the scattering of X-rays from atoms in crystal lattices. A problem which presents itself in this connexion is in a certain way similar to the problem discussed in the case of rock-salt.

A number of factors which determine the intensity of X-ray reflexions and which involve a certain amount of uncertainty in their numerical evaluation, assume definite values or become negligible for small angles of deflexion or, more exactly, for small values of $\sin \theta/\lambda$, where θ is the glancing angle of the reflexion and λ the wave-length. One of these factors is the quantity F , which we can define as the effective negative charge of the atom, which situated at its centre would be equivalent to the actual charge distributed in space for scattering radiation of the particular wave-length at the particular glancing angle θ *. F becomes equal to the actual charge for small values of $\sin \theta/\lambda$. Other factors are terms accounting for heat motion and for the Compton effect, which become negligible for small angles of deflexion.

On the other hand, extinction effects are greatest for the strong reflexions at small angles. They depend on the dimensions of the regular crystal units and on their distribution in the crystal and cannot be determined in a direct way.

* A more general definition of F can be given in which F is associated with the amplitude scattered from a plane of atoms, but for the purpose of the interpretation of the present experiments it is of greater interest to give to F the more special significance, rather than to introduce it in a phenomenological way.

It seemed, therefore, that a considerable simplification in the interpretation of the results could be obtained by measuring the reflexions at small glancing angles from a powder consisting of particles so small as to satisfy the conditions of negligible extinction. In this way we can avoid the superposition of too many factors, which render the interpretation of X-ray intensity measurements so difficult, and attempt to verify the fundamental assumptions before introducing them in more complex cases. The general evidence derived from the analysis of structures supports the classical relation making the contribution of each atom to the scattered intensity proportional to F^2 , but most of this evidence refers to light atoms, and not so much information is available with respect to the scattering from atoms of higher atomic number. Measurements for the intensity of scattering were therefore made for gold, silver, and aluminium, which all belong to the cubic face-centered type of crystals.

In pursuing these determinations a method for measuring the intensities had to be evolved so as to be adapted to the particular conditions of a powder. We have to refer to a few points in this connexion to account for the particular way in which the determinations were carried out.

Similar conditions present themselves when quantitative intensity measurements are required in connexion with the determination of structures; we discuss them, therefore, in a more general way than would be strictly necessary for the purpose of our experiments.

3. The effect of extinction* on the intensity of X-ray reflexions from the individual particles of a crystal powder depends mainly on the extinction in the particular crystal unit which is contributing to the reflexion, which Darwin calls primary extinction.

Darwin has given an approximate expression indicating the relative reduction of the intensity of the reflected radiation owing to the extinction in the reflecting unit. If m is the number of the reflecting planes and

$$q = N(e^2/mc^2)F\lambda^2/\sin^2\theta$$

measures the amplitude reflected from one plane, N being

* A general exposition of the phenomena of extinction in a single perfect crystal and in a crystal of "mosaic" structure has recently been given by Bragg, Darwin, & James, *Phil. Mag.* i. p. 897 (1926), and by P. Ewald, *Handbuch der Physik*, xxiv. (1926).

the number of atoms per unit volume, e and m being the charge and mass of the electron, c the velocity of light. Darwin's expression becomes

$$\frac{\tanh mq}{mq} \dots \dots \dots (1)$$

We give in Table I. the data calculated for the (111) reflexion for gold, silver, and aluminium, for which the expression (1) becomes equal to 99/100 or the extinction equal to 1 per cent., the last column gives the thicknesses corresponding to the numbers m . The F values used have been calculated according to Hartree*.

TABLE I.

Plane of reflexion.	$N \cdot 10^{-23}$	F .	q .	m .	Thickness $d \cdot 10^6$ cm.
Au (111)	5.94	72.7	12.8	135	3.2
Ag (111)	5.90	41.3	7.55	250	5.9
Al (111)	6.02	9.3	2.0	880	20.5

We can make sure of reducing this extinction effect below a given value by limiting the size of the crystal particles to the dimensions imposed for the individual crystal unit according to (1).

It will be noted that expression (1) increases very rapidly with mq , i. e., with the thickness of the reflecting crystal unit; on the other hand, this expression refers to the unit, not to the particle, and it might appear unlikely that the whole of one powder particle is perfect, i. e., acts as one single unit.

In discussing extinction effects in the case of a powder, it has been pointed out by the writer† that when the conditions for negligible extinction in the individual particle are satisfied, there still exists a particular extinction effect, which could better be described as the additive absorption effect of the various crystal forms. All possible crystal faces contribute to it according to the number of times p they are represented on the crystal form, and according to their scattering power. The additive effect is thus a discontinuous function of the wave-length, as this limits the total number of faces which can reflect, but it is the same

* D. R. Hartree, Phil. Mag. l. p. 289 (1925).

† Loc. cit.

for all reflexions and appears as an additive term in the absorption coefficient.

When making absolute determinations from a powder layer of finite thickness, the proper coefficient of absorption could be determined for the actual powder, in such cases where the effect is appreciable. But the measurement of absorption coefficients from powders is exposed to a serious source of error, owing to the varying density of a powder mass, and this raises a difficulty in all absolute intensity measurements from powders in which the coefficient of absorption has to be introduced in an explicit or implicit form.

Another reason which makes powders less suitable for absolute measurements is the weakness of the reflected beams; this involves that for absolute determinations two intensities in the ratio 1:10,000 or 1:100,000 have to be compared, so that absolute measurements seem to require very great precautions.

It was therefore decided not to undertake absolute determinations, but to limit ourselves to relative measurements. It will be seen that the conditions of reflexion from a powder lend themselves particularly well to such determinations.

4. If dV is a volume element of powder, so small that absorption can be neglected, θ the glancing angle with respect to a set of lattice planes corresponding to a certain reflexion, so that 2θ is the angle between the incident and the reflected radiation, and I the intensity of a parallel beam of X-rays falling upon the volume element, the radiation scattered for this reflexion in unit time is given by

$$dP = \frac{1}{2} I p \cos \theta Q dV. \quad (2)$$

$$\text{where } Q = \frac{e^4}{m^2 c^4} \cdot F^2 N^2 \frac{\lambda^2}{\sin^2 \theta} \frac{1 + \cos^2 2\theta}{2} e^{-\lambda^2 \frac{\sin^2 \theta}{\Lambda^2}} \quad (3)$$

The expression Q is the generally accepted value derived from classical theory, assuming that each electron scatters independently*. The exponential factor accounts for the heat motion of the atoms. A further factor should be added for the Compton effect, which limits the part of the incident radiation available for scattering†.

* C. G. Darwin, *Phil. Mag.* xliii. p. 800 (1922).

† Williams, *Phil. Mag.* ii. p. 657 (1926); Jauncey, *Phys. Rev.* xxix. p. 757 (1927).

This expression has to be integrated according to the conditions imposed by the particular method.

In the method used a beam of X-rays diverging from the focal spot of the anticathode, or from a slit near to it, falls on a flat layer of powder situated at a distance a from the point from which the X-rays diverge. The scattered radiation is observed at a distance b from the powder layer. Details of the arrangement have been described in another paper*, and certain focussing properties of it have been discussed. The glancing angle of incidence of the central beam being α and the glancing angle of emergence being β , we measure more conveniently not the quantity P , which is the radiation scattered according to the surface of a cone of semi-apex 2θ , but the part P_b of it, which falls at the distance b on a strip of unit height placed normally to the plane of deflexion in which the angles α and β are measured, and $\alpha + \beta = 2\theta$.

We have thus for the central beam

$$dP_b = \frac{I_p Q dV}{8\pi b \sin \theta} \quad \dots \quad (4)$$

Integrating for finite thickness z of the layer we have

$$P_b = \frac{I_p Q f}{8\pi b \sin \theta \mu (1 + \sin \alpha / \sin \beta)} \cdot \left(1 - \frac{1}{e^{-\mu z \left(\frac{1}{\sin \alpha} + \frac{1}{\sin \beta} \right)}} \right),$$

where f is the cross-section of the beam.

If the layer is sufficiently thick to absorb the incident radiation completely, and introducing X as the intensity of the divergent incident beam measured by the energy incident in unit time in the solid angle one and χ as the actual solid angle of a narrow incident pencil defined by the diaphragms of the instrument

$$P_b = X \frac{\mu Q \chi}{8\pi b \sin \theta} \cdot \frac{1}{\mu \left(1 + \frac{\sin \alpha}{\sin \beta} \right)} \quad \dots \quad (5)$$

The focussing condition requires for the central beam

$$\frac{\sin \alpha_0}{\sin \beta_0} = \frac{a}{b} = \text{const.} \quad \dots \quad (6)$$

to be satisfied for all angles of reflexion. We see, therefore,

* J. Brentano, Proc. Phys. Soc. Lond. xxxvii. p. 184 (1925). There the arrangement is described in view of making exact angular measurements; its advantages for quantitative intensity measurements are indicated, but not fully discussed.

that for a narrow pencil which satisfies the focussing condition the particular intensity factor of the instrument is the same for all angles of deflexion.

In the actual experiment the finite width of the incident beam introduces a certain range in the angles of incidence α . Further, while measuring a given reflexion the powder layer is rotated through a certain range. The result of both these facts is that the focussing condition is satisfied only in approximation.

In order to consider the effect of the rotation of the layer on the radiation scattered from its centre, we have to integrate over the range $2\alpha'$, where α' is the greatest deviation of the powder layer from the correct setting. Then

$$P_b = X \frac{pQ}{\mu \sin \theta} \cdot \text{const.} \int_{\alpha_0 - \alpha'}^{\alpha_0 + \alpha'} \frac{1}{\omega_a} \frac{d\alpha}{1 + \frac{\sin \alpha}{\sin \beta}}.$$

In this expression the constant in front of the integral contains factors which depend on the particular arrangement. The term ω_a accounts for the angular velocity of the powder layer, which in general varies with θ .

If for the small range $2\alpha'$, ω_a can be considered constant the expression becomes

$$P_b = X \frac{pQ}{\mu \sin \theta} \frac{\text{const.}}{\omega_a} \left(\alpha' + \frac{1}{2} \cot \theta \log \frac{\cos(\alpha_0 - \theta + \alpha')}{\cos(\alpha_0 - \theta - \alpha')} \right),$$

and when in this case it is arranged to measure various reflexions during equal times, α' becomes proportional to ω_a , and the effect of the rotation of the layer on the reflexion from a point near to its centre is expressed by the additive term. We can thus estimate its value for any given conditions.

* In measuring with a photographic method a rotating slit is employed which moves with uniform velocity in front of the photographic film and uncovers an angular extension η of it at one time. The integration of (4) gives

$$P_b = X \frac{pQX}{8\pi\mu b \sin \theta} \frac{t}{T} \frac{1}{\eta} \int_0^\eta \frac{d\eta}{1 + \frac{\sin \alpha}{\sin \beta}},$$

where t is the time during which any particular point of the film is exposed, and T is the total time for one swing of the layer. For each reflexion α and β extend over a certain range determined by η always satisfying $\alpha + \beta = 2\theta$. P_b is in this case an average effect over the time T .

By a similar reasoning we can estimate the effect of the finite angular extension ϵ of the incident beam in the plane of deflexion. It results that the effect of the larger and smaller values of α largely compensate one another except for small glancing angles. When making measurements at small glancing angles, ϵ must necessarily be small, in order that the whole incident beam may fall on the powder layer. So it is found that, in general, the experimental conditions are such as to allow to refer to expression (5). For relative measurements of different reflexions from a sufficiently thick layer keeping χ constant, we have then,

$$P_b = X \frac{pQ}{\sin \theta} \cdot \text{const.} \quad . \quad . \quad . \quad . \quad . \quad (7)$$

The quantity P_b in (5) is the energy entering into an ionization chamber in unit time, when the entrance slit at the distance b has the height one and is sufficiently wide to embrace the whole radiation scattered for the particular reflexion.

In the photographic record the quantity P_b is represented by the total blackening of the film taken for the whole width of the line. For the quantitative evaluation of photographic blackenings it is, of course, essential that the X-rays fall vertically on the film, which condition is satisfied with the apparatus. Different reflexions have also to be recorded for equal times.

It is desirable to make the incident beam diverging from the anticathode or from a point close to it, so that its intensity is uniform for the whole of its extension ϵ . In this case inequalities of the layer have less effect. This requires that a should be made somewhat larger than b .

5. In order to compare intensities of reflexion from different crystals, simple conditions are obtained by making measurements on composite layers containing both substances. We have then to consider that the expressions for P_b are obtained by an integration over a volume. In the case in which the experimental conditions allow us to use expression (7), and when X is the same for different reflexions, the ratio of two reflexions from a layer containing two substances in the proportion M_1/M_2 becomes

$$\frac{P_{b1}}{P_{b2}} = \frac{M_1 \rho_2 p_1 Q_1 \sin \theta_2}{M_2 \rho_1 p_2 Q_2 \sin \theta_1}, \quad . \quad . \quad . \quad . \quad . \quad (8)$$

where the quantities which refer to the one and to the other

crystalline substance are distinguished by the indices 1 and 2 and ρ are the densities.

As will be seen, the absorption coefficient and other constants which depend on the particular conditions of the measurement do not enter in this expression.

When only two lines or two groups of lines of similar intensity have to be compared the proportion of the two masses M_1/M_2 can be so adjusted as to make intensities of corresponding reflexions approximately equal. The shortcomings of the photographic method in comparing widely different intensities can thus be overcome to a considerable extent.

In the particular case of gold, silver, and aluminium, the lattice constants are 4.08 \AA ., 4.07 \AA ., and 4.06 \AA ., respectively. The reflexions fall, therefore, so near together that a comparison substance had to be used and measurements made from layers containing one of the metals and the comparison substance.

Nickel oxide, which had been employed as admixture in other measurements*, is in general a very suitable comparison substance in combination with Cu radiation, owing to its density and to the fact that the characteristic radiation of nickel is not excited by the radiation of copper. Its lattice constant is 4.1705 \AA ., and the metal and nickel oxide lines are thus so near that a proper determination of the background is rendered difficult. Therefore cadmium oxide was used, the lattice constant of which is 4.72 \AA . Its (200) reflexion falls very near to the (111) reflexion of the metals, so that the (220) reflexion of cadmium oxide was compared with the (200) reflexion of gold, silver, and aluminium.

6. It seemed to be of some interest to ascertain whether it would actually be necessary to have recourse to so small particles as indicated by Table I.

For gold and silver it is known that the reflexions obtained from sheets of these metals are broadened, and this has recently been made the subject of an investigation by Dehlinger†. It could be expected that in such cases the mechanical treatment of preparing a coarse powder would produce a powder with sufficiently small crystal units.

Fig. 1 (Pl. I.) shows comparative photographs taken from two composite layers consisting of equal parts by weight of

* Brentano & Dawson, *Phil. Mag.* iii. p. 411 (1927).

† U. Dehlinger, *Zeitschrift f. Kristallographie*, lxx. (5) p. 615 (1927).

gold and nickel oxide*. The gold contained as impurities about 2.2 per cent. of silver and 1 per cent. of copper in each case. In the first photograph (a) extremely fine fragments of gold were used, obtained from gold leaves of $5 \cdot 10^{-6}$ cm. thickness. In the second photograph (b) the gold consisted of fine filings obtained from a thin sheet. Since the spacing for gold is slightly less than the spacing for nickel oxide, the reflexions from the latter occur at smaller angles than those of the former; on the photographs the lines corresponding to smaller angles are on the left.

It will be seen that in the case of the coarse gold particles the gold reflexions are by far the weaker, indicating considerable extinction in particular for small angles. At larger angles the difference between corresponding reflexions from the two films is less pronounced, which is what should be expected for an extinction effect †.

It is possible that the extinction effect observed with the coarser gold particles is not entirely due to primary extinction, but in part produced by secondary extinction. It indicates, in any case, that small particles had to be adopted for the measurements.

To obtain these particles, foils of gold, silver, and aluminium were powdered with the addition of a volatile substance. Taking the thickness of the foils as indicating the maximum dimension of the crystal units to be expected in these particles, for gold, the less favourable case, the corresponding extinction for the (200) reflexion amounted to 3 per cent.

7. In applying expression (8) to the particular conditions of our experiments, a simplification can be introduced, as the same reflexions are compared in each case and the value of $\sin \theta$ is nearly the same for the three metals. Therefore, we can write

$$\frac{P_{61}}{P_{62}} = \frac{M_1 \rho_2 Q_1}{M_2 \rho_1 Q_2} \cdot \text{const.} \quad . \quad . \quad . \quad (9)$$

The P_6 values were measured from photographic records, and the photometry was carried out in the same way as for the measurements from rock-salt, but a more accurate

* This comparison of coarse and fine gold forms part of the early stages of this research undertaken in collaboration with Mr. W. E. Dawson, M.Sc., and I wish to express my indebtedness to him for his assistance.

† The exposure (b) (with coarse gold) was considerably longer than exposure (a) and the lines are darker. This does not show so much on the reproduction, but it accounts for certain nickel oxide lines appearing in (b) which are only faintly indicated in (a).

evaluation has been adopted in view of the different width of the lines obtained from different metals. The galvanometer deflexions taken for the various points of the lines were plotted in a logarithmic scale. By means of a suitable blackening curve it was then easy to express them in terms of X-ray intensities.

Fig. 2 shows examples of the curves so obtained. The ordinates in the upper curves represent the logarithms of the galvanometer deflexions, the ordinates in the lower curves represent the corresponding X-ray intensities, and their areas are proportional to the quantities P_0 . The scale of the abscissæ is chosen so as to obtain areas convenient for measurement. The agreement between different measurements taken with the same substances is 5 per cent.

Table II. represents the results obtained from a greater number of measurements using Cu K α radiation. The quantities referring to the metals gold, silver, and aluminium are marked by the index 200 of the corresponding reflexion; the quantities referring to the comparison substance are indicated by the index 220. The last column gives comparative values of Q for the three metals by introducing the ratio of the masses and the densities in (9).

TABLE II.

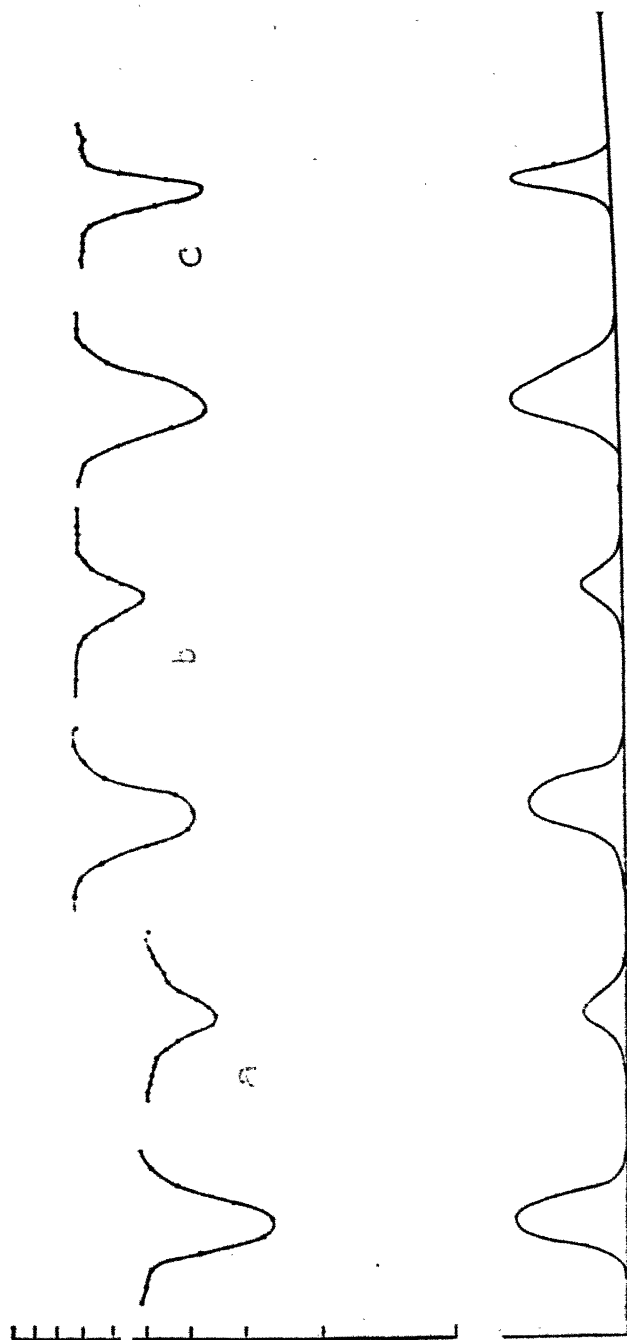
	ρ .	$\frac{P_{200}}{P_{220}}$	M_{200}/M_{220}	Q const.
Au	19.3	0.310	1.00	585
Ag	10.5	0.270	0.67	405
Al	2.58	0.109	1.00	1.6

8. When discussing these Q values we can neglect the small differences in the numbers N , owing to the close agreement between the lattice constants for the three metals, so that referring to equation (3) for the comparison of the reflexions from gold, silver, and aluminium, F^2 becomes proportional to Q .

We have calculated the F values for the (200) reflexions from the three metals according to Hartree*, assuming Stoner's distribution of electrons. The values so found are $F_{200}=69.55$ for gold, $F_{200}=38.65$ for silver, $F_{200}=9.23$ for aluminium. From calculation we obtain thus for the ratio,

* *Loc. cit.*

Fig. 2.



Photometry of (200) reflexions from gold (a), silver (b), and aluminum (c). The corresponding comparison reflexions are on the left.

gold and silver, $\frac{F_{Au}^2}{F_{Ag}^2} = 3.23$, while the ratio of the experimental Q values gives 1.44.

The discrepancy is too great to be easily attributable to extinction effects or to the approximative character of the calculation.

A particular anomaly in the scattering power has been brought into evidence by an experiment by Mark and Szillard*, and is discussed in a more general treatment of scattering phenomena by Kallmann and Mark†. This anomaly is associated with the excitation of characteristic radiation of the scattering atom by the incident radiation and is effective only when the wave-length of the scattered radiation is near to one of the absorption edges of the scattering atom. This phenomenon cannot account for the present discrepancy.

The possibilities present themselves that either a general falling off of scattering power takes place as compared with the value given by Thomson's expression, for those electrons which are in the vicinity of a heavy nucleus, or that for the elements of higher atomic weight definite orbits do not contribute to the scattering. Comparing the gold and silver values with those from aluminium we find from calculation $\frac{F_{Au}^2}{F_{Al}^2} = 56.8$ and $\frac{F_{Ag}^2}{F_{Al}^2} = 17.6$, while the ratio of

the experimental Q values gives 5.70 and 3.95 respectively. This indicates that on the latter hypothesis groups of electrons from gold and from silver should be excluded. It does not seem permissible to introduce the present experimental values in a treatment in which some factors, notably the factor for heat-motion, have been neglected for justifying any particular assumption as to the omission of the scattering from certain orbits. Determinations at low temperature and for different wave-lengths are in progress.

If we consider the experimental Q values without referring to equation (3), which is based on the assumption of independently scattering electrons and not on the continuous distribution of quantum-mechanics, and simply introduce the Q's to measure the scattering power per unit volume under the condition for (2) and (4), it appears that much closer agreement exists by comparing them with the calculated F values and not with their squares.

* Mark and Szillard, *Zeitschr. f. Phys.* xxxiii. p. 688 (1926).

† Kallmann and Mark, *Ann. der Phys.* lxxxii. p. 585 (1927).

We find from calculation, $\frac{F_{Au}}{F_{Al}} = 7.54$ and $\frac{F_{Ag}}{F_{Al}} = 4.2$,

the corresponding experimental ratios, 5.70 and 3.95, give thus a relative value for gold which is somewhat too small, but show very good agreement for the relative values of silver and aluminium.

Retaining for F its significance as "effective" negative charge, so as to account for the spacial distribution of the electrons, this would indicate a contribution from each atom proportional to its charge.

Here two remarks present themselves: one that when applying an expression for Q to the scattering from a volume, in which extinction and absorption are nil, it would be very satisfactory to find the contribution of the individual atom to the total intensity of one reflexion proportional to F and not to F^2 . In fact, F in such a case only determines the scattering from the individual unit of the pattern, so that a variation of F does not affect the range through which reflexion occurs, different from N in expression (3); the other that it is questionable whether an equation of this type can actually be applied to express the scattering when extinction is absent.

The two points are not so widely different as they appear, since, in considering the scattering from crystals, the scattering from one atom by itself has no physical meaning.

On the other hand, in making these remarks we must bear in mind that the general evidence from structure analysis and from absolute determinations on lighter elements is in agreement with (3) also in cases where this expression has been applied to measurements from microcrystalline mosaics and fine powders. It seems, therefore, of interest to discuss the present measurements in terms of this expression, when they indicate that the relations verified for lighter elements seem not to be satisfied in a general way.

The writer is indebted to Prof. W. L. Bragg, F.R.S., for various facilities, among which is the use of a transformer obtained by means of a grant of the Royal Society, and to the Leembruggen Trust for a special grant. He wishes in particular to express his thanks to Mr. W. E. Dawson, M.Sc., for his help in the earlier stages of this work, and to Mr. J. Adamson, M.Sc., for assistance received in the more recent experiments.

Manchester,
April 5th, 1928.

XII. *The Magnetic Energy of Permanent Magnets and of Linear Currents.* By H. V. LOWRY*.

SUPPOSE the field has an applied electric force E' and permanent magnetism I_0 , then using Maxwell's equations

$$\begin{aligned} \int (E'j) dv - \int (Ej) dv &= - \int (E - E', \text{curl } H - \frac{\partial D}{\partial t}) dv \\ &= - \int (\text{curl } E - E', H) dv + \int (E - E', \frac{\partial D}{\partial t}) dv + \int [EH]_n dS \\ &= \int (\frac{\partial}{\partial t} (B - I_0), H) dv + \int (E - E', \frac{\partial E}{\partial t}) dv, \quad \dots \quad (1) \end{aligned}$$

the integrals being taken over all space, so that

$$\int [EH]_n dS = 0.$$

In an isotropic medium of constant permeability and capacity the right-hand side of 1 becomes

$$\frac{\partial}{\partial t} \left\{ \frac{1}{2} \int \mu H^2 + K(E - E')^2 dv \right\}.$$

$\int (E'j) dv$ is the rate at which work is done on the field by the applied forces; $\int (Ej) dv$ is the rate of dissipation of energy; and hence the right-hand side of (1) represents the rate of increase of the electrical energy of the field. This energy is in two parts, the first of which definitely depends on the magnetic properties of the field. If the field contains permanent magnets and no currents, this part becomes

$$W = -\frac{1}{2} \int (I_0 H) dv$$

because $\int (BH) dv$ becomes zero in a magnetostatic field.

If the field contains no permanent magnets and the currents are steady and flow in circuits,

$$\frac{1}{2} \int \mu H^2 dv \text{ transforms to } \frac{1}{2} \sum i N = (T),$$

N being the total induction through a circuit carrying a current i .

If we regard the permanent magnets as made up of

* Communicated by the Author.

molecular currents, we can look on W and T as two different ways of uniting $\frac{1}{2} \int \mu H^2 dv$, just as

$$W_e = \frac{1}{2} \sum p_r e_r e_r \quad \text{and} \quad W_v = \frac{1}{2} \sum q_r v_r v_r$$

are different ways of writing the electrostatic energy $\frac{1}{2} \sum e V$.

From the magnetostatic point of view the force corresponding to the coordinate x is $\left(-\frac{\partial W}{\partial x}\right)$, and, as this is obtained by keeping I_0 constant, it is better to write it

$$\left(-\frac{\partial W}{\partial x}\right)_{I_0=\text{const.}}$$

But when the magnets are replaced by currents, the currents must be kept constant during the displacement δx in order that the equivalent magnetization shall remain constant. For two circuits

$$T = \frac{1}{2} \{ L_1 i_1^2 + 2 M i_1 i_2 + N i_2^2 \},$$

so that keeping L_1 and L_2 and the shapes of the two circuits constant

$$\delta T = \delta M i_1 i_2.$$

The equations that give the currents are

$$\frac{\partial}{\partial t} (L i_1 + M i_2) + R_1 i_1 = E_1$$

$$\text{and} \quad \frac{\partial}{\partial t} (M i_1 + N i_2) + R_2 i_2 = E_2.$$

In the displacement

$$i_2 \delta M = (E_1 - R_1 i_1) \delta t$$

and

$$i_1 \delta M = (E_2 - R_2 i_2) \delta t.$$

Hence the increase of energy of the circuit

$$\begin{aligned} E_1 i_1 + E_2 i_2 - R_1 i_1^2 - R_2 i_2^2 - X \delta x &= 2 i_1 i_2 \delta M - X \delta x \\ &= 2 \delta T - X \delta x. \end{aligned}$$

Therefore $2 \delta T - X \delta x = \delta T$.

We have therefore two expressions for the force X

$$X = \left(-\frac{\partial W}{\partial x}\right)_{I_0=\text{const.}} = \left(+\frac{\partial T}{\partial x}\right)_{i=\text{const.}}$$

These different expressions arise solely from the two
Phil. Mag. S. 7. Vol. 6. No. 34. July 1928. 0

different ways of writing $\frac{1}{2} \int \mu H^2 dv$, and are analogous to the electrostatic equations

$$X = \left(-\frac{\partial W}{\partial x} \right)_{V=\text{const.}} = \left(+\frac{\partial W_V}{\partial x} \right)_{I=\text{const.}}$$

If absolutely permanent magnets were possible the energy $2\delta T$ would have to be supplied from molecular sources.

We obtain the same result if we assume that the magnets have induced magnetization only, and that during a displacement this is kept constant by the application of an external magnetic force.

For such magnets the energy is $W' = -\frac{1}{2} \int (IH) dv$. In a displacement in which I is kept constant,

$$\delta W' = -\frac{1}{2} \int (I \delta H) dv.$$

To keep I constant in such a displacement an external magnetic force δH must be applied, and this will do work

$$-\int (I \delta H) dx = 2\delta W'.$$

Hence, as above, we have

$$2\delta W' - X \delta x = \delta W';$$

$$\text{therefore} \quad X = \frac{\delta W'}{\delta x}.$$

This expression for X is equivalent to the value

$$\left(\frac{\partial T}{\partial x} \right)_{I=\text{const.}}$$

It is only the gradients of the energy that occur in the equations of motion and in the expressions for the generalized forces. The potential energy of a system of magnets is not necessarily $-\frac{1}{2} \int \mu H^2 dv$, because its kinetic energy is $+\frac{1}{2} \int \mu H^2 dv$; both T and W are equal to $\frac{1}{2} \int \mu H^2$, and the equations

$$X = -\frac{\partial W}{\partial x} = +\frac{\partial T}{\partial x}$$

are consistent with this, because

$$\left(\frac{\partial W}{\partial x} \right)_{I=\text{const.}} + \left(\frac{\partial T}{\partial x} \right)_{I=\text{const.}} = 0.$$

The confusion arises because the quantities kept constant in the partial differentiation are often omitted.

XIII. *Chemical Interactions corresponding to the Constant of Mass Action, being a Function of the Volume and Masses of the Constituents, as well as of the Temperature and Catalytic Action.*—I. By R. D. KLEEMAN, B.A., D.Sc.*

§ 1. *Introductory Remarks.*

THE writer has shown † that, in general, the constant of mass action of a gaseous interacting mixture is a function of its volume and masses of the constituents as well as of the temperature. In a subsequent paper ‡ the differential equations were developed which determine the functional nature of the constant of mass action in any given case. They were applied to investigate some well-known reactions by the help of the gas equation

$$pv = MRT, \quad (1)$$

where p denotes the pressure of M mols of a pure gas at the volume v and absolute temperature T . In the particular cases considered, it was found that the constants of mass action are independent of the volumes of the reacting mixtures, as shown by experiment. The effect of the masses of the constituents on the constant of mass action was not investigated.

It was shown in a subsequent paper § that, strictly according to thermodynamics, the equation of a perfect gas is

$$pv = MRT\xi, \quad (2)$$

where ξ is a function of T , v , and M , which is practically equal to unity except for temperatures close to the absolute zero, and for very large volumes. It would follow, then, that strictly in all cases the constant of mass action of a mixture in the perfectly gaseous state is a function of the volume, notably when it is very large, and the masses of the constituents, as well as of the temperature, though it may be practically independent of these quantities except of the temperature over a large range of values. In this paper it will be shown that the constant of mass action may be appreciably a function of the foregoing three quantities for reactions

* Communicated by the Author.

† Phil. Mag. v. p. 263 (1928).

‡ Phil. Mag. v. p. 620 (1928).

§ Phil. Mag. v. p. 1191 (1928).

taking place under certain conditions, even when equation (1) is supposed to hold strictly.

§ 2. *The Functional Nature of the Constants of Mass Action of Gaseous Mixtures reacting under Certain Conditions, and Catalytic Action.*

If the reacting mixture involves the constituents a, b, \dots whose masses in gram atoms are M_a, M_b, \dots the differential equation of the reaction in respect to volume as independent variable is

$$v \frac{\partial p}{\partial v} - M_a v_a \frac{\partial p_a}{\partial v} - M_b v_b \frac{\partial p_b}{\partial v} - \dots = 0, \quad (3)$$

where p denotes the total pressure of the mixture, p_a, p_b, \dots the partial pressures of the constituents not in combination with each other, or the pressures they exert through membranes each of which is permeable to one of them, and v_a, v_b, \dots , the corresponding volumes per gram atom. If the constituents when isolated form certain molecules the form of the equation may be altered accordingly, examples of which have already been given. The application of the gas equation (1) gives besides

$$p = RT \Sigma C, \quad (4)$$

where ΣC denotes the sum of the concentrations of the various molecules. Similarly, for the partial pressures p_1, p_2, \dots , of the various molecules, we have

$$\left. \begin{aligned} p_1 &= RTC_1 \\ p_2 &= RTC_2 \\ &\dots \end{aligned} \right\}, \quad (5)$$

where C_1, C_2, \dots , denote their concentrations. The masses in gram atoms of the constituents are given by

$$\left. \begin{aligned} v \Sigma n_a C_{a_n} &= M_a \\ v \Sigma n_b C_{b_n} &= M_b \\ &\dots \end{aligned} \right\}, \quad (6)$$

where C_{a_n} denotes the concentration in mols of the molecules which contain n_a gram atoms of atoms a , etc. Besides there are a number of mass action equations, each of which may be written in the generalized form

$$KC_1 C_2 \dots = C_4 C_5 \dots \quad (7)$$

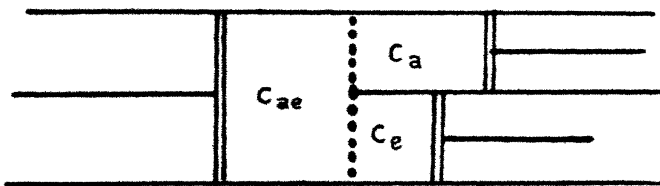
The differential equation with respect to the mass M_a as independent variable is

$$v \frac{\partial p}{\partial M_a} - M_a r_a \frac{\partial p_a}{\partial M_a} - M_b v_b \frac{\partial p_b}{\partial M_a} - \dots = 0, \quad (8)$$

and so on.

Now, the differential equations of the type (3) and (8) are derived by passing a mixture through a certain isothermal cycle. If the mixture consists of two constituents it is initially contained in the chamber C_{ae} of an apparatus shown diagrammatically in fig. 1, this chamber being separated from the chambers C_a and C_e by membranes, each of which is permeable to one of the constituents. An essential condition of the process is that in passing the mixture from the chamber C_{ae} into the chambers C_a and C_e , or *vice versa*, the pressures in the chambers are kept constant. We will

Fig. 1.



now vary this process by supposing that the walls of one of the chambers C_a and C_e —say C_a , is permeable to a gas contained in an adjacent infinitely large reservoir. Whatever the nature of the reaction now going on in this chamber, it is evident that the foregoing condition will still be satisfied, since the pressure in the chamber does not depend on its volume for constant pressures in the chambers C_{ae} and C_e . The general forms of the differential equations obtained will therefore be the same as before, but the forms of equations (4) and (5) may now be different. Now, if it can be shown by means of these equations that, corresponding to the first arrangement, the constant of mass action of the reacting mixture in the chamber C_{ae} is a function of the temperature only, it will be evident that with the second arrangement this may no longer be true. It follows, therefore, that a reaction taking place in one of the chambers C_a and C_e may affect catalytically the reaction in the chamber C_{ae} , causing the constant of mass action to become a function of the volume and masses of the constituents as well as of the

temperature. Examples of this will be considered in Sections 3, 4, and 6.

Instead of supposing that the chamber walls of the chamber C_a are permeable to molecules c , we may suppose that this is not the case, but that the chamber contains permanently a mass M_c of molecules c . In order to derive the differential equations in this case, we must now suppose that when the mixture is initially contained in the chamber C_{aa} the chamber C_a is at a volume V_{a1} , and contains molecules of the constituent a as well as molecules c . On transferring the mixture in the chamber C_{aa} into the chambers C_a and C_c we must further suppose that the pressures in the chambers C_{aa} and C_c only are kept constant.

Let us now pass the mixture through a cycle similar to the one used * to derive equation (3), to which the reader is referred for information. The external work done by the chamber C_a during the process (a) is now not $p_a v_a M_a$, but

$$\int_{V_{a1}}^{V_{a2}} p_a \cdot \partial V_a,$$

where V_{a1} and V_{a2} denote the volumes of the chamber at the beginning and end of the process. The work done by the chamber during the process (b) is not $p_a M_a \cdot \partial v_a$, but

$$p_{a2} \cdot \partial V_{a2},$$

where p_{a2} denotes the pressure when the volume is V_{a2} . The work done during the process (c) is

$$-\int_{V_{a1}}^{V_{a2}} p_a \cdot \partial V_a - \partial \int_{V_{a1}}^{V_{a2}} p_a \cdot \partial V_a,$$

instead of $-M_a v_a p_a - \partial(M_a v_a p_a)$. Finally, on equating the external work done, we obtain

$$v \frac{\partial p}{\partial v} - M_a v_a \frac{\partial p_a}{\partial v} - \frac{\partial}{\partial v} \int_{V_{a1}}^{V_{a2}} p_a \cdot \partial V_a + p_{a2} \cdot \frac{\partial V_{a2}}{\partial v} = 0. \quad (9)$$

If the last two terms in this equation, on substituting from equations (4), (5), and (6), assume a different functional form than the term $M_a v_a \frac{\partial p_a}{\partial v}$, which corresponds to no molecules c being present in the chamber C_a (compare with equation (3)), the molecules c in the chamber influence catalytically the reaction going on in the chamber C_{aa} . The constant of mass

action of the reaction is then necessarily a function of the volume and masses of the constituents, if it is a function of the temperature only when the molecules c are absent*.

§ 3. *The Catalytic Effect of the Molecular Volume of a Gas on the Constant of Mass Action of a Reaction.*

Suppose that the walls of the chamber C_a are permeable to molecules c in the gaseous state contained in an adjacent infinitely large reservoir. Let us further suppose that these molecules have a volume associated with them which is equal to b per c.c. If we suppose that we are dealing with a reaction between molecules a and c in the chamber C_{ac} , the chamber C_a will contain also molecules a , and the chamber C_c molecules c . The differential equation of the reaction in the chamber C_{ac} with respect to its volume v as independent variable is

$$v \frac{\partial p}{\partial v} - M_a v_a \frac{\partial p_a}{\partial v} - M_c v_c \frac{\partial p_c}{\partial v} = 0, \quad \dots \quad (10)$$

where M_a and M_c denote the masses in mols of the substances a and c , and v_a and v_c the volumes of mols in the chambers C_a and C_c at the pressures p_a and p_c respectively, and p denotes the total pressure of the mixture in the chamber C_{ac} . Let us next suppose that the molecules a and c in the chamber C_a do not interact chemically, in which case the pressure p_a of the molecules a is given by

$$p_a = \frac{RT}{v_a} \frac{1}{1-b} = RTC_a' \frac{1}{1-b}, \quad \dots \quad (11)$$

* It will be helpful to point out that the equation of state of the matter in the chamber C_a may be written $p_a = \phi_1(T, V_a, C_a)$, where C_a denotes the concentration of the uncombined molecules a in the chamber C_{ac} . Its form may be determined directly by experiment with the chamber C_{ac} containing only molecules a . The mass M_{a1} of molecules a in the chamber C_a is given by the equation $M_{a1} = \phi_2(T, V_a, C_a)$, whose form may also be determined by experiment. It should also be observed that M_a , the total mass of the substance a in the chamber C_{ac} at the volume v , is now a function of v , and that

$$\frac{\partial M_a}{\partial v} = - \frac{\partial M_{a1}}{\partial v} = - \frac{\partial M_{a1}}{\partial C_a} \frac{\partial C_a}{\partial v}.$$

The volume V_{a2} corresponds to the total and constant mass $M_a + M_{a1}$ of the substance a in the chamber C_a , and is given by the equation $V_{a2} = \phi_3(T, C_a)$, whose form is determined by experiment. Hence

$$\frac{\partial V_{a2}}{\partial v} = \frac{\partial V_{a2}}{\partial C_a} \frac{\partial C_a}{\partial v}.$$

where C_a' denotes the concentration of the molecules a in the chamber, $v_a = 1/C_a'$, and the factor $1/1-b$ expresses the effect of the volume of the molecules c on the pressure. If C_a denotes the concentration of the free molecules a in the chamber C_{ac} , the partial pressure they exert is equal to RTC_a . This pressure must be equal to the pressure in the chamber C_a , otherwise diffusion from one chamber to the other will take place, and hence

$$C_a = C_a' \frac{1}{1-b}, \dots \dots \dots (12)$$

which gives the relation between C_a and C_a' . The term $M_a v_a \frac{\partial p_a}{\partial v}$ in equation (3) may now be written

$$M_a v_a \frac{\partial p_a}{\partial v} = \frac{M_a RT}{C_a' (1-b)} \frac{\partial C_a'}{\partial v} = \frac{M_a RT}{C_a (1-b)} \frac{\partial C_a}{\partial v}$$

by means of equations (11) and (12) and since $v_a = 1/C_a'$. If the chamber C_a did not contain molecules c , the foregoing term expressed in terms of C_a would have the form $\frac{M_a RT}{C_a} \frac{\partial C_a}{\partial v}$. Hence, if in the latter case the constant of

mass action of the reaction in the chamber C_a is a function of the temperature only, this will not be the case when the chamber C_a contains molecules possessing molecular volume, the constant now being a function of the volume as well*.

Similarly, it can be shown, by means of the differential equations involving the masses of the constituents as independent variables, that the constant of mass action is now a function of the masses of the constituents. The molecular volume of the molecules c thus has a catalytic action on the reaction in the chamber C_{ac} through contact by means of the molecules a , which is exhibited by a change in the constant of mass action.

This effect should also occur if the reacting molecules themselves possess molecular volume, as is the case in practice. If this volume be known, its effect on the constant of mass action may easily be calculated by means of the differential equations given in Section 2. The same effect would be produced by the addition of an inert gas possessing molecular volume to the reacting mixture. The effect might be large enough to measure in practice.

* This will be immediately evident from the investigations in the second paper quoted. The conditions that K is independent of v for the cases considered are now obviously not satisfied.

§ 4. *The Effect of the Functional Form of the Constant of Mass Action of a Reaction on the Form of the Constant of another Reaction.*

Let us suppose that the molecules c in the chamber C_a in the arrangement of the preceding Section interact with the molecules a , and that the corresponding constant of mass action K_{ac} is a function of the volume of the chamber C_a , or what amounts to the same thing, a function of the volume v of the chamber C_{ac} . The term $M_a v_a \frac{\partial p_a}{\partial v}$ in equation (3) may then be written in the form

$$M_a v_a \left\{ \left(\frac{\partial p_a}{\partial v} \right)_{K_{ac}} + \left(\frac{\partial p_a}{\partial K_{ac}} \right)_v \frac{\partial K_{ac}}{\partial v} \right\}.$$

Since $\frac{\partial K_{ac}}{\partial v}$ occurs only once and represents an independent function it will not disappear from the equation. Hence, if the equation is solved, we finally obtain the constant of mass action of the reaction in the chamber C_{ac} expressed in terms of $\frac{\partial K_{ac}}{\partial v}$, which is a function of v . This shows that the reaction in the chamber C_a affects that in the chamber C_{ac} , and *vice versa*, and therefore the reactions will also affect each other if they take place in the same mixture.

§ 5. *The Effect of a Magnetic and Electric Field on the Constant of Mass Action of a Reaction.*

Let us suppose that a gaseous reaction between molecules a and c takes place in the chamber C_{ac} , and that the molecules a in the chamber C_a are subjected to a magnetic field. If the molecules a are paramagnetic, energy must be expended to take a molecule out of the field. The concentration of the molecules inside the field will therefore be greater than outside of it, since the velocities of the molecules are distributed according to Maxwell's law, and only those are able to escape whose velocities lie above a certain value. An analogous case is a liquid in contact with its vapour, the attraction of the liquid taking the place of the magnetic field. The pressure in the chamber C_a will therefore be given by

$$p_a = RT C_a' a, \quad . \quad . \quad . \quad . \quad . \quad (13)$$

where C_a' denotes the concentration of the molecules a and α a quantity less than unity depending on the strength of the field. The pressure of the free molecules in the chamber C_{aa} is RTC_{aa} , which must be equal to the pressure in the chamber C_a , otherwise diffusion from one chamber to the other will take place, and hence

$$C_a = C_a' \alpha. \quad . \quad . \quad . \quad . \quad . \quad (14)$$

The term $M_a v_a \frac{\partial p_a}{\partial v}$ in equation (3) may now be written

$$M_a v_a \frac{\partial p_a}{\partial v} = \frac{\alpha M_a RT}{C_a'} \frac{\partial C_a'}{\partial v} = \frac{\alpha M_a RT}{C_a} \frac{\partial C_a}{\partial v}$$

by means of equations (13) and (14) and since $v_a = 1/C$. If no magnetic field were present the value of α would be equal to unity. Thus, if the differential equation (3) is solved corresponding to a magnetic field existing in the chamber C_a , the constant of mass action of the reaction in the chamber C_{aa} appears a function of the volume. Similarly, it can be shown by using equations of the type (8) that the constant of mass action is a function of the masses of the constituents.

The same result is obtained on applying the field to the chamber C_{aa} . The value of α , it will be observed, will have different values for the different molecules. It will not be difficult to see from an inspection of equations (3), (4), (5), and (6), that the effect of the field on the constant of mass action is in this case different from that obtained by applying the field to both the chambers C_a and C_{aa} .

If we suppose that the magnetic field is applied to the three chambers C_a , C_{aa} , and C_{aa} at the same time, it will not be difficult to see that the effect on the constant of mass action is different from the previous cases considered. This indicates that the magnetic field produces a change in a molecule which gradually disappears when it wanders out of the field, as may happen in the first two arrangements.

If an electric field is applied instead of a magnetic field similar results are obtained.

§ 6. *The Effect of a Dense Substance on the Constant of Mass Action and Catalytic Action.*

If in the process to which equation (9) refers, the substance c in the chamber C_a does not obey the gas laws, the expression, taking into account that M_a is now a function of v ,

$$\left\{ v \left(\frac{\partial p}{\partial M_a} \right)_v - M_a v \left(\frac{\partial p_a}{\partial M_a} \right)_v \right\} \frac{\partial M_a}{\partial v} - \frac{\partial}{\partial v} \left(\int_{V_{a1}}^{V_{a2}} p_a \cdot \partial V_a + p_{a2} \frac{\partial V_{a2}}{\partial v} \right)$$

will involve quantities depending on the nature of the substance *c*. That this is so will be evident from supposing that the substance *c* in the chamber *C_a* is in the gaseous state, but possesses a considerable molecular co-volume, in which case it can easily be shown, similarly as in Section 3, that the above expression involves this co-volume. The constants depending on the substance *c* do not occur elsewhere in the equation than in the above expression, and also do not occur in the equations (4), (5), and (6) used to effect the solution of equation (3). They will be associated with factors which may be expressed as functions of the variables *v*, *M_a*, *M_c*, *M_a'*, *M_c'*, where *M_a'* and *M_c'* denote the masses of the constituents *a* and *c* in the chamber *C_a* when its volume is *V_{a1}*, and *v* denotes the volume of the reacting mixture in the chamber *C_a*, and *M_a* and *M_c* the masses of the constituents *a* and *c* it contains. Hence the solution of equation (3), from which the concentrations of the various molecules in the chamber *C_a*, may be determined*, when substituted in equation (7), gives the constant of mass action a function of the above variables. If the equation of state of the mixture in the chamber *C_a* under the changing conditions during the cycle be known, the calculations can actually be carried out. The differential equations involving the masses of the constituents as independent variables may similarly be used.

Thus, we have the very important result that a dense substance in contact with a gaseous reaction of which it occludes to a certain extent one or more of the constituents, renders the constant of mass action a function of the volume and masses of the constituents. A catalytic agent thus is not only likely to change the velocities of the various changes continually going on in the reacting mixture, but the value of the constant of mass action as well, and to an extent depending on the volume and masses of the constituents of the reacting mixture. The far-reaching nature of these results will be further discussed in a separate paper.

Shenectady, N.Y., U.S.A.

* *Loc. cit.*

XIV. *On the Theory of Light-scattering in Liquids.*

To the Editors of the Philosophical Magazine.

GENTLEMEN,—

IN a paper published in the *Phil. Mag.* v. pp. 498–512 (1928), under the title of “A Theory of Light-scattering in Liquids,” Prof. C. V. Raman and K. S. Krishnan refer to a new theory of light-scattering which they attribute to Dr. K. R. Ramanathan (‘*Indian Journal of Physics*,’ i. p. 413, 1927), and which, in their notations, leads to the formulæ:—

$$i = i_0 \frac{\pi^2}{2d^2} \cdot \frac{RT\beta}{N\lambda^4} (\mu^2 - 1)^2 \cdot \frac{6 + 6r}{6 - 7r},$$

$$r = \frac{2n_0 F}{N} \frac{RT\beta}{\left(\frac{\mu^2 - 1}{4\pi}\right)^2} + \frac{7}{3} n_0 F.$$

Now these formulæ have already been given by myself with equivalent notations (*C. R.* p. 212, Aug. 1925). In my work I named these “Formulæ type Vessot-King,” in order to remind us that Prof. Vessot-King (*Nature*, cxi. p. 667, 1923), was the first to give a molecular theory of light-scattering. This author implicitly supposed that the polarization-field had no fluctuation. In my paper mentioned above, I brought this hypothesis into full evidence, showing that it was sustainable, and that the disagreement between Vessot-King’s theory and those of Gans and Ramanathan was due to the fact that the latter replaced that hypothesis by others.

Krishnan’s experiments, instigated by my work mentioned above, having shown the superiority of the theory “type Vessot-King,” Dr. K. R. Ramanathan, wishing to correct his formulæ, simply adopted the hypothesis in question, only justifying it by qualitative reasons. He therefore fell again into the “Formulæ type Vessot-King” which I gave in my paper, without apparently adding anything. The same conclusions hold for the theory proposed by Prof. C. V. Raman and K. S. Krishnan, which has also, however, the special interest of giving a very suggestive explanation for the apparent difference of anisotropy which the molecules in a liquid or a gaseous state seem to offer.

To say the truth, the question of the fluctuations of the polarization field is still an open one; I will show, in a paper

to be published soon in the *Annales de Physique*, that these fluctuations exist, but that one can bring them in the calculations of the intermolecular field, which must be considered contrary to the opinion expressed some time ago by Dr. K. R. Ramanathan.

Collège de France, Paris.
March 20th, 1928.

Yours faithfully,
Dr. Y. ROCARD.

XV. *A Note on the Magnetic Field of a Rectilinear Circuit and the Attraction of a Straight Wire.* By J. A. TOMKINS, A.R.C.Sc., F.Inst.P. (Technical College, Bradford)*.

HAVING had occasion recently to consider at about the same time with different students, the apparently diverse problems of the magnetic field of a rectangular coil and the gravitational attraction of a straight wire, I was led to note that the relation between them was such that a simple geometrical construction for the one was, with a slight extension, applicable to the other. As the latter has not, so far as I am aware, been previously described, and the former, judging from its absence from most of the text-books, does not appear to be generally known, a brief account of it may be of interest. The geometrical construction referred to is that for the magnetic field of a long straight conductor which was described by Dr. G. F. C. Searle in 1891*.

Taking Ampère's formula $i \cdot ds \cdot \sin \theta / r^2$ for the magnetic force due to a current element ds , let NAB (fig. 1) be the conductor, ab the current element, and P the given point. From P drop the perpendicular PN, and with P as centre and radius PN draw a circle touching the wire at N. Join Pa, Pb, meeting the circle in d and e . Through d and e draw df , eg perpendicular to the diameter parallel to the wire and dh , ek perpendicular to PN. Through a draw ac perpendicular to Pb.

Then if $PN = a$, $Pb = r$, and the angle $PbN = \theta$, the magnetic force at P, perpendicular to the plane of the paper due to the current element ab , is

$$\frac{i \cdot ab \cdot \sin \theta}{r^2} = \frac{i \cdot ac}{r^2} = \frac{i \cdot de}{ra} = \frac{i}{a} \cdot \frac{fg}{a} = \frac{i}{a^2} \cdot fg.$$

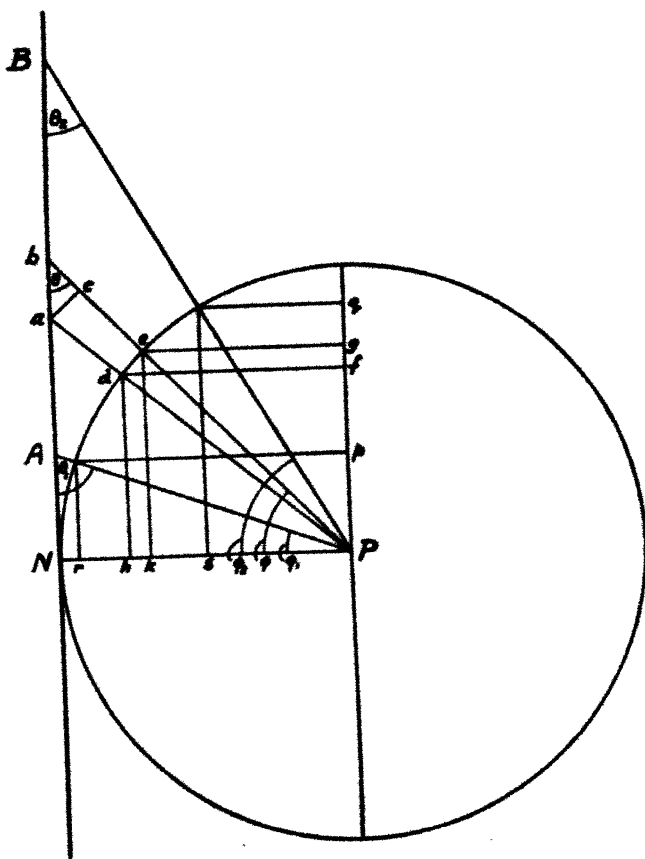
* Communicated by the Author.

† 'Electrician,' Dec. 4, 1891.

Hence, for the whole conductor, the magnetic force at P is

$$\frac{i}{a^2} \Sigma \overline{fg} = \frac{2i}{a}.$$

Fig. 1.



For a finite portion AB of the conductor, the contribution to the magnetic force at P will be

$$\frac{i}{a^2} \overline{pq} = \frac{i}{a} (\sin \phi_2 - \sin \phi_1).$$

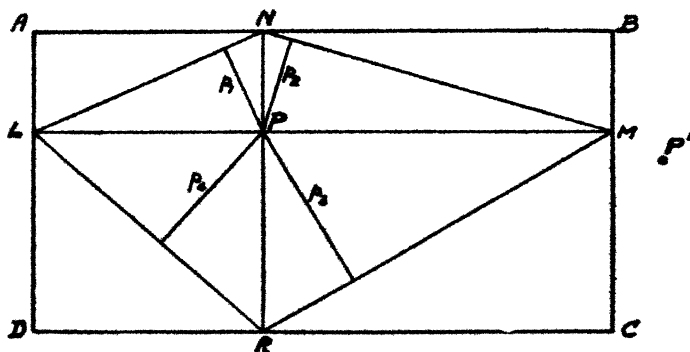
In the case of a thin straight wire of attracting matter, if ρ be the linear density, the attraction on unit mass at P,

due to an element of the wire, will be $\frac{G\rho \cdot ds}{r^2}$ along r , where G is the constant of gravitation. Hence the component perpendicular to the wire is $G\rho \cdot ds \cdot \sin \theta / r^2$ and that parallel to it $G\rho \cdot ds \cdot \cos \theta / r^2$.

Comparing these expressions with that for the magnetic field due to a current element, it will be seen that a similar method can be employed for their summation. Thus for an infinite wire the resultant force perpendicular to it is $2G\rho/a$, For a wire AB of finite length, the component perpendicular to it is obviously

$$\frac{G\rho}{a^2} \cdot p\bar{q} = \frac{G\rho}{a} (\sin \phi_2 - \sin \phi_1),$$

Fig. 2.



and that parallel to it is

$$\frac{G\rho}{a^2} \cdot r\bar{s} = \frac{G\rho}{a} (\cos \phi_1 - \cos \phi_2).$$

Returning now to the magnetic field of a circuit, the magnetic force at any point due to a rectilinear circuit can be calculated by the method given, whereas, with the usual circular coil, the calculation for points not on the axis involves the use of spherical harmonics or elliptic integrals. In the case of a rectangular circuit, the expression for the magnetic force at any point in its plane was, I believe, first derived by the late Prof. G. M. Minchin *, in a form which does not appear to be usually given.

Let $ABCD$ (fig. 2) be the rectangular circuit and P the given point. Through P draw the straight lines LM , NR ,

* *Ibid.* Sept. 6, 1895.

parallel to the sides. Then denoting LA and AN by a_1 and a_2 and the angles they subtend at P by ϕ_1 and ϕ_2 , the contribution of these adjacent portions to the magnetic force at P will be

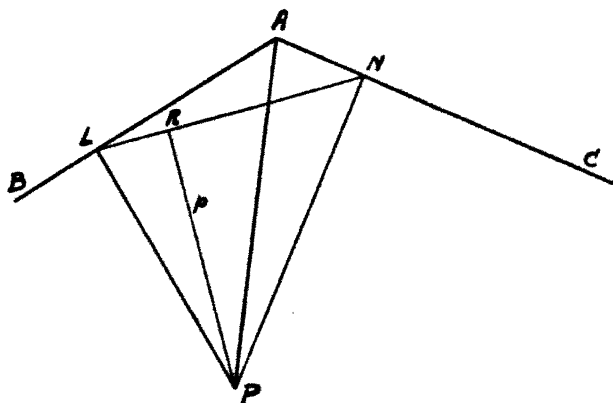
$$i \left(\frac{\sin \phi_1}{a_2} + \frac{\sin \phi_2}{a_1} \right) = i \left(\frac{a_1}{a_2 \sqrt{a_1^2 + a_2^2}} + \frac{a_2}{a_1 \sqrt{a_1^2 + a_2^2}} \right) \\ = \frac{i}{a_1 a_2 / \sqrt{a_1^2 + a_2^2}} = \frac{i}{p_1},$$

where p_1 is the perpendicular from P on LN.

Hence for the whole circuit the magnetic force at P is

$$i \left(\frac{1}{p_1} + \frac{1}{p_2} + \frac{1}{p_3} + \frac{1}{p_4} \right)$$

Fig. 3.



If the point is outside the circuit as at P', it will be seen that two of the perpendiculars, p_2 and p_3 , will be negative.

This result was obtained by Prof. Minchin from the consideration of the potential due to the equivalent magnetic shell, a more fundamental but less simple method than that given here, as it involves the rather troublesome calculation of the solid angle and the derivation of the magnetic force from the potential. Prof. Minchin also gave*, though without proof, a corresponding expression for the magnetic force at any point in the plane of a triangular coil, viz.,

$$i \left(\frac{\sin A}{p_1} + \frac{\sin B}{p_2} + \frac{\sin C}{p_3} \right).$$

* *Ibid.* Sept. 27, 1895.

where A, B, and C are the angles of the triangle, and p_1 , p_2 , and p_3 the perpendiculars from the given point on the lines joining the feet of the perpendiculars from the point on the sides.

But it can be easily shown that a similar expression holds for the magnetic force at a point in the plane of any rectilinear circuit.

For let BAC (fig. 3) be two adjacent sides of the circuit, PL and PN the perpendiculars on these two sides from the given point P, and PR the perpendicular on LN, the line joining the feet of these perpendiculars. Then the magnetic force at P due to the adjacent portions LA, AN of the circuit is

$$i \left(\frac{\sin \text{APL}}{\text{PL}} + \frac{\sin \text{APN}}{\text{PN}} \right).$$

But, since the points PLAN are concyclic, we have

$$\text{PAL} = \text{PNL} \quad \text{and} \quad \text{PAN} = \text{PLN}.$$

Hence

$$\sin \text{APL} = \cos \text{PAL} = \cos \text{PNL},$$

$$\text{and} \quad \sin \text{APN} = \cos \text{PAN} = \cos \text{PLN}.$$

Thus the expression becomes

$$\begin{aligned} & i \left(\frac{\cos \text{PNL}}{\text{PR} \sin \text{PLN}} + \frac{\cos \text{PLN}}{\text{PR} / \sin \text{PNL}} \right) \\ &= i \left(\frac{\sin \text{PLN} \cdot \cos \text{PNL} + \sin \text{PNL} \cdot \cos \text{PLN}}{\text{PR}} \right) \\ &= i \left(\frac{\sin \text{PAN} \cdot \cos \text{PAL} + \sin \text{PAL} \cdot \cos \text{PAN}}{\text{PR}} \right) \\ &= i \frac{\sin \text{LAN}}{\text{PR}}. \end{aligned}$$

Hence, for the whole circuit, the magnetic force at P may be written

$$i \Sigma \frac{\sin A}{p}.$$

The expressions for the rectangle and triangle are thus but particular cases of this more general theorem.

XVI. A new Method of determining the Mobility of Ions or Electrons in Gases. By R. J. VAN DE GRAAFF, B.Sc., Queen's College, Oxford*.

1. **I**N many of the experiments that have been made to determine the velocity of ions or electrons in the direction of an electric force, the velocity that is measured is in some cases an upper limit of the mean velocity and in others a lower limit. This may be due to the fact that the velocities of all the ions are not the same, and also to the fact that a group of ions tends to diffuse in all directions. In order to avoid these and certain other difficulties I have devised a method for measuring the mean velocity of a group of ions moving in a gas under a steady and uniform electric force.

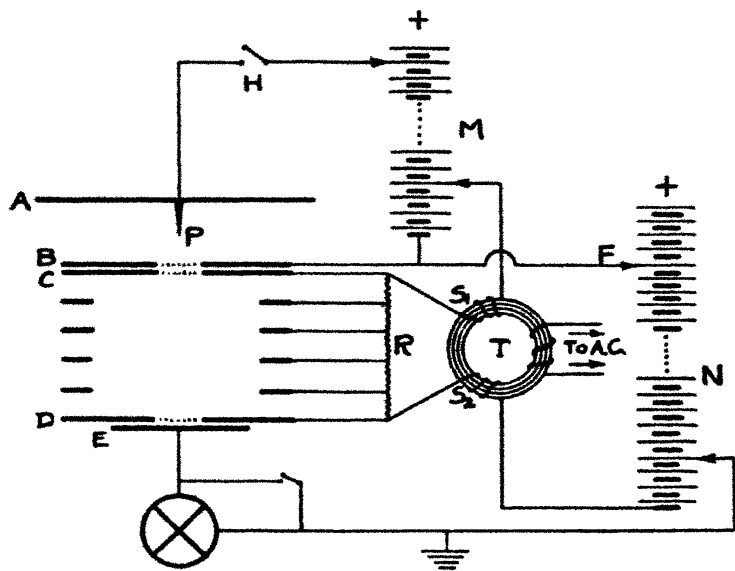
The principle of the method is the same as that used for the determination of the velocity of light by Fizeau, who employed a rotating toothed wheel as a periodic shutter to break up a beam of light into sections which travel a known distance and then again encounter the periodic shutter, which, depending on the time of arrival of the sections of the beam, either stops them or allows them to pass on. Thus the transmitted light may be observed as a function of the speed of rotation of the disk, and from this, taking into account the geometry of the apparatus, the velocity of light may be easily computed.

2. The apparatus used for the determination of the velocity of ions works in an analogous way. An oscillating potential in combination with grids gives the shutter effect corresponding with that of the rotating toothed wheel of Fizeau. The arrangement is shown diagrammatically in fig. 1. The plate A is maintained by the battery M at such a potential that a small glow-discharge is formed at the needle-point P, thus supplying to plate B ions of the sign whose velocity is to be measured. These, for the sake of clearness in description, may be assumed to be positive ions. Plates B, C, and D are provided, as shown, with central grids. The connexions to the batteries M and N maintain a steady potential of a few volts, opposing the passage of positive ions from plate B to plate C, and likewise from plate D to plate E. The plate E is connected to an electrometer for the measurement of the ionic current received through the

* Communicated by Prof. J. S. Townsend, F.R.S.

gas. As may also be seen from the diagram, the connexions through the batteries M and N furnish an electric field favouring the passage of positive ions from plate C to plate D, and between these plates are four equally-spaced rings connected to the resistance R, which is composed of a series of five equal high resistances. This arrangement provides, between plates C and D, a uniform field in which the velocity of positive ions is determined by measuring the time required for the ions to pass from plate C to plate D, a distance of 5 cm. It is evident then that, with no oscillating potential, positive ions cannot reach the plate E

Fig. 1.



connected to the electrometer, as the forces in the space between plates B and C, and in the space between plates D and E, are in the contrary direction.

In order to reverse these forces momentarily and at regular intervals, an oscillating current is supplied to the primary of a transformer T with two secondaries, S_1 and S_2 , which have the same number of turns and are wound in the same direction. A consideration of the connexions shown in fig. 1 shows that an oscillating potential is superposed over the steady potentials of the system of plates and rings connected to the resistance R. The connexions are arranged so that the potential of this system of plates and rings varies

as a whole, while the electric force between the plates C and D, where the velocity of the ions is determined, remains steady and is entirely unaffected by the oscillation. The oscillating potential is so adjusted that its maximum instantaneous value slightly exceeds the small, steady, opposing potentials between plates B and C and between plates D and E. Thus, when the oscillating potential is maximum negative, a group of positive ions will pass through the grid in plate B and on through the grid in plate C. After traversing the grid in plate C, the group moves under the action of the steady electric field with a uniform velocity toward plate D. If the group arrives at the grid of plate D when the oscillating potential is at its maximum positive value, some of the ions will pass through to the plate E and produce an electrometer deflexion. If, on the other hand, the group arrives at plate D when the oscillating potential is not near its maximum positive value, the ions will not pass through to plate E, but will be discharged on the grid of plate D. Thus it is seen that the current to the electrometer will be at a maximum when the velocity of the ions is such that the time required by a group of ions to pass from plate C to plate D is just equal to the time required for an odd number of half-cycles of the oscillating potential. Therefore the condition for a maximum current to the electrometer is that

$$W = \frac{d}{t} = \frac{2fd}{n} \quad . \quad . \quad . \quad . \quad . \quad (1)$$

where W is the velocity of the ions in the direction of the electric force; d is the distance apart of the plates C and D; t is the time of flight of the ions between the plates C and D; f is the frequency of the oscillating potential; and n is an odd integer representing the number of half-cycles elapsed during the time of flight of the ions from plate C to plate D. Thus the velocity of the ions in the electric field between the plates C and D may be found.

Laporte in some recent investigations* has used a method based on this principle, where a rotating wheel with a slit is used as a periodic shutter at each end of the space over which the ions are timed.

3. In order to simplify fig. 1 as much as possible, certain details of the apparatus are not shown. The connexions to the plates B, C, and D were provided with potentiometers for fine potential adjustment. Also a double switch was so

* M. Laporte, *Annales de Physique*, viii. p. 466 (Nov. 1927).

connected that in one of its positions the ends of the resistance R were connected as shown in fig. 1, while in the other position of the switch the ends of the resistance R were connected directly to the batteries M and N , and not through the secondaries of the transformer.

In taking the electrometer readings, the glow-discharge was first turned on by closing the switch H , then the oscillating potential was connected to the instrument for a definite period, say thirty seconds, by means of the double switch just described, after which the glow-discharge was turned off and the current to the electrometer measured by means of the induction-balance method due to Townsend, in which the insulated system connected to the electrometer is maintained at zero potential during the course of the experiment.

As a source of oscillating current for the primary of the transformer T , a small alternating generator of variable speed was used, the frequency being determined by means of a revolution counter.

The sides of the instrument, which was constructed principally of brass, were enclosed by a glass cylinder, the ends of which fitted into grooves in the end-plate A and in the base-plate. Both of these joints were coated on the outside by an elastic cement, which effectively rendered them airtight, as was shown by the fact that the instrument gave no indication of a leak when pumped out to a pressure of 0.001 mm. of mercury and left for a period of several days.

The point P , at which the glow-discharge was obtained, was constructed by sharpening a nickel wire to a needle-point.

The principle of split insulation was used in insulating the plate E , which was connected to the electrometer. Glass insulation was used throughout in order to prevent the introduction of impurity by the evolution of occluded gases from the insulating material. The electrical leads from the various plates and rings were taken out through the base of the instrument by means of copper-glass joints, from one of which a glass side-tube led to the apparatus from which the supply of gas was obtained.

The principal dimensions of the instrument were as follows:—The diameter of the inner plates and rings was 7.5 cm.; the distance from point P to plate B , 1.3 cm.; from plate B to C , 0.36 cm.; from plate C to D , 5.00 cm.; and from plate D to E , 0.45 cm. For the construction of the grids, plates B and C were thinned at the centre to a thickness of 0.45 mm., and plate D to a thickness of

0.26 mm. In the middle of the plates a series of parallel cuts were sawed through the metal. These cuts were 0.60 mm. wide and were separated by strips of metal 0.36 mm. wide, and covered on each plate an area approximately circular and 2.1 cm. in diameter.

The gas used in the experiments was hydrogen, generated by the electrolysis of barium hydrate, and passed into the apparatus by diffusion through a heated palladium tube fused into the glass-work of the apparatus. Before each series of experiments was begun, the whole apparatus was washed out many times with hydrogen. A Toepler pump and a McLeod gauge were connected to the apparatus and were separated from the instrument by taps and a liquid-air trap to prevent the diffusion of mercury vapour into the instrument. A large glass tube was connected to the instrument in order to provide a space in which an electrodeless discharge could be formed. The spectrum of this discharge was observed at intervals with a small direct-vision spectroscope, and no lines due to impurities were seen.

4. The electrometer readings may be taken according to either of two plans. In the first method the readings corresponding to various values of the potential between plates C and D were taken, while the frequency of the oscillating potential was kept constant. In the second method the electrometer readings may be taken with different frequencies of the oscillating potential, while the field of force between plates C and D is kept constant. The second of these plans is not so convenient experimentally as the first, where, between the various readings, only the connexion F on the battery N is changed.

The experimental results obtained by the first method may be shown by a curve, where the electrometer current is plotted as a function of the voltage V between the plates C and D. Two examples of these curves for positive ions are given in figs. 2 and 3. The curve, fig. 2, represents the results obtained with hydrogen at 94 mm. pressure, and the curve, fig. 3, with hydrogen at 181 mm. Assuming for the moment that the velocity is proportional to the electric force, the time of flight t of the ions is inversely proportional at any point on the curve to the voltage V , the abscissa of the point. Thus, in passing along the curve from right to left, the increasing time of flight becomes successively equal, first to one-half cycle of the oscillating potential, then to three half cycles, then to five, etc., and in each case the current passes through a maximum value, in agreement with

equation (1) above. If V_1 is the value of the voltage at the first maximum, corresponding to $n=1$, then the successive maximums should occur at $1/3V_1$, $1/5V_1$, etc. Inspection of

Fig. 2.

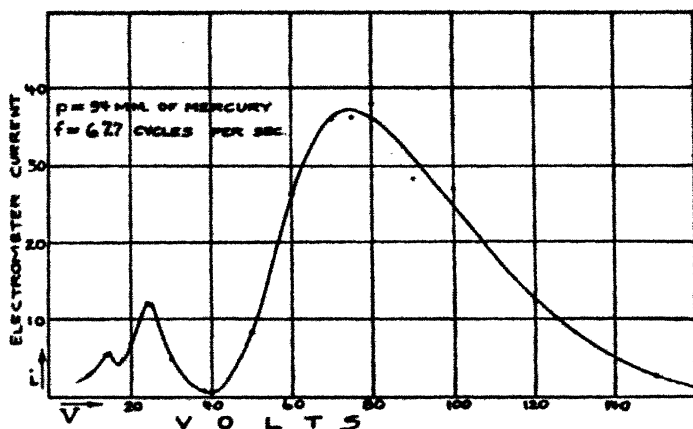
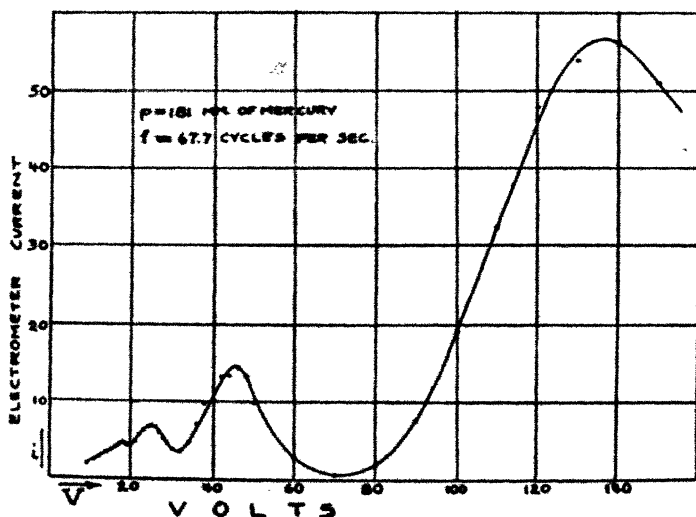


Fig. 3.



figs. 2 and 3 shows that this is the case within a few per cent., and the result confirms the assumption made above that the velocity of the positive ions is proportional to the electric force, within the range of the experiment.

As the origin is approached, it is seen that the maxima fall nearer and nearer together, until finally they become indistinguishable, due to diffusion and other causes. In fig. 3, for example, this occurs after the maximum corresponding to seven half cycles.

5. The velocities W of the ions may be found from the points of maximum current on the curves, the electric force being V/d . With hydrogen at 94 mm. pressure, the velocities W and the corresponding electric forces X obtained from the curve, fig. 2, are:—

W .	X .
677	14.8
226	4.84
135	2.96

With hydrogen at 181 mm. pressure, the values of W and X obtained from the curve fig. 3 are:—

W .	X .
677	27.2
226	9.04
135	5.00
96.7	3.60

If the mobility W_0 be defined as the velocity of the ions under an electric force of one volt per cm. in the gas at 760 mm. pressure, the velocity at the pressure p is

$$W = 760 \cdot W_0 \cdot \frac{X}{p}.$$

Using this relation, the values found for the mobility from the values of W_0 obtained with the two largest forces are 5.66 and 5.78 where the pressure was 94 mm., and 5.93 and 5.95 where the pressure was 181 mm. The mean of the above values gives $W_0 = 5.8$ cm. per second for positive ions in hydrogen.

The values obtained by different observers for the mobility of the positive ion in hydrogen vary, but most of these values lie between that of 5.34, obtained by Lattey and Tizard*, and that of 6.70 obtained by Zeleny†.

* R. T. Lattey & H. T. Tizard, Proc. Roy. Soc. A, lxxxvi. p. 349 (1912).

† J. Zeleny, Phil. Trans. A, cxcv. p. 193 (1900).

6. The method of determining mobilities described in this paper shows the presence of ions of a given velocity by a curve characterized by a series of maxima, whose sharpness and relative positions give a measure of the accuracy and reliability of the results. The accuracy of the experiments is not appreciably affected by diffusion and space-charge, as these tend not to shift the positions of the maxima, but merely to make them less sharp. The method is adapted to the investigation of cases where there may be present in the gas different kinds of ions having different velocities. Each kind of ion would then be shown by a separate series of maxima whose abscissæ would show the velocity and whose ordinates would show the relative number of ions of that kind.

The alternating-current generator used in the present experiments can be replaced by a valve oscillator capable of supplying potentials of higher frequency, which could be used to extend this method of investigation to the determination of the large velocities of free electrons, or of positive ions in gases at low pressures.

7. In conclusion, I have much pleasure in expressing my gratitude to Professor Townsend for his constant advice and inspiration throughout the course of this research.

XVII. *On the Magnetic Susceptibilities of Electronic Isomers.*

—Part II. By Professor S. S. BHATNAGAR, *J.Sc.(Lond.)*,
and R. N. MATHUR, *M.Sc.**

IN a previous paper in this Journal†, S. S. Bhatnagar and C. L. Dhawan gave an empirical equation which was found to give remarkably satisfactory results for the diamagnetic susceptibilities of some twenty electronic isomers. According to this equation

$$\chi_m = -2.85 \times 10^{10} \times (KR)^3, \quad . \quad . \quad . \quad (1)$$

where

χ_m = molecular diamagnetic susceptibility.

R = radius of the molecule calculated on the assumption of closest packing of the atoms constituting the molecule, by using Bragg's data for the diameter of atoms‡. (A complete account is given in the paper referred to above.)

* Communicated by the Authors.

† *Phil. Mag.* [7] v. p. 536 (1928).

‡ W. L. Bragg, *Phil. Mag.* xl. p. 169 (1920).

And K = an arbitrary constant, but which in a series of isomers is found to exhibit variations with the number of atoms in the isomers. (Its significance was considered in the paper referred to above, and has again been considered later on in this paper.)

According to Langevin's theory of atomic diamagnetism

$$\chi_{\text{At.}} = -\frac{e^2}{4mc^2} \sum_n \bar{r}^2, \quad \dots \dots \dots (2)$$

the summation being extended over the n electrons in the atom, and \bar{r}^2 being the mean square of the radius of the projected orbit in a plane perpendicular to the field. Multiplying (2) by Avagadro's number, we get

$$\chi_{\text{A}} = -\frac{e^2 N}{4mc^2} \sum_n \bar{r}^2.$$

And on substituting the values of constants in the equation, we get

$$\chi_{\text{A}} = -2.85 \times 10^{10} \sum_n \bar{r}^2. \quad \dots \dots \dots (3)$$

The resemblance between our empirical equation (1) and (3) is remarkable, but while (R^2) in (1) gives the square of the radius of the molecule, (r^2) in (3) is the mean square of the radius of the projected orbit in a plane perpendicular to the field. In order to make the resemblance closer, we take in (3) the mean square of the radius of the orbit itself, instead of the mean square of the radius of the projected orbit. If r_1 (components x_1, y_1, z_1) is the distance of an electron from the nucleus, then for an atom symmetrical in the sense that

$$\begin{aligned} \bar{x}_1^2 &= \bar{y}_1^2 = \bar{z}_1^2, \\ \Sigma \bar{r}^2 &= \frac{3}{2} \Sigma r_1^2. \end{aligned}$$

and equation (3) then becomes

$$\chi_{\text{A}} = -2.85 \times 10^{10} \times \frac{3}{2} \Sigma \bar{r}_1^2, \quad \dots \dots \dots (4)$$

and equation (1) can be written as

$$\chi_{\text{m}} = -2.85 \times 10^{10} \times \frac{3}{2} K R^2, \quad \dots \dots \dots (5)^*$$

where

$$K = \frac{2}{3} (K)^2.$$

The resemblance between Langevin's equation (4) and our empirical equation (5) is now closer than that between

* Equation (3) employed in the previous paper to this Journal has been modified to equation (5) in order to facilitate the theoretical interpretation of the values of K on the Langevin's concept of the theory of diamagnetism.

equations (1) and (4), and shows the significant fact that instead of extending the summation over all the electrons in the isomer, it has to be extended only over a fraction of them, given by the value of the constant K . It has been noted by several workers* that, in order to make the equation of Langevin applicable to all atoms, an effective value of n may have to be taken, and hence the constant K in our equation (whose value is different from n , and in the case of isomers of high values of n , much less than n) assumes particular significance. In this investigation the values of the diamagnetic susceptibilities of over twenty electronic isomers have been experimentally determined, and equation (5) is found to be applicable in all cases.

The apparatus used to determine the diamagnetic susceptibilities is Wilson's modification of Curie's Balance. The substance contained in a small glass tube, attached to a light aluminium system, is suspended in a non-homogeneous magnetic field by a thin silver ribbon. The force exerted by the field is balanced by the torsion of the suspension, and read off from a graduated torsion-head. A complete description of the experimental arrangement is given in a paper shortly to be communicated. The susceptibilities of the substances are calculated by the formula†

$$x = \frac{1}{M} \left[x_a M_a + (x_w m_w - x_a m_a) \frac{D - D_1}{D_2 - D_1} \right]$$

where x = susceptibility of the specimen.

M = mass of the specimen in grams.

x_a = specific susceptibility of air (210×10^{-7}).

M_a = the mass of air filling the same volume as the specimen.

x_w = the specific susceptibility of water (-7.25×10^{-7}).

m_w = mass of water filling the same volume as the specimen.

m_a = mass of air filling the same volume as water.

D = torsion due to specimen-tube + specimen.

D_1 = torsion due to specimen-tube alone.

D_2 = torsion due to specimen-tube + water.

Before determining the susceptibilities of the substances given in this investigation, substances of known susceptibility were used, and the results obtained were within the limit of the experimental error.

The radii of the isomers used in this communication, calculated according to the method given in the previous

* Stoner's 'Magnetism and Atomic Structures,' Chap. 14.

† Oxley, Proc. Roy. Soc. A, ci. pp. 264-279.

220 Prof. S. S. Bhatnagar and Mr. R. N. Mathur on the paper to this Journal, are given in Table I. and the remaining results in Tables II. and III. :—

TABLE I.

Substance,	Radius in Å.
BaCl ₂	2.183
CaBr ₂	1.876
*KI	3.475
*CsCl	3.425
Ethyl acetate	1.357
Butyric acid.....	1.367
*NaCl.....	2.825
*CaO	2.350
Methyl acetate.....	1.263
Propionic acid.....	1.263
*AgCl.....	2.825
*BaO	2.750
Anisol	1.532
Benzyl alcohol.....	1.532
CaSO ₄	1.422
K ₂ CO ₃	2.675
Cresol	1.532
Phenyl hydrazine	1.545
Toluidine	1.534
Methyl aniline.....	1.534
*NaF	2.450
*MgO	2.075
Isobutyraldehyde.....	1.305
Methyl ethyl ketone.....	1.305
Phenyl acetate	1.620
Methyl benzoate	1.620
Ethyl aniline.....	1.601
Dimethyl aniline	1.601
TeH ₂ O ₃	1.471
ZnSO ₄	1.051
Glycerine	1.323
Aniline	1.460

* In the case of substances marked with * the radii have been obtained by summation of the radii of the atoms. This is as it should be.

In Table II. the results obtained by calculation from equation (5) are tabulated against the experimental values, some of which are taken from the Physico-Chemical Tables of Landolt and Börnstein, and some determined experimentally.

TABLE II.

*Atomic number.	Names.	$-x_m \times 10^6$. Experimental.	$-x_m \times 10^6$. Calculated on equation (5).
28	NaCl.....	23.98	22.94
28	CaO.....	15.12	15.74
64	BaO.....	18.4	21.55
64	AgCl.....	40.13	31.99
20	NaF.....	11.76	10.95
20	MgO.....	6.73	7.83
68	K ₂ CO ₃	76.02	81.57
68	CaSO ₄	51.73	43.00
72	CsCl.....	47.12	48.94
72	KI.....	51.46	50.35
78	TeH ₂ O ₃	33.72	33.68
78	ZnSO ₄	43.58	42.44
40	Methyl acetate.....	39.78	41.8
40	Propionic acid.....	43.83	41.8
48	Ethyl acetate.....	59.7	60.4
48	Butyric acid.....	61.13	60.42
58	Anisol.....	72.79	72.79
58	Benzyl alcohol.....	67.60	72.79
58	Cresol.....	71.17	72.79
58	Phenyl hydrazine.....	67.82	70.21
58	Toluidine.....	88.69	73.00
58	Methyl aniline.....	82.74	73.00
40	Isobutylaldehyde.....	47.45	47.56
40	Methyl ethyl ketone.....	47.45	47.56
72	Methyl benzoate.....	83.23	82.9
72	Phenyl acetate.....	82.69	82.9
66	Ethyl aniline.....	89.3	89.4
66	Dimethyl aniline.....	89.66	89.4
50	Glycerine.....	56.12	53.3
50	Aniline.....	65.1	65.1

* The atomic number in the case of compounds has been taken to mean the sum of the atomic numbers of the elements in the compound.

Significance of K employed in equation (5).

K is an arbitrary constant. Its value for every two isomeric molecules is the same, as shown in Table III., where the values of *K* have been assembled together with the atomic numbers and the number of atoms in the isomers :—

TABLE III.

No. of atoms.	Atomic number.	Substance.	Value of <i>K</i> .
2	20	NaF.....	0.06
2	20	MgO	0.06
2	28	NaCl	1.5
2	28	CaO.....	1.5
2	64	AgCl	2.1
2	64	BaO.....	2.1
2	72	CsCl	2.2
2	72	KI	2.2
6	68	CaSO ₄	6.0
6	68	K ₂ CO ₃	6.0
6	78	TeH ₂ O ₃	8.194
6	78	ZnSO ₄	8.194
11	40	Methyl acetate	13.79
11	40	Propionic acid	13.79
13	40	Isobutylaldehyde	14.7
13	40	Methyl ethyl ketone	14.7
14	48	Ethyl acetate	15.32
14	48	Butyric acid	15.32
14	50	Glycerine	16.04
14	50	Aniline	16.04
16	58	Anisol.....	16.305
16	58	Benzyl alcohol	16.305
16	58	Cresol	16.305
16	58	Phenyl hydrazine	16.305
17	58	Toluidine	16.32
17	58	Methyl aniline	16.32
18	72	Methyl benzoate.....	16.44
18	72	Phenyl acetate	16.44
20	66	Ethyl aniline	18.34
20	66	Dimethyl aniline	18.34

A close examination of the above table shows three significant relations between the values of K :—

(a) The values of K increase with the number of atoms contained in the molecule. For example, in the case of molecules having three atoms the value of K is 2.5. For molecules having 13 atoms it is 14.7, and for molecules having 20 atoms it is as great as 18.34.

(b) The values of K for every two isomeric molecules are the same.

(c) In the case of groups of isomers having the same number of atoms in the molecule, the values of K increase with the atomic numbers of the groups. For example (CaSO_4 and K_2CO_3) and (TeH_2O_3 and ZnSO_4) are two groups of isomers having the same number of atoms (six) in the molecule but having different atomic numbers, 68 and 78 respectively. And the value of K in the latter group is greater than that in the former. Similar relations also exist between the groups of isomers having 2 and 14 atoms in the molecule.

Most of the experimental data have been taken from the unpublished work of Messrs. C. L. Dhawan and S. L. Luthra, to whom our thanks are due.

The values of K for the isomorphous series given in Table V. in the previous paper (*Phil. Mag.*, March 1928, vol. 5, No. 29) have not been discussed in this paper on account of the doubtful purity of these substances.

University Chemical Laboratories,
University of the Punjab,
Lahore, India.
23rd February, 1928.

XVIII. *Frequency Variations of the Triode Oscillator.* A
Reply to Lieut.-Col. Edgeworth, D.S.O., M.C., A.M.I.E.E.
By DAVID F. MARTYN, B.Sc., A.R.C.Sc.*

IN the April number of the Philosophical Magazine there appears a note by Lieut.-Col. K. E. Edgeworth under the above title, referring to a previous paper of mine (*Phil. Mag.*, Nov. 1927), also with the same title. Edgeworth remarks that it is obvious that I must have overlooked his

* Communicated by Prof. E. Taylor Jones, D.Sc.

previous paper on "Frequency Variations in Thermionic Generators," read before the Institute of Electrical Engineers (Wireless Section) on 6th January, 1926. He further claims that "So far as they cover the same ground, the experimental results appear to be in agreement, and the explanations offered are substantially the same. The main cause of frequency variations is associated with damping of one sort or another in the grid circuit, and, other things being equal, the magnitude of the frequency variation is proportional to the amount of damping. This type of frequency variation is referred to in my paper as a frequency variation of the first type."

At the outset I may state that I had read Edgeworth's paper before writing my own, although I did not see occasion to refer to it. Chief among my reasons for not doing so is the fact that the causes of frequency variation considered by Edgeworth in his paper are totally incapable of explaining the large frequency variations which I obtained. Indeed, investigation of Edgeworth's experimental results, and comparison with those of others, has led me to the conviction that his own results, as well as those of others, are explained completely by the grid current theory developed in my paper, and that the four causes of frequency variation considered by Edgeworth are of very minor importance.

It has been realized for a number of years that the frequency of the triode oscillator was not exactly $\frac{1}{2\pi\sqrt{L_1C_1}}$

but depended to some extent on the values of the anode and filament voltages of the triode and on the coupling between the coils. The extent of the frequency variation has been found to be, at most, 3 per cent. Several experimental investigations of these frequency variations were made, notably by Eccles and Vincent*; but, in spite of the great importance of the subject, both in wireless technology and in the laboratory, no attempted theoretical explanation was published until Edgeworth's paper appeared in March 1926. In October 1926, while using the simple "tuned-anode" oscillator, but with abnormal values for the coil inductances and the condenser capacity, I obtained extremely large variations of frequency, extending over several octaves, when the filament current or anode voltage of the valve was altered. In order to explain these effects I developed a mathematical theory of the oscillator which took account of the flow of grid current in the valve. By the aid of this

* Proc. Roy. Soc. xvi. & xvii. (1920).

theory, as described in my previous paper, I succeeded in explaining every type of frequency variation which I observed. It is Colonel Edgeworth's claim that the theory which he had put forward is capable of explaining these large frequency variations. We shall now proceed to analyse the four causes of frequency variation which he considered.

(1) The first cause of frequency variation is said to be due to "grid damping" *when there is a condenser across the grid coil*. Equations are developed giving the extent of the frequency variation. This is the cause of frequency variation which Edgeworth specifically claims to be capable of explaining the large frequency variations which I observed. In my experiments there was no condenser across the grid coil. On putting $C_2=0$ in Edgeworth's equation (no. 8 in the

paper) we find the frequency at once reduces to $\frac{1}{2\pi \sqrt{L_1 C_1}}$, so that *no frequency variations whatever occur!* Even if we allow for a considerable self-capacity in the grid coil, the frequency variation predicted by Edgeworth's theory is exceedingly small, and quite inadequate to explain the variations which I obtained experimentally.

(2) The second cause of frequency variation only applies when a "tuned-grid" oscillator is used, and hence need not be further considered.

(3) The third cause of frequency variation is due to the presence of resistance in the anode coil. This, however, has been previously worked out by Eccles*, and I have shown that it is much too small to account for the frequency variations which I observed.

(4) An effect due to harmonics, as worked out by Appleton and Greaves†. This effect also I have considered in my paper, and have shown to be exceedingly small and unimportant.

Summing up, then, we see that none of the four causes of frequency variation put forward by Edgeworth is capable even of explaining a frequency variation which in any way approaches the order of magnitude observed by Eccles and Vincent. Still less can they explain the very large frequency changes which I obtained. The correct magnitude of frequency variation is at once obtained, however, from the

* Proc. Phys. Soc. xxxi. (1919).

† Phil. Mag. xlv. (1923).

equations which I have put forward, based solely on the flow of grid current. It is a remarkable fact that, although from the text of his paper, Edgeworth appears to have realized that grid current was a factor of importance, yet in his theoretical treatment of the subject he has neglected it almost entirely, only considering it in the very minor role of introducing damping into an oscillatory grid circuit.

Edgeworth further suggests that the magnitude of the frequency variation can be increased indefinitely merely by increasing the "grid damping." Such procedure, however, merely results in the cessation of oscillations. The order of magnitude of the frequency variations which can be obtained with a given valve depends entirely upon the values of the

ratios $\frac{L_1}{C_1}$, $\frac{L_2}{L_1}$, $\frac{M}{L_1}$, as worked out in my paper under the heading "Conditions for Maximum Frequency Variation."

A careful comparison of the experimental results which I have obtained working with large variations at low frequencies, with those of other investigators working with small variations at high frequencies, has revealed the fact that there are no essential differences, other than magnitude, between the results. Since the theory based on grid current has been completely successful in explaining all my experimental results, there is every reason to believe that the same theory provides the explanation of all the frequency variations to which the oscillator is subject. In other words, when the resistances present are not large, and the frequency is not too high, *by far the most important cause of frequency variation is the flow of grid current, and all the types of variation which have been observed experimentally may be traced to this effect.*

One important consequence of this fact is that if we can succeed in eliminating grid current from the oscillator, then it should be possible to attain a frequency which will possess a very high degree of constancy. Previous experiments on the attempted elimination of grid current, described in my former paper, suggested that this was a difficult if not impossible matter. These experiments sufficed to indicate that the elimination of grid current was a problem which could not be solved merely by increasing the negative bias on the grid, the method usually recommended*. To test the possibility of having zero grid current in any particular circumstances, a series of measurements were made for the purpose of plotting V^2 (the square of the peak voltage across

* Moullin, 'Radio-Frequency Measurements,' p. 7.

the anode coil L_1 against I_g (the total grid current). If it is impossible to have the grid current zero, then we should expect these curves to pass through the origin. If, on the other hand, zero grid current is a possibility, then we should expect the curves to intersect the V^2 axis.

Some of the curves obtained showed a definite tendency towards cutting the V^2 axis, thus indicating that zero grid current was possible in these particular cases, while oscillations were occurring. An extensive series of observations were then made in order to find the best conditions for the elimination of grid current. The results may be summarized as follows :—

- (1) The high tension voltage should be as large as the valve can take without damage.
- (2) The coupling between the coils L_1 and L_2 must not be too loose.
- (3) The negative bias on the grid should be as large as possible.
- (4) The filament current should be as low as possible.
- (5) The inductance of the coil L_2 should be small.

In practice, the best method of procedure is first to set (1), (2), and (5) to appropriate values. Next the filament current is gradually reduced until oscillations cease. The value of (3) is then readjusted until oscillations recommence. The filament current is again reduced, and the same procedure followed repeatedly until the filament current is so low that oscillations will only occur for a very small range of grid bias variation. With the oscillator so adjusted, the filament current may be varied over an appreciable range without causing grid current to flow. This range decreases as the coupling is decreased. An improvement in the elimination of grid current is effected by inserting a small condenser in series with the grid coil L_2 . This condenser was found to increase the range of variation of filament current over which no grid current flowed. It acted by automatically adjusting the grid bias. Thus if the filament current was such as to cause a small current to flow to the grid, the condenser charged up negatively and so stopped the flow of grid current.

The conditions for the elimination of grid current having been determined, an oscillator was specially designed and set up, in order to find out how constant the frequency would be in these circumstances. In order to keep the high

frequency resistance of the coils low they were wound with Litzendraht wire. This wire is made up of a large number of well insulated strands. The two coils were wound on two ebonite cylinders of different sizes, so that one could be inserted inside the other, thus ensuring a close degree of coupling. The grid coil was several times smaller than the coil in the plate circuit. A small condenser of capacity 0.001 mfd. was inserted in series with the grid bias battery. The oscillator was adjusted in the manner described above, and the grid current eliminated. A quartz oscillator was set up, producing oscillations of a frequency very near to that of the valve oscillator. The two oscillators were loosely coupled by means of a single loop of wire in series with a pair of head telephones. A note of audible frequency was heard in the telephones. The frequency of this note could be determined by means of a monochord. In this manner a very small change of frequency of the valve oscillator could be measured. It was found that the frequency remained constant to one part in 100,000 *even when the filament current was deliberately varied*, so long as no grid current flowed. When the filament current remained steady, the frequency was, of course, constant to a much higher degree. There is no doubt that an oscillator so designed provides a source of frequency which is considerably more constant than that which is obtained from any of the complicated constant frequency circuits designed by Fromy * and others.

The only disadvantage is that the power generated is very low, but this, of course, is of little moment when the oscillator is to be used for heterodyne purposes, or as a master oscillator. For the purpose of making accurate physical measurements, the triode oscillator, with grid current eliminated, should be of great value.

The experimental work described above was carried out in the Research Laboratories of the Natural Philosophy Department of the University of Glasgow, with much appreciated financial assistance from the Department of Scientific and Industrial Research. I am greatly indebted to Professor E. Taylor Jones for much helpful advice and encouragement.

April 1928.

* *L'Onde Electrique*, 4e année, p. 433 (1925).

XIX. *On Hamilton-Jacobi's Differential Equation in Dynamics.*

To the Editors of the Philosophical Magazine.

GENTLEMEN,—

I HAVE just read Prof. J. Kunz's article "A Note on Hamilton-Jacobi's Differential Equation in Dynamics" in the January issue of your Magazine. I should like to remark that it has caused me (and probably many others of your readers) mild surprise. Unless I am mistaken, Prof. Kunz regards his manner of deriving Lagrange's equations, the equation of energy, and the Hamilton-Jacobi equation, as purely original, whereas it is surely already well known—granted the condition which Prof. Kunz should have (but has not) proved, viz., that

$$\int (E_k - E_p) dt = \int f(t, q_1, \dots, q_n, \dot{q}_1, \dots, \dot{q}_n) dt$$

is stationary along the actual trajectory, as compared with adjacent ones. This is easily shown by using the equations

$$(\bar{x}, \bar{y}, \bar{z}) = -\partial E_p / \partial (x, y, z). \dots \dots (1)$$

Now any text-book on the Calculus of Variations (*vide* Williamson's 'Integral Calculus,' pp. 430, 437, *et seq.*, or Whittaker, 'Analytical Dynamics,' pp. 266, 267) proves that the condition that

$$\int_{t_1}^{t_2} f(t, q_1, \dots, q_n, \dot{q}_1, \dots, \dot{q}_n, \ddot{q}_1, \dots, \ddot{q}_n, \dots) dt,$$

is stationary are

$$0 = \frac{\partial f}{\partial q_r} - \frac{d}{dt} \left(\frac{\partial f}{\partial \dot{q}_r} \right) + \frac{d^2}{dt^2} \left(\frac{\partial f}{\partial \ddot{q}_r} \right) - \frac{d^3}{dt^3} \left(\frac{\partial f}{\partial \ddot{q}_r} \right) + \dots (r=1, \dots, n)$$

together with certain terminal equations. In particular, if f contain derivatives of the q 's of order no higher than the first

$$0 = \frac{\partial f}{\partial q_r} - \frac{d}{dt} \left(\frac{\partial f}{\partial \dot{q}_r} \right) (r=1, 2, \dots, n). \dots (2)$$

Moreover, if f is quadratic in the \dot{q} , then

$$\begin{aligned}\frac{df}{dt} &= \frac{\partial f}{\partial t} + \Sigma \left(\dot{q} \frac{\partial f}{\partial q} + \ddot{q} \frac{\partial f}{\partial \dot{q}} \right), \quad \dots \dots \dots (3) \\ &= \frac{\partial f}{\partial t} + \Sigma \left\{ \dot{q} \frac{d}{dt} \left(\frac{\partial f}{\partial \dot{q}} \right) + \frac{d\dot{q}}{dt} \cdot \frac{\partial f}{\partial \dot{q}} \right\} \quad \text{by (2),} \\ &= \frac{\partial f}{\partial t} + \frac{d}{dt} \left(\Sigma \dot{q} \frac{\partial f}{\partial \dot{q}} \right),\end{aligned}$$

and if $\partial f / \partial t$ vanishes we have at once that

$$f - \Sigma \dot{q} \frac{\partial f}{\partial \dot{q}} = \text{constant}$$

is an integral, the so-called integral of energy. These results and also the method of their derivation are, I expect, familiar not only to all applied mathematicians but also to those who deal in the Calculus of Variations. So also will be the fact that

$$S = \int (E_k - E_p) dt$$

is a solution of the Hamilton-Jacobi equation

$$0 = H(q, \partial S / \partial q) + \partial S / \partial t.$$

(For all these results see, for example, Whittaker, 'Analytical Dynamics,' §§ 41, 143; Plummer, 'Dynamical Astronomy,' §§ 123, 128; Birtwistle, 'Quantum Theory of the Atom,' §§ 33, 34, 35, 39; Williamson, *loc. cit.* §§ 287, 292.)

Incidentally, there is an error in an important equation of Prof. Kunz. Instead of

$$\frac{d}{dx} \left(f - \Sigma y_r' \frac{\partial f}{\partial y_r'} \right) = \frac{\partial f}{\partial x} + \Sigma y_r' \frac{\partial f}{\partial y_r} - \Sigma \left\{ y_r'' \frac{\partial f}{\partial y_r'} + y_r' \frac{d}{dx} \left(\frac{\partial f}{\partial y_r'} \right) \right\}$$

it should obviously read on the right-hand side

$$\begin{aligned}\frac{\partial f}{\partial x} + \Sigma \left(y_r' \frac{\partial f}{\partial y_r} + y_r'' \frac{\partial f}{\partial y_r'} \right) - \Sigma \left\{ y_r'' \frac{\partial f}{\partial y_r'} + y_r' \frac{d}{dx} \left(\frac{\partial f}{\partial y_r'} \right) \right\} \\ = \frac{\partial f}{\partial x} + \Sigma y_r' \left\{ \frac{\partial f}{\partial y_r} - \frac{d}{dx} \left(\frac{\partial f}{\partial y_r'} \right) \right\}\end{aligned}$$

as in (3), though this mistake is corrected in the next equation.

97 Thornbury Road,
Osterley Park, Middx.
Feb. 28, 1928.

Yours faithfully,
ARTHUR J. CARR.

XX. *Optically Excited Iodine Bands with Alternate Missing Lines.* By Prof. R. W. WOOD, *For.Mem.R.S., The Johns Hopkins University*, and Prof. F. W. LOOMIS, *New York University*.*

[Plate II.]

THIS paper is a report of some direct experimental evidence that, as predicted by the wave mechanics, the rotational states of symmetrical molecules are divided into two classes between which transitions do not occur. These classes of states are those whose eigen-functions are respectively symmetrical and anti-symmetrical in the positional coordinates of the nuclei. The evidence has been obtained as the result of improvements in the technique of exciting iodine fluorescence.

It was shown by R. W. Wood in 1910⁽¹⁾ that if iodine vapour *in vacuo* is excited by monochromatic radiation—for example, the green mercury line,—the vapour emits a series of close doublets, 27 or more in number, spaced at nearly equal intervals on a frequency scale, the first doublet occurring at the wave-length of the mercury line, and the last in the remote red, brought out only by photography with a dicyanine plate. In 1920, when the methods of the Bohr theory of atomic spectra were first successfully applied to band spectra, Lenz⁽²⁾ showed that this series of doublets was unmistakable evidence for the selection principle for rotational quantum numbers, $j' - j'' = \pm 1$, whose introduction was the essential new step in the theory.

The accepted⁽³⁾ explanation of this series of fluorescent doublets is briefly as follows. All the iodine molecules which happen to absorb the narrow green mercury line are thereby lifted into one definite state, which happens to be $n' = 26$, $j' = 34$. Since the molecular vibration is anharmonic, the correspondence principle permits return transitions to any vibrational quantum number n'' . Thus the doublet which coincides with the green line (the zero-order doublet) corresponds to the vibrational transition $26 \rightarrow 0$, the first-order doublet to $26 \rightarrow 1$, etc. The possible values of the final rotational quantum number j'' are, however, strictly limited by the selection principle, $j'' = j' \mp 1$, to $j'' = 33$ or 35, and these correspond to the two members of each doublet. That is, the fluorescent series is picked out of the very complex emission spectrum by the limitation to a single excited state, and consists of one line from the R branch ($j'' = j' - 1$), one

* Communicated by the Authors.

232 Prof. R. W. Wood and Prof. F. W. Loomis on *Optically*
line from the P branch ($j''=j'+1$) of each band having
 $n'=26$.

If a little inert gas, say helium, is added to the iodine vapour, it was found by Wood and Franck that the fluorescent spectrum was enriched. The bands to which the doublets belong are apparently completely developed, and new bands corresponding to adjacent values of n' appear on each side of them. Obviously the iodine molecules, while in the excited state, make collisions of the second kind with helium atoms and undergo changes of n' and j' , the result being that there is no longer a single initial state for the emission of the fluorescent light, but a group of vibrational and rotational states clustering about the original one. The bands represent transitions from all these states.

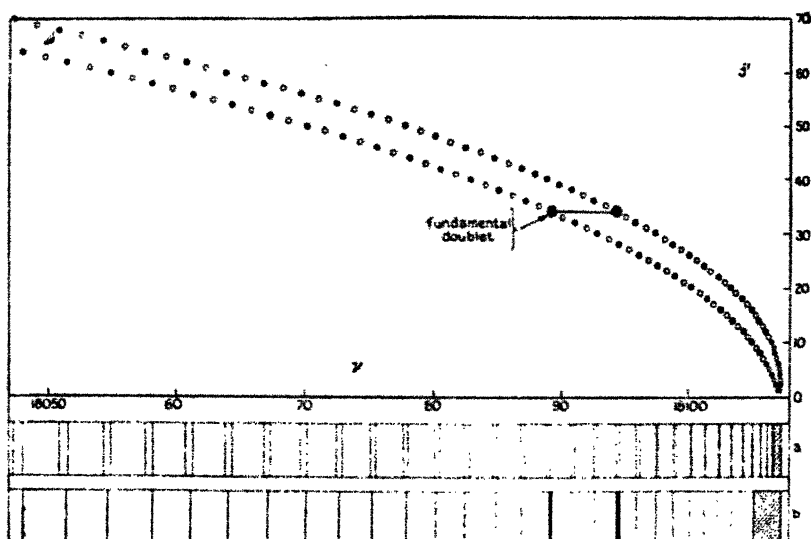
These bands are the subject of the present study. In order to be able to photograph them with a spectrograph of much higher resolution than heretofore, the iodine fluorescence is excited with a battery of four vertical Cooper Hewitt glass mercury lamps which gives a very powerful stimulation of the vapour. The lamps are arranged close together on a single stand, with just room enough between them for the vertical glass tube containing the iodine vapour. They are started by an auxiliary, by simply closing a switch, which is far more convenient than the older arrangement in which the lamp was lighted by tipping. The iodine tubes are about 50 cm. in length by 5 cm. in diameter, blown out at the top in the form of a thin clear bulb, and drawn off obliquely at the bottom, to prevent reflexion and secure a good background. The oblique cone at the bottom is painted black on the outside. With this arrangement it is possible to secure photographs in the second-order spectrum of a 6-inch plane grating with a lens of over 3 metres focus in about 15 hours.

Pl. II., fig. a, shows the spectrum obtained when the iodine is in the presence of helium at $\frac{1}{2}$ mm. pressure. The vibrational transition corresponding to each band which is brought out is marked at the head of the band. It will be noted that the bands with $n'=26$, that is, those containing the doublets, are strongest; those with $n'=25$ and $n'=27$ are fainter; those with $n'=24$ and $n'=28$ are very faint, and none are apparent with other values of n' . This means that most of the excited molecules which undergo collisions of the second kind suffer no change in n' ; some have n' changed by 1, a few by 2, and hardly any by more than 2.

Much larger changes take place in the rotational quantum number, as is shown by the development of the bands to some distance on each side of the doublets. But a more

interesting point, and the one with which we are here chiefly concerned, is that these bands contain fewer lines, in any given region, than the corresponding absorption bands. For instance, on Pl. II., figs. *b* and *e*, which are enlargements of the (26, 1) and (26, 3) bands in fig. *a*, and still more distinctly in figs. *c* and *f*, which were made in the third-order spectrum, it is plain that there are only two lines within the doublets; whereas Loomis's analysis⁽⁴⁾ of the absorption spectrum shows that there are actually ten absorption lines in this region, five on the R branch and 5 on the P branch. Compare fig. 1, the upper part of which is a Fortrat diagram of the (26, 1) band, and in which the circles, both full and

Fig. 1.



Above is a Fortrat diagram of the (26, 1) absorption band. Lines with even j' are indicated by solid circles, those with odd j' by hollow circles. (a) is a plot of the absorption lines having even values of j' . (b) is a plot of the centres of the lines of the fluorescent band as it appears when iodine is mixed with helium at 4 mm. pressure.

hollow, represent absorption lines. It happens that this band has not been measured in absorption, but its lines can be accurately calculated, by the combination principle, from those of the bands (26, 0), (29, 1), and (29, 0), which have been measured. The relation between the fluorescence and absorption bands is shown in the lower part of fig. 1. Here the upper spectrum has been obtained by projecting down from the Fortrat diagram the lines with even j'

j' (i. e., those represented by full circles); while the lower is a plot of the centres of the lines of the same (26, 1) band as it appears in fluorescence. Clearly, the fluorescence lines correspond exactly to the absorption lines with even j' , and the alternate lines are missing in the fluorescence band. It is true that each line in the R branch happens to lie so close to a line in the P branch that they are not quite resolved; but the spectra show plainly that the fluorescent lines far from the head are becoming broader. A special grating was therefore ruled for the work, exceptionally bright in the third-order spectrum. Only one or two satisfactory photographs have been made up to the present time, owing to troubles with the thermostat, for a more exact temperature control of the grating was necessary in this case. Pl. II., fig. *f*, shows the band associated with the third-order doublet (26, 3), the lines indicated by arrows being clearly resolved. The lines of the third-order doublet are 1.67 Å.U. apart, and the separation of the closest doublets marked by arrows is about 0.1 Å.U.

The lines marked by dots are "ghosts" of the strong doublet, and some of the lines correspond to weak doublets, which appear also when the iodine is *in vacuo*. They are "main" doublets due to the stimulation of fainter absorption lines, which lie within the region covered by the green mercury line. The band (25, 3) photographed in the third-order spectrum is reproduced in Pl. II., fig. *d*.

Table I. shows the correspondence between the frequencies of the lines of the (26, 1) band in absorption and fluorescence.

TABLE I.

Band (26, 1) in absorption.					In fluorescence.	
R branch.		P branch.		Average.	Intensity.	
j' .	ν .	j' .	ν .	ν .		
head	18107.43	—	—	—	18107.4	—
16 ...	18105.02	10	18105.13	18105.08	05.2	2
17 ...	04.66	11	04.77			
18 ...	04.26	12	04.39	04.32	04.2	3
19 ...	03.80	13	03.95			
20 ...	03.39	14	03.50	03.44	03.4	3
21 ...	02.91	15	03.03			
22 ...	02.42	16	02.56	02.49	02.3	2
23 ...	01.87	17	01.95			
24 ...	01.32	18	01.48	01.40	01.3	4
25 ...	00.74	19	00.98			

TABLE I. (*continued*).

Band (26, 1) in absorption.					In fluorescence.	
R branch.		P branch.		Average.	Intensity.	
<i>J</i> .	ν .	<i>J</i> .	ν .	ν .		
26 ...	00·14	20	00·32	00·23	00·1	4
27 ...	18099·50	21	18099·74			
28 ...	98·83	22	99·05	18098·94	18098·8	10
29 ...	98·10	23	98·39			
30 ...	97·46	24	97·03	97·54	97·5	4
31 ...	96·74	25	96·02			
32 ...	95·89	26	96·19	96·04	95·9	12 wide
33 ...	95·14	27	95·40			
34 ...	94·34	28	94·59	94·46	94·5	20 f.d.
35 ...	93·53	29	93·80			
36 ...	92·61	30	92·93	92·77	92·7	4
37 ...	91·75	31	92·04			
38 ...	90·85	32	91·11	90·98	90·9	4
39 ...	89·84	33	90·13			
40 ...	88·92	34	89·25	89·14	89·3	10 f.d.
41 ...	87·91	35	88·23			
42 ...	86·88	36	87·20	87·04	87·0	5
43 ...	85·82	37	86·18			
44 ...	84·76	38	85·10	84·93	85·0	3
45 ...	83·65	39	84·01			
46 ...	82·52	40	82·69	82·70	82·5	3
47 ...	81·36	41	81·76			
48 ...	80·17	42	80·56	80·36	80·3	4
49 ...	78·99	43	79·36			
50 ...	77·73	44	78·13	77·93	78·0	3
51 ...	76·45	45	76·88			
52 ...	75·17	46	75·60	75·38	75·3	3
53 ...	73·85	47	74·29			
54 ...	72·51	48	72·97	72·74	72·7	3 wide
55 ...	71·15	49	71·59			
56 ...	69·74	50	70·22	69·98	70·2	3 wide
57 ...	68·37	51	68·79			
58 ...	66·88	52	67·36	67·12	67·2	2 wide
59 ...	65·40	53	65·89			
60 ...	63·89	54	64·41	64·15	64·1	1 wide
61 ...	62·36	55	62·91			
62 ...	60·80	56	61·34	61·07	61·2	2 wide
63 ...	59·22	57	59·77			
64 ...	57·60	58	58·18	57·89	58·2	0 hazy
65 ...	55·98	59	56·56			

f.d.=fundamental doublet.

TABLE I. (*continued*).

Band (26, 1) in absorption.					In fluorescence.	
R branch.		P branch.		Average.	ν .	Intensity.
j' .	ν .	j' .	ν .	ν .		
66...	54.31	60	54.89	54.60	54.7	1 wide
67...	52.63	61	53.22			
68...	50.91	62	51.51	51.21	51.4	0 wide
69...	49.17	63	49.79			
70...	47.39	64	48.02	47.70	48.0	1 wide

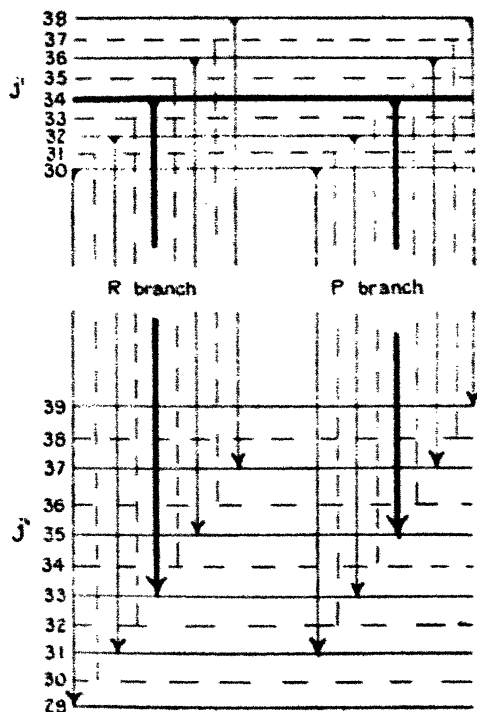
The absorption line frequencies are calculated from those of other bands which have been measured, by the relation $\nu(26, 1) = \nu(26, 0) + \nu(29, 1) - \nu(29, 0)$. In some cases they have been calculated by second-difference interpolation between the lines calculated by the above equation. The fluorescent lines in Table I. are those which appear in iodine mixed with helium at 4 mm. pressure. A few extra lines which do not belong to the (26, 1) band appear on Pl. II., fig. *b*, either interspersed among the lines of the band or as irregularities in the intensity distribution. These are fluorescent doublets, like the "fundamental" doublets, but due to the stimulation of absorption lines belonging to weak overlapping bands. They disappear entirely when the helium pressure is raised to 4 mm. They do not occur in the bands with $n' \neq 26$. They are of no interest in connexion with the subject of this paper.

It is evident, then, that the fluorescent spectrum contains only lines starting from states with even values of j' , the alternate lines being missing. Now, the original excited molecules, just after absorbing the light from the mercury arc, and before colliding with helium atoms, had $j' = 34$. It follows that, during collisions in which the electronic quantum number is unchanged, the rotational quantum number of an iodine molecule can only change by an even number.

This result, while incomprehensible on the classical Bohr-Lenz theory, is entirely in accord with the wave mechanics. According to the theory of Hund⁽⁵⁾, successive rotational states of a symmetrical molecule, such as I_2 , have alternately eigen-functions symmetric and anti-symmetric in the positional coordinates of the two nuclei. Moreover, since the symmetric and anti-symmetric eigen-functions correspond to different orientations of the spins of the two nuclei, and since these spins are very loosely coupled to the rest of the

atom, it is to be expected that transitions between symmetric and anti-symmetric states will be very infrequent. Also, it is to be expected that the eigen-functions will retain their characteristic symmetry, or anti-symmetry, even in an electric or a magnetic field or the field of a neighbouring atom, so that transitions from symmetric to anti-symmetric states will not even take place during collisions. In fact, Dennison ⁽⁶⁾ has recently solved the long outstanding problem

Fig. 2.



A few of the energy-levels and transitions associated with the fluorescent bands.

of the specific heat of hydrogen by assuming that such transitions do not occur in appreciable numbers, even during the time it takes to make a measurement of specific heats.

The situation is pictured in fig. 2, which shows a few of the rotational levels near those which are associated with a fundamental doublet. The level $j'=34$, which is the initial level for the emission of the fundamental doublet, is

238 *Optically Excited Iodine Bands with Missing Lines.*

represented by a very heavy line, as are the two transitions from this level which correspond to the fundamental doublet. The upper levels with even j' , which are those having the same character, let us say, for convenience, symmetric, as the level $j'=34$, are indicated by continuous lines. The levels with odd j' will then be anti-symmetric, and are indicated by dashed lines. Now Loomis's analysis of the absorption spectrum has shown that each band consists of one P and one R branch, and that it is therefore of the $^1s-^1s$ type, with $j'-j''=\pm 1$. Since transitions only occur between levels of the same symmetry character, it follows that in the lower state the rotational levels with odd j'' must be symmetric, and they are so indicated in the diagram. The transitions from the upper levels with even j' to the lower levels with odd j'' , i. e. those between symmetric states, are also represented by continuous lines. These are the transitions which result in the fluorescent spectrum. The transitions between anti-symmetric states are indicated by dashed lines. They occur, upward, in absorption, because both kinds of states are present in iodine vapour; but only those represented by continuous lines occur in the fluorescent spectrum, because the green mercury arc line happens to be absorbed by, and excite, a molecule in a symmetric state. Of course the words symmetric and anti-symmetric can equally well be interchanged in the above statements, so far as we know at present.

The writers have been unable to detect any signs of alternating intensities in the absorption bands of iodine. This doubtless means that the nuclear spin of the iodine atom is so high that the statistical weights of the symmetrical and anti-symmetrical states of the molecule are practically equal.

References.

- (1) R. W. Wood, *Phys. Zeitschr.* xi. pp. 1195-1196 (1910); *Phil. Mag.* xxxv. pp. 236-252 (1918).
- (2) Lenz, *Phys. Zeitschr.* xxi. p. 691 (1920).
- (3) National Research Council Committee Report on 'Molecular Spectra in Gases,' Chapter vi. The notation of this paper is that of the Report. Primed letters refer to the upper electronic state of the molecule, double-primed letters to the lower state. j is the quantum number associated with the total angular momentum of the molecule; n is the vibrational quantum number.
- (4) Loomis, *Phys. Rev.* xxix. pp. 112-134 (1927).
- (5) Hund, *Zeitschr. f. Phys.* xlii. p. 110-111 (1927).
- (6) Dennison, *Proc. Roy. Soc. A*, cxv. pp. 483-486 (1927).

XXI. *Notices respecting New Books.*

Introduction to Contemporary Physics. By K. K. DARROW.
(Macmillan & Co., St. Martin's Street, London. Price 25s. net.)

THE author has given an account of the state of present day physics, theoretical and experimental, more particularly with reference to the structure of the atom, and the phenomena of spectra. He has made accessible the theories and experimental results of recent investigators and provided an interesting and readable survey of these branches of modern physics. The earlier chapters of the book are devoted to the "experimental electron," the "experimental atom," and the classification of the elements and their properties, period, non-periodic, and irregular. The deflexions of alpha particles and electrons by atoms, the photo-electric effect, stationary states, and the atomic models, with the experimental evidence provided by the study of the X-ray and other spectra, are then considered. The electric discharge in gases, which has played so important a part in atomic structure, is treated in the final chapter. A useful index of subjects is appended.

Dr. Darrow has done a real service to students by introducing them to some of the problems of modern physics; for this reason, his book can be heartily commended to their notice.

Lectures on Theoretical Physics. By H. A. LORENTZ. Vol. I.
Aether Theories and Aether Models and Kinetical Problems.
(Macmillan & Co. Ltd., St. Martin's Street, London. Price 12s. 6d. net.)

PROFESSOR LORENTZ's lectures on Theoretical Physics at the University of Leyden, edited by his Dutch pupils, are here translated into English and thus made available to a wider circle of readers. The subject of the first course of lectures is Aether Theories and Models, edited by Prof. H. Bremekamp; theories of Fresnel, Planck, and others are brought under review, and one chapter devoted solely to the study of Kelvin's model of the quasi-rigid aether. A brief treatment of the attraction and repulsion of pulsating spheres is given in the later sections.

The lectures on Kinetical Problems, edited by Drs. Bruins and Reudler, are largely expositions of the classical researches of M. Knudsen and O. W. Richardson, the former on surface phenomena and the flow of rarefied gases through narrow tubes and orifices, the latter on the emission of electricity from hot bodies. There are two indexes giving sources and references to original papers.

The translators have accomplished their task with success and produced a readable English version of these important topics. English readers will await with interest the translation of the remaining volumes.

The Collected Papers of Spīnivasa Ramanujan. Edited by G. H. HARDY, P. V. SESHU AIYAR, and B. M. WILSON. Pp. xxvi + 355. (Cambridge: At the University Press. 1927. Price 30s. net.)

THE publication of a collected edition of the papers of the remarkable Indian mathematician, Ramanujan, has been made possible by the aid of contributions from the University of Madras, the Royal Society, and Trinity College, Cambridge. The Editors state in their preface that there is still a large mass of unpublished material left by Ramanujan in his notebooks, much of which should certainly be edited and published. For this purpose further monetary assistance would be required, and they express the hope that the present volume will enjoy sufficient success to make further publication possible. Enough is already known of Ramanujan's work to make detailed comment here unnecessary, but collected into one volume its genius and singular quality cannot fail to impress the reader. It is pleasing to recall that, before his early death in his thirty-third year, the merit of his work had been recognised by his election to the Fellowship of the Royal Society—he was the first Indian to receive this honour—and by his election to a Fellowship at Trinity College, Cambridge.

The papers are preceded by two biographical notices. Notes on the papers are contained in an Appendix, and a second Appendix gives extracts from Ramanujan's letters to Mr. G. H. Hardy.

The Phase Rule and its Applications. By ALEXANDER FINDLAY, M.A., D.Sc., F.I.C. Sixth Edition. Pp. xv + 326 with 165 figures. (London: Longmans, Green & Co. 1927. Price 10s. 6d. net.)

PROF. FINDLAY's volume on the phase rule and its applications forms the best introduction to the study of chemical equilibria. That a sixth edition has been called for is a recognition of its value. The treatment is non-mathematical and carries the student sufficiently far to be able to read with profit the more advanced works on the subject.

For the present edition a new chapter on the practical applications of equilibrium diagrams has been added, the chapter in previous editions on the equilibria between iron, carbon monoxide, and carbon dioxide being omitted to make room for it. The chapters dealing with equilibria in one and two component systems have been recast and largely rewritten with additions which include discussions of the nature of the equilibria in intensively dried systems and of Smits's theory of allotropy. The remainder of the volume has been carefully revised and brought up to date.

[The Editors do not hold themselves responsible for the views expressed by their correspondents.]

THE
LONDON EDINBURGH, AND DUBLIN
PHILOSOPHICAL MAGAZINE
AND
JOURNAL OF SCIENCE.

[SEVENTH SERIES.]

AUGUST 1928.

XXII. *General Solution of the Equation $\nabla^2\psi = \omega$ in n -dimensional Euclidean Space.* By A. J. CARR, M.A., formerly Lecturer in Mathematics, the Technical College, Bradford*.

IN a paper, "Note on Green's Lemma and Stokes's Theorem," which appeared in the Phil. Mag. for Sept. 1927, I postulated the existence in Euclidean space of n dimensions of the formula analogous to Green's Lemma for three dimensions in the form

$$\begin{aligned} & \iint \dots \int \sum_1^n \partial U_n / \partial x_i \cdot dx_1 dx_2 \dots dx_n \\ &= \iint \dots \int \sum_1^n (-)^{n-i} U_i J_i \cdot du_1 du_2 \dots du_{n-1}, \quad (1) \end{aligned}$$

where

$$J_i = \partial(x_1, \dots, x_{i-1}, x_{i+1}, \dots, x_n) / \partial(u_1, \dots, u_{n-1}).$$

This was arrived at by comparison with the previous results of the same article, and without attempting further to prove it, I set myself the same month that the paper was published the problem of finding a solution of the equation $\nabla^2\psi = \omega$ by its aid.

By pure but happy accident, two days after I had completed my solution to my satisfaction I discovered a handy little book, 'Vector Analysis and Relativity,' by Dr. F. D.

* Communicated by the Author.

Murnaghan (The Johns Hopkins Press, 1922). There I saw a rigorous proof of the foregoing formula, which, as it very fortunately turned out, now stands without need of correction (save that $dx_1 dx_2 \dots dx_n$ should be replaced by

$$du_1 du_2 \dots du_{n-1} du_n \partial(x_1 \dots x_n) / \partial(u_1 \dots u_{n-1}, u_n),$$

where $u_1, u_2, \dots u_{n-1}$ are any $n-1$ variables which serve to specify the $(n-1)$ -dimensional surface given by $u_n = \text{constant}$, otherwise this paper might have had to be destroyed.

As it is, I have made practically no alteration save that I have fallen into line with Murnaghan by speaking of a co-ordinate "spread" and using dV_{n-1} and dV_n in place of df and dr , as I had previously written them. I had also introduced the idea of direction-cosines and normals, which I find are the same as his direction-coefficients and normals; but as my viewpoint was somewhat different from his, I have not excised this part of my work.

Whereas, however, Murnaghan's small treatise is a fairly complete exposition of n -dimensional tensor analysis, I confined (and do confine) myself exclusively to orthogonal Cartesian coordinates. My U_s is the same as his (X_s) [$\equiv (-)^{n-s} X_{12 \dots r-1, s+1, \dots n}$], the X 's in the second member being (as his notation implies) components of an alternating covariant tensor of rank $n-1$ (p. 38). The advantage (for the purpose for which I shall use it) of the form (1) is that the right-hand member can conveniently be written

$$(-)^{n-1} \left(\left| U_s \frac{\partial x_2}{\partial u_1} \frac{\partial x_3}{\partial u_2} \dots \frac{\partial x_n}{\partial u_{n-1}} \right| \{ du_{n-1} \}, \quad (2)$$

where, as usual, $|a_1 b_2 \dots|$ denotes the determinant

$$\begin{vmatrix} a_1 b_1 & \dots \\ a_2 b_2 & \dots \\ \dots & \dots \end{vmatrix}$$

$$\text{and} \quad \{k_p\} \equiv k_1 k_2 \dots k_p.$$

Putting in (1)

$$U_s = \phi \partial \psi / \partial x_s - \psi \partial \phi / \partial x_n, \quad (2A)$$

we get

$$\begin{aligned} \int_{V_n} [\phi \nabla^2 \psi - \psi \nabla^2 \phi] dV_n \\ = \Sigma \int_{V_{n-1}} \left(\phi \frac{\partial \psi}{\partial \nu} - \psi \frac{\partial \phi}{\partial \nu} \right) dV_{n-1}, \quad (3) \end{aligned}$$

where the V_{n-1} are the $(n-1)$ -dimensional "spreads" bounding V_n the n -dimensional "region," and

$$\frac{\partial}{\partial \nu} = \sum \nu_i \frac{\partial}{\partial x_i}$$

denotes differentiation along the outward "normal" to V_{n-1} . This result is also given by Murnaghan (p. 71), where his dV_{n-1}

$$\begin{aligned} &= \sqrt{g} g^{ij} J_i J_j \\ &= \sqrt{\sum J_i^2} \end{aligned}$$

here, since $g=1$, $g^{ij}=1$ or zero, according as $i=j$, or $i \neq j$.

I myself derived the latter result in the somewhat more naïve manner which here follows.

Let

$$F(x_1, x_2, \dots, x_n) = 0 \quad (4)$$

be the equation to an $(n-1)$ -spread, and also, for brevity, let s be a dummy or umbral symbol (*i. e.* if it occurs twice in a term, that term is supposed to be summed for all values of s from 1 to n , thus obviating the necessity of writing \sum each time and at the same time clarifying the analysis) unless otherwise stated.

Then, if the straight line given by

$$x_s = \alpha_s + l_s r \quad (s = 1, 2, \dots, n),$$

and therefore having direction-cosines (l_1, l_2, \dots, l_n) , where $l_i l_i = 1$, cut (5), we have

$$0 = F(\alpha_1, \dots, \alpha_n) + r l_s \frac{\partial F}{\partial \alpha_s} + \frac{1}{2} r^2 \left(l_s \frac{\partial}{\partial \alpha_s} \right)^2 F + \dots$$

The line is a "tangent" if

$$F(\alpha_1, \dots, \alpha_n) = 0$$

and

$$l_s \frac{\partial F}{\partial \alpha_s} = 0, \dots \quad (5)$$

which shows that (α) lies on an $(n-1)$ -spread, the tangent-plane-spread to (4). In this lie *all* the straight lines whose $n-1$ equations are

$$\frac{x_1 - \alpha_1}{l_1} = \frac{x_2 - \alpha_2}{l_2} = \dots = \frac{x_n - \alpha_n}{l_n}.$$

This gives an $n-1$ -ply infinite number of straight lines for the $n-1$ -ply infinite choices of

$$l_1, l_2, \dots, l_{n-1} \quad (l_n = \sqrt{1 - l_1^2 - \dots - l_{n-1}^2}),$$

all of which, if they satisfy (5), are tangent lines to (5) and therefore also satisfy the equation

$$l_s \nu_s = 0. \quad (6)$$

Multiply (5) by λ , subtract (6); then, since all the l 's (except l_s , say) are independent, the condition that

$$l_s \left(\lambda \frac{\partial F}{\partial \alpha_s} - \nu_s \right) = 0$$

always, is that

$$\lambda = \frac{\nu_1}{\partial F / \partial \alpha_1} = \frac{\nu_2}{\partial F / \partial \alpha_2} = \dots = \frac{1}{\sqrt{(\partial F / \partial \alpha_s)(\partial F / \partial \alpha_s)}}.$$

Now assuming that, since the normal to dV_{n-1} makes an angle with the x -axis whose cosine is ν_s , the projection on the $(n-1)$ -coordinate plane-spread normal to that axis is

$$dV_{n-1,s} = \nu_s dV_{n-1},$$

we have

$$dV_{n-1}^2 = dV_{n-1,s} dV_{n-1,s};$$

where $dV_{n-1,s}$ is the counterpart in curvilinear coordinates of the element $dx_1 dx_2 \dots dx_{s-1} dx_{s+1} \dots dx_n$ in the original Cartesian system, and is therefore expressed by the usual formula for change of variables, namely

$$\begin{aligned} dV_{n-1,s} &= (-)^{n-s} \frac{\partial(x_1, \dots, x_{s-1}, x_{s+1}, \dots, x_n)}{\partial(u_1, \dots, u_{n-1})} du_1 \dots du_{n-1} \\ &= (-)^{n-s} J_s \{du_{n-1}\} \quad (s \text{ is not umbral}), \\ dV_{n-1}^2 &= J_s J_s \{du_{n-1}\}^2, \quad \dots \quad (7) \end{aligned}$$

where the u_{n-1} serve to specify the $(n-1)$ -spread. This, as has been before remarked, is also Murnaghan's result.

Thus, let us define a hypersphere whose centre is at the point (a_1, a_2, \dots, a_n) and whose "radius" is R , by the equation

$$F(x_1 \dots x_n) \equiv (x_s - a_s)(x_s - a_s) - R^2 = 0.$$

$$\begin{aligned} \therefore \nu_s &= (\partial F / \partial x_s) / \sqrt{\partial F / \partial x_p \cdot \partial F / \partial x_p} \\ &= (a_s - a_s) / R = \partial R / \partial \alpha_s; \end{aligned}$$

while the equations of the radius from the centre (a) to (α) give

$$\frac{\alpha_1 - a_1}{l_1} = \frac{\alpha_2 - a_2}{l_2} = \dots = R.$$

Hence $l_i = \nu_i$, and therefore the radius is normal to the surface of the hypersphere, so that $\partial/\partial\nu$ can be replaced by $\partial/\partial r$. The expression for dV_{n-1} will follow later.

We gather that, just as in three dimensions, we have

$$\int \left(\frac{\partial U}{\partial x_i} \frac{\partial V}{\partial y_i} \frac{\partial W}{\partial z} \right) dv = \Sigma \int (\nu_i U + \nu_i V + \nu_i W) df,$$

so here we always get that

$$\int (\partial U_i / \partial x_i) dV_n = \Sigma \int (-)^{n-1} U_i J_i \{ du_{n-1} \} = \Sigma \int \nu_i U_i dV_{n-1}.$$

Turning now to $\nabla^2\phi=0$, we find that a simple solution is

$$\phi = r_n^{-n+2}, \quad \dots \quad (8)$$

where, if

$$y_i = x_i - a_i,$$

then

$$r_n^2 = y_i y_i;$$

since

$$\frac{\partial}{\partial x_i} \left(\frac{1}{r_n^{n-2}} \right) = -(n-2) \frac{y_i}{r_n^n},$$

$$\frac{\partial^2}{\partial x_i^2} \left(\frac{1}{r_n^{n-2}} \right) = -\frac{n-2}{r_n^n} + n(n-2) \frac{y_i^2}{r_n^{n+2}},$$

and thus

$$\begin{aligned} \nabla^2(r_n^{-n+2}) &= -n(n-2)r_n^{-n} + n(n-2)r_n^{-n-2}y_i y_i \\ &= 0. \end{aligned}$$

Using this in (3), we find

$$\int_{V_n} \frac{\nabla^2\psi}{r_n^{n-2}} dV_n = \Sigma \int_{V_{n-1}} \frac{\partial}{\partial \nu} (r_n^{-n+2}\psi) \frac{dV_{n-1}}{r_n^{n-4}}, \quad \dots \quad (9)$$

provided $A(a)$ is a fixed point *outside* the region of integration V_n .

If, however, A be *inside* the region, then, since r_n^{-n+2} is now infinite at A , we adopt the usual method of surrounding A by a small hypersphere of radius ρ and centre A . If we use (2), the right-hand member of (9) will be found to reduce to

$$\begin{aligned} -(-)^{n-1} \int_0^{2\pi} d\theta_n \int_0^\pi \dots \int_0^\pi \left[\rho \frac{\partial \psi}{\partial \rho} + (n-2)\psi \right] \frac{\Delta_n}{\rho^n} \{ d\theta_{n-2} \} \\ \dots \quad (10) \end{aligned}$$

* It will now be seen why I deal only in Galilean coordinates for which ν_n behaves as a vector. It does not do so in generalized curvilinear space, nor is r_n^2 invariant. Cf. Eddington, 'Mathematical Theory of Relativity,' § 74, p. 179, and § 84, p. 198.

since we have seen that ρ is negatively normal to the surface of the hypersphere. Here

$$y_1 = \rho \cos \theta_1,$$

$$y_s = \rho \sin \theta_1 \sin \theta_2 \dots \sin \theta_{s-1} \cos \theta_s, \quad (s = 1, 2, \dots, n-1)$$

$$y_n = \rho \sin \theta_1 \sin \theta_2 \dots \sin \theta_{n-2} \sin \theta_{n-1};$$

and thus

$$y \cdot y = \rho^2.$$

Also

$$\Delta_n \equiv \begin{vmatrix} y_1 & y_2 & \dots & y_n \\ \frac{\partial y_1}{\partial \theta_1} & \frac{\partial y_2}{\partial \theta_1} & \dots & \frac{\partial y_n}{\partial \theta_1} \\ \dots & \dots & \dots & \dots \\ \frac{\partial y_1}{\partial \theta_{n-1}} & \frac{\partial y_2}{\partial \theta_{n-1}} & \dots & \frac{\partial y_n}{\partial \theta_{n-1}} \end{vmatrix}.$$

This determinant can be most easily evaluated by induction. For, if we put

$$y_n' \equiv y_n \cos \theta_n, \quad y_{n+1} \equiv y_n \sin \theta_n,$$

then

$$\begin{aligned} \Delta_{n+1} &\equiv \begin{vmatrix} y_1 & y_2 & \dots & y_n' & y_{n+1} \\ \frac{\partial y_1}{\partial \theta_1} & \frac{\partial y_2}{\partial \theta_1} & \dots & \frac{\partial y_n'}{\partial \theta_1} & \frac{\partial y_{n+1}}{\partial \theta_1} \\ \dots & \dots & \dots & \dots & \dots \\ \frac{\partial y_1}{\partial \theta_{n-1}} & \frac{\partial y_2}{\partial \theta_{n-1}} & \dots & \frac{\partial y_n'}{\partial \theta_{n-1}} & \frac{\partial y_{n+1}}{\partial \theta_{n-1}} \\ \frac{\partial y_1}{\partial \theta_n} & \frac{\partial y_2}{\partial \theta_n} & \dots & \frac{\partial y_n'}{\partial \theta_n} & \frac{\partial y_{n+1}}{\partial \theta_n} \end{vmatrix} \\ &\equiv \begin{vmatrix} y_1 & \dots & y_{n-1} & y_n \cos \theta_n & y_n \sin \theta_n \\ \frac{\partial y_1}{\partial \theta_1} & \dots & \frac{\partial y_{n-1}}{\partial \theta_1} & \frac{\partial y_n}{\partial \theta_1} \cos \theta_n & \frac{\partial y_n}{\partial \theta_1} \sin \theta_n \\ \dots & \dots & \dots & \dots & \dots \\ \frac{\partial y_1}{\partial \theta_{n-1}} & \dots & \frac{\partial y_{n-1}}{\partial \theta_{n-1}} & \frac{\partial y_n}{\partial \theta_{n-1}} \cos \theta_n & \frac{\partial y_n}{\partial \theta_{n-1}} \sin \theta_n \\ 0 & \dots & 0 & -y_n \sin \theta_n & y_n \cos \theta_n \end{vmatrix} \\ &= (-)^{2n-1} (-y_n \sin \theta_n) \Delta_n \sin \theta_n + (-)^{2n} y_n \cos \theta_n \Delta_n \cos \theta_n \\ &= y_n \Delta_n = y_n' \sec \theta_n \Delta_n. \end{aligned}$$

Thus, if

$$\bar{y}_k = y_k \sec \theta_k = \prod_{p=1}^{k-1} \sin \theta_p,$$

then

$$\begin{aligned}\Delta_n &= \bar{y}_{n-1} \Delta_{n-1} \\ &= \bar{y}_{n-1} \bar{y}_{n-2} \dots \bar{y}_2 \Delta_2.\end{aligned}$$

Now Δ_2 is calculated on the supposition that

$$y_1 = \rho \cos \theta_1, \quad y_2' = \rho \sin \theta_1.$$

Hence

$$\begin{aligned}\Delta_2 &= \begin{vmatrix} \rho \cos \theta_1 & \rho \sin \theta_1 \\ -\rho \sin \theta_1 & \rho \cos \theta_1 \end{vmatrix} \\ &= \rho^2.\end{aligned}$$

$$\therefore \Delta_n / \rho^n = \sin^{n-2} \theta_1 \sin^{n-3} \theta_2 \dots \sin^2 \theta_{n-3} \sin \theta_{n-2}.$$

If, in (10), we now put $\rho=0$, then (provided $\partial\psi/\partial\rho$ is finite always), since the hypersphere now becomes a point, the expression (10) reduces to

$$\begin{aligned}2\pi(-)^n(n-2)\psi_A \int_0^\pi \sin^{n-2} \theta_1 d\theta_1 \int_0^\pi \sin^{n-3} \theta_2 d\theta_2 \dots \\ \int_0^\pi \sin \theta_{n-2} d\theta_{n-2} \\ = 2\pi(-)^n(n-2)\psi_A \frac{\Gamma\left(\frac{n-1}{2}\right)\Gamma\left(\frac{1}{2}\right)}{\Gamma\left(\frac{n}{2}\right)} \cdot \frac{\Gamma\left(\frac{n-2}{2}\right)\Gamma\left(\frac{1}{2}\right)}{\Gamma\left(\frac{n-1}{2}\right)} \dots \\ \frac{\Gamma\left(\frac{3}{2}\right)\Gamma\left(\frac{1}{2}\right)}{\Gamma\left(\frac{4}{2}\right)} \cdot \frac{\Gamma\left(\frac{2}{2}\right)\Gamma\left(\frac{1}{2}\right)}{\Gamma\left(\frac{3}{2}\right)} \\ = 2\pi(-)^n(n-2)\psi_A [\Gamma\left(\frac{1}{2}\right)]^{n-2} / \Gamma(n/2) \\ = K_n \psi_A,\end{aligned}$$

where

$$\begin{aligned}(-)^n K_n &= 4\pi^{n/2} / (\tfrac{1}{2}n-2)! \quad (n \text{ even}) \\ &= (4\pi)^{(n-1)/2} (\tfrac{1}{2}n-3)! / (n-3)! \quad (n \text{ odd}).\end{aligned}$$

Finally, we get for a point *inside* the region that a solution of the equation $\nabla^2\psi = \omega$ is

$$K_n \psi_A = \int_{V_n} \frac{\omega dV_n}{r_n^{n-2}} - \Sigma \int_{V_{n-1}} \frac{\partial}{\partial \nu} (r_n^{n-2} \psi) \frac{dV_{n-1}}{r_n^{2n-4}}. \quad (11)$$

The equation (11) constitutes as complete a solution as we are ever likely to get without specifying further the nature of the $(n-1)$ -dimensional spreads. If, for example, ω is different from zero inside a hypersphere of radius R , and we take its "surface" for the outer bounding surface, there being no surfaces enclosed, then

$$\begin{aligned} dV_n &= \frac{\partial(y_1, y_2, \dots, y_n)}{\partial(\theta_1, \dots, \theta_{n-1}, r_n)} dr_n \{d\theta_{n-1}\} \\ &= (-)^{n-1} \frac{\Delta_n}{r_n} dr_n \{d\theta_{n-1}\}, \end{aligned}$$

and (11) becomes

$$\begin{aligned} K_n \psi_A &= (-)^{n-1} \int_0^{2\pi} d\theta_{n-1} \prod_{s=1}^{n-2} \left(\int_0^\pi \sin^{n-s-1} \theta_s d\theta_s \right. \\ &\quad \left. \left[\int_0^R \omega r_n dr_n - \frac{\partial(R^{n-2}\psi)/\partial R}{R^{n-3}} \right] \right) \quad (12) \end{aligned}$$

from (10).

Incidentally, this shows us that the element of surface of a hypersphere of radius R is, comparing equations (11) and (12), given by

$$dV_{n-1} = (-)^{n-1} (\Delta_n / R) \{d\theta_{n-1}\}. \quad (13)$$

This result can also be proved directly by using (7). For here J_n , if written down, will be found to reduce to

$$\left| \frac{\partial y_1}{\partial \theta_1} \cdot \frac{\partial y_2}{\partial \theta_2} \cdots \frac{\partial y_{s-1}}{\partial \theta_{s-1}} \cdot \frac{\partial y_{s+1}}{\partial \theta_s} \cdot \frac{\partial y_{s+2}}{\partial \theta_{s+1}} \cdots \frac{\partial y_n}{\partial \theta_{n-1}} \right|,$$

and by precisely the same method as that employed for Δ_n , the last determinant is

$$y_{n-1} \bar{y}_{n-2} \cdots \bar{y}_{s+2} \cdot \Delta_{s+2},$$

where in Δ_{s+2} we have

$$y_{s+1} = R \sin \theta_1 \sin \theta_2 \cdots \sin \theta_s \cos \theta_{s+1},$$

$$y'_{s+2} = R \sin \theta_1 \sin \theta_2 \cdots \sin \theta_s \sin \theta_{s+2},$$

and therefore

$$\begin{aligned} \Delta_{s+2} &= \frac{\partial(y_{s+1}, y'_{s+2})}{\partial(\theta_s, \theta_{s+1})} \\ &= y_s \bar{y}_{s+1}. \end{aligned}$$

Finally, since

$$\frac{\partial y_k}{\partial \theta_k} = -\bar{y}_{k+1},$$

we have

$$\begin{aligned} J_s &= (-)^{s-1} \bar{y}_2 \bar{y}_3 \dots \bar{y}_s y_s \bar{y}_{s+1} \bar{y}_{s+2} \dots \bar{y}_{n-1} \\ &= (-)^{s-1} y_s \cdot \Delta_n / R^2. \end{aligned}$$

Thus

$$\begin{aligned} dV_{n-1}^2 &= J_s J_s \{dV_{n-1}\}^2 \\ &= (\Delta_n^2 / R^2) \{d\theta_{n-1}\}^2, \quad . \quad . \quad . \quad (14) \end{aligned}$$

from which follows (13).

Also from this we see that

$$\begin{aligned} v_s &= (-)^{n-s} J_s \{d\theta_{n-1}\} / dV_{n-1} \\ &= y_s / R, \quad . \quad . \quad . \quad . \quad . \quad . \quad (15) \end{aligned}$$

just as before.

(Or we can argue thus. We have always (comparing (2) and (7))

$$v_s U_s dV_{n-1} = (-)^{n-1} \left| U_1 \frac{\partial y_2}{\partial u_1} \cdot \frac{\partial y_3}{\partial u_2} \dots \frac{\partial y_n}{\partial u_{n-1}} \right| \{du_{n-1}\}.$$

Of course this equation does not enable us generally to determine dV_{n-1} , which is independent of the U_s . But if the surface be that of a hypersphere, then using (15), we get, putting

$$U_s = \partial R / \partial x_s = y_s / R,$$

$$\frac{y_s}{R} \cdot \frac{y_s}{R} dV_{n-1} = (-)^{n-1} \left| \frac{y_1}{R} \cdot \frac{\partial y_2}{\partial \theta_1} \dots \frac{\partial y_n}{\partial \theta_{n-1}} \right| \{d\theta_{n-1}\},$$

$$\text{i. e.} \quad dV_{n-1} = (-)^{n-1} \Delta_n \{d\theta_{n-1}\} / R.$$

We also see that for the hypersphere

$$dV_n = \frac{\partial (y_1, y_2, \dots, y_n)}{\partial (\theta_1, \dots, \theta_{n-1}, R)} dR \{d\theta_{n-1}\},$$

and since $\partial y_s / \partial R = y_s / R$, this gives

$$\begin{aligned} dV_n &= (-)^{n-1} \frac{\Delta_n}{R} dR \{d\theta_{n-1}\} \\ &= dR dV_{n-1}, \end{aligned}$$

analogously to three dimensions.

Finally, if

$$\psi = O(R^{-m}) \quad (m > 1)$$

as

$$R \rightarrow \infty,$$

then

$$\lim_{n \rightarrow \infty} \frac{1}{R^{n-3}} \cdot \frac{\partial}{\partial R} (R^{n-2} \psi) = 0.$$

If such be the case, we write

$$K_n \psi_A = \int_{V_n} \frac{\omega dV_n}{r_n^{n-2}},$$

where the region now extends to infinity.

It would be both interesting and perhaps startling to discover that in the four dimensions, x, y, z, ict , this solution could replace Kirchhoff's solution of

$$\square \psi = \omega.$$

Yet this actually appears to be the case, as the following analysis will serve to show.

Firstly, we observe that here

$$\begin{aligned} r_4^{-n+2} &= r_4^{-2} \\ &= \frac{1}{2r} \left\{ \frac{1}{r-ct_1} + \frac{1}{r+ct_1} \right\}, \quad \dots \quad (17) \end{aligned}$$

where

$$r^2 = (x-x_0)^2 + (y-y_0)^2 + (z-z_0)^2,$$

$$t_1 = t-t_0,$$

is of the form

$$\phi = \frac{1}{r} \{ f(r-ct_1) + f(r+ct_1) \}.$$

and is therefore a well-known simple solution of the wave-equation.

Secondly, in (1), put

$$x_1 = x, \quad x_2 = y, \quad x_3 = z, \quad x_4 = ict_1, \quad u_3 = ict_1.$$

Then

$$\begin{aligned} \int \frac{\omega dV_4}{r_4^2} &= \int \frac{\omega}{r_4^2} \frac{\partial(x_1, x_2, x_3, x_4)}{\partial(u_1, u_2, u_3, u_4)} du_1 du_2 du_3 du_4,^* \\ &= -ic \int_{-\infty}^{\infty} \left\{ \int \omega dv \right\} \frac{dt}{r_4^2}, \end{aligned}$$

* As we are going to integrate with respect to u_4 first, it seems necessary to put this last in the Jacobian in order to ensure the correct equation for Stokes's Generalized Lemma. Vide Murnaghan, *loc. cit.* p. 35.

where

$$dv = \frac{\partial(x, y, z)}{\partial(u_1, u_2, u_4)} du_1 du_2 du_4$$

and

$$u_4 = \text{constant}$$

is the equation to the two-dimensional bounding surfaces S of the now three-dimensional solid region.

Also

$$J_1 = \frac{\partial(y, z, ict_1)}{\partial(u_1, u_2, ict_1)} = \frac{\partial(y, z)}{\partial(u_1, u_2)},$$

$$J_2 = \frac{\partial(x, z, ict_1)}{\partial(u_1, u_2, ict_1)} = -\frac{\partial(z, x)}{\partial(u_1, u_2)},$$

$$J_3 = \frac{\partial(x, y, ict_1)}{\partial(u_1, u_2, ict_1)} = \frac{\partial(x, y)}{\partial(u_1, u_2)},$$

$$J_4 = \frac{\partial(x, y, z)}{\partial(u_1, u_2, ict_1)} = \frac{1}{ic} \Sigma \frac{\partial(y, z)}{\partial(u_1, u_2)},$$

where

$$\dot{x} = dx/dt_1 \text{ etc.}$$

For internal points (1), (2 A), and (11) now give us

$$\begin{aligned} K_4 \psi_A + \int (-)^{i+j} J_i \left(\phi \frac{\partial \psi}{\partial x_i} - \psi \frac{\partial \phi}{\partial x_i} \right) du_1 du_2 du_3 \\ = \int \frac{\partial}{\partial x_i} \left(\phi \frac{\partial \psi}{\partial x_i} - \psi \frac{\partial \phi}{\partial x_i} \right) \frac{\partial(x_1, x_2, x_3, x_4)}{\partial(u_1, u_2, u_3, u_4)} du_1 du_2 du_3 du_4, \end{aligned}$$

$$K_4 \psi_A = -ic \int \left\{ \int \omega dr \right\} \frac{dt_1}{r_4^2} - S,$$

$$\begin{aligned} S = ic \Sigma \int dt_1 \int \Sigma \left[\left(\psi \frac{\partial \phi}{\partial x} - \phi \frac{\partial \psi}{\partial x} \right) \right. \\ \left. - \frac{\dot{x}}{c^2} \left(\phi \frac{\partial \psi}{\partial t_1} - \psi \frac{\partial \phi}{\partial t_1} \right) \right] \frac{\partial(y, z)}{\partial(u_1, u_2)} dS \end{aligned}$$

$$\begin{aligned} = ic \Sigma \int \int \left[\left(\psi \frac{\partial \phi}{\partial v} - \phi \frac{\partial \psi}{\partial v} \right) \right. \\ \left. - \frac{v}{c^2} \left(\phi \frac{\partial \psi}{\partial t_1} - \psi \frac{\partial \phi}{\partial t_1} \right) \right] d\Omega dt_1, \end{aligned}$$

$$K_4 = (-)^4 4\pi^{4/2}/(4/2-2)! = 4\pi^2.$$

Here ν is the resolved part of $(\dot{x}^2 + \dot{y}^2 + \dot{z}^2)^{1/2}$ along the two-dimensional spreads or surfaces in the three-dimensional region.

Also

$$\phi = -\frac{1}{2rc} \left\{ \frac{1}{(t_1 - r/c)} - \frac{1}{(t_1 + r/c)} \right\},$$

$$\frac{\partial \phi}{\partial t_1} = \frac{1}{2rc} \left\{ \frac{1}{(t_1 - r/c)^2} - \frac{1}{(t_1 + r/c)^2} \right\}.$$

So, writing

$$\phi = \frac{1}{2ct_1} \left\{ \frac{1}{r - ct_1} - \frac{1}{r + ct_1} \right\},$$

we get

$$\frac{\partial \phi}{\partial t_1} = -\frac{c^2 t_1}{r} \cdot \frac{\partial \phi}{\partial r}.$$

Hence we can integrate with respect to t_1 from $-\infty$ to $+\infty$ by the theory of residues*. Thus

$$ic \int_{-\infty}^{+\infty} f_1(t_1) \phi dt_1$$

$$= \frac{\pi}{2r} \left\{ f_1\left(\frac{r}{c}\right) - f_1\left(-\frac{r}{c}\right) \right\} - 2\pi c \Sigma R_1, \quad \dots \dots (19)$$

$$ic \int_{-\infty}^{+\infty} f_2(t_1) \frac{\partial \phi}{\partial t_1} dt_1$$

$$= -\frac{\pi}{2r} ([f_2'(t_1)]_{r/c} - [f_2'(t_1)]_{-r/c}) - 2\pi c \Sigma R_2,$$

$$ic \int_{-\infty}^{+\infty} f_3(t_1) \frac{\partial \phi}{\partial r} dt_1$$

$$= \frac{\pi}{2c^2} \left\{ \left[\frac{\partial}{\partial t_1} \left(\frac{f_3(t_1)}{t_1} \right) \right]_{r/c} - \left[\frac{\partial}{\partial t_1} \left(\frac{f_3(t_1)}{t_1} \right) \right]_{-r/c} \right\} - 2\pi c \Sigma R_3,$$

where ΣR_1 is the sum of the residues of $f_1(t_1)\phi$ at the various poles of $f_1(t_1)$ above the real axis; ΣR_2 of $f_2(t_1)\partial\phi/\partial t_1$ at those of $f_2(t_1)$, and ΣR_3 of $f_3(t_1)\partial\phi/\partial r$ at those of $f_3(t_1)$.

By means of these formulæ equation (18) becomes, after some reduction,

* Whittaker & Watson, 'Modern Analysis,' § 6·23, or MacRobert, 'Functions of a Complex Variable,' p. 65.

$$8\pi\psi_A = - \int \frac{[\omega]_1^2}{r} dv + S_1 + 4c \int \frac{\Sigma R}{r} dv + 4c \int \Sigma R_0 dS,$$

$$S_1 = \int \left\{ \left[\frac{1}{cr} \frac{\partial r}{\partial v} \frac{\partial \psi}{\partial t_1} - \psi \frac{\partial}{\partial v} \left(\frac{1}{r} \right) + \frac{1}{r} \frac{\partial \psi}{\partial v} \right]_1^2 \right. \\ \left. + \frac{1}{c^2} \left[2\dot{v} \frac{\partial \psi}{\partial t_1} + \psi \ddot{v} \right]_1^2 - \frac{2}{cr} \frac{\partial r}{\partial v} \left[\frac{\partial \psi}{\partial t_1} \right]_2 \right\} dS, \quad (20)$$

where

$$[F(t_1)]_1^2 = F(r/c) - F(-r/c),$$

and therefore

$$[F_1(t)]_1^2 = F_1(t_0 + r/c) - F_1(t_0 - r/c).$$

Also ΣR , ΣR_0 denote the sums of the residues of ω and the integrand of S respectively, *qua* functions of t_1 at their poles in t_1 , which are of the form $a + bi$, where b is positive.

I have written the first three terms in the surface integral so as to make it resemble Kirchhoff's integral. It will be noticed that, neglecting the first substitution of r/c for t_1 in S_1 and also in the volume integral, and omitting the last three terms of S_1 and the residue terms in the previous equation, we get precisely minus one-half of Kirchhoff's solution.

The reason for this apparent discrepancy is that in place of Kirchhoff's function

$$\frac{1}{r} F\left(t_1 + \frac{r}{c}\right),$$

I have written

$$-\frac{1}{2rc} f\left(t_1 + \frac{r}{c}\right),$$

where

$$f(x) = 1/x.$$

His $F(x)$ possesses the rather artificial property of being, together with all its derivatives, zero, except when $x=0$, and of giving

$$\int_{-\infty}^{+\infty} F(x) dx = 1.$$

My $f(x)$ arises more naturally, and although it has not the first property, which here is not necessary, it does give

$$\frac{1}{\pi i} \int_{-\infty}^{+\infty} f(x) dx = 1,$$

254 Mr. A. J. Carr on the General Solution of the
which is all that is required; for then

$$\frac{1}{\pi i} \int_{-\infty}^{+\infty} \xi(x) f(x) dx = \xi(0) + 2\Sigma R,$$

as per formula (19). The residues of $f(z)$ above the real axis must necessarily appear, as otherwise the function would be a constant, by Liouville's Theorem, and in this case the substitutions indicated by []² would render (20), and generally ψ_A , zero, and this is not a solution of the general equation with ω different from zero.

Equation (20) clearly represents two equal and opposite wave-trains. Moreover, it includes terms which indicate a normal velocity and acceleration. If we take $\dot{v}=c$, $\ddot{v}=0$, these disappear, but there is nothing that demands that \dot{v} is the wave-velocity, so it seems advisable to retain these terms.

Of course I do not pretend for a moment that Kirchhoff's classic solution no longer holds. It obviously must from the method of its derivation. My solution above must therefore be regarded presumably as an extension of his, or else an alternative one.

APPENDIX.

It was omitted to state that, if $\nabla^2\psi$ is finite at A,

$$\int \frac{\nabla^2\psi}{r_n^{n-2}} dV_n$$

is zero when taken over the small hypersphere of radius ρ . For, clearly then, writing $d\omega'$ for the surface-element with $\rho=1$, we have seen that

$$dV_n = r_n^{n-1} d\omega' dr_n.$$

Hence, if $\nabla^2\psi \leq k$, a finite quantity, at all points in the neighbourhood of A,

$$\begin{aligned} \int_0^\rho \frac{\Delta^2\psi}{r_n^{n-2}} r_n^{n-1} d\omega' dr_n &< k\omega' \int_0^\rho r_n dr_n \\ &= k\omega' \frac{1}{2}\rho^2 \rightarrow 0. \end{aligned}$$

Again, if

$$\lim_{r_n \rightarrow \infty} \omega r_n^p \leq C, \quad (p > 2)$$

then, R_1 being any finite quantity,

$$\int_{r_n=0}^{r_n=R_1} \frac{\omega}{r_n^{n-2}} dV_n \leq \int_{r_n=0}^{r_n=R_1} \frac{\omega}{r_n^{n-2}} dV_n + |K_n C| \int_{R_1}^R \frac{1}{r_n^p} r_n dr_n$$

Equation $\nabla^2\psi=\omega$ in n -dimensional Euclidean Space. 255
and the latter integral is

$$\begin{aligned} &= \frac{|K_n C|}{p-2} \left\{ \frac{1}{R_1^{p-2}} - \frac{1}{R^{p-2}} \right\} \\ &\rightarrow \frac{|K_n C|}{p-2} \cdot \frac{1}{R_1^{p-2}} \end{aligned}$$

as $R \rightarrow \infty$. Also this is a finite quantity; so that under these conditions

$$\int \frac{\omega}{r_n^{n-2}} dV_n,$$

taken over the whole of space, is a convergent integral, no assumption being made as to the *continuity* of ω .

Lastly, it is evident that the results throughout the whole paper entail that $n \geq 3$. For $n=2$, we proceed slightly differently, for then

$$J_1 = \frac{\partial y}{\partial u_1}, \quad J_2 = \frac{\partial x}{\partial u_1},$$

and formula (1) therefore becomes

$$\begin{aligned} &\iint \left(\frac{\partial U_1}{\partial x} + \frac{\partial U_2}{\partial y} \right) \frac{\partial(x, y)}{\partial(u_1, u_2)} du_1 du_2 = \\ &= \int \{ (-)^{2-1} U_1 J_1 + (-)^{2-2} U_2 J_2 \} du_1 \\ &= \int \left(U_2 \frac{\partial x}{\partial u_1} - U_1 \frac{\partial y}{\partial u_2} \right) du_1. \quad \dots (21) \end{aligned}$$

In the event of confusion arising as to which sign to take in replacing $dx dy$ by $\pm \partial(x, y)/\partial(u_1, u_2) du_1 du_2$, we will consider a typical example of finding the area of the circle $r=a$.

Here, put

$$U_1 = 0, \quad U_2 = y, \quad u_1 = \theta, \quad u_2 = r.$$

Then (21) becomes

$$\int_0^a dr \left[\int_0^{2\pi} \frac{\partial(x, y)}{\partial(\theta, r)} d\theta \right] = \int_0^{2\pi} \frac{\partial y}{\partial \theta} d\theta,$$

or

$$\int_0^{2\pi} \left(-\frac{1}{2} a^2 \right) d\theta = - \int_0^{2\pi} a^2 \sin^2 \theta d\theta,$$

which is seen to be true. Here, then, we replace the element of area by $-\partial(x, y)/\partial(\theta, r)$. This corresponds

with the previous expression for the dV_n of a hypersphere. Hence we see that the negative sign must be taken, rendering (21) as

$$\iint \left(\frac{\partial U_1}{\partial x} + \frac{\partial U_2}{\partial y} \right) dx dy = \int (U_1 dy - U_2 dx),$$

the usual Green's Theorem for two dimensions.

For the solution of

$$\frac{\partial^2 \phi}{\partial x^2} + \frac{\partial^2 \phi}{\partial y^2} = 0$$

we can take

$$\begin{aligned} \phi &= \lim_{n \rightarrow 2} \frac{r_n^{-n+2} - a^{-n+2}}{n-2} \dots \dots (22) \\ &= -\log_e (r/a). \end{aligned}$$

Hence (3) becomes, putting $a=1$,

$$\iint \omega \log_e r \, dx \, dy = \Sigma \int (\log_e r \cdot \partial \psi / \partial \nu - \psi / r \cdot \partial r / \partial \nu) \, ds$$

for external points, and for internal points we take the small circle of radius ρ , where

$$ds = \rho \, d\theta, \quad d\nu = -dr.$$

Since

$$\lim_{r \rightarrow 0} r \log_e r = 0,$$

the left-hand member is zero at A, while the right-hand member now reduces to

$$\psi_A \int_0^{2\pi} d\theta = 2\pi \psi_A.$$

This is really no new result, for, referring back to where K_n was first derived, we find that, on dividing ϕ by $n-2$ (which we have done here, (22)), we get

$$K_n' = 2\pi(-)^n [\Gamma(\frac{1}{2})]^{n-2} / \Gamma(n/2),$$

and putting $n=2$, we have at once

$$K_2' = 2\pi.$$

Hence,

$$\begin{aligned} 2\pi \psi_A &= \int \omega \log_e r \, dx \, dy \\ &+ \Sigma \int_c (\psi / r \cdot \partial r / \partial \nu - \log_e r \cdot \partial \psi / \partial \nu) \, ds, \end{aligned}$$

which is the analogue of (11).

We get Cauchy's Theorem if ω is zero, for this implies the existence of a function ϕ conjugate to ψ and satisfying the same differential equation.

Thus if

$$\begin{aligned}\psi_A + i\phi_A &= f(a) = \frac{1}{2\pi i} \int_c \frac{f(z)}{z-a} dz \\ &= \frac{1}{2\pi i} \int_c \frac{(\psi + i\phi)e^{i\zeta}}{|z-a|e^{i\theta}} ds \\ &= \frac{1}{2\pi i} \int_c \frac{\psi + i\phi}{r} e^{i(\zeta-\theta)} ds,\end{aligned}$$

then

$$\psi_A = \int_c \psi/r \cdot \sin(\zeta-\theta) ds + \int_c \phi/r \cdot \cos(\zeta-\theta) ds.$$

But

$$\begin{aligned}\partial r/\partial \nu &= \partial r/\partial x \cdot \partial x/\partial \nu + \partial r/\partial y \cdot \partial y/\partial \nu \\ &= (x-a)/r \cdot \partial y/\partial s - (y-b)/r \cdot \partial x/\partial s \\ &= \cos \theta \sin \zeta - \sin \theta \cos \zeta = \sin(\zeta-\theta).\end{aligned}$$

So the first term is

$$\int_c \psi/r \cdot \partial r/\partial \nu \cdot ds.$$

For the second term we notice that

$$\begin{aligned}0 &= [\log(r\phi)]_c^a = \int_c \partial(\log(r\phi))/\partial s \cdot ds \\ &= \int_c \phi [\sin \zeta \partial(\log r)/\partial y + \cos \zeta \partial(\log r)/\partial x] ds \\ &\quad + \int_c \log r [\sin \zeta \partial \phi/\partial y + \cos \zeta \partial \phi/\partial x] ds \\ &= \int_c \phi [\sin \zeta (y-b)/r^2 + \cos \zeta (x-a)/r^2] \\ &\quad + \int_c \log r [\partial x/\partial \nu \cdot \partial \psi/\partial x + (-\partial y/\partial \nu)(-\partial \psi/\partial y)] ds.\end{aligned}$$

$$\text{Hence } \int_c \phi/r \cdot \cos(\zeta-\theta) ds = - \int_c \log r \cdot \partial \psi/\partial \nu \cdot ds.$$

$$\text{So } 2\pi \psi_A = \int_c (\psi/r \cdot \partial r/\partial \nu - \log r \cdot \partial \psi/\partial \nu) ds.$$

This result is only to be expected since Riemann's proof of Cauchy's Theorem uses Green's Theorem in two dimensions*.

* MacRobert, *loc. cit.* § 27.

this reason that their results can only be regarded as approximations. Schmick's formula enables us to make estimates of the effective radii of electrolytic ions, but it does not offer a means of deducing the behaviour of a given ion in a given solvent from its behaviour in other solvents. In the present state of our knowledge of the liquid state, it seems, therefore, that a semi-empirical line of attack is the only one open to us.

It may be taken as a general rule that those solvents which yield electrolytic solutions consist of molecules which behave as dipoles in the gaseous state. If this is so, we should expect, as indeed we find to be the case, that in the liquid state these molecules would tend to form aggregates having comparatively small external fields; that is, the liquid would exhibit the properties characteristic of molecular association. As, moreover, thermal agitation would tend to break up these aggregates, the liquid should exhibit decreased association with rise of temperature, and the temperature coefficient of its dielectric constant should have a markedly higher value than that of a liquid whose molecules are not dipoles.

An ion placed in such a liquid would tend to orientate the solvent molecules round it, but this orientation would be destroyed by thermal agitation, and we have to consider the average condition of an ion as a case of equilibrium between electrostatic attraction and thermal agitation; its mobility will therefore be a function of its charge (ve) and the thermal energy of a molecule at the temperature of the experiment ($3k\theta/2$). But it will also depend on the dipolar moment of the solvent molecules, and we have no means of estimating this directly: it is, however, clear that the dielectric constant (D) of the solvent is a function of the moment of its molecules, and we may thus use this to represent the required factor.

Another factor which will influence the result is the size of the solvent molecules, and this, again, is unknown, for, even where information is available as to the size of molecules in the gaseous state, this does not enable us to state their average size when the liquid exhibits association. The kinetic theory, however, indicates that the viscosity of a liquid is a function of the dimensions of its molecules, and we can therefore assume that the mobility of an ion will be a function of the viscosity of the solvent (η). It must also depend on the dimensions of the ion, and we will therefore introduce a quantity σ which has the dimension of length

and is characteristic of the ion. We thus arrive at the conclusion that

$$l/Fe = f(ve, k\theta, D, \eta, \sigma) \quad \dots \quad (ii.)$$

Application of the method of dimensions shows that the required function must have the form

$$\frac{l}{Fe} = \frac{1}{\eta\sigma} \phi\left(\frac{3k\theta D\sigma}{2e^2}\right), \quad \dots \quad (iii.)$$

where ϕ indicates an unspecified function. Now, the fact that (a) certain ions, such as the tetraethylammonium ion, give values for $l\eta$ which are practically independent of D or θ , and that (b) the values of $l\eta$ for any ion tend towards constancy when D is small, suggest that $\phi(3k\theta D\sigma/2e^2)$ may have the form $A + B(3k\theta D\sigma/2e^2)^n$, where A and B are constants. An examination of the data showed that $l\eta$ could be expressed with remarkable accuracy by the equation

$$l\eta = \alpha + \beta(\theta D)^2, \quad \dots \quad (iv.)$$

where α and β are constants characteristic of the ion. Data for conductivities are more abundant than those for mobilities, and since $\lambda_0 = l + l'$, where l and l' are the mobilities of anion and kation respectively, it is easiest to test the equation in the first place in the form

$$\lambda_0\eta = (\alpha + \alpha') + (\beta + \beta')(\theta D)^2. \quad \dots \quad (iva.)$$

The values of α and β used in what follows have been deduced from the data of Kohlrausch⁽¹¹⁾ and his collaborators for aqueous solutions at 18° C., and from the results of Sir H. B. Hartley^{(14), (15)} and his colleagues for solutions in methyl alcohol at 25° C. In a comparatively small number of cases one or other of these failed to give the required information, *e.g.* no sulphate is soluble in methyl alcohol. In such cases α and β have been so chosen as to give the best agreement with all the reliable data available.

Table I. gives values for various salts in water at temperatures between 0° C. and 156° C., and also in methyl and ethyl alcohols. In many cases the conductivity has only been determined at a few concentrations, and extrapolation to zero concentration is therefore somewhat uncertain.

Similar remarks apply to the values for sodium iodide given in Table II.; here also it must be noted that some of the solvents, *e.g.* pyridine, are extremely hygroscopic, and that it is well known that small traces of water tend to raise

TABLE I.

		KCl.		NaCl.		NH ₄ Cl.		AgNO ₃ .		Ba(NO ₃) ₂ .		K ₂ SO ₄ .		MgSO ₄ .	
		Calc.	Expt.	Calc.	Expt.	Calc.	Expt.	Calc.	Expt.	Calc.	Expt.	Calc.	Expt.	Calc.	Expt.
Water	0°	79.70	82.02 (37), (40), (41)	66.76	68.75 (14), (16), (37), (42)	79.79	80.0 (1)	70.63	73.2 (3)	71.35	71.2 (41)	80.20	80.5 (26)	68.23	70.7 (41)
	7.1°	98.55	99.11 (18)	82.63	—	98.72	—	87.53	—	88.53	—	98.82	—	85.22	—
	10°	106.63	107.03 (26)	89.45	—	106.84	—	94.79	—	95.91	—	108.28	—	92.57	—
	18°	130.00	130.01 (21)	109.18	118.91 (21)	130.34	130.12 (21)	115.85	115.88 (21)	117.31	117.16 (21)	132.95	132.52 (21)	114.08	114.58 (21)
	25°	152.63	151.38 (27), (28)	127.36	127.59 (27)	152.10	—	131.44	134.12 (26)	137.26	134.6 (21)	156.08	153.85 (21)	134.36	—
	35°	183.73	182.39 (18)	154.69	155.75 (18), (19)	184.46	—	164.59	—	166.99	—	199.75	—	164.95	—
	50°	223.8	231.05 (26)	197.31	199.0 (17)	235.06	—	210.5	194.9 (26)	213.9	214 (26)	246.1	—	214.25	—
	75°	322.45	316.5 (28)	273.12	—	324.8	—	292.5	—	298.06	—	346.85	—	305.25	—
	100°	414.9	414 (26), (27)	352.7	358.5 (26)	418.8	415 (26)	379.25	395 (26)	387.4	385 (26)	455.5	455 (26)	404.7	426 (26)
	128°	519.4	519 (26)	443.2	—	525.3	—	478.45	—	480.95	—	582.4	—	522.5	—
Methyl alcohol {	140°	561.5	572 (26)	479.85	512 (26)	568.35	—	518.8	—	531.8	—	634.9	—	571.8	—
	150°	612.34	625 (26)	524.35	555 (26)	624.5	628 (26)	568.15	570 (26)	583.25	600 (26)	700.2	715 (26)	633.7	690 (26)
Ethyl alcohol {	15°	95.02	92 (6)	87.56	—	101.33	—	101.85	98 (6)	—	—	—	—	—	—
	25°	105.01	105.05 (14)	96.89	96.95 (14)	110.97	111.00 (14)	112.88	112.85 (14)	—	—	—	—	—	—
	18°	42.58	43.6 (34)	39.80	38.06 (36)	45.33	35.0 (12)	46.90	37.3 (9)	—	—	—	—	—	—
	25°	48.29	—	45.19	45.9 (11)	51.45	47.7 (11)	53.30	45 (38)	—	—	—	—	—	—

TABLE II.

Sodium Iodide.

$$\alpha + \alpha' = 0.4783; \beta + \beta' = 1.2468 \cdot 10^{-9}.$$

	θ	λ_0 calc.	λ_0 expt.	λ, η
Water	0	66.99	65.15 (36)	1.168
	18	109.59	109.59 (21)	1.1575
	25	128.44	128.31 (27), (30), (33)	1.146
Acetonitrile	25	177.4	173 (35)	0.6138
Methyl alcohol	25	106.67	106.7 (14)	0.5814
Ethyl alcohol.....	0	31.40	30.5 (7)	0.5405
	25	50.35	48.2 (7)	0.5239
	50	76.14	76 (7)	0.5328
Benzonitrile	25	44.2	51.6 (7)	0.6450
Propyl alcohol	0	14.02	13.5 (7)	0.5157
	30	30.21	28.2 (7)	0.4935
	62	57.48	54.2 (7)	0.4935
Acetone	0	134.3	139 (38)	0.5477
			131.4 (29)	
	25	166.8	184.6 (36)	0.5829
			176.2 (23)	
	50	204.2	227.5 (38)	0.5825
Methyl-ethyl-ketone	25	127.9	139 (7)	0.5587
Methyl-phenyl-ketone ...	25	28.05	35.6 (7)	0.6409
	0	36.34	40.8 (7)	0.6367
Pyridine	0	36.34	40.8 (7)	0.6367
	25	56.66	68.4 (7)	0.5974
	40	68.37	88.0 (7)	0.6372
	80	107.2	136 (7)	0.6283

the conductivity of solutions in some solvents. (Hartley, Applebey, and Garrod Thomas⁽¹³⁾ found that 0.1 per cent. of water increased the conductivity of a solution of lithium nitrate in pyridine by 33 per cent.) It is not therefore surprising that the experimental values given in such

solvents are higher than those given by the formula. In this table are given the experimental values of $\lambda_0\eta$ in order to emphasize the statement that $\lambda_0\eta$ is not constant for such a salt as sodium iodide.

TABLE III.
Tetra-ethyl-ammonium Iodide.
 $\alpha + \alpha' = 0.5624$; $\beta + \beta' = 0.7920 \cdot 10^{-2}$.

	α	λ_0 calc.	λ_0 expt.	$\lambda_0\eta$.
Water	0	56.97	58.0 (35)	1.040
	25	110.55	112.5 (29)	1.0045
Furfural	0	26.61	30 (35)	0.7426
	25	45.17	50 (35)	0.7470
Nitromethane	25	107.62	113.8 (29)	0.7078
Nitrobenzene	25	35.07	40 (35)	0.7318
Acetonitrile	25	187.46	193.7 (35)	0.6773
Propionitrile	25	148.56	165 (35)	0.6816
Methyl alcohol	0	77.65	88 (35)	0.7189
	25	115.23	124 (35)	0.6756
Ethyl alcohol	0	34.54	34.5 (39)	0.6113
	25	55.77	55.0 (35), (29)	0.5978
Cyanacetic ethyl ester ...	25	23.22	28.2 (35)	0.7050
Benzonitrile	25	48.80	56.5 (35)	0.7062
Acetyl-acetone	25	77.72	75.2 (35)	0.5866
			81 (29)	0.6320
Epichlorhydrin	25	58.09	62.1 (35)	0.6396
Acetone	0	150.9	166.4 (38)	0.6592
	25	187.8	209.0 (38)	0.6599
	50	230.7	246.2 (38)	0.6556
Methyl-ethyl-ketone	25	145.6	151.0 (29)	0.6068
Pyridine	25	65.60	78.5 (35)	0.6856
Methyl thiocyanate	25	90.91	96 (35)	0.6901
Ethyl thiocyanate	25	78.91	84.5 (35)	0.6550

TABLE IV.

Tetra-ethyl-ammonium picrate.

$$\alpha + \alpha' = 0.5627; \beta + \beta' = 0.000.$$

	θ	$10^{-4}(\theta D)^2$	λ_0 calc.	λ_0 expt.	$\lambda_0 \eta$
Water	0	580	31.38	31.0 (37)	0.5558
	18	549.9	53.22	53.35 (37)	0.5642
	100	425.5	199.4	197 (37)	0.5559
Methyl alcohol	0	104.9	68.87	72.5 (39)	0.5923
	25	82.8	103.25	102.9 (39)	0.5606
	56	70.9	150.1	153.4 (39)	0.5751
Ethyl alcohol	0	62.7	31.75	32 (39)	0.5670
	25	55.3	51.75	51.5 (39)	0.5598
	56	41.45	88.5	88.7 (39)	0.5636
Acetone	0	40.7	142.8	141.4 (38)	0.5601
	25	38.75	178.2	177.3 (38)	0.5598
	50	15.75	219.8	218.6 (38)	0.5594

Tables III. and IV. give corresponding values for tetra-ethyl-ammonium iodide and picrate.

Furfural is an interesting solvent, owing to its comparatively high dielectric constant (38), but it is troublesome to investigate, owing to its rapid polymerization. Agreement with Getman's results⁽¹⁰⁾ is fairly good, considering the experimental difficulties.

$$1/\eta = 67.1 : (\theta D)^2 = 1.197 \times 10^6.$$

Salt	LiI	NaI	KI	RbI	NH ₄ I	NEt ₄ I
Exptl. ...	35.24	40.70	43.10	45.00	46.10	48.40
Calc.	39.34	42.11	46.01	47.40	48.05	44.10

Results for some other solvents are collected below * (all at 25° C.).

* Values in brackets here and in Table V. are experimental.

	Aceto- nitrile.	Epichlor- hydriu.	Propio- nitrile.	Benzo- nitrile.	Nitro- benzene.	Nitro- methane.
KI	196.0 (203)	—	—	—	—	114.25 (127.8)
NaI	179.6 (160)	—	—	44.24 (50.3)	—	—
NMe ₄ I	199.5 (205)	60.27 (73.8)	155.0 (185)	—	—	—
NEt ₄ I	188.9 (200)	58.06 (66.8)	148.5 (163)	48.79 (56.5)	35.72 (40)	107.6 (113.8)
NPr ₄ I	—	51.42 (59)	142.0 (148)	43.32 (52.2)	31.98 (35)	—
NAm ₄ I	159.4 (163)	—	—	—	30.15 (33)	—
NMe ₄ Cl ...	—	54.71 (70)	—	—	—	—
NMe ₄ Br ...	—	57.09 (73.7)	—	—	—	—
NMe ₄ CNS ..	195.9 (223)	60.48 (74.7)	154.4 (187)	—	—	—
NMe ₄ NO ₃ ...	198.1 (220)	—	—	—	—	113.1 (125)

Finally, in Table V. are collected data for all those ions for which there are sufficient experimental results to justify their inclusion.

If the empirical equation

$$\ln \eta = \alpha + \beta (\theta D)^2 \quad . \quad . \quad . \quad . \quad (iv.)$$

is to be brought into line with the suggestions deduced by the method of dimensions, then we must have

$$l\eta = \alpha + \beta(\theta D)^2 = FeA/\sigma_1 + 9Fk^2\sigma_2 B(\theta D)^2/4e^3, \quad (v.)$$

whence

$$\alpha = 15.35 \times 10^{-8} \text{ A}/\sigma_1 \quad \text{and} \quad \beta = 0.121 \text{ B}\sigma_2, \quad (\text{vi.})$$

and, as the values of α lie between 0.19 and 0.62, so σ_1/A will lie between 81×10^{-8} and 23×10^{-8} , and σ_1 will be of atomic dimensions if A is a numerical constant of quite moderate magnitude. Similarly, the values of β lie between 0.0 and 0.89×10^{-9} , so that $B\sigma_2$ will lie between 0.0 and 0.735×10^{-8} , and σ_2 can also represent an atomic dimension if B has a moderate numerical value.

In fig. 1 three functions are shown plotted against atomic number; these are: (1) values of the atomic radius (σ)

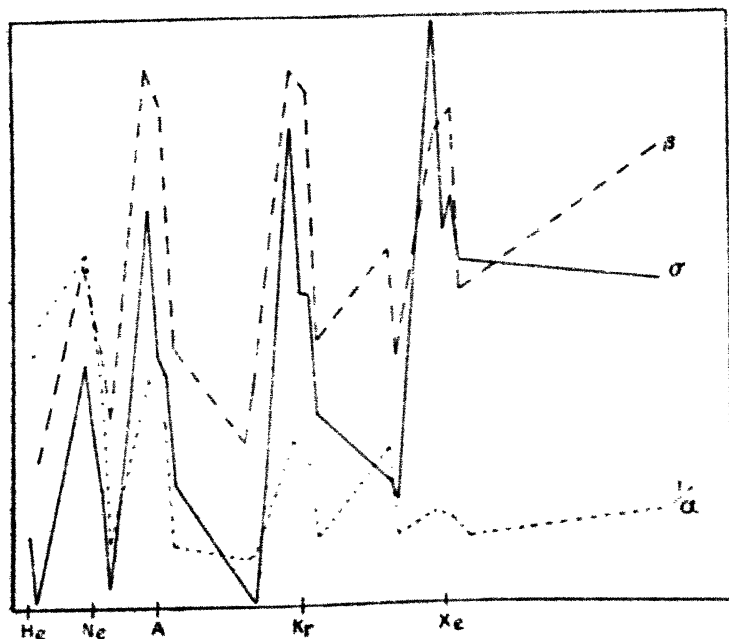
TABLE V. (See footnote on p. 264.)

	α	$10^4 \beta$	Water 18°	Water 25°	Water 100°	Acetonitrile 25°	Methyl alcohol 25°	Ethyl alcohol 25°	Acetone 25°
$1/\eta$			94.59	112.0	354.35	289	183.5	92.0	316.7
$10^{-3} D^{20}_D$			5.480	5.364	4.302	1.15	0.828	0.554	0.888
			<i>l.</i>	<i>l.</i>	<i>l.</i>	<i>l.</i>	<i>l.</i>	<i>l.</i>	<i>l.</i>
Li	0.1880	0.2919	33.31 (33.21)	38.69 (41.42)	120.5 (111.45)	—	39.12 (39.5)	18.88 (17.6)	63.44 (62.0)
P1701	.5941	46.89 (46.90)	—	—	—	40.24 (40.25)	—	—
Na2108	.4548	43.52 (43.27)	50.92 (50.63)	144.0 (145.8)	76.03 (89.4)	45.59 (45.6)	—	72.35 (88.7)
Mg2855	.3362	45.47 (45.41)	—	155.5 (177.0)	—	57.80 (57.7)	—	—
Cl2058	.8910	65.06 (65.65)	76.56 (76.57)	208.75 (206.9)	—	51.30 (51.3)	23.47 (21.4)	76.12 (104.7)
K2537	.8320	64.34 (64.34)	75.08 (75.10)	246.2 (202.25)	92.33 (96.4)	53.71 (53.7)	24.82 (24.6)	81.08 (69.7)
Ca2883	.4657	51.41 (51.42)	—	—	—	59.98 (60.0)	—	—
Cu2929	.3185	44.21 (44.23)	—	—	—	58.58 (58.6)	—	—
Zn2945	.3989	48.53 (48.54)	—	—	—	60.10 (60.1)	—	—
Br2305	.8463	67.74 (77)	70.05 (78.44)	216.8 (209.5)	96.07 (97.4)	55.77 (55.7)	25.73 (22.5)	83.59 (82.0)
Rb2417	.8551	67.9 (7)	78.43 (77.85)	—	—	57.35 (57.35)	—	—
Sr2827	.4756	51.39 (51.40)	—	—	—	59.10 (59.1)	—	—

Ag	2332	6125	53.66 (53.91)	62.96 (62.91)	176.95 (165.5)	—	52.10 (52.1)	24.57 (17)	—
Cd	2810	4490	49.85 (49.87)	—	—	—	58.38 (58.4)	—	—
I	2675	7920	66.35 (66.35)	77.52 (77.33)	—	103.62 (106.6)	61.11 (61.1)	28.65 (26.3)	94.43 (115.9)
Ca	2720	8235	68.42 (68.21)	79.91 (78.34)	221.9 (188.1)	—	62.42 (62.2)	—	—
Ba	2832	5496	55.27 (55.17)	64.72 (63.1)	181.1 (183.0)	—	60.31 (60.1)	—	96.43 (85.6)
Tl	2690	7660	63.15 (65.69)	76.13 (75.53)	—	—	61.00 (61.0)	—	—
NH ₃	2614	7706	64.67 (64.68)	—	210.1 (208.2)	—	59.67 (59.7)	27.98 (22)	92.25 (83.6)
NM ₂	3085	2030	—	46.75 (46.5)	—	95.90 (98.4)	59.68 (65.2)	28.49 (29.2)	100.19 (102.8)
NEt ₃	2949	—	27.89 (27.64)	33.02 (33.0)	104.5 (103.0)	86.22 (83.4)	54.11 (52.95)	27.13 (27.2)	98.39 (93.1)
NPr ₃	2265	—	—	25.37 (26)	—	—	—	—	71.74 (71.8)
NAm ₄	193	—	—	21.6 (18)	—	55.8 (50.4)	35.4 (25)	17.75 (16.7)	—
NH ₂ Et ₂	2862	1019	—	38.17 (38)	—	—	54.07 (57)	26.85 (25.7)	91.89 (91.4)
NH ₂ Bt	2441	1777	—	38.00 (38)	—	—	47.48 (47.5)	23.36 (20.9)	79.5 (92.4)
NO ₂	2380	7524	—	71.84 (71.85)	—	—	55.10 (55.1)	—	—
NO ₂	2735	9378	62.04 (62.05)	72.53 (72.56)	203.25 (202.0)	102.23 (121.6)	60.78 (60.8)	28.72 (26)	95.17 (109.8)
BrO ₃	2658	4482	48.37 (48.38)	—	—	—	55.58 (55.6)	—	—
ClO ₃	2910	5313	55.46 (55.08)	—	—	—	61.46 (61.5)	—	—
ClO ₄	3308	5125	58.42 (58.6)	68.50 (75.5)	198.7 (174.8)	—	69.58 (69.9)	—	112.97 (115.6)
SO ₄	6236	1850	68.63 (68.21)	80.99 (81.50)	249.3 (249.0)	—	—	—	—
CNS	2781	5002	56.89 (56.90)	—	188.1 (193.5)	90.97 (125.6)	59.99 (60.0)	28.60 (26)	95.32 (86.4)
Pic	2678	—	25.33 (25.5)	29.98 (30.7)	94.88 (93.5)	77.40 (78)	49.14 (49.9)	24.64 (24.2)	84.80 (84.2)

deduced from measurements of crystals⁽²⁾ and from the viscosities⁽³¹⁾ of the inert gases; (2) values of β ; and (3) values of $1/\alpha$ from Table V. It will be seen that in every case maxima occur at the halogens and alkali metals with minima between, but that in the cases of σ and β the maxima tend to increase in height with increasing atomic number. The reverse is true for $1/\alpha$; here the maximum at $Z=9$ is much higher than the rest, and, by the time $Z=53$ is reached, fluctuations of $1/\alpha$ with Z have almost died out.

Fig. 1.

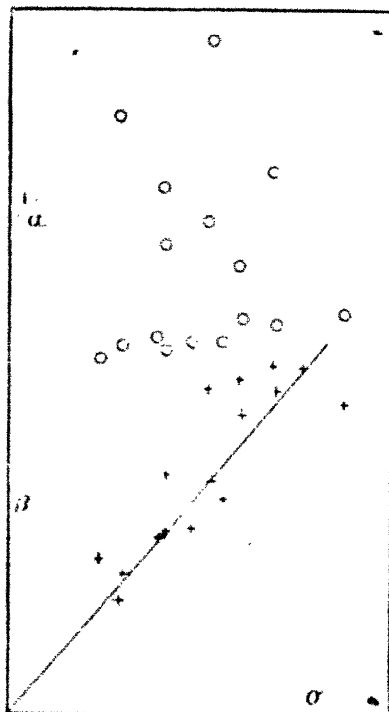


In fig. 2 Bragg's values for σ are plotted (i.) against β , and (ii.) against $1/\alpha$, and it is again evident that while β and σ appear to be intimately related for these elementary ions, the relationship between $1/\alpha$ and σ involves some other variable.

It must not, however, be assumed that the quantities denoted by σ_1 and σ_2 in equations (v.) and (vi.) are actual atomic radii; if they were, we should be led to the absurd conclusions (1) that the alkyl-ammonium ions have zero radius, and (2) that the ions ClO_2 and ClO_4 are smaller than Cl. These considerations drive us to the conclusions that σ_1

represents some function of the dimensions of an ion which approximates to the radius in the case of elementary ions. This is not unreasonable when we consider that in compound ions the effect of the ionic charge on the solvent is partly

Fig. 2.



screened by those parts of the ion which carry no charge, *e. g.* by the C_2H_5 groups round the charged N-atom in $N(C_2H_5)_4$.

References.

- (1) Bhattacharrya & Dhar, *Proc. K. Acad. West. Aust.* xviii. p. 373 (1916).
- (2) Bragg, *Phil. Mag.* ii. p. 258 (1926).
- (3) Born, *Z. für Phys.* i. p. 221 (1920).
- (4) Debye & Hückel, *Phys. Zt.* xxiv. pp. 187, 305 (1923).
- (5) Déguisne, *Wied. Ann.* lii. p. 604 (1894).
- (6) Dampwolf, *Phys. Zt.* v. p. 637 (1906).

270 *Influence of Solvent on Mobility of Electrolytic Ions.*

- (7) Duthoit & Duperthuis, *J. Chim. Phys.* vi. p. 728 (1908).
- (8) Duthoit & Nicollier, *Zt. Elektrochem.* xii. p. 643 (1906).
- (9) Duthoit & Rappeport, *J. Chim. Phys.* vi. p. 545 (1908).
- (10) Getman, *J. Phys. Chem.* xxviii. p. 212 (1924).
- (11) Goldschmidt, *Zt. phys. Chem.* lxxxix. p. 129 (1914; xcix. p. 128 (1921)).
- (12) Häggland, *J. Chim. Phys.* x. p. 210 (1912).
- (13) Hartley, Applebey, & Garrod Thomas, *J. C. S.* xciii. p. 538 (1906).
- (14) Hartley & Frazer, *Proc. Roy. Soc.* cix. p. 351 (1925).
- (15) Hartley & Raikes, *Trans. Farad. Soc.* xxiii. p. 393 (1927).
- (16) Hoskings & Lyle, *Phil. Mag.* iii. p. 487 (1902).
- (17) Jones & Clover, *Amer. Chem. J.* xliii. p. 187 (1910).
- (18) Jones & Douglas, *Amer. Chem. J.* xxvi. p. 428 (1901).
- (19) Jones & West, *Amer. Chem. J.* xxxiv. p. 357 (1905).
- (20) Kahlenberg, *J. Phys. Chem.* v. p. 339 (1901).
- (21) Kohlrausch, 'Landolt & Börnstein's Tables.'
- (22) Lorenz & Michael, *Zt. anorg. Chem.* cxvi. p. 161 (1921).
- Lorenz & Voigt, *ibid.* cxlv. p. 277 (1925).
- (23) McBain & Coleman, *Trans. Farad. Soc.* xv. p. 27 (1919).
- (24) Milner, *Phil. Mag.* xxiii. p. 551 (1912), and xxv. p. 743 (1913).
- (25) Nernst & Lob, *Zt. phys. Chem.* ii. p. 948 (1888).
- (26) Noyes, Melcher, Eastman, & Kato, *J. Amer. C. S.* xxx. p. 335 (1908), and xxxii. p. 157 (1910).
- (27) Ostwald & Nernst, *Zt. phys. Chem.* iii. p. 120 (1889).
- (28) Parker & Parker, *J. Amer. C. S.* xlvi. p. 312 (1924).
- (29) Philip & Courtman, *J. C. S.* xcvi. p. 1269 (1910).
- (30) Rabinowitsch, *Zt. phys. Chem.* xcix. pp. 338, 417 (1921).
- (31) Rankine, *Phil. Mag.* xlvii. p. 612 (1921), and xlv. pp. 280, 292, 508; *Proc. Roy. Soc.* lxxxviii. p. 575 (1913), and cvi. p. 83 (1924).
- (32) Schmick, *Zt. für Phys.* xxiv. p. 56 (1924).
- (33) Stearn, *J. Amer. C. S.* xlv. p. 670 (1922).
- (34) Stenquist, *Zt. Elektrochem.* xxv. p. 29 (1898).
- (35) Walden, 'Leitvermögen der Lösungen.'
- (36) Walden, *Ber.* xxxii. p. 2865 (1899); *Zt. phys. Chem.* iv. p. 207 (1906).
- (37) Walden & Ulich, *Zt. phys. Chem.* cvi. p. 49 (1923).
- (38) Walden, Ulich, & Busch, *Zt. phys. Chem.* cxxiii. p. 429 (1926).
- (39) Walden, Ulich, & Laun, *Zt. phys. Chem.* cxiv. p. 275 (1925).
- (40) Washburn & McInnes, *J. Amer. C. S.* xxxiii. p. 1686 (1911).
- (41) Whetham, *Phil. Trans.* cxciv. p. 321 (1900).
- (42) Wood, *Zt. phys. Chem.* xviii. p. 521 (1895).

Electrical Laboratory,
Oxford,

XXIV. *Factors governing the Appearance of the "Forbidden Line" 2656 in the Optical Excitation of Mercury.* By R. W. WOOD and E. GAVIOLA*.

[Plate III.]

THE appearance of the forbidden line 2656 of mercury in optically-excited vapour at room temperature in the presence of nitrogen at 3 or 4 mm. pressure has been described by Wood. Because of the importance which the appearance of this line has for the theory of spectra, a further investigation was made to determine the most favourable conditions for its development.

The forbidden line appears on the long wave-length side of the pseudo-triplet 2652, 2654, 2655, the relative intensities of which, if nitrogen or water vapour is present in the tube, are about 4 : 8 : 1. With dry nitrogen at a pressure of 3 to 6 mm. in the resonance tube, the intensity of the "forbidden line" is about equal to the intensity of 2655. That has been shown by Wood in pl. xiv. fig. 2, *Phil. Mag.*, Sept. 1927. In the course of the present investigation we have been able to increase the relative intensity of the "forbidden line" about five times, so that it can be obtained stronger than 2652 and nearly equal to the strongest line of the triplet 2654, see Pl. III. (In *vacuo* the relative intensity of the lines of the triplet is quite different.)

Wood has observed that the "forbidden line" appears only if nitrogen is able to bring up strongly the "water-band," which is due to OH produced by the dissociation of water molecules. This circumstance makes it appear probable that the transition $2^3P_0 - 1^1S_0$ is in some way connected with the presence of water vapour in the tube. The next step was to try the effect of different quantities of water vapour mixed with the nitrogen.

To accomplish this the bulb containing nitrogen, which was connected to the fluorescence tube by a fine capillary, was supplemented by another bulb containing copper-sulphate crystals which are in equilibrium with water vapour at a pressure of about 3 mm. at room temperature. If the stop-cock is opened, small quantities of water vapour can be introduced into the tube. A series of photographs taken with 5 mm. of nitrogen and increasing quantities of water vapour in the tube showed that the intensity of the "forbidden line" increases at first rapidly, until the water

* Communicated by the Authors.

vapour has attained a partial pressure of about $\frac{1}{2}$ mm., and then more slowly up to a pressure of 2 or 3 mm. At these higher pressures the intensity decreases rapidly with time owing to the formation of hydrogen, as we shall see later. The OH bands follow a similar course, except that while the "forbidden line" increases its relative intensity 3 or 4 times, the water band increases about 10 times.

The next step was to try whether water vapour alone, without the co-operation of nitrogen, was able to develop the forbidden line. The result was that if 2 or 3 mm. of water vapour were introduced into the tube the whole fluorescence, including the OH band and the "forbidden line," was at first very bright, but became rather faint in a few minutes. It was difficult to photograph the lines under those conditions, because it was necessary to renew the water-vapour charge every 2 or 3 minutes. Wood had observed in previous work that something similar occurred with nitrogen. The fluorescence intensity diminished with the time and the charge had to be renewed. He found that the reason for this was that hydrogen developed in the resonance tube, which could be detected with a small auxiliary discharge-tube connected with the resonance system, and hydrogen is known to be very active in destroying the fluorescence of mercury. With water vapour in the tube hydrogen was developed also, but much more rapidly than in the case of nitrogen, in which case the water vapour probably came from the walls of the tube. On the other hand, it was observed that if the tube was not completely evacuated before introducing the water vapour, so that about 0.1 mm. of air was left in it, the fluorescence remained bright for a much longer time before beginning to fade. Air was then able to compensate the action of hydrogen. To study the action of air a third very fine and long capillary was sealed in, in addition to the water and nitrogen capillaries. Its free end was sealed and could be opened to the air of the room by breaking its end. The capillary was made of such size that, with *vacuo* in the tube, it let pass in one minute a quantity of air sufficient to raise the pressure by 0.03 mm. Thus one could measure the quantity of air introduced by noticing the time that the capillary was open, from the moment when its end was broken until it was again sealed with a small gas flame. It was then observed that if, for instance, 2 mm. of water vapour had been in the tube, and the fluorescence became faint at the end of a few minutes if the air capillary was opened, the fluorescence intensity increased greatly until a maximum was reached. If now the capillary was sealed

the fluorescence remained bright for 3 or 4 minutes and then gradually faded again, returning, however, to its maximum on admitting more air. The quantity of air required to bring the visible fluorescence to a maximum was about 0.03 mm., and if the regenerating action of air is due to the neutralization of hydrogen by combination with oxygen, forming HO or H_2O , we see that about 0.012 mm. of free hydrogen was developed in the tube, since in 0.03 mm. of air only 0.006 mm. of oxygen is present. That such a small quantity of hydrogen is able to diminish the fluorescence at least 4 or 5 times is extremely interesting, and we shall see later the explanation of this fact.

If the air capillary is not sealed when the visible fluorescence becomes a maximum, but is left open for a few seconds more, permitting the entrance of an additional one or two thousandths of a millimetre of oxygen, fluorescence disappears entirely, and the tube is in the "dark state." If now it is left to itself, after a few minutes of darkness the fluorescence suddenly appears again and rises to a maximum value in a few seconds. The time that the tube remains "dark" seems to be proportional to the quantity of free oxygen in it. This surprising action of such a small quantity of oxygen in destroying the whole fluorescence was traced to the fact that the oxygen oxidizes all of the mercury vapour, which deposits as HgO on the walls of the tube as a yellow layer. While the tube is in the "dark state" no mercury vapour is present in the region illuminated by the arc. As long as free oxygen remains in the tube all the mercury vapour that is evaporating from the mercury drop at the bottom of the tube is immediately oxidized when it enters the region illuminated by the arc. The free oxygen is used so slowly by the evaporating mercury that the phenomenon might be used for measuring the velocity of evaporation of mercury. As soon as all of the free oxygen is consumed in this way the evaporating mercury vapour again fills the tube and the fluorescence reappears with full intensity. That the mercury vapour is really "cleaned up" by 0.001 mm. of oxygen has been tested by measuring the absorption of the line 2537 of the arc across the resonance tube. As soon as and as long as the tube is in the "dark state" 2537 is not absorbed at all, showing that no mercury vapour is present.

For the "cleaning up" of the mercury vapour by a few thousandths of a millimetre of oxygen it is necessary that some water vapour be present in the tube. If only mercury vapour is present and we introduce 0.001 mm. of pure

oxygen the fluorescence will diminish but little. In the presence of water vapour it disappears completely. The oxidation of mercury seemed then to be due to a catalyzing action of water vapour, and it was found that nitrogen is also able to catalyze that reaction, which explains why air destroys the fluorescence to a greater degree than oxygen. Now the principal and common action of nitrogen and water vapour on the optically-excited mercury is the bringing (by collisions) of a large number of excited atoms to the metastable condition with electrons on the 2^3p_0 level, where they accumulate, due to the long mean life of that state. The energy of the metastable atoms is probably the real catalyzer of the reaction. The conditions for the rapid oxidation of the mercury vapour are then (1) to have the necessary quantity of free oxygen, and (2) to have a large number of metastable atoms.

The necessary condition for the appearance of the forbidden line seems then to be the formation of a large number of metastable atoms. Water vapour, if no free hydrogen is present, is more efficient than nitrogen in bringing atoms to the metastable level. This has been proved by measuring the absorption of the arc line 4046, which is absorbed only by the metastable atoms, and 0.005 mm. of water vapour in the tube is sufficient to cause the reversal of 4046 if photographed with the large quartz Lummer-Gehrke plate, while 0.5 mm. of nitrogen is necessary to do the same.

On the other hand, the absorption line appears very narrow with 0.1 to 0.5 mm. of water vapour (only the core of the 4046 line is absorbed), while with 0.1 to 1 mm. nitrogen it appears to be much broader. For this reason a reversal of the line appears with water as soon as the absorption begins to be noticeable, while with nitrogen the absorption is at first nearly homogeneous for the whole width of the arc line, so that, in spite of the absorption, "reversal" does not appear. From the measurements of Stuart* and others, it is known that water vapour is more efficient than nitrogen in diminishing the intensity of the resonance line. The result of the collisions in both cases is to bring atoms from 2^3p_1 to 2^3p_0 . Water brings then by equal pressure more atoms to the metastable level than nitrogen. The broadening of the level 2^3p_0 in the case of nitrogen can be interpreted as showing that nitrogen is more efficient than water vapour in shortening the life of that level, and that collisions of the second kind with metastable atoms take place more often

* Stuart, *Zeits. f. Phys.* xxxii. p. 262 (1925).

with N_2 than with water. This diminishes the number of metastable atoms in the case of nitrogen, and by shortening the life of the 2^3p_0 state broadens the absorption line 4046. K. Donat* has found that metastable atoms are more sensitive to collisions with nitrogen than with argon. In our case water seems to act in a way similar to that of argon as observed by Donat. This may be the reason for the stronger development of the "forbidden line" with water than with nitrogen. It is of theoretical importance to know if there is a small spontaneous transition probability of the $2^3p_0 - 1^1S_0$ transition, i. e., if the intensity of the forbidden line is simply proportional to the number of metastable atoms, or if it is necessary to "disturb" the metastable atoms to obtain that transition, which otherwise would not occur. So far we cannot give a conclusive answer to this question. If a spontaneous transition probability exists, the intensity of the "forbidden line" in fluorescence should be proportional to the total absorption of 4046 under all conditions.

If disturbances are necessary the ratio $\frac{\text{intensity of 2656}}{\text{absorption of 4046}}$ should vary with changing conditions; for instance, if instead of nitrogen water vapour is used. This point will be investigated further.

The use of water vapour for bringing up the "forbidden line" has the disadvantage that under illumination it generates free hydrogen more rapidly than does nitrogen, and hydrogen is known to be very efficient in shortening the life of the metastable atoms as well as the intensity of the resonance line †. A very small quantity of free hydrogen diminishes considerably the intensity of 2656 and of the OH band. If water vapour is then used it is necessary to neutralize the free hydrogen every few minutes by admitting a suitable quantity of oxygen or air. On the contrary, a mixture of 2 or 3 mm. of nitrogen and 0.1 to 0.4 mm. of water vapour seems to be very efficient in developing the "forbidden line" and it remains bright for a long time. The way to maintain the fluorescence at maximum intensity is to have some oxide, for instance HgO , in the interior of the tube. If then water vapour or water and nitrogen is introduced, the free hydrogen that might develop will reduce the oxide and regenerate the water vapour ‡. The

* K. Donat, *Zeits. f. Phys.* xxix. p. 345 (1924). Also S. Loria, *Phys. Rev.* xxvi. p. 573 (1925).

† See Franck und Jordan, *Amregung von Quantensprünge durch Stöße*, p. 220. Dorgelo, *Physika*, v. p. 429 (1925).

‡ Franck und Cario, *Zeits. f. Phys.* xi. p. 161 (1922).

yellow deposit of mercury oxide that appears sometimes at the walls of the tube, absorbing strongly the ultra-violet light, can be reduced easily in this way. It is only necessary to introduce 1 mm. of hydrogen in the tube and to illuminate it for about 10 minutes. The yellow film disappears and small mercury droplets remain on the walls of the tube.

Pl. III. shows the relative intensity of the "forbidden line" in regard to the pseudo-triplet 2652, 2654, 2655. The photograph "a" was taken while 5 mm. of nitrogen and a little water vapour were in the tube, photograph "b" while the partial pressure of water vapour was increased to 2 mm. The considerable increment of 2655.8 is plainly shown. The exposure times of the reproduced photographs were about 7 minutes.

XXV. *On the Theory of the Pianoforte String.*

By DR. KULESH CHANDRA KAR*.

IN recent years a number of interesting papers have appeared on the vibrations of the pianoforte string, an account of which has been given in a previous article † by the author in collaboration with Messrs Ganguly and Laha. In that account we did not refer to the theory advanced some eight years ago by C. V. Raman and B. Banerji ‡, as we thought there were serious objections against that theory. Nowadays there appears to be a tendency amongst the experimental workers on the subject, like W. H. George § and others, to give more prominence to the theory than, we think, is due. In the circumstances it seems necessary to point out the mathematical errors that have crept in, which arise out of their misconceptions about the convergence of a Fourier's series.

The writer regrets the article could not be made ready for publication earlier owing to pressure of work.

Now, in their theory referred to above, Raman and Banerji have considered the motion of the string during the time of contact as that of a loaded string. Thus the motion

* Communicated by the Author.

† Kar, Ganguly, and Laha, *Phil. Mag.* v. p. 547 (1928).

‡ Raman and Banerji, *Proc. Roy. Soc. A*, vol. xcvi. p. 100 (1920).

§ W. H. George, *Phil. Mag.* vol. xlviii. p. 34 (1924); also *Proc. Roy. Soc.* vol. cviii. p. 293 (1925).

of the string during the time the hammer is in contact is given by the following equations of Lord Rayleigh* (Rayleigh, 'Theory of Sound,' vol. i. p. 204):

$$-M\lambda \sin \lambda a \sin \lambda b = \rho \sin \lambda l \text{ (frequency equation),} \quad (1)$$

$$\text{and} \quad y = \sum_r P_r \sin \lambda_r x \sin \lambda_r a \cos (c\lambda_r t - \epsilon_r) \quad . \quad . \quad (2a)$$

between $x=0$ and $x=a$,

$$y = \sum_r P_r \sin \lambda_r (l-x) \sin \lambda_r b \cos (c\lambda_r t - \epsilon_r) \quad . \quad (2b)$$

between $x=a$ and $x=l$,

where P_r, ϵ_r are arbitrary constants, a and b are the two parts into which the string of total length l is divided by the hammer or the load, c is the velocity of the wave along the string, M the mass of the hammer, and ρ the linear density of the string. As, however, the system is started into motion by initial velocity at $x=a$ by the hammer whose velocity just before contact is v , one set of arbitrary constants, say ϵ_r , will drop out and the equations will take the form:

$$y = \sum_r P_r \sin \lambda_r x \sin \lambda_r (l-a) \sin c\lambda_r t \quad . \quad (3a)$$

between $x=0$ and $x=a$,

$$y = \sum_r P_r \sin \lambda_r (l-x) \sin \lambda_r a \sin c\lambda_r t \quad . \quad (3b)$$

between $x=a$ and $x=l$,

and thus at $x=a$

$$y_0 = \sum_r P_r \sin \lambda_r a \sin \lambda_r b \sin c\lambda_r t \quad . \quad . \quad (3c)$$

The arbitrary constants P_r etc. of the above series can be evaluated from the initial conditions either directly or with the help of Art. 101 of Lord Rayleigh's 'Theory of Sound,' vol. 1. The second method, which will be called Rayleigh's method, has been followed by Raman and Banerji. In the present paper it seems advisable to give both the methods.

Rayleigh's Method.

It follows directly from equation (7) of art. 101 referred to above (with present notations):

$$y_0 = \sum_r \sin c\lambda_r t \cdot \frac{P_r^2 \sin^2 \lambda_r a \sin^2 \lambda_r b}{c\lambda_r \int \rho u_r^2 dx} \cdot Mv, \quad . \quad . \quad (4)$$

* Notations have been slightly changed.

where M is the mass of the load, i. e. hammer, v its velocity before impact, and

$$\int \rho u_r^2 dx = \rho \int_0^a P_r^2 \sin^2 \lambda_r x \sin^2 \lambda_r b dx + \rho \int_a^l P_r^2 \sin^2 \lambda_r (l-x) \sin^2 \lambda_r a dx. \quad (5)$$

Taking the value of $\rho \int u_r^2 dx$ as given in (5), we have from (4), after a number of transformations,

$$y_0 = \sum_r \frac{2v}{c\lambda_r} \sin c\lambda_r t \cdot \frac{1}{M \left(\frac{a}{\sin^2 \lambda_r a} + \frac{b}{\sin^2 \lambda_r b} \right) - 1}, \quad (6)$$

which is different from that obtained by Raman and Banerji*.

Direct Method.

From equations (3a) and (3b) we have on differentiating and putting $t=0$,

$$(\dot{y})_0 = \sum_r P_r \lambda_r c \sin \lambda_r x \sin \lambda_r b. \quad (7a)$$

between $x=0$ and $x=a$,

$$(\dot{y})_0 = \sum_r P_r \lambda_r c \sin \lambda_r (l-x) \sin \lambda_r a. \quad (7b)$$

between $x=a$ and $x=l$,

and hence, using the normal property of the function, we get

$$\int_0^a \rho(\dot{y})_0 \sin \lambda_r x dx = P_r \lambda_r c \rho \sin \lambda_r b \int_0^a \sin^2 \lambda_r x dx. \quad (8a)$$

$$\int_a^l \rho(\dot{y})_0 \sin \lambda_r (l-x) dx = P_r \lambda_r c \rho \sin \lambda_r a \int_a^l \sin^2 \lambda_r (l-x) dx. \quad (8b)$$

Remembering now that $(\dot{y})_0=0$ except at $x=a$, we have the left-hand sides of equations (8a) and (8b) equal to

$$\rho(\dot{y})_0 \sin \lambda_r a dx_1 \quad \text{and} \quad \rho(\dot{y})_0 \sin \lambda_r b dx_2$$

respectively.

Thus we have from (8a) and (8b)

$$\rho(\dot{y})_0 dx_1 = P_r \lambda_r c \rho \cdot \frac{\sin \lambda_r b}{\sin \lambda_r a} \int_0^a \sin^2 \lambda_r x dx, \quad (9a)$$

$$\rho(\dot{y})_0 dx_2 = P_r \lambda_r c \rho \cdot \frac{\sin \lambda_r a}{\sin \lambda_r b} \int_a^l \sin^2 \lambda_r (l-x) dx. \quad (9b)$$

* If, however, the Wad, i.e., the hammer, is taken as part of the string, then both the methods will give the same equation as that obtained by Raman and Banerji.

On adding (9a) and (9b), we get

$$Mv = P_r \lambda_r c \rho \left[\frac{\sin \lambda_r b}{\sin \lambda_r a} \int_0^a \sin^2 \lambda_r x dx + \frac{\sin \lambda_r a}{\sin \lambda_r b} \int_a^l \sin^2 \lambda_r (l-x) dx \right] \quad \dots (10)$$

Hence we have, after transformation,

$$P_r = \frac{2Mr \sin \lambda_r a \sin \lambda_r b}{\lambda_r c \rho \left\{ a \sin^2 \lambda_r b + b \sin^2 \lambda_r a - \frac{\sin \lambda_r a \sin \lambda_r b \sin \lambda_r l}{\lambda_r} \right\}} \quad \dots (11)$$

Substituting the above value of P_r in (3c), we have y_0 equal to that given in equation (6). Thus both the methods lead to the same result.

Now the above equation (6) gives the value of y_0 as an infinite series. And if λ 's in the different terms have simple ratios—in which case only is there great acoustical interest,—the sum will represent a Fourier's series. It is well known to mathematicians (*vide* Hobson, 'Theory of Functions of a

Real Variable, etc.,' p. 635 *et seq.*) that $\sum \frac{\sin c \lambda_r l}{\lambda_r}$ between $-\pi$ and $+\pi$ is a non-uniformly convergent series representing a discontinuous curve. And therefore it cannot be further differentiated term by term. It can be easily seen that the right-hand side of equation (6) is exactly of the same form as above except the factor*

$$\frac{1}{M \left(\frac{a}{\sin^2 \lambda_r a} + \frac{b}{\sin^2 \lambda_r b} \right) + 1} \quad \dots (12)$$

Now $\sin^2 \lambda_r a$, $\sin^2 \lambda_r b$ in the above expression vary from 0 to 1. If we take the minimum value 0, then the whole expression becomes zero. If, however, we take the greatest value, the expression becomes $\frac{M}{m-M}$, where m is the mass of the string. Thus the value of expression (12) cannot exceed $\frac{M}{m-M}$, and it has the same sign as $\frac{M}{m-M}$. The

* Raman and Banerji have got the value

$$\frac{1}{\frac{a}{M \left(\sin^2 \lambda_r a} + \frac{b}{\sin^2 \lambda_r b} \right) + 1}$$

value of (12) therefore varies between 0 and $\frac{M}{m-M}$ and does not change sign. If we take any possible value (say k) between the limits 0 and $\frac{M}{m-M}$ of the factor (12) for all the terms of the series, equation (6) becomes

$$y_0 = 2\pi\kappa \sum_r \frac{\sin c\lambda_r t}{c\lambda_r} \dots \dots \dots (13)$$

The right-hand side of equation (13) is convergent. But on differentiating term by term, the series thus obtained becomes divergent. Thus $\frac{dy_0}{dt}$ or $\frac{d^2y_0}{dt^2}$ cannot be obtained by differentiating equation (6) as has been done by the previous writers (*loc. cit.*) to obtain the pressure of the hammer.

In conclusion we may quote the remark made by Raman and Banerji about such a *divergent* series :—" . . . a difficulty arises in attempting to carry out a numerical summation of the series for all values of t , owing to the discontinuous nature of the function which the sum represents. This difficulty may, however, be evaded," etc.

Note added in proof.—Further results confirming the above view have been obtained. They will be very shortly ready for the press.

Physical Laboratory,
Presidency College, Calcutta,
March 1928.

XXVI. X-Ray Analysis of Silver Aluminium Alloys. By Prof. A. F. WESTGREN and A. J. BRADLEY, M.Sc., Ph.D.*

[Plate IV.]

THE silver aluminium system has been investigated by Petrenko †, who arrived at the equilibrium diagram reproduced in fig. 1. According to this, there should be

* Communicated by the Authors.

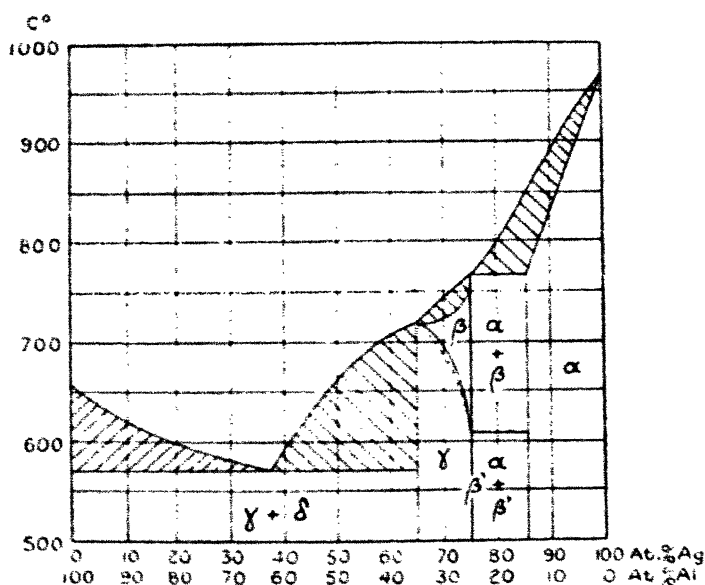
† *Zeitschrift f. anorg. Chemie*, xlv. p. 49 (1905)

two intermediate phases present in this system at ordinary temperatures, one corresponding to Ag_3Al and the other being a "mixed crystal" phase made up of Ag_3Al and Ag_2Al . Both should be formed through transformation in the solid state.

In the following the former phase is called β' and the latter γ . The solid solution of aluminium in silver is denoted by α , and the aluminium phase by δ .

In order to make an X-ray analysis of the system, we have produced a series of alloys by melting together pure

Fig. 1.



Equilibrium diagram of the Ag-Al-system according to Petrenko.

silver with electrolytic aluminium in different proportions. The composition of the specimens was controlled by chemical determinations of both silver and aluminium. Small pieces of the alloys were filed or crushed into fine powder, which was recrystallized by heating *in vacuo* for some minutes to a temperature about 100°C . below the melting-point. From these powders, photograms were taken in a set of focussing cameras constructed by G. Phragmén.

From the series of photograms reproduced in Pl. IV. it is evident that Petrenko's statement concerning the number

of intermediate phases present at ordinary temperatures is correct. Each phase gives a characteristic pattern of lines, and specimens containing two phases give the patterns corresponding to each phase, superimposed one upon the other. The phases corresponding to each alloy can thus be picked out by inspection. Evidently the β' phase corresponds exactly to the formula Ag_3Al with a very narrow range of homogeneity, alloys with 24 and 26 atomic per cent. of aluminium both containing another phase. The other intermediate phase is homogeneous in the range 27–40 atomic per cent. of aluminium.

The α - and δ -Phases.

The lattice parameter of pure silver was found to be 4.079 Å., in good agreement with the values given by W. L. McKeehan* (4.080 Å.), W. P. Davey† (4.079 Å.), and T. Barth & G. Lunde‡ (4.078 Å.). In a homogeneous α -phase specimen containing 19 atomic per cent. aluminium the lattice parameter had fallen to 4.056 Å., and in the saturated phase co-existent with β' it had fallen to 4.053 Å.

The δ -phase had in equilibrium with γ the same lattice parameter as pure aluminium, i.e. 4.042 Å., which proves that the solubility of silver in aluminium is very small.

The mean error of the parameter values given may be estimated at 0.002 Å.

The Phase Ag_3Al .

The β' -phase is in equilibrium with α in the range 20–25 atomic per cent. Al, and with γ in the 25–27 atomic per cent. Al. Its interference lines show no displacement, which proves that the phase is homogeneous in a range so narrow that it may be denoted by a mere line in the equilibrium diagram. An alloy, giving lines only of β' and showing interferences neither of α nor of γ , contained exactly 25 atomic per cent. Al. The phase must therefore be Ag_3Al .

Its structure is of considerable interest, being the same as that of the so-called β -modification of manganese, which

* Phys. Rev. (2) xx. p. 424 (1922).

† Phys. Rev. (2) xxv. p. 753 (1925).

‡ *Zeitschr. f. physik. Chemie*, cxxi. p. 78 (1926).

is stable at higher temperatures*. A comparison between the X-ray data of Ag_3Al , given in Table I., and those of β -manganese, given by Westgren and Phragmén†, shows a close similarity in structure.

In Table I. the intensity, I , of the interferences are denoted by st.=strong, m.=medium, w.=weak, and v.w.=very weak. $h_1 h_2 h_3$ are the Miller indices $\Sigma h^2 = h_1^2 + h_2^2 + h_3^2$, and θ is the deflexion-angle. The radiation used was FeK , with the wave-lengths $\alpha_1 = 1.932 \text{ \AA.}$, $\alpha_2 = 1.936 \text{ \AA.}$, and $\beta = 1.753 \text{ \AA.}$

TABLE I.
Power Photographs of Ag_3Al .

I.		Radiation.	$\sin^2 \frac{\theta}{2}$	$\sin^2 \frac{\theta}{2}$
m.	5	α	0.097	0.01940
w.	6	α	0.117	0.01950
m.	9	β	0.1435	0.01594
w.	10	β	0.160	0.01600
st.	{ 9	{ α	0.175	{ 0.01944
st.	{ 11	{ β	0.195	{ 0.01591
m.	10	α	0.2145	0.01950
m.	11	α	0.2725	0.01945
w.	14	α	0.2875	0.01597
w.	18	β	0.3205	0.01603
v.w.	20	β	0.350	0.01941
st.	17	α	0.370	0.01944
st.	18	α	0.389	0.01945
v.w.	20	α	0.395	0.01598
w.	25	β	0.408	0.01943
m.	21	α	0.415	0.01596
m.	23	β	0.4275	0.01943
w.	27	β	0.4325	0.01600
m.	29	β	0.4655	0.01605
v.w.	30	β	0.480	0.01600
m.	25	α	0.487	0.01948
st.	26	α	0.5065	0.01948
m.	27	α	0.526	0.01948
v.w.	35	β	0.562	0.01606
st.	29	α_1	0.5655	0.01950
m.	29	α_2	0.568	0.01950
v.w.	36	β	0.5785	0.01607
m.	30	α_1	0.585	0.01950
w.	30	α_2	0.587	0.01957
v.w.	37	β	0.5945	0.01605
w.	38	β	0.610	0.01606

* A. Westgren and G. Phragmén, *Zeitschrift f. Physik*, xxxiii. p. 777 (1925). A. J. Bradley, *Phil. Mag.* 1. p. 1018 (1925).

† *Loc. cit.*

TABLE I. (continued).
Power Photographs of Ag_3Al .

I.		Radiatio	$\sin^2 \frac{\theta}{2}$	$\sin^2 \frac{\theta}{2}$
v.w.	41	β	0.6585	0.01610
w.	34	a_1	0.663	0.01950
v.w.	34	a_2	0.666	0.01959
st.	35	a_1	0.682	0.01949
m.	35	a_2	0.685	0.01958
st.	36	a_1	0.702	0.01950
m.	36	a_2	0.705	0.01959
m.	37	a_1	0.721	0.01949
w.	37	a_2	0.724	0.01956
st.	38	a_1	0.7405	0.01948
m.	38	a_2	0.7435	0.01956
v.w.	40	a_1	0.780	0.01950
v.w.	49	β	0.7865	0.01605
m.	41	a_1	0.798	0.01946
m.	41	a_2	0.802	0.01956
v.w.	42	a_1	0.8185	0.01949
w.	43	a_1	0.838	0.01949
v.w.	43	a_2	0.841	0.01956
v.w.	53	β	0.8505	0.01605
v.w.	54	β	0.8665	0.01605
st.	45	a_1	0.876	0.01947
m.	45	a_2	0.880	0.01956
v.w.	46	a_1	0.896	0.01948
v.w.	56	β	0.898	0.01604
v.w.	57	β	0.914	0.01604
w.	59	β	0.946	0.01604
st.	49	a_1	0.954	0.01947
m.	49	a_2	0.9585	0.01956
st.	50	a_1	0.974	0.01948

The phase is cubic, and the strongest reflexions found correspond to the Σh^2 -values 9, 10, 11, 14, 18, 20, 26, 29, etc., just as in the β -manganese photograph. The edge of the elementary cube is calculated to be $6.920 \pm 0.003 \text{ \AA}$, and the density of the phase is found to be 8.74. A calculation of the number of atoms per unit cell on the basis of these data gives the value 20.01, i. e. 20.

Westgren and Phragmén could not definitely settle whether the number of atoms in the elementary cube of β -manganese was 20 or possibly 160. They found some faint interferences which could only be explained if the cube was large enough to contain the latter number of atoms. No interferences of this kind have been observed in the Ag_3Al photographs, and from the close analogy of this phase with β -manganese it may be concluded that the

latter substance has also 20 atoms in its elementary cube. The extra interferences observed were probably due to some oxide content or to some other slight contamination of the manganese powder investigated.

Very little can be said with regard to the structure of the compound Ag_3Al , which is probably too complex to be solved from a powder photograph alone. It is however clear that neither the 15 silver atoms nor the 5 aluminium atoms can form a group of equivalent points. It thus seems probable that the structure contains at least four independent groups of atoms, two containing silver atoms and two containing aluminium atoms. As an alternative solution, silver and aluminium atoms may be distributed at random throughout the structure: in which case the reason for the exact ratio of silver and aluminium atoms would be that the structure was stable only at a certain concentration of valency electrons*.

The γ -Phase.

This phase is close-packed hexagonal, a type of structure common in alloys. The lattice dimensions change continuously within the homogeneous range. As may be seen from Pl. IV., the interference lines are continuously displaced within this interval, but from 43 atomic per cent. Al and further on they have a constant position. From 43 to 100 atomic per cent. Al the lines of the γ -phase gradually decrease in intensity, while the Al-lines grow stronger as the Al-content rises. The X-ray data for the γ -phase are given in Table II.

The calculated values of the intensity, I , given in the table are deduced from the product of the relative occurrence of the reflecting planes and the square of the structure amplitude. The constants of the quadratic forms—

$$\frac{\lambda^2}{3a_1^2} \text{ and } \frac{\lambda^2}{4a_2^2}, \quad -\lambda = \text{wave-length, } a_1 \text{ and } a_2 \text{ are the lattice}$$

parameters—are given in Table III. This also contains the density values, the lattice dimensions, and the calculated number of atoms per elementary parallelepiped.

If the lattice dimensions given in the table be plotted diagrammatically against the concentration values, it is evident that the range of homogeneity of the γ -phase has the limits 27 and 40 atomic per cent. Al.

* Comp. Westgren and Phragmén, *Arkiv för matematik* etc., Stockholm 19 B, No. 12 (1926); *Zeitschr. f. Metallkunde*, xviii, p. 279 (1926).

TABLE II.
Powder Photographs of the γ -Phase.

I.		Radiation.	$h_1 h_2 h_3$	27 at. per cent. Al. $\sin^2 \frac{\theta}{2}$		43 at. per cent. Al. $\sin^2 \frac{\theta}{2}$	
Obs.	Calc.			Obs.	Calc.	Obs.	Calc.
v.w.	...	β	1 0 0	0.123	0.1237
w.	...	β	0 0 2	0.1455	0.1470
m.	3	α	1 0 0	0.1495	0.1502
m.	...	β	1 0 1	0.1595	0.1604
st.	4	α	0 0 2	0.178	0.1784
st.	18	α	1 0 1	0.1945	0.1948
w.	...	β	1 0 2	0.266	0.2668	0.269	0.2707
st.	6	α	1 0 2	0.325	0.3241	0.328	0.3286
v.w.	...	β	1 1 0	0.374	0.3744	0.3995	0.3711
m.	...	β	1 0 3	0.444	0.4442	0.4545	0.4545
st.	12	α	1 1 0	0.455	0.4551	0.4595	0.4596
w.	...	β	1 1 2	0.515	0.5164	0.516	0.5181
v.w.	...	β	2 0 1	0.530	0.5299	0.530	0.5316
st.	...	α	1 0 3	0.5395	0.5396	0.5515	0.5517
m.	18	α	1 0 3	0.5415	0.5416	0.5545	0.5544
w.	...	β	0 0 4	0.5675	0.5676	0.5875	0.5874
w.	...	β	2 0 0	0.607	0.6068	0.600	0.6004
v.w.	3	α	2 0 0	0.609	0.6082	0.603	0.6032
st.	...	α	1 1 2	0.6275	0.6275	0.629	0.6288
m.	24	α	1 1 2	0.6305	0.6299	0.632	0.6318
st.	...	α	2 0 1	0.650	0.6499	0.645	0.6453
m.	18	α	2 0 1	0.652	0.6525	0.648	0.6480
m.	...	α	0 0 4	0.690	0.6896	0.714	0.7140
w.	4	α	0 0 4	0.6925	0.6922	0.7175	0.7175
m.	...	α	2 0 2	0.7795	0.7792	0.7785	0.7789
w.	6	α	2 0 2	0.782	0.7822	0.7815	0.7825
w.	...	β	2 0 3	0.8185	0.8185	0.8245	0.8248
m.	...	α	1 0 4	0.841	0.8413	0.863	0.8641
w.	6	α	1 0 4	0.844	0.8445	0.8665	0.8683
w.	...	β	2 1 1	0.9095	0.9091	0.902	0.9019
w.	...	β	1 1 4	0.942	0.9420	0.958	0.9582

There is nothing in the photographs of the γ -phase to indicate that the Ag or the Al atoms are arranged in a regular way. They are evidently distributed quite at random at the points of the close-packed hexagonal lattice, thus forming a solid solution of a very simple structure*. There is consequently no reason to believe that the γ -phase contains an intermetallic compound with a formula such as Ag_2Al or Ag_3Al .

* Comp. Phil. Mag. (6) 1, p. 311 (1926).

TABLE III.
Lattice Dimensions and Number of Atoms per Elementary Parallelepiped in the γ -Phase.

Atomic per cent. Al.	Average Atomic Weight.	Density.	$\frac{\lambda^2}{3a_1^2}$.		$\frac{\lambda^2}{4a_2^2}$.		a_1 in Å.	a_2 in Å.	a_3/a_1 .	Number of atoms per Elementary Parallele- piped.
			K_{a_1}	K_{β}	K_{a_1}	K_{β}				
27	86.13	8.60	0.1517	0.1248	0.0131	0.0355	2.845	4.653	1.625	2.00
32	82.88	8.33	0.1512	0.1245	0.0436	0.0359	2.869	4.625	1.612	2.01
39	76.18	7.62	0.1504	0.1237	0.0445	0.0366	2.877	4.579	1.592	1.99
43	73.17	7.23	0.1501	0.1236	0.0446	0.0367	2.879	4.573	1.588	

The Phase stable at Higher Temperatures.

According to Petrenko there should be a phase present in the range 15–35 atomic per cent. Al, stable only at higher temperatures. The following observations have confirmed the correctness of this statement.

When specimens of alloys having the said composition were polished and electrolytically etched with nitric acid, a macroscopically visible granular structure was revealed. The size of the grains amounted to several millimetres. X-ray photograms obtained by reflexions against these surfaces showed, however, no single spots, as might have been expected, but continuous lines of a somewhat diffuse appearance, which is a proof that the large grains had been broken up into a very fine structure by some transformation in the solid state.

There are reasons for believing that the phase stable at higher temperatures has a structure analogous to the β -phase of the Cu-Zn-, Ag-Zn-, Au-Zn-, Cu-Al- and Cu-Sn-systems*, i. e. a body-centred cubic lattice; but to settle this it must be investigated in a camera designed specially for high temperature work. Attempts to obtain the phase at the ordinary temperature by quenching heated specimens failed.

Summary.

1. An X-ray analysis of the Ag-Al-system has confirmed the statement of Petrenko that it has two intermediate phases at ordinary temperature, both formed through transformation in the solid state.

2. As Petrenko also found, one of them is Ag_3Al . It is cubic, having an elementary cube with an edge of 6.920 \AA. , containing 20 atoms. *It is isomorphous with β -manganese.*

3. The other intermediate phase, which is homogeneous in a range from 27 to 40 atomic per cent. aluminium, is a solid solution of close-packed hexagonal structure. Its lattice dimensions change continuously from $a_1 = 2.865 \text{ \AA.}$, $a_2 = 4.653 \text{ \AA.}$, and $a_3/a_1 = 1.625$ when saturated with silver to $a_1 = 2.879 \text{ \AA.}$, $a_2 = 4.573 \text{ \AA.}$, and $a_3/a_1 = 1.588$ when saturated with aluminium.

One of the authors is indebted to the Royal Commissioners for the Exhibition of 1851, for a Senior Studentship which enabled him to undertake this investigation, which was carried out at the Metallographic Institute, Stockholm.

* Westgren and Phragmén, *loc. cit.* p. 3.

XXVII. Radio Transmission Formulæ. By G. W. KENRICK,
*Sc.D., Moore School of Electrical Engineering, University of
 Pennsylvania, Pa., U.S.A.**

EARLY studies of the problem of the propagation of electric waves over the surface of the earth considered the problem to be that of determining the field at any point on the surface of an isolated conducting sphere due to an oscillating doublet located at a given point P on its surface †. While these investigations were valuable contributions to theoretical optics, they led to a transmission formula giving an attenuation much greater than that experimentally observed.

The explanation of the departure is, of course, to be found in the important role played by the conductivity of the Kennelly-Heaviside layer.

Much successful work has recently been carried out with a view to explaining the phenomena of short-wave transmission by means of a study of the reflexion and refraction of electric waves by ions and electrons in a magnetic field, but less attention has been given to modifications produced in the classical Hertzian solution for the field at a distant point due to an oscillating doublet when multiple-order reflexions are considered.

G. N. Watson first attacked this problem in 1919 ‡, and obtained a solution for two concentric spherical shells of finite conductivity and sharply-defined boundaries. Dr. Watson's method of attack involved the setting down of Maxwell's equations and an investigation of their solution in terms of series expansions involving spherical or zonal harmonics.

While admirable from the point of view of the mathematician, the method of Watson was too involved to adapt itself to extension to the consideration of the gradually varying conductivity of the upper atmosphere and other related problems of considerable importance in short-wave transmission. For this reason, perhaps, the work of Watson is not frequently referred to by engineers and physicists

* Communicated by Dr. Balth van der Pol.

† H. M. MacDonald, *Proc. Roy. Soc.* lxxii. pp. 59-68 (1903); xc. pp. 50-61 (1914). G. N. Watson, *Proc. Roy. Soc. A*, xcv. pp. 83-99 (1918-19). J. W. Nicholson, *Phil. Mag.* xx. p. 172 (1910). B. van der Pol, *Phil. Mag.* xxxviii. p. 365 (1919). O. Laporte, *Ann. d. Phys.* lxx. p. 595 (1923).

‡ G. N. Watson, *Proc. Roy. Soc.* xcv. pp. 548-563 (1919).

Phil. Mag. S. 7. Vol. 6. No. 35. August 1928.

working in this field, who have adopted the optical point of view of directly-transmitted and singly- or multiply-reflected or refracted rays in their further studies of this problem.

A modification in the coefficient of the exponential in Austin's formula, suggested by Watson's analysis, has also apparently escaped attention, due, perhaps, to the fact that it is implicitly contained in Watson's expression for the Hertzian function rather than explicitly set down in an expression for the field.

Watson's formula involved physical hypotheses which while far from accurate in the general case, are nevertheless probably adequate to the treatment of long-wave communication, from which Austin's formula was originally derived. It is of interest to note that the results obtained by Watson may also be obtained with slight approximation by an application of the optical point of view of reflected rays.

It will be the purpose of this paper to derive such an expression for the field between two concentric conducting spheres by a direct summation of the reflected waves, and to consider the application of the formula thus derived to the problem of long-distance radio communication.

1. *Review of Classical Solution for the Oscillating Doublet.*

The classical problem of determining the field at a point P due to an electronic charge e vibrating at the origin, with an electric moment $A \sin \omega t$ (see fig. 1), gives for the electric and magnetic field intensities at the point P *

$$E_{\theta} = -\frac{\sin \theta}{\rho} A \omega^2 \sin \omega \left(t - \frac{\rho}{c} \right), \quad . . . (1)$$

$$E_r = 0, \quad (2)$$

$$H_{\phi} = -\frac{\sin \theta}{\rho} A \omega^2 \sin \omega \left(t - \frac{\rho}{c} \right). \quad . . . (3)$$

It is not unusual, although not strictly rigorous, to apply this theory to the case of a radio antenna †. Admitting this

* G. W. Pierce, 'Electric Oscillations and Electric Waves,' p. 432 *et seq.* (McGraw Hill, 1920).

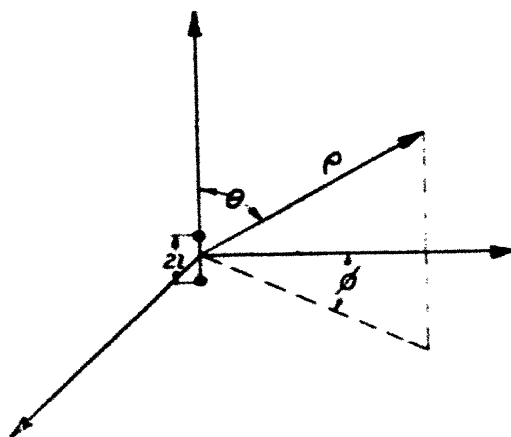
† Pierce's computations of radiation resistance for flat-topped loaded antennae make it possible to correct the results computed on the oscillating doublet theory if such a correction is desired in a particular case. (See text-reference above.)

approximation, we evaluate the constant A in terms of the antenna constants.

Thus we may write, where i is the antenna current in absolute electrostatic units, $2l$ the length of the doublet, e the electronic charge ($2le = A$),

$$i = \dot{q} = \frac{A\omega}{2l} \cos \omega \left(t - \frac{\rho}{c} \right). \quad . \quad . \quad . \quad (4)$$

Fig. 1.



If I represents the maximum amplitude of i , we may write $2lI = A\omega$, and hence (with appropriate choice of the axis of t)

$$E_{\theta} = -\frac{\sin \theta}{\rho} 2lI\omega \sin \omega \left(t - \frac{\rho}{c} \right). \quad . \quad . \quad . \quad (5)$$

Noting further that $\omega = \frac{2\pi c}{\lambda}$ gives

$$E_{\theta} = -\frac{\sin \theta}{\rho} \frac{4\pi clI}{\lambda} \sin \omega \left(t - \frac{\rho}{c} \right). \quad . \quad . \quad (6)$$

By the elementary theory of electrostatic images, the field is unaltered by the introduction of a perfectly conducting plane in the horizontal plane $\theta = \frac{\pi}{2}$ (see fig. 1). The solution given in equation (6) is therefore the solution for

the radiation from a doublet antenna of height l located at a point O on a perfectly-conducting plane where all quantities are expressed in absolute electrostatic units. For convenience we will let

$$\frac{4\pi clI}{\lambda} = K. \quad . \quad . \quad . \quad . \quad . \quad (7)$$

At this point it is of interest to note that, expressed in practical units (amp., km., volts), this value of K gives for E at the surface of the earth

$$E = \frac{120\pi I}{\rho\lambda}, \quad . \quad . \quad . \quad . \quad . \quad (8)$$

where

E = root mean square field in volts-km.,

I = root mean square antenna current in amp.,

ρ = distance in km.,

λ = wave-length in km.,

l = height of antenna in km.

2. Propagation of Waves between two Perfectly-conducted Planes.

We will now alter the conditions of the previous problem by introducing a second perfectly-conducting plane at a height h above the $\theta = \frac{\pi}{2}$ plane of fig. 1 (see fig. 2). We

require the field at a point P on the plane $\theta = \frac{\pi}{2}$ due to the doublet at O.

We may obtain this solution directly from optics in terms of a direct and a series of reflected rays, but it is perhaps more satisfactory to formulate the problem from the theory of images; i. e., we require a series of image doublets which will cause the tangential electric field at any point on the bounding planes to vanish. Such an infinite series of doublets is indicated in fig. 2.

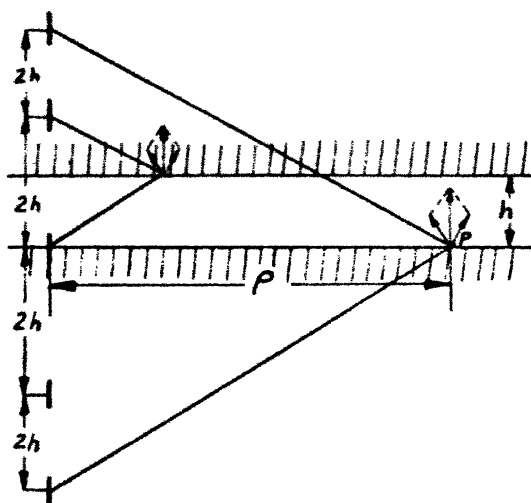
The resultant field at the point P is then obtained by taking the sum of the normal components of the electric fields due to each pair of symmetrically-located doublets*

* It will be noted that tangential components of electric force vanish as required.

and summing the components due to all the pairs of doublets. This gives for the resultant normal field at P

$$E_p = K \left[\frac{\sin^2 \theta_0 \sin \omega \left(t - \frac{\rho}{c} \right)}{\rho} + 2 \sum_{s=1}^{\infty} \frac{\sin^2 \theta_s \sin \omega \left(t - \frac{\sqrt{\rho^2 + 4s^2 h^2}}{c} \right)}{\sqrt{\rho^2 + 4s^2 h^2}} \right]. \quad (9)$$

Fig. 2.



Noting that $\sin^2 \theta = \frac{\rho^2}{\rho^2 + 4s^2 h^2}$, this may be written

$$E = K \left[\frac{\sin \omega \left(t - \frac{\rho}{c} \right)}{\rho} + 2 \sum_{s=1}^{\infty} \frac{\rho^2 \sin \omega \left(t - \frac{\sqrt{\rho^2 + 4s^2 h^2}}{c} \right)}{(\sqrt{\rho^2 + 4s^2 h^2})^3} \right]. \quad (10)$$

The evaluation of E for small $\frac{\rho}{h}$ may be carried out by

direct computation, as the terms in this case decrease in magnitude. For $\frac{\rho}{h} > 10$, however, this procedure is evidently laborious.

It may be shown, however, that under these conditions the probability is small that the mean E at any point P chosen at random will depart much from $\frac{1}{2} \sum_{s=0}^{\infty} E_s^2$; i. e.,

$$\bar{E}^2 \simeq \frac{1}{2} K^2 \left(\frac{1}{\rho^2} + 4 \sum_{s=1}^{\infty} \frac{\rho^4}{(\rho^2 + 4s^2 h^2)^2} \right), \quad (11)$$

where the units employed are absolute electrostatic units and K is as defined in equation (7).

We will now proceed to some purely mathematical manipulation which may be used to sum this infinite series. We begin by availing ourselves of the well-known identity obtained from product considerations †, i. e.,

$$\coth x = \frac{1}{x} + 2 \sum_{s=1}^{\infty} \frac{x}{x^2 + s^2 \pi^2}. \quad (12)$$

Changing variable, letting $\frac{\pi y}{2h} = x$, gives

$$\coth \frac{\pi y}{2h} = \frac{2h}{\pi y} + 2 \sum_{s=1}^{\infty} \frac{\frac{\pi y}{2h}}{\frac{\pi^2 y^2}{4h^2} + s^2 \pi^2}. \quad (13)$$

or

$$\frac{\pi}{4yh} \left(\coth \frac{\pi y}{2h} - \frac{2h}{\pi y} \right) = \sum_{s=1}^{\infty} \frac{1}{y^2 + 4s^2 h^2}. \quad (14)$$

Letting $y = \sqrt{x}$, we have

$$\frac{\pi}{4h\sqrt{x}} \left(\coth \frac{\pi\sqrt{x}}{2h} \right) - \frac{1}{2\sqrt{x}} = \sum_{s=1}^{\infty} \frac{1}{x + 4s^2 h^2}. \quad (15)$$

Differentiating both sides of this identity with respect to x gives

$$\frac{\pi}{8h(\sqrt{x})^3} \coth \frac{\pi\sqrt{x}}{2h} - \frac{\pi^2}{16h^2\sqrt{x}} \operatorname{csch}^2 \frac{\pi\sqrt{x}}{2h} - \frac{1}{2x^2} = \sum_{s=1}^{\infty} \frac{1}{(x + 4s^2 h^2)^2}. \quad (16)$$

* This, in the optical analogy, amounts to taking the resultant intensity of the light as the sum of its component intensities.

† See E. B. Wilson's 'Advanced Calculus,' p. 454.

Differentiating again, we have

$$\begin{aligned} & \frac{3\pi}{16h(\sqrt{x})^5} \coth \frac{\pi\sqrt{x}}{2h} + \frac{3\pi^2 \operatorname{csch}^2 \frac{\pi\sqrt{x}}{2h}}{32h^2 x^2} \\ & + \frac{\pi^3}{32h^3(\sqrt{x})} \left(\operatorname{csch}^2 \frac{\pi\sqrt{x}}{2h} \right) \left(\coth \frac{\pi\sqrt{x}}{2h} \right) - \frac{1}{x^2} \\ & = \sum_{s=1}^{\infty} \frac{2}{(x+4s^2h^2)^2}. \quad (17) \end{aligned}$$

If, now, we multiply both sides of this equation by $2K^2x^2$, set $x=\rho^2$, reverse the order of the members, and subtract $\frac{K^2}{\rho^2}$ from each side of the resulting equation, we have our required summation; i. e.,

$$\begin{aligned} K^2 \left(\frac{1}{\rho^2} + \sum_{s=1}^{\infty} \frac{4\rho^4}{(\rho^2+4s^2h^2)^2} \right) \\ = K^2 \left(\frac{3\pi}{8h\rho} \coth \frac{\pi\rho}{2h} + \frac{3\pi^2 \operatorname{csch}^2 \frac{\pi\rho}{2h}}{16h^2} \right. \\ \left. + \frac{\pi^3\rho}{16h^3} \left(\operatorname{csch}^2 \frac{\pi\rho}{2h} \right) \left(\coth \frac{\pi\rho}{2h} \right) - \frac{1}{\rho^2} \right). \quad (18) \end{aligned}$$

Substituting the value of K from equation (8), we may write for the root mean square field E , in practical units,

$$\begin{aligned} E = \frac{120\pi I}{\lambda} \left[\frac{3\pi}{8h\rho} \coth \frac{\pi\rho}{2h} + \frac{3\pi^2 \operatorname{csch}^2 \frac{\pi\rho}{2h}}{16h^2} \right. \\ \left. + \frac{\pi^3\rho}{16h^3} \left(\operatorname{csch}^2 \frac{\pi\rho}{2h} \right) \left(\coth \frac{\pi\rho}{2h} \right) - \frac{1}{\rho^2} \right], \quad (19) \end{aligned}$$

where h is the height of the Kennelly-Heaviside layer in kilometres and the other quantities are in the same units as in equation (8).

For $\frac{\rho}{h} \ll 1$ this equation becomes identical with equation (8), and represents an E inversely proportional to ρ . This is, of course, as it should be, as reflected waves will not be of importance at distances from the transmitter very small compared with h .

For $\frac{\rho}{h} \gg 1$, however, the term $\frac{3\pi}{8hp} \coth \frac{\pi\rho}{2h}$ governs, and the value of E given by the formula approaches

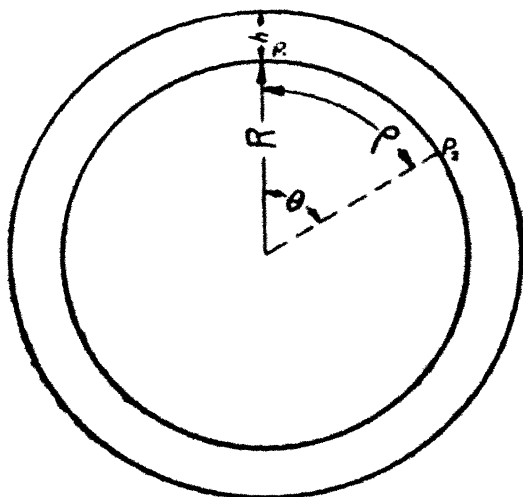
$$E = \frac{120\pi I}{\lambda} \sqrt{\frac{3\pi}{8hp}}.$$

In other words, E decreases only with $\frac{1}{\sqrt{\rho}}$ in this case.

3. Correction for Earth Curvature.

In the previous analysis we have found intensity at any point at a distance ρ from an oscillating doublet located at

Fig. 3.



the surface of one of two perfectly-conducting planes. This analysis may, with slight approximation, be extended to the case of two concentric conducting spheres separated by a distance small compared with their radii.

Thus, referring to fig. 3, showing two concentric conducting spheres, we require the intensity of the electric field E normal to the inner sphere at its surfaces at a point P_2 at a distance ρ from an oscillating doublet located at point P_1 on the surface of the inner sphere. If R is approximately 6400 km. and $h = 100$ km., we may, to a very good approximation, neglect the curvature of the great circle in computing the paths of the rays, thus reducing the problem to much the same form as in the plane case.

It does not follow, however, that we may likewise neglect the curvature of the small circles $R \sin \theta$ or $(R+h) \sin \theta$ on the surfaces of the inner and outer spheres respectively. This results in a focussing action in which the energy flowing out from the emitting doublet passes out, at a distance ρ from the doublet, through an area $2\pi R \sin \theta$ as contrasted with an area* $2\pi R \theta$ in the plane case. Now, the total energy passing through these surfaces† must, in the absence of attenuation‡, be equal to the total emitted energy of the doublet. It follows, therefore, that for a given ρ , if E_s^2 and E_p^2 are the squares of the field intensities in the sphere and plane cases respectively, we have, with slight approximation §,

$$\frac{E_s^2}{E_p^2} = \frac{2\pi\rho h}{2\pi R h \sin \theta} = \frac{\rho}{R \sin \theta} = \frac{\theta}{\sin \theta}.$$

Hence the formula for the mean square field E becomes in this case

$$E_s = \frac{120\pi I}{\lambda} \sqrt{\frac{\theta}{\sin \theta}} \left[\frac{3\pi}{8h\rho} \coth \frac{\pi\rho}{2h} + \frac{3\pi^2 \operatorname{csch}^2 \frac{\pi\rho}{2h}}{16h^2} + \frac{\pi^3\rho}{16h^3} \left(\operatorname{csch}^2 \frac{\pi\rho}{2h} \right) \left(\coth \frac{\pi\rho}{2h} \right) - \frac{1}{\rho^2} \right] \quad [\text{km., amp., volts, radians}]. \quad (21)$$

For this $\frac{\rho}{h} \ll 1$ reduces to

$$\frac{120\pi I}{\lambda\rho} \sqrt{\frac{\theta}{\sin \theta}} \quad \dots \dots \dots (22)$$

Equation (22) is readily recognized as the coefficient of Dr. Austin's transmission formula. Our analysis indicates

* Neglecting higher-order terms in $\frac{h}{R}$.

† We do not consider waves passing around the sphere more than once. These are not of practical interest, owing to attenuation.

‡ In cases of attenuation factors involving ρ only, this argument is still valid, as the same fraction of initial energy reaches the surface at a distance ρ .

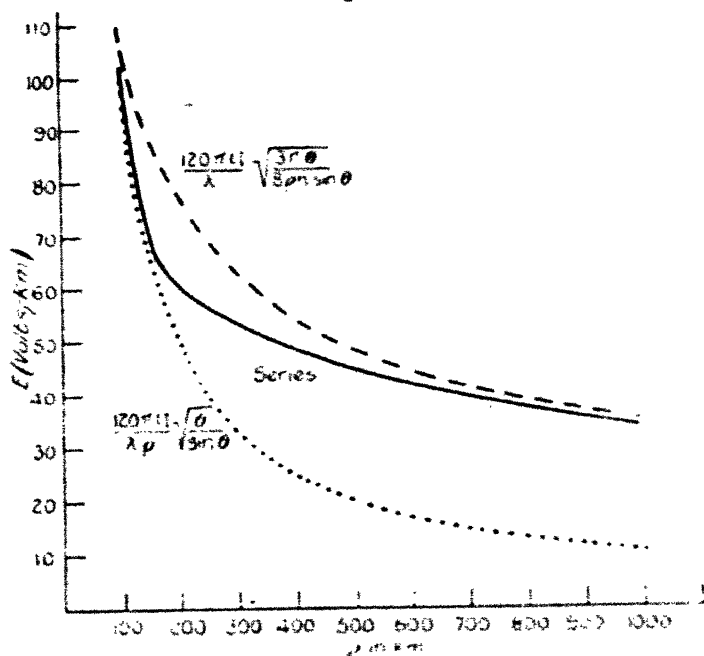
§ Our approximation consists in neglecting certain phase differences; i. e., we assume that $\int E_x H \cdot ds \sim E^2 (\text{area})$. At considerable distances from the transmitter, however, our wave is nearly plane, and this approximation is not seriously in error.

that when reflexions are considered, a more appropriate form of the coefficient for $\frac{\rho}{h}$ large would be

$$\frac{10 \pi l I}{\lambda} \sqrt{\frac{3 \pi \theta}{8 \rho h \sin \theta}} \dots (23)$$

Figs. 4 and 5 give plots of E as computed from equations (22), (23), and (11) * for the case $120 \pi l I = 10^4$ (a constant determined at the transmitting station), $h = 100$ km. The

Fig. 4.



Comparison of transmission formulae for infinite conductivity case (ρ small).

interval $\rho = 100$ to $\rho = 1000$ km. is shown in fig. 4, and the interval $\rho = 1000$ to $20,000$ km. is shown in fig. 5. For values of $\rho < 100$ (11) corresponds closely to (22), and for values of $\rho > 10,000$ to (23).

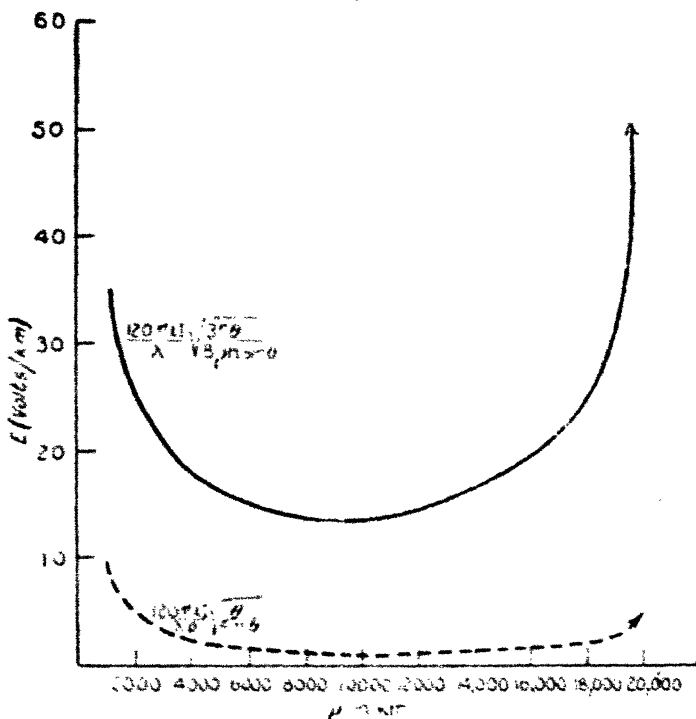
* Equation (11) must, of course, be modified to take account of earth curvature, and reduced to comparable practical units. This gives for E ,

$$E = \frac{120 \pi l I}{\lambda} \sqrt{\frac{\theta}{\sin \theta}} \left(\frac{1}{\rho^2} + 4 \sum_{s=1}^{\infty} \frac{\rho^s}{(\rho^2 + 4s^2 h^2)^{3/2}} \right)^{1/2} \dots (11b)$$

4. Modifications introduced by Finite Conductivity.

Thus far we have considered the propagation of waves between two perfectly-conducting sharply-defined planes or concentric spheres. It is not, however, difficult to modify equation (11) in such a manner as approximately to take into account attenuation due to finite conductivity and a non-sharply defined boundary at the upper conducting layer.

Fig. 5.



Comparison of transmission formulæ for infinite conductivity case (p large).

However, the problem of the series thereby introduced is not in general as simple as in the infinite conductivity case.

Thus, in the formulation of § 2, if we still consider the lower plane (corresponding to the earth) as perfectly conducting, and let r_s be the reflexion (or refraction) coefficient of a ray incident on the upper plane at an angle of incidence ϕ_s , we have, for the plane case,

$$E^2 = \frac{1}{2} K^2 \left(\frac{1}{\rho^2} + 4 \sum_{s=1}^{\infty} \frac{\rho^4 r_s^2}{(\rho^2 + 4s^2 h^2)^3} \right). \quad (24 a)$$

It will be noted that § 2 was not limited in its application to long-distance long-wave communications. The approximations of § 3 *et seq.*, however, need further investigation and modification before the above methods can be used to deduce a transmission formula applicable for short-wave communication over short or moderate distances. It will in particular be noted that the form of the reflexion coefficient of equation (24) distinctly does not hold under these considerations, although the possibility remains of employing a suitably-modified coefficient of reflexion, taking into account the non-metallic nature of the reflector and non-sharply defined boundary.

Another correction of importance when transmission over short or moderate distances is considered arises in connexion with the correction for earth curvature. Due to the shadow effect of the earth, according to our approximate treatment, the directly-transmitted wave (and, at sufficiently great distances, lower-order reflexions) would be suppressed. At long distances the effect of these terms is relatively unimportant. At short distances a term for term computation of equation (24) is possible. If, as an approximation, we modify the small directly-transmitted wave-term to the form it assumes in the MacDonald-Watson diffraction solution for the earth as an isolated conducting sphere, equation (24), modified further to take account of earth curvature in the reflexion terms, becomes *

$$E^2 = \frac{\theta}{\sin \theta} K^2 \left(\frac{A}{\rho} e^{-\frac{0.0073 \rho}{\sqrt{\lambda}}} + \sum_{r=1}^{\infty} \frac{\rho^4 r^4}{(\rho^2 + 4r^2 h^2)^2} \right). \quad (24b)$$

The complete theory of the determination of the quantity r as a function ϕ , the thickness of the conducting boundary, and the frequency involves the entire problem of the wave-length attenuation function of radio transmission, a discussion beyond the scope of the present article.

It is of interest, however, to note that, on the assumption of an ohmic conductivity and a sharply-defined boundary †, the reflexion coefficient may be approximately written in exponential form.

From usual optical theory we have, for a wave with its

* See reference † of page 289. Watson concludes that for this case the Hertzian function is of the order of $A (\sin \theta)^{-\frac{1}{2}} e^{-23.844 \lambda^{-\frac{1}{2}}}$, which in our notation is given above. A is a constant.

† A boundary may be considered as sharply defined, provided reflexion takes place in an interval small compared with a wave-length.

electric intensity vector in the plane of incidence, a reflexion coefficient given by *

$$\sqrt{r_s} = \frac{n^2 \cos \phi_s - \sqrt{n^2 - \sin^2 \phi_s}}{n^2 \cos \phi_s + \sqrt{n^2 - \sin^2 \phi_s}}, \quad \dots (25).$$

where

n = the relative index of refraction of the media ;

ϕ_s = angle of incidence.

For a large index of refraction n and a correspondingly large \sqrt{r} this may conveniently be written, by ordinary algebraic division, in the form

$$\begin{aligned} \sqrt{r_s} &= \frac{1 - \frac{\sqrt{n^2 - \sin^2 \phi_s}}{n^2 \cos \phi_s}}{1 + \frac{\sqrt{n^2 - \sin^2 \phi_s}}{n^2 \cos \phi_s}} \\ &= 1 - \frac{2\sqrt{1 - \frac{\sin^2 \phi_s}{n^2}}}{n \cos \phi_s} + \frac{2\left(1 - \frac{\sin^2 \phi_s}{n^2}\right)}{n^2 \cos^2 \phi_s} + \dots \quad (26); \end{aligned}$$

or to higher-order terms in $\frac{1}{n}$,

$$\sqrt{r_s} \simeq \epsilon^{-\frac{2}{n \cos \phi_s}} \dots \dots \dots (27).$$

For $\mu_1=1$, $\epsilon_1=1$, $\mu_2=1$ and a reflecting medium of specific conductivity γ , n becomes, for a wave of period T ,

$$n = \sqrt{\epsilon_2 + 2\sqrt{-1\gamma T}}. \quad \dots \dots (28)$$

For γ large, we have

$$n \simeq \sqrt{2\gamma T}/45^\circ \quad \dots \dots \dots (29)$$

and

$$|\sqrt{r_s}| \simeq \epsilon^{-\frac{1}{\sqrt{\gamma T} \cos \phi_s}} \dots \dots \dots (30).$$

Substituting equation (30) in (24 a), we have, for the plane case, noting that $\cos \phi_s = \frac{2sh}{\sqrt{\rho^2 + 4s^2h^2}}$,

$$\bar{E}^2 = \frac{1}{2} K^2 \left(\frac{1}{\rho^2} + 4 \sum_{s=1}^{\infty} \frac{\rho^4 \epsilon^{-\frac{\sqrt{\rho^2 + 4s^2h^2}}{h\sqrt{\gamma T}}}}{(\rho^2 + 4s^2h^2)^2} \right), \quad \dots (31 a)$$

* P. Drude's 'Theory of Optics' (Longmans, Green & Co., 1920).
G. W. Pierce, 'Electric Oscillations and Electric Waves.'

and from (24 b), for the case of the earth as a sphere,

$$E^2 = \frac{\theta}{\sin \theta} \frac{1}{2} K^2 \left(\frac{A}{\rho} e^{-\frac{0.0075 \rho}{\sqrt{\lambda}}} + 4 \sum_{s=1}^{\infty} \frac{\rho^s e^{-\frac{\sqrt{\rho^2 + 4s^2 h^2}}{4 \sqrt{\gamma T}} \rho}}{(\rho^2 + 4s^2 h^2)^s} \right). \quad (31b)$$

It is of interest to note that in equation (31) the attenuation factor of every term (except that for the ground-wave) involves the inverse square root of the wave-length. For lower-order reflexions and ρ large, moreover, $\sqrt{\rho^2 + 4s^2 h^2} \sim \rho$, making this approximation for the series as a whole, the corresponding value of E for the plane case reduces at large distances, in the units of equation (18) (γ measured in mhos./km.²), to

$$E = \frac{120\pi/I}{\lambda} \sqrt{\frac{3\pi}{8\rho h}} e^{-\frac{0.183 \rho}{4 \sqrt{\lambda} \sqrt{\gamma}}} \dots \quad (32)$$

Considerations of earth curvature are not essentially altered by the finite conductivity, since the exponential factor of attenuation is the same in both cases for equal values of ρ . With earth curvature taken into account, (32) becomes

$$E = \frac{120\pi/I}{\lambda} \sqrt{\frac{3\pi\theta}{8\rho h \sin \theta}} e^{-\frac{0.183 \rho}{4 \sqrt{\lambda} \sqrt{\gamma}}} \dots \quad (33)$$

Taking $h=100$ km. (effective height), an exponent of the order of 0.0015 is obtained for a γ of the order of about one-thousandth that of sea-water, certainly not an extravagant assumption for the upper-atmosphere conductivity.

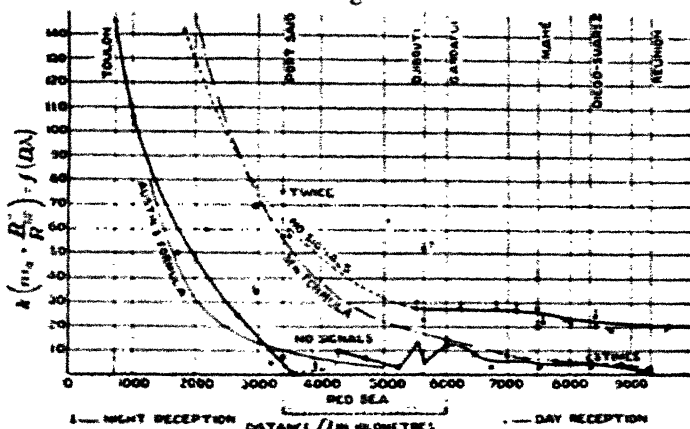
5. Summary of Results and Conclusions.

It thus appears that, under the hypothesis of reflexion of the metallic type, an assumption quite possibly justified at long wave-lengths, the inverse square root of the wave-length in the attenuation factor of the original Austin formula has considerable theoretical justification. This theory, however, suggests the desirability of a modification of the inverse first power of the distance in the coefficient of the exponential to an inverse square root. A slight change in the numerical constant in this coefficient is also indicated.

The writer has not the data at hand, nor is it within the scope of this paper, to enter into an elaborate statistical comparison of the closeness of accord with experimental data

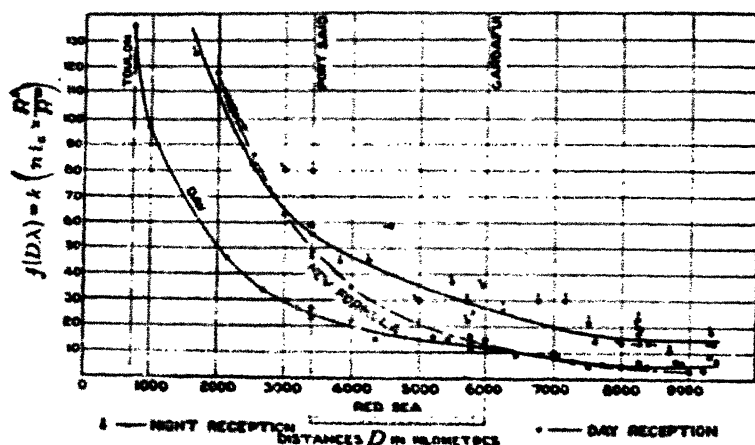
obtained by this formula, the original Austin formula, and a modification recently suggested by Dr. Austin. It will be noted, however, that the above formula gives much larger values than the Austin at large distances where fields predicted by the Austin formula have in general been found to be too

Fig. 6.



Curves of received signal strengths between Toulon and Réunion.
Transmission from Nantes on 9000 m.

Fig. 7.



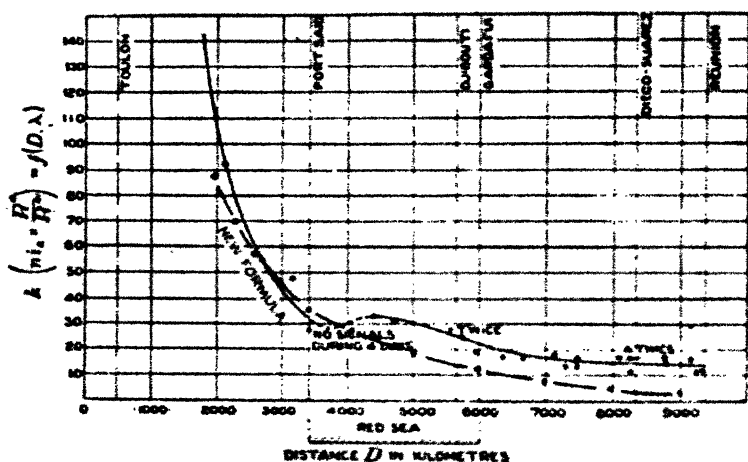
11,000 metre transmission (Lyons).

small to check with observed results. Some idea of the relative values of the fields predicted may be obtained from figs. 4 and 5, which plot the coefficients. Let us compare the formula with at least one piece of experimental data, however. Figs. 6, 7, and 8 show plots of some of the data

taken on the cruise of the 'Aldebaran' to the Antipodes*. The results obtained from the modified formula are plotted in the broken curves; the remaining curves are reproduced exactly as they appear in figs. 4 and 5 of the original article. The absolute scale of these curves does not seem to be available. The broken curves were obtained by multiplying the curve for the Austin formula plotted in fig. 4 of the original article by the ratio of the coefficient of the two formulae obtained from this paper (see, for instance, figs. 4 and 5).

It will be noted that the accord of our formula is distinctly better than that of the original. There is, of course, no

Fig. 8.



15,000 metre transmission (Lyons).

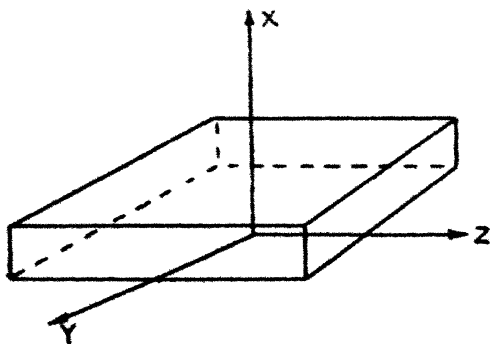
theoretical reason why the factor 0.0015 in the exponential term should not be subject to modification, and it seems indeed probable that the conductivity of the upper atmosphere is subject to daily and yearly variations. The results of this study indicate the desirability from a theoretical standpoint of seeking modifications in this constant and as indicated in the coefficient rather than in the power to which the wave-length appears in the exponent of the exponential, at least when long-distance long-wave transmission is under investigation.

* "Explorations Hertiennes entre Toulon et Tahiti," *Guierre Comptes Rendu de la Société Française des Electriciens*, pp. 247-268 (1920).

XXVIII. *Steady Flow of Heat in a Rectangular Parallelepiped.* By E. W. CHIVERS, B.Sc., East London College*.

WHILE considering a new method for determining Thermal Conductivities of Rocks, the necessity arose for the solution of the problem of the flow of heat in a rectangular prism heated at the top surface, and cooled to a fixed temperature at the lower surface, the other faces radiating heat to the surrounding air kept at the same fixed temperature. In Fourier's 'Theory of Heat' † the problem is treated in a simplified form, the prism considered being infinite in length. Carslaw deals with the problem in its

Fig. 1.



most general form, but arrives at a solution, which, as he says, does not lend itself to numerical calculation, and is not suitable for the evaluation of the thermal constants ‡.

Accepting Carslaw's proof that the temperature may be expressed as a Fourier series, the problem of finding the coefficients of the terms of the series may be conveniently solved by the following method suggested by Prof. Lees.

Consider a prism bounded by the planes

$$\begin{cases} x=0; & x=b, \\ y=-a; & y=+a, \\ z=-a; & z=+a. \end{cases}$$

* Communicated by Prof. C. H. Lees.

† Fourier, 'Theory of Heat' (Freeman's translation), p. 311.

‡ Carslaw, 'Fourier Series and Integrals,' p. 307.

Suppose the surface $x=b$ is kept hot at a constant temperature V .

Suppose the surface $x=0$ is kept cold at zero temperature.

Then if v is the temperature at any point (x, y, z) within the prism,

$$\frac{\partial^2 v}{\partial x^2} + \frac{\partial^2 v}{\partial y^2} + \frac{\partial^2 v}{\partial z^2} = 0. \quad (1)$$

Boundary conditions are :

$$\begin{cases} x=0; & v=0. & (a) \\ x=b; & v=V & (b) \\ y=\pm a; & -K \frac{\partial v}{\partial y} = hv & (c) \\ z=\pm a; & -K \frac{\partial v}{\partial z} = hv & (d) \end{cases}$$

where K = thermal conductivity of substance,
and h = emissivity of substance.

Assume a solution of equation (1) of the form

$$v = ae^{-m(x-b)} \cos ny \cos pz.$$

Differentiating and substituting in (1),

$$m^2 = n^2 + p^2$$

$$m = \pm \sqrt{n^2 + p^2}.$$

Applying boundary conditions (c) and (d) we have

$$-n \sin ny + \frac{h}{K} \cos ny = 0 \text{ when } y = -a \text{ or } +a,$$

$$-p \sin pz + \frac{h}{K} \cos pz = 0 \text{ when } z = -a \text{ or } +a,$$

$$\text{i. e.,} \quad \frac{ha}{K} = na \tan na \text{ and } \frac{ha}{K} = pa \tan na. \quad (2)$$

If now we put $\epsilon = na$ or pa , ϵ is given by the equation

$$\frac{ha}{K} = \epsilon \tan \epsilon.$$

This equation admits of an infinite number of solutions. Denoting these by $\epsilon_1, \epsilon_2, \epsilon_3$, etc., we have values of n and p satisfying (2) infinite in number and given by

$$\frac{\epsilon_1}{a}, \frac{\epsilon_2}{a}, \frac{\epsilon_3}{a}, \dots, \text{etc.}$$

Denote these by n_1, n_2, n_3 , etc.

Hence the general value of v is given by :

$$v = \sum_{n_2} \left(\sum_{n_1} a_1 e^{\pm \sqrt{n_1^2 + n_2^2} \cdot (x-b)} \cdot \cos n_1 y \right) \cos n_2 z.$$

In this particular case we have at $x=0, v=0$, hence

$$v = \sum_{n_2} \left(\sum_{n_1} a_1 \cdot \frac{\sinh \sqrt{n_1^2 + n_2^2} \cdot x}{\sinh \sqrt{n_1^2 + n_2^2} \cdot b} \cdot \cos n_1 y \right) \cos n_2 z,$$

or

$$\begin{aligned} v = & a_{11} \frac{\sinh \sqrt{n_1^2 + n_1^2} \cdot x}{\sinh \sqrt{n_1^2 + n_1^2} \cdot b} \cdot \cos n_1 y \cos n_1 z \\ & + a_{12} \frac{\sinh \sqrt{n_1^2 + n_2^2} \cdot x}{\sinh \sqrt{n_1^2 + n_2^2} \cdot b} \cdot \cos n_1 y \cos n_2 z \\ & + a_{21} \frac{\sinh \sqrt{n_1^2 + n_2^2} \cdot x}{\sinh \sqrt{n_1^2 + n_2^2} \cdot b} \cdot \cos n_2 y \cos n_1 z \\ & + a_{22} \frac{\sinh \sqrt{n_2^2 + n_2^2} \cdot x}{\sinh \sqrt{n_2^2 + n_2^2} \cdot b} \cdot \cos n_2 y \cos n_2 z \\ & + \dots, \text{ etc.} \end{aligned}$$

By symmetry $a_{12} = a_{21}$.

At $x=b, v = \text{constant temperature } V$.

$$\begin{aligned} \therefore V = & a_{11} \cos n_1 y \cos n_1 z + a_{12} (\cos n_1 y \cos n_2 z + \cos n_2 y \cos n_1 z) \\ & + a_{22} \cos n_2 y \cos n_2 z + \dots \\ & \dots + a_{pp} \cos n_p \cdot y \cos n_p \cdot z + a_{pq} (\cos n_p y \cos n_q z \\ & + \cos n_q y \cos n_p z) + a_{qq} \cos n_q y \cos n_q z + \dots \end{aligned}$$

To determine the coefficients $a_{11}, a_{12}, a_{21}, \dots$ etc.

To find the general coefficient a_{pq} multiply both sides of equation by $\cos n_p \cdot y \cdot dy$, and integrate from $-a$ to $+a$.

On left-hand side we have :

$$V \int_{-a}^{+a} \cos n_p \cdot y \cdot dy.$$

On right-hand side we have a series of terms involving an integral of the form

$$\int_{-a}^{+a} \cos n y \cos p y \cdot dy,$$

together with two other terms, viz.,

$$a_{pp} \int_{-a}^{+a} \cos^2 n_p y \cdot dy \cos n_p z + a_{pq} \int_{-a}^{+a} \cos^2 n_p y \cdot dy \cos n_q z.$$

Now

$$\begin{aligned} \int_{-a}^{+a} \cos n y \cos v y \cdot dy &= \int_0^a \cos (n-v) y \cdot dy + \int_0^a \cos (n+v) y \cdot dy \\ &= \left[\frac{1}{n-v} \cdot \sin (n-v) y + \frac{1}{n+v} \sin (n+v) y \right]_0^a \\ &= \frac{1}{2} \left\{ \frac{(n+v) \sin (n-v) a + (n-v) \sin (n+v) a}{n^2 - v^2} \right\} \end{aligned}$$

But every value of n satisfies

$$n \tan na = \frac{ha}{K}.$$

$$n \tan na = v \tan va.$$

\therefore

$$\therefore n \sin na \cos va - v \sin va \cos na = 0.$$

Thus the foregoing integral, which reduces to

$$\frac{1}{n^2 - v^2} (n \sin na \cos va - v \sin va \cos na)$$

is zero except in the case when $n=v$.

$$\begin{aligned} \therefore V \int_{-a}^{+a} \cos n_p y \cdot dy &= a_{pp} \int_{-a}^{+a} \cos^2 n_p y \cdot dy \cos n_p z \\ &\quad + a_{pq} \int_{-a}^{+a} \cos^2 n_p y \cdot dy \cos n_q z. \end{aligned}$$

Multiply both sides by $\cos n_q z \cdot dz$, and integrate as before, then

$$\begin{aligned} V \int_{-a}^{+a} \cos n_p y \cdot dy \int_{-a}^{+a} \cos n_q z \cdot dz &= a_{pp} \int_{-a}^{+a} \cos^2 n_p y \cdot dy \\ &\quad + a_{pq} \int_{-a}^{+a} \cos^2 n_p y \cdot dy \int_{-a}^{+a} \cos n_p z \cos n_q z \cdot dz. \end{aligned}$$

Second integral zero on integration.

$$\begin{aligned} \therefore 4V \int_0^a \cos n_p y \cdot dy \int_0^a \cos n_q z \cdot dz \\ &= a_{pp} \int_0^a (1 + \cos 2n_p y) dy \int_0^a (1 + \cos 2n_q z) dz, \\ 4 \cdot V \cdot \frac{\sin n_p a}{n_p}, \frac{\sin n_q a}{n_q} &= a_{pp} \left(a + \frac{\sin 2n_p a}{2n_p} \right) \left(a + \frac{\sin 2n_q a}{2n_q} \right). \end{aligned}$$

$$\therefore a_{pq} = 4V \cdot \left(\frac{\frac{\sin n_p a}{n_p}}{1 + \frac{\sin 2n_p a}{2n_p}} \cdot \frac{\frac{\sin n_q a}{n_q}}{1 + \frac{\sin 2n_q a}{2n_q}} \right) = 4V \cdot N_p N_q.$$

Hence

$$\begin{cases} a_{11} = 4 \cdot V N_1^2, \\ a_{12} = 4 \cdot V \cdot N_1 N_2, \\ a_{22} = 4V \cdot N_2^2. \end{cases}$$

Substituting for constants in general expression for v :

$$\begin{aligned} v = 4 \cdot V \left\{ N_1^2 \frac{\sinh \sqrt{n_1^2 + n_1^2} \cdot x}{\sinh \sqrt{n_1^2 + n_1^2} \cdot b} \cos n_1 y \cos n_1 z \right. \\ + N_1 N_2 \left(\frac{\sinh \sqrt{n_1^2 + n_2^2} \cdot x}{\sinh \sqrt{n_1^2 + n_2^2} \cdot b} \cos n_1 y \cos n_2 z + \cos n_2 y \cos n_1 z \right) \\ \left. + N_2^2 \frac{\sinh \sqrt{n_2^2 + n_2^2} \cdot x}{\sinh \sqrt{n_2^2 + n_2^2} \cdot b} \cos n_2 y \cos n_2 z + \dots \text{etc.} \right\}. \end{aligned}$$

where $n_1, n_2 \dots \text{etc.}$, are the roots of the equation

$$n \tan na = \frac{h}{K}.$$

The solution of this equation is most simply performed by obtaining an approximate solution by means of a graph and then solving more accurately by "trial and error."

E. g. Suppose specimen is of granite :

$$a = 2.5 \text{ cm.} \quad b = 2.5 \text{ cm.}$$

$$h = 0.0003. \quad K = 0.006.$$

$$na \tan na = 0.125.$$

Solving and substituting we have :

$$\begin{aligned} v = V \left\{ 1.0404 \frac{\sinh \sqrt{n_1^2 + n_1^2} \cdot x}{\sinh \sqrt{n_1^2 + n_1^2} \cdot b} \cos n_1 y \cos n_1 z \right. \\ - 0.02487 \frac{\sinh \sqrt{n_1^2 + n_2^2} \cdot x}{\sinh \sqrt{n_1^2 + n_2^2} \cdot b} (\cos n_1 y \cos n_2 z + \cos n_2 y \cos n_1 z) \\ \left. + 0.000595 \frac{\sinh \sqrt{n_2^2 + n_2^2} \cdot x}{\sinh \sqrt{n_2^2 + n_2^2} \cdot b} \cos n_2 y \cos n_2 z + \dots \text{etc.} \right\}, \end{aligned}$$

the coefficients all being expanded numerically.

XXIX. *Anti-Stokes Radiation of Fluorescent Liquids.**By R. W. Wood*.*

[Plate V.]

EXCEPTIONS to Stokes's law in the case of the fluorescing vapours of sodium, iodine, and other elements are the rule, as has been shown in numerous previous papers.

In the case of solutions of organic dyes it is less easy to show the phenomenon; in fact its existence was a matter of dispute for nearly a quarter of a century. The very careful photometric work of Nichols and Merritt established its existence, but the observations appear to have been extremely difficult, and so far as I know no photographs have ever been published showing the presence of anti-Stokes radiations in the case of solutions.

In preparing an article on fluorescence for the new edition of the *Encyclopædia Britannica* it appeared to be of interest to secure photographs establishing the reality of the phenomenon, and I was surprised at the ease with which results were secured.

A very dilute solution of fluorescein (alkali-salt), rendered slightly turbid with a precipitate of silver chloride, was illuminated in a square bottle with the beam of light issuing from the slit of a two-prism monochromator. The function of the silver chloride was to scatter a small portion of the monochromatic light so that the narrow spectrum band of the illuminating beam would appear superposed on the fluorescent spectrum. The slit of the prism spectrograph faced the fluorescent track from the side.

With blue light excitation the fluorescence was very bright and an exposure of half a minute was sufficient. A sodium flame was then placed behind the bottle for a few seconds for the purpose of securing a reference mark on the spectrogram. The result of this exposure is reproduced on Pl. V. fig. *a*, the exciting monochromatic band scattered by the silver chloride is at the left, while the D lines are at the right, the green fluorescent spectrum lying between the two. In figs. *b* and *c* the exciting band has moved up into the region of fluorescence, and the spectrum is seen well developed on the short wave-length side. The intensity of the fluorescence was much less in this case, exposures of four and five minutes being necessary. In fig. *d* the wave-length

* Communicated by the Author.

of the exciting band has increased to such a degree that fluorescence no longer manifests itself. Keeping in mind the principles of the quantum theory, the question presents itself as to where the energy comes from that makes the anti-Stokes radiation possible.

In the case of sodium and iodine vapours there is no difficulty. The absorbing molecule may be in states of vibration and rotation higher than the zero states, and after excitation may revert to the zero state. In this case the excess energy necessary for the anti-Stokes term or terms was stored in the molecule before it absorbed the monochromatic exciting radiation.

Or when in the excited state, say the 27th vibrational level, it may, by collision with another molecule, either of the same or a different gas, be carried to a higher vibrational and rotational level, and thus, on its reversion to the lower initial state, release more energy than it absorbed.

Both of the above processes will be facilitated by high temperature, for in the case of the first process there is a greater chance of a molecule being initially in a state higher than zero, and in the second case the energy which can be delivered by the colliding molecule will be greater. High temperatures favour the development of anti-Stokes lines in the case of iodine vapour excited to fluorescence by the green mercury line, as was shown by Pringsheim.

We might therefore expect that heating a fluorescent solution would favour the production of anti-Stokes radiation.

To test this point the monochromator was set to deliver radiation as in the case of fig. *b* (Pl. V.), i. e., to excite with a wave-length inside of the fluorescence band. A test-tube was filled with fluorescein solution at 0°, and the upper part heated to boiling with a bunsen flame. On holding the test-tube in front of the slit of the monochromator, and moving it up and down, the upper portion (at 100°) was seen to fluoresce with much greater intensity than the lower (at 0°). This was not the case with excitation by blue light. In general the effect of high temperature is to *decrease* the fluorescence of organic dyes. Some samples of rhodamine are non-fluorescent at 100° while shining brightly at room temperature.

There is another factor, however, which must be considered in this connexion. The absorption band advances towards the region of longer wave-lengths as the temperature is increased. This is a very general effect, and very obvious in the case of some coloured glasses. In the case of fluorescein the upper part of the solution (at 100°) is, by transmitted

light, of a slightly different tint from the lower (at 0°), the change of tint being from pale yellow to pale orange-yellow.

Interpreting this in the language employed in the case of iodine vapour, we might say that at the higher temperature the molecules were in a partially excited state, and that consequently less energy (as supplied by a radiation of longer wave-length) would be necessary to carry them to a definite upper level. Our knowledge regarding the absorbing mechanism in the case of these complicated molecules is too scant at the present time to warrant much speculation.

XXX. *The Measuring of Lags in Discharge.* By WILLIAM CLARKSON, Ph.D., M.Sc., *International Education Board Fellow, Physical Institute of the University of Utrecht* *.

1. *Introductory.*

WORK on lags in the occurrence of discharges through gases involves the determination of the dependence of the lag on various factors, of which, for example, voltage is one. Since fully to determine the relations sought numerous and comparable measurements must be made, quick and simple methods must be possible. They should also be utilizable at high voltages and be non-selective, recording all lags impartially. The present account describes two such methods used by the writer which fulfil the required conditions admirably.

2. "*Lags.*"

As a rule condenser, or "dynamic," discharges are studied, and indeed they present the most general case for this purpose. The sequence of events in the initiation of all dynamic discharges is the "striking" of the discharge (at some point on or beyond the threshold current characteristic), the subsequent "building-up" of the current with a traversal of the build-up region of the characteristic, till another point on the characteristic is reached and "extinction" occurs. Single condenser discharges exhibit these phenomena in the simplest form, and their study provides all the material essential for the elucidation of the problems involved.

* Communicated by Professor Ornstein.

Two types of lag must be distinguished, an interval between the application of the potential and the initiation of build-up, *i. e.*, a lag in "striking," and an interval between the discharge striking and the maximum current being attained—*i. e.*, a lag in "build-up." A lag in build-up is always present.

Since the voltage is a highly significant factor in lag variations it is necessary for their exact study that they be measured under definite or comparable voltage-time conditions. Normally the voltage throughout a lag in striking will be constant; its variation during the build-up period demands investigation.

It has been shown that during build-up of a condensed discharge the current increases continuously with time, very slowly at first, but subsequently at an ever-increasing rate, *i. e.*, in a somewhat exponential manner, until extinction takes place. In discharge-tubes the current, even after as much as 90–95 per cent. of build-up has transpired, is only some $10\mu\text{A}$. This means that for all but small condensers the voltage-fall in this period is almost negligible unless for very great lags, and that we commit but small (say at the most a 5 per cent.) error when we assume that the potential is constant, at its initial value, throughout build-up, and that then its fall to the extinction value is instantaneous.

3. Principles of Methods.

Two methods utilizing the foregoing properties of discharges have been developed. In each the quantity diverted by a system in parallel with the discharge-tube during the interval between the application of the condenser and the end of build-up being reached is measured.

With the applied potential being assumed constant (at V_m), this quantity is determined by:—

(A) The charging-up of a capacity K through a high resistance R , the increase in its voltage from V_0 , the initial value, to V_m , the final value, being found. The time extinction t is given by

$$t = KR \log_e \frac{V_m - V_0}{V_m - V_K}; \quad \dots \dots (1)$$

(B) The throw of a ballistic galvanometer (throw ϕ) of known constant K , the deflexion θ for the steady current produced by V_m being found. In this case

$$t = K \frac{\phi}{\theta}. \quad \dots \dots (2)$$

Both arrangements satisfy the following essential conditions: the quantity diverted from the discharge system is so small that the conditions of discharge are unmodified; this can be checked by the fact that on no-discharge V_K attains the value of V_M , and that they can be made insensitive to all voltages less than the extinction voltage in value, otherwise the "clear-up" lag and the remaining charge in the condenser would add to the throw of the galvanometer, or increase the value of V_K .

4. Electrostatic-Voltmeter Method. (Fig. 1.)

Method.—The diagram is practically self-explanatory. A condenser C is connected to a source of steady voltage,

Fig. 1.

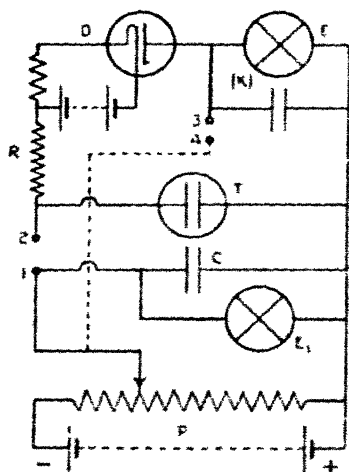
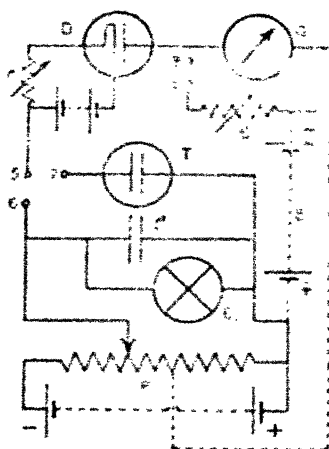


Fig. 2.



here diagrammatically a potentiometer P , and a voltage measuring device, here given as the voltmeter E_1 . It can be discharged through the discharge-tube T by closing the key 2, 1.

An electrostatic voltmeter E , shunted with a small condenser, forming a system of capacity K , is connected in parallel with the tube through a diode D , as valve, and a high resistance R .

E_1 is initially at V_0 , C at V_M . On closing 2, 1, C remains at V_M up to the end of build-up E , meanwhile charging up to V_K . The voltage of C then falls to its final value; E remains at V_K .

Precautions.—The following conditions must be observed :—

a. V_K must be higher than the extinction value. This can be obtained by choosing V_0 of suitable value. (To vary V_0 close 3, 4, adjust P.)

b. The diode resistance must be small compared with R and should be constant, that is, the filament current should be large and constant. In the writer's experience the correction for the valve resistance and characteristic could be neglected.

c. With R large and K small the quantities of electricity diverted from the discharge are negligible and the diode resistance relatively insignificant. The value of R should be the maximum consistent with K being great enough to be unaffected by the change of capacity of E on deflexion, and with V_K having a value such that the relation $V_K - V_0/V_K - V_K$ (see 1) is determined with sufficient accuracy. The writer has used circuits with $R=10-50$ megohms and $K=0.001 \mu F$. For resistances even pencilled ebonite may be used; some of the better grade "grid leaks," however, prove to be the most reliable.

d. The leakage of the system should be small. This is antagonistic to c. If it is constant, however, the rate of leak at V_K may be found and the correction applied for the interval between the discharge taking place and the reading of V_K , i.e., for a period of the order of 5-10 secs.

5. String-Electrometer Method.

The foregoing arrangement has been found to possess two sources of error in practice—the resistance of the voltmeter contacts, an incurable fault in most cases, and the "soaking-in" effects of the condenser at K . Substituting a string-electrometer for the electrostatic voltmeter avoids these errors.

The string is coupled with the diode side and the plates connected through suitable batteries to the other arm of the circuit. The string can be made quite taut, as but little sensitivity is needed, and thus the system, though relatively sensitive, is practically dead-beat. The capacity and the leakage of the electrometer being quite negligible, K is the capacity of the condenser in parallel, i.e., is constant, and as this may be a small air condenser, leakage effects may be eliminated and the soaking-in effects are quite avoided. Further, the value of R may be increased to almost any extent.

It was found that the new difficulties introduced were (a) determining the values of RC , and (b) measuring V_0 and V_K . For RC it was found easiest to calibrate the system directly with a contact of known duration; for (b) the electrometer was coupled through 3, 4 to the voltage supply, as shown. V_0 could be kept constant at a known value or determined afresh from E_1 , and a few readings of V_K from E_1 , while giving their values, also served to calibrate the instrument in this region. One advantage was that all voltages were read on the same instrument.

6. Ballistic Galvanometer Method. (Fig. 2.)

Method.— G is a ballistic galvanometer which can be shunted by a variable resistance S . One side is connected to the discharge-tube through a diode with variable filament current. In order to make the system insensitive to voltages less than the extinction value, the other terminal of the galvanometer was maintained at a higher potential than this by making its connexion through a battery B , as shown. Alternatively it may be connected permanently to a suitable point on the potentiometer.

With S out of the circuit (*i.e.* 8, 9 open) and the tube in (*i.e.* 5, 7 closed), a discharge is sent through T by momentarily closing 6, 5 and r adjusted until the diode conductivity is such that the throw ϕ of the galvanometer is of suitable value, *i.e.*, some few cms.; the smallest throw consistent with accuracy is best. The diode is now permitted to attain a constant state before final readings are made.

The tube T is now cut out of the circuit (5, 7 opened) and the shunt S included (8, 9 closed). S is now adjusted until the galvanometer deflexion on closing 6, 5 (*i.e.* for a voltage V_K) is of suitable proportions.

Knowing the values of the resistances of S and G , the values of the "throw" ϕ , and the deflexion θ , and the constant of the galvanometer system K , the duration of the discharge t may be found, as previously shown.

Precautions.—*a.* The more sensitive the galvanometer the less the charges diverted; the lower the resistance, however, the better. Extremes are unnecessary.

b. The diode must be well insulated so that the back-voltage due to B produces no deflexion of the galvanometer.

c. It is easiest to determine the constant of the galvanometer directly by giving contacts of known duration. This gives the constant for working conditions.

d. Measurements of ϕ and θ must only be made with the diode in a quite constant state. This necessitates waiting some minutes after varying r . On the other hand, once the diode is constant a range of throws of from 2 or 3 to 50 cm. is possible, i. e., a corresponding range of lag-values covered for the one filament current.

e. The method had one fault not contained in the preceding ones; on no-discharge or only a corona-discharge taking place the whole charge of C is thrown through the galvanometer. The effect has been found not to be serious; normally the probability of this occurring is absent in most cases. It is obviated in any case by making the contact at 6, 5 the minimum possible.

7. Conclusion.

Both the given methods fulfil the conditions for the study of lag phenomena. They are quick and reliable and normally give results under constant voltage conditions. They are accurate to the limit the dynamic characteristic allows, and if necessary may be corrected for the (say 5 per cent.) error this implies. Corrections, however, are superfluous; for one thing the readings are relatively correct, and in any case the lag under "constant" conditions shows greater variations.

Though for many purposes direct methods based on commutators, &c., or on the peak-voltage variations, are quite suitable, they determine only the extreme values of the lag and are not easily applicable to single discharges. The above methods record all lag variations impartially.

Further, by changing the minimum voltage to which the systems are sensitive the whole dynamic characteristic has been studied, the "clear-up" lag as well as the "build-up" lag. This is an interesting field.

The ballistic galvanometer method is suited to work at high voltages, the limit being fixed merely by the strength of the diode.

It is possible to combine both methods and to measure the quantity diverted into a condenser by the galvanometer throw. This method, however, is more complicated and has no obvious advantages.

The writer has great pleasure in recording his obligation to Professor Ornstein, and also to the International Education Board.

XXXI. *A Method of Determining the Absolute Zero of Temperature.* By J. R. COTTER, M.A.*

THE determination of the absolute zero is, from the theoretical point of view, not an experiment in thermometry, but in accurate calorimetry. This is pointed out in Lord Kelvin's article "Heat," in the ninth edition of the *Encyclopædia Britannica*. In that article Kelvin suggests that the thermodynamic scale might be realized by means of what he calls a steam thermometer, that is, a vapour-pressure thermometer containing a mixture of water and steam. Using Clapeyron's equation for the calculation, he required to know the pressure of saturated steam at various temperatures, and the latent heat, as well as the density, of steam, and the ratio of the densities of steam and water. He believed that Regnault's values for the vapour-pressure and latent heat would be sufficiently accurate, but had no data for the density of steam. He was unable to form an opinion whether this method would be more accurate than the use of the hydrogen or nitrogen thermometer, but he expresses confidence that the steam thermometer, once standardized, would be much more accurate and more easily reproducible than any other thermometer whatever.

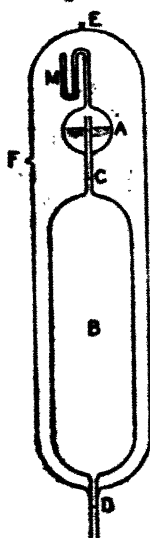
By a modification of Kelvin's method and the use of electrical calorimetry, the position of the absolute zero could, I believe, be found with a great degree of precision. In fig. 1, A is a small bulb which is connected to the much larger bulb B, and also to a small manometer M. The lower exit of B is connected to a tall mercury barometer capable of measuring a pressure of two or three atmospheres. A, B, and M are surrounded by a glass vessel, which can be exhausted. The whole apparatus is supposed to be enclosed in an accurate thermostat.

Now suppose that B is filled with mercury up to the mark C on the stem, and that A contains nothing but a liquid and its vapour, and that M contains the same liquid and its vapour in the closed limb. Water might be used, but probably a more volatile liquid such as benzene would be better. A naked heating-coil (not shown in the figure) is immersed in the liquid benzene in A. When all is at the temperature of the thermostat the benzene in the two limbs of M are at the same height. The vapour-pressure is then read off on the mercury barometer.

* Communicated by the Author.

To carry out an experiment the mercury is run out of B at a constant rate, the current in the heating-coil in A being simultaneously started. If the current-strength is properly adjusted to the flow of mercury the whole of the heat supplied by the coil will be employed in causing the mixture of benzene and its vapour to go through an isothermal expansion. Any lack of adjustment between the heat-supply and the change of volume will be at once revealed by the differential manometer M. When the mercury reaches the mark D the current is switched off and the outflow stopped simultaneously.

Fig. 1.



If v_1 is the volume of M and A down to the mark C, v_2 the volume of M, A, and B down to the mark D, Q the energy communicated in ergs, and T the (unknown) absolute temperature, then, exactly as in Clapeyron's equation,

$$\frac{dT}{T} = \frac{(v_2 - v_1)dp}{Q},$$

so that if a series of experiments is carried out at temperatures ranging from the freezing-point (T_0) to the boiling-point (T_{100}), we can find Q as a function of p and integrate equation (1), getting

$$\log \frac{T_{100}}{T_0} = (v_2 - v_1) \int \frac{dp}{Q}.$$

The advantages of this method are that only one volume, that of the bulb B from C to D, has to be measured; that the calorimetric conditions are ideal, since there is no radiation correction and no correction for the thermal capacity of the containing vessel; and that the heat-energy is directly obtained in ergs, so that Joule's equivalent is not required, as it would be in the method suggested by Kelvin. The only correction, beside the electrical ones, is that for the expansion of the globe B due to pressure and rise of temperature, and the usual barometer corrections.

In order to bring the mercury back from D to C it would be convenient to have a heating-coil wound round B. On warming B, and admitting air to the exhausted space, causing a cool current of air to pass in at E and out at F, the vapour in B would be dried, and the mercury could be slowly raised to C.

With this instrument the whole thermodynamic scale down to the lowest temperatures could be reconstructed by using a succession of suitable liquids. Some modification would be necessary below the freezing-point of mercury.

At present, the exact position of the absolute zero seems to be uncertain to about $0^{\circ}1$. Kamerlingh Onnes obtained the value $-273^{\circ}09$, while Henning and Heuse give $-273^{\circ}2$. Other calculations lie between these values.

XXXII. *Hamilton-Jacobi's Differential Equation in Dynamics.* By G. S. MAHAJANI*.

1. **I**N his note, published in the January number of this Magazine, Kunz claims to have derived the Hamilton-Jacobi equation directly from Euler's differential equation of the calculus of variation. This note is somewhat misleading, for, instead of deriving the Hamilton-Jacobi equation, what is really done is simply to verify that a particular function is a solution of it.

2. That the equations of a dynamical system are included in the single principle of least action is well enough known. In fact, as has been sometimes said, the test of any system being "dynamical" is the existence of some function which remains stationary. And because "the Lorentz" field-equations can

* Communicated by E. Cunningham, M.A.

be derived from the least-action principle, some claim that "electron theory" is nothing but the dynamics of the electron. Hence, every dynamical equation—in particular, therefore, the Hamilton-Jacobi's equation—must be capable of being derived from the differential equation of calculus of variations.

3. The logical order of steps in this process is as follows :—

$$\delta \int_{t_0}^t L(q, \dot{q}, t) dt = 0 ; \quad . \quad . \quad . \quad (I.)$$

from this we come to

$$\frac{d}{dt} \left(\frac{\partial L}{\partial \dot{q}_r} \right) - \frac{\partial L}{\partial q_r} = 0 ; \quad . \quad . \quad . \quad (II.)$$

$r = (1, 2, 3 \dots n)$

and from this to

$$\left. \begin{aligned} \dot{q} &= \frac{\partial H}{\partial p_r}, \\ -\dot{p} &= \frac{\partial H}{\partial q_r}, \end{aligned} \right\} . \quad . \quad . \quad . \quad (III.)$$

whence

$$\frac{\partial S}{\partial t} + H\left(q, \frac{\partial S}{\partial q}, t\right) = 0. \quad . \quad . \quad . \quad (IV.)$$

Now all these four systems are completely equivalent to each other, and the significance of the last is this :—

If we can find *any* solution for *S* of that equation, with the necessary number of constants, say

$$S = f(q_r, \alpha_r, t),$$

then the solution of the problem is

$$\left. \begin{aligned} p_r &= \frac{\partial f}{\partial q_r} \\ -\beta_r &= \frac{\partial f}{\partial \alpha_r} \end{aligned} \right\}$$

where " β 's" are also constants.

It must be remembered the integration constants (α), and the other constants (β), do not in general bear a simple interpretation. But there is one particular solution of the equation in which the constants appear significant. That

particular function is what is known as the Principal Function of Hamilton, viz. :

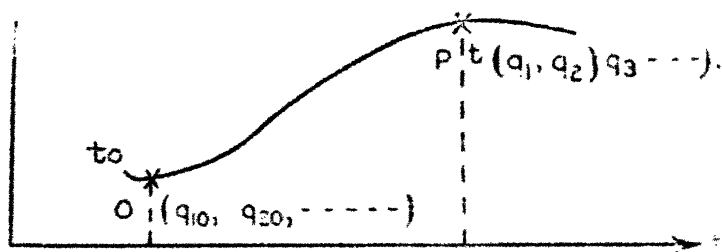
$$S = \int_{t_0}^{t_1} L dt.$$

What Kunz has done is simply to show that this function satisfies the Hamilton equation. But that certainly does not establish that *any* solution of the equation solves the dynamical problem—which, in fact, is the main point about that equation.

4. Whittaker has shown in his book on Dynamics that “all the differential equations which arise from problems in the calculus of variations with one independent variable can be expressed in the Hamilton form” (Article 110). We can, therefore, dispense with the Lagrangian Equation and get the Hamiltonian system directly from the Euler equation of Calculus of Variations. And then we establish the complete equivalence of (III.) and (IV.) above.

5. I shall conclude by proving that the Principal Function of Hamilton, $\int_{t_0}^{t_1} L dt$, satisfies (IV.) in a way which clearly brings out the significance of the constants.

Consider the trajectory in the n -dimensional space :—



Let the system be projected from O with velocity

$$(\dot{q}_{10}, \dot{q}_{20}, \dots, \dot{q}_{n0}).$$

Then $\int_{t_0}^{t_1} L dt$ is a definite function of the $2n$ initial constants (q_{r0}, \dot{q}_{r0}) and t . Alternatively, we can express it in terms of

$$(q_{r0}, q_r, t),$$

and in this form we denote it by

$$S(q_{r0}, q_r, t) = \int_{t_0}^{t_1} L dt.$$

Consider, now, an adjacent *varied* path having one-to-one corresponding but *contemporaneous* positions of points. Then

$$\begin{aligned}\delta S &= \int_{t_0}^t \delta L dt \\ &= \int_{t_0}^t \left(\frac{\partial L}{\partial q_r} \delta q + \frac{\partial L}{\partial \dot{q}_r} \delta \dot{q}_r \right) dt,\end{aligned}$$

which reduces to

$$\left[\delta q_r \frac{\partial L}{\partial \dot{q}_r} \right]_{t_0}^t,$$

since

$$\begin{aligned}\frac{d}{dt} \left(\frac{\partial L}{\partial \dot{q}_r} \right) - \frac{\partial L}{\partial q_r} &\equiv 0 \\ \delta S &= \sum p_r \delta q_r - \sum p_{r0} \delta q_{r0}, \\ \begin{cases} \frac{\partial S}{\partial q_r} = p_r, \\ \frac{\partial S}{\partial q_{r0}} = -p_{r0}. \end{cases}\end{aligned}$$

But, now, if we suppose t also to vary, we get

$$\begin{aligned}\frac{dS}{dt} &= \frac{\partial S}{\partial t} + \sum \frac{\partial S}{\partial q_r} \dot{q}_r, \\ i. e., \quad L &= \frac{\partial S}{\partial t} + \sum \frac{\partial S}{\partial q_r} \dot{q}_r \\ &= \frac{\partial S}{\partial t} + \sum p_r \dot{q}_r.\end{aligned}$$

$$\therefore \frac{\partial S}{\partial t} + (\sum p_r \dot{q}_r - L) = 0,$$

$$i. e., \quad \frac{\partial S}{\partial t} + H = 0.$$

Thus we see that $\int_{t_0}^t L dt$ is a solution of the Hamilton-Jacobi equation, and that the constants (q_{r0}) define the initial position of the system, and (p_{r0}) give the initial momenta.

XXXIII. *The Application of a Valve Amplifier to the Measurement of X-ray and Photo-Electric Effects.* By C. E. WYNN-WILLIAMS, M.Sc.*

IN a previous paper† a valve amplifier for ionization currents was described which could conveniently be used to replace an electrometer for the measurement of ionization currents of the order of 10^{-12} ampere. Such an instrument, it was shown, possessed certain advantages over other methods of measurement. Its usefulness, however, was limited in that it could not always be operated if an induction coil or similar impulsive high-potential apparatus was at work in its neighbourhood. For this reason, its use for the measurement of the ionization currents produced by X-rays was ruled out.

Subsequent investigations, however, have shown that, under certain conditions, and provided that suitable precautions are taken as to screening the apparatus, the difficulties in the way of using it for X-ray measurements can be overcome, and that, in addition, when employed in conjunction with a photo-electric cell, it can be used for photometric work. The object of the present paper is to explain how this can be done, for the guidance of any who desire to employ the amplifier either in connexion with X-ray measurements or photometric work.

In addition, the modifications of the amplifier described in the present paper may be found helpful in applications of the amplifier other than for X-ray measurements and photo-electric work.

For a full discussion of the theory of the amplifier the original paper‡ should be consulted. Here, a general account will suffice. Referring to fig. 1, C and D are two three-electrode valves whose anodes are connected, through resistances R_1 and R_2 , to H, the positive pole of the high-tension battery, the negative end of the latter being connected to A, the negative end of the valve filaments. A galvanometer G is connected across the two anodes. Considering only the plate currents i_1 and i_2 , and regarding the system as a Wheatstone bridge, balance will be obtained when $R_1/R_2 = X_1/X_2$, where X_1 and X_2 are the impedances of

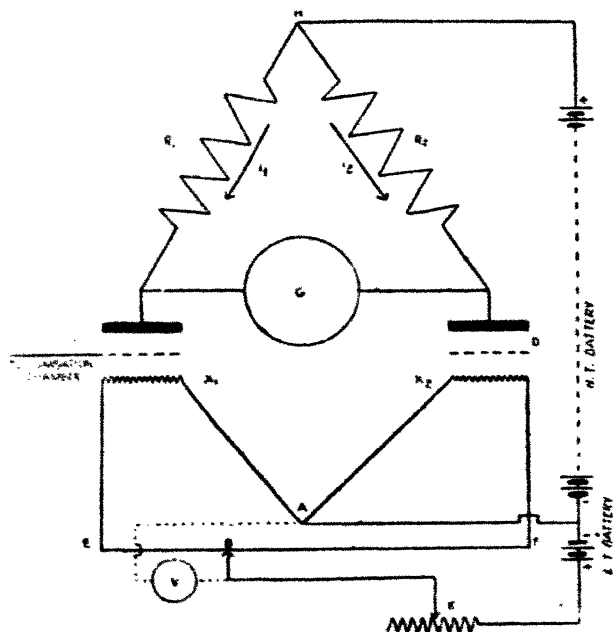
* Communicated by Prof. E. A. Owen, M.A., D.Sc.

† C. E. Wynn-Williams, *Proc. Camb. Phil. Soc.* xxiii. p. 811 (1927).

‡ *Loc. cit.*

the valves. The effect of driving an ionization current on to one of the grids—the other being left free, or “floating”—is to raise its potential, positively or negatively, and so alter the value of X_1 (or of X_2). This results in the bridge becoming unbalanced, and it can be shown that, provided the amplifier is operated with suitable values of high-tension and low-tension voltage, a small change E in the potential of

Fig. 1.



one of the grids will give rise to a galvanometer current of

$$E \times \frac{\mu}{2X + G \left(1 + \frac{X}{R}\right)}.$$

As the electrostatic capacity of, and leakage current from, the grid of a valve is usually very small, a small ionization current can raise the grid potential by an appreciable amount, and a current amplification factor—representing the ratio of the galvanometer current to the ionization current driven on to the grid—of the order of 10^5 can be obtained. The

amplifier may therefore be used to replace an electrometer, or extremely sensitive galvanometer, for certain types of work. To convey some idea of the sensitivity, while the characteristics of different valves of the same type vary considerably, in a particular case, using a reflecting galvanometer of sensitivity 200 mm./microamp., the system could be regarded as a quadrant electrometer of sensitivity about 6000 mm./volt and shunted by a leak of about 360 megohms. In this case the smallest current that could be measured (governed by the steadiness of the zero) was between 10^{-12} and 10^{-13} ampere. The scale was not strictly linear, but, if desired, could be calibrated without difficulty. For small positive ionization currents, however, the error introduced by assuming a linear scale could be ignored. A great advantage lay in the portability of the instrument, and also in the fact that high insulation of the ionization chamber was not necessary.

Compensation.—Unless two valves, identical in all respects, were used, such a bridge would be useless for the measurement of very small currents, owing to the fluctuations in potential of the batteries producing continuous and slightly different changes in the two plate currents and giving rise to a very unsteady zero. As the probability of obtaining a pair of valves—even of the same make and type—which are identical in every respect (*i.e.* as regards their various characteristic curves) to the degree required in the apparatus is extremely small, an artificial method of “matching” two ordinary valves has to be resorted to before a steady zero can be assured. Such a method was attained in the amplifier described in the original paper.

This can be accomplished very simply by the adjustment of the two series filament resistances FB and EB (fig. 1), which are actually the two portions of the slide wire EF. The theory, and the practical method of “compensating” the amplifier (or of rendering it immune from battery voltage fluctuations), are described in the original paper*. Here it is sufficient to say that, for any given filament voltage, there will usually be found one or more positions of the slider B on the wire at which a small change in the battery voltage produces no change in the galvanometer deflexion, and that it is a simple matter of trial and error to find a suitable combination of the position of the slider B and the filament voltage, the latter being adjusted by means of the rheostat K and the voltmeter V.

* *Loc. cit.*

Electromagnetic Disturbances.

Such a combination of amplifier and galvanometer can advantageously be substituted for an electrometer in certain types of work. In particular, it is very useful for radio-activity work. If, however, an induction coil be operated near it, or high-frequency surges are prevalent in the laboratory, the zero is rendered very unsteady by disturbances from these.

Each surge, or spark from an induction coil, radiates an electromagnetic wave, which induces an alternating potential on the insulated leads to either of the grids, resulting in the latter becoming charged alternatively positively and negatively. During the positive half-cycle, on account of the electron stream to the grid, the leakage current is greater than during the negative. Hence the grid acquires a mean negative charge during the "reception" of the disturbance, which leaks away after the wave-train has passed, behaving in this way like the "cumulative grid" rectifier used in radio-telegraphy or telephony.

In the original apparatus the valves and grid leads were enclosed in an earthed screening-box, which proved sufficient to protect the grid from hand-capacity effects. When, however, an induction coil was operated near the amplifier, the zero, in spite of the screen, was unsteady. In this case, as portions of the apparatus (*i. e.* batteries, resistances, etc.) were *outside* the box, the insulated leads entering the latter served to convey the potential surges through the electrostatic screen. Before the amplifier can therefore be used in a laboratory where high-frequency surges are prevalent, further attention must be paid to the screening.

Greater care is needed in screening a valve bridge than is the case when working with an ordinary electrometer, because of the rectifying action of the grid current. While, in the case of an electrometer, the high-frequency alternating surges *may* find their way to one pair of quadrants, despite the fact that most of the apparatus is enclosed in an earthed case, the mean value of the alternating potential will be zero, and will not cause any movement of the needle (unless, of course, the electrometer is being used idiostatically). On the other hand, in the case of high-frequency surges finding their way to the grid of a valve, the rectifying action of the grid current results in the mean value of the grid potential rising negatively and causing a change in the galvanometer current. Investigations were therefore made to ascertain whether, by careful screening, and ensuring that no wires

328 Mr. Wynn-Williams : *Application of a Valve Amplifier*
or leads remained outside the case, high-frequency surges from induction coils and transformers etc. could be sufficiently eliminated from the apparatus to render the zero steady enough for the measurement of X-ray ionization currents.

Arrangement of Apparatus.

In the original apparatus the anode resistances R_1 and R_2 consisted of plug-in resistance boxes of about 10,000 ohms. As it was necessary to enclose the anode resistances in the screening case, some form of variable resistance, controllable from outside the case, was desirable. An arrangement of this kind would also be more convenient from the point of view of rapid balancing, even were such screening unnecessary and the resistances left in the open.

As the change in resistance necessary to effect balance is small compared with the values of R_1 and R_2 , only portions of the latter need be variable and controllable from outside the case. The remaining portions can consist of fixed resistances.

In the arrangement adopted, the anode resistances consisted of three parts:—(1) Two fixed non-inductive wire resistances of 10,000 ohms * each, tapped at 2500, 5000, and 7500 ohms, the 7500 tapping being used. (2) A series of fixed resistance coils, of about 200 ohms each, attached to contact studs—connexion being made to the latter by wiper arms—serving to obtain an approximate balance. (3) A continuously variable 400 ohm resistance, of the type supplied for use as potentiometers in wireless receivers, which enabled a fine balance to be obtained. (2) and (3) were adjusted from outside the box by means of ebonite extension rods. Metal rods could, of course, be used for this purpose, but unless earthed to the case at the point of entry, they might possibly serve to conduct high-frequency surges into the box. For this reason the writer favours ebonite or some insulator for use as an extension rod.

The circuit employed was as shown in fig. 2 (a). It will be observed that the stud switch has two wiper arms, A and B, to which are connected the ends C and D of the 400-ohm potentiometer, thus bridging any consecutive pair of 200-ohm coils. This forms an effective resistance of 200 ohms, having a variable tapping E connected to the positive pole of the high-tension battery. By rotating either the pair of wiper arms AB of the stud switch, or the slider E of the potentiometer, the bridge can therefore be balanced. The total

* As supplied by Messrs. Varley & R. I. for wireless work.

resistance of the coils F, G, H, K, should be a little greater than 1250 ohms. Eight coils of 200 ohms each should therefore be suitable.

A simpler arrangement is shown in fig. 2 (b), which has the advantage that only one wiper arm is required on the stud switch. In this case the resistance of the coils may be increased from 200 ohms to a little under 400 ohms each, their sum being just greater than 2500 ohms. Other arrangements could be devised, but the one shown in

Fig. 2.

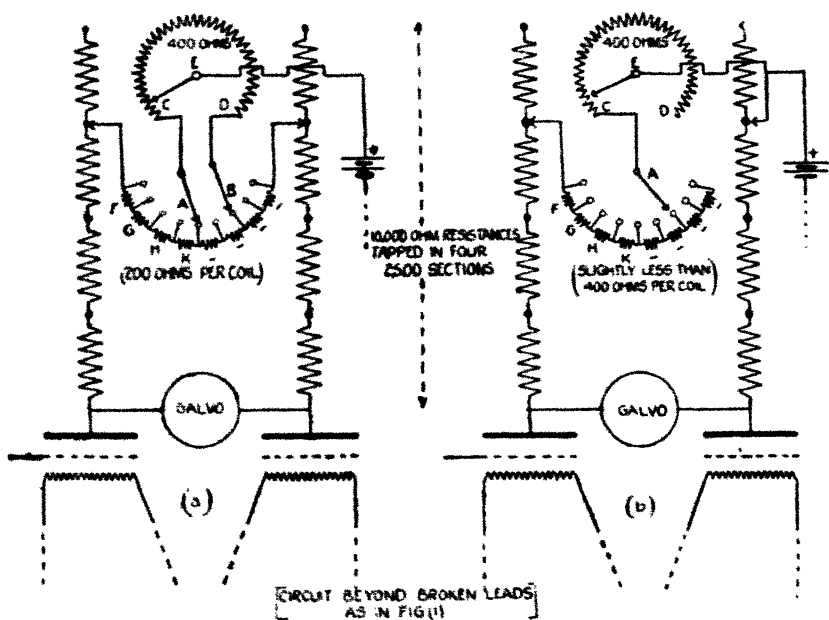


fig. 2 (a) will probably be found the most suitable. With the arrangement of fig. 2 (a), balance can be obtained in a few seconds with far less trouble than when plug-in resistance boxes are used. As a refinement, a smaller (say 10-ohm) resistance of a similar type to the potentiometer could be placed in series with the latter, to obtain a still finer control over the galvanometer, though this will not usually be found necessary.

It should be observed that it is not necessary to have the bridge actually balanced before use. Any arbitrary zero position of the galvanometer spot may be used. By slightly

debalancing, the zero can be moved to the most convenient position on the scale.

No other important changes were made in the circuit arrangements. The bridge was compensated as described on p. 817 of the original article, and used after a steady state of equilibrium was attained. The type of valve employed was, as in the original apparatus, "Osram 215," operated at a high-tension voltage of 60.

The valves, fixed and variable anode resistances, and leads to the grids were enclosed in one metal box, while the high- and low-tension accumulators, compensating slide-wire, and filament rheostat were enclosed in another. The connecting leads between the boxes passed through metal tubes soldered into the latter. The galvanometer—a reflecting pattern, fairly well damped, and of sensitivity about 200 mm/micro-amp.—was enclosed in a third box with a wire grid window, the leads from the galvanometer to the anodes passing, as before, through soldered-in metal tubes. The three boxes were close to one another, and were electrically bonded together in several places. All wires were completely enclosed in the boxes. The outer casing could be connected to earth, or left free, as desired. This was found to make no observable difference in the readings.

Practical Precautions.

The effect of substituting the valve bridge for the ordinary electrometer of an X-ray installation was investigated by connecting the collector of the ionization chamber, through its guard-tubes, to the grid of one of the valves. It was found, however, that the galvanometer zero was extremely unsteady whenever the induction coil supplying the X-ray tube was operated, regardless of whether the X-ray beam entered the ionization chamber or not. On disconnecting the lead from the grid, but leaving the apparatus in the same position relative to the coil and X-ray tube, the zero was found to be steady with the coil and tube in operation. This proves that here again the guard-tubes enclosing the leads to the ionization chamber, while providing sufficient electrostatic screening for ordinary electrometer work, were quite inadequate to prevent high-frequency surges from reaching the grid of the valve and causing unsteadiness.

To overcome this difficulty a simple ionization chamber was built into the side of the valve box, the high-tension electrode being connected to the positive pole of the 60-volt battery supplying the plate current of the valves, thus

dispensing with an extra battery and lead, while the collector was connected directly to the grid. An earthed metal tube with a copper gauze end window covered the whole chamber, leaving no wire or metal parts exposed that were not earthed to the case.

With this arrangement the zero was found to be unaffected by the operation of the coil and X-ray tube, while a large deflexion was obtained when a beam of X-rays entered the ionization chamber. If, however, the metal tube surrounding the chamber was not in perfect contact with the rest of the screening-box, the zero was very unsteady. Tin-foil had to be used to make a good joint, as soldering, while desirable, was not convenient with the particular arrangement used. This emphasizes the importance of ensuring that all metal parts of the screening-boxes etc. are in good contact with one another. For this reason the writer suggests that, rather than have the various parts of the apparatus in separate metal boxes, and the latter bonded together, it would be preferable, and more convenient, to enclose the whole—amplifier, batteries, galvanometer, and ionization chamber etc.—in one large metal case, and to direct the beam of X-rays into the chamber etc. through lead slits in the case.

Results obtained with X-rays.

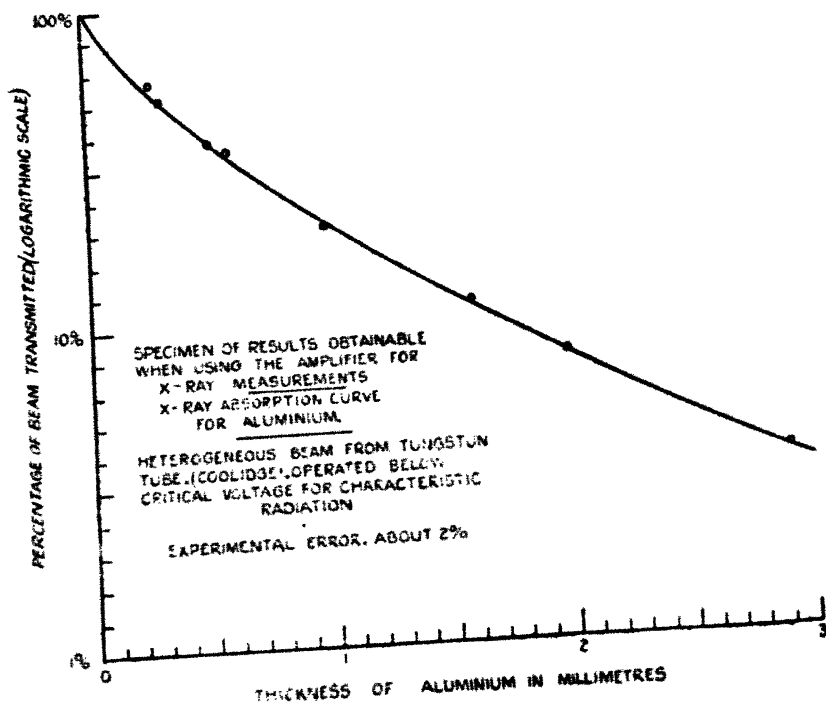
To obtain some idea of the nature of the results to be expected, the following test was carried out. A Coolidge tube, operated by an induction coil, was so arranged as to direct a beam of X-rays into the ionization chamber. The intensity of the beam was adjusted to give a full-scale deflexion of the galvanometer. As the grid of the amplifier (and hence the collector of the ionization chamber) must not be earthed, the usual electrometer method of taking the zero reading by earthing the collector cannot be employed. Instead, to obtain a zero reading the X-ray beam must be cut off, either by means of a lead shutter or by cutting off the coil.

A series of aluminium plates of various thicknesses were then interposed between the tube and the ionization chamber, and, in each case, the ratio of the galvanometer deflexion with the aluminium in position, to the deflexion with the full beam entering the chamber, was measured. It was found that there was a slight unsteadiness in the deflexion, due to the fact that the output of the tube was not quite constant. This, however, was only of the order of 2 per

cent. A slight creep of the zero (mentioned in the original paper) was also observed, but did not seriously affect the results, and could be allowed for.

The logarithm of the observed ratio was plotted as a function of the thickness of the aluminium, giving an X-ray absorption curve for the metal (fig. 3). As the tube was operated much below its critical voltage for characteristic radiation, the resulting line shows a slight curvature, due to

Fig. 3.



the beam being heterogeneous. The points, however, lie on a good line, especially considering that only one value was taken for each point and that the whole experiment did not occupy more than about twenty minutes. The scale was calibrated by a method described later, and found to be linear within the degree of accuracy obtainable in this experiment.

It is interesting to note that, if positive ionization currents are used (*i. e.* if the high-tension electrode of the chamber is

positive), the deflexions due to ionization currents, and those due to high-frequency surges picked up by the lead from the grid to the collector, are in opposite directions, a fact which is useful in deciding whether the amplifier is sufficiently well screened or not.

The effect of substituting a gas-tube supplied from the same coil for the Coolidge was next investigated. It was found that the output of the former was far too variable to give a steady deflexion, fluctuations of up to 100 per cent. being obtained. For work with such a tube some form of "integrating" indicator, such as an insulated electrometer etc., is evidently preferable to the valve bridge. The latter, however, might be useful for demonstrating the variation in the output of a gas-tube.

In the above tests, while the X-ray tube was close (about 2 feet) to the valve bridge, and in the open, the induction coil was several feet away. It is possible that, if the latter were situated near the amplifier, slight unsteadiness of the zero might be occasioned from the magnetic field of the coil, despite the most careful screening. Fortunately, however, in most X-ray installations it does not matter where the coil or transformer is situated, and it should not be difficult to arrange that it is several feet from the amplifier.

Photo-electric Effects.

Tests were carried out to ascertain whether the amplifier was suitable for measuring photo-electric currents. As a rough qualitative test, the apparatus and ionization chamber was set up as previously described, and a polished zinc plate attached to the collector of the chamber, the other electrode of the chamber being, as before, maintained at a potential of plus 60 volts by connexion to the high-tension battery supplying the anode currents. On allowing a beam of ultra-violet light from a mercury arc to enter the chamber, a large galvanometer deflexion was obtained, showing that the amplifier can be used to demonstrate the phenomenon of photoelectric emission.

For quantitative tests a potassium photo-electric cell was employed. The anode, or collector of the cell, was connected to one of the grids of the amplifier, and a suitable potential applied to the cathode from a separate battery, through a safety resistance. The cell was enclosed in a metal case, which was connected to the screening-case of the amplifier, and also to the guard-ring of the photo-electric cell. In this particular case the battery supplying the

334 *Valve Amplifier and X-ray and Photo-Electric Effects.*

potential to the photo-electric cell was outside the screening-case. If, however, trouble is experienced from high-frequency surges in the laboratory, it might be advisable to enclose it in the case also.

Light from a 60-watt metal filament lamp was admitted to the cell through a narrow slit in the outer screening-case. On gradually closing up the slit, by decreasing its length by means of a metal wedge placed across it and plotting the observed galvanometer deflexion as a function of the area of the slit remaining exposed, a curve was obtained which was practically a straight line, showing that the relation between the galvanometer deflexion and the current to the grid was approximately linear for small currents. This is the method of calibrating the scale referred to in the previous section.

Using this simple apparatus, it was possible to locate the positions of X-ray spectral lines on a photographic negative by moving the latter slowly across the slit and observing the galvanometer deflexion. This suggests that the amplifier, in conjunction with a comparatively low-sensitivity galvanometer, may be used with advantage to replace the electrometer, or high-sensitivity galvanometer, usually employed for photometer work in connexion with photo-electric cells. The advantages to be gained in such a case are: (1) high insulation of the leads etc. is unnecessary, (2) readings could probably be taken more quickly, and (3) the amplifier is much more portable and easier to set up than an electrometer.

It should be observed, however, that with such an arrangement, in taking zero readings, the grids (and hence the "collectors") must *not* be earthed. Instead, to obtain the zero reading the beam of light entering the cell should be cut off by means of a shutter, as described in the previous section in connexion with X-rays. It is also advisable, in choosing a galvanometer for the bridge, to see that it has a fairly high damping factor, as this will tend to mask any slight unsteadiness of the zero.

In conclusion, the writer desires to express his sincere thanks to Dr. E. A. Owen for offering facilities for carrying on this investigation at the Physics Laboratory of the University College of North Wales, Bangor, and also for the valuable suggestions made by him and his interest in the work. Further, he wishes to record his thanks to the various research students of the department for their assistance in carrying out tests of the amplifier with their X-ray and photo-electric apparatus.

XXXIV. *Notes on Active Nitrogen.* By ARTHUR EDWARD RUARK, Ph.D., Mellon Institute of Industrial Research, University of Pittsburgh, and Gulf Oil Companies*.

RECENTLY Okubo and Hamada† have published a paper on spectra excited by active nitrogen when it comes in contact with metallic vapours. Some of their results do not agree with those previously obtained by Ruark, Foote, Rudnick, and Chenault‡, and it seems of interest to examine the causes of this discrepancy. Okubo and Hamada used a discharge-tube which they describe as being similar to those used by Strutt and Fowler§ and by Mulliken||. The pressure-range in which these tubes were operated is not stated, but it may be inferred that it was of the order of several tenths of a millimetre, since this is the pressure which ordinarily gives the brightest afterglow when the Geissler tube is used to produce active nitrogen. On the other hand, Ruark, Foote, Rudnick, and Chenault used an electrodeless ring-discharge in a pyrex sphere about 30 cm. in diameter, because this discharge can be run at much lower pressures, of the order of .01 mm. (see p. 19 of our paper). Under these conditions, with a pressure ten to thirty times smaller than that which gives the best results in the ordinary discharge-tube, secondary effects are minimised. It is felt that this difference of pressure explains why we recorded fewer lines of thallium than Okubo and Hamada, and that it accounts, at least in part, for the fact that we obtained only the resonance line of cadmium at 3261 Å., and did not observe any spectral lines of sodium under the conditions described.

Because of possible secondary effects in the discharge used by Okubo and Hamada, such as collisions of the second kind between metal atoms and excited nitrogen molecules, it seems reasonable to say that their observation of the lines $2^3P-2^3P'$ of magnesium does not prove conclusively that two electrons can be displaced simultaneously to higher energy levels by the primary process which gives rise to metallic spectra at much lower pressures.

The writer and his colleagues recorded the mercury line $2^3P_1-6^3D_1$, which has an excitation potential of 10.0 volts. On the other hand, Okubo and Hamada state that they could

* Communicated by the Author.

† Phil. Mag. v. p. 372 (1928).

‡ J. O. S. A. & R. S. I. xiv. p. 17 (1927).

§ Proc. Roy. Soc. lxxxv. p. 377 (1911), and lxxxvi. p. 108 (1911).

|| Phys. Rev. xxxvi. p. 1 (1925), and previous papers.

not obtain any lines coming from levels higher than 4 D, with an excitation potential of 9.51 volts, even with exposures of 100 hours, although they were able to obtain the lines 2 P—4 D in four hours. It is probable that this discrepancy also is caused by the difference in pressure, although it is difficult to construct a detailed explanation in the present state of our knowledge.

The second positive bands of nitrogen were observed in some of our afterglow spectra. Okubo and Hamada have doubted our results, stating: "It may be questioned whether their sectorized disks operated satisfactorily and perfectly cut out the direct discharge or not." This objection is invalid. Careful tests were always made to be sure that the sectorized disks did cut out the direct discharge. It was easy to attain this condition since the disk was run slowly. Frequently it was so arranged that it made one revolution in five to ten seconds, and it was never run faster than one revolution per second.

Okubo and Hamada mention the existence of surface fluorescence of metals placed in the afterglow tube. This has been discussed by E. P. Lewis and others. The writer has observed a surface fluorescence of magnesium in active nitrogen as well as in mixtures of active nitrogen and helium. The distribution of the glow was not uniform, and it is believed to be associated with the presence of magnesium oxide or hydride on the surface. Small particles of magnesium in contact with active nitrogen glow with a bright white light. Presumably they become incandescent, although this cannot be stated with certainty.

Following Sponer, it is often assumed that active nitrogen owes its properties to the presence of neutral unexcited nitrogen atoms which combine in triple collisions with other molecules and atoms, exciting them by virtue of the heat of association which is transferred to them. Various theories may be advanced as to the subsequent history of the excited entities. It may be worth while to point out that a study of the absorption spectrum of activated nitrogen in the region where the absorption lines of the neutral nitrogen atom lie would provide evidence as to the presence of such atoms. The writer is not in a position to undertake such a test, and hopes this note will call it to the attention of someone equipped with suitable spectrographs.

It is a pleasure to thank Mr. Philip Rudnick for helpful comments.

Pittsburgh, Pa.,
May 8, 1928.

XXXV. *The Graphical Representation of the Stimulation of the Retina by Colours.* By FRANK ALLEN, Ph.D., LL.D., Professor of Physics, and A. J. FLEMING, M.A., University of Manitoba, Winnipeg, Canada*.

THE theory of colour vision formulated by Young is based upon the assumption of three fundamental colour sensations, red, green, and violet. Later exponents of this theory, such as Maxwell, Helmholtz, König, von Kries, McDougall, and Abney, have greatly expanded its scope, and applied it with more or less success to the explanation of the enormously varied phenomena of colour vision. All supporters of the trichromatic theory have agreed upon red and green as two of the primary sensations, but opinion has been divided between blue and violet as the third. The general principle of trichromasy is obviously not disturbed by such a change, though it is of course important to discover which of the two colours elicits the sensation in question.

Great and prolonged controversy has ensued on the number as well as the precise designation of the fundamental colour processes, and in particular many theorists have insisted upon the primary character of yellow and white. Indeed, some supporters of the three-components theory of Young, such as McDougall, and to some extent Abney, have felt the necessity of recognizing white as a fundamental sensation, largely because a greater or less amount of white is invariably associated with all colour perceptions.

If the judgment of consciousness alone is invoked, it would have to be admitted that the claims of yellow, blue, and white to equal recognition with red and green as primary sensations are well founded. These claims, however, are disturbed, if not refuted, by the experimental evidence that has accumulated. The yellow colour, for example, may be matched, except in saturation, by proper mixtures of spectral red and green lights. Experiment also has shown that spectral yellow will appear tinged with red or green according as the retina has previously been stimulated with green or red, respectively. As a sensation of yellow can also be obtained from the binocular mixture or fusion of red and green, it is clear that yellow cannot be a simple fundamental sensation. While Edridge-Green has presented a long series of reasons favouring the primary character of

* Communicated by the Authors.

yellow, more formidable evidence against that view has been collected by McDougall and by Parsons*.

In the case of white the evidence is also disturbing. White light may be dispersed into the spectral colours, and the colours may in turn be recombined to give white. Not only is this true for steady light, but it also occurs, as Newton originally showed †, in intermittent illumination by the spectral colours in succession, through the persistence of vision. Complementary colours also will give a white sensation devoid of any chromatic tinge. All colours, when excessively bright or very dim, approach whiteness in appearance. Flashes of white light may also give rise to chromatic effects of various hues.

In order to satisfy the claims of consciousness for the simple, and of experiment for the compound nature of yellow and white, some writers distinguish between psychological and physiological primaries. Both colours would therefore be recognized at once as psychologically simple and physiologically complex. Even should this distinction be admitted, the physiological complexity is of more fundamental importance and is far more, if not alone, susceptible of laboratory investigation.

To decide between blue and violet as the third primary involves different considerations from those affecting yellow and white. Young ‡ originally assumed blue to be the third sensation, but subsequently chose violet in its place. Burch believed his experiments indicated both colours to be primary sensations, thus making four. In his measurements to determine the sensation curves, Abney § used violet experimentally, and afterwards resolved this into red and blue components. The investigations of one of the writers || have clearly shown the blue of the spectrum to be a compound sensation and violet to be simple. Reasons will shortly be given whereby the confusion may be satisfactorily elucidated.

Both Young and Helmholtz assumed that every colour stimulated the three primary sensations but in unequal amounts. The latter ¶ represented his assumption by the well-known diagram in fig. 1.

* 'Colour Vision,' 2nd ed. pp. 276 & 311.

† 'Opticks,' Second Ed. p. 122; also, *Am. Journ. Physiol. Optics*, vol. vii. p. 446 (1926).

‡ Parsons, *loc. cit.* p. 209.

§ 'Researches in Colour Vision,' pp. 230 & 240.

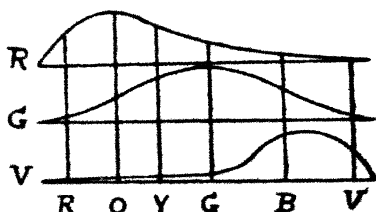
|| Allen, *Journ. Op. S. A. & R. S. I.* vol. vii. p. 583 (1923).

¶ 'Physiological Optics,' English ed. vol. ii. p. 143.

Abney * dissented in part from this assumption. "The red," he says, "stimulates only the red sensation in one part of the spectrum, whilst the violet stimulates both the red and blue, and not the green sensations. A green colour not only stimulates the green sensation, but it stimulates the red and blue sensations as well, as is shown in Helmholtz's diagram." The experimental evidence adduced by Allen, however, clearly showed that stimulation with all colours from the extreme red to the extreme violet invariably influenced the three colour sensations.

Abney † represented his conclusions by a different type of diagram from that employed by Helmholtz. He used three parallel vertical lines to represent the primary sensations, and a horizontal line to represent equal stimulation of

Fig. 1.



Helmholtz's representation of the colour sensations.

the three sensations to which, in conformity with his measurements, the white sensation is due.

A somewhat different graphical method has been used by the writers which seems to be very serviceable in representing the facts of colour perception.

In fig. 2 A, the action of red light upon the three sensations is shown by three unequal elevations, the highest representing the red, the next the green, and the lowest the violet sensation. The relative heights in this and the other diagrams, which represent relative degrees of excitation and not luminosities, are not drawn to any exact scale, though in many cases these could be obtained from the ordinates of the sensation curves of König, Exner, and Abney.

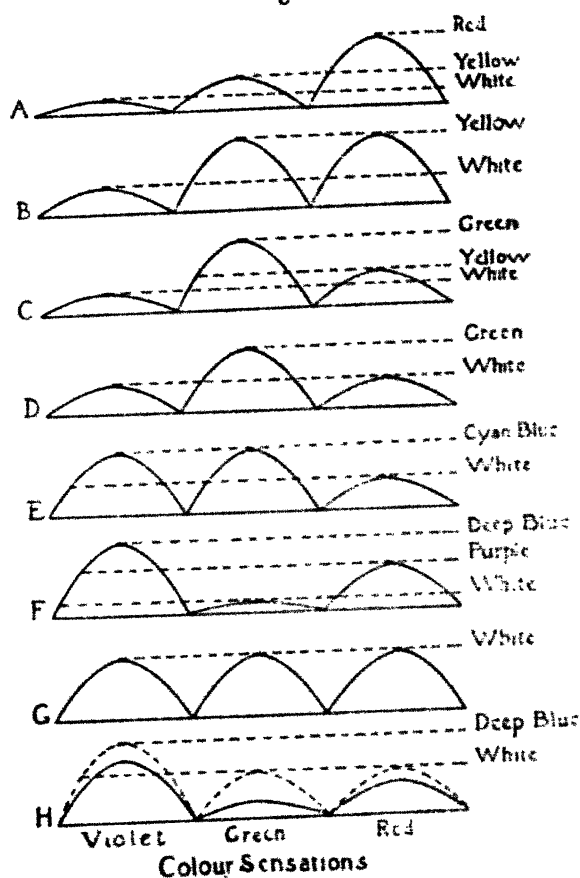
Thus from Abney's measurements of the "percentage composition of spectrum colours in terms of equal stimulus of sensations to form white," the exact scale of heights of the elevations can be found for the part of the spectrum for

* 'Researches in Colour Vision,' p. 231.

† *Ibid.* p. 232.

340 Prof. F. Allen and Mr. A. J. Fleming on the Graphical which his measurements are given in respect to the red, green, and blue colours. In his experiments Abney used the violet colour $\cdot 425 \mu$ and afterwards reduced this to equivalent amounts of red and blue.

Fig. 2.



A few typical selections are quoted here from his 'Researches in Colour Vision' (p. 368):—

λ .	B.S.	G.S.	B.S.
$\cdot 572 \mu$	47.2	51.2	1.6
$\cdot 527$	29.7	62.1	8.2
$\cdot 500$	16.8	47.1	36.1
$\cdot 477$	5.7	14.1	80.2
$\cdot 440$	2.32	0.15	97.5

If now a horizontal line is drawn parallel to the base at a height equal to the lowest elevation, which in this case is violet, it will represent equal degrees of stimulation of the three sensations, which cause the white sensation associated with the red colour, by which the saturation is reduced. A similar horizontal line drawn at the height of the next highest elevation, the green, will represent equal amounts of stimulation of the red and green sensations, which will be perceived together as yellow. For according to the sensation curves the intersection of those for red and green occurs between the wave-lengths 570μ and 580μ , which is the narrow yellow region of the spectrum. This means that equal stimulation of the red and green sensations is the cause of yellow. The remaining portion of the third elevation projecting above the yellow level represents the colour perceived as red.

Thus the perception of red rests upon a stratum of yellow and a substratum of white. The white diminishes the saturation, and the yellow confers on the red colour an orange tint. These recognized facts of colour vision, therefore, are fully represented by this diagram.

When the wave-length of the stimulus is shortened, the relative heights of the elevations are changed, both the violet and green being raised. The white and yellow levels will also be raised indicating the perception of a red colour with a diminishing saturation and an increasing orange tint. As the wave-length of the stimulating colour is made still shorter, a colour will be found which will excite equally both the red and green sensations. This may be represented by fig. 2 B, where there is no projecting part of an elevation above the yellow level. Yellow will therefore be perceived mingled only with the inevitable white.

After the yellow point of the spectrum is passed, the colours will stimulate the green sensation more than the red, as shown in fig. 2 C. As the red sensation is evoked more than the violet, a yellow line can still be drawn. Green, therefore, is perceived tinged with a yellow hue, mingled with the unsaturating white.

As the wave-length of the colour stimulus becomes shorter, its effect on the red sensation becomes less, while the violet is increasingly stimulated. A wave-length will therefore be found which will give equality of stimulation of the red and violet sensations, with a preponderance of green which is represented in fig. 2 D. The stimulation of the violet and red sensations will give a purple colour

which, when mixed with a proper amount of the complementary green, will appear white. Evidently, when this occurs green will be perceived mixed only with white. Abney found this to be the case with the wave-length $\cdot 515 \mu$.

Traversing the spectrum still farther towards the more refrangible end, a blue colour will be found that stimulates the green and violet sensations equally and the red to a smaller extent. This is shown in fig. 2 E, and represents the perception of the cyan blue of the spectrum.

With the violet colour the relative stimulation of the three sensations is somewhat altered. This is represented in fig. 2 F. In this case the red sensation is stimulated much more than the green and therefore a purple line can be drawn representing a stratum of this colour upon which the fundamental colour is superposed. As violet is the most saturated of all the colours*, the green elevation must be very low and in consequence the white line must be very close to the base. The excess of the real fundamental sensation represented by the part of the violet sensation above the purple level is not sufficiently powerful to do more than slightly alter the appearance of the purple.

Allusion has already been made to the difficulty of deciding whether blue or violet is the third primary sensation. From consideration of this graphical method of representation of the facts of colour vision, it occurred to the writers that the question could quite readily be settled in the satisfactory way of reconciling both points of view.

In the more refrangible half of the spectrum the colour changes from green to blue, then, at least in some eyes, to a much deeper blue or indigo, and finally to violet. It seems probable that if our sensations were only individually stimulated, the shortest visible wave-lengths would arouse only a sensation of still deeper blue instead of violet. These wave-lengths, however, possess the power of stimulating the red sensation as well as the deep blue, and hence we perceive a mixture of the two as the violet colour, which is represented in fig. 2 F. As additional evidence for this statement, the experiments of one of the writers† have shown that the wave-length $\cdot 410 \mu$ is quite as powerful in enhancing the green and red sensations as yellow, which is fully seven hundred times as bright.

* Helmholtz, 'Physiological Optics,' Eng. ed. vol. ii. p. 127.

† Allen, Journ. Op. S. A. & R. S. I. vol. vii. p. 596 (1923).

Houstoun* quotes Prof. S. P. Thompson as saying that "indigo was more akin to green than to violet," and adds that "in this opinion, I think, everyone will concur."

In testing the vision of a number of observers Houstoun found four who saw indigo as a special colour; "they all objected to the word indigo, and chose dark blue as a more suitable name for the new colour; they all said it was more like blue than violet. They estimated the boundary between it and blue at 4650 A. U."

These considerations appear to justify the conclusion that the third fundamental colour sensation is excited by the shortest visible wave-lengths at the violet end of the spectrum, but that the deep fundamental blue which is evoked in normal eyes is masked by always being mingled with a considerable portion of the more luminous red.

In this connexion it is important to note, according to Helmholtz †, that when the part of the ultraviolet spectrum, extending from the line L to R (3179μ), is rendered visible it is indigo-blue with low, and bluish-grey with higher, intensities.

Should this reasoning be correct it would appear to follow that if the red sensation could be inhibited from action the violet colour would then be perceived as a deep or a very dark blue. Possibly this might be accomplished by experiments involving fatigue of the red sensation, or by intermittent stimulation at such a rate that only the blue sensation would have time to be excited. Indeed, one of the writers, Allen, recalls that when experimenting on the critical frequency of flicker of the violet colour, a brilliant dash of pure blue colour was sometimes visible for an instant as the sector disk began to rotate, which quickly subsided into the normal violet hue. This phenomenon appears to be a combination of the pure blue sensation, excited before the red becomes active, with the five-fold "overshooting" or enhancement of its brightness that was shown to occur by Broca and Sulzer.

A readier method of testing this reasoning is afforded by the response of the colour blind to stimulation by violet. With this idea in view the recent book on 'Colour Blindness,' by Dr. Mary Collins, was examined in the hope that observations covering this point had been made. This work contains the exceedingly detailed study of ten cases of colour blindness, concerning nine of which it is definitely stated that

* 'Light and Colour,' pp. 8 & 9.

† 'Physiological Optics,' Eng. ed. vol. ii. p. 66.

violet was always matched with or perceived as blue, while it is remarked that the tenth case confused these two colours when they were separately viewed. In addition, two cases of anomalous trichromatic vision were described, one of whom also matched violet with blue. It is noteworthy that on viewing colours this person's eyes almost immediately became strongly and even painfully fatigued. This conforms to the suggestion of Hollenberg* that colour blindness is partly due to the inhibition of the enhancing reflex nervous impulses, leaving the depressing impulses unopposed. It is significant also that all the colour-blind cases, with one exception, perceived violet as *dark* blue, which is what would occur should the much more luminous red sensation fail to be excited. The exceptional case matched violet with a fairly light blue.

So uniform and complete is the evidence from this book that the writers feel great confidence in concluding that the third primary sensation is a blue of a deeper and darker hue than any found in the spectrum, and that it is excited by the short violet waves between the wave-length 425μ and the end of the spectrum. In this manner, therefore, the rival claims of violet and blue as the third primary colour sensation may be reconciled.

It has been observed that when the intensity of the spectrum is very high, only two colours, yellow and blue, are seen, which at still higher intensities also disappear leaving the spectrum white in every part. These facts may be thus represented diagrammatically.

When the retina is stimulated by a certain range of colours from red to some wave-length of green, the colours incline towards yellow as the intensity of stimulation increases. This is due to a gradual approach towards equality of action of the stimulus upon the red and green sensations. If, for example, the colour is red, after the primary red sensation is excited to a certain degree, the green sensation is then stimulated disproportionately, with the result that the hue of the original red light becomes yellowish. The deep blue sensation would also be increasingly stimulated. The proportion of white and yellow in the resulting sensation would consequently be gradually increased. In the diagram this condition would be represented by increasing the heights of the violet and green elevations more rapidly than the red, and the white and yellow levels in fig. 2 A would pro-

* Journ. Op. S. A. & R. S. I. vol. ix. p. 380 (1924).

gressively be raised leaving the projecting part of the red continually smaller.

In the same way the part of the spectrum from some wave-length in the green to the violet would gradually be seen as blue of diminishing saturation. In other words, under intense stimulation the spectrum would gradually appear to be composed of but two colours, yellow and blue, the red, green, and violet having disappeared*. With still more intense stimulation the yellow and blue colours will also disappear leaving only white; that is, the heights of the three elevations in the diagram would become equal and the white level would rise to their summits as in fig. 2 G. When, on the other hand, the intensity of stimulation is greatly reduced, the yellow and blue colours first disappear leaving only the fundamental red, green, and violet. Ultimately these are equally stimulated, causing every colour to appear white. This effect may be represented diagrammatically by greatly reducing the heights of the elevations in fig. 2 G, so that the yellow and blue levels cannot be distinguished from the white with which they finally coincide.

The peculiarities of colour perception in the peripheral regions of the retina have called forth for their explanation the theory of zones, which is based upon the assumption that the fundamental colour sensations in the periphery differ from those in the centre. The analysis of colour perception is sufficiently involved already. To complicate it still further by different hypothetical mechanisms in different parts of the retina can be justified only when every other explanation of the facts has failed. Since nowhere on the periphery do new colours unknown to central vision appear, it seems most reasonable to conclude that it is not the fundamental sensations that differ from zone to zone, but their relative excitations by the same stimulus. In the centre, red, for example, stimulates the red sensation in excess of the green and deep blue or violet; in the so-called yellow-blue zone, red stimulates the green sensation equally with the red, just as it does in the centre with high intensities, and thus yellow and not red is perceived; in the extreme periphery the red stimulus excites the three sensations equally and causes a resultant sensation of white. Similarly with all other colours, except that the more refrangible portion of the spectrum excites the deep blue and green sensations equally, and finally all three.

* Rivers, in Shafer's 'Text Book of Physiology,' vol. ii. p. 1079.

This explanation of the differences between central and peripheral colour vision is confirmed by the existence of four colours*, whose hues remain invariable, except in saturation, in whatever part of the retina they are viewed. Since, for example, in the periphery a considerable range of wave-lengths will elicit the sensation of yellow, the very narrow band of wave-lengths in the spectrum that excite yellow in central, can scarcely fail to do the same in peripheral, vision.

Despite the fact that the theory of zones has received the support of a number of eminent investigators†, the present writers are unable to see wherein the facts of peripheral vision are irreconcilable with the principles of the trichromatic theory of Young.

The unequal boundaries of the retinal colour fields are simply the limits at which colours cease to stimulate one sensation in excess, and begin to stimulate two equally. Nor is there any reason to expect, on the trichromatic theory, that the limits of such actions of one wave-length will coincide with those of another. As the relative degrees of excitation of the three sensations by any stimulus vary with the intensity of the colour, it would follow that the boundaries of the colour-fields would not be the same for all brightnesses.

When two colours fall simultaneously upon the same retinal area, their effects may also be graphically represented. If, for example, the colours are properly selected hues of red and green, the graphical representation is a combination of figs. 2A and 2C, which will give equal heights of the red and green elevations and a higher violet elevation as well. The white level, consequently, will be raised denoting a less saturated yellow than the yellow of the spectrum with which the colour mixture may be matched in hue. It follows, therefore, that in order to obtain a complete match between the composite and spectral yellows, the latter must be mixed with white light. Since stimulation with two colours will doubly affect the three sensations there will always be associated with mixtures a larger proportion of white light than with individual hues. Colours formed by mixtures will in consequence always be paler than the spectral colours with which they otherwise match.

In order to obtain a sensation of white, the three primary sensations must be equally stimulated. Since a single

* Parsons, 'Colour Vision,' 2nd ed. p. 75.

† Helmholtz, 'Physiological Optics,' Eng. ed. vol. ii. p. 451.

colour cannot do this at moderate intensities, at least two colours must be chosen. From the diagrams it is evident that the two colours must be on the two sides of the green sensation. The complementary of red, for example, must be capable of raising the violet elevation to the same level as the others, and therefore it must have some blue in it; that is, the complementary of red must be a bluish green. If the hue of the colour of longer wave-length is changed to orange and yellow, the red and green elevations become more nearly equal in height, and in order to obtain an equal height of the violet elevation the wave-length of the second colour must become shorter, thus making the complementary a deeper blue.

It is apparent from the diagrams that green cannot have a single spectral complementary, since no spectral colour can raise the red and violet elevations to the level of the green. This can only be accomplished by a combination of red and blue or violet. The complementary of green is therefore purple.

Helmholtz has thus summarised* the general effects obtained in colour mixtures. "Lastly," he says, "there is still to be considered the effect of mixing colours that are not complementary. Concerning this matter the following rule may be given: When two simple colours are mixed that are not so far apart in the spectrum as complementary colours, the mixture matches one of the intermediate colours in hue; being more nearly white in proportion as the two components are farther apart, and more saturated the nearer they are together. On the other hand, the mixture of two colours that are farther apart than complementary colours, gives a purple hue or a match with some colour comprised between one of the given colours and that end of the spectrum. In this case the resultant hue is more saturated when the two components are farther apart in the spectrum, and paler when they are nearer together; provided, of course, that the interval between them always exceeds that of a pair of complementary colours.

"For instance, when red, whose complementary colour is greenish-blue, is mixed with green, the result is a pale yellow, which for different proportions of the two components may pass either through orange into red, or through greenish yellow into green. A mixture of orange and greenish yellow may also match pure yellow, but it is more

* 'Physiological Optics,' Eng. ed. vol. ii. p. 128.

saturated than that produced by red and green. On the other hand, by mixing red and cyan-blue, we get pink (pale purple-red); and by changing the proportions of the mixture we can make this pink pass into red, or through violet and indigo-blue into cyan-blue. But red mixed with indigo-blue or, better still, with violet gives a saturated purple-red.

"Incidentally, too, it appears that in these mixtures the degree of saturation of the colours of the spectrum is different. Thus red mixed with green of equal brightness gives a reddish orange; and violet mixed with green of equal brightness gives an indigo-blue close to the violet. On the other hand, when equally saturated colours of the same luminosity are mixed, the resultant compound colour is about midway between the two components.

"No new colours are obtained by mixing more than two simple or homogeneous colours. The number of different colours is exhausted by mixing pairs of simple colours . . .

"Accordingly, with all possible combinations of systems of æther-waves of different frequencies of vibration, there is after all a comparatively small number of different states of stimulation of the organ of vision which can be recognized as different colour sensations."

These results can readily be inferred from the diagrams which have been considered. The three-fold nature of the response of the visual mechanism prohibits the experience of a saturated colour-sensation, except possibly, as McDougall has pointed out, by subjective vision in the case of after images*. With all colour mixtures the three primary sensations must be more evenly stimulated than with single colours, and hence the white level will be higher, or the saturation will be diminished. The farther apart in the spectrum the two component colours are, until they become complementary, the more nearly equal must be the stimulation of the three sensations, and in consequence the less the saturation. When the distance between the components becomes sufficient, equal stimulation of the sensations follows, the white level touches the tops of the elevations, and the distinctive hue of the mixture vanishes leaving only the white. When this complementary stage is passed the two outer sensations, red and violet, must be stimulated more than the green, if the components still recede from each other, with the result that the hue of the colour becomes a mixture of these two, which is purple. The intermediate

* Parsons, *loc. cit.* p. 122.

sensation, green, will be less and less excited as the components get farther apart, the white level will fall, and the resultant hue, as Helmholtz says, will appear more saturated.

The relative degrees of stimulation of the sensations must vary with the intensities of the components, and hence the specific results that Helmholtz gives in the second paragraph of the quotation can be fully accounted for and graphically represented.

The case mentioned by Helmholtz that violet mixed with green of equal brightness gives an indigo-blue close to violet, may be thus represented. The relative excitations of the three sensations by violet are shown by the continuous line in fig. 2 H. The violet, or rather the fundamental deep blue sensation, is stimulated most, the red next, and the green least. It will be recalled that Abney goes so far as to state that the green sensation is not at all excited by violet. The most *luminous* part of the violet colour is obviously the red component. Hence, if the green sensation be excited to the same degree as the red by the addition of green light, the effect of which is to bring the excitations up to the level of the dotted lines in the figure, the white level will touch the summits of the red and green elevations causing these hues to disappear, leaving only the real fundamental deep blue to be perceived, as Helmholtz observed, with a small admixture of white.

The sensitivity of the three primary sensations has been shown* to be under the control of the efferent nervous system through visual sensory reflex actions, which result from stimulation of the retina by all colours. By taking into account these induced changes in sensitivity many hitherto obscure phenomena of vision may be elucidated.

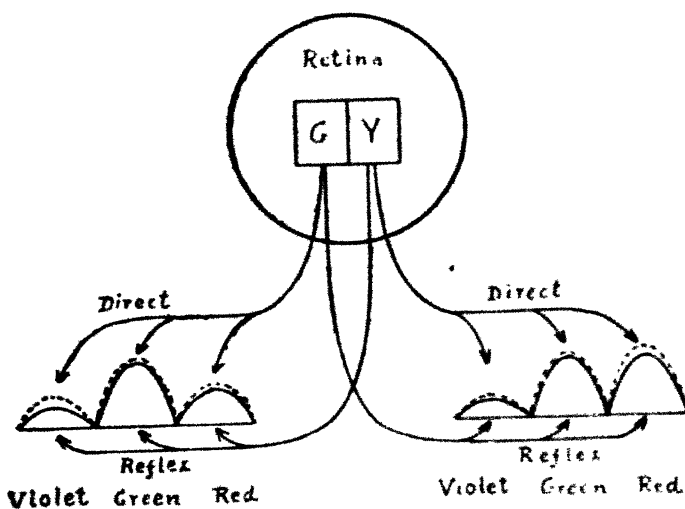
The most difficult problem in colour-vision has undoubtedly been the explanation of the mutual modification of colours by simultaneous contrast. The difficulty has been much increased by the discovery that binocular contrast exhibits the same modifications of colour as are found in unocular observations. When two patches of colour fall upon contiguous retinal areas each appears as if it were mixed with nearly the complementary of the other. That is, if green and yellow are the two contrasting colours, the yellow appears as if it were mixed with red, which is one of

* Allen, "On Reflex Visual Sensations," Journ. Op. Soc. Am. vol. vii. p. 583 (1923); also *ibid.* vol. xiii. p. 383 (1926).

the components of the purple complementary of green, and green appears as if it were mixed with blue, which is the complementary of yellow. The two colours thus appear as if they were moved away from each other in the spectrum.

Helmholtz believed that the effect was an illusion due to systematic deception of the judgment. Hering considered that the assimilation of one retinal substance on one part of the retina under the influence, for example, of green light, caused or facilitated the opposite process of dissimulation of the same substance in the adjoining regions. No method was suggested by which these opposing processes could thus

Fig. 3.



Unocular Simultaneous Contrast.

be brought into action, while the phenomena of binocular contrast were ignored. The explanations provided by all other theories of colour-vision, of which over sixty have been devised, have been equally unsuccessful. The reflex theory of one of the writers affords a clear physiological explanation which rests not upon hypothesis but upon abundant experimental evidence*.

The application of the principle of reflex inductive action to the problem of contrast is easily indicated by the aid of

* Allen, "On Reflex Visual Sensations and Colour Contrast," Journ. Op. Soc. Am. vol. vii. p. 913 (1923).

the diagram in fig. 3. If two contiguous patches of green and yellow colours upon a neutral grey background be observed, a similar pattern will be formed upon the retina. The *direct* action of the green light stimulus upon the three fundamental sensations red, green, and violet is shown at the left of the diagram. Each primary sensation is stimulated to an amount represented by the relative heights of the elevations as shown by the continuous line. The efferent nervous impulses caused by the *reflex* inductive action of the adjoining yellow light are represented by the arrows acting *under* the elevations, by which their sensitivities are increased. Since experiments show that the visual reflex actions elicited by a colour act upon all, but predominantly upon its complementary, sensations, the violet and green sensations, which together make blue, which is the complementary of yellow, will be much enhanced in sensitivity. The direct action of the green light will thereby stimulate them more than is normally the case. The degree of stimulation of the enhanced sensations may be denoted by the dotted line in the diagram. Blue will therefore be added to the green, thus modifying that colour by mixing it apparently with the complementary of yellow.

Similarly, yellow directly stimulates the three sensations in the manner indicated by the continuous line at the right side of the diagram. The reflex action of green enhances predominantly the complementary red and blue (purple) sensations, of which red is visually the more prominent. The yellow colour therefore stimulates the red sensation more than normally, as indicated by the dotted line, thereby causing yellow to become orange in appearance.

Thus by contrast green appears bluer and yellow more orange than they will ordinarily appear; or, in other words, they will assume the appearance of colours situated farther away from each other in the spectrum. As reflex inductive actions are not confined to one sensation but extend in varying degrees to all, the contrast modification will not be exactly, but only predominantly, the mixture of green and yellow with their complementaries.

As the reflex actions are transferred from one eye to the other with precisely the same effects, the explanation also holds for binocular contrast. In both cases the contrast effect will be seen as quickly as the ocular nervous mechanism can act.

XXXVI. *Photo-electric Thresholds of Potassium.*

By Miss JESSIE BUTTERWORTH, B.Sc.*

UNFORTUNATELY, in plotting the graphs of $\log \frac{C}{T^n}$ against $\frac{1}{T}$ and in computing the thresholds, in my recently-published paper †, centigrade temperatures were inadvertently used instead of absolute temperatures. The re-calculated thresholds are 7100 A.U. and 21,000 A.U., with a somewhat doubtful indication of a threshold at 10,000 A.U., and they are independent of the numerical value of n in $\log \frac{C}{T^n}$: at any rate, in the range of values between $\frac{1}{2}$ and 2.

The experiments have recently been repeated with a tube which was lined with a thick silver film, formed by reduction of silver nitrate. The film was in contact with one of the electrodes, and the potassium was deposited on it. This form of apparatus made it possible to verify that any positive emission from the glowing platinum wire was too small to be detected by the galvanometer. The curve obtained by plotting $\log \frac{C}{T^n}$ against $\frac{1}{T}$ was very similar to the earlier one, and yielded the values $\lambda = 9800$ A.U. and $\lambda = 20,000$ A.U. The highest temperature reached was unfortunately too low to bring out the threshold, which probably exists at about 7100 A.U.

XXXVII. *The Power Relation of the Intensities of the Lines in the Optical Excitation of Mercury.* By R. W. WOOD and E. GAVIOLA ‡.

IN previous work on the optical excitation of mercury by one of us §, it was observed that the line 3650 of mercury behaved in a quite anomalous way. Its relative intensity with regard to 3654 or 3663, for instance, could be varied over a large range by changing the conditions of the

* Communicated by Prof. William Wilson, F.R.S.

† Phil. Mag. [7] vi. p. 1, July 1928.

‡ Communicated by the Authors.

§ R. W. Wood, Phil. Mag., Oct. 1925, Sept. 1927.

excitation, but it was difficult to reproduce at will a given ratio of the intensities. It was found, for example, that the application of a magnetic field to the exciting lamp, to avoid reversal of the arc lines, increased the intensities of all of the lines of the optically-excited spectrum, but especially the line 3650. The increments of the lines due to the pressing of the arc discharge against the wall of the quartz tube by the magnet were :

Line 2537, four-fold; lines 3654, 3663, 5461, etc., eight-fold; line 3650, sixteen-fold *.

In the paper above referred to it was pointed out that the anomalous behaviour of 3650 was probably due to the fact that the line appears in fluorescence as the result of three successive absorption acts. Its intensity must then be proportional to the product of the intensities of the three exciting lines producing it, the absorption of which originates 3650. If the ratio of the intensities of the lines in the arc is constant, the product of the intensity of three arc lines is proportional to the cube of the arc intensity. 3650 should vary then with the cube of the intensity of the exciting light. On the other hand, nearly all of the other lines that appear in fluorescence are originated by two successive absorptions. Their intensity must then be proportional to the square of the intensity of the arc. And finally the intensity of the resonance line 2537 should vary directly with the intensity of the arc. This prediction has now been proved quantitatively in the course of the present work.

To observe the changes of the intensity of the different fluorescent lines as a function of the intensity of the arc exciting it, it was necessary to avoid the presence of foreign gases in the resonance tube, which have been found to influence the relative intensity of the lines. For that reason the measurements were made while the resonance tube was in communication with the pump, so that only mercury vapour at room temperature was present.

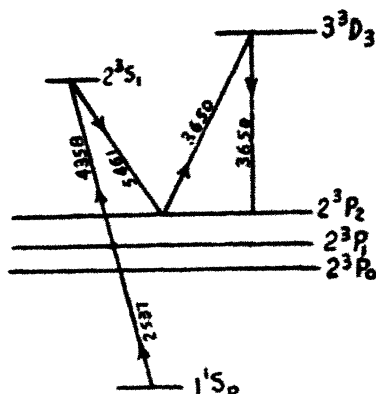
It was necessary to vary the intensity of the exciting light in a known amount, and in the same amount for all of the lines of the arc. Absorption filters cannot be placed between the arc and the tube because all filters absorb selectively.

One might vary the distance of the arc from the resonance tube, but in the case of a long narrow source of light in close proximity to the tube it is not easy to calculate the reduction accomplished in this way.

* R. W. Wood, *Phil. Mag.*, Oct. 1925, p. 784.

The rotating sector cannot be used, as was pointed out in the earlier paper, since there is no actual reduction of the light-intensity, except as integrated over time. A fine-wire gauze, used as a filter, accomplishes the desired result, however, since it is non-selective in its action. We employed a sheet of gauze which reduced the intensity of the light to one-fifth of its original value. The gauze can be employed only under such conditions that the illumination produced behind it is uniform, *i. e.* not with a point-source, in which case the field would be bright, but traversed by dark lines (the shadows of the wires). If the gauze is placed between the resonance tube and the spectroscope, all lines will be reduced to one-fifth of their original intensity; if placed between the arc and the tube, lines varying as the square of

Fig. 1. I



the intensity of the exciting light will be reduced to $1/25$, and lines varying as the cube to $1/125$ of their original value.

It was found that, if the gauze was held between the eye and the prism at the top of the resonance tube, the green fluorescence was still fairly bright (reduced to $1/5$), while, if the gauze was held between the arc and the resonance tube, practically no fluorescence was to be seen (reduced to $1/25$). When this method was applied with the spectrograph, we found, as was to be expected, that the lines 3650 and 3021 (three-stage absorption processes) were reduced to $1/125$ of their initial value.

Method of Measuring and Results.

Fig. 1 shows the experimental arrangement. An image of the cross-section of the resonance tube was thrown upon

the slit of a large quartz spectrograph by an achromatic quartz fluorite lens of 43-cm. focal distance. A photograph of about 20 minutes' exposure was taken, while a fine copper gauze that reduced the intensity of the arc 5 to 6 times was placed between the arc and the tube. On the same plate a series of exposures of increasing duration was then taken while the wire gauze was removed. By matching the photographs of the same line on the plate, with and without gauze, and noticing the corresponding times of exposure, one could calculate the decrease due to the gauze for each line. The following table gives the results obtained by using different gauzes and in different positions. The first column gives the number of times that 3650 decreases if the gauzes are introduced. The third column gives the same for 3654, which was selected on account of its close proximity to 3650, but any other of the lines that appear, as a result of two successive absorptions, could have been used as well. The second and the fourth column give the cube root of the decrease of 3650 and the square root of the decrease of 3654 respectively. If 3650 changes with the third power of the arc intensity, and 3654 with the second power, the numbers in the second and fourth columns should be equal and express the change of intensity of the exciting light. We see that the agreement is quite satisfactory.

Change of 3650.	$\sqrt[3]{\text{Change.}}$	Change of 3654.	$\sqrt{\text{Change.}}$
150 times	5.3	30 times	5.5
1200 ..	10.6	120 ..	11.0
240 ..	6.2	40 ..	6.3
150 ..	5.3	30 ..	5.5
240 ..	6.2	40 ..	6.3
400 ..	7.4	50 ..	7.1
480 ..	7.8	60 ..	7.7

The second and fourth columns of the table give at the same time the decrease that one should expect for the resonance line 2537. We convinced ourselves that 2537 changed apparently with the first power of the arc intensity; but accurate measurements were not made, because that line is very easily absorbed in the air of the room if especial care is not taken in keeping it free from mercury vapour.

Summing up, we can say that the intensities of the lines that appear in fluorescence are proportional to the square of the arc intensity, with the exception of 3650 and 3021, that change with the third power, and of 2537 and 2656 (forbidden

line $2^3p_0-1^1S_0$), that increase with the first power of the exciting light.

We saw at the beginning that Wood had found that the application of a magnet to the arc increased 2537 four times, 3654 eight times, and 3650 sixteen times. It is now possible to explain those changes. The four-fold increase of 2537 shows that the reversal of that line in the arc has been reduced by the magnet so as to increase four times the intensity of the core of the line. Only the core of the line is absorbed by the vapour at room temperature. This increase of 2537 brings four times as many atoms to the level 2^3p_1 . The line 3654 appears when no foreign gases are present, mainly as a result of the absorption of 3125. The fact that 3654 increases not only four times but eight shows that the intensity in the core of 3125 has been increased two times by the magnet. The same is true for 3650. The reversal of 3125 and 3650 in the arc without the magnetic field seems, then, to be about half as strong as the reversal of the resonance line 2537. This result is quite plausible.

XXXVIII. *A Suggested Method for extending Microscopic Resolution into the Ultra-Microscopic Region.* By E. H. SYNGÉ*.

IT is generally accepted as an axiom of microscopy that the only way to extend resolving-power lies in the employment of light of smaller wave-lengths. Practical difficulties, however, rapidly accumulate as light of increasingly small wave-length is brought into service, and probably little hope is entertained of arriving at a resolution much beyond $\cdot 1 \mu$, with, perhaps, $\cdot 05 \mu$ as an extreme limit.

Yet a method offers itself which lies a little outside the beaten track of microscopic work and raises various technical problems of a new kind, but which makes the attainment of a resolution of $\cdot 01 \mu$, and even beyond, dependent upon a technical accomplishment which does not seem impracticable at present. The idea of the method is exceedingly simple, and it has been suggested to me by a distinguished physicist that it would be of advantage to give it publicity, even though I was unable to develop it in more than an abstract way.

* Communicated by the Author.

I propose, therefore, to give a sketch of the method in principle, and will add something regarding the technical difficulties which seem to await the experimenter. Here, too, I only propose to deal with the principles involved in the various difficulties, and it must, of course, lie with the practical experimenter to say whether the suggestions I can offer really contain the solutions of the difficulties.

We shall suppose that a stained biological section, embedded in an ordinary medium, such as Canadian balsam, is attached to a microscope slide in the usual way, but not protected by any cover-glass. The exposed surface of this section is ground so that, over a small area, its divergence from a true plane does not anywhere exceed a fraction of 10^{-6} cm. The preparation of such a surface on the section is one of the technical difficulties which will be considered later

We shall suppose, also, that a minute aperture, whose diameter is approximately 10^{-6} cm., has been constructed in an opaque plate or film and that this is illuminated intensely from below, and is placed immediately beneath the exposed side of the biological section, so that the distance of the minute hole from the section is a fraction of 10^{-6} cm. The light from the hole, after passing through the section, is focussed through a microscope upon a photo-electric cell, whose current measures the light transmitted. The section is moved in its plane with increments of motion of 10^{-6} cm., so as to plot out an area, the intensity of the light-source being kept constant. The different opacities of the various elementary portions of the section, which pass in succession across the hole, produce correspondingly different currents in the cell. These are amplified and determine the intensity of another light-source, which builds up a picture of the section, as in telephotography, upon a moving photographic plate, the motion of the photographic plate being synchronized with that of the section. One would most simply plot out a square area of the section, with a side of, say, μ in length, by passing up and down in successive strips 10^{-6} cm. wide.

If it proved more convenient, the relative positions of the section and the plate containing the hole might be reversed, and the latter placed between the section and the objective of the microscope; but, in any case, it is essential that the hole and the exposed surface of the section should be as close to one another as possible. In the arrangement first described the section is, of course, beneath the glass slide to which it is attached.

This description will sufficiently indicate the principle of

the method. It remains to consider the most obvious technical difficulties. These seem to be four in number :—

- (1) The source of illumination, which must be of very great intensity.
- (2) The making of small adjustments of order 10^{-7} cm., which would be required in the vertical inter-adjustments of the section and the opaque plate, and the making of regular increments of motion of 10^{-6} cm. in the plane of the section, the conditions in both cases being such that friction cannot be entirely eliminated.
- (3) The planing of the biological section so that it presents a surface which does not diverge from a plane by more than a fraction of 10^{-6} cm.
- (4) The construction, in an opaque plate or film, of a hole whose diameter is of the order 10^{-6} cm.

(1) *The source of illumination.*—An ordinary carbon arc might be strong enough to give indications with a hole of 10^{-6} cm. diameter. But to obtain a refined gradation of shades, such as would be necessary for satisfactory results, one would require a light of greater intensity. This points to the employment of an arc enclosed in a chamber under a very high pressure. The method has been used by Lummer, who is said to have attained a brightness nearly twenty times as great as an ordinary arc, using a pressure of twenty-two atmospheres. But the advantages of light produced in this way are greater than would appear from this figure. For the very high temperature will move the energy maximum of the spectrum down towards the blue, where the photo-electric effect of the light is greatest. I do not know whether the method has yet been brought to a practical stage. But it seems certain that one can count on it, as requiring only technical improvements, to be available for the method of microscopy suggested.

It is, of course, essential that the intensity of the light reaching the section shall be kept constant during the experiment, which might last two or three hours. Various automatic devices would secure this, and I need not consider the question here.

(2) *The making of very small adjustments.*—The impossibility of eliminating friction renders the use of springs impracticable, and the simplest arrangement which suggested itself to me was a differential screw having an exceedingly

small difference between the pitches of the two nuts. If the pitch of one nut were 1 mm. and of the other $\frac{1}{25}$ inch, the screw would advance .016 mm. for each turn of the screw-head, and a worm and clicking spring arrangement, giving one click for each $\frac{1}{1800}$ of a rotation of the screw-head, would give increments of motion, of sufficient regularity, of 10^{-6} cm. each. I do not know whether the metric and inch units have ever been put together in this way, but I have been informed by a well-known firm of instrument makers that they could construct such a screw without difficulty.

For adjustments of the order of 10^{-7} cm., pitches of $\frac{1}{4}$ mm. and $\frac{1}{30}$ inch, or better $\frac{1}{16}$ inch, would probably be advisable. All parts of the instrument, where practicable, would be constructed of Invar, pieces being selected, if possible, with a zero coefficient of expansion.

(3) *The planing of the biological section.*—Plates of quartz glass can be ground, polished, and tested in pairs by means of interference fringes until the surface of each shows a divergence from a true plane of less than $\frac{1}{100}$ of a wavelength. Disks of 25 centimetres in diameter, of this degree of accuracy, were prepared by the U.S. Bureau of Standards in 1927. If ultra-violet light were used for the interference tests the practicable limit of accuracy would seem to be about 2×10^{-7} cm.

For obvious reasons, one could not apply such a method to produce a correspondingly plane surface on a biological section. But it seems possible to use plates of glass prepared in this way, which need not of course be as large as those mentioned, as the points of departure for a grinding device which should produce similar surfaces on a biological section embedded in any ordinary medium.

In principle the problem will be solved if we can construct a plate covered with emery grains, fixed in cement, in such a way that the summits of all the grains lie in the same plane, or do not rise above it by more than a fraction of 10^{-6} cm. in any case.

If we have such a plate and can move it in various directions in its plane, the emery grains will grind away any surface on which they impinge to a corresponding planarity. In fact, if we carry on the process for a long enough time, provided the emery grains do not break down, an even higher degree of planarity should be attainable in the section.

As regards the movement of the emery plate in the plane, it would probably be best that it should roll upon small

quartz spheres, which had themselves been ground and tested by interference fringes to a similar degree of accuracy—that is, to a fraction of 10^{-6} cm. The total inaccuracy might then be about 10^{-6} cm., but even so, if the process is carried on for long enough, a planarity to within a fraction of 10^{-6} cm. should be attainable in the section.

To prepare a grinding plate of this kind, it seems possible to make use of a glass plate which is accurately plane to within a fraction of 10^{-6} cm. If we take such a glass plate and, keeping it parallel to the base-plane of the emery plate, press it down very gently upon the emery particles before the cement hardens, their summits, if they do not pierce the glass, will lie in a plane to the required degree of accuracy. It would seem necessary to find a cement which does not alter its volume upon setting, and it might be advisable to use a plane plate constructed of a harder substance than glass, if it should be found difficult to avoid the emery particles piercing the glass. One would use only fine grains of emery, averaging, say, 5μ in diameter, and as it would only be necessary to grind away very small thicknesses of the comparatively soft material used in embedding the biological section, there should be little or no breaking-down of the emery points.

(4) *The construction of a hole of approximate diameter 10^{-6} cm.*—One finds holes in chemically deposited films of silver on glass, which approach this size, and these seem to indicate the way in which the problem may be dealt with. In the case of such films of silver the holes are presumably due to the presence, on the surface of the glass, of colloid particles of substances on which deposition of the silver does not take place. The extreme fragility of these silver films and the difficulty of cleaning them would, however, make them hardly suitable for the purposes in view, although it might be possible to use them.

When one turns to the question of employing films of more resistant metals “sputtered” in vacuum-tubes, it appears that minute holes do not here present themselves in the same way. The cathode particles, in fact, will not select their target, but will cover everything equally. We may suppose a number of colloid particles of some transparent substance, averaging 10^{-6} cm. in diameter, to be sprinkled on a plane glass slide, and that a film, about 10^{-6} cm. in thickness, of some metal with a high opacity, is then sputtered on the slide. Each of the transparent particles will be represented by a little monticle of the

metal, rising about 10^{-6} cm. above the general level of the film surface, and to obtain the holes which we require it will be necessary that we should plane down these little monticles. Here the method which has been proposed above for planing the biological sections seems to be again available. In fact, the differential screws should make it possible to approach the sputtered slide to the emery plate by stages of about 10^{-7} cm., and thus to plane down the monticles by successive thicknesses of similar amount. As we proceed in this way the larger of the transparent particles will be first exposed and these will provide us with holes whose advantages will depend upon the shapes of the particular particles. A particle which is pyramidal in form, or which consists of a congery of smaller particles forming a little pyramid, will obviously be the most suitable if the opacity of the film is sufficient.

The thickness of the film has been assumed to be 10^{-6} cm., and in the case of a metal as opaque as silver this should be just sufficient to allow of a hole 10^{-6} cm. in diameter being used. The light coming through a small area of the film around the hole will, of course, come to the same focus as the light which actually passes through the hole, and it will therefore be an advantage that the film should be sufficiently thick to make this accessory light of little consequence. Otherwise we should have to use a very high-power objective (so as to reduce this area), and this would have various inconveniences. If the film were 2×10^{-6} cm. thick we could disregard this accessory light to a large extent in the case of silver films. But in this case we should have to use larger transparent particles, and to obtain holes of diameter 10^{-6} cm. we should be dependent upon pyramidal particles. Since, however, some thousands, or even millions, of transparent particles might well be deposited on the slide initially, there would be no lack of holes to choose from, and if even a very small proportion of the particles or congeries were pyramidal, our requirements would be satisfied.

The final limitations of the method seem, indeed, to depend solely upon the limitations to the opacity of the films for light of various wave-lengths. For a film having the opacity of silver with respect to ordinary light, the practicable limit of resolution would seem to be about 0.05μ , or 0.04μ where a pyramid occurred in the most favourable configuration.

Since this degree of resolution should bring all living organisms within our scope an attempt to overcome the technical difficulties would seem to be justified. It appears to me, indeed, that most of these difficulties are reducible to

362 *Suggested Method for extending Microscopic Resolution.*

the question of sufficient funds. The most formidable, apart from such considerations, might be the preparation of the plate of emery grains.

Note.—So much depends on the attainment of absolutely true surfaces that it seems worth suggesting a method for testing these, which would make a still higher degree of accuracy possible than by the use of interference fringes.

If total reflexion is taking place at a surface, and if another surface is brought sufficiently close to it (*i. e.*, a distance from it of the order of a wave-length), the reflexion ceases to be total, a sensible part of the light passing through the second surface. The intensity of this transmitted beam is derivable, in the case of grazing incidence, from the expression $e^{-4\pi\sqrt{n^2-1}\cdot\frac{d}{\lambda}}$, and since a change of intensity of one part in a thousand is measurable by photo-electric apparatus, a difference of less than 10^{-8} cm., or even 10^{-9} cm., in the distance between two parallel surfaces should be measurable, provided, of course, that they are sufficiently close together. An ordinary reflected beam would probably serve as well as one within the angle of total reflexion (although the formula would not be the same), and it would be much more convenient to work with. By making a constant beam of light travel systematically, at a constant angle, over the two plates, when placed parallel a fraction of a wave-length apart, a picture might be built up automatically in a few minutes, as in telephotography, the reflected beam affecting a photographic plate directly or through the medium of a photo-electric cell. The relative intensities of shade in this photograph would obviously indicate the relative distances apart of the plates, since different intensities in the reflected beam correspond to differences in these distances. If an apparatus for producing this kind of chart were perfected—and it seems to present no difficulties—the production of quartz plates and spheres to an accuracy of 10^{-7} cm. could be placed upon a commercial basis, and this should make the whole microscopic apparatus a practicable instrument of the laboratory as far as expense was concerned.

An adaptation of the first part of the idea in this note would also serve for estimating the distance of the section from the opaque plate, as they come very close together.

Dublin,
May 25, 1928.

XXXIX. Notices respecting New Books.

Lehrbuch der Physikalischen Chemie, von Dr. KARL JELLINEK.
Fünf Bände. Erster Band: Grundprinzipien der Physikalischen Chemie. Die Lehre von Fluiden Aggregatzustand reiner Stoffe. Zweite, vollständig umgearbeitete Auflage. [Pp. liii + 966, mit 162 Tabellen und 337 Textabbildungen.] (Stuttgart: Ferdinand Enke, 1928. Preis, geh. M.82; geb. M.86.)

THE first edition of this volume appeared in 1914, shortly before the outbreak of war. The complete work was planned in four volumes, but owing to the conditions resulting from the war it was not found possible to publish the last two volumes. The two volumes which were published have been out of print for some time and a new edition has become necessary. At the same time the whole work has been replanned and is to appear in five volumes; the extensive recent developments in atomic theory, theories of crystal structure, quantum theory, relativity, etc., having necessitated increasing the size of the work. Not only so, but judging by the size of the first volume, the size of the volumes themselves will be increased. The second edition of Vol. I. contains 234 pages more than the first volume. This is due in part to the rapid growth of the subject—the volume covers the literature up to the end of 1926—and in part to the transference of a certain amount of material dealing with the fluid state from Vol. II. to Vol. I., so that the whole of the material concerning the fluid state is now contained in the one volume.

The author's summary of the contents of this volume is as follows:—

“Allgemeinste Gesetz des Stoffes und der Energie. Die Lehre vom fluiden Aggregatzustand reiner Stoffe (ganz verdünnte Gase, mässig verdünnte Gase, verdichtete Gase, Flüssigkeiten), experimentell, thermodynamisch und kinetisch behandelt.”

Although it would not be possible to summarise the contents more briefly yet precisely, this description does not convey an idea of the comprehensiveness with which the work has been planned both from the theoretical and from the practical viewpoints. Mathematics is not avoided where necessary: for those who can appreciate it, it is there; those who cannot must accept the formulae which are proved. Full descriptions of experimental methods and apparatus are given. References to the literature of the subject are included throughout, and detailed author and subject indexes amounting to 30 pages make it easy to obtain information on any particular point which is dealt with in the volume.

Because of its completeness and detailed treatment and in spite of—or perhaps also because of—its size, the volume is one which no physical chemist can afford not to have available for reference purposes.

The Higher Coal-Tar Hydrocarbons. By ARTHUR ERNEST EVEREST, D.Sc., Ph.D., F.I.C. Pp. xiii+334. (London: Longmans, Green & Co. 1927. Price 18s. net.)

THE importance of the derivatives of coal-tar hydrocarbons, as a source of synthetic colouring matters and because of the therapeutic value of some of them, has resulted in extensive investigations and an immense mass of literature. Most attention has been given to the derivatives of benzene, toluene, xylene, naphthalene, and anthracene. Comparatively little work has so far been done on the higher coal-tar hydrocarbons, and they offer a wide field for careful systematic research. The volume under review is concerned very largely with three groups of the higher hydrocarbons, the acenaphthene group, the fluorene group, and the phenanthrene group. These groups have not up to the present yielded many derivatives which are of commercial importance as a source of colours and intermediates. The aim of the author has been to collate the known facts concerning these groups in the hope that the many virgin fields for research which they offer may stimulate systematic work in them.

Spectroscopy. By E. C. C. BALY, C.B.E., M.Sc., F.R.S. Third Edition. (In four volumes.) Vol. III. [Pp. viii+532, with 6 plates and 60 figures.] (London: Longmans, Green & Co., 1927. Price 22s. 6d. net.)

THE third of the four volumes into which the third edition of Prof. Baly's text-book on spectroscopy is divided is concerned mainly with those developments of the subject which are the more immediate results of Bohr's theory. The size of the volume is a testimony to the remarkable developments in spectroscopy within recent years. Spectroscopists, both practical and theoretical, are under a debt of gratitude to Prof. Baly for the detailed descriptions of experimental work and the numerous tables of experimental results which are given in the volume. But although the practical aspect of the subject predominates, the principal advances in atomic theory are adequately described.

The volume is divided into four chapters of which the first, on series of lines in spectra, fills more than half the total number of pages. It contains an account of the early work of Rydberg, Kayser and Runge, Paschen and Ritz, of Bohr's theory and of the subsequent developments, leading up to modern work on series, the selection principle, doublets and multiples, etc. A summary of results connected with X-ray spectra is also included. The second and third chapters are devoted to the Zeeman and Stark effects respectively, which are discussed both from the theoretical and practical viewpoints: the anomalous Zeeman effect, Landé's rule of intensities, and the Paschen-Back effect are amongst the subjects dealt with. The fourth and final chapter contains an account of work on emission band spectra.

References to original publications and complete author and subject indexes increase the value of the volume.

A Treatise on the Analytical Dynamics of Particles and Rigid Bodies with an Introduction to the Problem of Three Bodies.

By Professor E. T. WHITTAKER, LL.D., Sc.D., F.R.S. Third Edition. [Pp. xiv. + 456.] (Cambridge: at the University Press, 1927. Price 25s. net.)

THE new edition of Prof. Whittaker's *Treatise on the Analytical Dynamics of Particles and Rigid Bodies* is, with the exception of the last two chapters, a reprint of the previous edition, with some corrections and additional references. The two chapters in which changes have been made are those dealing with the general theory of orbits and with integration by series. In view of the developments of this portion of the subject during the ten years which have elapsed since the publication of the second edition, these two chapters have been entirely rewritten and the new matter incorporated. The additions enhance the value of the treatise, which has proved invaluable to the more advanced students of theoretical dynamics during the past generation.

The Electrical Conductivity of the Atmosphere and its Causes. By VICTOR F. HESS, Ph.D. Translated from the German by L. W. CODD, M.A. Pp. xviii + 204 with 15 figures. (London: Constable & Co. 1928. Price 12s. net.)

A CONCISE but adequate account is given in this volume of the present state of knowledge of the ionization of the atmosphere and its causes. The apparatus and methods for determining the conductivity of the atmosphere, the average mobility of the ions, and the number of ions are described. The various phenomena which contribute to the observed ionization, both those of radioactive origin and those of non-radioactive origin, are considered in some detail. The processes which result in the destruction of ions are then dealt with. The question of how far the known causes of ionization are quantitatively sufficient to bring about the amount of ionization actually observed is then discussed for the layers of air near the earth over dry land, for the lower layers over the sea, and for the free atmosphere up to the neighbourhood of the upper limits of the troposphere. It follows from this discussion that the observed ionization is in all cases satisfactorily accounted for by the known causes of ionization. Finally, a section is devoted to the phenomena of the conductivity and ionization of the upper layers of the atmosphere.

A detailed account is given of the penetrating radiation (*höhenstrahlung*), including the original work up to the beginning of 1927. For the present translation, the sections dealing with this and with the phenomena in the highest layers of the atmosphere have been rewritten by the author and brought up to date.

The subject of the volume is of interest to those concerned with geophysics, meteorology, astronomy, geology, and radiotelegraphy. To all of these the present account will prove a valuable summary. References are given to the more important theoretical investigations and experimental results.

X-Rays: Past and Present. By V. E. PULLIN and W. J. WILTSHIRE.
229 pp., with 43 illustrations. (London: Ernest Benn. 1927.
Price 12s. 6d. net.)

IN the thirty years or so which have elapsed since their discovery, X-rays have exercised a very profound effect on physical and chemical investigation and have found many practical applications in medicine and surgery and in various branches of industry. They have always been of great interest to the general public, and the telling of their story in a manner that would interest the inquiring layman who is not possessed of any scientific training was well worth doing. This is a task which the authors, both radiologists with wide experience, have accomplished with conspicuous success.

After an account of early experiments, the researches of Crookes and others with the electric discharge tube are described, leading to an account of Röntgen's discovery. The early controversies as to the nature of X-rays are recounted, and the investigations of J. J. Thomson and others which led to the discovery of the electron are summarised. The development of modern ideas as to the nature and structure of the atom which has resulted from these and other investigations is explained in non-technical language. The phenomenon of the diffraction of X-rays by crystals, which finally settled the vexed question as to the nature of the rays, is then discussed. The remainder of the book deals with the numerous practical applications of X-rays and with the modern developments of X-ray tubes and apparatus.

This well-written account will bring home to the layman the important results which may accrue from research in pure science and will leave him with the conviction that there are many avenues as yet unexplored in which X-rays will be found to have practical application.

The Theory of Functions of a Real Variable and the Theory of Fourier's Series. By E. W. HOBSON, Sc.D., LL.D., F.R.S.
Vol. I. Third Edition. Pp. xv+736. (Cambridge: At the University Press. 1927. Price 45s. net.)

THE second edition of Prof. Hobson's treatise on the theory of functions of a real variable was double the size of the first edition, which appeared as a single volume in 1907, and was substantially a new book. Volume I. of the second edition appeared in 1921, Volume II. in 1926. The first volume has now gone into a third edition. The previous edition has been thoroughly revised, certain sections rewritten, and new matter, amounting in all to 65 pages, has been added. These additions have been made without changing the numbering of the sections, so that the references in Volume II. to sections in Volume I. are still applicable to the new edition.

The work as a whole is too well known to call for detailed comment. The present volume deals with numbers, the descriptive and metric properties of sets of points, transfinite

numbers and order types, functions of a real variable, the Riemann integral (in which the section on the Riemann-Stieltjes integral has been rewritten and enlarged), the Lebesgue integral (in which the sections dealing with the indefinite integral of a function of two variables have been considerably added to), and non-absolutely convergent integrals.

Prof. Hobson's treatise is the standard treatise on the subject in the English language, and he is to be congratulated upon the revisions and additions which are incorporated as new editions become necessary, so keeping the work thoroughly up to date. A list of additions and corrections to the second edition (1926) of Volume II. is given at the end.

The printing of the volume is in accordance with the highest traditions of the Cambridge University Press. The price of the new edition remains the same as that of the second edition.

Chemical Affinity. By L. J. HUDLESTON, M.C., B.Sc., A.I.C.
[Pp. vii + 138.] (London: Longmans, Green & Co., 1928.
Price 7s. 6d. net.)

THIS new volume in Messrs. Longmans, Green & Co.'s series of Monographs on Inorganic and Physical Chemistry deals with the important subject of the application of thermodynamic considerations to questions of chemical affinity. The treatment is elementary and assumes no previous knowledge on the part of the reader: it is therefore suitable as an introduction to the subject and to the study of more advanced treatises.

After preliminary considerations about energy, its conservation, degradation, and availability and about reversible and irreversible processes, the conception of entropy is introduced and explained. The importance of the heat content and free energy (following the terminology of Lewis) is then introduced and the measurement of free energy changes is discussed. The next chapter is devoted to reactions involving solutions, the important conception of "activity" introduced by Lewis being explained. In the following chapter, Nernst's heat theorem and various applications are dealt with. The final chapter contains a large number of illustrations of the application of the principles explained in the preceding chapters to practical problems. The author states that it is in this chapter "that the main purpose lies, and if this serves to assist research workers to learn how to survey their problems, to estimate the most favourable conditions for experiment, and to study the possibility of disturbance by side reactions, this purpose will, indeed, have been fulfilled." There are many to whom mathematical symbols have little meaning until translated into numerical data: all such will be grateful to the author for the variety of practical applications discussed in this chapter.

The volume is well written and clearly expressed, and the author has been judicious in his choice between what to include and what to exclude. The volume is well printed and the type is very clear.

Cambridge Tracts in Mathematics and Mathematical Physics:—

No. 23. *Operational Methods in Mathematical Physics.*
By HAROLD JEFFREYS, M.A., D.Sc., F.R.S. [Pp. vii+101.]

No. 24. *Invariants of Quadratic Differential Forms.*
By OSCAR VEBLEN, Professor of Mathematics, Princeton University. [Pp. viii+102.]

(Cambridge: at the University Press, 1927. Price 6s. 6d. net each volume.)

THE two new volumes of the series of Tracts in Mathematics and Mathematical Physics, published by the Cambridge University Press, are welcome additions to a valuable series.

No elementary connected account of Heaviside's powerful operational methods for solving differential equations in physics has hitherto been available. Dr. Bromwich and several other investigators have published papers dealing with Heaviside's methods and some of the applications, but the fact that more general use has not been made of them is due undoubtedly to the lack of a connected summary such as Dr. Jeffreys has now provided. The principles of the methods are briefly and simply explained, and the manner of applying them to practical problems is illustrated by a wide variety of applications—to electrical and other problems involving one independent variable, to wave-motion, to conduction of heat, to problems with spherical or cylindrical symmetry, to dispersion, and to problems involving Bessel functions. These illustrations bring home to the reader in a compelling manner the power of the method and its peculiar utility for physical problems in which the initial conditions are assigned.

The Tract by Professor Veblen bears the same title as No. 9 in the series by the late J. E. Wright, which has for some time been out of print. The earlier tract was published in 1908, before the development of the generalised relativity attracted widespread attention to the subject. The new orientation thereby given to the subject has to a large extent shaped the contents of this tract: practical applications to relativity, electromagnetic theory, dynamics, and the quantum theory have been omitted. Such are easily accessible to the student of physics. What he requires and what he is provided with in this tract is an account of the underlying differential invariant theory but oriented with a view to practical applications. The treatment has been made as elementary as the subject permits, and fundamental definitions have been carefully formulated.

[The Editors do not hold themselves responsible for the views expressed by their correspondents.]

THE
LONDON EDINBURGH. AND DUBLIN
PHILOSOPHICAL MAGAZINE
AND
JOURNAL OF SCIENCE.

[SEVENTH SERIES.]

SEPTEMBER 1928.

XL. The Direct Current Conductivity of Insulating Oils.
By D. H. BLACK, Ph.D., M.Sc., Research Laboratory
of International Standard Electric Corporation.*

IT has long been known that, in general, when a difference of potential is applied across two electrodes immersed in a liquid dielectric, the current falls off with time, the rate of fall depending on various conditions. As distinct from most solid dielectrics this absorption current in oils is not reversible, and has been called the "irreversible anomalous current." Although the absorption effect is not reversible, there are in some cases traces of a small back-effect. These, however, are usually attributed to chemical polarization of the electrodes, and their effect can be allowed for when taking measurements.

The purpose of this paper is to give a simple theory which seems capable of explaining the observed phenomena, and to show how this theory is strongly supported by experimental evidence.

An absorption current can conceivably be caused in two ways: (1) a change in the resistance between the electrodes; and (2) the formation of polarization potentials due to an accumulation of charges in the dielectric—a kind of space-charge effect. From the irreversible nature of the absorption, and more particularly from the form of the current/time relationship observed on reversing the applied potential, it is considered that (2) above plays little, if any, part in the

* Communicated by Sir E. Rutherford, F.R.S.

phenomena. Reasons for this are given towards the end of the paper.

Assuming, then, that absorption is due to an increase of resistance, the question arises as to whether this increase is due to the building-up of a resistance at one, or both, of the electrodes ("contact resistance"), or whether it is due to the withdrawal of the conducting particles from the liquid itself. It is well known that conducting particles, especially water, can be removed from a liquid dielectric by the application of an electric field. These effects are, however, chiefly observed in more or less impure liquids. While it is not denied that a similar action may take place in reasonably pure dielectrics, it is here assumed that the predominating factor is the formation of a contact resistance.

The phenomenon of contact resistance has been observed by several workers when dealing with solid dielectrics*, and Hartshorn† put forward a theory to account for the usual absorption effects and power losses on these grounds. In the case of liquid dielectrics it seems to have been assumed that such contact effects are not encountered; but in the light of the present work this seems to be far from correct. Various workers have recorded the presence of a contact or transfer resistance with ordinary electrolytic solutions‡, and the action of the electrolytic rectifier is thought to depend on such an effect§. More recently Bryson||, when working with molten glass, observed a similar effect, the resistance being largely due to the formation of a gas layer at one electrode. Therefore, even without further experimental support, the assumption that a contact resistance is formed in liquid dielectrics seems quite justified.

Any building up of a contact layer at an electrode is most probably due to the transportation of material by the current flowing, the rate at which it is being formed being proportional to the current. It is observed that if a film of oil which has had a voltage applied to it for some length of time is short-circuited, the extra resistance which has been built up gradually disappears and the oil returns to its initial state. Thus it is evident that there is a force which is tending to remove this contact resistance, and this may be

* *E.g.* Joffé, *Ann. der Phys.* lxxii. 6, p. 461 (1923).

† *Proc. Phys. Soc.* vol. xxxvii. p. 215 (1925).

‡ See, for example, Newberry, *Roy. Soc. Proc. A*, cxi. p. 182 (1926); Crowther and Stephenson, *Phil. Mag.* vol. 1. p. 1066 (1925).

§ See Meserve, *Phys. Rev.* xxx. p. 215 (1927).

|| *Journ. Soc. Glass Techn.* xi. p. 331 (1927).

termed its tendency to recombine. From the analogy with the case of chemical mass action it is reasonable to assume that the rate of recombination is proportional to the magnitude of the resistance layer present.

Let R_0 be the initial resistance of the oil between the electrodes; R_s the final steady value of the resistance after the application of a potential E ; R the resistance at time t after the application of the potential; I_0 , I_s , and I the corresponding values of the current; and r the increase in the resistance. Then $R = R_0 + r$ and $R_s = R_0 + r_s$. Applying the assumptions made above, we get

$$dr/dt = kI - lr, \dots \dots \dots (1)$$

k and l being constants. When a steady value has been reached, $dr/dt = 0$, and so

$$r_s = kI_s/l;$$

hence $R_s = R_0 + nI_s, \dots \dots \dots (2)$

where $n = k/l$. Therefore, if the values of R_s for different values of E are measured and graphed against the corresponding values of the current, the points should be on a straight line, cutting the axis $I = 0$ at the value of R_0 *.

Eliminating I by means of Ohm's law, we get

$$R_s = R_0/2 + \sqrt{n^2 E^2 + (R_0/2)^2} \dots \dots \dots (3)$$

If, by suitable switching arrangements, the time available for recombination is greater than the time the potential is applied, then the resistance ought to be decreased. A method is described later in which a commutator connected the potential across the film for a fraction of each revolution, the film being short-circuited for the remainder of the cycle. This was rotated at a speed which was sufficient for it to be assumed that the resistance remained constant throughout the cycle. If α is the fraction of one revolution during which the potential is applied, then

$$\frac{dr}{dt} = \alpha kI - lr, \dots \dots \dots (4)$$

and when $dr/dt = 0$,

$$R_s = R_0 + \alpha n I_s, \dots \dots \dots (5)$$

αI_s representing the average current flowing. Thus, while keeping the potential constant, values of R_s can be obtained

* It is of interest to note that Meserve (*loc. cit.*) obtains a similar relationship for the aluminium cell.

for different values of the average current by varying α . The relationship should still be linear.

If the absorption current observed in oils is due to the processes given above, then the value of R_0 obtained by varying the applied voltage should be the same as the initial value of the resistance obtained in taking an absorption curve, due allowance being made for the true capacity current. That is to say, both should give the true resistance of the oil itself. This has been found to be approximately correct in some cases; but in others the value of R_0 was found to be greater than the resistance observed fifteen seconds after the application of the voltage. The explanation suggests itself that R_0 is not the true resistance of the oil, but that there is a permanent contact effect at the electrodes which is independent of the passage of a current. The capacity and resistance effects of such a layer would conceivably give rise to absorption currents as outlined by Hartshorn*.

Whether R_0 is the true resistance of the oil or not, the values obtained for it by varying the thickness of the films by equal steps should differ by equal amounts. Also, since k and l would be expected to remain constant, the points obtained by graphing R , against I , should lie on a series of equidistant parallel lines.

If these deductions are correct, then on reversing the applied potential after the current had previously reached the steady state, the initial resistance would be the value of R , before reversal†. The contact layer which had been built up at the one electrode would be removed while a similar one was being built up on the other. The rate of removal of the previously-formed layer would be greater than the rate of formation of the new one, since in the former case the current and the forces of recombination would be both tending to remove the layer. Such a state of affairs does not lend itself to simple mathematical treatment, but it is evident that one would expect the current to rise to a maximum and then fall off to the value of I , before reversal.

So far, it has been assumed that a contact resistance is built up at one electrode only, but it is quite possible that one is formed at each electrode. It can easily be shown that in the latter case the relation between the resistance and the final current would still be linear. On reversing the applied potential, the rates at which the two films break

* *Loc. cit.*

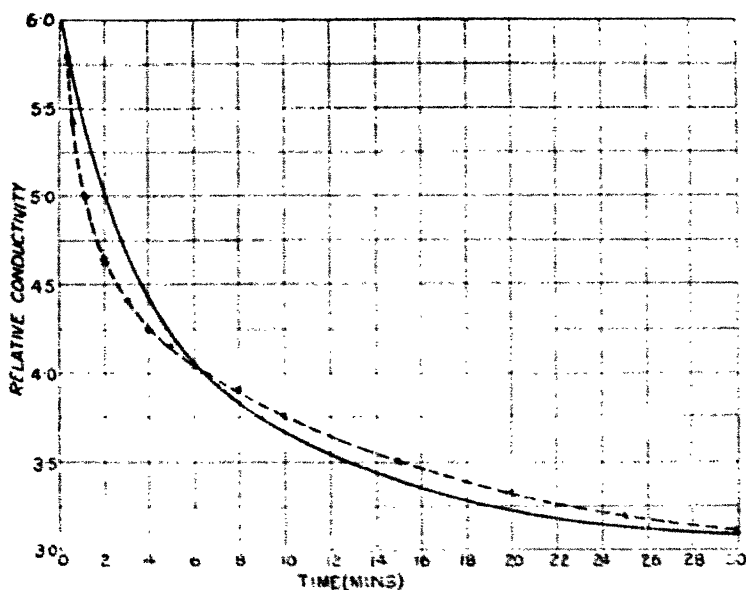
† The effect of the true capacity charges and discharges are not considered, as they would take place in a very small interval of time.

up might differ, and in that case one would expect to observe two maximum points. It is worth noting here that such a state of affairs is observed in some cases.

A comparatively simple equation connecting the resistance with the time of application of the potential can be found for the case in which a contact resistance is assumed to be built up at one electrode only, and the initial resistance is that of the oil itself. This is

$$t = -\frac{1}{l(R_s + r_s)} \left[R_s \log \frac{R_s - R}{r_s} + r_s \log \frac{R + r_s}{R_s} \right]. \quad (6)$$

Fig. 1.



Theoretical absorption curve. (Broken curve shows initial part of fig. 7.)

Fig. 1 shows the form of the curve obtained for the relationship between conductivity and time when $R_s = 3.33$, $R_0 = 1.66$, and $l = 0.06$. The broken curve shows the experimental values obtained on an oil as shown in fig. 7. By suitably adjusting the undetermined constants R_0 and l , a closer agreement between the observed and calculated values could be obtained. It is, however, felt that the above simple case is the exception rather than the general rule, and that the mathematical complications involved if contact effects take place at both electrodes and

if permanent contact effects are present make exact comparison between calculated and observed values extremely difficult.

Most workers on the subject seem to be of the opinion that the conductivity of liquid dielectrics is electrolytic in character. If such is the case, then the liquid may be considered as an electrolyte of practically infinite dilution, so that "ionic" dissociation may be considered as being complete. The conductivity of an electrolyte is proportional to the number of ions present and to their mobility. If dissociation is complete the number of ions will not change with temperature, and the conductivity should vary in the same way as the mobility. That is to say, one would expect the resistance of the liquid to be proportional to the viscosity. This applies to the resistance of the liquid itself; but should resistances be built up at the electrodes, one would not expect the measured resistance to vary in such a manner. It seems reasonable to assume that the value of k in equation (1) would not vary greatly with temperature; but one would expect the value of l to increase with temperature, just as the rate at which ordinary chemical reactions are known to increase. This would mean that the relative absorption would decrease as the temperature increased, and that the ratio of viscosity to final resistance would increase with temperature, the viscosity/temperature curve being much less steep than that for the resistance/temperature relation. Also, the value of the resistance measured at short time intervals after the application of the voltage and the value of R_0 obtained by varying the voltage across the film should change at a slower rate with the temperature than the ordinary final resistance measured under voltage.

It should be noted that the values of k and l are not to be expected to be similar for different liquids. In general it seems that for oils the greater the resistance of the oil itself the greater the value of the contact resistance built up for any given voltage. Thus the value of l seems to depend on the conductivity in such a way that the more ions there are present in the liquid the greater the tendency for the contact resistance to recombine. The reasons for this are not evident, but they may be connected with the results to be mentioned later dealing with the addition of moisture to oils. However, it is interesting to note that Crowther and Stephenson* observed a similar effect in ordinary electrolytes.

* *Loc. cit.*

Experimental.

The theory put forward above was developed from the consideration of experimental results obtained from insulating oils. The work, which is still in progress, was undertaken with a view to attempting to discover the fundamental nature of the electrical conductivity of liquid dielectrics. A great deal of time has been taken up in overcoming experimental difficulties, a description of which is too lengthy to be included here; and, so far, the results obtained have been mainly concerned with what may be termed the "anomalous effects" rather than with the conductivity of the oils themselves.

The oil under test was contained in a conical vessel forming one electrode and having an inner concentric electrode which was guarded at top and bottom. The vessel was sealed off from the atmosphere by means of two ground joints, and it was capable of being evacuated to comparatively low pressures. The film thickness could be accurately varied without opening the vessel in any way. The vessel and electrodes were constructed of brass, using bakelite for the necessary insulation, and the actual surfaces exposed to the oil were tinned to lessen any tendency to form sludge. The testing vessel was placed in an electrically-heated oven, the temperature of which could be regulated to keep the temperature of the oil film constant to within 0.1°C ., and by taking particular care the variations could be kept to 0.02°C . In general the resistance of the oil was measured by direct deflection methods, using a sensitive moving-coil galvanometer*.

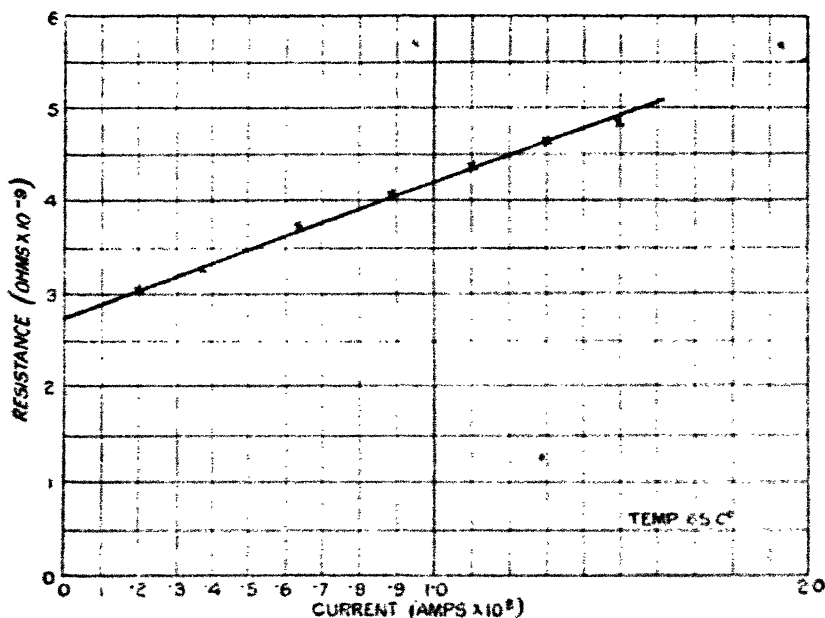
The liquids used were all oils of the paraffin series, and these were usually supplied in a carefully purified state. The only further treatment they received was vacuum drying when in the testing apparatus, this being usually carried out at a temperature of 60°C .– 70°C . The idea may be advanced that the vagueness of the constitution of the oils used detracts from the scientific value of the results; but it is very difficult to obtain liquids whose chemical constitution is definitely known and which are of sufficiently high resistivity to be considered as insulators. Moreover, since the effects studied do not deal with the nature of the oils themselves, but with

* It is obviously important to be able to measure the resistance of the oil films at very short intervals after the application of the potential. So far it has not been possible to do this, but it is hoped that a string galvanometer will be available in the near future when such observations will be attempted.

the electrode phenomena, it is thought that the constitution of the oils is, in the present case, of secondary importance.

Fig. 2 shows the straight-line relation between current and resistance for medicinal paraffin oil, and fig. 3 shows the same for a thin engine oil taken at several film thicknesses *. The curves were taken by varying the voltage in steps and leaving an interval of one hour at each change of voltage before taking a reading. In the latter case it will be observed that the points line on a series of equidistant parallel straight lines as indicated by the theory.

Fig. 2.

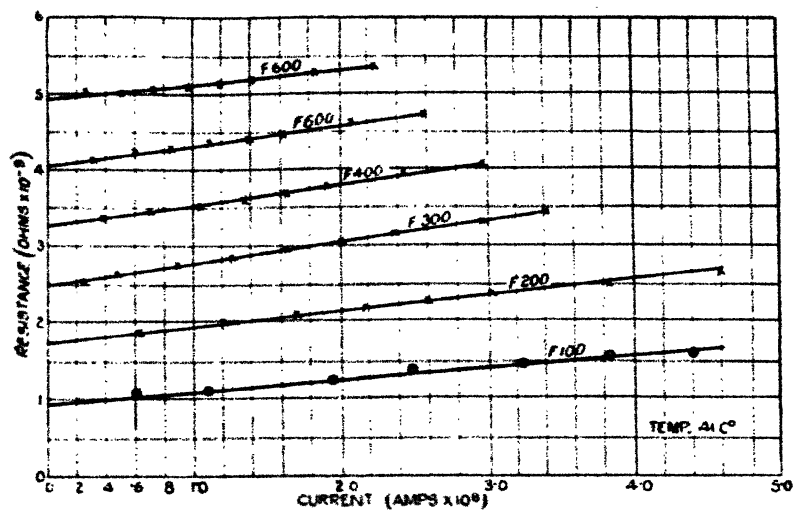


Relation between resistance and current for paraffin oil.

Fig. 4 is a diagram of the method used for increasing the proportion of the time of recombination to the time of current flow. The commutator consisted of a piece of heavy copper tubing, about 7 inches long and 3 inches in diameter, which was divided in two by a diagonal saw-cut. The two halves were mounted on a wooden cylinder supported on ball bearings. Two fixed brushes made contact with the two

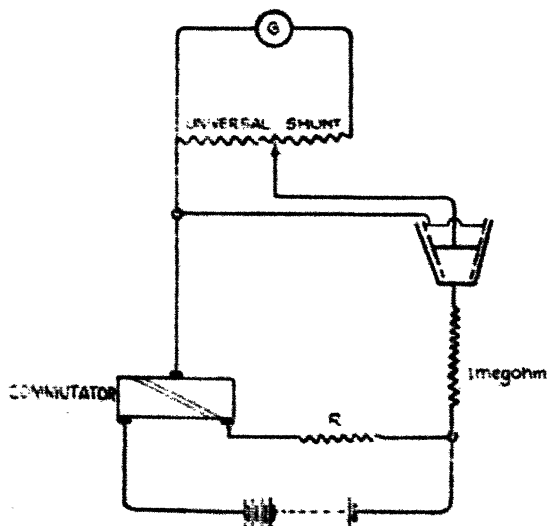
* The film thicknesses, when given, are expressed in divisions of the rotating head which varied the distance between the electrodes. The head was divided into 100 divisions, and 646 divisions on the head corresponded to 0.1 inch film thickness.

Fig. 3.



Relation between resistance and current for an engine oil.

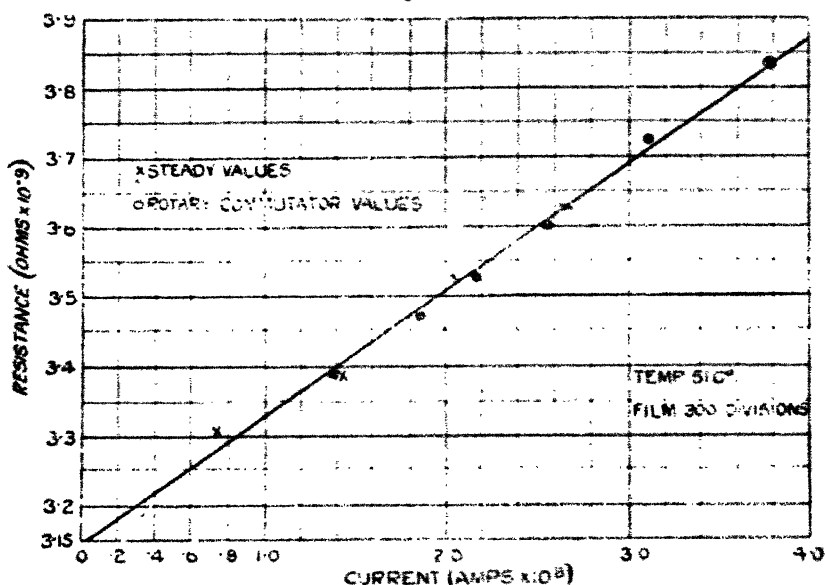
Fig. 4.



Connexions for rotary commutator.

segments, and a third brush could be adjusted so that the proportion of each segment which came into contact with it could be altered. The resistance R prevented the battery from being short-circuited while the movable brush made contact with both segments at once as it passed from one to the other. The value of R , 50,000 ohms, was small in comparison with the resistance of the oil film, and so did not affect the readings. Pure capacity and other reversible effects were eliminated, since both the charge and discharge currents passed through the galvanometer, but in opposite

Fig. 5.



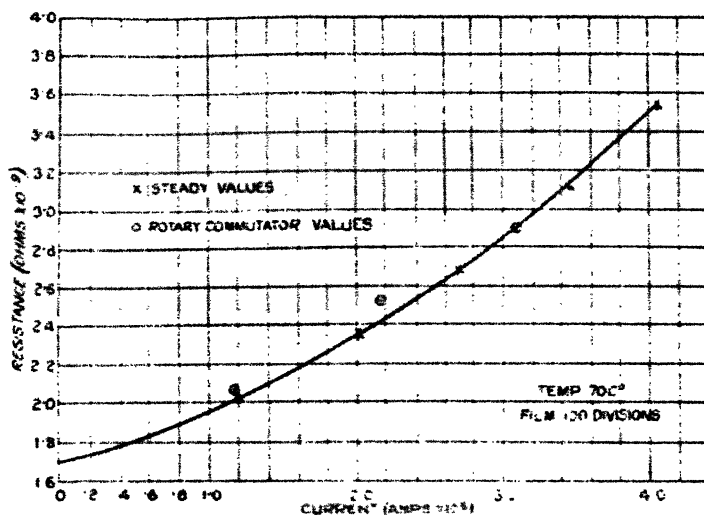
Showing agreement between values of resistance obtained by varying the voltage and by means of the rotary commutator.

directions. The commutator was run at a speed of from 1000 to 1200 revolutions per minute, and this gave a steady galvanometer deflexion. The method of obtaining the resistance values was quite straightforward, and fig. 4 shows that the resistance graphed against average current gives the same straight line as that obtained by varying the applied voltage.

While the general tendency seems to be for the resistance to have a linear relationship with the current flowing, yet such a simple state of affairs does not always exist. This is especially so in the case of freshly-prepared oil films, and

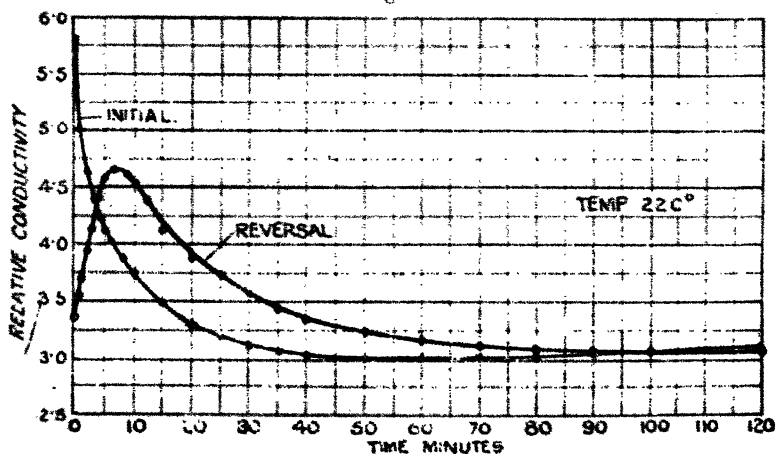
fig. 6 shows the resistance/current relationship for the same sample of oil as in fig. 5, but taken soon after the oil was introduced into the tester and also at different temperature and film thickness. It will be observed, however, that the

Fig. 6.



Showing non-linear relationship between resistance and current.

Fig. 7.



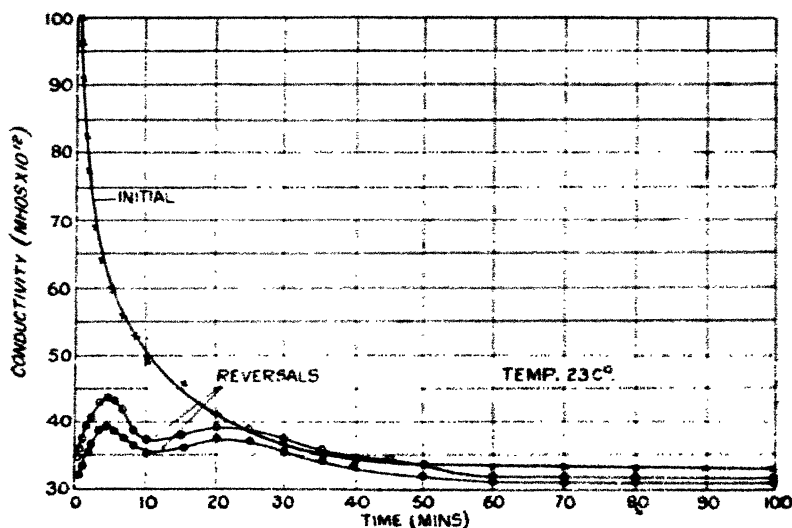
Relation between conductivity and time for transformer oil.

resistance values obtained by means of the rotary commutator lie approximately on the same curve as those obtained by varying the voltage.

Fig. 7 shows a typical absorption and reversal curve, the liquid being a transformer oil. It will be noticed that the curve obtained on reversal rises to a maximum and then falls away as indicated *. Fig. 8 is a similar curve showing the double maxima sometimes obtained on reversing the applied potential.

The resistance of an oil film sometimes varies according to the direction in which the current is flowing. This is easily explained by the theory, since the two electrodes may not have exactly similar surfaces, thus altering the values of k and l . This accounts for the fact that the two reversal

Fig. 8.



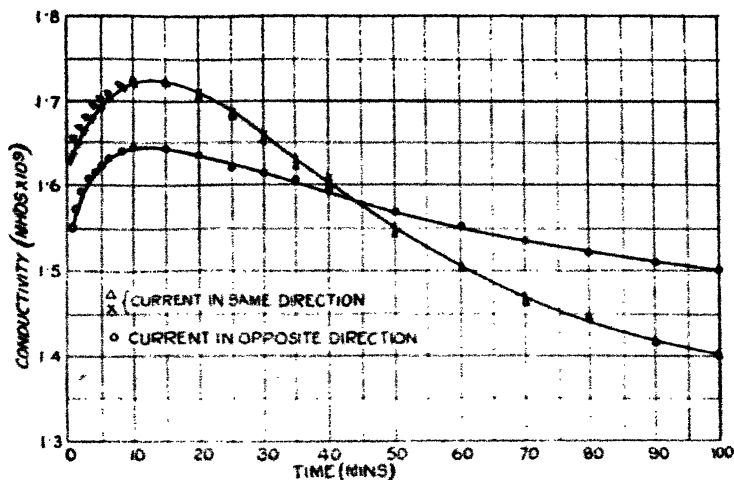
Conductivity-time curves showing double maxima on reversal.

curves in fig. 8 are not coincident. The phenomenon is shown more definitely in fig. 9. Curve I. shows the relationship with the current in one direction, and curve II. that with the current reversed. On reversing the current a second time the points obtained lie on curve I. once more.

Fig. 10 shows the ratio of viscosity to final resistance for medicinal paraffin. The points are plotted on a logarithmic scale for the sake of convenience. The fact that the resulting graph is a straight line may be of importance, but

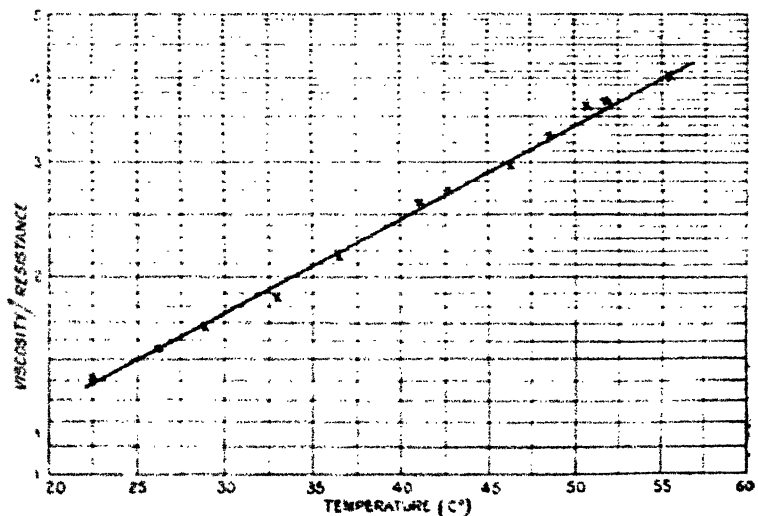
* Similar curves have been obtained for liquid bromine (Anderson, *Phys. Soc. Proc.* xl. p. 62, 1928) and for liquid sulphur (Black, *Proc. Camb. Phil. Soc.* xxii. p. 393, 1924).

Fig. 9.



Variation of conductivity with direction of current (transformer oil).

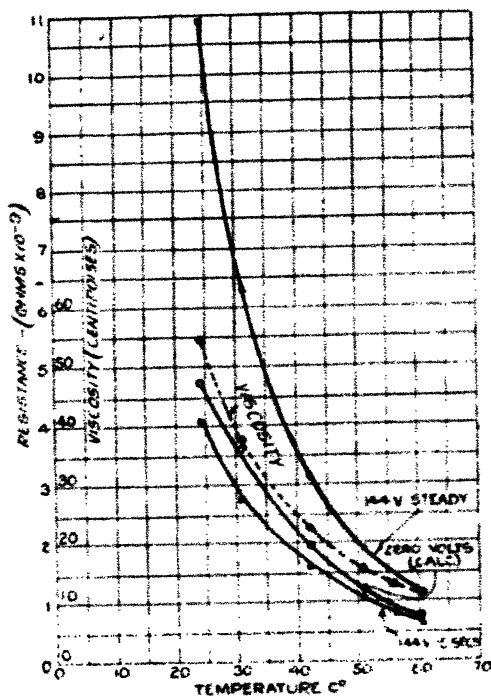
Fig. 10.



Variation of the ratio of viscosity to resistance with temperature (paraffin oil).

the main fact to notice here is that the resistance decreases much more rapidly than the viscosity. Fig. 11 shows the difference in the rate of change of resistance with temperature of an oil film of 0.46 inch thickness when measured 15 seconds after the application of the voltage and after a steady deflexion had been obtained; and in addition the values of R_0 obtained from the resistance/current relationships are shown for the different temperatures. It will be noticed

Fig. 11.



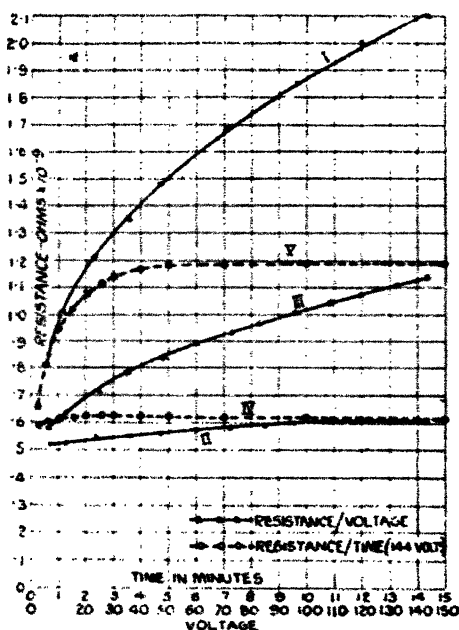
Effect of temperature on resistance and viscosity of an engine oil.

that the resistances measured after 15 seconds are less than the values of R_0 in each case, suggesting the presence of a contact resistance before the application of any voltage. The viscosity/temperature curve is seen to be more nearly parallel to the lower curves than to that obtained for steady values of resistance at 144 volts.

Some experiments have been made in an attempt to determine the effect of moisture on the resistance of an oil, and some of the results are of interest in the light of the

present theory. Moisture was brought into contact with the oil in the form of water vapour, at the same temperature as the oil, by connecting a small flask of water to the testing apparatus. The amounts absorbed were very small, and it was not found practicable to measure them with an ordinary chemical balance. In fig. 12, curve I. shows the resistance/voltage relationship before exposure to moisture, curve II. the same after 60 hours' exposure to moisture, and curve III. after 16 hours' vacuum drying after the exposure.

Fig. 12.



Showing effect of moisture on transformer oil (temp. $60^{\circ}\text{C}.$).

Curves IV. and V. show the resistance/time relationships at 144 volts corresponding to curves II. and III. respectively. The main effect of the moisture seems to be to reduce the value of the contact resistance built up without changing the resistance of the oil to any great extent, since all the five curves appear to cut the ordinate at approximately the same point.

It may be asserted that the above phenomena could also be explained by the assumption that space charges are set up in liquid dielectrics. However, this seems to be negatived

by two main facts :—(1) The absorption curve of an oil may take some hours to reach a steady value. If this were due to the gradual formation of a space charge, one would expect that, on removing the applied voltage and short-circuiting the film, the charge would take a similar length of time to disappear, and would give a residual current time curve comparable with the original absorption curve. Such is not observed in oils. (2) If a space charge is built up giving an opposing E.M.F., then on reversing the applied potential this space effect should be acting in the same direction, giving a larger current than that observed at the beginning of the original absorption curve. That such is certainly not the case is indicated by the reversal curves shown.

No mention has so far been made of the probable nature of the contact resistance. There is a certain amount of evidence to suggest that it exists in the form of a gas layer on one or both electrodes ; but until further experimental support is obtained it must be regarded as a tentative suggestion only.

Finally, it should be pointed out that, when a contact resistance is built up, the layer so formed may have a large capacity, and thus, when the final steady current has been attained, the combination of oil and contact layer may act as an ordinary two-layer dielectric, following ordinary Maxwellian theory. In the case of ordinary insulating oils, however, the residual effects so obtained would be small in comparison with the change in the resistance of the contact layer. It is conceivable that such an effect might be detected with an oil of very high specific resistance.

Summary.

A theory is put forward to account for the absorption current in liquid dielectrics. It is assumed that contact resistances are formed at one or both electrodes by the passage of an electric current, this causing the well-known decay of current with the time the potential has been applied across the electrodes. Experimental support of the theory is given, and it seems capable of explaining in a simple manner the anomalous conductivity phenomena observed in liquid dielectrics under D.C. stresses.

My thanks are due to the International Standard Electric Corporation for permission to publish these results.

I am also indebted to Mr. J. D. Cockcroft of the Cavendish Laboratory for much helpful criticism.

XL1. The Action of X-Rays on Colloidal Ceric Hydroxide.
*By J. A. V. FAIRBROTHER, B.Sc.**

INTRODUCTION.

IN a previous joint paper with Professor Crowther† we reported upon the action of X-rays on colloidal Iron, Copper, Silver, and Gold. It appeared that cationic sols, that is, sols in which the particles are attracted towards a negative pole, are coagulated, whilst anionic sols become more stable. Since then we have irradiated many more positive and negative sols and have found no exception to this rule. From the numerical investigation of a Bredig copper sol, it was suggested that coagulation was due to the destruction of the electrokinetic potential by ionization produced by the rays in the diffuse double layer surrounding the particles.

By measuring the viscosity changes produced in a viscous sol by X-rays, it was hoped to study and follow the changes taking place in the electrical state of the particles. The researches described in this paper were undertaken with this end in view.

Smoluchowski has developed the following formula for the viscosity of a colloidal solution :

$$\mu_s = \mu_w \left\{ 1 + 2.5 \phi \left[1 + \frac{1}{\lambda \mu_w r^2} \left(\frac{D\zeta}{2\pi} \right)^2 \right] \right\}.$$

μ_s and μ_w are the viscosities of the sol and water respectively.

ϕ is the volume of the particles in unit volume of the solution.

r is the mean radius of the particles.

λ the specific conductivity of the sol.

D the dielectric constant.

ζ the electrokinetic potential.

If it be assumed that ϕ , λ , and r remain constant, we can deduce a very simple relation between the viscosity of the sol and the electrical charge on the particles.

For
$$\frac{\mu_s}{\mu_w} = 1 + 2.5 \phi + K \zeta^2,$$

where K is a constant.

* Communicated by Professor J. A. Crowther, Sc.D.

† Crowther & Fairbrother, *Phil. Mag.* iv. August 1927.

If $\mu_{\phi 0}$ is the viscosity of the sol when the electrokinetic potential on the particles is destroyed, then

$$\frac{\mu_{\phi 0}}{\mu_x} = 1 + 2.5 \phi. \quad (1)$$

$$\therefore \frac{\mu_s}{\mu_x} - \frac{\mu_{\phi 0}}{\mu_x} = K \xi^2.$$

Now q , the charge on a particle, is proportional to ξ . It will also be proportional to $X - x$, where X is the X-ray dose required to discharge the particle completely, and x the dose which it has actually received.

Therefore

$$\frac{\mu_s}{\mu_x} - \frac{\mu_{\phi 0}}{\mu_x} \propto (X - x)^2. \quad (2)$$

We may conclude

- (1) That the curves obtained by plotting $\frac{\mu_s}{\mu_x}$ against x , the X-ray dose applied, should be parabolic in form.
- (2) That when all the particles have been discharged, the viscosity should be given by formula (1) above.

This formula is the one developed by Einstein relating the viscosity of a sol to the number of particles in unit volume, a formula in which no account is taken of the electrokinetic potential. If ϕ is small so that 2.5ϕ is negligible compared with unity, then

$$\mu_{\phi 0} = \mu_x,$$

and the viscosity of the sol should equal that of water.

Fernau and Pauli* have coagulated a positive ceric hydroxide hydrosol and denatured albumen with the rays from radium. This second observation has been repeated with X-rays†. In the case of ceric hydroxide hydrosol, they observed that the viscosity first decreased to a minimum, then rose rapidly, and that the sol finally set to a gel. This particular sol appeared well suited for such a research as we had in mind. Preliminary investigation showed it to be very susceptible to X-rays and to give marked viscous changes with varying doses.

* Fernau & Pauli, *Kolloid. Zeit.* xx. p. 20 (1917); *ibid.* xxx. p. 6 (1922).

† Fairbrother, 'British Journal of Radiology,' April 1928.

X-Rays on Colloidal Ceric Hydroxide.

EXPERIMENTAL DETAILS.

The experimental arrangements were similar to those described in the previous paper.

The source of radiation was a Shearer tube with a molybdenum anticathode, run at a P.D. of 55,000 volts and a current of 4 m.a. by means of a large induction coil and mercury break. The resultant beam consisted largely of molybdenum K-radiation with a mean coefficient of absorption in aluminium of 4.6.

The liquid to be exposed was contained in a small quartz boat 28 mm. by 9 mm. and 9 mm. deep. The beam completely filled the dish. 1 c.c. of liquid was always exposed, and filled the dish to a depth of 5 mm. An equal volume of the sol was placed in a similar dish and treated in exactly the same way. Both the exposed and control samples were sealed down under boxes, the tops of which were closed with thin glass cover-slips 0.2 mm. thick. By thus hermetically sealing the liquids, any changes brought about by exposure to the atmosphere were eliminated, and by comparing the exposed sample directly with the control, any changes brought about in the actual sealing process were eliminated also.

The viscosimeter consisted simply of a vertical capillary tube with an intermediate bulb of 1 c.c. capacity and a reservoir at the base. The liquid was sucked up from the reservoir, and the time taken for it to fall from a mark on the capillary above to a mark on the capillary below the bulb gave a measure of the viscosity. The instrument stood in a thermostat kept constantly at 20° C. The difference between the times taken by the exposed and control samples divided by the control time clearly gives the fractional change in viscosity. In these experiments the control time remained so constant that it was quite safe to assume that the changes in the exposed sample were due entirely to the radiation.

The intensity of the radiation was measured by means of an air-gap ionization chamber, so constructed that the volume of ionized gas between the plates was 1 c.c. A standard 1 mf. condenser was connected to the insulated plate of the chamber, and the radiation necessary to charge the condenser to a P.D. of 1 volt was taken as the unit of dosage, and will be referred to as a microcoulomb, or 1 mc. A dose of 1 mc. corresponds to a dose of 3000 e in the ionization chamber, where e is Friedrich's unit of dosage.

The window of the chamber was distant 10.75 cm. from

the focal spot of the tube. If the surface of the liquid is distant x cm. from the focal spot, the dose given to the exposed sample is $\left(\frac{10.75}{x}\right)^2$ mc. The time taken to apply a unit dose varied with the condition of the tube, but was usually about 20 minutes. In all sets of readings different doses were applied to the sol by varying the distance of the surface of the exposed sample from the focal spot. The dose measured in the ionization chamber was the same throughout any set of readings, so that the time taken to apply different doses was constant.

PREPARATION OF THE SOL.

About 5 gm. of ceric ammonium nitrate crystals were dissolved in 50 c.c. of distilled water. The solution was immediately poured into a glass bell-shaped dialyser covered with stiff parchment, and the whole stood in a dish of distilled water. Two factors are essential for successful preparation. First, dialysis must take place as uniformly as possible throughout the sol. This is ensured by using a large membrane surface. Secondly, the dialysis must be slow. For this reason, rather than remove the dialysate with a stream of running water, the dialyser stood in a dish of distilled water, which was removed every four or six hours. Under these conditions and after about three days a beautiful lemon-coloured viscous sol of ceric hydroxide is obtained. If this is now stored in a hard glass or quartz flask, a spontaneous increase in viscosity ensues, and the liquid eventually sets to a clear stiff gel. If this stock is diluted before gelling takes place, the viscosity continues to increase, though less rapidly, and by repeating the dilution a sol is obtained which is quite thick, and the viscosity of which may be considered to remain sensibly constant for a number of hours.

RESULTS.

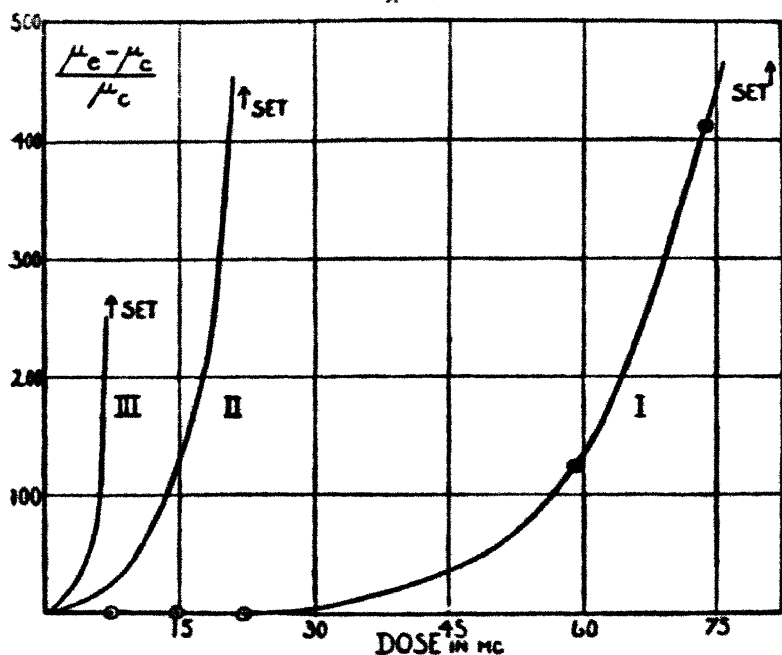
A. Susceptibility of the sol to X-rays with ageing. (Figs. 1 & 2.)

A solution of 5 gm. of ceric ammonium nitrate in 50 c.c. of distilled water was dialysed from November 26th to 29th, and the resultant sol stored in a quartz flask. When irradiated, it showed an increase in viscosity, the rate of increase becoming rapidly larger with increasing doses. Finally, the sol set to a gel. A similar viscosity increase takes place with age although two or more weeks elapse before the sol

sets. If μ_e and μ_c represent the viscosities of the exposed and control samples respectively, then $\frac{\mu_e - \mu_c}{\mu_c}$ is the percentage change in viscosity. In fig. 1 are plotted values of $\frac{\mu_e - \mu_c}{\mu_c}$ against the corresponding X-ray doses for the same sol on three different days.

(Curve I. was taken on December 1st, three days after completion of dialysis. Initially, the viscosity increase is

Fig. 1.



very small. It then increases rapidly and the sol gels with a dose of 81.1 mc.

The behaviour of the same sol on December 5th and 6th is given in curves II. and III. respectively. On December 5th it was set to a gel by a dose of 22.1 mc., and on December 6th by 7.4 mc. Thus, as the sol ages, its viscosity continually increasing, it becomes very much more sensitive to X-rays. The water value of the viscosimeter used was 7.2 seconds, and the control times on the three days December 1st, 5th, and 6th were 8.0, 10.3, and 11.0 seconds. If μ_w denotes the water value of the viscosimeter, then $\frac{\mu_e - \mu_w}{\mu_w}$ is the

percentage excess of the viscosity of the control over that of water. Throughout the experiments there was never found any appreciable difference between the viscosities of the stock sol and the control, so that the control time may be taken to mean as well the stock time.

The data for these curves are collected in Table I.

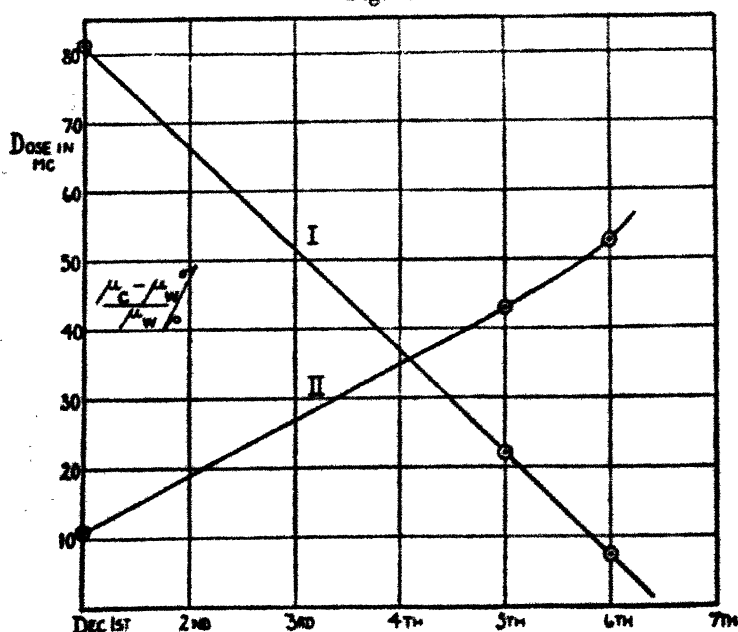
TABLE I.

Control time (seconds).	Date.	Gelling dose. (mc.).	$\frac{\mu_c - \mu_w}{\mu_w}$ %.
8.0	Dec. 1st	81.1	11.1
10.3	Dec. 5th	22.1	43.0
11.0	Dec. 6th	7.4	53.8

Time taken to apply to each dose = 40 minutes.

Water value of the viscosimeter = 7.2 seconds.

Fig. 2.



The straight line I. in fig. 2 is obtained by plotting the dose required to set the sol to a gel against the days. The fact that this dose decreases linearly with time suggests that the ageing effect and the action of the radiation are additive.

In curve II. $\frac{\mu_s - \mu_w}{\mu_w}$ is plotted against the time. The relation is almost a linear one over the period studied, but the curve begins to curve upwards, and would continue to do so more and more rapidly until finally the sol gelled.

B. Change in viscosity produced by the rays in sols of different concentrations. (Figs. 3 & 4.)

Portions of a fresh and rather viscous stock sol were diluted with distilled water to give solutions of one-half, one-third, one-quarter, and one-eighth the concentration. If the strength of the stock sol made by dialysing a solution of 5 gm. of ceric ammonium nitrate in 50 c.c. of water is denoted by S , then the concentrations of these new sols can be represented by $\frac{S}{2}$, $\frac{S}{3}$, $\frac{S}{4}$, and $\frac{S}{8}$. Samples of these sols were placed with the surface of the liquid distant 2.8 cm. from the focus of the tube, and a dose of 1 mc., as measured in the ionization chamber, given to each. Since the distance of the chamber window from the focal spot on the tube was 10.75 cm., the dose actually incident upon the surface of the liquid exposed was $\left(\frac{10.75}{2.8}\right)^2 = 14.75$ mc. This was the same for each sample. The percentage change in viscosity $\frac{\mu_s - \mu_c}{\mu_c}$ produced by this dose in each solution was plotted against the concentration. The resultant curve is given in fig. 3 and the data in Table II.

TABLE II.

Concentration.	μ_c (seconds).	μ_s (seconds).	$\frac{\mu_s - \mu_c}{\mu_c}$ %.
$\frac{S}{2}$	65.3	77.2	+18.3
$\frac{S}{3}$	34.9	36.2	+3.8
$\frac{S}{4}$	27.1	26.2	-3.5
$\frac{S}{8}$	19.8	19.0	-3.8

Water value of viscosimeter = 10.5 seconds.

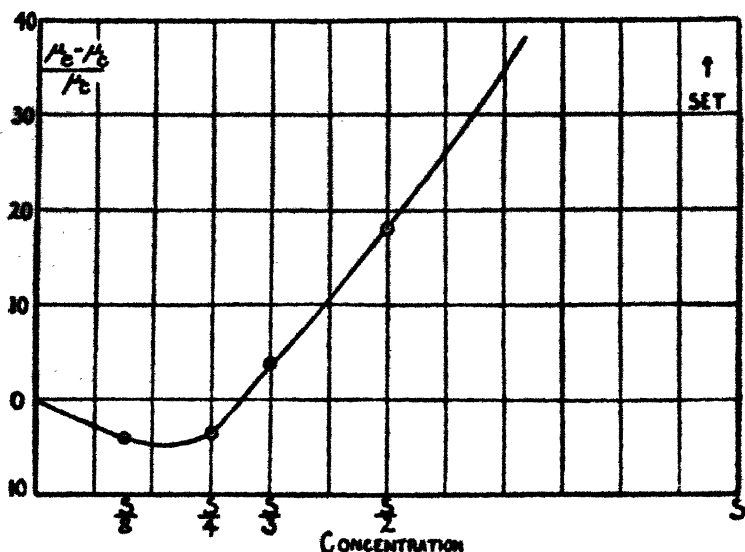
X-ray dose given = 14.75 mc.

Time taken to apply the dose = 20 minutes.

Sols of low concentration show quite a marked decrease in viscosity with a dose of 14.75 mc., whereas the stock solution from which the more dilute ones were prepared is set to a gel by the same dose.

In fig. 4 $\frac{\mu_{\text{exposed}}}{\mu_{\text{water}}}$ is plotted against varying X-ray doses for sols one-third, one-fourth, and one-sixth the stock concentration. These sols are denoted by $\frac{S}{3}$, $\frac{S}{4}$, and $\frac{S}{6}$. Each one was made on the day of investigation by diluting a portion of the same stock. Curves I. and IV. apply to the

Fig. 3.



sol of $\frac{S}{4}$, but curve IV. was taken two weeks after curve I.

The data for the curves of fig. 4 are set out in Table III.

According to the theory discussed in the introduction to this paper we should expect the curves obtained by plotting

$\frac{\mu_{\text{exposed}}}{\mu_{\text{water}}}$ against the X-ray dose to be parabolic in form.

Instead, the value of $\frac{\mu_{\text{ex}}}{\mu_{\text{w}}}$ decreases rapidly at first and then gradually approaches a limiting value. In the case of Curves I., II., and III. the limiting value is almost equal to unity, whilst that of curve IV. is not greater than 1.25.

TABLE III.

Distance of liquid surface from focus.	Dose (mc.)	I.		II.		III.		IV.	
		8 4 Jan. 24th.		8 6 Jan. 26th.		8 3 Jan. 27th.		8 4 Feb. 28th.	
		μ exposed (seconds).	$\frac{\mu \text{ exposed}}{\mu \text{ water}}$	μ ex.	$\frac{\mu \text{ ex.}}{\mu \text{ w.}}$	μ ex.	$\frac{\mu \text{ ex.}}{\mu \text{ w.}}$	μ ex.	$\frac{\mu \text{ ex.}}{\mu \text{ w.}}$
* —	0	17.30	1.697	15.39	1.510	25.72	2.521	52.80	5.130
6.30	2.90	—	—	11.40	1.118	—	—	—	—
5.30	8.24	13.14	1.289	10.40	1.020	16.10	1.579	15.20	1.480
3.30	21.26	10.75	1.054	10.21	1.021	11.01	1.168	16.12	1.580
2.60	29.50	10.73	1.052	10.22	1.002	11.43	1.123	30.65	3.005
2.30	43.62	10.35	1.015	11.27	1.104	13.87	1.360	gelled	∞
1.88	65.43	11.87	1.163	13.68	1.340	gelled	∞	—	—
† 2.3	87.24	30.96	3.018	18.90	1.854	—	—	—	—

Distance of ionization chamber window from the focus of the X-ray tube = 10.75 cm.

Water value of viscosimeter = 10.20 seconds.

Time taken to apply each dose = 30 minutes.

* Along this line μ exposed = μ control; the control time.

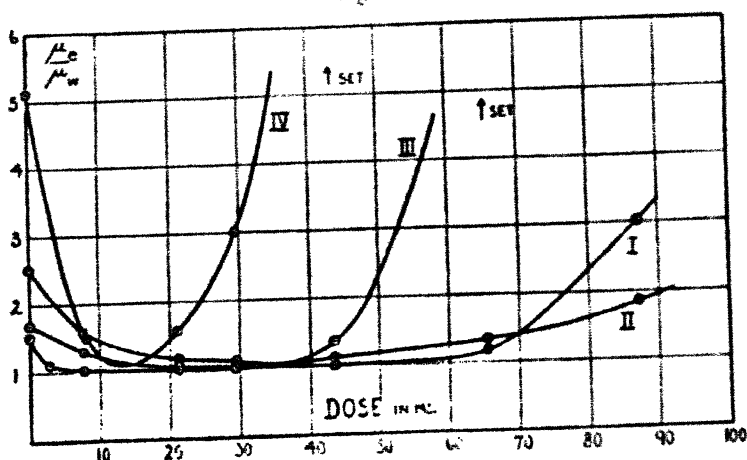
† Time taken to apply this dose = 60 minutes.

Table IV. gives the approximate dose, as deduced from the curves of fig. 4, necessary to produce the maximum decrease in viscosity in each of the sols investigated, and the date on which each curve was obtained.

TABLE IV.

	I.	II.	III.	IV.
	Jan. 24th.	Jan. 26th.	Jan. 27th.	Feb. 6th.
Dose in mc. producing maximum decrease in viscosity	45	33	35	13
Concentration	8	8	8	8
	4	6	3	4

Fig. 4.



If we regard the difference between the doses producing the maximum decrease in curves II. and III. as being insignificant, the difference lying within the limit of the error in reading the minimum points on the curves, then we can say that the dose required to produce the maximum lowering of the viscosity decreases with the age of the stock sol from which each of the solutions were made. This is in agreement with the observations made in Section A.

The fact that the curves are not parabolic must be due to a variation of one of the factors ϕ , λ , and r the mean radius of the particles, which, in the theory, were assumed to remain constant. Experiments described in Section C showed that

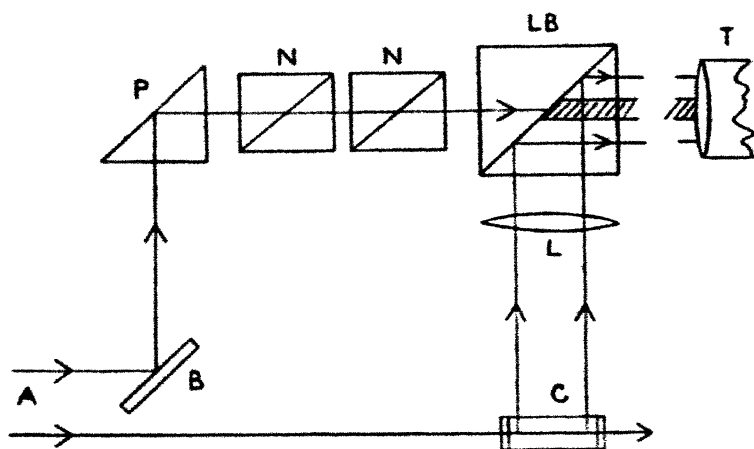
the mean radius of the particles was decreasing up to the position of minimum viscosity.

C. Change in size of the particles with varying doses of X-rays. (Figs. 5 & 6.)

In order to study the changes, if any, in the average size of the particles, use was made of the Tyndall meter, an instrument devised by Mecklenburg for comparing the intensities of two beams of light.

A parallel beam of light A (fig. 5), in this case a pointolite projected with Zeiss projecting apparatus, is allowed to pass

Fig. 5.

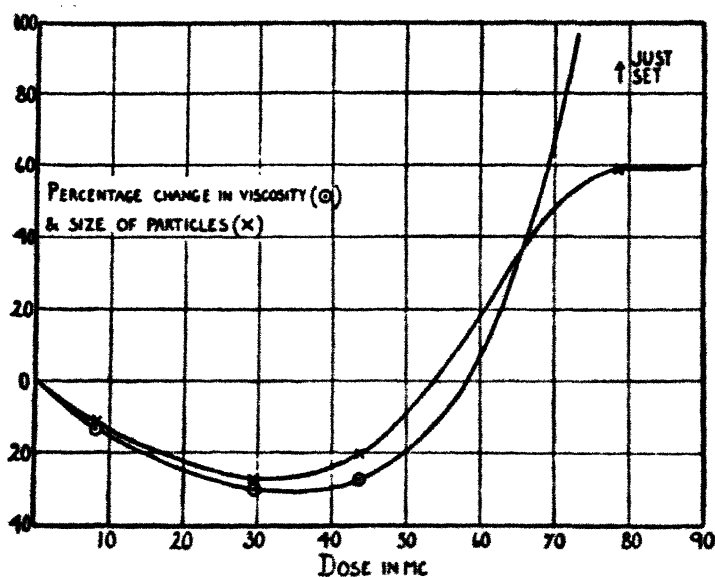


through the solution contained in a cylindrical glass tube C, closed at the ends with thin plate-glass. Half of the beam is diffusely reflected upwards by means of a plaster-of-paris slab B, and again made parallel to the original beam by means of a right-angled prism P. This beam then passes through two Nicol prisms NN and through the central spot of a Lummer-Brodhun cube LB, into the telescope T. The light scattered in the tube C is collected by the lens L and reflected as a parallel beam into the telescope. By rotating one of the nicols, the intensity of the upper beam can be cut down until equal to the lower, in which case a uniform field is seen in the telescope, the central spot disappearing entirely. The intensity of the upper beam is reduced by suitable filters until it is nearly equal to that of the beam of scattered light. In this case the principal planes of the

nicols make an angle of about 45° with one another when a uniform field is seen in the telescope and the accuracy of comparison of the beam is then a maximum. If θ_1 and θ_2 are the angles between the principal planes of the nicols for beams of intensities J_1 and J_2 when a uniform field is seen in the telescope, then

$$\frac{J_1}{J_2} = \frac{\cos \theta_1}{\cos \theta_2}.$$

Fig. 6.



The intensity of light scattered is given by

$$J \propto \frac{nv^2}{\lambda^4}.$$

n is the number of particles per c.c.

v^2 the mean of the squares of the volumes of the particles.

λ the wave-length of the incident light.

The concentration c of the sol is

$$c = n \cdot v \cdot \rho,$$

where ρ is the density of the particles, and for the same sol c remains constant, so that we may write

$$J_1 \propto \frac{v_1 c}{\lambda^4 \rho}, \quad J_2 \propto \frac{v_2 c}{\lambda^4 \rho}.$$

$$\frac{J_1}{J_2} = \frac{v_1}{v_2} = \frac{\cos \theta_1}{\cos \theta_2}.$$

In fig. 6 the percentage change in the average size of the particles and the percentage change in viscosity of the sol, which, in this case was one-fourth the concentration of the usual stock solution, are plotted against the X-ray doses. The data are given in Table V. It is rather surprising that the percentage decrease in the size of the particles from the origin to the minimum viscosity point is proportional, and, in fact, almost equal, to the fractional change in viscosity. After the minimum point is reached gelling sets in, and the particles show a maximum increase of about one and a half times their normal size.

TABLE V.

Distance of liquid surface from focal spot. (cm.)	Dose (mc.)	μ exposed (seconds).	μ control (seconds).	$\frac{\mu \text{ ex.} - \mu \text{ con.}}{\mu \text{ con.}} \%$	$\theta \text{ ex.}$	$\theta \text{ con.}$	$\frac{\cos \theta \text{ ex.}}{\cos \theta \text{ con.}}$	Percentage change in size of particles.
5.3	8.2	20.8	24.0	-13.3	61.3°	57.5°	.895	-11
2.8	20.5	17.2	24.6	-30.1	70.3°	62.2°	.72	-28
2.3	43.6	17.8	24.3	-26.8	66.5°	59.6°	.80	-20
2.1	78.6	Just set.	24.3	∞	33°	58°	1.59	+50

Water value of viscosimeter = 10.2 seconds.

Time taken to apply each dose = 30 minutes.

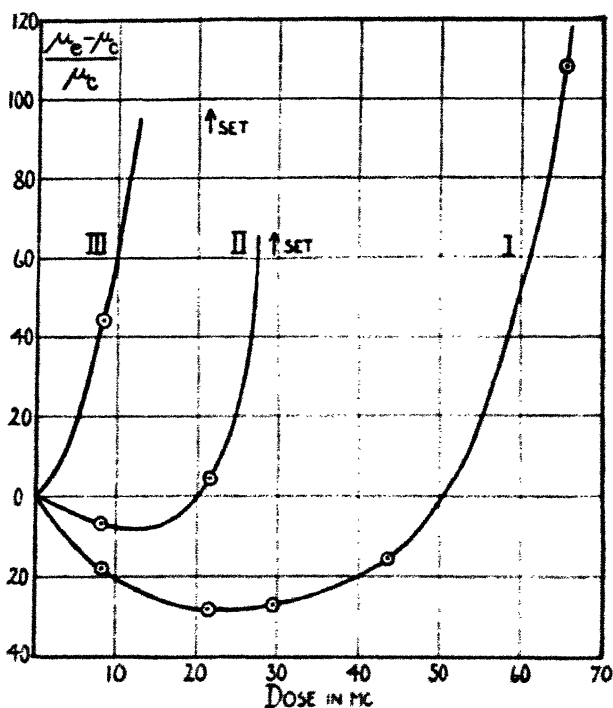
* Time taken to apply this dose = 45 minutes.

D. Gelling after the isoelectric point has been reached. (Fig. 7.)

Although it has not been definitely proved, it is reasonable and will be assumed that the position of minimum viscosity of the sol corresponds to the stage at which all the particles are discharged; that is, when the sol is at the isoelectric

point. The spontaneous setting which takes place after this point has been reached is not nearly so rapid as might be expected. Observations were made on a sol one-third the concentration of the standard stock sol. The percentage change in viscosity was plotted against the X-ray dose (curve I. fig. 7). The samples with which this curve was obtained were kept and measured again 21 hours and 92.5 hours after exposure (curves II. and III.). It is seen

Fig. 7.



that a sample which had suffered the maximum decrease in viscosity had only exceeded its original value by 4 per cent. after 21 hours. The sample with a dose of 29.5 mc., which was a little in excess of the completely discharging dose, had just set after 21 hours. It is quite safe to say that in the case of these sols of low concentration, the spontaneous setting which ensues after the minimum viscosity point has been reached takes at least several hours for completion. On the other hand, if irradiation is continued sufficiently beyond the isoelectric point, the sol sets immediately to a

clear stiff gel. The rays must be regarded therefore as accelerating the gelling process.

Data for the curves of fig. 7 are given in Table VI.

TABLE VI.

Distance of liquid surface from focal spot (clear). (cm.)	Dose (mc.)	μ exposed (seconds).	μ control (seconds).	$\frac{\mu_{ex} - \mu_{con.}}{\mu_{con.}}$ %	Percentage change after 21 hrs.	Percentage change after 92.5 hrs.
5.30	8.24	16.33	19.95	- 18.3	-6.73	+43.8
3.30	21.26	14.37	19.85	- 27.4	+4.44	Just set.
2.80	29.50	14.91	19.98	- 25.4		
2.30	43.62	16.80	19.96	- 15.8		
1.88	65.20	41.75	19.95	+108.5		

Time taken to apply each dose = 44 minutes.

Water value of the viscosimeter = 10.2 seconds.

DISCUSSION.

It was pointed out in the previous paper that the effect of the radiation on the solution is to liberate a number of fast β -particles, each of which produces several hundreds of pairs of ions. On account of the intense electric field surrounding the particles, the ions produced in the electrical double layer will be drawn out of the field before any appreciable recombination has taken place. If the number of β -particles lost by a colloidal micelle is less than the number of ions captured, its charge will be neutralized. Calculation shows that this condition is satisfied. The particles will therefore be discharged by the rays with a consequent decrease in the viscosity of the sol. In the case of a hydrophobic sol, coagulation and precipitation begin directly the isoelectric point is reached. The stability of hydrophilic sols depends also on a second factor, the hydration. The particles of such a solution must be regarded as being surrounded by a ring of attached water molecules. When their charges are neutralized, this hydration persists and prevents them aggregating and precipitating. Instead, they cling together, producing an increase in viscosity, eventually forming a rigid framework or lattice when the solution sets to a gel.

The spontaneous gelling which sets in directly the isoelectric point is reached for any number of particles will, in more concentrated sols, mask the initial decrease in viscosity. This is happening in the curves of fig. 1. In a less concentrated sol, however, the time taken for a discharged particle to find a partner will be very much longer, and if the exposure is not too prolonged we may expect to study the initial viscosity decrease before coagulation has set in to any appreciable extent. Such a study is made in Section B.

The ageing of the sols is due to a gradual diminution of the charges on the particles with consequent slow coagulation.

Since the size of a colloidal micelle must be taken to include the surrounding ring of hydrating water molecules, the decrease in size up to the isoelectric point may be due to a decrease in hydration. It seems probable that the hydration will depend upon the charge on the particles, and that the smaller their charge the smaller are the forces binding the water molecules.

Discussing the coagulation of a ceric hydroxide sol by radium radiation, Freundlich* states "that only the discharge and the decrease in viscosity appear to be caused by the radium radiation, for the rise in viscosity also occurs when the radium preparation is removed from the sol at the moment when the viscosity is at a minimum." In this research X-ray doses sufficiently in excess of that required to produce complete discharge will coagulate the sol immediately, and can be regarded as accelerating the gelling process, which in the case of the sol investigated in Section D would have taken several hours for completion.

SUMMARY.

(1) A quantitative study is made of the viscosity changes produced in ceric hydroxide hydrosol by X-rays.

(2) a. In sols of low concentration and with increasing X-ray doses the viscosity decreases to a minimum, then increases rapidly and the sol sets to a rigid gel.

b. In more concentrated sols the spontaneous increase in viscosity which takes place when the particles are discharged masks the initial decrease.

c. The sols become more sensitive to X-rays with age, and the doses required to produce the maximum decrease in viscosity and to set the sol to a gel

* 'Colloid and Capillary Chemistry,' p. 485.

become very much smaller, indicating that the charge upon the particles is decreasing.

(3) *a.* When the position of minimum viscosity is reached the sol sets spontaneously to a rigid gel within the course of a few hours.

b. An X-ray dose sufficiently in excess of that required to produce the maximum decrease will set the sol to a gel immediately.

(4) In a particular sol studied the particles decreased in size up to the position of minimum viscosity. The percentage decrease in size was almost equal to that in viscosity. Beyond the minimum point the particles increased in size, reaching a maximum at the setting point of 1.6 times the normal value.

In conclusion, I should like to thank Professor Crowther for his particular interest, kind help, and advice. He has intimated his intention, in a future paper, to review and comment upon the researches carried out in this laboratory during the past two years on the colloidal state of matter. I should also like to express my indebtedness to the Board of Scientific and Industrial Research for a grant which has made this work possible.

Department of Physics,
University of Reading,
June 8th, 1928.

XLII. *On the Thermal Measurement of X-ray Energy.* By J. A. CROWTHER, M.A., Sc.D., F.Inst.P., Professor of Physics in the University of Reading, and W. N. BOND, M.A., D.Sc., F.Inst.P., Lecturer in Physics *.

Introduction.

THE experiments described in this paper were commenced early in 1926 to determine the relation between the ionization produced by a beam of X-rays and the energy of the beam. The matter is of importance both from a theoretical and a practical aspect. In the first place, early experiments, as for example those of Rutherford and McCullung, indicated that the work spent per ion during

* Communicated by the Authors.

ionization by X-rays was considerably greater than the ionizing potential of the gas ionized, and it is desirable that this result should be tested further. In the second place, it is generally agreed that the most suitable method of measuring quantities of X-rays is by the ionization they produce in some suitable form of ionization chamber, and it is clearly desirable that experiments should be made to determine exactly what it is that an ionization chamber measures. At the time when we commenced our work there seemed to be no adequate data on this point, and it was hoped that such data might be supplied by the experiments we had in mind.

Neglecting secondary effects which may be produced by the presence of the electrodes used for measuring the ionization current, the number of electrons produced per unit volume of air by the passage of a beam of X-rays can depend only on two factors, the energy conveyed by the beam, and the wave-length of the radiation, and can be written in the form $I = \phi(E, \lambda)$. If the values of E and I can be determined for a sufficient number of values of λ , the nature of the function can be determined. The ionization, I , can be determined in some suitable ionization chamber, and the energy E by absorbing the radiation completely in a calorimeter and measuring the energy in the form of heat. This is what we set out to do.

The necessity for such measurements seems to have become apparent to other experimenters at about the same time, and during the progress of our experiments a number of such determinations have been published, amongst others by Kriegesmann*, Kircher and Schmitz†, Kulenkampff‡, and Rump§. It appeared at first sight that further work on our part might be superfluous. Unfortunately, however, there was such strong disagreement between the values published by the different authors that further investigation became imperative. Thus Kriegesmann finds that the work spent in producing a pair of ions varies from 87·8 volts for X-rays of mean wave-length 0·397 Å.U. to 132 volts for a wave-length of 0·166, and states that the "volts" required to produce an ion-pair increases as the wave-length diminishes. Kircher and Schmitz, on the other hand, give a value of 21 volts per ion-pair, and find that it is independent of the wave-length. Kulenkampff, in a very long and elaborate

* Kriegesmann, *Zeit. für Phys.* xxii. p. 542 (1925).

† Kircher & Schmitz, *Zeit. für Phys.* xxxvi. p. 481 (1926).

‡ Kulenkampff, *Ann. der Phys.* lxxix. p. 97 (1926).

§ Rump, *Zeit. für Phys.* xliii. p. 254 (1927), and xliv. p. 396 (1927).

paper, agrees that the energy spent is independent of the wave-length, but gives its value as 35 ± 5 volts per pair of ions. Finally, Rump gives values for the same quantity ranging from 300 volts for long wave-length radiation down to about 40 volts for filtered radiation from a hard tube. It was clear, therefore, that in spite of much recent work, the constant required was still in very considerable doubt. It was also clear that its determination was full of pitfalls, and that great care would be necessary to avoid both errors of measurement, and errors in evaluation of the constant from the measurements taken.

General Plan of the Experiment.

The radiation was produced by a Shearer tube working on a two-kilowatt transformer, and having a molybdenum anticathode. Two windows in the tube, closed with aluminium foil 1/20 mm. thick, allowed two narrow pencils of rays, one vertical, the other horizontal, to leave the tube. The horizontal beam passed through a small ionization chamber A, having parallel plate electrodes of aluminium. This chamber was used for comparison purposes only, as a means of eliminating the effect of fluctuations in the output; the actual measurements used in calculation were all made on the vertical beam. The tube was controlled by adjusting the supply of air to it by means of a micrometer air-leak. As the tube is self-rectifying its condition cannot be determined with any accuracy by means of a spark-gap, since the spark-gap measures only the peak potential in the circuit, which, in the case of a self-rectifying tube, occurs in the half wave which does not pass through the tube. The peak potential, when the tube is taking a current, will clearly be less, and may be considerably less than this. To overcome this difficulty a milliammeter with an open scale was inserted in the tube circuit, and an A.C. voltmeter was connected across the primary terminals of the transformer. It was found, experimentally, that a given pair of readings on these instruments corresponded to a definite state of the tube. If, for example, the voltmeter was set, by adjusting the primary resistance, to read 155 volts, and the milliammeter, by adjusting the leak, to read 3 milliamperes, the output from the tube was of definite quality and intensity, which was found to be reproducible at any time to an accuracy of at least 1 per cent. This method of regulating the tube is much more convenient than the use of a spark-gap, and seems to be at least as accurate.

The anticathode end of the tube was efficiently water-cooled. It was, however, of the utmost importance to prevent any thermal radiation from the tube from reaching the calorimeter in which the X-ray energy was measured. A "water-sheet" was therefore introduced between the tube and the calorimeter. This consisted of two parallel sheets of stout brass with a space about 1 mm. thick between them, through which a constant stream of water could be passed. A circular hole, 1.007 cm. in diameter, was pierced through the double sheet, the holes being covered with thin celluloid sheets to make the system watertight. This hole came immediately below the window of the tube, and served as the stop limiting the vertical beam passing into the calorimeter. Thus all the energy passing through the "water-sheet" passed directly into the calorimeter. Since it is convenient that the horizontal and the vertical beams should be of the same composition, sufficient thickness of cellophane was introduced into the horizontal beam to equalize the absorption of radiation in the vertical beam due to the water-sheet. The efficiency of the water screen is discussed in a later section.

After penetrating the water screen the vertical beam passed either into the calorimeter, which is described later, or into the ionization chamber which was used as a standard for the experiment. This chamber was furnished with a shutter, actuated by a carefully graduated micrometer screw, which limited the beam entering the chamber. The collecting electrode of this chamber could be connected, when desired, to the same electroscope as that attached to the comparison chamber A. A standard mica condenser could also be connected to the electroscope when necessary. The details of the ionization measurements will be discussed more fully in a later section.

The course of the experiments was as follows. The calorimeter was inserted in the path of the rays. The standard ionization chamber was cut out of the electroscope system, leaving the comparison chamber A attached to the electroscope and to the standard condenser. The tube was then excited, and kept working in its standard condition until the deflexion of the electroscope indicated a rise in potential of approximately one volt. The actual voltage was then measured by means of a potential divider in the usual way. The total charge which the X-rays had allowed to pass across the comparison chamber during the run could thus be measured. The condenser used was a subdivided microfarad, and the charge conveyed across the ionization chamber

in a single run was usually of the order of a microcoulomb. As evidence of the certainty with which the tube condition could be reproduced, it may be mentioned that the time taken to produce a charge of one microcoulomb on the condenser for a given setting of the tube did not vary by more than a few seconds in about eight minutes, over a period of some months.

In this way determinations were made of the heat produced in the calorimeter in relation to the charge conveyed across the comparison chamber. The calorimeter was now removed and the rays allowed to fall on the shutter of the standard chamber, which was now connected to the electro-scope system. The standard chamber was charged to a potential of opposite sign to that of the comparison chamber, and the area of the shutter was adjusted until a balance was obtained in the electroscope with the rays passing through both chambers. In order to increase the sensitivity, the condenser was removed from the system during balancing experiments. It was possible to balance the two currents to an accuracy of one part in a thousand. Balances on different occasions, however, were only consistent to about one per cent. These variations probably indicate the limits of certainty to which the tube conditions can be controlled.

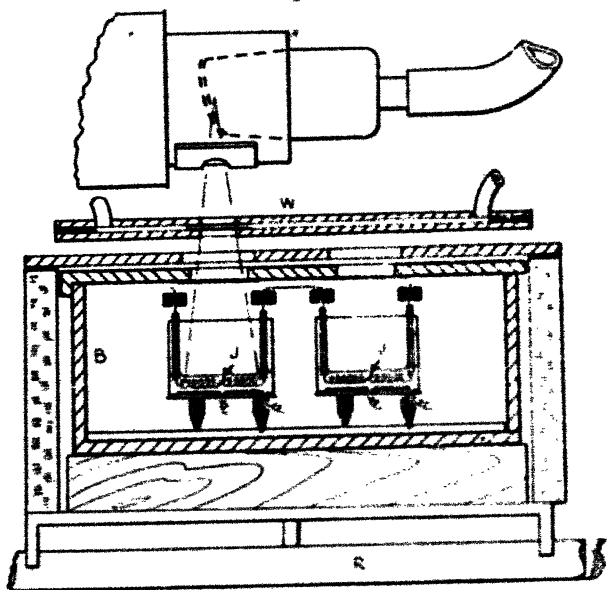
Assuming the whole area of cross-section of the vertical beam in the plane of the shutter to be known, the ionization which would have been produced if the whole of the X-ray energy which is absorbed in the calorimeter had passed through the standard chamber, is equal to the ionization as measured in the comparison chamber multiplied by the ratio of the cross-section of the whole beam to the aperture of the shutter. The results of these determinations are given in Tables III. and IV., and a more detailed account of the observations in the following section.

The Energy Measurements.

The accuracy of the energy measurements depends on our being able to absorb the whole of the incident X-ray energy, and to transform it into heat at the proper place. Owing to the phenomena of scattered, fluorescent, and corpuscular radiation, it is impossible to find a surface which will do this. The only reliable method is to pass the radiation into a box, the aperture of which subtends a sufficiently small angle at the surface on which the radiation actually falls. From the point of view of ease of measurement a thermocouple made of thin foil presents

many advantages. A suitably designed thermocouple will show a rise of one or two degrees when placed in a powerful beam of X-rays. It seemed, however, to be practically impossible to determine with any certainty what fraction of the X-ray energy would be lost by secondary radiation from the surface, using, as we were, heterogeneous beams. The fraction so lost would depend on the character of the radiation used, and from our estimates might conceivably be as high as 10 per cent. The calibration of such a thermocouple also presented difficulties. We decided, therefore, in favour of a calorimeter, using oil as the absorbing medium.

Fig. 1.



X-ray tube, "water-sheet," and calorimetric apparatus.

Calculation showed that, with the dimensions employed, the proportion of the energy lost was of the order of 1 per cent. Its exact determination was thus not of any great importance.

Actually, a pair of similar calorimeters was employed (fig. 1). Each calorimeter consisted of a vertical cylinder of thin plated copper, 2.8 cm. diameter and 2 cm. high, closed at the base by a plated copper sheet 1 mm. thick. The calorimeters, supported on short ebonite legs, stood side by side in a brass box B, 3 mm. thick, the top and one end of which were movable. The top of this box was pierced

by a pair of holes, each vertically over one calorimeter, the holes being covered with thin tissue-paper. The whole of this box could slide aside on rails R, so that the X-ray beam was no longer intercepted, but passed to a standard ionization chamber lower down.

The difference in temperature of the two calorimeters was estimated by a pair of thermo-junctions JJ, copper-eureka-copper (0.27 mm. diameter). Each calorimeter contained about $2\frac{1}{2}$ c.c. of light oil (such as is used in oil-immersed transformers), in which was located one of the thermo-junctions. The wire for a short distance on either side of the junction was wound into a horizontal helix, which, being in oil, should make the temperature of the junction at the centre fairly representative of that of the calorimeter. The eureka wire passed upwards out of one calorimeter through a glass tube, thence over an ebonite support and down through a second glass tube into the other calorimeter. The copper wires, similarly insulated, passed, without any joins, side by side to the galvanometer terminals. To avoid any possibility of the X-ray apparatus disturbing the galvanometer, the latter was situated in an adjoining room.

For purposes of calibration, a single-layer pancake coil of covered eureka wire, 0.27 mm. diameter, was fastened with shellac on the inside of the base of each calorimeter. The ends of these wires passed through ebonite in the base of the calorimeters, and at a short distance outside were joined to thin copper wires, which passed through ebonite bushes in the side of the brass box B, and there joined stout copper wires through which a small measured current could be supplied.

To screen the brass box, containing the calorimeters, from fluctuating supplies of heat, its sides were covered with asbestos board and cotton-wool, and its top with a cardboard sheet. (It rested below on a wood block.) Further to screen its top, and especially to prevent heat radiation from the X-ray tube from passing through the tissue-paper covered hole into the calorimeter, a "water-sheet" screen W was placed above. This consisted of two plates of brass (2 mm. thick), separated by a rubber edging, between which water was passed. Holes drilled in the brass sheets were covered with thin celluloid, so that a window was formed for the passage of the X-rays. Unlike the metal box B, the "water-sheet" was not movable, and its window formed a permanent stop, limiting the width of the X-ray beam. Any screens used to filter the rays were placed between the X-ray tube and this "water-sheet."

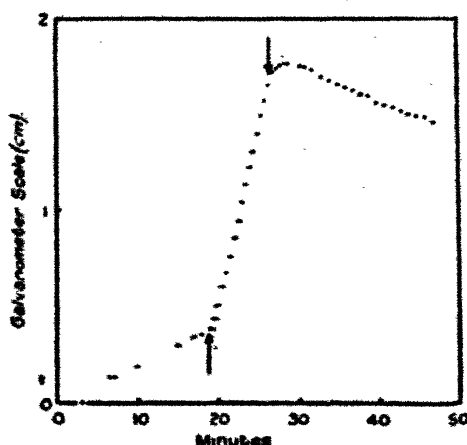
The copper wires from the thermo-junctions JJ were connected directly to a galvanometer of about 115 ohms resistance, giving about 23 mm. scale deflexion per micro-volt. As a result, a deflexion of $\frac{1}{10}$ mm. corresponded to about 10^{-4} °C. difference in temperature between the two calorimeters. In any experiment, the heating due to X-rays or to the current through the pancake coil was continued for about 7 minutes, and resulted in about $1\frac{1}{2}$ cm. galvanometer deflexion. Owing to the lag of the galvanometer and to the time required for heat diffusion in the calorimeter, the galvanometer did not attain its final rate of motion till about $1\frac{1}{2}$ minutes after the X-rays were started, or $2\frac{1}{2}$ minutes after the heating current through the pancake coil was started. To avoid the difficulty thus introduced, and to minimize any effects due to any slight fluctuation in the running of the X-ray tube, the total galvanometer movement, corrected for cooling, was deduced in each case. (At the same time, the total charge passed across the comparison ionization chamber was measured.)

When no heat was being supplied, the difference in temperature between the calorimeters decreased to half its value in about 8 minutes. The rate of cooling was, however, affected by slow heat waves, chiefly due to the X-ray tube and pumps. Therefore all subsidiary apparatus was put in action about an hour before any experiment, and the galvanometer reading was noted about every minute from considerably before till well after the experiment. (A typical set of results is shown in fig. 2.) The rates of galvanometer movement before and after the test were then used to deduce the total galvanometer reading corrected for cooling. The uncertainty in the value of any one cooling correction (the correction amounted on the average to about 20 per cent.) was minimized, and shown not to be large, by arranging to have the initial difference in temperature between the calorimeters varying in value and even in sign throughout a set of experiments.

For the heat calibration the resistance of the pancake coil (in the calorimeter in which X-rays were absorbed) was measured at the commencement and end of the experiments. The amount of the wire that was effective in producing heating of the calorimeter was able to be estimated to at least an accuracy of $\frac{1}{2}$ per cent. (see Table I.). The heating current was supplied by a 2-volt secondary cell, with about 230 ohms resistance in series. The current was measured by connecting a standard cell and table galvanometer across a

known part of this resistance; checks were obtained by changing the standard cell, changing the resistance box used, and by reversing the connexions of 2-volt and standard cells. The heat was supplied at about the same rate as in the X-ray experiments, and for about an equal time. A cooling correction was applied as in the main experiments, the pumps etc. being run during some tests and not during others. The corrected galvanometer deflexion for a joule of energy supplied to the calorimeter was thus estimated at various times during the course of the experiments, enabling the energy supplied during any X-ray absorption experiment to be deduced.

Fig. 2.



Thermal measurement of energy supplied by X-ray beam.
(Duration of X-ray heating indicated by arrows.)

The result of these experiments was:—

TABLE I.

Resistance of Calibrating Pancake Coil.

Rureka wire in calorimeter	9.46 ohms.
" " " ebonite.....	0.08 "
" " outside calorimeter	0.31 "

Assumed effective resistance producing heating of calorimeter,
 $9.46 + 0.08/2 = 9.50$ ohms.

TABLE II.

Heat Calibration Experiments.

Heating current 0.00848 amp. (i.e. drop in potential across 120 ohms arranged to equal e. m. f. of standard cell, 1.018 volts).

Rate of energy supply to calorimeter, $9.50(0.00848)^2 = 0.000684$ watts.

Duration (min.).	Galvanometer deflexion (cm.) corrected for cooling.	Corrected galvanometer deflexion (cm.) per joule supplied to calorimeter.
5	1.66	8.08
7.08	2.29	7.68
7	2.20	7.65
8	2.68 ₁	8.17
7	2.28	7.12
6	1.92 ₃	7.81
5	1.68	8.18
7	2.37 ₁	8.26
Mean.....		7.99 ± 0.06

TABLE III.

Thermal Measurement of Energy supplied by X-ray Beam.

Series.	Galvanometer deflexion (cm.) corrected for cooling.	Microcoulombs passed across comparison ionization chamber.	Galvanometer (cm.) Microcoulombs comparison.	Joules supplied by beam Microcoulombs comparison. $\left(\frac{E}{1}\right)$
I.	$\left\{ \begin{array}{l} 1.53 \\ 1.62 \\ 1.43 \\ 1.50 \end{array} \right\}$	$\left\{ \begin{array}{l} 0.542 \\ 0.545 \\ 0.567 \\ 0.545 \end{array} \right\}$	$\left\{ \begin{array}{l} 2.82 \\ 2.97 \\ 2.52 \\ 2.75 \end{array} \right\}$	0.346 ± 0.009 $(0.341)^*$
II.	$\left\{ \begin{array}{l} 2.15 \\ 2.07 \\ 2.00 \\ 2.01 \end{array} \right\}$	$\left\{ \begin{array}{l} 1.045 \\ 1.045 \\ 1.03 \\ 1.03 \end{array} \right\}$	$\left\{ \begin{array}{l} 2.05_1 \\ 1.98 \\ 1.94 \\ 1.95 \end{array} \right\}$	0.248 ± 0.003 $(0.244)^*$
III.	$\left\{ \begin{array}{l} 1.50 \\ 1.37 \\ 1.37 \\ 1.25 \end{array} \right\}$	$\left\{ \begin{array}{l} 1.10 \\ 1.105 \\ 1.075 \\ 1.035 \end{array} \right\}$	$\left\{ \begin{array}{l} 1.36_1 \\ 1.24 \\ 1.27_1 \\ 1.21 \end{array} \right\}$	0.159 ± 0.003 $(0.151)^*$

* The numbers in brackets are after applying a 1½-per-cent. correction for heat radiation, described in the next paragraph.

The above experiments seemed largely to have eliminated any error due to slow heat waves affecting the calorimeters unequally. It remains to test whether heat radiation in any appreciable amount was passing through the celluloid and flowing water that formed the window. The temperature attained by a screen of aluminium foil ($\frac{1}{10}$ mm. thick) that had been placed above the "water-sheet" to filter the X-ray beam was therefore measured. After copper-plating part of the lower face of the foil near the centre, a thermo-junction was soldered on. The running of the X-ray tube was found to cause the lower face of the foil to rise in temperature between 1° C. and $2\frac{1}{2}^{\circ}$ C., according to how good a thermal contact there was between the aluminium and the "water-sheet." That the measurement was not affected appreciably by heat conduction along the thermo-junction wires was shown by obtaining an almost identical result using much finer wires ($\frac{1}{15}$ mm. diam.). The aluminium foil was then heated electrically by a small coil placed above, and the heat reaching the calorimeter for a known temperature of the aluminium foil was measured (the X-ray tube not being run). When the foil was 19° C. above the temperature of the room, the amount of heat reaching the calorimeter was quite small compared with that received in the X-ray experiments. It was finally deduced that the heat radiation received from the foil during an X-ray absorption experiment amounted to rather less than 2 per cent. of the total heat measured.

Measurement of the Number of Ions produced.

As the experiments progressed, it became more and more clear that the real difficulties in the experiment would be concerned with the measurement of the ionization and not with the measurement of energy. The difficulty arises from the fact that the radiation from the anticathode of an X-ray tube is a mixed beam containing components of very different wave-length and absorbability. The beams used in our experiments, for example, contained components with a coefficient of absorption in cellophane ranging from more than 2.1 to something less than 0.4. Let us assume, as seems probable from the results of these experiments, that the number of ions produced by a beam of strictly homogeneous radiation is proportional to the energy absorbed from the beam in the ionization chamber. Since the coefficient of absorption is proportional to the cube of the wave-length, the ionization produced by the long-wave components in a mixed beam will be many times greater than

that due to the shorter wave-lengths, for equal intensities in the beam. Suppose, now, that to measure the absorbability of the radiation we insert a thin sheet of absorbing material in front of the ionization chamber. This will produce a marked absorption of the longer wave-length radiation, and, therefore, a large decrease in the measured ionization. The more penetrating radiation will have suffered little absorption in the sheet; but as its ionizing power is small, the presence of this penetrating radiation in the beam will not compensate for the loss of the softer radiation. In other words, the ionization method will overestimate the amount of energy absorbed from the beam. Consequently, any estimates of the fraction of the energy absorbed in an ionization chamber, made from coefficients of absorption so determined, will be seriously in error.

We were able to demonstrate this effect quite conclusively from our readings. It was found that the introduction of 0.2 mm. of aluminium into the beam from our tube reduced the measured ionization by 45 per cent. in a particular case. The energy of the beam as measured calorimetrically was, however, only reduced by 25 per cent. The discrepancy under actual experimental conditions may thus be very large. The point may seem to be so elementary as to be hardly worth making. It is, however, easily overlooked, and, in fact, several of the calculations in the papers on X-ray energy already mentioned are made on this basis, or on the basis of a mean wave-length calculated from such absorption measurements. This probably accounts for at least some of the differences in their results. Where the beam is a mixed one the attempt to translate coefficients of absorption into mean wave-lengths can serve only as a rough indication of the quality of the rays. Any calculations based on this method are liable to serious error.

As the fraction of the energy absorbed in the ionization chamber cannot be deduced from absorption experiments, we are reduced to determining the total number of ions formed by the complete absorption of the radiation. As a column of air 1 metre long would only absorb some 25 per cent. at most of the radiation employed, this determination cannot be made directly. We can, however, arrive at it indirectly as follows. If I is the intensity of the X-radiation, the ionization in a chamber containing air of mass per unit area dm will be $I \cdot dm$. The total ionization produced by the complete absorption of the beam is thus $\int_0^I I \cdot dm$. If I_0 is the initial intensity of the radiation, the ionization in

the ionization chamber, as measured in the energy experiments, is $I_0 \cdot \Delta m$, where Δm is the mass per unit area of the air in the chamber and is equal to $l\rho$, where ρ is the density of air, and l the length of the path of the rays through the chamber. The value of I , the intensity of the radiation, can be found in arbitrary units by using a small ionization chamber and measuring the ionization with gradually increasing thicknesses of the absorbing material between the chamber and the source of radiation. The area, α , of the curve obtained by plotting I against m will be the required integral, and $\frac{1}{I_0} \int_0^x I \cdot dm$ the required correcting factor.

In practice it is not possible to use air as the absorbing material, and the experiments were actually made using cellophane sheets. Cellophane is a convenient form of cellulose, and from its composition we might expect that its properties as regards X-ray absorption would not differ markedly from those of air. To obtain the true area of the curve, however, the ionization must be plotted not against the mass of cellophane employed, but against the mass of air which would produce the same absorption. This involves a knowledge of the relative absorbing powers of air and cellophane.

According to the makers, cellophane is pure cellulose, and the ratio of the mass absorption of cellophane to that of air should thus be calculable from the atomic coefficients of absorption. This calculation gave the value 0.84. Owing to the marked influence of traces of impurity of high atomic number on the absorption (the argon in the air accounts for 12 per cent. of the total absorption), it was deemed wiser to measure the required ratio directly. The rays were accordingly passed through a wide tube one metre in length, with thin cellophane windows, the tube being evacuated to any desired pressure. The ionization in a suitable chamber placed at the far end of the tube could be balanced against that in the standard chamber, by means of the adjustable shutter. A balance was first obtained with the tube full of air at atmospheric pressure. Five sheets of cellophane, each of mass per unit area 0.0243 gm./cm.², were interposed in the beam, and the chamber evacuated until the balance was restored. The reduction in pressure required was found to be 67.3, 67.3, and 67.5 cm. for the three classes of radiation used in our experiments, at a temperature of 19°C., giving a ratio of air to cellophane of 0.880, independent of the quality of the radiation. The experimental value was

employed in the calculations. The difference between the calculated and the experimental values is no doubt due to the presence of metallic impurities in the cellophane. This suggestion was confirmed by an "ash" test on the substance, which was found to yield about 0.4 per cent. ash, containing principally sodium and calcium as its metallic constituents. Each absorption curve was continued until the ionization had been reduced to 3 per cent. of its initial value, so that the true area of the curve could be determined without uncertainty as to the nature of the end radiation. The values so obtained for the factor $\frac{1}{I_0} \int_0^\infty I \cdot dm$ are given in the fourth column of Table IV.

A further correction is necessary to allow for the radiation scattered out of the direct beam. The ionization due to the scattered radiation is clearly not included in the ionization measurements. If E is the energy of the primary beam, μ the mass coefficient of absorption, and σ the mass coefficient of scattering, then the total energy S scattered out of a narrow pencil of rays is given by

$$S = \int_0^\infty \sigma E e^{-\mu m} dm = \frac{\sigma}{\mu} \cdot E.$$

Unfortunately, we cannot apply this relationship directly to our measurements, for, as we have already pointed out, the mean wave-length, however calculated, is only a very rough test of the quality of a heterogeneous beam, and the coefficients of absorption, as deduced from an absorption curve, are liable to be in very serious error.

The only adequate solution of the difficulty is to analyse the radiation spectroscopically. When the distribution of energy among the various wave-lengths is known, the relation already given can be applied separately to each constituent of the heterogeneous beam, and the value of S for the whole beam can thus be determined. Fortunately, Mr. L. G. Treloar has been engaged for some little time in this laboratory in analysing the radiation from a Shearer tube under different conditions, and we have been able to select from his results, which will shortly be published, distribution curves corresponding to the conditions of working in our experiments. In this way values were obtained for S/E for the three types of radiation used in our experiments. The total measured ionization is due to the absorption of $E-S$ units of energy, instead of the E units measured in the calorimeter, since S units have been scattered from the beam and produce their ionization

elsewhere. To obtain the true value of the energy spent per ion we must therefore multiply our measured energy by $\frac{E-S}{E}$. The calculated values of this ratio are given in column 5 of Table IV.

Although the method seems sound, the calculation of the scattering correction is probably the least satisfactory part of the work. The values for the scattering coefficient σ and the values of μ the mass absorption coefficients for different wave-lengths have been calculated from tables of values collected by Compton. In spite of the large amount of work which has been done on the subject, the values given by different authorities are not in very close agreement, and we have not felt justified in giving this correction to more than two significant figures. An error of 10 per cent. in estimating S/E only introduces an average error of about 3 per cent. into the correcting factor, and we consider that the latter should be correct to this amount. It may be mentioned that the coefficients used in calculating the scattering correction are the only data employed in our calculations which have not been directly measured in our experiments.

Measurements and Results.

It will be appreciated from the previous sections that the determination of the energy spent per ion for radiation of given quality involved a very considerable amount of experimental work. On the other hand, owing to the possibility of deterioration in the tube with prolonged usage, it was desirable that the experiments should not be unduly prolonged. It was decided, therefore, to concentrate on three standard beams: (I.), with the tube running at the highest potential at which it was possible to secure steady working, about 55,000 volts, and filtering the radiation through 0.3 mm. of aluminium; (II.), with the tube as in (I.), but with a filter of only 0.1 mm. of aluminium; and (III.), with the tube running at the minimum potential which would give a beam of sufficient intensity to measure calorimetrically. This radiation was also filtered through 0.1 mm. of aluminium. The water screen was, of course, present in all experiments. These limits were fixed by the capacity of the apparatus, and the average quality of the radiation in the three beams did not differ very widely, though the difference was appreciable. The initial mass coefficients of absorption in cellophane were 1.0, 2.0, and 2.6 respectively, but as we have already pointed out, the coefficient

of absorption is not a reliable index of the average quality of the radiation. A better estimate may perhaps be obtained from the area of the absorption curve. For homogeneous

radiation the value of $\frac{1}{I_0} \int_0^\infty I \cdot dm$ is equal to $\frac{1}{\mu}$. If we

write $\frac{1}{\bar{\mu}} = \frac{1}{I_0} \int_0^\infty I \cdot dm$, we can perhaps regard $\bar{\mu}$ as a

kind of mean coefficient of absorption, and the corresponding wave-length as a mean wave-length. The values of μ in air deduced in this way are respectively 0.86, 1.12, and 1.48. The wave-lengths which would correspond to these absorption coefficients if the radiation were homogeneous are 0.60, 0.68, and 0.75 Å.U. The range is not a very wide one. It is hoped to extend it in the near future, when more powerful apparatus is available.

The calculation of the energy expended by the rays for the production of a pair of ions was made as follows. The calorimetric measurements recorded in Table III. give the energy in joules collected by the calorimeter during the passage of one microcoulomb across the comparison chamber. This corresponds to the passage of one microcoulomb across the standard chamber when the aperture of this chamber is adjusted for compensation. The shutter reading, a , for this balance is given in column 3 of Table IV. The area of the aperture is the shutter reading multiplied by the width, d , of the aperture. If the whole beam had passed through the ionization chamber, the ionization produced would be increased in the proportion A/ad , where A is the cross-section of the beam at the level of the shutter. This area was determined geometrically, the necessary readings being made with a cathetometer. The value obtained this way was 12.96 cm.² Measurements made by exposing a photographic plate to the beam gave a value of 13.1 cm.² The two methods are thus consistent to 1 per cent.

The ionization produced in a layer of air of unit mass per unit area is obtained by dividing by the length, l , of the path of the rays in the ionization chamber, multiplied by ρ , the density of the air. The total ionization which would have been produced by the complete absorption of the beam is

obtained by multiplying by $\frac{1}{I_0} \int_0^\infty I \cdot dm = T$, the values

of which are given in column 4 of Table IV. The ionization is thus obtained in microcoulombs. The fraction of the whole energy used in producing this ionization is

$\frac{E-S}{E}$. Hence, since 1 ionic charge is equal to 1.591×10^{-12} microcoulombs, we have finally

$$\text{joules per microcoulomb} = \left(\frac{E}{I}\right) \times \frac{dA}{A} \cdot \frac{1}{l} \cdot \frac{E-S}{E} = \frac{E_J}{Q_M},$$

$$\text{ergs per ion pair} = \frac{E_J}{Q_M} \times 1.591 \times 10^{-12} \times 10^7,$$

$$\text{or "volts" per ion pair} = \frac{E_J}{Q_M} \times 10^6.$$

The values of the various quantities are given in Table IV. In calculating the last column, a small additional correction has been applied for the absorption of the beam in the column of air between the calorimeter and the standard ionization chamber. This correction varies from 1.5 per cent. in set I. to 3.6 per cent. in set III.

TABLE IV.

Series.	Joules per m.c. (measured) (E-I).	Aperture of shutter (a) (cm.).	$\int_0^L I. d\alpha$ =T.	Scattering correction (E-S)/E.	Energy per ion pair in "volts."
I.	0.341	1.128	1.168	0.71	44.2
II.	0.244	1.085	0.892	0.75	42.0
III.	0.157	1.292	0.675	0.78	43.3

A = area of beam at shutter = 12.96 cm.²

d = width of shutter = 0.665 cm.

l = length of path of rays in chamber = 3.125 cm.

ρ = density of air at 18° C. and 760 mm. pressure = 0.00120 gm./cc.

Discussion of Results.

The results of the experiments are collected in the last column of Table IV., and, on the whole, are in very satisfactory agreement. There is no evidence that the energy abstracted from a beam of X-rays for the production of one pair of ions varies with the quality of the radiation over the range of our experiments, and we are justified in combining the results of the three sets of experiments. The measurements of the constants for the apparatus are certainly correct to well within 1 per cent., and the same applies to the measurements from which columns 3 and 4 of Table IV.

were calculated, as these measurements were made by the balance method, which, for comparatively large ionization currents such as we had to deal with, is susceptible of very considerable accuracy. Assuming that the variations in the results are due mainly to the errors in the heating experiments (given in Table III.), we obtain for the energy spent per ion 41.2 ± 1.2 , 42.0 ± 0.5 , and 43.3 ± 0.8 volts. Taking the weighted mean of these observations we obtain as our final result 42.5 ± 0.4 volts per ion pair.

There are, however, two factors which might affect the mean value. The first is the scattering correction which has already been discussed in detail. The mass coefficient of scattering for air was taken as 0.164, and the coefficients of absorption for various wave-lengths were taken from the table of mean values given by Compton. Any errors in these coefficients would affect the three correcting factors to very much the same extent. Fortunately, the scattering correction is not a very large one, so that the accepted values used in the calculations would require to be in very considerable error to produce any appreciable error in our mean.

The remaining factor which has to be considered is the efficiency of the standard ionization chamber. It may be desirable, therefore, to describe it somewhat more minutely. The collecting electrode was an aluminium plate, 3 cm. square, furnished with an aluminium guard ring 9 cm. square. The charged electrode was an aluminium plate, also 9 cm. square, placed parallel to the first at a distance of 2 cm. The field across the centre of the electrodes was thus uniform to a high degree, and the mass of gas from which the electrons were collected could be determined with certainty.

The radiation passed centrally between the electrodes, the width of the beam being 0.8 cm. at the centre of the plates. The apparatus was so adjusted that any radiation which might be scattered from the water-cooled stop, which limited the beam, would not be able to reach the electrodes. It was found experimentally that the ionization current across the chamber became saturated with a potential of about 350 volts on the plate; a potential of about 500 volts was actually used during the experiments, giving a field of 250 volts per cm.

To obtain the full ionization produced by the rays, it is further necessary that the photo-electrons ejected by the radiation from the air shall be completely absorbed before reaching the electrodes. As it was somewhat difficult to obtain any reliable data on the range of the photo-electrons,

the matter was tested experimentally, the ionization current being measured, by the balance method, with different distances between the electrodes. It was found that the ionization current remained constant as the distance between the plates was increased from 1.9 cm. to 3.0 cm. At distances greater than 3 cm. the current began to diminish, owing to the impossibility of producing complete saturation with the potential available. We can assume, therefore, that there was no detectable loss of ions through photo-electrons reaching the electrodes before producing their full ionizing effect. Further experiments indicated that the ionization current was independent of the material lining the walls of the chamber. As far as our tests go, they indicate that the chamber was completely satisfactory.

It is interesting to compare the value obtained in these experiments with those obtained in other recent investigations. The very variable values obtained by Kriegesmann*, ranging from 282 to 87 volts per ion pair, are probably ascribable to the unsatisfactory method of computing the results. The very low value of 22 volts given by Kircher and Schmitz* is completely out of accord not only with our own results, but also with those of all other observers. We cannot suggest any explanation of this low value. Kulenkampff*, after a very elaborate and careful set of observations, suggests a value of 35 ± 5 volts per ion pair, and his work deserves consideration. The energy measurements were made by allowing the radiation to fall on a thin silver foil, the temperature of which was taken with a set of thermocouples. There is much to recommend this method from the experimental point of view. The reduction of the thermal capacity from the 2 or 3 grams required for a calorimeter, to perhaps $\frac{1}{10}$ gram or even less of the bare thermocouple, makes the temperature readings much easier. We abandoned it deliberately for two reasons: firstly, the impossibility of knowing what fraction of the incident energy might be re-radiated as scattered, fluorescent, and corpuscular radiation; and, secondly, the difficulty of calibrating such a system.

Both uncertainties seem to attach to Kulenkampff's work. Apparently no correction is applied for the re-radiated energy, though this might possibly amount to as much as 10 per cent. Two methods of calibrating the thermocouple system were tried, and differed by 10 per cent. The mean of these results was used in the calculations. If the higher,

* *Loc. cit.*

and apparently the more reliable, estimate had been taken, the final value would have been increased by about 5 per cent. These possibilities are probably covered by the very generous margin of ± 5 , which Kulenkampff allows to his mean value. The points which we have raised, however, indicate that the true value should lie somewhere near the upper limit of his range.

There remain finally the experiments of Rump*. Rump's values range, as we have already mentioned, from about 300 volts per ion for very soft rays, down to round about 42 volts per ion for heavily-filtered radiation from a hard tube. The large values given for the soft radiation are undoubtedly due to his unsatisfactory method of dealing with his observations, as we have already pointed out in an earlier section of the paper. It is only fair to Rump to state that he recognizes this in the concluding paragraphs of his paper; but as he had not taken the measurements necessary for a proper calculation, he has to be satisfied with suggesting that the lower values obtained with the filtered radiation are probably the more correct. The effect of filtration is to concentrate the radiation towards the short wave-length end of the spectrum, and thus to reduce its heterogeneity. His values for filtered radiation range from about 39 to 44 volts per ion pair, with a probable mean of about 42†. They are thus in close agreement with our results, although they apply to a very different part of the spectrum.

Summing up the discussion, we may conclude that the energy abstracted from an X-ray beam for the formation of a pair of ions is not very far removed from 42 volts, and that there is no evidence that this value varies with the wave-length of the radiation, though further evidence on this point is desirable. Since the ionization produced by X-rays is ascribed to the action of the photo-electrons produced by it, it is interesting to note that Meitner found for the energy spent per ion by β -radiation a value of 45 volts.

The ionization potential of the nitrogen and oxygen molecules is about 17 volts. The energy necessary to produce ionized atoms of nitrogen and oxygen from the molecule is, according to Smyth‡, respectively 28 and 23 volts. It is evident, therefore, that a very considerable portion of the energy of an X-ray beam is not spent in

* *Loc. cit.*

† He later (*loc. cit.*) reduces his estimate to 33 volts per ion pair.

‡ Smyth, *Proc. Roy. Soc. civ. A*, p. 121 (1923).

producing ions, but degraded in some other way. The most probable method seems to lie in the production of δ -radiation, the very low velocity electrons which are given off in considerable quantity from the surface of a solid on which a beam of X-rays falls. If we assume that the process of ionization commences with the projection from the molecule of a δ particle, the average energy of these particles would be $(42-17)$ volts, or 25 volts. Our knowledge of δ -radiation is very limited, but the velocities of the particles escaping from a solid surface are of this order of magnitude. Investigations on this point are now in progress in this laboratory, and may throw further light on the mechanism of X-ray ionization.

In conclusion we may consider, very briefly, the application of these results to the ionization method of measuring X-radiation. Assuming that the energy spent per ion is independent of the wave-length, the number of ions produced in an air ionization chamber is directly proportional to the energy absorbed in it, each pair of ions being accompanied by the absorption of 42.5 "volts" or 6.76×10^{-11} erg. The transference of 1 e.s.u. across the chamber thus indicates the absorption of 0.141 erg. Thus

$$I = 0.141 dE,$$

where I is the charge collected in e.s.u., and dE is the energy absorbed. If τ is the "true" mass absorption coefficient of the radiation, and dm the mass of air subjected to the rays in the chamber,

$$I = 0.141 E \cdot \tau \cdot dm,$$

or for 1 c.c. of air at 18° C. and normal pressure

$$I = 0.141 \times E \cdot \tau \times 0.00120 = 1.70 \times 10^{-4} E\tau.$$

It must, however, again be pointed out that this result can only be applied to homogeneous radiation, as measurements made in the usual way on the "coefficient of absorption" of a heterogeneous beam do not give even an approximately correct value for the energy absorption of the beam.

Summary.

- (1) The energy of a beam of X-rays has been measured by converting it into heat in a calorimeter.
- (2) The energy absorbed from the radiation for the formation of one pair of ions in air is 42.5 "volts."
- (3) This value is constant over the range of wave-lengths employed in the experiments.

(4) The quantity of electricity, I , measured in electrostatic units across 1 c.c. of air at 18°C . and normal pressure is given by

$$I = 1.70 \cdot 10^{-4} E\tau,$$

where E is the total X-ray energy in ergs which has passed through the gas, and τ is the "true" mass coefficient of absorption. The relation cannot be applied to a heterogeneous radiation, owing to the impossibility of determining τ for such radiation.

In conclusion, the authors wish to express their obligation to the Government Grants Committee of the Royal Society for a grant made to one of them (J. A. C.) for the purchase of essential apparatus.

Department of Physics,
The University, Reading,
June 9th, 1928.

XLIII. *Selective Adsorption from Gaseous Mixtures by a Mercury Surface formed in the Mixture.* By M. L. OLIPHANT, 1851 Exhibition Research Student*.

Introduction.

THIS paper presents experimental evidence which indicates that an expanding mercury surface selectively adsorbs carbon dioxide from a mixture of carbon dioxide with an excess of hydrogen or argon. The measurements show that within the limits of the experimental error the carbon dioxide so adsorbed forms a monomolecular layer over the surface of the mercury.

When a mercury surface expands or is created, fresh atoms of mercury find their way from the interior of the liquid to the free surface. It is improbable that the atoms of mercury are absolutely symmetrical in the sense that the forces on neighbouring atoms are independent of their orientation, and it is unlikely that the fresh atoms of mercury which enter the surface are all oriented in the same way. A surface which is freshly formed *in vacuo* will speedily rearrange its constituent atoms in such a way that the energy in the surface is a minimum. This rearrangement will take place very rapidly, so that it is impossible to

* Communicated by Sir E. Rutherford, O.M., F.R.S.

measure the resulting rapid fall in surface-tension, after the formation of the surface, by any ordinary means. However, when a surface is expanded in contact with a gas, a mercury atom which comes into the surface with an active "end" outward will possibly remain in such a condition for some time, as it is able to form a "compound" with a gas molecule which may have a life of several minutes. Thus the rearrangement of the surface to form one of the lowest energy will be delayed by the adsorption of a gas layer, and it becomes possible to measure the decrease in surface-tension from a very high initial value to a lower final value which is approached asymptotically. The changes in the surface-tension which measure directly the decrease in the free energy of the surface are accompanied by concomitant changes in the other surface properties. Thus Popesco* has shown that five seconds after the formation of a large drop of mercury in contact with a gas the surface-tension is above 500 dynes/cm., and that this falls exponentially to a final value of about 400 dynes/cm., the time taken varying with the gas. He has also shown that the photo-electric effect obtained at the surface with a given source of light shows changes which follow the same general course. Perucca† has demonstrated that the contact potential of the surface against platinum shows changes of the same character. He has observed that the time taken to reach equilibrium is longer with carbon dioxide than with hydrogen, indicating that the former gas is the more rigidly held at the surface.

On the other hand, Harkins‡, using the "drop-weight method" for measuring surface-tension, does not observe any large difference between the surface-tension of a drop formed *in vacuo* and one formed in a gas. This would indicate either that the gas is not adsorbed at the surface so as to interfere with its orientation, or that the assumed abnormally high initial surface-tension due to the random orientation in the fresh surface does not actually exist. One of the methods for measuring the surface-tension must give the wrong result, and the following experiments have been carried out in order to test whether the adsorption of gas does take place at an expanding mercury surface. The problem of the surface-tension of mercury remains unsolved, but these results give definite evidence in favour of the "large-drop method" as opposed to the "drop-weight method" for measuring this quantity.

* Popesco, *Ann. d. Phys.* iii. p. 402 (1925).

† Perucca, *C. R.* clxxv. p. 519 (1922).

‡ Harkins, *J. A. C. S.* 1920.

Langmuir* has measured the adsorption of gas at plane surfaces of mica and glass carefully packed into a vessel and separated so as to avoid capillary spaces. In this way he obtained a large area in a moderate volume, and was able to measure the fall in pressure of the gas when admitted at low pressure into the vessel maintained at very low temperatures. It is obviously not possible to apply this method to mercury, for there is no conceivable method by which a large surface of perfectly pure mercury could be created in contact with a very small volume of gas. For this reason use has been made of a comparative method only, whereby the change in composition of a mixture of gases is measured. Owing to the fact that some gases are apparently held to the surface by greater forces than those holding others, a surface which is exposed to a mixture of gases should become covered with an almost complete layer of the more closely-held gas, that is the gas whose life on the surface is longest. Thus, if a stream of mercury drops be allowed to fall down a column of a mixture of two gases, the more easily adsorbed should be largely removed from the top of the column and given up where the drops collect in a pool at the bottom. If it were possible to eliminate the effect of diffusion back and of the stirring action of the falling drops, it should be possible to deduce, from a knowledge of the change in composition of the gas at the top, or the bottom, and the total surface of the falling drops, the amount of the one gas transferred per square centimetre of surface. This yields at once the adsorption in molecules per square cm.

Schofield† has developed an ingenious method by which the disturbing effects may be eliminated and the adsorption measured in the case of liquids (ion adsorption from solution); and this is the basis of the method by which the present problem has been attacked.

Method.

Consider a stream of mercury drops falling through a column of gas and collecting together at the bottom. As the drop forms at the top, its surface is continually expanding so that the surface in contact with the gas is always one freshly formed. Gas is adsorbed at such a surface very readily, and if the atmosphere is a mixture of gases, one will in general be adsorbed more readily than the others; for instance, as we shall see later, carbon dioxide is selectively

* Langmuir, *Phys. Rev.* viii, p. 149 (1916); *J. A. C. S.* xl, p. 1361 (1918).

† Schofield, *Phil. Mag.* ser. 7, i, p. 641 (1920).

adsorbed from a mixture of this gas with hydrogen or argon.

When the drop separates, it carries this carbon dioxide down with it and gives it up when it merges with the pool of metal below, for there the surface contracts to zero. The concentration of this gas at the bottom therefore increases, while that at the top decreases, but a limit is soon reached when this concentration gradient ceases to grow, owing to the mixing action of the falling drops. This effect has been largely eliminated by using Schofield's flow method, as has already been mentioned. A stream of the mixed gases, fed into the column at the middle, divides there into an upward and a downward stream of equal velocity, which flow out from the immediate vicinity of the points at which the drops form and where they coalesce. This stream is quite slow, but is sufficient to sweep away the carbon dioxide carried down by the drops as fast as it is given up below, while the upper stream is correspondingly impoverished. The effect of the mixing of the gas over the length of the column is thus very largely eliminated, for it is only at the very beginning and end of the path that these effects would be serious, and here the gas is swept away from these disturbing influences as fast as it accumulates. A great disadvantage is that the concentration change is thereby rendered very much smaller than when the gas is at rest, and it becomes necessary to use a very sensitive method for measuring it. An attempt to detect it by means of the difference in heat conductivities due to the difference in composition in the case of a mixture of carbon dioxide and hydrogen proved abortive, and this method was abandoned for an improvised Rayleigh gas refractometer with tubes two metres long. At a concentration of 2 per cent. carbon dioxide in hydrogen this proved capable of detecting a change of .001 per cent., and except at the very highest concentrations, proved entirely satisfactory. The change measured is the difference in concentration of carbon dioxide in the two limbs of the apparatus, that is twice the change in concentration of either stream alone.

If V be the volume of mercury falling as drops in one second and N the number, the surface exposed to the gas per second is

$$A = 4\pi N \left(\frac{3}{4} \frac{V}{\pi N} \right)^{\frac{2}{3}}.$$

Now each square centimetre of this surface will adsorb, say, n molecules, so that the total number transferred each

second will be nA . If the volume of gas traversing the apparatus at a temperature T and pressure P be v , the total number of molecules passing per second will be

$$S = v \times \frac{6.06 \times 10^{23}}{22.4 \times 10^3} \times \frac{273}{T} \times \frac{P}{760}.$$

The transferred molecules will constitute part of the stream traversing the lower limb, and a correspondingly smaller number of carbon-dioxide molecules will traverse the upper. In either case the concentration change will be very nearly

given by $C = \frac{nA}{S} \times 100$, expressed as a percentage of the total volume passing. C is obtained from the interferometer, and knowing the other factors, n may be calculated. The measurements are carried out in practice in the following manner.

Experimental Details.

The apparatus was arranged as shown in fig. 1.

Mercury from the reservoir A, maintained at a constant level H, is delivered through a regulating tap T_1 to the stainless steel nozzle N fastened over the end of the glass tube with sealing-wax. This nozzle is perforated with twenty-five holes, each of which delivers about twenty drops per second. These drops fall down the tube F and collect in a pool at the bottom, whence the mercury flows out through the siphon S, finding its way through P_1 to the pump which returns it to the reservoir. The design of a pump which would circulate the mercury without contamination has proved the most tedious part of the investigation. An all-steel reciprocating pump proved unsuccessful, as it seized almost at once, owing to the impossibility of using any lubricant whatever. Abortive attempts at substituting a liquid (distilled water) piston for the steel were followed by a rotating design, which, after modification, worked very satisfactorily.

A drum D (fig. 2) of mild steel, lined throughout with sealing-wax after boiling in caustic soda and heating to a dull red, is mounted on the shaft of the motor M, and rotates at about 1400 revolutions per minute. The incoming stream of mercury is fed through the space between the inner and outer tubes of L, and falls through the hole H into the drum. The bent tube S scoops up mercury from the rotating shell of the metal which lines D, and delivers it through the axis of L to the reservoir. The compound tube L is clamped securely in a wooden block so that it passes

through the hole in the drum axially. This arrangement secures great rigidity and permits the construction of these parts of pyrex glass. The scooping action of S gives rise to

Fig. 1.

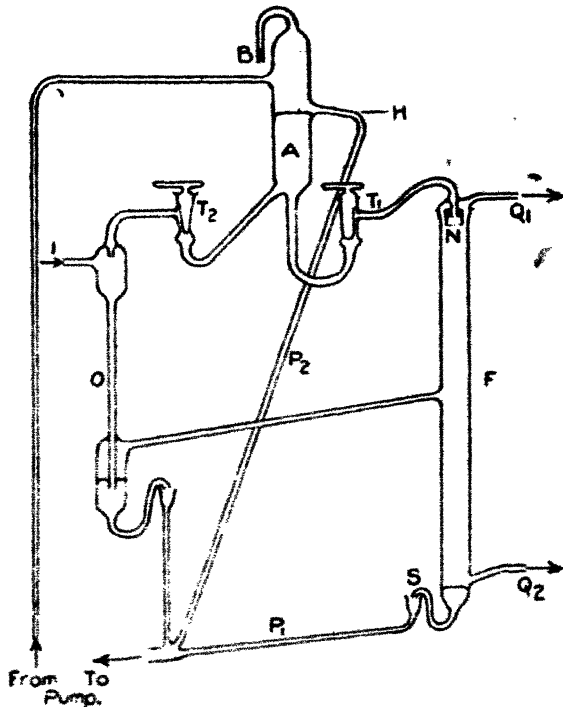
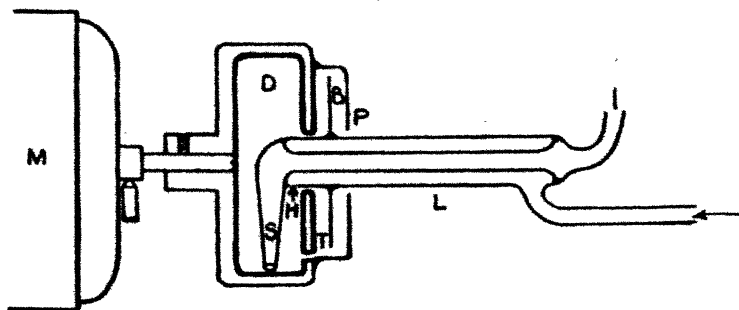


Fig. 2.



a spray of mercury drops in D, some of which escape through the clearance space between L and the drum. To avoid this a baffle B is stuck to the tube with sealing-wax and enclosed in a chamber P, a shallow glass dish, also fixed

with sealing-wax to the drum, and with a hole bored through the bottom. A small hole T is bored through the face of the drum at the periphery of this dish, and allows the mercury which collects in P to find its way back to the body of the pump. This circulating device runs smoothly and silently, and does not give rise to vibration of the bench to the extent that the reciprocating types did, while it possesses the great advantage of supplying a continuous stream of mercury whose rate of flow automatically adjusts itself to the rate at which mercury is supplied to the pump. In this way the level of the reservoir is maintained very constant, and the rate of dropping from the nozzle correspondingly so.

The mixture of gases which is to be used is fed at a constant rate into the centre of the fall tube F (fig. 1) by means of a Sprengel pump O with a fall of about 25 cm. The mercury for this pump is also supplied from the reservoir A through T₁, and after use is returned to the pump. The excess mercury supplied by the pump escapes down the overflow P₂.

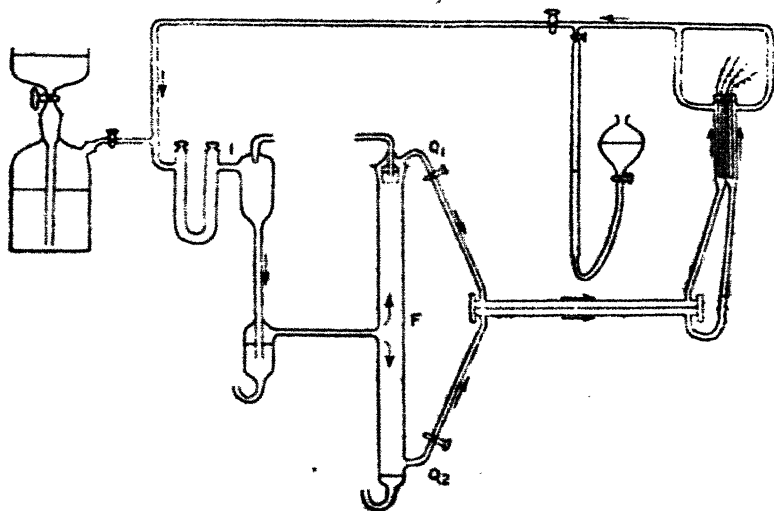
The stream of mixed gases divides at the centre, half passing upward and half down, thence through Q₁ and Q₂ to the two tubes of a Rayleigh interferometer. After traversing the interferometer the streams pass through two glass tubes down the axes of which fine platinum wires are sealed. These wires are heated by a current and balanced on a bridge, and they serve to maintain an equal rate of flow in each limb of the apparatus, any want of balance being rectified by adjusting the rate of flow. The difference in conductivity of the two streams, due to the slight difference in composition brought about by the adsorption, is not sufficient to affect the balance. The two streams then unite and are conducted back to the inlet I. A reservoir of the mixed gases is connected by a T-piece just before the stream reaches I and serves to maintain the pressure in the system at a constant value. A two-way tap connected at the same point allows the rate of flow to be observed at any instant by measuring the volume of gas collected in a burette in 10 seconds. The gas reservoir and the burette are filled with pure paraffin-oil in place of water in order to avoid loss of gas by solution. Just before entering at I the gas is thoroughly dried by passing over P₂O₅. A plan of the whole system showing the path of the gas through the apparatus is given in fig. 3.

The whole of the glass parts of the apparatus are of "pyrex," thoroughly cleaned with hot chromic acid and distilled water before assembling. The connexions and the

gas tubes are thick-walled pressure tubing which had been boiled in caustic soda and distilled water, and rubber-grease was smeared over the ends of all the glass tubes before pushing the rubber over. The mercury to be used is purified in the manner described by Burdon*, and is of similar quality to that used for other work on mercury surfaces in this laboratory. The apparatus was washed through with this mercury till that which escaped through S was good enough for distilled water to spread on it. In order to avoid effects due to temperature changes, the whole was assembled in an underground constant-temperature room.

The first mixture of gases used was one containing a

Fig. 3.



small proportion of carbon dioxide in hydrogen. Before commencing an experiment the apparatus was washed through with a slow stream of hydrogen for several hours, and then with the mixture of gases until the fringes in the interferometer showed no movement after one hour. During the preliminaries the mercury was not dropping in F.

Then the mercury is allowed to fall from the nozzle. The rate of dropping is determined by observing when the drops appear stationary and properly spaced at the nozzle when stroboscopically examined by means of an "Ashdown Rotoscope." This setting can be made an average for all twenty-five streams, and it can be reproduced to about 1 per cent. In most of the experiments the rate of flow of gas

* Burdon, *Proc. Phys. Sec. Lond.* xxxviii, p 148 (1926).

was about .24 cubic centimetre per second in each limb of the apparatus, and this remained constant for hours. Some time after commencing dropping the fringes begin to move and attain a constant deflexion after two hours. As this shift became greater than a few fringes, it was compensated by turning the compensating plate of the interferometer. The latter was calibrated for small variations about the particular composition used, so that the percentage composition change can be at once deduced from the fringe shift. By slightly warming the wax joint at P_1 (fig. 1) the collecting-tube could be slipped to one side and the mercury from S allowed to collect for a period of 10 or 20 seconds in a measuring cylinder. From the volume thus collected and the number of drops which have fallen in the period, the volume, and hence the area of a single drop, can be calculated. The total area of mercury surface exposed to the gas per second is therefore known, and the number of molecules adsorbed per square centimetre can be obtained from the other factors in the manner which has been indicated in discussing the method.

Results.

A typical set of observations is tabulated in Table I.

TABLE I.

Atmosphere 2 per cent. CO_2 in H_2 .

Temperature of mercury $16^{\circ}\cdot 1$ C.

Total pressure of gas inside apparatus: 79.0 cm. (P).

Temperature of gas 14° C.¹

Time. (Hrs., mins.)	Rate of flow. (c.)	Rate of dropping. (N.)	Volume of drops in 1 second. (V.)	Composition change (from fringe shift). (O.)
0.0	.24 c.c.	20.2 \times 25	1.54 c.c.	0 %
0.20	—	—	—	.002 ..
0.40	.25 "	20.1 ..	1.56 ..	.033 ..
1.0	—	—	—	.198 ..
1.20	—	—	—	.371 ..
2.0	.24 ..	20.1 ..	—	.400 ..
2.30	—	—	—	.400 ..
3.0	.24 ..	20.1 ..	1.53 ..	.400 ..
Average24 c.c.	20.1 \times 25	1.54 c.c.	Constant } .40 % change

Substitution of these quantities in the equation given earlier gives for the number of molecules of CO_2 adsorbed per square centimetre of mercury surface, at a temperature of $16^{\circ}\cdot 1$ C., from a 2 per-cent. mixture with hydrogen :

$$n = \cdot 5 \times 10^{15}.$$

Similar measurements have been made with $\cdot 5$, 5, 10, and 50 per cent. mixtures of the same gases. The whole of the measurements made on these mixtures are tabulated in Table II.

TABLE II.

Per cent. CO_2 in H_2 .	n .	Temperature.
$\cdot 5$	$\cdot 3 \times 10^{15}$	15° C.
2	$\cdot 5$..	16 ..
5	$\cdot 7$..	16 ..
10	$\cdot 7$..	$16^{\circ}\cdot 5$..
50	$\cdot 8$..	16 ..

The observations on the 2-per-cent. and the 5-per-cent. mixtures were repeated on different days and yielded identical results. The others are the result of only one experiment for each concentration, but it should be remembered that the factors which enter into the calculations are verified several times during any one run. Owing to the very much reduced sensitivity of the interferometer at the high concentrations, the last measurement is probably in error by as much as 20 per cent. either way, but it serves to indicate that the layer adsorbed is approximately the same, even at very high concentrations, namely about $\cdot 7 \times 10^{15}$ molecules per square centimetre.

For comparison with these, some experiments were carried out with similar mixtures of CO_2 and the inert gas argon in place of the hydrogen, and the results obtained are tabulated in Table III.

TABLE III.

Per cent. of CO_2 in argon.	n .	Temperature.
5	$\cdot 6 \times 10^{15}$	$14^{\circ}\cdot 5$ C.
10	$\cdot 6$..	15 ..
15	$\cdot 5$..	16 ..

Discussion of Results.

It is evident from the above that at all concentrations above about 2 per cent. carbon dioxide is adsorbed at a mercury surface to give a layer of very nearly the same density, namely between $\cdot 6$ and $\cdot 7 \times 10^{15}$ molecules per square centimetre. The diameter of a molecule of CO_2 , as given in the 'Smithsonian Physical Tables,' is $4 \cdot 2 \times 10^{-8}$ cm.; and if we assume the molecules on the mercury surface to occupy a square with this length of side, then in order to form a monomolecular layer over one square centimetre, $\cdot 6 \times 10^{15}$ molecules (very nearly) would be required. It therefore seems reasonable to assume that a monomolecular layer of CO_2 is normally formed at atmospheric pressure on a freshly-prepared mercury surface in a mixture of this gas with a much less easily condensable gas such as H_2 or argon, provided that the concentration of the CO_2 exceeds about 2 per cent.

The present work definitely establishes that adsorption does take place on an expanding mercury surface, and indicates that the forces involved are quite large, for the gas is retained while mercury drops fall through about 50 cm. It is improbable that the adsorption of this gas has a negligibly small effect on the surface-tension, and hence a method for measuring the surface energy should give very different values in a gas and in a vacuum. As has been pointed out, the "large-drop" method for measuring the surface-tension gives a very high initial value in a gas, which falls rapidly to a value considerably lower than the vacuum value. On the other hand, the "drop-weight" method of Harkins does not show these differences. It therefore seems probable that the values given by the former are more reliable than those given by the latter method. The results obtained by Perucca, who measured the change in the contact potential of a mercury surface against platinum in vacuum and after exposure to various gases, also support the view that the surface energy is very different in the two cases.

In this connexion it might be mentioned that measurements of the surface-tension of water and of aqueous solutions of salt by the capillary rise method, using a special technique for obtaining the height of the meniscus at very short intervals after the surface has been formed, have been made by Kleinmann* and others. These indicate that the

* Kleinmann, *Ann. d. Phys.* lxxx. p. 245 (1926). Schmidt und Steyer, *Ann. d. Phys.* lxxx. (1926).

initial surface-tension in contact with gases in considerably higher than for older surfaces.

These experiments were carried out in the Physical Laboratory of the University of Adelaide during 1927. The departure of the author for England interrupted the work at this stage, but it is hoped to be able to present at a later date further results obtained with a greater range of concentrations and with other gaseous mixtures.

In conclusion, I wish to express my sincere thanks to Mr. R. S. Burdon, to whose inspiration and continued help the success of these experiments is largely due.

XLIV. Evidence of the Anisotropy of the Carbon Atom. By
KATHLEEN LONSDALE (*née* YARDLEY), *D.Sc.(London)*,
Amy Lady Tate Scholar *.

IN a recent paper ⁽¹⁾ the writer has given the results of an X-ray examination into the structures of the fully-halogenated ethane derivatives, and has shown that in the solid state the molecule C_2Cl_6 , for example, has only one plane of symmetry and a pseudo-centre. This one symmetry plane passes through both carbon atoms and two of the halogen atoms, the other four being arranged in pairs at equal distances from the plane.

1. Assuming a truly tetrahedral distribution of the carbon atom valencies, the possible symmetries of the C_2Cl_6 molecule would be :

- (a) C_{3v} (rhombohedral),
- (b) D_3 (trapezohedral),
- (c) D_{3d} (ditrigonal scalenohedral),
- (d) C_{3h} (trigonal bipyramidal),
- (e) D_{3h} (ditrigonal bipyramidal),

according to the symmetry of the chlorine atoms and the relative arrangement of the two carbon atoms.

If, on the other hand, the four carbon valencies are not assumed to be alike, the symmetry of the C_2Cl_6 molecule may be reduced.

2. Assuming that there are three similar A valencies and one B valency, then combination between two similar carbon

* Communicated by Prof. R. Whiddington, F.R.S.

atoms and six similar chlorine atoms could take place in such a way as to give the molecule any of the above symmetries or else one of the following:—

- (a) A plane through both C atoms (*i. e.* parallel to the C—C bond) + a centre of symmetry.
- (b) Two planes, one parallel and one perpendicular to the C—C bond.
- (c) A plane parallel to the C—C bond (+ a pseudo-plane perpendicular to the bond).
- (d) A plane parallel to the C—C bond (+ a pseudo-centre).
- (e) A plane perpendicular to the C—C bond.
- (f) A dyad axis perpendicular to the C—C bond (+ a pseudo-plane perpendicular to the bond).
- (g) A dyad axis perpendicular to the C—C bond (+ a pseudo-centre).
- (h) A dyad axis perpendicular to the C—C bond (no pseudo-symmetry).
- (i) A centre of symmetry.
- (j) No symmetry.

It will be seen that one of these, (d), corresponds to the symmetry actually found.

3. Assuming that there are two similar A valencies and two similar B valencies in the carbon atom, then the C_2Cl_6 molecule might possess any of the symmetries (a)—(j) given for 2.

4. The same symmetries could exist if only two of the four carbon valencies were alike.

5. If all the carbon valencies were different, the C_2Cl_6 molecule could only have one of the symmetries 2 (f)—2 (j).

The experimental evidence, so far as this particular group of molecules is concerned, therefore points to the arrangement 2 (d), 3 (d), or 4 (d), in which the molecules would be of the type shown in fig. 1.

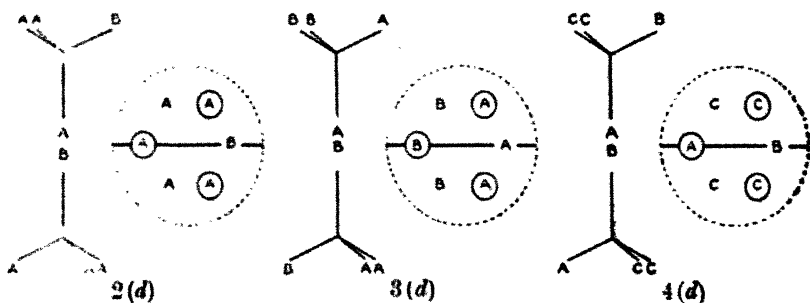
In each case the single bond between the carbon atoms is formed by the mutual sharing of two unlike valencies.

It should be pointed out that this crystallographic evidence only proves that the A, B, etc. valencies must differ slightly in a geometrical sense, although such a difference would probably imply further differences in physical and possibly in chemical properties. It is possible that in compounds where very heavy or extensive groups

are attached to a carbon atom the lack of symmetry of the carbon atom might easily be either masked or enhanced. There is a considerable amount of evidence, however, from other fields of work pointing to an anisotropy of the carbon atom.

In 1923 Main Smith⁽²⁾ published a table giving extra-nuclear electronic configurations based on chemical considerations. According to his arrangement two of the outer electrons of neutral carbon would occupy (2, 1) orbits and the remaining two (2, 2) orbits. In 1924 Fowler⁽³⁾ showed that the emission spectrum of C^+ (C II.) is similar to that of B (B I.), and concluded therefore that their electronic arrangements are similar; that is, that of the three outer electrons in C^+ , two move in (2, 2) orbits, while the electron which generates the spectrum traverses

Fig. 1.



a (2, 1) orbit. Independently of Main Smith, Stoner⁽⁴⁾ compiled a table similar to his, based principally on such spectroscopic evidence. The structure of neutral carbon was fully confirmed the following year by Millikan and Bowen⁽⁵⁾, who examined carbon spectroscopically as C^+ , C^{++} , C^{+++} , and showed conclusively that in neutral carbon there are two (2, 2) and two (2, 1) electrons.

This evidence shows that in all probability the carbon atom is of the type 3, possessing two A and two B electrons, rather than of the other geometrically possible types 2 or 4. These A and B valencies must surely be closely related to the existence of the two (2, 2) and two (2, 1) electrons in the neutral atom.

The structure of methane and of its derivatives has occupied considerable attention on the part of various workers. Methane crystallizes in the cubic system below

$-185^{\circ}8\text{ C.}$, but at a lower temperature still there is an enantiotropic transition into a doubly-refracting modification⁽⁶⁾. Similarly CCl_4 , which is cubic below -22° C. , becomes doubly-refracting at -47° C. ⁽⁷⁾, being presumably isomorphous with CBr_4 , which is cubic above 46° C. but monoclinic (pseudo-cubic) below that temperature⁽⁸⁾. Bridgeman⁽⁹⁾ has found three solid modifications of CCl_4 and of CBr_4 , one stable at atmospheric pressures (the regular form) and the other two at considerably higher pressures. This indicates that the useful symmetry of the carbon atom, in combination with other atoms in the solid state, may vary with temperature and pressure.

No complete X-ray analysis of the crystal structure has yet been given for any of these substances, but Mark⁽¹⁰⁾ has investigated the regular modifications of CBr_4 and Cl_4 by means of the powder method, and has placed them in the space-group T_d^1 (hexakistetrahedral), there being apparently one molecule in a unit cell, of side 5.67 \AA. in the case of CBr_4 , and 5.81 \AA. in the case of Cl_4 . For monoclinic CBr_4 , Mark found that the unit cell contained eight atoms of carbon and thirty-two of bromine, so that presumably polymerization had taken place, the molecule being at least C_2Br_8 . $\text{C}(\text{NO}_2)_4$, $\text{C}(\text{CH}_3)_4$ are also cubic⁽¹¹⁾ with low temperature doubly-refracting modifications. The regular forms of both of these have been examined by means of X-rays⁽¹²⁾. The molecule $\text{C}(\text{NO}_2)_4$ appears to possess trigonal symmetry, one NO_2 group being unique; $\text{C}(\text{CH}_3)_4$ possesses probable molecular symmetry T_d . Other symmetrically substituted methane derivatives crystallize with tetragonal or lower symmetry⁽¹³⁾. In 1923 Mark and Weissenberg⁽¹⁴⁾ published an X-ray examination of pentaerythritol, $\text{C}(\text{CH}_2\text{OH})_4$, the results of which (supposedly confirmed by Huggins and Hendricks⁽¹⁵⁾) have aroused much interest and controversy. These authors accepted the class C_4 given by Martin⁽¹⁶⁾, being unaware that Haga and Jaeger⁽¹⁷⁾ had shown by means of an excellent Laue photograph that the planes of symmetry supposed to intersect in the tetrad axis were non-existent. Various papers referring to this point followed^{(18), (19)}. X-rays can, in general, give no evidence as to the polarity of a crystal. Mark and Weissenberg assumed, after Martin, that pentaerythritol is polar, and then showed that in that case the only possible symmetry of the $\text{C}(\text{CH}_2\text{OH})_4$ molecule is C_4 . Thus the molecule would be of a pyramidal shape, the four valency directions of the carbon atom pointing along the edges of a tetragonal pyramid. Liebisch⁽²⁰⁾ had affirmed that the

pyro-electric test gave positive results for these crystals, and Giebe and Scheibe⁽²¹⁾ had recorded a positive result for the piezo-electric test. Armed with this evidence Weissenberg⁽²²⁾ and Reis⁽²³⁾ developed a new stereochemistry for the carbon atom, based on its possible non-tetrahedral form. Mark and Weissenberg's conclusions have not, however, remained unchallenged. I. Nitta⁽²⁴⁾ has repeated the X-ray investigation, and has shown that the results obtained are consistent with either a pyramidal (C_4) or a sphenoidal (S_4) symmetry of the $C(CH_2OH)_4$ molecule. This result has been confirmed by S. B. Hendricks⁽²⁵⁾ and by A. Nehnitz⁽²⁶⁾. The latter believes that the X-ray intensities observed favour the sphenoidal symmetry. On the purely crystallographic side I. E. Knaggs (*loc. cit.*) and later Schleede and Schneider⁽²⁷⁾ have been unable to detect any evidence of polarity in the crystal habit or by means of etch figures. Schleede and Schneider grew a number of crystals which appeared to show definite S_4 symmetry, the basal faces (001) and ($\bar{0}\bar{0}\bar{1}$) being rectangles whose long sides were crossed. Finally, H. Siefert⁽²⁸⁾ has very carefully reinvestigated the crystallographic properties of pentaerythritol. He obtained crystals which closely simulated C_4 symmetry, but which might have been formed by twinning of a lower class of symmetry. By cutting sections parallel to (001) at both ends of these bipyramids and etching on each of the four faces so obtained, he was able to prove that the bipyramids were formed of two interpenetrating bisphenoids and that the true crystal class is S_4 . He remarks that he obtained an apparent pyroelectric effect with the crystals, but that, since true pyroelectricity is impossible in the bisphenoidal class, the effect is probably only a manifestation of the piezo-electric effect, and quotes, in this connexion, the example of quartz (see R. E. Gibbs, *Science Progress*, lxxxviii. p. 613 (1928), for a brief summary of the properties of quartz), for which the existence of a true pyroelectric effect is also doubtful. Hettich and Schleede⁽²⁹⁾ have shown that piezo-electricity is compatible with S_4 symmetry, since its presence only indicates a lack of centro-symmetry.

Cooley⁽³⁰⁾ examined the fine structure of the band spectrum of methane, and found for the band at approximately 3.31μ , $\frac{\Delta}{\lambda} = 9.77 \text{ cm.}^{-1}$, whereas for the band at 7.7μ , $\frac{\Delta}{\lambda} = 5.41 \text{ cm.}^{-1}$. Dennison⁽³¹⁾ discussed these results on the basis of a tetrahedral molecule, and showed that the

observed difference in $\frac{\Delta}{\lambda}$ for the two bands may possibly be explained by the assumption that the CH_4 molecule possesses a resultant angular momentum fixed in direction in the molecule of the amount $\frac{1}{2}\left(\frac{h}{2\pi}\right)$. Guillemin⁽³²⁾, however, used Cooley's results to calculate the potential energies, (1) of a tetrahedral CH_4 molecule, and (2) of a pyramidal CH_4 molecule, and came to the conclusion that the pyramidal arrangement would be the more stable of the two. He assumed that the carbon was $-ve$ (and therefore polarizable) and the hydrogens $+ve$, an hypothesis which is by no means justified. He also accepted Grimm's⁽³³⁾ value of the CH_4 radius, which is about 10^{-8} cm., whereas Wasastjerna⁽³⁴⁾, whose calculations for other atoms have been fully confirmed by the latest X-ray results, gives as the radius of Kr, and therefore approximately of CH_4 , the value 1.76 Å. For CCl_4 , however, the tetrahedral arrangement is considered to be the more stable, and Guillemin suggests that a change from the pyramidal to the tetrahedral configuration may take place on substitution. Havelock⁽³⁵⁾ has used Guillemin's figures for the C—H distance to calculate the molecular refractivity and depolarization factors on the basis of a tetrahedral and a pyramidal arrangement of the methane molecule. In each case the values found are smaller than the experimental values, and Havelock suggests that is because Guillemin's figures are too small. Van Arkel and de Boer⁽³⁶⁾, independently of Guillemin, have made calculations for a CH_4 molecule in which the hydrogens, being $-ve$, are polarizable, and the carbon is $+ve$, and they have shown that the tetrahedral form is the more stable, both for CH_4 and also for CCl_4 .

Carbon tetraphenyl forms rather poor crystals, and its symmetry is not yet fully ascertained. Wahi⁽³⁷⁾ has placed it in the orthorhombic system as the result of an examination of its optical properties. W. H. George⁽³⁸⁾ has examined it by X-ray photographic methods, and has shown that the structure approximates closely to the tetragonal space-group D_{2d}^4 . The molecular symmetry is either S_6 or a close approximation to it. No other crystalline modification has been found at temperatures above -200°C .

Gerstcker, Mller, and Reis⁽³⁹⁾ have examined the compounds penta-erythritol tetra-nitrate and penta-erythritol tetra-acetate. They place the first in the space-group D_{2d}^4 and the second in C_{4v}^2 , with two molecules per unit cell in each case. The former compound could therefore only have

S_4 symmetry and the latter C_4 or S_4 symmetry. They give reasons, based on the crystal habit, for believing that the molecules of penta-erythritol tetra-acetate are pyramidal. I. E. Knaggs, however, has subsequently pointed out⁽⁴⁰⁾ that the space-group of the latter substance is most probably not C_{4h}^3 . Her examination of the crystals by ionization and by photographic methods failed to reveal any trace of odd orders of (001), and thus pointed to C_{4h}^4 as the true space-group and to S_4 as the only possible molecular symmetry. The writer, at Miss Knaggs's request, also examined the crucial plane very carefully by the ionization method, and confirmed the absence of odd order reflexions. It appears, therefore, that no case of a pyramidal arrangement of the carbon valencies has as yet been satisfactorily substantiated. The X-ray results so far obtained indicate that the carbon atom may be tetrahedral, trigonal, sphenoidal, or a close approximation to one of these symmetries.

Ebert and von Hartel⁽⁴¹⁾ have shown that many compounds of the type Cn_4 , such as $C(OCH_3)_4$, $C(OC_2H_5)_4$, $C(CH_2 \cdot O_2C \cdot CH_3)_4$, have measurable dielectric orientational polarizations in dilute benzene solution, and they have calculated the dipole moments of the molecules. They and Weissenberg⁽⁴²⁾ take these positive results as proof of the pyramidal structure of the molecules in question. It should be pointed out, however, that the existence of a dipole moment only shows that the molecules are not truly tetrahedral. It is difficult to see how they can even be truly sphenoidal, as indicated (in the case of $C(CH_2 \cdot O_2C \cdot CH_3)_4$) by the X-ray results. A carbon atom of the type postulated by the writer, having two A and two B valencies, would, however, possess a small dipole moment, which would probably be greater the more "elongated" the substituted groups. Williams and Krehma⁽⁴³⁾ have shown that the dipole moment of CCl_4 is negligible.

Further evidence for the anisotropy of the carbon atom comes from a consideration of the polarization factor for light scattered by methane, tetrachlormethane, etc. According to theory, if these substances were completely isotropic the depolarization factor should be zero. Cabannes and his collaborators^{(44), (45)} and Rayleigh⁽⁴⁶⁾ have found a small depolarization factor, even for the rare-gas atoms, He, Ne, Ar, Kr, Xe; for CH_4 Cabannes found⁽⁴⁷⁾ $\rho = 0.015$ and for CCl_4 ⁽⁴⁸⁾ $\rho = 0.0087$. Other investigators^{(49), (50), (51)} have obtained higher values for CCl_4 , but Cabannes is the only worker who has given results for both, and he states that the depolarization factor is definitely bigger for CH_4 .

than for CCl_4 . This he takes as conclusive proof that it is really the carbon atom which is anisotropic, since when the less refringent atoms of hydrogen are replaced by the much more refringent atoms of chlorine, the relative importance of the carbon atom and the consequent degree of anisotropy of the molecule will therefore be diminished.

A summary of much of the work in this and other fields has been given by V. Henri⁽⁵²⁾, who, however, has quoted Cabannes's results in support of Guillemin's pyramidal model for CH_4 and tetrahedral model for CCl_4 .

Application to Simple Crystal Structures.

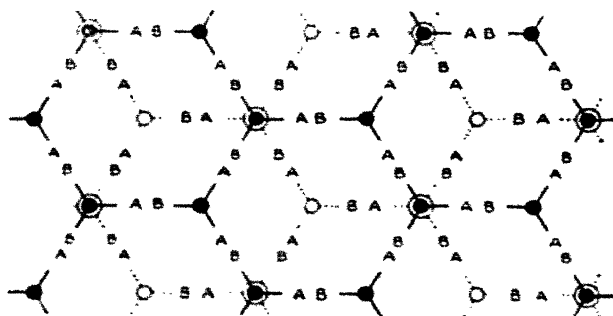
It is of interest to see how such a carbon atom as that suggested by the X-ray work on the C_2Cl_6 series, having two A and two B valencies, will fit in with the X-ray results for other carbon compounds. Diamond, of course, suggests itself first. Grimm and Sommerfeld⁽⁵³⁾ have pointed out that C, Si, Ge, and Sn all crystallize in the diamond type of lattice, and that, according to the Main Smith-Stoner classification, each of these contains two complete sub-groups of two electrons each, and requires an extra four electrons in order to reach the (2, 2, 4) grouping characteristic of the inert gases. The suggestion implied, that the electronic configuration must be similar in each of these crystalline substances, has been vigorously attacked by Hume-Rothery⁽⁵⁴⁾, who points out, however, that in diamond itself all the properties of the crystal indicate that the forces joining the carbon atoms in the lattice closely resemble those which bind together the atoms of a molecule. Thus the diamond is extremely hard, infusible below 3000°C ., and possesses a specific resistance of about 10^{+14} ohm-cm. The present writer⁽⁵⁵⁾ has shown that if C—C bonds in diamond are taken to resemble that in the molecule C_2Cl_6 , the cubic symmetry may be explained on the assumption that the (AB) electrons forming or contributing to the bond are absolutely mutually shared by the two carbon atoms in question. Carbon atoms of the AAAB or ABCC types referred to earlier could not fit into a strictly cubic lattice of the dimensions found, and even if a larger unit cell were assumed, the bonds linking the atoms together would not be all of one kind.

Graphite is a more difficult problem. The accepted structure, given independently by Hassel and Mark⁽⁵⁶⁾ and by Bernal⁽⁵⁷⁾, is one in which the carbon atoms lie in planes in which they form hexagonal nets. Half the atoms in one net lie normally above half the atoms of a net in the plane

beneath, while the other half lie normally above the centres of the hexagons of this net. Alternate nets lie atom for atom normally above each other. The tetrahedral symmetry of the carbon atom is thus lost, three of the valency directions lying in one plane, while the fourth is directed apparently at right angles to this plane. As Bernal points out, this result is inevitable in any graphite structure. Cleavage sheets of graphite possess considerable hardness and tenacity in their own plane, and it is therefore justifiable to assume that the linking between carbon atoms in this plane is similar to that in diamond (fig. 2), consisting entirely of (AB) junctions.

If the sharing is mutual, that is, if an (AB) junction is exactly equivalent to a (BA) junction, then the nets will be truly hexagonal. Bernal mentions a further difficulty,

Fig. 2.

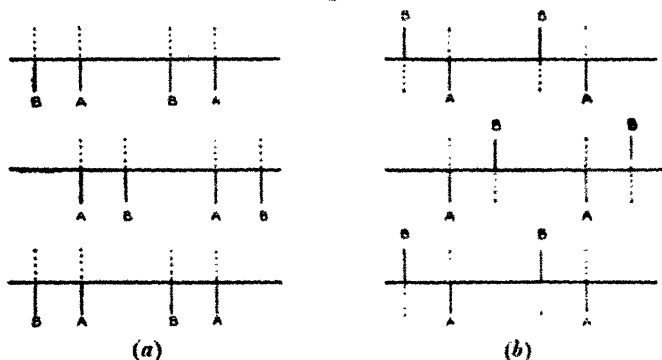


which is that the carbon atoms in graphite fall into two classes, according as to whether their nearest neighbours along the $[0001]$ direction are at a distance 3.41 or 6.82 Å., and, moreover, even the distance 3.41 is extremely large compared with the normal C—C distance (1.54 Å. in diamond, 1.42 Å. in the graphite cleavage planes). These difficulties are capable of explanation if the structure given in fig. 2 is correct; the projection of the structure on a plane at right angles to that of fig. 2 is shown in fig. 3 (a) or (b). The two types of carbon atoms are now clearly seen to be those which have an A-valency direction normal to the cleavage plane and those which have a B-valency direction normal (or possibly inclined) to that plane.

It is not known to what class graphite belongs, and therefore the space-group cannot definitely be fixed. Hassel and Mark give a list of possible space-groups, reducing them by means of arguments based on observed intensities.

Lane photographs and X-ray methods in general cannot distinguish between the classes D_{3h} , C_6 , D_6 , and C_{6h} . Hence it is impossible to say whether graphite is polar or non-polar. If it is non-polar, then the fourth valency or electron orbit must somehow be symmetrical about the cleavage plane. This is indicated by the dotted lines in the diagrams. The argument, of course, applies to any graphite structure. The junctions between atoms in successive cleavage planes are likely to be extremely weak, and, in fact, half of the carbon atoms may practically be regarded as unsaturated. Hence, probably, the ease with which graphite can combine with hydrogen to form a weak chemical compound and the tendency of various atoms to attach themselves to the surface of charcoal (which is hydrogenated graphite in a fine state of division).

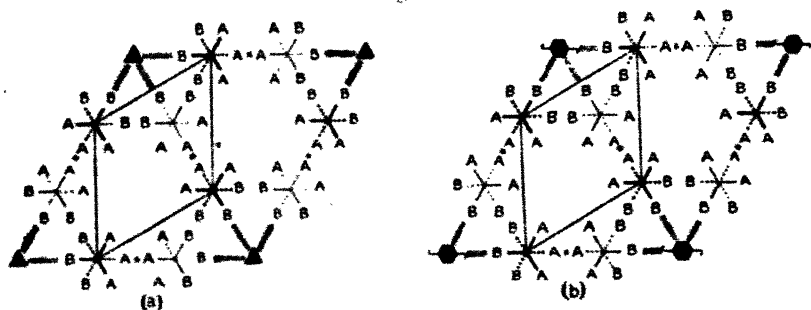
Fig. 3.



Another substance the crystal structure of which requires a closer investigation is ethane, C_2H_6 . Wahl showed⁽⁵⁸⁾ by the optical behaviour and the rhombohedral cleavage that at the temperature of liquid air ethane crystallizes in the hexagonal system. Mark and Pohland⁽⁵⁹⁾ pursued the investigation by means of the X-ray powder method, and showed that the unit cell, of size $4.46^2 \times 8.19^3 \text{ \AA}$, contains two molecules, characteristic points of which are approximately in the "close-packed" positions. The C—C bond lies along the principal axis, the distance between the carbons of one molecule being about 1.55 \AA . The positions of the H atoms could not be located. Niven⁽⁶⁰⁾ has suggested that in C_2H_6 all the (2, 2) electrons and two of the (2, 1) electrons of the carbon atoms are taken by the six hydrogen atoms to complete their (1, 1) orbits, while the remaining two (2, 1) electrons form a closed system of

two, thus making a bond between the two C atoms. If, as is almost certain, however, ethane is similar to hexachlor-ethane in the arrangement of the carbon valencies, the bond between the two C atoms would be formed by two unlike valencies. We must therefore see how such a molecule, having a plane through the two C atoms and two of the H atoms, together with a pseudo-centre, will fit into the structure recorded by Mark and Pohland. It is found, by examining every geometrical possibility, that in order to retain the hexagonal symmetry the unit cell must be at least three times the volume of that given by Mark and Pohland. This is not incompatible with their results, for they themselves say that the method they used was not sufficiently accurate to exclude the possibility of a unit cell larger than that given in their paper. Two possible

Fig. 4.



structures then present themselves, either of which is in agreement with the results found (fig. 4 (a) and (b)).

The cell indicated by the powder method is shown by full lines. The height of the cell remains unchanged, but its dimensions are now

$$(4.46 \times \sqrt{3})^2 \times 8.19 \text{ \AA.}^3,$$

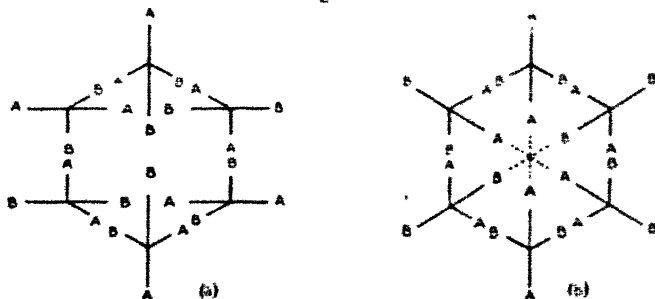
and it contains six molecules, each possessing a plane of symmetry.

In the case (a) no reflexion would be really absent, but planes of indices ($mm\bar{2}l$) where l is odd (referred to the cell given by Mark and Pohland) would have negligible odd orders. In the case (b) those orders would actually be absent. [In the true cell this would correspond to a halving of planes ($m0\bar{m}l$) where l is odd.] Now an examination of the experimental results shows that only one such reflexion is recorded, that from ($11\bar{2}3$), and even this weak reflexion

is very doubtful, since it coincides well within the limits of experimental error (given as 3 per cent.) with the reflexion from the (2022) plane. Until experimental data of much greater accuracy can be obtained using single crystals of ethane, it is not possible to say which of the above structures, if either, is true to the facts.

Another hydrocarbon which is of even greater importance is benzene. Unfortunately, X-ray results relating to crystalline benzene are most incomplete. Broomé⁽⁶¹⁾ has used powder and Laue methods to show that the unit orthorhombic cell contains four molecules, and Mark⁽⁶²⁾ quotes a dissertation by Schneefusz (Berlin, 1924—not available to the writer) in which the dimensions are verified and the space-group is given as Q_1^{11} , Q_1^{15} , Q_1^{16} , the molecule being apparently centro-symmetrical. Schneefusz has also

Fig. 5.



used X-ray methods to prove that C_6Cl_6 , C_6Br_6 , and C_6I_6 are centro-symmetrical, crystallizing in the monoclinic system. Similar results for C_6Cl_6 and C_6Br_6 were arrived at independently by Plummer⁽⁶³⁾. If the benzene ring of six carbon atoms persists with more or less distortion just as it exists in diamond or graphite, then again we must expect that the C—C bonds will consist of (AB) junctions. The existence of centro-symmetry definitely eliminates the Kekulé model with its three double bonds. Centro-symmetrical models, having no further symmetry, may be built up either on the Ladenburg or the Armstrong-Baeyer models (fig. 5 (a) and (b)).

By an extension of the fourth (internal) valencies, so that actual linking takes place within the ring, fig. 5 (b) could be made to represent the Claus model.

In conclusion, it may be stated that the structure here suggested for the carbon atom, in which two of the valencies are geometrically different from the other two, agrees with

the crystallographic determinations on various substances as least as well as, if not better than, the ordinary tetrahedral model, and is able to explain the curious lack of symmetry of many simple carbon compounds.

The writer wishes to express her indebtedness to the Council of Bedford College, London, for a scholarship enabling her to carry on research work at the University of Leeds.

Summary.

The possible symmetry of the carbon atom is investigated in the light of X-ray results on crystals of C_2Cl_6 and isomorphous compounds. A model is obtained having two A and two B valencies, geometrically different, and a comparison is made with the Main Smith-Stoner atom. Work in other fields is also quoted in favour of a non-tetrahedral carbon atom. A critical account is given of the controversy concerning pentaerythritol and other symmetrically substituted derivatives of methane, and it is shown that no case of a pyramidal carbon atom has yet been satisfactorily proved. It is found that the model now suggested will explain the symmetries, as determined by means of X-rays, of other simple carbon compounds, in some cases throwing light on anomalies revealed by such determinations.

References.

- (1) K. Yardley, *Proc. Roy. Soc. A*, cxviii. p. 449 (1928).
- (2) J. D. Main Smith, *Journ. Soc. Chem. Ind. (Chem. and Ind. Rev.)* xliii. p. 323 (1923).
- (3) A. Fowler, *Proc. Roy. Soc. A*, cv. p. 299 (1924).
- (4) E. C. Stoner, *Phil. Mag.* xlviii. p. 719 (1924).
- (5) R. A. Millikan and I. S. Bowen, *Phys. Rev.* xxvi. pp. 150, 310 (1925).
- (6) W. Wahl, *Proc. Roy. Soc. A*, lxxxvii. p. 377 (1912); xc. p. 1 (1914).
- (7) W. Wahl, *Proc. Roy. Soc. A*, lxxxix. p. 330 (1913).
- (8) — Zirnziebl. See P. Groth, *Chem. Kryst.* i. p. 230.
- (9) P. W. Bridgeman, *Phys. Rev.* iii. p. 153 (1914).
- (10) H. Mark, *Ber. Deut. Chem. Ges.* lvii. p. 1820 (1924).
- (11) W. Wahl, *Proc. Roy. Soc. A*, lxxxix. p. 333 (1913); lxxxviii. p. 359 (1913).
- (12) H. Mark and W. Noethling, *Zeit. f. Krist.* lxxv. p. 442 (1927).
- (13) I. E. Knaggs, *Trans. Chem. Soc.* cxxiii. p. 71 (1923).
- (14) H. Mark and K. Weissenberg, *Zeit. f. Phys.* xvii. p. 301 (1923).
- (15) M. L. Huggins and S. B. Hendricks, *Journ. Am. Chem. Soc.* xlviii. p. 164 (1926).
- (16) J. Martin, *Neues Jahrbuch f. Min.* vii. p. 1 (1890); cf. P. Groth, *Chem. Kryst.* iii. p. 385.
- (17) H. Haga and F. M. Jaeger, *Proc. Kon. Akad. Wetensch. Amst.* xviii. p. 1350 (1910).

- (18) H. G. Westenbrink and F. A. van Melle, *Zeit. f. Krist.* lxiv. p. 548 (1926).
- (19) H. Mark and K. Weissenberg, *Zeit. f. Krist.* lxv. p. 499 (1927).
- (20) T. Liebisch, *Grundriss der Phys. Kryst.* Leipzig, p. 141 (1896).
- (21) E. Giebe and A. Scheibe, *Zeit. f. Phys.* xxxiii. p. 760 (1925).
- (22) K. Weissenberg, *Ber. d. Deut. Chem. Ges.* lix. p. 1526 (1926); cf. H. Mark and K. Weissenberg, *Zeit. f. Phys.* xlvii. p. 301 (1928).
- (23) A. Reis, *Ber. Deut. Chem. Ges.* lix. p. 1543 (1926).
- (24) I. Nitta, *Bull. Chem. Soc. Japan*, i. p. 62 (1927).
- (25) S. B. Hendricks, *Zeit. f. Krist.* lxvi. p. 131 (1927).
- (26) A. Nehmitz, *Zeit. f. Krist.* lxvi. p. 408 (1928).
- (27) A. Schleede and E. Schneider, *Naturwissenschaften*, xv. p. 970 (1927).
- (28) H. Siefert, *Sitzungsber. Preuss. Akad. Wiss. Berlin*, p. 289 (1927).
- (29) A. Hettich and A. Schleede, *Zeit. f. Phys.* xlvii. p. 147 (1927).
- (30) J. P. Cooley, *Astrophys. Journ.* lxii. p. 73 (1925).
- (31) D. M. Dennison, *Astrophys. Journ.* lxii. p. 84 (1925).
- (32) V. Guillemin, jun., *Ann. der Phys.* lxxxi. p. 173 (1926).
- (33) H. G. Grimm, *Zeit. f. Electrochemie*, xxxi. 474 (1925).
- (34) J. A. Wasastjerna, *Comm. Phys.-Math. Soc. Scient. Fennicæ*, i. p. 38 (1923).
- (35) T. H. Havelock, *Phil. Mag.* iii. p. 433 (1927).
- (36) A. E. van Arkel and J. H. de Boer, *Zeit. f. Phys.* xli. pp. 27, 38 (1927).
- (37) W. Wahl, *Zeit. f. Phys. Chem.* lxxxviii. p. 129 (1914).
- (38) W. H. George, *Proc. Roy. Soc. A*, cxiii. p. 585 (1927).
- (39) A. Gerstäcker, H. Möller, and A. Reis, *Zeit. f. Krist.* lxvi. p. 355 (1928).
- (40) I. E. Knaggs, 'Nature,' cxxi. p. 616 (1928).
- (41) L. Ebert and H. von Hartel, *Naturwissenschaften*, xv. p. 669 (1927).
- (42) K. Weissenberg, *Naturwissenschaften*, xv. p. 662 (1927).
- (43) J. W. Williams and I. J. Krehma, *Journ. Am. Chem. Soc.* xlix. p. 1676 (1927).
- (44) J. Cabannes, *Ann. de Phys.* xv. p. 120 (1921).
- (45) J. Cabannes and A. Lepape, *Comptes Rendus*, clxxix. p. 326 (1924).
- (46) Lord Rayleigh, *Proc. Roy. Soc. A*, xcvi. p. 57 (1920).
- (47) J. Cabannes and J. Gauzit, *Journ. de Phys.* vi. p. 182 (1925).
- (48) J. Cabannes, *Journ. de Phys.* vii. p. 343 (1926).
- (49) Lord Rayleigh (Hon. R. J. Strutt), *Proc. Roy. Soc. A*, xcv. p. 155 (1919) (material of doubtful purity).
- (50) C. V. Raman and K. S. Rao, *Phil. Mag.* xlv. p. 625 (1923).
- (51) A. S. Ganesan, *Phil. Mag.* xlix. p. 1216 (1925).
- (52) V. Henri, *Chem. Rev.* iv. p. 189 (1927).
- (53) H. G. Grimm and A. Sommerfeld, *Zeit. f. Phys.* xxxvi. p. 36 (1926).
- (54) W. Hume-Rothery, *Phil. Mag.* iii. p. 301 (1927).
- (55) K. Yardley, *loc. cit.*
- (56) O. Hassel and H. Mark, *Zeit. f. Phys.* xxv. p. 317 (1924).
- (57) J. D. Bernal, *Proc. Roy. Soc. A*, cvi. p. 749 (1924).
- (58) W. Wahl, *Proc. Roy. Soc. A*, lxxxviii. p. 354 (1913).
- (59) H. Mark and E. Pohland, *Zeit. f. Krist.* lxii. p. 103 (1925).
- (60) C. D. Niven, *Phil. Mag.* iii. p. 314 (1927).
- (61) B. Broomé, *Phys. Zeit.* xxiv. p. 124 (1923); *Zeit. f. Krist.* lxi. p. 325 (1925).
- (62) H. Mark, *Ber. d. Deut. Chem. Ges.* lvii. p. 1820 (1924).
- (63) W. G. Plummer, *Phil. Mag.* i. p. 1214 (1925).

XLV. On the Radiation from the Inside of a Circular Cylinder.—Part II. *By* H. BUCKLEY, *M.Sc., F.Inst.P.*
(From the National Physical Laboratory *.)

IN the *Philosophical Magazine* for October 1927 † it was shown that the radiation per unit area from the inside of a uniformly heated infinite circular cylinder at temperature T° , taking into account multiple reflexions, was given by an integral equation of the form

$$\Phi(x_1) = \epsilon \sigma T^4 + \frac{1-\epsilon}{4} \left\{ \int_0^{x_1} \Phi(x) \frac{d^2}{dx^2} F(x_1-x) dx + \int_{x_1}^{\infty} \Phi(x) \frac{d^2}{dx^2} F(x-x_1) dx \right\},$$

where x and x_1 are measured from the end of the cylinder in terms of the radius, ϵ is the emissivity of the walls, and $\pi/2 \cdot F(x)$ is the radiation from a disk of radius unity and brightness unity to a parallel coaxial disk of radius unity at a distance x away, where

$$F(x) = \{x^2 + 2 - x(x^2 + 4)^{1/2}\}.$$

This equation merely expresses the fact that the radiation from any point of the cylinder is equal to the directly emitted radiation plus the reflected portion of the radiation received from the rest of the cylinder. Solutions of this equation were obtained by taking an approximation to the kernel $\frac{1}{2} \frac{d^2}{dx^2} F(x)$ in the form $\sum_1^n B_n e^{\beta_n x}$, where all the β 's are negative ‡. The approximation was also adjusted so that

$$\int_0^{\infty} \frac{1}{2} \frac{d^2}{dx^2} F(x) dx = \int_0^{\infty} \sum_1^n B_n e^{\beta_n x} dx = 1,$$

$$\text{i. e.,} \quad \sum_1^n (B_n / \beta_n) = -1.$$

The case considered was when $n=2$, but the extension to higher values of n is easily made and is obvious. It was also shown that for values of the emissivity greater than 0.25 (i. e., reflectivity less than 0.75) the approximate solution obtained with $n=2$ was quite satisfactory and that

* Communicated by Sir J. E. Petavel, K.C.B., F.R.S.

† Buckley, *Phil. Mag.* iv. p. 753 (1927).

‡ Whittaker, *Proc. Roy. Soc.* cxiv. p. 307 (1918).

even with $n=1$ the approximation was quite good. The approximate expressions for the kernel were

$$\frac{1}{2} \frac{d^2}{dx^2} F(x) = e^{-x} \quad \text{for } n=1$$

$$\text{and } \frac{1}{2} \frac{d^2}{dx^2} F(x) = 1.21e^{-1.14x} - 0.21e^{-3.40x} \quad \text{for } n=2.$$

The solutions in these cases were found to be

$$\Phi(x) = 1 + A_1 e^{a_1 x} + A_2 e^{a_2 x}$$

$$\text{and } \Phi(x) = 1 - (1 - \sqrt{\epsilon}) e^{-\sqrt{\epsilon} x},$$

where each side has been divided by σT^4 .

It is the purpose of this paper to consider the case of a finite cylinder, and also to apply the results obtained to deduce the brightness of the inside of a non-radiating diffusing cylinder of reflectivity ρ when illuminated by an infinite plane of brightness B and reflectivity zero at an infinite distance from the end of the cylinder. This is the problem of the brightness of a vertical circular shaft or light well illuminated by a uniform sky.

A solution is also obtained of the problem of the radiation from the inside of an infinite circular cylinder which has an infinite longitudinal slit parallel to the axis. This problem is of interest, since it approximates to the platinum black body primary standard of light employed by Ives*, except that emission and reflexion are considered to be perfectly diffuse instead of specular. In this case the solution is exact.

The Finite Radiating Cylinder.

The equation to be solved is

$$\begin{aligned} \Phi(x_1) = \epsilon + \frac{1-\epsilon}{2} \left[\int_0^{x_1} \Phi(x) \{ B_1 e^{\beta_1(x_1-x)} + B_2 e^{\beta_2(x_1-x)} \} dx \right. \\ \left. + \int_{x_1}^l \Phi(x) \{ B_1 e^{\beta_1(x-x_1)} + B_2 e^{\beta_2(x-x_1)} \} dx \right], \end{aligned}$$

where l is the length of the cylinder. It is obvious that the solution will be symmetrical about the mid-point of the cylinder, so that

$$\Phi(x) = \Phi(l-x).$$

This suggests that $\Phi(x)$ is of the form

$$\Phi(x) = A_0 + A_1 e^{a_1 x} + A_1 e^{a_1(l-x)} + A_2 e^{a_2 x} + A_2 e^{a_2(l-x)}.$$

* Ives, Journ. Frank. Inst. cxvii, pp. 147, 359 (1924).

On substituting this expression in the equation above, performing the integrations and equating the constant terms and the coefficients of $e^{a_1 x_1}$, $e^{a_2 x_1}$, $e^{\beta_1 x_1}$, and $e^{\beta_2 x_1}$ on each side of the equation, it is found that

$$A_0 = \epsilon - A_0(1 - \epsilon) \left(\frac{B_1}{\beta_1} + \frac{B_2}{\beta_2} \right),$$

$$1 = (1 - \epsilon) \left\{ \frac{B_1 \beta_1}{\alpha_1^2 - \beta_1^2} + \frac{B_2 \beta_2}{\alpha_1^2 - \beta_2^2} \right\},$$

$$1 = (1 - \epsilon) \left\{ \frac{B_1 \beta_1}{\alpha_2^2 - \beta_1^2} + \frac{B_2 \beta_2}{\alpha_2^2 - \beta_2^2} \right\},$$

$$0 = \frac{A_0}{\beta_1} - \frac{A_1}{\alpha_1 - \beta_1} - \frac{A_2}{\alpha_2 - \beta_1} + \frac{A_1 e^{a_1 l}}{\alpha_1 + \beta_1} + \frac{A_2 e^{a_2 l}}{\alpha_2 + \beta_1},$$

$$0 = \frac{A_0}{\beta_2} - \frac{A_1}{\alpha_1 - \beta_2} - \frac{A_2}{\alpha_2 - \beta_2} + \frac{A_1 e^{a_1 l}}{\alpha_1 + \beta_2} + \frac{A_2 e^{a_2 l}}{\alpha_2 + \beta_2}.$$

Four identical expressions are found from the coefficients of $e^{a_1(l-x_1)}$, $e^{a_2(l-x_1)}$, $e^{\beta_1(l-x_1)}$, and $e^{\beta_2(l-x_1)}$, as is to be expected. Furthermore, for $l \rightarrow \infty$ these equations become identical with those obtained in the previous paper for the case of the infinite cylinder.

The first of these equations gives $A_0 = 1$, since

$$\frac{B_1}{\beta_1} + \frac{B_2}{\beta_2} = -1.$$

The second and third show that α_1 and α_2 are given by the square roots of the roots of the quadratic in z ,

$$1 = (1 - \epsilon) \left\{ \frac{B_1 \beta_1}{z - \beta_1^2} + \frac{B_2 \beta_2}{z - \beta_2^2} \right\},$$

which is independent of l , so that the indices of the exponential terms in the solution for the finite cylinder are the same as those for the infinite cylinder. It can also be shown that $\epsilon_1 \alpha_2 = \sqrt{\epsilon} \beta_1 \beta_2$.

The coefficients, however, are different, and are given by the fourth and fifth equations when the values of α_1 and α_2 are substituted in them.

The numerical values of the approximate solutions for $n=2$ in the case of a cylinder whose length is eight times the radius are given below for various values of the emissivity.

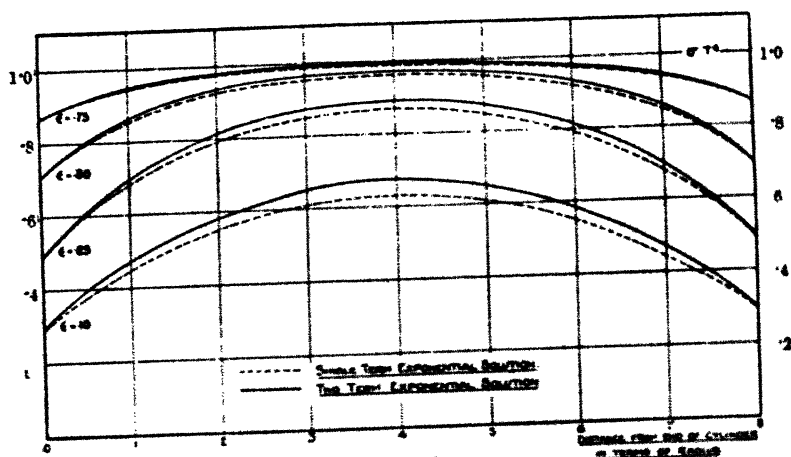
$$\epsilon = 0.75. \Phi(x) = 1 - 0.1399 e^{-0.980x} - 0.1399 e^{-0.980(8-x)} + 0.0059 e^{-3.425x} + 0.0059 e^{-3.425(8-x)},$$

$$\epsilon = 0.50. \Phi(x) = 1 - 0.3011 e^{-0.795x} - 0.3011 e^{-0.795(8-x)} + 0.0089 e^{-3.450x} + 0.0089 e^{-3.450(8-x)},$$

$$\epsilon = 0.25. \Phi(x) = 1 - 0.5064 e^{-0.558x} - 0.5064 e^{-0.558(8-x)} + 0.0080 e^{-3.470x} + 0.0080 e^{-3.470(8-x)},$$

$$\epsilon = 0.10. \Phi(x) = 1 - 0.6680 e^{-0.352x} - 0.6680 e^{-0.352(8-x)} + 0.0055 e^{-3.470x} + 0.0080 e^{-3.470(8-x)}.$$

Fig. 1.



Distribution of radiation from the inside of a uniformly heated finite cylinder.

The approximate solution for $n=1$ is given by

$$\Phi(x) = 1 - \frac{(1-\epsilon)\{e^{-\sqrt{\epsilon}x} + e^{-\sqrt{\epsilon}(l-x)}\}}{(1+\sqrt{\epsilon}) + (1-\sqrt{\epsilon})e^{-\sqrt{\epsilon}l}},$$

which, when $l \rightarrow \infty$ becomes

$$\Phi(x) = 1 - (1 - \sqrt{\epsilon})e^{-\sqrt{\epsilon}x},$$

and agrees with the value obtained previously.

These results are shown graphically in fig. 1. As before, the agreement between the two approximate solutions is quite good for values of ϵ greater than 0.25. It is to be anticipated that the solution for a three-term exponential

approximation to $\frac{1}{2} \frac{d^2}{dx^2} F(x)$ will be very close to that given by the two-term exponential approximation for the reasons discussed in the previous paper.

Circular Cylindrical Shaft or Light Well illuminated by a Uniform Sky.

Infinite Cylindrical Shaft.

The results obtained previously give the value of the radiation from any point x , of the infinite cylinder as

$$\Phi(x) = 1 + A_1 e^{a_1 x} + A_2 e^{a_2 x}$$

$$\text{or} \quad 1 - (1 - \sqrt{\epsilon}) e^{-\sqrt{\epsilon} x}.$$

If the end of the cylinder is closed by a circular disk of emissivity unity, and consequently of reflectivity zero, at the same temperature as the walls of the cylinder, the cylinder will approach the thermo-dynamic ideal of a constant temperature enclosure. Hence the radiation from every point on the walls of the cylinder is complete or black-body radiation. Thus, if $\theta(x)$ is the radiation from any point x in the cylinder when the end disk is in position, $\theta(x) = 1$.

Now let $\theta(x) - \Phi(x) = \Psi(x)$.

But $\theta(x) - \Phi(x)$ is merely the difference between what the walls radiate when the end disk is in position and what they radiate when it is not in position. What they radiate in each case is the radiation corresponding to the emissivity increased by multiple reflexion from the walls alone, since the disk at the end has zero reflectivity. Hence the difference $\Psi(x)$ is the radiation from the walls due to the radiation received by them from the end disk, increased by multiple reflexions from the walls.

$$\text{Hence} \quad \Psi(x) = -(A_1 e^{a_1 x} + A_2 e^{a_2 x})$$

$$\text{or} \quad (1 - \sqrt{\epsilon}) e^{-\sqrt{\epsilon} x}.$$

The same result is obtained if the end disk is replaced by an infinite disk having the same properties as the end disk but removed to an infinite distance. It also holds if the cylinder is not self-radiating, since what the walls radiate due to the presence of the disk is independent of what they radiate on their own account.

If, now, the infinite disk of unit emissivity be replaced by a uniform sky of brightness B , the sky can be regarded as

having zero reflectivity, so that the same result still applies if σT^4 is replaced by πB , and the reflectivity of the cylinder $(1 - \epsilon)$ replaced by ρ . Hence the radiation from the cylinder when illuminated by a uniform sky of brightness B , i. e. the brightness of the walls of the infinite cylinder, is given by

$$\Psi_B(x) = -\pi B(A_1 e^{a_1 x} + A_2 e^{a_2 x})$$

$$\text{or} \quad \pi B(1 - \sqrt{1 - \rho})e^{-\sqrt{1 - \rho}x}.$$

Finite Cylindrical Shaft.

The similar problem for a finite cylinder does not submit to such general treatment as is given above, and resort must be made to calculation.

The radiation directly received by a disk of radius r at a distance x from a radiating disk at the end of a cylinder of radius r is given by

$$\frac{\pi E}{2} \{x^2 + 2r^2 - x(x^2 + 4r^2)^{\frac{1}{2}}\}$$

$$\text{or} \quad \frac{\pi E}{2} \{x^2 + 2 - x(x^2 + 4)^{\frac{1}{2}}\},$$

where E is the radiation emitted per unit area of the radiating disk and x is expressed in terms of r .

Hence the radiation received per unit area by an elementary annulus of width dx at x is given by

$$-\frac{E}{4} \frac{d}{dx} \{x^2 + 2 - x(x^2 + 4)^{\frac{1}{2}}\} = -\frac{E}{4} \frac{d}{dx} F(x),$$

$$\text{but} \quad \frac{1}{2} \frac{d^2}{dx^2} F(x) = e^{-x} \text{ or } \{B_1 e^{a_1 x} + B_2 e^{a_2 x}\};$$

$$\therefore -\frac{1}{2} \frac{d}{dx} F(x) = e^{-x} \text{ or } \left\{ \frac{B_1}{\beta_1} e^{a_1 x} + \frac{B_2}{\beta_2} e^{a_2 x} \right\}.$$

Consider, now, a finite cylinder of length l , emissivity ϵ , closed at one end by a disk of emissivity unity, both disk and cylinder being at the same temperature. Then the radiation emitted at any point x on the cylinder is the radiation directly emitted, together with the reflected portion of the radiation received from the disk and from the rest of the cylinder.

$$\begin{aligned} \therefore \theta(x_1) = & \epsilon - \frac{1-\epsilon}{4} \frac{d}{dx} F(x) \\ & + \frac{1-\epsilon}{4} \left\{ \int_0^{x_1} \theta(x) \frac{d^2}{dx^2} F(x_1-x) dx \right. \\ & \left. + \int_{x_1}^l \theta(x) \frac{d^2}{dx^2} F(x-x_1) dx \right\}. \end{aligned}$$

For the single-term exponential approximation the equation becomes

$$\begin{aligned} \theta(x_1) = & \epsilon + \frac{1-\epsilon}{2} e^{-x} + \frac{1-\epsilon}{2} \left\{ \int_0^{x_1} \theta(x) e^{-(x_1-x)} dx \right. \\ & \left. + \int_{x_1}^l \theta(x) e^{-(x-x_1)} dx \right\}. \end{aligned}$$

Assuming that

$$\theta(x) = A_0 + A_1 e^{a_1 x} + A_1' e^{a_1(l-x)}$$

after substituting in the equation, performing the integrations, and equating on each side of the equation the constant terms and the coefficients of $e^{a_1 x_1}$, $e^{a_1(l-x_1)}$, e^{-x_1} , and $e^{-(l-x_1)}$ respectively, it is found that

$$\theta(x) = 1 + \frac{(1-\epsilon) \{ (1-\sqrt{\epsilon}) e^{-\sqrt{\epsilon}(l+x)} - (1+\sqrt{\epsilon}) e^{-\sqrt{\epsilon}(l-x)} \}}{(1+\sqrt{\epsilon})^2 - (1-\sqrt{\epsilon})^2 e^{-2\sqrt{\epsilon}l}},$$

which, when $l \rightarrow \infty$, gives $\theta(x) = 1$ as before.

But for the finite cylinder without the end disk,

$$\Phi(x) = 1 - \frac{(1-\epsilon) \{ e^{-\sqrt{\epsilon}x} + e^{-\sqrt{\epsilon}(l-x)} \}}{(1+\sqrt{\epsilon}) + (1-\sqrt{\epsilon}) e^{-\sqrt{\epsilon}l}};$$

$$\therefore \Psi(x) = \theta(x) - \Phi(x)$$

$$= \frac{(1-\epsilon) \{ (1+\sqrt{\epsilon}) e^{-\sqrt{\epsilon}x} - (1-\sqrt{\epsilon}) e^{-\sqrt{\epsilon}(2l-x)} \}}{(1+\sqrt{\epsilon})^2 - (1-\sqrt{\epsilon})^2 e^{-2\sqrt{\epsilon}l}},$$

which, when $l \rightarrow \infty$, gives

$$\Psi(x) = (1-\sqrt{\epsilon}) e^{-\sqrt{\epsilon}x}, \text{ as before.}$$

Thus the brightness of the walls of the finite cylinder when illuminated by a uniform sky of brightness B at one end is given by

$$\Psi_B(x) = \frac{\pi B \rho \{ (1+\sqrt{1-\rho}) e^{-\sqrt{1-\rho}x} - (1-\sqrt{1-\rho}) e^{-\sqrt{1-\rho}(2l-x)} \}}{(1+\sqrt{1-\rho})^2 - (1-\sqrt{1-\rho})^2 e^{-2\sqrt{1-\rho}l}}.$$

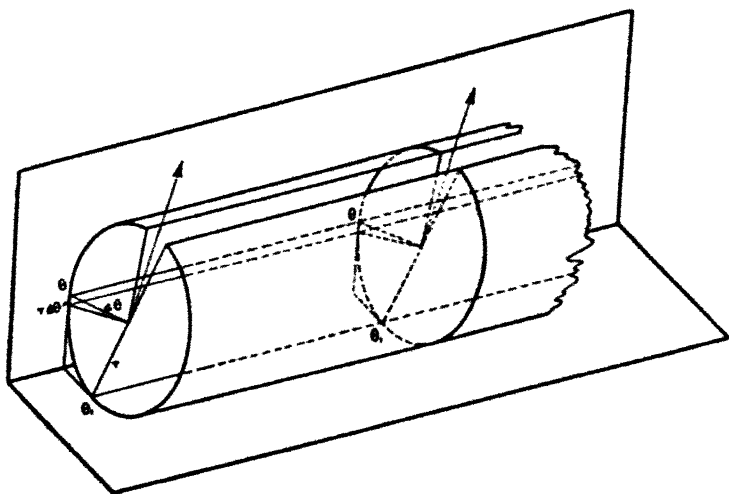
For the two-term exponential approximation the solution can be found by assuming that

$$\theta(x) = A_0 + A_1 e^{a_1 x} + A_1' e^{a_1(l-x)} + A_2 e^{a_2 x} + A_2' e^{a_2(l-x)},$$

and proceeding as before.

It should be noted that the approximate solutions obtained when the cylinder is not self-radiating are not as accurate as those obtained when the cylinder itself is radiating, since the former problem is solved by taking the difference between two solutions, of which at least one is an approximation. When the difference becomes small it may be considerably in error.

Fig. 2.



The Infinite Circular Cylinder with an Infinite Longitudinal Slit.

Consider an infinite cylinder with an infinite longitudinal slit parallel to the axis of the cylinder, subtending an angle 2ω at the axis as in fig. 2. It is obvious that the radiation emitted will be the same for all points on an elementary strip parallel to the longitudinal slit.

Let the origin of angular coordinates be taken as the line bisecting the slit. Then the radiation received per unit area at θ_1 from an infinite strip of width $r d\theta$ at θ is the same as the radiation from an infinite strip of width $r d\theta$ in the tangent plane at θ to the point θ_1 in the tangent plane at θ_1 .

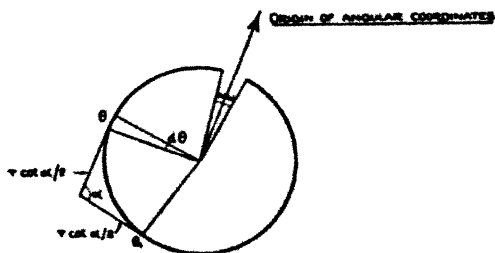
Now, α is the angle between the tangent planes at θ and θ_1 , so that it equals $\pi - (\theta_1 - \theta)$, while θ and θ_1 are situated at a distance $r \cot \alpha/2$ from the intersection of the two planes as shown in fig. 3.

The radiation to θ_1 from the area $r d\theta dy$ in the strip θ at a distance y from the plane normal to the axis of the cylinder and in which the receiving point θ_1 is situated is given per unit area by

$$\frac{\Phi(\theta) r d\theta dy}{\pi (4r^2 \cos^2 \alpha/2 + y^2)} \cdot \frac{r^2 \cot^2 \alpha/2 \cdot \sin^2 \alpha}{(4r^2 \cos^2 \alpha/2 + y^2)},$$

where $\Phi(\theta)$ is the total radiation per unit area from the

Fig. 3.



elementary strip at θ . The radiation from the infinite strip is therefore

$$\frac{\Phi(\theta)}{\pi} r^2 \cot^2 \alpha/2 \cdot \sin^2 \alpha d\theta \int_{-\infty}^{+\infty} \frac{dy}{(4r^2 \cos^2 \alpha/2 + y^2)}.$$

On putting $y = 2r \cos \alpha/2 \cdot \tan \beta$, this reduces to

$$\frac{\Phi(\theta)}{4} \cos \frac{\alpha}{2} d\theta = \frac{\Phi(\theta)}{4} \sin \frac{\theta_1 - \theta}{2} d\theta.$$

Hence the integral equation giving the required solution is

$$\Phi(\theta_1) = \epsilon + \frac{1-\epsilon}{4} \left\{ \int_w^\theta \Phi(\theta) \sin \frac{\theta_1 - \theta}{2} d\theta + \int_\theta^{2\pi-w} \Phi(\theta) \sin \frac{\theta - \theta_1}{2} d\theta \right\}$$

On differentiating twice with respect to θ_1 , it is found that

$$4\Phi''(\theta_1) = \epsilon - \epsilon\Phi(\theta_1),$$

so that

$$\Phi(\theta_1) = 1 + A \cos \frac{\sqrt{\epsilon}\theta_1}{2} + B \sin \frac{\sqrt{\epsilon}\theta_1}{2},$$

where A and B are undetermined constants. But from considerations of symmetry

$$\Phi(\theta) = \Phi(2\pi - \theta).$$

Hence

$$B = A \tan \sqrt{\epsilon}\pi/2.$$

Since the integral equation holds for all values of θ' ; $\omega < \theta' < 2\pi - \omega$ it holds for $\theta_1 = \pi$, so that

$$1 + A \cos \sqrt{\epsilon}\pi/2 + B \sin \sqrt{\epsilon}\pi/2 = \epsilon + \frac{1-\epsilon}{2}$$

$$\int_{-\pi}^{\pi} (1 + A \cos \sqrt{\epsilon}\theta/2 + B \sin \sqrt{\epsilon}\theta/2) \cdot \cos \theta/2 \cdot d\theta.$$

On integrating this equation and putting

$$B = A \tan \sqrt{\epsilon}\pi/2,$$

it follows that

$$A = \frac{-(1-\epsilon) \sin \omega/2 \cdot \cos \sqrt{\epsilon}\pi/2}{\sqrt{\epsilon} \cos \omega/2 \cdot \sin \sqrt{\epsilon}(\pi-\omega)/2 + \sin \omega/2 \cdot \cos \sqrt{\epsilon}(\pi-\omega)/2}$$

and

$$B = \frac{-(1-\epsilon) \sin \omega/2 \cdot \sin \sqrt{\epsilon}\pi/2}{\sqrt{\epsilon} \cos \omega/2 \cdot \sin \sqrt{\epsilon}(\pi-\omega)/2 + \sin \omega/2 \cdot \cos \sqrt{\epsilon}(\pi-\omega)/2}.$$

Hence

$$\Phi(\theta) = 1 - \frac{(1-\epsilon) \sin \omega/2 \cdot \cos \sqrt{\epsilon}(\pi-\theta)/2}{\sqrt{\epsilon} \cos \omega/2 \cdot \sin \sqrt{\epsilon}(\pi-\omega)/2 + \sin \omega/2 \cdot \cos \sqrt{\epsilon}(\pi-\omega)/2};$$

i. e.,

$$\Phi(\theta) = 1 - C \cos \sqrt{\epsilon}(\pi-\theta)/2,$$

where

$$C = \frac{(1-\epsilon) \sin \omega/2}{\sqrt{\epsilon} \cos \omega/2 \cdot \sin \sqrt{\epsilon}(\pi-\omega)/2 + \sin \omega/2 \cdot \cos \sqrt{\epsilon}(\pi-\omega)/2}.$$

Now,

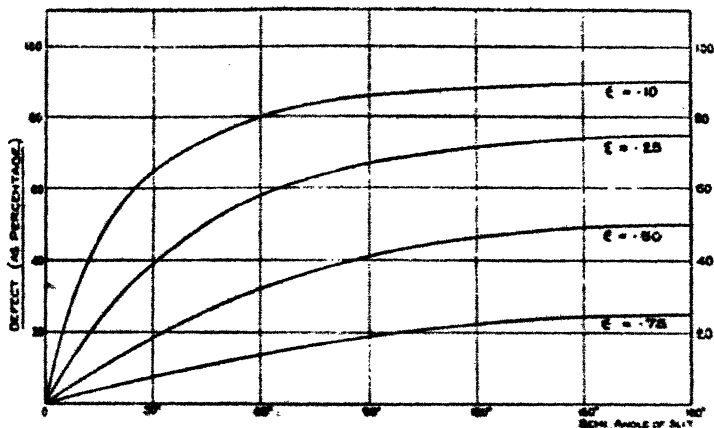
$$C \cos \sqrt{\epsilon}(\pi-\theta)/2$$

is the "defect" from black-body radiation as a function of θ and of ω , the semi-angle of the slit. This is shown graphically in fig. 4 for values of the emissivity of 0.10, 0.25, 0.50, and 0.75 for $\theta = \pi$, i. e., positions directly opposite the centre of the slit.

The solution of the inverse problem of the brightness of a similar cylinder of reflectivity ρ , illuminated by a uniform sky of brightness B , is easily obtained as

$$\Psi_B(\theta) = \frac{\pi B \rho \sin \omega/2 \cdot \cos \sqrt{1-\rho}(\pi-\theta)/2}{\sqrt{1-\rho} \cos \omega/2 \cdot \sin \sqrt{1-\rho}(\pi-\omega)/2 + \sin \omega/2 \cdot \cos \sqrt{1-\rho}(\pi-\omega)/2}$$

Fig. 4.



Defect of black-body radiation opposite slit in infinite cylinder.

Summary.

The paper is a continuation of a previous one in which the effect of multiple reflexion from the walls of a uniformly-heated infinite cylinder in building up black-body radiation is considered. The method is now applied to the case of a finite uniformly-heated cylinder, and an approximate solution is obtained. The results are of interest in showing how closely a uniformly-heated cylinder can approach the ideal black-body radiator.

It is also shown how the brightness of the inside of a non-radiating cylinder illuminated by a uniform sky can be deduced from the solution of the problem of the self-radiating cylinder. This is the case of a light well.

The problem of the radiation from the inside of a uniformly-heated infinite cylinder having an infinite longitudinal slit is also solved. In this case the solution of the integral equation is exact. The results are of interest in showing how closely a radiator of the type of Ives's primary standard of light approaches the ideal black-body radiator.

XLVI. *A Quartz Fibre Electrometer.* By D. R. BARBER,
*B.Sc., A.Inst.P., Research Student, Department of Physics,
 University College of the South-West of England, Exeter*.*

1. Introduction.

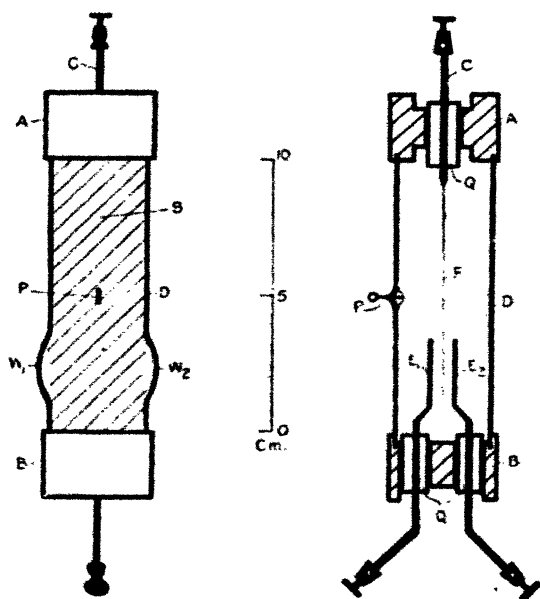
THE quantity of electricity which escapes from a charged body is very small, and it is necessary that the capacity of the instrument used to measure it should be small. This condition makes it advisable to use a small gold-leaf electroscope. It has been found that the gold leaf may be replaced by a single fibre of quartz, rendered conductive by the deposition of a suitable metallic film. In preliminary experiments the fibres employed, approximately 1 mil (2.5×10^{-2} mm.) diameter, were silvered by chemical deposition. This method ultimately proved unsatisfactory, the films becoming discontinuous a short time after their formation. Cathode disintegration of the metal "*in vacuo*" was finally adopted, and the "sputtered" fibres obtained by this method have proved very satisfactory. At first the electric field was applied between a single insulated plate and the containing case, the vertically suspended fibre being illuminated laterally and viewed through a microscope against a dark background. An "earthed" metal cylinder provided with windows formed the case of the instrument. It was found, however, that this type of electrometer suffered from two serious defects: (a) an erratic displacement of the fibre, which was independent of the electrical condition of the instrument, and was eventually traced to thermal radiations from the light-source, incident upon the fibre, causing the metal film and the quartz to dilate by unequal amounts. This effect was apparent even when reflected sunlight was used as the illuminant; (b) there was a non-linear relation between the P.D. applied to the fibre, and the resultant deflexion, except for very small field values. Under these conditions it would thus be necessary to calibrate the instrument over the entire working range. The design of the electroscope was therefore modified by using two parallel plates and direct illumination, i. e. the fibre was viewed against a bright background. The latter method, since it requires only a fraction of the illumination necessary in the former, does not give rise to any extraneous thermal effects.

* Communicated by Prof. F. H. Newman, D.Sc., F.Inst.P.

2. Description of the Instrument.

The instrument in its final form is shown diagrammatically in fig. 1. A silvered quartz fibre F is attached to a copper electrode C by a small globule of Wood's metal, and hangs symmetrically between the two electrodes, E_1 and E_2 , of sheet brass 2.5×2.0 cm. and separated by an air-gap 7.5 mm. wide. The leads from the plates pass through short lengths of quartz tube Q , cemented into the lower ebonite cap B and the fibre electrode is similarly insulated

Fig. 1.



by the quartz sleeve Q , cemented into the upper ebonite cap A . The case of the instrument is a glass tube D , 10.0 cm. long by 3.5 cm. diameter, provided with two windows W_1 and W_2 , slightly blown out in order to free the glass of air-bubbles, and, with the exception of the windows, it is coated on the inside with a film of silver, S . Contact with this is made by the platinum wire P , sealed through the glass, and terminating on the exterior in a loop electrode by means of which the silver coating is connected to earth. The ebonite cups were grooved concentrically to fit closely on to the cylindrical glass case, this method of assembly enabling the instrument to be easily dismantled, if the necessity arose

for subsequent modification in the relative position of fibre and plates.

Some trouble was experienced, initially, in mounting the fibre preparatory to the sputtering process, but after several ineffective trials, the following technique was adopted. The selected fibre was stretched across a rectangular glass frame, its two ends being cemented by means of shellac, and the frame was then held horizontally in a clamp, care being taken that the fibre was quite clear of the clamp edges. The electrode serving as the fibre support consisted of a straight copper wire, flattened at one extremity, and in this a fine groove was cut to receive the fibre. The wire was first fitted into its insulating sleeve and cap, and the tip was then "tinned" with Wood's metal, care being taken that the groove was completely filled with the metal. This tinned portion was then bent through an angle of about 20° , and the assembly clamped vertically beneath the fibre frame, in such a position that the wire was just in contact with, and parallel to, the fibre. A well-heated soldering-iron was placed against the under side of the wire, and the Wood's metal melted, a slight downward pressure being applied to the stretched fibre meanwhile, so that it sunk into its groove, this pressure being maintained until the molten metal solidified. The wire was finally straightened and the fibre cut to the requisite length, a fragment of glass being attached to its extremity to keep it taut when placed in the discharge-tube.

The discharge apparatus used for the cathode deposition of silver upon the fibre consisted of a vertical tube in which the fibre was suspended. Sealed to this was a horizontal side tube which served to connect the main tube to the exhaust system. The cathode of 60-mesh pure silver gauze formed a vertical cylindrical tube, concentric with, and entirely enclosing, the fibre and the "tinned" end of the copper electrode. A cup-shaped electrode of brass supported the cathode. The fibre having been lowered into position, its ebonite supporting cap was sealed down with wax and the tube evacuated. A 10 inch induction coil with a mechanical interrupter was used to excite the tube, and a continuous discharge was maintained for 30 minutes. Care was taken to protect the under surface of the insulating cap so as to prevent the possible formation of a silver deposit upon the ebonite surface. "Sputtering" of the silver readily occurred at a pressure of 5.0×10^{-4} mm. of mercury, and this pressure, after a sudden initial rise, remained constant throughout the period of discharge.

Fibres treated in this way were coated with a very uniform and coherent layer of metal, and a satisfactory electrical connexion between the fibre coating and the support was obtained. This is extremely important, since it was always at the junction of fibre and support that the chemically deposited layer, used in the earlier experiments, became discontinuous. Fibres coated by cathode disintegration showed practically no increase in diameter when examined under the microscope, and although no direct measurements have been made, it is estimated that these metallic films have an actual thickness of the order of 10^{-5} mm.

3. Calibration of the Instrument.

The instrument was calibrated directly by applying known P.D.'s to the fibre, with a constant field maintained between the two fixed electrodes.

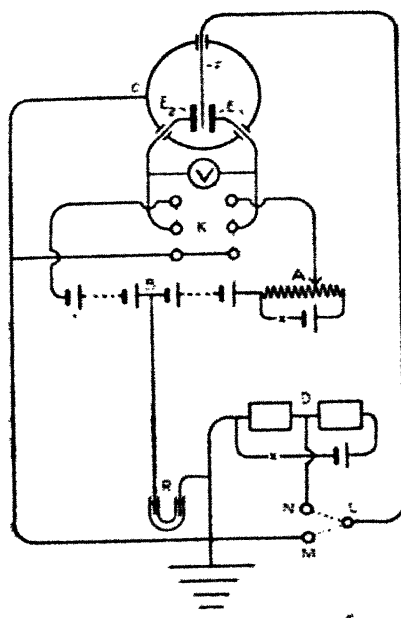
Measurements of the resultant deflexions were made by observations of the fibre image in the field of a telemicroscope, 25 divisions of the eyepiece scale corresponding to an actual displacement of 1.0 mm. Readings were taken, for a particular field value, corresponding to increasing fibre potentials over the range (0.0–2.1 volts), and these were repeated at measured plate voltages between 35 and 60 volts.

The circuit used for this calibration is shown in fig. 2. The two plates E_1 and E_2 of the electrometer are joined, through the double pole switch K , to the positive and negative terminals of a 60-volt H.T. battery B , whose centre-tapping is "earthed." The switch K is included in order that a P.D. may be applied to the plates simultaneously, as attempts to excite them separately invariably result in the fibre flying across the field and sticking to the plate. A commutator of the mercury contact type with its inter-connecting copper strips removed forms a convenient arrangement, and by using the two additional cups the electrometer plates may be "earthed" when no potential is applied to them. The adjustment is useful when obtaining the zero position of the fibre.

With the double-plate type of electrometer it is essential that the relative positions of fibre and electrodes remain unaltered whenever the electric field is applied, since any displacement which occurs entails re-calibration of the instrument. A potentiometer A joined in series with the battery B provides the necessary fine adjustment whereby the fibre may be restored to its zero position. This adjustment is made whenever the field is switched on previous to

making a series of observations. A voltmeter V is joined across the electrode leads, and measures the applied plate P.D. Varying potentials are applied to the fibre F by means of the potential divider D . Connexion from this to the fibre conductor is made by means of the mercury cups L , M , and N in a block of paraffin wax. When L and M are joined by means of an insulated "bridge" of copper wire, the fibre is "earthed." On breaking this circuit and joining L and N , connexion is made with D , and the fibre is raised to the required potential. The case C of

Fig. 2.



the instrument is "earthed," and a water resistance R is joined in series with the earth lead from the centre tapping of B , so that, in the event of the "earthed" fibre touching either of the plates, no short-circuit can occur.

4. Experimental Results.

The results obtained with the instrument were very consistent, and, as was anticipated, the relation between the potential applied to the fibre and the resultant displacement was found to be linear within the limits of experimental error.

The displacement period of the fibre was found to be comparatively short, the deflexion being complete in approximately 5 secs.

The results of the calibration are shown in fig. 3, and the sensitivity at different potential differences applied to the plates is given in Table I.

Fig. 3.

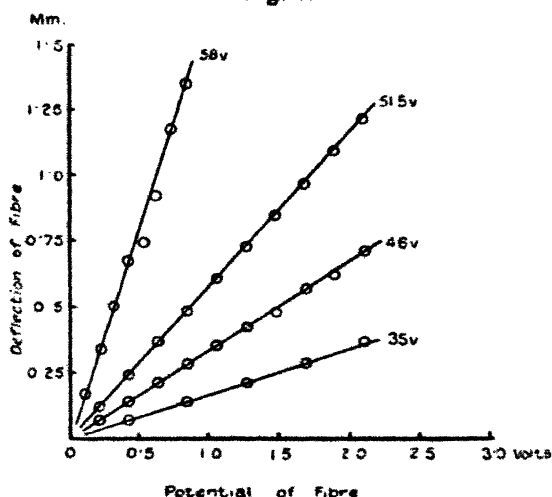


TABLE I.

P.D. applied to plates (volts).	P.D. range applied to fibre (volts).	Deflexion of fibre (mm.).	Sensitivity mm./volt.
35.0	0.42 -2.10	0.07-0.36	0.168
46.0	0.21 -2.10	0.07-0.70	0.330
52.0	0.21 -2.10	0.12-1.20	0.570
58.0	0.105-0.84	0.17-1.34	1.560
59.5	0.021-0.168	0.05-0.47	2.600

From the curves it will be seen that there is a linear relation between the potential applied to the fibre and the deflexion over the entire range of plate potential, viz. 36 to 60 volts.

At 58 volts, however, the calibration range becomes restricted, the fibre being unstable with an applied potential

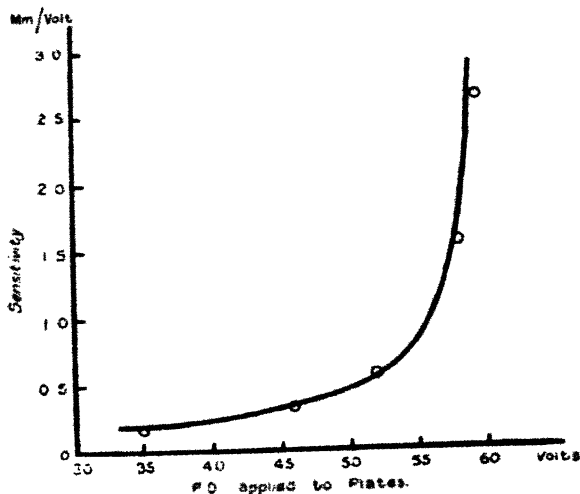
of 0.95 volt. This points to a critical value in the neighbourhood of 60 volts for the plate potential of the instrument described, and this result has been confirmed by interpolation, using the empirical relation found to exist between plate potential and mean sensitivity.

The capacity of the instrument, as measured by sharing its charge with a quadrant electrometer, was found to be approximately 3 cm.

5. Sensitivity of the Instrument.

Sensitivity has been defined as the actual displacement, in millimetres of the fibre, per unit potential applied to it

Fig. 4.



This has been adopted, since it makes direct comparison possible with the values found for other instruments. Using the above definition, we can express the relation between sensitivity S and plate potential V by the equation

$$S(V - 61) = -4.9.$$

This curve is reproduced in fig. 4. Putting $S = \infty$ in the above, we obtain a value of 61 volts for the critical plate potential difference, i. e. the potential at which the fibre becomes unstable.

It is interesting to compare the sensitivity values with those quoted for other electrometers of varying types.

Kaye*, using a modified form of Wilson's tilted leaf electroscope, obtained a sensitivity of 5.5 mm./volt over the range 0.8–1.20 volt, with a plate P.D. of 207 volts.

Using a double-plate electrometer in which a quartz fibre 0.003 mm. diameter was anchored at either end, Laby† found that with a plate P.D. of 60 volts, the plates being 1 cm. apart, 1 volt applied to the fibre gave a deflexion of 0.2 mm. As would be expected with a stretched fibre, this value of S is lower than that observed by the author, using the suspended fibre instrument. More recently Lindemann and Keeley‡ have devised a torsional quartz-fibre electrometer in which two silvered needles, capable of rotation about a horizontal axis, are mounted perpendicularly to the torsion fibre. These needles move in an electric field between two pairs of fixed plates, and their movement is constrained by the torsion of the suspended fibre. With a fibre 6μ diameter and 1.4 cm. long, the attached needles being 17μ diameter and 0.9 cm. long, a sensitivity of .76 mm./volt was obtained with a plate P.D. of 97 volts, the plate separation being 0.6 cm.

The high sensitivity obtained at comparatively low plate potentials, and the stability of the fibre over extended periods of observation, are advantages claimed for the present instrument.

6 Summary.

1. A description is given of a double-plate electrometer employing a single suspended quartz fibre as the moving system.

2. A method of rendering the quartz conducting by cathode disintegration of silver is given, with a description of the technique developed in handling and mounting the fibres.

3. The results of a direct calibration of the instrument are given, and compared with those obtained by other investigators using different types of electrometers.

In conclusion, the author wishes to thank Prof. F. H. Newman, D.Sc., and Mr. V. H. L. Searle, M.Sc., for their kindly interest and helpful suggestions throughout the course of this investigation.

* Kaye, G. W. C., *Proc. Phys. Soc.* vol. xxiii. pp. 209–218 (1911).

† Laby, T. H., *Proc. Camb. Phil. Soc.* vol. xv. pp. 106–113 (1909).

‡ Lindemann, F. A., and Keeley, T. C., *Phil. Mag.* vol. xlvii. pp. 577–583 (1924).

XLVII. *New Bands in the Secondary Spectrum of Hydrogen.*
By D. B. DEODHAR, M.Sc., Ph.D., Physics Research
Laboratory, King's College, London.*

IN the present paper it is proposed to deal with seven new bands in the secondary spectrum of hydrogen situated in the yellow region.

An attempt at suggesting possible groups of related lines in the yellow region was made by Kimura and Nakamura † by studying the electrodeless discharge of hydrogen, and recently Curtis ‡ grouped some prominent lines in that region under the heading of K, G, and H series. As to the relevance of the H group, Curtis himself appears to be uncertain. Curtis's K group consists of seven lines and the G group six lines. The second differences of the G's are rather irregular, though the second differences of the K's are good. Again, there is no relationship between the three groups.

It is now well known that the study of the spectrum of hydrogen under the conditions of excitation known as the first-type discharge lends a great help in picking out related lines on account of their selective enhancement or weakening of intensities in such a discharge. A study of the microphotograph of the first-type spectrum plate taken by Moll's self-registering photometer was made by the present author, at King's College, during the investigation on Fulcher systems, and it was seen that, in addition to the Fulcher group recently analysed by Prof. O. W. Richardson, the microphotograph possessed another distinct group situated in the yellow region. It appeared from the microphotograph that Curtis's K and G series were components of a system of seven bands. The bands are such that the successive corresponding lines in Curtis's K and G groups stand as P(2)'s and P(3)'s in each of the seven bands. Curtis's G group contains only six members. To these I have added 17729.30 (q) as the relevant seventh member. This line was picked up from the microphotograph, and it fits in as P(3) of the seventh band. Some Q branches were picked from the microphotograph, while the rest of the Q branches and R branches were developed by examining the behaviour of "condenser-discharge" lines in the first-type spectrum.

* Communicated by Prof. O. W. Richardson, D.Sc., F.R.S.

† Japan Journ. Phys. i. p. 86 (1923).

‡ Phil. Mag. i. p. 686 (1926).

The bands are named as D_1 , D_2 , D_3 , D_4 , D_5 , D_6 , and D_7 , and their properties and other details are given in Table I. The horizontal and vertical difference are given in Tables II. and III. respectively. In Table I. the band lines are represented by their wave-numbers, followed by (1) the intensity estimates given in the tables of Merton and Barratt*, Tanaka†, or Deodhar‡, and (2) the intensity estimate on the first-type plate. The lines from Tanaka's and Deodhar's tables are marked by the letters T or D underneath. The other letters denote the properties of the lines as given in Merton and Barratt's tables, with the notation H.P.=high pressure, L.P.=low pressure, C.D.=condensed discharge, He=Helium effect, Z=Zeeman effect, and S=Stark effect. These are followed by claims made by other systems. The first and second differences are given in the next two columns.

The line D_2 P(3) figures as Richardson's § 157 Q(4), but it is an unresolved doublet according to Merton and Barratt's tables. D_2 P(3) is claimed as 186 R(2) ||, but its intensity appears to be rather uncertain there. D_1 P(2) coincides with 201 R(2) ¶, but its intensity seems to be too great as a member of 201 R(m). Similarly, D_6 P(2) appears to be rather too strong to fit well in Richardson and Tanaka's series 81 R(m) **. It may be pointed out that Richardson and Tanaka think 81 R(7) to be double. The line D_2 Q(2) coincides with D_2 Q(5) and with Richardson's 156 Q(m); but the fact that it is extremely weakened in the first-type discharge favours its claim as D_2 Q(2) and D_3 Q(5) as well. D_2 Q(3) looks abnormal in intensity. However, its condensed discharge nature may favour its position there. D_2 Q(5) is also claimed as 156 Q(5) and 159 R(8) ††; Richardson thinks that the strength of the line can allow it to be a member of two series, and owing to its weakening in the first-type discharge, it seems reasonable that the line may have its place as D_2 Q(5) as well. 17812.35 figures as D_6 Q(4) and D_4 R(4). Its position as D_6 Q(4) appears to be more justifiable than its position as D_4 R(4). However, as this line is not claimed by more series, its assignment as D_4 R(4) may be retained for the present. The intensity of this line perhaps favours its

* Phil. Trans. A, ccxii. pp. 369-400.

† Roy. Soc. Proc. A, cviii. pp. 593-606 (1925).

‡ Ibid. cxiii. pp. 420-432 (1926).

§ Proc. Roy. Soc. A, cix. p. 240 (1925).

|| Ibid. p. 249 (1925).

¶ Proc. Roy. Soc. A, cvi. p. 663 (1924).

** Ibid. cvii. p. 617 (1925).

†† Ibid. cix. p. 246 (1925).

TABLE I.

$D_1 P(m)$		$D_1 Q(m)$		$D_1 R(m)$	
<i>m.</i>		<i>m.</i>		<i>m.</i>	
2.	16330.87 (o) (0) H.P. +, He +	1.	17139.43 (5) (1) C.D. + +	1.	17206.83 (1) (ab) 5 I, 4, Q(3)
3.	16331.32 (o) (o) > 90.35	2.	17108.44 (o) (1) > 30.99		> 29.27
4.	16764.15 (5) (< o) H.P. +, C.D. +, H.E. + +	3.	17068.60 (2) (< o) C.D. + +, H.E. + +		> 22.62
5.	16930.52 (o) (ab) > 139.63	4.	17013.55 (1) (ab) O.D. +	3.	17318.72 (o) (ab) He + +
		5.	16943.09 (1) (< o) C.D. +, He +	4.	17325.23 (qd) (ab) > 6.51
$D_2 P(m)$		$D_2 Q(m)$		$D_2 R(m)$	
<i>m.</i>		<i>m.</i>		<i>m.</i>	
2.	17130.36 (9) (6) I, P + +, C.D. + +	1.	17366.83 (1) (ab) D, R(1)	1.	17375.80 (o) (ab) > 40.74
3.	17025.82 (4) (4) L.P. + +, C.D. + +, 157 Q(4)	2.	17239.74 (3) (ab) O.D. + +, 156 Q(5)	2.	17416.54 (2) (ab) C.D. +
4.	16906.94 (q) (ab) T	3.	17292.55 (3) (4) O.D. + +, He + +	3.	17446.38 (o) (ab) > 29.84
5.	16774.72 (8) (4) H.P. +, C.D. +, He +, Z	4.	17151.52 (-) (ab) He + +, 201 R(q)	4.	17463.80 (q) (ab) T
		5.	17086.69 (2) (1) 156 Q(6), 159 R(8)		> 17.50

$D_3 P(m).$		$D_3 Q(m).$		$D_3 R(m).$	
$m.$		$m.$		$m.$	
2.	17278.89 (7) (7) L.P. + +, C.D. +	1.	17407.53 (o) (ab) 171 P(2)	1.	17512.36 (o) (prob. ab)
3.	17169.12 (5) (6) L.P. + +, C.D. + +, 183 R(2)	2.	17383.08 (q) (ab) He +	2.	17562.35 (o) (ab) C.D. + +, He + +
4.	17047.13 (5) (1) H.P. + +, C.D. + +	3.	17348.19 (2) (ab) C.D. + +	3.	17560.71 (rd) ³ (ab) D
5.	16915.38 (2) (1) H.P. + +, C.D. + +	4.	17299.42 () (o) H.P. + +, C.D. + +, He + +	4.	17623.32 (1) (ab) C.D. + +, He + +
		5.	17239.74 (3) (ab) C.D. + +, He + +, 156 q(5), D ₂ Q(2)		
$D_1 P(m).$		$D_1 Q(m).$		$D_4 R(m).$	
$m.$		$m.$		$m.$	
2.	17426.25 (8) (6) C.D. + +, 201 R(2)	1.	17557.13 (2) (o) D	1.	17634.50 (o) (ab) He + +
3.	17311.28 (7) (6) L.P. + +, C.D. + +	2.	17533.13 (rd) (ab) D	2.	17724.18 (q) (ab)
4.	17184.43 (1) (2) C.D. + +	3.	17501.57 (o) (prob. ab)	3.	17775.19 (1) (o)
5.	17051.64 (v) (ab) D	4.	17458.78 (1) (ab)	4.	17812.35 (4) (1) C.D. + +, D ₂ Q(4)
		5.	17404.99 (o) (ab)		

TABLE I. (continued).

$D_e P(m).$	$D_e Q(m).$	$D_e R(m).$
$m.$ 1. 17720-73 (rd) (ab) D 2. 17997.5 (-) (ab) T 3. 17854.50 (o) (ab) He++ 4. 17819.25 (-) (o) He++ 5. 17866.27 (2) (ab) C.D.+	$m.$ 1. 17720-73 (rd) (ab) D 2. 17997.5 (-) (ab) T 3. 17854.50 (o) (ab) He++ 4. 17819.25 (-) (o) He++ 5. 17866.27 (2) (ab) C.D.+	$m.$ 1. 17846.91 (o) (ab) He-, 187 Q(7), 4 L3, R(3) 2. 17909.9 (-) (ab) T 3. 17968.00 (2) (o) C.D.++, 83 Q(8) 4. 18000.57 (rd) (ab) D
$D_e P(m).$	$D_e Q(m).$	$D_e R(m).$
$m.$ 1. 17872.31 (7) (4) C.D.++, He++ 2. 17451.61 (7) (4) H.P.+, C.D.++, He++, 201 R(5) 3. 17018.72 (o) (ab) He++ 4. 17184.43 (1) (1) C.D.++, 5 Q4, Q6	$m.$ 1. 17872.31 (7) (4) C.D.++, He++ 2. 17451.61 (7) (4) H.P.+, C.D.++, He++, 201 R(5) 3. 17018.72 (o) (ab) He++ 4. 17184.43 (1) (1) C.D.++, 5 Q4, Q6	$m.$ 1. 18044.86 (o) (< o) C.D.++, He++ 2. 18140.19 (-) (ab) He++ 3. 18205.52 (o) (ab) L.P.++ 4. 18260.14 (1) (1)
$D_e P(m).$	$D_e Q(m).$	$D_e R(m).$
$m.$ 1. 17716.87 (3) (1) C.D.++, He++, 81 R(7) 2. 17591.33 (2) (o) C.D.++ 3. 17453.78 (1) (ab) C.D.++ 4. 17316.50 (3) (ab) C.D.++	$m.$ 1. 17716.87 (3) (1) C.D.++, He++, 81 R(7) 2. 17591.33 (2) (o) C.D.++ 3. 17453.78 (1) (ab) C.D.++ 4. 17316.50 (3) (ab) C.D.++	$m.$ 1. 18044.86 (o) (< o) C.D.++, He++ 2. 18140.19 (-) (ab) He++ 3. 18205.52 (o) (ab) L.P.++ 4. 18260.14 (1) (1)

allocation to more than one series. $D_3 R(3)$ is also given as $83 Q(8)^*$, but Richardson and Tanaka think it to be too strong for $83 Q(8)$.

The horizontal and vertical differences of $P(m)$, $Q(m)$, and $R(m)$ lines of all the bands are tabulated in Tables II. and III. It will be seen that the run of the horizontal differences in Table II. is fairly systematic except in one or two cases. The vertical differences assembled in Table III. show a very systematic variation for all the $P(m)$, $Q(m)$, and $R(m)$ lines of all bands.

TABLE II.

Horizontal Differences of $P(m)$'s, $Q(m)$'s, and $R(m)$'s.

$P(m)$.	$D_2 - D_1$.	$D_3 - D_2$.	$D_4 - D_3$.	$D_5 - D_4$.	$D_6 - D_5$.	$D_7 - D_6$.
$P(2)$	149.49	148.53	147.36	146.06	144.56	142.88
$P(3)$	144.30	143.30	142.16	140.33	139.72	137.97
$P(4)$	142.79	140.19	137.30	134.29	140.06	129.32
$P(5)$	144.20	140.66	136.46	132.59	132.97	119.75
$Q(1)$	127.40	140.70	149.60	163.60	181.68	205.53
$Q(2)$	131.30	143.34	150.05	164.37	182.21	207.10
$Q(3)$	133.95	145.64	153.38	162.93	186.49	207.53
$Q(4)$	137.97	147.90	159.36	160.47	193.10	208.37
$Q(5)$	143.60	153.05	165.25	161.28	198.84	210.19
$R(1)$	108.97	136.56	152.14	182.41	217.95	270.47
$R(2)$	120.44	145.81	161.83	185.72	230.29	277.00
$R(3)$	127.66	153.33	175.48	190.81	239.52	285.64
$R(4)$	138.57	159.52	189.03	188.22	259.57	298.79

TABLE III.

Vertical Differences of $P(m)$, $Q(m)$, and $R(m)$ lines.

	$P(2) - P(3)$.	$P(3) - P(4)$.	$P(4) - P(5)$.
D_1	99.35	117.37	133.63
D_2	104.54	118.88	133.22
D_3	109.77	121.99	131.75
D_4	114.97	126.85	132.59
D_5	120.70	132.89	134.29
D_6	125.24	132.55	142.28
D_7	130.45	141.20	151.85

* *Ibid.* cvii. p. 618 (1925).

TABLE III. (continued).

	Q(1) - Q(2).	Q(2) - Q(3).	Q(3) - Q(4).	Q(4) - Q(5).
D ₁	30.89	39.84	55.05	69.46
D ₂	27.09	37.19	51.03	64.83
D ₃	24.45	34.89	48.77	59.68
D ₄	24.00	31.56	42.79	53.79
D ₅	23.27	33.00	45.25	52.98
D ₆	22.70	28.72	38.64	47.24
D ₇	21.13	28.29	37.80	45.42

	R(2) - R(1).	R(3) - R(2).	R(4) - R(3).
D ₁	29.27	22.62	6.51
D ₂	40.74	29.84	17.50
D ₃	49.99	37.36	23.61
D ₄	59.68	51.01	37.16
D ₅	62.99	56.10	34.57
D ₆	75.33	65.33	54.62
D ₇	81.86	73.97	67.77

The P, Q, and R branches of all the bands obey the usual combination principle throughout, such as $Q(m+1) + Q(m) = P(m+1) + R(m)$. The accuracy with which the combination principle is obeyed shows the correctness of the associated branches; and the properties of the various lines and the manner in which the first differences vary from set to set appear to indicate that these seven bands are related to each other. This idea is further strengthened by looking to the systematic run of the ν_0 values from band to band and to the values of the moment of inertia assembled in Table VI.

Initial and Final Terms:—

We have, as usual,

$$R(m) = \nu_0 + F(m+1) - f(m), \quad \text{(i.) } (\overline{m+1} \rightarrow m)$$

$$Q(m) = \nu_0 + F(m) - f(m), \quad \text{(ii.) } (\underline{m} \rightarrow m)$$

and $P(m) = \nu_0 + F(m-1) - f(m), \quad \text{(iii.) } (\underline{m-1} \rightarrow m)$

In these equations ν_0 is the frequency of the origin of the band, and F and f stand for the initial and the final states respectively.

From these equations we see that

$$F(m+1) - F(m) = R(m) - Q(m) = Q(m+1) - P(m+1) \quad \text{(iv.)}$$

(Initial term difference)

$$f(m+1) - f(m) = R(m) - Q(m+1) = Q(m) - P(m+1). \quad \text{(v.)}$$

(Final term difference)

The initial and the final term differences of all the bands are tabulated in Tables IV. and V.

TABLE IV.

Initial Terms.

Band.	m .	$R(m)$ $-Q(m)$.	$Q(m+1)$ $-P(m+1)$.	Means.	Term diff.	2nd diff.
D_1	1 ...	127.40	127.57	127.48	$F(2) - F(1)$	> 59.89
	2 ...	187.66	187.08	187.37	$F(3) - F(2)$	> 62.39
	3 ...	250.12	249.40	249.76	$F(4) - F(3)$	> 62.36
	4 ...	311.68	312.57	312.12	$F(5) - F(4)$	
D_2	1 ...	108.97	109.38	109.17	$F(2) - F(1)$	> 67.59
	2 ...	176.80	176.73	176.76	$F(3) - F(2)$	> 67.44
	3 ...	243.83	244.58	244.20	$F(4) - F(3)$	> 67.92
	4 ...	312.28	311.97	312.12	$F(5) - F(4)$	
D_3	1 ...	104.83	104.19	104.51	$F(2) - F(1)$	> 74.66
	2 ...	179.27	179.07	179.17	$F(3) - F(2)$	> 72.73
	3 ...	251.52	252.29	251.90	$F(4) - F(3)$	> 72.23
	4 ...	323.90	324.36	324.13	$F(5) - F(4)$	
D_4	1 ...	107.37	106.88	107.125	$F(2) - F(1)$	> 83.55
	2 ...	191.05	190.29	190.67	$F(3) - F(2)$	> 83.31
	3 ...	273.62	274.35	273.98	$F(4) - F(3)$	> 79.38
	4 ...	353.57	353.15	353.36	$F(5) - F(4)$	
D_5	1 ...	126.18	125.19	125.68	$F(2) - F(1)$	> 86.96
	2 ...	212.4	212.89	212.64	$F(3) - F(2)$	> 88.37
	3 ...	301.50	300.53	301.01	$F(4) - F(3)$	> 80.57
	4 ...	381.12	381.84	381.58	$F(5) - F(4)$	
D_6	1 ...	162.45	162.84	162.64	$F(2) - F(1)$	> 97.43
	2 ...	260.48	259.06	259.07	$F(3) - F(2)$	> 93.98
	3 ...	354.53	353.57	354.05	$F(4) - F(3)$	> 94.05
	4 ...	447.79	448.61	448.20	$F(5) - F(4)$	
D_7	1 ...	227.39	227.06	227.22	$F(2) - F(1)$	> 102.58
	2 ...	330.38	329.22	329.80	$F(3) - F(2)$	> 102.83
	3 ...	432.64	432.62	432.63	$F(4) - F(3)$	> 106.09
	4 ...	538.21	539.05	538.63	$F(5) - F(4)$	

TABLE V.
Final Terms.

Band.	m.	$\frac{R(m)}{-Q(m+1)}.$	$\frac{Q(m)}{-P(m+1)}.$	Mean.	Term diff.	2nd diff.
D_1	1 ...	158.39	158.56	158.47	$f(2)-f(1)$	
	2 ...	227.50	226.92	227.21	$f(3)-f(2)$	> 68.74
	3 ...	305.17	304.45	304.81	$f(4)-f(3)$	> 77.60
	4 ...	382.14	383.03	382.58	$f(5)-f(4)$	> 77.77
D_2	1 ...	136.06	136.47	136.26,	$f(2)-f(1)$	
	2 ...	213.99	213.92	213.95,	$f(3)-f(2)$	> 77.69
	3 ...	294.86	295.61	295.23,	$f(4)-f(3)$	> 81.28
	4 ...	377.11	376.80	376.95,	$f(5)-f(4)$	> 81.72
D_3	1 ...	129.28	128.64	131.12,	$f(2)-f(1)$	
	2 ...	214.16	213.96	222.20	$f(3)-f(2)$	> 85.10
	3 ..	300.29	301.06	300.67,	$f(4)-f(3)$	> 86.61
	4 ...	383.58	384.04	383.81,	$f(5)-f(4)$	> 83.14
D_4	1 ...	131.37	130.88	131.12,	$f(2)-f(1)$	
	2 ...	222.61	221.85	222.23	$f(3)-f(2)$	> 91.11
	2 ...	316.41	317.14	316.77,	$f(4)-f(3)$	> 94.54
	4 ...	407.36	406.94	407.15	$f(5)-f(4)$	> 90.38
D_5	1 ...	149.41	148.42	148.91,	$f(2)-f(1)$	
	2 ...	245.40	245.89	245.64,	$f(3)-f(2)$	> 96.73
	3 ...	346.75	345.78	346.26,	$f(4)-f(3)$	> 100.62
	3 ...	434.30	434.82	434.56	$f(5)-f(4)$	> 88.30
D_6	1 ...	185.15	185.54	185.35	$f(2)-f(1)$	
	2 ...	289.20	288.38	288.79	$f(3)-f(2)$	> 103.44
	3 ...	393.17	392.21	392.69	$f(4)-f(3)$	> 103.90
	4 ...	495.03	495.85	495.44	$f(5)-f(4)$	> 102.75
D_7	1 ...	248.52	248.19	248.35	$f(2)-f(1)$	
	2 ...	358.67	357.51	358.09	$f(3)-f(2)$	> 109.74
	3 ...	470.44	470.42	470.43	$f(4)-f(3)$	> 112.34
	4 ...	583.63	584.47	584.05	$f(5)-f(4)$	> 113.62

perpendicular to the line joining the nuclei, h is Planck's constant, and c the velocity of light. The values of I' and I'' thus calculated are assembled in columns 10 and 11 of Table VI., while the values of ν_0 as derived from the P(2), Q(1), and R(1) members of each band are placed in columns 1, 2, and 3 of that table. The values of P and ρ are shown in columns 8 and 9.

It will be seen from Table VI. that the initial moment of inertia is larger than the final moment of inertia, and that it begins with a high value at D_1 and then steadily decreases as we go to D_7 . The highest value of the initial moment of inertia is 9.01×10^{-41} gm. cm.², and the lowest value is 5.34×10^{-41} gm. cm.². These two extreme values are nearly equal to those of some of the systems developed by Prof. O. W. Richardson in his recent paper "Structure," Part V. In that paper the maximum value of the moment of inertia of the excited hydrogen molecule (H_2) is found to be 11.35×10^{-41} gm. cm.² for an excited state for which the electron total quantum number is 5. These values are in the neighbourhood of Dieke's * value, which is about 8.2×10^{-41} gm. cm.². When the hydrogen molecule rotates in larger orbits as a result of it being greatly excited, it is quite reasonable to expect that it will have a large moment of inertia. In fact, Takahashi † has obtained a value as high as 20×10^{-41} gm. cm.² for the moment of inertia of an excited H_2 . Again, it may be pointed out that such high values of the moment of inertia of H_2 fit well with the results expected according to the Quantum theory of specific heat of hydrogen recently discussed by Van Vleck ‡.

From the above discussion it appears that the emitter of the bands set forth in the present paper is an excited hydrogen molecule (H_2). It appears from the majority of values of P and ρ that these bands are not of the half-quantum type. There are indications of a similar group of bands in the blue region of the spectrum having moments of inertia of the order involved in these bands. They are under investigation, and it is hoped to deal with them in another communication.

In conclusion, I should like to express my indebtedness to Prof. O. W. Richardson for suggesting this problem to me,

* Proc. Amsterdam Acad. Sci. xxvii. p. 490 (1924).

† Jap. Journ. Phys. ii. p. 95 (1923).

‡ Phys. Rev. xxviii. p. 995 (1926).

TABLE VI.—Band Constants.

Band.	ν_0 from Q(1).	ν_0 from P(2).	ν_0 from R(1).	F(2).	F(1).	f(2).	f(1).	P.	ρ .	Initial Moment of Inertia, $I'' \times 10^{-4}$ gm. cm. ² .	Final Moment of Inertia, $I'' \times 10^{-4}$ gm. cm. ² .
D ₁	17162.57	17162.39	17163.15	201.70	74.88	236.40	98.02	-0.56	-0.62	9.01	7.43
D ₂	17282.44	17282.19	17282.25	151.18	41.07	193.80	57.58	-0.114	-0.108	8.21	6.89
D ₃	17420.02	17420.31	17420.32	136.05	31.52	172.04	44.01	+0.072	-0.018	7.55	6.51
D ₄	17569.96	17570.42	17570.14	133.85	26.66	170.83	39.49	+0.194	+0.074	6.73	6.01
D ₅	17731.28	17734.87	17734.89	165.87	40.29	202.85	53.85	+0.028	-0.064	6.16	5.55
D ₆	17919.80	17919.25	17919.25	232.12	69.52	271.90	86.51	-0.209	-0.294	5.83	5.36
D ₇	18125.20	18125.20	18125.34	375.30	148.05	443.50	165.31	-0.689	-0.719	5.34	4.94

and for his encouragement and helpful criticism during the progress of this work.

Note added.—The following substitutions should be made in the wave-numbers of the band lines in the present paper in the light of the wave-length tables recently published by Gale, Monk, & Lee (*Astr. Phy. Journ.*, March 1928, pp. 89-113).

Substitute	In place of	Remarks.
D ₁ R (3) 17318.03 (o)	D ₁ R (3) 17318.72 (o)	17318.72, resolved by G. M. & L.
D ₂ P (5) 16774.42 (6)	D ₂ P (5) 16774.72 (8)	16774.72, resolved by G. M. & L.
D ₂ Q (1) 17404.90 (o)	D ₂ Q (1) 17407.53 (o)	
D ₃ R (1) 17508.99 (5) C.D. + +	D ₃ R (1) 17512.36 (o)	
D ₃ R (4) 17624.43 (o) Lee	D ₃ R (4) 17623.32 (1)	
D ₄ Q (4) 17457.57 (oo)	D ₄ Q (4) 17458.78 (1)	17458.78, resolved by G. M. & L.
D ₄ Q (5) 17407.51 (o)	D ₄ Q (5) 17404.99 (o)	
D ₅ R (3) 17964.86 (1)	D ₅ R (3) 17966.00 (2)	17966.00, resolved by G. M. & L.
D ₅ P (2) 17717.06 (3)	D ₅ P (2) 17716.87 (3)	17716.87, resolved by G. M. & L.
D ₅ P (4) 17459.76 (2)	D ₅ P (4) 17458.78 (1)	17458.78, resolved by G. M. & L.
D ₆ Q (3) 17853.78 (1)	D ₆ Q (3) 17850.99 (3)	
D ₆ R (2) 18142.91 (1)	D ₆ R (2) 18140.19 (—)	18140.19, resolved by G. M. & L.
D ₇ R (2) 18416.59 (o)†	D ₇ R (2) 18417.19 (rd)†	18417.19, resolved by G. M. & L.

Prof. Richardson states that there are no interferences between the strong lines of these bands and those of the unpublished extension of the New Bands in the Violet (see Richardson, *R. S. Proc. A*, vol. cxv. p. 528 (1927), Richardson & Davidson, '*Nature*,' June 30, 1928).

XLVIII. *Acoustics of Strings struck by a Hard Hammer.* By P. DAS and S. K. DATTA *.

IN the *Philosophical Magazine* for March 1928, Dr. Kar and his associates have commented on Das's † theory of struck string and its experimental verification by Datta ‡. The object of the present note is to show that their criticisms are without foundation, being based on misconceptions of theory and faulty experimentation.

In the first place they make the statement that the discontinuous changes in the pressure of impact with time are an "assumption" on which Das's theory is based. This is entirely erroneous, since these are not assumed but are the logical results of rigorous mathematical analysis. Further,

* Communicated by Prof. C. V. Raman, F.R.S.

† P. Das, *Proc. Ind. Ass. Cult. Soc.* vol. vii. pts. i. & ii. (1921).

‡ S. K. Datta, *Proc. Ind. Ass. Cult. Soc.* vol. viii. pt. ii. (1923).

identical results have been obtained by Professor C. V. Raman and Dr. B. Banerjee*, who solved the problem by an independent method. Apart from Datta's work, the experimental determination by George† of the pressure-time curve by the oscillograph method actually reveals these discontinuities, and the careful measurements by George and Beckett‡ of the energy lost by the hammer plotted against the striking-length have been shown by Das§ to be in remarkable agreement with the values calculated from his own formulæ.

In fact, a physical interpretation of these discontinuities can be easily given. When the hammer strikes the string the latter at once acquires the velocity v of the hammer, and the length of string set in motion in time δt is $2c\delta t$, where c = wave-velocity. If ρ be the mass per unit-length of the string, the momentum lost by the hammer in time δt is $2c\delta t\rho v$, so that the pressure at the instant $t=0$ is not zero but $2\rho vc$. When the pulse having velocity v returns to the hammer after reflexion from the nearer extremity, it is again reflected completely from the hammer, since the mass $\rho c\delta t$ of length $c\delta t$ of the string is infinitesimal compared with that of the hammer. The change of momentum in time δt is $\rho c\delta t \cdot 2v$, so that the pressure again increases by $2\rho vc$. This recurs with the period of vibration of the part of the string between the hammer and the nearer fixed end.

Dr. Kar and his co-workers adopt in their experiments a method which they borrow from Datta without acknowledgment. The details of their arrangements are, however, seriously defective. From the diagram and description appearing in their paper, it would seem that the string was stretched on two horizontal bridges and set in motion in a horizontal plane. It is obvious that there would be considerable slipping at the bridges, and the effective vibrating length of the string would be greater than the distance between the bridges. The overtones would be inharmonic, and points on the string usually regarded as nodes would hardly have a nodal character, so that in touching a so-called node the very overtone of which the amplitude is sought, is silenced. Their experimental results are thus unreliable and useless for the purpose of testing a theory. In this connexion we may point out that the large differences which they find in the amplitude of the fundamental with hammers of identical mass and velocity, but of different metals, are

* Raman and Banerjee, *Proc. Roy. Soc. A*, vol. xevii. (1920).

† W. H. George, *Proc. Roy. Soc. A*, vol. cviii. p. 284 (1925).

‡ George and Beckett, *Proc. Roy. Soc. A*, vol. cxiv. p. 111 (1927).

§ P. Das, *Ind. Journ. Phys.* vol. i. pt. iv. (1927).

doubtless spurious. George and Beckett*, in their recent very careful and accurate work did not find any notable changes in amplitude, either of the fundamental or of the overtones with hammers of different materials.

In calculating the amplitude of the harmonics, the upper limit T of the integral

$$\int_0^T F \sin n(t-t') dt' \quad [F = \text{pressure}]$$

was taken by Datta to be the intercept between $t'=0$ and the point where the pressure-time curve cuts the t' -axis. This procedure, which is questioned by Kar, is obviously justifiable. For, at the moment the contact between the string and the hammer ceases, the pressure F becomes zero. It is only if repeated contacts occur that such a procedure would be inadequate, and such cases have not so far been theoretically treated.

Finally, as an illustration of the imperfect appreciation of theory shown by Kar and his colleagues, we may refer to the paragraph (*Phil. Mag.* vol. v. p. 556, 1928) in which they express impulse in terms of grammes weight, and thus confuse its dimensions with those of force.

210 Bowbazar Street,
Calcutta,
25th April, 1928.

XLIX. *Magnetic Studies on Salts, with Particular reference to those with Complex Ions.* By LARS A. WELO (*The Rockefeller Institute for Medical Research*)†.

THIS paper is intended to be mainly a descriptive rather than an interpretative account of a study of the magnetic properties of a very large number of salts of various types. It seems, therefore, best to consider the results by groups according to the principal features which have been observed. A discussion of the significance of the results, in so far as a discussion seems possible or may be ventured upon, will then be given along with the appropriate experimental data.

* George and Beckett, *Proc. Roy. Soc. A*, vol. cxvi. p. 126 (1927).

† Communicated by the Author.

The salts, 124 in number, will be considered under the following main headings :—

1. Polynuclear salts of iron and chromium having very large negative values of θ in the Curie-Weiss law $K_a(T-\theta)=C$.
2. Iron salts having irregular and variable moments within the observed range of temperatures.
3. Miscellaneous salts of iron and chromium of normal ionic moment and with relatively small values of θ in the Curie-Weiss law.
4. Coordination compounds of chromium and cobalt previously studied by Rosenbohm at only one temperature.
5. A ferricyanide and the penta-cyano derivatives.
6. The Prussian blues.
7. Salts showing an anomalous temperature variation of the susceptibilities.
8. Diamagnetic and near diamagnetic salts of some transition elements.

GENERAL DISCUSSION OF THE METHODS EMPLOYED.

All of the salts were studied in the solid state in the form of powders. In the case of the paramagnetic substance, this necessitates susceptibility measurements throughout a range of temperature sufficient to make certain that

$\frac{1}{K_a} = f(T)$ is linear, and to permit the determination of the constants C and θ with the required accuracy. The apparatus was modelled after that described by Foëx and Forrer*, and need not be described in detail here. The magnetic field in the region occupied by the specimen was about 4000 gauss. As a rule, determinations of the susceptibilities were made at three temperatures: when the salt was at room temperature; when it was surrounded by melting ice; and when it was surrounded by solid CO_2 . The refrigerants were contained in the space between two coaxial glass tubes joined at one end. The real temperatures attained by the salts were not actually measured. This fact raises two questions. Does a specimen acquire a definite temperature each time that it is surrounded by the refrigerant, and, if so, by how much does this temperature differ from the actual temperature of the refrigerant? The first question was answered by comparing the values of θ

* Foëx & Forrer, *Journ. de Phys. et le Rad.* vii. p. 180 (1926).

obtained with a given salt in separate runs. Throughout the work many such were made. It was found that for values of θ not far from zero, they agreed within 2°C .

on the average. From the geometry of $\frac{1}{K_a} = f(T)$, it was calculated that with ice as a refrigerant the temperatures acquired by the salts were always the same to within 0.18°C ., and with solid CO_2 as a cooling substance they were constant to within 0.65°C .

A direct thermocouple determination of the difference between the temperature acquired by a sample and that of the solid CO_2 proved it to be 8.5°C . This was checked by measurements on Mohr's salt, $\text{FeSO}_4(\text{NH}_4)_2\text{SO}_4 + 6\text{H}_2\text{O}$, for which Foëx * has found $\theta = +22^\circ$. Using the nominal temperatures of 0°C . for ice, and -78.5°C . for CO_2 , θ appeared, in my measurements, to be -3° . The difference of 25° in θ leads again to a correction of 8.5°C . when solid CO_2 is used. In the same way the correction when ice is used turned out to be 2.4°C . When ice and solid CO_2 were used as cooling substances, the actual temperatures of the salts were therefore $2.4^\circ \text{C} = 275.5^\circ \text{K}$. and $-70^\circ \text{C} = 203.1^\circ \text{K}$., respectively, with the relatively small uncertainties noted in the previous paragraph.

Only very rarely were the ice points omitted and susceptibilities observed at only two temperatures. This was done only when the type of salt was one which would certainly

give a linear $\frac{1}{K_a} = f(T)$. The value of the moment observed served as a reliable check. A few salts were also studied at temperatures above that of the room by the use of a small electric furnace.

Mohr's salt, $\text{FeSO}_4(\text{NH}_4)_2\text{SO}_4 + 6\text{H}_2\text{O}$ served as a standard. Its magnetic constants have been carefully determined by Foëx †, so that its susceptibility at the calibration temperature can be calculated. The susceptibility values of Foëx agree with the Leiden data on the same salt to within 0.4 per cent. when adjusted to the same temperature. A further check on the standard was obtained by measuring $\text{Fe}_2(\text{SO}_4)_3(\text{NH}_4)_2\text{SO}_4 + 24\text{H}_2\text{O}$ in terms of it. The susceptibility observed was in essential agreement with the Leiden datum for this ferric salt. As a standard, Mohr's salt has the additional advantage of being uniform throughout a sample.

* Foëx, *Ann. de Phys.* xvi. p. 259 (1921).

† *Loc. cit.*

Commercial samples of CoCl_2 and NiCl_2 were seriously lacking in this respect.

The susceptibilities are given by the formula

$$K = \frac{v-v'}{v_1-v'} \frac{m_1}{m} \left(K_1 - \frac{k_a}{\delta_1} \right) + \frac{k_a}{\delta},$$

where

v = millivolts observed with specimen. (The compensating current was measured by a millivoltmeter used in connexion with a properly adjusted shunt.)

v_1 = millivolts observed with standard.

v' = millivolts observed with empty container (slight temperature variation known).

m and m_1 = the masses of the substance and standard, respectively.

δ and δ_1 = the densities of the substance and standard, respectively.

K_1 = susceptibility of the standard.

k_a = volume susceptibility of air.

Except for the very weak paramagnetics, the air correction is negligible and the formula reduces to

$$K = \frac{v-v'}{v_1-v'} \frac{m_1}{m} K_1.$$

The gram atomic susceptibilities are given by

$$K_a = KM - k_d,$$

where

M = molecular weight.

k_d = sum of gram atomic susceptibilities of constituents other than iron, chromium, cobalt, etc., as the case may be.

A list of the gram atomic susceptibilities of the constituents involved throughout the work may well be included here. Practically all are due to Pascal*.

$\text{C} = -6.0 \times 10^{-6}$	$\text{Cl} = -20.0 \times 10^{-6}$
$\text{H} = -2.9 \times 10^{-6}$	$\text{Br} = -31.0 \times 10^{-6}$
$\text{O} = -4.6 \times 10^{-6}$	$\text{I} = -45.0 \times 10^{-6}$
$\text{S} = -15.0 \times 10^{-6}$	$\text{Na} = -9.2 \times 10^{-6}$
$\text{N} = -5.5 \times 10^{-6}$	$\text{K} = -18.5 \times 10^{-6}$
$\text{Ca} = -15.8 \times 10^{-6}$	

* Pascal, 'Revue Générale des Sciences,' July 15, 1928.

The following values were used for certain groups:—

$$\text{H}_2\text{O} = -13.0 \times 10^{-6},$$

$$\text{NO} = -1.6 \times 10^{-6},$$

$$\text{and } \text{PO}_4 = -33.5 \times 10^{-6}.$$

Each time that the group CN occurs, a correction of $+0.8 \times 10^{-6}$ was applied. In some salts, Co and Cr appear in near diamagnetic ions. The values used were $+55.0 \times 10^{-6}$ and $+63.0 \times 10^{-6}$, respectively. According to Pascal, the atomic susceptibility of oxygen is to be taken as a variable in accordance with the nature of the chemical bonds. This variation is small, however, and was neglected in all paramagnetic salts.

The diamagnetic and near-diamagnetic salts were studied by the Gouy method, the forces being measured with a sensitive balance. The fields were about 11,000 gauss. The formula is the same as before, r , v_1 , and v' being replaced by f , f_1 , and f' . Water was used as a standard with $K_1 = -0.719 \times 10^{-6}$. With diamagnetic salts the air correction is not negligible. The density, if unknown, was taken to be that of a mixture of bromoform and benzene, in which the salt would just float. This procedure in the determination of the densities is rough, but permissible since the correction terms are small. The chief drawback with the Gouy method when applied to powders is that of obtaining uniform packing. Several measurements were necessary, repacking each time. To give the reader an idea of the accuracy attained with the diamagnetic salts, the table contains also the number of measurements made and the probable error.

$$E = \pm \frac{0.85}{n \sqrt{n-1}}.$$

The tables of data on the paramagnetic salts contain the specific susceptibilities adjusted to a temperature of 20°C . by means of the relation $K_a(T-\theta) = C$ with the values of C and θ as tabulated. The accuracy implied by the use of the second decimal place was not actually attained, even relatively. On the other hand, rounding off K to the first decimal place would not do justice to the relative accuracy of the measurements at the different temperatures as indicated by the closeness with which the points fall on straight lines in the plots of $\frac{1}{K_a}$ against T . Following the usual custom, the Weiss magneton numbers are also

tabulated as calculated by $p=14.07 \sqrt{C}$. The values of C and θ were computed by selecting any two temperatures, T_1 and T_2 , and observing the corresponding values of $\frac{1}{K_a}$ directly from the graphs of $\frac{1}{K_a}=f(T)$. It is readily seen that

$$C = \frac{T_1 - T_2}{\frac{1}{K_{a1}} - \frac{1}{K_{a2}}}$$

and

$$\theta = \frac{T_2 K_{a2} - T_1 K_{a1}}{K_{a2} - K_{a1}}.$$

I. Polynuclear Salts of Iron and Chromium with Large Negative Values of θ .

These unique and interesting salts, listed in Tables I., II., and III., were very kindly supplied by Professor R. Weinland, of the University at Würzburg*. All are acetates except Nos. 7 and 8 which are benzoates, Nos. 23 and 24 which are formates, No. 9 which contains pyrogallol groups, No. 10 which is a salicylate and No. 25 which is a propionate. The salts that were analysed for iron at this Institute at about the time of the magnetic measurements are indicated under "Remarks."

The results of the magnetic measurements are shown in Tables I., II., and III. and in figs. 1 and 2. Some of the salts listed in Table II. do not appear in fig. 2. To plot the values obtained would result in the superposition of, and confusion among, the lines. Likewise the curves obtained with the salts listed in Table III. are omitted. In all these omitted cases, the curves $\frac{1}{K_a}=f(T)$ were straight lines.

It appears that the iron and chromium ions in salts of this type have associated with them the normal values of C and p . The only clear-cut exception is the pyrogallol salt No. 9. It may be noted that this salt lacks the OH group which appears either once or twice in salts giving uniformly normal

* For a general index to the literature regarding salts of this type, see Professor Weinland's book, 'Einführung in die Chemie der Komplex-Verbindungen,' Stuttgart, 1919, pp. 345 ff. Particular papers that may be mentioned are: *Berichte*, xlii. p. 3881 (1909), xlv. p. 2662 (1912), and xlvii. p. 2763 (1914); *Zeit. anorg. Chem.* xcii. p. 81 (1916); cli. p. 271 (1926) and clii. p. 1 (1926). Also *Ann. der Chemie*, ed. p. 219 (1913).

TABLE I.—Polynuclear Salts of Iron.

Reference No.	SALT.	$K \times 10^6$ (20° C.).	C.	θ .	p .	Re- marks.
1	$\frac{1}{2}[\text{Fe}_2(\text{CH}_3\text{COO})_4(\text{OH})_2]\text{NO}_2 + \frac{5}{2}\text{H}_2\text{O}$	19.13	4.10	-577	28.5	
2	$\frac{1}{2}[\text{Fe}_2(\text{CH}_3\text{COO})_4(\text{OH})_2]\text{Cl} + \frac{1}{2}\text{H}_2\text{O}$	18.17	3.97	-603	28.0	Anal.
3	$\frac{1}{2}[\text{Fe}_2(\text{CH}_3\text{CNCOO})_4(\text{OH})_2]\text{ClO}_4 + \frac{5}{2}\text{H}_2\text{O}$	14.59	4.26	-607	29.0	
4	$\frac{1}{2}[\text{Fe}_2(\text{CH}_3\text{ClCOO})_4(\text{OH})_2]\text{NO}_2 + \frac{5}{2}\text{H}_2\text{O}$	14.38	4.05	-593	28.3	Anal.
5	$\frac{1}{2}[\text{Fe}_2(\text{CCl}_3\text{COO})_4(\text{OH})_2]$	9.27	4.05	-553	28.3	Anal.
6	$\frac{1}{2}[\text{Fe}_2(\text{CH}_3\text{COO})_4(\text{OH})_2(\text{COO})_2(\text{FeBr}_4)]$	27.90	3.64	- 89	26.8	Anal.
7	$\frac{1}{2}[\text{Fe}_2(\text{C}_6\text{H}_5\text{COO})_4(\text{OH})_2][\text{C}_6\text{H}_5\text{COO}](\text{ClO}_4) + \frac{1}{2}\text{H}_2\text{O}$	11.22	4.40	-695	29.5	
8	$\frac{1}{2}[\text{Fe}_2(\text{C}_6\text{H}_5\text{COO})_4(\text{OH})_2]\text{O}_6\text{H}_3\text{COO}$	28.00	1.74	+ 37	18.6	
9	$\frac{1}{2}[\text{Fe}_2(\text{C}_6\text{H}_5\text{O}_4)_4]\text{H}_2(\text{NH}_4)_2 + \frac{5}{2}\text{H}_2\text{O}$	24.58	3.46	-129	26.2	Anal.
10	$\frac{1}{2}[\text{Fe}_2(\text{C}_6\text{H}_4(\text{OH})\text{COO})_4(\text{OH})_2][\text{Fe}(\text{C}_6\text{H}_4(\text{O})\text{COO})_2] \cdot \text{C}_6\text{H}_4(\text{OH})\text{COO} + \frac{5}{2}\text{H}_2\text{O}$	35.64	4.20	+ 6	28.8	Anal.

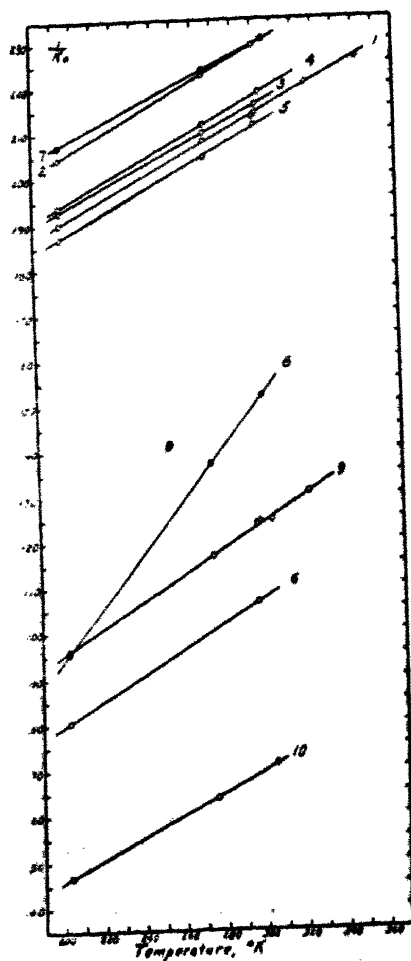
TABLE II.—Polynuclear Salts of Chromium.

Reference No.	SALT.	$K \times 10^6$ (20° C.).	C.	θ .	p .	Re- marks.
11	$\frac{1}{2}[\text{Cr}_2(\text{CH}_3\text{COO})_4(\text{OH})_2]\text{Cl} + \frac{5}{2}\text{H}_2\text{O}$	20.35	1.92	- 93	19.5	
12	$\frac{1}{2}[\text{Cr}_2(\text{CH}_3\text{COO})_4(\text{OH})_2]\{\text{CS}(\text{NH}_2)_2\}_3\text{Cl} + \frac{5}{2}\text{H}_2\text{O}$	16.54	1.93	-103	19.5	
13	$\frac{1}{2}[\text{Cr}_2(\text{CH}_3\text{COO})_4(\text{OH})_2\text{NH}_3]_2\text{H}_2\text{O}$	19.10	1.92	-116	19.5	
14	$\frac{1}{2}[\text{Cr}_2(\text{CH}_3\text{COO})_4(\text{OH})_2\text{NH}_3]\text{CH}_3\text{COO}$	22.95	1.91	-103	19.4	
15	$\frac{1}{2}[\text{Cr}_2(\text{CH}_3\text{COO})_4(\text{OH})_2\text{CNS}] + \frac{3}{2}\text{H}_2\text{O}$	21.77	1.91	-101	19.4	
16	$\frac{1}{2}[\text{Cr}_2(\text{CH}_3\text{COO})_4(\text{OH})_2]\{\text{CO}(\text{NH}_2)_2\}_2\text{Cl} + \frac{1}{2}\text{H}_2\text{O}$	20.08	1.87	- 89	19.2	
17	$\frac{1}{2}[\text{Cr}_2(\text{CH}_3\text{COO})_4(\text{OH})_2]\text{C}_6\text{H}_5\text{N}_3\text{NO}_2$	16.40	1.85	-100	19.1	Anal.
18	$\frac{1}{2}[\text{Cr}_2(\text{CH}_3\text{COO})_4(\text{OH})_2](\text{CH}_3\text{COO})_2 + \frac{1}{2}\text{H}_2\text{O}$	21.38	1.97	-106	19.7	
19	$\frac{1}{2}[\text{Cr}_2(\text{CH}_3\text{COO})_4(\text{OH})_2](\text{NO}_3)(\text{CH}_3\text{COO}) + \frac{2}{3}\text{H}_2\text{O}$	20.50	1.95	-111	19.6	
20	$\frac{1}{2}[\text{Cr}_2(\text{CH}_3\text{COO})_4(\text{OH})_2]\text{Cl}(\text{CH}_3\text{COO}) + \frac{1}{2}\text{H}_2\text{O}$	20.37	1.91	-105	19.4	
21	$\frac{1}{2}[\text{Cr}_2(\text{CH}_3\text{COO})_4(\text{OH})_2]\text{CO}_2(\text{CH}_3\text{COO}) + \frac{5}{2}\text{H}_2\text{O}$	19.23	2.06	-120	20.2	
22	$\frac{1}{2}[\text{Cr}_2(\text{CH}_3\text{COO})_4(\text{OH})_2](\text{C}_2\text{O}_4)(\text{CH}_3\text{COO}) + \frac{1}{2}\text{H}_2\text{O}$	18.15	1.93	- 92	19.5	
23	$\frac{1}{2}[\text{Cr}_2(\text{HCOO})_4(\text{OH})_2]\text{HCOO} + \frac{5}{2}\text{H}_2\text{O}$	25.08	2.02	-108	20.0	
24	$\frac{1}{2}[\text{Cr}_2(\text{HCOO})_4(\text{OH})_2]\text{Cl} + \frac{1}{2}\text{H}_2\text{O}$	24.60	1.82	- 93	19.3	
25	$\frac{1}{2}[\text{Cr}_2(\text{CH}_3\text{CH}_2\text{COO})_4(\text{OH})_2]\text{Cl} + \frac{5}{2}\text{H}_2\text{O}$	18.81	1.97	-114	19.7	
26	$\frac{1}{2}[\text{Cr}_2(\text{CH}_3\text{COO})_4(\text{OH})_2] + \frac{1}{2}\text{H}_2\text{O}$	21.55	1.92	- 44	19.5	
27	$\frac{1}{2}[\text{Cr}_2(\text{CH}_3\text{COO})_4(\text{OH})_2] + \frac{1}{2}\text{H}_2\text{O}$	24.00	1.79	+ 1	18.8	
28	$\text{Cr}(\text{CH}_3\text{COO})_3$	22.28	1.83	- 60	19.0	Anal.

TABLE III.—Mixed Polynuclear Salts.

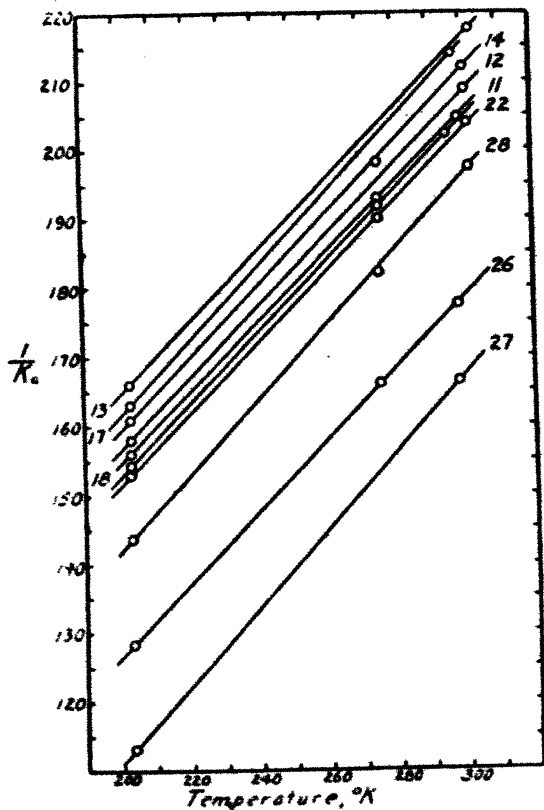
Reference No.	SALT.	$K \times 10^6$ (20° C.).	C.	θ .	p .
9	$[\text{Cr}_2\text{Fe}(\text{OH}_2\text{COO})_4(\text{OH})_2]\text{Cl} + 6\text{H}_2\text{O}$	16.80	8.00	-380	—
30	$[\text{Cr}_2\text{Fe}(\text{OH}_2\text{COO})_4(\text{OH})_2]\text{NO}_3 + 6\text{H}_2\text{O}$	17.15	9.38	-453	—
31	$[\text{Fe}_2\text{Cr}(\text{OH}_2\text{COO})_4(\text{OH})_2]\text{NO}_3 + \text{H}_2\text{O}$	18.81	7.69	-342	—

Fig. 1.



values of C and p and large negative values of θ . No significance can at present be attached to the salts No. 6 and No. 8. They are included in the table only as interesting variants. Structure complications make it difficult to decide just how to handle these two salts. For example, the measurements on No. 6 were handled on the questionable assumption that the contribution of the negative ion FeBr_4

Fig. 2.



is nothing. The low values of C and p given for No. 8 are probably related to the peculiar position of the oxygen as the salt is formulated. Not enough of salt No. 8 was at hand to make an analysis for iron. In view of the general excellence of the other salts as indicated by the agreement of our iron analyses with the formulae and published analyses, it is felt that the low values of C and p are not due to deficiency in iron.

In Table III. the C values apply to the whole trinuclear complex ion, and the p -values are omitted. In salt No. 29 (for analysis see *Berichte*, xlii. p. 3881 (1909)), C is approximately the sum of the normal values of C for the ferric and chromic ions. Assume $C=4.25$ for the ferric ion. For each chromic ion $C = \frac{8.00 - 4.25}{2} = 1.87$, leading to $p=19.2$,

which is in close agreement with $p=19.0$ as observed in simple chromium salts. A similar additive distribution is not possible for Nos. 30 and 31. No analyses on these salts could be found in the literature, and my own attempts to analyse the small quantities available failed. The probabilities are that the proportions of iron and chromium are not as formulated. Otherwise, we should have to conclude that the additive relations of the Curie constant observed when only iron or only chromium are the metals present, as in the salts of Tables I. and II., do not hold for the mixtures; and that the additivity observed with salt No. 29 is only a coincidence. The only thing that can be said, with certainty, about the mixed salts of Table III. is that the values of θ are negative and large, and intermediate between those found with iron alone and chromium alone.

Rosenbohm* has measured four hexa-formates of chromium of the type listed in Table II. at one temperature only. Jackson† recently considered these data, and tried to account for the apparent low moments by assuming that only two of the three chromium ions have the normal moment of 19 magnetons. The third chromium ion was assumed to be in another state of zero moment. Such an assumption is not necessary, in view of the results shown in Table II. To this Jackson has agreed in a private communication after having been informed of the present results.

The striking thing about these salts is, of course, the values of θ of the order -600 in the iron salts and -100 for those containing chromium. The problem of negative values of θ and of negative molecular fields is an old one and appears here in a particularly pressing form. They do not appear to be directly related to the existence of polynuclear ions. This possibility is eliminated by the fact that θ is only -129 in the pyrogallol salt, No. 9, and is $+6$ in the salicylate, No. 10; provided we accept the formulations given as representing their real nature. This consideration eliminates also a relation between θ and the

* Rosenbohm, *Zeit. f. Phys. Chem.* xciii. p. 711 (1919).

† Jackson, *Phil. Mag.* iv. p. 1070 (1927).

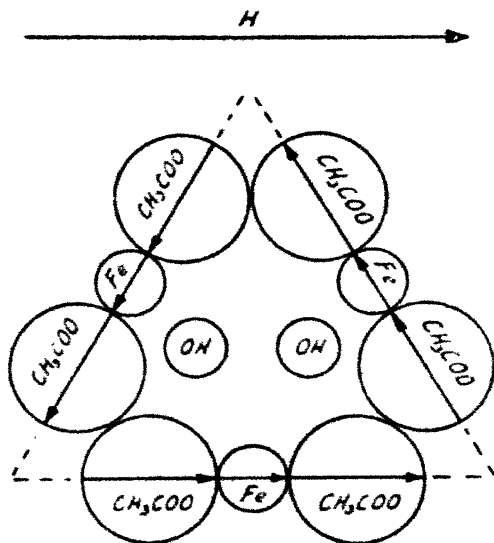
mass of the whole complex ion. Such a relation would be contrary to the theory of Oosterhuis *, if we are permitted to associate with J in his expression

$$\theta = \frac{-h^2}{24\pi^2 JK}$$

the moment of inertia of the whole complex ion. According to this theory, we should observe small values of θ in salts with large complex ions.

A possible way out is open to us if we recognize that the organic groups, CH_3COO , CHOO , $\text{C}_6\text{H}_5\text{COO}$, etc., are

Fig. 3.



themselves very probably permanent electric dipoles. We may then adopt and modify a point of view due to Debye †, which involves the assumption that the elementary magnets, that is, the iron and chromium ions, have permanent electric moments as well.

Let us consider as an example the typical polynuclear salt No. 1 $[\text{Fe}_2(\text{CH}_3\text{COO})_6(\text{OH})_2]\text{NO}_3 + 6\text{H}_2\text{O}$, and represent the complex ion by a model as in fig. 3. Since it is a plane

* Oosterhuis, Comm. Phys. Lab. Leiden, No. 31; Amst. Acad. p. 217, June 1913.

† Debye, *Handbuch der Radiologie*, Marx, Leipzig, 1925, vol. vi. p. 704 ff. Also 'Kinetic Theory of Gases,' Loeb, New York, 1927, p. 430.

model, it does not represent the true relative positions of the various parts, but it does serve to visualize the electrostatic control on the ferric ions. The model, as drawn, meets the requirement, however, of having no external resultant moment, either magnetic or electric. The complex ion as a whole, being fixed in the crystal lattice, does not rotate, but we shall adhere to the classical view that the ferric ions are capable of orientation by magnetic and electric fields. The magnetic axes of the ferric ions, which are not indicated in the figure, may or may not coincide with the permanent electric polarization.

It is immediately evident that the magnetization

$$I = N\mu_m \overline{\cos \phi}$$

induced by the magnetic field H and hence the susceptibility,

$$\frac{N\mu_m \overline{\cos \phi}}{H},$$

must be less than if there were no electrostatic control by the neighbouring organic groups. Consider salt No. 1 as an example. The gram atomic susceptibility was, at 20°C .

$$K_a = \frac{C}{T - \theta} = \frac{4.10}{293 + 577} = \frac{4.10}{870} = 4715 \times 10^{-6}.$$

A simple ferric salt having $\theta = 0$ and with the same Curie constant would have given

$$K_a = \frac{4.10}{293} = 14000 \times 10^{-6}.$$

The electrostatic control on the ferric ions in the case of the complex salt being considered has reduced the mean special value of $\overline{\cos \phi}$ to

$$\frac{4715 \times 10^{-6}}{14000 \times 10^{-6}} = 0.33 \text{ of its uncontrolled value.}$$

A similar calculation applied to a chromium salt, say, No. 11 $[\text{Cr}_2(\text{CH}_3\text{COO})_6(\text{OH})_2]\text{Cl} + 8\text{H}_2\text{O}$, shows that the postulated electrostatic control has reduced the susceptibility to 0.76 of its value without the control. A weaker control is indicated for the chromic ion, due presumably to a smaller electric moment μ_e .

Another question which must be considered is the influence of electrostatic control on the disorganization due to temperature agitation. The magnitude of the control is itself a

function of the temperature, owing to fluctuations in position and orientation of the controlling organic groups. But in any event the control which resists disorganization by temperature is, at every instant, exactly the same as the control which resists organization by the magnetic field. The temperature coefficient of the magnetization, or of the susceptibility, is therefore decreased in the same proportion as the magnetization or the susceptibility. But the temperature coefficient of susceptibility is, by experiment,

the quantity $-\frac{1}{T-\theta}$. Hence

$$\frac{K_a}{-\frac{1}{T-\theta}} = \text{a constant, which is the Curie-Weiss law.}$$

According to the view presented here, negative values of θ in the law $K_a(T-\theta)=C$ have a distinctly different origin from positive values. If the idea proves to be acceptable, it is of more importance than as a mere device to explain the frequent appearance of negative values. It removes what has been thought to be a difficulty in Debye's interpretation of molecular fields in ferromagnetics as being electric in nature. Debye's expression for ν in the equation for the effective field in ferromagnetics

$$H_e = H + \nu I$$

is

$$\nu = \frac{4\pi}{3} \frac{\mu_e^2}{\mu_m^2}.$$

It is of the observed order of magnitude in ferromagnetics, but cannot explain negative molecular fields or negative values of θ , since $\frac{\mu_e^2}{\mu_m^2}$ is essentially positive. On the view

proposed, there are no induced negative molecular fields. The fields which resist magnetization are provided by the permanent electric dipoles already present in the system.

It may be added that the hypothesis which has been briefly outlined provides the forces necessary for the existence of the aggregate of metallic ions and organic and hydroxyl groups which constitute the complex positive ion of the type $[\text{Fe}_3(\text{CH}_3\text{COO})_6(\text{OH})_2]$.

It would be interesting to study the magnetic behaviour of these polynuclear salts in solution, a line of work which I hope soon to undertake.

II. Iron Salts having Irregular and Variable Moments.

The results obtained with this group of salts are presented in Table IV. and fig. 4. They are commercial salts except the tetra-eugenol salt, No. 33, and the pyrocatechin salt, No. 34, which were supplied by Professor Weinland*. The work on No. 32 and on Nos. 35 to 39 was suggested by the irregular moments for ferric citrates and phosphates which have been calculated by Weiss from Pascal's measurements†. It was hoped that the values given there might be checked and definitely established. This could not be done, however. Even apparently analogous salts such as iron

TABLE IV.—Iron Salts with Irregular and Variable Moments

Reference No.	SALT.	$K \times 10^6$ (20° C.).	C.	θ .	p .	Re- marks.
32	FePO_4	71.40	3.82	- 60	27.5	Anal.
33	$\left\{ \begin{array}{l} [\text{Fe}(\text{C}_6\text{H}_5(\text{C}_6\text{H}_5)\text{OCH}_3\text{O})_4] \\ \text{K} \{ \text{C}_6\text{H}_5(\text{C}_6\text{H}_5)(\text{OCH}_3)(\text{OH}) \} \end{array} \right\}$	15.08	3.83	+ 24	27.5	"
34	$[\text{Fe}(\text{C}_6\text{H}_5\text{O})_2]_2\text{K} + 2.2\text{H}_2\text{O}$	33.82	3.56	- 3	26.5	"
	" "	2.81	+ 69	23.6	
35	Iron Pyrophosphate.....	20.72	4.81	-185	30.8	Anal.
36	Iron Ammonium Citrate.....	23.65	3.98	-169	28.0	"
37	Iron Magnesium Citrate.....	24.65	3.78	-157	27.3	"
38	Iron Potassium Citrate	23.52	2.67	- 24	23.0	"
39	Iron Tartrate and Ammonia	53.40	3.50	+ 63	26.3	"
	" "	3.04	+ 93	24.5	
	" "	2.66	+123	22.9	

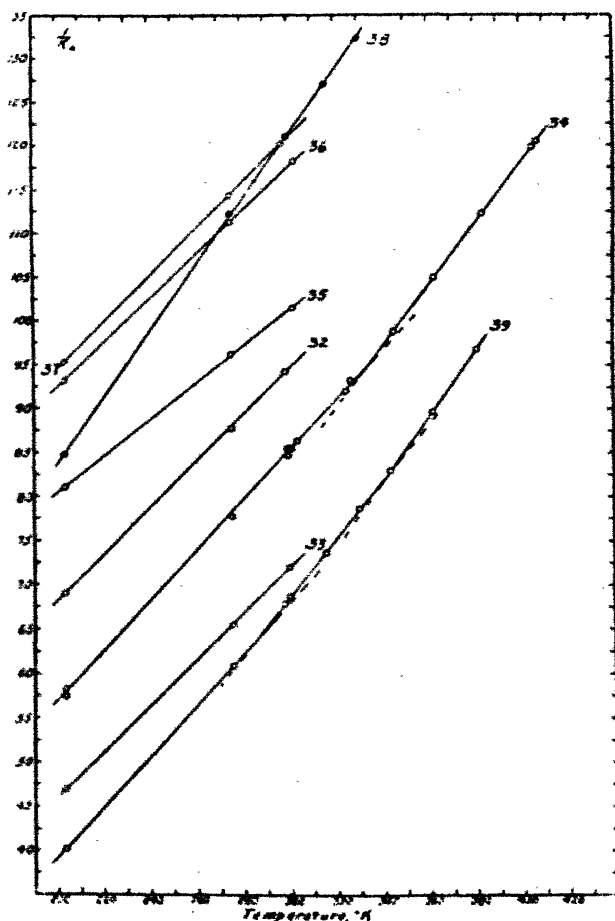
ammonium citrate and iron potassium citrate gave p values of 28 and 23 respectively. It is very doubtful whether these are the actual moments. It is more probable that the ferric ions in the pyrophosphate, the citrates, and the tartrate have the normal p values of about 29, but that the salts are mixtures of two or more components, each component being characterized by different values of θ in $K_a(T-\theta)=C$. Until the number of components and their proportions have been determined by complete chemical analyses, it cannot be stated that the iron does not appear with the

* See *Arch. d. Pharm. cclii.* p. 600 (1914); and *Berichte*, xlv. pp. 148 and 1113 (1912).

† Kuntz, "Theories of Magnetism," *Bull. No. 18*, Nat. Res. Council, p. 199.

normal moment of the ferric ion. A determination of iron alone is not sufficient. It should be stated that the salts, No. 32 and Nos. 35 to 39, were each analysed for iron three times by two different methods which checked to within 1 per cent.

Fig. 4.



The pyrocatechin salt undergoes a well-defined and reversible transformation at about 62° C. Considerable arbitrariness is involved in drawing curves through the points observed with iron tartrate and ammonia, and consequently in calculating C , θ , and p . Only the middle range is at all reliable, and here the apparent moment turns out to be far below the normal for ferric ion.

III. Miscellaneous Salts of Iron and Chromium.

The salts listed in Tables V. and VI. were, for the most part, obtained from Professor Weinland. The exceptions were the cupferon salt, No. 64, which was prepared by

TABLE V.—Miscellaneous Salts of Iron.

Reference No.	SALT.	K $\times 10^4$ (20° C.).	C.	θ .	p.	Remarks.
40	$[\text{Fe}(\text{HCOO})_2]\text{Cl} + \text{H}_2\text{O}$	60.17	4.18	- 55	28.8	Anal., formate.
41	$[\text{Fe}(\text{SO}_4)_2]\text{Na}_2 + 3\text{H}_2\text{O}$	30.44	4.15	+ 5	28.6	Anal.
42	$[\text{Fe}(\text{SO}_4)_2]\text{NH}_4$	50.72	4.00	- 2	28.1	
43	$[\text{Fe}(\text{PO}_4)_2]\text{H}_3(\text{NH}_4)_4 + \frac{1}{2}\text{H}_2\text{O}$	41.58	4.17	- 42	28.7	
44	$[\text{Fe}(\text{PO}_4)_2]\text{H}_2\text{Na}$	32.35	4.15	- 52	28.6	Anal.
45	$[\text{Fe}(\text{PO}_4)_2]\text{H}_4(\text{NH}_4)$	46.70	3.97	- 25	28.0	
46	$\text{Fe}(\text{H}_2\text{PO}_4)_3$	57.30	4.07	+ 12	28.4	Hypophosphite.
47	$[\text{Fe}(\text{C}_6\text{H}_5(\text{CHO})(\text{OCH}_3\text{O}))_3]\text{K}_2 + \text{H}_2\text{O}$..	17.15	4.33	+ 23	29.2	Vanillin.
48	$[\text{Fe}(\text{CrO}_4)_2]\text{K} + 2\text{H}_2\text{O}$	39.44	4.12	+ 4	28.5	
49	$[\text{Fe}(\text{C}_6\text{H}_5\text{O}_2)_3]\text{K}_2 + 2\text{H}_2\text{O}$	26.92	4.00	+ 20	28.2	Pyrocatechin.
50	$[\text{FeF}_6]_2\text{Na}_2$	52.25	4.15	- 119	28.6	M = 191.
51	$[\text{FeF}_6\text{OH}]_2\text{H}_2(\text{CN}_2\text{H}_5)_2 + 3\text{H}_2\text{O}$	41.95	3.97	+ 22	28.0	Anal., guanidine.
52	$[\text{Fe}(\text{SO}_4)_2]\text{H}(\text{C}_6\text{H}_5\text{N}) + 2\text{H}_2\text{O}$	39.15	3.96	+ 18	28.0	Pyridine.
53	$[\text{FeCl}_2(\text{C}_2\text{O}_4)_2]\text{H}(\text{C}_6\text{H}_5\text{N})$	40.00	4.13	- 65	28.6	M = 280.
54	$[\text{FeSO}_4(\text{C}_2\text{O}_4)_2]\text{H}_2(\text{C}_6\text{H}_5\text{N})_2$	28.90	4.07	- 22	28.4	M = 440.
55	$[\text{Fe}(\text{OH})_2(\text{C}_2\text{O}_4)_2]\text{H}(\text{C}_6\text{H}_5\text{N})$	42.30	4.07	+ 19	28.4	Anal.
56	$[\text{FeCl}(\text{OH})_2(\text{C}_2\text{O}_4)_2]\text{H}_2(\text{C}_6\text{H}_5\text{N})_2$	32.12	3.98	+ 19	28.1	Anal.
57	$[\text{Fe}(\text{CH}_3\text{COCHCOCH}_3)_2(\text{C}_6\text{H}_5\text{N})_2]\text{Cl}_2$...	37.92	4.15	+ 12	28.6	Acetyl acetate, pyridine.
58	$[\text{Fe}(\text{OH})_2(\text{CH}_3\text{C}_2\text{O}_4)_2]\text{H}(\text{C}_6\text{H}_5\text{N}) + 2\text{H}_2\text{O}$..	35.60	4.05	+ 20	28.3	Malonate.
59	$\frac{1}{2}[\text{Fe}_2\text{Cl}_4]\text{H}_2(\text{C}_6\text{H}_5\text{N})_2$	43.30	4.03	+ 19	28.2	
60	$[\text{Fe}(\text{C}_6\text{O}_4)_2]\text{H}_2(\text{C}_6\text{H}_5\text{N})_2$	15.20	4.33	+ 6	29.2	
61	$[\text{Fe}(\text{ClO}_4)_2]\text{C}_{11}\text{H}_{12}\text{N}_2\text{O}_6$	9.42	4.05	+ 20	28.3	Antipyrine.
62	$[\text{FeCl}_2]\text{C}_{11}\text{H}_{12}\text{N}_2\text{O}_6$	33.34	4.30	+ 12	29.1	Anal.
63	$[\text{FeSO}_4(\text{C}_2\text{O}_4)_2]\text{H}(\text{C}_6\text{H}_5\text{N})$	29.50	4.23	- 91	28.9	Anal., quinoline.
64	$[\text{FeSO}_4(\text{C}_2\text{O}_4)_2]\text{H}(\text{C}_6\text{H}_5\text{N})$	31.92	4.29	- 9	29.1	M = 441, cupferon.
65	$\text{Fe}(\text{CH}_3\text{COCHCOCH}_3)_2$	42.22	4.20	+ 14	28.8	Acetyl acetate.
66	$[\text{Fe}(\text{C}_6\text{H}_5(\text{O})\text{COO})_2]\text{K} + 4\text{H}_2\text{O}$	32.17	4.20	0	28.8	Salicylate.
67	$\text{Fe}(\text{C}_6\text{H}_5(\text{NOH})\text{CO})_2 + \frac{3}{2}\text{H}_2\text{O}$	28.75	4.21	0	28.8	Benzhydroxamate.
68	$\text{Fe}(\text{C}_6\text{H}_5\text{O}_2)_2$	38.68	4.15	0	28.6	Valerate.
69	$[\text{Fe}(\text{C}_6\text{H}_5(\text{OO})\text{C}_6\text{H}_5\text{O}_2)_2](\text{NH}_4)_2$	16.55	4.12	0	28.5	Anal., alizarine.
70	$\text{FeC}_2\text{O}_4 + 2\text{H}_2\text{O}$	68.80	3.33	+ 26	25.7	Anal., ferrous oxalate.
71	$\text{Fe}(\text{ClO}_4)_2 + 6\frac{3}{2}\text{H}_2\text{O}$	29.30	3.26	+ 1	25.4	Anal., ferrous perchlorate.
72	$\text{Fe}(\text{C}_6\text{H}_5\text{O}_2)_2 + \frac{1}{2}\text{H}_2\text{O}$	41.27	3.41	0	26.0	Anal., ferrous lactate.

Dr. Baudisch, the chromium salts Nos. 73, 78, and 79, loaned by Dr. Hendricks, and Nos. 46, 68, 70, 71, and 72,

which were of commercial origin. The plots of $\frac{1}{K_a} = f(T)$

are not shown. In each case where observations were made at various temperatures the relation was linear. Only in the cases of salts Nos. 66, 67, 68, 69, and 72 was a study of the temperature variation of the susceptibility omitted. The recorded values of $\theta=0$ are, therefore, not observed values, but were assumed. This assumption is justified by the fact that the values of C and p are the normal values of the type of ion involved.

TABLE VI.—Miscellaneous Chromic Salts.

Reference No.	SALT.	$K \times 10^6$ (20° C.).	C.	θ .	p .
73	$K_2Cr(CN)_6$	18.84	1.73	+17	18.5
74	$[Cr(C_2O_4)_3]K_4 + 3H_2O$	12.56	1.77	+12	18.7
75	$[Cr(OH)_6]Cr(SO_4)_3 + 2H_2O$	19.86	1.87	+13	19.2
76	$[Cr(OH)_4Cl]SO_4 + 3H_2O$	19.62	1.84	+15	19.0
77	$[Cr(NH_4)_3Cl]Cl_2$	24.80	1.73	+14	18.5
78	$[Cr(OH)_4Cl]Cl_3$ (blue)	22.42	1.77	+ 4	18.7
79	$[Cr(OH)_4Cl_2]Cl + 2H_2O$ (green) ..	22.60	1.70	+17	18.4

Unfamiliar organic groups may be identified by their names, which are found under "Remarks." Salts Nos. 50, 53, 54, and 64 had partly decomposed, so that they contained more iron than the formulæ indicate. The true molecular weights as determined by iron analyses are shown. It should be noted that the last three salts listed in Table V. are ferrous salts.

None of the salts listed in either table shows any features of any particular interest. To the first order of accuracy the Curie constants and the Weiss magneton numbers are normal, and the values of θ show no larger fluctuations than are found in the simpler salts. One salt that may be noted is the chromi-cyanide $K_2Cr(CN)_6$, No. 73. With Cr are associated 18.5 magnetons, approximately the usual 19 found with simple chromic salts, whereas the corresponding cobalt salt is diamagnetic, and the ferricyanide $K_3Fe(CN)_6$ gives the low magneton numbers 11.9 and 11.2 according to the temperature range.

It may also be noted that the salts $\text{Fe}(\text{ClO}_4)_3(\text{C}_{11}\text{H}_{12}\text{N}_2\text{O})_6$, No. 61, and $\text{Fe}(\text{CH}_3\text{COCHCOCH}_3)_3$, No. 65, are quite normal according to the present measurements. Magneton numbers of 50.3 and 32.4, respectively, have recently been reported for these two salts*.

IV. Coordination Compounds of Chromium and Cobalt.

Table VII. and fig. 5 contain the data observed with a series of chromium and cobalt coordination compounds

TABLE VII.
Chromium and Cobalt Coordination Compounds.

Reference No.	SALT.	$K \times 10^6$ (20° C.).	θ .	θ .	P .
80	$[\text{Cr}(\text{en})_3](\text{SCN})_3 + \text{H}_2\text{O}$	14.60	1.82	+10	18.9
81	$[\text{Cr}(\text{en})_3]\text{I}_3 + \text{H}_2\text{O}$	9.69	1.79	+13	18.8
82	$[\text{Cr}(\text{en})_3](\text{NO}_3)_3$	14.90	1.79	+15	18.8
83	$[\text{Cr}(\text{en})_3]\text{Cl}_3 + 4\text{H}_2\text{O}$	14.59	1.74	+15	18.5
84	$[\text{Cr}(\text{en})_2(\text{SCN})_2]\text{Br}$ (cis.)	16.18	1.71	+15	18.4
85	$[\text{Cr}(\text{en})_2(\text{SCN})_2]\text{Cl}$ (cis.)	18.15	1.70	+12	18.3
86	$[\text{Cr}(\text{en})_2(\text{SCN})_2]\text{Cl}$ (trans.)	18.15	1.70	+12	18.3
87	$\frac{1}{2}[\text{Cr}(\text{en})_3][\text{Cr}(\text{CN})_6] + \frac{3}{2}\text{H}_2\text{O}$	26.47	1.77	+17	18.7
88	$[\text{Cr}(\text{en})_3][\text{Co}(\text{CN})_6]$	13.38	1.75	+9	18.6
89	$[\text{Co}(\text{en})_3][\text{Cr}(\text{CN})_6]$	13.64	1.75	+14	18.6
90	$[\text{Cr}(\text{NH}_3)_6][\text{Co}(\text{CN})_6]$	16.68	1.78	+9	18.8
91	$[\text{Co}(\text{NH}_3)_6][\text{Cr}(\text{CN})_6]$	16.77	1.75	+15	18.6
92	$[\text{Co}(\text{en})_3][\text{Cr}(\text{C}_2\text{O}_4)_3]$	11.38	1.82	+13	19.0
93	$[\text{Co}(\text{en})_2\text{C}_2\text{O}_4][\text{Cr}(\text{en}(\text{C}_2\text{O}_4)_2)]$	11.38	1.85	+8	19.1

kindly loaned me by Professor P. Pfeiffer, of Bonn. To avoid superposition and confusion, some lines have been omitted from the figure. These data are of interest chiefly in that they verify, to a first approximation, the results of Rosenbohm†, who measured a very large number of salts of these types at one temperature only. In the main, the present results justify Rosenbohm's assumption of the simple Curie law $K_\theta T = C$, since θ is in all cases relatively small. Rosenbohm's conclusion that the geometrical and coordination isomers cannot be distinguished by magnetic means is confirmed.

* Berkman & Zocher, *Zeit. f. Phys. Chem.* cxxiv. p. 318 (1926).

† *Loc. cit.*

V. A Ferricyanide and some Ferric Penta-cyano Derivatives.

The data on this type of ferric salt are shown in Table VIII. and in fig. 6. The ferricyanide was a sample from

Fig. 5.

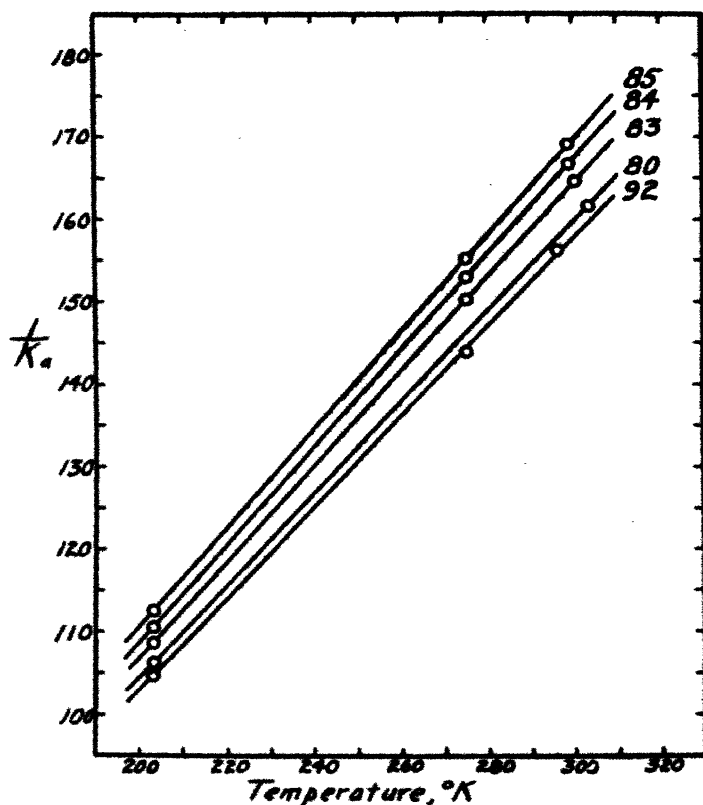
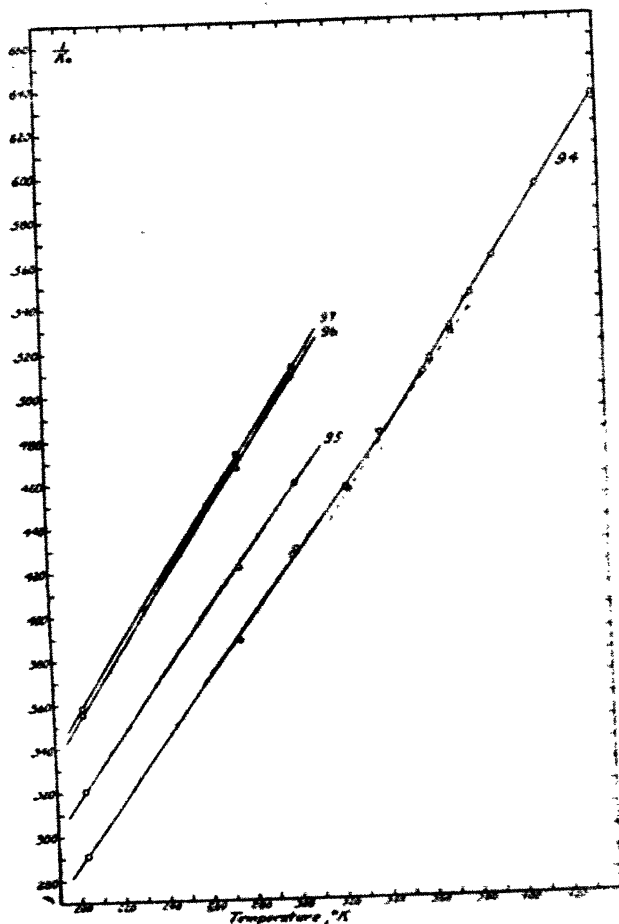


TABLE VIII.—Ferricyanide and Penta-cyano Derivatives.

Reference No.	SALT.	$K \times 10^6$ (20° C.).	C.	θ .	p .	Re- marks.
94	$K_3Fe(CN)_6$	6.97	0.720	- 6	11.9	
	"	0.636	+37	11.2	
95	$[Na_2Fe(CN)_5NH_2] + 2H_2O$...	7.43	0.707	-24	11.8	Anal.
96	$[Na_2Fe(CN)_5OH_2] + 2.6H_2O$...	6.38	0.641	-25	11.3	Anal.
97	$[Na_2Fe(CN)_5NO_2] + 2H_2O$..	5.60	0.639	-25	11.2	Anal.

Merck's, and the penta-cyano derivatives were made and analysed by Dr. Davidson at this Institute. These ferricyanide derivatives have been described by Hoffmann*, whose methods of preparation were largely followed in the preparation of the present samples. The main conclusion that

Fig. 6.

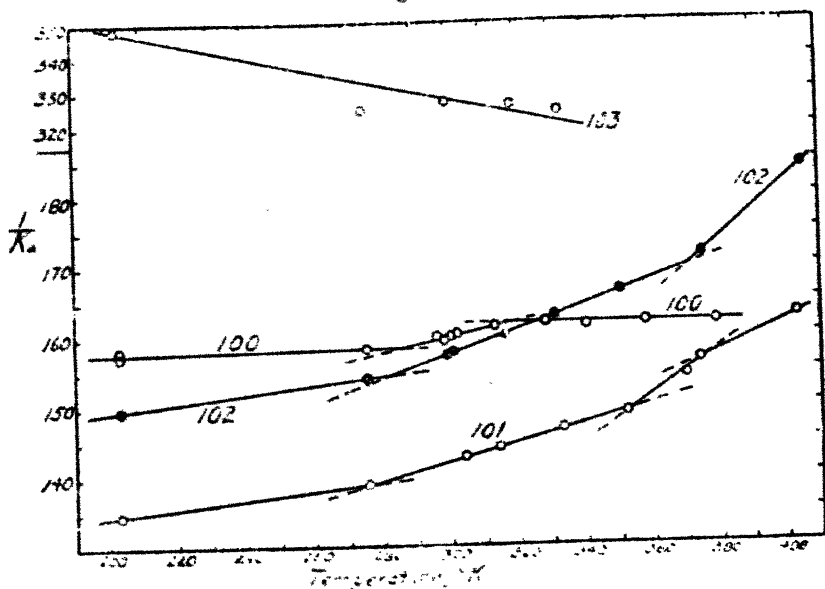


can be drawn from this part of the work is that the low moment found in the ferricyanide is retained without material alteration on substitution of other groups for the CN radicle. The moments observed in the penta-cyano compounds fall

* Hoffmann, *Ann. der Chem.* cccxii. p. 1 (1900).

within the limits 11.2 and 11.9 magnetons observed in $K_3Fe(CN)_6$ above and below its transformation point at $62^\circ C$. The fact that the amino salt, No. 95, appears with a higher moment than the aquo and nitro salts, Nos. 96 and 97, is not due to experimental errors. Each of them was measured twice, and they gave each time magneton numbers which agreed with the values of the table within 0.2 unit. It seems possible, in view of the two moments observed in the ferricyanide, that a suitable temperature range could be found in which the amino, the aquo, and the nitro salts would have identical moments.

Fig. 7.



Attention may be called to the fact that the specific susceptibilities of the ferric penta-cyano compounds listed in Table VIII. are from 62 to 78 per cent. of the values reported in a preliminary note * three years ago. A part of this discrepancy is due to the better quality of the salts used since. The present measurements were made on the third set of salts that have been prepared at this Institute. But the larger part of the discrepancy arises from my previous use of $K_3Fe(CN)_6$ as a standard, and from the fact that I had taken its susceptibility to be $K = +9.0 \times 10^{-6}$. This value

* Welo, 'Nature,' cxvi. p. 359 (1925).

due to Oxley* (corrected for the newer susceptibility of water, $K = -0.719 \times 10^{-6}$) seemed to be supported by those given in the physical tables, which are about 8 or 9×10^6 . At that time I was not aware of Ishiwara's† measurements on $K_3Fe(CN)_6$. His value of K at $21^\circ C.$ is $+7.08 \times 10^{-6}$, which is in as close agreement with $K = +6.97 \times 10^{-6}$, as shown in Table VIII., as can be expected from different samples.

Ishiwara studied $K_3Fe(CN)_6$ throughout a temperature range from $+21^\circ C.$ down to $-148^\circ C.$ When $\frac{1}{K_a}$ is plotted against T , his values fall very accurately on a straight line within the range $-12^\circ C.$ to $-118^\circ C.$ The values of C , θ , and p as determined by this straight line turn out to be 0.925 , -68 , and 13.5 respectively. Accordingly, $K_3Fe(CN)_6$ has still another transformation point at some lower temperature.

The magnetic data on solid $K_3Fe(CN)_6$ herein given are in fairly close agreement with those of Miss Collet‡, obtained with solutions. Her magneton numbers are 11.4 for concentrated solutions and 10.9 for the weak ones. A magneton number of 11 seems strange, in view of the number of the order 29 observed in simple ferric salts. But it may be recalled that the number 11 is associated with iron. We are reminded that the empirical Weiss magneton is, by definition, just one-eleventh of the atomic moment, at saturation, of pure iron.

Incidentally, it may be of interest to mention that $K_3Fe(CN)_6$, the amino salt, No. 95, and the aquo salt, No. 96, yield ferro-magnetic decomposition products on decomposition in air at $300^\circ C.$ The nitro salt, No. 97, was not tried. Qualitatively, these decomposition products behave just like oxidized precipitated magnetite§. The permeabilities are smaller, but of the same order of magnitude as in precipitated magnetite, and on heating to $600^\circ C.$ a non-reversible transformation takes place. Ferromagnetism does not appear on cooling again.

VI. Soluble and Insoluble Prussian Blue.

Soluble and insoluble Prussian blue will be very briefly considered in this paper, since the measurements and their

* Oxley, *Proc. Camb. Phil. Soc.* xvi. p. 107 (1910-1912).

† Ishiwara, *Sci. Rep. Tohoku*, iii. p. 303 (1914).

‡ Collet, *Compt. Rendus*, clxxviii. p. 987 (1924).

§ Welo and Bandisch, *Phil. Mag.* l. p. 399 (1925); Sosman and Posnjak, *J. Wash. Acad. Sci.* xv. p. 329 (1925).

significance to the disputed question of structure are being published elsewhere*.

Soluble Prussian blue is regarded as a potassium-ferric salt of hydro-ferrocyanic acid with the formula $K Fe [Fe(CN)_6]$, while insoluble Prussian blue is the ferric salt of the same acid with the formula $Fe_4 [Fe(CN)_6]_3$. It is well known that the ferrocyanides are diamagnetic, and we shall see in the last section of this paper that the paramagnetic contribution of the quadrivalent ion $Fe(CN)_6$, if any, is practically negligible. The measurements on the soluble blue were therefore computed on the assumption that only one of the two iron ions carries the magnetic moment. In the case of the insoluble blue, it was assumed that only four of the seven iron ions contribute to the paramagnetism of the compound. On the bases of these assumptions, it was found that the ferric ions have approximately the normal moments as observed in simple ferric salts. For the soluble blue, $KFe[Fe(CN)_6]$, the magnetic constants were: $C=4.05$, $\theta = +22$, $p=28.3$; and for the insoluble blue, $Fe_4[Fe(CN)_6]_3$, they were: $C=3.92$, $\theta = +15$, and $p=27.8$.

VII. Salts showing Anomalous Temperature Variation of $1/K_a$.

Of all the salts examined during the course of the work, only four were found to show irregularities in the curves $\frac{1}{K_a} = f(T)$ other than the frequent change of slope indicating a reversible transformation. No. 100 was a triglycolate $[Fe(OCH_2COO)_3]H_2(C_6H_5N) + 2H_2O$ with a susceptibility of $+15.4 \times 10^{-6}$ at $20^\circ C$. No. 101 was a diglycolate $[Fe(OCH_2COO)_2]H(C_6H_5N) + \frac{1}{2}H_2O$ whose susceptibility at $20^\circ C$. was $+24.1 \times 10^{-6}$. No. 102 was $[FeF_4]K$ with a susceptibility of $+37.3 \times 10^{-6}$ at $20^\circ C$. No. 103 was a polynuclear chloracetate of the type considered in the first part of this paper. Its formula was $\frac{1}{3}[Fe_3(CCl_3COO)_6(OH)_2] + \frac{1}{3}H_2O$, and its susceptibility at $20^\circ C$. was $+6.5 \times 10^{-6}$. The four salts were obtained from Professor Weinland†.

Nos. 100, 101, and 103 were analysed here at the time of the magnetic measurements. The curves obtained are shown in fig. 7. Values of C and p , calculated from the short middle portions of the curves, where they are apparently straight lines, yield values of these magnetic contents larger than the usual values for the ferric ion. The C values for Nos. 100,

* Davidson and Welo, *Journ. Phys. Chem.*, (in press).

† *Zeit. anorg. Chem.* cli. p. 271 (1926) and cl. p. 47 (1925).

101, and 102 are, respectively, 9.00, 7.20, and 5.51, leading to the magneton numbers 42, 38, and 33. With No. 103 no computations are possible.

These salts are unstable. It is quite certain that Nos. 101 and 102 contained ferro-magnetic decomposition products before being heated during the measurements. No. 101 became strongly ferromagnetic on being heated in air at 170° C. No. 102 became ferromagnetic on heating at 150° C., and very strongly so after being heated at 300° C. In both cases the decomposition products became simply paramagnetic after having been heated at 600° C. The decomposition products of Nos. 100 and 103, on the other hand, do not go through the ferromagnetic stage, but change directly to a paramagnetic condition which is not altered by heating at 600° C. The presence of a ferro-magnetic impurity in Nos. 101 and 102, due to decomposition, would account for the flatness of the curve $\frac{1}{K_a} = f(T)$ and large values of C and p , since the ferromagnetic part is relatively insensitive to temperature changes. Salts Nos. 100 and 103, which decomposed very rapidly at 75° C., were probably decomposing, during the measurements, into more paramagnetic forms at such rates as to make $\frac{1}{K_a}$ apparently constant in the case of No. 100, and fast enough to make $\frac{1}{K_a}$ decrease in the case of No. 103.

The true magnetic constants are therefore unknown. The glycolates, Nos. 100 and 101, could be diamagnetic for all that the present measurements tell us. It is more probable that the ferric ions carry the normal moments, but that the salts are characterized by large negative values of θ in the Curie-Weiss law. The glycolate groups would be expected to be electric dipoles, and might give rise to the magnetic behaviour observed in the polynuclear salts as described in Section I. of this paper.

A calculation readily shows that if the salt No. 103, $\frac{1}{3}[\text{Fe}_2(\text{CCl}_2\text{COO})_6(\text{OH})_2] + \frac{1}{3}\text{H}_2\text{O}$, is really of the same type as the polynuclear salts described previously, in which were found the usual ionic moment for the ferric ions, θ in the Curie-Weiss relation $K_a(T - \theta) = C$ would have to be at least -1100.

It is interesting to find that an anomalous behaviour in an iron fluoride has been noted before. Ishiwaru* studied

* *Loc. cit.*

$\text{FeF}_3 + \text{H}_2\text{O}$. It is indicated by him, however, that the chemical formula was a little doubtful. The susceptibility varied very little throughout the temperature range of -160°C . to $+170^\circ \text{C}$. Ishiwara's fluoride, $\text{FeF}_3 + \text{H}_2\text{O}$, and the present $[\text{FeF}_4] \text{K}$ were both, probably, contaminated by a ferromagnetic decomposition product.

TABLE IX.—Diamagnetic and Near-Diamagnetic Salts.

Reference No.	SALT.	No. of Measurements.	$K \times 10^6$.	$K_a \times 10^6$.	Remarks.
104	$\text{H}_4\text{Fe}(\text{CN})_6$	4	-0.328 ± 3	+ 5.0	
105	$\text{K}_4\text{Fe}(\text{CN})_6 + 3\text{H}_2\text{O}$	7	-0.408 ± 2	+ 5.0	
106	$\text{K}_4\text{Fe}(\text{CN})_6$	4	-0.366 ± 1	+ 4.1	
107	$\text{Na}_4\text{Fe}(\text{CN})_6 + 9.5\text{H}_2\text{O}$	4	-0.474 ± 3	- 1.0	Anal.
108	$\text{Na}_4\text{Fe}(\text{CN})_6$	3	-0.340 ± 1	- 2.0	
109	$\text{Ca}_4\text{Fe}(\text{CN})_6 + 10.5\text{H}_2\text{O}$	4	-0.465 ± 1	+ 8.3	Anal.
110	$\text{Na}_4\text{Fe}(\text{CN})_6 \cdot \text{NH}_3 + 4.2\text{H}_2\text{O}$	3	-0.379 ± 2	+ 18	Anal.
111	$\text{Na}_4\text{Fe}(\text{CN})_6 \cdot \text{SO}_3 + 8.8\text{H}_2\text{O}$	4	-0.398 ± 6	+ 31	Anal.
112	$\text{Na}_4\text{Fe}(\text{CN})_6 \cdot \text{NO}_2 + 7.5\text{H}_2\text{O}$	3	-0.364 ± 4	+ 36	Anal.
113	$\text{Na}_4\text{Fe}(\text{CN})_6 \cdot \text{OH}_2 + 2.3\text{H}_2\text{O}$	4	-0.229 ± 3	+ 52	Anal.
114	$\text{Na}_2\text{Fe}(\text{CN})_5 \cdot \text{NO} + 2\text{H}_2\text{O}$	5	-0.348 ± 4	- 4.0	Nitroprusside.
115	$[\text{Fe}(\text{C}_{10}\text{H}_6\text{N}_4)_2]\text{Pr}_2$	3	-0.069 ± 1	+ 196	Dipyridyl.
116	$\text{K}_4\text{W}(\text{CN})_6 + 2\text{H}_2\text{O}$	3	-0.365 ± 1	- 27	
117	$\text{K}_4\text{Mo}(\text{CN})_6 + 2\text{H}_2\text{O}$	3	-0.381 ± 1	- 5	
118	$[\text{Co}(\text{en})_2(\text{NH}_3)\text{Cl}]\text{Br}_2$ (levo) ...	5	-0.305 ± 1	+ 68	
119	$[\text{Co}(\text{en})_2(\text{NH}_3)\text{Cl}]\text{Br}_2$ (dextro) ...	5	-0.292 ± 1	+ 73	
120	$[\text{Co}(\text{en})_2(\text{NH}_3)\text{Cl}]\text{Cl}_2$ (racemic) ...	3	-0.324 ± 1	+ 69	
121	$\text{Co}(\text{C}_6\text{H}_5\text{NO}_2)_2$	Est.	+0.6	+400	Nitrobenzol.
122	K_2CrO_4	Est.	+0.04	+ 60	Anal.
123	$\text{K}_2\text{Cr}_2\text{O}_7$	Est.	+0.25	+ 60	Anal.
124	CrO_3	Est.	+3	+300	

VIII. Diamagnetic and Near-Diamagnetic Salts of Various Transition Elements.

The observed specific susceptibilities of these salts and the computed atomic susceptibilities of the metallic ions are tabulated in Table IX. The ferro-cyanides and the nitroprusside were commercial products. The hydro-ferrocyanic acid $\text{H}_4\text{Fe}(\text{CN})_6$ and the penta-cyano compounds were prepared by Dr. Davidson. The cyanides of tungsten and

molybdenum were loaned by Dr. Feldmann, of Hannover, as were the chromates by Dr. Hendricks. The dipyriddy iron salt and the nitrobenzol salt of cobalt are due to Dr. Bandisch and the cobalt amines are due to Dr. King. It is indicated that the susceptibilities of the last four salts were merely estimated. The apparatus used was not sensitive enough for diamagnetic measurements.

The important question with which we become concerned on examining the data of Table IX. is that of "residual paramagnetism independent of the temperature," a conception which it is difficult to reconcile with prevailing magnetic theory. It has been supposed that potassium ferrocyanide $K_4Fe(CN)_6 + 3H_2O$ is one of the compounds in which the metallic ion appears with a small positive residual susceptibility after correction for diamagnetism of the other constituents. $KMnO_4$, K_2CrO_7 , and the cobalt amines are familiar examples.

In view of the present results it is very doubtful if $K_4Fe(CN)_6 + 3H_2O$ belongs in this category. The best indication that it does not is the fact that the corresponding sodium salts Nos. 107 and 108 give residuals which are definitely not positive. Other points in the evidence against residual para-magnetism in iron in the ion $[Fe(CN)_6]$ are as follows:—

1. $H_4Fe(CN)_6$ apparently has a residual atomic susceptibility of $+5 \times 10^{-6}$, but it is known that the diamagnetic susceptibility of this acid is really more than -0.328×10^{-6} . The acid decomposes at ordinary temperature into the paramagnetic Prussian blue. The particular sample used, which gave $K = -0.328 \times 10^{-6}$ soon after preparation, was found, 22 months later, to be actually paramagnetic. Hence $K = -0.328 \times 10^{-6}$ is certainly too small, and does not represent the true diamagnetic susceptibility. An increase in K by 7.5 per cent. to $K = -0.352 \times 10^{-6}$ would remove the apparent positive residual of $+5 \times 10^{-6}$ for iron in $H_4Fe(CN)_6$.

2. The evidence is that the susceptibility of potassium ferrocyanide depends on the field strength. The present susceptibility of $K = -0.408 \times 10^{-6}$ was obtained with a field intensity of 11,000 gauss. This is in substantial agreement with Oxley*, who, however, does not state the

* *Loc. cit.*

field intensity. Ishiwara * used field strengths of about 2600 gauss, and found $K = -0.352 \times 10^{-6}$, which leads to a positive atomic susceptibility for iron of $+29 \times 10^{-6}$ as compared with about $+5 \times 10^{-6}$ in the present experiments. These distinct susceptibility values at different fields indicate the presence of a trace of ferromagnetic material.

3. The ferromagnetic traces suspected to be present in the ferrocyanides are the natural decomposition products. All of the ferrocyanides, the penta-cyano compounds and the nitro-prusside listed in Table IX. (the dipyriddy salt No. 115 was not tried), yield ferromagnetic decomposition products on being heated in air at 300°C . On heating to 600°C ., a non-reversible transformation takes place, and they become merely paramagnetic.

In connexion with the ferrocyanides, it is to be observed that the potassium and sodium salts were also measured in the dehydrated condition brought about by heating to constant weight in an atmosphere of nitrogen at 125°C . This was done, not so much to test for a direct magnetic effect of the water of crystallization, as to decide on the diamagnetic correction to apply for water. The correction as calculated from Pascal's additive law is -10.4×10^{-6} , whereas the observed molecular susceptibility for water is $-0.719 \times 10^{-6} \times 18 = -13 \times 10^{-6}$. Use of the latter value in computing K_a for hydrated potassium and sodium ferrocyanides leads to values of K_a which agree, within one unit, with the values of K_a found for the dehydrated salts. As an incidental matter, the conclusion is justified that water, as water of crystallization, is magnetically identical with water in the liquid state.

The ferrous penta-cyano compounds, although diamagnetic, yield positive residuals for iron which are larger than the residuals shown by the ferrocyanides. As has been pointed out, these salts give ferro-magnetic decomposition products, so that the observed diamagnetic susceptibilities are likely to be too low. It would be interesting to study these ferrous penta-cyano compounds over a range of low temperatures to see if there is present, also, a trace of the corresponding ferric salt which, as has been seen in Section V., is paramagnetic. Ishiwara has already shown that $K_4\text{Fe}(\text{CN})_6 + 3\text{H}_2\text{O}$ is free from any paramagnetic component, since the susceptibility was constant between room and liquid air temperatures.

* *Loc. cit.*

It is to be observed that the ferrous aquo salt No. 113, $\text{Na}_2\text{Fe}(\text{CN})_6\text{OH}_2$, falls into line with the other ferrous penta-cyano salts, in contrast to my previous results as presented in a letter to 'Nature'*. At that time it was thought to be paramagnetic and to approach in strength the ferric penta-cyano salts. This salt is especially likely to oxidize to the paramagnetic ferric form unless great precautions are taken.

The nitro-prusside, No. 114, is the only ferric penta-cyano compound so far known to be diamagnetic. It also yields a negative susceptibility for the iron in it. One is tempted to regard diamagnetism in this salt as being due to compensation of the moment associated with the ferric ion by that of the NO group. Quantitatively, however, there arises a discrepancy of 2 Weiss units, since the moment of the NO molecules is 9 magnetons.

No importance is to be attached to the susceptibility value and the positive residual found for the dipyriddy compound $[\text{Fe}(\text{C}_{10}\text{H}_8\text{N}_2)_3]\text{Br}_2$. Only one sample was available, and the quantity was too small to permit accurate measurements. It is included in the table merely as an additional example of a salt which is diamagnetic in spite of the presence of iron. The corresponding sulphate (instead of bromide) has been reported as diamagnetic by Berkman and Zocher†, but it is difficult to accept their value for the susceptibility, $K = -1.7 \times 10^{-6}$.

The cobalt amines containing the ethylene-diamine groups ($\text{en} = \text{NH}_2\text{CH}_2\text{CH}_2\text{NH}_2$) are diamagnetic, as Rosenbohm found them to be, but the mean value of the atomic susceptibility for the cobalt, $K_a = +70 \times 10^{-6}$, is a little higher than his value of $K_a = +60 \times 10^{-6}$. The lack of agreement seems to be outside of the experimental error. The samples were old, having been prepared in 1911. These salts do not yield ferromagnetic decomposition products, but they become paramagnetic on heating for a few minutes at 350°C . The presence of a small trace of a paramagnetic component is suggested by an observation on the salt $[\text{Co}(\text{en})_2\text{Cl}_2]\text{Cl}$, of the same lot as the cobalt amines and, presumably, prepared at about the same time. According to Rosenbohm, this salt should be diamagnetic. It was paramagnetic with $K = +11.3 \times 10^{-6}$.

The two chromates, Nos. 122 and 123, are seen to give positive residuals for chromium in close agreement with the

* *Loc. cit.*

† *Loc. cit.*

value $K_s = +63.3 \times 10^{-6}$ found by Weiss and Collet* in the dichromate $K_2Cr_2O_7$.

The value $K = +3 \times 10^{-6}$ for CrO_3 is too high on account of partial decomposition. For this substance Ishiwara found an initial susceptibility $K = +0.51 \times 10^{-6}$, and that the susceptibility rose to very high values on heating. On still further heating, CrO_3 became Cr_2O_3 and less magnetic with $K = 28.5 \times 10^{-6}$.

In conclusion, it may be remarked that salts such as the cobalt amines and the chromates, which seem to yield small positive residuals for the susceptibilities of the metals, need very careful studies as to the constancy of the susceptibilities when the temperature is varied. Miss Collett in collaboration with Weiss has studied a luteo cobalt salt and $K_2Cr_2O_7$, both as solids and in solution. The detailed results have not been given, as far as I know, but the published note gives the impression that the susceptibilities are constant only within very narrow limits. One element of difficulty in this problem of residual paramagnetism independent of the temperature is, of course, that of the proper diamagnetic constants to be used for correction. An equally difficult one is that of excluding or allowing for possible paramagnetic components.

It is a pleasure for me to express my thanks to those who have supplied me with material and who have, in other ways, contributed towards this work. I am especially grateful to Professor R. Weinland, Professor P. Pfeiffer, and Dr. D. Davidson for supplying so many salts of uniformly high quality. Dr. S. B. Hendricks, Dr. K. Feldmann, and Dr. V. King have also contributed many rare salts. Dr. O. Baudisch was largely instrumental in obtaining the material from abroad, and it is to him that I owe my interest in the subject of complex salts. Thanks are due to the General Electric Company for their kindness in lending the electromagnet.

Rockefeller Institute for Medical Research,
New York, April 12th, 1928.

* Weiss & Collet, *Compt. Rend.* clxxviii. p. 2146 (1924), clxxxi. p. 1057 (1925).

L. *The Surface Tension of Liquid Metals.*—Part III. *The Surface Tension of Mercury.* By L. L. BIRCUMSHAW, M.A., M.Sc.*

THE surface tension of mercury has been the subject of many investigations under very different conditions and by many different methods. The more recent work may be briefly reviewed. Stöckle† formed a drop of mercury in an enclosed vessel which could be evacuated or filled with a pure dry gas. Treating the surface of the drop as a convex mirror, he determined the position of an object and its image, from which the radius of curvature at the vertex was calculated. He obtained some very remarkable results, which are given in Table I.

TABLE I.

Gas.	t°.	Initial γ . mg./mm.	γ (after 1 hour). mg./mm.
Vacuum	15	44.4	44.4
Hydrogen	21	47.9	44.2
Air (dry)	17	48.5	43.7
Air (moist)	17	49.4	43.7
Carbon dioxide	19	49.0	44.4
Oxygen	23	48.7	44.0
Nitrogen	16	49.8	44.6

It was found that if a determination was made as rapidly as possible (in a few seconds) *in vacuo*, the value 44.4 mg./mm. was obtained, and this value was unchanged in one hour's time. If the drop were formed, however, in a gas, the initial value was much higher, but fell after a time to the value obtained *in vacuo*. Stöckle determined the fall of surface tension with time, and gives curves for all the above gases. It was found that the initial high values fell very rapidly in hydrogen (about 5 minutes), more slowly in carbon dioxide, and still more slowly in nitrogen, which required about fifty minutes for the value to fall to that obtained in a vacuum. He considered the effect to be due to the condensation of gas on the surface of the mercury. Stöckle's results are in general confirmed by

* Communicated by Sir J. E. Petavel, K.B.E., F.R.S.

† *Ann. d. Physik*, lxvi. p. 499 (1898).

Meyer*, who used the vibrating jet method, and therefore found higher initial values (51.5 mg./mm. in air and 56.5 in hydrogen).

Kalähne† formed stationary waves by means of the interference of two progressive circular wave systems in the surface of some mercury, and produced in this way what is, in effect, a plane reflexion grating. The wavelength of these small ripples is then equal to the constant of the grating, and this was measured, using sodium light. He obtained rather lower values than Stöckle, his highest being 44.0 mg./mm. at 18°.

Cenac‡ measured the surface tension of mercury in air and a vacuum at 0°, and found 437 dynes/cm. in air and 460 *in vacuo*. He used the drop-weight method and Lehnstein's corrections. A more recent determination by the same method by Harkins§ gave 476 dynes/cm. *in vacuo* and 465 in air.

Hogness|| found no difference in the surface tension of mercury in hydrogen when the pressure of the gas varied from 300 mm. down to a vacuum giving the green fluorescence of the glass with the electric discharge. No difference was detected when hydrogen was replaced by dry air.

Iredale¶, by means of the drop-weight method and mercury distilled into the apparatus *in vacuo*, obtained 456 dynes/cm. at 18–19° in air at atmospheric pressure (approx.), and as the pressure was decreased, the surface tension diminished to 410 dynes/cm. at 10^{-4} mm. Iredale suggests that there is some impurity present which lowers the surface tension, and this impurity is more effective in a vacuum. Removal of the taps in the apparatus, with their attendant lubricant, had no effect, however. In further experiments mercury was re-distilled twice in a current of air and then *in vacuo*. After distilling the metal into the apparatus, determinations were made as quickly as possible, and a value of 475 dynes/cm. was obtained at a pressure of 10^{-5} mm. On admitting air the value fell to about 460 dynes/cm., and after re-evacuating it fell to 410 dynes/cm. Experiments made with water-vapour in the dropping chamber gave a value of 411 dynes/cm., which is almost the same as that found for mercury *in vacuo*; the

* *Ann. d. Physik*, lxvi. p. 523 (1898).

† *Ann. d. Physik*, vii. p. 440 (1902).

‡ *Ann. Chem. et Phys.* p. 399 (1913).

§ *J. Amer. Chem. Soc.* xlii. p. 2539 (1920).

|| *J. Amer. Chem. Soc.* xliii. p. 1621 (1921).

¶ *Phil. Mag.* xlviii. p. 177 (1924).

suggestion is made that the adsorption of water-vapour from the glass is the cause of some of the anomalous results obtained. A further suggestion made by Iredale in this paper is that the pressure of air may raise the pressure of water-vapour necessary to form an adsorbed film.

In a further communication * Iredale has determined the surface tension of mercury by the measurement of a sessile drop. The mercury is distilled on to a glass plate enclosed in a glass chamber which can be evacuated. He uses the simple formula :

$$h^3 = a^3 = \frac{2\gamma}{\rho g},$$

where h is the distance from the maximum diameter of the drop to its vertex. Drops of about 1.5 cm. in diameter are employed. He found that the first few drops distilled over gave a low value, but that this rose after successive quantities were distilled, and he suggests that the first portions of the mercury tend to remove some impurity from the glass surface. From a measurement of eleven successive drops the surface tension rose from 430 to 465 dynes/cm., and after remaining for 24 hours *in vacuo* the value was found to be 446 dynes/cm. The admission of pure dry air to a mercury surface formed *in vacuo* does not alter its surface tension to any great degree, but unpurified air appears to lower it considerably, and the contamination is irreversible. Iredale considers that "when a surface is formed in air at atmospheric pressure the presence of the air may hinder the adsorption of the impurities, but the admission of air to a surface already formed in a vacuum does not appear to result in a de-sorption of impurities."

Popesco † has determined the surface tension of mercury by the previous method, and found a value of 436 dynes/cm. when the drop is formed and kept in a vacuum. If the drop formed *in vacuo* is exposed to a gas a decrease in the surface tension is observed. When a surface is formed in a gas the initial surface tension is greater than when formed *in vacuo*, but decreases after a time to the vacuum value. Popesco investigated these effects with different gases and at different pressures. It will be seen that he confirms in general Stöckle's results, and he ascribes these effects partly to adsorption and partly to the orientation of molecules in the liquid. Langmuir has shown that the initial velocity of

* Phil. Mag. xlix. p. 603 (1925).

† Ann. de Physique, iii. p. 402 (1926).

photo-electrons emitted from a mercury surface is modified similarly when the drop formed *in vacuo* is exposed to a gas. Popesco confirms this and points out the close parallelism between this phenomenon and surface tension.

Sauerwald and Drath* have recently made some determinations of the surface tension of mercury by the bubble-pressure method. These authors made experiments with a thick-walled glass capillary (0.61–1.28 mm.), a thin-walled glass capillary (0.035–0.05 mm.), and a thin-walled etched glass capillary. Their results are as follows ($t=19^\circ$):—

	γ .
Thick-walled capillary	465–480 dynes/cm.
Thin-walled capillary	453–476 "
Thin-walled capillary etched	465–474 "

A specially selected capillary with a thick wall gave results which varied from 469–479.8 dynes/cm., and a thin-walled etched silica capillary gave values from 469–477.5 dynes/cm. The influence of the depth to which the tube dipped in the metal was also investigated, and it was found that constant results were obtained when this exceeded 3 mm.

Burdon and Oliphant†, by the photography and measurement of a sessile drop, have repeated Popesco's work and confirmed his conclusions. They also found by means of the drop-weight method that mercury gives values when the drop is formed in air, which are only 1 per cent. higher than when the drop is formed *in vacuo*, and they consider that the drop-weight method fails to detect the differences between the air and vacuum values. They criticize the drop-weight method on the grounds that it is finally based on the value for the surface tension of water obtained by the method of capillary rise in glass tubes, and that the method has been based on determinations made with liquids of approximately unit density which are suspended from the outer circumference of a tube. They are doubtful as to whether the form of drop will be the same for liquids of high density, *e.g.* mercury which hangs from the inner circumference.

In view of the considerable divergence of the results found by previous workers, it was considered of interest to investigate the surface tension of mercury by means of the

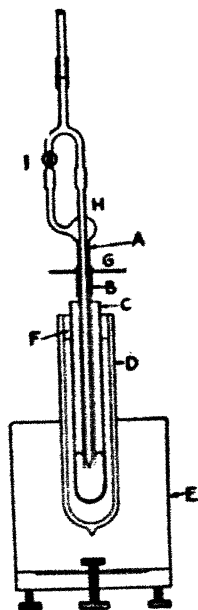
* *Zeit. Anorg. Chem.* cliv. p. 79 (1926).

† *Trans. Farad. Soc.* xxiii. p. 205 (1927).

maximum bubble pressure method under a number of different conditions, viz. :—

- (a) The use of tubes constructed of glass (soft).
- (b) The use of tubes constructed of silica.
- (c) The use of different gases for blowing the bubbles.
- (d) Varying the time of formation of the bubbles.
- (e) Different physical conditions of the surface of the ends of the tubes.

Fig. 1.



Experimental.

The apparatus is shown in fig. 1. It consists of an outer tube A 30 cm. long which fits tightly through the collar B. This collar carries a plate G, and through the top of the outer tube at H is fused a tube of smaller diameter which is drawn out to a capillary at its lower end. The ends of both tubes are ground carefully so that the cross-section of each is in the same plane, and this plane is parallel to the surface of the plate. The mercury is placed in the container * C,

* The glass container used had an internal diameter of 3.0 cm., and the internal diameter of the silica container was 2.7 cm.

which fits by means of a thick pad of cotton-wool F into a thermos flask D, which in turn is supported by a large wooden block E. The tubes are suspended in the mercury from a bracket attached to the plate, and this bracket is held by a heavy rigid iron stand. The stand, at its base, is supported on three levelling screws. By manipulating these the plate can be levelled up, when the ends of the tubes will be in a horizontal plane in the liquid. By closing or opening the tap I bubbles can be blown at will from the narrow or the wide tube. The procedure was, of course, the same as in the previous work*, viz. the difference in pressure required to detach a bubble, first from the wide and then the narrow tube, was measured. All the measurements were made at 20° C. The mercury in the container was placed in a thermostat for 15 minutes and rapidly transferred to the thermos flask. If the temperature of the room were kept at about 20°, then the temperature of the mercury, after a series of measurements had been made, was rarely found to have altered by more than 0.5°.

The mercury† was purified in the following manner:—A quantity of the metal was placed in a porcelain dish and floated on the surface of some mercury contained in a much larger dish. The whole was then covered with water containing a little sulphuric and nitric acids and electrolysed, using platinum wire electrodes with a current of 0.5 amp. for twenty-four hours. The mercury in the larger dish, which was the anode chamber, was then removed and dried. It was then distilled in air and finally in another still at a pressure of about 10 mm. of air.

The gases used were purified in the following manner:—

Hydrogen (generated electrolytically from caustic soda solution using an iron cathode) was dried, and passed through a silica tube at 600° to free the gas from traces of oxygen. It was then passed through a series of calcium-chloride tubes. Nitrogen was taken from a cylinder and passed over copper gauze heated to 600°, and a short length of iron gauze heated to 800°. The iron gauze had been previously oxidized and then reduced in hydrogen. The gas was then dried by passage over calcium chloride. Oxygen was taken from a cylinder and dried. Carbon dioxide was prepared from marble and hydrochloric acid; the gas passed through sodium-bicarbonate solution and dried through calcium-chloride tubes. In the actual determinations all these gases, with the exception of the carbon

* Phil. Mag. ii. p. 341 (1926).

† For the preparation of the mercury I am indebted to Mr. S. Watts.

dioxide, were finally (before entering the apparatus) passed through a tube immersed in solid carbon dioxide and acetone to remove the last traces of water. When carbon dioxide (gas) was used the final drying agent was phosphorus pentoxide.

In the first apparatus used the tubes (glass) had the following mean dimensions:—

External diameter of outer tube	1.156 cm.
Internal diameter of outer tube	1.009 "
External diameter of inner tube	0.0964 "

Perfectly concordant results were obtained with this apparatus, which gave:—

P wide.	P (narrow).	a^2 .	γ dynes/cm.
22.5	35.35	0.07477	497

The pressures are given in cms. of water. Experiments were then made to determine how the surface tension varied when the bubble was held on the end of the inner tube, at a pressure just below that at which it becomes detached, for various lengths of time. Normally about 40–50 secs. was taken to form and detach the bubble, and in these experiments the pressure in the bubble was developed to a value 3–5 mm. below that at which it was normally detached, held for various times, and in each case the final pressure at which the bubble was liberated was read. After each of these determinations the normal pressure (*i.e.* the reading obtained in the ordinary way in 40–50 secs.) was determined, and this practically never differed from the initial ordinary reading. It was found that the lowering of the pressure at which the bubble was detached always increased as the time the bubble was held on the end of the tube increased, but that the magnitude of the effect was hardly ever the same in experiments made on two consecutive days.

A large number of experiments were made and two series are given in Table II. The two series give (1) the smallest lowering obtained and (2) the highest.

TABLE II.

(1.)

Time (mins.).	P wide.	P narrow.	a^2 .	γ dynes/cm.
0	22.5	35.35	0.07477	497
5	22.5	35.25	0.07438	494
10	22.5	35.15	0.07399	492
15	22.5	34.95	0.07320	489
30	22.5	34.95	0.07320	489
60	22.5	34.7	0.07222	480

(2.)

Time (mins.).	P wide.	P narrow.	a^2 .	γ dynes/cm.
0	22.4	35.15	0.07419	493
10	22.4	34.8	0.07278	483
20	22.4	34.5	0.07152	475
30	22.4	34.4	0.07111	472
45	22.4	34.0	0.06947	461

The surface of the ends of the tubes in this apparatus was distinctly roughened. It had been ground with No. 3 emery. The ends were carefully polished with fine emery. On measurement the diameter of the inner tube was found to be 0.0982 cm. and the dimensions of the outer tube the same as before. The apparatus then gave the following:—

P wide.	P narrow.	a^2 .	γ dynes/cm.
22.05	34.8	0.07569	502

This result could be repeated to less than 0.5 per cent. (0.05 cm. in the pressure difference) any number of times.

A similar apparatus was constructed with silica tubes instead of glass. They had the following dimensions:—

Mean external diameter of outer tube ...	0.923 cm.
Mean internal diameter of outer tube ...	0.760 „
Mean external diameter of inner tube ...	0.1022 „

The ends of these tubes were carefully polished. Various values were obtained with this apparatus, four of which are as follows:—

P wide.	P narrow.	a^2 .	γ dynes/cm.
20.8	39.8		
20.8 (a)	39.4 (a)	0.10136	673
20.8	39.5		
20.8	39.8		

The result of one of these readings (a) has been calculated. The tubes were then etched for ten minutes in dilute hydrofluoric acid, when the diameter of the inner tube was found to be 0.1004 cm. Very high values were again obtained, as will be seen from the following readings, which also differ considerably among themselves:—

P wide.	P narrow.
21.2	36.6
21.2	37.7
21.2	36.8
21.2	36.5
21.2	36.6
21.2	36.9
21.2	37.8
21.2	38.0

The ends of the tubes were then roughened by grinding with No. 3 emery. The external diameter of the inner tube was then 0.0998 cm., and the following result was obtained :—

P wide.	P narrow.	a^2	γ dynes/cm.
22.1	34.65	0.07250	481

This result could be repeated any number of times. Experiments were then made holding the bubble on the end of the tube for various times, but practically no difference from the normal could be detected in the pressure required to liberate the bubble. These results are given below :—

Time (mins.).	P wide.	P narrow.	a^2 .	γ dynes/cm.
0	22.1	34.65	0.07250	481
15	22.1	34.60	0.07236	479
20	22.05	34.70	0.07307	485
30	22.05	34.6	0.07250	481

The glass apparatus used in the above work was unfortunately broken. A new one was constructed which had the following dimensions :—

Mean external diameter of outer tube...	1.007 cm.
Mean internal diameter of outer tube...	0.830 "
Mean external diameter of inner tube...	0.0990 "

The figures given by this tube (repeatable to 0.05 cm. in the pressure difference) were :—

P wide.	P narrow.	a^2 .	γ dynes/cm.
22.3	34.95	0.07451	495

This apparatus, unlike the first one used, gave practically no decrease in the reading when the bubble was held on the tube, as the following results show :—

Time (mins.).	P wide.	P narrow.	a^2 .	γ dynes/cm.
0	22.3	34.95	0.07451	495
5	22.3	34.95	0.07451	495
15	22.3	34.90	0.07420	493
30	22.3	34.90	0.07420	493

All the above determinations were made with hydrogen purified as described. Oxygen was next used. A very large number of determinations were made, but it was found to be impossible to obtain concordant readings, and most of these were very high. In some cases the normal reading was obtained a few minutes after placing the tube in the mercury, but the value rose rapidly after a short time. A

typical experiment is detailed below, the initial reading being taken ten minutes after the tubes were placed in the mercury.

Time.	P wide.	P narrow.	α^2 .	γ dynes/cm.
1.0 P.M.	22.25	34.85	0.07486	493
2.15 "	22.25	35.4		
	22.25	35.2		
	22.25	35.9		
	22.25	35.3		
3.0 "	22.15	36.1		
	22.15	36.1		
	22.15	35.8		
	22.15	35.6		
	22.15	35.9		
4.0 "	22.15	35.8		
	22.15	35.75		
	22.15	35.7		
	22.15	35.75		
	22.15	35.7		
5.15 ,	22.15	36.5	0.08192	544
	22.15	36.35		
	22.15	36.35		
	22.15	36.35		
	22.15	36.35		

The results obtained with this apparatus when using nitrogen and carbon dioxide, and the readings obtained when the bubble was held on the end of the tube for various times, are given in Table III.

TABLE III.

Nitrogen.

Time (mins.).	P wide.	P narrow.	α^2 .	γ dynes/cm.
0	22.1	34.85	0.07511	499
5	22.1	34.85	0.07511	499
15	22.1	34.85	0.07511	499
30	22.1	34.85	0.07511	499

Carbon Dioxide.

0	22.3	35.0	0.07480	497
15	22.3	34.8	0.07391	491
30	22.3	34.6	0.07301	485

When the bubbles were blown with moist hydrogen (hydrogen passed through water at 20°) the following result was obtained :—

P wide.	P narrow.	α^2 .	γ dynes/cm.
20.3	33.5	0.07611	505

The same result was obtained if a visible covering of water was placed on the mercury in the container.

With the silica tubes the values given in Table IV. were found:—

TABLE IV.

Nitrogen.

Time (mins.).	P wide.	P narrow.	α^2 .	γ dynes/cm.
0	22.1	34.75	0.07288	484
15	22.1	34.75	0.07288	484
30	22.1	34.80	0.07310	486

Carbon Dioxide.

0	21.95	34.5	0.07235	481
15	21.95	34.45	0.07202	479
30	21.95	34.4	0.07173	477

Oxygen.

0	22.5	34.8	0.07161	475
15	22.5	34.8	0.07161	475
30	22.5	34.8	0.07161	475

It will be seen that no appreciable decrease in the readings occurs when the bubbles are held on the end of the tube for as long as 30 minutes.

It was found that the time taken in the development of the maximum pressure of the bubble had no influence on the value obtained when the time was varied between 35 secs. and 2 mins. 30 secs. Variation within wide limits of the depth to which the tubes were immersed in the metal was also found to be without effect on the value.

The chief experimental results are given below in tabular form:—

	Hydrogen.	Nitrogen.	Carbon Dioxide.	Oxygen.
<i>1st glass tube.</i>				
Polished	502			
Roughened	495			
Bubble held 45 mins.....	461			
<i>2nd glass tube.</i>				
Roughened	495	490	497	No results.
Bubble held 30 mins.....	493	499	485	"
<i>Silica tube.</i>				
Polished	673			
Roughened	481	484	481	475
Bubble held 30 mins.....	481	486	477	475

Discussion.

Stöckle's experiments, which appear to have been carried out with great care, are very difficult to explain. It is easy to see, of course, that the presence of a gas might progressively lower the surface tension of a mercury surface, due to the time taken for the adsorbed gas film to reach equilibrium, but it is very difficult to imagine why different gases should reduce the value to that given *in vacuo*. It would have been expected that the initial (rapidly taken) value obtained in a gas would have approached that obtained in a vacuum, after which the surface tension would have diminished to some final equilibrium value. Nevertheless, it is extremely probable that the phenomena observed by Stöckle are genuine, as his results have been, in general, confirmed by Popesco and Burdon & Oliphant. They have been, however, chiefly noticed by workers who have used the "drop measurement" method. Harkins, Hogness, Cenac, and Burdon & Oliphant have found only small differences in the surface tension of mercury in air, and *in vacuo* when measured by the drop-weight method. This may be due to some extent to the relatively long time taken for the drops to form. An interesting explanation of Stöckle's results was first put forward by Bancroft ('Applied Colloid Chemistry,' 1921, p. 134). If we consider mercury to be a partially polymerized liquid, then the molecular modification which has the lowest surface tension will tend to be positively adsorbed at the surface, and equilibrium will be reached when a certain relation exists between the concentration of this modification in the surface layer and in the bulk of the liquid. The attainment of this equilibrium may take a definite time, and Bancroft suggests that it may be instantaneous when a mercury surface is formed *in vacuo*, but relatively slow in the presence of gases. Iredale, as previously stated, considers this lowering to be due to dirt or alkaline material derived from the glass which is much more rapid *in vacuo*. He also considers the possibility of moisture being the cause.

With regard to the results obtained in the present work, the following points call for special comment. It will be seen that distinctly higher results are obtained with glass tubes than with silica. This was found with both sets of glass tubes used, and the results obtained with these agree to less than 0.5 per cent. This value, nevertheless, is distinctly higher than that found by most workers on this subject. Sauerwald and Drath failed to detect any appreciable difference between glass and silica tubes, but the

highest value, 480 dynes/cm., obtained was with glass. A further interesting point is that with glass the same result is obtained whether the end (tip) of the tube is polished or roughened. In the case of the first glass apparatus the fall in surface tension noticed in holding the bubble on the end of the narrow tube was very variable, and in the second apparatus this effect was found to be almost absent. The only obvious explanation for these decreases is that they are due to traces of alkaline material (or dirt) left on the tube in spite of the cleaning treatment*. In view of the fact that they were only obtained with the first apparatus, the cause is more likely to be the specific nature of the glass, but this also may actually be due to surface alkali. The first glass tube was of pre-war German material, but the second was English soft alkali glass. When the bubbles were blown with nitrogen, a result was obtained which was practically identical with that recorded with hydrogen. No decreases on holding the bubble on the end of the tube were observed. When carbon dioxide was used the same normal result was obtained, but small decreases were found when the bubble was held on the end of the tube. With moist hydrogen a slightly higher value was obtained. This may be due to the fact that in this case the bubble does not form on the extreme circumference of the tube. It was also considered possible that, in the presence of so much moisture, the bubble actually formed on the inner circumference of the tube, the surface tension measured being the interfacial tension of mercury-water. Calculated on the inner radius, the figure 314 dynes/cm. was obtained, but the interfacial tension mercury-water, as determined by Harkins, is 375 dynes/cm., so that the above explanation appears to be unlikely.

With the apparatus made of silica the normal value obtained was, as previously stated, lower than that given by the glass apparatus. It is significant that with silica practically no decreases were observed on hanging the bubble on

* Before using the apparatus, the tubes were allowed to stand all night in a mixture of sulphuric and chromic acids, the acid mixture being drawn up into both tubes as far as the top of the bulb. The acid was then removed, the apparatus washed with freshly-distilled water, and then with acetone. The tubes were then inserted through the neck of a flask containing a small quantity of acetone. The latter was boiled and the lower parts of the tube were washed with condensed acetone. This treatment corresponds to "steaming," acetone being used instead of water. The tubes were then surrounded by a clean dry pyrex tube, and dry gas passed through first the inner and then the outer tube for at least two hours.

the end of the tube for a time as long as thirty minutes. This was found to be the case with all the gases used. Another interesting observation is that concordant normal values could not be obtained until the end of the tube had been roughened. This was established by a large number of experiments. Etching the tube with dilute hydrofluoric acid had little influence on the high readings obtained with the polished tubes, and observations of the surface under the microscope after etching showed that it was still very fine grained.

Curious results were obtained when oxygen was used for blowing the bubbles. With the glass apparatus sometimes correct readings were obtained immediately after placing the tubes in the mercury, but after a short time these readings were much too high. Moreover, the correct readings could not always be obtained in the early stages. With a silica apparatus this phenomenon was not observed. It was thought at first that these high values might be due to an oxide film produced on the surface of the tip of the tube which would cause the bubble to be formed nearer the inner circumference, or, of course, the high readings might have been due to real alteration in the surface tension of the mercury. In view of the fact that these observations were not repeated with a silica tube, however, this explanation appears improbable.

It appears from these experiments that values are obtained by the maximum bubble-pressure method for the surface tension of mercury which vary within small limits with the nature of the tube material. In the case of a silica tube the results also vary considerably with the physical condition of the end of the tube on which the bubble is formed. The use of different gases for blowing the bubbles does not appear to affect the results obtained.

The actual mechanism involved in the explanation put forward by Bancroft to explain Stöckle's results is, of course, very obscure. By making certain assumptions, however, it is possible to obtain a relation between the time required to reach equilibrium and the density of the gas.

The energy interchange between the liquid and the gas can only take place during a collision between gas and liquid molecules, so that if

k = the average loss (or gain) of kinetic energy of a gas molecule during a collision with a mercury molecule, and N = number of collisions per second per sq. cm. of surface, then the rate of communication of energy between

the gas and the liquid is equal to kN . If k is assumed to be equal $1/n$ th of the average kinetic energy of a gas molecule, then $kN = 1/n \left(\frac{1}{2} m \bar{v}^2 \right) N$, which is a quantity depending only on the condition of the gas and not on the time required to attain equilibrium at the surface. Therefore

$$kN = \frac{dE}{dT} = \frac{1}{n} \left(\frac{1}{2} m \bar{v}^2 \right) N,$$

$$\text{or} \quad E = \frac{1}{n} \left(\frac{1}{2} m \bar{v}^2 \right) NT,$$

where E is the energy in time T . E is the energy which is transferred to, or from, the liquid in the time required for the surface tension to change from the initial to the final value, and these two tensions presumably correspond with the dynamic and static surface tensions. E will therefore be a constant, and we have,

$$T = \frac{E}{\frac{1}{n} \left(\frac{1}{2} m \bar{v}^2 \right) N} \quad \text{or}^* \quad T \propto \frac{A}{m \bar{v}^2}.$$

Remembering that for any number of gases at the same temperature and pressure

$$m \bar{v}^2 = \text{a constant } c$$

$$\text{and} \quad \bar{v} = cm^{-\frac{1}{2}},$$

it is seen that

$$T \propto m^{\frac{1}{2}};$$

i. e., the time taken to reach equilibrium will be proportional to the square root of the density of the gas.

Stöckle found that the time required to reach equilibrium was much longer in nitrogen and carbon dioxide than in hydrogen. Popesco's figures for the surface tension, 5 seconds, 10 seconds, and 20 minutes after the formation of the drop, are given in the following table:—

	O ₂ .	N ₂ .	H ₂ .	CO ₂ .	SO ₂ .	NH ₃ .
5 secs.....	525	540	510	519	477	476
10 secs.....	505	524	477	509	438	450
20 mins.	438	447	445	455	—	448

Popesco's curves show a rapid fall of surface tension in the first twenty minutes, but from this time to 1 hour the fall is relatively gradual.

It is, of course, possible that the assumptions made in the above argument are unjustified, but, if not, the proportionality between the time for the surface tension to fall to the

* Ignoring variations in the value of n for different gases.

vacuum value and the density of the gas in which the mercury surface is produced do not appear to be in agreement with Popesco's results.

The remarkable phenomena observed by Stöckle and by Popesco cannot be considered to have been explained satisfactorily. The most interesting feature is that they appear to be peculiar to the "drop measurement method." It is possible that electrical effects, and the effect of gases on the rapidity with which mercury vapour attains equilibrium with the liquid * may ultimately be shown to be important.

Summary.

The surface tension of mercury has been determined by the method of maximum bubble pressure. Investigations were made regarding the influence of the material of the tube used, the physical condition of the surface of the end of the tube from which the bubble is blown, and the nature of the gas used for blowing the bubbles. The effect of hanging the bubble on the end of the tube for various lengths of time and the time taken to blow the bubbles has also been examined.

Glass tubes appear to give slightly higher results than tubes made of silica, and in the case of the latter it was found that roughening the ends (tips) of the tubes was essential before concordant results could be obtained. This did not appear to be necessary with glass tubes. The nature of the gas used for blowing the bubbles, with the exception of oxygen, has practically no influence on the values found. Results could not be obtained with oxygen when glass tubes were used, but with silica tubes concordant values were found. With one set of glass tubes used, hanging the bubble on the end of the tube for various lengths of time always resulted in a lowering of the figure found, and this lowering increased with the length of the time. With another glass apparatus this effect was practically absent.

The phenomena described by Stöckle and Popesco is discussed, with special reference to the possible polymerization and surface orientation in liquid mercury.

The author would like to thank Dr. W. Rosenhain, F.R.S., for his continued interest in this work; Mr. G. D. Preston, B.A., and Mr. J. H. Awbery, B.A., B.Sc., for a number of suggestions; and Mr. J. Trotter for assistance in the experimental part of the work.

* Rideal, 'Surface Chemistry,' chap. 2, p. 60.

LI. *On the Ultra-Violet Radiations emitted by Point Discharges.* By JOHN THOMSON, M.A., B.Sc., Houldsworth Research Student in the University of Glasgow*.

Introductory.

IN recent papers † it has been shown that ionizing electromagnetic radiations similar to those discovered by Wiedemann are emitted by the gas in the vicinity of metallic points charged to a high potential. That such radiations (or radiations of slightly longer wave-length) may be of first importance in determining the mechanism of the spark discharge has been suggested by J. Taylor ‡, and the present writer § has described results which appear to support his theory. The experiments described in the present communication were undertaken with a view to obtaining further evidence regarding the nature of these radiations and their relation to the discharge. The experiments are of a preliminary nature, since, as far as the writer is aware, no attempt has so far been made to investigate any part of this region of the spectrum at pressures comparable with atmospheric. The results obtained, however, fully justify further study of the phenomena exhibited.

Experimental Arrangements.

The final form of the apparatus used in the investigation is represented diagrammatically in fig. 1.

The tube containing the points E and F between which the discharge was to pass was cylindrical in form, the platinum electrodes being placed along the axis of the cylinder. The detecting and measuring apparatus was contained in a side-tube placed opposite one of the platinum points F, while the other two side-tubes were fitted with stop-cocks K, H. One tube was branched between the stop-cock K and the discharge-tube.

The detecting apparatus consisted essentially of a photo-electric cell, the insulated electrode of which was connected to a tilted electroscope or to a Dolezalek electrometer. C and D were two half-cylinders of brass of length 20 mm.,

* Communicated by Prof. E. Taylor Jones, D.Sc.

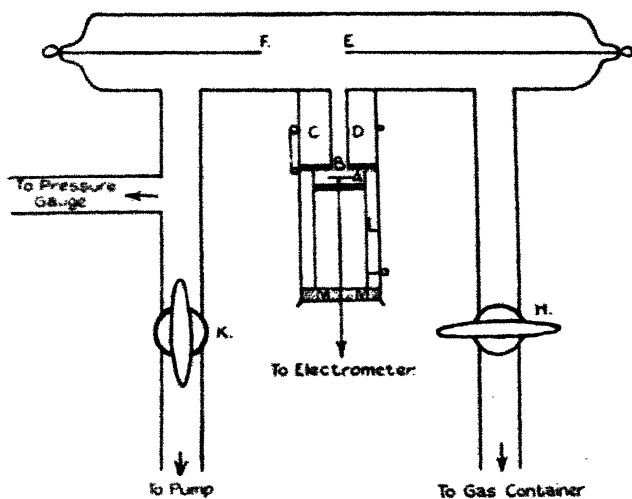
† C. E. Wynn-Williams, *Phil. Mag.* vol. i. p. 353 (1926); J. Thomson, *op. cit.* vol. v. p. 513 (1928).

‡ J. Taylor, 'Dissertation,' Utrecht (1927); *id.* *Proc. Roy. Soc. A*, vol. cxvii. p. 508 (1928).

§ J. Thomson, *loc. cit.*

sealed to the walls of the tube so that their faces formed the sides of a slot of width 4 mm. A potential difference of 560 volts was maintained between C and D during the course of the experiments. This strong electric field ($X=1400$ volts/cm.) was necessary in order to remove any ions which might drift or be projected down the slot towards the photo-electric cell. Theoretically the electric field was sufficiently strong to remove a simple positive molecular nitrogen ion projected into the slot with a speed of 3.10^7 cm./sec. Experiment showed that at pressures of 5 cm. of mercury and upwards no ions of any kind penetrated to the cell.

Fig. 1.



B was a circular piece of fine-mesh phosphor-bronze wire gauze placed across the tube and insulated from C and D by two half-cylindrical plates of ebonite. This gauze formed one electrode of the cell. Pressed against it was the brass cylinder L which contained the other insulated electrode A. This electrode consisted of a small rectangular copper plate covered on the side facing the slot with a thin film of copper oxide. The latter, though less sensitive to ultra-violet light than other substances, suffers less from "photo-electric fatigue," and consequently could be relied upon to give results which would be comparable over a long period. This plate was placed at a distance of about 2 mm. from the gauze and soldered to a thin copper wire which was imbedded in pure paraffin wax and led down the axis of the

cylinder L to the electroscope or electrometer. The latter was placed at a distance of about 2 metres from the tube itself. It will be observed, therefore, that the insulated electrode and the lead (surrounded by earthed tubing) from it to the measuring instrument were well shielded from effects due to induction. This was tested experimentally before any measurements were made. The insulation also was tested, and proved to be of high quality. Finally, the side-tube containing this apparatus was completely sealed at M with a mixture of beeswax and resin.

The detecting cell therefore consisted of the gauze B, the cylinder L, and the insulated plate A, while the slot between C and D limited the radiation affecting it to a small pencil from the immediate vicinity of the point E. The connexions to C, D, and B were made by platinum wires sealed into the glass tube.

The other side-tubes provided a means of controlling the nature and pressure of the gas in the discharge-tube. One tube was connected through a capillary to a gas container, while the other was connected to an oil-pump. The branch in the latter tube was sealed to a vertical tube dipping into mercury, so that the pressure of the gas could be measured almost directly at any time. Since pressure measurements did not require to be very accurate, such a gauge was sufficient for the purpose. All the connexions were sealed with the beeswax mixture which was found to be very satisfactory for work at pressures greater than 0.1 mm. of mercury.

The potentials relative to the earth of the half-cylinders C and D, and of the gauze B and the cylinder L, depended on the particular nature and purpose of each experiment. When observations were being made with the tilted electroscope to measure the photo-electric or ionization current, the half-cylinder C, the gauze B, and the cylinder L were all at earth potential, while the plate A was charged to ± 12 volts. In the later experiments in which the Dolezalek electrometer was employed, C, B, and L were maintained at ± 250 volts, while the plate A was initially at earth potential.

The current across the discharge-tube was supplied by a large induction coil (10-inch spark) used in conjunction with a motor mercury jet interrupter. Such an arrangement, when used to produce peak potential differences corresponding to spark lengths of less than half an inch in air at atmospheric pressure, gives a remarkably steady mean current through the secondary of the coil. This current was measured by a Gaiffe milliamperemeter, and could be

controlled to 0.1 milliampere. In order to eliminate as far as possible any inverse current through the coil, the battery E.M.F. in the primary circuit was kept as small as possible. Experiment indicated that the current at "make" was negligible.

Four gases were employed in the experiments to be described—oxygen, carbon dioxide, nitrogen, and hydrogen,—and of these, only the two latter were used in quantitative investigations. The hydrogen and oxygen were prepared by electrolysis; the nitrogen was prepared by the action of ammonium chloride on potassium nitrite in concentrated solution, and was purified by passing it through concentrated sulphuric acid and over red-hot copper filings; the carbon dioxide was prepared by the action of dilute hydrochloric acid on marble chips. No attempt was made to dry any of these gases.

The instruments used to measure the ionization and photo-electric currents have already been mentioned. The tilted electroscope, being easy to adjust, was used in the preliminary investigations, but all the quantitative experiments were performed with the Dolezalek electrometer. The suspension used in the latter was a fine quartz fibre which was thoroughly platinized by placing it near the platinum-wire cathode in a low-pressure discharge. The conductivity of the suspension was thus permanently ensured, and it was verified that the sensitivity of the instrument remained constant. During the work to be described, the deflexion of the needle due to one volt potential difference between the quadrants corresponded to 960 mm. on the scale, which was 3 m. from the instrument.

Ionization and Photo-Electric Currents in Different Gases at Atmospheric Pressure.

(1) *Oxygen*.—No results were obtained in oxygen on account of a peculiar phenomenon exhibited by the gas. As this phenomenon is one which might invalidate any ionization experiments carried out in this gas, it may be well at this point to describe it briefly.

With the apparatus described in the previous section and the tilted electroscope as the detector of ionization, the normal conductivity of the gas at A was observed. This was very small. Then a spark discharge at atmospheric pressure was passed across the gas between E and F, a current of 1 milliampere flowing for about one minute. The discharge was then discontinued, and again the leakage of the electroscope was observed. It was found that the gas in the

vicinity of the insulated electrode A had become conducting, the rate of leakage of the electroscope being about one hundred times as great as before. The apparatus was now allowed to stand, the same gas was being left in the tube, and the rate of leak of the electroscope was read at half-hour intervals. The leakage gradually and consistently decreased, until, twenty-four hours after the passing of the discharge, the rate of leak was the same as that observed at the beginning of the experiment.

On account of the strong electric field in the slot between the half-cylinders C, D, it was impossible for any charged particles to penetrate from the discharge between E and F to the plate A. Hence it must be concluded that the conductivity of the gas at A was caused by ionization which took place in the vicinity of A. This conclusion was verified by another experiment performed in a specially constructed tube, where all the ions directly produced by the discharge were immediately removed by a strong electric field. Spontaneous ionization of the gas continued to take place for some hours after the discharge had passed.

It is suggested that this ionization accompanies the gradual change of the O_2 molecule (and perhaps others) formed during the spark discharge to the normal O_2 molecule. It is immediately obvious that no experiments on the ionization produced by electromagnetic radiation could be performed in this gas with the apparatus described.

(2) *Carbon Dioxide*.—The ionization and photo-electric currents in this gas were exceedingly small. At atmospheric pressure the current at A was comparable with the normal leakage of the apparatus, and consequently any observations taken would be of little value. Even at the comparatively low pressure of 30 cm. of mercury the currents were still small, and investigation of the effects in carbon dioxide was therefore postponed until a later date.

(3) *Nitrogen*.—This gas, when purified, showed no signs of the phenomenon just described as occurring in oxygen, but a trace of oxygen in the gas was sufficient to give an observable effect. The nitrogen was therefore purified and repurified until all trace of the effect had vanished. The first experiment was made for the purpose of obtaining a table of ionization and photo-electric effects from the vicinities of the anode and cathode in the discharge-tube. It was hoped that this table might be comparable with that given in a former paper *

The tube was therefore filled with nitrogen at atmospheric pressure, all other gases having been excluded. The direction of the current in the primary of the coil was arranged so that E was the anode of the discharge, and readings were taken of the rate of leakage of the electroscope when the leaf, and therefore A, were charged to +12 and -12 volts relative to the earth. One milliampere was flowing from E to F. Then the direction of the current in the coil was changed, E becoming the cathode. The same readings were taken of the rate of discharge of A when charged to +12 and -12 volts. A great many difficulties were met with, one of the most important being the rise in temperature of the gas due to the discharge. Finally, the procedure adopted was to allow 15 minutes to pass between each reading of the ionization current, and to flood the discharge-tube with new gas before each reading. This allowed the tube to cool to room temperature between each discharge, and also eliminated any errors due to change in the chemical nature of the gas during the passage of the spark. The results, which have been verified with many samples of gas, are shown below ; the figures in the last column are accurate to about 5 per cent.

Potential of A in volts.	Nature of E.	Rate of discharge of A.
+12	Anode.	4
+12	Cathode.	5
-12	Anode.	9
-12	Cathode.	9

Comparing these results with those obtained under different conditions and described in the above-mentioned paper, it must be concluded that the radiations in the two cases are of the same nature and have the same origin. Briefly, the differences between the two tables are exactly such as might have been anticipated from the differences in the conditions. In the experiment just described a current of one milliamperere was flowing in the discharge ; in the former experiment the current was of the order of one microampere. The larger current might be expected (a) to intensify the radiations, (b) to partially level out the electric field in the gap, and so cause the intensity of the radiations from the vicinity of the cathode to increase. The first experiment was performed in air, the second in pure nitrogen. This appears to have caused little change in the total effect ; and since these radiations are molecular or atomic properties, this is just what might be expected.

(4) *Hydrogen*.—Pure hydrogen, like nitrogen, is free from the spontaneous ionization effect observed in oxygen. The experiments performed in nitrogen, which have just been described, were repeated in hydrogen, and the table shown below indicates the results. The currents in hydrogen were larger than those in nitrogen, and the figures in the last column can be compared directly with the corresponding figures for nitrogen.

Potential of A in volts.	Nature of E.	Rate of discharge of A.
+12	Anode.	4
+12	Cathode.	8
-12	Anode.	6
-12	Cathode.	16

Variation of Ionization and Photo-Electric Currents with Pressure in Different Gases.

The next series of experiments was designed to show how the effects of the radiations from each gas varied with the pressure of the gas. The experimental arrangements which have already been described were used, the Dolezalek electrometer being adopted as the current-measuring instrument. Readings were taken of the ionization and photo-electric currents at A, the insulated electrode, at different pressures, when one milliampere was flowing across the gas between E and F. Two sets of readings were taken: (i.) when the gauze B and cylinder L were at -250 volts relative to A; (ii.) when the gauze B and cylinder L were at +250 volts relative to A. In all cases E was made the cathode, as it was found that the currents from the anode were unsteady.

In case (i.) the currents measured by the electrometer represented the ionization currents at A. No photo-electric effect took place owing to the large negative potential of B; any photo-electrons emitted by B travelled to D under the action of the stronger electric field between B and D. Also since the field between A and B was 1250 volts/cm., the current measured was the saturation current for the gas, and was directly proportional to the number of ions formed between A and B.

In case (ii.) the currents measured by the electrometer represented the sum of the photo-electric and ionization effects, each giving its saturation current. Therefore, by subtracting the readings taken under conditions (i.) from the corresponding readings taken under conditions (ii.), it

was possible to obtain a measure of the pure photo-electric effects of the radiations.

The procedure while taking these observations was important, as on it depended the reliability of the results. It was as follows :—

(a) With the insulated quadrant of the electrometer earthed, and all the electrical connexions to C, D, B, and L broken, the discharge-tube was exhausted.

(b) The tube was flooded with the pure gas to the required pressure.

(c) The connexions to C, D, B, L were made and the discharge across EF was started, the current being adjusted to one milliampere.

(d) The pressure of the gas was observed.

(e) The electrometer quadrant was insulated, and the ionization current was read by noting the time taken by the image to move over 150 divisions on the scale.

(f) The quadrant was earthed and the pressure of the gas observed. The pressure at the time of reading the ionization current was the mean of the two observations.

(g) The discharge was stopped and the apparatus allowed to stand for 15 minutes.

This procedure was repeated with every observation of the current and pressure.

Hydrogen.—In fig. 2 below are given the curves obtained in hydrogen by the experiments just described. The ordinate represents in the case of curve (a) the ionization current, in the case of curve (b) the ionization current plus the photo-electric current. Curve (c) has been obtained by subtracting the ordinate of (a) from the ordinate of (b), and therefore represents the photo-electric current alone.

Nitrogen.—The corresponding curves for nitrogen are shown in fig. 3. Again (a), (b), (c) refer to ionization current, ionization current plus photo-electric current, and pure photo-electric current respectively. The scales in figs. 2 and 3 are the same, so that the relative effects in the two gases are shown directly.

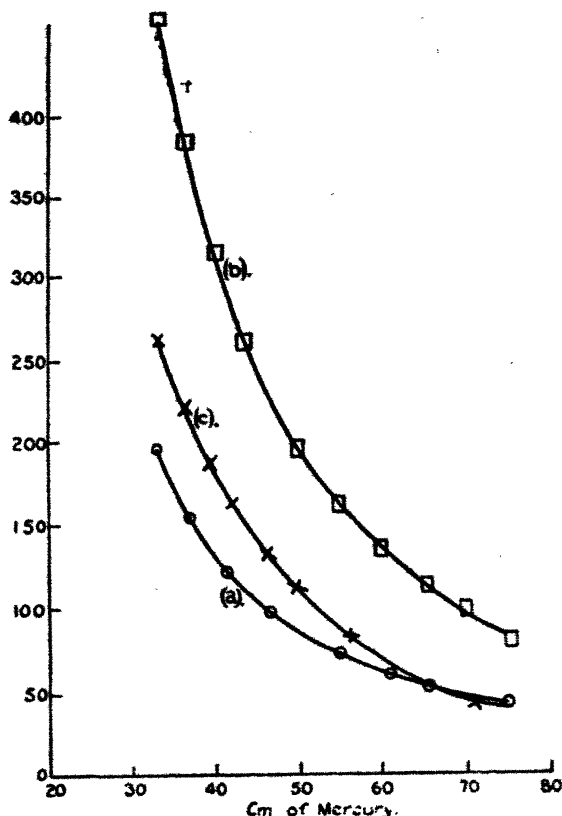
Variation of Ionization Current with Discharge Current.

The next experiments were performed to investigate how the ionization current at A varied with the current flowing between E and F, the pressure being kept constant. These observations were made in the same manner as those already described, viz. a new sample of gas was used at each reading, and the gas was kept at room temperature by allowing

a 15 minutes' pause after each observation. The results are indicated by the curves shown below (fig. 4), where the abscissa measures the current across EF in milliamperes, and the ordinate the ionization current in arbitrary units.

Curves (a) and (b) refer to nitrogen, (a) being taken at a pressure of 25 cm. of mercury and (b) at a pressure of

Fig. 2.



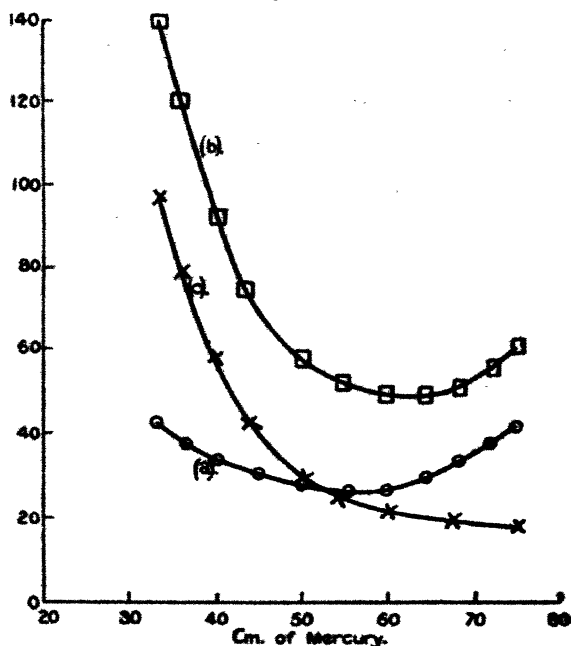
33 cm. Curves (c) and (d) refer to hydrogen. (c) was taken at 37 cm. and (d) at 48 cm. All these curves were obtained with the gauze system charged to -250 volts so that no photo-electric effect could take place.

Variation of Peak Potential across EF with Pressure.

The arrangement used for determining the peak potential across the discharge-tube was a spark-gap placed in parallel with the discharge. The electrodes of the gap were

zinc spheres of diameter 2.5 cm., carefully cleaned with fine emery-paper. The discharge across EF was maintained at one milliampere and the pressure of the gas was observed. Then the spark-gap was slowly closed until a spark just passed. The pressure of the gas was again observed and the discharge stopped. The parallel gap was measured to .005 cm. by means of a reading microscope. The pressure of the gas was the mean of the two readings taken. The results for this series of observations in nitrogen and

Fig. 3.



hydrogen are shown below (fig. 5), where the ordinate represents the peak potential across the gap in kilovolts, and the abscissa the pressure in cm. of mercury.

Discussion of Experimental Results.

The Ionizing Potentials of Hydrogen.—The ultra-violet spark spectra of hydrogen are well known. Under different conditions the gas emits two line spectra, stretching from 1670 to 900 A.U., and two continuous spectra. There is still considerable doubt as to the lowest ionizing potential of the gas. Many observers record ionization occurring at a

Fig. 4.

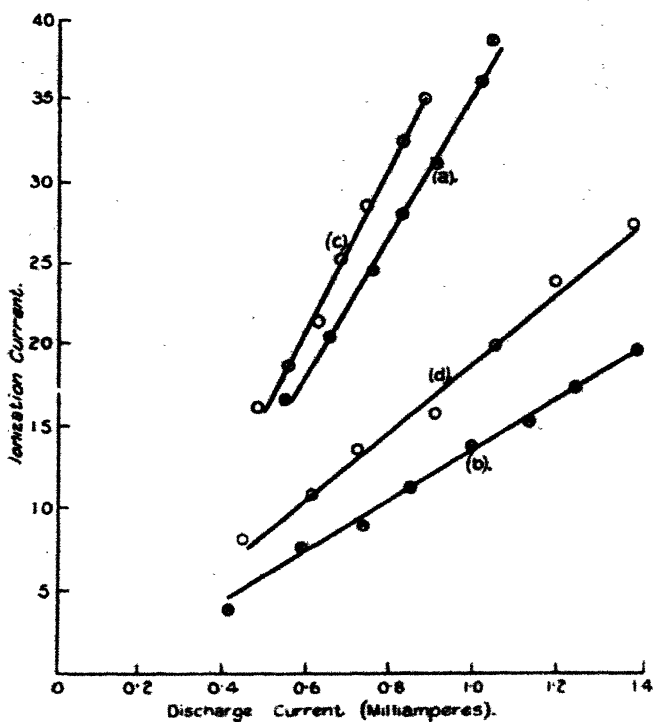
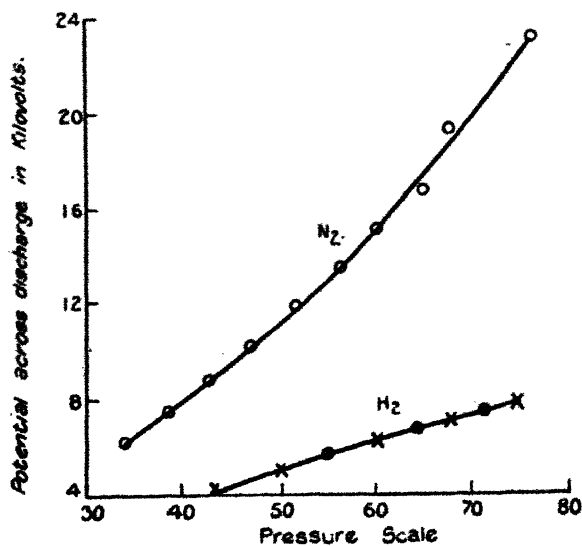


Fig. 5.



potential of 11 volts, but this value has been questioned by Horton and Davies*, who suggest that it is due to the presence of mercury vapour in the apparatus. The most generally accepted lowest value is 16 volts, which is said to correspond to the formation of H_1^+ and H_1^- from H_2 ; that is, to ionization plus dissociation. F. L. Mohler†, on the basis of his own experiments, concludes that "there is no evidence that hydrogen emits radiation which is capable of ionizing the normal molecule," and, as he points out, since no hydrogen lines have been observed beyond 885 A.U., this appears reasonable if the lowest ionizing potential is 16 volts. All the experiments performed in hydrogen and described in the present paper, however, indicate a strong ionization of the gas by its own radiations. Nor was this effect due to water-vapour content in the gas, for the same experiments were performed with identical results in gas which had been carefully dried. The water-vapour was only allowed to remain in the gas during the remainder of the experiments because it was found that it caused no perceptible alteration in any of the observations. Whether the observed ionization was due to the H_2 ion, or even to the H_1 ion, cannot be definitely stated. It seems improbable, however, that at pressures comparable with atmospheric such molecules should exist in sufficient numbers to account for the comparatively large currents which were measured. The conclusion suggested is that either hydrogen possesses a lower ionizing potential than the accepted one (16 volts), or the gas is capable of emitting radiations of shorter wavelength than those examined until the present. If the latter conclusion is correct, the radiations are molecular in origin, since the limit of the Lyman series, $N\left(\frac{1}{1^2} - \frac{1}{m^2}\right)$, which is the atomic radiation of greatest frequency, corresponds to a potential of 13.5 volts.

Variation of the Ionization Current with the Discharge Current, the Pressure being Constant.—The ordinates of the curves collected in fig. 4 measure the ionization currents at A. Since the pressure remained constant, and the currents measured were of saturation value, they may be taken to represent the intensities of the ionizing radiations. Therefore the curves show the variation of the intensity of the radiations with the current flowing between E and F. They indicate quite definitely that the intensity of these

* Phil. Mag. vol. xlv. p. 872 (1923).

† Proc. Nat. Acad. Sci. xii. p. 494 (1926).

radiations increases linearly with the discharge current. Therefore, if it is assumed that the mean frequency of the radiations does not change with change in the current density, it may immediately be stated that, since the potential across EF remains constant, *the pressure of the gas being constant, a constant fraction of the energy dissipated in the discharge (for the energies investigated) is transformed into ionizing electromagnetic radiation.*

Whether this remains true for very large or very small currents still remains to be investigated, but certain significant points emerge from a consideration of the curves already obtained. The gradients of the lines (a) and (c) are definitely greater than the gradients of the lines (b) and (d), while the curves, if produced, cut the discharge current axis at different points. The difference between the two sets of curves is that (a) and (c) were taken at a lower pressure than (b) and (d).

The fact that the gradients of the curves (a) and (c) are greater than the gradients of the curves (b) and (d) is suggestive. This means that, as the pressure diminishes, the same increase in the current density at E produces a larger increase in the radiations detected at A. This may be due to either or both of the following causes:—

(i.) Owing to the increase in the mean free paths of the gas ions with the decrease in the pressure, a greater percentage of the total number of ions carrying the current may excite radiation in the gas. If this is correct, the total intensity of the radiations at their source will increase as the pressure is diminished, a constant current being maintained across EF.

(ii.) The same change in the intensities of the radiations may occur at the source at all pressures, when the discharge current is changed by the same amount, but the change in the intensity at A will be smaller the higher the pressure, owing to the greater absorbing power of the gas.

No matter what the cause of these variations is, it is at least evident, as has been shown, that, for the currents investigated, $C = Li + M$, where C is the ionization current measured at A, and i is the current flowing across EF. L and M are constants when the pressure is constant, but L at least must be a function of the pressure, p . Taking the simplest assumption first, let

$$C = i\phi(p).$$

Then

$$\frac{\partial C}{\partial i} = \phi(p).$$

and therefore

$$\frac{\frac{\partial C}{\partial i}]_{p=p_1}}{\frac{\partial C}{\partial i}]_{p=p_2}} = \frac{\phi(p_1)}{\phi(p_2)} = \frac{C_1}{C_2}]_{i=\text{constant}} = \frac{m_1}{m_2},$$

where m_1 is the gradient of the line $C=i\phi(p_1)$, and m_2 is the gradient of the line $C=i\phi(p_2)$. But from the curves of figs. 2 and 3, $\frac{C_1}{C_2}$ may be determined. For the case of hydrogen $\frac{m_1}{m_2} = 2.9$, while $\frac{C_1}{C_2} = 1.7$ for corresponding pressures. Therefore C is not of the form $C=i\phi(p)$. The supposition that $C=(i-K)\phi(p)$ is no more tenable, for again

$$\frac{C_1}{C_2}]_{i=\text{constant}} = \frac{m_1}{m_2}.$$

It is therefore evident that the true form of the function must be

$$C = i\phi(p) - \psi(p). \quad . \quad . \quad . \quad (1)$$

Then

$$\frac{\partial C}{\partial i} = \phi(p)$$

and

$$\frac{m_1}{m_2} = \frac{C_1 + \psi(p_1)}{C_2 + \psi(p_2)}.$$

If

$$\psi(p_1) > \psi(p_2),$$

in general

$$\frac{m_1}{m_2} > \frac{C_1}{C_2}.$$

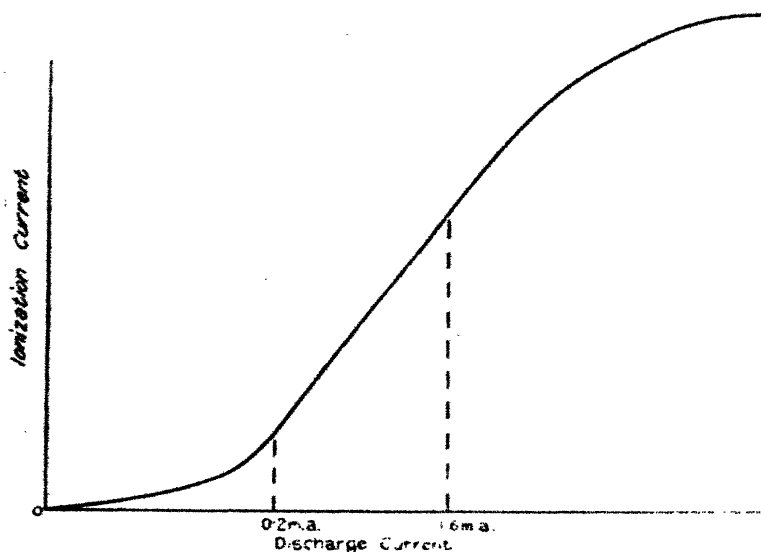
The graphs of fig. 4 indicate that $\psi(p_1) > \psi(p_2)$, and are therefore in agreement with this hypothesis. It may at this point be remarked that it is proposed in later work to evaluate $\psi(p)$ for many different values of p by observations similar to those shown in fig. 4. In this way it is hoped that the forms of both functions will be exhibited. Reasons will be given later which suggest that the form of $\frac{\phi(p)}{\psi(p)}$ should be interesting.

It must be observed that the theory which has just been given only applies to a limited range of discharge current (0.4 to 1.5 milliamperes). It is very improbable that the inear relation between C and i will hold for small currents;

as C would then be zero when $i = \frac{\psi(p)}{\phi(p)}$. Possibly the complete form of the C, i curve is as shown below in fig. 6.

Variation of Ionization and Photo-electric Currents with Pressure in Different Gases.—Figs. 2 and 3 represent the variation with pressure of the currents at A in hydrogen and nitrogen respectively. The pressures were varied from about 76 cm. of mercury to about 30 cm., as this region was the most difficult to investigate (owing to the small values of the currents) and at the same time the most interesting.

Fig. 6.



The curves in nitrogen are entirely different from those in hydrogen, except perhaps in the case of the curves giving the pure photo-electric effects, which are at least similar in form. The currents in hydrogen continually decrease with increase of pressure; both experimental curves in nitrogen exhibit a decided minimum at about 60 cm. of mercury.

As the problem of interpreting and, if possible, explaining these results is exceedingly complicated, it may be well to state at the outset in the most general terms the variables in the experiments. Broadly speaking, the variation with pressure of any radiations detected at A might be due to three factors, which are as follows:—

- (i.) Change in the total absorption of the gas between E and A.
- (ii.) Changes in the intensities of the radiations at their source E.
- (iii.) Changes in the frequencies of the radiations emitted at E.

Of these factors (i.) is likely to be of the greatest and (iii.) of the least importance, while (ii.) and (iii.) may be grouped together as changes in the character of the radiations from E.

Concerning the absorption of the gas between E and A, it is necessary to consider first how a monochromatic ultra-violet radiation of constant intensity I_λ at its source would vary in intensity at A as the pressure of the intervening gas is changed. It is well known that, for the visible spectrum and also for the X-ray region, the intensity at A might be represented by the expression $I_\lambda e^{-\alpha p}$, where p denotes the pressure of the gas, and α is a function of the frequency of the radiation. But for the region with which these experiments are concerned, namely that region producing intense ionization of the gas, this expression has not been verified; while for certain analogous cases concerned with the absorption of ultra-violet light by solutions, it is known that α is also a function of the concentration of the absorbing medium.

Let it be assumed, however, that the absorption of the radiation occurs according to the normal law. Let the loss of energy across a distance dx of the total distance EA be proportional to

- (i.) the intensity of the radiation at that point, I ;
- (ii.) the density of the gas at that point, ρ .

Also let the constant of proportionality (the absorption-coefficient) be a function of the wave-length of the light, $\phi(\lambda)$.

Then

$$dI = -\phi(\lambda)\rho I dx,$$

$$I = I_\lambda e^{-\phi(\lambda)kpx},$$

where $\rho = kp$.

But the ionization current C is proportional to the loss of energy, as the radiation passes through $2\frac{1}{2}$ mm. of the gas near A.

$$dI = -\phi(\lambda)kpI_\lambda e^{-\phi(\lambda)kpx} dx.$$

$$\therefore C = Kp\phi(\lambda)e^{-kpd\phi(\lambda)}, \dots \dots \dots (2)$$

where d is the distance EA.

Therefore, if the radiation from the vicinity of E were monochromatic, the current C would be a function of p of the form $C = ape^{-ap}$, having a maximum where $p = \frac{1}{a}$.

§. Needless to say, the radiations from A are not monochromatic, and the simple theory given above might be expected to be inapplicable to the experimental results on this ground alone. If, for example, the gas is supposed to emit a continuous spectrum, the absorption-coefficient in the above analysis will not take a mean value for the spectrum. As the pressure is diminished, the relative intensities at A of the different parts of the spectrum will vary, owing to the dependence of a upon λ . If the law of variation of spectrum intensity at the source is $I_\lambda = F(\lambda)$, then the intensity of the spectrum at A will be given by

$$I = F(\lambda)e^{-\phi(\lambda)kpd};$$

and if the spectrum is continuous between the limits $\lambda = \lambda_1$ and $\lambda = \lambda_2$ (analogous to an X-ray impulse spectrum* where the intensity at λ_2 is very small), the total effect at A in terms of ionization current is

$$C = K \int_{\lambda_1}^{\lambda_2} pF(\lambda)\phi(\lambda)e^{-kpd\phi(\lambda)}d\lambda. \quad (3)$$

Any attempts to evaluate $\phi(\lambda)$ and $F(\lambda)$ at this stage of the investigation must necessarily be purely hypothetical; but if it is assumed that the gas is a simple resonator of resonating wave-length λ_0 , then, where no damping coefficient is introduced,

$$\phi(\lambda) = \frac{N\lambda^4}{(\lambda^2 - \lambda_0^2)^2}.$$

Similarly, if it is assumed that the continuous spectrum is exactly analogous to the X-ray spectrum, beginning at $\lambda = \lambda_0$ and dying away towards $\lambda = 2\lambda_0$,

$$F(\lambda) = \frac{(2\lambda_0 - \lambda)(\lambda - \lambda_0)}{\lambda_0^2}$$

and

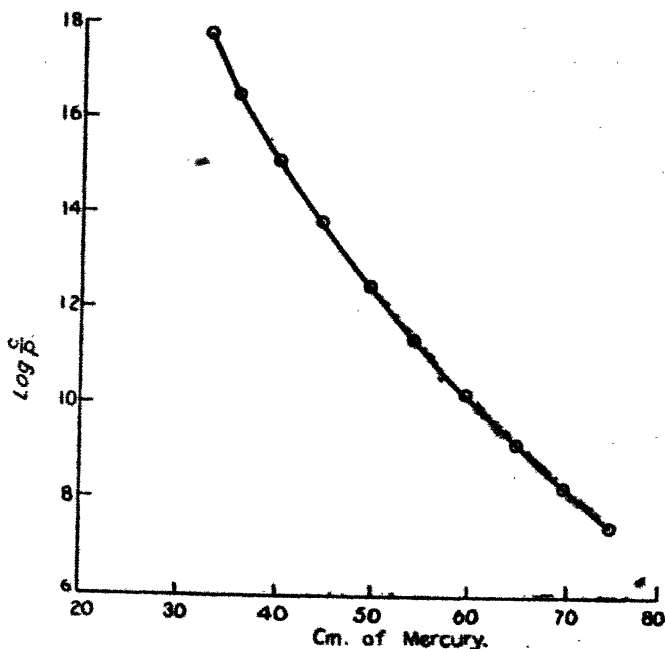
$$C = K \int_{\lambda_0}^{2\lambda_0} p \frac{(2\lambda_0 - \lambda)(\lambda - \lambda_0)\lambda^4}{\lambda_0^2(\lambda^2 - \lambda_0^2)^2} e^{-\frac{kpd\lambda^4}{(\lambda^2 - \lambda_0^2)^2}} d\lambda. \quad (4)$$

* C. T. Ulrey, *Phys. Rev.* ii. p. 401 (1918).

Neither equation (3) nor (4) can be used until more is known concerning the variables involved, and until they can be combined with the variations in intensity due to changes in the emissive power of the gas, for both are concerned wholly with absorption effects.

Qualitatively, however, the reduction of pressure might be expected by the above theory to increase the current C . Certainly no minimum is to be expected in the curve, although a maximum is predicted by equation (2) at a pressure probably much below those investigated in the

Fig. 7.



present experiments. The hydrogen curve (a) is not inconsistent with such a theory. The increase in the current with diminution of pressure is approximately according to the formula

$$C = Ape^{-\alpha p}, \quad \dots \dots (2)$$

a small but consistent increase in the coefficient α being evident. Fig. 7, below, exhibits the variation of $\log \frac{C}{p}$ with pressure for the curve (a) (fig. 2).

So far the variables (ii.) and (iii.) in the experiments have been neglected. The shape of curve (a) (fig. 2) has been examined wholly from the point of view of the absorption of the gas, and it has been implicitly assumed that the effects of variations in the intensities of the radiations at their source were negligible compared with the absorption effects. It now remains to be seen whether this assumption is justifiable or not.

Theoretically the reduction in pressure might be expected by increasing the mean free paths of the ions to increase the probability of excitation of the shorter wave radiations. On the other hand, the decrease in the potential necessary to carry the discharge which accompanied the decrease of pressure might cause a corresponding fall in the potential drops across the free paths of the ions. As the mean free path λ is inversely proportional to the pressure, and the potential, as shown from fig. 5, is approximately proportional to the pressure, the product $X\lambda$ might be expected to remain constant, on the assumption that the field X in the vicinity of E is proportional to the potential across EF. If, however, the field at E is that due to the normal cathode fall, and is independent of the pressure, the probability of radiation accompanying the impact of ions must be inversely proportional to the pressure. Again, if the radiations are due to the impact of ions on neutral molecules, another point must be considered. For a given ionic current the number of molecules in the gap EF and therefore the probability of radiation will be proportional to the pressure. If the radiations are due both to ionic and molecular collisions, the expression for the intensity at the source will be the sum of *two* functions of the pressure.

In the preceding investigation it was found that the current at A was given by equation (1) :

$$C = i\phi(p) - \psi(p), \dots \dots \dots (1)$$

where $\frac{d\psi}{dp}$ was negative. This indicates that an important

fraction of the radiation is due to the impact of ions on neutral molecules, since no other hypothesis could explain the existence of $\psi(p)$. If the simplest possible interpretation be given to the variation with pressure of the intensity I_λ of the radiations at their source

$$I_\lambda = Ai - \frac{B}{p}.$$

Then assuming the theory leading to equation (2),

$$C = (Aip - B)e^{-ap}$$

and $\phi(p) = Ape^{-ap}$, $\psi(p) = Be^{-ap}$.

No matter what functions of p are used in the expression for I_λ , since $C = pI_\lambda e^{-ap}$, it is quite reasonable to assume that the absorption term e^{-ap} will be the most important; this explains why the absorption effects could be considered alone in the case of hydrogen.

To return to the absorption of the radiations, in the case of curve (a) for nitrogen, the theory which has been sketched does not apply. The absorption of nitrogen cannot follow the simple laws which appeared to fit the case of hydrogen, or else the quality of the radiations from the discharge must vary with the pressure in a peculiar manner. It has certainly been observed that the visible radiations from the discharge in hydrogen are entirely different from those in nitrogen. The greater part of the spark in hydrogen is blue in colour, *and its colour does not alter as the pressure is diminished*. The spark in nitrogen at atmospheric pressure emits radiations of all colours, and consequently appears white, *but as the pressure is reduced the discharge becomes almost entirely red*. This may mean a shift of the maximum intensity of the radiations towards the red end of the spectrum; it may mean that the absorption of the gas has changed in such a way as to cut off the blue light. Neither explanation appears probable, but either is consistent with the curves (a) and (b) of fig. 3.

That the maximum intensity of the radiations should shift towards the red end of the spectrum as the pressure is diminished is contrary to the results obtained by L. Hamburger*, who found that for the visible spectrum the maximum of the emitted light from nitrogen shifted towards the ultra-violet as the pressure was diminished. His experiments were, however, performed at a very much lower pressure than those described in the present communication. It must also be observed that the curve (c) (fig. 3), which gives the variation with pressure of the intensities of the radiations producing the photo-electric effects at A, exhibits no minimum. Although the curve is not by any means exponential, there is a steady increase in the intensity as the pressure is reduced. This difference between the ionization-current

* K. Akad. Amsterdam, xx. Proc. 7, p. 1043 (1918).

curve and the photo-electric current curve must be significant. It indicates that if the anomalous variation in curve (c) is due to absorption, the anomalous absorption affects only the shorter wave radiations, and then it is difficult to see why the appearance of the discharge should alter as the pressure is reduced. On the other hand, it agrees well with the hypothesis that the maximum intensity of the radiations moves towards the infra-red, for then the photo-electric effect, being due to radiations of longer average wave-length than those causing the ionization effects, would suffer little change. On the whole, the evidence indicates that the difference between the curves for nitrogen and hydrogen is not due to the gases obeying different absorption laws, but is due rather to the difference between the modes of variation with pressure of the radiations emitted by the gases.

Summary.

Preliminary experiments are described showing :—

1. The variation with pressure of the ionizing and photo-electric radiations from hydrogen and nitrogen when the gases are excited by a discharge.
2. The variation of the intensity of these radiations when the pressure is kept constant and the discharge current is varied.

The curves obtained depend upon both absorption and emission variations, and an attempt is made to estimate the relative importance of the two effects, and so to separate them. Tentative explanations are offered of the various phenomena, and it will be a matter for further investigation to decide between them.

Reasons are put forward suggesting that the radiations are molecular in origin.

A spontaneous ionization phenomenon in oxygen is described and an explanation is offered.

In conclusion, the writer again wishes to express his thanks to Professor Taylor Jones for his encouragement and advice, which have proved invaluable. The work was performed in the Research Laboratories of the Natural Philosophy Department of the University of Glasgow.

LII. Mathieu Functions of Stable Type.

By E. L. INCE, M.A., D.Sc.*

1. Introduction.

THE general solution of the Mathieu equation †,

$$\frac{d^2y}{dx^2} + (\eta - 2\theta \cos 2x)y = 0, \quad \dots \quad (1)$$

is known from theoretical considerations to be of the form

$$y = Ae^{\mu x}\phi(x) + Be^{-\mu x}\phi(-x), \quad \dots \quad (2)$$

where $\phi(x)$ has the period π . The two main problems which arise are (a) the determination of η , for a given θ , such that the equation shall have a solution of assigned periodicity, and (b) the determination of μ when η and θ are given. The first problem has been solved by the present writer ‡, and tables of the functions of periods π and 2π will in due course be available. The second problem will now be considered.

When μ is a pure imaginary, the solution is said to be *stable*; otherwise it is *unstable*. When θ is zero, a stable solution exists for every positive value of η , but as θ increases, the probability that a solution with η chosen at random shall be stable diminishes rapidly. This is shown very clearly in fig. 1. The curves $a_0, b_1, a_1, b_2, \dots$ represent the determinations of η corresponding to the elliptic cylinder functions $ce_0(x), se_1(x), ce_1(x), se_2(x), \dots$. The regions between a_0 and b_1 , between a_1 and b_2 , and so on, for θ positive, and the symmetrical regions for θ negative, are the regions of stability, and since the bounding curves tend rapidly to coincidence, the above statement is justified. The diagram furnishes a rough guide as to whether the solution corresponding to any value-pair (θ, η) is stable or not. Naturally, in physical problems the stable solutions are the more interesting.

Several methods of determining the index μ have been

* Communicated by the Author.

† This form of the Mathieu equation differs slightly from the form generally in vogue, but it has been adopted as the standard in the computation of the elliptic cylinder functions which is now in progress. In the majority of physical applications η is positive.

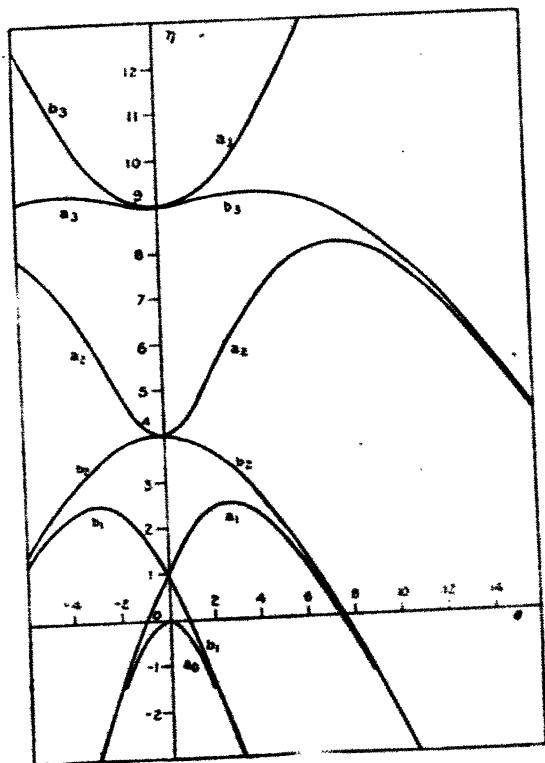
‡ Proc. Roy. Soc. Edin. xlv. pp. 20-29, 316-322 (1925-26); xlvii. pp. 294-301 (1927).

devised ; the latest is that due to Whittaker *. The essential point of his method is to express η and μ in the forms

$$\eta = F(\sigma), \quad \mu = G(\sigma),$$

where $F(\sigma)$ and $G(\sigma)$ are respectively even and odd Fourier series in σ whose coefficients depend only on θ . The first equation is solved numerically for σ ; the second then gives

Fig. 1.



μ immediately. This method is of practical value, and has, in fact, been applied to G. W. Hill's classical problem in the lunar theory. The numerical work is, however, laborious, and is complicated by the fact that in the stable case σ is either purely imaginary or a complex number of the form $\frac{1}{2}\pi + \pi i$. For that reason the following method is to be preferred in practice whenever the solution is known to be stable

* Proc. Edin. Math. Soc. xxxii. pp. 75-80 (1914).

2. The General Solution.

The Mathieu equation is satisfied by a solution of the form

$$y = \sum_{-\infty}^{\infty} e_r \cos(2r + \rho)x, \quad \dots \quad (3)$$

provided that the coefficients e_r satisfy the recurrence-relations

$$\{\eta - (2r + \rho)^2\}e_r = \theta(e_{r-1} + e_{r+1}) \quad \dots \quad (4)$$

for all integral values of r , and provided that these relations are consistent. There is evidently no loss of generality in assuming that $0 \leq R(\rho) \leq 1$, where $R(\rho)$ denotes the real part of ρ . When the solution is stable, ρ is real.

Equation (1) is unchanged if x is replaced by $\pi - x$. Consequently, when the solution (3) exists, there also exists the solution

$$\begin{aligned} y &= \sum_{-\infty}^{\infty} e_r \cos(2r + \rho)(\pi - x) \\ &= \cos \rho \pi \sum_{-\infty}^{\infty} e_r \cos(2r + \rho)x + \sin \rho \pi \sum_{-\infty}^{\infty} e_r \sin(2r + \rho)x, \end{aligned}$$

which is distinct from (3) except when ρ is an integer or zero.

With these exceptions, therefore, there is always associated with (3) the solution

$$y = \sum_{-\infty}^{\infty} e_r \sin(2r + \rho)x. \quad \dots \quad (5)$$

Conversely (3) is associated with (5) except when ρ is an integer or zero. These solutions are evidently distinct and form a fundamental pair. Thus, setting aside the special cases which arise when ρ is an integer or zero, equation (1) has a general solution of the form

$$y = A \sum_{-\infty}^{\infty} e_r \cos(2r + \rho)x + B \sum_{-\infty}^{\infty} e_r \sin(2r + \rho)x,$$

which is not essentially different from (2). The number ρ is determined by the condition that the recurrence-relations be consistent.

If $\rho = 1$, the recurrence formula for $r = n$ is the same as that for $r = -n - 1$, and it is an easy matter* to prove that

* Express e_{-1}/e_0 as a continued fraction in two distinct ways as in the following section; this shows that $e_{-1} = \pm e_0$, and the rest follows immediately.

$e_{-r-1} = \pm e_r$. If $e_{-r-1} = e_r$, then (5) becomes identically zero, and (3) may be written

$$y = \sum_0^{\infty} c_r \cos (2r+1)x,$$

where $c_r = 2e_r$. For $r \geq 1$, c_r follows the same recurrence-relation as e_r , but for $r=0$ the relation becomes

$$(\eta - \theta - 1)c_0 = \theta c_1.$$

The solution is thus a multiple of an elliptic cylinder function of the type $ce_{2m+1}(x, \theta)$. If $e_{-r-1} = -e_r$, (3) becomes identically zero, and (5) may be written

$$y = \sum_0^{\infty} c'_r \sin (2r+1)x,$$

where $c'_r = 2e_r$. The recurrence-relation for c'_r is the same as that for c_r when $r \geq 1$, but when $r=0$ it becomes

$$(\eta + \theta - 1)c'_0 = \theta c'_1.$$

Thus the solution is a multiple of an elliptic cylinder function of the type $se_{2m+1}(x, \theta)$. The case $\rho=1$ virtually includes the case where ρ is any odd integer.

If $\rho=0$, the recurrence-relation for $r=n$ is the same as that for $r=-n$, and it is easily proved that $e_{-r} = \pm e_r$. If $e_{-r} = e_r = \frac{1}{2}c_r$, (5) becomes identically zero and (3) may be written

$$y = \frac{1}{2}c_0 + \sum_1^{\infty} c_r \cos 2rx.$$

For $r \geq 1$, c_r follows the same recurrence-relation as e_r , but for $r=0$ the relation becomes

$$\eta c_0 = 2\theta c_1.$$

The solution is thus a multiple of an elliptic cylinder function of type $ce_{2m}(x, \theta)$. Similarly, if $e_r = -e_{-r} = \frac{1}{2}c'_r$, (3) disappears and (5) may be written

$$y = \sum_1^{\infty} c'_r \sin 2rx.$$

For $r \geq 1$ the recurrence-relation is as before, but with $c'_0 = 0$. The solution is thus a multiple of an elliptic cylinder function of type $se_{2m}(x, \theta)$. The case $\rho=0$ virtually includes the case where ρ is an even integer.

It is clear that in the general case $\sum e_r \neq 0$, for if the contrary were true, then both (3) and its first derivative would vanish for $x=0$, which is impossible since the origin is an ordinary point of equation (1). Thus, if necessary, the solutions (3) and (5) may be made definite by the assumption $\sum e_r = 1$.

3. The Conditions for Consistence.

The recurrence-relation (4) may be written in the form

$$\begin{aligned} \frac{e_r}{e_{r-1}} &= \frac{\theta}{\eta - (2r + \rho)^2 - \theta \frac{e_{r+1}}{e_r}} \\ &= \frac{-\theta(2r + \rho)^{-2}}{1 - \eta(2r + \rho)^{-2} + \theta(2r + \rho)^{-2} \frac{e_{r+1}}{e_r}}, \end{aligned}$$

and may consequently be expressed as an infinite continued fraction depending upon r , ρ , θ , and η . It will be useful to have a compact notation for an infinite continued fraction whose successive partial quotients are determined by a definite law; let

$$\Phi_n \frac{\alpha_r}{\beta_r}$$

represent the continued fraction *

$$\frac{1}{\beta_n} + \frac{\alpha_{n+1}}{\beta_{n+1}} + \frac{\alpha_{n+2}}{\beta_{n+2}} + \dots$$

Consequently

$$\left. \begin{aligned} \frac{e_n}{e_{n-1}} &= -\theta(2n + \rho)^{-2} \Phi_n \frac{-\theta^2(2r + \rho)^{-2}(2r + \rho - 2)^{-2}}{1 - \eta(2r + \rho)^{-2}} \\ &= -\theta(2n + \rho)^{-2} \Phi_n \frac{-\theta^2(2r + 2n + \rho)^{-2}(2r + 2n + \rho - 2)^{-2}}{1 - \eta(2r + 2n + \rho)^{-2}} \end{aligned} \right\} \dots (6)$$

But the recurrence-relation may also be written as

$$\begin{aligned} \frac{e_{r-1}}{e_r} &= \frac{\theta}{\eta - (2r + \rho - 2)^2 - \theta \frac{e_{r-2}}{e_{r-1}}} \\ &= -\frac{\theta(2r + \rho - 2)^{-2}}{1 - \eta(2r + \rho - 2)^{-2} + \theta(2r + \rho - 2)^{-2} \frac{e_{r-2}}{e_{r-1}}}, \end{aligned}$$

and consequently

$$\frac{e_{n-1}}{e_n} = -\theta(2n + \rho - 2)^{-2} \Phi_n \frac{-\theta^2(2n - 2r + \rho)^{-2}(2n - 2r + \rho + 2)^{-2}}{1 - \eta(2n - 2r + \rho)^{-2}} \dots (7)$$

Note that the leading numerator is unity. Note also that

$$\Phi_n \frac{\alpha_r}{\beta_r} = k_n \Phi_n \frac{k_r \alpha_r}{k_r \beta_r},$$

if both members converge.

The last equation may be transformed by the relation

$$\frac{e_n}{e_{n-1}} = \frac{\eta - (2n + \rho - 2)^2}{\theta} - \frac{e_{n-2}}{e_{n-1}}$$

into

$$\frac{e_n}{e_{n-1}} = \frac{\eta - (2n + \rho - 2)^2}{\theta} + \theta(2n + \rho - 1)^{-2} \frac{\Phi_2 - \theta^2(2n - 2r + \rho)^{-2}(2n - 2r + \rho + 2)^{-2}}{1 - \eta(2n - 2r + \rho)^{-2}} \quad (8)$$

When θ , η , n , and ρ are finite,

$$\alpha_r \rightarrow 0, \quad \beta_r \rightarrow 1$$

in each continued fraction, therefore each continued fraction converges; moreover, as n increases, each tends to the limit unity*.

The condition for the consistence of the recurrence-relations is that (6) and (8) should give equal values to e_n/e_{n-1} . In particular, when $n=1$, let

$$L = -\frac{e_1}{e_0} = \frac{\theta}{(\rho+2)^2} \frac{\Phi_0 - \theta^2(2r+\rho+2)^{-2}(2r+\rho)^{-2}}{1 - \eta(2r+\rho+2)^{-2}},$$

$$R = -\frac{e_1}{e_0} = \frac{\rho^2 - \eta}{\theta} - \frac{\theta}{(\rho-2)^2} \frac{\Phi_2 - \theta^2(2r-\rho-2)^{-2}(2r-\rho-4)^{-2}}{1 - \eta(2r-\rho-2)^{-2}}.$$

Then the condition of consistence is $L=R$.

In order to apply this condition in any particular case when θ and η are given, tentative values of ρ are inserted in the continued fractions, and L and R are calculated. The result indicates how ρ is to be adjusted to secure numerical equality between L and R . When this end has been attained, not only has the value of ρ been obtained to the desired degree of precision, but material has been accumulated from which the ratios of consecutive coefficients in the expansion of the solution may easily be deduced. How the method is carried out in practice will be shown in the following section.

4. Numerical Example.

When the use of the Mathieu functions becomes more general than it is in the present day, it will be necessary to have at hand tables showing the value of ρ for outstanding values of θ and η . These tables would indicate a suitable initial value of ρ , for any assigned value-pair (θ, η) , on

* Perron, 'Die Lehre von den Kettenbrüchen,' § 56.

which the accurate calculation of ρ would be based. As things are at present, every value of ρ must be calculated *ab initio*.

As an example of the method, consider the data

$$\theta = 2, \quad \eta = 3.$$

Fig. 1 shows that this value-pair lies in a region of stability. For any assumed value of ρ , L is calculated according to the following scheme :

$$\begin{array}{cccc} & \frac{\theta}{(\rho+4)^2} & \frac{\theta}{(\rho+6)^2} & \frac{\theta}{(\rho+8)^2} \dots\dots, \\ \frac{\theta}{(\rho+2)^2} & \frac{\theta}{(\rho+2)^2} \cdot \frac{\theta}{(\rho+4)^2} & \frac{\theta}{(\rho+4)^2} \cdot \frac{\theta}{(\rho+6)^2} & \frac{\theta}{(\rho+6)^2} \cdot \frac{\theta}{(\rho+8)^2} \dots\dots, \\ 1 - \frac{\eta}{(\rho+2)^2} & 1 - \frac{\eta}{(\rho+4)^2} & 1 - \frac{\eta}{(\rho+6)^2} & 1 - \frac{\eta}{(\rho+8)^2} \dots\dots, \\ \gamma_1 & \gamma_2 & \gamma_3 & \gamma_4 \dots\dots, \\ \phi_1 & \phi_2 & \phi_3 & \phi_4 \dots\dots, \end{array}$$

where

$$\gamma_r = \frac{\theta^2}{(\rho+2r)^2(\rho+2r+2)^2} \div \phi_{r+1},$$

$$\phi_r = 1 - \frac{\eta}{(\rho+2r)^2} - \gamma_r,$$

and finally

$$L = \frac{\theta}{(\rho+2)^2} + \phi_1.$$

The number of significant figures required diminishes as the scheme proceeds to the right. The scheme stops at the n th column if γ_n does not affect the last figure in that column. Similarly R is calculated according to the similar scheme :

$$\begin{array}{cccc} & \frac{\theta}{(\rho-4)^2} & \frac{\theta}{(\rho-6)^2} & \frac{\theta}{(\rho-8)^2} \dots\dots, \\ \frac{\theta}{(\rho-2)^2} & \frac{\theta}{(\rho-2)^2} \cdot \frac{\theta}{(\rho-4)^2} & \frac{\theta}{(\rho-4)^2} \cdot \frac{\theta}{(\rho-6)^2} & \frac{\theta}{(\rho-6)^2} \cdot \frac{\theta}{(\rho-8)^2} \dots\dots, \\ 1 - \frac{\eta}{(\rho-2)^2} & 1 - \frac{\eta}{(\rho-4)^2} & 1 - \frac{\eta}{(\rho-6)^2} & 1 - \frac{\eta}{(\rho-8)^2} \dots\dots, \\ \gamma_{-1} & \gamma_{-2} & \gamma_{-3} & \gamma_{-4} \dots\dots, \\ \phi_{-1} & \phi_{-2} & \phi_{-3} & \phi_{-4} \dots\dots, \end{array}$$

where

$$\gamma_{-r} = \frac{\theta^2}{(\rho - 2r)^2(\rho - 2r - 2)^2} \div \phi_{-r-1},$$

$$\phi_{-r} = 1 - \frac{\eta}{(\rho - 2r)^2} - \gamma_{-r},$$

and finally

$$R = \frac{\rho^2 - \eta}{\theta} - \frac{\theta}{(\rho - 2)^2} \div \phi_{-1}.$$

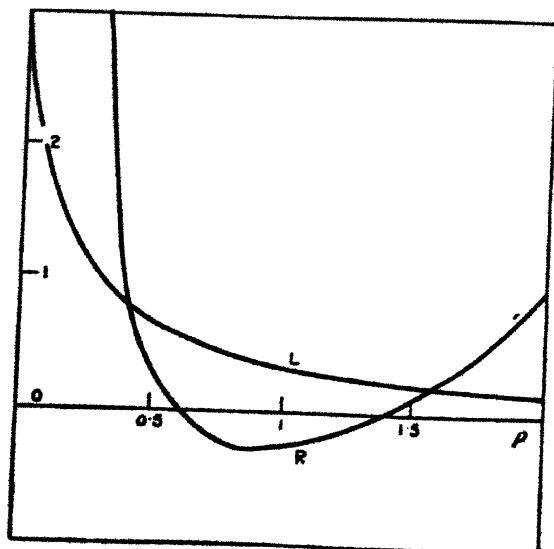
The method of procedure is as before.

As there was no indication as to the correct value of ρ , the following table was constructed :

ρ .	L.	R.
0.00	2.9010	-5.4011
0.25	1.1142	+5.1212
0.50	0.6630	+0.3065
0.75	0.4190	-0.2077
1.00	0.3438	-0.2559
1.25	0.2703	-0.1227
1.50	0.2197	+0.1157
1.75	0.1830	+0.4184
2.00	0.1553	+0.9457

The variation of L and R is illustrated in fig. 2.

Fig. 2.



Thus in the range considered there are two admissible values of ρ , whose sum is 2. The higher value is chosen to work with because the curves are flatter, and therefore interpolation is easier in its neighbourhood than in the neighbourhood of the other value.

By linear interpolation between $\rho=1.50$ and $\rho=1.75$ the value $\rho=1.5766$ is obtained. This gives

$$\rho=1.5766, \quad L=0.2072688, \quad R=0.2034813.$$

A second linear interpolation between $\rho=1.50$ and this value gives $\rho=1.5794$, leading to

$$\rho=1.5794, \quad L=0.2068352, \quad R=0.2067923.$$

Hence, if Δ denotes difference in the seventh decimal-place

$$\Delta\rho=28000, \quad \Delta L=-4336, \quad \Delta R=+33110.$$

Thus a more correct value of ρ is

$$\begin{aligned} \rho &= 1.5794 + \frac{L-R}{\Delta R - \Delta L} \Delta\rho \\ &= 1.579432. \end{aligned}$$

It has been remarked that the scheme of working gives not only the value of ρ to any desired degree of precision, but also the coefficients in the expansion of the solution. For this reason the figures in the scheme with the new value $\rho=1.579432$ will be given in full. The scheme for L reads as follows :

156099712	06424658	03481422	0217947	01492
765850432	01002887	00223670	0007588	000325
11127511	90363013	9477787	967302	9776
	236180	7847	333	—
754722921	90126824	9469940	966975	9776

$$L = 0.20683049.$$

The scheme for R is :

11.30728434	341346474	102346702	04861578	0282063	0184
15.96089651	3.85919481	034935685	00496543	0013685	00052
8.64539056	487980280	84647995	9272263	95769	972
	41534893	536341	14298	53	—
24.00628707	446445396	84111654	9257965	95716	972

$$\frac{\rho^2 - \eta}{\theta} = -0.25269728$$

$$-\frac{\theta}{(\rho - \eta)^2} + \phi_{-1} = 0.45952745$$

$$R = 0.20683017$$

Since L and R agree to the sixth place, ρ is correct to within a unit in the sixth place. A more precise value of ρ is

$$\begin{aligned}\rho &= 1.579432 + (L-R) \frac{\Delta\rho}{\Delta R - \Delta L} \\ &= 1.579432 + .00000032. \\ &= 1.57943227.\end{aligned}$$

The complementary value is

$$\rho = 0.42056773.$$

5. Determination of the Coefficients.

The coefficients will now be determined to six-place accuracy. Let $e_0 = 1$, then

$$\begin{aligned}e_1 &= -0.206830; \\ \frac{e_2}{e_1} &= -\frac{\theta}{(\rho+4)^2} \div \phi_1 = -\frac{.0642466}{.901268} = -0.0712846, \\ e_2 &= +0.014744; \\ \frac{e_3}{e_2} &= -\frac{\theta}{(\rho+6)^2} \div \phi_2 = -\frac{.034814}{.94699} = -0.036763, \\ e_3 &= -0.000542; \\ \frac{e_4}{e_3} &= -\frac{\theta}{(\rho+8)^2} \div \phi_3 = -\frac{.0218}{.967} = -0.0225, \\ e_4 &= +0.000012.\end{aligned}$$

Similarly

$$\begin{aligned}\frac{e_{-1}}{e_0} &= -\frac{\theta}{(2-\rho)^2} \div \phi_{-1} = -\frac{11.307264}{24.606287} = +0.459527, \\ e_{-1} &= +0.459527; \\ \frac{e_{-2}}{e_{-1}} &= -\frac{\theta}{(4-\rho)^2} \div \phi_{-2} = -\frac{.3413465}{.4464454} = -0.7645873, \\ e_{-2} &= -0.351349; \\ \frac{e_{-3}}{e_{-2}} &= -\frac{\theta}{(6-\rho)^2} \div \phi_{-3} = -\frac{.102347}{.841117} = -0.121680, \\ e_{-3} &= +0.042752;\end{aligned}$$

$$\frac{e_{-4}}{e_{-3}} = -\frac{\theta}{(8-\rho)^2} \div \phi_{-4} = -\frac{0.048516}{0.92580} = -0.052404,$$

$$e_{-4} = -0.002240;$$

$$\frac{e_{-5}}{e_{-4}} = -\frac{\rho}{(10-\rho)^2} \div \phi_{-5} = -\frac{0.02821}{0.9572} = -0.0295,$$

$$e_{-5} = +0.000066;$$

$$\frac{e_{-6}}{e_{-5}} = -\frac{\theta}{(12-\rho)^2} \div \phi_{-6} = -\frac{0.0184}{0.972} = -0.019,$$

$$e_{-6} = -0.000001.$$

The first solution of the Mathieu equation,

$$\frac{d^2y}{dx^2} + (3 - 4 \cos 2x)y = 0,$$

is therefore to six-place accuracy :

$$\begin{aligned} y = & \cos 1.579432x - 0.206830 \cos 3.579432x \\ & + 0.014744 \cos 5.579432x - 0.000542 \cos 7.579432x \\ & + 0.000012 \cos 9.579432x \\ & + 0.459527 \cos 0.420568x - 0.351349 \cos 2.420568x \\ & + 0.042752 \cos 4.420568x - 0.002240 \cos 6.420568x \\ & + 0.000066 \cos 8.420568x - 0.000001 \cos 10.420568x. \end{aligned}$$

The second solution is obtained by merely writing sine for cosine throughout.

6. Change of Sign of θ .

Fig. 1 is symmetrical about the η -axis, though it should be noted that in the negative half of the plane a_{2m+1} and b_{2m+1} are interchanged. Consequently, if the number-pair (θ, η) gives stability, so also does the number-pair $(-\theta, \eta)$. The Mathieu equation is unaltered if θ is replaced by $-\theta$ and x by $\frac{1}{2}\pi - x$, so if

$$y = A \sum_{-\infty}^{\infty} e_r \cos (2r + \rho)x + B \sum_{-\infty}^{\infty} e_r \sin (2r + \rho)x$$

is the general solution of (1), then the general solution of

$$\frac{d^2y}{dx^2} + (\eta + 2\theta \cos 2x)y = 0$$

is

$$y = A \sum_{-\infty}^{\infty} e_r \cos(2r + \rho)(\tfrac{1}{2}\pi - x) + B \sum_{-\infty}^{\infty} e_r \sin(2r + \rho)(\tfrac{1}{2}\pi - x) \\ = A_1 \sum_{-\infty}^{\infty} (-)^r e_r \cos(2r + \rho)x + B_1 \sum_{-\infty}^{\infty} (-)^r e_r \sin(2r + \rho)x,$$

where

$$A_1 = A \cos \tfrac{1}{2}\rho\pi + B \sin \tfrac{1}{2}\rho\pi, \quad B_1 = A \sin \tfrac{1}{2}\rho\pi - B \cos \tfrac{1}{2}\rho\pi.$$

Thus in general the only change in the fundamental solutions is a change in sign of the coefficients of odd rank. As before, the only exceptions arise when ρ is an integer or zero, in which cases A or B , and consequently A_1 or B_1 , are zero.

LIII. *On the Zeeman Resolution of the Oxygen Spectral Line at $\lambda 5577 \text{ \AA}$, the Auroral Green Line.* By Prof. J. C. McLENNAN, F.R.S., J. H. McLEOD, M.A.*, and RICHARD RUEDY, Ph.D.†

[Plate VI.]

IN previous publications⁽¹⁾ it has been shown that the green spectral line of the aurora and of the light of the night sky originates in oxygen in the atomic form in the upper atmosphere. A problem still outstanding is to determine just what electronic transition represented in the spectral scheme for oxygen is responsible for the production of this radiation at $\lambda 5577 \text{ \AA}$. A careful search for other spectral lines that might be associated with the green line has up to the present failed to elucidate the problem. A powerful method of classifying spectral lines is found in the character of the resolution experienced by the lines when the radiation giving rise to them is emitted by atoms in the presence of a magnetic field.

In 1927 McLennan, McLeod, and McQuarrie⁽²⁾ reported some visual observations on the Zeeman resolution of the oxygen green line in which it was seen that, viewed longitudinally, the green line was resolved into a doublet, the amount of whose separation appeared to be the same as that of the two outer components of a normal triplet.

* J. H. McLeod wishes to acknowledge his indebtedness to the Research Council of Canada for the grant of a Fellowship that enabled him to participate in this work.

† Communicated by the Authors.

The present paper deals with a more exact determination of the longitudinal Zeeman effect of the oxygen green line.

The necessary magnetic field was provided by a water-cooled solenoid shown diagrammatically in fig. 1. The coil was wound on a brass tube as shown, and consisted of ten layers of No. 16 B. & S. gauge enamelled single silk-covered copper wire. The layers were separated from each other by ebonite strips F each $\frac{3}{8}$ inch in thickness by $\frac{1}{8}$ inch in width, laid parallel to the axis of the coil and about 1 cm. from each other. These strips provided a series of open spaces running longitudinally to the coil between each layer of wire. The ebonite end-pieces B were perforated with many small holes to provide openings at each end of the spaces between the layers of the coil. When the coil was in operation tap water was forced through the spaces from one end of the coil to the other, so that every wire was bathed by flowing water. This method of cooling made it possible to pass a current of 30 amperes through the windings continuously, with a rise in temperature of the cooling water of only 9 or 10 degrees.

The length of the solenoid was 35 cm. and the total number of turns was 2390. The calculated field then for 30 amperes was 2620 gauss. Too much reliability should not be placed on this calculated value of the field for it could be that some current might leak through small cracks in the insulating enamel and so reduce the value of the field.

A comparison of the strength of the magnetic field at different points throughout the coil was made by means of a small search coil and a ballistic galvanometer. Fig 2 shows the graph obtained when deflexions of the galvanometer (proportional to the field strength) were plotted against distance through the solenoid. It is seen that for a distance of nearly 25 cm. in the central portion of the coil the field was within a few per cent. of being uniform. It was light emitted in the central portion of the solenoid that was used in the determination of the magnetic resolution of the green line.

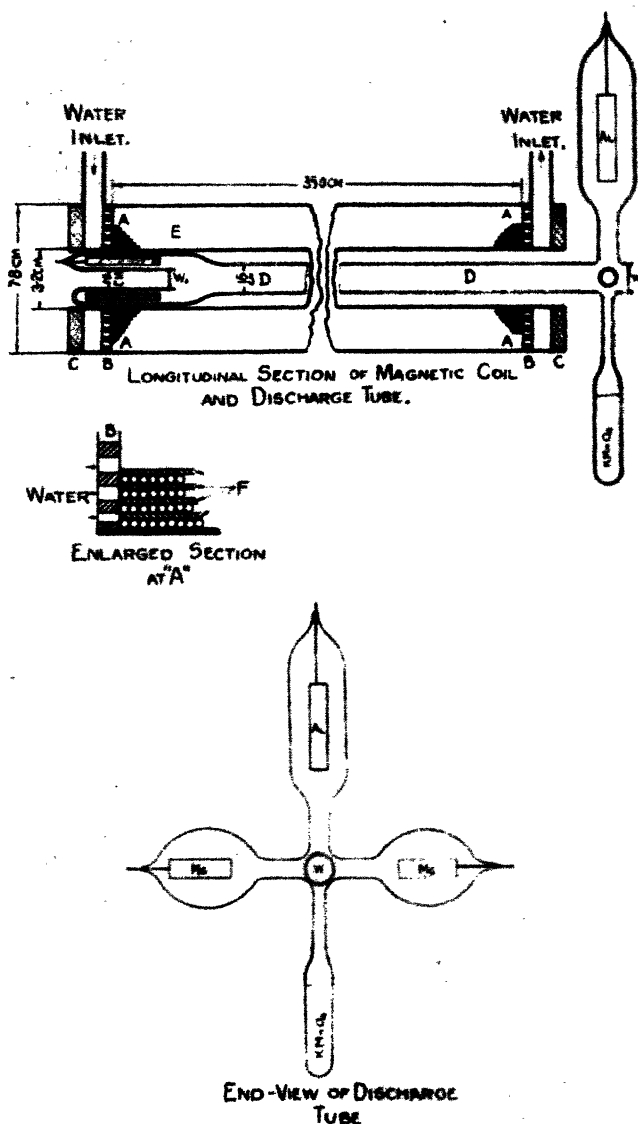
The green line radiation was produced in a tube containing a mixture of argon and oxygen. A current of about 30 m.a. from a 2000-volt D.C. motor-generator set was used to excite the tube.

A second tube containing neon gas was used to measure the strength of the magnetic field both before and after an exposure with the tube containing oxygen and argon was made. The yellow neon line at $\lambda 5852\text{\AA}$ was used as the standard.

560 Prof. McLennan, Mr. McLeod, and Dr. Ruedy :

Several conditions had to be fulfilled in the design of a suitable discharge-tube. It had to be designed so that it

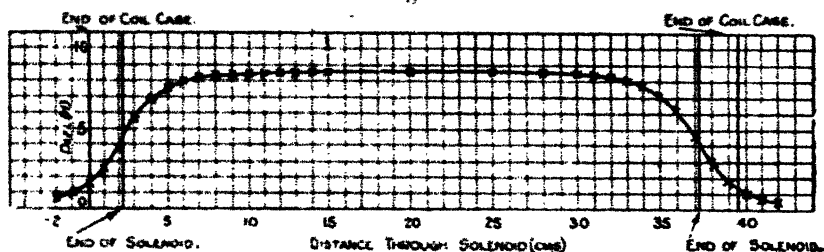
Fig. 1.



could be placed in or removed from the magnetic solenoid at will. In addition it had to be made so as to emit to the

resolving apparatus as much as possible of the light from that part of the tube which was in the uniform portion of the magnetic field and as little as possible from portions of the tube outside the field. At the same time no light was desired from the proximity of the electrodes. Fig. 1 shows the type of tube evolved to fulfil the conditions that have been enumerated above. By passing a heavy current between the magnesium electrodes shown it was possible to purify the gas to such a degree that the tube could be permanently sealed off from the pump and argon supply. A pair of aluminium electrodes was used to carry the existing current. By making one of them in the form of a cylinder and by placing it co-axially with the bore of the tube as shown at E it was possible to slide the discharge-tube into the solenoid to the position shown in fig. 1. Moreover, the discharge could be observed longitudinally through the hollow electrode. By having the window W_1

Fig. 2.



placed at the end of a re-entrant portion of the tube we were able to ensure that while light from the space in the tube in front of the window could pass out to the spectrograph, light from the space near the electrode was prevented from doing so. The tube and the solenoid were placed in the relative positions shown in fig. 1. A reference to fig. 2 will show that for a distance of about 25 cm. along the discharge-tube in front of the window W_1 the magnetic field was very nearly uniform. Farther along the discharge-tube than 25 cm. the magnetic field of course fell off in value, but that part of the tube was so far from the spectrograph that very little light from it could enter the spectrograph.

The resolving apparatus used consisted of a 45-plate echelon grating* with a constant deviation spectrograph to

* This instrument was presented to the Physical Laboratory of the University of Toronto by Messrs. Samuel and Benjamin of London and Toronto.

separate out the various spectral lines. The spectrograph slit and the edges of the echelon-plates were parallel and vertical. The constants of the echelon as given by the Adam Hilger Co., the makers, were as follows:—

Number of plates	45
Thickness of each plate	14.76 mm.
Width of step	1.0 mm.
Refractive indices :	

λ (Å.)	μ
6562.793	1.57185
5895.930	1.5759
5889.963	
4861.327	
4307.908	1.58581
	1.59417

From these constants the value of $\Delta\lambda$ max., the portion of the spectrum included between consecutive orders of the same line, was calculated. The two values used were $\Delta\lambda$ max. for λ 5577 Å = 0.336 Å and $\Delta\lambda$ max. for λ 5852 (Ne) = 0.376 Å.

The echelon was adjusted to give two orders of equal intensity for the line being photographed. This adjustment made it possible to get a measure of the displacement on the plate corresponding to $\Delta\lambda$ max., with a much shorter exposure of the plate than would have been the case if the maximum intensity had been thrown into one order.

Three photographs of the Zeeman resolution of the oxygen green line were made. Before and after each of these exposures a photograph of the Zeeman resolution of the yellow neon line at λ 5852 Å was taken in order to get a measure of the field strength. Pl. VI. fig. 1 shows a sample of a photograph of the Zeeman effect of the oxygen green line and Pl. VI. fig. 2 shows a similar one taken of the yellow neon line.

The duration of the exposure for the Zeeman effect of the green line was from 45 to 60 minutes and for the neon line it was from 4 to 8 minutes.

Back⁽³⁾ has shown that the neon line λ 5852 Å has for its Zeeman pattern the following $\frac{(0) 31}{30}$. By a measurement on the photographs of the separation Δx of the Zeeman components of the neon line and by a measurement of Δx max. between the orders, it was possible by simple calculation for us, knowing $\Delta\lambda$ max., to determine the field-strength. Table I. gives the actual results obtained.

TABLE I.

	Δx max. mm.	Δx mm.	$\Delta \lambda$ max. A.	$\Delta \lambda$ experi- mental.	H calculated from Neon Gauss.	H mean.	Current amps.	$\Delta \lambda$ calcul- ated.	Ratio: $\frac{\Delta \lambda \text{ exper.}}{\Delta \lambda \text{ calcd.}}$
Plates number one.	Neon.....	λ 5852 A	0.153	0.376	0.0886	2680	30.0		
	Oxygen.....	λ 5577 A	0.132	0.336	0.0711	2720	30.0	0.0794	0.895
	Neon.....	λ 5852 A	0.162	0.376	0.0926	2780	30.0		
Plates number two.	Neon.....	λ 5852 A	0.150	0.376	0.0863	2635	30.5		
	Oxygen.....	λ 5577 A	0.150	0.336	0.0774	2650	30.5	0.0774	1.000
	Neon.....	λ 5852 A	0.156	0.376	0.0888	2665	30.5		
Plates number three.	Neon.....	λ 5852 A	0.165	0.376	0.0938	2810	30.0		
	Oxygen.....	λ 5577 A	0.148	0.336	0.0751	2680	30.0	0.0785	0.937
	Neon.....	λ 5852 A	0.160	0.376	0.0856	2570	30.0		

Mean..... 0.96

The column headed "H mean" gives in each case the mean value of the magnetic field from the values obtained before and after the green line Zeeman effect was photographed. The column headed " $\Delta\lambda$ calculated" gives the separations between the outer components of a normal triplet for the field values given in the previous column. Finally, the last column gives the ratio of the observed $\Delta\lambda$ to the calculated $\Delta\lambda$ for a normal triplet.

The mean of the three results gives the magnetic separation of the oxygen green line to be 0.96 of the normal amount.

The neon lines were rather fuzzy, as can be seen from Pl. VI. fig. 2, and consequently it was difficult to judge just where the maximum of the line occurred. The determination of the field strength was therefore subject to error. Though there is little doubt that the total experimental error could have been as much as 4 per cent., we had no hesitation in concluding that the Zeeman separation of the green line was normal. Since parallel components would be absent for longitudinal observation, we take it that the oxygen green line at λ 5577 Å is resolvable magnetically into a *normal triplet*.

From the result that the magnetic resolution of the green line is a normal triplet, it is possible to determine with a considerable amount of definiteness the exact location of the oxygen green line in the spectral scheme for atomic oxygen.

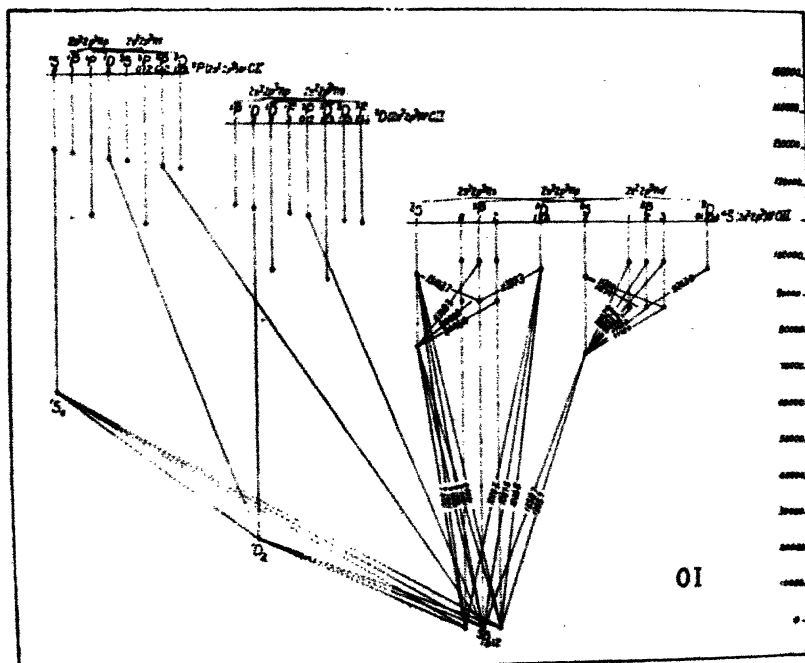
Fig. 3 is a diagram of this spectral scheme. It consists of three systems. Two of them have the metastable levels 1S_0 and 1D_2 for their lowest terms. The system with $^3P_{012}$ as its lowest term is well known. Those with 1S_0 and 1D_2 as lowest terms, as well as the one based more immediately on the $^3\bar{P}_{012}$ term, are systems predicted on the basis of the Hund theory. There is no possible place for the green line in the scheme having $^3\bar{P}_{012}$ for its deepest level, so we must confine our attention to the other two schemes.

A brief consideration of the energy relations involved enables one to limit further the position of the green line in the spectral term scheme of oxygen. An examination of fig. 3 will show that two spectral lines occur in that region of the oxygen spectrum that could be most easily photographed, if radiation covering it were included in the light coming to us from the night sky. They are at λ 4368 Å and λ 3947 Å. No such lines, however, have ever been observed in the spectrum of the light from the night sky.

From this fact it may be concluded, therefore, that, under the conditions that give rise to the emission of radiation from the night sky corresponding to the auroral green line, there is not sufficient energy available to raise the oxygen in the upper atmosphere to the atomic levels involved in the production of the wave-lengths $\lambda 4368 \text{ \AA}$ and $\lambda 3947 \text{ \AA}$.

It follows from this that there cannot be sufficient energy available to permit of electronic transitions to the low ^3P

Fig. 3.



Atomic levels of Oxygen.

levels of the $^1\text{S}_0$ system from higher ones in it or to the low ^3D levels of the $^1\text{D}_2$ system from higher ones in it.

Moreover, it is certain that an electron jump from any one of the low ^3P levels of the $^1\text{S}_0$ system to the $^1\text{S}_0$ level or from any one of the low ^3D levels of the $^1\text{D}_2$ system to the $^1\text{D}_2$ level would give rise to radiation far in the ultra-violet region. This follows from the fact that the resonance lines of the $^3\text{P}_{012}$ system are far down in the ultra-violet.

We are limited therefore to transitions from one or other of the metastable levels $^1\text{S}_0$ and $^1\text{D}_2$. These, it is well known, are usually classed as forbidden ones.

In 1927 ⁽⁴⁾ the authors pointed out that it would be necessary to include so-called "forbidden" transactions in our considerations when seeking for a place for the green line in the spectral term scheme for atomic oxygen.

Moreover, Bowen ⁽⁵⁾ has since shown that a number of the nebulium spectral lines result from electronic transitions ordinarily classed as forbidden ones. This furnishes conclusive evidence that metastable states are not absolutely stable ones, and that they, too, are states of excitation from which spontaneous transitions accompanied by the emission of radiation can occur.

The predicted Zeeman effects of all the transitions originating in the lower metastable states of the oxygen atom are given in Table II.

TABLE II.

Transition.	Zeeman Pattern.
$^1S_0 \rightarrow ^1D_2$	$\frac{(0) \ 1}{1}$.
$^1S_0 \rightarrow ^3P_0$	$\frac{0}{0}$.
$^1S_0 \rightarrow ^3P_1$	$\frac{(0) \ 3}{2}$.
$^1S_0 \rightarrow ^3P_2$	$\frac{(0) \ 3}{2}$.
$^1D_2 \rightarrow ^3P_0$	$\frac{(0) \ 1}{1}$.
$^1D_2 \rightarrow ^3P_1$	$\frac{(0) \ (1) \ 1 \ 2 \ 3}{2}$.
$^1D_2 \rightarrow ^3P_2$	$\frac{(0) \ (1) \ (2) \ 1 \ 2 \ 3 \ 4}{2}$.

It will be seen that two possible transitions could give rise to a normal triplet Zeeman effect. We may at once rule out the transition $^1D_2 \sim ^3P_0$ because if it were the transition that gave rise to the auroral green line the transitions $^1D_2 \sim ^3P_1$ and $^1D_2 \sim ^3P_2$ would certainly be present and would give rise to two spectral lines in the vicinity of $\lambda 5577 \text{ \AA}$. These have never been observed.

Therefore it is seen that the green line at $\lambda 5577, 341 \text{ \AA}$ in the spectrum of oxygen must have its origin in electronic transitions from 1S_0 metastable levels of oxygen atoms to 1D_2 ones.

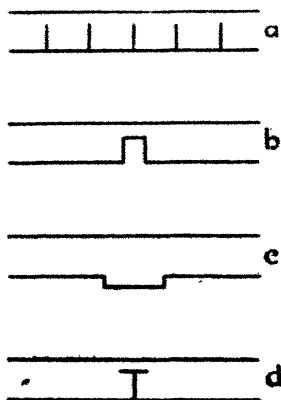
References.

- (1) McLennan & Shrum, Proc. Roy. Soc. A, cviii. p. 501 (1925).
McLennan, McLeod, and McQuarrie, Proc. Roy. Soc. A, cxiv. p. 1 (1927).
Cario, *Zeit. f. Physik*, xlii. p. 15 (1927).
McLennan and McLeod, Proc. Roy. Soc. A, cxv. p. 515 (1927).
- (2) McLennan, McLeod, and McQuarrie, Proc. Roy. Soc. A, cxiv. p. 1 (1927).
- (3) Back, *Ann. d. Physik*, lxxvi. p. 317 (1925).
- (4) McLennan, Ruedy, and McLeod, Trans. Roy. Soc. Canada, ser. iii. vol. xxi. section iii. (1927).
- (5) Bowen, 'Nature,' Oct. 1, 1927.

LIV. *The Effect on the Heat-flow through an Insulating Wall of Certain Modifications of Shape of its Isothermal Boundaries.* By F. H. SCHOFIELD, B.A., B.Sc.*

IN dealing with the steady flow of heat through a plane wall of insulating material, large in area in proportion to its thickness and with isothermal boundaries, it suffices

Fig. 1.



to treat the matter as one of two-dimensional flow between infinite parallel isothermals. It is proposed, on this basis, to investigate the effect on the heat-flow through such a wall due to certain modifications of one of its boundaries. The shapes dealt with are according to the sections shown in fig. 1. Of these (a) represents a series of thin projections, of equal depth and spacing, from one of the isothermals such

* Communicated by G. W. C. Kaye, Superintendent, Physics Department, National Physical Laboratory, Teddington, Middlesex.

as would correspond roughly to the metallic ribs of a ship projecting into a wall of insulation applied internally against its side; (b) and (c) represent single projections of finite width, respectively internal and external, such as would be encountered in a wall of insulation applied against a surface with either a projecting buttress or a recess; and (d) represents a single rib projection of T section. The solutions in these cases would, of course, apply where the modifications of one boundary are duplicated in the other as if by mirror reflexion about the mid-plane.

While the problems to be considered are thus stated in terms of heat-flow, it will readily be understood that they might equally well be expressed in relation to any other phenomenon which is subject to the Laplace equation. For example, the problems might be considered as those of the flow of electric current in long strips of metal of uniform thickness cut to the shapes indicated, or of the distribution of electrostatic charge and potential in the case of condensers of the appropriate cross-section extending to infinity in a plane perpendicular to that of the paper.

The method of solution employed is that of conformal representation, using the transformation found by Christoffel and Schwarz*.

I. A SERIES OF THIN RIBS.

In this case it is clear from considerations of symmetry that the flow lines from the tip of each rib, and from the points on the lower boundary, midway between the ribs, will be straight lines normal to the upper boundary. Hence it is only necessary to consider the rectangle formed by two such adjacent flow lines and the isothermal boundaries joining them. (See z plane, fig. 2.) This corresponds to the problem of the electrical resistance of a rectangular strip of metal with two electrodes supplied along the whole or portions of the sides—in the particular instance now under consideration the resistance of ABCD with electrodes along AD and BE—which has been treated generally by Moulton†. For our purpose it is convenient to follow a less general treatment than Moulton's and adopt the transformation shown in fig. 2. The linear dimensions l , m , and n of the z plane and l of the w plane are as indicated, while the

* For a discussion of this transformation with numerous examples, see J. J. Thomson's 'Recent Researches in Electricity and Magnetism,' chap. iii. (Clarendon Press, 1893.)

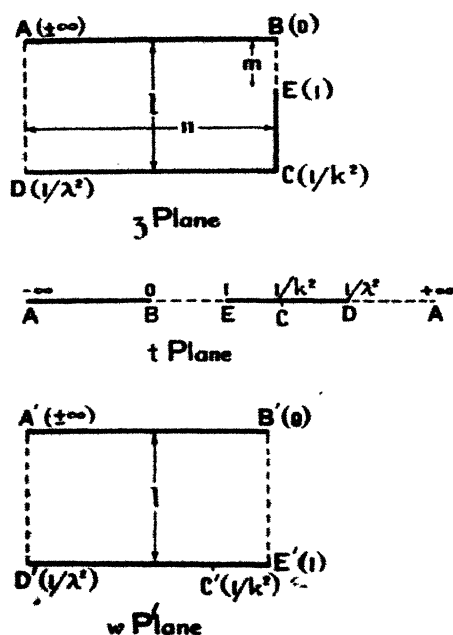
† Proceedings of London Mathematical Society, iii. p. 104 (1905). Also Jeans, 'Electricity and Magnetism,' 4th edition, p. 354.

lettering in brackets at the corners of the rectangles are the lengths along the real axis in the t plane, subject to the condition $\lambda < k < 1$. In fig. 2 and other similar diagrams the convention is adopted of showing the boundary isothermals and flow lines as full and dashed lines respectively.

The relation which converts the boundary ABCD, and the space inside it, into the real axis and upper half of the t plane, respectively is

$$dz/dt = Lt^{-1}(t-1/\lambda^2)^{-1}(t-1/k^2)^{-1}, \dots (1)$$

Fig. 2.



L being a constant. Putting $t = r^2/k^2$, we have

$$z = M \int \frac{dr}{\sqrt{1-r^2} \sqrt{1-r^2(\lambda^2/k^2)}} + N, \dots (2)$$

where M and N are constants. Calling B the origin and BC the real axis, N becomes zero, and we have

$$l = M \times K \pmod{\lambda/k}, \dots (3)$$

$$\text{and} \quad l/n = K/K' \pmod{\lambda/k}, \dots (4)$$

Hence combining (2) and (3) *,

$$z = (l/K) \operatorname{sn}^{-1}(k \sqrt{t}, \lambda/k), \quad \dots \quad (5)$$

and the length BE is given by

$$m = (l/K) \operatorname{sn}^{-1}(k, \lambda/k). \quad \dots \quad (6)$$

Similarly, the transformation from the w to the t plane yields

$$w = (l/K) \operatorname{sn}^{-1}(k \sqrt{t}, \lambda). \quad \dots \quad (7)$$

Hence from (5), (6), and (7),

$$\operatorname{sn}(Kz/l, \lambda/k) = k \sqrt{t} = \operatorname{sn}(Km/l, \lambda/k) \operatorname{sn}(Kw/l, \lambda). \quad (8)$$

The constants λ and k are known in terms of the dimensions l , m , n of the z plane through equations (4) and (6) above.

Hence the equation (8) gives the coordinates $(x+iy)$ of any point of the z plane in terms of the coordinates $(u+iv)$ of the corresponding point in the w plane, and so gives the distribution of flow lines and isothermals of the former plane in terms of the rectilinear distribution of the latter. The necessary calculation, involving the splitting of (8) into real and imaginary parts and solving for x and y , would be very laborious, and probably the simplest way of obtaining the z plane distribution would be to prepare two charts giving a series of orthogonal curves for constant values of p and of q in the relation †

$$P + iQ = \operatorname{sn}(p + iq),$$

and for the respective moduli λ and λ/k . Then the first chart would give P and Q for any desired values of u and v , and, after multiplying the former by the constant $\operatorname{sn}(Km/l, \lambda/k)$, the second chart would enable the values of Kx/l and Ky/l to be read off. It is not proposed to apply the method here, especially in view of the fact that the calculation of the distribution in the simpler case of a single rib in an infinite layer has been given by Lees ‡, and that, as will be shown below, this case gives a very close approximation to that of a series of ribs unless the gaps between them are comparatively small.

With regard to overall heat-loss, the flow across the strip of width l and length AB in the z plane is equal to the flow

* Since the function is to be inverted it is here written sn^{-1} in place of Legendre's F .

† See e. g. Dixon's 'Elliptic Functions.' Appendix A. (Macmillan & Co., 1894.)

‡ Proc. Phys. Soc. xxiii. p. 361 (1911).

across the strip of width l and length $A'B'$ in the w plane, where the flow is entirely normal. If there were no ribs such as EC in the z plane, the heat-flow from AB would also be normal, and hence we may regard the effect of inserting the ribs as equivalent to adding a length $2X$ per rib to the strip where X is given by

$$X = A'B' - AB = l \{ K'/K(\text{mod } \lambda) - K'/K(\text{mod } \lambda/k) \}. \quad (9)$$

From this equation we may readily deduce the "added length" for the marginal case of a single rib in an infinite layer. Thus putting $\lambda=0$ we have a zero modulus for both sets of elliptic functions, so that in each case $K=\pi/2$, and

$$K'(\text{mod } \lambda) = Lt_{\lambda=0} [\log (4/\lambda)]$$

and

$$K'(\text{mod } \lambda/k) = Lt_{\lambda=0} [\log (4k/\lambda)],$$

and from equation (6)

$$k = \sin (m\pi/2l).$$

Hence

$$\begin{aligned} X &= (2l/\pi) \log (1/k) \\ &= (2l/\pi) \log \operatorname{cosec} (m\pi/2l), \quad . \quad . \quad . \quad (10) \end{aligned}$$

which agrees with Lees's direct solution for this marginal case, while for the general equation (8) degenerates into

$$\sin (z\pi/2l) = \sin (m\pi/2l) \cdot \sin (w\pi/2l), \quad . \quad . \quad (11)$$

which is equivalent to Lees's equation.

The added length X for a series of ribs is calculated for known values of l , m , and n from equation (9) as follows:— From equation (4), using Legendre's Tables, we get the modulus λ/k : from (6) the argument k , and hence the other modulus λ . In the following table are set out the values of X/l for a series of values of n/l , taking the two cases where the depth of the rib ($l-m$) is respectively $\frac{3}{4}$ and $\frac{1}{2}$ of that of the layer.

It will be seen that in the two cases taken the error in the total heat transfer due to using the formula (10), applicable to the infinite case, becomes less than 1 per cent. when the semi-distance n between the ribs is slightly more than one-half of the thickness of the layer (see cols. 4 and 7 of Table I.). Hence in most practical cases each rib of a series, which may be of various depths and spacings, can be treated independently as a single rib in an infinitely long layer.

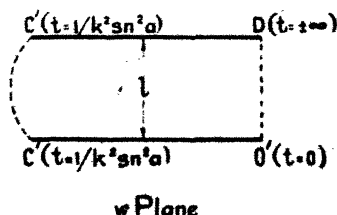
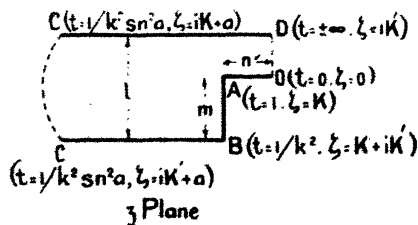
TABLE I.
 $2X$ = the "Added Length" per rib.

n/l	$l=4m.$			$l=2m.$		
	$X/l.$	Percentage diff. from ∞ case.		$X/l.$	Percentage diff. from ∞ case.	
		$100(X_{\infty}-X)$	$100(X_{\infty}-X)$		$100(X_{\infty}-X)$	$100(X_{\infty}-X)$
		X	$n+X$		X	$n+X$
Col. 1.	Col. 2.	Col. 3.	Col. 4.	Col. 5.	Col. 6.	Col. 7.
0.333	0.5070	20.6	12.4	0.1834	20.2	7.2
0.5	0.5731	6.7	3.6	0.2070	6.6	1.9
1	0.6098	0.3	0.1	0.2201	0.2	0.1
2	0.6116	0	0	0.2205	0	0
3	0.6120	0	0	0.2208	0	0
∞	0.6115	0	0	0.2206	0	0

II. THICK RIB OR BUTTRESS.

The diagram of this case is given in fig. 3 in the z and w

Fig. 3.



planes only, using the same conventions as before, but with a curved dotted line to indicate the flow line CC , which is

entirely at infinity. The transformation from the z to the t plane involves the third type of elliptic integral, and, with a view to obtaining the Jacobian form, we note that the infinity point C in the z plane gives rise to a term of the form $(t-b)^{-1}$ in the transformation. Hence b is conveniently put equal to $1/k^2 \operatorname{sn}^2 a$, while t is replaced by a new variable $\operatorname{sn}^2 \zeta$. Following a similar plan to that adopted in the previous case, the other corners of the polygon conveniently become as shown in the diagram, and the required transformation is given by

$$dz/dt = A(t-1)^{-1/2}(t-1/k^2 \operatorname{sn}^2 a)^{-1/2}t^{-1/2}(t-1/k^2)^{-1/2}. \quad (14)$$

Putting $t = \operatorname{sn}^2 \zeta$, and $M = -2Ak^3 \operatorname{sn}^2 a$, we obtain

$$\begin{aligned} \frac{dz}{d\zeta} &= M \left\{ \frac{\operatorname{cn}^2 \zeta}{1 - k^2 \operatorname{sn}^2 a \operatorname{cn}^2 \zeta} \right\} \\ &= M \left\{ 1 - \frac{\operatorname{dn}^2 a \operatorname{sn}^2 \zeta}{1 - k^2 \operatorname{sn}^2 a \operatorname{sn}^2 \zeta} \right\} \\ &= \frac{M}{k^2} \left\{ k^2 - \frac{\operatorname{dn} a}{\operatorname{sn} a \operatorname{cn} a} \left(\frac{k^2 \operatorname{sn} a \operatorname{cn} a \operatorname{dn} a \operatorname{sn}^2 \zeta}{1 - k^2 \operatorname{sn}^2 a \operatorname{sn}^2 \zeta} \right) \right\} \\ \therefore z &= \frac{M}{k^2} \left\{ k^2 \zeta - \frac{\operatorname{dn} a}{\operatorname{sn} a \operatorname{cn} a} \Pi(\zeta, a) \right\}. \quad (15) \end{aligned}$$

No integration constant is required if the origin is fixed at O, the real axis being OA. The values of the new variable ζ at the corners of the polygon are as shown in fig. 3, and, in order to obtain the finite dimensions l, m, n in the z plane, we proceed as follows:— l is the change in z as t passes through $1/k^2 \operatorname{sn}^2 a$ (or ζ passes through $iK' + a$), and is therefore given by

$$il = i \frac{\pi M \operatorname{dn} a}{2k^2 \operatorname{sn} a \operatorname{cn} a}. \quad (16)$$

This expression may also be obtained by use of (18), (19), and (20) below. Substituting in (15), we have

$$z = \frac{2l}{\pi} \left\{ \frac{k^2 \operatorname{sn} a \operatorname{cn} a}{\operatorname{dn} a} \zeta - \Pi(\zeta, a) \right\}. \quad (17)$$

To obtain the other dimensions in the z plane, use is made of the following relations of the Π function:—

$$\Pi(K, a) = KZ(a). \quad (18)$$

$$\Pi(K + iK', a) = KZ(a) + i\{K'Z(a) + a\pi/2K\}. \quad (19)$$

$$\Pi(iK', a) = i\{K'Z(a) + a\pi/2K \pm \pi/2\}. \quad (20)$$

Hence from (17), (18), and (19),

$$\frac{n}{l} = \frac{2K}{\pi} \left\{ \frac{k^2 \operatorname{sn} a \operatorname{cn} a}{\operatorname{dn} a} - Z(a) \right\} \dots \dots \dots (21)$$

$$-\frac{m}{l} = \frac{2K'}{\pi} \left\{ \frac{k^2 \operatorname{sn} a \operatorname{cna}}{\operatorname{dn} a} - Z(a) \right\} - \frac{a}{K}, \dots \dots \dots (22)$$

the signs in (22) being consistent with (16), (19), and (20).

The length BC is infinite by virtue of the value of $\Pi(iK' + a, a)$, and since we propose to obtain the difference between this length and a corresponding infinite length in the w plane, we analyse the function by means of the addition theorem, as follows:—

$$\begin{aligned} \Pi(iK' + a, a) &= Lt_{\epsilon=0} [\Pi(iK' + \epsilon + a, a)] \\ &= Lt_{\epsilon=0} \left[\Pi(a, a) + \Pi(iK' + \epsilon, a) \right. \\ &\quad \left. + \frac{1}{2} \log \left\{ \frac{1 + \frac{k^2 \operatorname{sn} a \operatorname{sn} a}{k^2 \operatorname{sn} \epsilon \operatorname{sn} (2a + \epsilon)}}{1 - \frac{k^2 \operatorname{sn} a \operatorname{sn} a}{k^2 \operatorname{sn} \epsilon \operatorname{sn} \epsilon}} \right\} \right] \\ &= \Pi(a, a) + i\{K'Z(a) + a\pi/2K\} \\ &\quad - \frac{1}{2} \log \operatorname{sn} 2a + Lt_{\epsilon=0} \left[\frac{1}{2} \log \operatorname{sn} \epsilon \right]. \end{aligned} \quad (23)$$

Hence BC is given by

$$\begin{aligned} BC &= OA + AB + BC - (OA + AB) \\ &= \frac{2l}{\pi} \left\{ \frac{k^2 \operatorname{sn} a \operatorname{cn} a}{\operatorname{dn} a} (a - K) + KZ(a) - \Pi(a, a) \right. \\ &\quad \left. + \frac{1}{2} \log \operatorname{sn} 2a - Lt_{\epsilon=0} \left(\frac{1}{2} \log \operatorname{sn} \epsilon \right) \right\} \dots \dots \dots (24) \end{aligned}$$

Converting to the Θ function by the relation

$$\Pi(a, a) = aZ(a) - \frac{1}{2} \log \frac{\Theta(2a)}{\Theta(0)},$$

and combining with equation (21), we obtain

$$\begin{aligned} BC &= \frac{l}{\pi} \log \left\{ \frac{\operatorname{sn} 2a \Theta(2a)}{\Theta(0)} \right\} - n \left(1 - \frac{a}{K} \right) \\ &\quad - \frac{l}{\pi} Lt_{\epsilon=0} (\log \operatorname{sn} \epsilon) \dots \dots \dots (25) \end{aligned}$$

This expression is infinite by virtue of the last term.

Turning now to the transformation which converts the w into the t plane, we have

$$dw/dt = t^{-1}(t - 1/k^2 \operatorname{sn}^2 a)^{-1}, \dots (26)$$

which yields on integration, for an origin O' and a real axis $O'C'$,

$$w = P \log \left\{ \frac{1 + k \operatorname{sn} a \sqrt{t}}{1 - k \operatorname{sn} a \sqrt{t}} \right\}, \dots (27)$$

the value of P being given by

$$il = P \log (-1) = P i \pi.$$

To obtain the length $O'C'$, we proceed in a similar way to that adopted in the case of the z plane, putting t equal to $1/k^2 \operatorname{sn}^2 (a + \epsilon)$ and taking the limit for $\epsilon = 0$.

Thus

$$\begin{aligned} O'C' &= Lt_{\epsilon=0} \left[\frac{l}{\pi} \log \left\{ \frac{\operatorname{sn}(a + \epsilon) + \operatorname{sn} a}{\operatorname{sn}(a + \epsilon) - \operatorname{sn} a} \right\} \right] \\ &= Lt_{\epsilon=0} \left[\frac{l}{\pi} \log \left\{ \frac{\operatorname{sn} a \operatorname{cn} \epsilon \operatorname{dn} \epsilon + \operatorname{sn} \epsilon \operatorname{cn} a \operatorname{dn} a +}{\operatorname{sn} a \operatorname{cn} \epsilon \operatorname{dn} \epsilon + \operatorname{sn} \epsilon \operatorname{cn} a \operatorname{dn} a -} \right. \right. \\ &\quad \left. \left. \frac{+ \operatorname{sn} a (1 - k^2 \operatorname{sn}^2 \epsilon \operatorname{sn}^2 a)}{- \operatorname{sn} a (1 - k^2 \operatorname{sn}^2 \epsilon \operatorname{sn}^2 a)} \right\} \right] \\ &= \frac{l}{\pi} \log \frac{2 \operatorname{sn} a}{\operatorname{cn} a \operatorname{dn} a} - \frac{l}{\pi} Lt_{\epsilon=0} \{ \log \operatorname{sn} \epsilon \} \dots (28) \end{aligned}$$

The last term of this equation is infinite and identical with the last term of (25).

Now, if the heat-flow from $OA + AB + BC$ had been "normal," that is to say, perpendicular to OA and BC , it would have been equivalent to that across a strip of width l and of length $BC + OA(l/l - m)$. Actually the heat-flow in question is equal to the normal flow across a strip of width l and of length $O'C'$, since this is the length in the w plane, where the flow is entirely normal, equivalent to $OA + AB + BC$ in the z plane. Hence the excess of the actual heat-flow from $OA + AB + BC$ over the hypothetical normal flow is equivalent to the addition to the strip of width l of a length X given by

$$\begin{aligned} X &= O'C' - BC - OA(l/l - m) \\ &= \frac{l}{\pi} \log \left\{ \frac{2 \operatorname{sn} a \Theta(0)}{\operatorname{cn} a \operatorname{dn} a \operatorname{sn} 2a \Theta(2a)} \right\} \\ &\quad + n \left(1 - \frac{a}{K} \right) - n \left(\frac{l}{l - m} \right). \dots (29) \end{aligned}$$

This equation, together with (21) and (22), which determine the constants k and a in terms of the dimensions l , m , and n of the z plane, gives the solution of the "added length" in the case under consideration.

It is useful to check the result by degenerating the solution to obtain known marginal cases involving two finite dimensions. Thus:—

Case 1: $n/l=0$.

This is obtained by making the modulus k equal to zero, for then

$$K=\pi/2 \quad \text{and} \quad K'=L_{k=0}[\log(4/k)].$$

Hence from equation (21), noting that $Z(a)=0$, we have

$$n/l=0,$$

while from (22), noting that k^2 is the lowest power of k in $Z(a)$ and that in the limit $k^2 \log k$ is zero,

$$\begin{aligned} -\frac{m}{l} &= \frac{2}{\pi} \log\left(\frac{4}{k}\right) \{k^2 \sin a \cos a - Z(a)\} - \frac{2a}{\pi} \\ &= -\frac{2a}{\pi}. \end{aligned}$$

Hence since $\Theta(2a)/\Theta(0)=1$, we have

$$\begin{aligned} X &= \frac{l}{\pi} \log \left(\frac{2 \sin a}{\cos a \sin 2a} \right) \\ &= \frac{2l}{\pi} \log \sec \left(\frac{m\pi}{2l} \right), \quad \dots \dots \dots (30) \end{aligned}$$

which agrees with (10) above, allowing for the fact that m of the last-mentioned equation is here replaced by $l-m$.

Case 2: $m/l=0$.

This is obtained by putting $k=1$. Then since $\operatorname{cn} a = \operatorname{dn} a = \operatorname{sech} a$ and $\operatorname{sn} a = Z(a) = \tanh a^*$, and, as will be shown below, $\Theta(2a)/\Theta(0) = \cosh 2a$, we have $m/l=0$ and $X/l=0$.

Case 3: $nl=\infty$.

This is obtained by putting $k=1$ and $a=K-\beta$, where β is a finite quantity, K of course being infinite. For the purpose of equations (21) and (22), we note that

$$\begin{aligned} \frac{\operatorname{sn}(K-\beta) \operatorname{cn}(K-\beta)}{\operatorname{dn}(K-\beta)} &= \frac{\operatorname{sn} \beta \operatorname{cn} \beta}{\operatorname{dn} \beta} = \tanh \beta, \\ Z(K-\beta) &= \beta/K = 0. \end{aligned}$$

* For these degenerations and those used in obtaining equation (30), see *e. g.* Dixon's 'Elliptic Functions,' chap. viii. (Macmillan & Co.)

So that

$$\frac{n}{l} = \frac{2K}{\pi} (\tanh \beta - \beta/K) = \infty \quad (31)$$

$$-\frac{m}{l} = \tanh \beta - 1 \quad (32)$$

From the latter equation

$$\tanh \beta = (l-m)/l \quad \text{or} \quad \beta = \frac{1}{2} \log \frac{2l-m}{m} \quad (33)$$

For the purpose of dealing with equation (29), we have

$$\frac{\Theta(2a)}{\Theta(0)} = \frac{\Theta(2\beta)}{\Theta(0)} = e^{-\beta^2/2K + \int_0^{2\beta} \tanh x \, dx} = e^{\log \cosh 2\beta} = \cosh 2\beta \quad (34)$$

$$\begin{aligned} \log \left\{ \frac{2 \operatorname{sn}(K-\beta) \Theta(0)}{\operatorname{cn}(K-\beta) \operatorname{dn}(K-\beta) \operatorname{sn}(2K-2\beta) \Theta(2K-2\beta)} \right\} \\ = \log \left\{ \frac{2 \operatorname{cn} \beta \operatorname{dn} \beta \Theta(0)}{k'^2 \operatorname{sn} \beta \operatorname{sn} 2\beta \Theta(2\beta)} \right\} \\ = 2 \log \frac{4}{k'} + 2 \log \frac{1}{2 \sinh 2\beta} \quad (35) \end{aligned}$$

$$\begin{aligned} \frac{n}{l} \left(1 - \frac{a}{K} \right) - \frac{n}{l-m} &= \frac{n}{l} \left(\frac{\beta}{K} - \frac{1}{\tanh \beta} \right) \\ &= \frac{2\beta}{\pi} (\tanh \beta + \coth \beta) - \frac{2K}{\pi} \quad (36) \end{aligned}$$

Using the last two equations, we have from (29)

$$\frac{X}{l} = \frac{2}{\pi} \log \frac{m(2l-m)}{4l(l-m)} + \frac{1}{\pi} \left(\frac{l}{l-m} + \frac{-m}{l} \right) \log \frac{2l-m}{m} \quad (37)$$

Putting $m = (l-b)$, this becomes

$$\frac{X}{l} = \frac{1}{\pi} \left\{ 2 \log \frac{l^2 - b^2}{4lb} + \frac{l^2 + b^2}{lb} \log \frac{l+b}{l-b} \right\} \quad (38)$$

which is identical with Lees's* direct solution for this marginal case.

Calculation of "Added Length."

The calculation of the "added length" in any particular case can be carried out by means of the Tables of Θ and

* Phil. Mag. xvi. p. 734 (1908).

allied functions due to Greenhill and Hippisley*. The functions are given for a series of values of the modulus k —for the most part for every 5° —and for every ninetieth part of K for the variable a . Expressed in terms of the notation used in the Tables, the variable r being equal to $90a/K$, equations 21, 22, and 29 become respectively

$$\frac{n}{l} = \frac{2K}{\pi} \left\{ \frac{k^2 A(r) B(r)}{k' C(r) D(r)} - E(r) \right\} \dots \dots \dots (39)$$

$$\frac{m}{l} = \frac{r}{90} - \frac{2K'}{\pi} \left\{ \frac{k^2 A(r) B(r)}{k' C(r) D(r)} - E(r) \right\} \dots \dots \dots (40)$$

$$\frac{X}{l} = \frac{1}{\pi} \log \left\{ \frac{2A(r) D(r)}{\sqrt{k'} B(r) C(r) A(2r)} \right\} + \frac{n}{l} \left(1 - \frac{r}{90} \right) - \frac{n}{l-m} \dots \dots \dots (41)$$

When $2r$ is greater than 90° , it can be shown that $A(2r)$ in equation (41) should be replaced by $B(s)$, where s is equal to $(2r-90)$.

The plan adopted in the present case is to take a constant depth m of the buttress, and obtain the values of X for a series of values of n . For this purpose, taking any modulus k , the value of r is found by trial giving the required ratio m/l , and using this value of r , the ratios of n/l and X/l are readily calculated. Curves have been obtained as above described for two values of m/l , namely $\frac{1}{2}$ and $\frac{3}{4}$, and are shown in fig. 4, which gives the calculated points and the appropriate modular angles. It will be observed from the curves, marked $B(\frac{1}{2})$ and $B(\frac{3}{4})$, that the asymptotic approach to the final value is extremely rapid.

III. RECESS.

The transformation from the t to the w plane is the same as for the previous case, while that for the z plane is identical with that employed by Carter† in dealing with a problem in magnetism illustrated below in fig. 9. Following the practice in the previous cases, we shall however adopt the slight modification of cutting the figure into two parts by the central flow line (see fig. 5), and hence obtain the following equation for the transformation from the z to the t plane.

$$dz/dt = At^{-\frac{1}{2}}(t-1)^{-\frac{1}{2}}(t-1/k^2)^{\frac{1}{2}}(t-1/k^2 \sin^2 a)^{-\frac{1}{2}}. \quad (42)$$

* 'Smithsonian Mathematical Formulæ and Tables of Elliptic Functions' (Publication No. 2672, Washington, 1922).

† Journ. Inst. Elect. Eng. vol. lxiv. p. 1117 (1926).

Fig. 4.

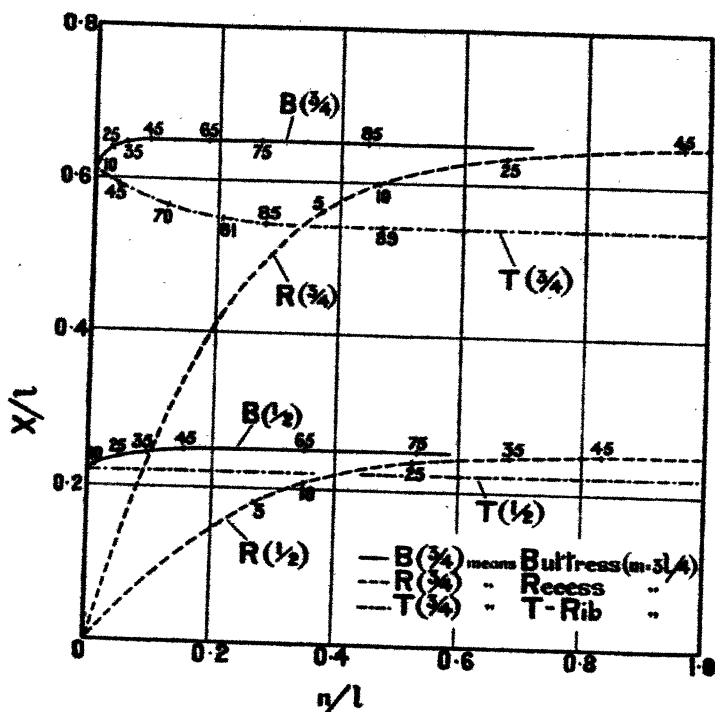
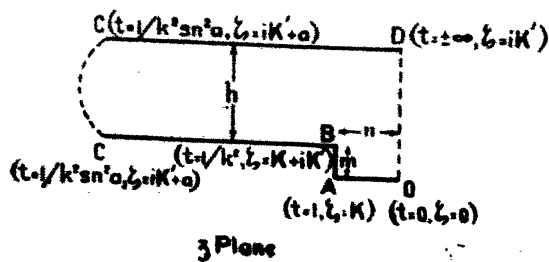


Fig. 5.



Putting $t = \text{sn}^2 \zeta$ and $M = -2Aksn^2 a$, we have, on integration, O being the origin and OA the real axis,

$$z = M \left\{ \zeta - \frac{\text{cn } a}{\text{sn } a \text{ dn } a} \Pi(\zeta, a) \right\}, \dots (43)$$

and for the finite dimensions h, m, n ,

$$h = \frac{M \text{cn } a \pi}{2 \text{sn } a \text{ dn } a} \dots (44)$$

$$\frac{m}{h} = \frac{2K'}{\pi} \left\{ \frac{\text{sn } a \text{ dn } a}{\text{cn } a} - Z(a) \right\} - \frac{a}{K} \dots (45)$$

$$\frac{n}{h} = \frac{2K}{\pi} \left\{ \frac{\text{sn } a \text{ dn } a}{\text{cn } a} - Z(a) \right\} \dots (46)$$

The expressions (44), (45), (46) agree with those given by Carter, but the remainder of the problem differs from that treated by him.

From (43) and (44) we have

$$z = \frac{2h}{\pi} \left\{ \frac{\text{sn } a \text{ dn } a}{\text{cn } a} \zeta - \Pi(\zeta, a) \right\}; \dots (47)$$

and hence using (23), (24), and (46),

$$\begin{aligned} BC &= \frac{2h}{\pi} \left\{ \frac{\text{sn } a \text{ dn } a}{\text{cn } a} (a - K) - (a - K)Z(a) \right. \\ &\quad \left. + \frac{1}{2} \log \frac{\text{sn } 2a \Theta(2a)}{\Theta(0)} - \text{Lt}_{\epsilon=0} \left(\frac{1}{2} \log \text{sn } \epsilon \right) \right\} \\ &= \frac{h}{\pi} \log \frac{\text{sn } 2a \Theta(2a)}{\Theta(0)} - n \left(1 - \frac{a}{K} \right) - \frac{l}{\pi} \text{Lt}_{\epsilon=0} (\log \text{sn } \epsilon). \end{aligned}$$

And since the length $O'C'$ is given by (28), we have for the "added length" X

$$\begin{aligned} X &= O'C' - BC - OA(h/h + m) \\ &= \frac{h}{\pi} \log \left\{ \frac{2 \text{sn } a \Theta(0)}{\text{cn } a \text{ dn } a \text{ sn } a \Theta(2a)} \right\} + n \left(1 - \frac{a}{K} \right) - \frac{nh}{h+m}. \end{aligned} \quad (49)$$

The solution given by equations (45), (46), and (49) may be checked, as before, by degeneration into marginal cases, thus:—

Case 1: $m/h = 0$.

This is obtained by putting $k = 1$, in which case X can be shown to be zero.

Case 2: $m/h = \infty$.

This is obtained by putting $k = 0$, which gives

$$\frac{n}{h} = \tan a, \quad \frac{m}{h} = \infty.$$

$$\begin{aligned} X_1 &= \frac{h}{\pi} \log \left(\frac{2 \sin a}{\cos a \cdot 2 \sin a \cos a} \right) + n \left(1 - \frac{2a}{\pi} \right) \\ &= \frac{h}{\pi} \log \left(\frac{k^2 + n^2}{h^2} \right) + \frac{2n}{\pi} \left(\frac{\pi}{2} - \tan^{-1} \frac{n}{h} \right) \\ &= \frac{h}{\pi} \log \left(\frac{k^2 + n^2}{h^2} \right) + \frac{2n}{\pi} \tan^{-1} \frac{h}{n}, \quad \dots \dots (50) \end{aligned}$$

which is equivalent to J. J. Thomson's* solution for this marginal case. It is to be noted that when $n = 0$, X becomes zero, as would be expected.

Case 3: $n/h = \infty$.

This is obtained by putting $k = 1$ and $a = K - \beta$, where β is a finite quantity, K of course being infinite. Following the procedure previously adopted, equation (49) degenerates into Lees's marginal case, *i. e.* equation (37) above.

Calculation of "Added Length."

The calculation in this case was carried out in the manner already described. In order to get a comparison with the previous case, which is of course identical with it when n is infinite, l is substituted for $(h + m)$, and curves calculated for the same values of m as before, namely $l/2$ and $3l/4$. The curves (see fig. 4) start from zero and approach their final value when n/l is of the order of unity.

IV. T-SHAPED RIB.

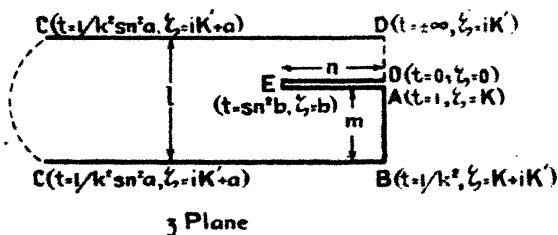
The w -plane diagram is identical with that used for the two preceding cases. The diagram in the z plane is as shown in fig. 6. Since we are concerned with both the upper and lower surfaces of OEA, these are shown separately for purposes of clearness, though, in fact, the projection OEA is infinitely thin. The third type of elliptic integral is again involved in the transformation from the z to the t plane, and hence the same sequence of descending values is adopted, as

* *Loc. cit.* p. 235.

before, for the points C, B, and A, namely $1/k^2 \operatorname{sn}^2 a$, $1/k^2$, and 1. Since it is not permissible to fix more than two absolute lengths along the axis in the t plane, or the ratios of three lengths, an arbitrary value has to be assigned to the point E, which must then be determined in relation to the constants k and a . The value at E must be less than 1, and, since the variable is to be changed to $\operatorname{sn}^2 \zeta$, the value in question is put equal to $\operatorname{sn}^2 b$. The required transformation is then

$$dz/dt = A(t - \operatorname{sn}^2 b)t^{-\frac{1}{2}}(t-1)^{-\frac{1}{2}}(t-1/k^2)^{-\frac{1}{2}}(t-1/k^2 \operatorname{sn}^2 a)^{-1}. \quad (51)$$

Fig. 6.



Putting $t = \operatorname{sn}^2 \zeta$ and $N = 2A k^3 \operatorname{sn}^2 a$, this yields on integration

$$z = N \left\{ \zeta \operatorname{sn}^2 b - \frac{1 - k^2 \operatorname{sn}^2 a \operatorname{sn}^2 b}{k^2 \operatorname{sn} a \operatorname{cn} a \operatorname{dn} a} \Pi(\zeta, a) \right\}, \quad (52)$$

no integration constant being required for the origin a and a real axis OE .

The points O and A being coincident in the z plane, we have, on putting $\zeta = K$,

$$0 = N \left\{ K \operatorname{sn}^2 b - KZ(a) \left(\frac{1 - k^2 \operatorname{sn}^2 a \operatorname{sn}^2 b}{k^2 \operatorname{sn} a \operatorname{cn} a \operatorname{dn} a} \right) \right\}. \\ \operatorname{sn}^2 b = \frac{Z(a)}{k^2 \operatorname{sn} a \operatorname{cn} a \operatorname{dn} a + k^2 \operatorname{sn}^2 a Z(a)}, \quad (53)$$

which gives the constant b in terms of a and k .

Then, since

$$l = N \frac{\pi}{2} \left\{ \frac{1 - k^2 \operatorname{sn}^2 a \operatorname{sn}^2 b}{k^2 \operatorname{sn} a \operatorname{cn} a \operatorname{dn} a} \right\}. \quad (54)$$

equation (52) may be written

$$\begin{aligned} z &= \frac{2l}{\pi} \left\{ \zeta \frac{\operatorname{sn}^2 b (k^2 \operatorname{sn} a \operatorname{cn} a \operatorname{dn} a)}{1 - k^2 \operatorname{sn}^2 a \operatorname{sn}^2 b} - \Pi(\zeta, a) \right\} \\ &= \frac{2l}{\pi} \{ \zeta Z(a) - \Pi(\zeta, a) \} \\ &= \frac{l}{\pi} \log \frac{\Theta(\zeta + a)}{\Theta(\zeta - a)}. \quad \dots \dots \dots (55) \end{aligned}$$

And for the finite dimensions m and n we have

$$\frac{m}{l} = \frac{a}{K}. \quad \dots \dots \dots (56)$$

$$\frac{n}{l} = \frac{1}{\pi} \log \frac{\Theta(b + a)}{\Theta(b - a)}. \quad \dots \dots \dots (57)$$

Further, we have

$$BC = \frac{l}{\pi} \left\{ \log \frac{\operatorname{sn} 2a \Theta(2a)}{\Theta(0)} - \lim_{\epsilon \rightarrow 0} (\log \operatorname{sn} \epsilon) \right\}; \quad (58)$$

so that the "added length," X , is given by

$$\begin{aligned} X &= O'C - (BC - OE) - OE(l/l - m) \\ &= \frac{l}{\pi} \log \left\{ \frac{2 \operatorname{sn} a \Theta(0)}{\operatorname{cn} a \operatorname{dn} a \operatorname{sn} 2a \Theta(2a)} \right\} - \frac{nm}{l - m}. \quad (59) \end{aligned}$$

The marginal cases of $n/l = 0$ and $n/l = \infty$ are dealt with below.

Case 1: $n/l = 0$.

This is obtained by putting $k = 0$, and equation (59) readily reduces to (30).

Case 2: $n/l = \infty$. ("Added Length" and Distribution.)

This marginal case does not appear to have been dealt with elsewhere, so that an independent derivation of the expression for the "added length" is given together with a computation of the flow line and isothermal distribution for one particular case ($m = 3l/4$). This calculated distribution, applying when $n/l = \infty$, allows an approximate idea to be formed of that applicable to a finite value of n , even when the latter is quite small, and is therefore useful in showing the nature of the flow in the neighbourhood of the sharp edge.

Referring to fig. 7, we have for the transformations to the t -plane from the z and w planes

$$dz/dt = Pt(t-1)^{-1}(t+a)^{-1} \quad (60)$$

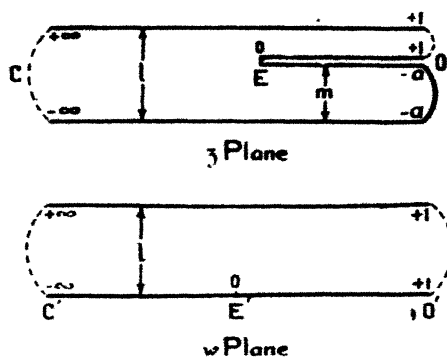
$$dw/dt = Q(t-1)^{-1} \quad (61)$$

Then, if E, E' and OC, O'O' are the respective origins and real axes, we have on integration and evaluation of the constants

$$w = \frac{l}{\pi} \log(1-t), \quad (62)$$

$$z = \frac{l-m}{\pi} \log(1-t) + \frac{m}{\pi} \log\left(1 + \frac{t}{a}\right), \quad (63)$$

Fig. 7.



where a is equal to $m/(l-m)$. Whence

$$EO = -\frac{l-m}{\pi} [\log(1-t)]_{t=1} - \frac{m}{\pi} \log\left(\frac{1+a}{a}\right). \quad (64)$$

$$EC = \frac{l}{\pi} [\log t]_{t=\infty} - \frac{m}{\pi} \log a. \quad (65)$$

$$E'O' = -\frac{l}{\pi} [\log(1-t)]_{t=1}. \quad (66)$$

$$E'C' = \frac{l}{\pi} [\log t]_{t=\infty}. \quad (67)$$

$$\therefore X = O'E' + E'C' - EC - EO(l/l-m)$$

$$= \frac{lm}{(l-m)\pi} \log \frac{l}{m} + \frac{m}{\pi} \log\left(\frac{m}{l-m}\right).$$

$$X/l = \frac{1}{\pi} \left\{ \frac{m}{l-m} \log \frac{l}{m} + \frac{m}{l} \log \frac{m}{l-m} \right\}. \quad (68)$$

For calculating the complete distribution, t must be eliminated from equations (62) and (63), so that the co-ordinates $(x+iy)$ of the z plane may be obtained in terms of those $(u+iv)$ of the w plane.

Thus from (62)

$$t = 1 - e^{u\pi/l} \{ \cos(v\pi/l) + i \sin(v\pi/l) \}, \quad . \quad . \quad (69)$$

while from (63)

$$x+iy = \frac{l-m}{l} (u+iv) + \frac{m}{\pi} \log \left[1 + \frac{(l-m) \{ 1 - e^{u\pi/l} (\cos(v\pi/l) + i \sin(v\pi/l)) \}}{m} \right]. \quad (70)$$

Hence

$$x = \frac{l-m}{l} \cdot u + \frac{m}{2\pi} \log(A^2 + B^2), \quad . \quad . \quad (71)$$

$$y = \frac{l-m}{l} \cdot v + \frac{m}{\pi} \tan^{-1}(B/A), \quad . \quad . \quad (72)$$

where

$$A = \frac{l - (l-m)e^{u\pi/l} \cos(v\pi/l)}{m}, \quad . \quad . \quad (73)$$

$$B = \frac{-(l-m)e^{u\pi/l} \sin(v\pi/l)}{m} \quad . \quad . \quad (74)$$

From these relations the coordinates of the points of intersection of the isothermals $v = 0, l/4, l/2, 3l/4$, and l , with the flow lines $u = 0, l/4, l/2 \dots$ have been calculated, and are shown in fig. 8. In order to show in greater detail the nature of the flow near the sharp edge, portions of the isothermals $v = l/8$ and $l/16$ and the flow line $u = 3l/8$ have also been calculated. It will be observed that at a comparatively short distance from the edge in either direction (see flow lines $u = \pm 5l/4$) the flow becomes practically normal.

Comparison of Boundary Distribution for 1-Ribs of Finite and Infinite Widths.

It is clear from the preceding section that the general distribution of flow lines and isothermals will be very similar in these cases, unless the width of the rib is small. An exact comparison of the distribution along the boundaries can however be made, that for the rib of infinite width being of course covered by the preceding section, and that for the

rib of finite width being deducible from equations (27) and (55). Thus from (27), since $P = l/\pi$ and $t = \text{sn}^2 \zeta$, we have

$$\text{sn } \zeta = \frac{\tanh (u\pi/2l)}{k \text{ sn } a},$$

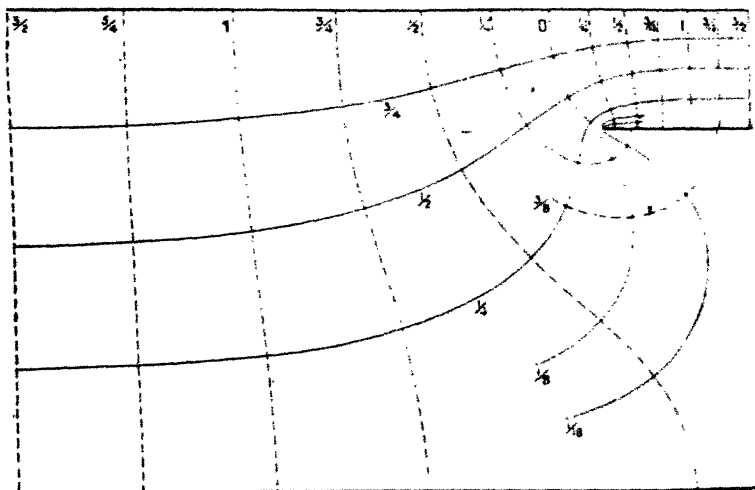
and the following deductions can be made as to boundary distribution:—

(a) *Lower Isothermal Boundary—along OE and EA (fig. 6).*

Here $v = 0$ and $y = 0$, so that

$$x = \frac{l}{\pi} \log \frac{\Theta(\zeta+a)}{\Theta(\zeta-a)}, \dots \dots \dots (75)$$

Fig. 8



where

$$\text{sn } \zeta = \frac{\tanh (u\pi/2l)}{k \text{ sn } a} \dots \dots \dots (76)$$

(b) *Lower Isothermal Boundary—along BC.*

Here $v = 0$, and the variable ζ is replaced by ϕ , where $\zeta = K + iK' - \phi$, so that

$$x + iy = \frac{l}{\pi} \log \left\{ \frac{\text{cn}(a-\phi) \Theta(a-\phi)}{\text{cn}(\phi+a) \Theta(\phi+a)} \right\} + im, \dots \dots \dots (77)$$

where

$$\frac{dn \phi}{cn \phi} = \frac{\tanh (u\pi/2l)}{\text{sn } a} \dots \dots \dots (78)$$

(c) *Upper Isothermal Boundary—along DC.*

Here $r = l$, and the new variable is given by $\zeta = iK' + \psi$, so that

$$x + iy = \frac{l}{\pi} \log \left\{ \frac{\operatorname{sn}(\psi + a) \Theta(\psi + a)}{\operatorname{sn}(a - \psi) \Theta(a - \psi)} \right\} - i(l - m), \quad (79)$$

where

$$\operatorname{sn} \psi = \operatorname{sn} a \tanh(u\pi/2l). \quad \dots \dots \dots (80)$$

The origin applicable to the finite case is O (fig. 6), while that for the infinite case is E. If we take E as a common starting-point for purposes of comparison, we have first to calculate for the finite case, from (75) and (76), the value of u at this point. The points of intersection, with the boundaries, of flow lines spaced at any desired intervals from the flow line through E, *e.g.* intervals corresponding to steps in u of $\pm l/2$, $\pm l$, etc., can then be calculated. This has been done with the result shown in the Table II. The depth of rib is the same as for fig. 8, *i.e.* $m = 3l/4$, and using a modular angle of 85° , the value of b is found to be 55.04° from (53) and $n/l = 0.280$ from (57).

It will be observed that, on the whole, there is a close agreement between the two cases given in Table II. The maximum divergence occurs where the infinite re-entrant portion of the one case is replaced in the other by the short re-entrant portion bounded by the upright line AB. Thus the flow line $u = l/2$ which in the infinite case falls on the lower boundary to the left of B, falls on the upright line AB in the finite case. The precise amount of the displacement in this region is indicated by the values given in Table II. for the flow line $u = 0.535l$, which actually passes through B in the finite case. The divergence along the portion of the lower boundary BC rapidly decreases as the distance from B increases. Along the portion of the lower boundary EO the agreement between the two cases is very close, while along the upper boundary the flow lines in the finite case are slightly displaced to the right (fig. 8), as would be expected.

With regard to the remainder of the boundary, expressions for the distribution of isothermals along OD (fig. 6) and of flow lines along AB could also be derived from equations (27) and (55).

It may be added that the cases of a finite buttress or recess could be dealt with in a similar way by use of equation (27) when combined with (17) or (43) respectively.

Calculation of "Added Length."

The calculation is made in a similar manner to that adopted in the preceding cases. From (56) we obtain directly the value r (or $90 a/K$) required to give the chosen

TABLE II.

Comparison of Boundary Distribution of Flow Lines for T-Ribs of Finite and Infinite Widths, each of depth $m = 3l/4$.

n/l	$u/$	x/l (origin E, direction EO negative) along		
		OD.	EO.	BC.
0.280	-1.0	-0.180	-0.184	—
∞		-0.179	-0.184	—
0.280	-0.5	-0.045	-0.068	—
∞		-0.044	-0.069	—
0.280	0	+0.120	0	—
∞		+0.122	0	—
0.280	+0.5	+0.378	—	— (on AB)
∞		+0.382	—	-0.187
0.280	+0.535	+0.402	—	-0.280 (B)
∞		+0.406	—	-0.053
0.280	+0.75	+0.559	—	+0.354
∞		+0.564	—	+0.374
0.280	+1.0	+0.769	—	+0.680
∞		+0.776	—	+0.692

ratio of m/l . b is then computed from (53), and n/l and X/l from (57) and (59) respectively. A series of values for the case of $m = 3l/4$ is given in fig. 4 (see curve marked T3/4), and it will be observed the "added length" shows a decrease with increase of the value of n , the final value as given by equation (68) being however reached very rapidly.

The case of $m = l/2$ admits of algebraic treatment, since it is obtained by putting $a = K/2$ or $r = 45^\circ$.

Thus, substituting the following values in (53),

$$\operatorname{sn}(K/2) = 1/\sqrt{1+k'}, \quad \operatorname{cn}(K/2) = \sqrt{k'/(1+k')},$$

$$\operatorname{dn}(K/2) = \sqrt{k'}, \quad Z(K/2) = (1-k')/2.$$

We find that $b = K/2$, while from (57)

$$\frac{n}{l} = \frac{1}{\pi} \log \frac{\Theta(K)}{\Theta(0)} = \frac{1}{\pi} \log \frac{1}{\sqrt{k'}}. \quad (75)$$

Hence, from (59),

$$\begin{aligned} \frac{X}{l} &= \frac{1}{\pi} \log \frac{2}{\sqrt{k'}} - \frac{1}{\pi} \log \frac{1}{\sqrt{k'}} \\ &= \frac{1}{\pi} \log 2; \end{aligned} \quad (76)$$

so that we have the curious result that, for the case of $m = l/2$, the "added length" is a constant independent of the value of n . This result is confirmed by the values given by equations (30) and (68) for the marginal cases of $n = 0$ and ∞ .

Comparison of "Added Lengths" of Buttress, T-Rib, and thin Rib.

The second of these cases differs from the first in that it has the additional re-entrant portion of sides EA, AB (see fig. 6). This re-entrant portion obviously produces a decrease in the total heat-flow, the precise magnitude of which for the two cases of $m = l/2$ and $3l/4$ is indicated by the distance apart of the B and T curves on fig. 4. The calculation of the complete curves, like those shown on fig. 4, for a series of values of m/l would be very laborious; but since the final value of the "added length" in either case is very nearly attained for comparatively small values of n/l , a close idea of the values in the two cases may be obtained by using equations (37) and (68), which give these final values, i. e. for $n/l = \infty$.

A series of values has accordingly been calculated on this basis, and is given in Table III., together with those obtained from equation (30) for the single thin rib which is the limiting form of both buttress and T-rib when $n/l = 0$.

It will be observed that, for values of m/l up to 0.5, the added length for the T-rib falls intermediate between those for the other two cases, while for greater values of m/l it is

less than for the others, being in the limit when $m = l$, one-half of the added length for either of the other cases.

TABLE III.

Comparison of "Added Lengths" of Buttress, T-Rib, and thin Rib.

m/l .	Values of X/l for		
	$n/l = 0$.	$n/l = \infty$.	
	Thin rib.	Buttress.	T-rib.
0.1	0.0079	0.0122	0.0115
0.25	0.050	0.065	0.060
0.5	0.221	0.250	0.221
0.75	0.611	0.650	0.587
0.9	1.181	1.222	0.929
$1 - \frac{1}{p}$ ($p \rightarrow \infty$)	$\frac{2}{\pi} \log p$	$\frac{2}{\pi} \log p^*$	$\frac{1}{\pi} \log p$

* Lees, Phil. Mag. xvi. p. 739 (1908).

GENERAL NOTE ON SIMILAR CASES.

The cases dealt with above fall under the general head of polygons, the boundaries of which consist of two isothermals, at different temperatures, together with two flow lines joining the ends of these isothermals. The method of solution consists in transforming, through an intermediate plane, the polygon into a rectangle, the opposite sides of which form the pair of isothermals or flow lines, as the case may be, and in which the complete isothermal and flow-line distribution is therefore rectilinear. According to the boundary conditions, the final rectangle will be finite, or semi-infinite or infinite along one axis, or infinite along one axis and semi-infinite along the other. The first case occurs when none of the two boundary isothermals or two boundary flow lines is situated entirely at infinity, while the other three cases occur respectively when one, a pair, or three of the boundary

isothermals or flow lines are so situated. There is also the special case where a boundary flow line or isothermal is of zero length, *e. g.* a point source. The rectangle appropriate to this case would be semi-infinite, the point isothermal or flow line of the z plane becoming the side of the rectangle at infinity. Examples of transformations from the w to the t plane applicable to the first three cases described above are equations (7), (27), and (62). It will be seen that the finite rectangle involves the first type of elliptic integral and the other cases simpler functions. In the fourth case, which is infinite along one axis and semi-infinite along the other, the rectangle becomes in fact one-half of the intermediate (t) plane, so that the final transformation to the w plane is rendered superfluous.

The transformation from the z to the t plane is, of course, more diverse in type and, as a general rule, more difficult of manipulation than that from the w to the t plane. It may, however, be pointed out that the cases of the buttress, recess,

Fig. 9.



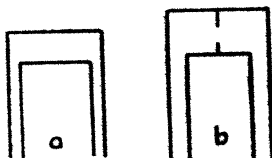
and T-rib treated above have the common feature of a z -plane transformation involving in part the third type of elliptic integral, and that this fact, together with the common w -plane transformation, has resulted in the first term in the expression for the "added length" being identical in the three cases (see equations (29), (49), and (59)).

Attention may also be drawn to the method, followed where appropriate throughout this paper, of deriving the z -plane transformation from a diagram obtained by dividing the figure by a line or lines of symmetry instead of using the complete original form. While this method of treatment has been of no immediate advantage in these particular instances, there are problems in which it results in considerable simplification, and in any event it serves to show the inter-connexion between cases apparently dissimilar. Thus, as already mentioned, Carter found it convenient, in dealing with the problem illustrated in fig. 9, to make use of the z -plane transformation applicable to fig. 1 (*c*), both these

figures giving the contour of fig. 5 on insertion of lines of symmetry. The boundary distribution of flow lines and isothermals would not be identical in the two cases, but this would not affect the z -plane transformation, but merely the second and simpler transformation from t to w plane

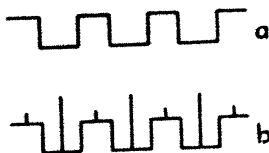
In a similar way the z -plane transformation applicable to fig. 5 will also apply to figs. 10 (a) and (b), in the latter case

Fig. 10.



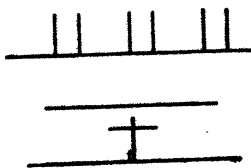
with the omission of either of the short upright lines if desired. Examples of problems covered by the z -plane transformation of fig. 3 are shown in fig. 11. Of these,

Fig. 11.



(a) and (b) are understood to have the second isothermal boundary at infinity, while in the case of (b) the alternate upright lines may be omitted if desired. Fig. 12 indicates problems governed by the z -plane transformation of fig. 6.

Fig. 12.



Finally, it may be pointed out that, since the complete system of the isothermals in any case is interchangeable with that of the flow lines, the solution of any problem gives that of the cognate problem obtained by effecting this interchange.

LV. *Experiments on a Ferromagnetic Compound of Manganese and Arsenic.* By L. F. BATES, B.Sc., Ph.D.,
Lecturer in Physics, University College, London*.

IN an examination of the thermal and magnetic properties of a ferromagnetic substance consisting of equal parts of manganese and arsenic, the writer† found that the specific heat of the substance rose from a value of 0.12 in the neighbourhood of 28° C. to a value of about 0.14 at 36° C., thence with increasing rapidity to a value of about 1.0 at 42° C., and then fell rapidly to a value of 0.13 at 45° C. The maximum value of the specific heat was found at 42.2° C. It was also found that the rate of decrease of the intensity of magnetization with rise in temperature, dl/dT , was a maximum at 42.2° C., whereas dI^2/dT was a maximum at 41.5° C. According to the Weiss theory of ferromagnetism, the specific heat of a ferromagnetic substance should exhibit a maximum at the temperature at which dI^2/dT is a maximum.

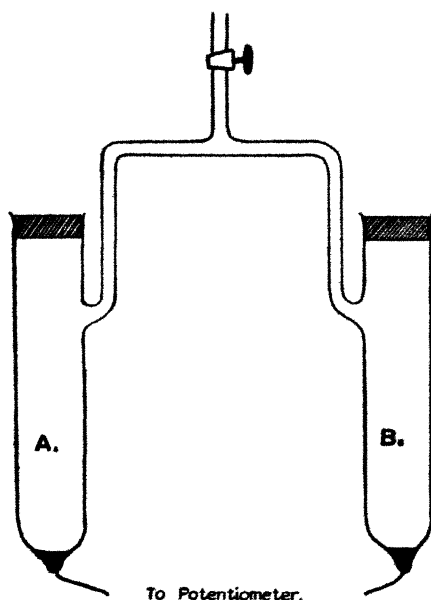
It was therefore hoped that further information would be obtained from experiments carried out on the following lines. A glass apparatus of the form shown in fig. 1 was constructed. Very short platinum wires were sealed through the lower ends of the vertical tubes. Some of the substance was placed in these tubes, so that the platinum leads were completely covered. The apparatus was then filled with a solution containing 40 c.c. of decinormal hydrochloric acid and 60 c.c. of distilled water, in which was dissolved 4.44 gm. of manganese chloride. A cork was fitted to each tube, and through that in tube A there passed a thermometer whose bulb rested in contact with the substance. The tube A was placed in a glass vessel containing paraffin and provided with an electrical heater, stirrer, and thermometer, whilst the tube B was placed in a glass vessel and surrounded with ice. The potential difference between the two electrodes was frequently determined as the temperature of the tube A was slowly raised. Curve *a* (fig. 2) shows a typical set of determinations, obtained after the substance had been in contact with the solution for some days. It will be observed that as the temperature rose the electrode A was at first positive with respect to the electrode

* Communicated by Prof. Alfred W. Porter, F.R.S.

† Bates, Proc. Roy. Soc. A, cxvii. p. 680 (1928).

B, the potential difference gradually reached a maximum and then decreased slowly, until in the neighbourhood of 40°C . it began suddenly to decrease, attained a minimum and negative value and again increased. The phenomenon was not a simple one, for the shape of the curve depended on the rate at which the temperature was raised during the set of observations. Thus curve *b* (fig. 2) shows the type of curve which was obtained when the temperature of the tube A was raised about four to five times as quickly

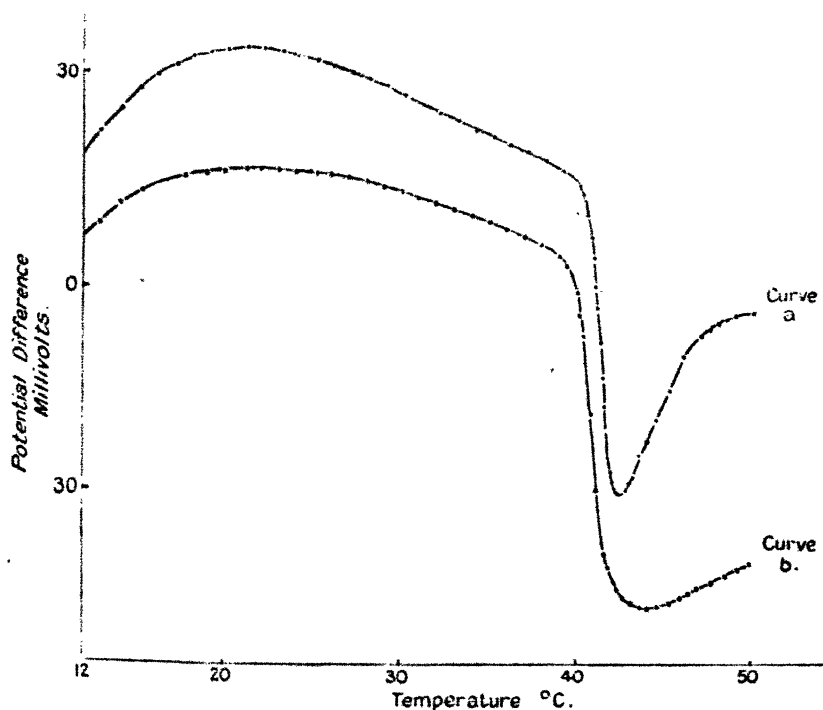
Fig. 1.



as in curve *a* (fig. 2). Curves of an intermediate form were obtained when the rate of rise of temperature was between the rates for curves *a* and *b*. Some further information was obtained from a set of observations made as follows. The temperature of tube A was raised slowly to 21°C ., and then maintained constant for forty-five minutes. During this interval of time the electrode A became considerably less positive. The temperature was then slowly raised to 29°C ., and the potential at the end of an equal interval of time again showed a considerable change in the same direction. This behaviour continued at each stationary temperature until a temperature of approximately 41°C . was reached,

where, during the forty-five minutes for which the temperature was maintained constant, the potential of the electrode A became considerably more positive. Similar changes were always observed when the temperature was above 41°C . These changes were no doubt due to polarization phenomena. When the temperature of the tube A was raised more and more quickly, the polarization phenomena would be less and less completely established, and this

Fig. 2



Note.—The ordinates of curve *b* have been displaced downwards by 30 millivolts.

would contribute a great deal to the differences between curves *a* and *b* (fig. 2). Now the substance exhibits pronounced temperature hysteresis, the ferromagnetic properties disappearing completely at 45°C . when the temperature is raised from 0°C ., and reappearing at 34°C . when the substance is cooled. The behaviour of the potential difference was therefore followed when the tube A was initially heated

to 54° C. and then allowed to cool. At 34° C. there was a sudden change in the potential of the electrode A, the electrode becoming more negative and reaching its most negative value at about 30° C., after which it became more positive. The changes, however, were very much less marked than those previously described. Such cooling experiments were difficult to carry out in a satisfactory manner, and the results were very difficult to interpret.

Discussion.

The above curves indicate in a striking manner the existence of a critical point in the neighbourhood of 42° C. Polarization phenomena, of course, make the interpretation of the results somewhat difficult. Let us assume, however, that we are dealing with a reversible electrode, and that q is the amount of heat liberated when an amount of the substance carrying unit charge of electricity goes into solution. Then the relation $T(d^2E/dT^2) = -dq/dT$ should be obeyed. Included in the quantity q is the energy of demagnetization, and thus dq/dT must contain the corresponding rate of change. According to Weiss this is directly proportional to dI^2/dT . Consequently, on this theory, $T(d^2E/dT^2)$ should exhibit a maximum at the temperature at which the value of dI^2/dT is a maximum. Naturally, this assumes that no complicated chemical changes obscure the maximum. The above curves show that a maximum value of $T(d^2E/dT^2)$ occurs just about 42° C. In the experiments on specific heat the maximum value of the specific heat was found at 42.2° C., whilst dI^2/dT was a maximum at 41.5° C. Since the substance was investigated in the form of a powder, it was conceivable that a lag in the apparatus used for the determination of the specific heat, or poor thermal conductivity of the substance, was responsible for the difference between the experimental and the theoretical temperatures of the maximum specific heat. The present results appear to indicate that the difference is a real one. It may be mentioned here that the experiments of Sucksmith and Potter* show that the specific heat may behave in a very different manner from that predicted by the Weiss theory. Their experiments were made at high temperatures, and experimental difficulties prevented them from finding whether the maximum

* Sucksmith & Potter, Proc. Roy. Soc. cxii. p. 157 (1926).

value of dI^2/dT actually coincided with that of the maximum value of the specific heat in their experiments. It has been suggested * that the atoms of ferromagnetic metals are associated in definite groups containing ions of different valencies which possess the same magnetic moments as the ions in solid salts and paramagnetic solutions, although it now appears very doubtful † that the magnetic carriers in paramagnetic solutions are simple ions. We can only say that the above results do not oppose this suggestion. On the theory of ferromagnetism recently put forward by Honda ‡ the loss of ferromagnetism would result from a re-orientation of the nuclei of the manganese and arsenic atoms in such a way that the resultant angular momentum of the group of atoms was no longer negligibly small. Presumably the energy supplied with rise in temperature would cause destruction or modification of the group so that the individual nuclei would be free to rotate, and the resultant angular momentum of the group would be too large to permit it to be orientated by an external magnetic field. Thus on Honda's theory the rate of change of the intensity of magnetization should correspond with the rate of supply of heat with rise in temperature; and this is what was shown in the previous experiments. However, it appears that the Honda theory would require the absence of the gyromagnetic phenomena which have been firmly established by the experiments of a large number of workers.

Summary.

Experiments are described which show the behaviour of the potential difference between a ferromagnetic substance, consisting of equal parts of manganese and arsenic, and a solution containing a manganese ion. Pronounced changes occur as the substance passes through its magnetic critical temperature.

It gives me much pleasure to acknowledge the kind interest with which Professor A. W. Porter, F.R.S., followed the course of this work.

* Stoner, Proc. Leeds Phil. Soc., Jan. 1926.

† Joos, *Annalen der Phys.* lxxxv. p. 641 (1928).

‡ Honda, *Zeit. für. Phys.* xlviii. p. 691 (1928).

LVI. *Notices respecting New Books.*

Cremona Transformations. By HILDA P. HUDSON, Sc.D. (Cambridge University Press. Price 42s. net.)

THIS volume gives a connected and comprehensive account of Cremona transformations in plane and space, with their applications to problems in higher geometry, especially to the resolution of singular points of curves and surfaces and the study of contact theories. Miss Hudson's researches, on both plane and space transformations, extend over a number of years, and her contributions to this branch of mathematics are well known. The bibliography shows in some measure the wealth of material largely incorporated in this work. Reference is made to Coble's report on Cremona transformations, and applications to algebra, geometry, and modular functions. All the important results of modern investigators are here collected and classified, and in this way valuable service has been rendered to workers in this special branch of geometry. An interesting chapter is devoted to the history and literature of the subject and attention drawn to problems which await solution. This volume is a worthy companion of the mathematical treatises already published by the University Press.

Theory of Vibrating Systems and Sound. By IRVING B. CRANDALL, Ph.D. (Macmillan & Co., St. Martin's St., London. Price 20s. net.)

Dr. CRANDALL's book is largely based upon the lectures given by him at the Massachusetts Institute of Technology, and presents, in the main, a mathematical treatment of the subject of Sound. Bessel functions of various kinds, with real, imaginary, and complex arguments, are in evidence in the study of vibrations of circular membranes, cylindrical tubes, vibrating strings, and the resistance coefficients for conduits. The chapter on radiation and transmission problems deals with the end corrections for a tube and the study of conical and exponential horns. The investigations of P. E. and W. B. Sabine in Architectural Acoustics are largely incorporated in the final chapter. Problems on the subject matter are given at the end of the chapters.

To those interested in acoustic research, the appendix giving the recent developments, both experimental and technical, will be helpful. Reference is made to original papers contributed during the last four or five years and include such diverse subjects as telephones, resonators, and transmitters, and the numerous devices introduced during the war for submarine signalling, sound-ranging, and direction-finding.

The Acoustics of Buildings. By A. H. DAVIS, D.Sc., and G. W. C. KAYE, D.Sc. (George Bell & Sons, York House, Portugal St., London. Price 15s. net.)

THIS volume on the behaviour of sound in buildings deals with the technical aspect of the subject. The introductory chapter on the production and measurement of sound is devoted to the analysis of sounds and the characteristics of speech, and describes some of the modern instruments for the measurement of sound intensity—Rayleigh's disk, the hot-wire microphone of W. S. Tucker, and the electrostatic microphone of Wentz. The practical applications of acoustic theory are considered under various headings; the reflecting characteristics of boundaries and the method adopted in their study—some excellent photographs illustrate the sound-pulse and ripple-tank methods; reverberation, with the methods for the measurement of absorption coefficients and the correctness of defects due to echoes and reverberation. The researches of W. C. Sabine and his successors in the Jefferson Physical Laboratory, and, within the last ten years, in the Sabine Laboratory, Geneva, Illinois, and those of F. R. Watson, investigated in the National Physical Laboratory, are reviewed in the section on the measurement of sound transmission. An interesting chapter on special types of auditorium traces the development of modern practice from the open-air theatre, Greek and Roman, and discusses the acoustic properties of buildings both in England and America. By bringing together many of the most recent results of applied acoustics, the authors have placed workers in this field under a considerable obligation.

Foundations of Euclidean Geometry. By H. G. FORDER, B.A. (Cambridge University Press. Price 25s. net.)

MR. FORDER has successfully accomplished the task of erecting Euclidean Geometry on a sound yet narrow basis and has provided a connected and "rigorous" account of modern investigations, with occasional references to non-Euclidean geometries. Axioms of order and congruence are first considered, circle and parallel axioms and the theorems of Pappus and Desargues. Then follow chapters on the Analysis Situs of plane polygons and polyhedra, the theory of areas and of volumes of polyhedra. The last two chapters are devoted to Pieri's set of axioms ("La Geometria Elementare") and to the discussion of the angle-sum of a triangle, with the related theory of non-Euclidean areas. References are also given to other investigations into the foundations of Geometry which differ from that given by the author, in particular the work of Weyl and Veblen. The book closes with useful lists of symbols and axioms of order, congruence, etc. The author rightly claims that a careful study of the volume should result in a general improvement of Geometrical teaching.

Practical Physics. By T. G. BEDFORD, M.A. (Longmans, Green & Co., 39 Paternoster Row, London. Price 10s. 6d. net.)

MR. BEDFORD'S wide and varied experience as Demonstrator in the Cavendish Laboratory has been drawn upon in the compilation of this excellent text-book of practical physics—a modern “Glazebrook and Shaw.” The large number of experiments described cover the elementary portions of the subject, properties of matter, heat, light, sound, magnetism, and electricity; many of the experiments require only the simplest kind of apparatus, but even with this slender equipment a considerable degree of accuracy can be obtained. Other experiments of a more advanced character given in the additional exercises at the end of each chapter are intended for those who have completed the preliminary course. Students who have mastered the book will be well fitted to undertake the experimental work in elasticity, optics, etc. in Dr. Searle's well-known volumes.

Electric Rectifiers and Valves. By Prof. A. GÜNTHERSCHULZE. Translated by N. A. DE BRUYNE, B.A. (Chapman & Hall, 11 Henrietta St., London. Price 15s. net.)

MR. DE BRUYNE'S book is both a translation and revision of Prof Güntherschulze's “Elektrische Gleichrichter und Ventile.” The first part of the book, the physical theory section, sets out the principles of valve-action and brings under review the introductory study of atomic structure, electric conduction in gases, electron production (photo-electric, thermionic, and glow), arc and spark discharges, and electrolytic rectifiers. The second part, technical section, opens with a chapter on the mathematical theory of valves, giving in particular the equations for various arrangements of valve circuits. Mechanical and electrolytic rectifiers are briefly noticed, followed by an account of the Wehnelt rectifier and the different types of mercury arc rectifiers. A table is given showing the useful ranges of different kinds of rectifiers. The publishers have rendered good service by adding this volume to their series of technical manuals.

[The Editors do not hold themselves responsible for the views expressed by their correspondents.]

THE
LONDON EDINBURGH. AND DUBLIN
PHILOSOPHICAL MAGAZINE
AND
JOURNAL OF SCIENCE.

[SEVENTH SERIES.]

OCTOBER 1928.

LVII. *The Separation of Isotopes and a Further Separation of Mercury by Evaporative-Diffusion.* By WILLIAM D. HARKINS, Ph.D., Professor of Physical Chemistry, University of Chicago, and BERNARD MORTIMER, Ph.D.*

I. INTRODUCTION : SEPARATION OF ISOTOPES BY
DIFFUSION.

THIS paper describes a method by means of which the isotopes of mercury may be partially separated by a process which is rapid in comparison with other processes which have been used elsewhere. The separation attained is of the order of 0.2 unit of atomic weight, but it would not be difficult, though it would be costly, to attain a separation of a unit if sufficient assistance were available for the work.

The only general method which has thus far proved successful in actually separating isotopes is that of diffusion. While a few isotopic atoms are separated from each other by the use of positive rays, they are almost immediately shot into paper or metal from which they cannot be segregated, so that no material, not even an unweighable amount, is separated. However, it seems probable that the current carried by the positive rays can be increased, at least with some elements, to such an extent as to give perceptible amounts of material. Isotopes may be separated by vaporization at a low pressure, but this is a diffusion process in which the surface acts as a membrane with pores of molecular dimensions.

* Communicated by the Authors.

The first work which was definitely shown to have given a separation of isotopes, that is, a change of the atomic weight of the element, is that of Harkins and Brooker*. They obtained an increase (ΔM) of 0.055 unit in the atomic weight of chlorine, in January 1920, by the diffusion of hydrogen-chloride gas through the walls of porous churchwarden pipe-stems at atmospheric pressure in the apparatus shown in fig. 1. The cut (C) was 8000, that is, the first of the final heavy fractions produced contained 1/8000 as much hydrogen chloride as was used for the initial diffusion. The procedure is shown diagrammatically in fig. 2. The materials used for the work were extremely pure hydrochloric and sulphuric acids, and sodium bicarbonate, and purifications were made both before and after the final diffusion. Five determinations of the change of atomic weight, made by an accurate method and arranged in the order of the determination, gave values (ΔM) of 0.052, 0.059, 0.057, 0.55, and 0.53 unit. Since intermediate purifications were made, and the hydrogen chloride was proved to be free from iodine and bromine, the fact that there is no general trend in one direction in the values shows that this was actually a separation of isotopes. The increase of atomic weight, based on the ordinary theory of diffusion, should have been 0.089, so the efficiency was 62 per cent.

Another separation begun even earlier, but completed later†, gave, with the same cut, an increase of atomic weight of 0.043 unit, or an efficiency of 48 per cent., while a separation of the light fraction‡ gave a decrease of 0.039 unit, with a mean efficiency of 66 per cent. These were both carried out by the use of churchwarden pipe-stems of the same general character as those used by Harkins and Brooker, and the general method used was the same.

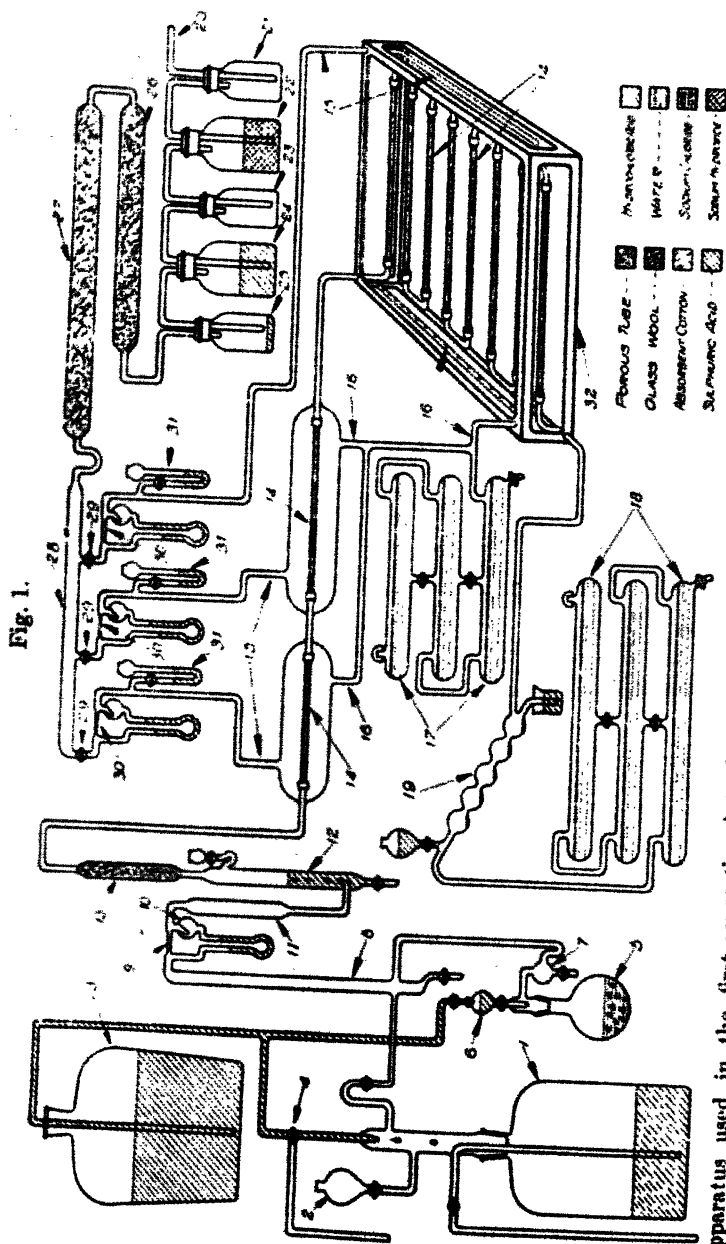
An increase in the diameter of the pores of the pipe-stems decreases the efficiency. For example, in the second separation of the isotopes of chlorine§ a cut of 12,000 gave an increase of atomic weight of 0.040 unit, with an efficiency of 36 per cent. The diffusions were carried out with great care, but it was found that the pores in the walls of the porcelain tubes, which were prepared specially for the work by the Bureau of Standards, had larger diameters, as

* 'Physical Review,' xv. p. 74 (Feb. 1920); 'Science,' li. p. 280 (1920); 'Nature,' cv. p. 230 (1920).

† Harkins & Liggett, J. Phys. Chem. xxviii. p. 74 (1924).

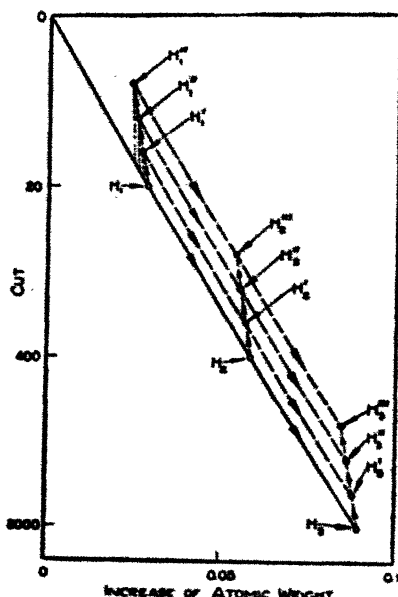
‡ Harkins & Jenkins, J. Am. Chem. Soc. xlviii. p. 58 (1926).

§ Harkins & Hayes, J. Am. Chem. Soc. xliii. p. 1083 (1921).



Apparatus used in the first separation into isotopes. Pure hydrogen-chloride gas, generated in flasks (1 or 5) on the left, passed through 12.2 metres of porous tubes of porous churchwarden pipe-stems (14), and the heavy fraction, which passed through the porous tubes, was absorbed by passing over water in the tubes 18. The first two tubes were included in separate jackets, while the remainder were in the large glass case 32. A swift air-current passed

Fig. 2.



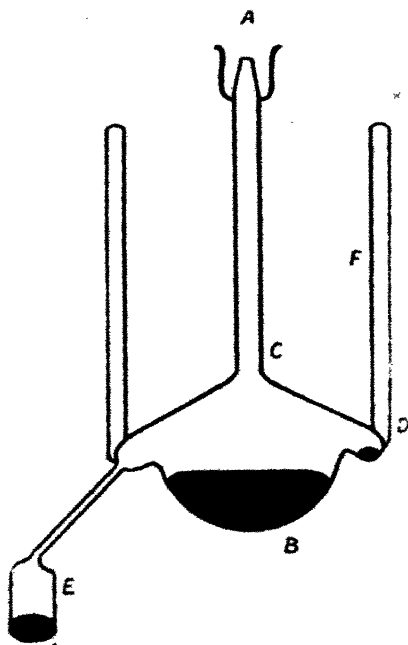
Theoretical increase of the atomic weight (x -axis) of chlorine with the cut (y -axis). The cut is the weight of the chlorine diffused divided by the weight of chlorine in the heavy fraction or undiffused residue. The number of the operation is plotted on a z -axis, so the lines represented by dashes, such as H_1' , H_2' , H_3' , are supposed to lie almost vertically above the line O , H_1 , H_2 , H_3 with the x, y plane horizontal. This line is slightly curved, though it appears to be straight. The original sample (0) is diffused with a cut of 20. The residue is represented at H_1 , while the diffusate is not shown, since it is treated in such a way as to give cuts of 2. The sample H_1 is now diffused, with a cut of 20 to give H_2 , while the remaining $19/20$ goes to H_1' . The sample H_2 is diffused, $1/20$ going to H_3 , and $19/20$ to H_2' . Thus H_2' contains the light fraction from H_2 , but it contains the heavy fraction from H_1' , since these are practically identical in atomic weight. As a result of the fact that H_2' contains two united fractions, it is much heavier than H_2 . For the reason that H_1' comes from H_1' , which is heavier, and H_2 from H_2 , which is lighter, the sample H' has 1.9 times the weight of H . The combined heavy fractions, H_3 , H_3' , H_4' , H_5' , contain 9 times the material of H_2 alone, yet their average atomic weight is only slightly less. The cut of 8000 referred to in the paper is that of the heaviest fraction H_{20} , while the atomic weights listed are those of the combined heavy fractions. Thus the greatest increase of atomic weight attained (for H_{20}) is slightly higher than that reported in the paper. The cut for H_{11}' , for example, is given by the intersection of the dotted line from H_{11}' and the line OH , that is, the point is the vertical projection of H_{11}' on the x, y plane.

revealed by microphotographs, than those of the churchwarden pipe-stems.

With pores of a given diameter the efficiency, with reference to the change of atomic weight produced by a given cut, increases as the pressure decreases. Thus at low pressures the efficiency increased to from 90 to 98 per cent.*, with diffusion walls of churchwarden pipe-stems.

It has been shown† that the value of a separation varies as the cube of the change of atomic weight attained. If

Fig. 3.



Cross-section of evaporator.

Apparatus for the separation of mercury into isotopes by vaporization at low pressures. B, heavy residue; E, light condensate; A, mercury-sealed joint for connexion to vacuum-pump; F, Dewar jacket for holding ice used for cooling.

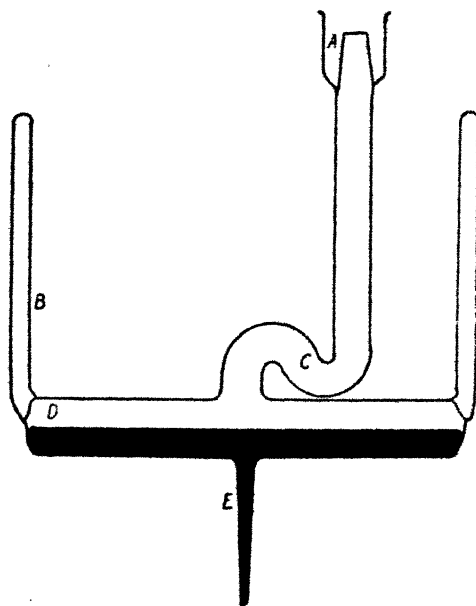
both heavy and light fractions are involved, then the value v varies as the sum of the cubes of ΔM . For example, seven months after Harkins and Broeker had attained an increase of 0.055 in the atomic weight of chlorine, Broensted and

* Harkins & Mann, unpublished work completed in 1922.

† Mulliken & Harkins, *J. Am. Chem. Soc.* xlv. p. 37 (1922); *Science*, liv. p. 359 (1921).

Hevesy obtained a minute increase of 0.006 unit and a decrease of 0.004 unit in the atomic weight of mercury. It is evident that this later separation had only about 1/600 the value of that secured earlier by Harkins and Broeker. Since Broensted and Hevesy* gave no evidence that their mercury was pure, Mulliken and Harkins† evaporated mercury (fig. 3) at low pressures and condensed it by cooling with ice and water. This gave a separation of 0.027 unit and an efficiency of separation which was found to be 80 per cent. with one type of apparatus, and proved to be 5 per

Fig. 4.



Apparatus, similar to that of fig. 3, for the experimental determination of the coefficient of separation (B) of mercury into isotopes. The distance from the upper surface of the mercury to the upper condensing surface D is kept small. This surface is cooled by liquid air or solid carbon dioxide held by the Dewar jacket B. The value of B was found to be 0.0060.

cent. higher than that of Broensted and Hevesy. Thus the efficiencies proved to be of the same order of magnitude with ice water and with liquid air as cooling agents.

What was assumed to be an efficiency 100 per cent. was obtained by the use of a special evaporator, with the

* Broensted & Hevesy, 'Nature,' cvi. p. 144 (1920).

† *Loc. cit.*

evaporating and condensing surfaces close together, as given in fig. 4. The cooling was produced by solid carbon dioxide and toluene.

Table I. gives the change of atomic weight (ΔM) obtained in four later separations of mercury into isotopes, and includes the results obtained in the work of the present paper.

TABLE I.

Later Separations of the Isotopes of Mercury, with their Relative Values.

	+M.	-M.	V+.	V-.	Value.
Broensted and Hevesy * ...	0.046	0.052	0.2 c.c.	0.2 c.c.	1.00
Harkins and Madorsky † ...	0.052	0.044	0.28	0.32	1.40
Mulliken ‡	0.0504	0.0512	22.00	22.00	121.00
Harkins and Mortimer	0.0962	0.0931	7.50	8.00	276.00

The *value* of the separation as given in the last column gives an estimate of the relative time necessary to produce the change of atomic weight obtained and the amount of material secured in the extreme fractions, that is, those which differ most in atomic weight. The relative value of the separations secured by Mulliken and by Harkins and Mortimer would be even higher if account were taken of the values of the intermediate fractions.

That large end fractions have a much greater value than those which are small may be illustrated as follows. The total separation obtained in the work described in this paper is 0.189 unit of atomic weight. However, the heaviest and lightest fractions contain about 100 grams each. By the use of a small unit of the general type described later, the atomic weight of the heaviest fraction could be increased by 0.022 unit in less than an hour, and by a few hours' work that of the light fraction could be decreased as much, so that in less than a day the total separation could easily be increased to 0.23 unit, and from the other heavy fractions this could in a few days be increased to more than 0.25 unit. This involves only the reduction of the volume of the end samples to about 0.2 c.c. That is, in the work of Broensted and Hevesy, and that of Harkins and Madorsky, the total separation attained would have been only about 0.05 unit of atomic weight if they had kept the samples as large as in

* Broensted & Hevesy, *Phil. Mag.* xliii. p. 31 (1922).

† Harkins & Madorsky, *J. Am. Chem. Soc.* xlv p. 591 (1923).

‡ Mulliken, *ibid.* p. 1592.

the present work. Their aim was to crowd all of the value in terms of change of atomic weight *alone* into the final fractions, which means that the work could not be continued farther in a systematic way; while in the present work the purpose has been to leave as uniform a set of fractions as possible over the whole interval, so that the progress of a later much greater separation may be continued without interruption.

The separation coefficient of zinc is about three and a half times that for mercury, so it would seem that it would prove a more satisfactory element to use if a rapid separation is desired. The attempts to separate the element into isotopic fractions have, however, given less favourable results. Thus Egerton and Lee* obtained values of $\Delta M = 0.017$ and $-\Delta M = 0.018$, while Harkins and Buckner† were able to increase the atomic weight by only 0.027 unit.

II. APPARATUS FOR THE RAPID SEPARATION OF MERCURY INTO ISOTOPIC FRACTIONS.

In the attempt to obtain an apparatus which would separate isotopic fractions of mercury very much more rapidly than in earlier work, Harkins and Madorsky developed the steel apparatus shown in fig. 5. The annular trough which holds the mercury is heated by a coil of nichrome wire, upon which it rests. Fig. 6 shows a similar, larger, apparatus in which the heating is secured by a coil of wire sheathed with steel, which lies at the bottom of the mercury. By the use of the smaller unit the separation of 0.1 unit at atomic weight, already mentioned, was obtained. The large unit was used only enough to prove that it gives a high efficiency with large amounts of mercury. In this apparatus a speed of evaporation of about 100 c.c. (more than 1 kg.) per hour gives an efficiency of 90 per cent. or more in the separation of isotopic fractions, if the pressure is kept between 0.001 and 0.0001 mm. of mercury.

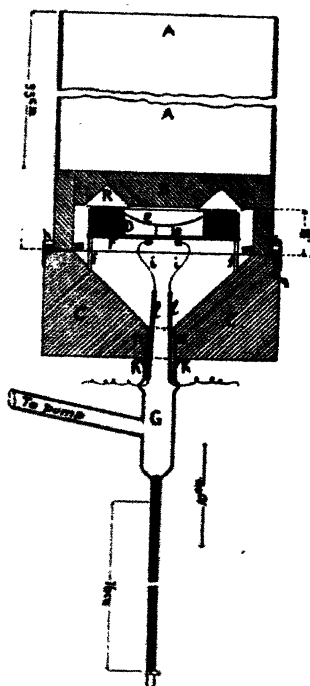
The light fraction of the mercury may be allowed to flow in a constant stream from the lower end of the glass tube at the bottom of the apparatus. This tube is bent at the bottom in such a way that it retains a column of mercury of barometric height, even if the stop-cock is kept open. This bend is not shown in the diagram. The mercury which flows from this tube is always about 0.004 unit of atomic weight lighter

* Egerton & Lee, Proc. Roy. Soc. ciii. A, p. 499 (1923).

† Harkins & Buckner, Unpublished work, begun in 1921 and completed in 1924.

than that present at the time in the trough. To prevent too much lag, this tube is made from a moderately narrow capillary.

Fig. 5.

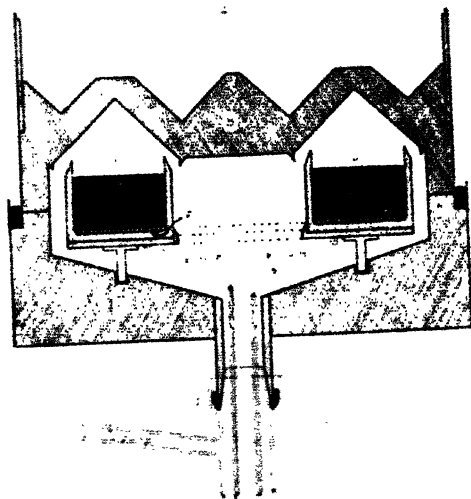


Steel vacuum apparatus for the separation of mercury into isotopes by vaporization at low pressures. B and C, parts of steel apparatus; A, mercury seal for vacuum; A, brass cylinder for ice and salt; D, annular steel trough of 190 c.c. capacity and 98 sq. cm. area of mercury surface; E, watch-glass with hole in centre for catching light fraction from inside eaves of condensing roof R. The mercury flows constantly into G, which ends below in a capillary tube of barometric height. This is bent at the bottom in such a way that mercury remains in the capillary with the stop-cock open. The heating coil F is directly underneath the trough D. In the newer models the platinum wires enter through insulating plugs through the steel base. The trough D is supported by glass rods *f*. When in operation the apparatus requires almost no attention, except for emptying the light fraction from the graduated cylinder in which it is collected about every half hour, and filling the cylinder with ice every two hours. The vacuum should be kept at about 0.0001 mm. of mercury. The apparatus has a small conical roof (not shown) at B which is used when it is desired to work with much smaller amounts of mercury. In this case a small circular trough is set on an independent heating unit in the centre of the apparatus, and the larger annular trough D is not used.

After this steel apparatus, with its attached mercury diffusion pump, backed by an oil-pump, is once set up, it is almost "fool proof," since it can be operated by a workman with almost no training. The only necessity is to keep the pressure in the apparatus sufficiently low while it is operating. With a battery of from six to twelve such units a comparatively rapid separation of the mercury may be secured.

The apparatus described above gives a separation of the mercury into samples of different density by a *diffusion* of atoms of mercury from liquid mercury, through the surface

Fig. 6.



Apparatus like fig. 5, except that the heating wires (F) are encased in steel and are in the mercury, but very close to the bottom of the trough. The area of the mercury exposed is also much larger.

of the liquid, which acts as a membrane with pores of molecular dimensions, into the gaseous phase above. If an efficiency of separation of 100 per cent. is to be attained, no atoms of mercury can be allowed to pass from the gaseous phase into the surface.

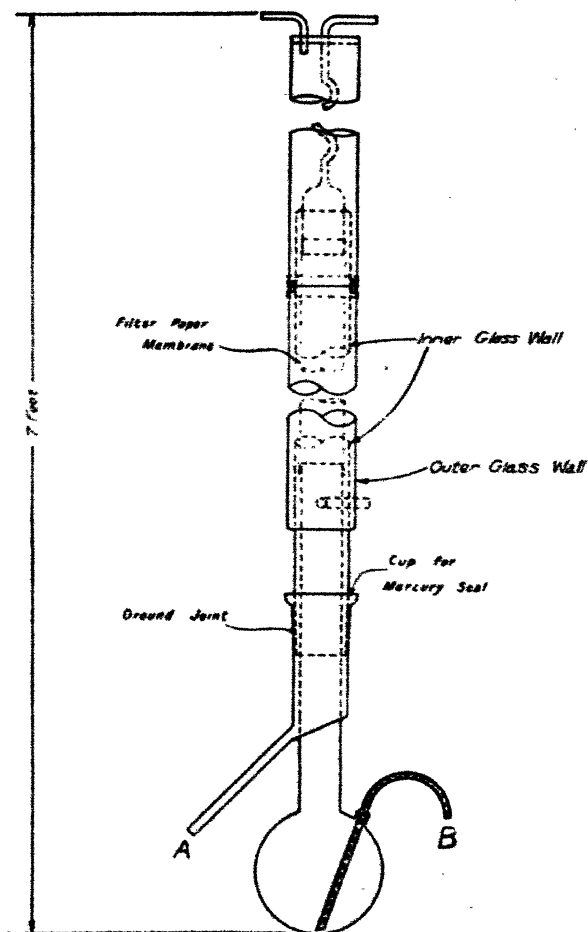
The great disadvantage of the method of evaporation at low pressures is that a considerable quantity of liquid must be used if a large area of surface is obtained, while in gaseous diffusion through a membrane a small amount of material may be diffused through a large area, which increases greatly the speed of the separation. The former method has the

additional disadvantage that a lower pressure is necessary for the same efficiency.

Combined Diffusion through a Membrane and Vaporization at Low Pressure.

In 1921 one of the writers (Harkins) constructed an apparatus which was intended to combine the separation of isotopic fractions by vaporization at low pressure with a

Fig. 7.



Apparatus for the separation of the isotopes of mercury by a combined evaporative-diffusion from the surface of mercury in the flask, and diffusion through a membrane of filter-paper. At B and A glass springs are sealed, and these lead into capillary tubes of barometric height filled with mercury. The complete unit is about 10 ft. high.

diffusion through a membrane, so that both processes might be brought about by one operation. Mercury vapour from a flask with a wide vertical neck was passed upward into a vertical tube of porous porcelain. The latter was surrounded by a double jacket of glass, between the walls of which cold water was caused to flow rapidly. The mercury condensed on the inner wall. The porcelain wall was found to possess certain disadvantages with respect to its use as a membrane. Its considerable thickness made the passage of the vapour comparatively slow. It was found, too, that if the porcelain tube was not heated by a heating coil of wire around it, mercury condensed near the outer surface, and this stopped the passage of the vapour.

An ideal membrane should be extremely thin and have extremely fine pores. The best membrane found in these respects is filter-paper (Whatman paper No. 5 was used), which, however, suffers from the great disadvantage that it is not durable. Nevertheless, six units with filter-paper tubes were built by Mulliken*, who in a few weeks of irregular operation obtained light and heavy fractions of 300 grams of mercury each, with a difference of atomic weight of 0.102 unit, an extremely large separation for so short a time.

The units used in our work were much more convenient than, though they were almost identical with, those used by Mulliken. The only important change was the substitution of a lower ground-glass joint (fig. 7) for a glass seal. This, however, reduced the time of changing the filter-paper in a single unit from 20 to 8 hours.

Six such units, set up on a single low bench and heated by extremely large Meker burners, were used. An asbestos-lined, well-ventilated iron hood, with a two-piece removable top, was fitted around each flask, in order to secure the uniformity of heating essential to keep the efficiency of the process constant.

III. THEORY OF THE SEPARATION OF ISOTOPES BY DIFFUSION.

In connexion with his work on the separation of the rare gases of the atmosphere, Lord Rayleigh† developed equations for the increase of density of the heavy fraction, or residue. These equations were put into a much simpler

* R. S. Mulliken, *J. Am. Chem. Soc.* xlv. p. 1502 (1923).

† Rayleigh, *Phil. Mag.* (5) xlii. p. 493 (1896).

form by Mulliken and Harkins*, who also developed relations for the change of density of the diffusate, that is, of the light fraction. Their general equation is

$$(1-k) \log C = k (\log (x_1)_0 - \log x_1) - \log (x_2)_0 + \log x_2. \quad (1)$$

A simpler equation,

$$\Delta M = \frac{(M_2 - M_1)^2 x_1 x_2}{cM} \ln C = D \ln C, \quad \dots (2)$$

gives a good approximation. Here $k = c \sqrt{\frac{M_1}{M_2}}$, in which c is commonly assumed to be equal to 2, x_1 and x_2 are the mol fractions of the isotopes present, and M is the mean molecular weight. The increase of molecular weight for a certain cut varies as the square of the difference of the two molecular weights, and inversely as the mean molecular weight. A more accurate coefficient is designated as B , or

$$\Delta M = B \ln C. \quad \dots (3)$$

For n identical operations the change of atomic weight of the diffusate (light fraction) is

$$\Delta M = -B \left(1 - BH \ln \frac{C}{C-1} \right) \ln \frac{C}{C-1}, \quad \dots (4)$$

in which

$$B = \frac{(1-k) x_1 x_2 (M_2 - M_1)}{x_1 + k x_2} \quad \dots (5)$$

and

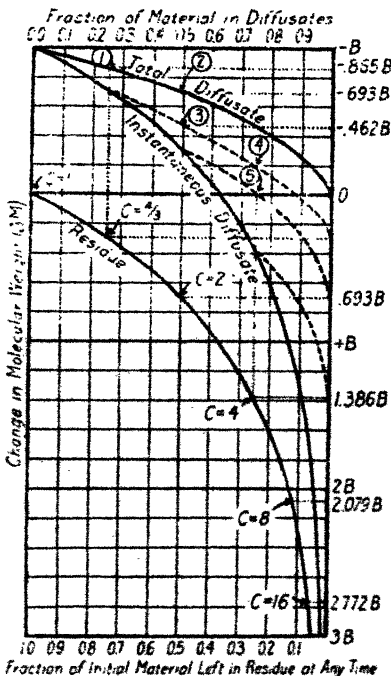
$$H = \frac{x_1 - x_2}{2 x_1 x_2 (M_2 - M_1)} \quad \dots (6)$$

The progress of a separation of isotopes up to a cut of 16 is shown in fig. 8. Equation (3) holds for any number of isotopes, but it is obvious that the expression for B is much more complicated than that given in equation (5). Fig. 9 shows the change of relative density of a number of isotopic materials as the cut progresses up to ten billion.

The above equation (3) shows the dependence of the atomic weight change on the separation coefficient B . In all known cases the coefficient B is small, which necessitates very rapid and systematically repeated operations if a large separation is to be obtained in a reasonable time. The efficiency of each individual operation is important, and is

* *Loc. cit.*

Fig. 8.

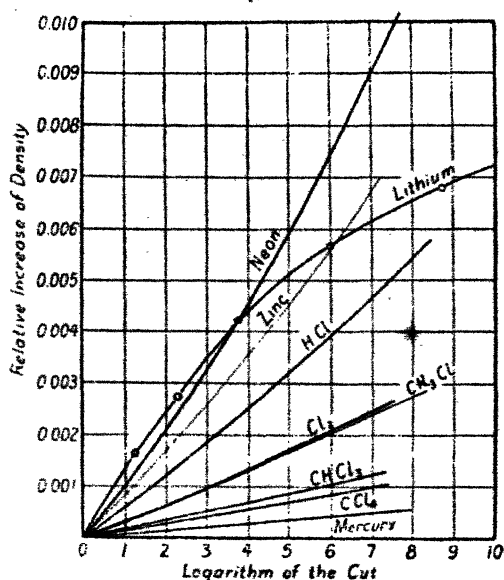


Generalized plot showing atomic or molecular weight of fractions obtained during a 100-per-cent. efficient diffusion or irreversible evaporation of a mixture of isotopes. The ordinates are expressed in terms of the "separation coefficient" B as a unit; this has a different numerical value (usually about 0.003 to 0.02) for each element. The value of B changes slightly with M . The symbol C stands for the "cut" or ratio of quantity of material in the residue at any time to the initial quantity; for any abscissa on the lower scale, the "cut" is merely the reciprocal quantity. The "instantaneous diffusate" curve gives at any point the composition of the material which is at any instant diffusing or evaporating from residual material corresponding to the same abscissa. Note that this curve has exactly the same form as the residue curve, and differs only in an upward displacement of the ordinates by B units. Each point on the "total diffusate" curve gives the average composition of the material which has diffused or evaporated from the beginning up to that point. The various dotted curves give the composition of fractions of the total diffusate beginning at various points after the beginning of the operation. The meaning of the total diffusate curves can be made clearer by a few examples. Thus, Point 1 gives the composition of the diffused or condensed fraction for the interval 0-25 per cent.; Point 2, for the interval 0-50 per cent.; 3, for 25-50 per cent.; 4, for 25-75 per cent.; 5, for 50-75 per cent. Taken in connexion with the residue curve, the total diffusate curves show how the original material can be divided efficiently into isotopic fractions. For example, the

curves show that the diffusate might be collected in fractions as follows: 0-25 per cent., $M = -0.865 B$; 25-50 per cent., $M = -0.462 B$; 50-75 per cent., $M = 0$. If the operation were stopped here, the residue would have the atomic or molecular weight $M + 1.386 B$, if M is the original atomic or molecular weight. The initial value of B is 0.0060 for mercury, 0.0095 for hydrogen chloride, 0.0049 for chlorine, about 0.002 for potassium, and 0.02 for zinc.

secured in the present apparatus by combining in successive steps two different methods of separation. The superposition of an efficient molecular diffusion on an inefficient evaporation accomplishes the effect of increased efficiency.

Fig. 9.



Relative increase of density $\frac{\Delta \rho}{\rho}$ with the logarithm of the cut.

The increase of molecular weight is equal to $\frac{M \cdot \Delta \rho}{\rho}$.

In any single diffusion the residue is enriched in the heavier isotopes, and the diffusate is enriched in the lighter isotopes. For the "instantaneous" diffusate the change in atomic weight (fig. 8) possible in this one operation is $\Delta M = -B$. Obviously, then, since B is small, large decreases of atomic weight can be secured only by repeated operations by subjecting the diffusate to many diffusions. With the residue on the other hand, large increases can be secured in a single operation by starting with sufficient

material and making a large cut. This is clearly shown by the equation which applies to the residue, $\Delta M = B \ln C$, in which ΔM depends directly on C , the cut. For an extended separation, however, regularly spaced intermediate fractions are vital, as a study of systematic fractionation will show, and so a compromise between the various attenuating factors must be sought. A cut of two is a good practical compromise for systematic fractionation. In this case

$$-\Delta M = +\Delta M = EB \ln 2 = 0.693 BE,$$

an equal and opposite change being effected in each operation. The efficiency of the process is then controlled largely by the diffusion rate, and by some artificial factors* whose effects have been very greatly minimized in the operation of the present apparatus.

IV. SYSTEMATIC FRACTIONATION.

Suppose a symmetrical fractionation procedure to be used for the division of an initially homogeneous sample into a set of fractions, all of some minimum size Q_0 , spaced at equal ΔM intervals on both sides of the initial composition M_0 . The simplest procedure† would consist of a series of individual operations, in each of which a fraction of size $2Q_0$ and composition M is divided into two fractions of size Q_0 and composition $M \pm EB \ln 2$. A study of the fractionation procedure shows that when the first $n-1$ pairs of fractions have already been produced, a total of n^2 additional unit operations will be required to produce the n th pair of fractions without permanently using up or increasing in size any of the previously-produced fractions. An example will help make this clear.

For simplicity consider the case where the inventory of the fractions of mercury is as follows:—

L3, L2, L1, zero mercury, H1, H2, H3; each of size Q_0 . L with a suitable number following designates the light fractions, and H with a suitable number designates the

* Before the scheme of systematic fractionation was in effective use, efficiency was lost by combining fractions if they differed by less than six parts per million. In the later operation there was no need for this, since the fractions were regularly twenty parts per million from each other. The loss in efficiency occurring whenever a unit is emptied and refilled was minimized by shaking the unit so that very little mercury adhered to the condenser walls, and by adjusting the siphon so that the flask emptied completely.

† Mulliken, J. Am. Chem. Soc. xlv. p. 1601 (1923) gives essentially the same discussion.

heavy fractions ; thus L1 has been produced by one diffusion by a cut of two on ordinary mercury, and H2 has been produced from ordinary mercury by two cuts of two. It is desired to produce L4 and H4, and the theory indicates that n^2 or 4^2 additional unit operations will be necessary without permanently using up any of the previously-produced fractions.

The first step is to start with a volume of ordinary mercury of size $2Q_0$ and diffuse half of it at some previously determined rate so that the diffusate will have the composition L1 and the residue the composition H1. At this point the H1 is added, and the diffusion is continued. After a cut of two has been made on this mercury, the diffusate is ordinary mercury and the residue is H2. To this the H2 is added, and the process repeated. The diffusate is now H1 and the residue is H3. With the addition of the H3 and the final diffusion, the diffusate has the composition H2 and the residue has the composition H4, provided none of the previously-mentioned causes of low efficiency was operative. These four operations have produced the H4, but have used up the H3.

The same procedure is carried out with the light mercury, with this difference : between each diffusion the unit must be emptied and refilled, thus consuming at least 50 per cent. more time to carry out the same number of operations. Since the L1 was produced at the same time as the H1, only three operations are necessary to produce the L4. By these seven distinct diffusions we have produced L4 and H4, but have used up L3 and H3, so that the inventory would be :

L4...L2, L1, zero, H1, H2, ...H4.

Applying the same reasoning to the production of L3 and H3 shows that five distinct diffusions are necessary ; to supply the L2 and H2 used up in this last process, only three diffusions are required ; and, lastly, an additional diffusion replaces the L1 and H1 used to produce L2 and H2. The inventory would now be :

L4, L3, L2, L1, zero, H1, H2, H3, H4 ;

and the total number of operations required to produce the L4 and H4 without using up any of the intermediate fractions is $7+5+3+1=16$, or 4^2 as the theory indicated. The total volume of mercury diffused in producing this n th pair of fractions is $Q=Q_0 \times 2^n$. Thus, if Q_0 is 50 c.c., as in this case, Q equals 800 c.c.

The corresponding time expended in producing the n th pair is evidently

$$t_n = n^2 \frac{(Q_0)}{(D)}, \quad \dots \quad (I.)$$

where D is the rate of production of the light fraction. Now

$$\Delta M = \pm nEB \ln 2, \quad \dots \quad (II.)$$

so that

$$t_n = \frac{(\Delta M)^2 Q_0}{E^2 B^2 (\ln 2)^2 D} \quad \dots \quad (III.)$$

The time required to produce a pair of extreme fractions is thus proportional to the *square* of the difference between its composition and that of the original raw material, and *inversely* proportional to the squares of the efficiency and of the separation coefficient. Since, in the production of extreme fractions, intermediate fractions of some minimum size must be maintained, the time of production of any extreme fraction should be taken to include the total time of production of all intermediate fractions.

$$t = t_1 + t_2 + \dots + t_n = (1^2 + 2^2 + 3^2 \dots + n^2) Q_0/D$$

or

$$t = \frac{n(n+1)(2n+1)}{6} \frac{Q_0}{D} \quad \dots \quad (IV.)$$

This equation can be used to calculate the *operating time** required to obtain any given fraction of composition ΔM , if the corresponding value of n is calculated from equation (II.). The *actual* working time required will be about *three* times this, because of the considerable time needed for repair and replacement of units, of loss of time when the units are not in operation together, of time required in starting and stopping the apparatus and in emptying and refilling units, and because of low efficiency when the air-pressure suddenly increases, thus changing the diffusion rate.

For $n=1$, t has the value $n^3 Q_0/D$; for $n=5$, t has the value $0.44 n^3 Q_0/D$; for $n=10$, $t=0.385 Q_0/D$; and for $n=\infty$, $t=n^3 Q_0/D$. Approximately, then, t is proportional to n^3 , except for the smallest values of n . We had above, $\Delta M = \pm nEB \ln 2$ (equation (II.)), giving for t

$$t = \frac{K (\Delta M)^2 Q_0}{DE^2 B^2} \quad \dots \quad (V.)$$

* Actually, it is much simpler to calculate the time by dividing the total volume which must be diffused by D , and then making the allowances suggested.

Equation (V.) shows the rapidly mounting difficulty of increasing ΔM , even by systematic fractionation; it shows the great effect of the value of B , the separation coefficient, on the possibility of obtaining a large difference in atomic weight in a moderate time; also B varies with ΔM , and there is a slight progressive decrease in the separation as it approaches completion. This shows the importance of using a method and apparatus which can deal with small intermediate fractions (Q_0), yet operate at high speed (D). Also, for a given $\Delta M/B$, t is a minimum if DE^3/Q_0 is a maximum.

V. ACTUAL FRACTIONATION SCHEME EMPLOYED *.

Because the systematic fractionation scheme on a cut of 2 had not yet been put into effective operation when this research was undertaken, considerable time was consumed in getting the fractions regularly spaced, once the efficiencies for various rates had been determined. The change in composition for diffusate and residue for a cut of two was determined for rates of 30 c.c. per hour, 40 c.c., 50 c.c., 60 c.c., and 70 c.c. per hour. At 30 c.c. per hour the rate of production of the light fraction is much too slow; at 70 c.c. per hour the life of the membrane is considerably shortened, offsetting the increased rate of production †. The practical compromise in this case was a rate of diffusion of 50 cc. (680 g.) per unit per hour on a cut of 2, in which the change in atomic weight between diffusate and residue is 0.008 unit; that is, the diffusate is 0.004 unit lighter and the residue is 0.004 unit heavier than the original material. Substitution of this value in the equation $\Delta M = 0.693 EB$ gives an efficiency of 92 per cent. This method of systematic fractionation requires a minimum number of fractions, and eliminates entirely calculations of composition.

A set of sixteen heavy fractions differing from each other by 0.004 unit of atomic weight, and a set of fifteen light fractions the same interval apart, were secured after much

* The mercury produced by Mulliken, total difference of atomic weight equal to 0.102 unit, was used in this work. The writers had cooperated in its production. The separation already attained corresponded to 12 heavy and 11 light fractions. This was increased to 25 light and 25 heavy fractions. However, many of the original 23 fractions had been used up, so much work was done in getting a complete set of these initial fractions.

† To renew a membrane takes eight hours.

diffusion, and combination of fractions less than 0.002 unit apart. At this stage the inventory was noted :

Heavy Fractions.			Light Fractions.		
c.c.			c.c.		
2550	H1	884	L1
559	H2	354	L2
199	H3	510	L3
100	H4	60	L4
108	H5	210	L5
196	H6	152	L6
49	H7	100	L7
47	H8	100	L8
49	H9	149	L9
50	H10	50	L10
54	H11	51	L11
52	H12	54	L12
47	H13	50	L13
51	H14	50	L14
54	H15	55	L15
47	H16			

The object now was to achieve the largest possible separation with this material most efficiently, that is, with the expenditure of the least time. Recourse was had to a critical detailed study of this phase of systemic fractionation. The schemes actually employed on the light and heavy side are shown in full in figs. 10 and 11. These will help to illustrate the general procedure, and will serve to clarify the important considerations.

Sunier * has shown, in his careful study of this process, that there are three factors of prime importance: (1) the starting-point; (2) the number of rows worked; and (3) the ratio of the number of cubic centimetres diffused to the number of cubic centimetres yield of the end fraction †. In general the analysis of the first two rows is an accurate guide to determine the starting-point. This was done for a number of distinct starting-points.

The first case considered was that of H2 as the starting-point for the final diffusions on the heavy side. For the

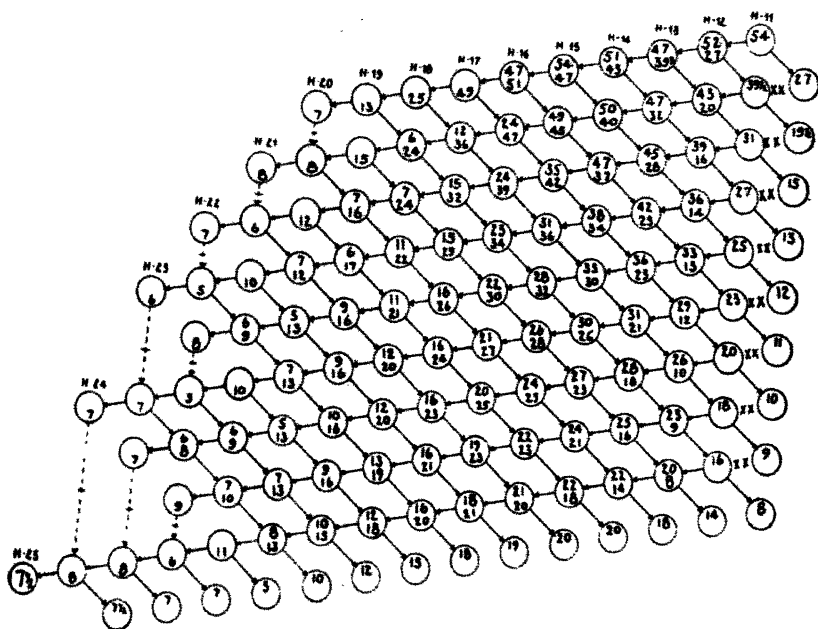
* Sunier, Doctor's Dissertation, Univ. of Chicago, Dec. 1927.

† In these final diffusions a small 200 c.c. flask was used instead of the 500 c.c. one, and it was safe to run the residue down as low as 5 c.c. (see p. 619).

first row worked, the number of cubic centimetres diffused is 1646 and the yield is 7 c.c., the ratio of 1646 to 7 being very high. For the second row the volume diffused drops to 1356 c.c. and the yield rises to 7.75 c.c., but the ratio is still too high.

The next case examined was H8. The intermediate starting-points were rejected upon application of the preliminary test, which is as follows: to produce H20 from H6, for instance, requires 20-6, or 14 cuts of 2 on H6. The

FIG. 10.



Actual fractionation scheme used on the heavy fraction.

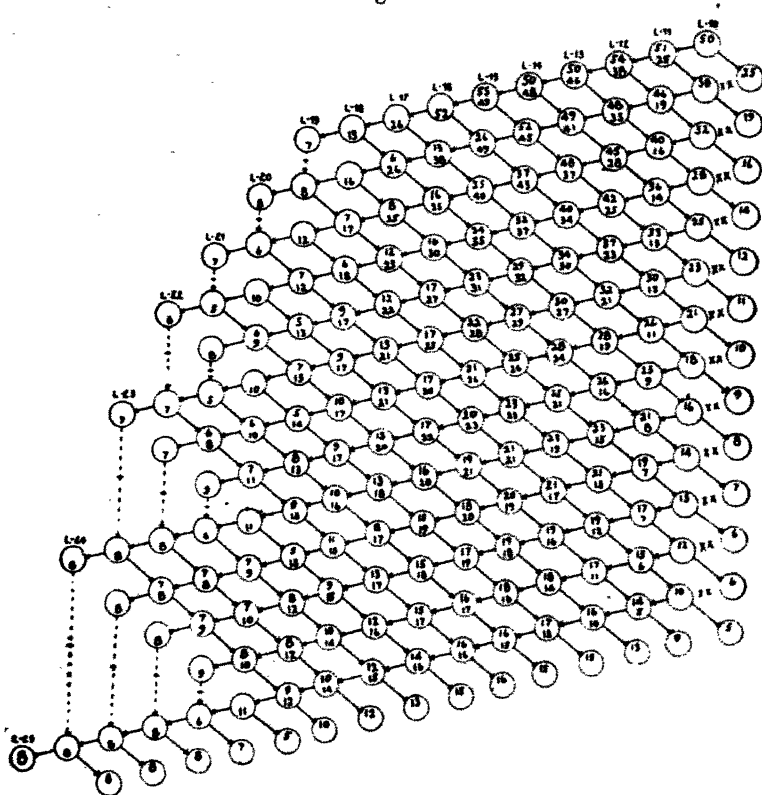
yield of H20 from H6 only in this process would be given by

$$\frac{\text{initial volume of H6}}{2^{14}}, \text{ a very small quantity. Of course,}$$

much of the material is reworked into the scheme, so that the test is not a rigorous one, but it can be used safely as a first approximation. For H8 the figures are for the first row 432/7 and for the second row 399/7.75, a considerable decrease in the volume diffused with no diminution in the yield. By elimination of other starting-points, H11 was

decided upon as the most practical and satisfactory from every point of view. In this case the ratio for the first row is 297.5 to 7, and for the second row the ratio is 262.5 to 8. In all the cases considered more material is produced in the second row than in the first row. These considerations bring out clearly the value of working more than one row.

Fig. 11.



Actual fractionation scheme used on the light fraction.

A similar examination was made of the light fraction. By a similar process of reasoning and calculating, L10 was chosen as the most practical starting-point. Before the final diffusions were begun, the densities of the starting fractions were checked to provide a means of determining just what loss of efficiency is experienced in working with small volumes. This factor was balanced somewhat by a lower diffusion rate which tends to increase the efficiency.

VI. DISCUSSION OF THE FRACTIONATION SCHEME EMPLOYED.

A. *The Heavy Fraction.*

The inventory of the heavy fractions used was :

c.c.	
54	H11
52	H12
47	H13
51	H14
54	H15
47	H16

These volumes appear as the figures in the upper part of the first six circles of the first row. The lower figure in the circle is the volume of mercury resulting from the previous diffusion. The directed arrows show where the products of each diffusion go. (The broken arrows at the end of the rows indicate the addition of mercury of identical composition before another diffusion is carried out.) Consider H12 in the first row. When half of the 54 c.c. of H11 has been diffused, the residue, 27 c.c., has the same composition as the 52 c.c. of H12. This latter volume is then added to the flask, and the diffusion is continued. Thus in any circle the upper figure represents the stock on hand, and the lower figure represents the volume resulting from the previous diffusion. The diffusion of H12 gives 39.5 c.c. of H13 as residue, and 39.5 c.c. of H11 as diffusate. The stock of H13 is added to the flask, and the process of diffusion on a cut of two is continued down through the entire row. It is understood, of course, that with the heavy fraction the process is continuous, that is, that no emptying of the unit is required between diffusions.

The 39.5 c.c. of H11 is introduced into the flask of a second unit, and the second row of this fractionation scheme is started only one diffusion behind row one. In this manner the mercury is used as quickly as it is produced. After the first row has been worked completely, the second row is only a step behind, so that the 7 c.c. of H20 which had been produced in row 1 is added to the H20 produced on the completion of row 2, and the diffusion is carried one step beyond, yielding H21. This general procedure is carried out throughout the entire fractionation, as many rows as possible being worked simultaneously.

The completion of nine full rows yielded 7.5 c.c. of H25 and the following fractions :—

c.c.		c.c.	
7.5	H23	18	H16
7	H22	19	H15
7	H21	20	H14
5	H20	20	H13
10	H19	18	H12
12	H18	14	H11
15	H17	124.5	H10

In addition there is the complete inventory of fractions from H9 down to ordinary mercury which was left untouched in this scheme.

B. The Light Fraction.

Very much more work was required to achieve the same relative separation of the light fraction, because of the more frequent emptyings and refillings necessary. To minimize the time spent in doing this, the order of progress of the fractionation scheme was modified.

The light fractions used were :

c.c.	
50	L10
51	L11
54	L12
50	L13
50	L14
55	L15

The first operation of the first row consists in diffusing half of the 50 c.c. of L10, obtaining 25 c.c. of L11 and 25 c.c. of L9. The flask is then emptied as nearly completely of L9 as possible, and all of the L11, 76 c.c., is introduced *. Two diffusions are carried out on this fraction before the flask need be emptied. The first of these yields 38 c.c. of L12 as diffusate, and 38 c.c. of L10 as

* This mixing of unlike fractions is unavoidable. The quantity remaining behind in the flask and adhering to the condenser walls is very small, yet its effect is to lower the efficiency of the process sufficiently to tell on the density. Every precaution, short of using a new apparatus for each set of diffusions, was exercised to minimize this loss of efficiency.

Separation of Isotopes by Evaporative-Diffusion. 625

residue. Another cut of two is made on the residue, after which the flask is emptied. By these two diffusions the second operation of the first row and the first operation of the second row of the fractionation scheme are consummated without emptying the unit. In the meantime the L12 had been introduced into another unit and the diffusion started, so that this unit uses the material which the first unit is producing. Thus the application of the fractionation scheme to the light fraction was down and backward, instead of out and forward, as on the heavy side. Essentially the progress of the light fraction is the same as the progress of the heavy, although more time is consumed, especially at either end of the scheme. This is due to the many more emptyings and refillings demanded.

The completion of thirteen full rows yielded 8 c.c. of L25 and the following fractions :—

c.c.		c.c.	
8 L23	15 L15
8 L22	16 L14
8 L21	15 L13
7 L20	15 L12
5 L19	13 L11
10 L18	9 L10
12 L17	148 L9
13 L16		

In addition there is the complete set of fractions from L8 down to ordinary mercury which this scheme does not embrace.

VII. THE DENSITY DETERMINATIONS.

The mercury used had been purified by prolonged agitation with nitric acid, followed by 5 distillations in a current of air at low pressure according to the method of Hulett and Minchin*, who claim that a single distillation gives a completely pure product. The first and last portions were rejected in each distillation, and a final distillation *in vacuo* was made.

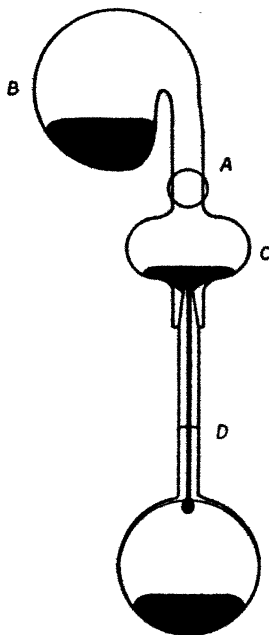
Before the final density determinations were made on L25 and H25, they were further purified. Two additional distillations, by the method indicated above, were carried out, and

* Hulett & Minchin, *Phys. Rev.* xxi. p. 388 (1905).

the middle portion from the second distillation was collected separately for the density determination *.

The pycnometer used was a small one, patterned after that devised by Harkins and Mulliken (fig. 12). The filling

Fig. 12.



Pycnometer.—The mercury is put into the bulb B; the pycnometer D is then put in place. The apparatus is evacuated by means of a mercury condensation pump. The mercury is moved in B by rotating the apparatus around the side-tube A, which connects with the vacuum-pump by means of a ground-glass joint. When a very low pressure has been attained the mercury is spilled over into C. Air is then admitted through A, and the bulb and stem of the pycnometer are filled completely with mercury. The pycnometer is then put in a thermostat at a temperature slightly above 25°. Later it is put into a thermostat at 25°·000, and the meniscus comes almost exactly to the fine mark at D. This is caused by the choice of just the proper temperature higher than 25°. The small deviation from the mark is determined by a cathetometer. By this means the relative density may be easily determined to one part in two million in the larger of the pycnometers used: in the smaller to better than 3 parts in a million.

* Additional evidence for the purity of this mercury is furnished by Dr. F. A. Jenkins, who recently completed an accurate study of the spectra of samples H16, H25, L15, and L20, the results of which are as yet unpublished. In a private communication he has informed the

device was slightly modified by the introduction of a ground joint, to allow greater ease in handling and filling the pycnometer. By filling it at a low temperature, and then allowing the mercury to overflow at a suitable temperature, calculated previously from the dimensions of the pycnometer and the coefficient of expansion of mercury, the meniscus would come approximately to the mark at 25°·000 C. Its distance from the mark was then measured by means of a travelling microscope fitted with a telescope objective, and the observed weight of the filled pycnometer is corrected accordingly. The pycnometer held 17·67110 grams of ordinary mercury. The details of the density determinations and the precautions observed are essentially those given in full by Mulliken and Harkins*.

Results of the Density Determinations.

Weight of pycnometer + dish	Average.....	14·25046
Weight of pycnometer + ordinary mercury + dish	1st	31·92155
	2nd	31·92152
	3rd	31·92158
	Average.....	31·92155
Weight of mercury		17·67110

Determinations of Density of H25.

	Weight of pycnometer + H25 + dish.	Weight of H25.	Atomic weight change.
1st determination (corrected)	31·93000	17·67955	+0·0959
2nd " " "	31·93005	17·67960	+0·0964
3rd " " "	31·93004	17·67959	+0·0963
4th " " "	31·93001	17·67956	+0·0960
5th " " "	31·93001	17·67956	+0·0960
		Average	+0·0962

From this the atomic weight of H25 is 200·706.

writers that in all his work, using various methods of exciting the spectrum, no lines other than those of mercury were ever recorded. We may regard this as a searching confirmation of the absence of metallic impurities, especially in the heaviest fraction, where even a slight impurity of the original mercury would be expected to accumulate.

* *Loc. cit*

Determinations of Density of L25.

	Weight of pycnometer + L25 + dish.	Weight of L25.	Atomic weight change.
1st determination (corrected)	31.91338	17.66293	-0.0927
2nd " " "	31.91335	17.66290	-0.0931
3rd " " "	31.91334	17.66289	-0.0932
4th " " "	31.91333	17.66288	-0.0933
5th " " "	31.91335	17.66290	-0.0931
Average			-0.0931

The atomic weight of this L25 is 200.517.

Discussion and Results.

There has been obtained 7.5 c.c., or 101.96 grams of H25 of atomic weight 200.706, an increase of 0.0962 unit. The efficiency of these final diffusions with the smaller volumes is only slightly less than that which was obtained with larger quantities. On the basis of the previously-determined efficiency of 92 per cent., the theoretical change in atomic weight would have been, for H25, 0.100 unit. The actual operative efficiency was 88 per cent. That is, in these last 14 cuts of 2, the residue, in each cut, became heavier by only 0.0038 unit, instead of 0.004 unit, a difference which is within the limits of accuracy of the density determinations. Of course, with the heavy fraction there is some *favourable* mixing of unlike fractions. For example, on completion of the first row of the fractionation scheme the flask is emptied of H20, and H11 is introduced to start another row. This mixing is very favourable, and doubtless served to reduce the loss of efficiency, even though the quantity of H20 which remains behind is very slight (see footnote, p. 616).

For the heavy fraction 8 c.c., or 108.76 grams, of L25 of atomic weight 200.517 has been obtained, with a decrease of 0.0931 unit of atomic weight. The unavoidable mixing of unlike fractions, unfavourable in this case, is reflected in the lowered efficiency. Although a smaller flask was used throughout all the latter work, this factor was not enough in itself to maintain the efficiency of the evaporation and diffusion. The theoretical change in atomic weight would have been 0.100 unit, but was only 0.0931 unit, an efficiency of 85.6 per cent. To be sure, the slower diffusion rate operative with the smaller fractions contributed somewhat to maintain the efficiency determined for larger volumes.

The existence of appreciable quantities of mercury of densities different from ordinary mercury under the same conditions offers opportunities for the investigation of the variation of properties with isotopic composition.

The lightest and heaviest fractions of the mercury ($\Delta M = 0.189$) were used by Dr. F. A. Jenkins* for the study of the wave-lengths of the lines $\lambda\lambda 5461, 4359, 4078,$ and 4047 . The intensities of the satellites were also compared. No differences were detected by the use of the 8-inch plane grating in the fifth order, or by the 30-plate Michelson echelon. Specimens of isotopic mercury have been given to the Bureau of Standards for the determination of their electrical conductance.

With isotopic chlorine ($\Delta M = +\Delta M = 0.055, -\Delta M = 0.04$) Dr. Jenkins found a shift in the direction of higher frequency for the heavy fraction. This is in accord with what was found for lead by Harkins and Aronberg†, and later by Merton‡. However, the *relative* difference in the atomic weights of the isotopic chlorine used was about three times that for the mercury, which may account for the difference in the results of the spectroscopic investigations.

Dr. Jenkins has calculated for us the change in composition of the mercury attained in the end fractions of our separation on the basis of a total change of 0.18 unit of atomic weight, which is slightly *less* than that actually obtained. The results of these calculations are given below. Recently Aston§ has succeeded in resolving the components of the mass-spectrum group of mercury, and gives the following atomic weights, with a rough estimate of the proportions:—

198 (4) 199 (5) 200 (7) 201 (3) 202 (10) 204 (2).

Assuming that the bracketed numbers represent approximately the relative numbers of atoms of each isotope, we can calculate the change in these values corresponding to a given change in atomic weight. For the best samples of mercury used in this investigation, the atomic weight differed by more than 0.18 unit. In the fractional diffusion by which these were produced the material was always cut in half, one of the resulting fractions serving as the material for the succeeding diffusion. This operation was repeated 25 times for the "heavy" fraction (atomic weight

* Jenkins, *Phys. Rev.* xxix. p. 54 (1927).

† Harkins & Aronberg, *Proc. Nat. Acad. Sci.* iii. p. 710 (1917).

‡ Merton, *Proc. Roy. Soc. A*, c. p. 84 (1921).

§ 'Nature,' cxvi. p. 208 (1925).

change +0.1), and 20 times for the "light" fraction (atomic weight change -0.08). For each of the final fractions we may apply the theoretical equations of Mulliken and Harkins* to determine the change in average molecular weight, and in relative quantity, of any pair of isotopes. Five suitably chosen pairs give a complete solution and the new isotopic composition. In obtaining the values of Table II., pairs were chosen such that the average molecular weight of each was as near as possible to that of ordinary mercury, since these decrease in amount during the fractionation at almost exactly the same rate as the total quantity of mercury. Allowance was also made for the change in the rate of separation as it progresses, since this becomes appreciable in the relatively large changes brought about for the lightest and heaviest isotopes.

TABLE II.

Isotope	198.	199.	200.	201.	202.	204.
Initial percentage	12.90	16.13	22.58	9.68	32.26	6.45
Percentage in light fraction...	14.09	17.01	23.00	9.52	30.65	5.73
Percentage in heavy fraction .	11.51	15.03	21.96	9.83	34.23	7.45

The absolute values are, of course, not as accurate as the table indicates, but are given merely to show the relative changes. The latter we may assume to be qualitatively correct, and indicate changes of 27 and 20 per cent., respectively, of the initial proportions of isotopes 204 and 198.

VIII. SUMMARY.

(1) A comprehensive survey of the separation of isotopes actually achieved has been made, and the possibilities of any larger separations have been discussed. The difference of atomic weight between samples of mercury as obtained in this work is 0.189 unit, the largest difference in atomic weight yet achieved by artificial means.

(2) The apparatus developed by Harkins and Mulliken was modified by the introduction of a ground joint between the flask and condenser, which greatly reduced the time of repair and replacement of the filter-paper membrane.

(3) The theory of isotopic resolution by evaporation and diffusion is briefly reviewed. It is shown that the change in atomic weight, ΔM , depends largely on the separation coefficient, the cut, and the efficiency.

* Journ. Am. Chem. Soc. *lxiv.* pp. 47, 51 (1922).

(4) The details of the method of systematic fractionation, with cuts of 2, used in this work, are given in detail. The time required for the production of any extreme fraction, allowing for the time necessary to build up the intermediate fractions, is given by $t = K(\Delta M)^3 Q_0 / DE^3 B^3$, in which K is a constant, B the separation coefficient, E the efficiency, and D the rate of production of the light fraction. Study of this equation shows the difficulty of obtaining large values of ΔM , especially if B is small, as it is with mercury.

(5) The completion of nine full rows of the fractionation scheme applied to the heavy fraction yielded 101.96 grams of H25, 0.0962 unit of atomic weight heavier than ordinary mercury, and a set of 23 fractions each 0.004 unit heavier progressively than ordinary mercury. The completion of thirteen full rows of the fractionation scheme applied to the light fraction yielded 108.76 grams of mercury 0.0931 unit lighter than the ordinary element; in addition there is the corresponding set of 23 fractions, each progressively 0.004 unit lighter than ordinary mercury.

(6) The existence of this isotopic mercury affords an opportunity for the investigation of the variation of properties with isotopic composition.

University of Chicago,
April 9, 1928.

LVIII. *The Relation between Kinematic Pairs and Links in a Mechanism.* By WILLIAM J. WALKER, D.Sc., Ph.D., University of the Witwatersrand, Johannesburg*.

THE usual discussion in treatises and text-books on kinematics of machinery regarding the relationship between the number of pairs and number of links in a mechanism leads to the formula

$$L = 2P - 4, \dots \dots \dots (1)$$

where L is number of links and P number of pairs.

This formula, which is based upon a somewhat arbitrary elimination of certain pairs in any mechanism, necessitates, for complicated mechanisms especially, a careful tabulation of all pairs and elements, in order to arrive at the correct

* Communicated by the Author.

632 *The Relation between Kinematic Pairs and Links.*

number of pairs P in the mechanism to be inserted in formula (1). In other words, P in that formula does not represent the actual number of pairs in a mechanism. Clearly, therefore, a formula involving P as the actual number of pairs in any mechanism, a number easy to compute without tabulation, is a desirable feature in any system of machine analysis. The following investigation of this problem leads to such a formula, and will be found to fit the link-pair relationship for any definite mechanism, however complicated.

In every case the building-up of connected chains in a mechanism consists in the addition of three turning pairs and two links for every additional quadric chain after the first. It might appear at first sight that three extra links are required, but since one of these must be a fixed link, this may be considered as embodied in the fixed link of the first or primary chain. Hence the P series for all mechanisms is

$$P=4, 7, 10, 13, \dots \text{etc.},$$

the general member of which is given by

$$P=4+3(n-1),$$

where n equals number of quadric chains. Similarly, the link series is given by

$$L=4, 6, 8, 10, \dots \text{etc.},$$

the general member of which is

$$L=4+2(n-1).$$

Eliminating n between these two equations for P and L gives

$$L = \frac{2P+4}{3} \dots \dots \dots (2)$$

The only point to be borne in mind when applying this formula is that when a number of links l furnish elements at a common point of conjunction, the number of pairs at such point of conjunction should be $l-1$. This follows naturally from the fact that one of the l links may be considered to furnish one common element, completing the pairs for the remaining $l-1$ elements.

With this strictly logical observance, formula (2) will be found of general applicability to all mechanisms.

LIX. *The Photoelectric Properties of Thin Films of the Alkali Metals.* By N. R. CAMPBELL. (Communication from the Staff of the Research Laboratories of the General Electric Company, Limited, Wembley.)

SUMMARY.

THE thin films mainly studied are those produced by depositing an alkali metal on some other material, driving it off by heat, and subjecting the remaining film to a discharge in hydrogen. By this process photoelectric cathodes can be produced that have very remarkable and stable sensitivity to red light; photoelectric currents can be obtained with light of $\lambda 8000 \text{ \AA}$ of the same order as those obtained in normal potassium cells with light of $\lambda 4500 \text{ \AA}$. The sensitivity depends very greatly on the material on which the film is deposited.

The observations are closely related to those of Ives on the photoelectric properties of thin films and to those of the many workers who have investigated the effects of gas films on photoelectric emission. The surfaces concerned almost certainly consist of a succession of monomolecular layers, similar to those of caesium and oxygen on tungsten (Langmuir and Kingdon) or of barium and oxygen or other gases (Rydé). But the conditions of their formation are exceedingly complex, and little progress has been made towards an analysis of their constitution.

The observations seem to have an important bearing upon attempts to correlate thermionic and photoelectric emission.

(1) *Origin of the Experiments.*

THE accidental interchange of the connexions of a gas-filled potassium photoelectric cell led to the observation that the photoelectric threshold of the anode lay much further towards the red end of the spectrum than that of the cathode. The area of the anode was much less than that of the cathode, yet, when the cell was exposed to diffused light through a red screen, the emission from the small electrode was greater than that from the large. It appeared at once that if the large electrode could be made as sensitive to red light as the small, the resulting cell would be very useful,

for it would make photoelectric measurements as easy at the red end of the spectrum as at the blue end.

Further inquiry showed that the difference between the two electrodes (it has been found in almost all the gas-filled cells from various sources that have been examined) arises primarily from the thickness of the layer of potassium covering them. The large electrode is covered with a massive layer, the smaller with a thin film acquired by condensation of the vapour at room temperature. The difference arising from this cause is reinforced by the passage of a discharge in hydrogen according to the Elster-Geitel sensitizing process, which doubtless has the effect (among others) of producing a gas film on the surface. Accordingly the study of the remarkable red sensitivity of the anodes of normal cells would naturally follow paths that have been partially explored by previous workers. For Ives* has studied the photoelectric properties of thin films and shown that their threshold may lie further towards the red than that of the massive material; and many workers† have shown that the removal of gas films may transfer the threshold towards the blue, and consequently that the formation of suitable layers may transfer it towards the red. Unfortunately, however, I have been unable so far to relate these observations closely to those of others and thereby to explain them; the facts that will be set forth are at present practically useful rather than theoretically significant. Accordingly it will be better to describe them as part of a completely unknown field rather than as particular illustrations of established principles.

(2) *The First Experiments.*

All the earlier experiments were made in cells of a normal type shown in *Phil. Mag.* iii. p. 947, fig. 1*b* (1927). The photoelectrically active layer is deposited on the metallic coating of a shallow cup forming the bottom of the cell, which is the cathode; a nickel gauze parallel to it serves as anode. It may possibly be relevant to record that the cells were made of borosilicate glass with molybdenum leading-in wires. During, or after, manufacture the cells could be exposed to the light from a tungsten source at about 2700° K. with the interposition of screens. The screens

* H. E. Ives, *Astrophys. J.* lx. p. 209 (1924).

† The latest are H. Klumb, *Zeit. J. Phys.* xlvii. p. 652 (1928); R. Fleischer, *Ann. d. Phys.* lxxxii. p. 75 (1927).

were those of the Wratten monochromatic series, usually No. 70, which transmits wave-lengths longer than λ 6400 Å, and No. 75, which transmits wave-lengths between λ 5400 Å and λ 4550 Å. The photoelectric current was measured by a galvanometer.

A typical experiment consisted of three or four stages each leading to a different state of the cathode. After the cell had been evacuated for an hour at 400° C., the active metal, usually potassium, was distilled into it; no elaborate precautions were taken to ensure chemical purity. The metal was deposited on the metallic coating by heating the remainder of the cell by a flame. The cathode thus covered with a thick layer of the active metal is in state A. Sometimes hydrogen was introduced at this point and the metal sensitized by the discharge; the sensitized state of the thick layer is A'. In the next stage the thick layer is driven from the cathode by the application of a small flame and deposited on the walls; a window for the entrance of the light is preserved at the top of the cell by warming it. When the thick layer evaporates from the cathode a marked change in appearance spreads over its surface; the end of the evaporation can therefore be determined sharply. The cathode is now left covered with a very thin film, such as Ives studied, which is quite invisible. If the cell is left to cool, further distillation of the potassium is apt to occur, and a visible layer may be formed again on the cathode or may obscure the window. Accordingly it is convenient to introduce hydrogen to a pressure of about 1 mm. as soon as the layer has been driven from the cathode; the gas equalizes temperatures within the cell and directs condensation to the upper portion; the window, if obscured, can be cleared again without deposition of the metal on the cathode. The cathode is now in state B. Last, the thin layer is sensitized by passing a discharge of a few milliamperes through the hydrogen with the cathode of the cell as the cathode of the discharge. The cell is now in state B'.

The photoelectric current excited by the light incident on the cell through the two screens was measured in each state. If gas was present, allowance was made for absorption of the electrons or ionization by collision, so that the numerals given, termed for brevity the red sensitivity and the blue sensitivity, are proportional to the photoelectric emission under the red and blue light. Since comparisons between the sensitivities in the various states alone are in question, no useful purpose would be served by reducing

the readings further; they are given in scale divisions. The following table gives some typical results:—

TABLE I.

State.	Blue sensitivity.	Red sensitivity.
A (thick layer)	70	< 1
A' (thick layer sensitized)	480	3
B (thin layer)	400	23
B' (thin layer sensitized)	450	600

(3) The Conditions of Red Sensitivity.

The features to which attention should be directed are these. The sensitization of the thick layer produces an increase of the red sensitivity as well as of the blue; in fact the ratio of the sensitivity in A' to the sensitivity in A is greater for the red than for the blue. The substitution of the very thin film for the thick layer reduces slightly the blue sensitivity, but increases the red; the blue sensitivity is still, however, far the greater. Sensitization of the thin film changes the blue sensitivity little, but produces an enormous increase in the red sensitivity.

If the experiment is repeated, either on another similar cell or by driving the potassium again to the cathode of the same cell and repeating the cycle, these features will recur. But the values of all the sensitivities may differ by factors as large as 2. It has been found impossible to obtain quantitative consistency, however great the precautions taken to repeat the conditions, and therefore the effects of changes in the procedure cannot be established certainly unless they are large. Nevertheless, some conclusions concerning the various states can be established.

Little need be said about states A and A', for they are well known. The blue sensitivity in state A can be increased by repeated distillation of the active metal, but no appreciable red sensitivity can be induced even when the greatest care is taken to secure chemical purity. During the passage of the discharge which produces state A' both sensitivities rise to a maximum and then fall. This maximum seems independent of the pressure of the gas or the current carried by the discharge. In general it increases with the sensitivity in the preceding state A, but the correlation is not perfect. The red sensitivity in A' is more variable than the blue.

State B is presumably the nearest approximation in these experiments to the state studied by Ives (*loc. cit.*); the sensitivity may therefore be expected to change with the time since the thin layer was formed. Some variation of the nature described by Ives is usually found, but the changes that I have observed are much smaller than his. A steady state is reached in about half an hour after the thick film is driven off; all statements refer to this steady state. The sensitivities in this state are very variable, but no connexion could be found with the procedure employed in producing it. They do not seem to depend directly on the temperature to which the cathode is heated (so long as it is sufficient to drive off the film and insufficient to soften the glass), or on the time for which the temperature is maintained, or on the presence of hydrogen while the cathode cools.

In state B' there is also sometimes an initial variation with the time since the cessation of the discharge, leading to a final steady state. (Such variations are also found in state A'.) It generally consists in a fall of both sensitivities and of the ratio of the red to the blue, but sometimes it is wholly absent. The nature and the duration of the discharge may have a marked influence on the final sensitivity, but their influence is very complex. Any discharge produces some increase in red sensitivity; the occurrence of any visible glow for a second will produce a marked effect; it is not necessary even that the surface to be sensitized should be the cathode; some sensitization will be produced if it is the anode. Further, in some circumstances a discharge of whatever nature, enduring only for a few seconds, will produce the full sensitivity of state B', which is unaffected by further passage of the discharge; the circumstances in which sensitization is thus independent of the nature of the discharge are, in general, those in which the greatest red sensitivity is attained. In other circumstances the red sensitivity depends greatly on the duration and the direction of the discharge; the sensitivity produced will now be greater if the active metal is the cathode of the discharge than if it is the anode, and there will be an optimum time of discharge that gives the greatest sensitivity, but this time will vary very greatly in different experiments.

States A and A', being those of thick layers of the active metal, are independent of the material on which the layer is deposited (as might be expected), except in so far as it may influence the purity of the metal. But states B and B' depend very greatly on this material. The results given in

Table I. (p. 636) were obtained when the underlying material of the cathode was silver, deposited chemically; experiments were also made with platinum, deposited from a platinizing solution, and with copper electroplated on silver. With platinum both the blue and red sensitivities and the ratio of the red to the blue are somewhat smaller than with silver; with copper the blue sensitivity is smaller but the red sensitivity very much greater. Lesser variations of the same kind can be produced by treatments that might be expected to change the surface composition of the cathode, although its main bulk is unaffected. Thus, if potassium is distilled repeatedly from a silver cathode, the red sensitivity in states B and B' will be reduced; at the same time, as has been noted, the blue sensitivity in state A and both the blue and red sensitivities in state A' will be somewhat increased. This treatment might be expected to remove electronegative impurities (*e.g.* oxygen) from the surface. On the other hand, if oxygen is admitted to the cell and then removed, the red sensitivity is likely to be increased. Similar changes in platinum are not so easily produced. They can be produced in copper, but not so regularly; again, oxidation of the surface seems favourable to red sensitivity, reduction unfavourable. The greatest red sensitivities were obtained when the copper was deliberately oxidized in air before the cell was pumped.

The nature of the active metal is, of course, also important, but here the relations are not those that might have been anticipated. In states A and A' the red sensitivity of caesium is much greater than that of potassium, but this is by no means true of states B and B'. The difference between states A and A', on the one hand, and states B and B' on the other, is much greater with sodium and potassium than with caesium and rubidium, and so is the difference between state A and state A' or between state B and state B', produced by sensitization. The greatest red sensitivities have been obtained with potassium on copper; sodium in state B' on copper gives as great a red sensitivity as any that I have been able to produce with caesium in any circumstances. The sensitivities, both red and blue, of caesium in state B' are so small that it is not certain that they are due to caesium rather than to traces of other alkali metals present as impurities.

Table II. summarizes some of the more important results. The three columns of figures give the photoelectric emission from various cells when similarly exposed to the light from the same tungsten source at 2700° K. through the red and

blue screens and without any screen at all. The first part of the table refers to the various alkali metals prepared in the normal manner, the cathode being covered with thick layers sensitized in hydrogen (state A'); the second part refers to various cathodes in state B'. Each cell is a favourable specimen of its class, but never the most sensitive that has been prepared.

TABLE II.

Cell.	No filter.	Photoelectric Emission.	
		Red filter ($\lambda > 6400 \text{ \AA}$).	Blue filter ($\lambda 5400-4550 \text{ \AA}$).
State A'.			
Sodium.....	2150	<0.2	40
Potassium.....	6300	<0.2	255
Rubidium.....	2250	0.4	126
Cæsium.....	830	3.7	21
State B'.			
Potassium on silver.....	950	42	23
Sodium on copper	735	14	17
Potassium on copper ...	2050	328	31
Rubidium	700	21	20
Cæsium	76	7	1.5

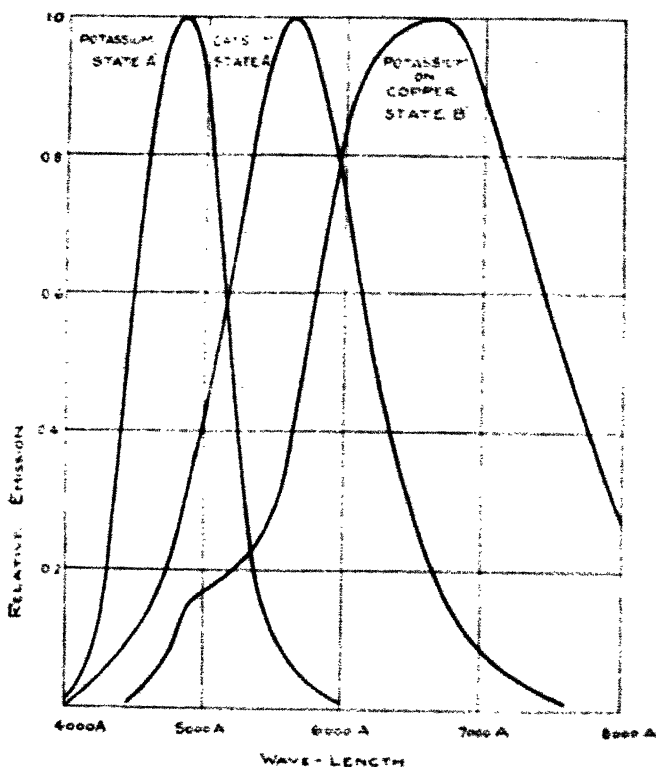
The table suggests that if maximum sensitivity throughout the whole range of the visible spectrum is required, a combination of the normal potassium cell (state A') and a potassium-on-copper cell (state B') should be used. Closer inquiry confirms this suggestion. No cell has been found which is more sensitive than both of these two at any part of the spectrum; cæsium cells, generally said to have their maximum sensitivity in the yellow, are not more sensitive than the potassium-on-copper cells even in this region.

(4) *Relation between Frequency and Sensitivity.*

So far the results have been stated in terms of the purely empirical magnitudes, red and blue sensitivities, depending upon the particular source and screen employed. For theoretical purposes they should be expressed by the relation between the frequency and the ratio of the photoelectric emission to the energy of (or possibly to the number of quanta in) the incident light. Some measurements have been made with spectrally resolved light from a source of

known energy distribution, but I do not propose at present to report them. For some unexpected difficulties have appeared, and the examination of the results of other workers on the alkali metals in states A and A' reveals serious discrepancies; it is of no use to publish further discrepant measurements unless the reason for the discrepancy can be made clear.

Fig. 1.



The Photo-Electric Properties of Thin Films of the Alkali Metals.

But it may be useful to give a few results which, while still empirical, are rather more complete. In fig. 1 the emission excited by the light issuing from the slit of a certain monochromator is plotted against the nominal wave-length. Each abscissa corresponds to light of the same quality in each curve, but the ordinate scale is different for each curve, unit emission for each curve being taken to be that for the nominal wave-length that gives maximum

emission. Curves are given for potassium and caesium in state A' and for potassium-on-copper in state B'.

It will be seen that there is every evidence that the increase in red sensitivity characteristic of the change from state A' to state B' represents a shift of the threshold towards the longer wave-lengths and not a mere change in the ratio of finite sensitivities. If a curve for potassium-on-silver in state B' were added, it would appear again that the threshold depends on the underlying material as well as on the active metal. In the curve for potassium-on-copper there are signs of an irregularity in the neighbourhood of $\lambda 5000 \text{ \AA}$; this may be compared with the double maxima shown in similar experiments by Richardson and Young on oxidized potassium sensitized by the hydrogen discharge*. But the irregularity is not so great as they found and it does not always appear; it probably indicates that the surface is not homogeneous.

(5) *A Practical Difficulty.*

It appears, then, that the potassium-on-copper cell is likely to be of great practical utility, but it has one drawback that must be mentioned. It cannot be filled with argon or other rare gas and used as a gas-filled cell, because the presence of these gases, and still more the passage of a discharge through them, destroys the red sensitivity†. On the other hand, they can be filled with hydrogen, and it is possible to obtain as great magnifications by ionization by collision in hydrogen as in argon, though they are less stable. But, as Elster and Geitel found long ago, the hydrogen gradually disappears; this was their original reason for using an inactive gas rather than hydrogen. The difficulty can be overcome partially by attaching a palladium tube to the cell through which hydrogen can be added, but this is not wholly convenient. The absorption of hydrogen is being investigated and some more convenient solution may be found. It displays some remarkable features; thus the absorption is much more rapid and persistent when the potassium is deposited on copper than when it is deposited on silver. But this matter must be left over for the present.

* O. W. Richardson & G. F. A. Young, *Proc. Roy. Soc. A.* cvii. p. 386 (1925).

† I have never seen a record of the fact, but many users of photo-electric cells must know that a similar change occurs with potassium in state A'. In an ordinary argon-filled cell, standing unused for some time, the blue sensitivity decreases while a red sensitivity develops. The passage of a discharge through the cell for a few seconds increases the blue sensitivity, but very greatly decreases the red sensitivity.

(6) *Second Series of Experiments.*

When it was clear that surface gas films were playing a large part in the process it became desirable to make experiments in conditions such that the films could be removed or controlled by the usual high vacuum technique. Accordingly cells were constructed in which the cathode consisted of a plate, well separated from the walls, which could be heated by radiation or by electronic bombardment from a tungsten filament placed behind it; the anode was again a parallel nickel gauze. The following materials were used as cathodes, each in a different cell: carbon, aluminium, iron, nickel, cobalt, copper, zinc, molybdenum, silver, tungsten, platinum, gold. In the first experiments with such cells the cathode was freed from gas as far as possible by heating before the first deposition of the active metal. State B was then produced by driving off the active metal with gentle heat, and state B' by the discharge. Potassium was used exclusively as the active metal.

To my surprise and disappointment, the development of red sensitivity proved more and not less complex, less and not more controllable, in these cells than in the type used at the outset. Moreover there were some outstanding differences between the two series of experiments. The variations of the sensitivity with the time were now much larger; in state B they were in accordance with those to be expected from the work of Ives. As the plate cooled, both blue and red sensitivities rose to a maximum and then declined; the changes in the red sensitivity were much greater than those in the blue; the maximum ratio of red to blue sensitivity occurred at about the same time as the maximum of either. Ives seems to have investigated these changes only for one metal, platinum; his comparisons of different metals refer only to the state finally attained; my experiments suggest that if he had followed the earlier stages he would have found far more difference between the various metals in the stage of maximum sensitivity than he found in the final stage. As regards the final stage my results concerning the difference between the various metals are not wholly in accordance with those of Ives, but then I have not been able to obtain complete consistency in different experiments. Ives does not say if he experienced any difficulty in repeating his results quantitatively.

In state B' similar changes occur, but more slowly. The maximum red sensitivities observed with silver, copper, and platinum (the metals common to the two series) were of the same order as those found in the simple cells, but these

high red sensitivities were never permanent. Both blue and red sensitivities, and the ratio of the red to the blue, decayed; finally they were not always higher than those obtainable in the final stage of state B.

Again the effects of the discharge were far more complex. Sometimes the state was attained in which any discharge would produce almost immediately the full red sensitivity, but now sometimes the discharge would actually decrease, instead of increasing, both the red sensitivity and the blue. An apparently exact repetition of the same experiment would sometimes produce qualitatively different results. With the molybdenum cathode the passage from B to B' was often produced by the mere presence of hydrogen; the red sensitivity increased greatly as soon as the gas was introduced, and no further increase could be produced by the discharge. Indications of sensitization by hydrogen without the discharge were observed with other metals, but in none so markedly.

Attempts to reproduce the old results were made by admitting oxygen and other gases to the plate, in the hope of forming a suitable gas film on it. The addition of oxygen, especially to some metals, increased the red sensitivity obtainable in the consequent following states B and B', but it did not make the sensitivity permanent or the effects of the discharge less complex and inconsistent. Permanency could only be attained by avoiding from the outset all attempts to free the plates from gas and by following as nearly as possible the procedure used in the simple type of cell.

(7) Results of Second Series.

In spite of all these irregularities regular differences between different materials for the cathode could be established. For instance, if they are compared on the basis of the maximum red sensitivity occurring in state B' at some time after the discharge, and if the greatest value obtained for this maximum in a series of experiments is taken, then it appears that the order of this red sensitivity is somewhat as follows: copper, zinc—cobalt, nickel—gold, molybdenum, silver, platinum—iron, tungsten, aluminium, carbon. Here the cathode is supposed to have been freed from gas as completely as possible by heating before the deposition of the potassium. It is highly improbable that all surface films were removed in all cases; thus aluminium cannot be freed from surface oxide by bombardment, zinc evaporates at a temperature certainly too low to remove gas from other

metals, and it is well known that it is almost impossible to remove the gas absorbed in the interior of copper. Indeed it is possible that from no metal was the gas perfectly removed, for the conditions were not ideal.

If, on the other hand, no attempt is made to remove surface gas, if the cell is simply baked, leaving the cathode covered, in some cases, with a visible layer of oxide, then the order is rather different. Thus iron comes up into the third group and gold into the second, but copper and zinc are still better than all others.

Some subsidiary observations may be added which may be relevant when explanation is sought. When the potassium was first distilled into the cell a visible layer would often form on every part of it except the cathode; the anode gauze would be covered by a brilliant metallic layer, while the neighbouring cathode remained unaffected. The cathode cannot have failed to condense the vapour because, being thermally insulated, it became hot, for the anode is equally insulated and of smaller thermal capacity. But if the potassium were distilled repeatedly from one part of the cell to another, with intervals of cooling (in order that the cathode might remain cool), the metal would always finally condense on the cathode. The reason for this behaviour must be doubtless sought in the work of Knudsen and his successors, and in particular of Cockcroft*, who has shown that the critical temperature for the condensation of vapours upon imperfectly clean surfaces is particularly high. For when the vapour refused to condense there was always reason to believe that the cathode was not clean, and, once it had condensed, it would always condense again readily.

When there was difficulty in condensing the vapour on the cathode it always displayed some photoelectric sensitivity before the visible layer of the active metal appeared. But in no case was the red sensitivity thus developed before full condensation as great as that developed after condensation and subsequent evaporation. Ives (*loc. cit.*) records no difference† between the properties of films formed by slow condensation and those formed by removing a thick film; probably there is no difference if the surface on which condensation occurs is clean, but there certainly may be a difference if it is not.

* J. D. Cockcroft, Proc. Roy. Soc. A, cxix. p. 293 (1928).

† Except with gold, which is permanently altered in appearance by the deposition of the active metal. My observations here agree entirely with his.

A few attempts were made to determine whether the temperature at which the visible layer of potassium disappears from the cathode was independent of the material on which the layer is deposited. The measurements were very rough, but they disclosed no great variation between different materials. It should be recorded that state B' is always destroyed, at least partially, by heating the cathode to the temperature at which the passage from A to B occurred; that is to say, state B persists at temperatures at which state B' is unstable.

(8) *Some Theoretical Considerations.*

The main object of this paper is to draw attention to a large class of interesting and practically important facts requiring further investigation. But a brief mention of some of the more obvious theoretical conclusions that they suggest may be desirable.

There can be no doubt about the general nature of states B and B'. The surface of the cathode in these states is compounded of the actual metal, the underlying material, hydrogen, and some other substances (of which oxygen is probably one) in such a manner that the photoelectric properties of the compound surface are affected by all these constituents, but that its work function may be less than that of any of them. A few years ago a suggestion that such a compound surface consisted of patches might have been plausible, but to-day it is certainly more plausible to suggest that it consists of a succession of monomolecular layers and is similar to the surfaces compounded of caesium, tungsten, and oxygen studied by Langmuir and his associates* or to those more complicated surfaces, in which barium is an element, that Ryde† has studied so exhaustively. Of course, neither Ives's experiments nor my own provide any evidence as cogent as that provided by these workers that the layers are truly monomolecular, but the onus of proof would seem to rest on anyone who would maintain that there is not an essential similarity.

Nevertheless there are differences, the chief of which is the far greater irregularity of my observations. The explanation may possibly lie in less perfect experimental conditions;

* I. Langmuir, *Phys. Rev.* xxi. p. 380 (1923); I. Langmuir and K. H. Kingdon, *Proc. Roy. Soc. A*, cvii. p. 61 (1925).

† J. W. Ryde. Paper not yet published. Ryde had reached his main conclusions before the beginning of these experiments, which were very greatly influenced by his work.

I may not have avoided sufficiently the presence of disturbing substances. But it must be remembered that my most regular results were obtained in the conditions apparently least perfect, namely in the simple cells from which the observations started. It is more likely that the difference lies in the conditions of temperature; all thermionic measurements are made at temperatures that destroy or modify profoundly the photoelectric sensitivity; the peculiarly variable surfaces that are studied here may not exist at all at these temperatures. Further, the surface compounded of monomolecular layers may be in a state of dynamical rather than statical equilibrium; interchange of material between the cathode and its surroundings may be proceeding constantly. In thermionic experiments the cathode is always hotter than the walls, in photoelectric experiments it is at the same temperature. The state of the photoelectric cathode may be influenced to a greater degree than the thermionic by variations in the state of the walls, which are very difficult to control; indeed some evidence, though it is not so far conclusive, has been obtained of a correlation between the state of the walls and the sensitivity of the cathode. Again, if the equilibrium is dynamical, the small sensitivity of caesium in state B' may be explained; the vapour-pressure of the metal may be so high that very few molecules are present on the surface at any one time. These questions must obviously be examined by experiments at different temperatures.

Concerning the exact nature or the order of succession of the monomolecular layers little can be suggested at present. Oxygen is almost certainly a constituent of some at least of the surfaces, and in state B' hydrogen ions are almost certainly another. For since normally any kind of discharge in hydrogen will produce an increase in red sensitivity, while the mere presence of hydrogen will not, the conclusion is almost inevitable that the primary function of the discharge in sensitization is the provision of hydrogen ions. Measurements have been made recently on sensitization by means of the Townsend discharge, supported by photoelectric emission from the cathode, in which the number and energy of the ions can be controlled and ascertained. The results are not very easy to analyse and, once more, will be reserved for the present, but they are consistent with the view that the change from state B to state B' is intimately connected with the arrival of hydrogen ions at the cathode. The irregular effects of the discharge are probably due to changes, other than mere ionization, that it produces; thus it may heat the

cathode or sputter material from the cathode and deposit it on the walls, or from the walls and deposit it on the cathode.

According to this view states A and A', the unsensitized and sensitized states of thick layers, must be essentially similar to states B and B'; the only difference is that in states A and A' the material of the underlying cathode is the same as that of one of the superimposed monomolecular layers. The remarkable observations of Richardson and Young (*loc. cit.*), in which they obtained great red sensitivities and a threshold in the infra-red by subjecting an oxidized potassium surface to the hydrogen discharge, are essentially similar to my own; they probably realized a state B' of potassium on potassium. The threshold that they observed was not that of potassium; that is to say, it was not that of a cathode consisting uniformly of potassium from a homogeneous interior to a boundary at which the electrons are emitted free to move under small external fields. Such a cathode is obtainable, if at all, only when the most strenuous endeavours are made to free the surface from gas; the observations of Fleischer* suggest that its threshold lies well towards the blue end of the spectrum.

These remarks are relevant when attempts are made to relate the thermionic and photoelectric properties of such metals as potassium. It is clearly very difficult to ensure that the two properties studied experimentally are those of the same surface. But a more general consideration concerning the relation of thermionics and photoelectricity may be offered; it was suggested to me in conversation by Mr. R. H. Fowler. The difference between the thermionic emission from different substances is often regarded as determined wholly by the work function. But another property must enter, namely, the emission coefficient; that is to say, the ratio between the number of electrons acquiring energy greater than the work function to the number emerging from the surface during any period. If the cathode is completely homogeneous the neglect of the emission coefficient may be justified. For then the surface will probably consist electrically of a simple rapid change of potential, all in one direction; if the emission coefficient varies from one metal to another, its variation is likely to be correlated closely with that of the work function. But if the cathode is not homogeneous, if there are several superimposed monomolecular layers at its surface, this correlation may be absent, for the work function is determined by the total change of potential through the whole series of layers,

* R. Fleischer, *loc. cit.*

while the emission coefficient may well be determined by the manner in which the change occurs. The potential may have maxima and minima within the series of layers, and these are likely to effect the emission coefficient, though they may not affect the work function.

In photoelectric emission the work function corresponds, of course, to the threshold; the emission coefficient is probably represented by the sensitivity for frequencies considerably greater than that of the threshold. In my experiments the work function is determined roughly by the red sensitivity, the emission coefficient by the blue sensitivity. Table II. (p. 639) shows that the two sensitivities are not at all closely correlated; it is not true, even in the most general way, that the cathode with the lower frequency for its threshold has the greater emission for higher frequencies; indeed, if films of the same active metal on different cathode materials are compared, the converse of this proposition is more nearly true. The mutual independence of red and blue sensitivities accords well with the theory that the surfaces are composed of successive layers; it shows also that any relation between the variation of the thermionic emission with the temperature and the variation of photoelectric emission with the frequency is likely to be far more complicated than is indicated by any of the theories that have been proposed hitherto.

*LX. Chemical Interactions corresponding to the Constant of Mass Action being a Function of the Volume and Masses of the Constituents as well as of the Temperature, and Catalytic Action.—II. By R. D. KLEEMAN, B.A., D.Sc.**

§ 1. *Introductory Remarks.*

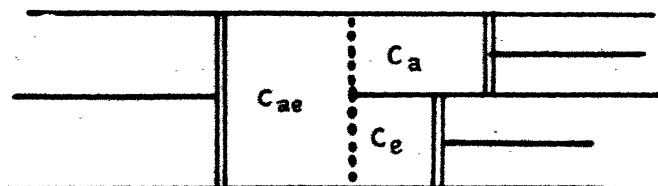
IN a previous paper † the writer has investigated some of the conditions under which the constant of mass action is a function of the volume of the gaseous interacting mixture and the masses of the constituents, as well as of the temperature. This paper is a continuation of the investigation. The reader should acquaint himself with the matter in the paper quoted.

The investigations in question are based on differential equations obtained by means of a certain isothermal cycle

* Communicated by the Author.

† Phil. Mag. vi. pp. 195-203 (1928).

which may be varied somewhat depending on the given conditions. The cycle usually involves a chamber containing the reacting gaseous mixture, separated from a number of other chambers by membranes, each of which is permeable to one of the constituents. If this number is two the apparatus has the form shown diagrammatically in the figure.



§ 2. The Effect of Small Dissociation on the Constant of Mass Action of a Gaseous Mixture.

Suppose that a mixture of M_a mols of molecules a and M_e mols of molecules e at the pressure p is contained in the chamber C_{ae} of the apparatus shown in the figure, whose volume is v . The chambers C_a and C_e are separated from the chamber C_{ae} by membranes permeable to molecules a and e respectively, the pressures in these chambers will accordingly be denoted by p_a and p_e , and the corresponding volumes of mols of molecules a and e by v_a and v_e respectively. The differential equation of the reaction with respect to the volume v as independent variable is *

$$v \frac{\partial p}{\partial v} - M_a v_a \frac{\partial p_a}{\partial v} - M_e v_e \frac{\partial p_e}{\partial v} = 0. \quad (1)$$

Let us suppose that the pressure of the free molecules a in the mixture is extremely small. The equation of state of the molecules a in the chamber C_a is then not given by

$$p_a v_a = RT, \quad (2)$$

where T denotes the absolute temperature, but by †

$$p_a v_a = \xi_a RT, \quad (3)$$

where ξ_a is a function of v_a and T , or

$$\xi_a = \phi_0(v_a, T). \quad (4)$$

ξ_a differs very little from unity except when v_a is very large, being then less than unity. For the molecules in the chamber C_{ae} , whose concentration is not small, ξ may be

* Phil. Mag. v. pp. 620-629 (1928).

† Phil. Mag. v. pp. 1191-1198 (1928).

taken equal to unity. It will now be evident from a previous investigation* of the solution of the differential equation (1) that K the constant of mass action is now obtained a function of v , even if we suppose that the other free molecules obey the orthodox gas law.

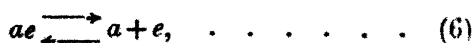
Similarly, it can be shown by means of the differential equation †

$$v \frac{\partial p}{\partial M_a} - M_a v_a \frac{\partial p_a}{\partial M_a} - M_e v_e \frac{\partial p_e}{\partial M_a} = 0 \quad . \quad . \quad (5)$$

of the reaction, in which M_a is the independent variable, that the constant of mass action is a function of M_a , and so on.

A similar result can be shown to hold for other reactions in which the concentration of one or more of the constituents is very small.

Let us, for example, consider the reaction between equal numbers of mols of molecules a and e ,



in which the concentrations of the free molecules a and e are extremely small.

The equation (29) in a previous paper ‡ can now easily be shown to have the form

$$\frac{\partial C_a}{\partial v} = \left(\frac{M_a}{v} \right) \frac{C_a}{C_a v - 2M_a \xi_a}, \quad . \quad . \quad . \quad (7)$$

supposing that $\xi_e = \xi_a$, and taking into account that $v_a = \xi_a/C_a$, where C_a denotes the concentration of the molecules a in the chamber C_{ae} §. If this equation is solved and the expression obtained for C_a substituted in the equation

$$K \left(\frac{M_a}{v} - C_a \right) = C_a^2, \quad . \quad . \quad . \quad (8)$$

also given in the paper quoted, the functional form of K in respect to v is obtained.

Since the constant of mass action can be determined only from concentration measurements, and it is difficult to measure small partial concentrations, it will be difficult to prove this result and others of the same kind experimentally.

* Phil. Mag. v. pp. 621-622 (1928).

† Loc. cit.

‡ Phil. Mag. v. pp. 626-627 (1928).

§ The gas equation (2) applies to the molecules a in the chamber C_{ae} since the total molecular concentration is not small, while the gas equation (8) applies to the molecules a in the chamber C_a . Since the pressure of these molecules is the same in the two chambers (otherwise diffusion from one chamber to the other would take place), it follows that $v_a = \xi_a/C_a$.

The constant of mass action under these conditions, it will be recognized, is very small. In a previous paper* the writer showed that the constant of mass action is approximately a function of the temperature only when the dissociation is small. The result is based on the supposition that equation (2) holds exactly. Since this is not the case the quoted result must be modified somewhat accordingly.

§ 3. *The Catalytic Effect of a Surface Absorbing Substance on the Constant of Mass Action of a Reaction.*

Let us suppose that the surface of the walls of the cylinder of the chamber C_a absorbs some of the gaseous molecules a in contact with it till a point of saturation is reached. This absorption we will suppose consists simply of the deposition of a layer of molecules on the surface which can be removed by mechanical means, such as passing another solid substance over the surface. The mass of molecules a deposited per cm.² is a function of the pressure p_a of the molecules and the temperature, and it may therefore be written $\phi(T, p_a)$. The total mass M_a' absorbed is therefore equal to

$$M_a' = A \cdot \phi(T, p_a), \quad . \quad . \quad . \quad . \quad (9)$$

where A denotes the area of the exposed surface of the cylinder.

Let us next suppose that the mixture of molecules a and e in the chamber C_{ae} is passed through the first of the two cycles described in a previous paper†. The process (a) of this cycle consists in passing the mixture into the chambers C_a and C_e at constant pressures, during which the external work

$$M_a'' v_a p_a + M_e v_e p_e - p v$$

is done, where M_a'' denotes the mass of molecules a in the chamber C_a at the end of the process, which are not deposited on the chamber walls. In the process (b) the chambers C_a and C_e are increased in volume by a small amount, during which the work

$$M_a'' p_a \cdot \partial v_a + p_a v_a \cdot \partial M_a'' + M_e p_e \partial v_e$$

is done, where M_a'' must be considered a variable since it depends on A and p_a . In the process (c) the substances a and e are returned to the chamber C_{ae} at constant pressures, giving rise to the external work

$$-(M_a'' v_a p_a + M_e v_e p_e - p v) - \partial(M_a'' v_a p_a + M_e v_e p_e - p v),$$

* Phil. Mag. v. pp. 263-271 (1928).

† Phil. Mag. v. pp. 620-629 (1928).

where M_a'' , as before, must be considered a variable. The deposited molecules a are shaved off during the process by the piston of the chamber C_a . In the last process (d) the volume of the mixture is decreased by ∂v , giving rise to the external work

$$-p \cdot \partial v.$$

On equating to zero the total external work done, we obtain the equation

$$v \frac{\partial p}{\partial v} - M_a'' v_a \frac{\partial p_a}{\partial v} - M_e v_e \frac{\partial p_e}{\partial v} = 0, \quad \dots (10)$$

which has the same form as the equation (1) obtained in the paper quoted, where M_a is replaced by M_a'' . Now

$$M_a'' = M_a - M_a' = M_a - A \cdot \phi(T, p_a) \quad \dots (11)$$

by equation (9). Hence equation (10) be written

$$v \frac{\partial p}{\partial v} - \{M_a - A \cdot \phi(T, p_a)\} v_a \frac{\partial p_a}{\partial v} - M_e v_e \frac{\partial p_e}{\partial v} = 0. \quad (12)^*$$

The other equations which are used with this equation to obtain a solution, which are given in the paper quoted, do not contain $A \cdot \phi(T, p_a)$, since when the mixture is completely in the chamber C_{ae} no molecules a are deposited on a surface. It follows, therefore, from the investigation in this paper that the solution of (12) will give K a function of v , M_a , and M_e , as well as of T , whose form with respect to v is determinate. The form with respect to M_a and M_e is determined by two equations given by the second cycle, which may be obtained from equation (12) on substituting ∂M_a and ∂M_e in succession for ∂v . *Thus a solid substance which condenses a gaseous substance on to its surface has a catalytic effect on the constant of mass action of a reaction involving the gaseous substance.*

The expression for K will also involve A . This signifies that a continual deposition and evaporation of molecules a in the chamber C_a takes place during which they undergo a process of activation at the surface, which changes their chemical behaviour. This activation of the molecules when not in contact with the surface will gradually disappear. Hence the average extent of activation of a mass of gaseous molecules will depend on the area A of the activating surface. This result is the theoretical explanation of the

* If the deposition is supposed to take place on the surface of the chamber C_{ae} and we suppose that the mass $A \cdot \phi(T, p_a)$ is deposited while the mass M_a is in the gaseous state, the corresponding differential equation, as can easily be shown, is obtained from equation (12) on changing the sign of the term $A \cdot \phi(T, p_a)$

result observed long ago that the activity of a catalytic agent depends largely on the area of the exposed surface.

§ 4. *The Catalytic Effect of a Bulk Absorbing Substance on the Constant of Mass Action.*

Let us suppose, as was done in a previous paper*, that the walls of the chamber C_a are permeable to molecules c which are contained in an adjacent reservoir of infinite dimensions. The presence of the molecules c may affect the nature of the molecules formed from the molecules a in the chamber, especially if the molecules c are in a dense or liquid state. It is well known that dissociation or polymerization of the molecules of a gas absorbed by a liquid or solid may take place. The osmotic pressure p_a' of the molecules a in the chamber C_a is under these conditions equal to αp_a , where p_a is the pressure in the chamber C_{ae} , and α is a quantity which may be greater or less than unity. α is evidently a function of p_a and T , and we may therefore write

$$p_a' = p_a \alpha = p_a \cdot \psi_1(T, p_a). \quad . \quad . \quad (13)$$

The volume v_a' of a mol of the molecules a in the chamber C_a may be written

$$v_a' = \psi_2(v_a), \quad . \quad . \quad . \quad (14)$$

where v_a is the volume when the molecules c are absent.

If the mixture is passed through the first of the cycles described in a previous paper†, the same differential equation in form as before is obtained, where p_a' and v_a' take the place of p_a and v_a , or

$$v \frac{\partial p}{\partial v} - M_a v_a' \frac{\partial p_a'}{\partial v} - M_c v_c \frac{\partial p_c}{\partial v} = 0, \quad . \quad . \quad (15)$$

which becomes

$$v \frac{\partial p}{\partial v} - M_a \cdot \psi_2(v_a) \frac{\partial \{p_a \cdot \psi_1(T, p_a)\}}{\partial v} - M_c v_c \frac{\partial p_c}{\partial v} = 0, \quad (16)$$

by means of equations (13) and (14). From the second cycle two additional equations may be obtained in which the independent variables are M_a and M_c .

The subsidiary equations that are used to solve these equations are independent of the molecules c in the chamber C_a . It follows, therefore, that the expression obtained for the constant of mass action will contain the functions ψ_1 and ψ_2 . An examination of the investigation in the paper quoted will

* Phil. Mag. vi. pp. 195-203 (1928).

† Phil. Mag. v. pp. 620-629 (1928).

show that in that case the constant of mass action is a function of the volume and masses of the constituents as well as of the temperature. Thus, for example, equation (15) in that paper, which corresponds to the reaction

$$2ae = a_2 + e_2, \quad . \quad . \quad . \quad . \quad . \quad (17)$$

now becomes

$$\int \left\{ \psi_2 \left(\frac{1}{C_a} \right) \frac{\partial \{ RTC_a \cdot \psi_1(T, RTC_a) \}}{\partial C_a} + \frac{1}{C_a} \right\} \partial C_a \\ = \log \frac{1}{v} + \psi_2(M_a, T). \quad . \quad (18)$$

If this is integrated and the expression obtained for C_a substituted in the equation

$$K \left(\frac{M_a}{v} - C_a \right) = C_a^2, \quad . \quad . \quad . \quad . \quad (19)$$

obtained from equations (10) and (11) in the paper quoted, the functional nature of K with respect to v is obtained.

It will be of interest to consider the special case corresponding to the concentration of the substance a in the chamber C_a obeying Henry's law, in which case we have $p_a' = \alpha_1 p_a$ and $v_a' = v_a / \alpha_1$ where α_1 is a constant. Equation (15) now reduces to the same form it would have if no molecules c were present in the chamber C_a . Hence under these conditions the molecules c have no catalytic effect on the constant of mass action.

§ 5. *The Functional Nature of the Constant of Mass Action of Electrolytes.*

Let us suppose that the apparatus in the figure is placed in a solvent to which the walls are permeable, and that the chamber C_{ae} contains a mass M of a solute which dissociates in part into positive and negative ions. Let us also suppose that the membranes separating this chamber from the chambers C_a and C_e are permeable to the positive and negative ions respectively. The pressures p_a , p_e , and p now denote the osmotic pressures of the segregated ions, and of the mixture of undissociated solute and ions, respectively.

The ions in a solution due to the dissociation of an added solute, behave as a whole like uncharged molecules as far as their intrinsic pressure is concerned, since the repulsion the ions of one sign exert upon each other can be shown to be balanced by the attraction the ions of opposite sign exert upon each other. Thus consider the solution divided into two parts A and B by an imaginary plane. Let the negative

ions in A repel the negative ions in B with a force F . The positive ions in the two parts will then repel each other also with a force F . Hence the part A repels the part B with a force $2F$. But the negative ions of A attract the positive ions of B with a force F , and the positive ions of A attract the negative ions of B with a force F , or the two parts attract each other with a force $2F$. This force of attraction neutralizes the force of repulsion. Thus the total effect of the electric charges of the ions on their intrinsic pressure is zero. As a first approximation the ions may therefore be taken to behave like uncharged molecules, and hence, if the concentration is not too large, the osmotic pressure of the mixture of solute and ions in the chamber C_{ae} approximately obeys the gas laws.

The pressures of the positive and negative ions in the chambers C_a and C_e are equal to the pressures of the corresponding ions in the chamber C_{ae} . For, if that were not so, diffusion from one chamber to the other would take place. We may therefore write

$$p_a = p_e = CRT \quad . \quad . \quad . \quad . \quad (20)$$

for these pressures, where C denotes the concentration of the positive and negative ions in the chamber C_{ae} .

Some information about the concentration of the ions in the chambers C_a and C_e may be obtained from the following considerations:—Let us suppose that each molecule of solute in the chamber C_{ae} is dissociated into two ions, each of which carries a charge e , and let them be transferred at constant pressures into the chambers C_a and C_e . The external work done on the system is

$$pr - 2p_a v_a M,$$

where v_a denotes the volume of a mol of ions in both the chambers C_a and C_e , and M the mass in mols of the original solute. But since the solute is completely dissociated, and the pressure of each kind of ion is the same in the chambers C_a , C_e , and C_{ae} , the foregoing work may be written

$$2p_a(v - Mv_a).$$

If the volume of each of the chambers C_a and C_e at the end of the process is the same as that of the volume of the chamber C_{ae} at the beginning, $v - Mv_a = 0$, and hence the foregoing work is zero. But it cannot be zero, and has besides a positive value, since this operation involves the separation of positive from negative ions. It follows, therefore, that

$$Mv_a < v,$$

or the concentrations of the ions in the chambers C_a and C_e are greater than the corresponding concentrations in the chamber C_{ae} . Since the work of separation of the ions in the chamber C_a from those in the chamber C_e against electrical attraction increases with their concentrations and these concentrations increase with the corresponding concentrations in the chamber C_{ae} , the above work done increases with increase of the latter concentrations. Hence the ratio Mv_a/v decreases with decrease of v . We may therefore write

$$v_a = v_e = \frac{\alpha_2}{C}, \quad . \quad . \quad . \quad . \quad . \quad (21)$$

where α_2 is a function of C which is smaller than unity, and which decreases with an increase of C .

The reason for this difference in concentrations is probably that when the ions are of one sign and two ions approach one another they decrease in speed on account of the repulsion they exert upon each other, and the average velocity of translation is thus smaller than would otherwise be the case. The concentration corresponding to a given pressure will then be greater than when the particles are uncharged. The effect is the opposite to that existing with uncharged molecules, in which case the attraction they exert upon each other increases their average velocity of translation*. This would be for large concentrations considerably greater than that corresponding to the gaseous state. The latter velocity a molecule has when it passes through a point in the substance at which the forces of the surrounding molecules neutralize each other. In the case of a mixture of equal numbers of positive and negative ions the decrease in velocity when two similarly charged ions approach each other is compensated by the increase when two ions oppositely charged approach each other.

The osmotic pressure p of the mixture in the chamber C_{ae} is given by

$$p = RT(C_s + 2C) = RT\left(\frac{M}{v} + C\right), \quad . \quad . \quad (22)$$

where $\frac{M}{v} - C = C_s$, the concentration of the undissociated solute. On substituting for p, p_a, p_e, r_a , and v_a in equation (1)

* 'A Kinetic Theory of Gases and Liquids,' by R. D. Kleeman, Chap. II. (John Wiley & Sons, New York). Phil. Mag., July 1912, p. 100.

from equations (22), (21), and (20), and taking into account the equations $M_a = M_s = M$, we obtain

$$\frac{\partial C}{\partial v} = \frac{MC}{(Cv - 2Ma_2)v} \quad \dots \quad (23)$$

This equation, together with the mass action equation

$$KC_s = K\left(\frac{M}{v} - C\right) = C^2, \quad \dots \quad (24)$$

determines the functional form of K . An equation may be obtained from this equation by differentiation with respect to v , which may be written

$$\begin{aligned} \frac{\partial K}{\partial v} &= \left[\frac{\partial}{\partial v} \left(\frac{C^2 v}{M - Cv} \right) \right]_C + \left[\frac{\partial}{\partial C} \left(\frac{C^2 v}{M - Cv} \right) \right] \cdot \frac{\partial C}{\partial v} \\ &= A_1 + B_1 \frac{\partial C}{\partial v}, \quad \dots \quad (25) \end{aligned}$$

and by the help of which the properties of K may conveniently be investigated.

Let us first consider the case corresponding to the dissociation of the solute in the chamber C_{as} being small, in which case C is small. The quantity α_2 in equation (23) is then

equal to unity. If the expression for $\frac{\partial C}{\partial v}$ given in that case by equation (23) is substituted in equation (25), we obtain

$\frac{\partial K}{\partial v} = 0$, as has already been shown in a previous paper*.

Thus in the case of weak electrolytes K is a constant at constant temperature, which agrees with the facts.

If, however, the ionic concentration is large, as with strong electrolytes, α_2 is less than unity. Now, the values of A_1

and B_1 in equation (25) are positive, and the value of $\frac{\partial C}{\partial v}$

given by equation (23) is negative when $\alpha_2 = 1$. These values, we have just seen, reduce the right hand side of equation (25) to zero. When α_2 is less than unity the

negative value of $\frac{\partial C}{\partial v}$ given by equation (23) is greater than that corresponding to $\alpha_2 = 1$. In that case the value of $\frac{\partial K}{\partial v}$ given by equation (25) is negative. This agrees with the

* Phil. Mag. v. pp. 620-629 (1928).

facts according to which $\frac{\partial K}{\partial v}$ in the case of strong electrolytes has decided negative values. This is indicated by the values of K given in the Table (see p. 659), where the first column gives the volume in litres of the solution containing a mol of KCl , the second column the value of Cv , and the third column the values of K calculated by equation (24)*.

A further test of the theory may be made by calculating the value of α_2 given by equation (23) corresponding to different ionic concentrations in the chamber C_{ae} . Its values should be less than unity and decrease with increase of concentration. Thus it was obtained from the Table that, corresponding to the volumes 7500 and 1.5, α_2 has the values .98 and .88 respectively. Corresponding to the volume 7500 the value of α_2 is nearly equal to unity, as we would expect should be the case at such low concentrations. A striking confirmation of the theory is thus obtained.

If the functional form of α_2 were known equation (23) could be integrated, and hence the functional form of K be determined from equation (24). But the exact form of α_2 cannot at present be predicted theoretically. We may therefore proceed to determine the functional form of K empirically from the values of K and v given in columns 1 and 3 of the Table. If we write

$$K = \frac{2.35}{v^{.5459}}, \quad \dots \dots \dots (26)$$

and calculate the values of K corresponding to the various values of v in the first column of the Table, the values given in the fourth column are obtained. A more complicated formula for K would no doubt give a better agreement with the facts †. The exponent of v in the foregoing equation is approximately equal to $\frac{1}{2}$, which is probably not accidental but has an important significance.

* Table taken from 'A Treatise on Physical Chemistry,' p. 557, edited by H. S. Taylor (D. van Nostrand Co., New York), which was compiled from figures by Kohlrausch and Maltby, *Wiss. Abh. tech. Reichsanstalt*, iii. p. 157 (1900).

† Strictly equation (26) should be written $K = a + \frac{b}{v^c}$, where a is the limiting value of the constant of mass action when the concentration is infinitely small, and which accordingly is a function of the temperature only. But since the value of a is small in comparison with a large range of values of the other term, its value probably cannot be determined very accurately from this equation.

TABLE.

v lit.	Q_v	K	$\frac{2.35}{v^{0.459}}$
∞	1.000	—	—
10,000	.9936	.0154	.0154
5,000	.9912	.0223	.0225
2,000	.9862	.0352	.0371
1,000	.9802	.0485	.0542
500	.9723	.0681	.0790
200	.9577	.1084	.1303
100	.9424	.1542	.1892
50	.9234	.2221	.2892
20	.8910	.3642	.4582
10	.8624	.5405	.6686
5	.8310	.8154	.9761
2	.7883	1.434	1.610
1	.7565	2.350	2.350

It appears, therefore, that *when an electrolyte dissociates easily into ions the constant of mass action is a function of the volume of the solution as well as of the temperature.* This signifies that *either the chance of a molecule dissociating into ions depends on its previous encounters with other molecules, or that the chance of two ions of opposite sign combining on collision depends on previous encounters with other ions and molecules, or that both effects occur.*

Shenectady, N.Y.,
U.S.A.

LXI. *Covalency, the Paramagnetism of Oxygen and Stereochemistry.* By H. F. BIGGS, M.Sc., M.A., Demonstrator in Physics in Oxford University*.

LONDON'S† theory of covalency suggests so many more researches both theoretical and experimental than I shall be able to carry out, that I venture to publish the following somewhat speculative considerations.

London shows by very general arguments as to symmetry that two atoms will form a homœopolar or covalent link

* Communicated by Prof. Townsend, F.R.S.

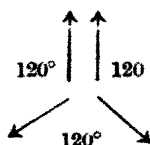
† *Zts. f. Phys.* xlv. p. 455 (1928).

when each possesses an unpaired electron, if these electrons are in corresponding orbits but spinning opposite ways. The "correspondence" of the orbits includes angular momentum and orientation, but perhaps not radial motion. Further, in any atom in a group of orbits with the same azimuthal quantum number the unpaired electrons all spin the same way.

London writes for the six outer or L electrons of the oxygen atom :

	<i>s</i>	<i>p</i>		
<i>l</i>	0	1		
No. of electrons	2	2	1	1

where *l* is the old azimuthal number (*k*) minus one. The two unpaired electrons in differently oriented orbits are the valency electrons. Now, if the axes of the four *p*-orbits are arranged thus :



the resultant is one unit of angular momentum, giving a P term, while the two spins, combining in the same direction to give again one unit, may make an angle of 0° , 120° , or 180° with the doubled orbit, giving a final resultant $j=2, 1$, or 0 respectively, thus forming a triplet P term as seems to be required by observation. There is nothing new in this ; it is only a consistently geometrical statement of the known model. If we now form an oxygen molecule we place two such atoms in the same orientation, which will be symmetrical to the line of their nuclei. The odd spins then go out in pairs (forming the bonds), but we are left with a resultant *orbital* angular momentum of 2 units. Since this is due to electrons describing *p*-orbits, we may suppose that in a magnetic field the whole molecule will be oriented parallel, perpendicular, or anti-parallel to the field, giving a Stern-Gerlach triplet, with splitting-factor 2, if we assign

one Bohr magneton to each p -orbit. This gives the right value for the paramagnetism of oxygen on Sommerfeld's* quantization of Langevin's Theory, namely :

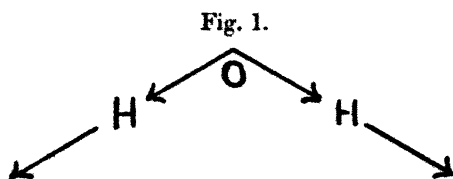
$$\chi = \frac{2^2 + 0^2 + (-2)^2}{2} \frac{N\beta^2}{kT},$$

$$\kappa = 1.42 \times 10^{-7} \text{ at } 20^\circ \text{C. ; } (\kappa_{\text{obs.}} = 1.44 \times 10^{-7}),$$

where χ is the molecular susceptibility and κ the volume susceptibility, N is Lohschmidt's number and β is one Bohr magneton, while the numerical fraction represents the mean square of the component of magnetic moment parallel to the field.

Van Vleck's† detailed theory also needs only a slight modification to fit this model, for we obtain the same result if in his formula (27) or (28) we put the spin-number s equal to zero, and instead of σ_k^2 write $\sigma_k(\sigma_k + 1)$, as is justified by his own reasoning (p. 606, *l. c.*).

The 120° between the orbits of the p -electrons in the oxygen atom has now obvious applications in chemistry, for the water molecule must be drawn thus :



which gives a dipole moment and may underlie the hexagonal structure of ice. We here make the natural assumption that when two atoms are joined by a single bond, the line of nuclei is the common axis of the valency orbits. A closed chain of three atoms suggests itself for ozone, but we have then to assume that *parallel orbits may give rise to a bond, even when the spins are not directly opposed*, since otherwise no closed chain of an odd number of atoms could be formed by London's covalent links.

For the nitrogen atom we should have two paired s -electrons, and the three p -orbital axes making 120° with each other in a plane. The nitrogen molecule would then obviously be neutral (or diamagnetic), while the NO molecule would have one orbital magneton and one spin

* 'Atombau,' 4th edition, pp. 639 and 641.

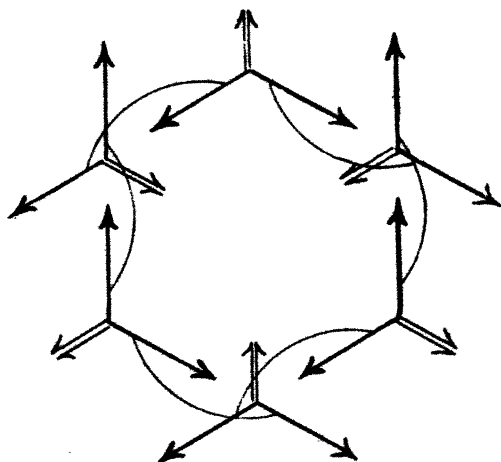
† Phys. Rev. xxxi. p. 587 (1928).

magneton, presumably parallel or anti-parallel, which, when quantized as for O, would give for the susceptibility

$$\chi = \frac{2^2 + 0^2 + 0^2 + 0^2 + 2^2 + 0^2}{6} \frac{N\beta^2}{kT}, \quad \kappa = .71 \times 10^{-7} \text{ at } 20^\circ \text{C.},$$

or half the value for oxygen. This number is also obtained by Van Vleck, but it does not agree with the available observations ($\kappa_{\text{obs.}} = .61 \times 10^{-7}$), and Van Vleck accounts for the discrepancy by introducing another factor depending on the temperature, which for nitrogen will have the required value of 0.85 at ordinary temperatures, while for oxygen it is practically unity, the distinction between the

Fig. 2.



two cases being due to the energy intervals being comparable to kT in the case of nitrogen but not in that of oxygen. In the case of the present model, however, this distinction can hardly be supposed to hold, and therefore the agreement of the model with observation must be regarded as unsatisfactory.

Carbon, again, is given by London one s -electron and three unpaired p -electrons, which I arrange at 120° with each other in a plane. If, then, one of the p -bonds is used up on a hydrogen atom, the axes of the remaining two valency orbits of each CH radical will form an angle of 120° . Six such radicals can now combine without strain to form a plane regular hexagon as in fig. 2, where the whole arrows

represent orbital axes, the half arrows spin axes, and the curved lines bonds between electrons whose orbits are parallel but whose spins make 120° with each other. The spins may also be alternately in opposite directions as we go round the ring. All this time we are conveniently neglecting the six *s*-electrons, but I suggest that since there is nothing directional about the *s*-state (it is really not an orbit at all), the direction of spin is free, and the bond can have perhaps an attractive but no directive effect, and may be neglected in building simple molecules. The only strong reason I can think of against such an assumption is that the hydrogen molecule is apparently held together by *s*-electrons. In most other cases when an atom has a single outer electron in an undoubted *s*-state, as in the case of the alkalis, this electron does not form a covalency, but drops off. In graphite the *s*-electron would form the bond normal to the planes of cleavage, accounting for the lubricating properties of the substance.

Diamond and the aliphatics, on the other hand, seem quite inexplicable on this model, and all four L-electrons must have $l = 1$ and have their orbit-axes pointing in tetrahedral symmetry. If this is correct, the inert gases might also be taken to have their outer electrons arranged in pairs with the axes of their orbits in tetrahedral symmetry.

Such a model is, of course, contrary to the accepted spatial quantization, which only allows three different *p*-orbits; but it does not seem necessary that in the quantization of a system of several electrons the only possible states of the individual electrons should be those of an electron in a system or "ring" by itself. The geometrical method of atom-building, however, though it justifies this model, does not account for the fact that we never get an *s*-electron when we have four *p*-electrons in tetrahedral symmetry.

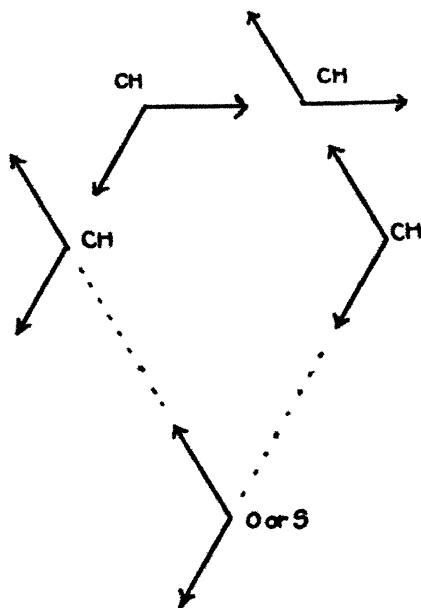
The apparent anomaly, that if benzene is forced to take up two *additional* atoms of hydrogen the C_6H_8 behaves as a far more unsaturated substance than C_6H_6 , may now be readily explained; for the additional atoms cannot be added without upsetting the hexagonal symmetry of the carbon atoms concerned, so that the unstrained plane structure of the ring is lost, and it is natural to suppose that the other carbon atoms revert to the tetrahedral type and become actively tetravalent. That the "aromatic" properties of benzene, hexagonal angles, and apparent trivalency of carbon are associated is shown by a consideration of furan or thiophen, which I draw as in fig. 3. These have properties very similar to those of benzene, and,

again, their *addition* products have no aromatic properties, but are analogous to cyclohexane.

London's hypothesis is also supported by some of the facts of catalysis. The magnetic metals are the strongest catalysts, and seem to produce their effect with only small energy change, presumably by their power of orienting the reacting molecules so that they have a greater concentration in a position favourable to reaction with each other at the surface of the metal than in the body of the gas.

A partial interpretation can now be given of the effect * of hydrogen in diminishing the paramagnetism of palladium

Fig. 3.



The magnitude of the effect is of a far higher order than the diamagnetism of hydrogen: 7.8×10^{-8} per c.c. at room temperature against 2×10^{-10} . A quantitative agreement cannot be obtained till we know something more of the mechanism of the absorption of the hydrogen; but it is evident from a comparison of the value just given with the susceptibilities of O_2 and NO that the order of magnitude is consistent with the neutralizing of two magnetons of palladium per molecule of hydrogen absorbed.

* Biggs, *Phil. Mag.* xxxii. p. 131 (1916).

LXII. *Crystal Structure of Calcium* *

By C. D. NIVEN, M.A. †.

IN endeavouring to grow crystals of calcium, some were obtained which definitely showed that Hull was right in ascribing a cubic structure to calcium, and a brief description of the work will be given in the following paragraphs.

As calcium reacts with glass or other siliceous substance it is necessary in heating calcium to use containing vessels of iron. At first, an endeavour was made to make crystals by Bridgeman's ‡ method. An iron tube was closed at one end by screwing on a cap, and pieces of calcium were dropped in. The air was then evacuated and the iron tube closed at the top by a rubber tube and clamp. The end at which the calcium was lying was then lowered into a furnace. It was found that after heating strongly and cooling, the calcium took on the appearance of having been melted, but yet it had not run to the bottom of the tube. Calcium was also placed in a pyrex glass tube and heated, although it attacked the walls of the tube very badly, making them quite black, yet when the tube was broken crystals of metal could be found inside on the walls of the tube. It appeared from this that calcium had a very low distillation temperature, and that it might be quite possible to get crystals by distillation.

The furnace which had been previously used by Professor McLennan and the author in distilling lead was accordingly fitted up again. Improvements were made in regard to keeping the outer case of the furnace cool. A window was put into the side so as to see the furnace as it heated, and the molybdenum strip was replaced by a new form of heating element. This consisted of a piece of nichrome wire wound round an iron crucible. The crucible consisted of a piece of half-inch iron rod about two inches long, bored out so that the walls were about $1/32$ inch thick. In order to insulate the nichrome wire from the iron, alundum powder was mixed up with water glass to form a thin paste, and smeared over the outside of the iron crucible. It was allowed to dry overnight, preferably in a warm place. About 17 turns of nichrome wire (18-wire gauge) were

* This work was carried out with the aid of a Fellowship from the National Research Council of Canada.

† Communicated by Prof. J. C. McLennan, F.R.S.

‡ Proc. Amer. Acad. of Arts & Sci. ix. p. 305 (Oct. 1925).

coiled round the crucible, the turns being closer together at the bottom than at the top, and in order to keep in the heat more of the water glass preparation was put on the outside. At first a small condenser was arranged just above the mouth of the crucible, but it was found that a little iron lid, with a hole through it for evacuation purposes, served quite sufficiently to condense the distilled calcium.

The current was read on an ammeter, and tests were made with currents from 10 to 15 amperes.

It was easy to see with the naked eye that the crystals formed were not hexagonal as H. Moissan * had concluded. The four-sided pyramids could easily be seen, yet it was hard to say definitely whether they were tetragonal or cubic. To do this it was necessary to make a goniometer measurement, which was very kindly performed by Professor A. L. Parsons, of the Mineralogical Department, University of Toronto. The values of ρ and ϕ found are given in the table, and clearly demonstrate that the crystal was a rhombic dodecahedron. The crystals of calcium were found to stand considerable exposure to the atmosphere.

ρ ...	45° 00'	45° 09'	45° 03'	45° 05'
ϕ	180° 02'	359° 56'	90° 01'	270° 00'

In conclusion, I should like to express my sincere thanks to Professor Parsons for his kind assistance in identifying the crystal form, and to Professor McLennan for stimulating suggestions throughout the work.

The Physical Laboratory,
University of Toronto.

LXIII. *Electrical Conductivity of Arsenic and Antimony at Low Temperatures* †. By Prof. J. C. McLENNAN, F.R.S., C. D. NIVEN, M.A., and J. O. WILHELM, M.A. ‡

AT the present time it is generally conceded that superconductivity is a property only of certain elements. In view of this fact the efforts of the authors of this com-

* *Comp. Rend.* cxxvi. p. 1753 (1898).

† This work was carried out with the aid of a grant of a Fellowship from the National Research Council of Canada to C. D. Niven.

‡ Communicated by the Authors.

munication have been directed recently towards finding the actual temperature-resistance curves at low temperatures of the metals investigated, rather than towards merely trying whether a particular metal was superconducting or not. Most experimenters seem to have been bent on finding superconductors, so that a great deal of work has been done on the more electropositive metals at very low temperatures, while very little has been done on such metals as arsenic and antimony. So far as theory is concerned this has not been advantageous, as the electropositive elements have fewer valency electrons and are therefore simpler; yet, before any theory can be complete, it must apply to those metals with higher valency and more complicated crystal structure. With this in mind, the authors carried out the work described below on arsenic and antimony.

Arsenic.

As crystal structure has undoubtedly a certain bearing on the electrical resistance of a piece of metal, it was thought desirable, if possible, to get a single crystal of arsenic, and a considerable amount of time was spent in this connexion. Arsenic, when heated, sublimates before it melts, and on this account it was not possible to make crystals by Bridgeman's* method, which, briefly, consists of lowering the metal contained in a glass tube slowly out of a furnace into the cool air of the room. When this was done the metal condensed much too rapidly and a deposit that was not a crystal was formed. It was quite impossible to prevent this condensation by merely lowering the tube slowly. But the experiments made in attempting to do this suggested to us two methods of making crystals of arsenic, one of which was subsequently adopted.

Before we describe the different tubes in which the metallic arsenic was contained, a short description of the furnace used will be given, as the detailed construction of it was a little different from that of the one Bridgeman used. Instead of taking a quartz tube and winding resistance wire round it, we took six porcelain heating coils as used in domestic room-heaters, and placed these on end. In order to hold them in position, pieces of channel-shaped porcelain were tied round them with wire and the whole embedded in fireclay inside two channel-shaped pieces of asbestos used for lagging steam pipes. The terminals of the six heating coils were connected in parallel to two heavy brass rods suitable for carrying the current. The whole

* Proc. Am. Acad. of Arts and Sc. ix. p. 305 (Oct. 1925).

thing was then placed inside a sheet tin case, which had a hole in the top and in the bottom. Asbestos was packed in to hold the furnace central in the case, and the top was then soldered on. The case was in turn mounted on a wooden stand, so that it could turn and thus allow the furnace to lie in a vertical or a horizontal position. In using this type of furnace it is important to note that the temperature reached with a given current is very different when the furnace is standing in a vertical position with the ends open, from what it is when in a horizontal position, owing to the fact that in the vertical position there is a strong circulation of air.

There was no particular reason for constructing the furnace out of these heating coils beyond the fact that there was no quartz of the required size on hand at the time, and there was no reason for leaving the little air space between the porcelain packing and the coils, except that it was thought that the air space would conduct away a little less heat than fireclay or porcelain. Yet these two factors contributed to making the temperature of the furnace uneven along the inside. Wherever there was a junction of two heaters, the temperature was a little lower than in the middle of a single heater. Although it was by accident that the furnace was constructed with this unevenness of temperature, it was subsequently found to be the key to getting crystals to grow.

The tubes in which the arsenic was placed were made at first as follows. A piece of pyrex glass about 8 inches long and 0.75 cm. in diameter was sealed up at one end. A smaller tube was sealed into the side and bent round till the small tube pointed along the axis of the larger. The end of the smaller tube was sealed up, and the arsenic placed in the pocket formed at the bottom of the larger tube; the whole tube was then evacuated and sealed off at the top. It was hoped that when the tube was suspended, the arsenic would slowly distil to the bottom and form a crystal there. Instead of this happening, it was found that, while some of the arsenic found its way to the lower parts of the short tube and condensed merely on the side, yet a crystal was formed in the bend of the small tube. It was noticed, too, that the mass of arsenic in the pocket gradually took on a crystal-like appearance against the glass. The "arrangement" of the mass of arsenic into a crystal was similar apparently to the phenomenon observed by Langmuir in making copper crystals. This method of holding the metal at a high temperature until a crystal is formed, appeared therefore to have possibilities in the case of arsenic, but we did not pursue the method, as it was found possible to get a large

enough crystal out of the small tube for measuring change of resistance with temperature. The actual crystal measured was taken from a tube such as the one just described. Even when the tube was suspended for a long time in the furnace it was noted that the arsenic did not all distil into the small tube at the bottom, and at first it seemed surprising that the crystal referred to above was formed near the top of the small tube at all. It was concluded that if the furnace had been made of one piece instead of a number of small pieces this could not have happened; but because of the particular way in which our furnace was accidentally constructed, cool parts existed at the junctions of the heated coils. The temperature at such a point must have been sufficiently high for the slow formation of the crystal, and not too high to cause it to distil away again from that part of the tube.

Subsequently the furnace was turned into a horizontal position and merely a straight tube containing arsenic at one end was pushed in. The arsenic sublimed from the warmer part of the tube to the cooler part which lay opposite a junction of two coils in the furnace. Various methods were employed to try and improve on the type of tube for forming the crystal, such as introducing a current of air in an inner tube inside the tube containing the arsenic; the condensation, however, was too rapid, with the result that a number of small crystals were formed instead of a single large one. The improvement that seemed necessary was to construct a furnace with two chambers which could be regulated separately and fitted with thermometers to tell just the correct temperatures for the best formation of crystals, but as our object was mainly to get a single crystal for electrical measurements and not to grow large crystals, we did not continue farther with the work.

The crystal to be measured was clamped between two copper jaws at either end. Four wires leading to the four jaws comprised the two current leads and the two potentiometer leads. Crystals formed from the vapour of a substance display their facets and thus differ as a general rule from crystals formed by slow cooling of molten metal. In one of our crystals the direction of the hexagonal axis could be easily seen. Measurements were made on this crystal between room temperature and the temperature of liquid helium along the hexagonal axis.

Antimony.

No trouble was experienced in making a crystal of antimony from molten metal. In spite of the fact that antimony has a melting-point nearly as high as pyrex glass,

it was found that a fine bore tube did not cave in at the temperature of molten antimony and that it was possible to obtain a long thin single crystal by the method used by Bridgeman in pyrex glass. The temperature resistance curves of a crystal of antimony prepared in this way and also of a chip off a mass of metal were investigated between room temperature and the temperature of liquid helium.

Results of Measurements.

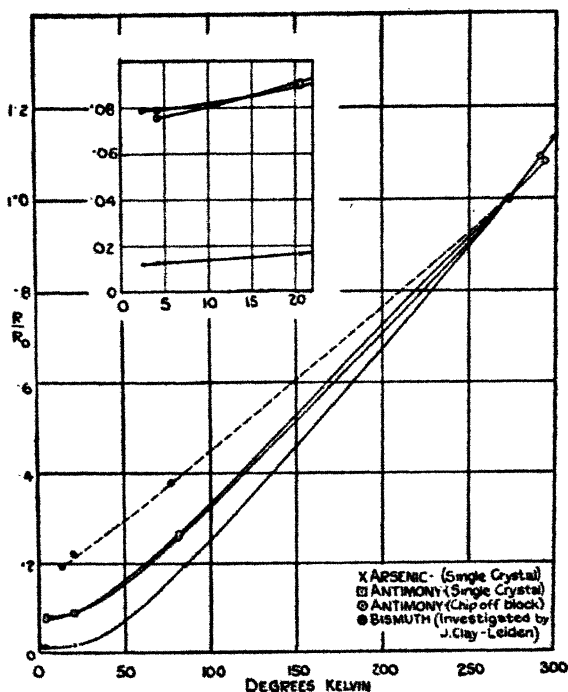
In the work previously published by the authors, graphs, showing the variation of electrical resistance with temperature, have been constructed measuring specific resistances along the resistance axis. In this communication, however, the more usual practice of using the ratio of the resistance at any temperature to the resistance at 0°C . will be adopted. We do this because we wish to compare our results with Clay's*. The results of the measurements are given in the table, and these are presented in graphical form in the diagram.

Crystal of Arsenic.					
Degrees Kelvin.	Ohms.	R/R_0			
298	1.25×10^{-3}	1.13			
273	1.11	1.00			
85	.216	.195			
20.6	.018	.0162			
4.2	.014	.0127			
2.42	.014	.0127			

Chip of Antimony.			Crystal of Antimony.		
Degrees Kelvin.	Ohms.	R/R_0	Degrees Kelvin.	Ohms.	R/R_0
294	8.28×10^{-4}	1.08	291	7.97×10^{-3}	1.09
273	7.66	1.00	273	7.32	1.00
82	2.03	.265	82	1.90	.260
20.6	.696	.0909	20.6	.656	.0896
4.2	.580	.0760	4.2	.579	.0791
			4.43	.581	.0794

* Diss. Leiden, 1908, p. 51.

By studying the diagram below we can reach some rather interesting conclusions. (1) The resistance temperature curve of the antimony crystal is not very different from that of the piece off the mass of metal. (2) The curves arrange themselves as would be expected from the arrangement of the metals in the periodic table. (3) The temperature resistance curve for arsenic resembles that of many other pure metals. At the same time there is a very decided



departure from the law stating that the electrical resistance is proportional to the absolute temperature. (4) Our results show that in the case of both arsenic and antimony resistance at low temperatures approximates to a definite residual value. This property is common to most pure metals. The arsenic crystal was measured to 2.42°K. , and the antimony crystal to 2.43°K. ; neither was found to be superconducting.

On the graph we have drawn the curve for bismuth according to Clay's results; bismuth appears to be unique in its behaviour, since, so far as is known, it is the only

672 Prof. McLennan, Messrs. Niven and Wilhelm on the

pure metal that has a value of R/R_0 greater than 0.3 at the temperature of liquid air. The value 0.3 is what would be expected if the linear relation connecting resistance and temperature held good. In general, metals have a value of R/R_0 in liquid air less than 0.3, and in this respect both arsenic and antimony follow the general behaviour of other metals.

The Physical Laboratory,
University of Toronto.
June 30th. 1928.

LXIV. *The Resistance of Cæsium, Cobalt, and Chromium at Low Temperatures.* By Prof. J. C. McLENNAN, F.R.S., C. D. NIVEN, M.A. *, and J. O. WILHELM, M.A. †

Cæsium.

ALTHOUGH a great deal of work has been done on the conductivity of the alkali group of metals in regard to variation with both temperature and pressure, yet data were not available on cæsium and rubidium below the temperature of liquid air at the time when Onnes and Tuyn† published their "Data concerning the Electrical Resistance of Elementary Substances at Temperatures below $-80^{\circ}\text{C}.$ " Last year the authors of this communication published some data on rubidium at low temperatures, so that only cæsium remained to be measured.

The cæsium was run into a fine capillary tube similar to that used in measuring potassium and sodium, as described in another paper§. Measurements were made at room temperature and at the temperature of liquid air, liquid hydrogen, and liquid helium. By assuming the value for the specific resistance given in Smithsonian Tables and by neglecting any change in the dimensions of the cæsium due to contraction with change of temperature, the values of the specific resistances were calculated. The results are given in Table I. and reproduced graphically in the diagram (p. 674).

* This work was carried out with the aid of a Fellowship from the National Research Council of Canada to C. D. Niven.

† Communicated by the Authors.

‡ Leiden Communications Supplement, No. 58.

§ Phil. Mag. iv. p. 386 (Aug. 1927).

TABLE I.

Cæsium.			Chromium (aged).		
Degrees Kelvin.	Ohms.	Specific Resistance.	Degrees Kelvin.	Ohms.	Specific Resistance.
290	75.34×10^{-3}	205	292	5.59×10^{-3}	17.2
82	18.50	5.04	80	.655	2.01
20.6	4.69	1.28	20.6	.260	.80
4.2	1.32	.359	4.2	.258	.79
2.2	1.19	.324	2.25	.258	.79

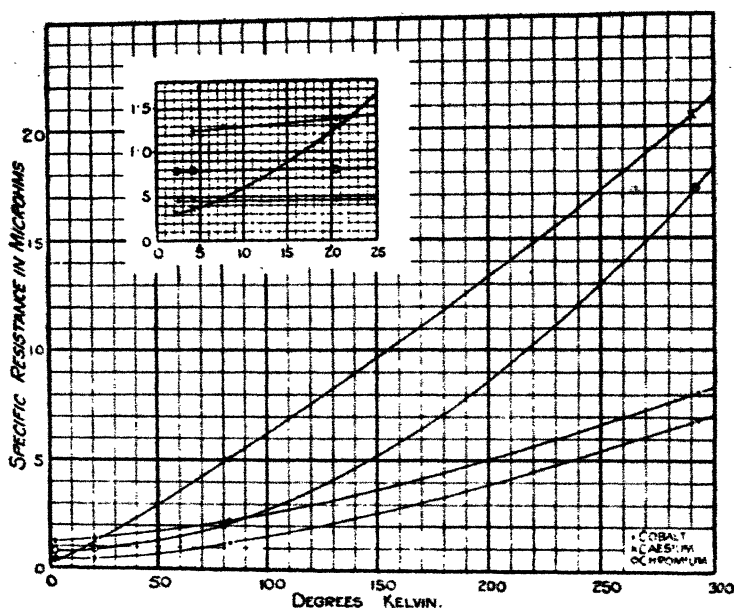
Cobalt (unaged).			Cobalt (aged).		
Degrees Kelvin.	Ohms.	Specific Resistance.	Degrees Kelvin.	Ohms.	Specific Resistance.
293	1.80×10^{-3}	8.07	293	2.11×10^{-3}	6.85
83	.495	2.22	83	.382	1.24
20.6	.313	1.37	20.6	.143	.46
4.2	.277	1.24	4.2	.140	.45
			2.5	.140	.45

P. W. Bridgeman* found that cæsium was very compressible, and also that the electrical resistance passed through a minimum with increasing pressure, and on this account cæsium appeared to be an interesting member of the alkali group to measure at low temperatures. The resistance of nearly all pure metals, other than superconductors, approaches a certain limiting value, so that in general at very low temperatures the resistance of a pure metal is independent of the temperature. In this respect cæsium stands out as different from most pure metals. A glance at the diagram shows that the resistance of cæsium continues to decrease with temperature below 4° K.

In Table II. values of R/R_0 —i.e., the ratio of the resistance at any temperature to the resistance at 0° C.—are

* Am. Acad. Proc. lx. pp. 385-421 (Oct. 1925).

given for sodium, potassium, rubidium, and caesium at the temperatures of liquid hydrogen and helium. It can be observed from these figures that the three metals, sodium, potassium, and rubidium, all approach a certain limiting value. Had caesium behaved like rubidium a limiting value



of about $\cdot 046$ might perhaps have been expected. Spectroscopic data give the following electronic configurations* for the alkalis.

TABLE II.

	Sodium.	Potassium.	Rubidium.	Cæsium.
0° C.	1	1	1	1
Liquid hydrogen ...	$\cdot 015$	$\cdot 027$	$\cdot 057$	$\cdot 067$
Liquid helium	$\cdot 004$	$\cdot 007$	$\cdot 038$	$\cdot 018$
Liq. hel. red. pr. ...	$\cdot 004$	$\cdot 007$	$\cdot 038$	$\cdot 017$

* See paper by McLennan, Smith, and McLay, Proc. Roy. Soc. A, cxii. p. 76 (1926).

Sodium 2 : 2.6 : 1.

Potassium... 2 : 2.6 : 2.6 - : 1.

Rubidium ... 2 : 2.6 : 2.6.10 : 2.6 - - : 1.

Cæsium..... 2 : 2.6 : 2.6.10 : 2.6.10 - : 2.6 --- : 1.

When the valence electron is stripped off the core is left complete in the case of sodium, potassium, and rubidium, but in the case of cæsium the fourteen 4_s electrons are missing. It is highly probable that this accounts for the compressibility of cæsium, and it is not improbable that it accounts too for the temperature gradient of the electrical resistance persisting right down to very low temperatures. This explanation would be more feasible if rubidium had had a limiting resistance comparable with that of sodium or potassium, but measurements do not indicate that this is the case. Cæsium was not superconducting at the temperature of 2.2° K.

Cobalt and Chromium.

A group of elements that seem so far to have been rather neglected in work on electrical conductivity are those grouped round iron. Doubtless this was due to the difficulty in obtaining pure samples, but last year, through the kindness of Mr. C. C. Paterson, a piece of pure chromium was obtained from the General Electric Company of England, and this year some pure cobalt was obtained from the Belgo-American Trading Corporation, New York. The cobalt was cut into a strip and aged in a vacuum for about four hours at a dull red heat. Measurements were made on an aged and on an unaged sample. The results of the measurements are given in Table I. and reproduced in graphical form in the diagram. It may easily be seen that the ageing had the effect of merely shifting the temperature resistance curve down in the direction of the resistance axis. The value found for the specific resistance of the aged cobalt at 20° C. was 6.85 microhms per c.c., and the specific resistances at different temperatures were calculated from this value. The specific resistance of the unaged piece of cobalt was found to be 8.07 microms per c.c. at 20° C.

The work on chromium has been described in a previous paper, but at the time when that paper was written it was not possible to get the final measurement in liquid helium and so the results are repeated here with that reading added. The chromium was measured at 2.25° K. and the cobalt at

2.5° K. ; neither was found to be superconducting. It was found that both cobalt and chromium had very small temperature gradients below the temperature of liquid hydrogen. It appeared, in fact, that the resistance of cobalt or chromium at low temperature was almost independent of temperature.

TABLE III.

	Chromium.	Iron.	Cobalt.	Nickel.	Copper
R/R_0 at liq. air	·132	·0848	·202	·180	·144
R/R_0 at liq. hydr.	·059	·0113	·075	·085	·0015
Sp. resist. at 273° K....	15.25	8.85	6.15	6.93	1.59
Sp. resist. at 20.6° K....	·90	·101	·46	·59	·0024

The value 6.85 microhms for the specific resistance of cobalt at 20° C. is much lower than the value given in Smithsonian tables, but is close to the accepted specific resistance for nickel at 20° C., namely 7.5. The value given for iron is 8.8. In Table III. values of R/R_0 are given for chromium, iron, cobalt, nickel, and copper at the temperature of liquid hydrogen. From these values and the specific resistances of the metals at 0° C., the specific resistances at liquid hydrogen temperature were calculated. The values are given in the lowest line of the table. The values for R/R_0 at liquid helium temperature for iron, nickel, and copper were not given in Onnes and Tuyn's data, and the original papers had not become accessible at the time of writing, so that it has not been possible to calculate the specific resistances at liquid helium temperature.

In comparing the specific resistances of different elements it is customary to compare the values either at room temperature or at 0° C. When the values differ widely it is not of much importance what temperature is taken for the comparison, but if the specific resistances are close together the order of magnitude may change at different temperatures. It is therefore of importance to decide what temperature should be chosen for comparing specific resistances ; it seems almost obvious that the ideal temperature for making a comparison would be the absolute zero. Measurements cannot be made at that temperature, but on account of the

fact that the temperature gradient is practically zero for many metals at low temperatures, one can employ measurements at slightly higher temperatures to make comparisons.

It was with this in view that the last line in Table III. was calculated. It appears that although iron is a poorer conductor than either cobalt or nickel at room temperature, yet at low temperature it is much superior. No measurements have been made on manganese, and therefore it is perhaps rather too early to press conclusions. Nevertheless, the figures seem to indicate that as one passes from chromium to copper, the resistance falls from a high value for chromium to a low one for iron, and then rises again for cobalt and nickel and falls eventually to a very low value for copper. This increase in the value of the specific resistance for iron is very interesting from the point of view of atomic structure. If the electron configuration for iron be taken as $2 : 2.6 : 2.6 : 6 : 2$, when the valence electrons are stripped off, a system of six 3_s electrons is left. This is a comparatively stable system, although of course ten 3_s electrons are required for complete stability. On the other hand, when two valence electrons are stripped off cobalt and nickel, a system of seven and eight 3_s electrons is left. In the case of copper, when one valence electron is stripped off, all the ten 3_s electrons are present, and an excellent conductor results. It appears then, for a metal to be a good conductor, the electron systems of the core must be completed. If this be so, the reason for the resistance of iron being small at low temperatures can be accounted for if six 3_s electrons form a fairly stable system. Hund, in dealing with the magnetic properties of the rare earths, found that when six electrons had filled into the 4_f system, the magnetic susceptibility fell almost as if fourteen electrons had completed the system. In offering this explanation for the behaviour of the electrical conductivity of the iron, cobalt, and nickel group, the possibility of any of them having three valence electrons has not been considered. It must be admitted that an assumption has been made here, but it seems a very reasonable one. The point that is stressed throughout this communication, both in connexion with the alkalis and with the iron group, is the importance of the structure of the core of the atom on the electrical conductivity of a pure metal.

LXV. *The Effect of Cadmium as an Impurity in Lead on the Conductivity of Lead.* By Prof. J. C. McLENNAN, F.R.S., C. D. NIVEN, M.A.*, and J. O. WILHELM, M.A.†

A GREAT deal of effort has been expended on obtaining pure metals for the investigation of electrical resistance at low temperatures because the important effect of impurities on electrical resistance has always been borne in mind by any experimenters in investigating whether a metal were a superconductor or not. Indeed, when a metal did not turn out to be a superconductor it was always doubtful whether or not the little impurity—which is nearly always present even in the purest attainable samples of a metal—was sufficient to account for the small resistance at very low temperatures. Recently, opinion has strongly favoured the idea that a residual resistance may be expected for most metals at the lowest temperatures. At the same time, if resistance at higher temperatures is so greatly affected by an impurity, two questions seemed to us to be worthy of investigation, firstly, whether or not a slight impurity in a superconductor spoilt its superconductivity at the superconducting temperature, and secondly, whether the temperature at which the superconductivity appeared changed with the amount of impurity.

In entering this field the authors of this communication realized the enormous complications that could arise in the results. When the metals are mixed to form an alloy they may either form a mechanical mixture or they may form a solid solution, or they may form a chemical combination. If a mere mechanical mixture were formed the mean conductivity might be expected, and when one of the constituents became superconducting probably the whole alloy would. On the other hand, if a solid solution were formed a totally different curve might be expected from the temperature-resistance curve for the pure metal, and it might be that the superconducting property disappeared altogether. Again, there was always the possibility that a solid solution at room temperature might undergo a change at low temperatures, and this introduced a further complication.

Very little work has been done on alloying superconductors. Some work has been done at Leiden‡ by

* This work was carried out with the aid of a grant of a fellowship from the National Research Council of Canada.

† Communicated by the Authors.

‡ Leiden Comm. No. 181.

Tuyn and Kamerlingh Onnes on an alloy of tin and lead, but the authors have not come across any other work. An alloy of tin and lead is an alloy composed of two superconductors, and it is not surprising at first sight that the alloy should have been found superconducting. Yet on further consideration this does not seem a necessary consequence of the mere fact that the original metals were superconductors. Had the metals formed a solid solution or chemical compound, why should we expect the alloy to be superconducting?

The problem of superconductivity has not been treated satisfactorily by any theory up to the present, and on this account there seemed to be no reason for not collecting data and ascertaining some empirical facts about the effect of adding impurities to a superconductor on its resistance at low temperatures, even though they could not be clearly interpreted.

Apart from the complications attendant on the formation of solid solutions and compounds, we realized that before any conclusions could definitely be drawn from our method of attack a great deal of work might be necessary. There are five superconductors, and with each of these probably 6 or 8 different metals should be alloyed. For each of these combinations a whole series of alloys should be prepared and have their resistance-temperature curves determined. The results, therefore, communicated in this paper must be looked upon as a mere beginning of what may be expected from a somewhat extensive programme, yet we think them of sufficient interest to publish, as they show that a metallic impurity in a superconductor will not necessarily eliminate the property of superconductivity.

The alloying metal chosen by us was cadmium and the superconducting metal was lead. We chose lead as it was possible for us to get a very pure sample of that metal from the Bureau of Standards. In some ways lead was awkward to measure at low temperatures as it became superconducting about 7°K . On this account great care had to be taken in handling the helium liquefier. It was necessary for conditions to be upset sufficiently at the nozzle so that liquid helium would not "make," and so that the temperature remained constant. A helium gas thermometer at the side of the liquefier indicated when the temperature was steady. The temperatures were read on a constant thermometer. In reading the temperatures we assumed that the temperature-resistance curve for constantan was linear between the temperatures of liquid helium and liquid

hydrogen. This assumption is justified from work by Onnes and Holst*. Due to the difficulties of holding the temperature constant and in reading its absolute value accurately, the value found for the superconducting temperature of pure lead was a little lower than what we found it two years ago, and on this account we measured the resistance of a piece of pure lead along with that of the pieces of alloyed metal. We were thus able to tell if the alloy were superconducting at the same temperature as the pure metal or not. This question was of much greater interest to us than the question of fixing the absolute value of the temperatures by which superconductivity appeared.

The cadmium was distilled as a precaution in case it was not pure, and alloys containing about 0.1, 1, and 3 per cent. of cadmium were prepared as follows:—The lead and cadmium were accurately weighed out and placed in a pyrex glass tube which was evacuated and sealed off. The tube was heated until the metals melted, and was then well shaken. In order to measure the specific resistance a part of the alloy thus formed was run into a glass tube of about 2 mm. bore through a fine constriction to keep back any surface contamination. If the dimensions of the sample were to be accurately determined, it was important to get the alloy to solidify in the tube free from pit-marks, and the tube was, therefore, placed in a furnace we had formerly used for making crystals and not merely heated in a bunsen flame. It was very important to get the glass broken off without damaging the surface. The cross section of each sample thus obtained was measured in five different places in a length of about 4 cm. The length was taken between two steel points which carried the "potentiometer" leads. In this way the specific resistances of the alloys we prepared were measured at room temperature, and we were thereby enabled to represent the temperature-resistance curves of different alloys on the same diagram.

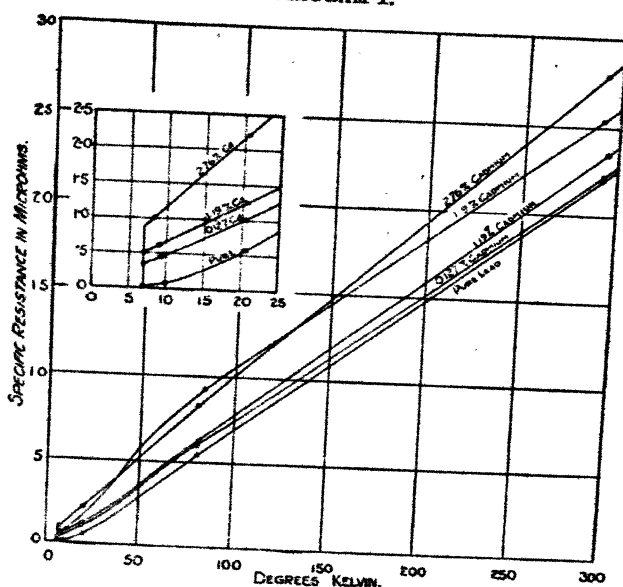
The remaining portion of each alloy was run into a fine glass tube and used for obtaining data for the resistance-temperature curves. The dimensions in this case were of no consequence; it was of greater importance to get a reasonably high value for the resistance. Pieces of two different alloys and a piece of pure lead were mounted on a piece of red fibre, and wires were soldered on in such a way that the samples were connected in series. A pair of tapping-off or "potentiometer" leads were soldered to each

* Leiden Comm. No. 141 a.

piece of metal. With this arrangement of wiring three metals could be measured with eight leads. This was a rather important point because we had only a small tube through which to bring all our wires out from the helium liquefier; in addition we had to bring out wires from the constantan thermometer.

Measurements were made at room temperature and at the temperature of liquid air and liquid hydrogen. As described above, measurements were made in the helium liquefier with the conditions upset, and it was found to our surprise that all the alloys which we had prepared were superconducting

DIAGRAM I.



at a temperature very near to that at which the pure lead was superconducting. The results of the measurements of the three alloys containing 0.127 per cent., 1.19 per cent., and 2.76 per cent. of cadmium are given in graphical form in Diagram I. A glance at the diagram shows that the curves for the alloys containing 0.127 and 1.19 per cent. of cadmium at higher temperatures run approximately parallel to the curve for pure lead, and in this respect are markedly different from the alloy containing 2.76 per cent. This appeared to us to be rather interesting, and we decided to make up an alloy containing about 2 per cent. cadmium.

As apparently all the alloys we had made so far were superconducting, we thought it would also be interesting to make up an alloy with a larger impurity still, such as 5 per cent.

Two alloys were therefore prepared, one containing 5.19 per cent. of cadmium and the other 1.88, and wires of them were mounted on the piece of fibre in place of two other alloys. They were measured at room temperature, and at the temperature of liquid air, and liquid hydrogen, and finally in the helium liquefier. With the experience we had had previously we succeeded in improving our

Specific resistances of Lead-Cadmium Alloys

Pure Lead.		0.127 % Cadmium.		1.19 % Cadmium.				2.76 % Cadmium.	
Degrees Kelvin.	Sp. resist.	Degrees Kelvin.	Sp. resist. before.	Degrees Kelvin.	Sp. resist. before.	Degrees Kelvin.	Sp. resist. after.	Degrees Kelvin.	Sp. resist. before.
293	22	293	22.2	292	25.4	294	23.5	293	27.9
81	5.46	81	5.97	84	9.27	81	6.29	81	8.34
20.6	.582	20.6	1.09	9	.620	20.6	1.24	20.6	2.22
10	.079	7.2	.359	7.2	.511			8.4	1.01
7.2	.028		Superconducting.		Superconducting.			7.2	.356
	Superconducting.								Superconducting.

technique considerably. In the first place we had learned how to control the liquefier so that the temperature remained steady for a fair length of time, and in the second place we took the leads from the pure lead to the pair of terminals on the potentiometer that we had previously been using for the standard resistance. The batteries were sufficiently constant so that when once the current was known by a measurement of the standard resistance, there was no further need of having the latter attached to the potentiometer. By having the pure lead leads attached to these terminals it was possible to switch instantaneously from the

pure lead to an alloy; and thus, at the superconducting temperature, comparisons could be made between the pure lead and an alloy with the assurance that the temperature had not changed in the meanwhile.

With these improvements we were able to show that while the resistance of an alloy dropped suddenly at the temperature at which lead was superconducting it did not completely vanish. The 5.19 per cent. alloy became superconducting at four-tenths of a degree below the superconducting temperature of lead, and the 1.88 per cent.

before and after cooling to 7° K.

1.88 % Cadmium.				5.19 % Cadmium.			
Degrees Kelvin.	Sp. resist. before.	Degrees Kelvin.	Sp. resist. after.	Degrees Kelvin.	Sp. resist. before.	Degrees Kelvin.	Sp. resist. after.
294	26.2	294	25.3	294	21.9	294	18.8
84	8.02	225	18.8	84	8.09	225	14.2
20.6	1.75	85	7.19	20.6	1.92	85	5.29
12.7	1.06	20.6	1.54	12.7	0.97	20.6	1.08
9.1	0.90			9.1	0.82		
7.3	0.87			7.3	0.78		
7.2	0.048			7.2	0.12		
7.0	Superconducting.			7.0	0.024		
				6.8	Superconducting.		

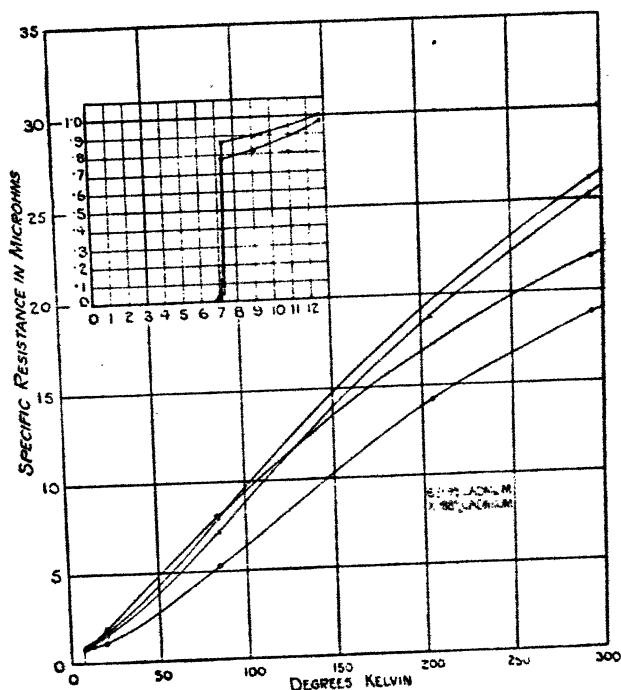
alloy at two-tenths below. This seemed to point to the fact that the amount of cadmium affected the temperature at which the resistance of an alloy entirely vanished, but did not affect the temperature at which the phenomenon of superconductivity started to make its appearance.

From the measurements the specific conductivities were calculated and the graph was plotted. It was found that the 5.19 per cent. alloy had a very decided curvature at higher temperatures, i.e., between liquid air and room temperature, and as a rough guide in drawing the curve it was decided to take a measurement in alcohol cooled

684 *The Effect of Cadmium as an Impurity in Lead.*

with liquid air down to about 220° K. When this was done, and the corresponding point put on the graph, it was found that we had to draw a curve with three bends in it to pass through the points. It was concluded that some mistake had been made, and as a precaution the readings in liquid air of the 1.88 per cent. and the 5.19 per cent. alloys were repeated. Neither of the readings when repeated agreed with the previous readings. Repeat measurements

DIAGRAM II.



were made at room temperature, and these did not agree with the original measurements either. Finally repeat measurements were made in liquid hydrogen. The results were plotted for both the alloys (1.88 and 5.19) and we found that for each alloy there were two curves. The curves are shown in Diagram II. We think the change in resistance is due to the cooling to very low temperatures—a sort of ageing effect has probably taken place. This is supported by work we have done on ageing cobalt and chromium, which showed that ageing had the effect practically of shifting the temperature-resistance curve

down in the direction of the resistance axis. In the case of the alloys here in question the approximately constant difference of resistance seems to exist only above the temperature of liquid air.

Repeat measurements were made on the alloy containing 1.19 per cent. cadmium, and when these were plotted the constant difference of resistance was again apparent. The measurement in hydrogen for this alloy was made after the measurement in the helium liquefier, so that the reading for the hydrogen temperature before the cooling to 7° K. is not known. Readings are given in the table in two columns under the headings "after" and "before"—*i. e.* after the alloy had been in the liquefier and before. No "after" readings are available for the 0.127 per cent. and 2.76 per cent. alloys, as these resistances had been taken off the piece of fibre before this ageing phenomenon had been observed.

We do not wish to press any conclusion as we should first like to investigate much more thoroughly this strange ageing phenomenon. New questions at once arise; for instance, what temperature is necessary for the effect to take place? or, has time any influence on the ageing? or again, will cooling a second time to the superconducting temperature produce a further change? Until such questions be answered it is premature to say whether the effect is due to a separation of a solid solution into components or merely to some alterations in crystal structure. At all events, since a cadmium-lead alloy containing as much as 5 per cent. of cadmium was found to be superconducting, it is highly probable that there is a continuous chain of lead atoms in the superconducting state of the alloy.

LXVI. *Experimental Evidence of the Existence of Aggregates of Active Deposit Atoms in Gases containing Radon.* By Prof. E. L. HARRINGTON, Ph.D., University of Saskatchewan, Canada *.

[Plate VII.]

MILLE C. CHAMIÉ† recently described experiments giving photographic evidence that radioactive material of various kinds when introduced into mercury exists in the form of aggregates rather than as individual atoms, regardless

* Communicated by Sir E. Rutherford, O.M., P.R.S.

† Mlle C. Chamié, *C. R.* clxxxiv. p. 1243 (1927).

of the method employed in activating the mercury. Later experiments * definitely indicated that these aggregates were in general not due to the association of radioactive atoms within the mercury, at least not solely, but actually existed as such before the introduction of the radioactive material into the mercury. In these experiments the aggregates were obtained from surfaces exposed to emanations and from surfaces activated in various solutions. From both theoretical and practical standpoints it is important to know whether in the case of surfaces exposed to emanations the aggregates form in the body of the gas and are deposited as such, or whether the process of aggregation takes place with atoms deposited individually on the surface exposed.

Certain work by Mme Curie †, by Makower and Russ ‡, and a number of others point definitely to the former process, though the latter may also function. This report has to deal with a somewhat different line of experimental investigation of this problem.

Experimental Methods and Results.

Since Mme Curie's work indicated a part played by gravity in the distribution of the active deposits on surfaces exposed to emanations, it was believed that by centrifuging tubes containing radon the distribution of active deposit on the walls should be affected. The experimental arrangement for measuring the distribution is indicated in fig. 1. Air-radon § mixtures were introduced into tubes such as T, and the latter mounted in such a way as to be adjustable in position along a vertical guide S provided with a scale. Two lead blocks LL situated between this guide and a gamma ray electroscope E were separated by a space of 1 cm., thereby forming virtually a slit. This limited the gamma radiation reaching the electroscope to that due to the portion of the tube immediately in front of the opening. The rate of fall of the electroscope leaf over a certain range of the telescope scale was taken as the relative activity of that portion of the tube in front of the slit.

Curve A of fig. 2 shows as a typical case the distribution of activity along a tube enclosing an air-radon mixture at atmospheric pressure, and containing 15 millicuries of radon.

* *Id.*, *ibid.* clxxxv. pp. 770, 1277 (1927).

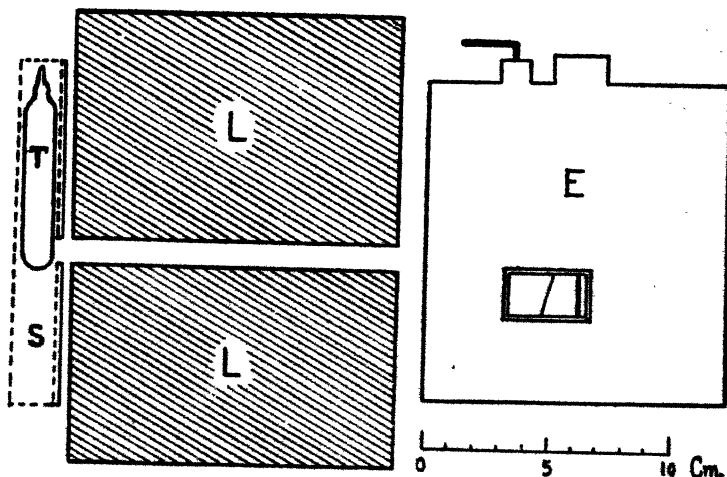
† Curie, *Radioactivité*.

‡ Makower and Russ, *Phil. Mag.* xix. p. 100 (1910).

§ The writer is indebted to Mr. G. R. Crowe for assistance rendered in connexion with the radon supply.

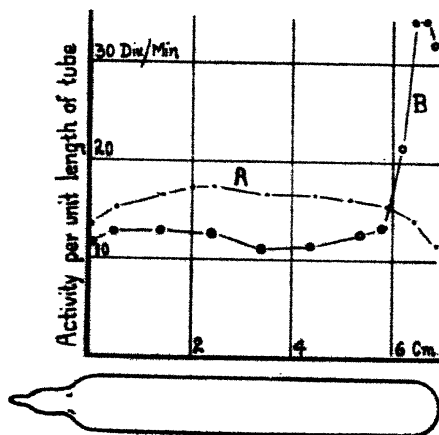
The ordinate at any point indicates the activity per unit of length of the corresponding portion of the tube. After determining the activity distribution in the tube it was

Fig. 1.



Experimental arrangement for determining the distribution of activity along a tube.

Fig. 2.



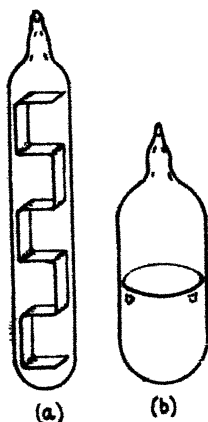
Curves showing the effect of centrifuging on the distribution of activity along a tube.

placed in a motor centrifuge (rounded end of the tube pointing outward) and centrifuged at about 1750 revolutions per minute for a period usually of the order of 30 minutes.

Since the circle described by the outer end of the tube had a radius of 15 cm., the centrifugal force acting on the particles near the end of the tube was about 500 times that exerted by gravity on the same particles. In view of the short mean life of some of the products, the advantage of this method over one depending on gravity is obvious.

Curve B of fig. 2, representing data taken immediately after the centrifuging, indicates the definite change in distribution caused thereby, obviously due to active material being thrown to the outer end of the tube. The magnitudes of the effects produced by centrifuging varied from unobservable ones to effects considerably greater than that shown in fig. 2. They increase with the partial

Fig. 3.



Tubes used to show that aggregates exist in suspension in the body of the gas containing radon.

pressures of radon and of water-vapour and with the total pressure, and depend somewhat on the shape of the tube. It is of interest to note that Mme Curie found a similar dependence on these factors in her work on the effect of gravity.

It is likely that in all cases a part of the effect of centrifuging is due to aggregates loosely attached to the wall being dislodged and thrown to the outer end of the tube. But the fact that the filter through which the radon mixture is removed always shows some activity, and the results shown by the following experiment, indicate that a definite portion of the material affected must come from the body of the gas. A strip of brass about 5 mm. wide was bent and inserted into a tube as indicated in fig. 3 (a); the

horizontal portions of the strip, or the "steps" of the "ladder," effectually divide the length of the tube into such short sections that any material dislodged from the walls of the tube during centrifuging would be unlikely to reach the middle portions of the steps. In one case the tube was centrifuged during the entire time (45 minutes) the radon-air mixture was in the tube, and in another case the radon was left in the tube overnight before centrifuging. In each case after removing the radon the tube was opened and the middle portions of the steps were cut out and laid on a photographic plate—the first step with the upper face up, the next with the upper face down, the next up, and so on alternately until the steps were all lying side by side in a row on the plate. This was then covered by another sensitive plate and left for about 10 minutes. On development each plate showed a row of alternately darker and lighter spots, and in every case the darker spots were due to exposure to the upper faces of the steps, *i. e.* to the faces pointing towards the axis of rotation of the centrifuge. On repeating the experiment but omitting the centrifuging, spots of uniform density were obtained.

The tube shown in fig. 3 (*b*) was used in a further test of the same sort. Here the tube was divided by a circular mica partition. After the centrifuging and removal of the radon the mica was placed on one photographic plate and covered by another. The results showed the upper face to have received the greater deposit. Fig. 4 (Pl. VII.) shows a greatly enlarged view of a portion of the plate exposed to the upper face, and indicates that in addition to a general distribution the active material is collected in aggregates distributed at random.

These experiments pointed definitely to the conclusion that the aggregates existed in suspension in the gas, and the size of these atomic groups, as suggested by their photographic action, indicated the probability of seeing them ultramicroscopically. Mme Curie (*l. c.*) and others have indeed reported having observed very persisting clouds in chambers containing gases including emanations and water-vapour. For a test of this a small brass chamber was constructed and filled with a radon-air mixture, and then examined ultramicroscopically by an arrangement similar to that described by Whytlaw-Gray*. Intense illumination, carefully adjusted, was required to make the particles visible, when they appeared as tiny "stars" exhibiting

* Whytlaw-Gray, *Proc. Roy. Soc. cii.* p. 600 (1913).

Brownian movements and drifting with the convection currents. An electric field, established between the central wire and the brass case by connexions to the D.C. mains, quickly swept the particles to one side. Even when the field had been left on for some time, only a comparatively short time, say 10 or 15 minutes, was required to elapse before particles again began to appear in the field of the microscope. The variations in the intensities of the "stars" and their activities in Brownian movements suggested a certain variation in their sizes. The particles visible in a freshly-filled chamber seemed to have higher mobilities than those visible later, but, except at first, little change with time was noticeable. This is due no doubt to the attainment of a condition of equilibrium in which the particles seen range in size from the smallest visible to the largest permitted by gravity to remain in suspension, new aggregates forming and growing and old ones disappearing owing to gravity or diffusion. Work along this line is being continued.

The question as to whether the particles detected ultra-microscopically are aggregates of radioactive atoms or merely dust requires consideration. In the first chamber used the radon-air mixture introduced had been previously used in a number of experiments like those described above, and this involved its being filtered a number of times through a cotton-wool plug; and it was again filtered as it was introduced into the brass chamber. Moreover, the application of the electric field should have disposed of any dust escaping all these filterings. However, the second chamber used was constructed as a miniature Wilson expansion chamber. It contained some water and was filled with filtered air only. Attempts to see particles were all unsuccessful; but when this same chamber was filled with a radon-air mixture similarly filtered, the particles were visible at once. Neither repeated expansions nor electric fields temporarily applied could permanently rid the field of particles, though such treatment should certainly have removed any dust. As further evidence on this point, it may be mentioned that, in some of the experiments on centrifuging first described above, the same tube, remaining hermetically sealed, was used on successive days without any apparent change in the definiteness of the effect produced by centrifuging.

The above experimental results are entirely in agreement with the experimental evidence obtained by others, and all considered together leave little doubt as to the actual existence of aggregates of radioactive atoms in suspension

in gases containing emanation. Certain other experiments, of which the details are considered unessential, will be mentioned in connexion with the next section.

It was felt that photographic evidence of these aggregates, obtained by methods similar to those described by Chamié (l. c.) or by Mühlestein* would be useful. The sensitive plates were "infected" in the following manner. As soon after the removal of the radon mixture as convenient the tubes were opened and the inner surfaces rubbed by a wire or a small steel ball mounted on a wire. The latter, bearing a certain amount of loosely adhering active material, was then tapped on the plates. These, on being developed, indicated that the spots of the gelatine actually touched became heavily infected, but there was also a scattering of independent and well-separated aggregates obtained elsewhere on the plate. Slow plates and slow development were found best. Fig. 5 (Pl. VII.) is a microphotograph showing the random distribution of aggregates thus obtained on the plates. Figs. 6 and 7 (Pl. VII.) show individual haloes at a still greater magnification. The "radiant" appearance is due to individual alpha particles from the aggregate passing through the air for different distances before striking the gelatine layer. When by a suitable arrangement a layer of mercury was left on the plate during exposure, all alpha particles except those having paths wholly within the gelatine were absorbed. The tracks of the alpha particles thus obtained are substantially equal in length, and define a circle having a radius equal to the range in gelatine of the alpha particles involved. Figs. 8 and 9 (Pl. VII.) show different magnifications of the circles thus obtained. Measurements on one hundred different diameters and involving many different circles and plates gave a mean value of approximately 53 microns as the actual radius of the circles on the original plates. Any plate will in general show circles having wide variations in the number of tracks radiating from the centres, some with only a few isolated tracks and others with so many as to make a solid black circle. The numbers of atoms in the aggregates must vary similarly, but the actual sizes of the aggregates are in general much too small to affect appreciably the diameters of the circles obtained.

Discussion.

The tendency of radioactive atoms to form aggregates was observed early in the course of experimental study by

* Mühlestein, *Archives des Sciences*, 5th, iv. p. 38 (1922).

different observers*. As to whether in the case of emanations this aggregation took place in the body of the gas or on the surfaces exposed to the emanations seemed less certain. No doubt existed as to the presence of the active deposit atoms in the gas containing the emanation, and in the light of the results obtained by others together with those described above. The obvious conclusion would seem to be that these atoms exist, at least in part, in the form of aggregates in suspension in the body of the gas.

Evidence as to the nature of the particles is more indirect, but yet suggestive. The importance of the presence of water-vapour raises the question as to whether the particles observed are minute drops of water incorporating a load of radioactive atoms or whether they are aggregates of the latter, including or absorbing water-vapour molecules to an extent determined by the partial pressure of the water-vapour. Those who have held the former view as to their nature have had to assume the presence of chemical compounds of some sort, say nitrogen oxides due to the action of the emanation on the air, in order to account for the persistence of these drops in an unsaturated atmosphere. But Mme Curie† was able to observe the gravity effect also in carbon dioxide and in hydrogen, and the present writer, in the course of experiments on centrifuging gases containing radon, substituted argon for air in certain cases without any observable change in the nature of results. This would seem to preclude the probability of any chemical action being essential to the formation of the particles. Vapour-pressure considerations would scarcely support the idea of the formation of minute drops of water in a non-saturated atmosphere in the absence of chemical compounds of some sort‡. That the effect persists even at very low vapour-pressures was seen from the following test. A tube containing the usual radon-air mixture with saturated water-vapour and also giving a marked effect of centrifuging was mounted with its lower end dipping 1 centimetre into a mixture of ether and carbon dioxide snow during the period of attaining equilibrium. The distribution of activity along the tube was then determined, after which it was returned to its former position long enough to offset the effect of any rise of temperature occurring during the taking of the observations.

* For detailed references consult Curie, *Radioactivité*; Rutherford, 'Radioactive Substances and their Radiations'; or Meyer and Schweidler, *Radioaktivität*.

† Mme Curie, *Radioactivité*, vol. i. p. 371, figs.

‡ See Poynting and Thomson, 'Properties of Matter,' 2nd ed. p. 166.

It was then centrifuged and again tested with the usual positive indication of active material having been thrown to the outer end. A second trial with argon substituted for the air gave like results. The vapour-pressure in these cases was certainly much too low to permit the formation of drops, and any excess water was frozen to the bottom of the tube before the tube was centrifuged. In the ultramicroscopic study mentioned above the observed particles were removed by an electric field temporarily applied, and from the vapour-pressure considerations referred to above one would expect that if any later condensation takes place it would be on the water surfaces already formed. It would appear then most unlikely that the new particles that appeared later were drops of water. Furthermore, Rutherford and others have found that for the greater part the active deposits carry positive charges. It is known from observations made with the Wilson expansion chambers that drops of water form more readily on dust particles or on negative ions than on positive ions, and in these experiments there could have been no shortage of available negative ions. These and certain other considerations have led the writer to the conclusion that the particles observed in non-saturated gases containing radon are not drops of water, but are aggregates of active deposit atoms. In saturated atmospheres no doubt both types of particle may exist.

The Origin of the Aggregates.

It would appear that particles might originate in either or in both of two ways. In the first place, the photographic evidence clearly proves that these aggregates do exist on surfaces which have been exposed to emanation. Makower and Russ (*l. c.*) and Lawson*, among others, have definitely proved the reality of the "aggregate recoil"—in other words, that when a member of an aggregate of radioactive atoms, say on a plate, ejects an alpha particle in the direction of the plate, not only the parent atom, but the entire aggregate containing this atom, may be thrown from the plate by recoil. This, then, offers one way of accounting for the aggregates found in suspension in the gas.

It appears probable, however, that most of the aggregates are actually formed in the gas itself. In the experiments described above there were atoms of radon and of subsequent members of the series, molecules of air or water-vapour, and

* Lawson, *Wien. Ber.* cxxvii. p. 1315 (1918); cxxviii. p. 795 (1919).

of unknown other kinds present in the tubes employed. This mixture was subjected to the intense ionizing action of alpha, beta, and gamma rays and of recoil atoms, and there must have resulted a corresponding variety of ions, some positive, some negative. That atoms of active deposit generally carry positive charges has been repeatedly observed, and that a considerable number carry negative charges was indicated by the following test:—Three long narrow plates were mounted parallel to and symmetrically about the axis of a glass tube into which the usual radon-air mixture was introduced to a pressure nearly atmospheric. Two of these plates were connected to the terminals of a 200-volt D.C. line, and the third left insulated. After due exposure the plates were removed and placed on a photographic plate. The latter on being developed showed that the cathode had received a much heavier deposit than the anode, but that the anode had received a very definitely greater deposit than the third plate. Since, then, active deposit ions of unlike sign do exist, there must be combinations between them in addition to the many other kinds of combinations possible with such a variety of ions. If in any combination only molecules of gases are involved, these molecules should separate at once and be as independent as they are normally. But if the ions, whether simple or cluster ions, included two or more atoms of radioactive or other substance normally existing as a solid under the conditions of the experiment, there appears to be no obvious reasons why these should separate. On the contrary, every consideration indicates that they should remain together. Moreover, at least a certain proportion of the molecules of air, or especially of water-vapour, included in the uniting ions would be expected to remain in the resulting group or particle because of the tendency of such molecules to become absorbed on solids. Therefore in such a mixture of ions the probability of combinations of permanent nature is very high. Once a nucleus of an aggregate is formed, the chance of further acquisitions increases with the growth of the aggregate, since its mobility and therefore its chance of reaching the wall must decrease, and its probability of being struck by other particles or molecules must increase with its size. This growth should continue until it is removed by diffusion, by electric field, or by gravity.

Whether the aggregates known to exist on the surfaces exposed to emanations originate thus or actually form on the wall will not be discussed here; but this theory would explain the experimentally observed fact that these aggre-

gates are, at least in many cases, but loosely attached to the activated surface.

On this theory the rate of growth of an aggregate would increase with the number of atoms of active deposit, of molecules of vapours, and of any other substance not able to leave a combination once formed. These deductions appear to fit known experimental facts, and in particular to explain the part water-vapour may play, even in a non-saturated atmosphere, in the formation of these aggregates.

Summary.

Experimental evidence is given of the existence of aggregates of atoms of active deposit in mixtures of radon and air, also of radon and argon, including in either case more or less water-vapour. The evidence is both direct and indirect. Photographic evidence as to the nature and variety of these aggregates is included.

Suggestions as to the possible origin of these aggregates seem to account for the facts experimentally obtained by various observers.

The writer is grateful to the University of Saskatchewan for the grant of a leave of absence, and particularly indebted to Professor Sir Ernest Rutherford for his kindness in granting him the privilege of working in the Cavendish Laboratory, for suggesting the problem, and for his interest and many suggestions during the course of the work. He would acknowledge also the valuable assistance given by Dr. Chadwick, who had much to do with providing the facilities and materials required.

Cavendish Laboratory,
June 23, 1928.

LXVII. *Molecular Cohesion.* By G. A. TOMLINSON, B.Sc.*

[Plate VIII.]

(1) **T**HE amount of well-established knowledge concerning the nature and origin of interatomic forces is very limited. Within recent years the theoretical aspect of the question has received much attention, and a number of interesting and suggestive results have been obtained by mathematical methods. It is generally agreed, however, that the problem of atomic forces has not been solved, and

* Communicated by Sir J. E. Petavel, K.B.E., F.R.S.

even on the more restricted question of the relation between the force and the distance, different workers are not at all in agreement. It is known that atoms or molecules in any of the states of matter can exert a powerful attraction on one another when very close together, and there is reason to believe that the effective field of the attraction force is at the most only a small multiple of the dimensions of the molecule. Thus in liquids the force becomes negligible at distances of the order eight times the normal distance between the molecules.

For equilibrium to exist among the atoms of a solid, we are compelled to suppose that the atoms also exert a repulsive force on each other, a force about which there appears to be hardly any positive knowledge, except that the sum of the repulsive forces must be in balance with the sum of the attractive forces. There is reason to think that the repulsion falls off at a considerably greater rate than the attraction as two atoms separate, and therefore has a smaller field. Simple considerations of the stability of the atoms in the solid require this to be so.

Several distinct atomic attractive forces must be recognized, such as the force of chemical affinity, the binding force in polyatomic molecules, and the cohesive attraction exerted generally by all atoms or molecules. The cohesive force is some rapidly diminishing inverse function of the distance between the atoms, and very varied suggestions have been made as to the probable law of force. Many years ago, Sutherland* gave reasons for believing that gaseous and liquid molecules attract according to an inverse fourth-power law. He also published a kinetic theory of solids† in which the same law is assumed. Chatley‡ has suggested that the attraction in the case of solids follows an inverse sixth-power law. Järvinen§ considers that molecules attract according to a law, force $\frac{m^2}{d^5}$, in which m is

the mass of the molecule. Kam|| arrives at a conclusion favouring an inverse square law, and Antonoff¶ from surface-tension phenomena suggests an inverse fourth power. Lennard-Jones** finds for the inert gases that the most probable index is -5 . In his Cantor lectures on the

* Phil. Mag. xxiv. and xxvii. (1889).

† Phil. Mag. xxxi. (1891).

‡ Proc. Phys. Soc. xxvii.

§ Zeit. Phys. Chem. 1914.

|| Phil. Mag. xxxvii.

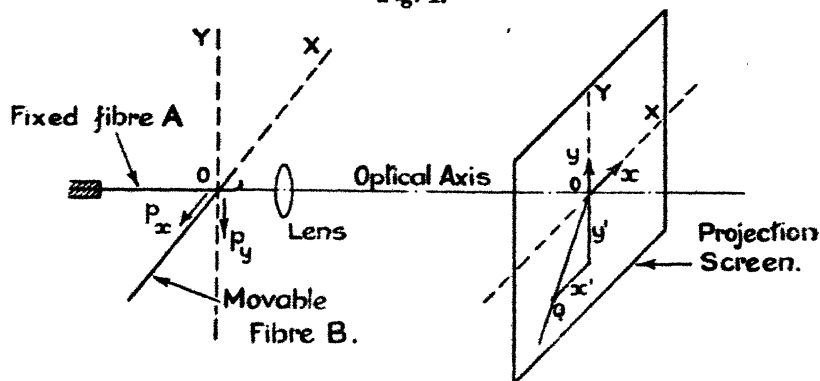
¶ Phil. Mag. xxxvi.

** Proc. Roy. Soc. cxii.

structure of metals, Rosenhain* mentions an inverse cube law as a probable description of the forces between metallic atoms. Finally, Edser† has suggested that it is necessary to consider a higher index than any of those already mentioned, and regards -8 as being more probable.

(2) The present paper gives a description of some experiments in which the force of adhesion between fibres and spheres of glass or quartz can be observed and measured. The results obtained experimentally are then compared with those to be expected by calculation, if the molecular attraction follows a law $F = Kd^{-n}$, different integral values being allotted to the index n . There is no very strong *a priori* reason for thinking that the force between two atoms can be described by a simple inverse law, such as the above, in which

Fig. 1.



n is an integer; but, on the other hand, as the above references show, there is such diversity of opinion as to the approximate law of force, indices of 2, 3, 4, 5, 6, and 8 being suggested by different writers, that any evidence in support of a particular integral index may be considered to be a small advance in our knowledge of the nature of the attraction.

If two freshly-drawn fibres of glass or quartz are brought into contact, they are found to adhere, and, on separating the fibres, the force of adhesion causes a measurable elastic deflexion of the fibres. Similarly, the force of adhesion of two fused spheres can be observed if the spheres are flexibly supported, as, for example, by a piece of piano wire. Measurements of the force were made in the following way. One fibre, A (see fig. 1), was supported as a cantilever in a

* Cantor Lectures, 1925.

† Brit. Ass. Rep. 1922.

horizontal optical projector, its direction coinciding with the optical axis. The tip of the free end of the fibre was bent upwards and was focussed at the screen. A second fibre, B, was held below the first at right angles to it, and this fibre could be moved in two directions, OX and OY, at right angles. The two fibres were brought into contact, when they adhered, and then they were drawn apart until they separated. The deflexion of the fixed fibre at the point of separation was marked on the screen, from which the force of adhesion can be found by calibrating the stiffness of the fibre with light wire riders.

The fixed fibre A can be deflected either downwards in the direction OY by a force normal to the contact surfaces, or horizontally along OX by a tangential frictional force. If the measured deflexions of the fixed fibres in the two cases are y and x , and λ denotes the stiffness of the fibres in dynes per cm. deflexion and μ is the coefficient of friction between the fibres, then the force of adhesion in the two cases is

$$p_x = \frac{\lambda x}{\mu},$$

$$p_y = \lambda y.$$

The first case may be called free adhesion, since the normal force between the fibres is solely that due to adhesion, no external normal force being applied. The second case may be called the limiting adhesion when the fibres are separated. It was always found that p_x was considerably greater than p_y . A typical example of adhesion measurement is given below.

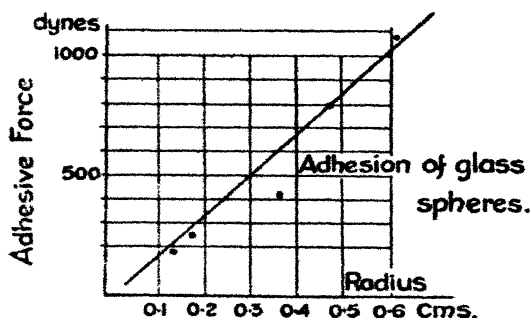
Material	drawn quartz fibres.
Radius	0.006 cm.
Stiffness	= 3.33 dynes per cm.
Deflexion	$y = 0.204$ cm.
	(mean of 78 readings).
"	$x = 0.52$ cm.
	(mean of 61 readings).
Coefficient of friction	0.58.
Free adhesion force	$p_x = 2.98$ dynes.
Limiting adhesion force ...	$p_y = 0.68$ dynes.
Ratio	$\frac{p_x}{p_y} = 4.4.$

The coefficient of friction was determined by mounting two much stiffer fibres in the same way. The fibres were

pressed together by a normal force which was found from the deflexion y' of the fibre (fig. 1). The fixed fibre was then pulled tangentially through a distance x' until slipping occurred. A group of such points was obtained and a mean line, OQ, was drawn through them. From the slope of this line the coefficient was found. The fibres used were freshly drawn and comparable in every way, except as regards diameter, with those used in the adhesion measurements, so that the value of μ is probably closely the same in both cases. Stiff fibres were used to ensure that the applied force was far larger than the forces concerned in adhesion.

Some further experiments were made in which the limiting adhesion (p_y) was measured for freshly-blown glass spheres of various radii. Some results obtained, each being the mean of a considerable number of observations, are shown in fig. 2.

Fig. 2.



The curve indicates that the adhesion force is proportional to the radius of the sphere. The observations do not fall very exactly on the mean straight line, but, having in view the nature of the measurements, there appears to be sufficient consistency to support the conclusion that the relation is linear. With the spheres, quite large adhesion forces are observed. Thus with the largest spheres of 1.22 cm. diameter the force slightly exceeds 1 gm. weight.

(3) Before considering the experimental results further, the cause of the observed force will be discussed shortly. It is necessary to establish securely that the force is one of molecular cohesion. It is possible that a force similar to that observed might be due to electrification. This has been tested by discharging any electrification by strong ionization with radium both before the fibres touch and also while adhering together with a force applied tending to separate

them. The ionization was found to have no effect on the force. Another possible cause is the presence of an adsorbed film of liquid. Against this must be placed the fact that the force exerted by the fibres is always found to be at its strongest just after they have been cleaned by heating to a bright red in a flame. The force is found to diminish slowly with time, and in making the measurements the fibres were actually repeatedly re-heated. The magnitude of the measured forces also appears to be altogether too large for an explanation depending on the surface tension of a liquid film to be satisfactory.

More positive evidence that the force is due to cohesion can be obtained by examining the surface of glass that has been in contact. Fig. 3 (Pl. VIII.) shows an enlarged photograph of a piece of clean glass plate which has been very lightly stroked with a fused glass sphere. It will be seen that, as the sphere moves, a succession of flakes have been torn out of the plate, and at each tear the sphere jumps a short distance clear of the plate, its track being clearly shown as a broken line. A similar effect has been described by Hardy in his work on lubrication. This experiment conclusively shows that strong cohesion occurs at the contact.

(4) The experiment with the adhering fibres will next be considered in some detail, as facts of some interest can be deduced from the results. In the condition of free adhesion the attraction between the fibres results in a normal pressure, $p_x = 2.98$ dynes, which will produce a small elastic indentation, the contact area being a circle the radius of which is 3.4×10^{-5} cm., calculated by the usual equation of Hertz. In the second case of limiting adhesion the force exerted is 0.68 dyne, and there is no residual pressure reaction between the fibres, which are just on the point of separating and are in a purely geometrical contact. The last statement can be substantiated experimentally by observing the behaviour of the fibres as they approach each other. It is found that the fibres adhere quite suddenly without any external pressure being applied, which is shown by the absence of any deflexion of the fixed fibre. There is no doubt that adhesion has occurred, as the minute vibrations of the fibre are immediately checked, and, further, if the movable fibre is now withdrawn, it draws the fixed fibre with it. Hence the molecular attractions acting at the instant of geometrical contact are sufficient to draw the fibres together into the condition of complete free adhesion.

A similar conclusion is reached by reasoning from the equilibrium of the two fibres. In general, three forces are acting: (a) an external separating force F ; (b) an elastic reaction, the sum of a large number of molecular repulsions $\Sigma(R)$; and (c) a cohesive attraction, the sum of a large number of molecular attractions $\Sigma(A)$.

For equilibrium we must have

$$F + \Sigma(R) = \Sigma(A).$$

The bodies are in equilibrium for all values of F from zero in free adhesion to p_y , the limiting normal force, since F can be continuously increased in the experiment from zero upwards. Hence, if a small increment dF of the external force produces a relative displacement of the fibres of amount dx , we must have

$$\begin{aligned} dF + d\Sigma(R) - d\Sigma(A) &= 0 \\ \text{or} \quad \frac{dF}{dx} &= \frac{d\Sigma(A)}{dx} - \frac{d\Sigma(R)}{dx}. \end{aligned}$$

Since the attractive and repulsive forces must both diminish to zero with increasing distance between the bodies, $\frac{d\Sigma(A)}{dx}$ and $\frac{d\Sigma(R)}{dx}$ are essentially of opposite sign to $\frac{dF}{dx}$, and it follows, therefore, that for all positions of equilibrium $\frac{d\Sigma(R)}{dx}$ must be numerically greater than $\frac{d\Sigma(A)}{dx}$.

Initially, in free adhesion, $\Sigma(R)$ and $\Sigma(A)$ are equal; hence the above considerations lead us to expect that $\Sigma(R)$ will continuously decrease relative to $\Sigma(A)$ as the fibre is steadily deflected, until finally $\Sigma(R)$ approaches zero and $\Sigma(A)$ has the limiting value p_y as measured, after which the fibres separate.

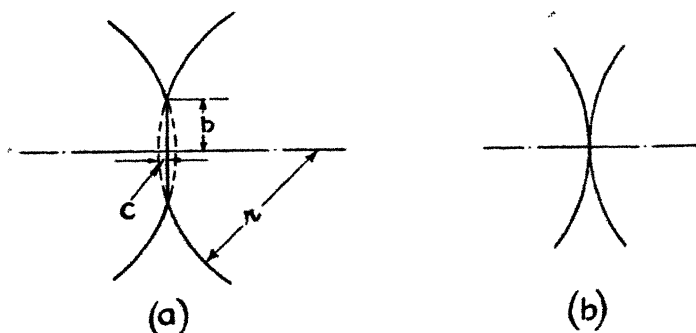
The experiment thus demonstrates that the molecules of a solid exert a cohesive attraction through space on other molecules. Actual contact is not necessary for cohesion to be operative, defining contact as the approach of the molecules sufficiently near to give rise to a repulsive reaction force. It is interesting to find this direct experimental evidence that the molecule of a solid thus possesses a certain small field of attraction, such as matter in the liquid and gaseous states is known to possess.

The experiment further appears to throw a little light on the nature of the repulsion force between molecules. Present conceptions of the structure of the atom compel us to

postulate the existence of a repulsion field, and a number of workers in mathematical physics arrive at the conclusion that this repulsion field falls off much more rapidly than the cohesive attraction field. The behaviour of the fibres described above appears to furnish some direct experimental evidence that the repulsion certainly has this property, although no quantitative information can be derived about the relative rates of change of the attraction and repulsion. However, since practically nothing is known at present about the atomic repulsion, it would appear that any knowledge, however slight, that is based on experimental observations is worthy of note.

Some information of a qualitative kind can be derived from the experiment as to the range of the field of attraction. For this purpose it is convenient in imagination to

Fig. 4.



substitute two spheres of twice the radius of the fibres for the two crossed cylinders, the two cases being identical as regards mean curvature over the small region concerned around the point of contact. Fig. 4 then shows the condition of the two bodies (a) in free adhesion and (b) in geometrical contact as in limiting adhesion. The exact form taken by the bodies in case (a) is unknown, but by making the simple assumption that the deformation takes the form of a small circular flat of radius $b = 3.4 \times 10^{-5}$ cm., the dimension c in the figure is found to be 4.8×10^{-8} cm., which is comparable with atomic dimensions. The force of adhesion in this case was found to be 4.4 times as great as the force in case (b), and the experiment thus gives a general indication of the rapidity with which the attraction diminishes as the distance separating the molecules is increased.

(5) An attempt will next be made to interpret the experimental results on the basis of a simple inverse law of molecular attraction

$$\text{Force} = \frac{K}{a^n}$$

with a view to finding what integral value of n is in best agreement with the results.

It is not possible to calculate the force of adhesion between the fibres in either of the cases, but we can calculate the ratio of the forces by making certain assumptions, and this ratio, assigning different possible values to n , can be compared with the ratio 4.4 found experimentally.

We shall first attempt to show that there is a lower limit to the possible values of n , this limit being 4 if cohesive attraction is supposed to reside in the surface molecules, and 6 if all the molecules of the two bodies are exerting attractions similar to gravitating particles. The first of these alternatives appears to be the more probable, and conforms with the present view held by many, that cohesion is an electrical force accompanying the structure of the atom, adhesion being due to the cohesion fields of the unsymmetrical surface molecules.

In order to derive an expression in a simple way for the total force of attraction between the fibres, we shall substitute for the crossed fibres a plane and a sphere of the same radius as the cylinders. This artifice is justified by the knowledge that the effective force is confined to those atoms in a small region round the contact, of dimensions comparable with molecular dimensions, and the sphere and plane are identical as regards mean effective curvature with the crossed cylinders. We shall in the first place determine the adhesion force with the sphere and plane in geometrical contact, on the assumption that only the surface molecules exert cohesive attraction.

It is necessary in the first place to determine the force exerted normal to its surface by a plane on a single molecule at a distance a from the surface. Let e be the mean distance between the molecules. Then we may either find the total attraction on the single molecule by infinitesimal methods, taking the source of attraction as being continuous over the surface or throughout the body, or we may find the arithmetical sum of the separate attractions treating each molecule as a discrete point for this purpose.

The integration method strictly is not correctly applicable, since it is known in advance that a is of the same order as e ,

but the result is more useful being in algebraic form, and it has been found by actual trial to differ only very little from that obtained by the arithmetical summation.

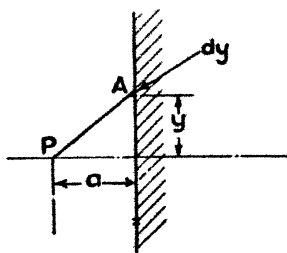
Taking firstly a surface distribution of attracting matter, let s be the number of molecules per unit area. In fig. 5 let P be the position of the external molecule, then the normal attraction of a ring element of the surface of radius y is

$$\frac{2\pi Ksy dy}{(PA)^n} \times \frac{a}{PA},$$

and the attraction of the whole surface is

$$F = 2\pi Ksa \int_0^\infty \frac{y \cdot dy}{(a^2 + y^2)^{\frac{n+1}{2}}} \dots \dots \dots (1)$$

Fig. 5.



Making the substitution $y = a \tan \theta$, this becomes

$$F = \frac{2\pi Ks}{a^{n-2}} \int_0^{\pi/2} \sin \theta \cos^{n-2} \theta d\theta \dots \dots \dots (2)$$

The definite integral is a pure number which will be denoted β .

The attraction between the plane and the sphere can now be found by dividing the spherical surface into elements parallel to the plane and at a distance x from it, having a width dx measured along the common normal.

The normal attraction to the plane of an element, by equation (2), is

$$\frac{2\pi Ks\beta}{x^{n-2}} \times 2\pi sr dx,$$

or the total attraction is

$$4\pi^2 s^2 K\beta r \cdot \int_0^{n\pi} \frac{dx}{x^{n-2}} \dots \dots \dots (3)$$

It may be postulated that two molecules at the point of geometrical contact cannot be closer together than two molecules are in the interior of the solid. The value of the lower limit is therefore taken to be e .

The attraction between two molecules falls off so rapidly with increasing distance that the integration need only extend over a small cap of the sphere, and the upper limit has been written as a multiple of e where me is small compared with r , but is sufficiently large compared with e itself. Equation (3) shows that no integral value of n less than 4 is admissible. It is necessary, to be consistent with what is known experimentally about adhesion, that the integral should be zero at the upper limit. For values of n less than 4 this is not the case, and we should arrive at the result that the adhesive force at the contact was a function of the dimensions of the body other than the curvature at the point of contact.

The total attraction between the sphere and plane will next be found on the second assumption, namely that all the molecules of the body exert attractive forces.

As before, we shall first find the attraction of the plane body on a single molecule at a distance a from the surface by dividing the body into plane elements of thickness dx at a distance x from the single molecule.

Then, by equation (2), the attraction of any element is

$$\frac{2\pi K\beta S dx}{x^{n-2}},$$

where S is now the number of molecules in unit volume. The whole attraction on the molecule is then

$$2\pi K\beta S \int_a^\infty \frac{dx}{x^{n-2}} = \frac{2\pi K\beta S}{n-3} \times \frac{1}{a^{n-3}}, \quad (4)$$

and the total attraction of the sphere and plane body is

$$\frac{2\pi K\beta S}{n-3} \int_e^{me} \frac{\pi y^2 S dx}{x^{n-3}}.$$

As we are concerned only with a small region near the point of contact, we may put

$$y^2 = 2rx,$$

and the attraction becomes

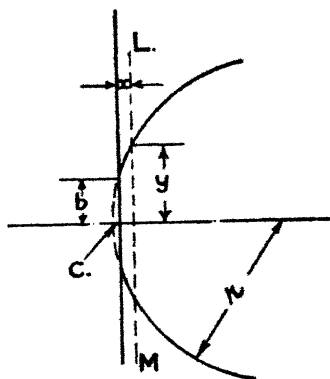
$$\frac{4\pi^2 S^2 K\beta r}{n-3} \int_e^{me} \frac{dx}{x^{n-4}}. \quad (5)$$

In this case, for similar reasons, no integral value of n less than 6 can be accepted.

(6) We shall next take the experimental result that the ratio $\frac{p_x}{p_y} = 4.4$, and compare this with the values that can be computed for this ratio on assigning various values to the index n . Dealing firstly with the case in which cohesion is assumed to be a surface phenomenon, the force of free adhesion, as in fig. 6, may be divided into two parts: p_1 for the circular area of contact of radius b , and p_2 for the remainder of the sphere.

It can be shown that p_2 is independent of b , the radius of the contact circle, when b is small compared with the radius

Fig. 6.



of the sphere. If any plane section is taken, such as LM in fig. 6, of radius y , the area of the spherical cap is

$$A = 2\pi r(c + x),$$

$$\text{or} \quad \frac{dA}{dx} = 2\pi r.$$

The attraction on any ring element of the surface is a function of the area of the element and the distance x whatever the law of attraction may be. Between any values x and $x + \delta x$ there is a constant increment of area independent of the value of y . Hence the total attraction is independent of the value of b . It therefore follows that p_x is equal to p_y , the total attraction occurring in the case of limiting adhesion of fig. 4 (b), which corresponds to the

particular case of $b=0$; and this has already been found by equation (3) to be

$$p_z = p_y = 4\pi^2 s^2 K r \beta \frac{1}{(n-3)e^{n-3}} \dots (6)$$

To find the value of p_1 , let it be assumed that the atoms in contact are separated by a mean distance e . Then, neglecting a small edge effect, the adhesion of these surfaces can be found from equation (2), and is

$$p_1 = \frac{4\pi^2 s^2 K \beta b^2}{2e^{n-2}} \dots (7)$$

Hence
$$\frac{p_1 + p_z}{p_z} = \frac{p_z}{p_y} = 1 + \frac{(n-3)b^2}{2re} \dots (8)$$

In taking the ratio, all the unknown terms disappear, and if an average value such as 3×10^{-8} cm. is assumed for e , the ratio can be found for various assumed values of n as given below:—

n	2	3	4	5	6	7	8
$\frac{p_z}{p_y}$	2.2	1	4.2	7.4	10.6	13.8	17.0

The value of n yielding a result nearest to that found by experiment is 4. It is of interest to note that both the table and the form of equation (8) again show that no index under 4 can possibly give a result in agreement with experiment, an index 3, for example, giving $p_z = p_y$ whatever the values of b and r may be. The rate of variation of p_z/p_y with n is unfortunately not large enough, for values of n greater than 3, to say with any finality that an index exceeding 4 is also not possible, but it may be said that 4 is the most probable value.

If a similar calculation is made on the second assumption that all the molecules throughout the solid are effective in causing adhesion, the following result is obtained:—

$$\frac{p_1 + p_z}{p_z} = \frac{p_z}{p_y} = 1 + \frac{n-5}{n-4} \times \frac{b^2}{2re}, \dots (9)$$

and this gives numerical values as below:—

n	4	5	6	7	8	9
$\frac{p_z}{p_y}$	—	1	2.6	3.13	3.4	3.56

These results are not very conclusive for values of n over 5, but, on the other hand, the assumed distribution of molecular forces is somewhat improbable, as already stated. Equation (9) indicates that 6 is the minimum value of n , which would be consistent with the experiments.

(7) Various workers in mathematical physics have advanced the conception that the atom behaves as an electric doublet when in close proximity to another atom. This view has been successfully applied to the theory of specific inductive capacity from which the electrical moment of the doublet has been calculated in certain cases. It is interesting to note that this conception leads at once to an inverse fourth-power law of attraction, and at the same time offers a partial explanation of the universal property of atoms to exert cohesion. If the doublet hypothesis is assumed to be correct, an interesting result is obtained on comparing some of the calculated electrical moments with the corresponding value found for glass, which may be derived from the present experiments on adhesion in the following manner. The constant K can be determined by assuming the attraction to follow an inverse fourth-power law on the doublet theory and as indicated, although somewhat indecisively, by the experiments described.

The force of attraction between two spheres of radius r can be derived from equation (3) above, and is

$$p_y = \frac{2\pi^2 s^2 K r}{3e}, \dots \dots \dots (10)$$

and in fig. 2 the measured adhesion of glass spheres is given. It may be noted that equation (10) shows that a linear relation should exist between the force and the radius, a result approximately found by experiment. From the curve in

fig. 2 the mean value of $\frac{p_y}{r}$ is 1650; hence the constant K is given by

$$K = \frac{3e}{2\pi^2 s^2} = \frac{p_y}{r} = 250 \frac{e}{s^2}.$$

If we suppose the molecules to be closely packed hexagonally in the surface, each is at a distance e from its neighbours,

and s has a value $\frac{2}{\sqrt{3}e^2}$. The particular type of arrange-

ment assumed does not greatly affect the estimate of K , and this value of s will be assumed. Close packing in square

formation, for example, gives a value $1/e^2$ for s which differs only slightly from the above. Using the first value of s , we have

$$K = 187 e^5.$$

Assigning an approximate value 3×10^{-8} to e , the value of K is 0.45×10^{-35} . The force between two doublets of moment M at a distance x apart varies between $\frac{6M^2}{x^4}$ when end on and $\frac{3M^2}{x^4}$ when broadside on. If the force of cohesion follows a law

$$F = \frac{K}{x^4},$$

we shall have K varying from $6M^2$ to $3M^2$,

$$\text{or } M \text{ varying from } \sqrt{\frac{K}{6}} \text{ to } \sqrt{\frac{K}{3}}.$$

Taking the above value of K , we find M to lie between 1.22×10^{-18} and 0.86×10^{-18} .

Sir J. J. Thomson* gives the following values of the calculated electrical moment:—

$$M = 2.1 \times 10^{-18} \quad \text{for } H_2O,$$

$$M = 1.5 \times 10^{-18} \quad \text{for } NH_3.$$

These values are derived from measurements of the variation of the specific inductive capacity with temperature.

The agreement in the order of magnitude of the electrical moments is remarkable, and appears to justify the tentative suggestion that cohesion is perhaps the attraction of two molecular doublets. This view also lends support to the idea that only the surface atoms exert attraction on external atoms. The field of an interior atom, it is reasonable to suppose, is absorbed by a neighbouring atom, and only the unsymmetrical surface atoms have any appreciable field extending beyond the boundary of the body into space. The molecular theory of magnetization provides an analogy in this respect.

The electrical moment of a doublet is the product of a quantity and a length, and a doublet theory of atomic attraction would be quite untenable if this length should be found to exceed the known atomic dimensions. The quantity concerned in the product cannot be less than the electror

* 'The Electron in Chemistry,' p. 49.

charge q , and hence a maximum possible value $\frac{M}{q}$ can be calculated for the length of the doublet.

Taking the higher value 1.22×10^{-18} for M , this gives a maximum length of 0.2×10^{-8} cm., or about $1/15$ of the diameter of the atom, and the doublet theory thus involves no inconsistency with respect to the size of the atom.

(8) The probability that the cohesive attraction follows an inverse fourth-power law can be subjected to a further indirect test by calculating the tenacity of glass. For this purpose the tenacity will be considered as equivalent to the cohesive attraction, with an inverse fourth-power law, between two imaginary plane faces inside the material. The attraction of one plane for a single molecule of the other face can be obtained from equation (2), and is given by

$$\frac{2\pi Ks}{3e^2},$$

and the attraction of the faces per unit area is therefore

$$F = \frac{2\pi Ks^2}{3e^2}.$$

If, as before, a close packing of molecules is assumed and s has a value $\frac{2}{\sqrt{3}e^2}$, we have

$$F = \frac{8\pi K}{9e^6} \dots \dots \dots (11)$$

An estimate of this in the case of glass, using the previous values of K and e , is

$$F = 1.7 \times 10^{10} \text{ dynes per sq. cm.}$$

This value is much greater, about twenty times, than the tenacity usually found for glass, but it is generally recognized that the actual tenacity of materials as found by tensile tests is always far short of the ideal tenacity which the cohesion forces would impart. Griffith*, however, has obtained some remarkably high tenacities for drawn glass fibres, and some of his results exceed the above amount, though generally this calculated tenacity is of the same order as Griffith's experimental results.

The mechanism of rupture in tension is so imperfectly understood at present, especially in crystalline materials

* Phil. Trans. ccxxi.

such as the metals, that it is hardly safe to base any conclusions on comparisons of actual and ideal tenacities. In the case of glass, which has an amorphous structure, this objection perhaps has less weight, as Griffith has clearly shown that tenacities approaching the ideal value can be actually realized. There is, however, an interesting relation in the case of metals which has not been mentioned previously as far as the writer is aware. Table I. gives the crystal lattice constant and the closest approach of the atoms for a group of seven metals, all of which crystallize in the face-centred cubic system. Values of $1/e^6$ are given in

TABLE I.

Metal.	Lattice constant.	Closest approach of atoms e .	$1/e^6$.	Tenacity f dynes per sq. cm.	Ratio $\frac{f}{1/e^6}$.
Nickel	3.54×10^{-8}	2.505×10^{-8}	40.5×10^{44}	5.3×10^9	0.131×10^{-25}
Copper	3.60	2.540	37.1	4.3	0.116
Platinum ...	3.92	2.780	21.6	3.3	0.152
Silver	4.06	2.876	17.65	2.9	0.164
Aluminium ..	4.05	2.660	18.3	2.3	0.126
Lead	4.92	3.480	1.78	0.21	0.118
Gold	4.08	2.680	17.55	2.3	0.131

column 4, and, as the table is purely comparative, e has been taken as the closest approach of the atoms. Together with these, the measured tenacities of the metals are given and the ratio of the tenacity to $1/e^6$.

It will be seen that this ratio is approximately constant for the series of metals, though the tenacities concerned cover a fairly wide range. It should be remarked that this relation is based entirely on experimental determinations of e and f . The relation appears to be definite enough to suggest that a rational basis underlies the empirical result. Some care must be exercised in attempting to interpret the result, as various considerations become involved. Thus, for example, if we suppose the expression of equation (11) to give the ideal tenacity, assuming the inverse fourth-power law of atomic attraction to hold, we obtain a rational

explanation of the index 6 in the relation $fe^6 = \text{constant}$, but only subject to two conditions, viz. that the measured tenacity is nearly the same fraction of the ideal tenacity, and that the cohesion constant K is nearly the same for all the metals concerned. The first of these is not an unreasonable supposition for a group of pure metals having identical crystal lattices. Nor is there any obvious intrinsic objection to the second condition, as the table itself shows that, with the high index 6 comparatively small, variations in the lattice constant can in themselves account for wide differences in tenacity without the necessity for supposing large variations in the atomic constant.

For the present it would be unsafe to say more than that the empirical relation is not opposed to the inverse fourth-power assumption, but as definite evidence in favour it can only be accepted with some reserve.

The author wishes to record his thanks to Sir Joseph Petavel, Director of the National Physical Laboratory, and to Mr. J. E. Sears, Superintendent of the Metrology Department, for their kind interest and encouragement.

1st August, 1928.

LXVIII. *The Reflexion of Electrons from an Aluminium Crystal.* By D. C. ROSE, Ph.D., 1851 Exhibition Senior Student*.

THE development of the new wave mechanics has recently directed considerable attention to experiments on the scattering of particles. One of the outstanding features of the theory is that it indicates that a particle of mass m may be treated as a wave-like disturbance of wavelength $\lambda = \frac{h\sqrt{1-\beta^2}}{mv}$, where v is the velocity of the particle,

or considering the particle as a wave, the velocity of propagation of energy. It is connected with the phase velocity v_p by the relation $v_p v = c^2$. This means that, if suitable conditions could be found, a beam of particles might be expected to have the properties of a ray of light.

If such is the case, the most obvious method of testing the theory is by looking for refraction or diffraction of

* Communicated by Sir E. Rutherford, P.R.S.

beams of particles by methods similar to those used in studying radiation of corresponding wave-length. The diffraction phenomenon would be expected to exist for α -particles, β -particles, electrons, positive ions, or such moving particles. The wave-length corresponding to an α -particle is of the order of 10^{-13} cm. and is therefore too short to be studied by ordinary methods. Similarly, owing to the high velocity of β -rays and the large mass of positive rays, the wave-lengths corresponding to these are in general too short to be measured easily. For an electron, however, the corresponding wave-length may be brought into the X-ray region by giving it a suitable velocity. The wave-length associated with a 100-volt electron is 1.2 \AA . It would therefore be expected that the phenomenon of the diffraction of X-rays by a crystal grating might be observed with a beam of electrons. In the present paper an experiment is described in which a beam of electrons has been diffracted in an aluminium crystal in a manner similar to that used for the analysis of X-ray beams.

Two methods of studying such a beam of electrons are available. The first method corresponds to the Laue method of examining crystal structure by X-rays. As it is generally known, if a narrow beam of X-rays strikes a crystal face normally and the intensity of the scattered beam is measured in all directions, sharply defined diffracted beams occur whose direction is connected by a simple relation with the crystal structure, its orientation with respect to the incident beam and the wave-length. G. P. Thomson⁽¹⁾ showed that such diffracted beams could be found by passing a narrow beam of cathode rays through thin metal foils. Davisson and Germer⁽²⁾ have also performed such an experiment with electrons. They bombarded the face of a nickel crystal cut parallel to a (111) plane with a beam of electrons at normal incidence. As the electrons could not penetrate through the crystal, they could only examine the region on the same side of the crystal as the incident beam. Several diffracted beams of electrons were found which correspond to Laue beams. These did not occur exactly in the position calculated from the known structure of nickel and the wave-length corresponding to the beam of electrons. They could, however, be brought into agreement by assuming that the crystal was contracted somewhat in the direction of the incident beam. A more correct explanation seems to be the assumption of an index of refraction for these waves in the metal. This point will be discussed later.

The other method of studying the diffraction of electrons is analogous to the Bragg method of analysing a beam of X-rays. If a narrow beam of X-rays impinges on a crystal making an angle θ with one of the planes of the crystal structure, the rays scattered from successive planes one behind the other build up a sharp beam in the position of normal reflexion, also at an angle θ with the crystal plane. The wave-length and the angle θ are connected by the well known formula

$$n\lambda = 2d \sin \theta, \quad . \quad . \quad . \quad . \quad . \quad (1)$$

where n is the number of wave-lengths in the path difference between rays from two successive planes in the crystal, or the order of the reflected beam, and d is the spacing between the planes.

In the experiments described here an attempt was made to obtain a reflected beam of electrons by replacing the X-ray beam in the Bragg method by a beam of electrons. The apparatus was built and mostly assembled before the results of Davisson and Germer were published. Although the results obtained in this experiment were not as accurate as those of Davisson and Germer, they seemed worth putting forward because they confirm the theory, using a different crystal and a Bragg method of analysis*.

Apparatus and Method of Experiment.

The apparatus was essentially similar to a Bragg X-ray spectroscope, the beam of X-rays being replaced by a beam of electrons. The arrangement of the filament and slits is shown in figs. 1 and 2. The important dimensions are, roughly, slits A to B 2.5 cm., slits E to F 1.4 cm., and slits B and E were about 1.4 cm. from the axis marked with a small circle. The size of these slits was about 1 by 4 mm. With this arrangement a slightly divergent beam of electrons (about three degrees) was defined by slits A and B. In order to obtain good definition of the reflected beam it would be advantageous to make the slits as fine as possible. Much finer slits than the above were tried when the apparatus was first set up, but it was found that the intensity of the scattered beam defined by slits E and F was too small to be measured satisfactorily. Hence the apparatus was dismantled and the slits enlarged to the above mentioned sizes. The accelerating potential was put on between the filament and slit A. The

* At the time of writing Davisson and Germer have published some preliminary results of experiments with a nickel crystal by the Bragg method. Proc. Nat. Acad. xiv. p. 317 (1928).

space around the crystal was sufficiently shielded to protect it from fields due to the charging of the surfaces of the containing glass bulb. While runs were being taken A, B, C, D, the crystal and framework of the apparatus, were kept at the same potential. A retarding potential was placed between slits D and E to analyse the reflected beam. The

Fig. 1.

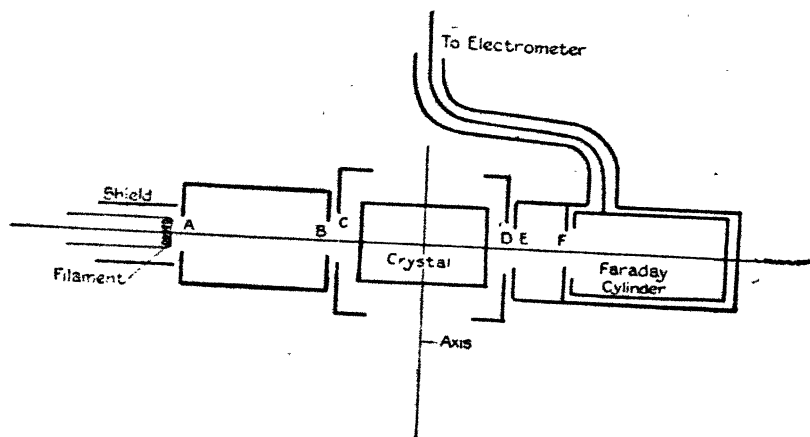
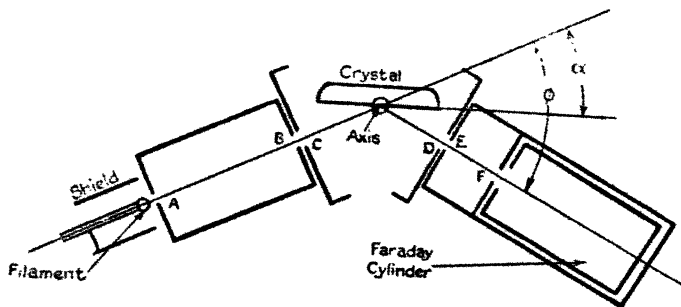


Fig. 2.



primary beam could be analysed by putting a retarding potential between slits B and C and using the whole frame and rest of the apparatus as a collector.

The crystal was loaned to the author by Professor G. I. Taylor. It was already cut with one face, about 7×14 mm. in size, parallel to a (111) plane. It was so arranged in the

apparatus that it could be rotated about an axis lying in that face, perpendicular to the direction of motion of the primary electron beam. The crystal was so orientated that one of the rows of atoms in its surface lay parallel to the axis of rotation, that is, one of the sides of the equilateral triangle formed by adjacent atoms in a (111) plane (face-centred cubic) of the crystal was parallel to the axis of rotation. The collector, which consisted of a Faraday cylinder inside an earthed shield, and the slits D, E, F, and G could be rotated about the same axis. The lead from the Faraday cylinder was carried up into the line of the axis of rotation in a quartz tube and out of the apparatus by a side tube in the same line. It was insulated with quartz except at the glass seal, and shielded by an aluminium tube outside the quartz all the way. The main frame was of aluminium. The shield around the filament and the first slit A were of mild steel as they got very hot during the experiments. The other slits were made of aluminium, except those in the collector, which were made of brass heavily nickel-plated. The bearings were steel on steel. The crystal and collector were rotated by means of an electromagnet acting on soft iron slugs in side tubes off the main containing bulb. These slugs were on the ends of shafts which turned worm and pinion drives. These in turn turned the crystal holder and collector independently about the same axis by means of a complicated system of bearings.

The fact that some of the parts of the apparatus, including most of the screws holding it together, were of steel meant that very low voltages could not be used with any accuracy owing to the probability of magnetic deflexion of the electron beams. However, the steel parts were kept as far away as possible from positions that would affect the results and were carefully demagnetized before being assembled. The magnetic rotating mechanism was also demagnetized between each reading by passing alternating current through the electromagnet and drawing it away from the apparatus slowly. Tests with a magnetometer showed that the field near the crystal, even under the worst conditions, could not have been much greater than the earth's field. As it was not intended in the first place to work below about 100 volts, and also because the steel parts in the apparatus would make compensation difficult, no attempt was made to compensate for the earth's field. A calculation shows that the error due to this could hardly be greater than about 1 degree for 100 volt electrons. This is the same magnitude as errors due to other causes.

The crystal face was prepared by polishing with fine emery, then etching with caustic soda until all traces of the polished layer were removed. It was then washed and dried and put in the apparatus without touching the prepared surface in any way. This surface, as would be expected after the etching, was rough and pitted. The electrons would not be expected to penetrate very far into the crystal without losing their identity with the primary beam or a considerable part of their energy. Since the reflexion effect, which the experiment was designed to study, is the interference or building-up of waves scattered by successive layers of atoms in the crystal structure, it is essential that the surface layers of atoms should be in the natural position defined by the crystal structure. Hence it was thought that it would be more advisable to leave the rough-etched surface exposed to the electron beam rather than to attempt to obtain a smooth surface. It is well known that an aluminium surface which has been exposed to air is always covered with a thin layer of oxide. However, it was hoped that this oxide layer would be so thin that it would not spoil the results, and that it would be advantageous in helping to prevent amalgamation with what mercury vapour got into the apparatus. In the experiments of Davisson and Germer the nickel crystal was treated much more rigorously. They heated their crystal by electron bombardment until the nickel distilled freely in vacuum. They found that their diffracted beam became very diffuse or disappeared if they allowed the pressure in their apparatus to increase to about 10^{-4} mm. This effect was ascribed to the absorbed gas molecules on the surface of the crystal. Considering the trouble they had with gas layers in the surface of their crystal it seems that no definite results should have been expected in the present experiment.

The metal parts of the apparatus, with the exception of the crystal, were vacuum ovened before assembly. The whole apparatus was assembled in a glass bulb about 5 inches in diameter with a $2\frac{1}{2}$ -inch neck and various side tubes to bring out the connecting leads and turning mechanism. The bulb was connected to a fast mercury-diffusion pump. This pump was backed by the Gaede type of rotary mercury pump and a Fleuss oil pump. Between the bulb and the diffusion pump there was a potassium-mercury trap, a liquid-air trap, and a mercury cut-off. The liquid-air trap was used while the apparatus was running. The potassium trap was intended to keep mercury vapour from reaching the apparatus overnight when there was no liquid air. The

pressure during the runs was of the order of 10^{-6} mm. Overnight it would increase to about 10^{-3} mm. This increase in pressure was probably due to the potassium trap giving off hydrogen. There was a phosphorus-pentoxide trap between the mercury vapour pump and the backing pumps, but this was separated from the apparatus overnight by the mercury cut-off. Possibly enough water vapour came off the walls and metal parts of the apparatus to produce this increase in pressure when it was reduced by the potassium. It was not due to a leak, as it did not occur before the potassium was run in. This effect made the intensity of the reflected beam slightly variable from day to day. However, as the object of the experiment was to find the position of the peaks rather than their intensity, it was not thought necessary to go to further refinements. Sets of curves for a given voltage were taken together during one continuous run, and repetitions showed exactly similar results.

The bulb was made of soda glass and so arranged on a stand that an electric oven could be lowered over it. This would heat the whole apparatus to about 300 degrees centigrade while the pumps were running. It was usually given about two days outgassing before taking a series of observations. The angles were read by means of a scale outside the glass bulb. The collector and crystal holder were arranged with a pointer so that the angle was read by the position of the line of sight defined by a point on end of the axle which supported the crystal holder and the pointer on the scale. The zero position could be found by adjusting the crystal so that the beam of light from the filament just grazed its surface. Variations in the thickness of the glass bulb would cause inaccuracies in the scale reading, but as the pointer and scale were as close to the glass as possible, the one on the inside and the other on the outside, the error would be reduced to a minimum. The angles could be read easily to better than half a degree. The peaks were much wider than this so more accurate measurements were quite unnecessary. The current was measured by timing the deflexions of a spot of light reflected from the mirror of an ordinary Dolezalek electrometer.

Results.

The procedure was as follows:—Setting the accelerating potential at say 122 volts, the crystal was set so that its surface made a small angle with the incident beam, then the current was measured in the collector at various points over

the range of angles (angle ϕ , fig. 2) from zero to about 120 degrees taken from the line of the incident beam as the zero line. It would be expected that sharp maxima would occur in the intensity distribution when the incident angle, that is the angle between the face and the incident beam, and the reflected angle were equal and connected with the voltage by relation (1) and

$$\lambda = \frac{h}{mv}, \text{ neglecting the relativity correction,}$$

$$\text{or} \quad \lambda = \sqrt{\frac{150}{V}},$$

where V is the accelerating potential of the incident beam.

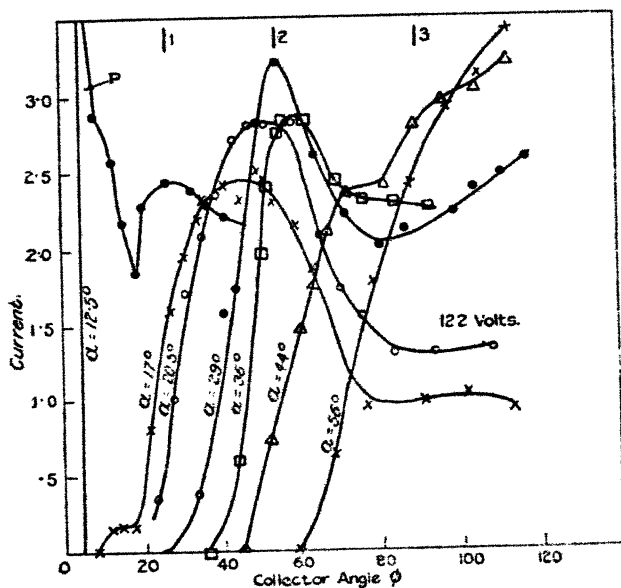
The electrons forming this peak should have the velocity of the incident beam. It was found that in order to get sufficient current in the collector it was necessary to have it from 20 to 40 volts positive with respect to the filament. This was due to the fact that the retarding potential was placed between slits D and E rather than just in front of the Faraday cylinder. These slow electrons would be deflected by any lack of symmetry in the retarding field and also any slight magnetic fields. Hence the analysis of the reflected beam is more a function of the position of the slits and of the retarding potential than of the velocity of the beam itself. This was shown in the following way:—The crystal and collector were set at the zero position so that some of the primary beam went past the crystal directly into the collector. An analysis of this beam by slits D and E showed that the current decreased roughly linearly for retarding potentials varying from about 20 to 30 volts below the accelerating potential to a retarding potential equal to the accelerating potential which stopped all the electrons. On the other hand, an analysis of the whole primary beam by a retarding potential between slits B and C showed that it was homogeneous to about 3 volts. This corresponds to the filament potential drop. Hence it seems reasonable to assume that very few electrons get into the collector except those which were allowed to pass through slit E with velocities greater than 20 volts. The primary bombarding current was about 10^{-7} amp., and the currents measured in the collector were of the order of 10^{-13} amp.

Fig. 3 shows a typical set of curves for 122 volts accelerating potential. They are plotted in the manner the readings were taken, that is, each curve represents the variation of the current in the collector for different values of the collector angle ϕ and one value of the crystal angle α .

The first high peak P which occurs when the crystal is set at a small angle is due to the fact that the incident beam was wider than the angular width of the crystal face when set at this grazing angle. As a result part of the primary beam gets past the crystal directly into the collector. This happens until the collector is turned sufficiently far around to be out of range of the primary beam. The short lines at the top represent the calculated position of the various orders of X-ray reflexion of the corresponding wave-length.

It is seen that there is a definite peak in the curve where the first order is expected, but it is so close to the incident

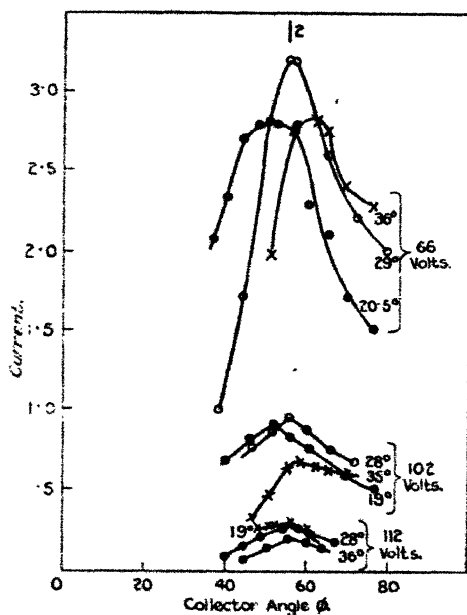
Fig. 3.



beam that its position cannot be located with any accuracy. However, there is a sharper peak at the expected position of the second order. This peak was examined very carefully for accelerating potentials of 122 volts. It was found that this peak could be located more accurately than the others. With a wide incident beam and a low resolving power due to the relatively small number of layers taking part in the reflexion the peak would be expected to cover a considerable range of incident angles. For this reason a peak occurs in the neighbourhood of the expected position for positions of the crystal anywhere near the correct reflecting angle.

However, the peak which occurs in a position such that the angle of incidence is equal to the angle of reflexion is always sharper and more intense than the others. Such a peak is seen in fig. 3 in the curve for which $\alpha = 28^\circ.5$. This peak is taken as representing the reflected beam of electrons of 122 volts initial energy. The curves shown in fig. 3 were taken with the collector 37 volts positive with respect to the filament. That the peaks should be associated with the full accelerating voltage is shown by measurements of the position of the second order peak at different retarding potentials, as given in fig. 4. This figure

Fig. 4.

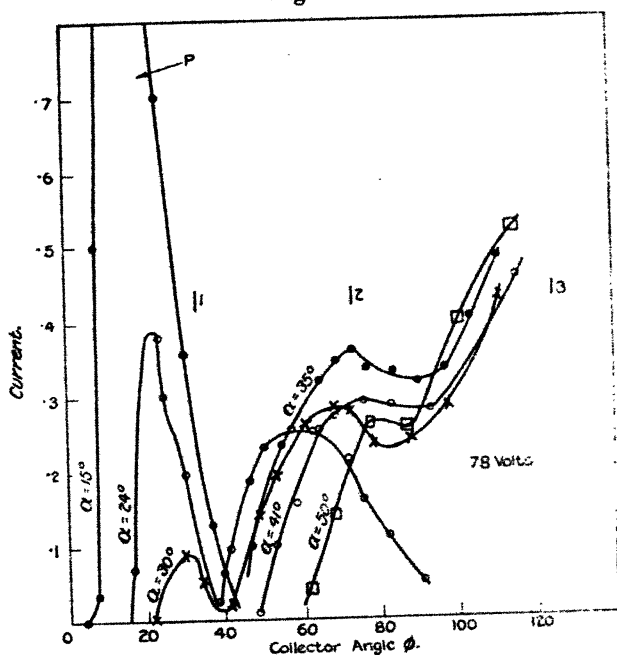


shows three curves for each retarding potential 85, 102, and 112 volts. One of the three was taken with the crystal set in as nearly as possible the correct position for wave reflexion and another curve was taken with the crystal set on either side of that position. The curves show that the position of the peak does not vary with the retarding potential, and therefore should be associated with the full accelerating potential rather than some potential between it and the retarding potential. The curves at the bottom of the figure, taken with a retarding potential of 112 volts, all show the peak in the same position. This is what would be expected with a finer analysis of the beam, but as the current was too

low to obtain very consistent readings no great significance should be given to this set. The third order position in fig. 3 is indefinite for a reason that will appear when the results obtained with higher voltages are discussed.

Fig. 5 shows a similar set of curves for 78 volts and a retarding potential of 65 volts. Here the first order appeared plainly, but is still at too small an angle to be located accurately. The currents were also so small as to be difficult to measure reliably. Lower voltages were tried with

Fig. 5.



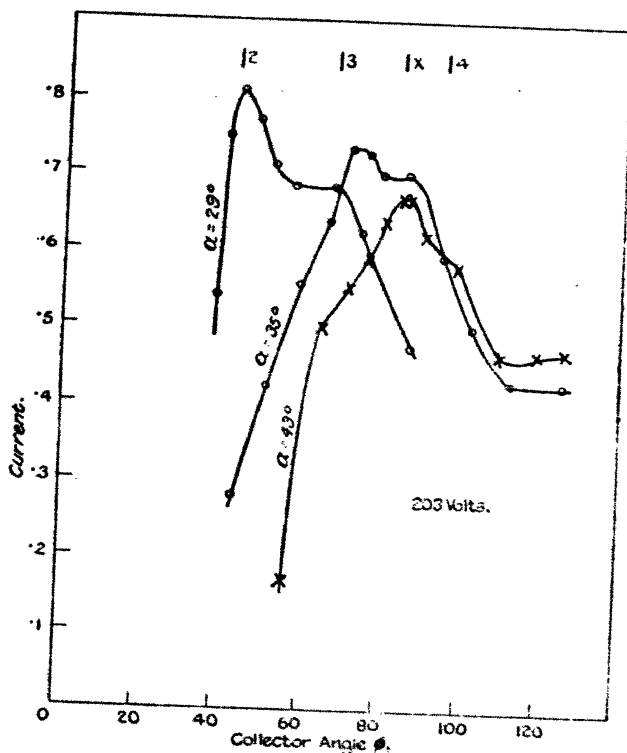
still lower retarding potentials, and peaks representing the first two orders were obtained. However, owing to the uncertainty due to the effects of small magnetic fields they can only be used to indicate that the peaks move in the right direction with varying voltages.

Higher voltages were tried, and in fig. 6 three curves are shown for an accelerating potential of 203 volts and a retarding potential of 164 volts. The curve showing the second order alone is not shown, but the existence of the second order is indicated by the curve with $\alpha = 29^\circ$. The third order is shown as a definite bump. Between the

third and fourth orders another peak occurs, marked X, which makes it impossible to separate these orders enough to give accurate results. Curves for 243 volts with a retarding potential of 306 volts show a similar peak. At this voltage the fourth order is plainly indicated, and a possible fifth order. These are shown in fig. 7.

Very little can be said about the relative intensity of the various orders. The first order is weak, no doubt due

Fig. 6.

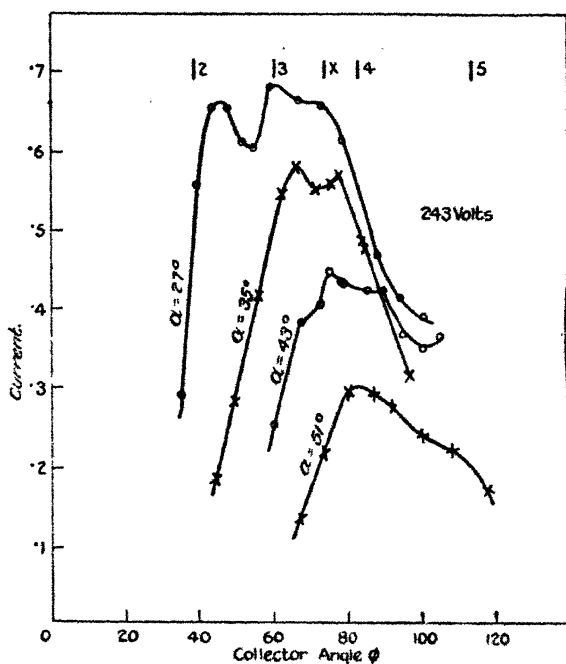


to the fact that it occurs at such small angles that only part of the primary beam is effective. The second is the strongest and therefore the one whose position can be located most accurately. The third is ambiguous because of the extra peak, and the fourth is very weak.

What causes the extra peak marked X is uncertain, but it is most likely due to contamination of the surface by gas or by the layer of aluminium oxide. Assuming that the extra peak is a first order reflexion the grating constant,

which it represents, would be 0.65 \AA . This is smaller than the accepted radius of an aluminium atom. However, on some of the curves for lower voltages there is a mere indication of another peak which might be the first order of this reflexion. This would then represent a spacing of 1.3 \AA . There is hardly enough information obtainable from this to associate it with any definite spacing in a corundum crystal, because it gives no information about the orientation except that the planes causing the reflexion are parallel to (111) planes in the aluminium crystal. The position of

Fig. 7.



these peaks is shown in Table II. The position of the peaks marked first order is very uncertain, as they are indicated only by the fact that for the lowest voltages tried one or two points were a little off the smooth line. A more accurate analysis of such peaks might give some information about the transition layer between aluminium and aluminium oxide.

Table I. gives a summary of all the peaks found which can be associated with the aluminium (111) plane spacing, $d = 2.34 \text{ \AA}$. Column 2 gives the angle θ in relation (1), which is half the angular position of the peaks shown in

figs. 3 to 7. Beside each angle is given the limits of possible error in locating the peak from the curves. Column 4 shows the wave-length calculated from the voltage, and

TABLE I.

Volts.	Angle of peak. θ .	Order. n .	Wave-length. $\sqrt{\frac{150}{V}}$.	Wave-length. $\frac{2d \sin \theta}{n}$.
56	25 \pm 4	1	1.64	1.98 \pm 0.30
56	42 \pm 4	2	1.64	1.57 \pm 0.14
62	21 \pm 2	1	1.56	1.68 \pm 0.15
62	42 \pm 3	2	1.56	1.57 \pm 0.14
78	16 \pm 4	1	1.39	1.29 \pm 0.32
78	37 \pm 2	2	1.39	1.41 \pm 0.07
83	16 \pm 4	1	1.35	1.29 \pm 0.32
83	36 \pm 2	2	1.35	1.38 \pm 0.07
122	14 \pm 3	1	1.11	1.13 \pm 0.24
122	28.5 \pm 1	2	1.11	1.12 \pm 0.04
164	25 \pm 2	2	0.96	0.99 \pm 0.07
164	45 \pm 7	3	0.96	1.10 \pm 0.14
203	21.5 \pm 2	2	0.86	0.86 \pm 0.08
203	35 \pm 3	3	0.86	0.89 \pm 0.06
203	50 \pm 5	4	0.86	0.89 \pm 0.06
243	23 \pm 4	2	0.79	0.91 \pm 0.15
243	33 \pm 3	3	0.79	0.85 \pm 0.07
243	46 \pm 4	4	0.79	0.84 \pm 0.06

TABLE II.

Volts.	Wave-length.	Angle.	Spacing.	Order.
56	1.64	36 \pm 6	1.4	1
62	1.56	30 \pm 6	1.5	1
203	0.86	43 \pm 4	1.3	2
243	0.79	38 \pm 4	1.3	2

column 5 the wave-length calculated from the angle and grating constant. This calculation assumes the index of refraction to be unity. It should be noted that the most accurately measured peak is the second order peak at

122 volts. Considering all sources of inaccuracies the possible error for this peak should not be greater than about 7 per cent.

Discussion.

The results of this experiment indicate that electrons can be diffracted by a crystal grating in the manner suggested by the wave theory. Table I. indicates that they agree with the theory within the accuracy of the experiment. This fact does not agree with the results of Davisson and Germer⁽²⁾. They found two types of diffracted beams. The first type is due to rows of atoms in the surface layer of the crystal acting as a plane diffraction grating. These are spoken of as surface diffracted beams. The second are those which correspond to Laue X-ray beams, as explained previously. These are depth diffracted beams, or considering a set of planes in the crystal as reflecting the waves when the angle and wave-length are such that they satisfy relation (1), they may be called depth reflected beams. These so-called depth diffracted beams, in the case of Davisson and Germer's experiment, may also be considered as positions of maximum intensity in the surface diffracted beam. Such maxima exist because more layers than one are effective in producing the beam. If a large number of layers was effective the beams would be all suppressed except the one at the position of this maximum. These depth diffracted beams should occur in the same directions as Laue X-ray beams of the same wave-length. The results of Davisson and Germer did show a set of depth diffracted beams arranged with a three-fold symmetry around the direction of the incident beam corresponding to a set of X-ray beams. However, they did not occur at the same angles that X-ray beams of the same wave-length would have occurred. They could be made to fit the corresponding set of X-ray beams by assuming a contraction of the crystal in the direction of the incident beam by a factor of about 0.7. This contraction factor varied for different beams. Patterson⁽³⁾ pointed out that by a different association of the electron beams with the Laue beams the two could also be made to agree by assuming an expansion factor in the same direction.

Eckart⁽⁴⁾ and Bethe⁽⁵⁾ have suggested what seems to be a much more satisfactory explanation of the difference in position between electron beams and corresponding X-ray beams. It is the assumption of an index of refraction for the de Broglie waves in the metal. Bethe shows that the existence of this index of refraction may be due to the

surface potential of the metal by the following reasoning. A more complete expression for the wave-length is

$$\lambda = \frac{h}{\sqrt{2m(E - V)}}$$

where E is the kinetic energy of the incident beam and V may be taken as the potential through which the electron must pass in going through the surface of the metal. From this it is easily seen that the refractive index is

$$n = \frac{\lambda_{\text{vac}}}{\lambda_{\text{metal}}} = \sqrt{1 - \frac{V}{E}}.$$

Now in order to prevent free electrons from streaming out of the metal the surface potential must be in a direction which accelerates the electron as it passes in through the surface and retards it as it passes out. This would mean that the velocity of the electron would be increased, hence the phase velocity decreased and the wave-length decreased. This means that the index of refraction should be greater than unity. This index of refraction should also vary with the accelerating potential. Using the results of Davisson and Germer, Bethe has calculated the value of the surface potential and obtained an average value of about 15 volts. He also points out that this is the order of the value expected on the Sommerfeld theory of conduction. In Davisson and Germer's later results, using a Bragg type of reflexion, they show some uncertainty as to the order of their peaks and give two sets of refractive indices, one greater and the other less than unity. The set having values greater than unity is probably the correct value. The indices vary from 1.14 to 1.01 for voltages from 28 to 585. A calculation of the surface potentials from this data gives an average value of about 14 volts.

The results of the present experiment fit the theory assuming an index of refraction of unity. Assuming an error equal to the estimated accuracy of the experiment (7 per cent.) for the second order peak at 122 volts, the refractive index would be 1.013. This would correspond to a surface potential of between three and four volts. The other peaks are not sufficiently accurate to give a reliable estimation of the surface potential. If the supposed second order peak were really a third order the surface potential would be about 35 volts. No matter which way one takes it, it seems unreasonable that there should be such a difference between nickel and aluminium.

There are possible explanations of the divergence between the results of the present experiments and those of Davisson and Germer, but they can all be ruled out with a fair amount of certainty. It might be that the residual magnetic fields in the present experiments were stronger than it was thought. Considering the precautions taken this seems very unlikely. Again, no correction was made for the diffuse background scattering, as the curves did not give sufficient information about it. It is, however, unlikely that such a correction would change the position of the peaks sufficiently to account for the divergence. It is also conceivable that the magnetic properties of the nickel crystal in the experiments of Davisson and Germer have some effect on the results, but it is very doubtful if such an effect would be noticeable as the fields would have to be very intense and so arranged that they would not interfere with the three-fold symmetry.

Summary.

Experiments have been performed in which electrons have been reflected by the planes of an aluminium crystal in the manner suggested by the wave theory. The apparatus was similar to a Bragg X-ray spectroscope having the beam of X-rays replaced by a beam of electrons. It would be expected that a beam of electrons would be reflected in a manner analogous to X-rays when the accelerating potential, spacing constant of the crystal, and angle of reflexion were connected by the usual relations

$$\lambda = \frac{h}{mv}$$

and

$$n\lambda = 2d \sin \theta.$$

Four different orders of reflected beams were found whose position agreed with that predicted by theory within the accuracy of the experiment. Two orders of another set of beams were found, which are attributed to aluminium oxide or some other contamination of the surface of the crystal. A comparison is made between these experiments and those of Davisson and Germer (*Phys. Rev.* xxx. p. 705, 1927), who obtained different results with a nickel crystal. Their results differed from those predicted, but could be explained by the assumption of a refractive index.

In conclusion I would like to thank Prof. G. I. Taylor for making this experiment possible by lending me the

aluminium crystal with the required information about the position of its principal planes. I should also like to thank Prof. Sir Ernest Rutherford and Dr. J. Chadwick for interest and advice.

References.

- (1) G. P. Thompson, *Proc. Roy. Soc. A*, cxvii. p. 600 (1927).
- (2) Davisson and Germer, 'Nature,' 16th April, 1928, and *Phys. Rev.* xxx. p. 705 (1927).
- (3) Patterson, 'Nature,' cxx. p. 46 (1927).
- (4) Eckart, *Proc. Nat. Acad.* xiii. p. 519 (1927).
- (5) Bethe, *Naturwissenschaften*, xix. p. 333 (1928), and xviii. p. 786 (1927)

LXIX. *The Raman Spectra of Scattered Radiation.* By R. W. WOOD*. (Communication No. 7 from the Loomis Laboratory, Tuxedo.)

[Plate IX.]

THE very important and surprising discovery recently announced by Professor C. V. Raman and K. S. Krishnan opens up a new field in the study of molecular structure.

They found that if various transparent media, such as fluid organic compounds, crystals, and even water, are illuminated with monochromatic light, the spectrum of the light scattered by the medium shows, in addition to the line of the illuminating radiation, other bright lines the wave-lengths of which depend upon the nature of the medium. This at first sight might appear to be no different from fluorescence, but a closer inspection, as Prof. Ramsay showed, compels us to admit that the phenomenon is quite different and wholly new.

The difference may be well illustrated by the case of crystalline quartz, which is one of the substances which I have studied and which will be more fully described later. This substance, when illuminated by light of practically any wave-length in the region below the green mercury line, gives a companion line of wave-length greater than that of the exciting line (about 90 Å.U. in the case of excitation by

* Communicated by the Author.

the violet mercury line 4358). If the spectrum of the scattered light is photographed with a quartz spectrograph, we find every strong line or group of lines reproduced exactly by faint lines or groups of lines about 90 \AA.U. on the long wave-length side. Now Raman has shown that the frequency difference between the companion line and the exciting line is constant, and equal to the frequency of an infra-red absorption band. This means that the light-quantum gives up a portion of its energy to the molecule, raising it to an excited state, and then passes off with diminished energy, recording itself in the spectrograph as a line of greater wave-length. An explanation of the phenomenon on the classical theory would have been difficult, to say the least, and it appears to me that no more convincing proof of the quantum theory of light has been found up to the present time. The line which I have found with quartz corresponds to the absorption band at 21μ . Two other lines, much fainter and closer to the exciting line, indicate absorption bands at 49 and 80μ respectively. No trace of a line corresponding to the band at 8.5μ has been found up to the present time. This is perhaps to be expected, as this band would correspond to a higher state of excitation which would be less probable than excitation to lower vibrational states. My spectrum of the quartz emission shows Hg 3125-3131 and 3650, 3654, 3663 beautifully duplicated. In the case of benzol, Raman found that a line of shorter wave-length than that of the exciting line was also present with the same frequency difference (measured against the exciting line) as was the case with one of the lines of longer wave-length. This could mean only that the impinging quantum of violet light (4358) gathered up some energy from a molecule already in an excited state, and then rebounded as a quantum of greater energy which recorded itself on the ultra-violet side of the exciting line. The line was so faint that it did not appear on the reproductions of his photographs, but a curve made with a recording photometer showed a very small hump at the right place. Employing higher dispersion I find a double line at this point, a matter which will be more fully discussed later on. In the case of carbon tetrachloride I find anti-Stokes terms (shorter wave-length lines) almost as strong as the corresponding lines of longer wave-length, the group being reproduced as a "mirror-image," regarding the exciting line as the mirror (Pl. IX. fig. b). With improved methods of illumination I have been able to record the stronger Raman lines with an exposure of only a few minutes.

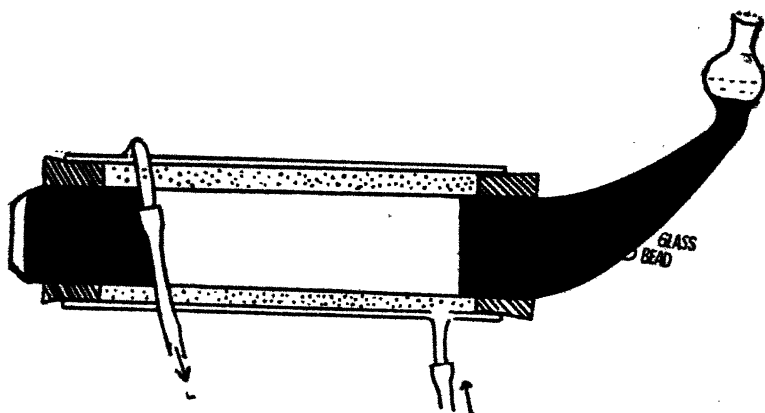
Apparatus and Methods.

Raman illuminated his fluids in spherical glass bulbs, concentrating the light of a mercury arc at the centre of the bulb by means of a large lens, and photographed the spectrum of the illuminated area viewed end-on.

This method of excitation is very inefficient in comparison with that which I have employed in recent investigations of resonance spectra; in which the arc is brought into close proximity with the resonance tube.

The apparatus used in the present work is the outcome of a number of trials, and can hardly be improved upon. The illumination is so powerful that the strongest Raman lines can be photographed with an exposure of a few minutes.

Fig. 1.



The tube is water-cooled, and if filters are to be employed for the removal of certain portions of the spectrum of the exciting light, the colouring material can be dissolved in the water operating the cooling system.

It is shown in fig. 1, and consists of a glass tube of 3 cm. internal diameter, blown flat and rather thick at one end, like the bottom of a bottle, and drawn off into an oblique cone at the other. The flat bottom is ground plane and polished, or is made sufficiently good optically by cementing a thin cover-glass to the ground surface with Canada balsam. Bulbs were used at first, but they act as spherical short-focus lenses when the tube is filled with liquid and are unsatisfactory, since only a single section of the tube can be brought to a focus. A small bead of glass is fused into the wall of

the sloping cone as nearly as possible in coincidence with the tube's axis. This bead, when backed by a lamp, is visible as a bright star when viewed through the other end of the tube, and is of great assistance in adjusting the tube parallel to the axis of the collimator—a very important matter. With the tube filled with liquid, it is impossible, without the bead, to send a ray of light down its axis, on account of refraction by the oblique wall.

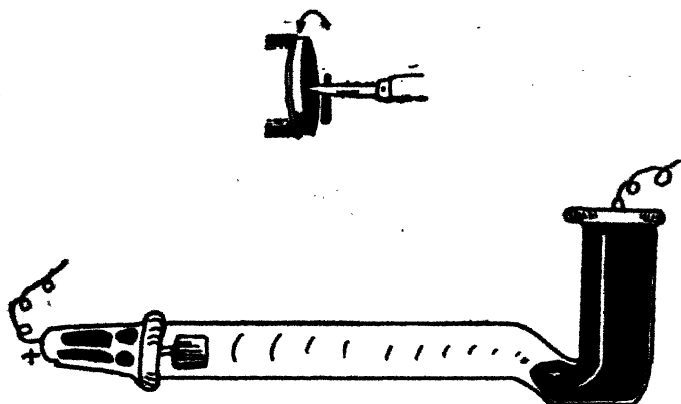
The tube is painted on the outside with black paint (the new celluloid enamel paint for automobiles is best), as shown in fig. 1, taking care not to cover the bead, and surrounded by a second glass tube provided with side tubes for the in- and out-flow of the water. The seals at the ends are made from rubber stoppers in the following way, a method not as well known as it should be. A stopper of size sufficient to allow it to be slipped easily for two-thirds of its length into the large tube is inserted snugly into a short length of brass tubing, preferably made slightly conical on the inside to fit the stopper. This is mounted in a lathe and spun rapidly. A pen-knife with a long thin blade made very sharp at the point is moistened with glycerine, and rested, cutting-edge up, on a tool support adjusted parallel and very close to the protruding face of the stopper. The point is now pressed lightly against the stopper, marking a circle, which should be of a diameter equal to that of the inner tube. The blade is now pressed through the stopper, taking care to keep it parallel to the axis of rotation and tangential to the circle which is being cut. It will go through the stopper in a few seconds, giving a clean-cut ring with a central plug, which is easily pushed out after removing the stopper from the brass tube. It is possible to make rings a millimetre or two in thickness from stoppers 4 or 5 cm. in diameter. The position of the knife blade with respect to the rotating stopper is shown in fig. 2.

The exit tube for the water must be on the top of the outer tube, and be bent sharply down as shown, so that the tube of the mercury arc can be brought down to within a centimetre or two of the tube, as shown in fig. 1. Without the cooling system most of the fluids studied would have been raised to the boiling-point in a few minutes.

Water was delivered from an iron pail with a brass tube soldered through the side close to the bottom, and a glass stop-cock in circuit with the rubber tube controlled the flow, insufficient cooling being indicated by the rise of the fluid in the small bulb surmounting the oblique cone. The quartz mercury arc must be mounted in some type of support free

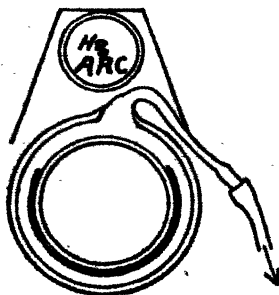
from metal supports on the underside, so that it can be brought down almost in contact with the upper surface of the water jacket. Two reflectors augment the illumination, one of them above the arc, and resting on the quartz tube,

Fig. 2.



the other, bent to a hemi-cylinder of slightly less diameter than that of the inner tube, clamps around the latter on the underside. These reflectors were made of very highly-polished sheet aluminium of about the thickness of writing-paper (a commercial product). An alternative method

Fig. 3.



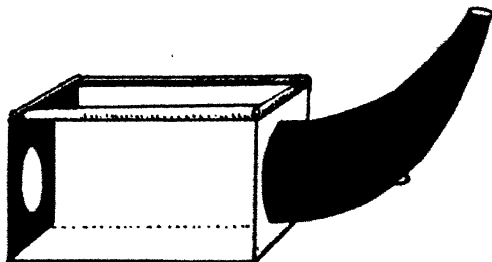
would be to silver the inner tube on the lower surface. The disposition of the reflectors is shown in fig. 3.

By this arrangement practically the entire emission of the quartz arc is thrown into the inner tube, and the intensity is

still further increased by reflexion back from the cylindrical reflector.

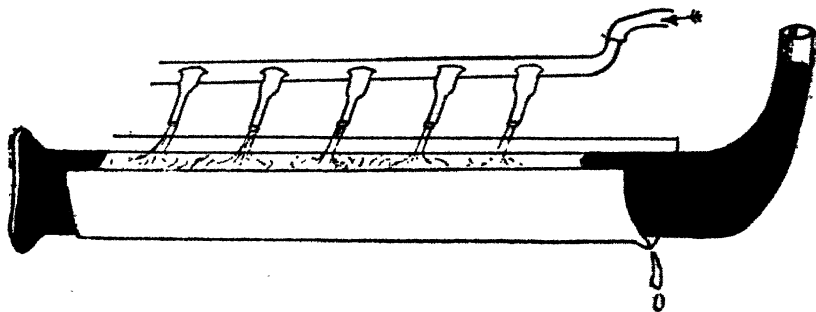
In the case of solids, such as quartz, calcite, or glass, the method employed is shown by fig. 4. The front face of the block is painted black, with the exception of a circular aperture and a bent cone of glass cemented to back face with

Fig. 4.



picein wax : this cone is filled with glycerine and is painted black ; a glass bead is provided for collimation. On the upper face four small glass rods are attached with surgeon's tape : these form a wall to retain the pool of water, constantly renewed by a small stream, which keeps the block cold. The block is mounted at a slight angle on a sheet of

Fig. 5.



the reflecting aluminium, so that the water overflows on the cone side and the front window remains clear, the water being carried away by a tin gutter. A third and simpler arrangement is shown in fig. 5. This was employed in the excitation of fluids in a quartz tube by the total radiation of the arc. The end of the tube was blown out into a thin bulb the front of which was then flattened in the flame. The

tube rested in a cylindrical gutter of the highly reflecting aluminium previously described, the cooling being effected by five jets of water which played continuously against its upper surface. This tube, like the block of quartz, was mounted at a slight angle to prevent the water from running out of the upper end of the gutter. The water-jet tubes point in a nearly horizontal direction just under the edge of the aluminium reflector which covers the lamp. The brilliancy of the light scattered by pure dust-free liquids under these conditions is very surprising, and it is hard to believe that the fluid is not turbid.

The aiming of the spectrograph is a matter of great importance if scattered light from the walls of the tube is to be avoided. It is best accomplished in the following way. Two diaphragms are formed by perforating two rather large squares of black cardboard with holes about 1 cm. in diameter. These are mounted in clamp stands about 30 cm. apart, with the holes in line with the axis of the tube. An incandescent lamp with a frosted bulb is placed close to the glass bead, and the screens adjusted so that the bead is visible centrally placed when viewed through the two holes. The spectroscope is now placed with its slit about 20 cm. from the first screen, the collimator pointing through the two holes at the illuminated bead. Before bringing the spectroscope into place, it is well to light the arc and make sure that only the illuminated fluid is visible through the two holes when the eye is moved about over the first hole. Next, bring the eye up to the region where the spectrum is focussed, and, with the slit wide open, adjust the instrument to such a position that the illuminated bead is seen exactly at the centre of the camera lens. It will be coloured, of course, the colour depending upon the position of the eye. Remove the incandescent lamp and mount a lens of about 18 cm. focus close to the first screen. The lens forms an image of the hole in the second screen on the slit of the instrument, and on placing the eye at the focus, the whole field of the instrument should appear illuminated with green light when the pupil of the eye is in the position of the green mercury line. The slit is now closed and the exposure made. This method of aiming a spectroscope will be found useful in the case of many other investigations.

Experimental Results.

An important point to be settled is the relative intensity of scattering for the exciting and modified wave-lengths.

To accomplish this we must be sure that only light scattered by a dust-free and pure fluid enters the spectrograph. I have made only a rough preliminary examination of this point in the case of some of the strongest Raman lines, and found that the ratio of scattering is of the order 1 : 500. This determination was made by making a series of exposures of varying time and picking out the two which gave the modified and unmodified lines of the same intensity. We will now take up the results obtained with a selected few of the liquids and solids examined up to the present time. Wave-length determinations have not been made of all of the plates, as preparations are now under way for photographing the spectra with a prism spectrograph of 40 foot focus. The photographs were made with a constant deviation Bausch and Lomb one-prism spectrograph of 50 cm. focus, with a comparison spectrum of iron running across the centre. The spectrograph was kept at a constant temperature by a toluene thermostat, as in some cases exposures of several hours were necessary.

It was at once apparent that still higher dispersion was desirable, as some of the lines were found to be bands sharp on the long wave-length side and shaded off towards the violet.

Turning now to Pl. IX., we find at the top the spectrum of the quartz mercury arc used for the excitation of the materials. It was much over-exposed for the purpose of bringing all of the fainter lines, which otherwise might be mistaken for Raman lines, on the spectrograms. Below this is the spectrum scattered by carbon tetrachloride, which has been reproduced of full width, showing the lines both above and below the iron comparison spectrum. The other prints have been trimmed narrower, showing iron on one side only.

Carbon tetrachloride.

This is perhaps the most striking photograph of all, on account of the great intensity of the modified lines of wave-length shorter than that of the exciting line. Immediately to the right of the 4358 line of mercury we find a strong triplet with the lines spaced thus |||, while to left, and symmetrically placed, the same triplet reversed thus |||, this being the anti-Stokes group. We find in addition a close double line further along towards the green region. This same complete set of lines will also be seen to the right of the violet 4047 line, the Raman lines being indicated by

ink dots below the spectrum. Still more remarkable is the appearance of the groups, both Stokes and anti-Stokes, excited by the green line 5461, also indicated by dots. Raman reported that he found no trace of excitation in any case by this line, as might be expected from the Rayleigh law of scattering, but in the case of carbon tetrachloride, chloroform, and some other substances the green line produces strong scattering of modified lines. One of the anti-Stokes lines is in coincidence with a very faint mercury line, which appears much intensified by the superposition of the Raman line. The wave-lengths and frequencies are given in the following table :—

Carbon Tetrachloride.

λ of Exciting Line.	Freq. of Exciting Line.	λ of Modified Line.	Freq. of Mod. Line.	Frequency Difference.
4046.8	247039	4082.0	244909	2130
		4098.3	243932	3107
		4127.7	242491	4548
		4174.4	239488	7551
		4179.6	239190	7849
4077	245161	4155.0	240606	4555
4358	229383	4317.3	231561	-2178
		*4400.2	227199	2184
		4299.45	232523	-3139
		*4419.0	226240	3143
		4272.6	233984	-4601
		*4447.05	224805	4578
		*4507.35	221798	7585
		*4513.7	221484	7899
4347	229953	4328.8	227794	2159
		4407.5	226823	3130
		4435.6	225386	4567
4339	230393	4426.9	225829	4564

The triplet and doublet previously mentioned are indicated by stars. We find in this table the wave-lengths of the modified lines excited by the fainter mercury lines in the vicinity of 4046 and 4358 (shown on the upper spectrum of Pl. IX., and better resolved because of less exposure in the lower spectra). The frequency differences in the right-hand columns have been arranged slightly

displaced, so that those which belong together can be seen at a glance. Anti-Stokes lines are indicated by a minus sign.

We see from the table that we are dealing only with the five frequency differences corresponding to the five lines previously mentioned. The maximum and minimum values are 2184 and 2130, 3143 and 3107, 4601 and 4548 for the triplet, and the average of all values for the doublet are 7570 and 7875, these two last being the frequencies corresponding to wave-lengths 13.2μ and 12.2μ . Now, Coblentz's

Fig. 6.



curve of the infra-red absorption of carbon tetrachloride shows complete absorption between 12.5μ and 13.5μ . This curve is reproduced (fig. 6).

The close double line at λ 4507 and 4513 thus corresponds to this absorption band, and proves that it is in reality a double band. The other three frequency differences correspond to absorption bands at 46μ , 32μ , and 22μ , a region difficult or impossible to investigate by absorption methods. An attempt to find these by the method of residual rays will be made in the autumn, if they cannot be found in the literature, which seems unlikely.

I have given the full set of values in this and some of the following cases, as they form such a complete verification of

the theory of Professor Raman, and show the value of the method for the investigation of the remote infra-red absorption region by the study of modified lines in the visible part of the spectrum.

Chloroform.

The modified lines of this substance are shown in spectrum *c* of Pl. IX. They occur in pairs, the anti-Stokes terms are strong, and they are excited by the green line as well as by the violet lines. The values are given in the following table:—

Chloroform.

λ of Exciting Line.	Freq. of Exciting Line.	λ of Modified Line.	Freq. of Mod. Line.	Frequency Difference.
4347.5	229953	4397.4	227343	2610
		4417.7	226299	3654
		4477.1	223296	6654
4358	229383	4408.8	226756	2627
		4308.4	233040	-2657
		4427.1	235716	3667
		4289.9	233040	-3657
		4489.4	222684	6699
		4234.3	236100	-6717
		4507	221815	7658
4046.8	247039	4089.7	244448	2591
		4159.1	240369	6670
		4174.1	239465	7574
4077.8	245161	4191.9	238488	6673

The average values of the frequency differences are 2621, 3655, 6682, and 7571, corresponding to infra-red absorption at 38.15μ , 27.93μ , 14.96μ , and 13.20μ respectively. Coblentz gives complete absorption at 12.5μ .

Benzol.

Coming now to a ring molecule, we find that the modified lines of shorter wave-length than that of the exciting line are absent or so faint that they come out only with very long exposure. Spectrum *d* was made with this substance. To bring out the faint lines it is necessary to distil the

substance, as it contains an impurity which causes a strong continuous spectrum (probably fluorescence) in the blue and green region.

If a spectrogram is made of the residue left in the flask, this spectrum is so strong that the Raman lines are practically wiped out.

It was with benzol that Raman found his anti-Stokes line at 4178.5, so faint, however, as to be almost invisible, and reproduced in his paper only by a very small hump on the microphotometer curve. With long exposure I have found two lines at this point very close together, one of wavelength 4177.3 excited by 4358, and another of $\lambda = 4190$ excited by 4046.

The source of excitation of these lines was determined by filtering out the 4046 line from the light of the arc by adding chromate of potassium (*not* bichromate) to the water supplying the cooling system. The amount to be added depends upon the thickness of the layer of water between the tubes, and is best determined by adding increasing amounts to the water in the pail until the 4538 line scattered by the liquid in the inner tube shows a trace of weakening. This can be done visually or, better, photographically. Under these conditions 4046 is practically removed. The 4358 line can be removed, permitting excitation by 4046 and lines of shorter λ by means of fluorescein. The out-flow runs into a second pail on the floor, from which the upper pail is replenished. These two substances were used in the case of a number of other substances in which there was doubt about the origin of the modified lines.

On examination of the benzol spectrogram with a high-power magnifier, it was at once evident that the strong line at 4618.8 (indicated by a dot) was in reality a sharply-shaded band, very intense and sharp on the side towards the red. This line is originated by the 4046 excitation, as was found by Raman and verified by the chromate of potassium filter.

Benzol was the only substance for which wave-lengths were determined by Raman (at least in his first paper), and as they were made without an iron comparison spectrum from the mercury lines as standards, they are remarkably good. The values given in the following table are probably a little more accurate, and eight or ten lines not found by Raman are given. The increase of accuracy results from the use of about double the dispersion employed by Raman and the presence of the iron comparison spectrum.

Benzol (with intensities of stronger lines estimated).

λ of Exciting Line.	Freq. of Exciting Line.	λ of Modified Line.	Freq. of Mod. Line.	Frequency Difference.
4330	230393	4533.5	220514	9879
4347.5	229953	4542.1	220101	9852
4358.3	229383	4476.7(3)	223316	6067
		4525.8	220896	8487
		4555.8(5)	219439	9944
		5029.6(4)	198768	30515
		4681.7	213538	15845
		4687.1	213297	16086
		4594.7(3)	219581	11702
		4177.3	239322	-9939
4046.8	247039	4147.7	241024	6015
		4190.5	238568	8471
		4215.7(10)	237142	9897
		4090.8	244382	2654
	(band)	4618.8(8)	216446	30593
		4322.9	231261	15778
		4327.3	231026	16013
4077.8	245161	4180.9	239116	6045
		4215	239142	8019
		4248.9(4)	235289	9872
		4123.7	242491	2670
		4657.5	214648	30513
4108.1	243353	4282.2	233459	9894
3650	273883	4109.7	243317	30566
3654	273535	4115.1(4)	242945	30590
3662.9	272937	4125.5(4)	242326	30605

The last three lines represent the reproduction of the mercury ultra-violet triplet in the violet region, the first member falling a trifle on the long wave-length side of the mercury line 4108. It is scarcely resolvable from this in the reproduction.

The frequency difference 30564 corresponds to an absorption band at 3.27μ (Coblentz gives 3.25μ), 15812 to a band at 6.30μ , and 16050 to a band at 6.23μ (Coblentz 6.25μ).

Toluol and Monochlor benzol.

Raman spectra of these two compounds are shown on Pl. IX. (*e* and *f*). The chlorine compound became milky under the action of the light, and consequently the mercury lines were very strongly scattered, none of the lines to the right of 4915 Hg being Raman lines. The spectra are quite similar in appearance, owing to the similarity of the two molecules, chlor benzol being regarded as toluol with the CH_3 replaced by chlorine.

Partial determinations only of the wave-lengths of these substances have been made at the present moment, and it does not seem worth while to publish them, as it is expected that spectra under vastly higher dispersion will be obtained very shortly. Benzol, toluol, and xylol appear to have lines in common.

The spectrum of xylol is reproduced (spectrum *g*) excited by the total radiation of the arc, and spectrum *h* excited with 4046 removed by the chromate of potash. As will be seen, some strong lines in the group to the right of 4358 are due to 4046. Below these are reproduced spectra of ether, methyl alcohol, and ethyl alcohol. Spectra have also been made of bisulphide of carbon, sulphuric acid, water, nitrobenzol, and a number of other substances, but the plates have not yet been measured.

Quartz.

The lines scattered by a large block of very clear crystal quartz are reproduced (spectrum *l*), the Raman lines being indicated by dots. The frequency difference for these three lines (wave-lengths 4448.3, 4397.4, and 4382) are 4632, 2040, and 1246, corresponding to absorption bands at 21.58 μ , 49 μ , and 80.3 μ .

Residual-ray methods show a band of metallic absorption at 20.7 μ , which is given by the 4448.3 line. So far as I know, definite bands of longer wave-length have not been observed. Quartz is moderately transparent at 56 μ and also between 100 and 300 μ .

No trace has been found as yet of a Raman line corresponding to the well-known absorption band at 8.5 μ .

Calcite.

Modified lines have been obtained with calcite (Iceland spar) also. The frequency differences in this case were 10870, 17302, and 2802, corresponding to infra-red absorption at 9.19 μ , 5.78 μ , and 35.7 μ . So far I have been able to find record only of bands at 11.3 μ , 6.46 μ , and 30.3 μ .

Preparations are under way at the moment for a record with a very large and clear crystal with which observations can be made in several directions.

The observations on calcite were made with a very clear natural rhomb measuring $4 \times 5 \times 2$ inches, backed by a reflector and surmounted by a pool of running water.

The wave-lengths of the lines excited by 4358 are given in the following table, together with the corresponding absorption bands (calculated) in the infra-red. Such absorption bands as have been observed are given in the last column :—

Modified line.	μ (cal.).	μ (obs.) residual rays.
4386.45	68	
4387.35	65.9	
4389.15	62	
4412 (strong).....	35.67	30.3
4498.2 (faint)	14	11.3
4574.6 (very strong).....	9.18	6.46

The calculated absorption bands in this case are of considerably longer wave-length than those observed by the method of residual rays.

Rock-salt.

No lines have been found with rock-salt up to the present time.

In conclusion, I wish to express great obligation to Mr. H. M. O'Bryan, who determined the wave-lengths and rendered much assistance in picking out the lines which belonged together.

Loomis Laboratory, Tuxedo, N.Y.
Sept. 8th, 1928.

LXX. *The Equation of State of a Perfect Gas.*

To the Editors of the Philosophical Magazine.

GENTLEMEN,—

IN a paper that appeared in the June number of the Philosophical Magazine, the writer showed from thermodynamical considerations of the zero of entropy that the equation of a perfect gas, or the limiting equation of state

of the substance when the volume is infinitely large, is strictly

$$pv = MRT\xi,$$

where ξ is a function of the volume v , absolute temperature T , and mass M in mols. The proof may be given an improved form which will now be pointed out. The term $p(v_2 - v_1)$ in equation (3) may be written $p_2 v_2 - p_1 v_1$, where p_1 and p_2 denote the pressures in the condensed and vaporous states respectively. Equation (6), which applies to $T = 0$, may then be written

$$\left(\frac{\partial w}{\partial T}\right)_v = v_2 \left(\frac{\partial p_2}{\partial T}\right)_{v_2} - v_1 \left(\frac{\partial p_1}{\partial T}\right)_{v_1} = 0.$$

Now $\left(\frac{\partial p_1}{\partial T}\right)_{v_1} = 0$ at $T = 0$ (Phil. Mag. iv. p. 262, 1927),

and hence

$$v_2 \left(\frac{\partial p_2}{\partial T}\right)_{v_2} = 0.$$

The rest of the argument is the same as before.

The result may also be obtained independently of considerations of the zero of entropy. The writer has shown (J. Franklin Inst. 206 (5) p. 692, 1928) that a non-atomic gas at infinite volume near in temperature to the absolute zero has a maximum specific heat whose value is abnormally large, which depends on the fact, deducible from Clapeyron's equation, that the internal heat of evaporation at $T = 0$ is zero. Thus the specific heat c_v at constant volume is a function of the temperature, and this will therefore also hold for γ , the ratio of the specific heats. Now the temperature scale of a perfect gas thermometer coincides with the thermodynamical scale of temperature only if γ is a constant, and hence these scales strictly do not coincide. Therefore, if the temperature, as measured by the perfect gas thermometer, is expressed in terms of the temperature T on the thermodynamical scale, the equation of a perfect gas becomes

$$pv = RT \cdot \phi(T').$$

It can now be shown similarly as before that the function ϕ also involves the volume v .

Yours faithfully,
R. D. KLEEMAN.

[The Editors do not hold themselves responsible for the views expressed by their correspondents.]

THE
LONDON, EDINBURGH, AND DUBLIN
PHILOSOPHICAL MAGAZINE
AND
JOURNAL OF SCIENCE.

[SEVENTH SERIES.]

SUPPLEMENT, NOVEMBER 1928.

LXXI. *Ionization Measurements of γ -Rays.*
By J. A. CHALMERS, B.A., *Queens' College, Cambridge* *.

1. *Introduction.*

MEASUREMENTS on γ -rays can only be carried out by measuring some property of the secondary β -rays they release from matter. Various properties are available, and, in particular, the most direct information is yielded by measurements of the number ^{(1), (2)} or the energy ⁽³⁾ of the β -rays; but such experiments, owing to their length and difficulty, are not available for a great deal of the work on γ -rays. The work has largely been carried out by measurement of the ionization produced in the gas in a chamber, and thus it is of great importance to consider what meaning may be attached to such measurements.

Since the ionization is a tertiary effect, being produced by the secondary β -rays, it is clear that ionization measurements cannot be expected to give direct information about the primary γ -rays. Though it has long been recognized, *e.g.* by Bragg ⁽⁴⁾ in 1910, that ionization from γ -rays is a complex phenomenon, yet many workers have, in default of other data, been forced to assume that ionizations measure either number of quanta [*e.g.* Ahmad ⁽⁵⁾, Kohlrausch ⁽⁶⁾, etc.]

* Communicated by Sir E. Rutherford, P.R.S.

or γ -ray energy [*e. g.* Miss Szmidt⁽⁷⁾, Ellis and Wooster⁽⁸⁾, and others in connexion with the RaB/RaC γ -ray energy ratio].

The variation with frequency of the ionization per quantum is conveniently termed the "ionization function," and clearly might depend on the conditions used, *e. g.* on the shape, size, and material of the chamber, on the gas contained, on the relative positions of the source and chamber, etc.

Ionization measurements of γ -rays may be divided into two main classes: (a) the comparison of sources having the same spectral distribution of γ -rays, as in measurements of standards and of decay periods; and (b) the comparison of γ -rays of different qualities; this includes the standardization of thorium, and other, sources in terms of radium, *e. g.*⁽⁸⁾, and also all absorption measurements, as the frequency distribution must be altered by absorption. Measurements of class (a) cannot be affected by the conditions used, but those of class (b) may be so affected. The simplest case to consider is that of the comparison of two homogeneous γ -ray beams, and this can easily be extended to more complex cases; what we can actually measure are J_1 , J_2 , the ionizations produced by N_1 , N_2 quanta respectively of the two beams; if I_1 , I_2 are the values of the ionization function of the electroscope for the two frequencies of the γ -rays, then $J_1 = N_1 I_1$, $J_2 = N_2 I_2$. If we keep the external conditions unaltered, the relative number of quanta will be unaltered, *i. e.* $\frac{N_1}{N_2}$ is constant; so $\frac{J_1}{J_2} \propto \frac{I_1}{I_2}$, and hence we can investigate the change in $\frac{I_1}{I_2}$, the ratio of the values of the ionization function for two frequencies.

2. Objects and Nature of Experiments.

The objects of the experiments carried out were to demonstrate as simply and unambiguously as possible the effect of the ionization function on γ -ray measurements, to obtain an idea of the magnitude and to see how it must influence past and future γ -ray ionization work. The source used was a radium standard of 7.65 mgm. giving γ -rays almost entirely from RaB and RaC; this is particularly suitable as there are two distinct groups of γ -rays, from RaB and RaC respectively, of considerable frequency

difference, while each group is itself heterogeneous. Thus, if we can measure the relative ionizations of the two groups, or of two parts of the same group, we should expect the results to be dependent on the conditions if the ionization function has any appreciable effect. For measuring the ionizations a gold-leaf electroscope of a normal type was used, the leaf being suspended inside the chamber investigated.

To vary the relative intensities of rays of different frequencies in the beam, absorption in lead sheets up to 3 cm. in thickness was used; the results can be plotted as the logarithm of the ionization against the thickness of absorber. It was found, as is well known, *e.g.* ⁽⁹⁾, that beyond about 1.8 cm. the points lie well on a straight line, *i.e.* that the absorption is exponential. The slope of the line gives the absorption coefficient of the RaC rays, and the intercept on the axis of zero absorption gives, *vide* ⁽⁷⁾, the fractions of the total ionization due to the RaB and RaC γ -rays. For the complete description of the absorption curve, it is necessary to find also the absorption coefficient of the RaB rays by subtracting the effect of the RaC rays.

It is not possible to make use of a change in ionization function due to altering the shape or size of the chamber or the relative positions of source and chamber, for, as has been pointed out by Keetman ⁽¹⁰⁾ and others, the absorption curves are here altered owing to differences in the γ -rays entering the chamber, because of scattering. We are here concerned with the difference in the effects of similar beams of γ -rays, so we must keep all conditions outside the chamber constant. The changes in conditions that remain available are alterations of the gas or pressure inside the electroscope, and change of lining of the electroscope. The first experiments carried out were concerned with the effect of pressures above atmospheric; but, to an accuracy of about 4 per cent. in relative ionizations, the absorption curves showed no definite alteration for pressures up to $2\frac{1}{2}$ atmospheres, so description of the experimental arrangement is needless. The variation of the gas in the chamber was carried out in one instance by using CO₂ in place of air, and the effect was inappreciable; but there are considerable features of interest in other work on the subject; Rutherford and Richardson ⁽¹¹⁾ and Richardson ⁽¹²⁾ used methyl iodide in the chamber, and increased the effect of the RaB γ -rays to 85 per cent. of the total effect, as compared with 10–20 per cent. for air; they also noticed that the absorption coefficient for the RaC rays is different

with methyl iodide from that with air ; these results will be considered later together with the results of the present experiments. The alteration of lining was next investigated, and lead and aluminium were used ; eight different arrangements could be obtained by changing the base, walls, and top. Work on the variation of lining has previously been carried out by Bragg⁽⁴⁾, Keetman⁽¹⁰⁾, Sutherland and Clark⁽¹²⁾, and others ; Bragg and Keetman found variation, with the γ -rays used, of the relative ionizations for different linings ; Sutherland and Clark found variation with the position of the source ; and Keetman made some measurements of absorption curves, in which he found the soft rays more effective with a lead lining than with zinc or paper linings. These results will also receive further consideration.

3. *Experimental Arrangements.*

Owing to the great effect of the particular geometrical form of the apparatus used, this must be described in some detail, and its general form can be best seen from the diagram (fig. 1).

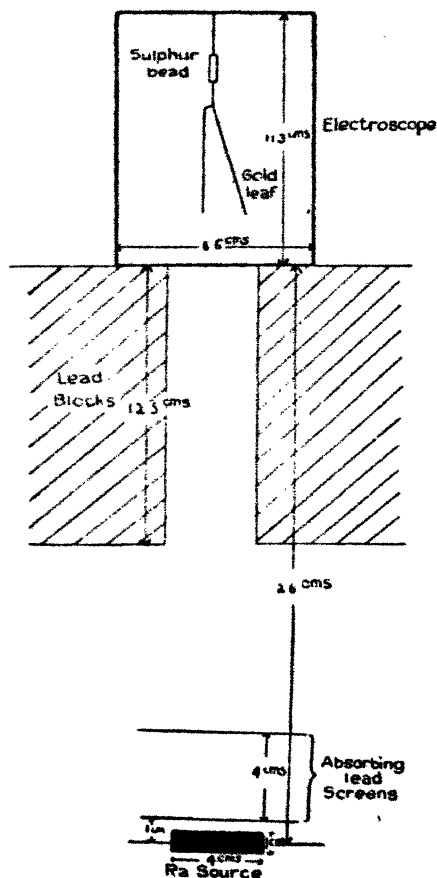
The electroscope was a cylindrical brass vessel with axis vertical ; the base was 4 mm. thick and the walls 2 mm. The electroscope was covered with 2-3 mm. of lead to exclude stray scattered γ -rays, which were further decreased by the position of the electroscope in front of a glass window. The lead linings were 1.53 mm. thick, the aluminium lid and base linings 1.63 mm., and the wall linings 3.26 mm. To change the linings the lid was completely removed.

The lead blocks enclosed a rectangle about $2\frac{1}{2} \times 5$ cm. ; the absorbing screens were rectangular, and all within the limits of 10×8 cm.² and 6×6 cm.² ; the source was cylindrical, of diameter about 1 cm. and length about 4 cm. The geometry of the apparatus was so arranged that the only γ -rays able to impinge on the side walls were those scattered in the base ; this obviously is the best arrangement for theoretical discussion, but the canalization, necessary to ensure this result, reduces the intensity considerably, and would not in general be desirable. To ascertain the effect of allowing the γ -rays to hit the sides of the chamber, another set of experiments, referred to as Set II., was carried out, when the distance from the source to the base of the electroscope was 18 cm., the thickness of the lead blocks 4 cm., and the square enclosed of side about $4\frac{1}{2}$ cm. Set II. represents more nearly the

disposition of the apparatus in the normal use of a γ -ray electroscope. Other conditions were similar in the two sets.

The sensitivity of the electroscope did not remain quite constant, and so readings were taken with a standard absorber [1.69 mm. of lead] between readings with other absorbers; each group between standards contained cases

Fig. 1.



of large and small absorption intermingled, to eliminate systematic changes.

Readings were corrected in the usual way for natural leak, and the results represented by plotting $\log I/I_0$ against absorbing thickness, where I_0 is the corrected rate of leak for the standard absorber, obtained, for the time when I was measured, by interpolation between the two standard readings.

The best straight line on the logarithmic curve, for points beyond 1.8 cm. absorption, is drawn, and from the slope and intercept we can obtain the absorption coefficient and fraction of ionization due to soft rays. Since the drawing of the best line is subject to some errors, no very great accuracy can be claimed for the results, and there may be 3-4 per cent. error in the absorption coefficients and 10-15 per cent. error in the fraction due to soft rays.

The experiments carried out were intended mainly to show the alterations in the absorption curves, but the results obtained can also be used to give rough values of J/J' , the relative ionizations for two linings. For any one lining the accuracy of relative ionizations is about 1 per cent., but in comparing two linings there is the possibility of a change in capacity, so results for J/J' cannot be relied on to more than 10 per cent. The voltage sensitivity remained fairly constant at about $\frac{1}{3}$ micrometer division per volt, with a microscope giving a magnification of about 20 diameters; the capacity was about 5 cm., but could not be measured very accurately. The values given represent the current in volts per minute for zero absorption.

In addition to the table of results the complete absorption curves for two cases are given in the accompanying graph (fig. 2). The two cases chosen are those for wholly lead and wholly aluminium linings in Set II.; this pair is chosen since they best show up one of the features of which mention will be made.

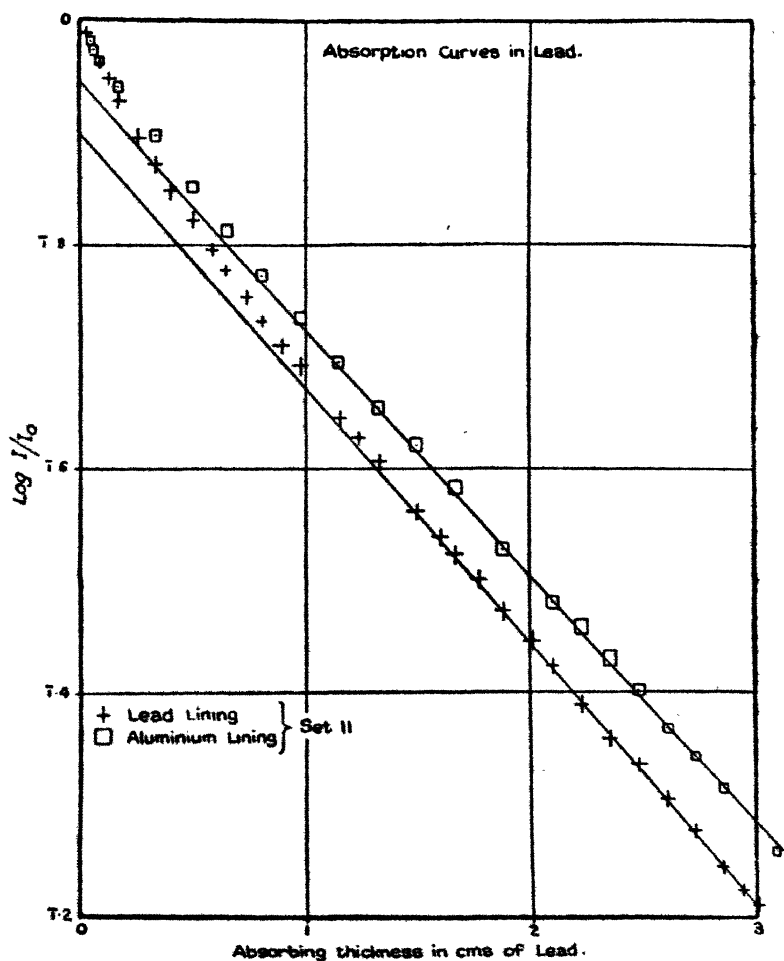
4. Table of Experimental Results.

Conditions.			SET I.			SET II.	
Base.	Walls.	Top.	Fraction due to soft rays.	Absorption coefficient of hard rays.	Volts per min. for zero absorption.	Fraction due to soft rays.	Absorption coefficient of hard rays.
←	Pb	→	.25	.50	43.4	.185	.54
←	Al	→	.12	.51	20.7	.06	.52
Pb	← Al →		.19	.51	19.8	.20	.51
Al	Pb	Al	.19	.51	43.2	.265	.50
← Pb →		Al	.22	.50	36.5	.22	.53
Al	← Pb →		.20	.52	53.4	.26	.52
← Al →		Pb	.20	.50	28.6	.16	.52
Pb	Al	Pb	.26	.49	27.2	.19	.52

5. Discussion of Experimental Results.

It is at once obvious from the table, and, perhaps, more obvious from the graph, that the absorption curves are very materially altered by changing the lining. It must be

Fig. 2.



emphasized that all conditions, except the lining, are kept identical throughout one set. Although we may not be able to define what γ -rays actually are entering the electroscope, we can be confident that for any one absorption, in one set, the same beam of γ -rays enters the electroscope no

matter what may be the lining; no correction has been made for absorption of γ -rays in the base, which is thicker than the maximum range of the secondary β -rays; such a correction would tend to accentuate the differences noticed between absorption curves for different linings.

Considering first the values of the absorption coefficient, there does appear in Set II., though not in Set I., to be some evidence that the presence of lead increases the absorption coefficient, but the accuracy of the values is scarcely sufficient to be regarded as definite; where ^{(11), (12)} methyl iodide causes the soft rays to be more accentuated than in the present experiments, there is definite evidence of a change in absorption coefficient.

Turning to the results for the soft fraction, or, which amounts to the same thing, the RaB/RaC ionization ratio, there can be no doubt that the replacement of aluminium by lead gives an increase, which may be as much as a factor of 2:1. Now, as previously emphasized, the beam of γ -rays must be the same in each case, so the RaB/RaC ratio of energies or quanta must be the same; thus, if any one electroscope did measure energies or quanta, then no other electroscope would do so. So we can say that no electroscope is likely to measure a definite property of the γ -rays.

As regards the relative total ionizations, we see that a lead top or wall increases ionization, but a lead base causes a decrease which is less than that accountable for by extra absorption in the base.

Since the geometry is altered in passing from Set I. to Set II., we cannot make a direct comparison, for we have not similar beams of γ -rays entering the electroscope. It is, however, noticeable, as might be expected, that the lead walls have more effect in Set II. than in Set I.

6. *Explanation of Results.*

Up to this, the ionization has merely been considered as an indirect result of the passage of the γ -rays; but, for any explanation of the results, it is necessary to consider in some detail the various processes involved between the passage of the primary γ -rays and the ionization produced. The γ -rays may be absorbed photo-electrically or scattered according to the Compton effect, in the metal or in the gas, and will in each case give rise to a secondary β -ray; the β -rays produced in the metal may emerge into the gas,

the chance of so doing depending on their place of origin, energy, and direction of emission, and on their chance of absorption before emergence. The β -rays, when travelling in the gas, will lose energy which appears as ionization, the amount depending on the velocity of the β -rays; when they strike the walls of the electroscope the β -rays may be absorbed or they may be scattered back [reflected], the chance depending on their velocity. Also, γ -rays which have been scattered will possibly again give β -rays later. For a complete analysis of the problem it would be necessary to use: (a) the laws of scattering and absorption of X-rays and their conversion into β -rays; (b) the laws of the passage of the β -rays through matter, including scattering and loss of energy; and (c) the relation of the energy lost by β -rays in a gas to the ionization produced. Besides the great amount of calculation involved, there are so many features of uncertainty in the laws that the calculation of the ionization function is not, at present, practicable; rough approximations will be considered later. But, fortunately, the main features can be given a qualitative explanation without such calculations.

To simplify the discussion, we must take the RaB and RaC rays each to form a homogeneous group of X-rays. Experimentally we find J_1/J_2 the ratio of the soft and hard ionizations; if N_1N_2 are the number of quanta and I_1I_2 the ionization functions, then $J_1/J_2 = N_1I_1/N_2I_2$; without the calculations mentioned we cannot obtain I_1/I_2 theoretically, and without a knowledge of N_1/N_2 we cannot obtain I_1/I_2 from experiment. All data for N_1/N_2 , except Kovarik's⁽²⁾, which is only obtained indirectly, are derived from ionization measurements, *i.e.* depend on N_1I_1/N_2I_2 . If primed and unprimed letters refer to two different linings, then experimentally we can obtain $\frac{J_1}{J_2}$ and $\frac{J_1'}{J_2'}$, *i.e.* $\frac{N_1I_1}{N_2I_2}$ and $\frac{N_1I_1'}{N_2I_2'}$, since $\frac{N_1}{N_2}$ is unaltered, the geometry being the same. Hence we can get $\frac{J_1/J_2}{J_1'/J_2'} = \frac{I_1/I_2}{I_1'/I_2'}$, and no knowledge of $\frac{N_1}{N_2}$ is now needed.

We are now in a position to consider the explanations advanced by previous workers, in particular Bragg⁽⁴⁾ and Keetman⁽¹⁰⁾. Bragg's work is concerned with different linings, without alteration of the quality of the γ -rays, *i.e.* he is concerned only with the variation with lining of

the ionization function for one beam, not, as in the present experiments, with the change of the relative values for two beams. His theory is that the ionization is proportional to: (a) the mass absorption coefficient of the lining, and (b) the total range in the lining of the secondary β -rays. We shall see that other factors are also concerned, but Bragg's theory contains the most important features. Keetman measured the relative ionizations in lead- and paper-lined chambers for γ -rays from Ra(B+C), MsTh and RdTh in each case filtered and unfiltered; by considering the ionization to depend only on the chances of absorption in the gas and metal, he obtains an explanation which, though incomplete, is adequate to account for his experimental results.

To account for the experimental results, we must compare, in turn, pairs of conditions where one part alone of the lining is altered from aluminium to lead. As above, if suffices 1 and 2 refer to soft and hard rays, and the primed and unprimed symbols to the two lining conditions, we find experimentally the ratio $\frac{J_1}{J_2} \frac{J'_1}{J'_2}$, where J 's represent

ionizations. This, we have seen, is equal to $\frac{I_1}{I_2} \frac{I'_1}{I'_2}$, where

I 's represent the ionization functions. Since the ionization is due to the secondary β -rays, and these can have different origins, we must divide each I into four parts, A, B, C, and D, corresponding to photo-electric effect and Compton effect in the metal, and the two effects in the gas respectively.

$$\text{So } \frac{I_1}{I_2} \frac{I'_1}{I'_2} = \frac{A_1 + B_1 + C_1 + D_1}{A_2 + B_2 + C_2 + D_2} \times \frac{A'_1 + B'_1 + C'_1 + D'_1}{A'_2 + B'_2 + C'_2 + D'_2}$$

We know theoretically ⁽¹⁴⁾ that for γ -rays the chance of photo-electric effect varies with wave-length according to a power between 2.5 and 3, and Ahmad ⁽⁵⁾ has shown variation with the 4th power of Z , the atomic number. We can use approximately an extrapolation of the $\lambda_0 Z^4$ law ⁽¹⁵⁾, valid for X-rays, and compare this with the law for the Compton effect ^{(16), (17)}, where variation with wave-length is small, and with Z of the first power. Thus we see that photo-electric effect is negligible for air and aluminium, compared with the Compton effect, but of the same order for lead; this is verified by Ahmad's ⁽⁵⁾ separation of the effects proportioned to Z and to Z^4 . So, with air in the electroscope, we may neglect the "C" terms, while for a lining wholly of aluminium we may also neglect the "A" terms.

As the simplest case for detailed consideration, we will take the replacement of an aluminium base lining by one of lead, the rest of the lining being taken, for definitiveness, to be aluminium, though the arguments apply equally to the other cases. If the unprimed and primed symbols refer to the aluminium and lead base linings respectively, and the suffices 1 and 2 to the RaB and RaC γ -rays, then the measured RaB/RaC ratios give, as we have seen, a value for

$$\frac{I_1}{I_2} \frac{I_1'}{I_2'}, \text{ where } I\text{'s are ionization functions or ionizations per}$$

quantum. In Set I. this is, in the case considered, equal to .4 approximately, and we have to account for this. Since the lead base absorbs the γ -rays more than does the aluminium base, and this is more effective for the soft rays,

this alone would make $\frac{I_1}{I_2} \frac{I_1'}{I_2'}$ equal to about 1.3*. So the

remaining effect, accountable for by the partition of I into A, B, C, D, must give, if acting alone, a value for

$$\frac{I_1}{I_2} \frac{I_1'}{I_2'} \text{ of } \frac{.4}{1.3} = .3, \text{ and we must account for this value,}$$

if I 's are now ionizations per quantum reaching the top of the base lining. The ionizations due to Compton absorption in the gas and top [and also in the walls when the argument is extended to Set II.] will be unaffected by the change of base lining; so, including the effect from the top lining with that from the gas, $D_1 = D_1'$, $D_2 = D_2'$. It can be shown that the ratio of ionizations due to Compton effect in the base for the two γ -rays is the same for both linings,

$$\text{i. e. } \frac{B_1}{B_2} = \frac{B_1'}{B_2'}, \text{ but this is considerably less than the ratio for}$$

* Using priming and suffices as before, let $\mu_1 \mu_2 \mu_1' \mu_2'$ be absorption coefficients, x, x' the thicknesses of the base lining, and $N_1 N_2$ the numbers of quanta at the under side of the base lining. Then the numbers of quanta at the upper side of the base lining will be:

$$N_1 e^{-\mu_1 x}, N_2 e^{-\mu_2 x}, N_1 e^{-\mu_1' x'}, N_2 e^{-\mu_2' x'}. \text{ If this alone affected } \frac{I_1}{I_2} \frac{I_1'}{I_2'},$$

it would give a value of

$$\frac{e^{-\mu_1 x}}{e^{-\mu_2 x}} \frac{e^{-\mu_1' x'}}{e^{-\mu_2' x'}} = e^{(\mu_1' - \mu_2')x' - (\mu_1 - \mu_2)x}.$$

Using the values

$$\mu_1 = .57 \text{ cm.}^{-1}, \mu_2 = .13 \text{ cm.}^{-1}, \mu_1' = 2.9 \text{ cm.}^{-1}, \mu_2' = .51 \text{ cm.}^{-1}, \\ x = .163 \text{ cm.}, x' = .153 \text{ cm.},$$

this gives

$$e^{.94 \times 1.53 - .44 \times 1.63} = e^{.29} \text{ approximately } = 1.3.$$

photo-electric effect, $\frac{A_1'}{A_2'}$. This shows certainly that

$\frac{I_1/I_1'}{I_2/I_2'}$ will be less than 1, and we can obtain the expected

* Neglecting the change of γ -ray intensity in the β -ray range [though this can be brought in by altering " f " later], the base lining may be considered to be a homogeneous though non-isotropic source of Compton secondary β -rays. For any given γ -ray the energy of the β -ray ejected at any angle is independent of the metal. Experiments have been carried out by W. Wilson⁽¹⁸⁾, Varder⁽¹⁹⁾, Madgwick⁽²⁰⁾, and others on the ionization due to homogeneous β -rays after passage through various thicknesses of absorber, using different metals and β -ray velocities; the resulting curves cannot be directly used, for they depend on the electro-scope used, but they show two general results of considerable use: (a) the "range" of the β -rays, in electrons per sq. cm., is nearly the same for all metals for one β -ray velocity; (b) the form of the curve is nearly the same with change of abscissal scale, for one metal for all velocities; that is to say, the area under the curve is equal to the product of the ionization for zero absorption, the range, and a factor " f " which depends only on the metal and not on the velocity.

Since β -rays are produced at all distances under the surface, the total ionization due to β -rays ejected at angles from θ to $\theta + d\theta$ will be this area mentioned; this is $f \cdot k d\theta \cdot i \cdot R \cos \theta$, where $k d\theta$ is the chance in unit distance [1 electron per sq. cm.] of one quantum causing the ejection of a β -ray at this angle, i the ionization produced by one such β -ray ejected at the surface, and R the range [in electrons per sq. cm.] [k , i , and R all depend on θ , but the suffix is omitted]. Using lead in place of aluminium, k , i , and R are unaltered, depending only on the Compton effect, which is an electronic, not atomic, property; so the ratio of ionizations will be f/f' . Integrating for all angles, we get

$$B_1/B_1' = f/f'. \quad \text{Similarly } B_2/B_2' = f/f'. \quad \text{Thus } \frac{B_1}{B_2} = \frac{B_1'}{B_2'}.$$

Now, turning to the " A' " terms, we can use priming to refer to photo-electric effect, for the Compton effect is the same for the two linings, except for " f 's." If E_1, E_2 are the energies of Compton electrons at θ for γ -rays of frequencies ν_1, ν_2 , we have⁽²¹⁾: $E_1/E_2 = (\nu_1/\nu_2)^n$, where $1 < n < 2$. If E_1', E_2' are photo-electric energies, $E_1'/E_2' = \nu_1/\nu_2$. If we assume that $R \cos \theta \propto \nu^m$, then

$$R_1 i_1 \cos \theta / R_2 i_2 \cos \theta = (\nu_1/\nu_2)^{mn} \quad \text{and} \quad R_1' i_1' \cos \theta / R_2' i_2' \cos \theta = (\nu_1/\nu_2)^m$$

Hence

$$B_1/B_2 = (\nu_1/\nu_2)^{mn} \cdot \sigma_1/\sigma_2,$$

where σ_1, σ_2 are Compton absorption coefficients, and

$$\sigma_1/\sigma_2 = (\nu_1/\nu_2)^p,$$

where $-1 < p < 0$. But

$$A_1'/A_2' = (\nu_1/\nu_2)^m \cdot r_1/r_2,$$

where r_1, r_2 are photo-electric absorption coefficients, and

$$r_1/r_2 = (\nu_1/\nu_2)^r,$$

where $-3 < r < -2.5$ ⁽¹⁴⁾. So

$$\frac{A_1'/A_2'}{B_1'/B_2'} = \left(\frac{\nu_1}{\nu_2}\right)^{m+r} / \left(\frac{\nu_1}{\nu_2}\right)^{mn+p} = (\nu_1/\nu_2)^{m(1-n)+r-p}.$$

value of .3 by a rough calculation * of the relative magnitudes of the ionizations from different sources; since considerable approximations have been made, as much reliance cannot be placed on this agreement as might at first be expected, but it does show that the relative magnitudes are not far wrong. The same argument can be applied to all cases of the replacement of the aluminium base by lead, and a very similar effect is shown in the replacement of the aluminium top lining by one of lead; since the Compton electrons are all ejected forward, those emerging from the top lining must have been scattered back, and so it is not possible to apply this preceding

Now $1-n$ and r are negative, p is $< -r$, so we can deduce that $A_1'/A_2 > B_1'/B_2'$.

If β is the β -ray velocity, then, neglecting high-order terms in β , $E \propto \beta^4$ and i for unit distance $\propto \beta^{-2}$; we can say that i probably $\propto \beta^s$, where $-3 < s < -1$. So $R i \cos \theta \propto \beta^{4+s}$ or $\propto E^{2+2/s}$. Thus $m = 2 + \frac{1}{2}s$.

$$\text{So} \quad \frac{A_1'}{A_2'} \cdot \frac{B_1'}{B_2'} = \left(\frac{v_1}{v_2} \right)^{(2+\frac{1}{2}s)(1-n)+r-p} = \left(\frac{v_1}{v_2} \right),$$

where the outside limits for t are $-5\frac{1}{2} < t < -2\frac{1}{2}$. But $v_1/v_2 = \text{approx. } \frac{1}{2}$, so we get

$$3^{5\frac{1}{2}} > \frac{A_1'}{A_2'} \cdot \frac{B_1'}{B_2'} > 3^{2\frac{1}{2}} \quad \text{or} \quad 500 > \frac{A_1'}{A_2'} \cdot \frac{B_1'}{B_2'} > 15.$$

* The mean energy of the Compton electrons can be found from the theoretical values ⁽²¹⁾ of the numbers and total energies of the Compton electrons; if α is the value of $.024/\lambda$ [λ in \AA], the mean energy E is $\frac{\alpha^2}{1+2\alpha} m_0 c^2$. For the RaC rays, $\alpha = 1.5$ nearly, so $E_2 = \frac{(1.5)^2}{4} m_0 c^2$, while E_2' , the energy of the photo-electron, is $\alpha m_0 c^2$; thus $E_2/E_2' = 3.75$; then, as before,

$$R_2 i_2 \cos \theta / R_2' i_2' \cos \theta = (E_2/E_2')^m,$$

where $\frac{1}{2} < m < 1\frac{1}{2}$, giving $.23 < R_2 i_2 \cos \theta / R_2' i_2' \cos \theta < .61$. Using Ahmad's ⁽⁵⁾ values of σ_2 , r_2 per atom of lead as 13.8×10^{-24} and 7.2×10^{-24} respectively, $.44 < B_2'/A_2' < 1.16$.

$B_2 = k i_2 R_2 \cos \theta \cdot f$; $D = k i_2 d$, where d is the height of the electro-scope in electrons per sq. cm. Thus $B_2/D_2 = R_2 \cos \theta f/d$; similarly $B_1/D_1 = R_1 \cos \theta f/d$. So

$$\frac{B_1}{B_2} \cdot \frac{D_1}{D_2} = \frac{R_1}{R_2} = (E_1/E_2)^2 = (v_1/v_2)^{2n},$$

where $1 < n < 2$. There is, in addition, the part of the ionization due to Compton effect in the top; hitherto we have considered this with D , but it must now be treated apart. This effect can only be due to Compton electrons scattered back; we know ^(22, 23) that reflexion at aluminium gives about 30 per cent. of the initial ionizing power, but the rays are less penetrating, so R is less. We will take this as approximately $\frac{1}{5} B$. From Varder's ⁽¹⁹⁾ ranges we can get R for electrons of the mean energy

analysis directly. For the change of wall lining from aluminium to lead there are two opposing effects; first, there is that of γ -rays scattered from the base; here, in the same way as for the base, the presence of lead increases the RaB/RaC ratio. On the other hand, there is an effect due to reflexion of β -rays at the walls; it is known^(22, 23) that β -rays are more readily reflected by lead than by aluminium; the faster the β -ray the greater is the energy loss on reflexion, and hence the greater the loss of ionizing power, for the fraction reflected varies slowly with velocity; since more energy is lost by β -rays from the hard γ -rays and more energy is lost at aluminium walls, we see that this would give a decrease in the RaB/RaC ratio when lead replaces aluminium for the wall lining. The two opposing effects give in some cases an increase and in some a decrease of the ratio.

We have seen how the general results for the RaB/RaC ratio can be explained qualitatively for Set I.; similar considerations can be applied to Set II., bearing in mind that the γ -rays from the source are falling directly on the walls. The absorption coefficients can be dealt with similarly, most simply by considering two groups of RaC γ -rays; then we should expect to find a higher absorption coefficient where there is a higher RaB/RaC ratio. This is not noticeable in Set I., but may be found in Set II.; but, if there is a small inaccuracy in drawing the line, this will, at the same time, increase the RaB/RaC ratio and decrease the absorption coefficient, or *vice versa*. The definite change of absorption coefficient in the work of Rutherford and Richardson⁽¹¹⁾ with methyl iodide is explained by photo-electric effect in the gas, i. e. by the "C" terms here negligible.

of the Compton electrons, and, using for θ the angle corresponding to the mean energy, we get $B_2/D_2 = 3'$ approximately. In order to make calculations, we use

$$\frac{A_1'}{A_2'} / \frac{B_1'}{B_2'} = 100, \quad \frac{B_2'}{A_2'} = 1, \quad \frac{B_1}{B_2} / \frac{D_1}{D_2} = \frac{1}{30}, \quad f = \frac{1}{2}, \quad \text{and} \quad f' = \frac{1}{2}.$$

Then

$$\begin{aligned} \frac{I_1}{I_2} / \frac{I_1'}{I_2'} &= \frac{B_1 + D_1}{B_2 + D_2} / \frac{A_1' + B_1' + D_1'}{A_2' + B_2' + D_2'} \\ &= \frac{B_1 + B_1 \times \frac{30}{3 \times \frac{1}{2}} + \frac{B_1}{5}}{B_2 + \frac{B_2}{3 \times \frac{1}{2}} + \frac{B_2}{5}} / \frac{100B_1' + B_1' + B_1' \times \frac{30}{3 \times \frac{1}{2}} + \frac{B_1'}{5}}{B_2' + B_2' + \frac{B_2'}{3 \times \frac{1}{2}} + \frac{B_2'}{5}} \\ &= \frac{1 + 20 + \frac{1}{2}}{1 + \frac{2}{3} + \frac{1}{5}} / \frac{100 + 1 + 30 + \frac{1}{5}}{1 + 1 + 1 + \frac{1}{5}} = .3 \text{ approximately.} \end{aligned}$$

Turning to the results for relative intensities in the two electroscopes, these can also roughly be explained *, though the agreement is only to 20 per cent. ; bearing in mind the difficulty in connexion with the capacity, this is quite satisfactory.

It is possible to use the same approximations, as have given the above agreement with experiment, to obtain a value of the RaB/RaC energy ratio ; this gives a value of about $\cdot 10$ †, in good agreement with accepted values, *e.g.* ⁽³⁾; this might make it appear desirable to carry out the calculations in more detail, but at present there is so much margin of doubt in the fundamental laws used that we must wait until further experimental data can give the laws more definitely. Though the approximations used are very rough, they give a satisfactory explanation of other results, and so may justifiably be applied to the calculation of the RaB/RaC ratio.

7. Electroscope Measurements.

As suggested by the arguments in the introduction, γ -ray ionization measurements are very considerably influenced by the ionization function. Ionization measurements, particularly with electroscopes, are exceedingly convenient for γ -ray work, but electroscopes can only measure ionizations, and we have seen the difficulty of correlating ionizations with definite properties of the beam. By considering various types of γ -ray measurements, we will illustrate the uses and limitations of the electroscope.

An interesting type of measurement to consider is that of the comparison of radium and thorium standards by means of γ -rays ; since the γ -rays are of different hardness, it has long been recognized that the comparison must depend on the amount of filtration, and comparisons are always given as measured through a certain thickness of lead ; but, since the

* For hard rays in the wholly aluminium electroscope, the ionization is $\cdot 88 \times 20 \cdot 7$ volts/minute ; with a lead base, it is $\cdot 81 \times 19 \cdot 8$. This gives a ratio experimentally of $18 \cdot 2/16 \cdot 0 = 1 \cdot 14$. In the preceding calculations, $I_2/I_1' = \frac{28}{15} B_2/\frac{16}{5} B_2'$, but $B_2/B_2' = f/f' = 3/2$; so $I_2/I_1' = 7/8$; correcting for absorption in the base, this gives $\cdot 68/\cdot 74 = \cdot 92$.

† For a wholly aluminium electroscope, $N_1 I_1/N_2 I_2 = 12/\cdot 88$ experimentally. From the previous calculations, $I_1/I_2 = \frac{106}{5} B_1/\frac{28}{15} B_2$ and $B_1/B_2 = (\nu_1/\nu_2)^{mn+p}$. With the same kind of approximations as before, $B_1/B_2 = \frac{1}{25}$. Whence we get $I_1/I_2 : \cdot 452$; so $N_1/N_2 = \cdot 30$ and $E_1/E_2 = \cdot 10$.

γ -rays are of different qualities, the electroscope used will have an effect, and so a comparison of γ -ray activities of radium and thorium sources should include a specification of the electroscope used, as well as of the thickness of lead. An important determination of this type is the ratio of the number of α -particles from radium and thorium when the γ -ray activities, measured through a certain thickness of lead, are equal; this has been carried out by Shenstone and Schlundt⁽⁵⁾, and by Watson and Henderson⁽²⁴⁾, but their results are not absolute, depending as they do on the electroscope used; but, since Watson and Henderson required their results for work on the heating effect of α -rays⁽²⁵⁾, and they used the same electroscope for the purpose of measuring the strengths of sources in the two experiments, so they are justified in using the results. Any other property of the sources would have been equally useful, but the γ -ray ionization is most convenient. This forms a good example of the way in which ionization measurements may be applied without error, even though they are concerned with γ -rays of different qualities.

As seen from the present experiments, and from previous work on the subject, the RaB/RaC ratio depends very largely on the electroscope used. It also appears probable that absorption coefficients are similarly affected; since absorption coefficients are made the basis of much theoretical work, *e. g.*^{(5), (6), (26)}, it is useful here to consider them more fully; if we can measure quanta, N , or energies, E , as well as ionizations, J , we can obtain the three absorption coefficients μ_N , μ_E , and μ_J , from $N = N_0 e^{-\mu_N x}$ etc. With a homogeneous beam of γ -rays, μ_N , μ_E , and μ_J would be equal, but no such beam can be obtained, and if obtained would soon become heterogeneous by scattering; thus μ_J can never be equal to μ or μ_E , and this is the reason why absorption coefficients for ionizations cannot be used to give energy values, *e. g.*⁽³⁾.

The most interesting of the deductions from absorption coefficients is that of Kohlrausch⁽⁶⁾. Using γ -ray intensities deduced from Thibaud's⁽²⁷⁾ results, and the accepted absorption laws^{(15), (16)}, he calculates the expected absorption coefficients, and finds divergences from those from ionization measurements; he is tacitly assuming that each quantum produces equal ionization, thereby neglecting the ionization function, but it is unlikely that this will produce sufficient effect to account for his divergences, which must still be traced to the absorption laws.

From these experiments it is also possible to obtain

information to guide in the choice of an electroscope for a particular purpose; from the absolute values, we see that the greatest ionization is produced in an electroscope with an aluminium base and the rest of lead; this, then, is the type to be chosen for the greatest sensitivity. If the presence of the soft rays will cause difficulties, either directly or due to such factors as transient equilibrium, then these can be minimised by the use of a wholly aluminium lining; for β -ray measurements it is desirable to diminish the γ -ray effect, and here again the completely aluminium electroscope is desirable.

The next question of importance is to consider whether any experimental arrangement can be devised by which the effect of the ionization function can be either eliminated or rendered easily calculable. Moseley and Robinson⁽²⁸⁾ used a very thin-walled electroscope in air and assumed the ionization inside to be equal to that in an equal volume of air; hence, knowing the absorption coefficient of air, it is possible to obtain the γ -ray energy by integrating the ionization over all space; but their basic assumption is not justifiable exactly, and other difficulties occur. Ahmad⁽⁵⁾ allowed the γ -rays to fall in succession on a number of parallel lead plates with air between; if all the secondary β -rays emerge from the plates, if we can neglect loss of energy at reflexion of the β -rays, and if all the γ -rays are absorbed, then ionization will be proportional to energy, but these conditions are not fulfilled. To obtain a method which allows ionization functions to be easily calculated, we are faced with the difficulty of obtaining a definite value for the ionization due to a single secondary β -ray; with a very large ionization chamber, or high gas-pressure, the ionization might be due to its whole energy, but here we will have difficulties due to the "D" terms, from Compton absorption in the gas. With a small chamber, or low pressure, and poorly reflecting walls we might expect the ionization to depend on $1/\text{energy}$, but it is impossible completely to eliminate the effect of reflexion. So we see it is not easy to devise an electroscope suitable for direct measurement of the γ -rays. It seems that electroscope measurements, while ideal for the comparison of similar beams of γ -rays, may only be used for beams of different quality when it is realized that ionizations are the only factors measurable. When there is any question of deducing some definite property of γ -ray beams, *e.g.* energy or quanta, then ionization measurements are only in general useful for giving a very rough indication of the value (*e.g.* Aston⁽²⁹⁾).

8. Summary.

The ionization produced in a chamber is only dependent on primary γ -rays through the agency of the secondary β -rays, and hence may not measure any definite property of the γ -ray beam; experiments have been carried out which show striking alterations in the relative ionizations of the RaB and RaC γ -rays when the electroscope lining is altered, the γ -ray beam being the same. A qualitative and a very rough quantitative explanation are given, using well-known ideas of absorption and scattering of β - and γ -rays. This demonstrates the part of an "ionization function" in γ -ray measurements, and the consequences of this are considered in relation to past work and in connexion with the limitations necessary in the use of ionizations to measure γ -rays.

It is a great pleasure to thank Professor Sir Ernest Rutherford, who suggested the problem, for his interest, and Dr. C. D. Ellis, who is responsible for many of the ideas embodied in this work, for his constant help and advice.

References.

- (1) Hess & Lawson, *Wien. Ber.* cxxv. p. 585 (1916).
- (2) Kovarik, *Phys. Rev.* xxiii. p. 559 (1924).
- (3) Ellis & Wooster, *Phil. Mag.* l. p. 521 (1925).
- (4) Bragg, *Phil. Mag.* xx. p. 385 (1910).
- (5) Ahmad, *Proc. Roy. Soc. cv.* p. 507 (1924); cix. p. 206 (1925).
- (6) Kohlrausch, *Phys. Zeit.* xxviii. p. 1 (1927).
- (7) Miss Szmidt, *Phil. Mag.* xxviii. p. 527 (1914).
- (8) Shenstone & Schlunt, *Phil. Mag.* xliii. p. 1038 (1922).
- (9) Soddy & Russell, *Phil. Mag.* xix. p. 725 (1910).
- (10) Keetman, *Ann. der Phys.* lii. p. 709 (1917).
- (11) Rutherford & Richardson, *Phil. Mag.* xxv. p. 722 (1913).
- (12) Richardson, *P. R. S.* xci. p. 396 (1915).
- (13) Sutherland & Clark, *Proc. Phys. Soc.* xxxiv. p. 51 (1921).
- (14) Oppenheimer, 'Nature,' cxviii. p. 771 (1926).
- (15) Richtmyer & Warburton, *Phys. Rev.* xxii. p. 539 (1923).
- (16) Compton, *Phys. Rev.* xxi. p. 483 (1923).
- (17) Dirac, *P. R. S.* cxi. p. 405 (1926).
- (18) W. Wilson, *P. R. S.* lxxxii. p. 612 (1909); lxxxvii. p. 310 (1912).
- (19) Varder, *Phil. Mag.* xxix. p. 725 (1915).
- (20) Madgwick, *Proc. Camb. Phil. Soc.* xxiii. p. 970 (1927).
- (21) Compton & Hubbard, *Phys. Rev.* xxiii. p. 441 (1924).
- (22) Kovarik, *Phil. Mag.* xx. p. 849 (1910).
- (23) Kovarik & W. Wilson, *Phil. Mag.* xx. p. 866 (1910).
- (24) Watson & Henderson, *Proc. Camb. Phil. Soc.* xxiv. p. 133 (1928).
- (25) Watson & Henderson, *P. R. S.* cxviii. p. 318 (1928).
- (26) Gray & Cave, *Trans. Roy. Soc. Can.* xxi. p. 163 (1927).
- (27) Thibaud, *Journ. de Phys.* xxxiv. p. 807 (1925).
- (28) Moseley & Robinson, *Phil. Mag.* xxviii. p. 327 (1914).
- (29) Aston, *Proc. Camb. Phil. Soc.* xxiii. p. 935 (1927).

LXXII. *The Heartbeat considered as a Relaxation Oscillation, and an Electrical Model of the Heart.* By BALTH. VAN DER POL, D.Sc., and J. VAN DER MARK*.

[Plates X.-XII.]

1. *Relaxation Oscillations.*

THE equation $\ddot{v} - \alpha(1-v^2)\dot{v} + \omega^2 v = 0 \dots\dots\dots (1)$

is representative of an oscillatory system of which the resistance is a function of the elongation. When α is a positive quantity the system has a resistance which for a small amplitude is negative. Therefore, the position

$$v=0$$

is unstable. When, further,

$$\alpha^2 \gg \omega^2, \dots\dots\dots (2)$$

it is obvious that as long as

$$v^2 \ll 1,$$

the variable v will initially leave the value $v=0$ in an aperiodic way, but when later

$$v^2 > 1,$$

the resistance has changed its sign and has become positive and, therefore, v will have the tendency to go back again towards $v=0$. The possibility of (1) even with the condition (2) having still a purely periodic solution is made plausible by the above considerations, and a full description of the solutions of (1) was given by one of the present authors some years ago†.

It followed from the research mentioned that the fundamental period T_{rel} of the solution of (1) with the condition (2) is

$$T_{rel} = 1.61 \frac{\alpha}{\omega^2}.$$

* Communicated by the Authors. A more detailed account of these considerations will appear in the next issue of *L'Onde Electrique*.

† Balth. van der Pol, Phil. Mag. ii. p. 978 (1926); *Jarhb. d. dr. Tel. (Zs. f. Hochfreq. Technik)* xxviii. p. 178 (1926), xxix. p. 114 (1927).

If (1) is taken to represent an electrical oscillation

$$\alpha = \frac{R}{L},$$

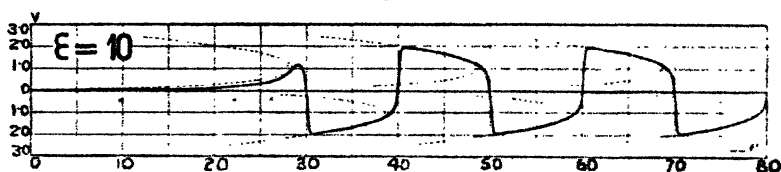
$$\omega^2 = \frac{1}{LC},$$

and thus

$$T_{\text{rel}} = 1.61 RC,$$

and therefore the fundamental period of the new oscillations is, apart from the numerical constant, given by a time constant or relaxation time, and for this reason the name *relaxation oscillation* was suggested. In fig. 1 (taken from the paper mentioned above) the solution of (1) is depicted, and it is seen that the "wave form" deviates very considerably from the sinus function.

Fig. 1.



Graphical representation of the solution of equation (5) with the condition $\epsilon = \alpha/\omega = 10$. In this case the equation represents a "relaxation oscillation" which is characterized *a. c.* by its form departing in a very marked way from a sinus curve. Sudden jumps are seen to occur periodically.

A further research of the behaviour of a relaxation system under the influence of an impressed periodic electromotive force of small amplitude revealed very remarkable synchronization properties*.

In fact it was found that, when this E.M.F. was near resonance, the *free* relaxation period of the system could be varied over a wide range (of the order of an octave), the system continuing to vibrate with the impressed period. Also the system was found very easily to synchronize on a *subharmonic* of the impressed E.M.F., *i. e.*, when the frequency of the latter was ω_0 , the fundamental frequency of the "forced" oscillation in the system was ω_0/n , n being any whole number up to 100 or 200. These relaxation

* Balth. van der Pol and J. van der Mark, "Frequency Demultiplication," 'Nature,' Sept. 10th, 1927.

oscillations therefore enable us to realise a *frequency demultiplication*. The experiment showed that the amplitude of the relaxation oscillation could not considerably be influenced by the external E.M.F. Therefore, the frequency of a relaxation oscillation can easily be influenced by an external periodic E.M.F., while the amplitude is quite "rigid." Exactly the reverse is the case with systems obeying (1) but with the condition

$$\alpha^2 \ll \omega^2,$$

as, e. g., a triode oscillator under the influence of an impressed E.M.F. *

Summarizing the properties of relaxation oscillations we have :

- (a) their *time period* is determined by a time constant or relaxation time ;
- (b) their *wave form* deviates considerably from a sinus, and, as very steep parts occur, many higher harmonics of pronounced amplitude are present ;
- (c) a small impressed periodic force can easily force the relaxation system in step with it (*automatic synchronization* even on subharmonics) while under these circumstances,

- (a) the amplitude is hardly influenced at all.

Though relaxation oscillations were originally derived in the way outlined above, it will be clear that they are to be found in many realms of nature, for there are many different types of relaxation time. We are mostly used to find a decay phenomenon to occur only once in a special experiment, and it is typical in the case of relaxation oscillations to find such an asymptotic occurrence to repeat itself periodically. Obviously this automatic periodic re-occurrence of such a typical aperiodic phenomenon is closely related to the presence of some form of energy source which is to be found behind the negativity of the resistance of (1).

Some instances of typical relaxation oscillations are : the æolian harp, a pneumatic hammer, the scratching noise of a knife on a plate, the waving of a flag in the wind, the humming noise sometimes made by a water-tap, the squeaking of a door, the multivibrator of Abraham and Bloch †, the

* This synchronisation property of a triode oscillator was first found by W. H. Eccles and J. H. Vincent, British Patent Spec. clxiii. p. 462, application date Febr. 17th, 1920. The theory of this phenomenon is to be found in Balth. van. der Pol, Phil. Mag. iii. p. 65 (1927).

† Abraham & Bloch, *Ann. de Physique*, xii. p. 237 (1919).

tetrode multivibrator*, the periodic sparks obtained from a Wimshurst machine, the Wehnelt interrupter, the intermittent discharge of a condenser through a neon tube, the periodic re-occurrence of epidemics and of economical crises, the periodic density of an even number of species of animals living together, and the one species serving as food for the other†, the sleeping of flowers, the periodic re-occurrence of showers behind a depression, the shivering from cold, menstruation, and, finally, the beating of the heart‡.

In all these examples the frequency of these periodic phenomena is not determined by the product of an elasticity and a mass but by some form of relaxation time.

That the frequency of these periodic phenomena is not rigidly constant is due to the fact that a relaxation time is determined *a. o.* by some form of resistance, and it is a well-known fact that outer circumstances may much easier influence a resistance than a mass or elasticity.

2. Schematic Dynamical Representation of the Heart.

In applying the theory of relaxation oscillations to the beating of the heart we will consider the heart as a system of three degrees of freedom: the *sinus*, the *atrium* (*auricle*), and the *ventricle*. As normally the two auricles beat in exact synchronism and the same can be said of the two ventricles, we will further speak of *the auricle* and *the ventricle*.

When we consider the heart as having three degrees of freedom only, it will be obvious that we exclude at the outset those movements of the heart which can only be described by partial differential equations. For instance, we cannot find back the finite velocity of propagation of contraction over the wall of the heart. We therefore shall not consider flutter or fibrillation, as these phenomena are directly connected with progressing and standing waves.

Returning to the view of the heart having the above-mentioned three degrees of freedom only, we consider each of them to be able to perform a relaxation oscillation by itself, each of the three having its own natural period. Moreover, a coupling exists between the *sinus* and the *auricle*, the former acting on the latter. Another coupling

* Phil. Mag. li. p. 991 (1926).

† Volterra, *Accad. Lincei, Atti* (1926).

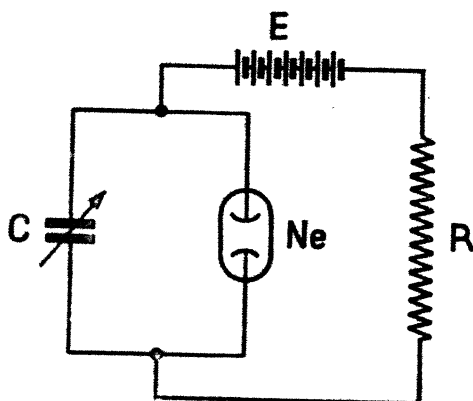
‡ The view that heart beats belong to the type of relaxation oscillations was first expressed two years ago by Balh. van der Pol (Phil. Mag. ii. p. 992 (1926)).

exists between the auricle and the ventricle, which coupling is realized through the existence of the bundle of His.

In a normal heart both the couplings mentioned have the peculiarity that they transmit a stimulus in one direction only, *i.e.*, from the sinus to the auricle, and from the auricle to the ventricle, respectively. These couplings are therefore in the normal heart of a unidirectional character. In an electrical model to be described later on, these two couplings are therefore represented by two triodes, which do not amplify at all, but which were simply inserted in order to provide a unidirectional instrument.

The purpose of this paper is to give a general connected view of the heartbeats considered as relaxation oscillations. The properties of these oscillations, which have lately been studied,

Fig. 2.



A system capable of producing relaxation oscillations. It consists of a neon lamp *Ne*, a condenser *C* of approximately 1 microfarad, a resistance *R* of the order of 1 megohm, and a battery of about 180 volt.

enable us to consider the rhythm of the heart from a new general point of view, giving a logical connected account of the heart-rhythm. According to this new theory some anomalies of the heart-rhythm can be predicted, which, so far as the authors are aware, have not yet been observed or recognized in the human heart.

3. *Electrical Model of the Heart.*

In constructing a model of the heart according to the theory expounded above, various systems capable of producing relaxation oscillations could be chosen. As a very

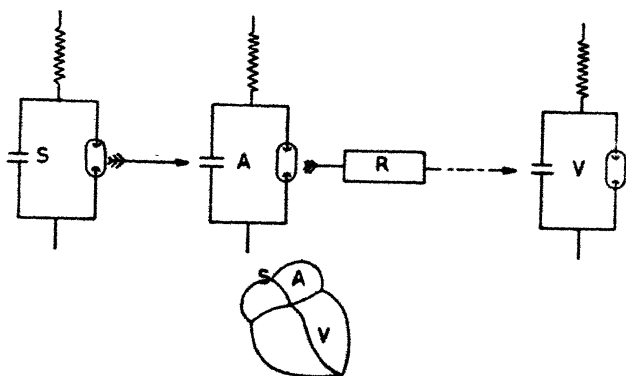
practical example, which is also well suited for demonstrations, an intermittent discharge through a neon tube can be made use of. Such a system is depicted in fig. 2, where E is a battery of say 150 to 200 volts, R a resistance of the order of 1 megohm, and C a capacity of the order of one microfarad.

As the charging-up time of the condenser is given by the product of the capacity C and the resistance R , the time period T_{rel} of this relaxation oscillation will be about

$$T_{rel} \doteq CR = 10^{-6} \cdot 10^{+6} = 1 \text{ sec.}$$

We therefore see the neon lamp to give a short flash once about every second.

Fig. 3.



Schematic representation of the heart by three relaxation systems: S (=Sinus), A (=Auriculum), and V (=Ventriculum). R is a retardation system representing in the model the finite time necessary for a stimulus to be transmitted through the A-V bundle.

In fig. 3 the heart is represented by three such systems, where the first one S stands for the sinus, A for the atrium, and V for the ventricle. Between A and V a rectangle R is drawn representing a retardation system imitating the finite time taken for a stimulus to be transmitted from the atrium through the atrio-ventricular-bundle to the ventricle. In our electrical model this retardation is brought about by the action of a fourth neon tube, which therefore takes care that the ventricular systole sets in somewhat later than the corresponding auricular one. However, any other retardation system could be chosen, and we want to stress the fact that the working of our model

is independent of the type of system used for this retardation.

A photo of the complete instrument is given in fig. 4 (Pl. X.), where it is seen that the three neon tubes S, A, and V of fig. 3 are brought to the front of the instrument, each flash corresponding to the activity of the respective part of the heart.

At the back of the instrument three keys are mounted, with which a short electrical impulse can be given to the systems S, A, and V of fig. 3, thus causing extrasystolæ of the sinus, auricle, and ventricle respectively. Moreover, the coupling between A and V (the auricle and ventricle) can be varied at will, thus imitating the beautiful experiments of Erlanger of gradually clamping the bundle of His.

The whole model consists of resistances and capacities only, and no intended inductances are introduced in the system.

Electrocardiograms could be taken from this artificial heart by adding the current impulses in the auricle and

Fig. 5.



Typical electrocardiogram of the artificial heart. The P top and the QRS complex are clearly visible. The T top however is missing, due to insufficient definite data at hand as regards its origin.

in the ventricle; a further filtering circuit was used to remodel somewhat the form of the impulses, which were registered, after amplification, with a Cambridge oscillograph. Obviously this filter circuit had no influence on the working of the model, and is not used for ordinary demonstration purposes.

A typical electrocardiogram of our artificial heart, working in a normal way, is shown in fig. 5, where the P top and QRS complex is plainly visible, while the T top is missing. As the origin of the T top in the electrocardiogram of the human heart is not quite certain yet, we could not insert a representing mechanism for it.

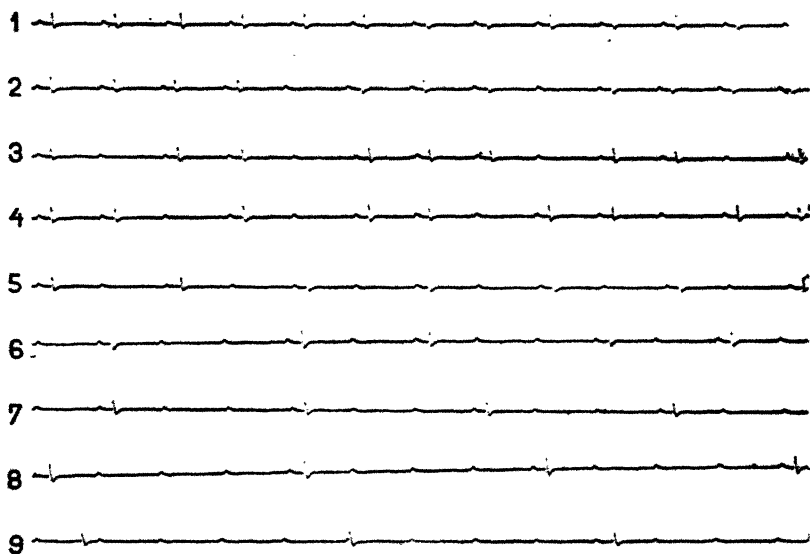
4. Observations and Measurements made with the Electrical Model.

4 a. Heart block.—In fig. 6 we give nine films taken with our model giving the effect of gradually decreasing the coupling between auricle and ventricle, thus imitating the experiments of Erlanger on clamping the bundle of His.

Film No. 1 gives the normal heart beat ; No. 2 shows an occasional failure of the ventricle ; in No. 3 these failures become more frequent ; in No. 4 we approach the case of 2:1 *heart block*, which stage is reached in film No. 5. In No. 6 we have alternatively 2:1 and 3:1 block. Further, we see in Nos. 7 and 8, respectively, 3:1 and 4:1 block, till at last in film No. 9 the coupling has become zero, which gives *complete heart block*.

A typical case of *sino-auricular block* is given in fig. 7 (Pl. X.), where the first film gives the normal heart beat and the second shows clearly the block just mentioned.

Fig. 6.



Electrocardiograms from the artificial heart obtained by gradually reducing the coupling between the A and V system (clamping the bundle of His). The development of 2:1, 3:1, and 4:1, as well as complete heart block, is clearly shown.

4b. *Extra systolæ*.—When our heart model beats in the normal way we can impress a small electrical impulse on the ventricle. If this is done directly after a ventricular systole we find that nothing happens. The ventricle therefore is still in its *refractory period*: the condenser of the V system is not yet charged up to such a potential that the extra E.M.F., superimposed upon it causes the total potential to reach the flashing potential of the neon lamp. When we repeat the same experiment slightly later,

after a ventricular systole, we find a flash of the V system. to occur; the ventricle has now passed its refractory state. When this flash occurs and we have therefore excited a ventricular extrasystole, the condenser discharges through its neon tube in a normal way down again to the potential where the gas discharge breaks, and thus we find back the famous law of "*all or nothing*": a stimulus has either no effect at all or it causes a complete systole to occur. When we investigate into the magnitude of the stimulus necessary to cause a ventricular extrasystole as a function of the phase of the ventricular cycle, we find this stimulus to decrease exponentially with an increasing phase, as was to be expected. The magnitude of the stimulus E necessary to produce an extra systole as a function of the time t , counted from the moment of a former systole, is therefore represented by the formula

$$E = Ae^{-\frac{t}{CR}} - B,$$

which follows directly from the manner in which a condenser is charged through a resistance. No doubt a similar law applies to the real heart.

Consider fig. 8 (Pl. XI.), where the film No. 1 again represents the electrocardiogram of our artificial heart beating in the normal way. Film No. 2, however, shows a *ventricular extrasystole* given shortly before an impulse from the atrium arrives. It is clearly seen that the next following auricular systole finds the ventricle still in the refractory period, so that it does not cause a normal ventricular systole. When, as in No. 3, the ventricular extrasystole is caused to occur earlier in the ventricular cycle, the next coming auricular systole *does* have effect and causes the normal ventricular systole, so that here we have the case of an "*interpolated*" *ventricular systole*.

Again in fig. 9 (Pl. XI.), film 1 represents the normal working of the heart. In film 2 an *auricular extrasystole* is caused. Here, again, the auricular extrasystole is followed after the normal time by a ventricular systole, but a *compensatory period* is found after this auricular extrasystole, so that the next one comes at the normal time rigidly determined by the frequency of the sinus. Film 3 represents the same case, but with the difference that the auricular extrasystole was excited a little earlier than in film 2. Therefore the auricular extrasystole finds the ventriculum still in its refractory period, and under these

circumstances therefore the auricular extrasystole is *not followed* by a ventricular one.

Fig. 10 (Pl. XII.), No. 1, gives the normal heart beat. Film No. 2 represents a case of a *sinus extrasystole*. It is clearly seen that the original rhythm has been lost, as is the case in the human heart.

Finally, we reproduce in fig. 11 (Pl. XII.) an electrocardiogram of the human heart, taken in three normal positions 1, 2, and 3, with the same special amplifier used in the experiments with the artificial heart and also with the same Cambridge oscillograph, which has a shorter natural time period and therefore responds quicker than the string galvanometer.

This amplifier, which had the property of amplifying the very low frequencies of say one half period per second or less, as well as the higher frequencies, enabled us to make visible the real human heart beat as periodic flashes of a neon tube. This neon tube flashed twice in each heart cycle, when it was connected to the output side of the amplifier, the input side being connected to the two hands of the patient.

5. *Final Considerations and Suggestions of new Possibilities.*

The very close analogy between the working of our model and the beating of the mammalian heart leaves no doubt that the view expressed in the former paragraphs of regarding the heart beat as a relaxation oscillation is correct. Therefore, without going into the detailed nervous and physical-chemical action of the heart, it can safely be concluded that what ultimately determines the period of the heart is a *diffusion time* (a relaxation time). As mentioned above, the model described represents a first approximation only to the action of the heart, and it could be extended in several directions, thus assigning to the heart more than three degrees of freedom only.

Moreover, a reduction of the electromotive force of the battery connected to the model reduces the "tonus," and soon a point is reached where our electrical heart does not beat any more. The system under these conditions closely shows, so far as the response to an external stimulus is concerned, the behaviour of an ordinary muscle. In fact, a cross-striated *muscle* can be represented by what may be called a "*relaxation cable*," about which we hope to report in another communication.

In conclusion, we give some further possible disorders mainly obtained mathematically and which were all verified

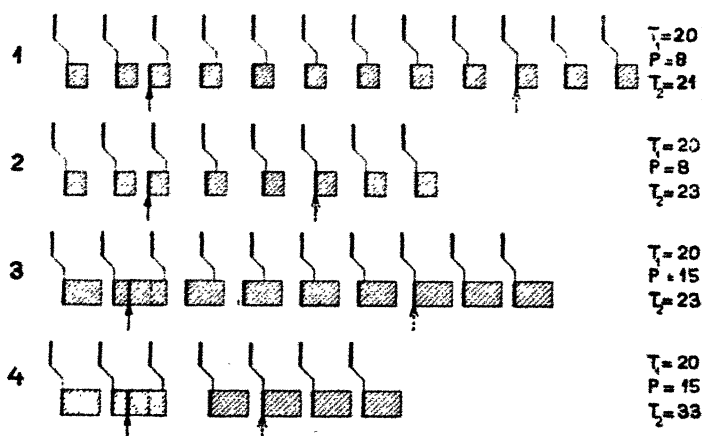
with the aid of our model. Possibly these anomalies either have or will be found in the human heart as well.

It follows from the considerations expounded above that there are two possibilities that may cause a partial heart block:

- (a) the amplitude of the stimulus arriving through the A-V bundle at the ventricle is smaller than normal;
- (b) the natural relaxation period of the ventricle is prolonged.

Both causes may result in exactly the same working of the heart, though means may be found to distinguish between the two.

Fig. 12.



Transient periods elapsing after a ventricular extrasystole is given at the moment indicated by the first arrow. Only at the moment indicated by the second (dotted) arrow is the normal periodic action of the heart resumed. This figure gives the course of events calculated and verified experimentally with the aid of the model, and with the condition that the free natural relaxation period T_2 of the ventricle is larger than that (T_1) of the auricle.

But also an acceleration of the natural free ventricular period may result in anomalies, which bear some resemblance to a combination of heart block with ventricular extrasystolæ. Especially these anomalies occur when the free relaxation period of the ventricle is slightly greater or slightly smaller than the period of the sinus and when the conduction through the A-V bundle is reduced. Let, *e.g.*, fig. 12

represent the auricular and ventricular systolæ. The shaded portions following the ventricular systolæ represent the duration of the refractory period as determined *a.o.* by the amplitude of the stimulus arriving from the A-V bundle. Calling:

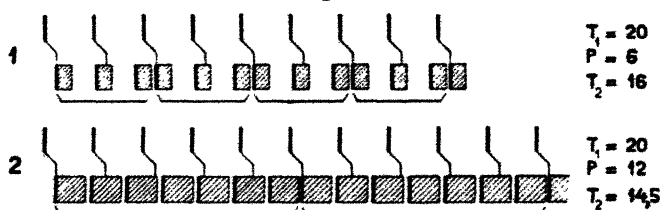
T_1 = period of the stimulus arriving from the A-V bundle.

T_2 = free relaxation period of the ventricle.

P = length refractory period.

Fig. 12, Nos. 1, 2, 3, and 4 represent different effects of extrasystolæ. The durations of T_1 , T_2 , and P are given at the side of the figures in arbitrary units. In this fig. 12 $T_1 < T_2$. Under these circumstances a ventricular extrasystole may temporarily disturb the rhythm (mathematically: transients). The extrasystole is everywhere indicated by

Fig. 13.



Some possibilities (derived theoretically and verified with the aid of the model) when the free natural relaxation period T_2 of the ventricle is slightly smaller than the auricle period T_1 . The shaded portions indicate (like in fig. 12) the refractory period of the ventricle. Especially No. 1 shows the possibility that the fundamental period of the rhythm in this case is *not* equal to the period of the auricle, but is twice as long. Here *three* ventricular systolæ occur in the time of only *two* auricular systole. The last ventricular systole in each fundamental period resembles somewhat to cause a retrograde beat of the auricle.

an arrow, while the dotted arrows give the beginning of normal working of the heart again. The anomalies of figs. 12 and 13 have been derived on the basis of a strict unidirectional conduction through the A-V bundle, and it will be clear from these figures that some of the anomalies resemble somewhat "retrograde beats."

It is seen from fig. 12, No 1, that with the numbers as given in the figure, it takes the time of 7 auricular systolæ after the extrasystole before the normal rhythm is restored again. For the special instant of the extrasystole of No. 2 and for the corresponding T_1 , T_2 , and P, the transient period

lasts about three auricular beats. Again, in Nos. 3 and 4, it takes respectively about 5.5 and 2.5 auricular periods before the normal action is restored again.

Finally, in fig. 13, two possible anomalies are depicted. Here, $T_1 > T_2$, i. e., the natural ventricular free period is shorter than the auricular period. Thus the possibility arrives that the fundamental period of the complete system consists of a whole number of auricular systolæ, i. e., the phenomenon repeats itself exactly only after, e. g., 4 or 5 or 6 auricular beats. This fundamental period is indicated by the brackets underneath each drawing. We therefore find the possibility of a, e. g., 2 : 3 block and a 5 : 7 block. We are not aware whether these phenomena occur in the real heart.

From the fact that, when

$$T_1 > T_2,$$

a forced ventricular beat can only occur when the stimulus from the A-V bundle arrives at the ventricle when the latter is outside its refractory period, it follows that the fundamental period T , where

$$T = nT_1,$$

is determined by the following two *Diophantic inequalities*

$$R < (nT_1 - mT_2) < T_2,$$

where both n and m are whole numbers and n the smallest possible one satisfying the inequalities.

Eindhoven, Natuurkundig Laboratorium
der N. V. Philips' Gloeilampen-fabrieken.
May 1928.

LXXIII. *On the Adsorption of the Alkali Metals on a Mercury-Vacuum Interface.* By R. STEVENSON BRADLEY, B.A.*.

THE adsorption of vapours on the surface of mercury has recently excited considerable interest; the corresponding case of adsorption of metals dissolved in mercury has not yet been studied.

The most interesting amalgams, and those for which most results are available, are those of the alkali metals. Both

* Communicated by Prof. R. Whytlaw-Gray.

Schmidt * and Oppenheimer † have published values for the surface tension of alkali metal amalgams at low concentrations. The publication by Bent ‡ and Hildebrand of the activities of the dissolved metals enables the Gibbs surface excess Γ to be calculated.

$$\Gamma = \frac{-d\sigma}{2 \cdot 303 RT} d \log a_2,$$

where σ is the surface tension, a_2 the activity of the dissolved metal.

Hildebrand's equations refer to pure alkali metal as the reference state; when the latter is transferred to infinitely dilute amalgams they become

$$\log \frac{a_2}{N_2} \text{ Cs} = \frac{15620}{T} N_2$$

$$\log \frac{a_2}{N_2} \text{ K} = \frac{11630}{T} N_2$$

$$\log \frac{a_2}{N_2} \text{ Na} = \left(\frac{3930}{T} + 6 \cdot 84 \right) N_2,$$

where N_2 is the mol fraction of dissolved metal. This transference is equivalent to the omission of the constant C , which disappears on differentiating. There appears to be a misprint on p. 3024 of Hildebrand's paper; the coefficients of N_2 should be changed in sign in the three equations for

$$\log \frac{a_2}{N_2}.$$

The temperature has been taken as 18°C . Schmidt worked at about 18°C ., Oppenheimer at 20°C . Temperature variations of a few degrees do not affect the values for a_2 .

When σ is plotted against $\log a_2$ a straight line is obtained, and this constancy of Γ down to the lowest concentrations used and over a concentration range of over a hundredfold for sodium, and over tenfold for potassium and caesium, suggests that a unimolecular surface layer is formed, even at 0.0007 per cent. of the alkali metals. At still lower concentrations the curve must bend sharply, and run nearly parallel to the axis of $\log a_2$.

In Tables I., II., and III., the fourth column gives the value of σ read off from the graph at the corresponding value of $\log a_2$.

* *Ann. der. Physik*, xxxix. p. 1108 (1912).

† *Zeitschr. f. Anorg. Chem.* clxi. p. 98 (1928).

‡ *J. Amer. Chem. Soc.* xlix. p. 3011 (1927).

TABLE I.

Sodium Amalgams.

Wt. % Na.	σ .	$-\log a_2$.	corrected σ .
0.0002	435.5	4.76	435.2
0.0007	424.2	4.21	426.1
0.0022	418.8	3.71	417.7
*0.019	404.0	2.75	401.7
*0.025	399.0	2.62	399.4
0.049	393.3	2.28	393.7
0.067	391.3	2.12	391.0
0.124	384.4	1.77	385.3

GRAPH I.

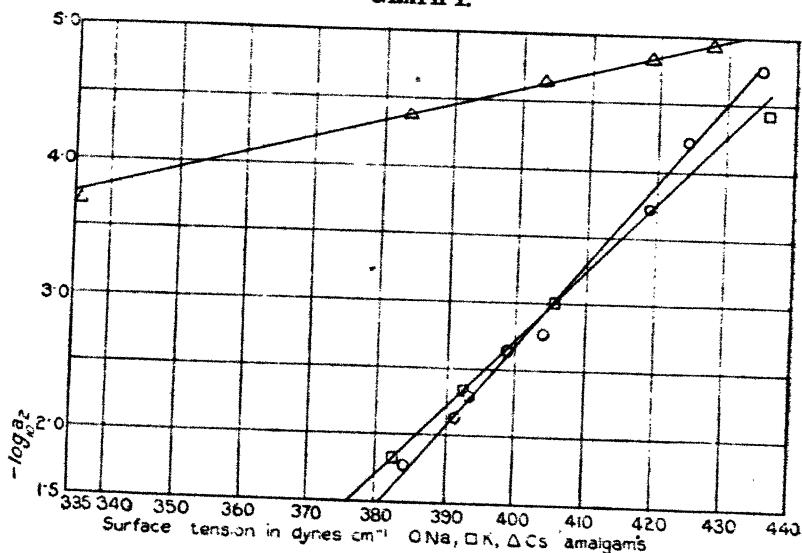


TABLE II.

Potassium Amalgams.

Wt. % K.	σ .	$-\log a_2$.	corrected σ .
0.0007	436.0	4.44	433.9
0.0018	405.1	3.00	405.4
0.0068	392.3	2.32	392.3
0.0135	388.4	1.88	383.6
0.015	382.5	1.81	382.3

* Values are those of Oppenheimer.

TABLE III.

Cæsium Amalgams.

Wt. % Cs.	σ .	$-\log a_2$.	corrected σ .
0.0008	427.6	4.92	426.2
0.001	418.8	4.82	418.5
0.0016	403.1	4.62	403.1
0.0028	383.5	4.37	383.6
0.0131	335.4	3.69	332.0

From the straight lines values of Γ may readily be calculated; for sodium, potassium, and cæsium we find for

$\frac{1}{\Gamma}$ in A.U. per atom the values,

55.4

47.9

14.7

These afford an interesting confirmation of the view that the deviations of the alkali metal amalgams from the perfect solution are to be attributed to compound formation. Bragg* gives for the atomic radii of sodium, potassium, and cæsium the values 1.77, 2.07, and 2.37 A.U. respectively, whilst Kolkmeyer† assigns 1.51 A.U. to mercury. We may assume that for sodium amalgams each atom of the surface is surrounded by six others. The area occupied by each atom may be taken as that of the circumscribing hexagon. This gives for the area occupied by the complex $\text{Na}-\text{Hg}_6$, in which each sodium atom is surrounded by a ring of six mercury atoms, the value 58 A.U. There are thus roughly six mercury atoms to one sodium atom on the surface. For potassium the ratio is less. This agrees with the freezing-point data of Kurnakow‡, the stability of the compounds $\text{R}-\text{Hg}_4$, $\text{R}-\text{Hg}_2$, being greater, as measured by the degree of sharpness of the maxima, for sodium than for potassium. The value 14.8 A.U. for cæsium is less than that of the circumscribing hexagon 22.0 A.U. The constancy of Γ with varying concentrations makes the possibility of a poly-molecular layer unlikely, so that presumably the cæsium atoms are more tightly packed than in the crystal.

* Phil. Mag. xl. p. 169 (1920).

† *Rec. Trav. Pays Bas*, xliii. p. 677 (1924).

‡ *Zeitschr. f. Anorg. Chem.* xxiii. p. 489 (1900).

Summary.

For the amalgams of the metals sodium, potassium, and caesium at low concentrations $\frac{d\sigma}{d(\log a_2)}$ is constant. Values of Γ , the surface excess, are in agreement with compound formation in the surface-layer, roughly to the extent of Na-Hg₂ for sodium, rather less for potassium. Caesium atoms alone occupy the surface of caesium amalgams.

The University,
Leeds.

LXXIV. *On the Application of Tensor Analysis to Physical Problems.* By FRANCIS D. MURNAGHAN, *Professor of Applied Mathematics, Johns Hopkins University**.

ALTHOUGH the methods of tensor analysis are generally admitted to be of great power and usefulness from a theoretical point of view, these methods are not commonly applied to problems in what may be called the older physics, the simple reason being that they are supposed to lead to expressions of too high a degree of complexity. We propose to treat in this paper the problem of determining the form of the stress-equations of elasticity in any system of curvilinear coordinates, orthogonal or not, and we trust that a comparison of our method with that given in Love's standard treatise† for the special case of orthogonal curvilinear coordinates will show that the methods of tensor analysis are not only more general but easier to follow than the method given there.

Before proceeding to a consideration of the particular problem with which we wish to support our thesis, it is necessary to point out that in physics we measure quantities that are usually different from the quantities met with in tensor analysis. Thus we say in the latter theory that if a set of n quantities X^r are the components of a contravariant tensor of the first rank in a coordinate system x , then the

* Communicated by the Author.

† A. E. H. Love, 'The Mathematical Theory of Elasticity,' 3rd edition, pp. 87-89.

components in any other coordinate system \bar{x} are given by the equations

$$\bar{X}^r = X^a \frac{\partial \bar{x}^r}{\partial x^a} \quad (a \text{ is a summation symbol}).$$

If we wish to give a geometrical interpretation to this description of a tensor, we may consider, from the x coordinate system, the family of level surfaces $\bar{x}^r = \text{const.}$; then the n expressions $\partial \bar{x}^r / \partial x^a$ are, at any point x , the covariant components of the gradient vector to that particular level surface of the family which passes through the point in question. The magnitude of this gradient vector is

$$\left(g^{ab} \frac{\partial \bar{x}^r}{\partial x^a} \frac{\partial \bar{x}^r}{\partial x^b} \right)^{\frac{1}{2}},$$

where the g^{ab} are the contravariant components of the metrical tensor, and, in accordance with the formulæ of transformation for the components of a contravariant tensor, this is simply $(\bar{g}^{rr})^{\frac{1}{2}}$. Upon dividing our equation for \bar{X}^r by this magnitude, we see that the ratio $\bar{X}^r / (\bar{g}^{rr})^{\frac{1}{2}}$ is the resolved part of the tensor \bar{X}^r in the direction of the gradient vector to the \bar{x}^r coordinate surface. Now, it is these resolved parts of tensors, *i. e.* these scalar quantities, with which we actually deal in physics. Since the gradient vector of any surface has the direction of the normal to the surface, drawn in the direction towards which the constant of the surface is increasing, the resolved part of the tensor \bar{X}^r in this direction may be conveniently represented by the symbol \bar{N}_r , and we have the relation

$$\bar{X}^r = (\bar{g}^{rr})^{\frac{1}{2}} \bar{N}_r.$$

If, then, we wish to translate a theorem of tensor analysis which involves the components of a contravariant tensor of the first rank into a form suitable for the practical purposes of physics, we should replace each component \bar{X}^r of the tensor by $(\bar{g}^{rr})^{\frac{1}{2}} \bar{N}_r$, where \bar{N}_r denotes the resolved part of the tensor in the direction of the normal to the coordinate surface $\bar{x}^r = \text{const.}$, the normal being drawn in the direction towards which \bar{x}^r is increasing. Similarly, if we consider the formulæ of transformation for the components of a covariant tensor of rank one, namely,

$$\bar{X}_r = X_a \frac{\partial x^a}{\partial \bar{x}^r},$$

we see that the n quantities $\partial x^a / \partial \bar{x}^r$, which appear as

coefficients in the r th of these formulæ, are the contravariant components of a tensor which is tangent to the \bar{x}^r coordinate curve, i. e. the curve along which all the coordinates \bar{x} , save \bar{x}^r , are constant. The magnitude of this tensor is

$$\left(g_{a\beta} \frac{\partial x^a}{\partial \bar{x}^r} \frac{\partial x^\beta}{\partial \bar{x}^r}\right)^{\frac{1}{2}},$$

or simply $(\bar{g}_{rr})^{\frac{1}{2}}$, since the g_{rs} are the covariant components of the metrical tensor. Upon dividing our equation for \bar{X}_r by this magnitude, we see that the ratio $\bar{X}_r/(\bar{g}_{rr})^{\frac{1}{2}}$ is the resolved part of the covariant tensor \bar{X}_r in the direction of the tangent to the \bar{x}^r coordinate curve through the point in question, the tangent being supposed drawn in the direction in which \bar{x}^r is increasing. This resolved part may be conveniently denoted by \bar{T}_r , and we then have the equation

$$\bar{X}_r = (\bar{g}_{rr})^{\frac{1}{2}} \bar{T}_r.$$

If, then, we wish to translate a theorem of tensor analysis, which involves the components of a covariant tensor of rank one, into a form which is of practical utility for physics, we must replace each covariant component \bar{X}_r by $(\bar{g}_{rr})^{\frac{1}{2}} \bar{T}_r$, where \bar{T}_r denotes the resolved part of the tensor in the direction of the tangent to the \bar{x}^r coordinate curve through the point in question, the tangent being drawn in the sense in which \bar{x}^r is increasing.

As examples of what we mean, let us consider two particular results:—

(a) In tensor analysis we have, associated with any contravariant tensor field X^r of rank one, a scalar quantity known as its divergence. The formal expression for this divergence is

$$\frac{1}{\sqrt{g}} \frac{\partial}{\partial x^a} (\sqrt{g} X^a)^*.$$

We rewrite this expression in the form

$$\frac{1}{\sqrt{g}} \frac{\partial}{\partial x^a} (\sqrt{g g^{aa}} N_a).$$

When the curvilinear coordinate system x is orthogonal, we may put

$$(ds)^2 = (dx')^2/h_1^2 + (dx'')^2/h_2^2 + \dots + (dx^n)^2/h_n^2,$$

* Here, as elsewhere throughout this paper, summation symbols are denoted by Greek letters.

so that

$$g_{rr} = (1/h_r)^2; \quad g_{rs} = 0 \quad (r \neq s); \quad g = (1/h_1 h_2 \dots h_n)^2$$

and

$$g^{rr} = h_r^2; \quad g^{rs} = 0 \quad (r \neq s).$$

On substituting from these equations, we obtain the familiar formula for the divergence of a vector field in orthogonal curvilinear coordinates, namely

$$h_1 h_2 \dots h_n \left\{ \frac{\partial}{\partial x^1} (N_1/h_2 \dots h_n) + \frac{\partial}{\partial x^2} (N_2/h_1 h_3 \dots h_n) + \dots \right. \\ \left. + \frac{\partial}{\partial x^n} (N_n/h_1 \dots h_{n-1}) \right\}$$

(see Love, *loc. cit.* p. 54, eq. 37). It should be observed that when the coordinates are orthogonal the gradient vector to the coordinate surface x^r has the same direction as the coordinate line x^r , so that we could have written T_r instead of N_r in the expression for the divergence.

(b) Associated with any covariant vector field X_r we have an alternating covariant tensor field of rank two, which is known as the curl of the given tensor field. Its components X_{rs} are defined by the equations

$$X_{rs} = \partial X_s / \partial x^r - \partial X_r / \partial x^s.$$

In accordance with our remarks above, the X_r which occur on the right-hand side of these formulæ must be replaced by $(g_{rr})^{\frac{1}{2}} T_r$, but it is necessary to find out what physically measured quantities are described by the components X_{rs} of the alternating covariant tensor of rank two. From the formulæ of transformation we have

$$\bar{X}_{rs} = X_{\alpha\beta} \frac{\partial x^\alpha}{\partial \bar{x}^r} \frac{\partial x^\beta}{\partial \bar{x}^s} = 'X_{\alpha\beta} \frac{\partial (x^\alpha, x^\beta)}{\partial (\bar{x}^r, \bar{x}^s)},$$

where the prime indicates that the summation labels α and β run over all pairs, without repetition, out of the n labels 1 to n . The $n(n-1)/2$ Jacobian determinants may be said to define an element of area on the (\bar{x}^r, \bar{x}^s) coordinate surface, *i. e.* the surface on which all the coordinates \bar{x} , save \bar{x}^r and \bar{x}^s , are constant. The magnitude of this element of area is, by definition, the square root of

$$'(g_{\alpha\lambda} g_{\beta\mu} - g_{\alpha\mu} g_{\beta\lambda}) \frac{\partial (x^\alpha, x^\beta)}{\partial (\bar{x}^r, \bar{x}^s)} \frac{\partial (x^\lambda, x^\mu)}{\partial (\bar{x}^r, \bar{x}^s)},$$

where the summation labels (α, β) and (λ, μ) run, independently, without repetition over all pairs out of the n labels 1 to n . If we introduce the symbol

$$g_{pq,rs} = \begin{vmatrix} g_{pr} & g_{ps} \\ g_{qr} & g_{qs} \end{vmatrix} = g_{pr}g_{qs} - g_{ps}g_{qr},$$

this is a covariant tensor of rank four, which is alternating in the first two labels (pq) and also in the last two (rs) . Our expression for the magnitude of the element of area takes the form

$$\left\{ g_{\alpha\beta, \lambda\mu} \frac{\partial(x^\alpha, x^\beta)}{\partial(\bar{x}^r, \bar{x}^s)} \frac{\partial(x^\lambda, x^\mu)}{\partial(\bar{x}^r, \bar{x}^s)} \right\}^{\frac{1}{2}},$$

or simply $(g_{rs,rs})^{\frac{1}{2}}$, from the formulæ of transformation for a covariant tensor of rank four. If, then, we divide our equation for \bar{X}_{rs} by this magnitude, the result is the flux of the alternating tensor X_{rs} through the element of area of the (\bar{x}^r, \bar{x}^s) coordinate surface divided by the magnitude of this element of area. We shall denote this by \bar{T}_{rs} , and may call it the resolved part of the tensor X_{rs} in the direction of the (\bar{x}^r, \bar{x}^s) coordinate surface. We have the equation of connexion

$$\bar{X}_{rs} = (g_{rs,rs})^{\frac{1}{2}} \bar{T}_{rs},$$

or, in the x coordinate system,

$$X_{rs} = (g_{rs,rs})^{\frac{1}{2}} T_{rs} = (g_{rr}g_{ss} - g_{rs}^2)^{\frac{1}{2}} T_{rs}.$$

Hence the desired, physically useful, form of the equations of definition of the curl of a covariant tensor field of rank one is

$$T_{rs} = (g_{rr}g_{ss} - g_{rs}^2)^{-\frac{1}{2}} \left\{ \frac{\partial}{\partial x^r} (g_{ss}^{\frac{1}{2}} T_s) - \frac{\partial}{\partial x^s} (g_{rr}^{\frac{1}{2}} T_r) \right\}.$$

In the special case of orthogonal curvilinear coordinates this takes the form

$$T_{rs} = h_r h_s \left\{ \frac{\partial}{\partial x^r} (T_s / h_s) - \frac{\partial}{\partial x^s} (T_r / h_r) \right\}$$

(cf. Love, *loc. cit.* p. 55, formulæ 38).

We now proceed to a consideration of the stress-equations of elasticity theory. The rôle of the stress-tensor is that of associating with any element of area at a point a vector which is the stress, or force, per unit area, across that element. In the usual presentation of the theory the stress-tensor is given as a tensor of the second rank, and when

rectangular Cartesian coordinates are used the nine components are denoted by the scheme

$$\begin{pmatrix} X_x & X_y & X_z \\ Y_x & Y_y & Y_z \\ Z_x & Z_y & Z_z \end{pmatrix}.$$

Thus X_y , for example, denotes the x -component of the stress across an element which is placed perpendicular to the y -axis. It is assumed that the stress-tensor is symmetric, so that we have the three relations

$$Y_z = Z_y; \quad Z_x = X_z; \quad X_y = Y_x.$$

The stress-equations are

$$\partial X_x / \partial x + \partial X_y / \partial y + \partial X_z / \partial z = \rho(\ddot{x} - X),$$

$$\partial Y_x / \partial x + \partial Y_y / \partial y + \partial Y_z / \partial z = \rho(\ddot{y} - Y),$$

$$\partial Z_x / \partial x + \partial Z_y / \partial y + \partial Z_z / \partial z = \rho(\ddot{z} - Z)$$

(cf. Love, *loc. cit.* p. 33), and it is our purpose to rewrite these equations when the coordinates in use are any set of curvilinear coordinates whatever.

Since the rôle of the stress-tensor is to set up a correspondence between elements of area and vectors, the stress-tensor must be covariant of rank two and contravariant of rank one; in all, it is of rank three, and it is alternating in the two covariant labels. Denoting it by $X_{pq}{}^r$, we have

$$X_{qp}{}^r = -X_{pq}{}^r.$$

The vector, or contravariant tensor of rank one, associated by means of the stress-tensor with any element of area is

$$X^r = 'X_{\alpha\beta}{}^r d(x^\alpha, x^\beta),$$

where the $n(n-1)/2$ Jacobian determinants $d(x^\alpha, x^\beta)$ serve to define the element of area. In order, however, to conform with the usual practice of representing the stress-tensor as a tensor of rank two, we multiply the triply-labelled tensor $X_{pq}{}^r$ scalarly by the alternating tensor ϵ^{imn} , whose components have the values $\pm 1/g^{1/2}$ or zero, and arrive in this way at the contravariant tensor of rank two,

$$X^{rs} = \frac{1}{2} \epsilon^{\alpha\beta} X_{\alpha\beta}{}^r = (X_{pq}{}^r) / \sqrt{g}.$$

Here p and q are the two labels which are different from s ,

arranged so that the arrangement (*s p q*) is an even rearrangement of the standard order (123). Explicitly

$$X^{1r} = (X_{23}^r) / \sqrt{g}; \quad X^{2r} = (X_{31}^r) / \sqrt{g}; \quad X^{3r} = (X_{12}^r) / \sqrt{g}.$$

This doubly-labelled tensor X^{rr} may be called the contravariant stress-tensor of rank two. It is then apparent that the stress-equations already given are merely the rectangular Cartesian form of the tensor-equation

$$X^{aa}{}_{,a} + F^a = 0,$$

where the symbol $X^{aa}{}_{,a}$ means that we first take the covariant derivative $X^{rr}{}_{,t}$ of X^{rr} and then contract with respect to the labels *r* and *t*. The tensor F^a is the contravariant presentation of the tensor whose components in rectangular Cartesian coordinates are

$$\rho(X - \ddot{x}), \quad \rho(Y - \ddot{y}), \quad \rho(Z - \ddot{z}).$$

We shall call this the force tensor per unit volume, in accordance with D'Alembert's scheme of reducing a dynamical problem to a static one by including amongst the forces acting on the system the reversed inertial forces. As far as tensor analysis goes, the problem is over; the stress-equations in any coordinate system whatever are

$$X^{aa}{}_{,a} + F^a = 0.$$

In order, however, to put this result in a form which may be useful in practice, we must ask ourselves how the components X^{rr} of the contravariant stress-tensor are connected with the stresses which are actually measured. In order to answer this question, we shall first consider the stress-tensor in the form in which it actually arises, *i. e.* in its triply-labelled form X_{pq}^r . When a transformation to any other coordinate system \bar{x} is made, the components of the stress-tensor become

$$\bar{X}_{pq}^r = 'X_{\alpha\beta}^{\gamma} \frac{\partial(x^{\alpha}, x^{\beta})}{\partial(\bar{x}^p, \bar{x}^q)} \frac{\partial \bar{x}^r}{\partial x^{\gamma}},$$

where the prime indicates that the summation labels (α, β) run over the three pairs (2, 3), (3, 1), and (1, 2) without repetition. If we divide this equation through by the magnitude

$$\left\{ g_{\alpha\beta, \lambda\mu} \frac{\partial(x^{\alpha}, x^{\beta})}{\partial(\bar{x}^p, \bar{x}^q)} \frac{\partial(x^{\lambda}, x^{\mu})}{\partial(\bar{x}^p, \bar{x}^q)} \right\}^{\frac{1}{2}}$$

of the element of area of the (\bar{x}^p, \bar{x}^q) coordinate surface and also by the magnitude

$$\left\{ g^{is} \frac{\partial \bar{x}^r}{\partial x^s} \frac{\partial \bar{x}^r}{\partial x^s} \right\}^{\frac{1}{2}}$$

of the contravariant tensor $\partial \bar{x}^r / \partial x^s$, which is tangent to the \bar{x}^r coordinate line, we obtain the resolved part of the stress, i. e. force per unit area, across the element of area of the (\bar{x}^p, \bar{x}^q) coordinate surface, in the direction of the \bar{x}^r coordinate line. This resolved part of the stress may be denoted by the symbol $\overline{pq, r}$, and our equation for $X_{pq}{}^r$ is equivalent to

$$\bar{X}_{pq}{}^r = \sqrt{(\bar{g}_{pp}\bar{g}_{qq} - \bar{g}_{pq}^2)} \bar{g}^{rr} \overline{pq, r}.$$

Upon multiplying this through by $1/\bar{g}^{\frac{1}{2}}$, we find

$$\bar{X}^{rr} = \sqrt{(\bar{g}_{pp}\bar{g}_{qq} - \bar{g}_{pq}^2)} \bar{g}^{rr} \bar{g} \widehat{sr},$$

where (s, p, q) is an even rearrangement of $(1, 2, 3)$ and \widehat{sr} denotes precisely the same physically measured thing as $\overline{pq, r}$. Dropping now the bars, we see that

$$X^{rr} = \sqrt{(g_{pp}g_{qq} - g_{pq}^2)} g^{rr} / g \widehat{sr} = \sqrt{g^{ss} g^{rr}} \widehat{sr},$$

since

$$g^{ss} = (g_{pp}g_{qq} - g_{pq}^2)/g.$$

These are the expressions that must be substituted for X^{rr} in the equations $X^{ss}{}_{,s} + F^s = 0$ to make them practically useful. Even when this is done, there is one further step to take. Since the F^s are the components of a contravariant tensor of rank one, we write them in the form

$$F^s = (g^{ss})^{\frac{1}{2}} N_s,$$

and obtain the desired form of the stress-equations:

$$\left. \begin{aligned} (g^{ss})^{-\frac{1}{2}} X^{ss}{}_{,s} + N_s &= 0, \\ X^{rr} &= \sqrt{(g_{pp}g_{qq} - g_{pq}^2)} g^{rr} / g \widehat{sr} \\ &= \sqrt{g^{ss} g^{rr}} \widehat{sr}. \end{aligned} \right\}$$

Here (s, p, q) is an even rearrangement of $(1, 2, 3)$, and N_s denotes the resolved part of the force-tensor along the normal to the coordinate surface $x^s = \text{const.}$ We may put this result in a somewhat more explicit form. Thus, from the formula for covariant differentiation, we have

$$X^{rr}{}_{,s} = \partial X^{rr} / \partial x^s + X^{sr} \Gamma_{st}{}^t + X^{sr} \Gamma_{st}{}^r,$$

where the Γ_{pq}^r are the Riemann-Christoffel three index symbols of the second kind. Hence

$$\begin{aligned} X^{\alpha}_{;\alpha} &= \partial X^{\alpha\alpha} / \partial x^{\alpha} + X^{\beta\alpha} \Gamma_{\beta\alpha}^{\alpha} + X^{\alpha\beta} \Gamma_{\beta\alpha}^{\alpha} \\ &= \partial X^{\alpha\alpha} / \partial x^{\alpha} + X^{\beta\alpha} \Gamma_{\beta\alpha}^{\alpha} + X^{\alpha\beta} \frac{\partial}{\partial x^{\beta}} \log \sqrt{g} \\ &= \frac{1}{\sqrt{g}} \frac{\partial}{\partial x^{\alpha}} (\sqrt{g} X^{\alpha\alpha}) + X^{\beta\alpha} \Gamma_{\beta\alpha}^{\alpha}. \end{aligned}$$

In the particular case of orthogonal curvilinear coordinates, where

$$(ds)^2 = (dx^1)^2/h_1^2 + \dots + (dx^n)^2/h_n^2,$$

$$\Gamma_{11,1} = \frac{1}{2} \partial g_{11} / \partial x^1 = -(\partial h_1 / \partial x^1) / h_1^3;$$

$$\Gamma_{11}^1 = g^{11} \Gamma_{11,1} = -(\partial h_1 / \partial x^1) / h_1;$$

$$\Gamma_{11,2} = -\frac{1}{2} \partial g_{11} / \partial x^2 = (\partial h_1 / \partial x^2) / h_1^3;$$

$$\Gamma_{11}^2 = g^{22} \Gamma_{11,2} = (h_2^2 \partial h_1 / \partial x^2) / h_1^3;$$

$$\Gamma_{12,1} = \Gamma_{21,1} = \frac{1}{2} \partial g_{11} / \partial x^2 = -(\partial h_1 / \partial x^2) / h_1^3;$$

$$\Gamma_{12}^1 = \Gamma_{21}^1 = g^{11} \Gamma_{12,1} = -(\partial h_1 / \partial x^2) / h_1;$$

$$\Gamma_{12,3} = 0; \quad \Gamma_{12}^3 = g^{33} \Gamma_{12,3} = 0,$$

$$X^{11} = h_1^{-2} \widehat{11}; \quad X^{12} = h_1 h_2 \widehat{12}; \quad X^{13} = h_1 h_3 \widehat{13}, \text{ etc.}$$

Since the contravariant stress-tensor is symmetric, these equations show that $\widehat{sr} = \widehat{rs}$. On putting $s=1$, the first of our three equations becomes

$$\begin{aligned} N_1 + \frac{1}{h_1} \left\{ h_1 h_2 h_3 \left[\frac{\partial}{\partial x^1} (h_1 \widehat{11} / h_2 h_3) + \frac{\partial}{\partial x^2} (\widehat{12} / h_3) + \frac{\partial}{\partial x^3} (\widehat{13} / h_3) \right] \right. \\ \left. - h_1 \widehat{11} \partial h_1 / \partial x^1 - 2 h_2 \widehat{12} \partial h_1 / \partial x^2 - 2 h_3 \widehat{13} \partial h_1 / \partial x^3 \right. \\ \left. + h_1^2 \widehat{22} (\partial h_2 / \partial x^1) / h_2 + h_1^2 \widehat{33} (\partial h_3 / \partial x^1) / h_3 \right\} = 0, \end{aligned}$$

i. e.

$$\begin{aligned} N_1 + h_1 h_2 h_3 \left\{ \frac{\partial}{\partial x^1} (\widehat{11} / h_2 h_3) + \frac{\partial}{\partial x^2} (\widehat{12} / h_3 h_1) + \frac{\partial}{\partial x^3} (\widehat{13} / h_1 h_3) \right\} \\ + \widehat{12} h_1 h_2 \frac{\partial}{\partial x^2} (1/h_1) + \widehat{13} h_1 h_3 \frac{\partial}{\partial x^3} (1/h_1) \\ - \widehat{22} h_1 h_2 \frac{\partial}{\partial x^1} (1/h_2) - \widehat{33} h_1 h_3 \frac{\partial}{\partial x^1} (1/h_3) = 0 \end{aligned}$$

(cf. Love, *loc. cit.* p. 89, formula 19).

It would be somewhat pedantic to point out that the argument as outlined here is applicable to tensors of any rank provided they are *alternating*. Indeed, it may not be too much to say that alternating tensors suffice for physics; the underlying reason therefore being that the elements of content, *i. e.* area, volume, etc., are described by means of Jacobian determinants, which are in their very nature alternating. The obvious rejoinder to such a remark is a reference to the contravariant stress-tensor X^{rs} , which is, as we have remarked above, symmetric. However, the stress-tensor should really be regarded in its triply-labelled form X_{pq}^r , the doubly-labelled form X^{rs} being artificial. To say that $X^{22}=X^{33}$, for instance, is to say that $X_{12}^3=X_{31}^3$, or, equivalently, that $X_{12}^3+X_{13}^3=0$, since the stress-tensor is alternating in its covariant labels. Expressed in tensor form, this says that the result of contracting the triply-labelled stress-tensor is the zero-tensor, *i. e.*

$$X_{pa}^a = 0.$$

A similar remark would apply to the symmetrical tensor G_{rs} , which, in Einstein's theory, vanishes in space at points free from matter. This may be presented as a tensor of rank four, G_{lmn}^r , which is alternating in the covariant labels. The condition of symmetry is

$$G_{lma}^a = 0.$$

LXXV. *A General Theorem on Screened Impedances.* By
RAYMOND M. WILMOTTE, B.A. (of the National Physical
Laboratory)*.

SUMMARY.

FOR accurate measurements, especially at high frequencies, it is necessary that all impedances and apparatus used should be surrounded by metal screens kept at definite potentials. By this means, the leakage and capacity effects to earth can be rendered perfectly definite, and the apparatus electrically independent of the surrounding objects. Even when this is done, there is some ambiguity regarding the value of the impedance of the apparatus. The impedance is

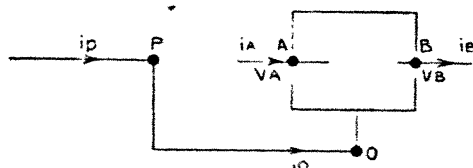
* Communicated by the Author.

the ratio of the potential difference across the apparatus to the current. Now, both the potential difference and the current depend on the potential of the screen; moreover, the current may be measured at various points. One of the most usual values of the impedance is obtained when the screen is kept at the same potential as the terminal where the current is being measured, but is not directly connected to that terminal. On this definition of impedance it would be natural to expect that there would be two possible values, depending on which terminal is kept at the potential of the screen. In this paper the curious result is obtained that these two values are equal, and certain limitations are considered. This general result is of considerable importance, as it makes it unnecessary to connect the apparatus in any special way, so long as the screen is kept at the same potential as the terminal at which the current is measured.

Introduction.

CAPACITY effects to earth have brought about the universal use of metal screens surrounding any apparatus which is to be used for accurate measurements, especially at

Fig. 1.



high frequencies. The only case in which it is legitimate to do without metal screens is when the impedance of the apparatus is small.

Generally, then, an impedance has three terminals—one at each end, and one on the screen. Let these be A, B, and O respectively, as shown in fig. 1.

The value of the impedance is the ratio of the potential difference between A and B to the current. This will depend on the potential at which the shield O is kept relatively to A or B, and the point at which the current is measured. The screen S is usually connected to some point P in the circuit. This point P is not necessarily directly connected to A or B, but is instrumental in fixing the potential of O relative to A or B. For any setting

of the potential of the screen O relative to A, there will be two possible values of the impedance, namely,

$$\frac{V_A - V_B}{i_A} \quad \text{and} \quad \frac{V_A - V_B}{i_B}$$

If the screen O is given the same setting of potential but relative to B instead of to A, there should be another two values for the impedance :

$$\frac{V_{A'} - V_{B'}}{i_{A'}} \quad \text{and} \quad \frac{V_{A'} - V_{B'}}{i_B}$$

It is proved in the next paragraph that the only setting of the potential of O which will make two of these values equal in the general case is when the potential of O is made equal to that of A or B, then

$$\frac{V_A - V_B}{i_A} = \frac{V_{A'} - V_{B'}}{i_{B'}} \dots \dots \dots (1)$$

For any special case, of course, some of the values of the impedance can be made equal by suitable settings of the potential of the screen ; for instance, if there is absolute symmetry about the centre of the impedance, it will also be found that

$$\frac{V_A - V_B}{i_B} = \frac{V_{A'} - V_{B'}}{i_{A'}}$$

In this particular case, then, the values of the impedance can be reduced to two.

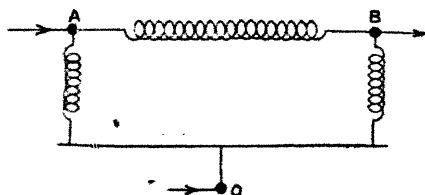
The importance of the equality (1) in the general case is that the impedance of any piece of apparatus can be given without stating which terminal should be kept at the potential of the screen. The potential of the screen must be kept at the potential of one of the terminals A or B, and the screen must not be directly connected to that terminal. This latter condition is necessary, for if the point P coincides with A, the current measured would not be I_A , but I_P .

The condition, that the screen should be kept at the potential of one of the terminals while there is no direct connexion between the two, happens to be a very frequent condition of bridge measurements where a Wagner earth is used. It would be convenient, therefore, to standardize this particular value of the impedance so that only when other values are required should it be necessary to state the conditions of measurement.

Two other values, sometimes required, occur when the screen is directly connected to one of the terminals. That is, P coincides with either A or B . If P coincides with A , the current I_B should be measured and not I_P . The reason for this is that, owing to the comparatively large size of the screen, appreciable current may flow *via* the earth to the screen from other apparatus in the circuit, and the current I_P will depend not only on the potential difference between A and B , but also on the circuit arrangement. On the other hand, the current i_B is independent of the circuit, being equal to $(i_A + i_0)$.

The three common values of an impedance can be represented diagrammatically by a network of three impedances, as shown in fig. 2. This method of representation may be useful in some cases (*e. g.*, a condenser) in order to gain a physical conception why the different values exist; but, in general,

Fig. 2.



this is unnecessary, since in any case the complete data of the impedance of a piece of apparatus used in such a way that the screen is kept by some means or other at the potential of one of the terminals, must consist of at least three values.

The above results have been stated for a special case in a previous paper by L. Hartshorn and the author*, but no proof was given and the result was not generalized, nor were the limitations considered.

Proof.

Consider the impedance made of a network of admittances interconnecting the points 1, 2, 3, ... n , such that Y_{rs} is the admittance joining the points r and s . The points 1 and n correspond to the terminals of the apparatus. Let a current I_1 enter at the point 1 and I_n leave at the point n . Let V_1 ,

* L. Hartshorn & R. M. Wilmette, "Note on Shielded Non-inductive Resistances," J. Sci. Inst. iv. pp. 33-37 (1926).

V_2, V_3, \dots, V_n be the potentials of the junction points of the admittances. Let the screen be denoted by the point 0.

Since the total current entering a junction point is zero, we have

$$\begin{aligned} I_1 &= (V_0 - V_1)Y_{01} + (V_2 - V_1)Y_{12} + (V_3 - V_1)Y_{13} + \dots \\ &\quad + (V_n - V_1)Y_{1n} \\ &= -V_1 \sum_{r=0}^{r=n} (Y_{1r}) + V_2 Y_{12} + V_3 Y_{13} + \dots + V_n Y_{1n} + V_0 Y_{01}. \end{aligned}$$

Similarly,

$$\begin{aligned} 0 &= V_1 Y_{12} - V_2 \sum_0^n (Y_{2r}) + V_3 Y_{23} + \dots + V_n Y_{2n} + V_0 Y_{02} \\ &\dots \dots \dots \\ -I_n &= V_1 Y_{1n} + V_2 Y_{2n} + V_3 Y_{3n} + \dots - V_n \sum_0^n (Y_{nr}) + V_0 Y_{0n}. \end{aligned}$$

Eliminating V_2, V_3, \dots, V_{n-1} from the first $(n-1)$ equations, we obtain

$$I_1 \nabla = V_1 \nabla_1 + V_n \nabla_n + V_0 \nabla_0, \quad \dots \quad (2)$$

where

$$\nabla = \begin{vmatrix} -\sum_0^n (Y_{2r}), & Y_{23}, & \dots, & Y_{2,n-1} \\ Y_{23}, & -\sum_0^n (Y_{3r}), & \dots, & Y_{3,n-1} \\ \dots & \dots & \dots & \dots \\ Y_{2,n-1}, & Y_{3,n-1}, & \dots, & -\sum_0^n (Y_{r,n-1}) \end{vmatrix}$$

and

$$\nabla_r = \begin{vmatrix} Y_{1r}, & Y_{12}, & Y_{13}, & \dots, & Y_{1,n-1} \\ Y_{2r}, & -\sum_0^n (Y_{2r}), & Y_{23}, & \dots, & Y_{2,n-1} \\ Y_{3r}, & Y_{23}, & -\sum_0^n (Y_{3r}), & \dots, & Y_{3,n-1} \\ \dots & \dots & \dots & \dots & \dots \\ Y_{n-1,r}, & Y_{2,n-1}, & Y_{3,n-1}, & \dots, & -\sum_0^n (Y_{r,n-1}) \end{vmatrix}$$

It should be noted that both ∇ and ∇_n are symmetrical with respect to 1 and n , that is, 1 and n can be interchanged without changing their value. This symmetry does not

exist in ∇_0 or ∇_1 . The following relation can also be shown to obtain

$$\nabla_0 + \nabla_1 + \nabla_n = 0. \quad (3)$$

Now let V_0 , the potential of the screen, be given a certain value between V_1 and V_n , so that it can be written in the form

$$V_0 = V_1 + k(V_n - V_1), \quad (4)$$

where k is a constant.

Equations (2), (3), and (4) reduce to

$$\frac{I_1}{V_n - V_1} = \frac{\nabla_n - k \cdot \nabla_0}{\nabla}. \quad (5)$$

The left-hand side of this equation is the admittance of the apparatus with the screen at a potential $k(V_n - V_1)$ above that of the point 1, and the current measured at the point 1. This value of the admittance will only be equal to the value when the screen is at a potential $k(V_n - V_1)$ above the point n and the current measured at n , if the right-hand side of equation (5) is symmetrical with respect to 1 and n . This will only occur for either of the two conditions:

- (a) that ∇_0 be symmetrical with respect to 1 and n , or
- (b) that $k=0$, that is, $V_0 = V_1$.

The first of these conditions will only occur in special cases, while the second only means that the potential of the screen must be kept at the potential of one of the terminals. The admittance in this latter case is

$$\frac{\nabla_n}{\nabla}.$$

The effect on the admittance of measuring the current at the other terminal is equivalent to putting $k=1$ in equation (5). The admittance is then

$$\frac{\nabla_n - \nabla_0}{\nabla}.$$

This is not symmetrical with respect to 1 and n in the general case unless ∇_0 is symmetrical. There will, therefore, generally be two values for this admittance, depending on which terminal is kept at the potential of the screen.

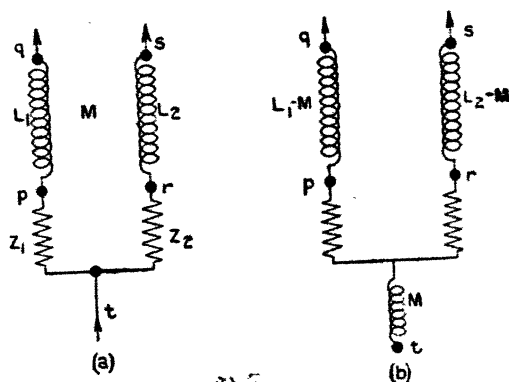
It may be noted that in the proof no restriction whatever was imposed on the nature or magnitude of the admittances, so that the result will hold even if the admittances to the

screen are not capacitative. Nor were there any limitations to the number of admittances. The existence of distributed admittances, therefore, will not invalidate the result.

Limitations.

In the proof given in the last paragraph, it has been tacitly assumed that the values of the admittances are the same whether $V_0 = V_1$ or V_n , although, admittedly, the current distribution will have altered. In other words, the potential difference between any two consecutive junction points must be proportional to the current flowing directly between those two points. It would appear, therefore, that mutual inductances within the apparatus would

Fig. 3.



invalidate the theorem. That this is so in a general case can be proved by working out a simple network. There, is, however, a condition in which the presence of mutual inductances does not affect the result, and these cases are so general that they will almost invariably be found in practice.

A mutual inductance, as in fig. 3 (a), between two coils pq and rs , which are joined at the point t through impedances Z_1 and Z_2 , can be exactly represented by the network of impedances shown in fig. 3 (b), so long as the current in Z_1 is the same as that in L_1 and the current in Z_2 is the same as that in L_2 . Such a mutual inductance, if present in an apparatus, can be replaced by its equivalent network, so that the theorem will still hold, as the assumption on which it depends is accurately correct.

In practice it often happens that the currents in Z_1 and L_1 , or Z_2 and L_2 , are not absolutely equal owing to small stray capacity effects. These will cause a deviation to the first order of small quantities. If, moreover, the mutual inductance is also small, the error will depend on the product of the capacity and the mutual inductance, and will only be of the second order.

Another effect that may invalidate the theorem is the presence of eddy currents. This is purely due to a mutual inductance between a coil and a lump of metal, and can be treated as an ordinary mutual inductance. The theorem will still be correct, therefore, if the coil is connected to the lump of metal through an impedance carrying the same current as the coil.

The final cause, owing to which the theorem will fail, is closely connected with the exact definition of potential difference. The lines of electric intensity are not solely due to the distribution of charges or current alone, but to a combination of the two. Any alteration of one which is not followed by a similar alteration in the other will affect the lines of flow of the displacement current in the dielectric, and will cause an alteration in the distribution of the capacities. In a general case, the distribution of capacities will differ with the potential of the screen. In all practical cases, however, this effect will be quite negligible, with certain exceptions, when the size of the apparatus is comparable to the wave-length.

10th July, 1928.

LXXVI. *On the Penetration of an Electric Field through Wire-gauze.* By W. B. MORTON, M.A., Queen's University, Belfast*.

IN a method which has been frequently used for the investigation of the mobilities of gaseous ions, the apparatus consists of a cylindrical vessel which is divided into two compartments by a partition of wire-gauze. Ions are generated in one compartment and are acted upon by a steady electric field which pushes them through the meshes of the gauze into the other compartment. Here they come under the influence of an alternating field. If this is strong

* Communicated by the Author.

enough, and the alternations slow enough, ions leaving the gauze will be carried to the plate which forms the other boundary of the field before they are turned back by the reversal of the electric force. The plate is connected to an electrometer; so that the current reaching it can be measured for different values of the alternating P.D. The mobility can be deduced from the value of the smallest field which can produce a current between gauze and plate.

The values arrived at by different workers vary rather widely and several suggestions have been made to account for this. Among these there is one on which special emphasis has been laid by Loeb*, namely, that a source of error is to be found in the interpenetration of the two fields through the meshes of the gauze. It is the object of the present note to examine this as a purely mathematical problem, with a view to finding an upper limit to the importance of this source of error. Any disturbance of the applied field due to the presence of the ions will be neglected and the ions will be supposed to move along the lines of force with a velocity proportional to the strength of the field at each point.

It seems obvious that the effect of the penetration of fields will be increased by each of the following three modifications of the actual experimental arrangement. These at the same time reduce the problem to a form easily tractable:

- (1) Remove one set of wires of the gauze, so transforming it to a grating.
- (2) Reduce the wires to mathematical lines.
- (3) Consider only ions which move along lines of force midway between the wires.

In this way we shall arrive at a disturbance of the theoretical result greater than that to be expected under the actual conditions. It will appear that, even after this exaggeration, the error is only a small one. We require, to begin with, the field of a freely charged grating of thin parallel wires. This is contained in Maxwell's solution of the problem of electric screening by a grating. It may also be obtained as the limit of the case of plane strips regularly spaced in their own plane. It is easy to verify that the relation

$$\sin(x + iy) = \sin \delta \cosh(\phi + i\psi),$$

where ϕ is the potential, gives the field of a series of strips in the plane $y=0$ with spacing π , the breadth of a strip

* Loeb, Journ. Franklin Inst. v. 193, p. 771 (1923).

being 2δ . The force at a great distance from the grating is unity. The straight line of force $\psi=0$, $x=\frac{\pi}{2}$ passes through the centre of a space, the magnitude of the force along it is $\sinh y/(\cosh^2 y - \sin^2 \delta)^{\frac{1}{2}}$, the line $\psi=\frac{\pi}{2}$, $x=0$ passes through the middle of a strip, magnitude of force is $\cosh y/(\sinh^2 y + \sin^2 \delta)^{\frac{1}{2}}$. Making $\delta=0$, we find that the force due to a freely charged grating of thin wires, in a plane midway between wires, varies as $\tanh y$, when the distance between wires is π , or as $\tanh(\pi y/s)$ when the spacing is s . By superposing a uniform field perpendicular to the plane of the grating, we obtain a field which has values E_1, E_2 at great distances on the negative and positive sides respectively. The expression for the force along the midway line is then

$$\frac{1}{2}(E_2 + E_1) + \frac{1}{2}(E_2 - E_1) \tanh(\pi y/s).$$

We take E_1 , on the negative side, to be the steady auxiliary field which pushes the ions through the gauze, and E_2 , on the positive side, the alternating force by which the mobility is measured. The equation of motion of an ion is got by equating dy/dt to k times the above expression, where k is the mobility.

Two methods have been adopted in practice as regards the alternating field: (1) the "square-wave" plan, in which, by means of a commutator, the force E_2 is suddenly changed from a constant value in one direction to a constant value in the opposite direction; (2) the sine-wave method, in which E_2 is given by an alternator. In the first case the equation of motion can be integrated; in the second case the variables cannot be separated, and recourse must be had to either arithmetical or geometrical methods. I have used the latter to obtain approximations which are, perhaps, close enough for the present purpose.

(1) When E_2 is constant the integral is

$$2\pi k E_1 E_2 t$$

$$= s \{ (E_2 + E_1) \eta - (E_2 - E_1) \log (E_2 e^\eta + E_1 e^{-\eta}) \} + \text{const.}$$

in which η is written for $\pi y/s$.

Suppose the force to continue at the constant value E_2 for time T in the direction which moves the ion away from the gauze. Then the distance, if the gauze introduced no

disturbance of the field, would be $kF_2T=c$, say. Put $\pi c/s=\gamma$. We want to compare with c the actual distance reached in time T by an ion which starts from the plane of the gauze, or to compare η with γ . Writing p for the ratio E_2/E_1 , we arrive at the result :

$$(p+1)\eta - (p-1)\{\log(pe^\eta + e^{-\eta}) - \log(p+1)\} = 2\gamma.$$

The disturbance vanishes when $E_1=E_2$, or $p=1$. It will be seen that the above equation then gives $\eta=\gamma$.

The equation becomes simpler when $e^{-\eta}$ can be neglected, and this is allowable in the conditions of experiment. $e^{-\eta}$ is less than $\cdot 01$ when $\eta > 4\cdot 6$, or $y > 1\cdot 5$ s. The relation now reduces to

$$\eta = \gamma - \frac{1}{2}(p-1)\{\log(p+1) - \log p\}.$$

This shows that the correction to the distance depends only on the ratio of the field-strengths on the two sides of the gauze. When p is large $(\gamma - \eta)$ approaches the limit $\frac{1}{2}$; this means that the travel of the ion is shortened, owing to the openings in the grating, by $\cdot 159$ of the spacing. As the auxiliary field is increased up to equality with the main field, the shortening of the range decreases to zero, and when $E_1 > E_2$, $p < 1$, there is an increase in the distance travelled. This increase, $(\eta - \gamma)s/\pi$, approaches infinity for $p=0$, but the approach is so slow that, even when the auxiliary field is 100 times the other, $(\eta - \gamma)$ is only $2\cdot 28$, i. e. the increase in travel of the ion is $\cdot 726$ of the spacing. If the force E_2 is now reversed in direction and maintained constant for another period T , it is obvious that the ion will not return quite to its original position at the grating, for its motion at the end of the journey will be opposed by the penetrating field. Its final position is given by the equation

$$(p+1)\log(pe^\eta - e^{-\eta}) - (p-1)\eta = 2p\log p - (p-1)\log(p+1).$$

This cannot be simplified, because it is not now permissible to neglect $e^{-\eta}$. The following values have been calculated :—

$E_2/E_1 = \cdot 01$	$y/s = \cdot 840$
$\cdot 1$	$\cdot 471$
1	$\cdot 153$
10	$\cdot 023$
∞	0

Under a continued succession of simple reversals in the field the ions would work their way across any distance. To prevent this, and to ensure that all ions which do not reach the plate are swept back to the gauze, it is usual to make the reversed force greater than the direct. The above figures show that, from the purely electrostatic point of view, a comparatively slight degree of asymmetry in the alternations would be sufficient to secure this. That other considerations must enter into the matter is shown by some results given by J. S. Rogers in a recent paper*. To get definite measurements he found it necessary to make the reverse force greater by 25 per cent., although he was working with a continuous plate instead of gauze.

With the reversed field there will be a plane of zero force near the grating which acts as an impassable barrier to the returning ions. The position of this is given by

$$y/s = -\log p/2\pi.$$

It thus lies on the positive or negative side according as p is less or greater than unity, as is otherwise obvious. Some values are given below:—

$E_2/E_1 = \cdot 01$	$y/s = \cdot 753$
$\cdot 1$	$\cdot 367$
1	0
10	$-\cdot 367$

(2) When the alternating force varies in a simple harmonic manner, $E_2 \sin 2\pi nt$ is to be put for E_2 in the equation of motion. The "undisturbed" distance travelled by an ion during the positive half-period is now $c = kE_2/\pi n$. Let p again represent E_2/E_1 and put $\pi y/s = \eta$, $\pi c/s = \gamma$, $2\pi nt = \xi$. The differential equation is then

$$(4p/\gamma) d\eta/d\xi = p \sin \xi (1 + \tanh \eta) + (1 - \tanh \eta).$$

When the auxiliary field is very weak (p large), this approaches the integrable form:

$$(4/\gamma) d\eta/d\xi = \sin \xi (1 + \tanh \eta),$$

which leads to the following equation for the value reached by η when $\xi = \pi$, beginning with $\eta = 0$ for $\xi = 0$,

$$\eta - \frac{1}{2}e^{-2\eta} = \gamma - \frac{1}{2}.$$

As before, the exponential can be neglected, so that, exactly as in the former case, the range is shortened by $s/2\pi = \cdot 159$.

* Phil. Mag. v. p. 888 (May 1928).

For the general case an approximation to the truth can be got by the method of "isoclines". The plane of $(\xi\eta)$ is covered with a family of curves, the loci of points where $d\eta/d\xi$ has a definite value and an integral curve drawn which crosses each of these at the right slope. In the account of this method given by M. d'Ocagne in his 'Calcul Graphique et Nomographie' it is pointed out that a more definite mode of approximation is obtained when the integral curve is built up of pieces of parabolas, with vertical axis, between each pair of isoclines*. He gives a construction by which, when the point on one isocline is known, the corresponding point on the next can be found. This depends on the fact that two tangents to a parabola intersect on a vertical midway between the verticals through the points of contact. A much simpler construction to the same end is provided by another parabolic property. If two tangents to a parabola make with the perpendicular to its axis angles $\tan^{-1}m_1$, $\tan^{-1}m_2$, then it is easily shown that the chord joining their points of contact makes with the same direction the angle $\tan^{-1}\frac{1}{2}(m_1+m_2)$. The desired construction can therefore be quickly carried out by drawing a succession of chords between consecutive isoclines, the tangent of the slope of the chord being the mean of the values belonging to the isoclines†.

In the present case, if we write θ for $(4p/\gamma) d\eta/d\xi$, the equation of a isocline is

$$p \sin \xi = (\theta - 1 + \tanh \eta) / (1 + \tanh \eta).$$

A definite value having been assigned to p , the above curves were drawn, each marked with its θ . This diagram could then be used for any plate-distance; the slopes on the curves being found by dividing θ by the assumed value of $4p/\gamma$.

In practice the axis of ξ was divided in degrees, and this changed the factor $4p/\gamma$ into

$$720p/\pi\gamma = 720sp/\pi^2c = 72.97ps/c.$$

To simplify the arithmetic, round numbers were taken for this magnitude, such as would give reasonable values for c/s .

It was not necessary to carry on the construction for the full range of motion. Above the level of $\eta=2.5$ to 3 the isoclines run up as vertical straight lines. Once this region is reached the further course of the integral curve is

* *Loc. cit.* p. 156.

† I owe this suggestion, and the carrying out of the work of drawing, to my brother, Mr. F. Morton.

of sine-form and the remaining distance can be calculated. The curved portions of the isoclines could therefore be drawn on a large scale, covering the region in which the disturbing effect of the openings of the grating is felt. If the sine-motion is taken to begin on isocline θ , it is easy to show that the total value of η is got by adding to the height already reached the amount

$$\left\{ 1 + \sqrt{1 - \frac{\theta^2}{4p^2}} \right\} \pi c/2s.$$

The ions which reach the greatest distance are no longer those which start at $\xi = 0$. When $E_2 > E_1$ we must take those which leave the gauze when the combined field there is zero, i. e. $\xi = -\sin^{-1}(E_1/E_2)$. For $E_2 = E_1$ this becomes $\xi = -90^\circ$, the alternating force has its greatest backward value. For $E_2 < E_1$ the greatest range continues to be attained by ions starting at this epoch. The following numerical results have been obtained :—

$$\begin{array}{ll} E_2 = E_1 & \left\{ \begin{array}{l} c/s = 14.6 \\ \quad \quad 36.5 \end{array} \right. \quad \begin{array}{l} (y-c)/s = .44 \\ \quad \quad .49 \end{array} \\ E_2 = 2E_1 & \left\{ \begin{array}{l} c/s = 14.6 \\ \quad \quad 36.5 \end{array} \right. \quad \begin{array}{l} (y-c)/s = .66 \\ \quad \quad .07 \end{array} \end{array}$$

The numbers are only rough approximations, for the method is not capable of much accuracy, but they are perhaps sufficient to show that the error is again of the order of the spacing. On the whole, therefore, it appears probable that the interpenetration of the fields is not a source of serious error in the measurements.

I am indebted to Prof. J. J. Nolan for suggesting this investigation and for references to the experimental work.

LXXVII. *Quantum Theory and the Analysis of Observations.*
By F. J. SELBY, C.B.E., M.A. *

THE aim of science is to give a simple description of our perceptions. The description must itself be in terms of perceptions; the field to be described widens as, with various aids, our perceptions are extended.

* Communicated by the Author.

In our description we employ certain conceptions, abstractions, defined more or less accurately in terms of our perceptions. Thus in physics we employ the conceptions length, time, mass, and we say that all physical quantities are measurable in terms of these three conceptions, *i. e.* in terms of certain arbitrary units of length, time, mass.

As we attempt, however, to increase the exactness of the description of our perceptions, of our observations, we find that we cannot define these conceptions with absolute precision. Our unit of length may be the distance between two marks on a bar, but the mark is not a Euclidean line and has indefinite boundaries. We may employ a wavelength of light as our unit, but, as we shall see, this again cannot be precisely defined as an object of perception. Time, likewise, is not susceptible of exact definition as a physical quantity. Mass presents similar difficulties; its very definition, indeed, has always proved somewhat intractable, though the accuracy with which mass can be measured, in terms of an arbitrary unit, is not less high than the accuracy of measurement of time and space.

Einstein has suggested that our observations are mainly of coincidences in time and place. A complete observation of any physical phenomenon involves, however, all the three quantities above mentioned. I will direct attention especially to observations involving, directly or indirectly, the use of the eye; but the statement is true of all observations, with the aid of whatever sense they are made.

In the observation of any natural phenomenon, any "event," we are accustomed to differentiate between three things: the entity, external to ourselves, which is the object of our observations; the means, mechanism, sense organ, by which the observation is made; and the subjective self, mind, consciousness, which receives and records the observation. There is no observation in which these three are not involved; there is no perception in which the relative contributions of the three can be entirely separated. They form a trinity in unity: three incomprehensibles and yet one incomprehensible.

My main aim is to consider the methods of analysis of the more delicate observations of modern physics, in which electrons and protons, waves and radiation are involved. In all such observations the eye, as sense-organ, is directly or indirectly concerned. We may employ intermediate mechanisms, photographic plates, thermopiles, photo-electric cells, electrometers as energy receivers and recorders; but

in our interpretation of intensities, in our energy measurements, we base ourselves on comparisons in which the eye is the ultimate judge. It would be easy to conceive an analysis based on a definition of mass derived, say, from the sense of touch; this would not affect the principles I wish to educe or the main features of my argument.

In these refined observations, where we are reaching the limits of perception, we find that it is no longer possible to maintain the differentiation between the three aspects of our trinity. There is interaction between the observed phenomenon and the observing mechanism; the perception is further conditioned by the limitations which restrict the response of mind and consciousness. Some partial discrimination between subjective and objective may still be possible; complete separation of the three components of the trinity will probably remain for ever beyond human capacity, though we are continually extending our means of observation, and there is no need to be dogmatic. We have enlarged the world of our perceptions, but they still set the boundaries to knowledge.

Let us examine now a simple case of observation to which the foregoing ideas are applicable. I will take the example, of much interest of late years in relation to the quantum theory, of the hydrogen spectrum. We will suppose the radiation from glowing hydrogen gas to be refracted by a prism, the resulting spectrum being observed by the eye. Using the ideas of modern wave mechanics, the energy from the glowing hydrogen, after passing through a narrow slit, is conveyed in wave-groups to the prism; it does not "pass through" the prism, but is dispersed by it, and after both surface and internal losses, due to the prism, travels on in a number of divergent wave-groups to the eye. Let us suppose the eye to be receiving from one selected direction a single sequence of these wave-groups. The energy transferred to the retina—no doubt by resonance, since the loss of energy is small—is seen as a spectrum "line," so called, actually a spectrum band of small width and of a definite brightness. I have, of course, not followed the whole course of events in detail: I have selected the changes on which I wish for the moment to concentrate attention. The theories of Planck and Bohr tell us that these changes are not continuous in character: they take place by discrete amounts, quanta; they are finite changes, brought about by resonance, from one stationary state to another. The transfer of the energy to the retina is one of these changes and

of the same nature as the rest : it takes place by quanta. But let us examine the phenomenon from the receiving end ; consider its aspect from the point of view of the eye and the conscious mind behind it. It would be in accord with our general experience to suppose that there is a *minimum sensible*, a minimum disturbance below which no effect is produced on the consciousness ; a minimum change, also, which is perceptible, which may (or may not) be of identical amount. The eye receives a succession of wave-groups associated with a certain frequency, the group or beat frequency : it responds by resonance, after a very brief interval : the natural measure of the response is therefore of dimensions energy \times time, *i. e.* of action. Let us suppose that there is a certain minimum of response, the quantum of action, which is perceptible by the eye and the mind behind it. We can now trace back our phenomenon to its objective end, but we must retain our quantum of action as an indivisible unit. We realize at once the reason for the appearance of the quantum in all visual phenomena ; it is inherent in ourselves. Planck's constant h , Bohr's quantum of action, cannot but be identical with it*, since any transfer of energy to the eye as a receiving mechanism will be governed by the usual quantum laws. Indeed, it is difficult to suppose that there could be two independent quanta involved in phenomena.

Let us continue our analysis. Reception by the eye of the light from the single hydrogen "line" is associated with a definite frequency, the group or beat frequency. The eye is comparable with a heterodyne receiver, capable of responding over a certain range of frequencies ; the range is no doubt different for different eyes, as the range of audibility is different for different ears. The group frequency is related to the wave frequency by the Rayleigh formula. If we denote the energy received in the usual manner by $\int I d\lambda$, we realize that the wave-length is a conception, an abstraction, merely ; it is one of the boundaries of an integral field. But it is clear that we can think in terms of the ordinary wave theory ; and the conclusions reached with the aid of that theory hold good. We note, in passing, that the wave-group has no definite boundaries : it dies away rapidly from a maximum, but may be supposed to extend to infinity in either direction : a succession of

* We can conceive that the *minimum sensible* may be a submultiple of h , but there would appear to be no means of perceiving such a distinction.

wave-groups is a succession of maxima, of singularities, in a wave-field.

In considering next the dispersion of the hydrogen light by the prism, we can adopt the usual wave theory ; but we must bear in mind in our analysis that we are dealing with indivisible quanta of action, and frame our conceptions accordingly. The transfers of energy which take place again occur by resonance.

Tracing our phenomenon further back to the radiating atom, we have the option of treating it by the methods of particle mechanics, or by the new methods of wave mechanics. We must, however, recognize that our particle is comparable with the wave-group, the singularity in a wave-field, and has no definite boundaries. Newton's corpuscular theory of light and the wave theory combine to form a more comprehensive whole.

Let us return to the ideas with which we started. To describe our perception of an event, we make use of three conceptions—length, time, and mass ; or we may say length, time, and action. There is a natural, indivisible, unit of action, the quantum. Expressed in terms of mass, the dimensions of this quantum are MV^2T or MVL , where V is velocity, of dimensions L/T . If, now, we choose arbitrary units of mass and length, say the mass of the electron and the wave-length of the red cadmium line, there is a corresponding definite value of V which is not infinite ; we must not suppose V to become infinite without at the same time supposing M or L to become infinitely small. We are, in fact, dealing with a "complementarity," to use Bohr's term with a somewhat different significance, a trinity in unity, and we must adjust our conceptions accordingly. We thus reach what we may call an extended theory of relativity, which includes quantum theory, in which length, time, and mass are inter-related and the quantum of action is an invariant.

Let us now suppose that in the observation of any phenomenon we wish to follow the changes of some quantity Φ . Our quantum, wave-group, electron or proton is capable of motion in three directions and of rotation about three axes in space. Let its position or configuration at any instant be determined by the variables $x, y, z, \theta, \phi, \psi$. Other variables involved are t and $n\hbar$, where n , however, must be an integer, \hbar being Planck's constant, the quantum of action. Our quantity Φ is a function of these variables :

$$\Phi(x, y, z, \theta, \phi, \psi, t, n\hbar).$$

Experience indicates that, as a first approximation in considering the changes of Φ , we can neglect differential coefficients of higher order than the second. The changes will thus be given by a differential equation of the form

$$f'' \frac{\partial^2 \Phi}{\partial \xi_r \partial \xi_r} + f_r \frac{\partial \Phi}{\partial \xi_r} + f_0 = 0,$$

where ξ denotes any one of the variables and the f 's are functions of any or all of the variables*. Our procedure is to try to fit solutions of this equation to the phenomena, remembering that n can only change by integral steps.

Various methods of obtaining solutions of this equation in particular cases have been devised by Bohr, Heisenberg, Schrödinger, de Broglie, Dirac, and others, and remain applicable without modification with the conceptions introduced above. It is very instructive to realize how the experimenter, by inductive reasoning, has been led to introduce into his conceptions, in order to explain observed phenomena, the "subjective" unit, the quantum, which was unavoidably involved in the limitations of his powers of perception.

I do not propose to follow my subject further in the present note. Much no doubt remains to be done in the devising of rapid methods of calculation applicable in the analysis of observations of the kind to which attention has been devoted, but already good progress has been made. It is hoped that the foregoing may assist the physicist who has not acquired the mathematical technique to grasp at least the *rationale* of the procedure which is being followed. He will find much further information in Bohr's article published in 'Nature' on April 14th, to which this note may be regarded as a corollary.

I have been concerned with microscopic or, I might say, sub-microscopic phenomena. In dealing with macroscopic or statistical phenomena we can employ the usual procedure; it is only at the surfaces of bodies, or at the boundaries of our field, that we may need to resort to the more complicated technique of the new methods.

* Repetition of suffixes implies summation, as in relativity notation.

LXXVIII. *The Continuous Spectrum of Hydrogen.* By F. H. NEWMAN, D.Sc., F.Inst.P., Professor of Physics, University College of the South-West of England, Exeter*.

[Plate XIII.]

1. Introduction.

THE origin and exact character of the continuous spectrum of hydrogen, which has been investigated by many observers, still remains uncertain. In some cases this type of spectrum possesses the peculiar characteristic of occurring without the presence of either atomic or molecular lines, and an explanation of this fact has been advanced by Kaplan†, who suggests that when the hydrogen molecule in the first electronic state possesses more than 0.50 volt vibrational energy, it may split into two atoms with emission of energy as radiation, the value 0.50 volt being derived from the observed short wave-length limit of this continuous spectrum. The absence of observed lines is due to the fact that transitions from the initial excited state of the molecule to lower ones give rise to lines lying far down in the ultra-violet region.

This spectrum, which is quite distinct from that one which begins at the limit of the Balmer series and continues towards the shorter wave-lengths, appears in celestial spectra in the absence of the Balmer lines and the secondary spectrum, and its limit on the red side is always at wave-lengths greater than $\lambda 3646$; for example, as an absorption spectrum it begins in α Cygni at $\lambda 3710$, having a maximum intensity at $\lambda 3660$, approximately, and in Vega it commences at $\lambda 3800$, its maximum being at about $\lambda 3710$.

Crew and Hulburt‡ found this type of spectrum to be of similar character, although of differing intensity, in a number of sources, including a long hydrogen tube constructed after the manner of Wood with the light coming end-on through a quartz window from the central portion only, an ordinary discharge-tube, the separate striations of the positive column, the condensed spark in hydrogen at pressures above atmospheric, and in the water spark. In all cases it was of appreciable intensity near $H\alpha$, rising slowly to a maximum in the rear ultra-violet, and descending slowly in intensity from $\lambda 3000$ to $\lambda 2200$.

* Communicated by the Author.

† Nat. Acad. Sci. Proc. xiii. p. 760 (1927).

‡ Phys. Rev. xxviii. p. 936 (1926).

Adopting Bohr's theory, a continuous spectrum extending into the ultra-violet should begin at the limit of the Balmer series, λ 3646, and it may be noted that Herzberg*, using the electrodeless ring discharge in hydrogen, has obtained this type of spectrum, the intensity variation in the continuum being continuous with that in the Balmer series. The wave-number at the beginning of this spectrum corresponds to the energy set free in the fall of an electron from rest at infinity into the second orbit. If such an electron possesses additional energy of its own, it gives up more energy when it is bound than one at rest, and this energy appears as radiation of wave-length less than that corresponding to the Balmer series limit. Since the initial kinetic energy of the electrons, external to the atom, varies from one electron to another, it is evident that the resulting radiations constitute the continuous spectrum beginning at the limit of the Balmer series and extending towards the ultra-violet. This theory is based on the assumption that the atomic orbits extend to infinity; but originally it was supposed that the size of the orbit system is restricted by the density of the radiating gas, and from this Wright† has inferred that it is necessary to substitute for the orbit at infinity the largest orbit in effective operation. Into this orbit, therefore, will enter electrons of all energies from zero upward. An electron thus entering the effective orbit and having zero initial kinetic energy will, on transfer to the second orbit, give rise to radiation of wave-length which forms the limit of the continuous spectrum on the red side; and it is to be expected, therefore, that the continuous spectrum would begin somewhere on the less refrangible side of the last visible line in the Balmer series, and that there should be an overlapping of this series and the continuous spectrum. As Nicholson‡ has pointed out, however, numerous experiments now show that the number of lines in the Balmer series available for observation is not determined necessarily by the density of the gas; and he cites his experiments made in conjunction with Merton§, in which they observed fourteen sharp lines of the series in a tube filled mainly with helium at 42 mm. of mercury pressure, such that the radius of the hydrogen atom emitting the last member on this Bohr theory was twice the average distance apart of the atoms. Wood's experiments with long

* *Phys. Zeits.* xxviii. p. 727 (1927).

† *Nature*, cix. p. 810 (1922).

‡ *Roy. Astron. Soc. Monthly Notices*, lxxv. p. 253 (1925).

§ *Proc. Roy. Soc. A*, xvi. p. 116 (1919).

discharge-tubes also preclude any correspondence between the number of lines visible and the density of the gas.

Nicholson supposed that this spectrum arises from the actual binding of stray electrons by the atoms, the electron having any kinetic energy in excess of that required for its motion in the path of the atom which it enters, the excess being emitted as radiation, so that the wave-numbers of the resulting radiation will form a continuous set, giving rise to a continuous spectrum. If the law of the distribution of velocity among these electrons which are thus captured is that deducible from the kinetic theory, the law of intensity throughout this continuous spectrum can be calculated and compared with that found experimentally. Crew and Hulburt* calculated this energy distribution by statistical methods, and found that the relative intensity involves an unknown probability, a_n , that the atom exists through the n th orbit, the region beyond being unquantized. When a_n is evaluated, approximately, from general physical considerations, the formula agrees qualitatively with the relative intensity throughout the spectrum obtained from the hydrogen stars and laboratory sources.

2. Experimental.

The author has found another method by which this continuous spectrum may be produced at very low pressures, viz. by means of the electric arc passed between cold electrodes in a rarefied hydrogen atmosphere. An intermittent electrical discharge is passed between two iron electrodes in a discharge-tube, and between one of these electrodes and a third one a potential difference of 200 volts is applied continuously. The tube contains hydrogen at a pressure of 10^{-3} mm. of mercury, and on passing the electrical discharge an arc through the gas may be produced. The resulting radiation shows no trace of iron lines, provided that the arc is allowed to continue for a few seconds only, otherwise owing to the heavy current through the gas, which may amount to 10 or more amperes, the electrodes quickly reach a sufficiently high temperature to emit the ordinary iron arc lines. The radiation emitted, which is pale blue or whitish in colour, has been examined and photographed through a quartz window by means of a quartz spectrograph. It has been found that the resulting spectrum varies according to the condition of the gas; but in all cases, and in spite of the low pressure, only a few of the Balmer lines actually

* *Loc. cit.*

appeared, those of wave-length shorter than H_β not being visible on the photographic plates.

If the hydrogen was not dried, the water bands, particularly those at $\lambda 3064$ and $\lambda 2811$, were prominent together with a few Balmer lines, but there was no continuous spectrum. On the other hand, when the gas was dry the water bands were absent and the continuous spectrum became very marked, being accompanied by the secondary hydrogen lines. It was difficult to estimate with any degree of exactness the limit of this continuous spectrum on the red side; but the average value of this limit, taken from numerous spectrograms of various exposures, gave the value $\lambda 4690$, approximately, the last line of the Balmer series which could be detected on the plates being H_δ , $\lambda 4102$. Thus, if ν_1, ν_2, ν_3 represent the wave-numbers of the limit of the continuous spectrum on the red side, the limit of the Balmer series and the last detectable line of this series, respectively,

$$\nu_3 - \nu_1 = \nu_2 - \nu_3,$$

$$\text{or} \quad 24373 - 21320 = 27420 - 24373,$$

$$3053 = 3047.$$

Although these numbers are only approximate, the result suggests that the margin of overlap of this continuous spectrum and the last observed Balmer line is equal to the interval between this line and the theoretical limit of the series. This supports Wright's view of the phenomenon; but it must be remembered that on the whole comparatively few electrons of approximately zero velocity are to be expected on the kinetic theory, and as these determine the limit at the red end of the spectrum, this limit will necessarily be ill-defined.

An interesting feature of the spectrograms is the effect of water-vapour on the appearance of this continuous spectrum. If the water bands are prominent the continuous spectrum is absent, as shown at I. (Pl. XIII.), whereas it becomes more and more intense as the bands disappear (II., Pl. XIII.).

The continuous spectrum may not arise from the interaction of an electron with the nucleus of a free atom: the atom may be influenced directly by other atoms or ions; for example, it may arise from the molecules, and Herzberg* suggests that the experimental conditions of excitation accord best with the view that the breaking-up of molecular ions H_2^+ is the cause.

The present experiments show that association of water molecules with the hydrogen atoms and molecules opposes the continuous spectrum excitation, and suggests that it is associated with the atoms, and certainly not with molecular aggregates. It must be noted, however, that this does not necessarily mean that the hydrogen molecules are ineffective in the emission. The restricted outer orbits may be part of a molecule.

In connexion with this type of spectrum, there is the case of iodine in which an emission spectrum has been photographed by Steubing* and which appears as a continuous band, even at the highest resolution. Franck† has explained this from the electro-negative behaviour of the iodine atom with its tendency to perfect itself into an eight-shell by taking up an external electron, but in this case the iodine atom need not be ionized to attract the foreign electron; the electron affinity suffices to effect the assimilation of the foreign electron, even in the case of the neutral iodine atom. In this phenomenon the continuous character of the spectrum also corresponds to the continuous distribution of the initial kinetic energy of the assimilated electron.

LXXIX. *The Electric Arc in Gases at Low Pressures.* By
F. H. NEWMAN, D.Sc., F.Inst.P., Professor of Physics,
University College of the South-West of England, Exeter‡

1. Introduction.

A NEW type of electric arc in high vacua has been described by the author§ in which with cold electrodes an arc could be started and maintained in various gases at very low pressures, provided that an initial electrical discharge was passed between one of the "arc" electrodes and a third electrode placed within the discharge-tube. There were two separate effects: first the ordinary arc in which the current reached 10–15 amperes, and secondly a brilliant glow discharge during which a very small current passed through the tube. Both of these effects could be excited at such low gas-pressures that there was practically

* *Zeits. f. Phys.* v. p. 428 (1921).

† *Ann. d. Phys.* lxi. p. 693 (1921).

‡ Communicated by the Author.

§ *Phil. Mag.* ii. p. 796 (1926).

no luminosity due to the electrical discharge. Later, Ratner * observed a very similar arc carrying many amperes which could be maintained in a vacuum as high as 10^{-3} mm. of mercury. For example, he found that at 10^{-3} mm. pressure a potential difference of 60 volts was sufficient to start the arc, at 5×10^{-2} mm. 120 volts was necessary, while at 1 mm. pressure a potential difference of 230 volts was not sufficient. It is evident, however, that the requisite voltage not only depends upon the gas-pressure, but also upon the distance between the electrodes. The latter may be of any metal, and the arc shows the usual current voltage characteristics. In some respects it is unilateral in that the polarity of the arc must bear some relationship to the polarity of the auxiliary electrical discharge, the arc only passing if the electric fields are in the same direction. Ratner has also found a similar unilateral relationship, although he noted, in addition, that the arc strikes independently of the direction of the field between the two "arc" electrodes when the third electrode, which is concerned solely with the electrical discharge, is the anode.

The formation of such an arc, passing practically unlimited currents, is interesting and surprising because the very low pressure in the tube made it almost impossible for the discharge to pass, and there was no sign of luminosity, the tube walls fluorescing under the cathode ray action. Occasionally a brilliant white glow was formed between the "arc" electrodes, but it was a momentary effect, existing prior to the starting of the arc proper. During this glow the electrodes remained cold, the actual current passing being but a small fraction of an ampere.

These effects indicate that the mechanism of the arc is entirely different from that of the ordinary electrical discharge, and further investigations on the actual conditions necessary for this arc to be started have been made.

2. Experiments.

The actual apparatus used was similar to that described in the previous paper, and although the effects can be produced with any type of metallic electrodes, iron rods were employed in all the experiments, chiefly because thick rods of this metal were available. With such heavy currents as were passing, these electrodes became very hot after the current had been flowing for a short time-interval, and finally it was found necessary to water-cool the electrodes to prevent the

* 'Nature,' cxx. p. 548 (1927).

wax, by means of which they were sealed into the discharge-tube, from softening. Another difficulty, due to the intense heat generated, was the liberation of gas from the walls of the vessel and from the electrodes with resultant increase of pressure within the vessel. To overcome this a large reservoir was sealed to the tube so that this gas emitted did not materially change the pressure in the apparatus while the arc was passing.

When the arc was first started the radiation emitted was entirely that from the gas molecules within the vessel, but the electrodes rapidly became red-hot and the characteristic radiation from the iron quickly made its appearance, the electrodes then becoming incandescent. As a rule, however, the arc was allowed to persist only for a short interval, as, once started, it is easily maintained, and it is the actual process of striking that is interesting and worthy of study. In passing, it may be noted that this method is very convenient and useful for starting and maintaining an iron arc in a very high vacuum, if it is desired to study the iron lines *in vacuo*.

The lowest applied potential difference with which it was possible to strike the arc was 108 volts, but it started most consistently at 200 volts, and the current which could be passed varied from 0.4 ampere upwards. Below this limiting value it was impossible to maintain the arc. Another factor which greatly influenced the process of starting was the type of electrical discharge employed. If the latter was feeble it was ineffective. A momentary discharge produced by temporarily switching in the induction coil commutator proved to be the best means of starting the arc. Thus a very high potential difference from the coil is necessary, and the most consistent results were obtained when the secondary discharge was unidirectional. The arc would not strike at pressures above 10 mm. of mercury, and worked better at lower pressures, particularly those within the range 10^{-2} – 10^{-3} mm.

In order that the arc may occur, the gas present must be ionized, and for this energy is required. This comes from electrified bodies which have acquired high velocities under the electric force from the transient electrical discharges, the initiation of the latter being due to stray electrons or electrified atoms, particularly to stray electrons. Before these electrons can ionize the gas, a time must elapse which is large in comparison with the time-interval between one collision of the electron with a molecule of the gas and the next, since before the electron can ionize it must obtain from the electric

field energy greater than the ionizing potential of the gas, and this energy must be conveyed to an electron in a molecule before an electron can be liberated. Thus there is produced a fairly copious supply of electrons which, under the further influence of the field due to the applied potential difference, form more ions by collisions, provided that the mean free path of the electrons is so large that they attain energy equivalent to the ionizing potential of the gas through which the electric arc passes. It seems, therefore, that the function of the electrical discharge is to provide those electrons which are ordinarily supplied by the incandescent electrode of the ordinary arc, or by the incandescent filament of a low-voltage arc.

In connexion with the initial ionization in a gas, Sir J. J. Thomson* has given an account of experiments on the radiations inside a closed vessel containing gas at a low pressure through which an electrical discharge is passed. These experiments indicate that the passage of the electrons through gases gives rise to Röntgen rays which may be of far higher frequency than any of the characteristic radiation of the gas. For example, he finds that, when electrons formed by a potential difference of 1500 volts are sent through hydrogen, Röntgen radiations having a frequency corresponding to 1500 volts were detected. The type of radiation at constant pressure depends upon the means used to send the discharge through the tube; for example, it depends upon the nature of the interrupter and its working. This is to be expected, as the potential difference between the electrodes often depends upon the nature of the discharge.

In addition, some of the radiation within the discharge-tube is of an exceedingly absorbable type, so absorbable that it is practically stopped by the equivalent in mass of a layer of air a few millimetres thick at atmospheric pressure. He supposes that this soft radiation produces the ionization in the negative glow.

At the lower gas-pressures the electrons, owing to their greater mean free path, have large amounts of energy, and they give radiations over a larger range of frequency than those with smaller amounts, although the density of the energy is not so great. At each collision the fast electrons may not produce much more radiant energy than the slow ones, but they are able to make many collisions with atoms and molecules before their energy is so

* *Phil. Mag.* xlix. p. 761 (1925).

much reduced that they are unable to generate Röntgen radiation. Hence the total amount of radiant energy produced by a fast electron will be much greater than that formed by a slow one, with the resultant increased ionizing effects. Thus we should expect a greater concentration of the electrons at the lower pressures; and this explains why the arc in the present experiments can be started more easily and consistently as the pressure is reduced. As Thomson * has shown, the radiation from the cathode rays is a mixture of soft radiation with quanta represented by a few volts, together with much harder radiation whose quanta may be comparable with a hundred volts. In addition there is the softer type of radiation produced by the positive rays. Seeliger † has shown that the total number of ions produced by a positive ray does not vary much either with the speed of the ray or with the gas-pressure; and this suggests that the ionization is due, not to the energy of translation of the particle, but to energy internal to it, such as might be represented by supposing the particle to contain a limited number of undischarged radiation quanta. These excite the ionization. The experiments made by Thomson ‡ on the electrodeless ring discharge show the existence of such radiations of wave-lengths shorter than those of visible light.

3. *The Effects of Foreign Bodies on the Arc.*

After the arc electrodes had been used for some time, it was impossible to start the arc, and on examining the electrodes they were found to be coated with a film of oxide arising from the decomposition of carbon-monoxide and carbon-dioxide gases, which are very difficult to remove from the vessel. If the electrodes were withdrawn and scraped, the arc could be produced as before. On the other hand, it was found that when patches of fused salts, such as potash, soda, sodium chloride, and calcium carbonate, were placed at the ends of the electrodes, the arc would strike more readily and consistently, this effect being, in fact, the reverse to that produced by the film of oxide on the metal. In addition, it was noted that usually a brilliant spot appeared on the cathode, even in the absence of any fused salt, and that this spot continuously changed its position, as it does in the mercury arc.

The effect of the fused salts can be explained by an

* *Phil. Mag.* ii. p. 674 (1926).

† *Phys. Zeits.* xii. p. 839 (1912).

‡ *Loc. cit.*

abnormal local heating, brought about by the bombardment with the positive ions. The salt, or a small part of it, is raised to incandescence, with the result that it emits a copious supply of electrons; and we have, therefore, a thermionic source similar to that of an incandescent cathode, only on a small scale. As a result the starting of the arc is facilitated. As opposed to this effect, the oxide film prevents these positive ions from bombarding the cathode, and, accordingly, there is no local heating-effect at the small particles of impurities, which exist even in the purest of iron. Thus the arc cannot be started.

These experiments seem to prove conclusively that this phenomenon of the cold electrode arc is due mainly to the localized heating-effect at these foreign particles which gives a copious supply of electrons from such local sources. Anything that shortens the life of the electron will increase the difficulty of getting the arc, but anything that reduces the number of collisions, required by one electron to detach another from a molecule, will facilitate the arc starting. It has been found that a thin deposit of sulphur is formed on the walls of the discharge-tube after the experiments have been continued for some time, this sulphur coming from the iron electrodes. Now, sulphur is very strongly electronegative, and, presumably, a sulphur molecule would be likely to capture an electron in collision, so that, although the vapour-pressure of sulphur is exceedingly low, the presence of this element would diminish the life of the electrons. The various gases present in the tube, such as nitrogen, hydrogen, etc., combine with the sulphur, and if these products, like sulphur, possess the power of capturing electrons, then the ionization in the tube is decreased, and this precludes the starting of the arc. On the other hand, complexes formed by aggregation, such as are produced by traces of moisture, facilitate the production of the arc. This may be explained by the electron detaching an electron more easily from one of these aggregates than from a single molecule. The moisture appears to act as a catalyst for the arc as it does in many cases of chemical combination. The existence of these aggregates is suggested by some experiments of Thomson*. The ordinary electrical discharge through gases produces also other modifications of the gases which only persist for a short time. In some cases, for example, with nitrogen and oxygen the existence of these modified forms is shown by the visible after-glows. We also

* Phil. Mag. iv. p. 1128 (1927).

know that the discharge and the arc can be maintained with lower applied potential differences than those required to start them, and this fact can be explained by the discharge and arc producing systems which are more easily ionized than the normal molecules.

It is evident, therefore, that in the present experiments the initial electrical discharge gives rise to two effects which facilitate the starting of the arc. In the first place it produces intense local heating of impurities lying on the surface of the cathode with resulting thermionic emission, and in the second place modifications of the gas arise, these modifications being more easily ionized than the gas in the normal state.

LXXX. *The Motions of Electrons in Ethylene.* By J. BANNON, *B.Sc.*, and H. L. BROSE, *M.A., D.Phil., F.Inst.P.* *.

IN an address given by Professor Townsend at the centenary celebration of the Franklin Institute in Philadelphia, September 1924, the type of instrument used in the present research has been fully described. The instrument affords a ready and accurate means of determining the velocity W in the direction of the electric force, and the velocity of agitation U of electrons in gases. It has been found that in nitrogen, hydrogen, and oxygen†, amongst other gases, these velocities depend only on the ratio of the electric force Z to the gas pressure p . A similar result has been obtained for ethylene, especially for values of Z/p greater than 5. Exceptionally tedious was the work on this gas, which appeared to alter as a result of making observations. This alteration manifested itself solely as an increase both in W and U .

In Table I. the values of Z and p , with the corresponding values of k and W , are given, where k represents the ratio of the mean kinetic energy of agitation of an electron to the mean kinetic energy of a molecule of a gas at 15°C . The numbers given are the means of several experiments, which are in good agreement. For values of Z/p , equal to

* Communicated by Prof. J. S. Townsend, F.R.S.

† J. S. Townsend & V. A. Bailey, *Phil. Mag.* xlii. p. 875 (Dec. 1921); H. L. Brose, *Phil. Mag.* i. p. 543 (1925).

and less than 5, the values of k increase appreciably as the pressure is reduced. This indicates the presence of some ions at the higher pressures, for, within any particular region of relative velocities of electrons and molecules, the number of ions formed is a function of the number of collisions. A direct method of testing for ions, used by Townsend and Bailey, is to apply a horizontal magnetic field of intensity about ten times that necessary for the determination of W . In the case of ethylene, for Z/p equal to 1.26, such a field sufficed to deflect about 90 per cent. of

TABLE I.

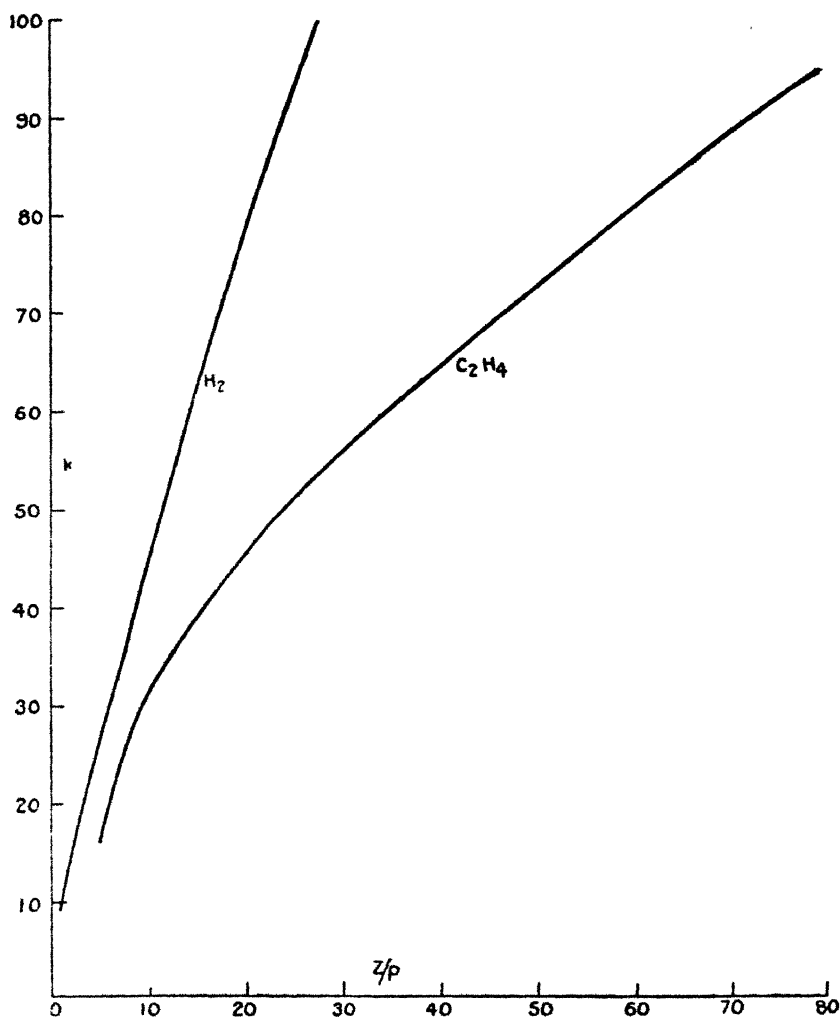
Z/p .	Z , volts per cm.	p , mm.	k .	$W \times 10^{-5}$, cm. per sec.
1.26	4.88	3.87	2.07	23.3
2.47	9.52	3.86	4.51	39.5
2.53	4.90	1.94	5.70	38.8
5.03	19.56	3.89	13.5	50.5
4.95	9.65	1.94	15.4	53.3
5.00	4.85	.97	16.25	55.2
10.1	38.8	3.86	28.7	58.5
10.2	18.9	1.85	30.1	59.8
10.1	9.7	.96	32.5	62.2
20.2	39.1	1.93	43.8	64.8
20.1	19.3	.96	45.9	68.3
20.1	9.55	.475	45.5	67.8
40.3	38.7	.96	64.5	89.2
40.0	19.0	.475	63.4	87.8
49.9	23.7	.475	71.8	103.3
80.0	38.0	.475	95.0	144.5

the electric charge on to one of the outer electrodes, and at least 98 per cent. for Z/p equal to 80. Hence, even for the lowest ratio of electric force to pressure the current was due almost entirely to free electrons. The magnetic field acts as an analyser, separating the comparatively slowly-moving, massive ions, which suffer little deflexion, from the small rapidly-moving electrons. As ions were beginning to make themselves evident, and as k was approaching unity, measurements were not made below the value 1.26 for Z/p .

The curves given in figs. 1 and 2 represent the values of k and W for various values of Z/p . For the sake of com-

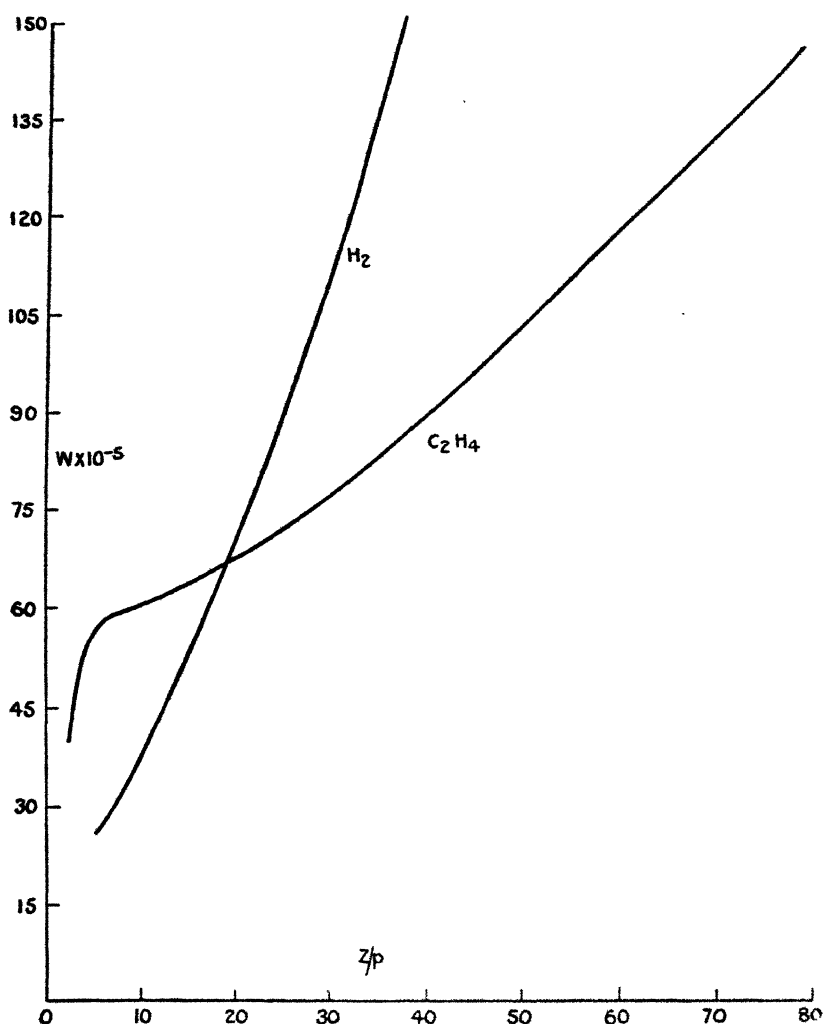
parison the curves for hydrogen and oxygen are inserted. The values of k and W , as read from the ethylene curves, for the various values of Z/p are given in the first three

Fig. 1.



columns of Table II. In the other three columns are given the values of U , the root mean square velocity of agitation of an electron, L , the mean free path of an electron in the gas at 1 mm. pressure, and λ , the fraction of the mean kinetic

Fig. 2.



energy of an electron lost in a collision with a gas molecule.
 U , L , and λ are calculated from the formulæ

$$U = 1.15 \times 10^7 \sqrt{k},$$

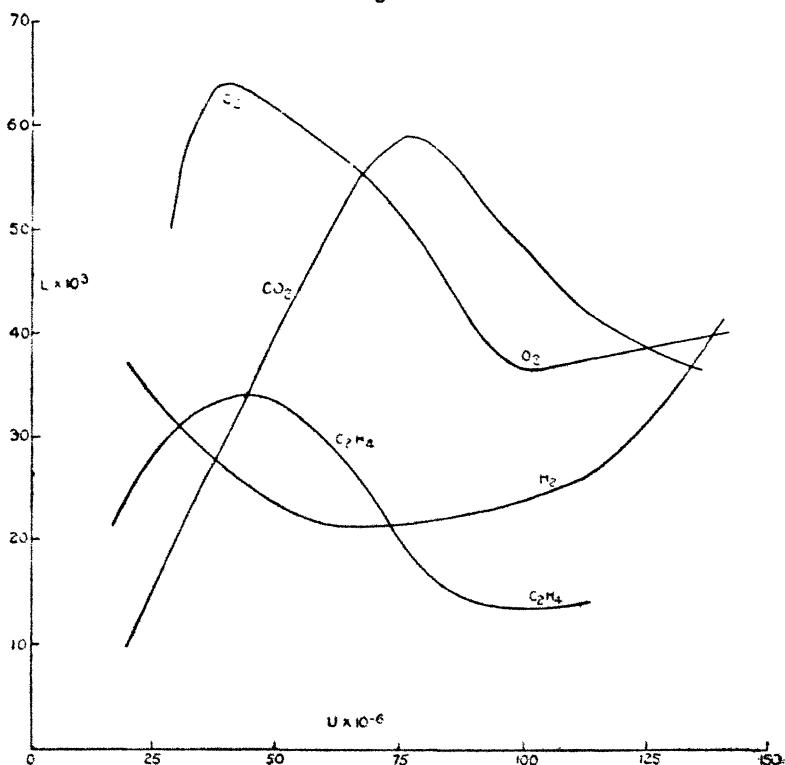
$$W = .815 \frac{Z}{p} \times \frac{e}{m} \times \frac{L}{U},$$

$$\lambda = 2.46 \frac{W^2}{U^2}.$$

TABLE II.

$Z/p.$	$k.$	$W \times 10^{-6}.$ cm./sec.	$U \times 10^{-6}.$ cm./sec.	$L \times 10^3.$ cm.	$\lambda \times 10^4.$
1.26	2.07	23.3	16.6	2.14	488
2.5	5.3	39.3	26.5	2.92	541
4	11.0	49.6	38.1	3.28	416
5	15.0	54.0	45.3	3.42	348
6	19.3	56.0	50.5	3.30	303
10	31.3	60.3	64.3	2.71	217
20	45.3	67.6	77.4	1.83	187
40	64.4	88.7	92.3	1.43	227
60	80.2	116	102	1.38	319
80	95.0	145	112	1.42	408

Fig. 3.



For ethylene, the variation of L with U is shown very strikingly in fig. 3. This curve, like the curves of oxygen and carbon dioxide, has a very definite maximum, with a less definite minimum.

From the sixth column of Table II. it is seen that the percentage energy lost by an electron in collision varies for the most part between 2 and 5. The minimum fraction of energy is lost by the electron when its agitational velocity is in the region of 77×10^6 cm. per sec., which is equivalent to the volt-velocity 1.7.

The acquisition of new properties by the gas, either as the result of exposure to ultra-violet light or of collisions with electrons (with or without an electric field), was the outstanding difficulty which presented itself. The extent of the change is indicated by data given in Table III. The results are set down in the order in which observations

TABLE III.

Sample.	Date.	Z/p.	p.	k.	W $\times 10^{-5}$. cm./sec.
(a).....	23rd May, 1927	5	.97	16.3	54.8
		40	.97	64.75	89.5
		5.1	.955	19.4	
	24th May, 1927	5.1	.95	20.2	59.1
		40.3	.95	68.9	91.0
	25th May, 1927	5.2	.94	23.3	62.0
		40.0	.936	71.0	98.2
(b)	30th May, 1927	20.3	1.88	44.4	64.1
		2.6	1.88	12.25	40.0
(c)	7th April, 1928	10.2	.95	34.2	
		5.1	.95	23.5	
(d)	9th March, 1928	10.0	1.06	34.8	
		5.1	1.06	23.4	

were made. For sample (a) the first two measurements of k for the ratios Z/p equal to 5 and 40 respectively are quite in keeping with those shown in Table I. The third, which followed immediately, shows a large increase of k for a Z/p equal to 5.1. Further increases in the values of k are recorded on the following day, and on the third day k has reached the value 23.3 for the ratio 5.2 and 71 for the ratio 40. A steady increase in the values of W is also noticeable. For sample (b) the first reading gives a value of k for Z/p equal to 20.3 in accordance with Table I. The reading for the ratio 2.6, however, is more than double that to be expected. The four readings for sample (b) were taken within the same hour. Similar remarks apply to (c) and (d) as to (b).

For the purpose of obtaining trustworthy results for ethylene, it was necessary to renew the gas in the instrument

about every three hours, and to make observations from the lowest value of Z/p upwards. To check the accuracy of values obtained in this way the following method of procedure was adopted. The instrument was thoroughly exhausted and, say, 4 mm. of gas were admitted. Readings for k and W were rapidly taken for Z/p equal to 1.26, the instrument was again exhausted, and fresh gas admitted at 4 mm. pressure. This time the ratio was made 2.5. Under similar conditions readings for all other ratios were obtained.

A second difficulty arose from contamination of the reflector used in focussing the ultra-violet light on the copper target. It was necessary to clean it about once every three days, when using the instrument at the rate of six hours a day. That ethylene was responsible there can scarcely be a doubt, because (a) the effect never occurred when either hydrogen or pentane was used, and (b) the effect was not experienced in working with either hydrogen or ammonia in a second instrument having a reflector made from exactly the same materials in the same workshop.

Both difficulties seem to have arisen, therefore, as a result of the nature of ethylene. The amount of polymerization was negligible, as the decrease in pressure of the gas in the instrument was not more than one per cent. per day. If the molecule decomposed, it could not do so in a way to give free hydrogen, as there would then be a marked increase in pressure. But if the molecule lost one carbon atom, and changed into the saturated hydro-carbon methane, this would account for the variation in k and W , for the contamination of the reflector, and for the fact that the pressure of any particular quantity of gas never increased. The slight decrease in pressure noticed throughout the work was traced to the drying agent phosphorus pentoxide, which absorbs ethylene at the pressures of the experiments and parts with it again when the pressure is reduced.

Estimations based on the electron currents used, the drift and agitational velocities, and the mean free paths show that electron collisions may account for slow changes in the values of k and W for any fixed value of Z/p , but not for the rapid changes observed to occur in one or two hours. Hence the view that ultra-violet light—with perhaps the help of an electric field—may cause rapid change appears tenable.

The electron currents used were of the order 10^{-12} ampere.

The ethylene used in the above experiments was generated by dropping ethyl alcohol into a flask highly exhausted of

air, and containing orthophosphoric acid at a temperature of about 230°C . Oils and other impurities such as alcohol vapour were extracted by passing the gas into traps maintained at the temperature of carbon dioxide snow. A solution of $\text{Na}_2\text{S}_2\text{O}_3$ served the purpose of extracting traces of oxygen. Bubbling through sulphuric acid helped in part to dry the gas, which, after it had passed over phosphorus pentoxide, was finally stored in flasks containing the same drying agent. In the generating and purifying processes the apparatus used was made entirely of glass. Different samples of gas were prepared, and the results from all were in good agreement.

We wish to express our warm thanks to Prof. V. A. Bailey for valuable assistance during the course of the work.

Physics Department,
University of Sydney.

LXXXI. *On the Best Correction Factors for Harmonic Coefficients.* By ALBERT EAGLE, B.Sc., Lecturer in Mathematics in the Victoria University of Manchester*.

CORRESPONDENCE in connexion with my paper, "On the Relations between the Fourier Constants of a Periodic Function and the Coefficients determined by Harmonic Analysis," in the Philosophical Magazine (Jan. 1928, p. 113) makes it desirable to add a few words by way of justification of the use of the suggested correction factors.

It need hardly be pointed out that the ordinary method of harmonic analysis makes no attempt to arrive at the most *probable* value of the harmonics from the given data, but only to determine them on the assumption that there are no harmonics present of a higher order than the number of ordinates per half period chosen for the analysis. The justification of the use of correction factors lies simply in the fact that we are not justified in making any such presumption about the higher harmonics; and that if these *are* present, they will necessarily render the values obtained for the lower harmonics erroneous. The tables of correction factors in my paper are all founded on *reasonable assumptions* about the amplitudes of these higher harmonics; but if it is

* Communicated by the Author.

known, in any particular case, that all the higher harmonics are absent, then certainly no correcting factors are required, and to apply them would be erroneous.

With p ordinates per half period, if we assume that harmonics higher than the $2p$ th are absent—which is assuming the presence of harmonics up to twice the order that ordinary harmonic analysis assumes—the relations between the true Fourier constants and the obtained coefficients become

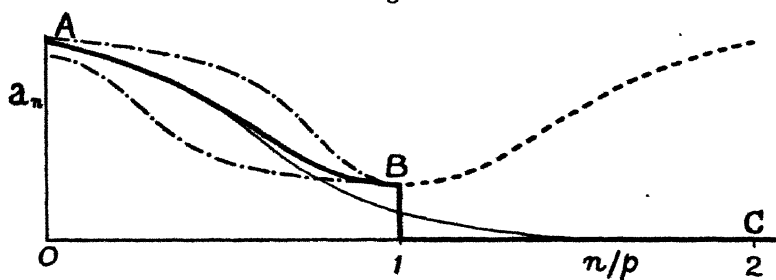
$$a_n = a_n + a_{2p-n}$$

and

$$b_n = b_n - b_{2p-n}$$

exactly ; which shows that the coefficient a_n needs correcting by subtracting from it the value of a_{2p-n} , and similarly for b_n .

Fig. 1.



In many cases, instead of using the tables of correction factors, the following graphical method will be sufficiently accurate ; while it is both more instructive and at the same time allows individual judgment being made to suit special cases. Let us plot the obtained coefficients a_n against n/p , and suppose that the thick line in fig. 1 represents the smooth curve through these points between $n/p=0$ and 1, continued by a line representing zero between $n/p=1$ and 2. The effect of applying correction factors is to assume that the coefficients should lie, not on the heavy broken line ABC, but on the thin line AC which reduces the ordinates to the left of $n/p=1$, and increases the (zero) ordinates an equal distance to the right by the same amount.

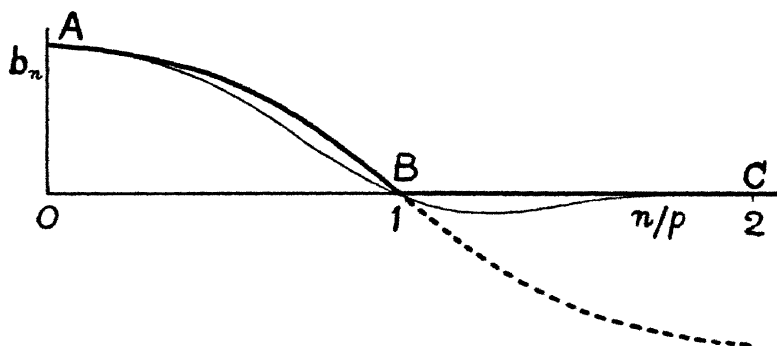
Similarly, when b_n is plotted against n/p , let the smooth curve through them be given by the thick line in AB in fig. 2. This line necessarily intersects the axis at $n/p=1$ since b_p is identically zero. The effect of the correction factors in this case is likewise to replace the thick broken line

ABC by the thin line ABC, which, at B, has half the slope of the heavy line.

The harmonics actually present in the function being analysed are obviously much more likely to follow the thin lines in figs. 1 and 2 than the heavy broken lines; but, just as obviously, if the thick lines AB ran tangentially into the axis at or before $n/p=1$, no corrections would be needed.

Some readers do not see how the second half of my Tables III. A and III. B * can be applied since ordinary harmonic analysis only gives harmonics up to the p th. But it is made clear, I think †, that the harmonic coefficients between the p th and the $2p$ th are to be taken as given by $a_{p+n} = a_{p-n}$ and $b_{p+n} = -b_{p-n}$. The dotted lines in figs. 1 and 2 show

Fig. 2.



these coefficients as continued by these relations; and the thin line between $n/p=1$ and 2 may be obtained by multiplying the ordinates of the dotted curves by the correction factors in the second half of the tables, just as the thin line between $n/p=0$ and 1 may be obtained by multiplying the ordinates of the heavy lines over this range by the correction factors in the first half of the tables.

It may happen that the points corresponding to a_n and b_n are too irregular to draw a smooth curve through them. If this is only due to a varying phase-angle, a smooth curve, of the nature of that in fig. 1, may be obtained by plotting $\sqrt{a_n^2 + b_n^2}$ against n/p . The correction factors then indicated when the corresponding thin line is drawn are then to be applied to both a_n and b_n .

* *Loc. cit.* p. 131.

† *Loc. cit.* p. 129, near bottom.

If the points on this latter curve are too irregular to draw a smooth curve through, there is nothing to give any indications about the harmonics between the p th and the $2p$ th, and consequently no correction factors should be applied.

It is easily found that adopting the correction factors in the last column of Table III. B makes the tangent to the thin line in fig. 1 at $n/p=1$ cut the axis at $n/p=1+0.15\sqrt{\pi}\equiv 1.266\dots$ In many cases this is a very suitable slope; but in some cases, such as those in which the thick line AB in fig. 1 takes the form of either of the dot-and-dash lines, the most naturally-flowing thin line AC having, as it must have, at least 5-point contact with the thick lines at A and C, will have a slope considerably different from this at $n/p=1$. In this case it is better to take the corrections from this sketched-in line than from the tables; but use can still be made of Table III. B if desired, since all the functions in it contained an arbitrary constant to which a particular value was assigned. By the property of the functions*, if we find graphically that $n/p=1+q$ is the best intercept for the tangent to the thin line at $n/p=1$, the correction factors in Table III. B may still be used, provided that (in the case of the last column) any given value in the table is not attributed to its actual $n/p\equiv 1-x$, say, but to a value of $n/p=1-qx/0.266$. Or, in other words, the correction factor to be applied for any given value of $n/p\equiv z$, say, is the value given in the table for $n/p=1-0.266(1-z)/q$; which is easily obtained if the function has been graphed.

There is no reason why in any work on harmonic analysis the diagrams in figs. 1 and 2 should not be attempted to be drawn, as they are exceedingly instructive and give much valuable information about the function being analysed. If it is objected that in much work only the first few harmonics are the subject of interest, and that harmonics up to $n=p$ are not of sufficient interest to justify their calculation, it may be pointed out that, when harmonics up to $n=p/2$ have been obtained, those from $p/2$ to p may be obtained by merely differencing two groups of terms that were added for the lower coefficients. After this, the diagrams, if it is possible to draw them, give a rational estimate of harmonics up to $n=2p$.

The limited accuracy of harmonic analysis must not be overlooked. Thus, suppose each ordinate was subject to a probable experimental error of ϵ , then, if the function

* *Loc. cit.* p. 128.

analysed possessed no symmetry so that it was necessary to use $2p$ ordinates spread over a whole period, it is easily found that the probable error of all the harmonic coefficients is ϵ/\sqrt{p} except in the case of the first and last cosine coefficients, $\frac{1}{2}a_0$ and $\frac{1}{2}a_n$, where it is $\epsilon/\sqrt{2p}$. The effect of this is to replace the thick lines A and B in figs. 1 and 2 by a band within which the values are uncertain.

LXXXII. *A Determination of the Stefan-Boltzmann Radiation Constant using a Callendar Radio Balance.* By F. E. HOARE, *A.R.C.S., B.Sc.*.*

1. *Introduction.*

ACCORDING to the Stefan-Boltzmann law the rate of emission of radiation from a fully radiating surface to surroundings at the absolute zero is proportional to the fourth power of the absolute temperature of the surface.

That is

$$E' = \sigma T_1^4.$$

$$E' = \text{radiation in ergs/cm.}^2/\text{sec.}$$

$$T_1 = \text{absolute temperature of radiator.}$$

$$\sigma = \text{radiation constant.}$$

If the radiating surface is in surroundings at T_2 Abs. which are themselves full radiators, then

$$E = E' - E'' = \sigma(T_1^4 - T_2^4).$$

$$E'' = \text{radiation received from surroundings.}$$

$$E = \text{net radiation of the surface.}$$

There have been a large number of determinations of the value of σ since the law was established thermodynamically by Boltzmann†; the agreement between different observers, however, is not good.

2. *Description and Theory of Radio Balance.*

The present paper describes some experiments which were made with the Radio Balance designed by Professor Callendar‡. It is designed as an instrument to give an absolute measure of radiation, the receiver being an

* Communicated by Prof. H. L. Callendar, F.R.S.

† *Ann. der Phys.* xxii. pp. 31 and 291 (1884).

‡ *Proc. Phys. Soc.* xxiii. p. 1 (1910).

almost perfect "black body" so that no correction for reflexion is necessary.

In this instrument the radiation is received through a small circular aperture, caught in a copper cup 3 mm. in diameter and 8 mm. long, and is balanced or determined in absolute measure by the heat absorbed or liberated by the Peltier effect in a thermocouple through which a measured current is passed.

The Peltier couple is of iron-constantan and is soldered in the bottom of the cup, which itself is mounted in a tubular thermopile consisting of twelve couples to indicate small changes in the temperature of the cup. The lower junctions of the tubular pile are fastened to a small copper block screwed to the base of a thick hollow copper cylinder 3 cm. by 3 cm. internal measurements. The pile and cup are duplicated to compensate external disturbances, such as changes in the temperature of the surroundings. The piles and couples belonging to either cup are connected in opposition and the pile circuit is completed through a sensitive galvanometer. The deflexion of the galvanometer is proportional to the difference in temperature of the cups.

When taking a reading the radiation is allowed to be incident in one of the cups whilst the other is screened. The current through the Peltier couples is adjusted until the galvanometer, in series with the thermopiles, shows no deflexion from its zero position. The cup first exposed is then screened, the other cup exposed and at the same time the current through the couples is reversed. This should leave the balance unchanged. The method of reversal accurately eliminates the small Joule effect. If P is the value of the Peltier effect in millivolts and C is the current in milliamperes required to balance the radiation, the radiant energy received is equal to $2 PC$ microwatts or $20 PC$ ergs/sec.

In practice, owing to the impossibility of making two soldered joints exactly alike, there will be a slight deflexion of the galvanometer on changing the cup exposed to the radiation and the direction of the Peltier current, but the equivalent microwatts can be calculated if the sensitivity of the galvanometer is known in microwatts generated at the Peltier junctions to cause one scale division deflexion.

This is obtained by shielding the balance cups from radiation and reversing a known current c milliamperes through the junctions, the galvanometer deflexion D being taken. The sensitivity is given as

$$s = 2 Pc/D \text{ microwatts per scale division,}$$

P being the Peltier coefficient in millivolts at the balance temperature.

If D' is the steady galvanometer deflexion when radiation is incident upon cup 1 which is also being cooled by the passage of a current of C milliamperes through the Peltier junction, and D'' is the steady deflexion when cup 2 is exposed and the direction of the current reversed, then the radiation received by either cup is given by

$$2 PC + (D' - D'')s,$$

$(D' - D'')s$ being measured in the direction of the deflexion due to passing from cup 1 to cup 2 exposed to the radiation with no current through the junctions.

The exact theory of the method of balancing the radiation and of reversal to eliminate the Joule effect is fully discussed in the paper already cited.

Assuming that the radio balance is adjusted so that its receiving aperture of area a sq. cm. is coaxial with the aperture of radius r in the water-cooled diaphragm serving to define the source, and that d is the distance in cm. between the planes of the apertures, the radiant energy E' in ergs/sec. or microwatts, depending on the units used for σ , entering the aperture from the source at temperature T_1 Abs. is given in terms of the radiation constant by the equation

$$E' = \frac{\sigma a T_1^4 r^2}{d^2 + r^2}.$$

If the source is replaced by one of equal area at a temperature T_2 Abs. the energy E'' received from the source is given by the same expression with T_2 in place of T_1 .

The quantity observed is the difference

$$E = E' - E'' = 2 PC + (D' - D'')s - D_0 s \text{ microwatts,}$$

where D_0 is the deflexion of the galvanometer measured in the same direction as $(D' - D'')$, when first cup 1 and then cup 2 is exposed to the source at T_2 Abs.

Hence

$$\sigma = \frac{\{2 PC + (D' - D'' - D_0)s\}(d^2 + r^2)}{ar^2(T_1^4 - T_2^4)} \text{ microwatts/cm.}^2/\text{degree}^4.$$

Actually the balance has two apertures which are arranged to be equidistant on either side of the axis of the radiating aperture and the same distance from the aperture. This displacement of the centres of the receiving apertures by an amount b from the axis diminishes the radiation received in

the ratio d^2/d^2+b^2 on account of the increase of distance between the source and receiver centres and in the same ratio again because of the obliquity of the apertures. With the distances at which the measurements were made this correction is very small and is applied sufficiently accurately by the addition of the constant $2b^2$ to the factor (d^2+r^2) in the previous expression for σ .

Hence

$$\sigma = \frac{\{2PC + (D' - D'' - D_0)s\}(d^2 + r^2 + 2b^2)}{ar^2(T_1^4 - T_2^4)} \text{ microwatts/cm.}^2/\text{degree}^4.$$

3. Calibration of the Radio Balance.

The Radio Balance was calibrated by finding the values of the Peltier coefficients under similar conditions to those in which it was used.

Two small heating coils were made in the following manner. A pair of copper leads were soldered to 32 cm. of S.W.G. 40 double silk-covered manganin wire at one end and an exactly similar pair at the other, so that the potential and current leads joined the manganin wire at the same place. S.W.G. 38 double silk-covered copper wire was used for the leads to keep the conduction losses small. One pair of leads was then pulled through a glass capillary tube of about 2.5 mm. external diameter and 3 cm. long, so that the soldered join to the manganin wire was just inside the tube and thus insulated by it. The manganin wire was then wound back on the glass tube to a distance of about 6 mm. from the end. By having a double layer of wire all the 32 cm. of wire was wound on this length. The remaining soldered joint was insulated and the coil held together by a coat of shellac dissolved in absolute alcohol, which was allowed to become thoroughly dry before the coil was used. The other coil was made in a similar manner, and the resistance was made to agree to less than 1 part in 1000 with that of the first coil by careful adjustment and testing with a potentiometer. The resistance of each coil was approximately 9 ohms; when complete and the shellac thoroughly dry they fitted tightly into the cups of the Radio Balance, the top of the coil being at least 2 mm. below the top of the cup. The coils were put one in each cup of the Radio Balance and a little vacuum oil was put in to make a better thermal connexion between the coils and the walls of the cups. This is very necessary, for if there is a large resistance to the flow of heat from the coil to the cup

the values obtained for the Peltier coefficients will be too large.

The current was made to flow through one of the coils and one pair of leads connected to the other coil. In this manner, by having the same current through the leads of each coil, the heating effects in the leads are accurately compensated.

The method of taking observations was to balance the heating effect in one coil against the cooling effect of the Peltier couple in one cup and the heating effect in the other. The current was then sent through the second coil and one pair of the leads to the first coil, and the current in the Peltier circuit reversed simultaneously. Knowing the current in the coil circuit and the potential across the coil the microwatts expended in the coil can be deduced.

If

W = microwatts expended in coil,

$(D' - D'')s$ = scale microwatts,

C = current in Peltier circuit in milliamperes,

the value of P is given by

$$P = \frac{W - (D' - D'')s}{2C} \text{ millivolts.}$$

This is the value of P at the temperature of the Radio Balance.

The currents in the coil circuit and the Peltier circuit were found by measuring the potentials across known standard resistances of approximately one ohm each, which had been carefully compared with N.P.L. standards.

The potentiometer used for potential measurements in all these experiments was the direct reading type 0-90 millivolts as made by the Cambridge Inst. Co. The scale, which read to one microvolt, was adjusted by means of a Weston standard cell which had been compared with N.P.L. standards. This cell was a hermetically sealed H type and the E.M.F. was taken as

$$1.0183 \text{ volts at } 20^\circ \text{C.}$$

with a temperature correction given by

$$V_t = V_{20} - 0.0000406(t - 20),$$

where t is the temperature of the cell in degrees centigrade.

The temperature of the Radio Balance was measured with a specially constructed mercury thermometer which fitted right into the body of the instrument. The thermometer was graduated in half-degrees centigrade and no difficulty was experienced in estimating to a tenth of a degree. The

temperature was varied by varying the temperature of the room, closing all the windows and doors and turning the heating apparatus full on for the higher temperatures, and leaving the windows and doors open, but carefully screening the Radio Balance from draughts, for the lower temperatures.

The values found for the Peltier coefficients were as follows :—

Temp. °C. ...	15°	17°	19°	21°	23°	25°
P millivolts...	14.85	14.98	15.11	15.25	15.38	15.51

These results are represented by the equation

$$P_t = P_{20} + 0.066(t - 20).$$

In the series of values obtained for P the deviation from a straight line when P was plotted against t was always less than 1 in 1000.

4. Arrangement of Apparatus.

The source of radiation used in these experiments was a wire-wound electric furnace, the temperature of which was measured with a platinum resistance thermometer.

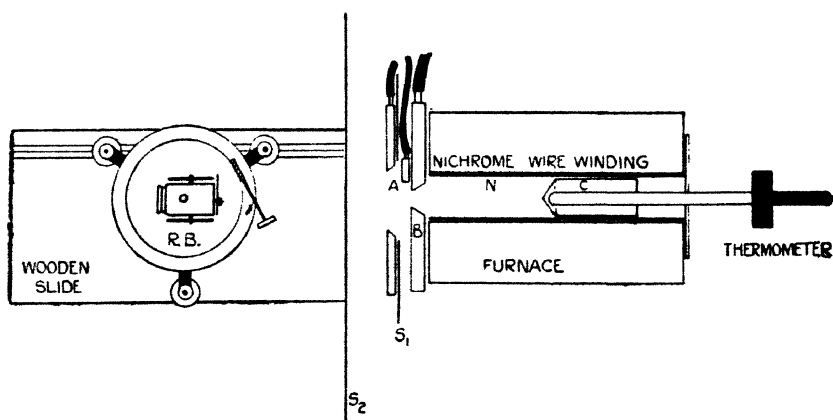
A heating solenoid of nichrome wire was wound on a quartz cylinder of about one and three-quarter inches internal diameter, the wire being wound closer at the ends than in the middle in order to compensate for the heat losses from the ends of the tube. This tube was surrounded with other concentric tubes and wrappings of insulating material. Into the quartz tube fitted fairly closely a nickel cylinder a sixteenth of an inch thick. This cylinder extended the whole length of the tube and no part of it was visible when taking readings. A nickel block with one end turned up to a blunt cone loosely fitted into this tube, so that the cone end was approximately in the centre of the furnace. The cone end of the nickel block formed the radiating surface and was made this shape to prevent direct reflexion into the Radio Balance. The other end of the nickel block was bored to take a platinum resistance thermometer, the coil being completely enclosed in the block and near the radiating surface. On the end of the furnace was fitted a water-cooled diaphragm made of brass and blackened, the water space between the back and front being half an inch. The aperture in the diaphragm could be closed with a water-cooled shutter mounted directly in front of the diaphragm. The diameter of the diaphragm was a little greater than that of the end of the furnace in order that no radiation from the heated parts

of the furnace could affect the Radio Balance. It is important that the flat side of the water-cooled diaphragm should be towards the receiver and the bevelled side towards the furnace to prevent any possible reflexion of heat by the bevel into the receiver. The receiving apertures of the Radio Balance were similarly bevelled with the flat side towards the source.

5. Measurements.

The diameters of the apertures in front of the cups were measured with a Hilger measuring microscope reading to 0.0001 cm.

Figure showing General Arrangement of Furnace and Radio Balance.



A. Movable Water-Cooled Shutter.
B. Water-Cooled Diaphragm.
C. Nickel Block.

N. Nickel Cylinder.
S₁, S₂. Screens.
R.B. Radio Balance.

The mean of 52 measurements for the diameter of aperture 1 gave 0.2099 cm. diameter or 0.03464 sq. cm. area.

For aperture 2 the mean of 50 measurements gave 0.2083 cm. diameter or 0.03411 sq. cm. area.

The mean area was taken as $a = 0.03411$ sq. cm.

The value of b was obtained by measuring with the same microscope the shortest distance between the apertures and adding the mean diameter of the apertures to this distance.

The value found was $b = 0.579$ cm.

The diameter of the aperture in the diaphragm was measured, whilst water was flowing through it, with a Cambridge Inst. Co. travelling microscope reading to 0.0001 cm.

The value found as a mean of 38 measurements was $2r = 2.0527$ cm.

The distance between the source and the receiver, which is the distance between the opposing flat surfaces, was measured with a micrometer distance piece reading to 0.0001 cm.

The current in the Peltier circuit was measured by taking the potential across a standard resistance as previously described.

The platinum thermometer used for measuring the temperature of the furnace was of the usual type as made by the Cambridge Inst. Co., having a fundamental interval of approximately one ohm.

The thermometer was used in conjunction with a Callendar Griffiths' bridge and a sensitive coil galvanometer. The bridge was calibrated by the usual substitution method and the small corrections found were applied to the coils. After the experiments had been proceeding for some time the coils were again calibrated. This calibration agreed with the previous one to the accuracy obtainable by this method.

The fundamental interval of the thermometer was determined about once a week during the course of the experiments and showed a slight change of 0.0003 ohm over this period. The ice point changed by 0.0005 ohm in the same period.

The temperature was calculated from the equation

$$pt = \frac{R - R_0}{R_{100} - R_0} \times 100,$$

and corrected to the gas scale by the equation

$$t - pt = d(t - 100)t.$$

pt = temperature on platinum scale.

t = temperature on centigrade scale.

$$d = 1.5 \times 10^{-4}.$$

When taking a reading the Callendar Griffiths' bridge was set to correspond with a previously decided temperature and the bridge galvanometer spot kept within limits corresponding to a fifth of a degree centigrade on either side of the balance position by hand manipulation of four rheostats in series with the furnace and the 110 volt mains.

The temperature of the water circulating in the diaphragm was measured to a tenth of a degree centigrade on inflow and outflow with mercury thermometers totally immersed in the stream. The mean of these temperatures was taken as T_p . The difference between the two thermometers rarely exceeded 0.5° C.

6. Method of taking Observations.

The Radio Balance was placed on a long wooden slide with a groove to take the feet of the instrument, in order that it could be moved along the axis through the centre of the radiating aperture. The slide and the Radio Balance were carefully levelled and centred, using a spirit level and steel rules. At no point was the centre of the Radio Balance more than 2 mm. off the horizontal axis through the centre of the radiating aperture; and the error introduced by this is much less than 1 part in 1000 for the distances used.

To prevent extraneous radiation from reaching the Radio Balance two screens were placed between the source and the receiver. The one nearer the furnace was water-cooled, having a central aperture of 10 cm. and was 5 cm. from the furnace. The other was of tin plate with a 4 cm. aperture situated 15 cm. from the furnace. Both screens were blackened on the side towards the receiver, and the apertures were arranged to be coaxial with the radiating aperture.

The Radio Balance apertures were exposed or screened by moving a shutter in close contact with the plane of the apertures and a screen on the front of the instrument. Both the shutter and the movable screen were blackened on the side remote from the furnace and gilded on the other.

The Radio Balance having been set with the plane of its apertures at a known distance from and parallel to the plane of the aperture in the water-cooled diaphragm, the latter was covered with the water-cooled shutter. First one cup of the receiver and then the other were exposed to the radiation from the shutter and surrounding bodies at a temperature T_2 . The small galvanometer deflexion on changing from one cup to the other was noted. This is D_0 in the expression given previously for σ . The shutter was then removed and one cup of the Radio Balance exposed to the radiation from the nickel block, the current through the Peltier junctions being adjusted so that the difference in temperature of the cups was very small. Galvanometer readings were taken every minute for five successive minutes, the potential across the standard resistance being taken at the same time. The second cup was then exposed to the radiation, the Peltier current reversed and a similar series of readings taken. The mean of each series was used in calculating the value of σ .

The temperature of the Radio Balance and the inflow and outflow temperatures of the water were taken before and after each set of readings, and found to be very constant.

7. Results.

Mean area of Radio Balance apertures... 0·03437 sq. cm.
 Diameter of water-cooled aperture 2·0527 cm.
 Displacement of balance aperture centres 0·579 cm.
 from axis.

The following table gives the value of $\sigma \times 10^5$ in ergs/sec./cm.²/degree⁴ :—

Date 1928.	Temp. furnace.	Temp. water.	Temp. Radio Balance.	Total micro-watts.	Dist. of furnace.	Value of $\sigma \times 10^5$.
April 26 ...	786·00° C.	16·5° C.	21·3° C.	200·15	36·041 cm.	5·751
" ...	"	"	21·3	200·37	"	5·758
" ...	777·20	"	21·0	261·74	31·010	5·758
" ...	"	"	21·1	260·73	"	5·735
" ...	"	"	21·1	371·10	26·029	5·756
" ...	"	"	21·1	370·53	"	5·747
April 27 ...	716·55	16·9	19·7	291·69	26·033	5·749
" ...	"	"	19·7	291·57	"	5·747
" ...	"	"	19·7	203·88	31·071	5·720
" ...	"	"	19·6	204·27	"	5·731
" ...	"	"	19·3	151·85	36·053	5·733
" ...	"	"	19·2	152·10	"	5·742
June 8 ...	772·27	19·3	22·0	541·70	21·195	5·681
" ...	"	"	21·6	361·02	26·072	5·723
" ...	"	"	21·6	359·23	"	5·694
" ...	"	"	21·5	257·04	31·008	5·760
" ...	"	"	21·5	256·02	"	5·737
June 9 ...	831·85	19·4	20·5	318·90	30·992	5·730
" ...	"	"	20·5	320·14	"	5·752
" ...	"	"	20·6	452·03	26·070	5·736
" ...	"	"	20·6	451·71	"	5·732
" ...	"	"	20·6	237·00	35·985	5·725
" ...	"	"	20·6	237·18	"	5·729
June 10 ...	985·51	19·6	20·0	400·76	35·963	5·734
" ...	"	"	20·0	400·50	"	5·727
" ...	"	"	20·0	536·35	31·159	5·763
" ...	"	"	20·0	535·76	"	5·756
" ...	"	"	20·0	763·51	26·072	5·747
" ...	"	"	19·6	1154·5	21·089	5·692
" ...	"	"	19·7	1156·7	"	5·703
June 11 ...	821·47	19·1	19·6	307·05	31·077	5·744
" ...	"	"	19·9	304·39	"	5·694
" ...	"	"	19·4	227·96	35·975	5·713
" ...	"	"	19·2	229·90	"	5·762
" ...	"	"	19·0	176·23	41·085	5·758
" ...	"	"	19·1	175·73	"	5·741
" ...	"	"	19·2	431·41	26·195	5·738
" ...	"	"	19·4	431·28	"	5·736

Mean value of $\sigma = 5·735 \times 10^{-5}$ erg/sec./cm.²/degree⁴.

8. *Discussion of Methods.*

The condition which is theoretically necessary in a determination of the radiation constant is that both the source and the receiver should be full radiators or "black bodies."

In the foregoing experiments this condition has been realized as far as is possible in experimental work of this description, by having constant temperature enclosures with good radiating walls and apertures small in comparison with the dimensions of the enclosure.

Keene* has been the only other observer using a similar method to determine the radiation constant who has endeavoured to obtain "black body" conditions in radiator and receiver. In his paper he states that owing to the water-cooled diaphragm on the furnace being in the reverse direction to that used above, his mean value of 5.89×10^{-5} c.g.s. units may be as much as 2 per cent. high, through heat reflected from the bevel re-entering the receiver. A range of only 23°C. ($1097^{\circ}-1120^{\circ}$) was used, and the distance between the source and receiver was only varied by 0.023 cm. The receiver was an aniline Thermoscope of rather high thermal capacity which was calibrated by an electrical method.

Coblentz† has made a determination of this constant using a modified Ångström Pyrheliometer. His value 5.722×10^{-5} c.g.s. units, is the mean of a large number of results using different receivers, but all of similar construction. The variation in the values of σ is about 4 per cent., after a correction for reflexion, separately determined, has been applied to the observed values.

Other experimenters using different methods, such as the ratio of emissivities, have obtained a value for σ of the order of 5.7×10^{-5} c.g.s. units. These results have not been discussed in detail here as the principles of the methods used differ from those of the methods already mentioned.

Lewis and Adams‡ have used the theory of ultimate rational units in order to calculate the value of σ . Using data based upon the electronic charge e , the gas constant R and the Faraday equivalent F , they obtain the value 5.7×10^{-5} c.g.s. units for the radiation constant.

More recently Millikan§ using Planck's equation for the distribution of energy in the spectrum of a "black body,"

* Proc. Roy. Soc. lxxxviii. p. 49 (1913).

† Bull. Bur. Stds. xii. p. 503 (1916).

‡ Phys. Rev. (2) iii. p. 92 (1914).

§ Phil. Mag. xxxiv. p. 1 (1916).

has calculated the value of σ . The value he obtains is $5.72 \pm .034 \times 10^{-5}$ c.g.s. units.

From a critical examination of the values of σ obtained by a variety of methods, it now seems well established that the value of this constant lies in the range 5.70 to 5.75×10^{-5} c.g.s. units.

9. Conclusion.

The concordance of the results obtained with the Radio Balance under widely differing conditions shows that the method used for evaluating the absolute measure of radiation is extremely satisfactory, and that the instrument is well suited for this purpose. It has the further advantages of being easy to manipulate, quickness in working, and accuracy in the necessary measurements.

I wish to express my gratitude to Professor Callendar for the continual advice he has given me, and the kindly interest he has shown throughout the course of the experiments.

LXXXIII. *Note on a Type of Determinantal Equation.* By
R. C. J. HOWLAND, M.A., M.Sc., *University College,*
London *.

EQUATIONS of the type

$$\begin{vmatrix} a_{11}-\lambda, & a_{12}, & \dots\dots\dots, & a_{1n} \\ a_{21}, & a_{22}-\lambda, & \dots\dots\dots, & a_{2n} \\ \cdot & \cdot & \cdot & \cdot \\ a_{n1}, & a_{n2}, & \dots\dots\dots, & a_{nn}-\lambda \end{vmatrix} = 0. \quad (1)$$

occur frequently in vibration and other problems, and in many such problems not more than two, the highest, values of λ are of interest.

When equation (1) is expanded, the coefficient of $(-\lambda)^n$ is unity; that of $(-\lambda)^{n-1}$ is the sum of the diagonal elements; while that of $(-\lambda)^{n-2}$ is the sum of $n(n-1)/2$ determinants of the second order, and is readily calculated. The remaining coefficients, however, appear as the sums of determinants of the third or higher orders. Experience shows that the calculation of such determinants, using a

* Communicated by the Author.

calculating machine, is not only laborious, but is of a type in which it is easy to fall into error.

It is the object of the present note to show that the equation may also be solved by an application of the root-squaring method *. The calculations involved are about as extensive as those needed for the direct solution, but they are of a kind better adapted to the calculating machine, and for this reason the method may prove to have some advantage in practice.

In order to form an equation whose roots are the squares of those of (1), we first form a new equation from (1) by changing the sign of λ and then multiply the two determinants in matrix fashion, rows by columns. This gives the new equation in the form

$$\begin{vmatrix} A_{11}-\lambda, & A_{12}, & \dots, & A_{1n} \\ A_{21}, & A_{22}-\lambda, & \dots, & A_{2n} \\ \cdot & \cdot & \cdot & \cdot \\ A_{n1}, & A_{n2}, & \dots, & A_{nn}-\lambda \end{vmatrix} = 0 \quad \dots \dots (2)$$

where

$$A_{rs} = \sum_{t=1}^n a_{rt} a_{ts}.$$

Since A_{rs} consists of a sum of simple products, its calculation is of a type to which a calculating machine is well adapted.

The process is now repeated with equation (2), and continued until the roots are so far separated that the first two can be estimated from three terms only of the equation ; these, as we have seen, are readily calculated.

Consider, for example, the equation

$$\begin{vmatrix} 25-\lambda, & 38, & 39, & 31, & 17 \\ 38, & 64-\lambda, & 69, & 56, & 31 \\ 39, & 69, & 81-\lambda, & 69, & 39 \\ 31, & 56, & 69, & 64-\lambda, & 38 \\ 17, & 31, & 39, & 38, & 25-\lambda \end{vmatrix} = 0. \quad \dots \dots (3)$$

which occurred in a problem of the whirling of a shaft.

* Whittaker & Robinson, 'The Calculus of Observations,' pp. 106 *et seq.* (London, 1924).

The first two roots of this equation were found to be 239.5 and 14.55. The first three terms of the expanded equation are

$$\lambda^5 - 259\lambda^4 + 4705\lambda^3 \dots = 0. \quad (4)$$

If the highest root is estimated from the coefficient of λ^4 only, we obtain $\lambda_1 = 259$. If the second root is estimated from the ratio of the coefficients of λ^3 and λ^4 , the result is 18.2.

A first application of the root-squaring process to (3) gives

$$\begin{vmatrix} 4840 - \lambda^2 & 8336 & 9558 & 8224 & 4727 \\ 8336 & 14398 - \lambda^2 & 16560 & 14285 & 8224 \\ 9558 & 16560 & 19125 - \lambda^2 & 16560 & 9558 \\ 8224 & 14285 & 16560 & 14398 - \lambda^2 & 8336 \\ 4727 & 8224 & 9558 & 8336 & 4840 - \lambda^2 \end{vmatrix} = 0$$

The first three terms of this equation are

$$\lambda^{10} - 57601\lambda^8 + 1.350 \times 10^7 \lambda^6 \dots = 0. \quad (5)$$

From the coefficient of λ^8 we now estimate the first root as

$$\lambda_1 = \sqrt{57601} = 240,$$

while the ratio of the coefficients of λ^6 and λ^8 leads to

$$\lambda_2 = \sqrt{1350/5.76} = 15.3.$$

The approximation is already quite good.

In repeating the process, it is necessary to work to seven or eight figures if the coefficients are to be accurate to three or four. The resulting determinant is therefore rather long and will not be written down. It leads to the equation

$$\lambda^{20} - 3.291 \times 10^9 \lambda^{16} + 1.569 \times 10^{14} \lambda^{12} - \dots = 0. \quad (6)$$

From this we have

$$\lambda_1 = (3.291 \times 10^9)^{\frac{1}{4}} = 239.5,$$

$$\lambda_2 = (1.569 \times 10^5 / 3.291)^{\frac{1}{4}} = 14.78.$$

The error in λ_2 is about 1.6 per cent., and, since the frequency depends on $\sqrt{\lambda}$, the error in this will be less than 1 per cent. Thus the first two roots are obtained with sufficient accuracy for most practical purposes.

In practice it is necessary to judge the degree of approximation that has been reached by watching the

convergence of the sequence of estimates given by the successive equations such as (4), (5), and (6). The three successive estimates of λ_2 , namely 18.2, 15.3, 14.78, indicate a rapid convergence to a value not very different from the last of them. Such an indication can usually be accepted with confidence, since it is generally known that the roots of the initial equation are real and well separated, conditions which are known to be sufficient to make the process a rapidly convergent one.

LXXXIV. *Heaviside's Formulæ for Alternating Currents in Cylindrical Wires.* By T. J. P. a. BROMWICH*.

IT was certainly due to Heaviside† that two correlated problems of this type were fully solved in terms of Bessel-functions; but of late years text-books have usually given the much less convenient solutions, obtained later‡ by Lord Kelvin in terms of the *ber* and *bei* functions. Lord Kelvin himself had certain numerical results tabulated from his formulæ, being (apparently) unaware that equivalent values had been previously tabulated by Heaviside: in other respects Lord Kelvin was fully aware of the importance of Heaviside's work. It is, in fact, due to Heaviside's work that we obtain the (now commonplace) view that the seat of the electromagnetic energy is the surrounding medium: that this energy gradually soaks into the conducting wire, and is there used up in heating the wire.

Hitherto (so far as I know) no proofs have been given of Heaviside's formulæ given in § 2 below; thus, although the results are some 40 years old, it may be of service to provide proofs, and at the same time to direct attention to the advantages obtained by using these formulæ.

§ 1. *Preliminary Formulæ.*

In Heaviside's discussion of an alternating current flowing along a cylindrical wire, the fundamental equations are (writing p for $\partial/\partial t$):

$$\frac{4\pi}{\sigma} E_1 = -\frac{\partial H_2}{\partial z}, \quad \frac{4\pi}{\sigma} E_3 = \frac{1}{r} \frac{\partial(rH_2)}{\partial r}, \quad -\mu p H_2 = \frac{\partial E_1}{\partial z} - \frac{\partial E_3}{\partial r},$$

* Communicated by the Author.

† Papers, vol. i. p. 362; and vol. ii. p. 97.

‡ Lord Kelvin himself refers repeatedly to the work done by Heaviside in this connexion.

where $(E_1, 0, E_3)$ and $(0, H_2, 0)$ denote the electric and magnetic forces (in cylindrical coordinates r, θ, z), and σ, μ are the specific resistance and permeability of the wire. In most practical applications the fields are independent of z and the familiar methods of solution give

$$E_1 = 0, \quad E_3 = AI_0(qr), \quad H_2 = \frac{4\pi}{\sigma q} AI_1(qr),$$

where $q^2 = 4\pi\mu p/\sigma$.

Without going further into the general theory of such operational symbols*, we may pass at once to the case of alternating currents, for which (assuming a time-factor $e^{i\pi}$) we can write simply

$$p = i\pi.$$

Then $q^2 = 4\pi i\mu p/\sigma = (4\pi i\mu/\sigma) e^{i\pi/2}$,

and so $qr = r \sqrt{4\pi i\mu/\sigma} e^{i\pi/4}$.

The total current in the wire is

$$C = \int_0^a \frac{2\pi}{\sigma} E_3 r dr = \frac{1}{2} a H_2(a) = \frac{2\pi A a}{\sigma q} I_1(qa),$$

and the effective resistance is accordingly given by

$$\frac{E_3(a)}{C} = \left(\frac{\sigma}{\pi a^2} \right) \frac{qa I_0(qa)}{2 I_1(qa)}.$$

When $p=0$ this expression reduces to $\sigma/\pi a^2 = R$, the steady current-resistance; but in general it is an operator, and is called by Heaviside the *resistance-operator*.

§ 2. Certain Series derived from Bessel Functions.

Let us write $qr = x e^{i\pi/4}$,

where x is real, and put $I_0(qr) = u$;

also let v denote the complex number conjugate to u .

It will be convenient to write further

$$\xi = \log x, \quad x = e^\xi,$$

so that

$$\frac{d}{d\xi} = x \frac{d}{dx} \quad \text{and} \quad \frac{d^2 u}{d\xi^2} = x \frac{d}{dx} \left(x \frac{du}{dx} \right) = r \frac{d}{dr} \left(r \frac{du}{dr} \right)$$

* For a convenient introduction (with references to Heaviside's work and to earlier papers of my own) the reader may consult Dr. H. Jeffreys's Tract (No. 23 of the Cambridge Mathematical and Physical Tracts, 1927).

Now the differential equation for $I_0(qr)$ gives

$$r \frac{d}{dr} \left(r \frac{du}{dr} \right) = q^2 r^2 u = \iota x^2 u = \iota e^{2\xi} u,$$

and so the final equation for u in terms of ξ is

$$\frac{d^2 u}{d\xi^2} = \iota e^{2\xi} u. \quad . \quad . \quad . \quad . \quad . \quad (1)$$

Since ξ is real, we can obtain the equation for v by changing the sign of ι in (1), and then we have

$$\frac{d^2 v}{d\xi^2} = -\iota e^{2\xi} v. \quad . \quad . \quad . \quad . \quad . \quad (2)$$

Consider now the actual formula for u : from the familiar series for $I_0(qr)$ we see that

$$u = 1 + \frac{\iota x^2}{2^2} - \frac{x^4}{2^2 \cdot 4^2} - \frac{\iota x^6}{2^2 \cdot 4^2 \cdot 6^2} + \frac{x^8}{2^2 \cdot 4^2 \cdot 6^2 \cdot 8^2} + \dots,$$

from which it is evident that the formulæ are simplified by writing *

$$x^2 = 4z, \quad \log z = \zeta, \quad \text{so that} \quad 2\xi = \zeta + \log 4 \quad . \quad (3)$$

Then we have

$$u = 1 + \frac{\iota z}{1^2} - \frac{z^2}{1^2 \cdot 2^2} - \frac{\iota z^3}{1^2 \cdot 2^2 \cdot 3^2} + \frac{z^4}{1^2 \cdot 2^2 \cdot 3^2 \cdot 4^2} + \dots, \quad (4)$$

and the equations (1) and (2) reduce to the forms

$$u'' = \iota e^\zeta u, \quad v'' = -\iota e^\zeta v, \quad . \quad . \quad . \quad . \quad (5)$$

where accents denote differentiation with respect to ζ .

Multiply equations (5) by u, v and add: then we have

$$uv'' + u''v = 0,$$

which may be written

$$\frac{d^2}{d\zeta^2}(uv) = 2u'v'. \quad . \quad . \quad . \quad . \quad . \quad (6)$$

Differentiate (6) again and the result will be

$$\frac{d^3}{d\zeta^3}(uv) = 2(u''v' + u'v'') = 2\iota e^\zeta(uv' - u'v). \quad . \quad . \quad (7)$$

The function on the right-hand side of (7) is of importance

* This z is the same as Heaviside's (Electrical Papers, vol. ii. p. 91). Also $u = M + \iota N$, $v = M - \iota N$ in his notation.

in the future work; and to obtain a convenient notation, it may be noted that from (4) we have

$$\begin{aligned} u &= 1 + \epsilon^{\zeta} + O(e^{2\zeta}), & v &= 1 - \epsilon^{\zeta} + O(e^{2\zeta}), \\ u' &= \epsilon^{\zeta} + O(e^{2\zeta}), & v' &= -\epsilon^{\zeta} + O(e^{2\zeta}). \end{aligned}$$

Thus $uv' - u'v = -2\epsilon^{\zeta} + O(e^{2\zeta}).$

It is therefore convenient to use the real function w defined by

$$2w = \epsilon(uv' - u'v), \quad . \quad . \quad . \quad . \quad (8)$$

so that the first term in w is ϵ^{ζ} .

It will now be seen that (7) reduces to

$$\frac{d^2}{d\zeta^2}(uv) = 4\epsilon^{\zeta}w. \quad . \quad . \quad . \quad . \quad (9)$$

Also $\frac{dw}{d\zeta} = \frac{1}{2}\epsilon(uv'' - u''v) = \epsilon^{\zeta}(uv). \quad . \quad . \quad . \quad (10)$

Remembering the form of (4) we see that

$$uv = 1 + \frac{1}{2}\epsilon^{2\zeta} + O(e^{4\zeta}).$$

Thus we can assume that

$$\left. \begin{aligned} uv &= 1 + A_1\epsilon^{2\zeta} + A_2\epsilon^{4\zeta} + A_3\epsilon^{6\zeta} + \dots \\ w &= \epsilon^{\zeta}(1 + B_1\epsilon^{2\zeta} + B_2\epsilon^{4\zeta} + B_3\epsilon^{6\zeta} + \dots) \end{aligned} \right\}, \quad . \quad . \quad (11)$$

and so, substituting in (9) and (10), the coefficients A_n, B_n are given by

$$2^3A_1 = 4, \quad 4^3A_2 = 4B_1, \quad 6^3A_3 = 4B_2, \dots \left. \right\}. \quad . \quad (12)$$

and $3B_1 = A_1, \quad 5B_2 = A_2, \quad 7B_3 = A_3, \dots \left. \right\}$

From (12) it is easy to see that

$$\left. \begin{aligned} A_1 &= \frac{1}{2}, \quad \frac{A_2}{A_1} = \frac{1}{2^3} \cdot \frac{1}{6}, \quad \frac{A_3}{A_2} = \frac{1}{3^3} \cdot \frac{1}{10}, \quad \frac{A_4}{A_3} = \frac{1}{4^3} \cdot \frac{1}{14}, \dots \\ \text{and} \\ B_1 &= \frac{1}{6}, \quad \frac{B_2}{B_1} = \frac{1}{2^3} \cdot \frac{1}{10}, \quad \frac{B_3}{B_2} = \frac{1}{3^3} \cdot \frac{1}{14}, \quad \frac{B_4}{B_3} = \frac{1}{4^3} \cdot \frac{1}{18}, \dots \end{aligned} \right\}. \quad (13)$$

Thus, from (11) and (13), we find the first pair of fundamental series

$$uv = P_1 = 1 + \frac{z^2}{2} \left(1 + \frac{z^2}{2^3 \cdot 6} \left(1 + \frac{z^2}{3^3 \cdot 10} \left(1 + \frac{z^2}{4^3 \cdot 14} \left(1 + \dots \right. \right. \right. \right. (14)$$

$$\text{and} \quad w = \frac{t}{2}(uv' - u'v) = zP_2, \quad \left. \begin{array}{l} \text{where} \\ P_2 = 1 + \frac{z^2}{6} \left(1 + \frac{z^2}{2^3 \cdot 10} \left(1 + \frac{z^2}{3^3 \cdot 14} \left(1 + \frac{z^2}{4^3 \cdot 18} (1 + \dots) \right) \right) \right) \end{array} \right\} \quad (15)$$

It is useful to note the numerical values of these successive denominators, which are in (14):

$$2, \quad 48, \quad 270, \quad 896, \dots$$

$$\text{and in (15):} \quad 6, \quad 80, \quad 378, \quad 1152, \dots$$

The next series which it is useful to obtain is

$$u'v' = \frac{1}{2} \frac{d^2}{d\zeta^2}(uv) = \frac{1}{2} \frac{d^2 P_1}{d\zeta^2}, \text{ from (6).}$$

On differentiating (14) this gives

$$u'v' = z^2 P_3,$$

where

$$P_3 = 1 + \frac{z^2}{2 \cdot 6} \left(1 + \frac{z^2}{2^2 \cdot 3 \cdot 10} \left(1 + \frac{z^2}{3^2 \cdot 4 \cdot 14} (1 + \dots) \right) \right) \left. \right\} \quad (16)$$

Here the denominators are found to be

$$12, \quad 120, \quad 504, \quad 1440, \dots$$

Finally we shall use also

$$uv' + u'v = \frac{d}{d\zeta}(uv) = \frac{dP_1}{d\zeta},$$

and from (14) this gives

$$uv' + u'v = z^2 P_4,$$

where

$$P_4 = 1 + \frac{z^2}{2^2 \cdot 6} \left(1 + \frac{z^2}{2 \cdot 3^2 \cdot 10} \left(1 + \frac{z^2}{3 \cdot 4^2 \cdot 14} (1 + \dots) \right) \right) \left. \right\} \quad (17)$$

The sequence of denominators is here

$$24, \quad 180, \quad 672, \quad 1800, \dots$$

It may be convenient to note that corresponding terms in these four series are arranged in order of numerical magnitude, so that

$$P_1 > P_2 > P_3 > P_4.$$

It may also be of interest to observe that the four series are connected by the simple identity

$$P_1 P_3 - P_2^2 = \frac{1}{4} z^2 P_4^2, \text{ so that } P_1 P_3 > P_2^2. \quad (18)$$

In fact we have

$$\frac{1}{4}(uv' + u'v)^2 - \frac{1}{4}(uv' - u'v)^2 = (uv)(u'v'),$$

or
$$\frac{1}{4}(z^2 P_4)^2 + (z P_2)^2 = P_1(z^2 P_3),$$

and, on division by z^2 , this reduces to (18).

As a direct verification, we find that (up to z^4)

$$\begin{aligned} P_1 P_3 &= 1 + \left(\frac{1}{2} + \frac{1}{12}\right) z^2 + \left(\frac{1}{96} + \frac{1}{24} + \frac{1}{1440}\right) z^4 + \dots \\ &= 1 + \frac{7}{12} z^2 + \frac{19}{360} z^4 + \dots, \\ P_2^2 &= 1 + \frac{1}{3} z^2 + \left(\frac{1}{36} + \frac{1}{240}\right) z^4 + \dots \\ &= 1 + \frac{1}{3} z^2 + \frac{23}{720} z^4 + \dots \end{aligned}$$

Thus, on subtracting, we see that

$$\begin{aligned} P_1 P_3 - P_2^2 &= \frac{1}{4} z^2 + \frac{1}{48} z^4 + \dots \\ &= \frac{1}{4} z^2 \left(1 + \frac{1}{12} z^2 + \dots\right), \end{aligned}$$

while $P_4^2 = 1 + \frac{1}{12} z^2 + \dots,$

so that the general formula (18) is verified as far as terms in z^4 .

For comparison with Heaviside's work it is convenient to observe that he writes

$$M + \iota N, \quad M - \iota N$$

for u, v respectively.

Thus in the notation used above, we find that,

$$\left. \begin{aligned} P_1 &= M^2 + N^2 \\ z P_2 &= \frac{1}{2} r (M N' - M' N) \\ z^2 P_3 &= \frac{1}{4} r^2 (M'^2 + N'^2) \\ z^2 P_4 &= r (M M' + N N') \end{aligned} \right\} \dots \dots (19)$$

where, in (19), as in Heaviside's formulæ, the accents refer to differentiations of M, N with respect to r :

Actually the functions M, N are identical with those for which Lord Kelvin introduced (at a later date) the notation *ber, bei*; but neither he nor any others (of those who have worked at the subject in ignorance of Heaviside's formulæ) gave the formulæ (18) and (19).

§ 3. *Applications to longitudinal alternating currents.*

In Heaviside's operational method we write

$$q^2 = 4\pi\mu p/\sigma, \quad . \quad . \quad . \quad . \quad . \quad (20)$$

where, as above, $p = d/dt$, and σ, μ are the specific resistance and the permeability. Thus if we write R for the steady-current resistance per unit length of the wire, we have

$$R = \sigma/\pi a^2,$$

$$\text{and} \quad q^2 a^2 = 4\mu p/R.$$

In the case of alternations of frequency $n/2\pi$, we can write effectively $p = in$, taking q then as a complex with a positive real part.

$$\text{Thus} \quad q^2 a^2 = 4\mu in/R,$$

$$\text{or} \quad qa = \sqrt{\frac{4\mu n}{R}} e^{i\pi/4}.$$

That is, in the notation of § 2,

$$x = 2\sqrt{\mu n/R},$$

$$\text{or}^* \quad z = \mu n/R. \quad . \quad . \quad . \quad . \quad . \quad (21)$$

Heaviside has shown that the resistance-operator of the wire (per unit length) is given by the formula (see § 1)

$$\frac{1}{2}Rqa I_0(qa)/I_1(qa), \quad . \quad . \quad . \quad . \quad . \quad (22)$$

which reduces to R , as it should, when the current is *steady*, so that we can write $p = 0$ or $q = 0$.

It is usual for numerical work to express the resistance-operator in the form

$$R' + L'p. \quad . \quad . \quad . \quad . \quad . \quad (23)$$

and then to call R', L' the *high-frequency resistance and self-inductance*, per unit length of the wire.

Using the notation of (4), (5), we find from (22) and (23),

$$R' + L'p = R \left(\frac{qa}{2}\right)^2 \frac{u}{u'} = R \frac{iz}{2} \frac{1}{u'v'} \{ (uv' + u'v) + (uv' - u'v) \}.$$

* In vol. i. of his Papers, Heaviside uses the alternative notation,

$$y = (4z)^2,$$

but this seems less convenient in most applications.

On substituting from (15)–(17) we see that

$$\frac{R'}{R} = \frac{P_2}{P_3} \quad \text{and} \quad \frac{L'n}{R} = \frac{\frac{1}{2}zP_4}{P_3}, \quad \dots \quad (24)$$

the two formulæ given by Heaviside*.

For example, let $z=10$ or $\mu n=10R$.

Then $P_2=44\cdot507$, $P_3=17\cdot755$, $P_4=7\cdot8454$,

and so $\frac{R'}{R} = \frac{44\cdot507}{17\cdot755} = 2\cdot507$, $\frac{L'n}{R} = \frac{39\cdot227}{17\cdot755} = 2\cdot212$.

It is not difficult to deduce Lord Kelvin's formula for R'/R from (24); we see, from (19), that

$$\frac{R'}{R} = \frac{P_2}{P_3} = \frac{2z}{r} \left(M \frac{\partial N}{\partial r} - N \frac{\partial M}{\partial r} \right) / \left\{ \left(\frac{\partial M}{\partial r} \right)^2 + \left(\frac{\partial N}{\partial r} \right)^2 \right\}.$$

To compare with Kelvin's actual formulæ, we must express the differentiations in terms of x ; and using (3), this gives†

$$\frac{R'}{R} = \frac{x}{2} \left(M \frac{\partial N}{\partial x} - N \frac{\partial M}{\partial x} \right) / \left\{ \left(\frac{\partial M}{\partial x} \right)^2 + \left(\frac{\partial N}{\partial x} \right)^2 \right\},$$

where $M = \text{ber } x$, $N = \text{bei } x$.

A table, calculated by Dr. Magnus MacLean, is given in Lord Kelvin's paper and will be found in Prof. Fleming's book (*loc. cit.* p. 103). As an example we may take $x=4$, for which $z=4$; then (15) and (16) give

$$P_2=4\cdot2229, \quad P_3=2\cdot5168,$$

so that $P_2/P_3=1\cdot6779$, while the tabular value is 1·6778.

An alternative method, when $|z|$ is large, is to use the asymptotic formula for I_0 , namely‡

$$I_0(qa) = \frac{e^{qa}}{\sqrt{2\pi qa}} \left\{ 1 + \frac{1}{8qa} + \frac{1\cdot9}{2(8qa)^2} + \dots \right\}.$$

* Papers, vol. ii. p. 98; they are naturally equivalent to Lord Kelvin's, but they are more simple to work with.

† Lord Kelvin, Math. and Phys. Papers, vol. iii. p. 491; see also Prof. J. A. Fleming, 'Electric Wave Telegraphy,' 4th ed. p. 101 (1919); and Pidduck's 'Electricity,' 2nd ed. p. 399 (it is perhaps useful to note that the table given in the first edition is erroneous).

‡ Other methods are given in § 6 below; I originally devised these in 1908–1909, but they may have been used earlier by Heaviside.

Then, by logarithmic differentiation, we see that

$$\frac{I_1(qa)}{I_0(qa)} = 1 - \frac{1}{2qa} - \frac{\frac{1}{8(qa)^2} + \frac{9}{64(qa)^3} + \dots}{1 + \frac{1}{8qa} + \frac{9}{128(qa)^2} + \dots}.$$

Thus *, on taking the reciprocal, we see that

$$\frac{qa}{2} \frac{I_0(qa)}{I_1(qa)} = \frac{qa}{2} \left\{ 1 + \frac{1}{2qa} + \frac{3}{8(qa)^2} + \frac{3}{8(qa)^3} + \dots \right\}, \quad (25)$$

and proceeding as before, we find that if

$$qa = s(1 + \iota), \quad \text{or} \quad s = \sqrt{2z} = \sqrt{2\mu n/R}, \quad (26)$$

then (22), (23), and (25) give

$$\left. \begin{aligned} \frac{R'}{R} &= \frac{s}{2} + \frac{1}{4} + \frac{3}{32s} + O\left(\frac{1}{s^3}\right) \\ \frac{L'n}{R} &= \frac{s}{2} - \frac{3}{32s} - \frac{3}{32s^2} + O\left(\frac{1}{s^3}\right) \end{aligned} \right\} \dots \quad (27)$$

Although (25) was known to Heaviside † at a later date, yet he never seems to have used more than the first terms in (27)—which constitute the extremely rough approximation due to Lord Rayleigh.

For example, with $z=10$, we have $s = \sqrt{20} = 2\sqrt{5}$, and so (27) gives

$$\begin{aligned} \frac{R'}{R} &= \sqrt{5} + \frac{1}{4} + \frac{3}{320} \sqrt{5}, \text{ nearly} \\ &= 2.236 + .25 + .021 = 2.507, \end{aligned}$$

while

$$\frac{L'n}{R} = \sqrt{5} - \frac{3}{320} \sqrt{5} - \frac{3}{640},$$

to the same order

$$= 2.236 - .021 - .005 = 2.210.$$

These two values agree extremely well with those found from (24) above ‡.

Similarly, with $z=20$, $s=10\sqrt{2}=14.142$, and then we find that

$$R'/R = 7.071 + .25 + .006 = 7.327,$$

while the value 7.325 is found in Kelvin's table.

* See, for instance, my book on 'Infinite Series' (2nd ed.) Art. 117. For more details see § 6 below.

† 'Electromagnetic Theory,' vol. iii. p. 371. (See § 6 below.)

‡ This example was given by Heaviside (Papers, vol. ii. p. 99), but he found a discrepancy through using the rough approximation of Rayleigh, $R' = L'n = (2.236)R$, corresponding to the first terms in (27).

§ 4. Lord Kelvin's method of evaluating R' .

This depends on a different physical principle; it is of some historical interest, and affords a useful check, although longer (and less fundamental) than Heaviside's method*.

Let E_3 , w denote the electric force and current parallel to the axis; then the rate of heating (per unit length) is

$$\int_0^a E_3 \bar{w} \cdot 2\pi r dr,$$

where \bar{w} is the complex conjugate to w .

Now, if H_2 is the magnetic force (in circles round the axis) we have

$$4\pi r w = \frac{\partial}{\partial r} (r H_2), \quad 4\pi r \bar{w} = \frac{\partial}{\partial r} (r \bar{H}_2), \quad \text{and} \quad \mu p H_2 = \frac{\partial E_3}{\partial r}.$$

Using these results, we can integrate by parts, and then the formula for the rate of heating becomes

$$\frac{1}{2} \left[r E_3 H_2 \right]_0^a - \frac{1}{2} p \int_0^a \mu H_2 \bar{H}_2 dr.$$

The last term gives zero on the average, since it is a perfect differential with respect to t ; thus we can take the rate of heating as the time-average of

$$\frac{1}{2} a (E_3 \bar{H}_2)_{r=a}.$$

Now, at $r=a$, we have

$$E_3 = (R' + L'p)C, \quad \text{and} \quad 2\pi a \bar{H}_2 = 4\pi \bar{C},$$

where C is the total current and \bar{C} is its conjugate complex.

Thus our result is the average of $(R' + L'p)(C\bar{C})$, and so the final estimate of the effective resistance is again equal to R' .

§ 5. The correlated problem of a coil surrounding a central core.

It is proved by Heaviside† that the effective resistance and self-inductance are then given by

$$R_1' + L_1'p = L_1p \left\{ \frac{2I_1(qa)}{qaI_0(qa)} \right\},$$

* It is perhaps necessary to caution readers against the version of this method given on pp. 102, 103 of Prof. Fleming's book: the slip made there is often to be found in energy-calculations when complex variables are used to represent the electric and magnetic fields. The fallacy lies in the assumption that the square of the intensity is equal to the square of the corresponding complex; but it is evident that $(x^2 + y^2)$ is far from being equal to $(x + iy)^2$, and the former is not even equal to the real part of the latter.

When the square of the intensity is needed, it is necessary to multiply the complex by its conjugate; that is, $(x + iy)$ by $(x - iy)$ gives $x^2 + y^2$.

† See, for instance, Papers, vol. ii. p. 99; as a matter of rapid calculation we can obtain all the necessary results (except for small points of detail) by an interchange of the electric and magnetic fields in § 1.

the expression in brackets simply being the reciprocal of that used in the original problem.

Now, in the notation used before, this bracket is equal to

$$\begin{aligned}\frac{4}{(qa)^2} \frac{u'}{u} &= \frac{1}{2\iota z} \left\{ \left(\frac{u'}{u} + \frac{v'}{v} \right) + \left(\frac{u'}{u} - \frac{v'}{v} \right) \right\} \\ &= \frac{1}{2\iota z} \left(\frac{z^2 P_4}{P_1} + 2\iota \frac{z P_2}{P_1} \right) \\ &= \frac{P_2}{P_1} + \frac{z P_4}{2\iota P_1} \dots \dots \dots (28)\end{aligned}$$

Writing $p = \iota n$ as before, we see that now

$$\frac{R_1'}{L_1 n} = \frac{z P_4}{2 P_1}, \quad \frac{L_1'}{L_1} = \frac{P_2}{P_1}, \quad \dots \dots \dots (29)$$

which agree with Heaviside's formulæ (91*h*) and (92*h*).

When $|z|$ is large, we can replace (28) by a formula corresponding to (25), which gives

$$\frac{2I_1(qa)}{qaI_0(qa)} = \frac{2}{qa} \left\{ 1 - \frac{1}{2qa} - \frac{1}{8(qa)^2} - \frac{1}{8(qa)^3} - \dots \right\}. \quad (30)$$

Then, if we write, as in (26), $qa = s(1 + \iota)$, the formula (30) becomes

$$-\frac{LR_1'}{L_1 n} + \frac{L_1'}{L_1} = \frac{1 - \iota}{s} - \frac{1}{2\iota s^2} + \frac{1 + \iota}{16s^3} + \frac{1}{16s^4} + \dots \dots \dots (31)$$

It follows that

$$\left. \begin{aligned}\frac{R_1'}{L_1 n} &= \frac{1}{s} - \frac{1}{2s^2} - \frac{1}{16s^3} + O\left(\frac{1}{s^5}\right) \\ \frac{L_1'}{L_1} &= \frac{1}{s} + \frac{1}{16s^3} + \frac{1}{16s^4} + O\left(\frac{1}{s^5}\right)\end{aligned}\right\} \dots \dots \dots (32)$$

As an illustration we may take, as before, $z = 10$, $s = \sqrt{20} = 2\sqrt{5}$, for which we find that

$$P_1 = 198 \cdot 2, \quad P_2 = 44 \cdot 507, \quad P_4 = 7 \cdot 8454.$$

Then (29) gives the values

$$\frac{R_1'}{L_1 n} = \frac{39 \cdot 227}{198 \cdot 20} = \cdot 1979, \quad \frac{L_1'}{L_1} = \frac{44 \cdot 507}{198 \cdot 20} = \cdot 2245.$$

And from (32) we find that

$$\begin{aligned}\frac{R_1'}{L_1 n} &= \frac{1}{2\sqrt{5}} \left(1 - \frac{1}{320} \right) - \frac{1}{40} = \cdot 2229 - \cdot 0250 = \cdot 1979, \\ \frac{L_1'}{L_1} &= \frac{1}{2\sqrt{5}} \left(1 + \frac{1}{320} \right) + \frac{1}{6400} = \cdot 2243 + \cdot 00016 = \cdot 2245.\end{aligned}$$

§ 6. Asymptotic series for use when $|qr|$ is large.

These formulæ are due (probably) to Heaviside; the first place in which they occur in a complete form is in his 'Electromagnetic Theory,' vol. iii. p. 371.

In the first place, no confusion with § 2 need arise if we write x for what is there called qr ; so that x is now a complex number (of phase $\frac{1}{4}\pi$). Then*

$$I_0(x) = \frac{1}{\sqrt{2\pi x}} \left[e^x \left\{ 1 + \frac{1}{8x} + \frac{1 \cdot 9}{2! (8x)^2} + \dots \right\} + \epsilon e^{-x} \left\{ 1 - \frac{1}{8x} + \frac{1 \cdot 9}{2! (8x)^2} + \dots \right\} \right],$$

the sign of ϵ in the second term being positive, since the imaginary part of x is also positive.

In order to obtain a formula for $I_0(x)/I_1(x)$ which is of a reasonable type, we must restrict x so that the second term is small compared with the first.

This requires that $e^{-2\xi}$ shall be small where $x = \xi(1 + \iota)$; for a relative order of $1/1000$, $\xi \geq 3 \cdot 5$, and so $|x| \geq 5$, say; for the order $1/10,000$, we take $\xi \geq 4 \cdot 6$ and $|x| \geq 7$ (roughly).

It is then evident that expansions in descending powers of x of the types used in (25) and (30) are possible: to find the sequence of coefficients, write

$$u = I_0(x)/I_1(x), \quad . \quad . \quad . \quad . \quad . \quad (33)$$

where again there is no risk of confusion with the former u . Then it is easy to verify that

$$\frac{du}{dx} = 1 + \frac{u}{x} - u^2 = 1 + \frac{1}{4x^2} - \left(u - \frac{1}{2x}\right)^2. \quad . \quad (34)$$

Thus, if we try the series

$$u = 1 + \frac{1}{2x} + \frac{A_2}{x^2} + \frac{A_3}{x^3} + \dots,$$

we find from (34), the identity

$$\begin{aligned} & \frac{1}{2x^2} + \frac{2A_2}{x^3} + \frac{3A_3}{x^4} + \frac{4A_4}{x^5} + \dots \\ & = - \left(1 + \frac{1}{4x^2}\right) + \left(1 + \frac{A_2}{x^2} + \frac{A_3}{x^3} + \dots\right)^2. \end{aligned}$$

* See, for instance, my 'Infinite Series,' 2nd ed. p. 353; the result is due to Stokes. But it should be noted that in the formula given for $I_n(x)$ in my book, n must be an integer.

Thus

$$\begin{aligned} \frac{1}{2} &= -\frac{1}{4} + 2A_2, & 2A_2 &= 2A_3, & 3A_3 &= 2A_4 + A_2^2, \\ 4A_4 &= 2A_5 + 2A_2A_3, & 5A_5 &= 2A_6 + 2A_2A_4 + A_2^2 \dots, \\ \text{or} \quad A_2 &= \frac{3}{8}, & A_3 &= \frac{3}{8}, & A_4 &= \frac{63}{128}, & A_5 &= \frac{27}{32}, \quad . \quad (35) \end{aligned}$$

and in addition, $A_6 = \frac{949\frac{1}{2}}{512}$ (as given by Heaviside).

Similarly, if we write $v = 1/u$ in the equation (34), we find that

$$\frac{dv}{dx} = 1 - \frac{v}{x} - v^2 \quad v = 1 - \frac{1}{2x} - \frac{B_2}{x^2} - \frac{B_3}{x^3} - \dots, \quad (36)$$

and so

$$\begin{aligned} \frac{1}{2x^2} + \frac{2B_2}{x^3} + \frac{3B_3}{x^4} + \frac{4B_4}{x^5} + \dots \\ = 1 + \frac{1}{4x^2} - \left(1 - \frac{B_2}{x^2} - \frac{B_3}{x^3} - \dots\right)^2. \end{aligned}$$

Thus

$$\begin{aligned} \frac{1}{2} &= \frac{1}{4} + 2B_2, & 2B_2 &= 2B_3, & 3B_3 &= 2B_4 - B_2^2, \\ 4B_4 &= 2B_5 - 2B_2B_3, & 5B_5 &= 2B_6 - 2B_2B_4 - B_3^2 \dots, \\ \text{so that} \quad B_2 &= \frac{1}{8}, & B_3 &= \frac{1}{8}, & B_4 &= \frac{25}{128}, & B_5 &= \frac{13}{32}, \quad . \quad (37) \end{aligned}$$

and apparently * $B_6 = \frac{536\frac{1}{2}}{512}.$

LXXXV. On the Investigation of Predischarges.

[Plate XIV.]

To the Editors of the Philosophical Magazine.

GENTLEMEN,—

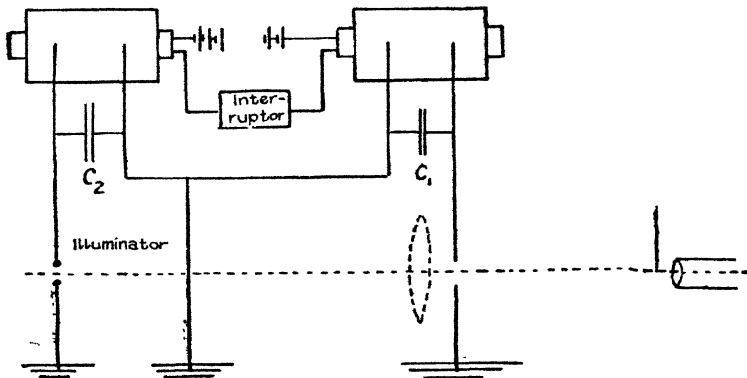
IN the May number of the Phil. Mag. [7] v. p. 1698 (1928), Prof. Harvey A. Zinszer, Hanover College, writes that the "Schlieren" method of Toepler and Mach has not been made use of hitherto in the investigation of the life-history of the spark. He is also of opinion that the

* The last coefficient is given by Heaviside as $\frac{69}{64} = \frac{552}{512}$; but I have checked the value given above in other ways.

"Schlieren" method as employed by Toepler, Mach, and Wood is not qualified for the investigation on the life-history of the spark.

Already in 1922 I published * photographs of brush-discharge "Schlieren," and showed that the "Schlieren" method has been useful in giving more precise information about the life-history of the spark. I believe that I have reason to say that by the dispositions of Toepler and Wood I got pictures which, in spite of their smallness, render the most subtle details more sharply than the shadow method of Foley, which has been used by Prof. Zinszer. Therefore I send you three photographs (Pl. XIV. figs. 1-3) with the request to publish them in your Magazine.

Fig. 4.



The Experimental Disposition.—The "Schlieren" apparatus was set up and adjusted in the usual manner described by Toepler. But to obtain a delay between the illumination-spark and the discharge to be examined, a method was employed which differs from those made hitherto by Toepler and Mach for photography of sound-waves. By an oscillatory discharge in the oscillatory circuit of the sound-spark the tension of the illumination-spark is considerably raised in a wholly determined phase of the first oscillatory circuit, and thus led Toepler and Mach to the installation of the illumination-spark in a fixed interval of time after the sound-spark. But this method is not adaptable for the investigation of pre-discharges, where the well-defined oscillations are wanting. Therefore I used two big inductors (fig. 4), and fastened their primary spools one after the

* *Phys. Zeitschr.* xxiii. p. 193 (1922).

other to the same interrupter. The condenser of the interrupter had to be enlarged correspondingly, so that the light arc of the interrupter was small and short. At every interruption of the primary circuit both secondary spools receive a shock by which the capacities C_1 and C_2 lying near them are charged. According to the period of the oscillatory circuit T_1 and T_2 , which depend on the self-inductions of the secondary spools and the capacities C_1 and C_2 , the one discharge will take place earlier than the other one.

Besides the two pointed electrodes (left +, right -) and the "Schlieren," some light equidistant lines are to be seen on the photographs (Pl. XIV. figs. 1-3). They are caused by the diffraction of the light by thin threads of quartz, which are spread before the lens at the distance 1 cm. from one another, so that the dimensions of the discharge may be easily read.

Results of the Observation.—The experiments were undertaken in order to determine which of the pre-discharges, the positive or the negative, is the more important for long sparks. Therefore the experiments always began with sparks, and then only passed over to pre-discharges by means of magnifying the electrode distance. Upon the illustrations we can see distinctly that the discharge under the given experimental conditions consists principally of a positive brush discharge. The negative part of the discharge is upon all photographs very much smaller, on the average about six times smaller, than the positive one. The middle length of the positive brush discharges amounted to 2.4 cm. at the tension of 32-35 kilovolts and an electrode distance of 5 cm. The middle length of the negative discharge is only 4 mm.; besides, the longest positive discharge was 5.5 cm. long and the longest negative only 1.0 cm. For the calculation of the middle length, only such plates were taken on which positive and negative "Schlieren" were to be seen simultaneously; 105 such photographs were obtained. It can further be demonstrated that by a change of the tension the length of the positive part of the discharge is more influenced than the length of the negative part.

Finally it may be mentioned that on moving plates, if several oscillations of the illumination-spark are employed, we can observe the temporal change of the discharge "Schlieren." The time-intervals can be estimated by the velocity of the plates. By this manner it could be fixed that the "Schlieren" rendered on figs. 1-3 (Pl. XIV.) had been

taken about $4-8 \cdot 10^{-4}$ sec. after the discharge. After $1 \cdot 10^{-3}$ sec. the "Schlieren" pictures were already indistinct, and after $2 \cdot 10^{-3}$ sec. nothing at all was to be distinguished.

Results.—By means of brush-light "Schlieren" it is demonstrated that with the long sparks—where the electrode distance is much larger than the radius of curvature of the electrodes—the spark track is produced by the positive pre-discharge.

Riga University.
June 20, 1928.

Yours faithfully,

FR. TREY,
Dr. Phil.

LXXXVI. *Electrical Properties of Neon.* By J. S. TOWNSEND, M.A., Wykeham Professor of Physics, Oxford, and S. P. MACCALLUM, M.A., Fellow of New College, Oxford*.

1. **T**HE experiments on the electrical properties of neon and helium which were made in the Electrical Laboratory, Oxford, have shown that in the development of large currents the photoelectric effect of radiation from the gas is very small compared with the effect of ionization by collision†, but the apparatus used in those experiments was not suitable for the determination of the coefficients α and β , which occur in the formula for the rate of increase of the current with the distance between the electrodes in a uniform electric field.

A new type of apparatus (fig. 1) with parallel plates was therefore made to determine the coefficients α and β , which also provided a means of comparing the effect of the radiation from the gas with other processes of ionization.

It was found to be of considerable advantage to have the apparatus enclosed in a long transparent envelope, so that a high frequency discharge could be used to examine the spectrum of the gas and to remove impurities.

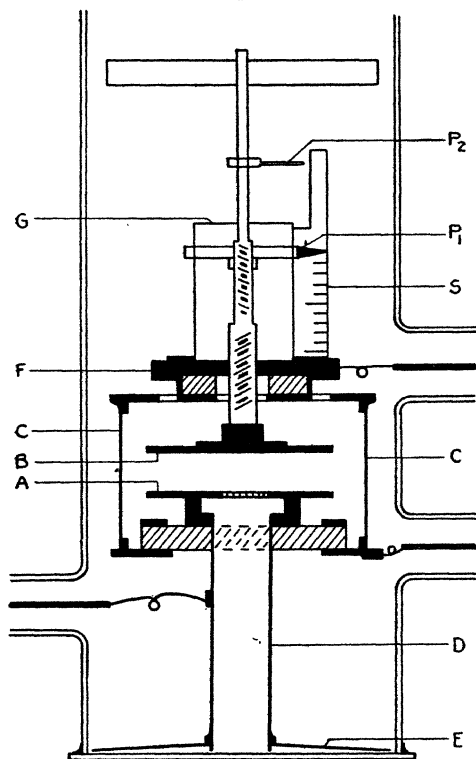
A quartz cylinder 23 cm. long and 5.8 cm. in diameter was therefore used to contain the apparatus. Flat quartz plates were fused to the ends of the cylinder, and the ultra-violet light from an external spark gap was introduced

* Communicated by the Authors.

† J. S. Townsend and C. M. Focher, *Phil. Mag.* ii. (Aug. 1926).
Phil. Mag. S. 7. Vol. 6. No. 38. *Suppl. Nov.* 1928. 3 K

through the lower quartz plate, as shown in figs. 1 and 2. All the metal parts were of nickel, except the small bar magnet which was used to rotate the micrometer screw, and the molybdenum rods with the lead seals in the side tubes for connecting to the electrodes.

Fig. 1.



The quartz side tubes and lead seals were made very carefully by Messrs. Mullard, and the joints were perfectly air tight.

It was thus possible to heat the apparatus to a high temperature to remove impurities from the quartz and metal surfaces. The experiments* on the effect of the high frequency discharge in removing small traces of im-

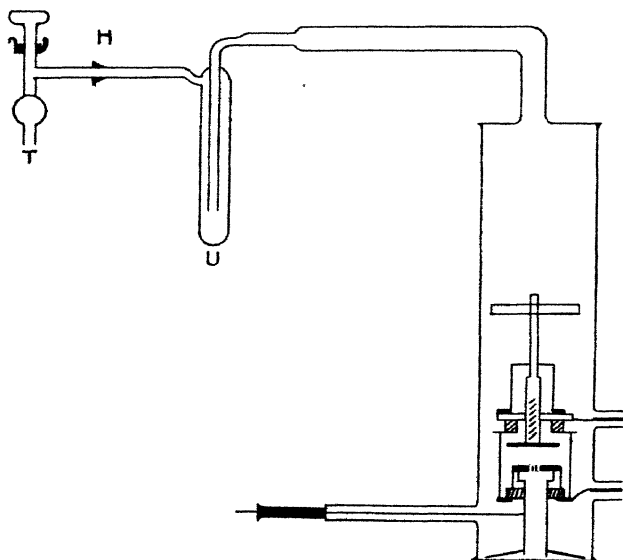
* J. S. Townsend and S. P. MacCallum, *Phil. Mag.* v. p. 695 (April 1928).

purities from neon which have already been described, were made with this apparatus.

The effects of small traces of impurities on the sparking potentials in diatomic gases have been determined by Meyer * and Dubois †. Many experiments on this subject are described in a recent paper by Prey ‡.

2. The arrangement of the electrodes is shown in fig. 1. They consisted of two parallel plates A and B, 3.5 cm. in diameter, and a cylinder C 4.5 cm. in diameter; a grid was formed by a set of parallel saw cuts .5 mm. wide and

Fig. 2.



1 mm. apart in the centre of the lower plate, through which the ultra-violet light passed and fell on the upper plate. A tube D about 6 cm. long and 1.2 cm. in diameter was screwed to the base of the plate A, and a thin plate E, 5.2 cm. in diameter, was screwed over the lower end of the tube.

The ultra-violet light from the external spark gap passed through the tube to the grid in A, and the cylinder C was screened from the light by the plate E.

* E. Meyer, *Ann. de Phys.* lviii. p. 297 (1919), and lxv. p. 335 (1921).

† E. Dubois, *Ann. de Phys.* (9) xx. (Sept. and Oct.) 1925.

‡ B. Prey, *Ann. de Phys.* lxxxv. p. 381 (1928).

The base of the plate A was fixed to quartz rods of rectangular section, and the ends of the rods were fixed to a flange on the lower end of the cylinder C.

The upper plate B was fixed to a spindle with a micrometer screw of one millimetre pitch, which rotated in a threaded hole in the metal plate F. The upper part of the spindle was reduced so as to pass freely through a small guiding hole in the cross-piece G, which was fixed to F. A short rod of soft iron was fixed to the upper end of the spindle, and the distance between the plates was adjusted by turning the iron rod with a horseshoe magnet.

The metal plate F was mounted on two quartz rods, the ends of the rods being fixed to a flange on the upper part of the cylinder C.

The four quartz rods supporting the two parallel plate electrodes were firmly clamped in positions adjusted so as to have the two plates exactly parallel.

The distance between the plates was given by a pointer P_1 on the scale S. The pointer was fixed to a small metal plate with a screw thread fitting a left-handed screw on the upper part of the spindle between F and G. Thus for one revolution of the spindle the plate B moved one millimetre, while the pointer moved two millimetres, so that the divisions of the scale were two millimetres apart and were easily seen through the quartz cylinder. The pointer P_2 was fixed to the spindle, and the distance between A and B was adjusted exactly by setting P_2 in a certain position.

The connexions to the plates A and B and the cylinder C were made with molybdenum rods through long quartz side tubes with lead seals.

All the metal parts were carefully cleaned and heated to a temperature of 500°C . in a vacuum before being assembled.

3. When fixed in position in the quartz cylinder the metal plate E rested on the quartz plate that closed the end of the cylinder, as shown in fig. 2. A quartz tube about 1.2 cm. in diameter was sealed in the upper end of the cylinder, and led through a pair of coaxial quartz tubes U to the tap T. The quartz and glass tubing were connected by a ground joint H, which was made air tight with a hard elastic cement.

The arrangement of the apparatus used to purify the gas, comprising a quartz tube containing copper oxide with an electric heater and a glass tube containing charcoal cooled with liquid air, has been described in the accounts of other

experiments which were made in the laboratory with helium and neon *.

The pure gas was admitted to the apparatus through the tap T (fig. 2), and it was intended to cool the tubes U with liquid air in order to prevent impurities from diffusing into the tap. This, however, was not found to be of much advantage. If charcoal is used in the tubes the neon is slowly absorbed when the tubes are cooled, so that in making experiments at different pressures time is wasted in waiting for the pressure to become steady. Without charcoal there is no appreciable change in the electrical properties for one or two days, when the tubes are kept cool with liquid air. When the tubes were not cooled a small change was observed after the gas had been five or six hours in the apparatus, but the amount of impurity was so small that it could be completely removed in less than one minute by a high frequency discharge in the upper part of the cylinder. This method of purifying the gas was found to be effective in removing the amount of impurity that accumulates in the gas after being one or two days in the apparatus.

4. The calculations of the ionization coefficients α and β are greatly simplified when the sparking potential V is known in terms of the product of the gas pressure p and the distance S between the plates.

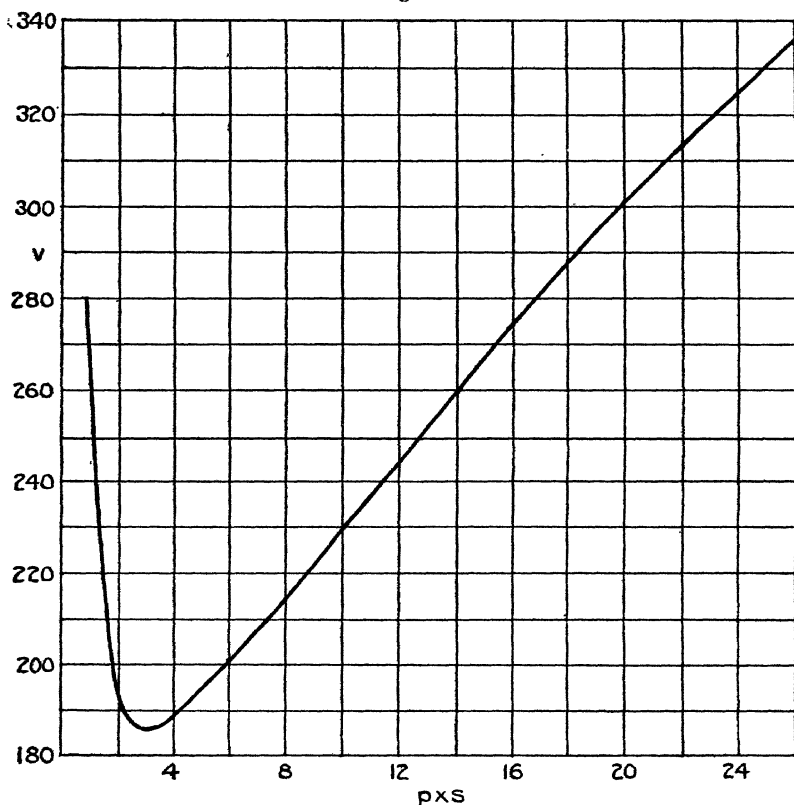
A battery of small accumulators was used to determine the potentials with a potentiometer to adjust the potential to one fifth of one volt. The connexions to the plates were made through high resistances with a galvanometer in one of the lines. The cylinder C may be insulated or connected to a point of the battery where the potential is nearly midway between the potentials of the plates. The current in the gas was observed either by the galvanometer or by the glow in the gas which was seen through a narrow slit in the cylinder C. A set of measurements were made with the plates 5 mm. apart and with 36 different pressures of the gas from 1.8 to 52 mm. The experiments were made with different specimens of pure gas within one or two hours after the gas was admitted to the apparatus. In these cases no change was observed in the sparking potential after the high frequency discharge was passed through the gas in the upper part of the quartz cylinder. The same values of V were obtained, generally within half a volt, with

* J. S. Townsend and C. M. Fochen, *Phil. Mag.* ii. p. 474 (August 1926); H. G. L. Huxley, *Phil. Mag.* v. p. 721 (April 1928).

other specimens of gas that were used in the course of the investigations. The results of these experiments are given by the curve (fig. 3), where the ordinates are the values of V in volts, and the abscissæ the product of the pressure p and the distance S between the plates.

The experiments which have been quoted * in describing the effect of the high frequency current in removing

Fig. 3.



V = sparking potential in neon in volts.

p = pressure of gas in millimetres.

S = distance between the plates in centimetres.

impurities from the gas, indicate the degree of accuracy that may be obtained in measurements of the sparking potentials with different specimens of the gas. The results taken from a curve drawn on a large scale are given in

* J. S. Townsend and S. P. MacCallum, *loc. cit.*

Table I. for definite values of the product $p \times S$ above and below the point of minimum sparking potential, which was 186 volts near the point where $p \times S = 3$. The ratio $X/p = V/(p \times S)$ is given in the third column of the table.

TABLE I.

Neon.—Sparking potentials for parallel plates.

$p \times S$.	V.	X/p .	$p \times S$.	V.	X/p .
26	336	12.9	6	202	33.7
24	325	13.5	5	194	38.8
22	313	14.2	4	189	47.2
20	301	15.0	3	186	62.0
18	288	16.0	2.5	187	75
16	274	17.1	2.0	194	97
14	260	18.6	1.6	206	129
12	244	20.3	1.2	236	197
10	229	22.9	1.0	271	271
8	214	26.7			

5. No change was observed in the sparking potential with a fresh quantity of pure gas after it had been in the apparatus for a few hours, but after one or two days there was a change of several volts. This was due to an impurity, in an amount so small that in most cases it could not be observed in the spectrum of the high frequency discharge. Occasionally a slight discoloration of the glow was noticed for one or two seconds after the discharge was started, but the discharge acts so quickly in removing the impurity that after about half a minute all traces disappear and the sparking potential is brought back to the value obtained with the pure gas and remains at that value for two or three hours.

The high frequency discharge thus provides a simple means of removing small traces of impurities, and the gas used in an experiment may be tested by finding the sparking potential before and after a high frequency discharge is passed through the gas.

As a rule the tubes U were not cooled with liquid air, and no experiments were made with gas that had been in the apparatus for more than two days, as the impurity is not

completely removed by the high frequency discharge when it is allowed to accumulate for long periods. In these cases the quartz cylinder was heated and the gas was pumped out while the apparatus was hot, and washed out once or twice with pure gas before making measurements.

It is necessary to have gas at a considerable pressure, about 10 or 20 mm., in the apparatus when the quartz cylinder is heated, in order to conduct the heat to the electrodes, otherwise some impurity may be driven on to the electrodes.

When these precautions were observed very consistent results were obtained. The experiments were frequently repeated with different specimens of gas, and there was no disagreement in the results greater than the errors that occur in measuring the electrometer currents or in reading the pressures with ordinary gauges.

6. In determining the photoelectric currents, the upper plate was connected to an electrometer with a set of condensers of small capacity to form an induction balance in order to maintain the plate close to the zero potential while the current was flowing. The lower plate was connected to the positive terminal of a battery of small accumulators, the negative terminal being connected to earth. The cylinder C was maintained at a fixed potential by connecting it to earth or to a point of the battery where the potential was less than half that of the lower plate.

The photoelectric currents n were measured with a constant electric force X and different distances x between the plates. The electrons set free from the upper plate by ultra-violet light from an external spark gap acquire energy as they move in the direction of the electric force, and after a certain point the atoms of the gas are ionized and the current increases continuously with the distance x . This effect takes place gradually, and there are no points at which the current changes abruptly until the sparking distance S corresponding to the force X is reached.

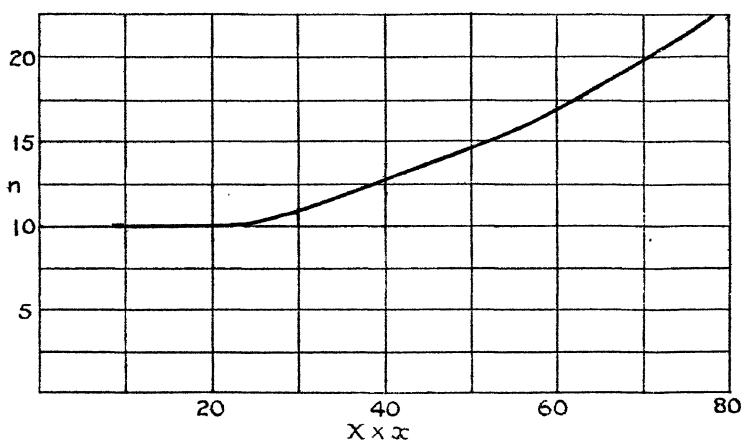
The initial stages of the process of ionization by collision may be observed with a force of 100 volts per centimetre and distances from 2 to .7 mm. between the plates. With this force the largest increases in current are obtained with a pressure of about 2.5 mm. In this case [$p = 2.5$, $X = 100$] the increase in current is about one per cent. of n_0 [the number of electrons set free per second by the ultra-violet light] when the plates are 2 mm. apart, and the potential of the lower plate 20 volts, but the current

does not attain the value $2n_0$ until the plates are about 7 mm. apart where the potential is 70 volts.

For a given value of the ratio of the electric force X to the gas pressure p the ratio n/n_0 depends only on the potential $x \times X$, and for each value of the ratio X/p the currents may be represented in terms of the potentials by a curve.

The curve corresponding to the case where $X/p = 30$ is given in fig. 4, the ordinates being the currents n and the abscissæ the potentials $X \times x$ in volts, the ordinate corresponding to n_0 being taken as 10. Thus, if the force were

Fig. 4.



Photoelectric currents in neon [$X/p = 30$].

X in volts per centimetre, x in centimetres.

100 volts per centimetre and the pressure 3.3 mm., the ratio n/n_0 would be 1.8 when the plates are 6.3 mm. apart and the potential 63 volts.

The rate of increase of the current in the initial stages, where n/n_0 is less than 2 for different values of the ratio X/p , is indicated by the ratios N_6/N_2 given in Table II. The current N_2 was obtained with plates 2 mm. apart and the potential 20 volts, and N_6 with plates 6 mm. apart and the potential 60 volts with the gas at different pressures p . The ratio X/p is given in the last column of the table, X being 100 volts per centimetre, and p the pressure in millimetres of mercury.

TABLE II.
X = 100 volts per centimetre.

<i>p.</i>	N_0/N_2 .	X/p .	<i>p.</i>	N_0/N_2 .	X/p .
7.35	1.43	13.6	1.61	1.71	62
6.50	1.48	15.4	1.165	1.60	86
5.54	1.54	18.1	.772	1.45	129
4.30	1.64	23.3	.633	1.38	158
3.32	1.73	30.1	.520	1.30	192
2.30	1.78	43.5			

7. When the electrons have traversed a certain distance x' in the direction of the electrical force the currents obtained with a constant electric force and a constant gas pressure are given in terms of the distance x between the plates by the formula

$$n = \frac{n_0(\alpha - \beta)e^{(\alpha - \beta)(x - \delta)}}{\alpha - \beta e^{(\alpha - \beta)(x - \delta)}} \quad . \quad . \quad . \quad . \quad (1)$$

for distances from x' to S , where S is the distance at which a spark is obtained.

Within this range the electrons and positive ions attain a steady motion, in which α and β are constant and independent of x . The lower limit x' is greater than the distance δ that occurs in the formula, but it is not a sharply defined point and it depends on the pressure of the gas.

If 2 mm. be taken as the shortest distance between the plates at which the currents are measured, the values of n are in agreement with the above formula for the range of distances from $x = .2$ to $x = S$, with pressures greater than 1.5 mm., when the electric force is 350 volts per centimetre. Somewhat smaller pressures may be taken with smaller forces, but if the pressure be reduced to one millimetre the currents with the plates 2 mm. apart are not in accordance with the formula, even with forces as low as 250 volts per centimetre.

In order to obtain the constant values of α and β the plates must be at distances such that the product $p \times x$ is greater than .3.

In neon there is no considerable range of distances where the current is given approximately by the formula $n = n_0 e^{\alpha x}$, which shows that the coefficient β is not very small compared with α . With this gas the simplest method of finding

α/p and β/p in terms of X/p is to determine $(\alpha - \beta)$ and the ratio $\beta/(\alpha - \beta)$ from measurements of the currents.

Equation (1) may be written in the form

$$n = n_0 \frac{e^{(\alpha - \beta)(x - \delta)}}{1 + \gamma - \gamma e^{(\alpha - \beta)(x - \delta)}}, \quad \dots \quad (2)$$

where $\gamma = \beta/(\alpha - \beta)$, and since n/n_0 is infinite when x is the sparking distance S , the following relation between δ and S is obtained :

$$(1 + \gamma)e^{(\alpha - \beta)\delta} = \gamma e^{(\alpha - \beta)S},$$

so that equation (2) becomes

$$n = \frac{n_0}{\gamma} \times \frac{1}{e^{(\alpha - \beta)(S - x)} - 1}. \quad \dots \quad (3)$$

This equation shows that $(\alpha - \beta)$ may be found from measurements of the ratios of the currents n , but in order to determine γ it is necessary to determine the ratio n/n_0 of a current n in the range from x' to S to the current n_0 due to electrons set free from the negative electrode by the ultra-violet light from the external spark gap.

8. Let n_a, n_b, n_c be three currents obtained with a constant electric force X and constant pressure p , with the distances a, b , and c between the plates where $(b - a) = (c - b)$. Three equations are thus obtained, from which n_0/γ and S , which occur in equation (3), may be eliminated and the following formula for $(\alpha - \beta)$ is obtained :

$$e^{(\alpha - \beta)(a - b)} = \frac{y_2(y_1 - 1)}{(y_2 - 1)}, \quad \dots \quad (4)$$

where y_1 is the ratio n_b/n_a and y_2 the ratio n_c/n_b .

In one set of experiments the currents n_2, n_4 , and n_6 were determined with the distances 2, 4, and 6 mm. between the plates, the electric force being 250 volts per centimetre and the gas at pressures from 1.7 to 7.4 mm. The results of the experiments are given in Table III., $(\alpha - \beta)$ being obtained by equation (4) from the ratios n_4/n_2 and n_6/n_4 .

The figures in the second and third columns show that the process of ionization represented by the coefficient β has a marked effect even at the distance of 4 mm. between the plates, since the ratios n_6/n_4 are considerably greater than the ratios n_4/n_2 . Since the steady motion in which α and β are independent of x is not attained in the distance $x = .2$ with pressures less than 1.6 mm., it is necessary to increase

TABLE III.

X = 250 volts per centimetre.

p .	n_4/n_2 .	n_6/n_4 .	$\frac{\alpha-\beta}{p}$.	$\frac{X}{p}$.
1.7	2.18	2.66	1.87	147
2.07	2.29	3.03	1.58	120
2.40	2.42	3.40	1.46	104
4.0	2.51	3.73	.92	62.5
5.5	2.41	3.61	.62	45.5
7.4	2.36	3.05	.48	33.8

the electric force in order to obtain the values of $(\alpha-\beta)/p$ that correspond to larger values of X/p .

The results of experiments with the same distances between the plates, 2, 4, and 6 mm., where the force X was greater than 250 volts per centimetre, are given in Table IV., n_4/n_2 and n_6/n_4 being the ratios of the currents.

TABLE IV.

X.	p .	n_4/n_2 .	n_6/n_4 .	$\frac{\alpha-\beta}{p}$.	$\frac{X}{p}$.
300	1.7	2.50	3.6	2.14	177
300	1.96	2.63	4.7	1.87	153
300	4.4	3.22	15.1	.98	68.2
300	6.0	3.18	13.0	.715	50.0
350	1.68	2.73	5.3	2.25	208
350	2.05	3.10	9.7	2.07	170
350	25	2.12	2.47	.126	14
350	44	1.50	1.59	.035	8
350	50	1.45	1.48	.031	7
420	35	2.21	2.70	.093	12
440	44	1.96	2.34	.060	10
176	44	1.13	1.14	? .015	4
110	44	1.11	1.12	? .010	2.5

The experiments with the gas at the pressures from 25 to 50 mm. were made in order to obtain the values of $(\alpha-\beta)/p$ corresponding to small values of the ratio X/p . In these cases it is necessary to have very large pressures as the forces

must be large in order to have large changes in the current when the distance between the plates is changed. A considerable increase in the current with the distance x is obtained with large pressures and small forces as shown by the values n_4/n_2 and n_6/n_4 in the two last experiments recorded in Table IV., but the values of $(\alpha-\beta)$ deduced from them are not accurate, as a small error in the measurement of the current gives rise to a large error in $(\alpha-\beta)$.

9. In order to show that the formula (2) gives the currents up to the distance S , at which a spark is obtained, the electric force was increased so that at the distance c , $X \times c$ is the sparking potential V . In this case $n_c/n_b = \infty$ and equation (4) becomes

$$e^{(\alpha-\beta)(b-a)} = \frac{n_b}{n_a} - 1 \quad . \quad . \quad . \quad (5)$$

$(b-a)$ being equal to $(c-b)$ as before.

The last experiment recorded in Table III. where the pressure was 7.4 mm. may be taken as an example to show that the same value of $(\alpha-\beta)$ is obtained over the range of distance from $x=2$ to $x=8$. With this pressure the sparking potential is 200 volts when the plates are .8 mm. apart, the electric force being 250 per cm. as in the measurements of the currents n_2 , n_4 , and n_6 .

Thus according to equation (5), $(\alpha-\beta)$ is obtained by the relation

$$e^{(\alpha-\beta) \times 2} = \frac{n_6}{n_4} - 1 = 2.05,$$

and from the ratios n_4/n_2 and n_6/n_4 equation (4) gives

$$e^{(\alpha-\beta) \times 2} = \frac{(n_4/n_2 - 1)}{(n_6/n_4 - 1)} \times \frac{n_6}{n_4} = 2.02.$$

In most of the experiments in which $X \times c$ was taken as the sparking potential the values of X/p were not the same as those in the above tables.

In one set of experiments the currents n_3 and n_5 were measured with the plates 3 mm. and 5 mm. apart and the force adjusted to the value $V/7$, V being the sparking potential with the plates 7 mm. apart as given by curve 1. The results of these experiments are given in Table V., the values of $(\alpha-\beta)$ being obtained by the formula (5). In this table p is the pressure of the gas in mm., V the sparking potential in volts corresponding to the product $p \times S = .7 \times p$, and $X/p = V/(\cdot 7 \times p)$.

It will be noticed that n_5/n_3 is nearly constant (about 3.2) in these experiments where the currents n_3 and n_5 are measured at the distances $3S/7$ and $5S/7$, the number $2S(\alpha-\beta)/7$ as obtained by equation (5) is $\log(2.2)$ and $S(\alpha-\beta)$ is thus found to be 2.76 for values of X/p from 13 to 53. This indicates a simple relation between the curves giving $(\alpha-\beta)/p$ in terms of X/p and the sparking potential V in terms of $p \times S$, since $\frac{\alpha-\beta}{p} = \frac{2.76}{p \times S}$ and $X/p = V/pS$.

The results of the various determinations of $(\alpha-\beta)/p$ in terms of X/p given in Tables III., IV., and V., are shown by the lower curve fig. 5, where the ordinates

TABLE V.

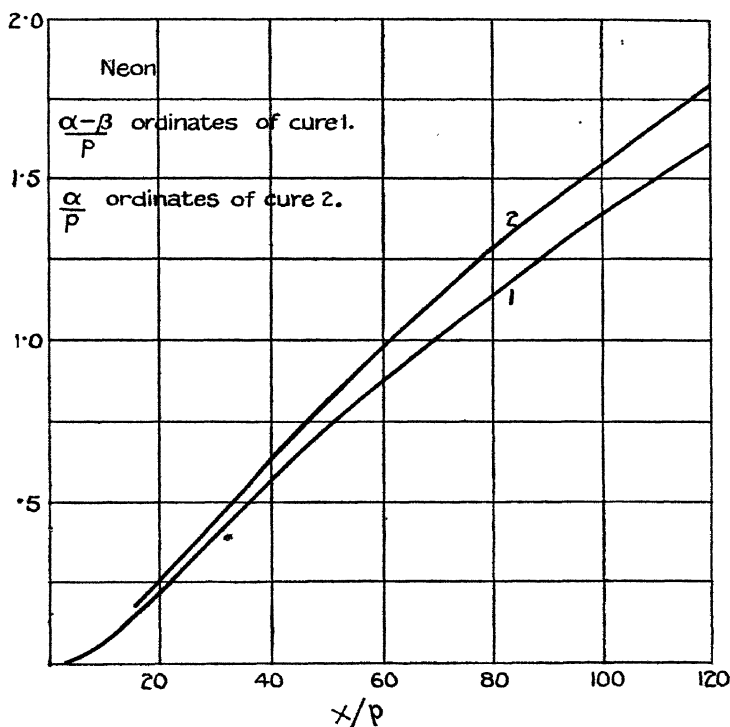
p .	V .	n_5/n_3 .	$\frac{\alpha-\beta}{p}$.	$\frac{X}{p}$.
5	187	3.25	.80	53.5
6.5	191	3.18	.60	42.0
8	198	3.20	.49	35.5
14	227	3.21	.28	23.2
16.4	241	3.12	.23	21.0
18	248	3.15	.213	19.7
27	295	3.19	.145	15.6
37.5	338	3.18	.106	13.0

represent $(\alpha-\beta)/p$ and the abscissæ X/p . The points found experimentally were plotted on a large diagram and a continuous curve drawn through them in the ordinary manner. The values of $(\alpha-\beta)/p$ for certain values of X/p obtained from the curve are given in Table VI., and the degree of accuracy may be seen by comparing the results with the numbers given in Tables III., IV., and V.

10. The quantity γ may be found by equation (3) from measurements of the ratio n/n_0 , n being the current at a distance x within the range where the currents have been found to be in agreement with equation (3). For this purpose the value of n may be taken at the distance x between the plates where the potential difference is 60 volts and $x \times p$ greater than .3. The currents n_6 obtained at the distance 6 mm. with a force of 100 volts per cm. given in Table II. may therefore be used to calculate γ , n_2 being

equal to n_0 (except in the experiments with the pressures 3.32 and 2.30 mm. where n_2 differs by about 1 per cent. from n_0). It will be observed that the quantity $(\alpha - \beta)(S - x)$ which occurs in equation (3), may be written as the product $\left(\frac{\alpha - \beta}{p}\right)\left(1 - \frac{60}{V}\right) \times pS$ where each factor has been found in terms of X/p , V , and $p \times S$ being given in terms of X/p , as

Fig. 5



X in volts per cm., p in mm. of mercury.

shown in Table II. The values of $(\alpha - \beta)/p$, V , $p \times S$, corresponding to the values of X/p given in Table II., are given in Table VI., also the values of n_2/n_0 . The values of $1/\gamma = (\alpha - \beta)/\beta$ obtained by equation (3) are given in the last column of the table, n being the current at the distance x where the potential difference between the plates is 60 volts.

The numbers in the last column show that with a constant electric force X , the ratio $\alpha/\beta [= 1 + 1/\gamma]$ increases with the

TABLE VI.

X/p .	V.	$p \times S$.	$\frac{\alpha - \beta}{p}$.	$\frac{n_3}{n_0}$.	$\frac{1}{\gamma}$.
13.6	325	24	.115	1.43	12.2
15.4	296	19.2	.145	1.48	12.1
18.1	264	14.6	.190	1.54	11.5
23.3	226	9.7	.275	1.64	10
30.0	207	6.9	.395	1.75	10.5
43.5	191	4.4	.63	1.80	10.2
62.1	186	3.0	.90	1.72	9.0
86	190	2.2	1.22	1.60	8.4
129	206	1.6	1.70	1.45	8.5
158	219	1.38	1.94	1.38	8.2
192	233	1.22	2.18	1.30	8.1

pressure. Near the point corresponding to the minimum sparking potential, $X/p=62$, β is approximately equal to $\alpha/10$, thus the ratio β/α is much greater in neon than in other gases.

The values of α/p and β/p are given in Table VII., and α/p is represented in terms of X/p by the curve 2, fig. 5.

TABLE VII.

X/p .	$\frac{(\alpha - \beta)}{p}$	α/p .	β/p .
200	2.25	2.53	.28
160	1.95	2.19	.24
120	1.60	1.79	.19
100	1.40	1.57	.17
80	1.15	1.29	.14
60	.88	.99	.10
50	.72	.80	.076
40	.57	.63	.060
30	.39	.43	.038
25	.31	.34	.031
20	.220	.240	.020
15	.140	.152	.012
12.5	.100	.108	.008
10	.058	—	—
7.5	.030	—	—

11. In order to compare the photoelectric effect of radiation from the gas with the effect of ionization by the collisions of electrons with atoms of the gas, the current i from the cylinder C to the lower plate A (figs. 1 and 2) was measured while the current n was flowing from the upper to the lower plate. In these experiments the cylinder and the upper plate were at zero potential and the lower plate maintained at a positive potential.

It is difficult to estimate the proportion of the radiation from the gas that falls on the upper plate and on the cylinder. In neon the velocity of agitation of the electrons is large compared with the velocity in the direction of the electric forces, so that the current between the plates tends to spread out towards the edges, and this effect is of importance in considering the points in the gas from which the radiation originates. An approximate calculation shows that with the plates 6 mm. apart the amount of radiation falling on the upper plate is about the same as that falling on the cylinder.

The current from the lower plate to the cylinder was, in all cases, small compared with the current between the plates. The ratio $i/(n-n_0)$ increased with the distance between the plates, and when the distance was 6 mm. this ratio was about .01 to .015, depending on the pressure.

Hence the photoelectric effect due to radiation from the gas must be small compared with the increase in conductivity due to the process of ionization represented by the coefficients α and β .

In neon the rate of diffusion of electrons is large, and as the main current n tends to spread out towards the edges of the plates some of the positive ions may move along the lines of force from the lower plate to the cylinder. The current between the lower plate and the cylinder, due to radiation from the gas, may there be much less than one per cent. of the increase of the current $(n-n_0)$ between the plates.

The fact that there was a small current between the lower plate and the cylinder shows that with the larger distances between the plates the current n between the plates is slightly smaller than it would have been if plates of larger diameter had been used.

A corresponding effect was observed in finding the sparking potentials for different pressures and distances between the plates. For a given value of the product $p \times S$ the sparking potentials were the same within one volt with the plates 4, 5, or 6 mm. apart, but with larger

distances between the plates the sparking potential increased with the distance. With the plates 7 mm. apart the sparking potentials were two or three volts greater than those obtained with the smaller distances for the same values of the product $p \times S$. For this reason the sparking potentials used in these investigations were those obtained with the plates 5 mm. apart, as given in Table I.

12. The ratio α/X , as shown by the numbers given in Table VII., has a maximum value near the point where $X/p=60$, which is approximately the value of X/p for the minimum sparking potential. Thus for a given force X there is a certain pressure $[X/60]$ at which ionization due to the collisions of electrons with atoms of the gas has a maximum effect.

The number of atoms ionized per centimetre by electrons moving in a uniform electric field is indicated by the formula $n=n_0 e^{\alpha x}$ for the rate of increase of the number of electrons with the distances x . On an average each electron ionizes one atom of the gas in moving a distance x_1 in the direction of the force when $e^{\alpha x_1} = 2$ or $\alpha x_1 = .693$. Thus the potential required to double the current, $X \times x_1$ is $.693 \times X/\alpha$. The minimum value of this potential is near the point $X/p=60$ where $X \times x_1$ is 42.5 volts. At the point $X/p=30$ the potential $X \times x_1$ is 48.5, and at $X/p=120$, $X \times x_1$ is 46.2. The fact that $X \times x_1$ increases as the pressure is increased above the value corresponding to $X/p=60$ shows that the loss of energy of electrons in collisions with atoms that are not ionized increases. The number of atoms which can radiate energy is thus increased in comparison with the number that are ionized, and if the process of ionization represented by the coefficient β were due to radiation the ratio β/α should increase as the pressure is increased. This is contrary to the experimental results which show that β/α increases as the pressure is diminished. With a constant electric force X , the ratio α/X diminishes as the pressure is reduced below the value corresponding to $X/p=60$, and since the kinetic energy of the electrons increases as the pressure is reduced, the energy of the electrons in collisions with atoms that are ionized must increase. Thus as X/p increases the electrons acquire energy greater than the minimum amount required to ionize atoms of the gas.

Taking these points into consideration the results of the experiments may be examined more closely by the method that has already been described*. In another paper we

* Phil. Mag. vol. xiv. pp. 445 and 1071 (1923).

propose to continue the investigations on these lines and to compare the properties of neon and helium, when the experiments with helium are completed with the quartz apparatus.

13. The experiments are in agreement with the hypothesis that the process of ionization represented by the coefficient β is due to positive ions. It is impossible to decide from the determinations of the currents between parallel plates which of the two effects, that of ionizing atoms of the gas, or that of setting free electrons from the negative electrode, is the more important *. Huxley's experiments on discharges between coaxial cylinders show that with small values of \bar{X}/p the principal effect of the positive ions is probably due to their actions in ionizing atoms of the gas †. The large values obtained for the coefficient β are in agreement with Huxley's experiments, which showed that the velocity of the positive ions increases rapidly with the electric force.

14. There are other points in connexion with these experiments which are of interest in considering the electrical properties of the atoms of the gas.

It cannot be supposed that the gas contained impurities in amounts that had an appreciable effect on the conductivity. The effects of small traces of impurities which get into the neon when it is kept in the apparatus increase continuously and are easily detected. When impurities are present in small amounts (which may not be observed spectroscopically), the effect on the conductivity is proportional to the amount of the impurity. For example, if a change of 2 volts were observed in the sparking potential after the gas had been 5 hours in the apparatus, a change of 4 volts was observed after 10 hours. Similar continuous changes are obtained in the values of the coefficients α and β . The fact that the impurities may be removed by two completely different methods which bring the gas to a state in which the same definite values of the sparking potential and of each of the coefficients α and β is obtained, shows that these coefficients are as characteristic of the pure gas as the lines of the spectrum.

In general it is difficult to determine the amount of an impurity required to produce a given change in the electrical properties of a monatomic gas.

With neon at a few millimetres pressure a very large

* 'Electricity in Gases,' pp. 330-332.

† H. G. L. Huxley, *Phil. Mag.* v. p. 721, April (1928).

change is produced with mercury vapour at 10^{-3} mm. pressure, and it is quite certain that gas with which the experiments were made did not contain mercury vapour at one hundredth of that pressure.

The large effect which impurities do produce in monatomic gases may be due to the fact that the velocity of agitation U of the electrons becomes very large in comparison with the velocity W in the direction of the electric force. In moving a distance x in the direction of the electric force the number of collisions an electron makes with molecules is Ux/Wl , where l is the mean free path between collisions with molecules. Thus the probability of collisions occurring with molecules which are present in small quantities increases with the ratio U/W , and a small number of molecules which are more easily ionized than atoms of a monatomic gas may have a large effect in increasing the conductivity.

15. The increase of conductivity due to ionization by collision is easily observed even when an electron collides with many atoms of the gas, as it moves in the direction of the electric force. With the gas at 44 mm. pressure, and the force 110 volts per centimetre, there is a 10 per cent. increase in the current when the distance between the plates is increased 2 mm. as shown by the figures in the last experiment recorded in Table IV.

The value of X/p in that experiment is about the same as in the luminous column of an electrodeless discharge in a tube 4 cm. in diameter with the neon at 1 mm. pressure. In this case the red lines of the spectrum are very intense, and the colour of the luminous column is a brilliant red.

The value of X/p in electrodeless discharges may be increased either by reducing the pressure of the gas or by reducing the diameter of the tube. Whichever method be adopted it is found that the colour of the discharge gradually changes from red to yellow. Hence the number of collisions which excite radiation in the red end of the spectrum diminishes in comparison with those which excite radiation of shorter wave-length, as X/p increases, or, as the kinetic energy of the electrons increases.

Thus with the smallest forces and largest pressures with which currents may be obtained, the energy of the electrons is not limited by critical properties of atoms to a value near the first resonance potential, which would prevent them acquiring energy in such amounts as are required to excite radiation in the visible spectrum or to ionize atoms of the gas.

Since the electrons acquire these amounts of energy when the ratio X/p is as small as 2.5, they must acquire energy in amounts much greater than that represented by the minimum ionizing potential when the pressure is reduced and X/p is increased to values of the order 10, or 20.

The experiments on the determination of the sparking potentials with the parallel plates show that the processes of ionization which maintain continuous currents sufficiently large to produce a luminous effect which is easily seen in the gas, are the same as those determined by the coefficients α and β in the experiments with small photoelectric currents. The small continuous currents of the order 10^{-7} ampere which are obtained with a battery of accumulators are maintained with the potential difference of $X \times S$ where S is the value of x for which the denominator of the fraction in equation 3 becomes infinite.

Thus the process of ionization represented by the coefficients α and β supply electrons at the rate which is required to maintain a continuous current of the order 10^{-7} ampere, and the collisions of the type which produce luminosity in these discharges must be supposed to occur also in the photoelectric currents*. Hence in all cases, however small the ratio X/p , the electrons acquire sufficient energy to ionize atoms of the gas and to cause atoms to radiate the long-waved light at the red end of the spectrum.

16. The sparking potentials have also been determined for helium with the improved form of apparatus in the quartz cylinder. As in neon, the sparking potentials were higher in the pure gas than in the gas with small traces of impurities, and the impurities are removed by the electrodeless discharge. The sparking potentials in pure helium are given in Table VIII. in terms of the product $p \times S$, the minimum potential being 223 volts near the point where $p \times S = 4$.

TABLE VIII.

$p \times S$	1.6	2	3	4	5	6	8	12	16
V.	360	280	230	223	225	232	249	287	324

V = sparking potentials in helium in volts.

S = distance between the plates in cm.

p = pressure of the gas in mm.

* 'Electricity in Gases,' p. 428.

These potentials are much higher than those found in earlier experiments. The method which was usually adopted to detect impurities, with a spectroscopic tube, is not sufficiently sensitive to indicate small traces of impurities which may have a considerable effect on the sparking potentials.

LXXXVII. *The Crystal Structure of Cu_9Al_4 . (δ Copper-Aluminium.)* By Dr. A. J. BRADLEY*.

[Plate XV.]

THE alloy system Cu-Al has been investigated thermally and microscopically by several independent investigators. The most recent work is that of Stockdale†, who has also made a special study of the alloys rich in copper‡. X-ray methods have been employed by several workers§, the most complete investigation by this method being that of Jette, Westgren, and Phragmén||. The results obtained by the latter do not entirely agree with the equilibrium diagram proposed by Stockdale for alloys with between 16 and 30 per cent. of aluminium. We have recently made an examination of some alloys in this range, which confirms neither of the above results, but corroborates the results of further work, done recently by Westgren and Phragmén, and communicated privately to us.

The most important point settled by this recent investigation is that Stockdale's δ -phase actually only extends over the range between 16 and 19 per cent. of aluminium. Beyond 19 per cent. of aluminium the photograms become rather difficult to interpret, and it was evident that the most satisfactory way to tackle the problem was to start by determining the way the atoms were arranged in the δ -phase, with between 16 per cent. and 19 per cent. of aluminium.

The clue to the crystal structure of the δ -phase is given by the close resemblance between the photograms of this phase and those obtained from alloys of copper and zinc containing between 61 and 69 per cent. of zinc. The structure of the

* Communicated by Prof. W. L. Bragg, F.R.S.

† Journ. Inst. Metals, xxxi. p. 275 (1924).

‡ Journ. Inst. Metals, xxviii. p. 273 (1922).

§ Owen & Preston, Proc. Phys. Soc. Lond. xxxvi. p. 14 (1923); Jette, Westgren, & Phragmén, Journ. Inst. Metals, xxxi. p. 193 (1924).

|| *Loc. cit.*

latter alloys was found by Bradley and Thewlis*, and in the present paper an attempt has been made to trace out the relationship between the two structures.

Data.

Jette, Westgren, and Phragmén (*loc. cit.*) obtained single crystals of alloys with 16 per cent. of aluminium, large enough to use for a Laue photograph. This showed that the crystal symmetry was cubic, the class being T^d , O , or O^h .

We have taken powder photographs of various alloys within the range 16–19 per cent. aluminium, and find that all the lines fit in with the assumption that the structure is cubic. The results obtained from two photographs are given below, in Table I. Copies of these photographs are shown in Pl. XV. together with a film of copper-zinc taken

TABLE I.

Σh^2 .	Radiation.	ALLOY A.			ALLOY B.		
		$\sin^2 \theta$ Obs.	$\sin^2 \theta$ Calc.	Intensity.	$\sin^2 \theta$ Obs.	$\sin^2 \theta$ Calc.	Intensity.
5	K α	·039	·039	m.-w.	·039	·039	m.-w.
6	K α	·047	·047	m.	·047	·047	m.
9	K α	·071	·071	m.	·070	·070	m.
12	K α	·095	·094	w.	·093	·094	w.
14	K α	·111	·110	w.	·109	·109	w.
18	K α	·141	·141	v.v.st.	·140	·141	v.v.st.
22	K α	·174	·172	m.	·172	·172	m.
24	K α	·189	·189	m.	·187	·188	m.
26	K α	·205	·204	w.	·202	·203	w.
27	K α	·213	·212	w.	·211	·211	w.
29	K α	·228	·227	v.w.	·227	·227	v.w.
33	K α	·260	·259	v.w.	·259	·258	v.w.
36	K α	·284	·282	v.st.	·281	·281	v.st.
38	K α	·299	·298	w.	·298	·297	w.
41	K α	·323	·321	v.w.	·320	·320	v.w.
42	K α	·331	·329	v.w.	·329	·328	v.w.
46	K α	·362	·360	m.	·360	·360	w.
48	K α	·378	·376	m.	·375	·375	m.
50	K α	·393	·392	m.	·391	·391	w.
52	K α	·408	·407	v.w.			
54	K α	·424	·423	v.st.	·422	·422	v.st.
56	K α	·441	·439	w.			
62	K α	·487	·486	v.w.			
66	K α	·518	·517	st.	·515	·516	st.

* Proc. Roy. Soc. A, cxii. p. 678 (1926).

TABLE I. (*cont.*).

Σh^2 .	Radiation.	ALLOY A.			ALLOY B.		
		$\sin^2 \theta$ Obs.	$\sin^2 \theta$ Calc.	Intensity.	$\sin^2 \theta$ Obs.	$\sin^2 \theta$ Calc.	Intensity.
68	Ka	·534	·533	w.	·531	·531	w.
70	Ka	·550	·548	v.w.	·546	·547	v.w.
72	Ka	·566	·564	st.	·562	·563	m.
74	Ka	·581	·580	v.w.	·578	·578	v.w.
76	Ka	·596	·595	w.	·594	·594	v.w.
78	Ka	·612	·611	w.	·609	·610	v.w.
81	Ka	·634	·635	v.w.			
82	Ka	·642	·642	v.w.			
90	{ Ka ₁	·704	·704	m.	·704	·703	m.
	{ Ka ₂	·708	·707	m.			
98	{ Ka ₁	·767	·767	m.	·764	·764	m.
	{ Ka ₂	·771	·770	m.			
102	{ Ka ₁	·798	·798	m.	·795	·795	m.
	{ Ka ₂	·802	·802	m.			
104	{ Ka ₁	·814	·813	v.w.			
	{ Ka ₂	·818	·818	v.w.			
106	{ Ka ₁	·829	·829	v.w.			
	{ Ka ₂	·833	·833	v.w.			
108	{ Ka ₁	·845	·845	m.	·842	·842	m.
	{ Ka ₂	·849	·849	m.			
110	{ Ka ₁	·860	·860	v.w.			
	{ Ka ₂	·865	·865	v.w.			
114	{ Ka ₁	·892	·892	st.	·889	·889	st.
	{ Ka ₂	·896	·896	st.			
117	{ Ka ₁	·915	·915	v.w.			
	{ Ka ₂	·920	·920	v.w.			
118	{ Ka ₁	·923	·923	w.			
	{ Ka ₂	·927	·928	w.			
120	{ Ka ₁	·938	·938	st.	·936	·936	st.
	{ Ka ₂	·943	·943	m.			
122	{ Ka ₁	·954	·954	m.			
	{ Ka ₂	·959	·959	w.			

for comparison. In each case the radiation employed was obtained from a hot cathode tube with a copper anticathode, the β -radiation being cut off by the use of a nickel screen. Only one β -line can be observed on each film, corresponding to the strongest α -line. At the ends of the photograms the α -doublet is clearly resolved. Only measurements from lines which are resolved have been used for the determination of the lattice dimensions. By this means it has been possible to get a high degree of accuracy in these calculations.

The number of atoms per unit cell was found to be the same in the copper-aluminium structure as in the copper-zinc structure, namely, 52. The data from which this figure was obtained are given in Table II.

TABLE II.

Radiation.	$\frac{\sin^2 \theta}{\Sigma h^2}$	Length of Unit Cell.	Density.	Per cent. Al.	Mean At. Wt.	Atoms per Unit Cell.
α_1	·007821	8·691	6·74	17·85	51·26	52·3
α_2	·007860	8·691				
α_1	·007799	8·704	6·64	18·66	50·81	52·2
α_2	·007741	8·703				

The values of $\frac{\sin^2 \theta}{\Sigma h^2}$, shown above, are the mean of all values from the lines where the α -doublet is resolved.

Derivation of the Structure of δ Cu-Al from the γ Cu-Zn Type.

The similarity between the copper-aluminium and copper-zinc photograms, which has been pointed out by Westgren and Phragmén, is so great that there can be no doubt that the structures are very closely related. The differences are, however, sufficiently marked to show that the structures are not quite the same in every respect. By carefully studying the difference it has been found possible to assign a structure to δ Cu-Al by a slight modification of the copper-zinc structure. The structure so obtained has the requisite symmetry shown by the Laue photograph. Starting out from the assumption that the structure of δ Cu-Al is based on the γ Cu-Zn type of structure, a variety of possible modifications suggest themselves. A choice between these possibilities has been made, taking the intensities of the lines as the sole guide for this purpose. The validity of the structure ultimately found rests on the excellent way in which it explains the observed intensities, including the differences in intensity of corresponding lines on the copper-aluminium and the copper-zinc photograms.

The 52 atoms in the unit cube of the copper-zinc type of structure are divided among four groups of structurally equivalent atoms, which may be called A, B, C, and D atoms

respectively. There are eight A atoms, eight B atoms, twelve C atoms, and twenty-four D atoms. The A and D atoms are zinc, the B and C atoms are copper, so that there are 32 zinc atoms and 20 copper atoms. The relative proportions of the two constituents in the copper-aluminium alloy is quite different, there being about twice as many copper atoms as aluminium atoms. The distribution of the atoms in δ Cu-Al must therefore be quite different from that in the γ Cu-Zn alloy.

This fact gives a possible explanation of the differences in the intensities in the photograms of the two alloys. The photograms differ in two ways. The relative intensities of the lines on the γ Cu-Zn photogram are not in every case the same as those of corresponding lines on the δ Cu-Al photograms. There are, moreover, some additional lines on the Cu-Al photograms which, for the most part, belong to planes with $h+k+l$ odd, indicating that the unit cube is primitive and not body-centred, as in the case of γ -brass.

These intensity changes cannot be accounted for by supposing that the *positions* of the atoms have suffered a slight *displacement*, the effect of which would be to produce a slight change in the least deviated reflexions and a much larger change in the most deviated reflexions. This is just the reverse of what one observes. It is therefore safe to conclude that the atoms, as a whole, occupy almost identical positions in the two alloys. The intensity changes must be ascribed to the differences in the distribution of atoms of the two species, and they can therefore be utilized in order to find how the copper and aluminium atoms are distributed.

The first condition imposed by the reflexions is that the unit cube of δ Cu-Al must be primitive. In order to see how this change from the γ Cu-Zn type can be brought about, it is only necessary to consider what arrangement is responsible for the γ Cu-Zn structure being body-centred. The γ Cu-Zn structure is body-centred because there is for every atom with coordinates $x y z$, a corresponding atom with coordinates $x + \frac{1}{2} y + \frac{1}{2} z + \frac{1}{2}$, and each of these pairs of atoms is of the same kind. If they were of different kinds the unit would be primitive. Thus the unit cube of the Cu-Al structure will be primitive, provided that, in at least one of the four groups of atoms, an atom with coordinates $x y z$ is aluminium and an atom with coordinates $x + \frac{1}{2} y + \frac{1}{2} z + \frac{1}{2}$ is copper. In other words, each group of atoms, A, B, C, D, may itself consist of two structurally independent sets of atoms. There are, therefore, eight possible independent sets of atoms in the δ Cu-Al structure.

Assuming that the coordinates of the atoms in the copper-aluminium structure are the same as those in the copper-zinc structure, the 52 atoms of the δ Cu-Al structure can be divided into eight sets of atoms with the coordinates shown in Table III. This division of the atoms is the only one consistent with the observed symmetry, and no other arrangement based on the γ Cu-Zn type is possible for δ Cu-Al.

From Table III. it is seen that the 52 atoms of the unit cube of Cu-Al may be divided into 4 A_1 atoms, 4 A_2 atoms, 4 B_1 atoms, 4 B_2 atoms, 6 C_1 atoms, 6 C_2 atoms, 12 D_1 atoms, and 12 D_2 atoms. A detailed examination of the differences

TABLE III.

The Coordinates of the Atoms in δ Cu-Al.

A atoms.

Subgroup 1.

$$(a\ a\ a), (a\ -a\ -a), (-a\ a\ -a), (-a\ -a\ a).$$

Subgroup 2.

$$(\frac{1}{2}+a\ \frac{1}{2}+a\ \frac{1}{2}+a), (\frac{1}{2}+a\ \frac{1}{2}-a\ \frac{1}{2}-a), (\frac{1}{2}-a\ \frac{1}{2}+a\ \frac{1}{2}-a), (\frac{1}{2}-a\ \frac{1}{2}-a\ \frac{1}{2}+a).$$

B atoms.

Subgroup 1.

$$(-b\ -b\ -b), (-b\ b\ b), (b\ -b\ b), (b\ b\ -b).$$

Subgroup 2.

$$(\frac{1}{2}-b\ \frac{1}{2}-b\ \frac{1}{2}-b), (\frac{1}{2}-b\ \frac{1}{2}+b\ \frac{1}{2}+b), (\frac{1}{2}+b\ \frac{1}{2}-b\ \frac{1}{2}+b), (\frac{1}{2}+b\ \frac{1}{2}+b\ \frac{1}{2}-b).$$

C atoms.

Subgroup 1.

$$(c\ 0\ 0), (-c\ 0\ 0), (0\ c\ 0), (0\ -c\ 0), (0\ 0\ c), (0\ 0\ -c).$$

Subgroup 2.

$$(\frac{1}{2}+c\ 0\ 0), (\frac{1}{2}-c\ 0\ 0), (0\ \frac{1}{2}+c\ 0), (0\ \frac{1}{2}-c\ 0), (0\ 0\ \frac{1}{2}+c), (0\ 0\ \frac{1}{2}-c).$$

D atoms.

Subgroup 1.

$$(d\ d\ e), (d\ -d\ -e), (-d\ d\ -e), (-d\ -d\ e).$$

$$(d\ e\ d), (d\ -e\ -d), (-d\ e\ -d), (-d\ -e\ d).$$

$$(e\ d\ d), (e\ -d\ -d), (-e\ d\ -d), (-e\ -d\ d).$$

Subgroup 2.

$$(\frac{1}{2}+d\ \frac{1}{2}+d\ \frac{1}{2}+e), (\frac{1}{2}+d\ \frac{1}{2}-d\ \frac{1}{2}-e), (\frac{1}{2}-d\ \frac{1}{2}+d\ \frac{1}{2}-e), (\frac{1}{2}-d\ \frac{1}{2}-d\ \frac{1}{2}+e).$$

$$(\frac{1}{2}+d\ \frac{1}{2}+e\ \frac{1}{2}+d), (\frac{1}{2}+d\ \frac{1}{2}-e\ \frac{1}{2}-d), (\frac{1}{2}-d\ \frac{1}{2}+e\ \frac{1}{2}-d), (\frac{1}{2}-d\ \frac{1}{2}-e\ \frac{1}{2}+d).$$

$$(\frac{1}{2}+e\ \frac{1}{2}+d\ \frac{1}{2}+d), (\frac{1}{2}+e\ \frac{1}{2}-d\ \frac{1}{2}-d), (\frac{1}{2}-e\ \frac{1}{2}+d\ \frac{1}{2}-d), (\frac{1}{2}-e\ \frac{1}{2}-d\ \frac{1}{2}+d).$$

$$a=0.10_3, b=0.16_7, c=0.35_3, d=0.30_3, e=0.04_7.$$

between the Cu-Al and the Cu-Zn photograms enables us to find out which of these atoms are copper and which are aluminium.

There are nine different ways in which the atoms may be distributed with approximately the given proportions of copper and aluminium atoms. These are tabulated below.

TABLE IV.

Possible Ways of placing the Aluminium Atoms
in δ Cu-Al.

(a) With 15.9 per cent. aluminium.

- (1) 4 A₁, 4 A₂, 4 B₁, 4 B₂.
- (2) 12 D₁, 4 A₁.
- (3) 12 D₁, 4 A₂.
- (4) 12 D₁, 4 B₁.
- (5) 12 D₁, 4 B₂.
- (6) 6 C₁, 6 C₂, 4 A₁.
- (7) 6 C₁, 6 C₂, 4 B₁.

b) With 18.4 per cent. aluminium.

- (8) 12 D₁, 6 C₁.
- (9) 12 D₁, 6 C₂.

A detailed examination of the nine possible solutions is given below, in which it is shown that arrangement (3) is the only possible solution.

Method of Elimination.

The possible solutions based on the γ Cu-Zn type of structure fall into three classes, according to the degree in which they fit in with the observations. In the first place, solution (1) can be ruled out without any detailed consideration, since it is a body-centred arrangement, which would give no reflexions from planes with $h+k+l$ odd. The remainder require fuller treatment, but, with the exception of (3) and (4), only reflexions from planes with $h+k+l$ odd need be considered in order to show that these solutions must be rejected. This greatly shortens the arithmetical work and only leaves (3) and (4) for a final detailed treatment.

Table V. gives the calculated values of $\frac{NS^2}{\sum h^2}$ for a number of planes with low indices with $h+k+l$ odd. For these calculations we have taken the scattering power of each atom to be proportional to its atomic number, so that if Cu + Al = 1, Cu-Al = 0.38, and 2 Cu = 1.38.

The structure amplitudes for planes with $h+k+l$ odd are as follows:—

A atoms,

$$S = (4 \cos ha \cos ka \cos la - 4i \sin ha \sin ka \sin la)(X_A - Y_A).$$

B atoms,

$$S = (4 \cos hb \cos kb \cos lb + 4i \sin hb \sin kb \sin lb)(X_B - Y_B).$$

C atoms,

$$S = (2 \cos hc + 2 \cos kc + 2 \cos lc)(X_C - Y_C).$$

D atoms,

$$\begin{aligned} S = & (4 \cos hd \cos kd \cos le - 4i \sin hd \sin kd \sin le \\ & + 4 \cos hd \cos ke \cos ld - 4i \sin hd \sin ke \sin ld \\ & + 4 \cos he \cos kd \cos ld - 4i \sin he \sin kd \sin ld)(X_D - Y_D). \end{aligned}$$

X and Y are numbers proportional to the scattering powers of the atoms in the respective sub-groups. Hence, if atoms in corresponding sub-groups (*e. g.* both A_1 atoms and A_2 atoms) are of the same kind, they contribute nothing to the value of S, but if the first set were copper and the second set aluminium, there might be a difference effect giving rise to a reflexion.

TABLE V.

Σh^2 .	Observed Intensity.	$\frac{NS^2}{\Sigma h^2}$								
		(1)	(2)	(3)	(4)	(5)	(6)	(7)	(8)	(9)
3	—	—	10	2	2	12	2	3	8	13
5	m.	—	3	10	11	3	1	1	5	8
9	m.	—	12	23	19	21	2	4	39	4
11	—	—	5	—	2	5	1	—	3	1
13	—	—	1	0	—	4	—	1	1	7
17	—	—	2	1	2	—	2	—	—	—
19	—	—	—	4	3	1	1	1	4	1
21	—	—	4	1	2	6	1	2	8	1
25	—	—	4	—	4	3	1	1	1	3
27	w.	—	4	7	6	3	1	2	8	5
29	v.w.	—	—	4	2	1	1	—	1	2
33	v.w.	—	11	10	9	14	1	1	12	13
35	—	—	7	2	7	3	—	—	2	4

Table V. shows clearly that only solutions (3) and (4) are possible. In order to decide between these two possibilities,

we require to consider the intensities of planes for which $h+k+l$ is even. In these cases S is given by the same formula as above, but $X-Y$ is replaced by $X+Y$. Table VI.

gives the calculated values of $\frac{NS^2}{\sum h^2}$, for the two possible solutions. In each case the value of line 18, the strongest line on the film, is put as 100. It seems that column 5 is in somewhat better agreement with the observed intensities than column 6, so that solution (3) is indicated as the true structure.

No attempt has been made to get a more accurate evaluation of the parameters, because the good agreement already obtained between the observed and calculated values indicates that the parameters of the copper-zinc structure are very closely adhered to, and with eight parameters to fix, a more accurate evaluation would be very difficult.

The observed and calculated values of the copper-zinc intensities are given in Table VI. for comparison with the values for copper-aluminium. This table may be compared with the copies of the photograms. It is evident that the differences in the distribution of the atoms in the two alloys completely account for the differences in the photograms.

Description of the Structure.

The structure of δ copper-aluminium containing 16–19 per cent. of aluminium is cubic, with 52 atoms per unit cell. These atoms have almost the same positions as the 52 atoms in the copper-zinc structure, containing 61–69 per cent. zinc. There are 16 aluminium atoms and 36 copper atoms in the “ideal” alloy, so that it may be represented by the stoichiometric formula Cu_9Al_4 , corresponding to a composition with 15.9 per cent. of aluminium. In alloys containing a slight excess of aluminium, aluminium atoms appear to replace copper atoms in a haphazard fashion, so that there is no appreciable difference in character between a 16 per cent. alloy and a 19 per cent. alloy.

The coordinates of the atoms are given in Table III. The copper atoms consist of 4 A_1 , 4 B_1 , 4 B_2 , 6 C_1 , 6 C_2 , and 12 D_2 atoms. The aluminium atoms consist of 4 A_2 atoms and 12 D_1 atoms. The structure can be best understood if the two subgroups of atoms (*e.g.* the A_1 and the A_2 subgroups) are considered separately. Each subgroup of atoms containing atoms A_1 , B_1 , C_1 , and D_1 , forms part of a cluster of 26 atoms grouped around the centre of the unit cell. A similar cluster of 26 atoms, such as A_2 , is grouped about the

TABLE VI.

Σh^2 .	Cu_3Zn_8 .		Cu_9Al_4 .		
	Observed Intensity.	$\frac{NS^2}{\Sigma h^2}$.	Observed Intensity.	$\frac{NS^2}{\Sigma h^2}$.	$\frac{NS^2}{\Sigma h^2}$.
				Case 3.	Case 4.
(1)	(2)	(3)	(4)	(5)	(6)
3	—	—	—	0.4	0.4
4	—	0	—	0.1	0.9
5	—	—	w.-m.	1.9	2.3
6	—	0.6	m.	3.9	1.1
8	—	0.1	—	0.1	0.0
9	—	—	m.	4.3	3.9
10	—	0.2	—	0.3	0.6
11	—	—	—	0.1	0.3
12	m.	5.0	w.	2.2	2.5
13	—	—	—	0.0	0.3
14	m.	3.9	w.	1.8	3.3
16	—	0	—	0.0	0.1
17	—	—	—	0.2	0.5
18	v.v.st.	100	v.v.st.	100	100
19	—	—	—	0.7	0.6
20	v.w.	0.7	—	0.3	0.9
21	—	—	—	0.1	0.3
22	m.-st.	9.7	m.	6.9	11.5
24	m.	5.8	m.	7.2	7.2
25	—	—	—	0.0	0.7
26	m.	4.1	w.	1.9	5.4
27	—	—	w.	1.3	1.2
29	—	—	v.w.	0.7	0.4
30	w.	1.3	—	0.5	0.3
31	—	0.8	—	0.5	0.9
33	—	—	v.w.	1.8	1.8
34	—	1.0	—	0.2	0.6
35	—	—	—	0.4	1.4
36	st.-m.	9.7	v.st.	12.7	10.3

corners of the unit cell. Thus we have around the centre of the unit cube 14 copper atoms and 12 aluminium atoms; and around the corners of the unit cell 22 copper atoms and 4 aluminium atoms.

The essential difference between the δ Cu-Al structure and the γ Cu-Zn structure is that in the latter case the cluster of atoms at the centre of the unit is the same as that at the corners of the unit cell. In this way the structure of Cu₅Zn₈ is analogous to a body-centred cube, whereas that of Cu₉Al₄ is analogous to the CsCl type of structure. This relation between the two structures is shown in Table VII.

TABLE VII.

Alloy.	Atoms in Centre Cluster.	Atoms in Corner Cluster.
Cu ₅ Zn ₈	Cu—4 B, 6 C. Zn—4 A, 12 D.	Cu—4 B, 6 C. Zn—4 A, 12 D.
Cu ₉ Al ₄	Cu—4 B, 6 C, 12 D. Al—4 A.	Cu—4 A, 4 B, 6 C. Al—12 D.

The structure of Cu₉Al₄ has the symmetry of the T^d class like that of Cu₅Zn₈, but the space-group is not the same, being T_1^d in the former alloy, and T_3^d in the latter case.

Summary.

(1) Powder photographs of δ copper-aluminium containing 16–19 per cent. aluminium show a cubic structure with 52 atoms per unit cell.

(2) The space-group is T_1^d , and there are eight sets of structurally equivalent atoms.

(3) There are 36 copper atoms and 16 aluminium atoms in each unit cube, corresponding to the formula Cu₉Al₄.

(4) The structure is essentially of the CsCl type, each lattice point being replaced by a cluster of 26 atoms, with tetrahedral symmetry. The cluster around the centre of the unit cell contains a different number of aluminium atoms from that around the corners of the unit cell.

(5) The coordinates of the atoms are not appreciably different from those in the alloy Cu₅Zn₈.

The author is indebted to Prof. W. L. Bragg, F.R.S., for his kind interest in this work, and to the Royal Commissioners for the Exhibition of 1851 for a Senior Studentship, enabling the work to be carried out.

LXXXVIII. *The Energy Losses of Electrons in Hydrogen.*
 By H. JONES, B.Sc.,* and R. WHIDDINGTON, M.A., D.Sc.,
 F.R.S., *Cavendish Professor of Physics, The University of*
Leeds †.

Introduction.

THE energy lost by an electron of determined velocity, suffering effective collision with a normal hydrogen molecule, is not to be deduced with any precision from the results of electron impact experiments which have hitherto been made‡. Since the ultra-violet spectrum of H_2 has been successfully analysed the energy levels of the molecule are known with accuracy, and it becomes interesting to examine the relation between these and the energy lost by electrons of various known velocities, and also the frequency with which certain excitation processes occur.

In essence the experimental method adopted consists in the passing of a beam of electrons through the gas under investigation and analysing the resulting stream by means of a magnetic spectrum device. As might be anticipated the issuing beam contains groups of definite energy, the determination of the energy differences between these groups and the relative number of electrons in each being the object of the experiment. No attempt was made to investigate the electron streams scattered in different directions. Only those electrons flung off in approximately their original direction are examined in these experiments, those scattered in different directions being made the subject of a separate investigation now in progress.

Apparatus.

The essentials of the apparatus are indicated in the accompanying diagram (fig. 1). Electrons from the filament F are accelerated towards the grid G by a suitable electric field and traverse the collision space included between G_1 and a second grid G_2 ; thereafter the composite beam is accelerated again by a second suitable electric field between G_2 and a slit system S_1S_2 , after which the fine beam so produced is deflected in a uniform magnetic field before affecting the

* Communicated by the Authors.

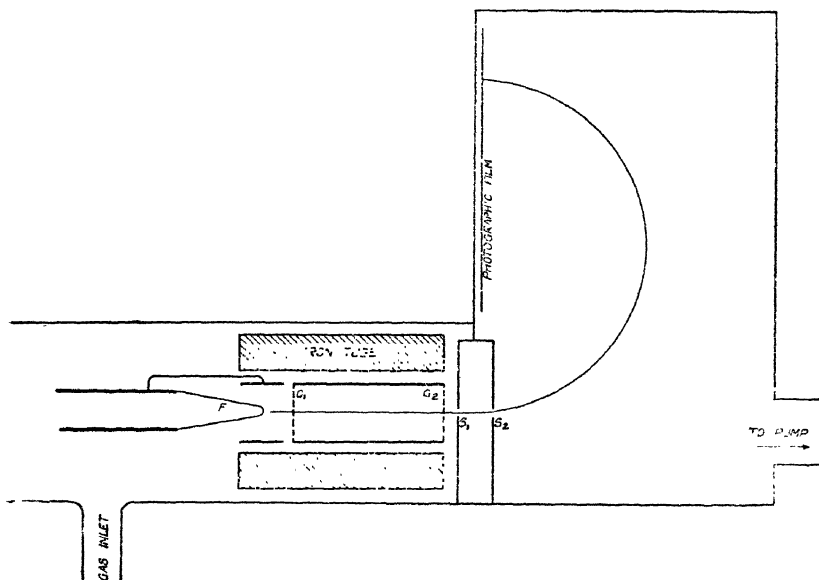
† In receipt of a maintenance grant from the Department of Scientific and Industrial Research.

‡ Franck and Jordan, 'Anregung von Quanten Sprünge durch Stöße,' p. 256.

photographic film. Since in operation the pressure in the collision space was usually about 10^{-2} mm. Hg., whilst in the camera it had to be kept at not more than 10^{-4} , a fast working pump system was chosen, viz., a Kaye Backhurst steel diffusion pump backed with a Pfeiffer rotary oil pump. This combination is very satisfactory for rapid evacuation.

The magnetic field across the camera was produced by two large coils measuring 31.5 cm. long, 23 cm. high, 15.5 cm. wide, separated by a distance of 9 cm. Calibration in the usual manner showed the field to be 22.0 gauss per ampere, and to be sufficiently uniform over a considerable region at

Fig. 1.



the centre. On account of the comparatively high values of the field employed (13 gauss) and the circumstance that the apparatus pointed north and south, it was not considered necessary to compensate for the earth's field.

The hydrogen was admitted to the all-glass apparatus through the gas-inlet shown in fig. 1, and every care was taken to ensure the purity of the gas supplied, which, electrolysed from barium hydroxide in a eudiometer, passed *via* an all-metal needle valve through the collision space G_1G_2 .

It was found convenient to have, in this part of the apparatus, the usual pentoxide tube drying arrangements,

the hydrogen being stored in a large glass reservoir at a pressure of a few centimetres of mercury, a liquid air-trap of ample dimensions intervening immediately before the above-mentioned gas inlet.

A Pirani gauge found a place on this side of the apparatus and proved to be particularly convenient for adjusting the pressure balance at any desired value, calibrated by reference to a permanently connected McLeod gauge. The Pirani readings were usually regarded as sufficient, but for the determination of the probability of excitation at high voltages, where a very accurate knowledge of the pressure is of first importance, a reading was taken directly on the McLeod gauge for each photograph.

To obtain enough photographic effect with electrons of velocity below, say, 200 volts, it is necessary to use some form of suitably sensitized films. Eastman duplitized X-ray films washed in a solution of vaseline in ether—of suitable strength—were employed *. By sensitizing large sheets and cutting off the films for use across the direction in which the sheet had been dipped, it was possible to obtain films along whose length the grease was of approximately uniform density. The necessity for the application of grease (or any fluorescent substance) must always make the comparison of intensities of widely different parts of the film somewhat uncertain. In the present experiments only portions of a few millimetres in extent were ever considered.

The Cathode and Slit System.

The principal problem in technique was that of obtaining a well-directed electron beam passing through a distance of some 3 cm. in the gas, then entering the camera, across which a uniform, or very nearly uniform, magnetic field must exist.

Two general possibilities are obvious. One may, or may not, use a compensating device over the collision space. Both methods have been tried. In the first case when no compensation is applied the electron stream in the gas follows its natural circular path of radius appropriate to the potential and magnetic field. The cathode for this purpose is introduced through a side tube inclined at about 50° to the base of the camera. For initial velocities greater than, say, 50 volts, this arrangement was fairly satisfactory for obtaining energy differences, but was not suitable for low

* G. F. Brett, Proc. Leeds Phil. & Lit. Soc. 1925.

velocities or for intensity measurements, and was not, therefore, our final choice.

Compensation may be effected by coils or by an iron cylinder suitably placed. A number of trials of both schemes led to the final adoption of a cylindrical iron shield placed in the manner shown in fig. 1.

The presence of so much iron produces a rather serious lack of uniformity in the field across the camera, a difficulty met by sacrificing the main advantage of focussing (shortness of exposure) by using two narrow slits. The first slit was 2 mm. long and 0.025 mm. wide, the second was 8 mm. long and 0.5 mm. wide, separated by a distance of 5 mm., the second being in the same plane as the photographic film, whilst the line joining the two slits was accurately at right angles to this plane. Care was taken to see that the two slits were parallel and that their direction was that of the magnetic field. In this way—since the field between the two slits is reduced by the presence of the iron—electrons which are moving perpendicular to the face of the first slit enter the camera and strike the photographic film normally. This arrangement was found to give lines of considerable sharpness.

The filaments which have been used throughout were of pure tungsten wire designed to carry a current of 0.2 ampere. They were in general 3 mm. long and were bent in hairpin form, bringing the central portion close to the grid G_1 .

The total fall of potential down the filament and leads under working conditions, *i. e.*, at the temperature generally used, was 1.24 volts, but on account of the "end effect" it could be seen that only the middle portion glowed at all vigorously. In addition, the grid—a closely-wound flat tungsten spiral—was placed at a distance of not more than 1 mm. from the centre of the filament. Consequently, the fall of potential down the effective portion could not have been more than 0.2 or 0.3 volt.

The copper cylinder surrounding the filament and connected to the negative end serves to prevent electrons passing directly to the iron cylinder. An advantage of using very small filaments consuming little energy is that exposures can be extended to any length without appreciable heating up of the apparatus. An equally important advantage is that dissociation as a result of contact with the glowing tungsten is reduced to an almost negligible amount.

When the velocity of the electrons entering the camera is below about 25 volts the photographic effect, even

with sensitized films, becomes very weak. In addition to which, external disturbances, *e.g.*, the earth's field, become relatively much more effective. This limitation has been overcome in these experiments by applying a permanent accelerating potential of 75 volts between the grid G_2 at the end of the iron cylinder and the face of the first slit of the camera. It is essential that the grid and the slit face—which are separated by about 1 mm.—shall be parallel, otherwise the electrons entering the first slit will not be moving in such a direction as to pass through the second. This, of course, applies only when the velocity of the electrons passing through the second grid is small, say one or two volts. When it is greater than this there will always be a certain number of those scattered in the collision space able to enter the camera, even when the grid and slit face are not quite parallel.

To obtain photographs giving information about the excitation probability in the neighbourhood of the critical potential requires that electrons, which after suffering effective collision, thus having velocities of one or two volts, shall in general pass a distance of one or two cm. inside the iron cylinder. The dimensions of this cylinder were such that an electron of 1-volt velocity moving within it with the external magnetic field 13.2 gauss followed a path of radius greater than 40 cm. From this it will be seen that the shielding is sufficiently complete for the present purpose. This is borne out by the photographs obtained at low voltages.

The thermionic current was measured with a Weston galvanometer of sensitivity 29×10^{-5} ampere per division. A 2-volt lamp was placed in the high-tension circuit to act as a fuse. As a rule arcing did not occur with the filament and grid separated by not more than 1 mm. unless the pressure was raised beyond 0.01 mm. Hg.

It is essential after introducing a film into the camera to continue the evacuation for not less than an hour and a half. This was necessary on account of moisture and any vapours given off by the film arising from the application of grease. After this time a reading of the McLeod gauge in general showed the pressure to be less than 10^{-4} mm. Hg., at which pressure the magnetic spectrum was found to consist of one sharp line only. There was no difficulty experienced by adjustment of the needle valve in obtaining a pressure balance of gas very close to the desired value, and in this state the apparatus was allowed to stand for five or ten minutes; the reading of the Pirani would then be taken and

the exposure made. With the small filaments used no sensible change in the pressure could be observed during exposures lasting up to fifteen minutes.

The question of the purity of the hydrogen is clearly of such importance that, although the greatest care was taken to exclude impurities, it was nevertheless thought advisable to obtain check photographs with air and oxygen*. These photographs obtained with high electron velocities were, even to a casual inspection, quite unlike those obtained with pure hydrogen under similar conditions when a single well-defined line is obtained. At velocities below 20 volts, the photographs with H_2 indicate the frequent occurrence of an additional energy loss of a smaller amount. The very characteristic dependence of the intensity of the line corresponding to this lower loss on the velocity of the impacting electrons, particularly the fact that the line completely vanishes for high velocities, removes any doubt concerning its origin.

Related to the question of impurities is that of the relative number of atoms and molecules at any instant in the collision space. As pointed out by Franck and Jordan†, the conditions favouring a maximum percentage of molecules are: (1) low pressures, (2) the use of suitable metal surfaces, (3) low temperatures, (4) extreme purity of the gas, (5) the removal of gas layers from the walls of the collision space. In the present experiments the first four points were fairly well complied with, but the last condition was not, since it did not appear practical to bake out the metal parts before each exposure. Favouring a large percentage of molecules was the circumstance that a continuous stream of gas was being passed through the collision space. It is to be expected then that the energy losses shown in the photographs are related to the molecular, not the atomic, levels. With hydrogen, as the numerical results will show, this is the case.

Calculation of Data from Photographs.

As already pointed out, the photographs of the magnetic spectrum with gas present, of which just a single illustrative

* The figures give the energy losses of the primary electrons in volts, and the remarks refer to the corresponding lines on the photographs.

Oxygen .. 16.1 (weak), 13.0 (strong), 10.8 (weak), 8.1 (strong).

Air 13.6 (very strong), 8.6 (very strong).

These results are only approximate, the lines on the air photograph being probably combinations of lines due to both oxygen and nitrogen lying in this neighbourhood.

† Franck and Jordan, *loc. cit.* p. 259.

example is reproduced here (fig. 2), usually consist of several separated lines or bands, the least deviated line corresponding to the full velocity electrons which may have come directly from the filament or more usually by way of one or more elastic reflexions. It is convenient to express any other lower velocity line in terms of the energy difference in volts between it and the full velocity line.

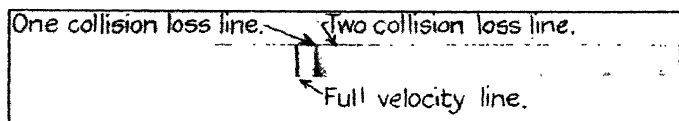
In the initial experiments when the focussing device was employed, which makes use of a very wide second slit, the velocity corresponding to a line at a distance l from the bottom of the film is

$$V \text{ (volts)} = \frac{H^2}{8 \cdot 10^8} \cdot \frac{e}{m} \{a^2 + (b+l)^2\}$$

a = distance between the two slits.

b = distance from the centre of the second to the bottom of the film.

Fig. 2.



In the final apparatus the second slit was also narrow and much closer to the first. In addition, the presence of the iron cylinder reduces very considerably the field in its immediate neighbourhood, and to a lesser extent over the whole region of the camera. Consequently, a being now effectively zero may be dropped out of the equation, b was measured and found to be 0.75 cm. The equation used was thus

$$V = K (\cdot 75 + l)^2.$$

The constant K being determined by calibration for the small range of the film which was actually used. This was done for two values of the magnetic field employing 13.20 and 16.28 gauss, the total applied potential being in the first case varied from 80 to 100 and in the second case in the neighbourhood of 150 volts. From these two measurements the two values of K were found in the usual manner. The error in the determination of differences can be estimated by observing that the first factor of

$$\delta V = 2K (\cdot 75 + l)\delta l$$

can be found to within 1 per cent., as shown by the values of V calculated from l , and the second part can also be determined to less than 1 per cent. The error to be expected in measurements of energy losses is thus somewhat greater than 1 per cent. The values given in Table I. bear this out fairly well, as most of them can be included within the mean value ± 0.2 volt.

When the adjustment of the cathode with respect to the camera slit system is satisfactory and no gas is present in the collision space, then, as can readily be seen, the single lines obtained corresponding to the applied accelerating potential will consist of two parts, which in general will be approximately superimposed. First, the electrons issuing from an almost point source move down towards the camera in very nearly straight lines, and the mark due to the direct beam will have a width limited by the length of the first slit, *i. e.*, 2 mm. Secondly, a number of electrons will suffer collision at the metal boundary or slit walls and may, in general, have all directions as they pass through the first slit; thus these will produce a line of uniform density stretching across the whole of the exposed part of the film. When gas is present this "uniform" line will be enhanced by the elastic, or almost elastic, collisions which occur with the gas molecules. As might be expected, it was only in exceptional cases that the alignments (including in addition that of the magnetic field) were sufficiently accurate to bring the part due to the direct beam into the centre of the film. The portion due to the direct beam is very much more intense than the second part and, as indicated here, is usually slightly higher up the film, but by an amount which is certainly not more than a few tenths of a volt. It is, however, a point of considerable interest, since in almost all the photographs which have been measured or photometered, the intense part due to the direct beam was at either one or other edge of the uniform line, and, consequently, all measurements referring to losses are made to the centre, *i. e.*, the point of maximum intensity of this last-mentioned part, and may thus be less than the true value by any amount up to 0.4 volt. With hydrogen present at the pressures usually employed, this line should be due mainly to electrons which have been reflected from the surface of the metal walls rather than to electrons which have suffered collision with the gas molecules; but for those cases in which the alignment was accurate, the uniform part of the full velocity line must arise from electrons scattered by the gas, since any reflected at the cylinder walls would subtend too great an angle to

register on the film. This is borne out by the fact that, in such cases, the uniform portion of the line is of the same order of intensity as the line due to electrons which have suffered effective collision. From this it follows that the numerical value of the loss at high voltages given in Table I. can only be regarded as setting a lower limit to the energy loss, the upper limit, however, being not greater than 0.4 volt beyond this value. Fortunately, less ambiguous results can be obtained for the true amount of energy lost by fast electrons from the photographs showing the effect of double collision—a point mentioned later in more detail.

Results.

The photographs obtained with hydrogen can most easily be described by considering them in three groups.

- (1) Those obtained with high electron velocities, above 50 volts and moderate gas pressures, *i. e.*, not greater than 10^{-2} mm. Hg.
- (2) Those obtained at high velocities about 150 volts and higher gas pressures of the order of 3×10^{-2} mm. Hg.
- (3) Those obtained with low velocities, below 25 volts, and moderate pressures.

TABLE I.

Photo.	Pressure, mm. Hg.	Velocity in collision space, volts.	Total final velocity, volts.	Energy loss, volts.
1	0.007	16	91.0	12.13
2	0.009	17	93.2	12.38
3	0.011	17	92.0	12.53
4	not measured.	24	98.0	12.18
5	„	24	98.0	12.08
6	„	24	97.8	12.03
7	0.009	25	97.0	12.21
8	0.009	26	89.0	12.53
9	0.009	30	103.8	12.31
10	0.008	50	98.0	12.22

Mean Energy loss = 12.26 volts.

(1) Of these photographs a number were chosen which appeared the most suitable for measurement, both on account of the clearness of the lines and because of the definiteness with which the conditions of the exposure were known, and the results of the measurement of all these are given in Table I. The loss given here is the only one which appears with certainty on photographs taken at high velocities; it also appears, however, at low velocities, and, consequently, the measurements given are not restricted merely to the former case. It may be that part of the small variations to be observed in Table I. is due to the distance between the points of maximum intensity of the full velocity line and of the loss line expressed in volts actually varying slightly under different conditions, a variation due perhaps to the small losses of energy which the electrons suffer either in collision with the gas molecules or by reflexion at the metal surfaces during "elastic" collision. Photographs taken with high electron velocities and low gas pressures all show a single well-defined loss line of considerable intensity, in addition, of course, to the full velocity line. It appears hardly necessary to mention that what may be called purely instrumental effects such as lack of uniformity of the magnetic field, fall of potential down the filament, contact potential differences and such like, cannot directly affect the magnitude of the energy differences. To the low velocity side of this 12 volt loss line, as appears on some of the photometric curves, there is an indication of another line or edge at about 14 or 15 volts. This corresponds possibly to the edge of the continuous absorption spectrum as given by Dieke and Hopfield at 14.53 volts, and is considered later.

(2) The photographs obtained in this group at high gas pressures were intended primarily to furnish values of the excitation probability at high velocities (see p. 902), but they can also be used to provide the correction for the error which is introduced by the slight uncertainty of the full velocity line. These photographs (one of which is reproduced) show two loss lines: the first very strong, being the one already considered, which arises from electrons having suffered a single effective collision; the second being due to electrons which have suffered two such effective collisions. The true value of the energy lost by the electron in this particular type of collision will be given by the voltage separation between the first and second loss lines, whilst the difference between the first and the full velocity line will give

a value like the mean of Table I. Measurements made on five photographs of this sort showed that the true energy loss was 0.36 volts greater than the mean value of the separation between the first loss and the full velocity line. The resulting value of the energy lost in collision is then 12.6 volts to within the accuracy of these experiments, which may be estimated for the mean as about 1 per cent.

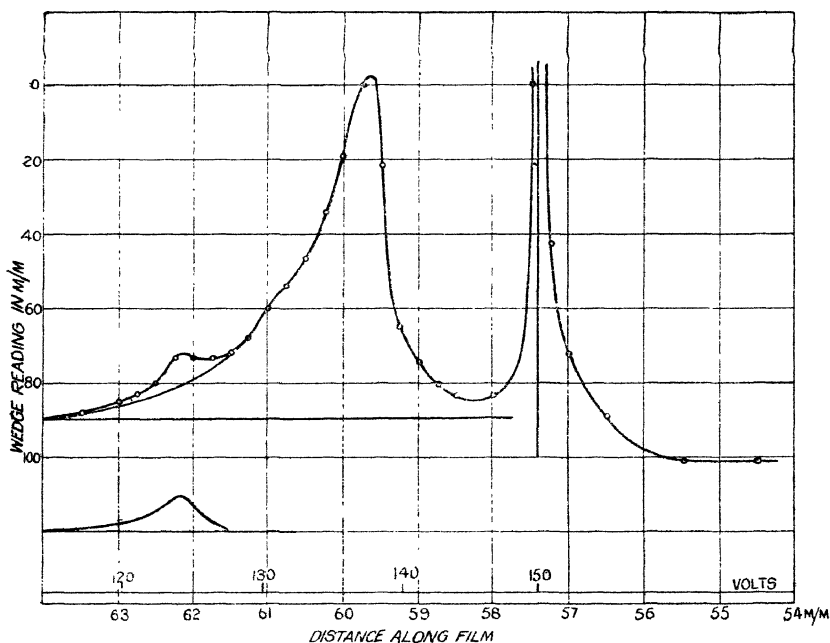
(3) Photographs obtained at low excitation velocities differ from those taken at high velocities, the change being a gradual one as the accelerating potential is reduced.

In this apparatus, where only the electrons which are flung forward through a very small angle are examined, the change is first to be observed at approximately 26 volts. At this potential a faint line appears at a distance corresponding to a loss of 9.1 volts. Naturally as the line is faint at this voltage, the accuracy of the measurement is small, and the value given might be in error by a few tenths of a volt. At lower potentials the intensity of this line increases very greatly, until at 18 or 16 volts it is comparable in intensity with the line at 12.6 volts. At still lower potentials from 13 to 14 it again vanishes, a number of photographs being obtained at these very low potentials, and on none, although the 12.6 line can always be seen, does the other appear. When the velocity was below that required to stimulate the 12.6 loss, the photographs showed only the single line corresponding to the applied accelerating potential, but to the low velocity side of this there was, in general, a very faint shading extending a distance of some 4 or 5 volts. At potentials about 16 volts, *i. e.*, the lowest at which this second loss occurred strongly, there exists shading between this line and the full velocity line. The point of maximum intensity corresponding to this loss does not appear to be a definitely fixed value independent of the excitation conditions. The photographs (1, 2, 3, and 23) show this line strongly and clearly, and the differences in the value of the loss are certainly due to the actual displacement of the point of maximum intensity. That this displacement is due to extraneous causes is made untenable by the fact that the measurements of the 12.6 (or direct mean 12.26) line on the same photographs give normally good values. These results are not as surprising as may at first sight appear when it is observed that this loss is probably connected with the dissociation of the molecule. Table II. gives the loss in volts corresponding to the maximum of this line. The measurements for this table have been taken from

TABLE II.

Photo.	Pressure, mm. Hg.	Velocity in collision-space, volts.	Total velocity, volts.	Loss, volts.	Ratio of Intensities.
23	0.007	16	90	8.64	
1	0.007	16	91	7.30	0.24
2	0.009	17	93.2	8.62	0.13
3	0.011	17	92	8.13	0.17
24	0.010	18	81.5	9.03	
8	0.009	26	89	9.59	0.03

Fig. 3.



photometric curves similar to fig. 3 which has been obtained from the spectrum reproduced above.

Besides the determination of the energy-loss, estimates have been made of the relative intensities of the two "lines" for a few different voltages. This has been done by comparing the areas under the two maxima on the photometric curves corresponding to the 12.6 and the lower loss.

As the photographic effect of slow electrons occurs through the intermediary action of the fluorescent grease

with which the films are sensitized, the intensity of the blackening will be related to the number of electrons in the beam, in the same way as the blackening depends upon the intensity of light in the ordinary case. If the blackening is not too intense, the photographic density may be taken as proportional to the intensity of the incidental light. Since the distance along the wedge of the photometer employed is proportional to the photographic density, and as the ordinates of the photometric curves are just the wedge-readings, these will be proportional to the number of electrons in the beam producing the mark. Thus the relative number of electrons having suffered the 12.6 and the lower loss will be given directly by the ratio of the areas on the photometric curves under their respective maxima. In the last column of Table II. are given the values of these ratios for a few cases. The photographs from which these ratios were obtained differed from those taken for ordinary energy-loss measurements only in that special care was taken to obtain a perfectly steady thermionic current and to measure this and the time of exposure (usually 4 or 5 minutes) accurately. The greatest difficulty in making measurements of intensities was that of obtaining a suitable reference line on the photometric curves. During an exposure the whole of the film is slightly darkened by electrons which are scattered within the camera. Moreover, all those electrons which are scattered near the slits (and most of them should be, since the gas is leaking through this way into the camera) will strike the film somewhere below the line corresponding to the applied potential. Consequently, it does not appear justifiable to use the flat part of the curve beyond the full velocity line as the reference level, rather should that part be regarded as the true zero which becomes flat below the loss line. In the treatment of the graphs, such as that shown, the centre of the full velocity line was first drawn, being determined from the upper part of the corresponding peak. This latter was then made symmetrical and the right-hand side of the first loss peak constructed by subtracting the ordinates. The left-hand part of this peak was then extrapolated to the base-line, and the right-hand side of the second loss peak determined as in the first case. For the curves referring to photographs taken at high velocities for the determination of the probability of excitation in which the second line is much fainter than the first, the adopted method was to extrapolate the curve of the first line, subtract the ordinates, and construct the curve of the second line from these. In addition, it is known that the second curve must be of the same form as the first, with

the ordinates diminished in a certain constant ratio. This serves as a check on the extrapolation.

Determination of the Probability of Effective Collision.

Although at the present time there are a few quantitative results on the probability of excitation by electron impact for electron velocities in the neighbourhood of the excitation potential, yet there appears to be no data giving the value of this probability for velocities exceeding the critical potential by some 100 volts. Seeliger and his collaborators have determined the relative excitation probabilities (or quantities closely allied) for these velocities by spectroscopic means. The experiments described here give a direct method for measuring the value of this probability at high velocities. Results are given for the $A \rightarrow C$ transition of the hydrogen molecule at a velocity of 150 volts.

The essential feature of the method is the obtaining on a single photograph of two lines, one due to electrons which have suffered a single effective collision, the other to electrons which have suffered two effective collisions. As will be readily seen, the ratio of the intensities of these two lines, a knowledge of the gas-pressure and the path-length, is sufficient to determine the absolute value of the probability of excitation.

The work of Lenard and others shows that a fast electron is deflected from its path or loses energy when it passes within the boundary determined by the gas kinetic radius of the molecule. This is equivalent to putting the mean free path of a fast electron equal to $4\sqrt{2}$ times the molecular mean free path.

Now let p be the probability that an encounter (as just defined) shall result in the stimulation of the molecule to a certain state, and the flinging off of the electron in approximately the same direction as that of approach. If the path-length in the gas be d the probability that an electron shall suffer one and only one encounter is $\frac{d}{\lambda} e^{-\frac{d}{\lambda}}$, where λ is the electron mean free path. Thus for the intensity of the first line we put

$$I_1 = \text{const. } p \cdot \frac{d}{\lambda} e^{-\frac{d}{\lambda}}.$$

The probability that an electron shall suffer its first encounter between x and $x + \delta x$, lose energy, and be flung off in the same

direction is $pe^{-\frac{x}{\lambda}\frac{\delta x}{\lambda}}$. The probability that it shall then suffer one and only one encounter in the remaining distance is $\frac{d-x}{\lambda}e^{-\frac{d-x}{\lambda}}$. Multiplying together and integrating from 0 to d , and multiplying by p , we have for the intensity of the second line

$$I_2 = \text{const. } p^2 \frac{d^2}{2\lambda^2} e^{-\frac{d}{\lambda}},$$

the constant in each case clearly being the same.

$$\therefore p = \frac{2\lambda}{d} \cdot \frac{I_2}{I_1}.$$

The quantity p which is determined by the experiment is not the true excitation probability; but for high electron velocities it approaches this within 1 or 2 per cent. as the results of Langmuir and also of Dymond show. This conclusion can also be drawn from many of the photographs obtained in these experiments. As already explained, when the alignment is such as to bring part of the direct beam into the camera, there is produced a short, very intense line, superimposed on the uniform part of the full velocity line. It is found that there is a corresponding increase of intensity in the 12.6 loss line at the same position. The meaning of this clearly is that the beam composed of the electrons which have lost 12.6 volts, expands only a little at high velocities from the original full velocity beam. In other words, most of the electrons are flung through only a very small angle when suffering effective collision at high velocities.

Table III. gives the values of the excitation probability taken from the only photographs which were photometered. It appears that it is of the order of 1 or 2 per cent. The mean of the first four values relating to an electron velocity of 150 volts is 0.015.

Relation between the Energy Losses of the Electrons and the Spectroscopic Term Values of H_2 .

The result of an electron impact with an atom, as far as energy interchanges are concerned, can be given a straightforward interpretation. The energy lost by the electron is very nearly equal to the energy difference between two states of the atom. In the case of an impact with a molecule,

it is still true, of course, that the energy is conserved, but that gained by the molecule will in general be distributed between the electronic and the nuclear states. The process of excitation, according to Franck *, occurs in the first place by the change of the electronic state, the nuclear motion being affected only indirectly as a result of the sudden change of binding. This picture has been justified to some extent by Condon †. When the stimulation occurs by the impact of a fast electron, say of 100 volts or more, it is to be expected that the molecule will be raised to some higher electronic state and that the primary electron will have lost this energy and passed on before the nuclei respond to the altered binding. Thus it is to be expected that the energy lost by a fast electron in collision with a gas-molecule will be equal to the change of energy due to the transition of the

TABLE III.

Photo.	Velocity, volts.	Ratio of Areas.	Pressure ‡, mm. Hg.	Excit. Prob. <i>p</i> .
18.....	150	0.053	0.0275	0.011
19	150	0.073	0.0204	0.020
20.....	150	0.056	0.0207	0.015
21.....	150	0.057	0.0255	0.013
22.....	98.8	0.060	0.0245	0.014

electronic state plus vibrational energy of an amount corresponding to the potential energy of the two nuclei in the higher electronic state, but with their original separation.

In order to estimate the amount of the vibrational energy imparted to the molecule, one only needs to draw the curve showing the energy of the molecule in a particular electronic state for various separations of the nuclei. When the band spectrum has been sufficiently analysed so that the vibrational and rotational constants are known, it is possible to do this for small values of $(r-r_0)$, where r_0 is the equilibrium

* Franck and Jordan, *loc. cit.* p. 252.

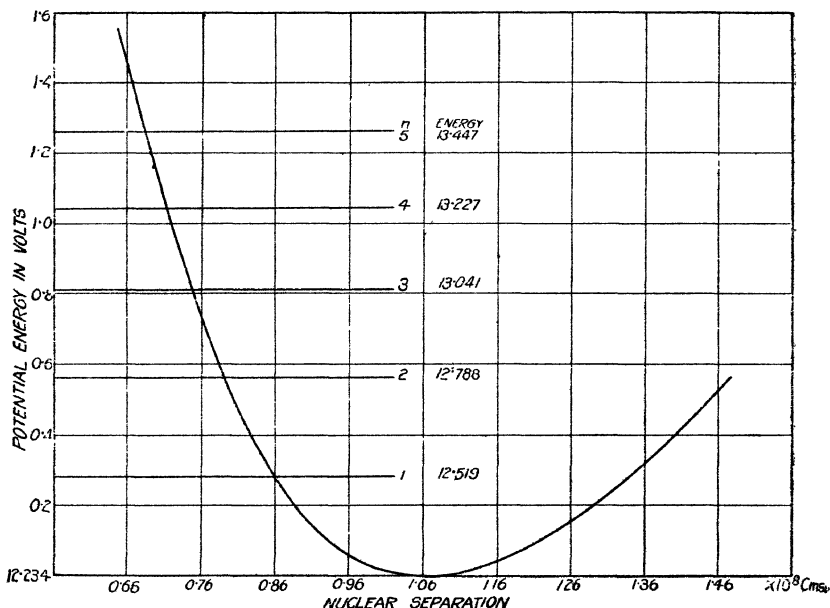
† Condon, Proc. Nat. Acad. Sc. xiii. p. 466 (1927).

‡ Owing to the smallness of p , the gas-pressure was raised in these experiments to the greatest practicable value so as to make λ as small as possible. This greatest pressure was found to be about 0.03 mm., the limit being set by the necessity of (1) preventing too rapid a leak through the slit into the camera; (2) providing the filament with a reasonably long life; (3) guarding against too frequent arcing between filament and grid.

separation. If the force between the two nuclei be expanded as a power series in $(r-r_0)$ the first three coefficients k_1 , k_2 , k_3 can be obtained from the band constants. Using the numerical data recently collected by Birge *, fig 4 referring to the C state of H_2 has been drawn showing the relation between the potential energy and the nuclear separation.

It is seen that when the nuclear separation in this state is equal to that in the normal A state, i. e., 0.76 A.U., the potential energy due to the displacement of the nuclei

Fig. 4.



=0.74 volt. It appears, then, that a collision with a fast electron resulting in the transition to the C state will involve the stimulation of vibrational motion and that the most probable values of the vibrational quantum-numbers are $v=2$ or 3. The point of maximum intensity on the photographs would be expected, therefore, to correspond to a loss of some value between 13.0 and 12.78, the precise position depending on the relative numbers which lose one or other of these values. Actually the adopted mean from the given measurements lies at 12.6 volts, but this is sufficiently near

* Birge, Proc. Nat. Acad. Sc. xiv. p. 12 (1928).

to make it likely that this line is rightly allocated to the C state. Still more convincing evidence on this point is that Hori, when examining the ultra-violet emission spectrum of H_2 stimulated by electrons of velocity varying up to 200 volts, found that only the bands corresponding to the C \rightarrow A transition were emitted at all strongly. It is noteworthy that unless there be some factor in the process of excitation by electron impact which tends to make one, or perhaps two, neighbouring vibrational levels much more probable than the rest, then our photographs would not show anything like a line at all, since the vibrational levels of the C state, according to Dieke and Hopfield * extend from 12.23 to 14.53 volts.

The complete absence of any line at 4.34 volts for high electron velocities may be regarded as additional direct evidence for the already well-established fact that high-velocity electrons are ineffective for producing dissociation by direct means, *i.e.* by yielding up just sufficient energy to carry this process out without simultaneous excitation of some electronic state.

A review of the older work on the measurement of critical potentials in hydrogen reveals, at all events, one feature which appears reliable, in that it is common to most observations. This is the existence of a strong radiation potential in the neighbourhood of 12.6 to 12.9 volts. It is to be remembered that the energy losses measured in this way are those sustained usually by electrons whose velocity is in the immediate neighbourhood of the excitation potential considered. Nevertheless, since the photographs obtained at low velocities (13 or 14 volts) still show the line corresponding to the A \rightarrow C transition (though of much reduced intensity), it appears that the above-mentioned critical potentials arise in the same way as the lines on our photograph, *i.e.*, by stimulation to the C state.

As already mentioned, at high velocities, apart from the 12.6 volt line (and the shading to the low-velocity side), there appears nothing else of noticeable intensity. Now the next lowest after the ground state is the 2^1S state, or the B of Dieke and Hopfield's notation. The non-vibrating level of this lies at 11.1 volts beyond the normal state. It appears, then, that the excitation of this state must be relatively very infrequent. This is in agreement with Hori's observation that the Werner bands always appear much more strongly than the Lyman bands even at low velocities. As

* Dieke and Hopfield, *Zs. f. Phys.* xl. p. 299 (1926).

a reason for this, it may be suggested that since the equilibrium separation of the nuclei for the 2^1S state is 1.55 A.U. , and that of the normal 1^1S state 0.76 A.U. , when excitation to the 2^1S state occurs by the action of a fast electron, the potential energy imparted to the nuclei, as a result of the altered binding, will be great, corresponding to a displacement of 0.79 A.U. Thus, if an impact with a fast electron is to result in the transition to the B electronic state, then this must be accompanied by the stimulation of a vibrational state of high quantum-number, or more likely by dissociation. Now according to Dieke and Hopfield, the limit of the B state is common with that of the C state, and lies at 14.53 volts . It would thus appear that is the significance of the increased intensity in the shading to the low-velocity side of the 12.6 volt line lying at 14 to 15 volts , which is especially prominent on the photographs taken at high velocities, as appears from the photometric curves. The products of the dissociation at 14.53 volts are given by Dieke and Hopfield as a neutral atom and an atom in the first quantum state, *i. e.*, the 10.15 state, this giving a value of 4.38 for the dissociation potential. If the energy imported as a result of the collision be somewhat less than 14.5 volts , the molecule may be left in the B state with strong nuclear vibration. It is generally considered that returns from such states to the ground A state will result in dissociation and the emission of the continuous spectrum. In a word, then, collisions of fast electrons resulting in the stimulation of the B state might be expected, first, not to require 11.1 volts , but something in the neighbourhood of 14 , and, secondly, to result not in the stimulation of the Lyman bands, but rather in that of the continuous spectrum.

The photographs obtained at low velocities appear to be rather surprising, but the large number taken under various conditions, and even with different forms of apparatus, forces one to the conclusion that low speed electrons may lose energy as a result of collision with some form of hydrogen of an amount much greater than the dissociation potential, but less than the first excitation stage of either the atom or the molecule. Moreover, for given conditions (mainly the accelerating potential) there is one value of the energy loss much more probable than any other. This is shown by the maximum to be seen on the photometric curves. It is especially to be noticed that when the accelerating potential is less than 14 or 15 volts , this loss of energy does not occur with sufficient frequency to produce a noticeable line on the photographs. Thus it would appear possible for it to be made

evident by the critical potential methods, since the number of electrons losing this energy increases gradually as the velocity is increased, without there being any well-defined threshold potential.

It was at first suggested * that this effect might correspond to the excitation of H_3 , as relatively large quantities of H_3^+ are known to exist under the discharge conditions employed. The rare appearance of the loss below about 15 volts suggested that H_2^+ was in some way connected with its occurrence, and this it is known is necessary to the formation of H_3 .

It seems more likely, however, that this line appearing at low velocities is intimately connected with the dissociation of the diatomic hydrogen molecule. The fact that the most probable loss, *i. e.*, the loss corresponding to the point of maximum intensity, is not a definite amount, but increases as the velocity of the primary electrons increases from 16 to 20 volts, makes it unlikely that it corresponds to any particular excitation state of any kind of molecule.

When the initial velocity of the electron, suffering collision with the molecule, corresponds very nearly to the energy separation of the two states between which the transition occurs, it might be expected that the electron and molecule will remain in interaction for a time sufficiently long to allow the nuclear motion to affect the amount of energy finally lost by the electron. The energy lost under consideration may be due, therefore, to an excitation process, which finally results in the dissociation of the molecule and the emission of radiation which forms part of the continuous spectrum. It is interesting to notice in this connexion that Oldenberg † has found that the continuous spectrum, but not the Lyman bands, is strongly excited by electron impacts in pure hydrogen, but when argon is present Lyman bands appear strongly and the continuous spectrum very weak. The two thus appear to be closely related and probably due to the same initial electronic excitation, *i. e.*, to the B state. The essential difference is, according to Oldenberg, that with argon present (the excitation occurring then by collisions of the second kind with the excited argon atoms) the vibrational energy is limited to that of the third state, whilst in the other case high vibrational states may occur, and therefore dissociation in the resulting transition which produces the radiation of the continuous spectrum. The work of

* Jones and Whiddington, Proc. Leeds Phil. & Lit. Soc., July 1928.

† Oldenberg, *Zs. f. Phys.* xli. p. 1 (1927).

Hughes and Skellett* shows that dissociation occurs almost certainly as a result of a simple process, *i. e.*, not a secondary effect, and, moreover, that the dissociation does not set in until the electrons have a velocity of 11 or 12 volts, and increases for higher potentials. These results fit with the observation first made by Horton and Davies† of the excitation of the continuous spectrum at low velocities. They gave tentatively as the lower limit for excitation 12·6 volts.

Finally, then, it appears that (1) the loss not being a definite one, independent of the excitation conditions, suggests that it is connected with dissociation; (2) results like those of Hughes and Skellett indicate that dissociation is connected with the emission of the continuous spectrum, since there appears no other way of accounting for the balance of energy, and does not occur until the electrons have a velocity of about 12 volts; (3) Oldenberg's results may be taken to indicate that the continuous spectrum is intimately connected with the excitation of the B electronic state, and this, as has been previously mentioned, would apparently require the impacting electron to have an initial velocity somewhat greater than the 11·1 volts necessary to stimulate the B_0 state. This fits, then, with the non-occurrence of the loss at very low potentials, and may be taken to support the attribution of this loss to a dissociation process.

Summary.

Experiments are described in which the energy losses of electrons in hydrogen of controllable velocity are measured, and also the relative number in the different energy groups. The results of the measurement of the photographs and their photometric curves may be summarized as follows:—(1) By far the most probable effect of a collision between an electron of 50 volts or more velocity and a hydrogen molecule is the excitation of the C state with a certain amount of vibrational energy. (2) The probability of effective collision at 150 volts is in the neighbourhood of 1 or 2 per cent. (3) At low velocities, smaller losses, the upper limit of which is 8 or 9 volts, varying slightly with the primary electron velocity, are observed, and the suggestion is made that these are connected with the dissociation of the molecule and the excitation of the continuous spectrum. (4) There is no loss of about 11·1 volts to be found, indicating that the B_0 and other low vibrational B states cannot be stimulated directly

* Hughes and Skellett, *Phys. Rev.* xxx. p. 11 (1927).

† Horton and Davies, *Phil. Mag.* xlv. p. 872 (1923).

by electron impact. (5) There is no indication, except at very low velocities (8 to 10 volts) when it is very faint, of a loss occurring which might be connected with direct dissociation.

The cost of part of the apparatus used in this investigation has been defrayed by a grant from the Royal Society.

The University, Leeds.

LXXXIX. *The K X-Ray Absorption Edge of Iron.*

By GEO. A. LINDSAY and H. R. VOORHEES*.

[Plate XVI.]

Introduction.

RECENT work in X-ray absorption spectra has shown that on the short wave-length side of the edge there often exists a complicated appearance which has been called the fine structure, or multiple structure of the edge. Early investigators were Stenström†, Fricke‡, and Hertz§. Lindh||, in an extended study of the K absorption edges of sulphur, chlorine, and phosphorus, found one or two secondary edges. Coster and Van der Tuuk¶ reported a secondary edge very close to the K edge of argon. Van Dyke and one of the writers** found a more complicated structure for the K edge of calcium than had previously been observed for any element. Nuttall††, working in this laboratory, has recently shown a structure for the potassium and chlorine K edges which is also very complicated.

The valence of the element affects the position of the absorption edge. In the work of Lindh there appeared a progressive shifting of the edge towards shorter wave-lengths as the valence of the element became higher.

The present work was undertaken for the purpose of extending the knowledge of the structure of the K absorp-

* Communicated by J. M. Nuttall, M.Sc.

† Stenström, Diss. Lund, 1919.

‡ Fricke, Phys. Rev. xvi. p. 202 (1920).

§ Hertz, *Zeits. für Phys.* iii. p. 19 (1920).

|| Lindh, Diss. Lund, 1923.

¶ Coster and Van der Tuuk, *Zeits. für Phys.* xxxvii. p. 367 (1926).

** Lindsay and Van Dyke, Phys. Rev. xxviii. p. 613 (1926).

†† Nuttall, Phys. Rev. xxxi. p. 742 (1928).

tion region and also with the hope of showing the effect of valence on this structure. With this in view, iron was chosen because of its convenient wave-length, because of the fact that crystals containing iron are plentiful, and also because iron has two valencies.

Experimental Procedure.

Two methods were used to obtain the absorption: first, crystals containing iron were used both as diffracting crystal and as absorbing medium; second, screens were made and placed in the path of the beam in the usual manner. The first method has the advantage of forming a very uniform absorber, and of permitting more radiation to reach the plate. It is a very desirable method for long wave-lengths and when good crystals are obtainable. On the other hand, if the crystals are poor and if suitable absorbing screens can be made, the second method gives better results. While crystals containing iron are plentiful, they have not especially good surfaces, and hence in this work the better results were obtained by the second method.

Many of the crystals used were not common in X-ray work, and it was therefore necessary to obtain the crystal-grating constants. This was done by precision measurements on the $\text{CuK}\alpha$ line, as outlined by Siegbahn*. The natural faces of the crystals were used, but in some cases these were polished in an effort to eliminate some of the surface irregularities. This polishing no doubt sacrifices to some extent the sharpness of the fine structure. The absorbing screens were made by mixing the finely-pulverized compound with collodion and spreading the mixture out in thin films to dry. In this manner screens of suitable thickness could readily be obtained. One of the crystals used in the first method was lepidomelane, a mica which contains iron, and which can be split into sheets as thin as 0.01 mm. These sheets served as excellent absorption screens for the second method. The screens for metallic iron were made by rolling a piece of pure electrolytic iron which was obtained from the General Electric Co., through Professor W. P. Davey. The rolling was done between pieces of copper, and fairly uniform screens as thin as 0.01 mm. were made.

A sylvite (KCl) crystal was used in the absorbing screen method. This crystal gave very good reflexion. Its dispersion is somewhat greater than that of calcite.

* Siegbahn, 'Spectroscopy of X-Rays,' pp. 62-64.

A Siegbahn vacuum spectrograph was used for photographing the edges. The reference line used on all the plates was the $\text{FeK}\beta$ line. The WL_2 line was also near, and served as a check. The distance from absorption edge to reference line was measured on a comparator having a least count of 0.005 mm.

In measuring the edge the cross hair of the comparator microscope was brought up just to the point where the blackening begins to decrease. The practice has commonly been to add to this reading one-half the width of the slit. It was found, however, that this correction gave abnormally low wave-lengths in cases where the dispersion of the crystal was small. If no corrections were made, the values for the edge by the two methods were found to agree much better. It was also found that the edge was much less sharp for metallic iron than for the compounds, even though other conditions were the same. This shows that factors other than slit-width may determine the sharpness of the edge. From these considerations it was thought best to omit the correction for the width of the slit. The width of the slit in the crystal method was 0.126 mm. In the screen method, where stronger reflexion could be obtained, it was narrowed to 0.043 mm. This aided in the resolution of some of the details of the structure.

The curves shown in this work are microphotograms taken on a Moll microphotometer. The lens system was modified so as to utilize more of the height of the plate, thus eliminating most of the fluctuations due to the coarse grain of the X-ray plates.

Experimental Details.

The predominant features of the multiple structure are as follows: first, a very sharp principal absorption edge; second, an intense white-line absorption immediately to shorter wave-lengths; third, several secondary regions of absorption, which also sometimes appear as white lines of less intensity. The more striking appearance of the first white line is, however, partly due to the fact that there is less contrast at the secondary edges. The microphotograms show that in many cases the secondary absorptions are really as intense as the principal white line. The blackening between the secondary absorptions by no means approaches in intensity that on the long wave-length side of the principal edge. In the tables this principal edge, which is the one always measured, is designated simply as the K edge. It forms the long wave-length boundary of the principal white line. The short

wave-length boundary is far less distinct. The secondary edges, that is the long wave-length sides of the secondary white lines or bands, are denoted by K_1 , K_2 , K_3 , etc. Certain faint and narrow absorptions that are often found near the secondary edges are designated as K_1' , K_2' , etc. K_1' is between K and K_1 , K_2' is between K_1 and K_2 , and so on. The structure is quite similar for all the compounds of iron.

✍ The structure for metallic iron differs from that for the compounds in that the principal edge is less sharp, as is revealed by the microphotogram of fig. 3 (Pl. XVI.), and there is no white line absorption of note until the K_2 edge is reached. The multiple structure covers a much greater range than in the case of the compounds.

Results of the Crystal Method.

The following crystals were used as diffracting crystals and at the same time as absorbers:—

(1) Iron pyrites, FeS_2 ; (2) Arsenopyrite, AsFeS ; (3) Hematite, Fe_2O_3 ; (4) Epidote, $\text{HCO}_2(\text{Al, Fe})_3\text{Si}_3\text{O}_{13}$; (5) Lepidomelane, $(\text{K, H})_2(\text{Mg, Fe})_2(\text{Al, Fe})_2(\text{SiO}_4)_3$; (6) Magnetite, Fe_3O_4 .

A summary of the results of the crystal method is given in Table I. The values shown for any one crystal are the average from several plates. The fainter edges are given in parentheses. Fig. 1 (Pl. XVI.), shows a representative plate of this method taken with iron pyrite. In the reproduction of the plate fainter detail is perhaps not evident, but it may be seen in the accompanying microphotogram of the same plate.

The summary of the data shows that the bivalent iron, as it occurs in iron pyrites and arsenopyrite, gives the same wave-length value for the principal edge. The white line for these two compounds measured 7 x.u. in width. Close study of the clearer plates shows, however, that this white line is separated in the middle by a very narrow black line. This indicates the presence of a K_1' edge in this mid-position. Such an edge was found later for the bivalent iron in the absorption-screen method. This faint K_1' edge is probably less distinct in the crystal method because of the wider slit used in that method. The remaining structure of these two crystals is quite the same for both, except that the pyrite crystal, which gave the better reflexion, shows the K_2' and K_3 edges faintly, while in the other they cannot be detected. The hematite and epidote crystals contain trivalent iron. The wave-length of the principal

TABLE I.—Summary of Data for Crystal Method.
 λ = wave-length in x.u. ΔV = energy difference in volts.

Crystal.	λ $\Delta \nu/R$ ΔV	Edges, λ .	White-line width.	K_1 .	K_1' .	K_1 .	K_2' .	K_2 .	K_3' .	K_3 .	K_4' .
Pyrite, FeS_2 (Val. = 2).	λ $\Delta \nu/R$ ΔV	1738.7	7.1 (4.4)* 2.15 (1.33) 29.2 (18.0)	1724.4 4.34 58.9	(1733.2) (1.47) (22.6)	1724.4 4.34 58.9	(1718.2) (6.25) (84.7)	1710.9 8.52 (15)	...	1698.5 (12.4) (168)	1687.5 15.9 215.0
Arseno-pyrite, AsFeS_2 (Val. = 2).	λ $\Delta \nu/R$ ΔV	1738.7	6.7 (4.0)* 2.03 (1.21) 27.5 (16.4)	1723.9 4.50 61.0	(1732.8) (1.79) (24.2)	1723.9 4.50 61.0	...	1712.4 8.05 109.0	1707.9 9.45 128.0	...	1687.1 16.0 217.0
Hematite, Fe_2O_3 (Val. = 3).	λ $\Delta \nu/R$ ΔV	1737.2	4.3 1.30 17.6	1725.8 3.47 46.9	...	1725.8 3.47 46.9	...	1711.5 7.88 107.0	(1707.0) (11.2) (151)	...	(1686.6) (15.7) (213)
Epidote (Val. = 3).	λ $\Delta \nu/R$ ΔV	1737.2	4.6 1.9 18.8	1726.1 3.88 45.7	...	1726.1 3.88 45.7	...	1713.3 7.32 99.0	...	1696.2 12.7 172	...
Lepidomelane (Val. = 2 & 3).	λ $\Delta \nu/R$ ΔV	1737.5	4.6 1.39 18.8	1723.5 4.26 57.8	...	1723.5 4.26 57.8	...	1714.1 7.16 97.0	1709.4 8.62 117.0	1695.9 129 174	1689.7 14.8 201.0
Magnetite (Val. = 2 & 3).	λ	1737.6									

Faint signs in parentheses.

* Probable separation point in the white line; barely discernible.

edge for these crystals was 1.5 x.u. shorter than for the bivalent forms. The white line was here found to be 4.4 x.u. in width.

The lepidomelane and magnetite crystals contain both bivalent and trivalent iron. The reflexion from the magnetite crystal was so poor that only the principal edge could be measured. The lepidomelane gave very strong reflexion, but its grating constant was large, and the dispersion was only 55 x.u. per mm. The detail was as sharp as in the crystals having iron of only a single valence.

Results of the Absorption-screen Method.

The absorption-screen method was more fruitful of results because of the excellent reflexion of the (KCl) crystal used. The slit was now narrowed in order to aid resolution. The dispersion for this sylvite was slightly greater than for calcite.

Absorbing screens were made of the following compounds:—ferrous carbonate, FeCO_3 ; ferric oxide, Fe_2O_3 ; ferrous ferric oxide, Fe_3O_4 ; ferric chloride, $\text{FeCl}_3 \cdot 6\text{H}_2\text{O}$; ferrous ammonium sulphate, $\text{FeSO}_4(\text{NH}_4)_2\text{SO}_4 \cdot 6\text{H}_2\text{O}$; and a mechanical mixture of the last two. Thin sheets of lepidomelane were also used as screens, and the metallic iron screen, made as described above, gave the absorption for the uncombined element.

The mineral siderite (FeCO_3) and ferrous ammonium sulphate were chosen because they are rather stable compounds.

Table II. shows a summary of the data obtained by the absorption-screen method, while figs. 2 and 3 (Pl. XVI.) show plates of Fe_3O_4 and metallic iron respectively with their microphotograms. In the case of the mechanical mixture it may be seen that the principal edge is like that for bivalent iron. We should expect this, for if the structures due to both forms are present, the edge due to the trivalent iron would fall in the intense white line due to the bivalent iron, and hence would not appear. Where the bivalent and trivalent iron are both in a single compound, as in the lepidomelane and magnetite, no evidence of a superposition of the two spectra could be found. The wave-length of the principle edge was intermediate between that for the two forms of iron. The white line was very narrow and a distinct K_1' edge was observed. These features indicate that the iron is held in these compounds in such a way as to show neither bivalent nor trivalent spectral characteristics. It rather appears that the iron ions are all alike.

TABLE II.—Summary of Absorption-screen Method. KCl. Crystal.
 λ = wave-length in KCl. ΔV = energy difference in volts.

Screen.	Edges, K.	White-line width.	K_1	K_2	K_3	K_4	K_5	K_6
Ferric oxide, Fe_2O_3 .	λ $\Delta \nu/R$ ΔV	3.9 1.19 16.0	1725.6 3.41 46.1	...	1713.3 9.9 97.5	...	1704.5 9.9 135.0	1686.5 15.6 212.0
Ferric chloride, $FeCl_3 \cdot 6H_2O$.	λ $\Delta \nu/R$ ΔV	3.5 1.06 14.4	1725.5 3.44 46.6	...	1714.9 6.71 90.8	...	1707.1 9.1 124.0	1692.0 13.9 188
Ferrous carbonate, $FeCO_3$.	λ $\Delta \nu/R$ ΔV	9.7 82 11.1	1728.4 2.89 39.1	...	(1716.0) (6.69) (90.7)	...	1709.5 8.7 118.0	1689.5 15.0 203.0
Ferrous ammonium sulphate, $FeSO_4(NH_4)_2 SO_4 \cdot 6H_2O$.	λ $\Delta \nu/R$ ΔV	2.7 82 11.1	1728.0 2.86 38.7	...	1716.8 6.80 85.3	...	1706.2 9.6 130.0	1695.9 12.8 174.0
Mixture of $FeCl_3 \cdot 6H_2O$ & $FeSO_4(NH_4)_2 SO_4 \cdot 6H_2O$.	λ $\Delta \nu/R$ ΔV	3.6 1.39 14.8	1726.8 3.25 44.0	...	1716.5 6.42 87.0	...	1707.2 9.3 126.0	1695.2 13.1 177.0
Lepidomelane.	λ $\Delta \nu/R$ ΔV	2.9 84 11.9	1727.6 2.95 39.9	...	1713.8 7.19 97.4	1709.8 8.44 114	1699.3 11.7 159.0	1689.8 14.7 200.0
Ferrous-ferric oxide, Fe_3O_4 .	λ $\Delta \nu/R$ ΔV	3.3 1.00 13.5	1726.3 3.38 45.6	...	1715.2 6.79 92	...	1704.7 10.1 136.0	1688.1 15.3 208.0
Fe, metallic.	λ $\Delta \nu/R$ ΔV	...	1726.7 3.82 51.8	1721.1 5.64 75.0	1715.2 7.36 100.0	1706.9 9.9 135.0	1701.3 11.7 158.0	1690.9 14.9 202.0
								1663.0 17.4 236.0
								(1614.0) (40.7) (551)

Values in parentheses are for faint edges.

Probably the most interesting portion of this work is the spectrum obtained with the screen of pure metallic iron. According to earlier views, which attributed the structure of the edge to the effect of the outer orbits, one should expect to find only a very limited structure for the absorption edge of a neutral element. On the contrary, our plates showed as many as a dozen secondary edges for metallic iron, the structure being distinct to more than 300 volts from the principal edge, with less distinct indications for several hundred volts further. This is a much greater range than has been observed before for the structure of any absorption edge.

It is of note that there is no white-line absorption at the principal edge for metallic iron. As may be observed from the photometer record of fig. 3 (Pl. XVI.), the slope of the edge is more gradual than for the compounds, and the K_1' and K_1 edges appear faintly on this slope. The first appearance of the usual white-line absorption is at the K_2 edge. The wave-length of the principal edge was found to be greater than for either of the ionized forms. Our value of 1739.3 x.u. for this edge is about 0.7 x.u. less than that given by Lindh.

Theoretical Considerations.

Kossel's theory of the fine structure was that the ejected electron may stop in the outer unoccupied orbits of the atom, and thus give rise to secondary edges, depending on the particular orbit in which the transition ends. The edge of shortest wave-length would thus correspond to complete removal of the electron, while the edge of longest wave-length would correspond to a transition to the innermost possible virtual orbit. This theory would account for a structure in the case of metallic iron of only a few volts in width, and at the most for not over 50 volts in the case of the trivalent Fe ion. The structure for the metallic iron here found is even more extended than for the compounds. We therefore think it very likely that multiple simultaneous ionization of the atom occurs under the action of the X-ray beam. G. Wentzel* predicted such a multiply-ionized condition in his discussion of the origin of certain non-diagram lines. Nuttall† gives this multiple ionization as the probable explanation of his results.

* G. Wentzel, *Ann. der Phys.* lxvi. p. 437 (1920).

† J. M. Nuttall, *loc. cit.*

When we attempt to calculate the position of any one of the secondary edges from the standpoint of multiple ionization, we find it difficult because of our lack of knowledge of the transition process in the outer part of the atom. However, since the portion of the spectrum corresponding to the virtual orbits is confined to a narrow region, it is possible to compute the *general* position of the absorption from a knowledge of the energy-levels of the atom.

If the iron atom has one of its K electrons removed to an outer level, its nucleus and K shell *together* then act, in so far as the outer electrons are concerned, like the corresponding parts of a cobalt atom. If an M electron were now to be ejected, it would require energy about equal to that for ejection of an M electron from a cobalt atom, which is about 104 volts for an M_I electron, 64 volts for an M_{II} or M_{III} electron, and 10 volts for an M_{IV} or M_V electron. If the K electron were entirely removed from the atom, these values would be somewhat more. Now, if one of these M electrons is ejected simultaneously with a K electron, the total energy absorbed will be approximately equal to the sum of that required to eject the K electron from the iron atom and the second M electron from a cobalt atom. If the M electron stops in some of the outer orbits, this energy value will be somewhat less. Thus, by choosing the proper number of electrons to be ejected and the proper stopping-places, it is possible to calculate values which will agree with almost any observed edge. The only point possible to make here at present is that that these computed values agree roughly with the structure found for iron. Thus the value for the K_1 edge is but slightly under the value computed for the ejection of a K electron together with an M_{II-III} electron; the K_2 edge is somewhat less than the computed value for the ejection of a K electron with an M_I electron. Further comparison is hardly worth while until more elements are investigated and until causes for variation in the fine structure are found.

From the multiple ionization viewpoint one might expect to find an absorption corresponding to the simultaneous ejection of a K and an L electron. Many trials were made with different absorption-screens and varying period of exposure to show such an effect. Several plates were obtained which showed two faint edges in the proper location to correspond to the ejection of an L_{II} or L_{III} electron with the K electron.

Kossel's theory will now be compared with the results obtained. According to tables of electron configuration, it

would appear that the N_{II} level is the first one in which a K electron might stop if the selection rule is obeyed. The absorption of energy sufficient to remove the K electron to this level may be considered as the cause of the principal edge. The energy necessary to remove the electron from this N_{II} level to infinity ought to be in the case of metallic iron about equal to the first ionizing potential for cobalt. The first ionizing potential of cobalt is given by Sur* as slightly over 8.5 volts. This would be the width of the virtual orbit effect, and if the white line is thus explained, it should not be more than this width for metallic iron. No evidence of a white line was found, but 8.5 volts would be equivalent to only about 0.2 mm. on our plates, and so narrow a white line might be practically obliterated by the radiation on either side. Applying the same reasoning to bivalent iron, it is found that the width of the white line should correspond approximately to the third ionizing potential of cobalt, which we are probably safe in assuming is not over 35 volts. This would be equal to a width of 8.5 x.u. If we ignore the division of the white line in the case of pyrite and arsenopyrite by the faint K_1' edge, then the entire width of the white line is about 7 x.u. The intense portion of the white line is much narrower than this.

Similarly, the limits for the virtual orbit effect for trivalent iron would be about equal to the fourth ionizing potential of cobalt, which we assume is not far from 50 volts. This is much greater than the observed width of the white line for trivalent iron. A width of 50 volts would reach about as far as the K_β edge.

It may be, however, that the white line is only another manifestation of multiple ionization, since the second ejected electron might also stop in one of the innermost unoccupied orbits. We could then think of the principal K edge as corresponding to a complete ejection of a K electron, and of the white line as the additive effect of M electrons, moved to higher levels. This view of the principal edge, however, is not in conformity with the low values of $\Delta\nu/R$ for the interval between the L_I edge and the L_{γ_4} line obtained by Miss Chamberlain and Lindsay†. Andrewes, Davies, and Horton‡ are also of the opinion that the principal absorption edge corresponds to the removal of the electron to the first possible unoccupied orbit.

* Sur, Phil. Mag. iv. p. 36 (1927).

† Chamberlain and Lindsay, Phys. Rev. xxx. p. 369 (1927).

‡ Andrewes, Davies, and Horton, Roy. Soc. Proc. cx. p. 64 (1926).

Summary.

The multiple structure for iron, both as a metal and in compounds, has been demonstrated to extend over a range considerably greater than that of any structure previously reported. The magnitude of this range is best explained by simultaneous ejection of electrons from outer orbits together with the K electron. Kossel's hypothesis appears satisfactory only as a possible explanation of the white-line absorption. As has been found previously, the principal edge shifts to shorter wave-lengths as the valence increases. The effect of valence on the multiple structure is small. When bivalent and trivalent iron are mechanically mixed, the expected superposition of the two patterns can be detected, but when the two valencies were in the same chemical compound, as in lepidomelane, no such overlapping could be found.

University of Michigan,
Ann Arbor, Michigan.
June 1928.

XC. *Measurements of the Velocity of Sound in Air, Nitrogen, and Oxygen, with special reference to the Temperature Coefficients of the Molecular Heats.* By W. G. SHILLING, M.C., D.Sc., and Prof J. R. PARTINGTON, M.B.E., D.Sc.*

THE method of experiment and the apparatus used are essentially the same as those described in a previous communication†. Except in a few matters of detail, no further description is necessary. Description of the determination of the tube constant has necessarily been amplified in reply to adverse criticism of previous work‡.

Preparation of the Gases.

Air.—The method of purification of the air used in the experiments is described in the previous communication§.

Nitrogen.—Nitrogen, containing as impurities only 0.3 per cent. (by volume) of oxygen and 0.1 per cent. helium and neon, was obtained from the British Oxygen Company.

* Communicated by the Authors.

† Phil. Mag. iii. p. 273 (1927).

‡ J. A. C. S. l. p. 627 (1928).

§ Phil. Mag. iii. p. 273 (1927).

The oxygen was removed by passage over reduced copper heated in a small electric furnace. The rare gases were not removed. The gas was dried by stick sodium hydroxide and phosphorus pentoxide.

Oxygen.—Electrolytic oxygen containing only 0·2 per cent. hydrogen was obtained from the British Oxygen

TABLE I.
Gases at Room Temperature.

No.	Air 20° C.		Nitrogen 19·5° C.		Oxygen 23·6° C.	
	Length.	$\lambda/2$ cm.	Length.	$\lambda/2$ cm.	Length.	$\lambda/2$ cm.
6	34·05	5·675	—	—	—	—
7	39·65	5·664	—	—	—	—
8	45·40	5·675	46·20	5·775	—	—
9	51·00	5·6 6	52·00	5·777	—	—
10	56·60	5·659	57·80	5·780	54·40	5·440
11	62·25	5·663	63·50	5·773	59·80	5·436
12	68·05	5·665	69·35	5·778	65·20	5·433
13	73·65	5·671	75·10	5·777	70·55	5·427
14	79·40	5·673	80·85	5·775	76·00	5·428
15	85·10	5·673	86·65	5·776	81·40	5·427
16	90·75	5·672	92·50	5·781	86·80	5·425
17	96·45	5·673	98·20	5·776	92·25	5·426
18	102·10	5·672	104·05	5·780	97·70	5·428
19	107·80	5·673	109·70	5·774	103·15	5·429
20	113·45	5·672	115·50	5·775	108·60	5·430
21	119·15	5·673	121·25	5·774	114·00	5·429
22	124·85	5·675	127·00	5·777	119·40	5·427
23	130·65	5·680	132·80	5·774	125·00	5·434
24	136·25	5·677	138·70	5·779	130·40	5·433
25	141·85	5·674	—	—	135·80	5·432
26	—	—	—	—	141·40	5·438
Means.....	5·671		5·776		5·431	

Company. The hydrogen was removed by passage over heated platinized asbestos, and the gas then dried by calcium chloride and phosphorus pentoxide.

Measurements were then made, as described in the previous paper, at temperature intervals covering the range from room temperature up to 1100° C. Tables I. to III. give typical sets of measurements. The mean cold-junction temperature is given at the top of the table. The three columns for each gas contain the number of half wave-lengths, the corresponding mean half wave-length, and the temperature in

TABLE II.
Gases at about 460° C.

No.	Air 17·6° C		Nitrogen 17·4° C.		Oxygen 19·9° C.	
	$\lambda/2$ cm.	M.V.	$\lambda/2$ cm.	M.V.	$\lambda/2$ cm.	M.V.
0	—	3·920	—	3·798	—	3·930
5	—	—	8·898	3·762	8·370	3·965
6	8·810	3·974	8·889	3·882	8·367	3·985
7	8·815	3·974	8·887	3·862	8·368	3·985
8	8·817	3·935	8·894	3·864	8·374	3·995
9	8·820	3·980	8·895	3·890	8·378	3·965
10	8·825	4·005	8·897	3·870	8·373	3·955
11	8·828	4·005	8·901	3·844	8·382	3·920
12	8·830	3·975	—	—	8·380	3·970
Means...	8·821	3·971	8·894	3·846	8·374	3·963
C. J.		79		78		90
Temp....		4·050		3·924		4·053
		460° C.		446° C.		460° C.

TABLE III.
Gases at about 980° C.

No.	Air 15·8° C.		Nitrogen 17·2° C.		Oxygen 20·2° C.	
	$\lambda/2$ cm.	M.V.	$\lambda/2$ cm.	M.V.	$\lambda/2$ cm.	M.V.
0	—	9·940	—	9·758	—	9·800
4	11·319	9·950	11·892	9·760	10·760	9·905
5	11·321	9·917	11·910	9·810	10·764	9·930
6	11·324	10·015	11·927	9·960	10·760	9·950
7	11·321	9·960	11·930	9·860	10·803	9·945
8	11·330	9·910	11·930	9·800	10·804	9·900
9	11·336	9·820	11·918	9·790	10·784	9·805
10	11·332	9·800	11·899	9·785	10·787	9·815
Means...	11·326	9·914	11·915	9·815	10·780	9·881
C. J.		71		77		93
Temp....		9·985		9·892		9·974
		981° C.		973° C.		980° C.

millivolts respectively. At the foot of each table is added the cold-junction correction and the equivalent temperature in degrees centigrade.

The velocities of sound shown in Table IV. have been calculated from measurements over the whole temperature

TABLE IV.

True Velocities of Sound in metres per second.

Temp. °C.	Air.	Nitrogen.	Oxygen.
0	331·4	—	—
Room *	340·8	347·6	323·8
100	387·2	394·1	367·4
200	435·6	443·3	413·5
300	478·9	487·4	454·8
400	518·4	527·5	492·3
500	555·1	564·7	527·4
600	589·3	599·4	559·9
700	621·5	632·3	590·8
800	651·7	663·0	619·8
900	680·8	692·3	647·3
1000	708·4	720·6	674·7

* Room temperatures as follows: Air 15·7° C.; Nitrogen 16·7° C.; Oxygen 16·5° C.

TABLE V.

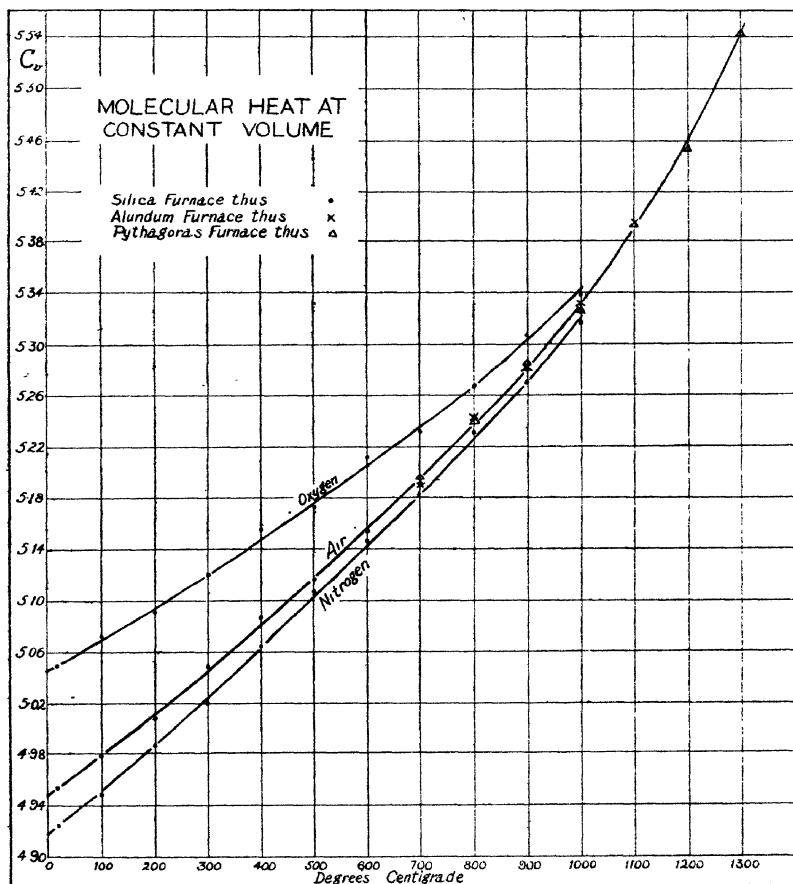
Values of the Physical Constants employed.

Constant.	Gas.		
	Air.	Nitrogen.	Oxygen.
Molecular weight, M	28·98	28·02	32·00
Critical temperature, T_c ...	132·6	126·5	154·25
Critical pressure, p_c	39·3	33·0	50·2
Viscosity at 0° C., η_0	0·000176	0·000167	0·000193
Density at 0° C., ρ_0	0·001293	0·001251	0·001429
$\epsilon = \kappa/cv\eta$	1·772	1·765	1·867
Ratio, c_p/c_v	1·403	1·405	1·395
Sutherland constant, S ...	119·4	113	132
Thermal conductivity, κ .	0·0522	0·052	0·057
Specific heat, c_v (approx.)	0·1701	0·1760	0·1582
The gas constant, R	$\left\{ \begin{array}{l} 8·3157 \times 10^7 \text{ ergs per } ^\circ\text{C., or} \\ 1·9875 \text{ cal. per gm. mole.} \end{array} \right.$		

range by the method already described. Table V. gives the values of the various physical constants used in the calculation of the factors required to reduce the experimental results.

If the constants in Table V. are used, the values given in Table VI. are obtained. Equation numbers at the heads

Fig. 1.



of the columns refer to equations fully explained in the previous paper. Berthelot's Equation of State has been used throughout.

From the values given in Tables IV. and VI. the results given in Table VII. are obtained.

The values of C_v are given graphically in fig. 1, which, in

TABLE VI.
Constants for Air, Nitrogen, and Oxygen.

Temp. °C.	Air.			Nitrogen.			Oxygen.		
	ϕ by (2).	$C_p - C_v$ by (3).	Eqn. 81 †.	ϕ by (2).	$C_p - C_v$ by (3).	Eqn. 81 †.	ϕ by (2).	$C_p - C_v$ by (3).	Eqn. 81 †.
0 ...	1.00072	1.997	—	1.00057	1.998	0.52	1.00145	1.999	—
Room *.	1.00044	1.996	0.561	1.00020	1.996	0.56	1.00105	1.998	0.565
100 ...	0.99969	1.991	0.707	0.99955	1.991	0.700	1.00003	1.992	0.709
200 ...	0.99947	1.989	0.867	0.99935	1.989	0.859	0.99967	1.990	0.861
300 ...	0.99944	1.989	1.020	0.99933	1.988	1.008	0.99957	1.989	1.026
400 ...	0.99945	1.988	1.165	0.99937	1.988	1.151	0.99956	1.988	1.161
500 ...	0.99949	1.988	1.306	0.99941	1.988	1.289	0.99957	1.988	1.317
600 ...	0.99953	1.988	1.442	0.99946	1.988	1.432	0.99960	1.988	1.455
700 ...	0.99956	1.988	1.573	0.99950	1.988	1.553	0.99962	1.988	1.590
800 ...	0.99959	1.988	1.702	0.99954	1.987	1.679	0.99965	1.987	1.719
900 ...	0.99962	1.987	1.827	0.99957	1.987	1.803	0.99967	1.987	1.847
1000 ...	0.99965	1.987	1.950	0.99960	1.987	1.923	0.99969	1.987	1.971
1100 ...	0.99967	1.987	2.070						
1200 ...	0.99969	1.987	2.188						
1300 ...	0.99971	1.987	2.304						

* Room temperatures as given in Table IV.

† See p. 293 of the previous communication.

TABLE VII.

C_v , C_p and C_p/C_v for Air, Nitrogen, and Oxygen up to 1000° C.

Temp. °C.	Air.			Nitrogen.			Oxygen.		
	C_v .	C_p .	C_p/C_v .	C_v .	C_p .	C_p/C_v .	C_v .	C_p .	C_p/C_v .
Room *.	4.952	6.948	1.4029	4.923	6.919	1.4054	5.049	7.046	1.3955
100 ...	4.978	6.969	1.4000	4.948	6.939	1.4024	5.072	7.064	1.3928
200 ...	5.006	6.995	1.3974	4.987	6.976	1.3989	5.089	7.079	1.3910
300 ...	5.048	7.037	1.3939	5.019	7.008	1.3962	5.120	7.108	1.3884
400 ...	5.087	7.075	1.3908	5.068	7.056	1.3923	5.158	7.152	1.3850
500 ...	5.117	7.105	1.3885	5.111	7.099	1.3890	5.174	7.162	1.3842
600 ...	5.156	7.144	1.3855	5.148	7.136	1.3861	5.216	7.204	1.3811
700 ...	5.190	7.178	1.3830	5.177	7.165	1.3839	5.232	7.220	1.3799
800 ...	5.246	7.234	1.3789	5.234	7.221	1.3797	5.270	7.258	1.3771
900 ...	5.280	7.267	1.3764	5.282	7.269	1.3763	5.310	7.297	1.3742
1000 ...	5.323	7.310	1.3734	5.317	7.304	1.3738	5.335	7.322	1.3721

* Room temperatures as given in Table IV. The results are in all cases given to one place of decimals further than that for which validity is claimed.

926 Dr. W. G. Shilling *and* Prof. J. R. Partington *on the*
the case of air, shows also the results of some further
measurements to be described later.

From the smoothed curves of fig. 1 the following values
(Tables VIII. and IX.) have been deduced :—

TABLE VIII.

Molecular Heats at Constant Volume.

Temp. °C.	Air.	Nitrogen.	Oxygen.
0	4.95†	4.92	—
Room*	4.95	4.92	5.05
100	4.98	4.95	5.07
200	5.01	4.99	5.09
300	5.04	5.02	5.12
400	5.08	5.06	5.15
500	5.12	5.10	5.18
600	5.16	5.14	5.21
700	5.20	5.18	5.24
800	5.24	5.22	5.27
900	5.28	5.27	5.30
1000	5.33	5.32	5.34
1100	5.39	—	—
1200	5.46	—	—
1300	5.54	—	—

TABLE IX.

Molecular Heats at Constant Pressure.

Temp. °C.	Air.	Nitrogen.	Oxygen.
0	6.94†	6.92	—
Room*	6.95	6.92	7.05
100	6.97	6.94	7.06
200	7.00	6.97	7.08
300	7.03	7.01	7.11
400	7.07	7.05	7.14
500	7.11	7.09	7.16
600	7.15	7.13	7.19
700	7.19	7.17	7.23
800	7.23	7.20	7.26
900	7.27	7.26	7.29
1000	7.32	7.30	7.32
1100	7.38	—	—
1200	7.44	—	—
1300	7.53	—	—

* Room temperatures as given in Table IV.

† From the assumed velocity at 0° C.; $V=331.4$ m./sec.

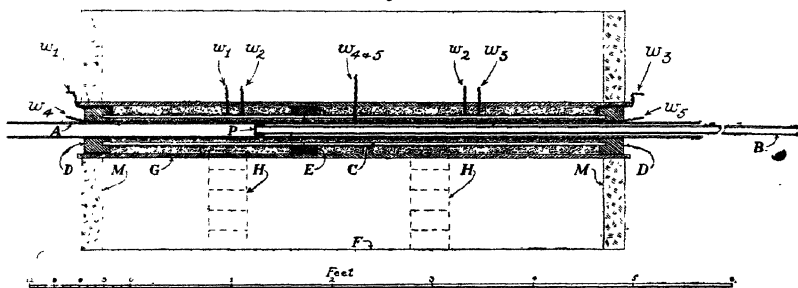
Measurements at Temperatures above 1000° C.

Experimental data for specific heats in the temperature region between 1000° C. and 2000° C. are very scanty. Above this temperature interval measurements can be made by explosion methods. Apparatus can be devised so that most of the other methods of experiment may be used for moderate temperatures approaching 1000° C.

A furnace capable of being maintained at temperatures over 1000° C. is obviously the only modification required before the method already described can be extended. Attempts were first made to use alundum tubes with windings of pure platinum. These failed for several reasons, although results, tabulated later, were obtained from 700° C. to 1100° C.

It was impossible to obtain alundum tubes in lengths greater than three feet. The consequent joints and the high coefficient of thermal expansion of alundum caused

Fig. 2.



mechanical difficulties too great to be overcome in a furnace six feet long. In addition, alundum is so extremely porous that it is necessary to surround the alundum tube containing the gas with an outer jacket of fireclay, so that the furnace tube could be surrounded by a layer of the gas under investigation. A further drawback was the roughness of the inner walls of the furnace tube. Until these had been polished with a carborundum mop it was impossible to make satisfactory measurements. The intensity of the sound-waves was reduced almost to nothing by the time they had reached the centre of the furnace. At a temperature just above 1100° C. the forces of expansion caused the inner tube to fracture in several places. The furnace was dismantled and a new one designed to incorporate several improvements suggested by experience.

A section of the new furnace drawn to scale is shown in fig. 2. The central tube, A, is 2100 cm. long, has a bore

of 4 cm. and a wall thickness of 0.5 cm. It was made of "Pythagorascompo" by W. Haldenwanger of Spandau. The tube had a smooth semi-glazed inner surface, was perfectly straight, of circular cross-section, and would stand a working temperature of 1650° C. At 1200° C. it is practically impervious, even to hydrogen. Hence it was unnecessary to surround the tube with an atmosphere of the gas under investigation. The ends could therefore be left to slide freely in fireclay collars, D, D, so that no strain due to expansion or contraction occurred.

Surrounding this tube was a three-inch bore tube, C, of alundum which carried a second, booster, winding of platinum. Alundum was employed here because this tube, which was in two lengths, was recovered intact from the previous furnace. Recesses in the collars, D, D, supported the ends of this tube concentrically with the inner tube whilst the junction of the two pieces was carried by a fireclay ring, E. Surrounding and supporting the whole was a heavy fireclay tube, G, of six-inch bore made by the Morgan Crucible Company of Battersea. This outer tube was in three sections supported by asbestos brick pillars, H, H, at the junctions. Each section was slit longitudinally into two halves to facilitate assembly of the furnace.

The resistor of the furnace was pure platinum ribbon of cross-section 1 in. \times 0.001 in. To wind the inner tube, two lengths of twelve feet of this material were used, the central ends being brought out to a common terminal. For the loan of this platinum and for making necessary repairs we are much indebted to Messrs. Johnson & Matthey.

Splitting the windings enabled the temperature of each half of the furnace to be adjusted independently and current to be used economically. Leads from the ribbon consisted of six strands of 26 S.W.G. platinum wire welded in six different places to the end inch of the ribbon. The six wires were twisted together and brought out as one wire, which was long enough in all cases just to extend for one inch beyond the outer fireclay tube. To extend these leads to terminals on the outer furnace casing, copper rods $\frac{3}{8}$ in. diameter were used, the platinum being clamped into a hole drilled for one inch into the end of the rods. The sectional drawing shows how the windings and leads were spaced. An accurately-measured spacing of $\frac{5}{16}$ in. between turns was allowed on all windings.

The cascade winding on the alundum tube consisted of two lengths of 10 ft. $4\frac{1}{2}$ in. and one length of 20 ft. 9 in. of ribbon similar to that used on the inner tube. The long length

covered the centre half of the furnace, whilst the two end quarters were separately wound. Experience had shown that with such an arrangement of windings uniform temperatures could be obtained along the whole furnace tube. More heat is required near the ends of the furnace to balance the greater heat-loss. The leads were made exactly as for the centre heating coils, and are shown in fig. 2.

As a further control to balance end-losses, two heaters of nichrome strip wound on alundum formers were inserted near the ends of the furnace. These are not shown on the drawing, but each was wound on a former measuring six inches long and having a bore of five inches. This was fitted over the alundum tube carrying the second platinum winding, but inside the fireclay tube. Each heater was wound with about six yards of 0.0625 in. \times 0.006 in. nichrome strip, and was capable of dissipating 400 watts per second.

The platinum windings were coated with a thin cement of pure alundum, dried and recoated, the operation being repeated until a uniform coating several millimetres in thickness was obtained. The annular spaces between the inner and central, central and outer tubes were filled with alundum grain. In the previous furnace the space next to the outer fireclay tube had been left filled only with the gas under investigation. This was done partly to prevent contamination by the atmosphere of the gas used, and partly to ensure more uniform distribution of temperature by convection and diffusion effects. It was found, however, that the furnace functioned much better when the second set of windings was well lagged.

The whole core of the furnace was held concentrically in a large rectangular outer casing by means of the asbestos brickends, M, M. The outer casing (2 ft. 6 in. \times 2 ft. 6 in. \times 5 ft. 4½ in.) consisted of a heavy iron frame lined with uralite boards. The whole of the remaining space inside the box was filled with lumps of crude bauxite. Owing to the weight of lagging—nearly one ton—the bottom framework of the furnace must consist of I-iron of cross-section at least 4 in. \times 2 in. It was found that L-iron slowly twists and sags, with consequent strain on the furnace tube.

A twelve-kilowatt, low-voltage, shunt-wound dynamo supplied the energy for the furnace. Each of the five platinum heating-coils was arranged in a separate circuit, with the exception of coils w_1 and w_2 (see fig. 2), which were run in series. When necessary a shunt resistance could be placed across one of these coils by direct connexion to the

furnace terminals. Adjustment of the end temperatures was, however, more easily effected by using the nichrome end boosters, which could be run from the 240-volt D.C. power circuit. Each platinum winding had as a controlling resistance a six-step series of one-ohm coils in series with a six-step vernier which had a total resistance of one ohm. The resistances were made of 12 S.W.G. nichrome wire. This fine adjustment of the resistance, together with the variable voltage of the dynamo, gave excellent control of the furnace temperature. A total of 3.3 kw. was required to reach a uniform temperature of 1000°C . throughout the furnace tube.

Temperature measurements were made by means of a Foster Optical Pyrometer of the disappearing filament type. Experiments kindly undertaken for us by the Foster Instrument Company of Letchworth showed that the instrument would record temperatures accurately if sighted down the piston tube and focussed on the piston face. When the piston is pushed into the furnace, it is necessary to read a temperature near the left-hand side of the furnace (see fig. 2) whilst sighting through the central part of the furnace. The latter is generally at a slightly higher temperature than that of the ends of the furnace. Messrs. Foster & Company carried out experiments on a disk maintained at 850°C . Direct readings were made and also readings when the pyrometer was sighted through a tube six feet long and one inch bore, with its central part maintained at 1200°C . Both readings were the same, as was also the reading through the tube after it had been cooled down. The differences of temperature used in these experiments were very much greater than any which would normally occur. It was found, however, that a tube of six feet length should not be less than $\frac{3}{4}$ -inch bore if the readings were to be consistent. The piston tube, B (fig. 2), was therefore designed to have a bore of 24 mm. The wall thickness was 4 mm. and the length 2 metres. It was made of Pythagorascompo, and the piston head, P, was formed and made in one piece with the tube. As in the previous work, the face of the piston was made as thin as possible to reduce the temperature lag of the back upon which the pyrometer was sighted.

The pyrometer and the open end of the piston tube were rigidly fixed to a sliding platform, so arranged that the pyrometer was always focussed on the back surface of the piston face. The whole platform was arranged to slide by means of a three-point bearing on two steel rods placed parallel to the axis of the furnace. A pointer attached to

the platform showed the scale-reading corresponding to the position of the piston in the furnace.

The end fittings of the furnace were of the same pattern as those described in the previous communication*. The only difference was that the piston fittings had to be enlarged. Water-cooling was arranged on the syphon system from a ten-gallon drum placed on top of the furnace. This was done to be independent of an intermittent water-supply.

With the silica apparatus, contraction of the piston rod as it was pulled out of the furnace could be neglected. A maximum correction of 0.7 mm. would be necessary if the whole 1.5 metre length of the piston were pulled out at 1000° C. and cooled to 20° C., assuming the coefficient of expansion of silica to be 5.0×10^{-7} . At the higher temperatures the full length of the scale could not be used, so that the maximum correction would be of the order 0.5 mm., which is the limit to which measurements could be made at these temperatures.

The coefficient of linear expansion of alundum is 4.8×10^{-6} , and that of pythagoras material is of the same order. The necessary correction was made directly at each reading, since a known length of the tube was pulled out. After passing the water-cooled gland and remaining exposed to the air for the time required for each measurement, the rod was practically at room temperature. The temperature drop was assumed to be from the temperature actually measured at the particular point down to room temperature. Since all the movements are of the same length and the variations in temperature along the furnace are small, this method gives the corrections to well within the required limits. The cooled length was measured from the gland to the reading index. On the furnace side of the gland the temperature equilibrium remains the same throughout a series of measurements, so that no contraction or expansion of the rod occurs in this region. This assumption is based on the behaviour of the telephone end of the furnace, where any disturbance of temperature equilibrium would be shown by a changed zero reading. This point has been fully discussed elsewhere †.

The makers state that the coefficient of linear expansion of pythagorascompo is the same as that of hard porcelain. Mellor and also Rieke state that the higher the firing

* Phil. Mag. iii. p. 273 (1927).

† See p. 283 of the previous communication.

temperature the lower is the coefficient of expansion of porcelains. Figures given by Holborn and Grüneisen, Bedford, and Rosenthal for Berlin porcelain vary between 3.03×10^{-6} and 3.6×10^{-6} , whereas Scheel gives 2.8×10^{-6} . A value of 3.5×10^{-6} has been taken for our calculations, since the coefficient of expansion increases slowly with temperature, but will probably be slightly lower than that of hard porcelain, since pythagorascompo is fired at a very high temperature.

The maximum correction from room temperature to the maximum temperature reached (just above 1300°C.) is therefore about 6.8 mm. for the pythagorascompo tube and about 9.0 mm. for the alundum tube, allowing contraction on the full 1.5 metre length. The need for these corrections is obvious.

Results.

After initial calibrations of the furnace tube, experiments with both the alundum and the pythagorascompo furnaces were begun at 700°C. to obtain an overlap to the temperature region already explored.

Measurements with the alundum tube had only progressed as far as 1100°C. when the furnace tube collapsed under the strain due to expansion.

The second furnace tube was quite successful, and measurements had been made up to 1300°C. , when the piston tube was accidentally broken. Owing to labour troubles in the German porcelain industry a long wait for replacements ensued, so that it is thought advisable to publish results as far as they go. There seems to be no reason why this method of experiment should not be successful to the limit of the apparatus. The furnace tube will stand a working temperature of 1650°C. , and may even be used for a short time up to 1700°C. With a closely-adhering layer of alundum cement to prevent volatilization, the platinum should remain intact at 1650°C.

Table X. compares the velocities of sound obtained :

1. In the old silica furnace.
2. In the alundum furnace.
3. In the pythagorascompo furnace.

The corresponding values of C_p are tabulated in Table XI. and are compared graphically in fig. 1.

Of the three series that with furnace 2 is considered the least reliable, since only a few sets of measurements were

taken before the furnace collapsed. Final values of C_v and C_p have been added to Tables VIII. and IX.

Fig. 1 shows the excellent agreement between the three independent sets of measurements. There is a tendency for the values of C_v to rise more sharply from 1000° C. upwards. This is confirmed by the values calculated by one of the authors* from considerations of gaseous equilibria. The

TABLE X.

True Velocities of Sound in Air in metres per second.

Temp. °C.	1.	2.	3.
700	621·51	621·57	621·42
800	651·71	651·71	651·75
900	680·77	680·74	680·70
1000	708·42	708·24	708·36
1100	—	734 40	734·39
1200	—	—	759·54
1300	—	—	783·18

TABLE XI.

Values of C_v for Air.

Temp. °C.	1.	2.	3.
700	5·190	5·187	5·197
800	5·246	5·246	5·243
900	5·280	5·282	5·284
1000	5·323	5·331	5·326
1100	—	5·394	5·393
1200	—	—	5·453
1300	—	—	5·544

curve of fig. 1 is similar to those for oxygen and nitrogen in fig. 2 of the above reference.

The Tube Correction.

Our method of calculation has recently been criticised by Cornish and Eastman †, who state that our results are worthless unless recalculated. They state that an explanation of

* Trans. Far. Soc. xxii. p. 377 (1927).

† J. A. C. S. i. p. 627 (1928).

the results may be that our frequency was not correctly determined. As has already been described*, the frequency of our oscillator was determined for us at the National Physical Laboratory. A copy of the tables of results included with the certificate is set out in the reference given. In addition, a steel bar standard was made up and calibrated at the National Physical Laboratory. This standard had a frequency very near that of the oscillator. The exact frequency of the latter could be estimated to one part in ten thousand in a few seconds by comparison with the steel standard. The standard wave-meter referred to was used to check the approximate frequency before the oscillator was sent to be calibrated.

In the later work with the alundum and pythagorascompofurnaces, the oscillator was modified in detail and all switches excluded. The changes reduced the total capacity of the circuit, causing the frequency to rise slightly. For the new frequency another steel standard was prepared. The oscillator used by Cornish and Eastman is essentially the same as ours except that less precautions were taken to ensure constant frequency. They used ordinary wireless condensers to obtain their capacity. These are relatively unstable and usually have a considerable temperature coefficient. No mention is made of any precautions taken to ensure a constant inductance. The calibration tables for our instrument showed that it is essential to maintain the anode current of the valve constant if a constant frequency is necessary. For this purpose we included a vernier resistance and a milliammeter in our filament circuit. In Cornish and Eastman's work this point seems to have been overlooked. Cornish and Eastman's determination of frequency seems to involve the counting of beats up to a possible maximum of 600 in two minutes. We have not attempted to count this number of beats in the time stated.

Since the tube correction in Cornish and Eastman's work agrees, by coincidence, with the theoretical equation given by Kirchhoff and Helmholtz, the former workers claim "overwhelming evidence" that the equation is universally true. Only a summary of the evidence against this claim need be given here, as the fallacy of the Kirchhoff-Helmholtz equation is too well established to need discussion. There is no evidence in the literature that *large* amounts of dust were used, as stated by Cornish and Eastman, unless for the express purpose of determining the effect of large

* Phil. Mag. iii. p. 273 (1927) (see p. 279 for tables).

excesses of dust. Kundt* introduced up to 10 gm. of lycopodium powder in some of his experiments. The effect of excess dust is quite small. Schneebeli†, Seebeck‡, Kayser§, Müller||, and Sturm¶ all obtained proof that the law of Kirchhoff and Helmholtz does not hold. In addition, we have Kirchhoff's own admission that the law could not hold unless the tube were perfectly smooth. Thiesen** has given a special treatment for the case of closed resonators. The factors obtained by Dixon and his co-workers†† also show that the Kirchhoff-Helmholtz equation has no general application. Finally, our own work on this subject has satisfied us that the only possible way to obtain an accurate tube correction is to determine it experimentally. This we have done throughout all our work, a point which Cornish and Eastman have ignored entirely.

To determine this correction the wave-length of sound in pure air at an accurately-measured temperature at, or near, that of the room is determined. Since the frequency of the note is known, the product *frequency* \times *wave-length* gives the apparent velocity of sound in air at the measured temperature. Great care must be taken to measure actually the temperature within the furnace tube, since the amount of lagging round the furnace renders it useless simply to measure room temperature. The lagging renders the tube immune from sudden small changes in room temperature. A calibrated thermometer pushed down the piston tube was used to measure this temperature. A thermometer with moderate lag was chosen so that in the few seconds required to withdraw it and read the temperature the error could not be greater than 0.1° C.

The true velocity of sound in pure air at the measured temperature was then calculated from the velocity at 0° C. on the assumption that velocities are proportional to the square root of the absolute temperature. Strictly speaking, the velocities are proportional also to $\sqrt{\gamma}$, but the difference for such small temperature differences is negligible. Hence the difference *True Velocity*—*Actual Velocity* is accurately known.

* Pogg. *Annalen*, cxxxv. pp. 337 & 527 (1868).

† Pogg. *Annalen*, cxxxvi. p. 296 (1869).

‡ Pogg. *Annalen*, cxxxix. p. 104 (1870).

§ *Ann. Phys.* ii. p. 218 (1877).

|| *Ann. Phys.* xi. p. 331 (1903).

¶ *Ann. Phys.* xiv. p. 822 (1904).

** *Ann. Phys.* xxiv. p. 401 (1907).

†† Proc. Roy. Soc. A, c. p. 1 (1921); cv. p. 199 (1924).

Our tube correction is of the form *

$$V' = V[1 - ck], \quad . \quad . \quad . \quad . \quad . \quad (1)$$

where

V' = the measured velocity in the tube,

V = the true velocity in free air,

k = the tube constant,

c = a factor given by

$$c = \sqrt{\frac{\eta_0 T \left[1 + \frac{S}{273} \right] \sqrt{1 + \frac{t}{273}}}{\rho_0 \times 273 \left[1 + \frac{S}{T} \right]}} \left[1 + \sqrt{\epsilon} \left[\frac{\gamma - 1}{\sqrt{\gamma}} \right] \right] \quad . \quad . \quad . \quad (2)$$

in which

η_0 = the viscosity at 0°C. ,

ρ_0 = the density at 0°C. ,

T = the absolute temperature,

t = the temperature in degrees centigrade,

S = the Sutherland constant,

$\epsilon = \kappa/\eta c_v$ = thermal conductivity / (viscosity \times sp. ht.),

$\gamma = C_p/C_v$ = the ratio of the specific heats.

Helmholtz and Kirchhoff † represented the velocity of sound in tubes by

$$V' = V[1 - c/2r \sqrt{(\pi N)}], \quad . \quad . \quad . \quad (3)$$

where

V = the true velocity in the free gas,

V' = the velocity in the tube,

N = the frequency of the note used,

r = the radius of the tube.

Helmholtz states that the constant c is the viscosity of the gas, but, according to Kirchhoff, c depends on the heat-exchange between the gas and the walls of the tube, and may be represented by

$$c = \sqrt{\alpha} + [V/b - b/V] \sqrt{\beta},$$

in which

b = the Newtonian velocity of sound, $\alpha = \eta/\rho$, and $\beta = \kappa/\rho c_v$, where η is the coefficient of viscosity, κ the coefficient of

* See 'Specific Heats of Gases,' pp. 50-55.

† Pogg. *Annalen*, cxxiv. p. 177 (1868).

thermal conductivity, ρ the density of the gas, and c_v the specific heat at constant volume. Substituting these values for α and β above, writing $\epsilon = \kappa/\eta c_v$, and remembering that

$$V/b = \sqrt{C_p/C_v} = \sqrt{\gamma},$$

we have

$$c = \sqrt{(\eta/\rho)} \left[1 + \sqrt{\epsilon} \left(\frac{\gamma-1}{\sqrt{\gamma}} \right) \right]. \quad . \quad . \quad . \quad (4)$$

The variation of η with temperature is then assumed to be given by Sutherland's equation*, and the density to be inversely proportional to the absolute temperature. When these additions are made, equation (2) above is obtained. This equation, which is Kirchhoff's equation neglecting only the effect of r and of N , takes no account of the nature of the inner surface of the tube nor of the thermal properties of the material of which it is made. Sturm (*loc. cit.*) showed definitely that the material of which the tube is made affects the velocity of sound in it. The experimental constant k (equation (1)) is necessary to correct for the effect of the various factors which cannot be determined theoretically. The assumption must then be made that the tube correction does not depend on the temperature. This assumption admittedly contains the weakness that the thermal conductivity of the tube, and hence the heat-exchange between it and the gas, may change with temperature. The difference must be extremely small, but it is unfortunate that sufficient thermal data are not available to apply the correction. It seems reasonable to assume that the nature of the inner surface of the tube does not change at temperatures well below the softening point of the material of which it is made.

For the various tubes used the following values of k were found :—

Tube.	A.	B.	C.	D.
k	0·0168	0·0186	0·00713	0·00136

Tube A. The short silica tube first used (see Trans. Far. Soc. xviii. p. 386, 1923). With this furnace an oscillator having a frequency of 2947 vibrations per second was used.

Tube B. The long silica tube used for experiments up to 1000° C. (see Phil. Mag. iii. p. 273, 1927). The frequencies used in these experiments were between 2992 and 3006 per second, changes being due to renewal of valves. Each frequency was accurately determined for a given anode current

* Phil. Mag. xxxvi. p. 507 (1893).

by the steel bar method as recommended by the National Physical Laboratory. In the experiments on steam, described in the last communication, the tube constant was found to have changed slightly. The change, which was the only one ever recorded throughout this work, may be ascribed to the fact that steam was the last of a series of six gases to be investigated in the same tube. The constant used was 0.0180 instead of 0.0186.

Tube C. The alundum furnace tube, using a frequency of 2992.

Tube D. The pythagorascompo tube, used with slight improvements to the oscillator and a change of frequency to 3018.5 per second.

The values of C_v , plotted in fig. 1, show the results obtained with tubes B, C, and D. Tubes B and C have, respectively, correction factors approximately ten times and three times greater than that demanded by Kirchhoff's formula, whilst that of tube D is less than the theoretical value. From the excellent agreement of the final values of C_v for the three tubes, we thus confirm previous workers' conclusions that the Kirchhoff-Helmholtz formula cannot be applied generally.

The differences in the tube constants can be explained qualitatively by a consideration of the nature of the tubes. The two factors mentioned by Kirchhoff probably account for the greater part of the differences. They are (a) the nature of the inner surface of the tube, (b) the heat-exchange between the tube and the gas. Tube B was of silica with a glazed inner surface, whilst the surface of C was very rough. Tube D had a very uniform and smooth surface, but was not glazed as in the case of B. The thermal conductivities of the tubes B, C, D are respectively 0.00082, 0.00833, and 0.00169. The measurements are comparative and are taken from the Norton Company's handbook *. Thermal conductivity seems to play a relatively large part. Thus, the excellent surface of the silica tube B is more than counterbalanced by its very low thermal conductivity. Hence a large correction factor. With the alundum tube the thermal conductivity is very high, but the extremely rough and porous surface increased what would otherwise probably have been a very small factor. The pythagorascompo tube—a mixture of aluminium oxide and fireclay—had a conductivity probably greater than that given above, which is the value for fireclay. It had an excellent inner surface. Hence the very small correction factor. The metal tubes used by

* 'Norton Refractory Laboratory Ware,' 1926, p. 9.

Cornish and Eastman would have very high thermal conductivity and presumably a fairly smooth surface. The tube correction thus might easily have coincided with the theoretical value, but coincidence with theoretical values in a single piece of research work does not seem to us sufficient grounds for dismissing as entirely wrong the work of many previous investigators and for claiming overwhelming evidence in favour of the minority. Particularly does this apply when the limitations of the theory were pointed out by its originator.

Summary.

The molecular heats of air, nitrogen, and oxygen have been determined over a temperature 0°C. to 1000°C. by a method depending on the measurement of the velocity of sound in the chemically pure gases. Further measurements for air up to 1300°C. are added, and a reply is given to criticism of the method of determining the tube constant.

Chemistry Department,
East London College,
University of London.

XCI. *The Effect of Refraction on Electron Diffraction.*

By G. P. THOMSON, M.A.*

IN a very valuable and important paper on the diffraction of electrons by thin metal films, E. Rupp† considers that his results can be best explained by attributing a refractive index to the metal for electron waves and calculates its value in certain cases. These values have recently been used by Rosenfeld and Witmer‡ in a theoretical paper. While the hypothesis that a metal shows a refractive index for electrons is intrinsically probable, and seems by far the best way of accounting for some of Davison and Germer's experiments with reflected electrons, it appears that there is an oversight in Rupp's method of calculation which greatly modifies the conclusions which can be drawn from his experiments. The problem is as follows:—Electrons are assumed to be guided by waves whose wave-length in free space is $\lambda = h/nw$. They pass at normal incidence through a thin film of metal and are diffracted by the atoms of the crystals composing it, a pattern being formed analogous to

* Communicated by the Author.

† E. Rupp, *Ann. der Phys.* lxxxv. p. 981 (1928).

‡ Rosenfeld and Witmer, *Zeit. f. Phys.* xlix. p. 534 (1928).

a Debye-Scherrer pattern for X-rays. How will the pattern be modified if the wave-length in the metal is not λ but $\lambda' = \lambda/\mu$ where μ is a quantity analogous to an optical refractive index? When $\mu=1$ the electrons are reflected whenever they are incident on a crystal plane at an angle θ satisfying Bragg's law

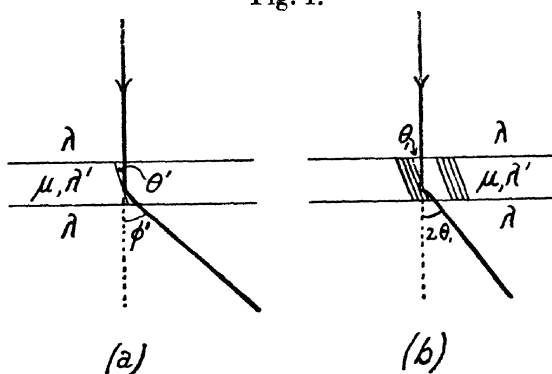
$$n\lambda = 2d \sin \theta,$$

and a diffracted beam occurs with a deviation $\phi = 2\theta$. If $\mu \neq 1$ this becomes (fig. 1, a)

$$n\lambda/\mu = 2d \sin \theta',$$

and this is the relation (in my notation) which Rupp uses to find θ' the new angle of reflexion. For the deviation he

Fig. 1.



takes $2\theta'$, and it is here that the error lies. If the wave-length is modified in the metal, there must, by Huyghen's principle, be a bending of the rays on emergence. In the actual case where the incidence is normal there is no bending on entering the metal, but λ becomes λ' and the deviation in the metal is $2\theta'$, which is the angle of incidence on the second surface. The angle of refraction ϕ' is given by

$$\sin \phi' = \mu \sin 2\theta'.$$

Comparing with the case where $\mu=1$,

$$\sin \theta / \sin \theta' = \mu$$

and

$$\begin{aligned} \sin \phi' / \sin \phi &= \mu \sin 2\theta' / \sin 2\theta = \cos \theta' / \cos \theta \\ &= \sqrt{4\mu^2 d^2 - n^2 \lambda^2} / \mu \sqrt{4d^2 - n^2 \lambda^2}. \end{aligned}$$

Thus for θ, θ' small the effects compensate, and for larger angles the small effect is in the opposite direction to that given by Rupp's calculation.

It has been suggested that the diffraction actually observed in these and similar experiments occurs at the inner surfaces of holes in the metal film (fig. 1, *b*). While holes are undoubtedly present in the films I used, and may have occurred in Rupp's films also (see, for example, Smekal's paper in the 'Transactions of the Volta Centenary' on the imperfection of crystals), it does not seem likely that these really play an important part. If the rays were really reflected from planes parallel to the inner face of one of these holes, the effect of refraction would be expressed by a formula found by Darwin * for the analogous case with X-rays, namely,

$$\theta_1 - \theta = \frac{\mu - 1}{\sin \theta \cos \theta},$$

where θ_1 is the new glancing-angle outside the metal, and $\mu - 1$ is small. Now in my experiments † with electrons of the order of 40,000 volts, θ_1 was of the order $\frac{1}{50}$, thus

$$(\theta_1 - \theta)/\theta \sim 50^2(\mu - 1).$$

But Bragg's law held in its simple form to better than 1 part in 50, thus

$$|\mu - 1| < \frac{1}{50^3}.$$

The theoretical formula

$$\mu = \sqrt{1 + \Phi/E},$$

where E the kinetic energy of the electron and Φ the potential of the metal, then gives $|\Phi| < .7$ volt. This is very small compared with the 18 volts found by Davison and Germer and with any theoretically probable value. In addition there is very little difference between patterns taken with my original films which had obvious holes, and with films which I have been using recently made by spluttering, which appear quite continuous under the microscope.

In criticizing Herr Rupp's calculations of the effect of the refractive index I should like to emphasize that I am not trying to minimize the importance of the exceedingly beautiful work he has done in showing that comparatively slow electrons can show well-marked diffraction patterns through metal films. The supposed effect of refractive index is only a few per cent. in any case, and Herr Rupp himself says

* C. G. Darwin, *Phil. Mag.* xxvii. p. 320 (1914).

† 'Nature,' cxx. p. 802 (1927); *Proc. Roy. Soc. A*, cxvii. p. 600 (1928).

that it is on the limit of the accuracy of the experiments. The discrepancy left, when the calculation is made as indicated above, may perhaps be accounted for by a slight systematic error in the measurement of the electron velocities.

Aberdeen,
Sept. 27, 1928

XCII. Notices respecting New Books.

Handbuch der Radiologie: Vierter Band, Dritter Teil. "Gluhelektroden," von O. W. RICHARDSON; "*Technische Anwendung der Gluhelektroden,"* von H. RUKOP; "*Flammenleitung,"* von ERICH MARX. Zweite Auflage. [Pp. xvi + 724, mit 190 Figuren und Abbildungen im Text.] (Leipzig: Akademische Verlagsgesellschaft m.b.H., 1927. Price, brosch. M.48; geb. M.50.)

THE third part of the second edition of Bd. iv. of the 'Handbuch der Radiologie' comprises three monographs. The first is a translation, by Prof. A. Karolus, of Richardson's well-known work on the emission of electricity by hot bodies. This has been brought up to date where necessary by a 32 page appendix, contributed by E. Rupp. The second monograph, by Prof. Rukop, written for the new edition of the Handbuch, is an account of the technical applications of thermionic emission. It is naturally concerned to a large extent with the theory and the various practical applications of the triode valve and of tubes with special characteristics—tubes with multiple grids, tubes used in conjunction with magnetic fields, &c. Extending to 138 pages, this monograph deals with the subject in a very comprehensive manner.

The third monograph, by the Editor of the Handbuch, deals with the conduction of electricity in flames. Since the appearance of the first edition, the theory of temperature ionization, advanced by M. N. Saha to explain the phenomena of stellar spectra, has gained general acceptance. This theory was shown by H. A. Wilson and Noyes to be applicable to the problem of conduction in flames. A full account of the theory and of its applications to electrical conduction in flames has been included in the new edition; the theory has enabled some matters, which were controversial at the time of the first edition, to be settled and the relevant sections have therefore been omitted. The monograph provides a valuable summary of the present position of practice and theory with respect to the phenomena of electrical conduction in flames.

Although the process of subdivision has been carried further in the second edition than the first, there does not appear to be any particular advantage in publishing these three monographs in one volume. If each were obtainable separately the sales would undoubtedly benefit.

The Theory of Probability. By the late WILLIAM BURNSIDE, Sc.D., LL.D., F.R.S. [Pp. xxx+106.] (Cambridge: At the University Press. 1928. Price 10s. 6d. net.)

THE late Professor Burnside became interested in the theory of probability during the period of the war, his first paper on the subject, published in 1918, being concerned with a military question. His interest in the subject grew, and other papers on topics related to the theory of probability appeared from time to time. Finally, he set out to prepare a systematic account of the theory. The draft was completed before a serious illness in 1925; although it contained all the issues which he proposed to discuss, additions and amplifications were intended, but remained unwritten. A number of notes, elucidating or establishing statements in the text were planned: only one was written, and no memoranda were left indicating the nature of the remainder. In these circumstances the draft has been published, under the editorship of Dr. A. R. Forsyth, exactly as it was written and has been prefaced by the obituary notice written by Dr. Forsyth for the Royal Society.

The account of the theory occupies only 100 pages and possesses the conciseness and precision characteristic of Prof. Burnside's writings. In the introductory chapter, the rule for calculating calculable probabilities is properly enunciated, and the method of estimating probability discussed. Direct, indirect and approximate methods of calculating probabilities are dealt with successively, with numerous illustrative examples. Two chapters are devoted to the probability of causes and to probabilities connected with geometrical questions. The final chapters deal with the theory of errors and with Gauss's law of errors. The volume forms a valuable addition to the literature concerned with the theory of probability.

XCI. *Proceedings of Learned Societies.*

GEOLOGICAL SOCIETY.

[Continued from vol. v. p. 1263.]

April 4th, 1928.—Prof. J. W. Gregory, D.Sc., F.R.S.,
President, in the Chair.

THE following communication was read:—

1. 'The Analcite-Syenites and Associated Rocks of Ayrshire.'
By George Walter Tyrrell, A.R.C.Sc., Ph.D., F.R.S.E., F.G.S.,
Lecturer in Geology in the University of Glasgow.

The analcite-syenites of Ayrshire occur in differentiated intrusions along with analcite-olivine-dolerites or crinanites, as stratiform bands, schlieren, and veins. The principal occurrence is at Howford Bridge, Mauchline, where analcite-syenite forms a considerable

part of the sill. In the remaining three described occurrences (Dippol Burn, Trabboch Burn, and Prestwick) the analcite-syenite is restricted to schlieren and veins.

The Howford Bridge, Dippol Burn, and Trabboch Burn occurrences form sills intrusive into the Permian lavas and tuffs of the Mauchline basin; the Prestwick sill is intruded into sediments of Coal-Measure age. They all belong to the widespread suite of analcite-bearing igneous rocks of late-Carboniferous and Permian age in the West of Scotland.

The constituent minerals of these rocks are labradorite, sodic plagioclase, potash-oligoclase, olivine, titanaugite, ægirine, soda-amphiboles, ilmenite, along with analcite and certain zeolites. The most noteworthy mineralogical feature is the abundant occurrence of analcite, thomsonite, natrolite, and prehnite, which must be regarded as late primary crystallizations from the magma.

Petrographically the rocks are divided into: (A) Olivine-analcite-dolerite (crinanite), constituting the major portions of all the described occurrences; (B₁) Analcite-syenite, a coarse-grained, comparatively basic type, which occurs as bands, schlieren, and veins; and (B₂) Analcite-syenite, a perfelsic type, rich in analcite and other zeolites, and with abundant ægirine and soda-amphibole. This variety is found chiefly as veins. Analyses of crinanite and analcite-syenite illustrate the chemistry of these rocks.

The analcite-syenite differentiate is found towards the interior parts of the sills. The petrographical variations within the various intrusive bodies are ascribed to simple crystallization-differentiation aided by the gravitative settling of titanaugite-ilmenite intergrowths. Several reaction-series, continuous and discontinuous, have been traced, and these have been combined in a Goldschmidt diagram showing at one and the same time the parallel courses of crystallization and differentiation. It is shown that a certain amount of lime is probably stored up in the residual liquor, along with the usual soda, potash, silica, water, and volatile constituents, leading to the final crystallization of analcite, soda-lime zeolites, and prehnite.

An hypothesis for the development of schlieren and veins in the sills under discussion by the effects of the varying incidence of the pressure due to the superincumbent column of rock, upon a crystal-mesh filled with interstitial liquid, is framed. The liquid is believed to be progressively driven towards the centre of the sill, and also laterally towards those places where the pressure is compensated in various ways, so that free contraction of the crystallizing mass can take place. The great development of analcite-syenite within the Howford Bridge sill is shown to be concomitant with the impoverishment of the associated crinanite in analcite; whereas in the other three sills, which contain relatively small developments of analcite-syenite, the crinanitic portions are relatively rich in analcite.

[The Editors do not hold themselves responsible for the views expressed by their correspondents.]

THE
LONDON EDINBURGH, AND DUBLIN
PHILOSOPHICAL MAGAZINE
AND
JOURNAL OF SCIENCE.

[SEVENTH SERIES.]

NOVEMBER 1928.

XCIV. *The Escape of Heat from a Harmonically Oscillating Hot Wire.* By R. S. MAXWELL, M.A., B.Sc.*

1. INTRODUCTION.

THE problem of the escape of heat by free convection from a thin cylindrical wire at rest has been studied by Langmuir † and others, while King ‡ has carried out an exhaustive research, both theoretically and experimentally, on the case when the stationary wire is cooled by a stream of air passing it with a certain velocity, *i. e.* cooling by forced convection. When the wire is not at rest the problem is considerably more complicated, and up to the present no complete mathematical analysis has been brought forward. A considerable amount of experimental work has, however, been done on the subject by Tucker and Paris § in connexion with their Hot-Wire Microphone. They measured the escape of heat from the electrically-heated wire when subjected to an alternating air-current. The converse effect, that of a hot wire oscillating in still air, has been dealt with by Richards ||. In both cases the wire is cooled,

* Communicated by Prof. A. W. Porter, F.R.S.

† Langmuir, *Phys. Rev.* xxxiv. pp. 401-422 (1912).

‡ King, *Phil. Trans. Roy. Soc. A*, ccxiv. pp. 373-430 (1914).

§ Tucker & Paris, *Phil. Trans. Roy. Soc. A*, ccxxi. pp. 389-430 (1921).

|| Richards, *Phil. Mag.* xlv. pp. 926-934 (1923).

and consequently its resistance alters. It is shown that the change can be divided into two categories :—

- (a) A lowering of the resistance of the whole wire.
This is known as the steady drop.
- (b) A periodic change of resistance.

The object of the present work is to investigate these two resistance changes under varying conditions, and also to bring forward, at any rate approximately, a mathematical theory which will explain the observed effects.

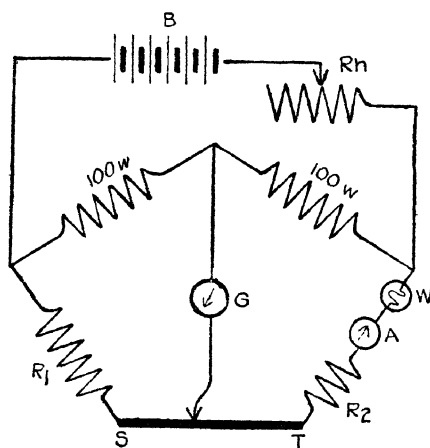
2. EXPERIMENTAL WORK.

(a) *Steady Drop.*

(1) *Description of Apparatus.*

The experiments were made with the very fine platinum wire—diameter 0·0006 cm.—in the grid of a Tucker hot-wire

Fig. 1.



microphone. This grid was mounted on one prong of an electrically-maintained tuning-fork, and a compensating weight was mounted on the other prong, so that the fork would vibrate evenly. The tuning-fork and grid were completely enclosed in a large wooden box, so that all extraneous draughts were excluded.

The grid (W) was arranged in one arm of a Wheatstone's network, so that its resistance could be measured, and a milliammeter (A) was also included in the circuit. The electrical connexions are shown in fig. 1.

The method of taking observations was as follows. A rheostat (Rh) in the battery circuit was adjusted until the heating current through the grid had reached some definite value—say 30 milliamperes—when the fork was at rest, and the resistance of the grid was then measured. A long straight wire (ST) which had previously been calibrated, with an adjustable contact to the galvanometer, was used to obtain an accurate point of balance.

When the fork was set in vibration, the resistance of the grid decreased as it became cooled, and the new resistance was measured by balancing the network again. In order to prevent much alteration of the grid heating current, the total resistance $R_1 + R_2$ in the two resistance boxes was kept constant throughout a given series of readings.

The resistance of the grid was measured for various values of the amplitude of the fork, keeping the heating current constant. Nine such series of readings were taken for different values of the heating current: the resulting curves are shown in fig. 2.

The amplitudes were measured by means of a microscope with an eyepiece scale which was calibrated against a linear steel scale.

(2) Numerical Calculations.

(α) *Temperature*.—Within the accuracy covered by these experiments, there is a linear relationship connecting the resistance of the grid when at rest with the excess temperature of the hot wire of the grid over that of the surrounding atmosphere.

If R_0 = resistance of grid at atmospheric temperature and R_θ = resistance of grid at a temperature excess of θ_1 above that of the atmosphere, then

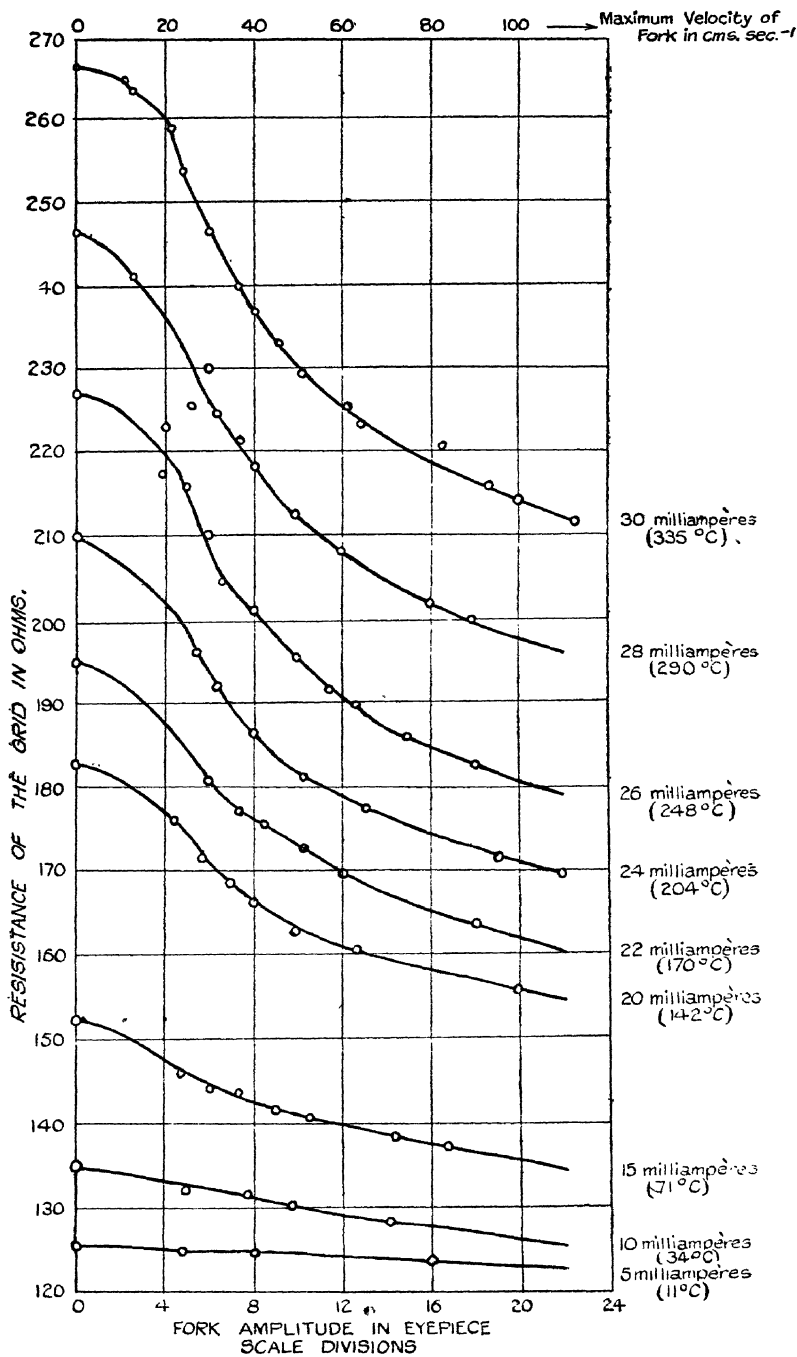
$$R = R_0(1 + \alpha\theta_1), \dots \dots \dots (1)$$

where α is the temperature coefficient of resistance of the wire of the grid.

Table I. shows the resistance of the grid when at rest for different heating currents. On extrapolating the resulting graph, it is found that the resistance of the grid at atmospheric temperature, *i. e.* when no current is flowing in the wire, is 120 ohms.

The last column in the table gives the excess temperature (θ_1), calculated with the aid of equation (1) and assuming $\alpha = 0.00367$ for platinum.

Fig. 2.



From the graph obtained on plotting $R\theta$ against θ_1 it is found that 1 ohm is equivalent to 2.24°C ., i. e. that a decrease in the resistance of the grid of 1 ohm corresponds to a fall in temperature of the wire of 2.24°C .

(β) *Velocity*.—The change in the steady drop when the heating current is unaltered is due to the relative movement of wire and air, and is a function of the velocity of the wire through the air. This of course is not constant throughout the cycle, but the maximum velocity (V) can easily be found.

TABLE I.

Heating current (i), milliamps.	Resistance of grid when at rest (R), ohms.	Excess temperature above atmospheric (θ), $^\circ\text{C}$.
30	267	335
28	247	290
26	228	248
24	210	204
22	195	170
20	183	142
15	152	71
10	135	34
5	125	11,
(0)	(120)	—

If
and $\left\{ \begin{array}{l} n = \text{frequency of fork} \\ y_0 = \text{amplitude } ,, \quad ,, \\ V = 2\pi ny_0. \end{array} \right\} \dots (2)$
then

Now, the frequency of the fork used during the experiments was 96 vibrations per second. The eyepiece scale of the microscope was calibrated against a steel millimetre scale, and it was found that one eyepiece scale-division was equivalent to $7.5 \times 10^{-3}\text{ cm}$. Therefore for one eyepiece scale-division

$$y_0 = 7.5 \times 10^{-3}\text{ cm.}$$

$$\therefore V = 2\pi \times 96 \times 7.5 \times 10^{-3}\text{ cm.}$$

$$= 4.52\text{ cm. sec.}^{-1}$$

Values of the maximum velocity (V) for various values of the amplitude are given in Table II.

(γ) *Steady Drop*.—The experimental values found for the steady drop (Δ) from the graphs of fig. 2, with the help of Table I., are tabulated in Table II. for various known conditions of temperature and velocity.

TABLE II.

Experimental Values of Δ in $^{\circ}\text{C}$. for Microphone Grid.

Amplitude.		Maximum Velocity (V) in cm. sec. ⁻¹ .	Temperature excess (θ_1) in °C.									
Eye-piece scale-divisions.	cm.		335	290	248	204	170	142	71	34	11	
— 2	0.015	9.0	2	7	4	6	6	4	3	2	0	
4	0.030	18.1	12	22	16	17	17	15	12	4	1	
6	0.045	27.1	41	46	43	36	32	27	18	7	1	
8	0.060	36.2	66	64	58	53	43	38	22	9	1	
10	0.075	45.2	81	77	72	63	50	45	26	11	2	
12	0.090	54.3	92	86	82	70	57	48	28	13	2	
14	0.105	63.3	100	94	90	75	63	54	30	15	3	
16	0.120	72.4	109	101	95	80	67	57	34	16	4	
18	0.135	81.4	112	105	100	83	72	60	36	18	4	
20	0.150	90.5	118	110	104	88	76	63	38	20	6	

(b) *Oscillatory Changes.*

The first experiments which were undertaken with a view to investigating the harmonic changes of resistance of the grid made use of a telephone receiver which was coupled inductively with the grid heating circuit. In addition to the fundamental the octave could be heard distinctly, and there was also evidence of higher harmonics. A vibration galvanometer was afterwards introduced in place of the telephone, and the presence of these harmonics was confirmed.

The instrument used was a Tinsley Moving Coil Vibration Galvanometer with a bifilar suspension. The suspended system had three adjustments, which could be varied to alter its natural frequency :

- (1) The length of the suspension.
- (2) The tension of the wires.
- (3) The distance apart of the two wires.

When these were adjusted to make the natural frequency of the system equal to the frequency of the alternating current passing through the galvanometer, the latter was said to be "tuned." In this state resonance occurred, and the spot of light broadened out into a wide band. During these experiments the distance apart of the two wires remained fixed, and the tension and length adjustments gave a range from about 85 to 500 cycles per second. Scales had been engraved on the torsion head and on the side of the case near the sliding bridge, so that it was possible to record definite positions for the tension and length of suspension respectively. Thus any particular condition could be repeated at will. The galvanometer had been calibrated for frequency by passing alternating currents of known frequencies through it and noting the positions of the bridge reading and torsion head.

The grid heating current, which was known to have a complex wave form, was passed through the vibration galvanometer, and the adjustments were made throughout the whole of the above range. The harmonics present in the current could then be picked out at once, because when the galvanometer became tuned to any one component, resonance was observed. The frequency of the component was then found from the calibration curves.

The results of this analysis showed that, denoting the frequency of the tuning fork by n , the grid heating current had a series of harmonic constituents whose frequencies were given by $2n$, $3n$, $4n$, and in one case for a very low fork $5n$, in addition to the fundamental. For these experiments on the oscillatory changes several forks were used, of frequencies varying from 68 to 167 vibrations per second, but in most cases the fork of frequency 96 vibrations per second was used as in the experiments on the steady drop. The experiments were repeated for a straight platinum wire of diameter .001 cm. mounted horizontally on the fork, and similar results were obtained, the harmonics being found as before.

A distinction must be made between the two cases, when the wire is vibrating (*a*) vertically, *i. e.* in its own convection current, and (*b*) horizontally. In (*a*) the fundamental and the octave appeared to be of approximately the same magnitude, but in (*b*) the octave was by far the most predominant harmonic present. This distinction is important on theoretical grounds, and is discussed in detail in section 4. The higher components of frequency $3n$, $4n$, etc. were observed to have considerably smaller amplitudes than the

fundamental and octave, although it proved impossible to measure any of these amplitudes with a great degree of accuracy. Attempts to make such measurements were made both directly and by means of photographing the wave form with the help of a rotating mirror, but they proved unsuccessful because the galvanometer could not be tuned sufficiently far away from the several resonance points to give a faithful reproduction of the wave form of the current, unless it was made too insensitive.

Photographs were taken of the vibrations of the prong of the fork to see whether the motion was accurately sinusoidal. Light from an arc was passed through a small diaphragm reflected from a mirror attached to the prong of the fork and from a rotating mirror, and finally was focussed on to the photographic plate. Several photographs were taken, and these showed that the prong was moving with simple harmonic motion, as was to be expected.

3. THEORETICAL CONSIDERATIONS.

(a) *General.*

The rate of loss of heat from a thin oscillating hot wire depends on several factors.

Heat Supplied.—If the wire is heated electrically, then the rate of heat supplied is E^2/R , where E is the e.m.f. in the heating circuit, and R is the resistance of the wire. If E is measured in volts, and R in ohms, then the rate of heat supplied will be measured in watts.

As the resistance of the wire is large compared with any other resistances in the circuit, the potential drop across the ends of the wire may be regarded as constant, and will not be affected by the oscillation.

Radiation.—In the treatment which follows, the loss of heat due to radiation will be ignored because Langmuir* has shown that for fine wires such as those used in the experimental work it is negligibly small.

Thermal Capacity of the Wire.—The thermal capacity (ϵ) is defined as the mass of the wire (m) multiplied by its specific heat (c).

Then $\epsilon d\theta$ represents the amount of heat added to or taken away from the wire for a change of temperature $d\theta$.

In the analysis given below the convention is adopted that

* Langmuir, *Phys. Rev.* xxxiv. pp. 401–422 (1912).

θ is reckoned positive for a lowering of temperature, and therefore

$\epsilon d\theta$ = amount of heat taken away from the wire
for a drop in temperature of $d\theta$.

Hence $\epsilon \frac{d\theta}{dt}$ = rate at which heat is taken away from the wire.

Free Convection.—If the wire is *at rest*, and is heated electrically, then it will take up a certain definite equilibrium temperature when the rate of heat lost by free convection is exactly equal to the rate of heat supplied by the electric current.

Let θ_1 = excess temperature of the wire above that of the surrounding atmosphere ;

E = e.m.f. in the heating circuit ;

R_1 = resistance of the wire at temperature θ_1 .

Then
$$\frac{E^2}{R_1} = H \theta_1, \quad . \quad . \quad . \quad . \quad (3)$$

where H is the free convection constant.

Forced Convection.—When the wire is cooled by being placed in a current of air, the phenomenon is called forced convection, and the escape of heat from the wire is dependent upon the velocity of the imposed draught. This may be treated as completely equivalent to the case when the wire is caused to move through still air with a definite velocity.

King* has derived two formulæ which give the heat-loss per cm. (W) from a wire of diameter d in a *steady* air-current of velocity V :

$$W = A'\theta_1 + B'V^{\frac{1}{2}}d^{\frac{1}{2}}\theta_1, \quad . \quad . \quad . \quad . \quad (4)$$

$$W = a'\theta_1 / \log \frac{b'}{\sqrt{Vd}}, \quad . \quad . \quad . \quad . \quad (5)$$

where A' , B' , a' , and b' are constants, and θ_1 is the excess temperature of the wire above that of the surrounding air.

He found a critical value $Vd = 0.0187$, where V is measured in cm./sec. and d in cm.

When $Vd > 0.0187$, *i. e.* for high velocities or thick wires, equation (4) must be used.

When $Vd < 0.0187$, *i. e.* for low velocities or thin wires, equation (5) is applicable.

The critical velocity for any wire is denoted by V_c .

* King, Phil. Trans. Roy. Soc. A, ccxiv. pp. 312–432 (1914).

An attempt has been made here to see whether King's formulæ can be adapted to the case when the wire is subjected to an oscillating draught, or, what is equivalent, to the case where the wire itself vibrates when mounted on a tuning-fork.

Let y = displacement of the prong of the tuning-fork, and consequently of the wire.

By experiment the motion is found to be simple harmonic, say $y = y_0 \sin pt$, where p is the pulsance of the imposed vibration = 2π times the frequency.

The velocity (v) of the wire at any time is given by

$$v = \frac{dy}{dt} = py_0 \cos pt,$$

but as the cooling of the wire is assumed to be independent of the direction of motion, the speed of the wire through the air at any moment can be written $py_0 |\cos pt|$ *, or $V |\cos pt|$, where V is the maximum value of the velocity, i. e. $V = py_0$.

For generality the escape of heat due to forced convection may be written $h(\theta_1, V |\cos pt|)$, and the appropriate formulæ (4) or (5) can be applied in special cases.

Differential Equation.—The general differential equation governing the escape of heat from the hot wire when it is oscillating can now be written down.

As before, let θ_1 = temperature excess of the wire above that of the surrounding atmosphere.

When the wire is set in vibration it is cooled by forced convection, and its temperature drops.

Let θ equal the divergence of the temperature from θ_1 at any time t , and let θ be regarded as positive when measured in a downward direction.

Then

$$\epsilon \frac{d\theta}{dt} = H(\theta_1 - \theta) + h((\theta_1 - \theta), V |\cos pt|) - \frac{E^2}{R_1(1 - \alpha\theta)},$$

. (6)

where α is the temperature coefficient of resistance of the material of the wire.

Since θ is small, equation (6) may be written

$$\epsilon \frac{d\theta}{dt} = H(\theta_1 - \theta) + h((\theta_1 - \theta), V |\cos pt|) - \frac{E^2}{R_1}(1 + \alpha\theta)$$

. (7)

* The expression $|\cos pt|$ is used to signify the numerical value of $\cos pt$ without regard to sign. The function $|\cos pt|$ is thus always positive.

In the following sections the applications of this equation will be considered.

(b) *High Velocities.*

In this case King's formula for the rate of loss of heat due to forced convection may be written

$$W = (\beta V^{\frac{1}{2}} + \gamma)(\theta_1 - \theta),$$

where β and γ are constants having the same meaning as in King's paper.

Equation (4) now becomes

$$\begin{aligned} \epsilon \frac{d\theta}{dt} &= H(\theta_1 - \theta) + (\beta V^{\frac{1}{2}} |\cos pt|^{\frac{1}{2}} + \gamma)(\theta_1 - \theta) - \frac{E^2}{R_1}(1 + \alpha\theta) \\ &= -\left((H + \gamma) + \frac{E^2}{R_1}\alpha\right)\theta + \left((H + \gamma)\theta_1 - \frac{E^2}{R_1}\right) \\ &\quad + \beta V^{\frac{1}{2}} |\cos pt|^{\frac{1}{2}} \theta_1 - \beta V^{\frac{1}{2}} |\cos pt|^{\frac{1}{2}} \theta. \quad (8) \end{aligned}$$

The last term is of a smaller order than the other terms, and to a first approximation it may be omitted. When an approximate value for the temperature θ has thus been obtained, it may be substituted in this small term, and the equation can then be solved to a higher degree of accuracy.

The equation may now be written in the simple form :

$$\frac{d\theta}{dt} = -a\theta + b + c\{|\cos pt|\}^{\frac{1}{2}}, \quad \dots \quad (9)$$

where

$$a = \frac{1}{\epsilon} \left[(H + \gamma) + \frac{E^2}{R_1} \alpha \right],$$

$$b = \frac{1}{\epsilon} \left[(H + \gamma)\theta_1 - \frac{E^2}{R_1} \right],$$

and

$$c = \frac{1}{\epsilon} \beta V^{\frac{1}{2}} \theta_1.$$

The function $\{|\cos pt|\}$ is not in a form suitable for integration. It may, however, be expressed as a Fourier Series, and the numerical values of the different coefficients can be found by graphical integration.

If T is the periodic time of the oscillation, then the required limits of the function must be $t=0$ and $t=T$, because after this everything will be repeated.

For brevity let x be written in place of pt ; then, when $t=0$, $x=0$, and when $t=T$, $x=2\pi nT=2\pi$, and the limits now become 0 and 2π .

The Fourier Series may be written down :

$$\begin{aligned} \{|\cos x|\}^{\frac{1}{2}} &= a_0 + a_1 \cos x + a_2 \cos 2x + \dots a_n \cos nx \\ &\quad + b_1 \sin x + b_2 \sin 2x + \dots b_n \sin nx. \end{aligned}$$

It is known that

$$a_0 = \frac{1}{2\pi} \int_0^{2\pi} \{|\cos x|\}^{\frac{1}{2}} dx,$$

$$a_n = \frac{1}{\pi} \int_0^{2\pi} \{|\cos x|\}^{\frac{1}{2}} \cos nx \, dx,$$

and
$$b_n = \frac{1}{\pi} \int_0^{2\pi} \{|\cos x|\}^{\frac{1}{2}} \sin nx \, dx.$$

The numerical values of these coefficients were determined by plotting the graph of the function within the integral sign for different values of x between the required limits, and finding the area enclosed between the curve and x -axis.

It was found that

$$a_1 = a_3 = a_5 = \dots a_{2n-1} = 0,$$

$$b_1 = b_2 = b_3 = \dots b_n = 0,$$

$$a_0 = 0.757,$$

$$a_2 = 0.330,$$

$$a_4 = -0.111,$$

$$a_6 = 0.080,$$

$$a_8 = -0.006.$$

Therefore

$$\begin{aligned} \{|\cos x|\}^{\frac{1}{2}} = & 0.757 + 0.330 \cos 2x - 0.111 \cos 4x \\ & + 0.080 \cos 6x - 0.006 \cos 8x + \dots \end{aligned}$$

Equation (9) now becomes

$$\begin{aligned} \frac{d\theta}{dt} = & -a\theta + b + c\{0.757 + 0.330 \cos 2pt - 0.111 \cos 4pt \\ & + 0.080 \cos 6pt - 0.006 \cos 8pt + \dots\} \quad (10) \end{aligned}$$

The solution of (10) is

$$\begin{aligned} \theta = & \frac{b}{a} + c \left\{ \frac{0.757}{a} + \frac{0.330}{\sqrt{4p^2 + a^2}} \cos(2pt - \phi_2) \right. \\ & - \frac{0.111}{\sqrt{16p^2 + a^2}} \cos(4pt - \phi_4) + \frac{0.080}{\sqrt{36p^2 + a^2}} \cos(6pt - \phi_6) \\ & \left. - \frac{0.006}{\sqrt{64p^2 + a^2}} \cos(8pt - \phi_8) \right\} + Ae^{-at}. \quad (11) \end{aligned}$$

The last term dies out as t becomes large, and may be ignored so far as periodic solutions are concerned.

The mathematical analysis shows :

(1) A steady drop in temperature (Δ), given by

$$\Delta = \frac{b + ca_0}{a},$$

and (2) a series of harmonics of frequency $2n, 4n, \dots$, of which the octave is the most predominant.

If this value of θ is substituted in the last term of equation (8), no new terms are introduced, but there is a small change in the values of the constants.

(c) *Low Velocities.*

For low velocities it is necessary to use the form of King's formula given in equation (5), and when applied to an oscillatory draught equation (7) becomes

$$\epsilon \frac{d\theta}{dt} = H(\theta_1 - \theta) + \frac{a'}{b' \log \sqrt{V |\cos pt|} d} (\theta_1 - \theta) - \frac{E^2}{R_1} (1 + a\theta) \quad \dots \dots (12)$$

The solution of this equation shows temperature changes of just the same form as those given by equation (11).

(d) *Critical Velocity.*

It is important to calculate the critical velocity (V_c) corresponding to King's value $Vd = 1.87 \times 10^{-2}$ for the actual wire used in the experimental work.

In this case $d = 6 \times 10^{-4}$ cm.

$$\begin{aligned} \therefore V_c &= \frac{1.87 \times 10^{-2}}{6 \times 10^{-4}} \\ &= 31.2 \text{ cm. sec.}^{-1}. \end{aligned}$$

This velocity marks the boundary between the high and low velocity formulæ, and this must be kept in mind during the succeeding sections.

4. COMPARISON OF THEORY WITH EXPERIMENT.

(a) *Steady Drop.*

It is possible to calculate values of the steady drop Δ by means of equation (11), using the appropriate values of β and γ as given by King* in his paper. The values thus found are not in sufficient agreement with those obtained experimentally to be given in detail in this paper, but they are of the same order of magnitude. Furthermore, in both cases

* *Loc. cit.* pp. 420 and 422.

the steady drop is found to increase with temperature and with velocity.

It must be remembered, however, that the experimental conditions were by no means the ideal conditions demanded by the theory. For one thing, instead of a straight wire stretched between two fixed supports, the crumpled wire of a microphone grid was used. There are three loops in such a grid, and as the grid was clamped in a vertical position, it is quite possible that the convection current from one part of the wire impinged upon another part, thus lowering the resistance of the grid as a whole*. Again, since the wire was not straight, it was very difficult to measure its length with any degree of accuracy. The value adopted -0.7 cm.—was found by observing the grid with a microscope and measuring those portions of the wire which would be effective in contributing freely to the convection current. But since the calculated value of Δ increases with increase of length of wire, this uncertainty is bound to introduce a small error.

The wires used in this experiment were very much smaller than any used by King in his experiments on forced convection with steady draughts, and it may be that his formulæ will not bear extrapolation to such fine wires. For example, the term depending upon the velocity does not appear to have a sufficiently great coefficient to cause the theoretical value of the steady drop to increase sufficiently for the greater velocities, and it is possible that other formulæ could be devised which would fit the experimental curves better; but it does not seem worth while pursuing this line until the theoretical conditions are more accurately realized.

There is yet another factor affecting the cooling of the wire which should be noticed. It has been shown above (p. 957) that the critical velocity below which the high velocity formula given by equation (8) will not hold is given by $V_c = 31.2$ cm. sec.⁻¹. Now, in the analysis put forward the actual velocity of $v = V \cos pt$ has been replaced by a mean velocity $a_0 V$, where $a_0 = 0.757$. Actually, however, the velocity varies between the limits $v = V$ and $v = 0$, the velocity falling to zero twice during each complete vibration of the fork. Thus, even if V is considerably greater than V_c , the actual velocity v must be less than V_c during certain portions of the cycle, and it cannot be expected, on this ground alone, that the theoretical equation would show exact agreement with the experimental results.

* Cf. Tucker & Paris, p. 396.

The last error which must be considered is that arising from neglecting the term $\beta V^2 |\cos pt|^{\frac{1}{2}} \theta$. If this term is worked out numerically, using the values of θ already obtained, it is found that, for the case where it could have the greatest possible effect, the error is less than 10 per cent., which is smaller than some of the other errors which have been considered above.

(b) Oscillatory Changes.

Effect due to the heating-up of the surrounding air :—

The mathematical analysis given in Section 3 does not indicate the presence of the fundamental, or the odd harmonics. This is because the theoretical treatment is concerned entirely with the free and forced convection from a hot wire vibrating in cool air, and no account has been taken of the general heating-up of the air in the neighbourhood of the wire. As in King's analysis, it has been assumed that the wire is always moving into air of atmospheric temperature. In this case, if the wire is vibrating with frequency $n = p/2\pi$ there are two positions, one at each end of the swing, in every complete vibration, when the wire is at rest. The cooling is thus identical in the two halves of the cycle, and is periodic with a frequency $2n$. Hence it follows that on this theory the *octave* is the most important term.

In practice, however, it is essential to take into account the heating-up of the surrounding air; and this depends upon the general convection current of the heated air which rises from the hot wire. There are two quite distinct cases :—

(a) *Hot wire vibrating vertically*.—As the wire moves upwards it travels with the convection current; as it moves downwards it travels against it. Thus it is quite clear that the escape of heat from the wire to the air is different for the two motions; consequently, any term arising from this convection effect will be periodic with the frequency of the fork, and the *fundamental* note occurs.

(b) *Hot wire vibrating horizontally*.—The motion of the wire is at right angles to the convection current; the heated air escapes upwards, and so does not affect the cooling of the wire further. This case approximates more to the simple theory, and the *octave* predominates.

The effect of considering this heating-up of the air near the wire is to introduce a periodic term of the same frequency as that of the driving-fork. There is no evidence

available concerning the physical nature of this term, but since it is periodic, it should be possible to represent it as a Fourier series containing all the harmonics. In any case, the fundamental is probably the predominating term, and without in any way being dogmatic in the matter, it is of interest to see the effect of introducing a term $d \cos pt$ to be added on to (9), which then becomes

$$\frac{d\theta}{dt} = -a\theta + b + c \{ |\cos pt| \}^{\frac{1}{2}} + d \cos pt. \quad . \quad . \quad . \quad (13)$$

$$\begin{aligned} \therefore \theta = \frac{b}{a} + c \left\{ \frac{0.757}{a} + \frac{0.330}{\sqrt{4p^2 + a^2}} \cos(2pt - \phi_2) \right. \\ \left. - \frac{0.111}{\sqrt{16p^2 + a^2}} \cos(4pt - \phi_4) + \dots \dots \dots \right\} \\ + \frac{d}{\sqrt{p^2 + a^2}} \cos(pt - \phi_1), \quad . \quad . \quad . \quad . \quad (14) \end{aligned}$$

the decaying exponentials being ignored as before.

If, now, this value of θ is substituted in the last term of (8), terms of the type

$$\begin{aligned} \cos(pt - \phi_1) \cos 2Kpt \\ = \frac{1}{2} \cos(\overline{2K+1} - \phi_1) + \frac{1}{2} \cos(\overline{2K-1} + \phi_1) \end{aligned}$$

arise for all integral values of K . Thus the complete equation becomes

$$\begin{aligned} \theta = \gamma_0 + \gamma_1 \cos(pt - \chi_1) + \gamma_2 \cos(2pt - \chi_2) \\ + \gamma_3 \cos(3pt - \chi_3) + \dots, \quad . \quad . \quad . \quad (15) \end{aligned}$$

which agrees with the experimental results in indicating the presence of a steady drop and the full series of harmonics.

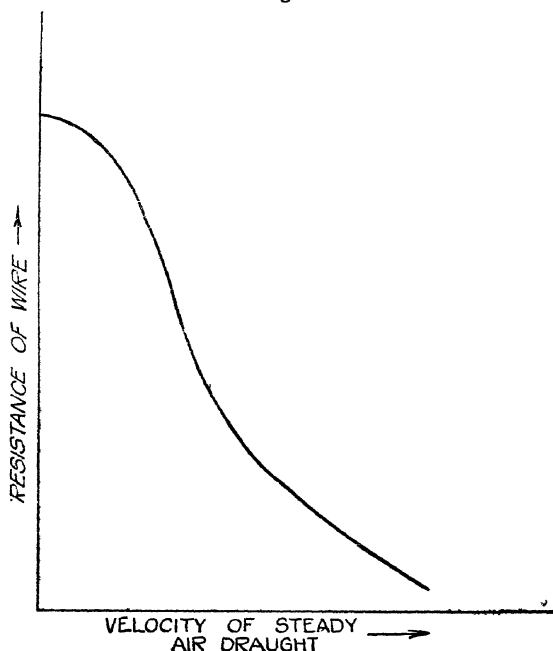
5. WIRE COOLED BY A STEADY DRAUGHT OF VERY LOW VELOCITY.

It appears permissible in conclusion to discuss briefly some of the difficulties which occur in dealing with King's formula for loss of heat when the velocity of the cooling draught is small.

The experimental curves found for the cases when the draught is steady, and when it is oscillatory, are very similar in character, and the difficulties which underlie their interpretation are more or less the same in both cases; so it is convenient merely to consider the simpler case, namely that in which a hot wire is subjected to a small steady cooling draught.

Thomas*, in his researches on the hot-wire anemometer, obtained a series of curves of the type shown in fig. 3 for a straight wire cooled by a steady draught. Richards†, using a microphone grid, and E. G. Richardson‡, using a grid constructed of thicker wire, have both obtained curves of the same type. This curve should be compared with those shown in fig. 2, which were obtained by the writer for oscillating draughts. The curve is concave to the V axis for very small velocities; indeed, it is approximately parabolic near the R axis, but it becomes convex to the V axis

Fig. 3.



as the velocity increases. Tucker and Paris§ obtained only the parabolic portion of the curve, using a microphone grid, but their velocities never exceeded 5 cm. per sec.

In every case the point of inflexion occurred when the velocity was far below the critical velocity V_c for the wire in question; therefore it appears that the experimental curve for low velocities is made up of two distinct parts.

* Thomas, *Phil. Mag.* xxxix. pp. 505-534 (1920). See fig. 8.

† *Loc. cit.* p. 927. See fig. 1.

‡ *Proc. Roy. Soc. A*, cxii. pp. 552-541. See fig. 2.

§ *Loc. cit.* p. 408. See fig. 7.

Thomas also found that "the velocity at which the change of curvature of the respective graphs occurs is greater the larger the heating current employed." This statement is also true for oscillatory draughts, as may be seen on examination of the graphs given in fig. 2.

Turning now to King's formula, given in equation (5),

$$W = \frac{a'\theta_1}{b' \log \frac{V}{d}}, \quad \dots \dots \dots (5)$$

it will be of interest to work it out numerically for a given temperature and for a series of velocities.

Preserving the notation, used by King, the constants a' and b' may be written

$$a' = 2\pi\kappa,$$

$$b' = 2bV,$$

$$\text{where} \quad b = \frac{\kappa e^{(1-\gamma)}}{s\sigma V}$$

and κ = thermal conductivity of air

$$= 5.2 \times 10^{-5} \text{ calories (cm.)}^{-1} \text{ (sec.)}^{-1} \text{ (}^\circ \text{C.)}^{-1},$$

$$\sigma = \text{density of air} = 1.3 \times 10^{-3} \text{ (grm.) (cm.)}^{-3},$$

s = specific heat per unit mass of air

$$= 1.71 \times 10^{-1} \text{ calories (grm.)}^{-1} \text{ (}^\circ \text{C.)}^{-1},$$

$$\gamma = \text{Euler's Constant} = 0.57721.$$

$$\therefore e^{(1-\gamma)} = 1.52.$$

\therefore Numerically

$$\begin{aligned} b' &= \frac{2 \times 5.2 \times 10^{-5} \times 1.52}{1.3 \times 10^{-3} \times 1.71 \times 10^{-1}} \\ &= 7.15 \times 10^{-1} *. \end{aligned}$$

For the wire in the microphone grid $d = 6 \times 10^{-4}$.

$$\therefore \frac{b'}{d} = 1.19 \times 10^3.$$

Now consider a particular temperature excess above atmospheric temperature, say $\theta_1 = 335^\circ \text{C}$. The heat-loss (W) will be given in watts per cm. of wire.

* This constant b' will be unaffected by a change of units from calories per second into watts, as long as κ and s are both measured in the same units. It is of the dimensions of a length.

In this case κ must be expressed in watt units, i. e.

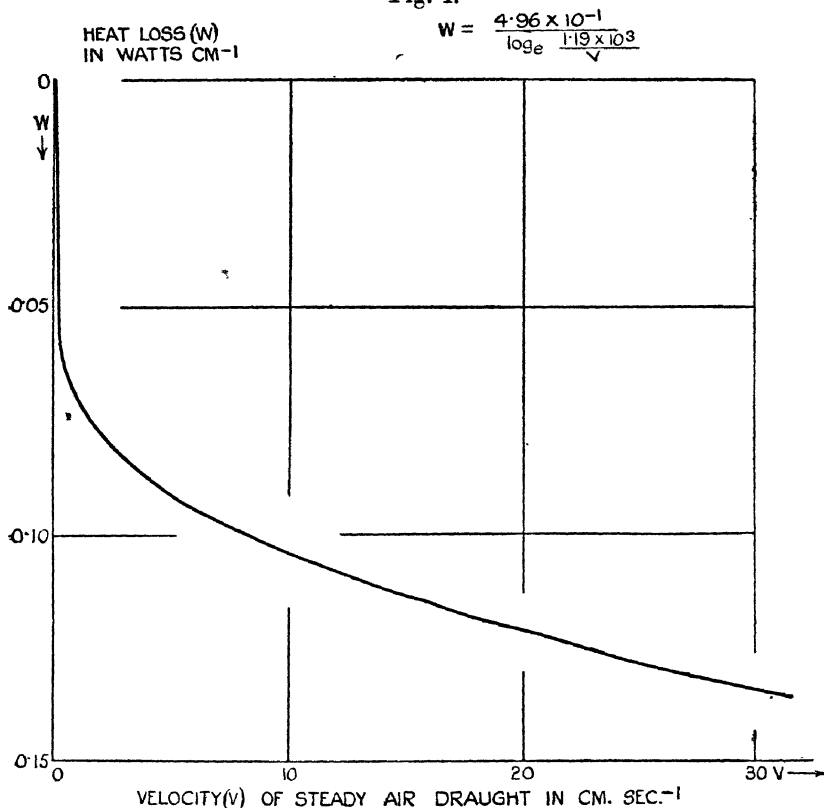
$$\kappa = 2.37 \times 10^{-4} \text{ watts (cm.)}^{-1} (\text{°C.})^{-1}$$

$$\text{and } a'\theta_1 = 2\pi \times 2.37 \times 10^{-4} \times 3.35 \times 10^2 \\ = 4.96 \times 10^{-1}.$$

$$\therefore W = \frac{a'\theta_1}{\log_e \frac{b'}{\sqrt{Vd}}} = \frac{4.96 \times 10^{-1}}{\log_e \frac{1.19 \times 10^3}{V}} \text{ watts cm.}^{-1}.$$

The resulting graph is shown in fig. 4.

Fig. 4.



It can be seen from equation (5) that a graph plotted for a wire at a different temperature would be of exactly the same shape, because the only difference would be in the value of θ_1 . Hence the graph of fig. 4 must be regarded as typical of the theoretical values predicted by King.

The question which must be faced is how to reconcile the theoretical curve shown in fig. 4 with the experimental

curve in fig. 3, for very small velocities, *i. e.* to explain the "parabolic" portion of the experimental curve. No attempt at a quantitative analysis is here put forward, but perhaps the following qualitative suggestions may throw some light on this rather complicated phenomenon.

Consider a hot wire at rest in absolutely still air. Then any heat which is lost must be lost by free convection. Let a very slowly moving air-stream pass across the wire. If the velocity of this stream is sufficiently slow, the wire will still lose heat almost entirely by free convection, and any loss due to forced convection must be extremely small. As the velocity increases, the loss of heat due to forced convection will also increase, and for a time such an increase will be fairly rapid. Such a state of affairs would be represented by the "parabolic" portion of the curve which has been found by all observers. When the velocity is increased still further, the forced convection would have become an appreciable factor in the cooling of the wire, and would increase less rapidly. This would correspond to the point of inflexion in the graph of fig. 3. For velocities higher than this and below V_c , King's low-velocity formula would hold, as shown in fig. 4.

The weakness in the above argument is that it differentiates so clearly between free and forced convection at these very low velocities. It is probably impossible to separate these two phenomena in practice, because they are both so intimately connected with the loss of heat from the wire.

Very little seems to be known about this portion of the subject, which appears to offer a field for further research.

6. SUMMARY.

An electrically-heated platinum wire was mounted upon the prong of an electrically-maintained tuning-fork of frequency n . The hot wire was cooled, owing to the periodic motion through the air, and superimposed upon the steady fall in resistance; there was also a periodic change, with a corresponding periodic change in current. This current was analysed by means of a vibration galvanometer, and was found to contain harmonics of frequency $2n$, $3n$, and $4n$ in addition to the fundamental.

The escape of heat from the wire is due to the following factors :—

(1) The Free Convection effect, which is the same whether the wire is at rest or in motion, except in so far as it depends

on the temperature of the wire, which is, of course, lowered when the wire is vibrating.

(2) The Forced Convection effect which depends upon the velocity of the wire through the air, and which gives rise to

(a) The steady drop in resistance.

(b) Periodic changes of resistance of frequencies $2n$, $4n$, $6n$.

The magnitudes of (a) and (b) depend upon the temperature and diameter of the wire and the velocity of the cooling draught.

(3) The effect due to the heating-up of the surrounding air, which causes the fundamental and probably all the rest of the harmonics to be present.

A mathematical theory is developed which is found to account qualitatively for the observed results.

The writer's thanks are due to Mr. R. C. Richards for some very helpful criticism, and to Prof. A. W. Porter, F.R.S., for his assistance and general direction throughout this research.

Carey Foster Laboratory,
University College, London.
July 1927.

XCV. *The Electrical Conductivity of Metals as a Function of Pressure according to the Sommerfeld Electron Theory.*
By A. T. WATERMAN, Ph.D., Assistant Professor of Physics, Yale University, U.S. National Research Fellow at King's College, London *.

IN a recent paper Houston† has made a noteworthy contribution to Sommerfeld's‡ theory of electrical conductivity in metals by working out the dependence of the mean free path upon temperature, pressure, and other variables. This is done by recognizing the wave nature of the electron, and thus treating the problem after the method used by Debye§ for the interference of X-rays.

* Communicated by O. W. Richardson, F.R.S.

† *Zeits. f. Phys.* xlviii. p. 449 (1928).‡

‡ *Zeits. f. Phys.* xlvii. p. 1 (1928).

§ *Ann. d. Phys.* xliii. p. 19 (1914).

The result shows very fair agreement with observation for the temperature gradient of the conductivity, qualitative agreement for the pressure gradient, and the correct order of magnitude for the conductivity itself, as well as several other interesting applications.

In the case of the effect of hydrostatic pressure upon the electrical conductivity of metals, Houston has merely given an approximate formula, and has briefly pointed out that its application is qualitatively correct. When subjected to quantitative calculation, this formula is found only to give the right order of magnitude for the pressure coefficient of resistance, as seen in Table I. (p. 969.). The accuracy of Bridgman's data * for the pressure coefficients of metals, however, warrants a more exact formula, which may be deduced as shown below.

The formula given by Houston † for the specific resistance of a metal is

$$\rho = 9 \left(\frac{8\pi}{3} \right)^{4/3} \frac{\epsilon^2 m^2 L^{2/3} Z^{2/3} \phi(x) H(c)}{h k \theta d^{1/3} A^{2/3}}, \quad . \quad . \quad . \quad (1)$$

where L = Loschmidt number,

Z = number of free electrons per atom,

θ = characteristic temperature,

d = density,

$$\phi(x) = \text{Debye function } 1/x \int_0^x \xi d\xi / (e^\xi - 1),$$

$$H(c) = (1 + 2c)/(1 + c) - 2c \log(1 + c)/c, \quad c = \lambda^2/(4\pi b)^2$$

(λ = electronic wave-length, b = constant determining the range of the ionic field).

Houston's approximation for the pressure effect lies in the assumptions: first, that the Poisson ratio is independent of pressure, so that $\theta = \text{const. } d^{-1/6} \kappa^{-1/2}$, where κ = compressibility; and secondly, that the temperature is high enough, so that $\phi(x)$ may be replaced by T/θ . Then $\rho = \text{const. } H\kappa$, writing H for $H(c)$, and for the pressure coefficient

$$1/\rho \, d\rho/dp = \partial \log \kappa / \partial p - \partial \log H / \partial p. \quad . \quad . \quad . \quad (2)$$

The first term on the right may be evaluated from the experimental data for the fractional change in volume

* Proc. Amer. Acad. lii. p. 571 (1917).

† Loc. cit. eq. (29).

$\Delta V/V_0$ under pressure, given in the form $\Delta V/V_0 = Ap + Bp^2$. From this we readily derive

$$\frac{\partial \log \kappa}{\partial p} = \frac{2B}{A + 2Bp} - \frac{A + 2Bp}{1 + Ap + Bp^2},$$

or, at zero pressure,

$$(\partial \log \kappa / \partial p)_0 = 2B/A - A.$$

The remaining term, $\partial \log H / \partial p$, is evaluated in the derivation given below.

The approximations underlying eq. (2) may be avoided by adopting Gruneisen's* method, as applied by him to Wien's conductivity theory †, for the derivation of the pressure coefficient of resistance. The feature of this method consists in distinguishing between the adiabatic and the isothermal pressure variation. Since the derivative at constant entropy of any function of θ/T vanishes,

$$(\partial \phi(x) / \partial p)_s = 0,$$

so that, taking the logarithmic derivative of eq. (1) at constant entropy, we have

$$(\partial \log \rho / \partial p)_s = (\partial \log H / \partial p)_s - (\partial \log \theta / \partial p)_s - \frac{1}{3} (\partial \log d / \partial p)_s, \quad (3)$$

assuming $\partial Z / \partial p = 0$.

In order to transform from adiabatic to isothermal conditions, we use the relation

$$\left(\frac{\partial}{\partial p} \right)_s = \left(\frac{\partial}{\partial p} \right)_T + \left(\frac{\partial}{\partial T} \right)_p \left(\frac{\partial T}{\partial p} \right)_s.$$

Also $(\partial \log \theta / \partial p)_s = 1/T (\partial T / \partial p)_s$, $d(\log d) = -d(\log V)$; and, since measurements involve the actual resistance R instead of the specific resistance,

$$(\partial \log R / \partial p)_T = (\partial \log \rho / \partial p)_T - \frac{1}{3} (\partial \log V / \partial p)_T.$$

Hence

$$\begin{aligned} \left(\frac{\partial \log R}{\partial p} \right)_T &= \left(\frac{\partial \log H}{\partial p} \right)_T \\ &\quad + \left(\frac{\partial T}{\partial p} \right)_s \left[\left(\frac{\partial \log H}{\partial T} \right)_p - \frac{1}{T} - \left(\frac{\partial \log R}{\partial T} \right)_p \right]. \end{aligned}$$

But

$$(\partial T / \partial p)_s = T/C_p (\partial V / \partial T)_p.$$

* *Verh. d. deutsche Phys. ges.* xv. p. 186 (1913).

† Columbia Univ. Lectures, 1913.

Hence, finally :

$$\left(\frac{\partial \log R}{\partial p}\right)_T = \left(\frac{\partial \log H}{\partial p}\right)_T + \frac{1}{C_p} \left(\frac{\partial V}{\partial T}\right)_p \left[T \left(\frac{\partial \log H}{\partial T}\right)_p - 1 - T \left(\frac{\partial \log R}{\partial T}\right)_p \right].$$

Writing $\alpha = (\partial \log R / \partial T)_p$, $\beta = (\partial \log V / \partial T)_p$, c' = specific heat per gram, the pressure coefficient of resistance becomes

$$\frac{1}{R} \left(\frac{\partial R}{\partial p}\right)_T = \left(\frac{\partial \log H}{\partial p}\right)_T - \frac{\beta}{c'd} \left[1 + T \left(\alpha - \frac{\partial \log H}{\partial T} \right) \right]. \quad (4)$$

For the two derivatives of $\log H$:

$$(\partial \log H / \partial p)_T = B / H (\partial c / \partial p)_T,$$

where

$$B = 1 + 2/(1+c) - 2 \log (1+c)/c,$$

$$c = 1/(4\pi b)^2 (8\pi/3m)^{\frac{2}{3}},$$

where n = number of free electrons per cubic centimetre.

Then

$$\left(\frac{\partial c}{\partial p}\right)_T = -\left(\frac{8\pi}{3}\right)^{\frac{2}{3}} \frac{1}{8\pi^2 b^2 n^{\frac{2}{3}}} \left[\frac{1}{3} \left(\frac{\partial \log n}{\partial p}\right)_T + \left(\frac{\partial \log b}{\partial p}\right)_T \right].$$

Taking n equal to the number of atoms per c.c., as done by Sommerfeld, if b varies under pressure directly as the mean atomic separation, or $b \propto n^{-\frac{1}{3}}$, then

$$(\partial \log b / \partial p)_T = -\frac{1}{3} (\partial \log n / \partial p)_T \quad \text{and} \quad (\partial c / \partial p)_T = 0,$$

so that

$$(\partial \log H / \partial p)_T = 0.$$

If b remains constant under pressure, say $b = a\delta_0$, where δ_0 = mean atomic separation at zero pressure, then

$$\left(\frac{\partial \log H}{\partial p}\right)_T = -\left(\frac{8\pi}{3}\right)^{\frac{2}{3}} \frac{B}{H} \frac{K}{24\pi^2 a^2 \delta_0^2 n^{\frac{2}{3}}}, \quad \dots \quad (5)$$

where $K = -1/V (\partial V / \partial p)_T$ = compressibility.

Similarly for $(\partial \log H / \partial T)_p$; if $b \propto n^{-\frac{1}{3}}$, $(\partial \log H / \partial T)_p = 0$; if $a = a\delta_0$ = constant, then

$$\left(\frac{\partial \log H}{\partial T}\right)_p = \left(\frac{8\pi}{3}\right)^{\frac{2}{3}} \frac{B}{H} \frac{\beta}{24\pi^2 a^2 \delta_0^2 n^{\frac{2}{3}}}, \quad \dots \quad (6)$$

where $\beta = 1/V (\partial V / \partial T)_p$ = thermal expansion coefficient.

Taking $a = \frac{1}{6}$, i. e. $b = \frac{1}{6}\delta$, with Houston, Table I. gives the observed pressure coefficients, $1/R (\partial R / \partial p)_T$, and the

values computed by eq. (4), both for $b = \text{constant}$ and for $b \propto n^{-\frac{1}{3}}$. The last column shows the values of the pressure coefficient as computed from Houston's formula, eq. (2), which uses $b = \frac{1}{6}\delta_0 = \text{constant}$.

TABLE I.

$$\frac{1}{R} \left(\frac{\partial R}{\partial p} \right)_T \times 10^{-12} \text{ (C.G.S.)}.$$

(All values negative unless otherwise indicated.)

Element.	Calc. ($b \propto n^{-1/3}$).	Calc. ($b = \text{const.}$).	Obs.	Calc. (Houston).
Li	-23	- 38	+ 6.9	+12
Na	43	68.0	- 68	+ 7.0
K	72.5	128	200	+10
Cu	3.2	4.2	2.05	- 5.6
Ag	4.8	6.2	3.7	6.7
Au	3.5	4.4	3.2	9.5
Mo	0.88	1.52	1.36	4.5
W	0.76	1.32	1.31	9.5
Ni	2.40	3.0	1.61	7.0
Pd	2.32	3.0	2.02	6.9
Pt	1.92	2.40	2.02	9.4
Al	6.0	7.9	4.25	2.1
Cd	7.5	11.6	10.8	5.3
Fe	2.30	3.4	2.5	—
Pb	12.2	15.7	14.7	5.1

The general agreement is best for the values calculated by the formula here developed, eq. (4), for the case $b = \text{constant}$, *i. e.* the range of the ionic field practically unaffected by pressure. The agreement may be considered fairly satisfactory, considering the necessarily approximate treatment of the field of an ion involved in Houston's theory. The present method apparently does not account for the positive pressure coefficient of Li, unless the value of b as a fraction of δ_0 differs markedly from that of other substances. If $b \propto n^{-\frac{1}{3}}$, there is on this theory (and also in Houston's formula) no possibility of a positive pressure coefficient. Houston's formula gives positive pressure coefficient for Li, Na, and K; for the other elements the pressure coefficient

is negative and in most cases considerably higher than the observed values.

I wish to express my indebtedness to the United States National Research Council and to the International Education Board for the opportunity of study at King's College, London, and my sincere thanks to Prof. O. W. Richardson for his continued interest and encouragement.

King's College, London.
August 24th, 1928.

XCVI. *The Variation of Velocity Amplitude close to the Surface of a Cylinder moving through a Viscous Fluid.*
By N. A. V. PIERCY, *D.Sc.*, and E. G. RICHARDSON, *B.A., D.Sc., Ph.D.**

1. *Introductory.*

IT has been tentatively suggested † that the discrete eddies appearing in the wake of a body moving through a viscous fluid beyond the range for streamline flow, may grow into being from the coalescence of neighbouring vortices during their passage over the surface of the body. Experiments directed towards investigating the matter in the case of an ogival wedge ‡ in a stream, showed comparatively steady motion near to the surface through the vortex sheet cast off from it. The counter suggestion was therefore made that the periodic motion in the wake was due to the rolling up of the vortex sheets some distance behind the body.

An exploration of the fluctuation of velocity adjacent to the surface of a circular cylinder, placed with its axis across the stream, has recently been carried out in the aerodynamics laboratory at East London College. The results differ from Messrs. Fage and Johansen's experiments at the back of a wedge and tend rather in support of Prof. Levy's view, with the proviso that the cumulative process is limited to a small area of the surface.

2. *Nature of Investigation.*

A quantity that is roughly proportional to the amplitude of the velocity fluctuation was observed at short intervals round twelve circles, concentric with the cylinder and

* Communicated by the Authors.

† Levy, *Phil. Mag.* ii. p. 844 (1926).

‡ Fage and Johansen, *Phil. Mag.* v. p. 417 (1928).

separated from its surface by distances ranging from 0.0025 cylinder diameters to one hundred times that amount. The readings were found to be sufficiently consistent to permit of the construction of contours, and the results to which these pointed were in part checked by an alternative method. The second method, in which the periodicity was made audible, it is thought may prove of general use in experiments of this nature.

3. Apparatus and Methods.

The smooth aluminium cylinder, turned to 4 inches diameter, reached from wall to wall of a 4-foot wind-channel. It was supported in bearings at the walls so as to permit of orientation about its long axis without interrupting the air-stream. The hot wire was of platinum, 0.001 inch diameter and 1.0 inch long, and was fastened between the ends of two thin brass rods, which were threaded through insulating bushes fitted along parallel diameters of the cylinder and projected an adjustable distance from its surface. These rods served as leads for a current of about 0.5 amp.

The quasi-periodic variation in resistance of the hot wire due to its heating and cooling in the fluctuating stream, induced oscillatory e.m.f.'s in the secondary coil of a step-up transformer connected with a vibration galvanometer of unifilar type. The instrument was set considerably out of tune with the frequency of the motion and thus acted as a string galvanometer which was not critically damped. Various tests, reported elsewhere*, confirmed that in this use of the instrument the amplitude of the oscillation of the string could be regarded as roughly proportional to the amplitude of the velocity fluctuation, assuming nearly constant frequency and speed. The refinement of allowing for the variation of mean velocity was not attempted.

In the alternative method, the oscillatory e.m.f.'s induced in the secondary of the transformer were amplified until they were capable of producing an audible note of corresponding frequency in a telephone receiver. We used a three-valve resistance-capacity coupled amplifier in which the secondary of the transformer with its oscillating e.m.f. formed the "grid-bias" of the first valve (fig. 1).

To illustrate the use of this method, some estimates were

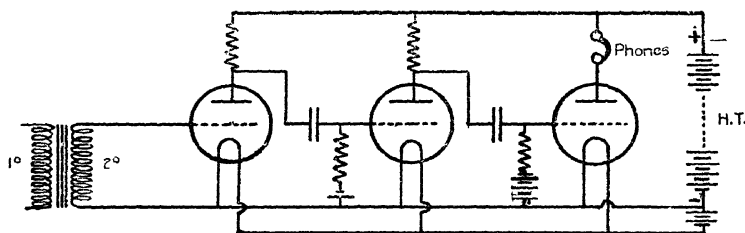
* In a paper submitted by us to the Aero. Res. Comm. See also Relf and Simmons, *Phil. Mag.* xlix. p. 509 (1925); and Tyler, *Phil. Mag.* v. p. 449 (1928).

made of the frequency in the wakes of a few thin rods, as follows :—

Velocity, V.	Diameter, D.	Frequency, <i>n</i> .	$\frac{V}{nD}$.
400	0.12	600	5.55
562	0.51	215	5.10
400	0.24	315	5.83
562	0.24	413	5.68
400	0.40	186	5.40
562	0.40	265	5.20

The above values of *n* were determined by comparing the note heard with a note in the sonometer. The results are in agreement with those obtained by other means *. The path

Fig. 1.



Arrangement of Audible Method.

of the vortices was traceable downstream by means of the 'phones, while a diminishing intensity of sound showed a damping out. By choosing suitable cylinders the critical value of Reynolds's number could be found, the channel speed being gradually increased until a note became audible.

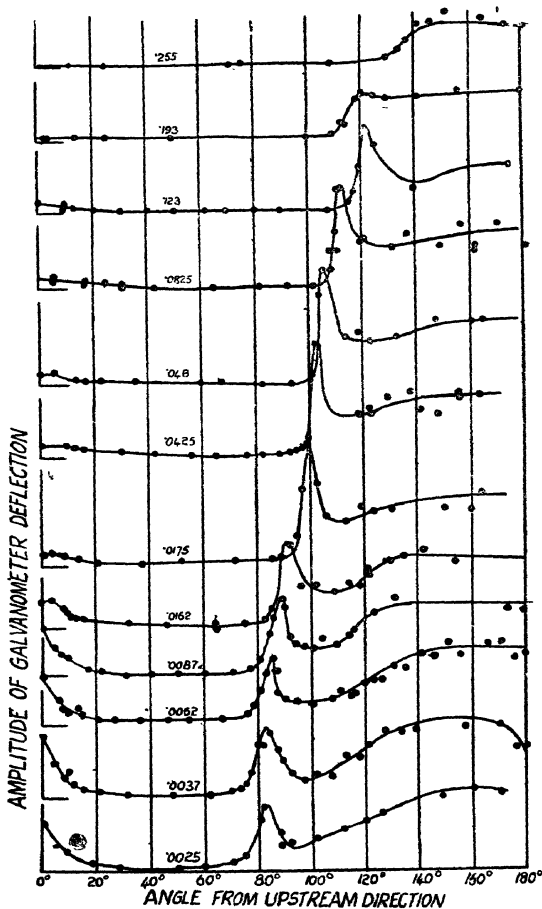
4. The Results.

The readings obtained with the vibration galvanometer are given in fig. 2, plotted in cylindrical coordinates. The numbers attached to the curves give the distance of the wire from the boundary—constant for each curve—expressed in terms of the diameter of the cylinder. From these curves and those of fig. 3, contours of equal galvanometer amplitude have been prepared and are shown in fig. 4. The

* Richardson, Proc. Phys. Soc. xxxvii. p. 178 (1925).

numbers attached to the contours are proportional to the width of the band of light thrown upon the scale less its static width. The peculiar form of the contours near the front of the cylinder led to the more detailed exploration in this region recorded in fig. 3.

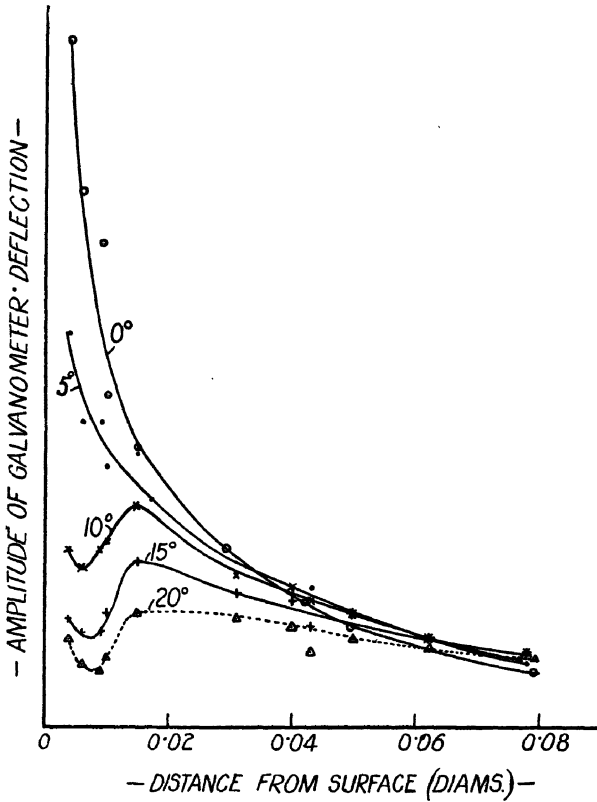
Fig. 2.



Amplitude of deflexion of vibration galvanometer with the hot wire, various constant distances from the surface, as marked on the curves in cylinder diameters.

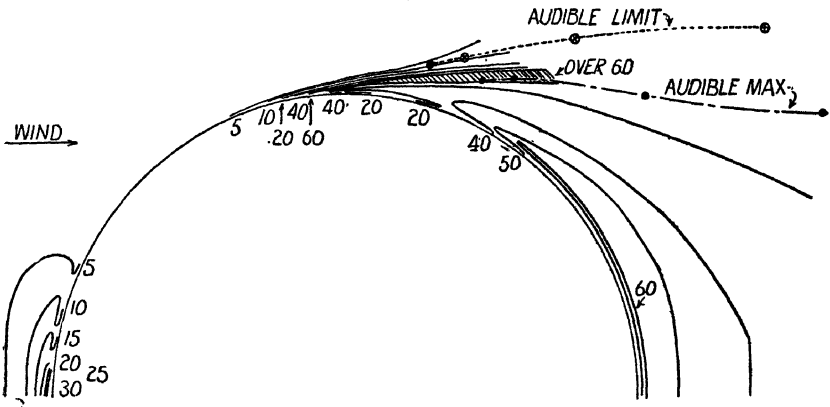
It will be seen that the front stagnation point is a centre of disturbance, which, however, is damped out in the air as

Fig. 3.



Exploration by vibration galvanometer near front stagnation point.
The angles are measured from the upstream direction.

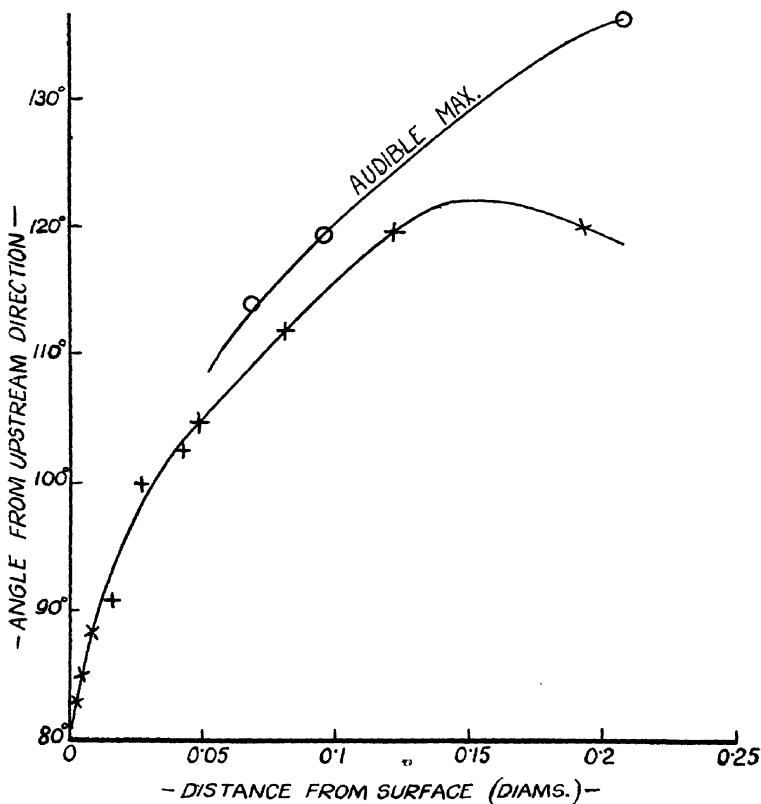
Fig. 4.



Contours of equal deflection amplitude of vibration galvanometer. The numbers are proportional to the width of the band of light observed on the scale. Curves are added showing where the eddying produced an audible note and maximum intensity of sound.

it flows out of the region. The reading close to the surface again begins to have an appreciable amplitude at an angle of 60° with the upstream direction. From there, the amplitude rapidly increases, reaching a maximum at an angle of about 80° . After this sharp peak, it as rapidly decreases, and is then built up more gradually to a large value that extends round the back of the cylinder. These features are

Fig. 5.



Locus of peak values of velocity amplitude, as determined by the vibration galvanometer method (crosses) and the audible method (circles).

similar in many ways to those that we have found close to the upper surface of an aerofoil*, so that it is likely that they apply to cylinders differing widely in section.

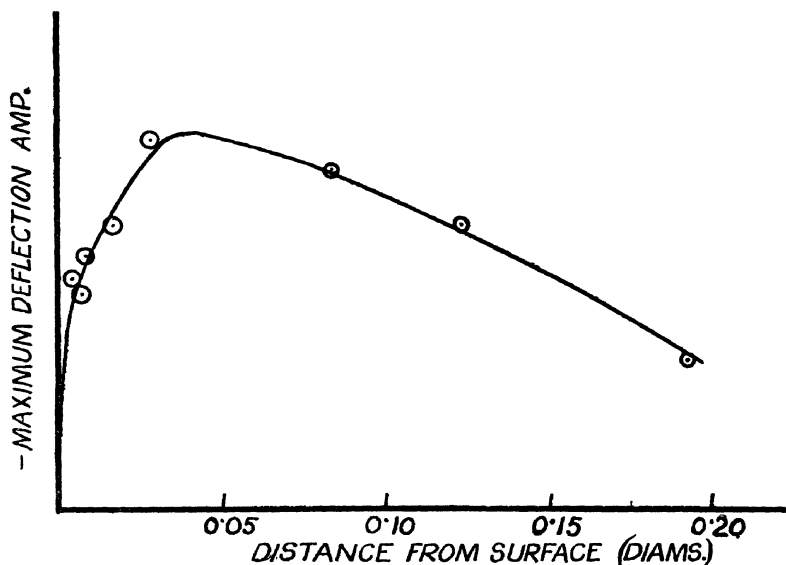
The peaks of fig. 2 mark the position of a wedge of large velocity amplitude, which is shaded in fig. 4. Within this

* *Loc. cit.* Aero. Res. Comm.

wedge the low frequency rumble discernible in the telephone receivers, using the second method of experiment, attained maximum intensity. In fig. 4 is also drawn a contour along which the periodic motion became audible.

Fig. 5 gives the position of maximum amplitude found by the vibration galvanometer and for comparison includes that indicated by the other, or telephone, method. Fig. 6 shows the variation of maximum amplitude with distance from the surface of the cylinder. From the latter figure it will be observed that at a very short distance from the surface the

Fig. 6.



Variation of maximum velocity amplitude with distance from surface, as determined by the vibration galvanometer method.

amplitude reaches half-way towards a maximum, which itself occurs, according to this method, at no greater distance from the surface than 0.04 cylinder diameter.

5. *Conclusions.*

These experiments show that the turbulence in the region of the front stagnation point of a circular cylinder is not carried by the fluid round the surface. The velocity appears steady over about one-third of the surface facing the wind. Well before the shoulder of the section is reached, however, turbulence sets in anew, and rapidly increases to a maximum,

or peak, value. A wedge-shaped funnel of high velocity amplitude almost abuts on the surface here. This may possibly form a species of exhaust duct for coalesced vortices, such as Prof. Levy envisages, but in that case the vortices are collected from only a small area on the neighbouring surface. The experiments might well be developed at some time to take account of variation of mean velocity.

Dr. Piercy has pleasure in acknowledging assistance from the Keddey Fletcher-Warr Studentship Fund, and from the Dixon Fund, both of the University of London, which enabled this investigation to be carried out.

XCVII. *On the Dynamics of an Electron.*

By D. MEKSYN.*

I. SPACE AND TIME IN PHYSICS.

§ 1. *The General Principle of Relativity and Motion of Electrons.*

AN attempt to apply the General Principle of Relativity to the motion of Electrons is met at the outset with insurmountable difficulties. It appears as if the problem is inherently self-contradictory. As a matter of fact, the track of an electron in an electromagnetic field is a curvilinear one; on the other hand the space, as follows from the law of motion of an electron, is not curved (unless a gravitational field exists); hence the motion cannot be a free one, as it should be according to the General Principle of Relativity.

It seems that this contradiction is intimately connected with the conception of Space and Time in the Principle of Relativity.

§ 2. *Space and Time in Geometry and in the Special Theory of Relativity.*

Space and Time are considered in the Special Theory of Relativity and in Geometry to be a physical Entity *sui generis*, which imposes its metrical laws upon solid bodies located in it. So, for instance, we could conceive two spaces (and times) which are similar in every respect, except that the dimensions of the first are, say, only half of the second

* Communicated by H. T. Flint, D.Sc.]

one. If we transfer a solid body from the second space into the first one, the latter will cause the body to shrink and take only half the size that it had previously. Such a change in dimensions of Space can be brought about, according to the Special Theory of Relativity, if we set a body in motion.

Until the appearance of the Principle of Relativity it was usually held that space had three dimensions, and its metric was given by Laws of Geometry. The Special Principle of Relativity has discarded the conception of a three-dimensional space and one-dimensional time, but has accepted the idea of Geometry that space is a kind of objective physical Entity which imposes its metrical laws upon solid bodies; therefore the Theory of Relativity has drawn the conclusion that, because it follows from Lorentz's transformations that the space dimensions of a fourfold system decrease if the latter is set in motion, a solid physical body which belongs to a moving system will shrink in its space dimensions.

§ 3. *Geometrical or Rigid Space.*

What, however, is meant by Space in Geometry is as follows:—There exist solid physical bodies which possess some metrical properties; they have finite dimensions (length, surface, volume); they do not change their dimensions if transferred from one part of space into another.

Now, it appears that it is possible to account by deduction for all metrical properties of solid bodies, if we construct an appropriate system of reference, a "space," in such a way that all metrical properties of solid bodies (length, surface, volume) are properties of the space itself, and every element of length is expressed by some definite (quadratic) function of three appropriately chosen directions in space.

Hence, rigid bodies do not change their size if transferred from one part of Geometrical Space into another, not because the latter is homogeneous, but conversely the Geometrical Space is homogeneous for bodies which do not change their dimensions by such transfer.

It does, of course, not follow that there is no objective space, or that this space has no metrical properties of its own. (We do not touch upon this question here; what it is necessary to notice is that the Geometrical Space, which gives us the metrical properties of solid bodies, is something quite different from the objective space (if we admit its existence).)

§ 4. *Four-dimensional or Kinematical Space.*

The idea of Space in Geometry will become clearer if we turn our attention to classical kinematics. It was built up upon different lines than Geometry.

In Geometry, as we have seen, all metrical properties of solid bodies are properties of the space itself.

In classical kinematics, side by side with metrical properties of Space, it was necessary to introduce some quantities which do not belong to the space (velocity and acceleration). The classical kinematics has lacked the unity of design which characterized Geometry.

The achievement of the Special Principle of Relativity was to restore this unity. The four-dimensional space is constructed in such a way that all kinematical elements of motion appear as metrical forms of the space itself; so velocity is the tangent of the angle between time axes, and acceleration is the radius of curvature of the four-track.

§ 5. *Dynamical Space.*

If we turn our attention to the dynamics of the Theory of Relativity we notice that here again the above-mentioned unity is not maintained; the fundamental quantities of dynamics, momentum, and Energy appear not as metrical properties of the Space itself, but, so to say, as properties brought into the space.

It is clear, therefore, that the natural generalization of the Special Theory of Relativity is to construct a dynamical space in which momentum and energy would be properties belonging to the Space itself.

§ 6. *Electricity and Gravitation.*

Before proceeding further we must bear in mind the divergence between an Electromagnetic field and a field of Gravitation. An isolated mass-point possesses a field of Gravitation, and it is usually held that an isolated charged mass-point has also an Electromagnetic field. We think, however, that the latter appears only if there are at least two electrons at a finite distance.

Hence, in the corresponding fundamental form this must be brought out by appearance of cross-terms of different spaces rather than by a change in the fundamental form of every space separately.

II. THE FUNDAMENTAL FORM OF DYNAMICAL SPACE.

§ 7. *Lagrange's Equations in the Special Theory of Relativity.*

The idea of a dynamical space is not a new one. Such space is used in Lagrange's equations. Lagrange's space, however, is built up in conformity with the old kinematics, i. e. in it the time coordinate is separated from Space. This ought to be modified in such a way that time shall appear symmetrically with Space; this is necessary to bring it into agreement with the Special Theory of Relativity.

Lagrange's equations are :

$$\frac{d}{dt} \frac{\partial T}{\partial \dot{x}_k} - \frac{\partial T}{\partial x_k} = Q_k. \quad . \quad . \quad . \quad (1)$$

In the classical Mechanics T is the kinetic Energy; but in the Theory of Relativity T is the so-called kinetic Potential, a quantity which has neither a dynamical nor a metrical meaning.

The first step to be made is to bring Lagrange's equations in the Special Theory of Relativity into such a form that it shall contain only metrical quantities.

For one material point this is easily done. If the fundamental form is

$$ds^2 = dt^2 - dx^2 - dy^2 - dz^2, \quad . \quad . \quad . \quad (2)$$

where t is chosen in light seconds. Lagrange's equations become in a variational form

$$\delta \int_{\tau_0}^{\tau_1} (m ds + V d\tau) = 0, \quad . \quad . \quad . \quad (3)$$

where V is the potential Energy. The Geometrical interpretation of (3) is that the four-track is a geodesic line on some surface $V=0$. If V disappears the track is a geodesic line of a free space.

In the case of several material points we consider the fundamental form

$$ds^2 = \sum_{k=1}^{k=n} m_k (dt_k^2 - dx_k^2 - dy_k^2 - dz_k^2), \quad . \quad . \quad (4)$$

which has $4n$ dimensions. It is easily seen that Lagrange's equations become

$$\delta \int_{\tau_0}^{\tau_1} \left(ds + \frac{1}{\sqrt{\sum_k m_k}} V d\tau \right) = 0; \quad . \quad . \quad (5)$$

as a matter of fact, from (5) we obtain

$$m_k \frac{d}{d\tau} \left(\frac{dx_k}{ds} \right) + \frac{1}{\sqrt{\sum_k m_k}} \frac{\partial V}{\partial x_k} = 0. \quad . \quad . \quad (6)$$

There are in all $4n-1$ independent equations and only $3n$ given space projections of force, so that we are left with $n-1$ time projections which we can dispose.

We define them from the following $n-1$ equations :

$$dt_k^2 - dx_k^2 - dy_k^2 - dz_k^2 = dt_l^2 - dx_l^2 - dy_l^2 - dz_l^2 ; \quad . \quad (7)$$

they are evidently equivalent to

$$X_k dx_k + Y_k dy_k + Z_k dz_k - T_k dt_k = 0, \quad . \quad . \quad (7a)$$

where $X_k Y_k Z_k T_k$ are the projections of the force.

From (7) the denominator in (6) becomes

$$ds = \sqrt{\sum_{l=1}^{l=n} m_l \cdot (dt_k^2 - dx_k^2 - dy_k^2 - dz_k^2)},$$

or inserting (ds) in (6) we obtain

$$m_k \frac{d}{d\tau} \left(\frac{dx_k}{\sqrt{dt_k^2 - dx_k^2 - dy_k^2 - dz_k^2}} \right) + \frac{\partial V}{\partial x_k} = 0,$$

which is the law of motion.

The expression $\sqrt{\sum m_k}$ in (6) appears to be rather disappointing, as it has had hitherto no dynamical meaning ; it need not, however, trouble us, because it will later disappear in the rigorous laws of motion.

What we have to notice is, that for several material points the law of motion is a geodesic line of a $4n$ dimensional space.

§ 8. *The Electromagnetic Field and the Form of Space.*

We turn our attention to the case of an Electromagnetic Force. Lagrange's equations for an electron are

$$\frac{d}{dt} \frac{\partial}{\partial \dot{x}_k} (T - M) - \frac{\partial}{\partial x_k} (T - M) = 0, \quad . \quad . \quad (8)$$

where T is the kinetic Energy,

$$M = e_1 (\phi - u_1 F - v_1 G - w_1 H), \quad . \quad . \quad (9)$$

$-\phi$ is the scalar, F, G, H the vector potential of Force, e_1 the charge, and u_1, v_1, w_1 the velocity of the electron.

To find now the fundamental form of space, we must bear in mind two points:

- (1) In (8) the kinetic and potential Energies appear perfectly symmetrically.
- (2) Lagrange's expression (1) for the equations of Motion becomes a geodesic if T is a quadratic function of \dot{x}_k .

Hence our task will be achieved if we transform (9) into a quadratic expression.

Suppose that the external field is produced by one moving electron whose coordinates, charge, and velocity are

$$x_2, y_2, z_2, t_2, \quad e_2, \quad u_2, v_2, w_2.$$

Then (9) becomes

$$M = \frac{e_1 e_2}{r} (1 - u_1 u_2 - v_1 v_2 - w_1 w_2), \quad . \quad . \quad . \quad (10)$$

where

$$r = \sqrt{(x_1 - x_2)^2 + (y_1 - y_2)^2 + (z_1 - z_2)^2}.$$

This expression for M suggests at once the expression for the fundamental form of space in this case. It is

$$\begin{aligned} ds^2 = & m(dx_4^2 - dx_1^2 - dx_2^2 - dx_3^2) \\ & + \frac{e_1 e_2}{r} (dx_4 dx_8 - dx_1 dx_5 - dx_2 dx_6 - dx_3 dx_7) \\ & + M(dx_8^2 - dx_5^2 - dx_6^2 - dx_7^2). \quad . \quad . \quad . \quad (11) \end{aligned}$$

In the general case where the external force is produced by $n-1$ electrons, *i. e.* in the case of the n electron problem, if we denote the mass, charge, and coordinates of the k th electron respectively by

$$m_k, \quad e_k, \quad x_{k+1} \quad x_{k+2} \quad x_{k+3} \quad x_{k+4}, \quad . \quad . \quad . \quad (12)$$

we obtain the following expression for the fundamental form

$$\begin{aligned} ds^2 = & g_{\mu\nu} dx_\mu dx_\nu \\ = & \sum_{k=1}^{k=n} m_k (dx_{k+4}^2 - dx_{k+1}^2 - dx_{k+2}^2 - dx_{k+3}^2) \\ & + \sum_{k,l=1}^{k,l=n} \phi_{kl} (dx_{k+4} dx_{l+4} \\ & - dx_{k+1} dx_{l+1} - dx_{k+2} dx_{l+2} - dx_{k+3} dx_{l+3}), \quad . \quad (13) \end{aligned}$$

where

$$\left. \begin{aligned} k \neq l \text{ and } \phi_{kl} &= \frac{e_k e_l}{r_{kl}} \\ r_{kl} &= \sqrt{(x_{k+1} - x_{l+1})^2 + (x_{k+2} - x_{l+2})^2 + (x_{k+3} - x_{l+3})^2} \end{aligned} \right\}, \quad (14)$$

or

$$\phi_{kl} = \frac{e_k e_l}{c^2 r_{kl}}$$

if c is the velocity of light.

The Equation of Motion will be

$$\delta \int ds = 0, \quad . \quad . \quad . \quad . \quad . \quad . \quad . \quad . \quad (15)$$

or a geodesic line in $4n$ dimensional space, which we proceed to discuss.

III. THE TWO-ELECTRON PROBLEM.

§ 9. The Form of Space.

We consider the problem of 2 electrons. The fundamental form for this particular case is

$$\begin{aligned} ds^2 &= m(dx_4^2 - dx_1^2 - dx_2^2 - dx_3^2) \\ &+ \frac{eE}{r}(dx_4 dx_8 - dx_1 dx_5 - dx_2 dx_6 - dx_3 dx_7) \\ &+ M(dx_8^2 - dx_5^2 - dx_6^2 - dx_7^2) \dots \dots \dots (16) \end{aligned}$$

A glance at this expression shows us that it satisfies the physical conditions of an electromagnetic Field. The eight-dimensional space is split up into two four-dimensional spaces which are Euclidean, but taken as a whole this space is not Euclidean because of the cross terms. Hence an electron will not move in a straight line.

§ 10. The Fundamental Tensor.

The discriminant g is equal to

$$g = \begin{vmatrix} g_{11} & . & . & . & g_{15} & . & . & . \\ . & g_{22} & . & . & . & g_{26} & . & . \\ . & . & g_{33} & . & . & . & g_{37} & . \\ . & . & . & g_{44} & . & . & . & g_{48} \\ g_{51} & . & . & . & g_{55} & . & . & . \\ . & g_{62} & . & . & . & g_{66} & . & . \\ . & . & g_{73} & . & . & . & g_{77} & . \\ . & . & . & g_{84} & . & . & . & g_{88} \end{vmatrix} \quad . \quad (17)$$

and is split up into four separate determinants.

Or

$$g = (g_{11}g_{55} - g_{15}^2)(g_{22}g_{66} - g_{26}^2)(g_{33}g_{77} - g_{37}^2)(g_{44}g_{88} - g_{48}^2), \quad (18)$$

and the contravariant tensor $g^{\mu\nu}$ is equal to

$$\left. \begin{aligned} g^{11} &= \frac{g_{55}}{g_{11}g_{55} - g_{15}^2} \dots, & g^{55} &= \frac{g_{11}}{g_{11}g_{55} - g_{15}^2}, \\ g^{15} &= \frac{-g_{15}}{g_{11}g_{55} - g_{15}^2} \dots, & g^{48} &= \frac{-g_{48}}{g_{44}g_{88} - g_{48}^2}, \end{aligned} \right\} \dots \quad (19)$$

in our particular case

$$\left. \begin{aligned} g_{11} &= g_{22} = g_{33} = -g_{44} = -m, \\ g_{55} &= g_{66} = g_{77} = -g_{88} = -M, \\ g_{15} &= g_{26} = g_{37} = -g_{48} = -\frac{eE}{r}, \end{aligned} \right\} \dots \quad (20)$$

where

$$m, e, x_1 x_2 x_3 x_4, \text{ and } M, E, x_5 x_6 x_7 x_8$$

relate respectively to the Electron and Proton.

§ 11. *The Equation of Motion* is, as we have seen, a geodesic line of this space, or

$$\frac{d^2 x_\alpha}{ds^2} + \{\mu\nu\alpha\} \frac{dx_\mu}{ds} \frac{dx_\nu}{ds} = 0. \quad \dots \quad (21)$$

In the general case of an eight-dimensional space, there are 288 three-index symbols, but in our case the number reduces to 136, and, if $g_{\mu\nu}$ does not depend upon time, to 102.

The only symbols which do not vanish are

$$\left. \begin{aligned} \{\alpha\alpha', \alpha\} &= g^{\alpha\alpha'} \frac{\partial g_{\alpha\alpha'}}{\partial x_\alpha}, \\ \{\alpha\nu, \alpha\} &= \frac{1}{2} g^{\alpha\alpha'} \frac{\partial g_{\alpha\alpha'}}{\partial x_\nu} \quad (\text{but } \{\alpha\alpha', \alpha\} = 0), \\ \{\mu\mu', \alpha\} &= -\frac{1}{2} g^{\alpha\alpha'} \frac{\partial g_{\mu\mu'}}{\partial x_\alpha} - \frac{1}{2} g^{\alpha\alpha'} \frac{\partial g_{\mu\mu'}}{\partial x_{\alpha'}}, \\ \{\mu\alpha', \alpha\} &= \frac{1}{2} g^{\alpha\alpha'} \frac{\partial g_{\alpha'a}}{\partial x_\mu}, \end{aligned} \right\} \quad (22)$$

where $(\alpha' - \alpha) = 4$.

There are in all 8 equations ; the first four give us the motion of the electron ; the last four, of the proton.

If we write out the equations (21) and insert the values of the 3-index terms, we obtain the following expressions :—

$$\begin{aligned}
 & \left. \begin{aligned}
 & \frac{d^2 x_1}{ds^2} + g^{11} \left(\frac{\partial g_{51}}{\partial x_2} V_5 - \frac{\partial g_{26}}{\partial x_1} V_6 \right) V_2 + g^{11} \left(\frac{\partial g_{51}}{\partial x_3} V_5 - \frac{\partial g_{37}}{\partial x_1} V_7 \right) V_3 \\
 & + g^{11} \left(\frac{\partial g_{51}}{\partial x_4} V_5 - \frac{\partial g_{48}}{\partial x_1} V_8 \right) V_4 + g^{15} \left(\frac{\partial g_{71}}{\partial x_7} V_1 - \frac{\partial g_{37}}{\partial x_5} V_3 \right) V_7 \\
 & + g^{15} \left(\frac{\partial g_{15}}{\partial x_6} V_1 - \frac{\partial g_{26}}{\partial x_5} V_2 \right) V_6 + g^{15} \left(\frac{\partial g_{15}}{\partial x_8} V_1 - \frac{\partial g_{48}}{\partial x_5} V_4 \right) V_8 \\
 & + g^{15} \left(\frac{\partial g_{15}}{\partial x_1} V_1 + \frac{\partial g_{15}}{\partial x_2} V_2 + \frac{\partial g_{15}}{\partial x_3} V_3 + \frac{\partial g_{15}}{\partial x_4} V_4 \right) V_1 \\
 & + g^{11} \left(\frac{\partial g_{15}}{\partial x_5} V_5 + \frac{\partial g_{15}}{\partial x_6} V_6 + \frac{\partial g_{15}}{\partial x_7} V_7 + \frac{\partial g_{15}}{\partial x_8} V_8 \right) V_5 = 0, \\
 & \dots \dots \dots \\
 & \frac{d^2 x_4}{ds^2} + g^{44} \left(\frac{\partial g_{84}}{\partial x_1} V_8 - \frac{\partial g_{15}}{\partial x_4} V_5 \right) V_1 + g^{44} \left(\frac{\partial g_{84}}{\partial x_2} V_8 - \frac{\partial g_{26}}{\partial x_4} V_6 \right) V_2 \\
 & + g^{44} \left(\frac{\partial g_{84}}{\partial x_3} V_8 - \frac{\partial g_{37}}{\partial x_4} V_7 \right) V_3 + g^{48} \left(\frac{\partial g_{48}}{\partial x_5} V_4 - \frac{\partial g_{15}}{\partial x_8} V_1 \right) V_5 \\
 & + g^{48} \left(\frac{\partial g_{48}}{\partial x_6} V_4 - \frac{\partial g_{26}}{\partial x_8} V_2 \right) + g^{48} \left(\frac{\partial g_{48}}{\partial x_7} V_4 - \frac{\partial g_{37}}{\partial x_8} V_3 \right) V_7 \\
 & + g^{48} \left(\frac{\partial g_{48}}{\partial x_1} V_1 + \frac{\partial g_{48}}{\partial x_2} V_2 + \frac{\partial g_{48}}{\partial x_3} V_3 + \frac{\partial g_{48}}{\partial x_4} V_4 \right) V_4 \\
 & + g^{44} \left(\frac{\partial g_{84}}{\partial x_5} V_5 + \frac{\partial g_{84}}{\partial x_6} V_6 + \frac{\partial g_{84}}{\partial x_7} V_7 + \frac{\partial g_{84}}{\partial x_8} V_8 \right) V_8 = 0.
 \end{aligned} \right\} \dots \dots (23)
 \end{aligned}$$

§ 12. The equations (23) could be brought in a form which will at once show their relation to the usual equations of Motion of an electron.

Let F , G , H , $-\phi$ be the vector potential ; then the electromagnetic force is

$$\left. \begin{aligned}
 \alpha &= \frac{\partial H}{\partial y} - \frac{\partial G}{\partial z} \dots, \\
 X &= -\frac{\partial F}{\partial t} - \frac{\partial \phi}{\partial x} \dots
 \end{aligned} \right\} \dots \dots (24)$$

From the values of g_{15} , g_{26} , we see that (except for a constant factor)

$$\left. \begin{aligned} g_{15}V_5 &= -eF_p, & g_{26}V_6 &= -eG_p, & g_{37}V_7 &= -eH_p, \\ & & & & g_{48}V_7 &= +e\phi_p, \\ g_{51}V_1 &= -EF_e, & g_{62}V_2 &= -EG_e, & g_{73}V_3 &= -EH_e, \\ & & & & g_{84}V_4 &= +E\phi_e, \\ & & & & . & . & . \end{aligned} \right\} \quad (25)$$

where the subscripts p and e denote that it is the vector-potential due to the proton (and, hence, acting on the electron) and the electron respectively.

We also denote the velocity of the electron and proton :

$$V_1 V_2 V_3 V_4 = V_e, \quad V_5 V_6 V_7 V_8 = V_p. \quad (26)$$

If we make use of (24) and (25), the equations (23) become

$$\left. \begin{aligned} \frac{d^2 x_1}{ds^2} &= -g^{11}e [X_p V_4 + Y_p V_2 - \beta_p V_3] \\ &\quad -g^{15}E [X_e V_8 + Y_e V_6 - \beta_e V_7] \\ &\quad -g^{11} \left(\frac{\partial g_{15}}{\partial x_5} V_5 + \frac{\partial g_{15}}{\partial x_6} V_6 + \frac{\partial g_{15}}{\partial x_7} V_7 + \frac{\partial g_{15}}{\partial x_8} V_8 \right) V_5 \\ &\quad -g^{15} \left(\frac{\partial g_{15}}{\partial x_1} V_1 + \frac{\partial g_{15}}{\partial x_2} V_2 + \frac{\partial g_{15}}{\partial x_3} V_3 + \frac{\partial g_{15}}{\partial x_4} V_4 \right) V_1, \\ \frac{d^2 x_4}{ds^2} &= g^{44}e [X_p V_1 + Y_p V_2 + Z_p V_3] \\ &\quad + g^{48}E [X_e V_5 + Y_e V_6 + Z_e V_7] \\ &\quad -g^{44} \left(\frac{\partial g_{84}}{\partial x_5} V_5 + \frac{\partial g_{84}}{\partial x_6} V_6 + \frac{\partial g_{84}}{\partial x_7} V_7 + \frac{\partial g_{84}}{\partial x_8} V_8 \right) V_8 \\ &\quad -g^{48} \left(\frac{\partial g_{48}}{\partial x_1} V_1 + \frac{\partial g_{48}}{\partial x_2} V_2 + \frac{\partial g_{48}}{\partial x_3} V_3 + \frac{\partial g_{48}}{\partial x_4} V_4 \right) V_4. \end{aligned} \right\} \quad (27)$$

1. Let us consider the case of a steady electromagnetic field. Or we assume that $M \rightarrow \infty$ and the velocity of the proton is

$$V_5, V_6, V_7 \rightarrow 0.$$

Then

$$g^{11} = -\frac{1}{m}, \quad g^{44} = +\frac{1}{m}, \quad g^{15} = g^{26} = g^{37} = g^{48} = 0,$$

and (27) becomes :

$$\left. \begin{aligned} m \frac{d^2 x_1}{ds^2} &= e [X_p V_4 + Y_p V_2 - \beta_p V_3], \\ m \frac{d^2 x_4}{ds^2} &= e [X_p V_1 + Y_p V_2 + Z_p V_3], \end{aligned} \right\} \quad (28)$$

Now the four-velocity can be transformed as follows :—

$$ds^2 = m(dx_4^2 - dx_1^2 - dx_2^2 - dx_3^2) + \mathbb{M}(dx_8^2 - dx_5^2 - dx_6^2 - dx_7^2) \\ + \frac{e\mathbb{E}}{\alpha}(dx_4dx_8 - dx_1dx_5 - dx_2dx_6 - dx_3dx_7) ;$$

to the first order of approximation the last term may be omitted because $\frac{eE}{r}$ (or $\frac{eE}{rc^2}$, if c is the velocity of light) is small in comparison with the mass of an electron; also, the force acting on the electron satisfies to the first approximation the equation (7 a); hence we have

$$dx_4^2 - dx_1^2 - dx_2^2 - dx_3^2 = dx_8^2 - dx_5^2 - dx_6^2 - dx_7^2, \quad (29)$$

as this does not impose new conditions on the variables.

Whence

$$\begin{aligned} ds^2 &= (m + \mathbb{M})(dx_4^2 - dx_1^2 - dx_2^2 - dx_3^2) \\ &= (m + \mathbb{M})(dx_8^2 - dx_5^2 - dx_6^2 - dx_7^2). \end{aligned}$$

The factor $\sqrt{M+m}$ appears twice in the denominator of the left and the right side of (28) (in the electric force through the vector potential, and in the velocity) ; hence it drops out from the equation of Motion, and they become, if we divide both sides by V_4 ,

[illegible]

where u, v, w is the three-velocity, and

$$d\tau^2 = dx_4^2 - dx_1^2 - dx_2^2 - dx_3^2.$$

These are the usual equations of motion for the electron.

2. In the general case, as is seen from (27), the force consists of four parts. Two of them are due to the direct action of the proton, and the other two forces to the reaction on the proton, due to the electromagnetic force of the electron.

The first one is the usual Lorentz's force, the second one is some new force; it is equal to

$$-g^{11}(\text{grad } g_{15} \cdot V_p)V_5 - g^{15}(\text{grad } g_{15} \cdot V_e)V_1.$$

3. From the equations of motion (21) a remarkable consequence follows concerning the number of degrees of freedom of an electron.

As is known,

$$\frac{dx_a}{ds} \left\{ \frac{d^2 x^a}{ds^2} + \{\mu\nu\alpha\} \frac{dx^\mu}{ds} \frac{dx^\nu}{ds} \right\} = 0, \quad . \quad . \quad (31)$$

or there are only $4n-1$ independent equations for n electrons. If we assume that the proton has three degrees of freedom, then we are left with $4n-4$ equations for $n-1$ electrons; or an electron has four degrees of freedom.

The fourth degree of freedom is in the direction of time, or, better, it is the kinetic energy, which is not equal to $m \frac{dt}{d\tau}$, as the Special Theory of Relativity gives, but has

to be found from the equations of Motion.

Our assumption (29) about the connexion between different times is only an approximate one. We must choose one time (of the proton) as an independent variable, and find all others from the equations of motion.

4. The so-called vector potential of Electrodynamics is the covariant velocity in the dynamical space.

For instance,

$$\frac{dx_5}{ds} = -m \frac{dx^5}{ds} - g_{15} \frac{dx^1}{ds},$$

which, for the particular case where the proton is at rest, is proportional to the vector potential of the electron

$$\frac{dx_5}{ds} = eF_e.$$

§ 13. The Wave Equation

$$g^{\mu\nu} \phi_{,\mu\nu} = g^{\mu\nu} \left(\frac{\partial^2 \phi}{\partial x_\mu \partial x_\nu} + \{\mu\nu, \alpha\} \frac{\partial \phi}{\partial x_\alpha} \right) = 0 \quad . \quad (32)$$

is rather complicated. We consider here the simple instance, when $g_{15} = g_{26} = g_{37} = 0$, or of a purely electric field. For

this case $\dot{\phi}_{\mu\nu} = \frac{\partial^2 \phi}{\partial x_\mu \partial x_\nu}$, except for the expression

$$\phi_{48} = \frac{\partial^2 \phi}{\partial x_4 \partial x_8} + \frac{1}{2} \left[g^{11} \frac{\partial g_{48}}{\partial x_1} \frac{\partial \phi}{\partial x_1} + g^{22} \frac{\partial g_{48}}{\partial x_2} \frac{\partial \phi}{\partial x_2} + g^{33} \frac{\partial g_{48}}{\partial x_3} \frac{\partial \phi}{\partial x_3} + g^{55} \frac{\partial g_{48}}{\partial x_5} \frac{\partial \phi}{\partial x_5} + g^{66} \frac{\partial g_{48}}{\partial x_6} \frac{\partial \phi}{\partial x_6} + g^{77} \frac{\partial g_{48}}{\partial x_7} \frac{\partial \phi}{\partial x_7} \right]. \quad (33)$$

We neglect, however, the cross terms in (33), because from the expression of ϕ , which we shall take, the second term for the Hydrogen Atom is only $\sim 10^{-10}$ of the first one.

So that the wave equation becomes

$$g^{11} \frac{\partial^2 \phi}{\partial x_1^2} + \dots + g^{44} \frac{\partial^2 \phi}{\partial x_4^2} + g^{55} \frac{\partial^2 \phi}{\partial x_5^2} + \dots + g^{88} \frac{\partial^2 \phi}{\partial x_8^2} + 2g^{84} \frac{\partial^2 \phi}{\partial x_4 \partial x_8} = 0. \quad (34)$$

Inserting in (34) the values of the tensor $g^{\mu\nu}$, we obtain after easy transformations

$$\frac{1}{m} \left(\frac{\partial^2 \phi}{\partial x_1^2} + \frac{\partial^2 \phi}{\partial x_2^2} + \frac{\partial^2 \phi}{\partial x_3^2} \right) + \frac{1}{M} \left(\frac{\partial^2 \phi}{\partial x_5^2} + \frac{\partial^2 \phi}{\partial x_6^2} + \frac{\partial^2 \phi}{\partial x_7^2} \right) + \left\{ -\frac{1}{m} \frac{\partial^2 \phi}{\partial x_4^2} - \frac{1}{M} \frac{\partial^2 \phi}{\partial x_8^2} + \frac{2V}{Mm} \frac{\partial^2 \phi}{\partial x_4 \partial x_8} \right\} = 0, \quad (35)$$

where $V = -\frac{Ee}{r}$ is the electrostatic potential.

This can be brought (under special assumptions) to Schrödinger's wave equations. Let us take for ϕ the expression

$$\phi \equiv \psi \cdot e^{\frac{2\pi}{h} \{ (m+E_1)x_4 + (M+E_2)x_8 \} i}, \quad \dots \quad (36)$$

or we assume in conformity with de Broglie's ideas that *not only Energy due to motion of an electron passes a frequency $\frac{E}{h}$, but also Energy due to the rest-mass has a frequency.*

For the Hydrogen Atom $\frac{E_1}{m} = V^2 \approx 10^{-5}$; hence E_1^2 , E_2^2 could be neglected in comparison with mE_1 , ME_2 , and E_1 .

E_2 in comparison with m and M . Under such approximation we easily obtain from (35) (36) the equation for ψ :

$$\frac{1}{m} \left(\frac{\partial^2 \psi}{\partial x_1^2} + \frac{\partial^2 \psi}{\partial x_2^2} + \frac{\partial^2 \psi}{\partial x_3^2} \right) + \frac{1}{M} \left(\frac{\partial^2 \psi}{\partial x_5^2} + \frac{\partial^2 \psi}{\partial x_6^2} + \frac{\partial^2 \psi}{\partial x_7^2} \right) + \frac{8\pi^2}{h^2} \left[\frac{M+m}{2} + (E_1 + E_2) - V \right] \psi = 0. \quad (37)$$

We can now transform (37) as follows:—Let us change the variables:

$$\left. \begin{aligned} x &= x_1 - x_5 & (m+M)\xi &= mx_1 + Mx_5, \\ y &= x_2 - x_6 & (m+M)\eta &= mx_2 + Mx_6, \\ z &= x_3 - x_3 & (m+M)\zeta &= mx_3 + Mx_7. \end{aligned} \right\} \quad (38)$$

Using (38), we obtain from (37):

$$\frac{1}{m} \left(\frac{\partial^2 \psi}{\partial x^2} + \frac{\partial^2 \psi}{\partial y^2} + \frac{\partial^2 \psi}{\partial z^2} \right) + \frac{1}{m+M} \left(\frac{\partial^2 \psi}{\partial \xi^2} + \frac{\partial^2 \psi}{\partial \eta^2} + \frac{\partial^2 \psi}{\partial \zeta^2} \right) + \frac{8\pi^2}{h^2} \left[\frac{M+m}{2} + (E_1 + E_2) - V \right] \psi = 0, \\ \mu = \frac{mM}{m+M}. \quad (39)$$

Let us assume for ψ :

$$\psi = f(x, y, z) g(\xi, \eta, \zeta); \quad (40)$$

hence

$$\frac{1}{\mu} g \nabla_{xyz}^2 f + \frac{1}{M+m} f \nabla_{\xi, \eta, \zeta}^2 g + \frac{8\pi^2}{h^2} f g + \left[\frac{M+m}{2} + (E_1 + E_2) - V \right] f g = 0. \quad (41)$$

$$\text{Let} \quad \frac{1}{m+M} \nabla^2 g = -\frac{4\pi^2}{h^2} g. \quad (42)$$

From (41) and (42) we obtain

$$\frac{1}{\mu} \nabla^2 f + \frac{8\pi^2}{h^2} [(E_1 + E_2) - V] f = 0, \quad (43)$$

which is Schrödinger's equation.

The radiation function is

$$\psi = \psi e^{\frac{2\pi}{h} (M+m+E_1+E_2)it}, \quad (44)$$

because to the first order of approximation

$$x_4 = x_8 = t,$$

the rest time.

§ 14. *The Metric of Space.*

The bearing of the fundamental Form of Space to Einstein's gravitational tensor $G_{\mu\nu}$ and G is as follows:—

To the first order of approximation (or neglecting the squares of $g_{aa'}$ and $g^{aa'}$ in comparison with g^{aa}) we obtain

$$G_{\mu\nu} = \frac{1}{2} g^{\sigma\rho} \left(\frac{\partial^2 g_{\sigma\rho}}{\partial x_\mu \partial x_\nu} + \frac{\partial^2 g_{\mu\nu}}{\partial x_\rho \partial x_\sigma} - \frac{\partial^2 g_{\mu\sigma}}{\partial x_\rho \partial x_\nu} - \frac{\partial^2 g_{\rho\nu}}{\partial x_\mu \partial x_\sigma} \right). \quad (45)$$

We have to take for our approximation only $\sigma = \rho$; hence

$$G_{\mu\nu} = \frac{1}{2} g^{\sigma\sigma} \left(\frac{\partial^2 g_{\mu\nu}}{\partial x_\sigma^2} - \frac{\partial^2 g_{\mu\sigma}}{\partial x_\nu \partial x_\sigma} - \frac{\partial^2 g_{\nu\sigma}}{\partial x_\mu \partial x_\sigma} \right), \quad (46)$$

and we obtain

$$\left. \begin{aligned} G_{11} &= -g^{55} \frac{\partial^2 g_{15}}{\partial x_1 \partial x_5}, \\ G_{12} &= -\frac{1}{2} g^{55} \frac{\partial^2 g_{15}}{\partial x_1 \partial x_5} - \frac{1}{2} g^{66} \frac{\partial^2 g_{26}}{\partial x_2 \partial x_6}, \\ &\dots \dots \dots \\ G_{15} &= \frac{1}{2} \left\{ g^{11} \frac{\partial^2 g_{15}}{\partial x_1^2} + g^{22} \frac{\partial^2 g_{15}}{\partial x_2^2} + \dots + g^{88} \frac{\partial^2 g_{15}}{\partial x_8^2} \right\} \\ &\quad - \frac{1}{2} g^{11} \frac{\partial^2 g_{15}}{\partial x_1^2} - \frac{1}{2} g^{55} \frac{\partial^2 g_{15}}{\partial x_5^2}. \end{aligned} \right\} \quad (47)$$

From (47) it is easily seen that $G_{\mu\nu} = 0$ only if $G_{\mu\nu} = \text{const.}$, or if there is no electromagnetic connexion between the electrons.

The gravitational invariant G is equal to

$$\begin{aligned} G &= g^{\mu\nu} G_{\mu\nu} \\ &= -2g^{11} g^{55} \left(\frac{\partial^2 g_{16}}{\partial x_1 \partial x_5} + \frac{\partial^2 g_{15}}{\partial x_2 \partial x_6} + \frac{\partial^2 g_{15}}{\partial x_3 \partial x_7} - \frac{\partial^2 g_{15}}{\partial x_4 \partial x_8} \right). \end{aligned}$$

Hence $\zeta = 0$ for our fundamental Form.

My thanks are due to Dr. H. T. Flint, for his criticism and help in the writing of this paper.

Wheatstone Laboratory,
King's College, London.

XCVIII. *An Example of Operational Methods.*

To the Editors of the Philosophical Magazine.

GENTLEMEN,—

SINCE the publication of Dr. Jeffreys's Tract* on Heaviside's operational methods, several enquiries have reached me, from which it would seem that a few additional easy examples may be found of interest to students of these methods. One such has suggested itself from reading a leader in 'The Times' (of the 8th June) on the effect of the *deep-earth-temperature*: it seems that, roughly speaking, when this temperature is below 47° Fahr. pulmonary diseases are prevalent; and above 57° Fahr., infantile diarrhoea is to be feared. The mathematical problem suggested is the following:—*Suppose the air outside a conductor (having a plane face) to be kept at temperature v_0 , and the deep-temperature in the conductor to be v_1 . Find the temperature at the surface, allowing for radiation.*

Take the face of the conductor as $x=0$, and the positive direction of x to be inside the conductor: then, using the notation explained in my paper†, we have (inside the conductor)

$$v = v_1 + (v_2 - v_1)e^{-qx},$$

where v_2 is the temperature at $x=0$ and $q^2 = p/k$, $p = \partial/\partial t$. The correct form of the surface-condition is uncertain, but we may use an equation similar to that which holds at a metal surface, namely

$$\frac{\partial v}{\partial x} = h(v_2 - v_0).$$

Thus

$$q(v_1 - v_2) = h(v_2 - v_0),$$

or

$$v_2 = \frac{hv_0 + qv_1}{h + q}.$$

An exact calculation of v_2 can be made in terms of error-functions (by means of the formulæ on p. 96 of Dr. Jeffreys's Tract): but in problems of this kind, as remarked by

* 'Operational Methods in Mathematical Physics' (No. 23 of the Cambridge Tracts), 1927.

† Proc. Camb. Phil. Soc. vol. xx. p. 411 (1921).

Heaviside ('Electromagnetic Theory,' vol. ii. pp. 14-16), there are two easy series which may be found, the first being suitable when t/τ is small, the second when t/τ is large, where τ is the time-interval given by $1/\tau = h^2 k$.

In the present problem exact values of the constants h , k are not available, but if we make estimates on the lines of Lord Kelvin's article * on "Conduction of Heat" (Encyclopædia Britannica, 9th ed., vol. xi. pp. 580, 586), it seems not unreasonable to take τ to be from 40 to 50 hours. Thus the solution to be aimed at corresponds to the hypothesis that t/τ is small; or, in the symbolic calculations, we may treat h/q as small. This gives the result

$$\begin{aligned} v_2 &= v_1 + (v_0 - v_1) \left(\frac{h}{q} - \frac{h^2}{q^2} + \frac{h^3}{q^3} - \dots \right) \\ &= v_1 + (v_0 - v_1) \left\{ \frac{2}{1} \sqrt{\frac{t}{\pi\tau}} - \frac{t}{\tau} + \frac{2 \cdot 2}{1 \cdot 3} \frac{1}{\sqrt{\pi}} \left(\frac{t}{\tau}\right)^{3/2} - \frac{1}{2!} \left(\frac{t}{\tau}\right)^2 \right. \\ &\quad \left. + \frac{2 \cdot 2 \cdot 2}{1 \cdot 3 \cdot 5} \frac{1}{\sqrt{\pi}} \left(\frac{t}{\tau}\right)^{5/2} - \frac{1}{3!} \left(\frac{t}{\tau}\right)^3 + \dots \right\}. \end{aligned}$$

The series converges for all values of t , but is convenient for calculation only if $t/\tau \leq \frac{1}{2}$ (as a rough guide).

However, in the application suggested, the interval t is not likely to exceed 7 hours, and t/τ may be taken as about $\frac{1}{4}$; this gives roughly $\frac{1}{3}$ as the value of the series in the brackets. This shows, for instance, that if the maximum outside temperature is 90° , and the deep-temperature is 54° , the surface-temperature would not be likely to rise above 66° . These numbers make no pretensions to great accuracy; but they do seem to confirm the conclusions of the 'Times' that *the deep-earth-temperature is of more importance than the air-temperature in determining conditions of health at the surface of the earth.*

I am, Gentlemen,

Your obedient servant,

Cambridge,
8th June, 1928.

T. J. I'A. BROMWICH.

* Reprinted in volume ii. of Kelvin's 'Mathematical and Physical Papers.'

XCIX. *The Potential Function due to certain Plane Boundary Distributions.* By C. FOX, M.A.(Camb.), D.Sc.(Lond.)*.

§ 1. *Introduction.*

THE object of this paper is to give the potential function throughout space when either the potential or (in an electrical problem) the charge is known over (i.) a plane and (ii.) two parallel planes. The method is illustrated by application to several problems: for example, the guard-ring, the freely-charged elliptic disk, and the problem of the potential field arising from an infinite conductor bounded by two parallel planes with two elliptical disk electrodes, applied so that the join of their centres is perpendicular to the bounding planes. When the two axes of the elliptical disks are equal, so that they become circular, the last problem becomes identical with that of Nobili's† rings, first solved by Riemann.

The method consists in applying a theorem, due to Neumann, as follows:

$$2\pi f(r, \phi) = \int_0^\infty u \, du \int_{-\pi}^\pi \int_0^\infty f(R, \Phi) \times J_0[u \sqrt{R^2 + r^2 - 2Rr \cos(\Phi - \phi)}] R dR d\Phi, \quad (1.1)$$

provided that the following conditions ‡ are satisfied:—

(i.) $f(R, \Phi)$ is a bounded function of the real variables R and Φ whenever $-\pi \leq \Phi \leq \pi$ and $0 \leq R$, and is such that

$$\int_{-\pi}^\pi \int_0^\infty f(R, \Phi) R^2 dR d\Phi$$

exists and is absolutely convergent.

(ii.) $f(R, \Phi)$ as a function of R is of bounded variation in the interval $(0, \infty)$ for every value of Φ lying between $\pm\pi$, this variation being an integrable function of Φ .

(iii.) If $\Omega(R, \Phi)$ denote the total variation of $F(R, \Phi)$ in the interval (r, R) , let $\Omega(R, \Phi)$ tend uniformly to zero with

* Communicated by the Author.

† The solution of this problem with references is given in Gray, Matthews, and MacRobert's 'Bessel Functions,' p. 144, § 3, 1922 ed.

‡ Since writing this paper I have discovered that condition (ii.) is superfluous, whilst condition (i.) can be replaced by another which is satisfied by all the functions that occur here. The proofs have not yet been published.

respect to Φ as $R \rightarrow r$ throughout the whole interval $(-\pi, \pi)$, with the exception of values of Φ in a number of sectors the sum of whose angles may be assumed arbitrarily small.

(iv.) If (r, ϕ) is a point of discontinuity of $f(R, \Phi)$, then $f(r, \phi)$ on the left-hand side of (1.1) must be replaced by the mean value of $f(R, \Phi)$ taken round a small circle with the point (r, ϕ) as centre. We assume that this mean value is finite.

This theorem is proved in Watson's 'Bessel Functions' *, where it is also shown that the order of the integrations on the right-hand side of (1.1) with respect to R and Φ may be interchanged.

Thus (1.1) can be written

$$2\pi f(r, \phi) = \int_0^\infty u \, du \int_{-\pi}^\pi \int_0^\pi f(R, \Phi) \times J_0[u \vee \{R^2 + r^2 - 2Rr \cos(\Phi - \phi)\}] R d\Phi dR. \quad (1.2)$$

The conditions above are too narrow †, as we shall show by an example later on. We shall also make use of the fact that in cylindrical coordinates

$$e^{\pm uz} J_0(ur) \quad . \quad . \quad . \quad . \quad . \quad (1.3)$$

is a solution of Laplace's equation. On changing the origin in the plane $z=0$ to the point (R, Φ) , it follows from (1.3) that

$$e^{\pm uz} J_0[u \vee \{R^2 + r^2 - 2Rr \cos(\Phi - \phi)\}]. \quad . \quad (1.4)$$

is also a solution of Laplace's equation.

§ 2. The Potential Field arising from a Known Plane Distribution.

2.1. If the value of the potential ‡ over the plane $z=0$ is given by $f(r, \phi)$, which satisfies the conditions of § 1, then the potential function V throughout space is given by

$$2\pi V = \int_0^\infty e^{\mp uz} u \, du \int_{-\pi}^\pi \int_0^\pi f(R, \Phi) \times J_0[u \vee \{R^2 + r^2 - 2Rr \cos(\Phi - \phi)\}] R dR d\Phi, \quad (2.11)$$

* P. 470.

† See footnote ‡, p. 994.

‡ Cylindrical coordinates are used throughout the paper.

or by

$$2\pi V = \int_0^\infty e^{\mp uz} u du \int_0^\infty \int_{-\pi}^\pi f(R, \Phi) \\ \times J_0[u \sqrt{R^2 + r^2 - 2Rr \cos(\Phi - \phi)}] R d\Phi dR, \quad (2.12)$$

whichever is more convenient, the upper or lower sign being taken according as z is positive or negative. These formulæ follow immediately from (1.1) and (1.2) on putting $z=0$.

As an illustration, consider the case of a unit point charge at the origin for which

$$f(r, \phi) = r^{-1}.$$

Conditions (i.) and (ii.) of § 1 are both violated; nevertheless, on substituting in (2.12) we get the correct result, showing, I think, that the conditions of § 1 are too narrow. The calculations are as follows:—

We have

$$2\pi V = \int_0^\infty e^{\mp uz} u du \int_0^\infty \int_{-\pi}^\pi \\ \times J_0[u \sqrt{R^2 + r^2 - 2Rr \cos(\Phi - \phi)}] d\Phi dR. \quad (2.13)$$

Also it is known that *

$$J_0[u \sqrt{R^2 + r^2 - 2Rr \cos(\Phi - \phi)}] \\ = J_0(uR)J_0(ur) + 2 \sum_{m=1}^\infty J_m(uR)J_m(ur) \cos m(\Phi - \phi), \quad (2.14)$$

and that we may integrate term by term with respect to Φ . Hence (2.13) becomes

$$V = \int_0^\infty e^{\mp uz} u du \int_0^\infty J_0(uR)J_0(ur) dR. \quad (2.15)$$

Now †

$$\int_0^\infty J_0(uR) dR = u^{-1}$$

and ‡

$$\int_0^\infty e^{-uz} J_0(ur) du = (r^2 + z^2)^{-\frac{1}{2}}. \quad (2.16)$$

if $z \geq 0$. Hence (2.15) reduces to

$$V = (r^2 + z^2)^{-\frac{1}{2}}$$

* Watson, 'Bessel Functions,' pp. 127–128.

† Watson, *loc. cit.* p. 391 (1).

‡ Watson, *loc. cit.* p. 384 (1). For the case $z=0$ we use (1), p. 391.

for all values of r and z . This, it is well known, is the potential due to a unit charge at the origin.

2.2. If the charge at the point (r, ϕ) in the plane $z=0$ is given by $f(r, \phi)$, which satisfies the conditions of § 1, then the potential at the point (r, ϕ, z) is given by

$$V = \int_0^\infty e^{\mp uz} du \int_{-\pi}^\pi \int_0^\infty f(R, \Phi) \\ \times J_0[u\sqrt{R^2 + r^2 - 2Rr \cos(\Phi - \phi)}] R dR d\Phi, \quad (2.21)$$

the upper or lower sign being taken according as z is positive or negative. The order of the integrations with respect to R and Φ may be interchanged.

To prove this from Neumann's theorem, § 1,

$$\int_0^\infty u du \int_{-\pi}^\pi \int_0^\infty f(R, \Phi) \\ \times J_0[u\sqrt{R^2 + r^2 - 2Rr \cos(\Phi - \phi)}] R dR d\Phi$$

converges when considered as an integral with respect to u . Hence

$$\int_0^\infty e^{\pm uz} u du \int_{-\pi}^\pi \int_0^\infty f(R, \Phi) \\ \times J_0[u\sqrt{R^2 + r^2 - 2Rr \cos(\Phi - \phi)}] R dR d\Phi$$

converges uniformly with respect to z . We may then differentiate the right-hand side of (2.21) under the integral sign, and so

$$\left(\frac{\partial V}{\partial z}\right)_{z=0} = -2\pi f(r, \phi)$$

on using Neumann's theorem once again. But for a plane distribution

$$\left(\frac{\partial V}{\partial z}\right)_{z=0} = -2\pi\sigma,$$

where σ is the intensity of charge per unit area. Also there is only one potential function which gives rise to a given charge distribution. Hence this potential must be given by (2.21).

As an illustration, consider the elliptic disk whose semi-axes are a and b . The charge * at (R, Φ) is proportional to

$$\left\{ 1 - \frac{R^2 \cos^2 \Phi}{a^2} - \frac{R^2 \sin^2 \Phi}{b^2} \right\}^{-\frac{1}{2}},$$

where R varies from 0 to the positive root of

$$1 - \frac{R^2 \cos^2 \Phi}{a^2} - \frac{R^2 \sin^2 \Phi}{b^2} = 0,$$

and Φ varies from $-\pi$ to π . For other values of R the charge is zero. If we let

$$\Psi^2 = \frac{a^2 b^2}{b^2 \cos^2 \Phi + a^2 \sin^2 \Phi}, \quad \dots \quad (2.22)$$

then

$$f(R, \Phi) = K \left\{ 1 - \frac{R^2}{\Psi^2} \right\}^{-\frac{1}{2}},$$

where K is a constant. From (2.21) the potential function* throughout space is

$$V = \int_0^\infty e^{\mp uz} du \int_{-\pi}^\pi \int_0^\Psi \left\{ 1 - \frac{R^2}{\Psi^2} \right\}^{-\frac{1}{2}} \times J_0[u \sqrt{R^2 + r^2 - 2Rr \cos(\Phi - \phi)}] R dR d\Phi, \quad (2.23)$$

the upper or lower sign being taken according as z is positive or negative.

The integral on the right of (2.23) with respect to R can be evaluated in terms of hypergeometric functions defined by

$$\begin{aligned} {}_p f_q(\alpha_1, \alpha_2, \dots, \alpha_p; \rho_1, \rho_2, \dots, \rho_q; x) \\ = \sum_{n=1}^{\infty} \frac{\Gamma(\alpha_1 + n) \Gamma(\alpha_2 + n) \dots \Gamma(\alpha_p + n)}{\Gamma(\rho_1 + n) \Gamma(\rho_2 + n) \dots \Gamma(\rho_q + n)} \frac{x^n}{n!}. \end{aligned}$$

On using the power series for the Bessel function and integrating term by term, a process which is known to be permissible for a power series, we have

$$\begin{aligned} \int_0^\Psi \left\{ 1 - \frac{R^2}{\Psi^2} \right\}^{-\frac{1}{2}} J_m(uR) R dR \\ = \frac{1}{2} \sqrt{\pi} \Psi^2 \left(\frac{1}{2} u \Psi \right)^m {}_1 f_2 \left(\frac{1}{2} m + 1; m + 1, \frac{1}{2} m + \frac{3}{2}; -\frac{1}{4} u^2 \Psi^2 \right). \end{aligned} \quad \dots \quad (2.24)$$

* $f(R, \Phi)$ is not of bounded variation in an interval which includes the value $R = \Psi$, thus violating (ii.), § 1. This difficulty is easily overcome by taking the range of integration with respect to R in (2.23) to be $(0, \Psi - \epsilon)$, and then letting $\epsilon \rightarrow 0$. There is no difficulty in showing that this limit is given by the right-hand side of (2.23). But see the footnote † on p. 994.

Now substitute (2.14) in (2.23). The series in (2.14) being uniformly convergent with respect to R , we may interchange the order of summation and integration. On using (2.24) and simplifying the first term, (2.23) becomes

$$\begin{aligned} V = & K \int_0^\infty e^{\mp uz} du \int_{-\pi}^\pi \Psi \frac{\sin u \Psi}{u} J_0(ur) d\Phi \\ & + \sqrt{\pi} K \int_0^\infty e^{\mp uz} du \int_{-\pi}^\pi \Psi^2 \sum_{m=1}^\infty \left(\frac{1}{2} u \Psi\right)^m, \\ & \times {}_1F_2\left(\frac{1}{2}m+1; m+1; \frac{1}{2}m+\frac{3}{2}; -\frac{1}{4}u^2\Psi^2\right) \\ & \times J_m(ur) \cos m(\Phi-\phi) d\Phi. \quad \dots \quad (2.25) \end{aligned}$$

It is not difficult to show that this series converges with the same rapidity as $\sum_{m=1}^\infty m^{-2}$.

When $a=b$ the disk is circular. We then have from (2.22) $\Psi^2=a^2$, and it can be seen that all the integrals with respect to Φ vanish except the first, giving us

$$V = 2\pi K a \int_0^\infty e^{\mp uz} \sin au J_0(ur) \frac{du}{u},$$

which, it is well known*, is the formula for the potential field due to a freely-charged circular disk of radius a .

To obtain the potential of the elliptic disk itself it is sufficient to find the potential of the origin, *i.e.* we make $r=z=0$ in (2.25). We then get

$$\begin{aligned} V &= K \int_0^\infty du \int_{-\pi}^\pi \Psi \frac{\sin u \Psi}{u} d\Phi \\ &= 2K \int_0^\infty du \int_0^\pi \Psi \frac{\sin u \Psi}{u} d\Phi, \quad \dots \quad (2.26) \end{aligned}$$

since Ψ is always positive.

Again, since

$$\int_0^\infty \frac{\sin u \Psi}{u} du$$

* Gray, Matthews, and MacRobert's 'Bessel Functions,' pp. 141-142.

is uniformly convergent with respect to $\Psi(>0)$, we may interchange the order of integration of (2.26), when we get

$$\begin{aligned} V &= 2K \int_0^\pi \Psi d\Phi \int_0^\pi \frac{\sin u \Psi}{u} du \\ &= K\pi \int_0^\pi \Psi d\Phi \\ &= K\pi ab \int_0^\pi \frac{d\Phi}{\{b^2 \cos^2 \Phi + a^2 \sin^2 \Phi\}^{\frac{1}{2}}}, \end{aligned}$$

an integral well known in the theory of elliptic functions.

§ 3. The Potential Function due to two Parallel Plane Distributions.

3.1. If we are given that in the plane $z=-c$ the potential at the point (R, Φ) is $f(R, \Phi)$, whilst at the same time in the plane $z=c$ the potential at the point (R, Φ) is $F(R, \Phi)$ both of these functions satisfying the conditions of § 1, then the potential V in between the two planes $z=\pm c$ is given by

$$\begin{aligned} 2\pi V &= \int_0^\infty u \frac{\sinh u(c-z)}{\sinh 2uc} du \int_{-\pi}^\pi \int_0^\infty f(R, \Phi) \\ &\quad \times J_0[u\sqrt{R^2+r^2-2Rr\cos(\Phi-\phi)}] R dR d\Phi \\ &\quad + \int_0^\infty u \frac{\sinh u(c+z)}{\sinh 2uc} du \int_{-\pi}^\pi \int_0^\infty F(R, \Phi) \\ &\quad \times J_0[u\sqrt{R^2+r^2-2Rr\cos(\Phi-\phi)}] R dR d\Phi. \end{aligned} \quad \dots (3.11)$$

We may change the order of integration with respect to R and Φ .

As an illustration consider the problem of the guard-ring. In this problem $V=0$ over the whole plane $z=c$, and $V=a$ constant, K say, over a circular disk in the plane $z=-c$ of radius a and centre on the z axis, whilst $V=0$ over the rest of the plane $z=-c$. Thus $F(R, \Phi)=0$, whilst $f(R, \Phi)=K$ when $R<a$, and $f(R, \Phi)=0$ when $R>a$. Hence

$$\begin{aligned} 2\pi V &= \int_0^\infty u \frac{\sinh u(c-z)}{\sinh 2uc} du \int_0^\pi \int_0^\pi K \\ &\quad \times J_0[u\sqrt{R^2+r^2-2Rr\cos(\Phi-\phi)}] R dR d\Phi \\ &= 2\pi K \int_0^\infty u \frac{\sinh u(c-z)}{\sinh 2uc} du \int_0^a J_0(ur) J_0(uR) R dR \end{aligned}$$

on using (2.14) and integrating with respect to Φ . But on using the Taylor's series for $J_0(uR)$ and integrating term by term, we get

$$\int_0^a R J_0(uR) dR = \frac{a}{u} J_1(au).$$

The potential function between the two planes $z = \pm c$ then reduces to

$$V = aK \int_0^\infty \frac{\sinh u(c-z)}{\sinh 2uc} J_1(au) J_0(ur) du.$$

3.2. If we are given that the intensity of charge at the point (R, Φ) on the side of the plane $z = -c$ facing $z = +c$ is $f(R, \Phi)$ per unit area, and that the intensity of charge at the point (R, Φ) on the side of the plane $z = c$ facing $z = -c$ is $F(R, \Phi)$ per unit area, then the potential function between the two planes $z = \pm c$, corresponding to this distribution, is given by

$$\begin{aligned} V = & 2 \int_0^\infty \frac{\cosh u(c-z)}{\sinh 2uc} du \int_{-\pi}^\pi \int_0^\infty f(R, \Phi) \\ & \times J_0[u\sqrt{R^2 + r^2 - 2Rr \cos(\Phi - \phi)}] R dR d\Phi \\ & + 2 \int_0^\infty \frac{\cosh u(c+z)}{\sinh 2uc} du \int_{-\pi}^\pi \int_0^\infty F(R, \Phi) \\ & \times J_0[u\sqrt{R^2 + r^2 - 2Rr \cos(\Phi - \phi)}] R dR d\Phi. \end{aligned} \quad (3.21)$$

Formulae of this type can also be used to solve the following problem. An infinite conductor is bounded by two parallel planes $z = \pm c$, and two elliptical electrodes are applied to these planes. To simplify the analysis we shall assume that the centres of the disks lie on the axis of z , that both the ellipses have semi-axes a and b ($a > b$), that both the major axes are in the plane $\Phi = 0$, and that the potential of the plane $z = 0$ is zero. The last assumption does not entail any loss of generality.

The disks being at constant potential, the charge at a point (R, Φ) on one of them at any instant is proportional to

$$\left\{ 1 - \frac{R^2 \cos^2 \Phi}{a^2} - \frac{R^2 \sin^2 \Phi}{b^2} \right\}^{-\frac{1}{2}},$$

whilst at other points on the planes $z = \pm c$ the charge is zero.

Again, if V is the potential function of the system (V must, of course, be a solution of Laplace's equation), the rate of flow from the upper disk, say, to the medium is $-k \frac{\partial V}{\partial z}$ with $z=c$.

We must therefore have

$$k \frac{\partial V}{\partial z} = 0, \quad \text{for } z = \pm c \text{ and } (R, \Phi) \text{ a point outside either of the elliptical electrodes,}$$

$$k \frac{\partial V}{\partial z} = K \left\{ 1 - \frac{R^2 \cos^2 \Phi}{a^2} - \frac{R^2 \sin^2 \Phi}{b^2} \right\}^{-\frac{1}{2}}, \quad \text{for } z = \pm c$$

and (R, Φ) a point inside either of the electrodes,

where K is a constant. If we assume that the disk in the plane $z=c$ is at positive potential whilst that in the plane $z=-c$ is at a negative potential (*i. e.* the flow of the electricity is in the negative direction of the z axis), then the total flow S , say, from the upper disk to the medium is given by

$$S = K \iint \left\{ 1 - \frac{R^2 \cos^2 \Phi}{a^2} - \frac{R^2 \sin^2 \Phi}{b^2} \right\}^{-\frac{1}{2}} R dR d\Phi,$$

taken over the area of the upper disk. Putting

$$R \cos \Phi = ar \cos \phi \quad \text{and} \quad R \sin \Phi = br \sin \phi,$$

the integral on the right-hand side is easily evaluated when we get

$$S = K \cdot 2\pi ab.$$

Hence we may write, with the notation of (2.22) :

$$\frac{\partial V}{\partial z} = \frac{S}{2\pi abk} \cdot \left\{ 1 - \frac{R^2}{\Psi^2} \right\}^{-\frac{1}{2}}, \quad \text{for } z = \pm c$$

and (R, Φ) a point inside either of the electrodes.

The potential function is then given by

$$\begin{aligned} 2\pi V = & -\frac{S}{2\pi abk} \int_0^\infty \frac{\cosh u(c-z)}{\sinh 2uc} du \int_{-\pi}^\pi \int_0^* \left\{ 1 - \frac{R^2}{\Psi^2} \right\}^{-\frac{1}{2}} \\ & \times J_0[u \sqrt{R^2 + r^2 - 2Rr \cos(\Phi - \phi)}] R dR d\Phi \\ & + \frac{S}{2\pi abk} \int_0^\infty \frac{\cosh u(c+z)}{\sinh 2uc} du \int_{-\pi}^\pi \int_0^* \left\{ 1 - \frac{R^2}{\Psi^2} \right\}^{-\frac{1}{2}} \\ & \times J_0[u \sqrt{R^2 + r^2 - 2Rr \cos(\Phi - \phi)}] R dR d\Phi, \end{aligned}$$

which, after simplification, becomes

$$2\pi V = \frac{S}{2\pi abk} \int_0^\infty \frac{\sinh uz}{\cosh ac} du \int_{-\pi}^\pi \int_0^\Psi \left\{ 1 - \frac{R^2}{\Psi^2} \right\}^{-\frac{1}{2}} \\ \times J_0[u\sqrt{\{R^2 + r^2 - 2Rr \cos(\Phi - \phi)\}}] R dR d\Phi. \quad (3.22)$$

When $a=b$ this becomes identical with the problem of Nobili's rings. In this case $\Psi=a$, and the integrals with respect to Φ and R can be evaluated just as for (2.23). The result is

$$V = \frac{S}{2\pi a^2 k} \int_0^\infty \frac{\sinh uz}{\cosh uc} \sin au J_0(ur) \frac{du}{u},$$

agreeing with Riemann's solution*.

In (3.22) put $R^2 = \Psi^2 v$, when we get

$$2\pi V = \frac{S}{2\pi abk} \int_0^\infty \frac{\sinh uz}{\cosh uc} du \int_{-\pi}^\pi \int_0^1 (1-v)^{-\frac{1}{2}} \\ \times J_0[u\sqrt{\{\Psi^2 v + r^2 - 2\Psi r^{\frac{1}{2}} r \cos(\Phi - \phi)\}}] \frac{1}{2} \Psi^2 dv d\Phi. \\ \dots \dots \dots (3.23)$$

By making a and b tend to zero, we can find the potential field when the electrodes become very small. We have

$$\Psi^2 = \frac{a^2 b^2}{a^2 \cos^2 \Phi + b^2 \sin^2 \Phi} \rightarrow 0, \quad \text{as } a, b \rightarrow 0,$$

and it is not difficult to show when $-c < z < c$, that the limit of the right-hand side of (3.23) is the same as

$$\frac{S}{4\pi k} \int_0^\infty \frac{\sinh uz}{\cosh uc} du \lim_{\substack{a \rightarrow 0 \\ b \rightarrow 0}} \int_{-\pi}^\pi \frac{ab d\Phi}{a^2 \cos^2 \Phi + b^2 \sin^2 \Phi} \int_0^1 (1-v)^{-\frac{1}{2}} \\ \times J_0(ur) dv.$$

But

$$\int_{-\pi}^\pi \frac{ab d\Phi}{a^2 \cos^2 \Phi + b^2 \sin^2 \Phi} = 4 \int_0^{\pi/2} \frac{\frac{b}{a} \sec^2 \Phi}{1 + \frac{b^2}{a^2} \tan^2 \Phi} d\Phi \\ = 4 \tan^{-1} \left(\frac{b}{a} \tan \Phi \right) \Big|_0^{\pi/2} = 2\pi$$

* Gray, Mathews & MacRobert, *loc. cit.* pp. 144-146.

if b/a is neither zero nor infinite. Hence

$$\lim_{\substack{a \rightarrow 0 \\ b \rightarrow 0}} \int_{-\pi}^{\pi} \frac{ab \, d\Phi}{a^2 \cos^2 \Phi + b^2 \sin^2 \Phi} = 2\pi,$$

and so (3.23) becomes in the limit :

$$V = \frac{S}{2\pi k} \int_0^{\infty} \frac{\sinh uz}{\cosh uc} J_0(ur) \, du, \quad . \quad . \quad (3.24)$$

provided that a and b tend to zero in such a way that $\lim b/a$ is neither zero nor infinite and $-c < z < c$.

The case $z = \pm c$ presents considerable analytical difficulty, but if we use the fact that the potential function is continuous, then the potential on the plane $z=c$ is given by

$$\lim_{z \rightarrow c} \frac{S}{2\pi k} \int_0^{\infty} \frac{\sinh uz}{\cosh uc} J_0(ur) \, du,$$

and, with the help of the asymptotic expansion of the Bessel Function, it is not difficult to show that this is equal to

$$\frac{S}{2\pi k} \int_0^{\infty} \frac{\sinh uc}{\cosh uc} J_0(ur) \, du.$$

Similarly for the case $z = -c$. Hence (3.24) is the potential function for $-c \leq z \leq c$.

It is interesting to note that the result is independent of the shape of the electrodes* as they shrink to zero, provided $\lim a/b$ is neither zero nor infinite, that is, provided that the ellipses do not shrink into straight lines.

§ 4. *The Introduction of a Unit Point Charge.*

4.1. When the planes in the preceding problems are all occupied by conducting matter, the potential functions can also be found if a point charge is introduced. We shall assume that this charge is positive, of strength unity, and situated at the point (z', r', ϕ') .

To find the field due to a point charge situated in the presence of a plane of conducting material at $z=0$ charged to the potential $f(R, \Phi)$ at the point (R, Φ) , we add the expression

$$\begin{aligned} & \{(z-z')^2 + r^2 - r'^2 - 2rr' \cos(\phi - \phi')\}^{-\frac{1}{2}} \\ & - \{(z+z')^2 + r^2 + r'^2 - 2rr' \cos(\phi - \phi')\}^{-\frac{1}{2}} \quad (4.11) \end{aligned}$$

* (3.24) is the same as the solution of the similar problem for circular electrodes (see Gray, Mathews, and MacRobert, *loc. cit.* p. 146).

to (2.11), using the upper or lower sign in (2.11) according as z' is positive or negative. If z' is positive, the potential throughout the space $z < 0$ is zero, whilst if z' is negative, the potential throughout the space $z > 0$ is zero.

To prove this, (4.11) is evidently a potential function which vanishes at $z=0$ and which has an infinity at $z=z'$, $r=r'$, $\phi=\phi'$, due to a unit point charge.

4.2. To find the field due to a unit charge at (z', r', ϕ') in the presence of a plane of conducting matter at $z=0$ charged to intensity $\frac{1}{2}f(R, \Phi)$ per unit area at the point (R, Φ) , we add the expression

$$\{z-z'\}^2 + r^2 + r'^2 - 2rr' \cos(\phi - \phi')\}^{-\frac{1}{2}} + \{(z+z')^2 + r^2 + r'^2 - 2rr' \cos(\phi - \phi')\}^{-\frac{1}{2}}. \quad (4.21)$$

to (2.21), using the upper or lower sign in (2.21) according as z is positive or negative. If z' is positive, the potential throughout the space $z < 0$ is zero, whilst if z' is negative the potential throughout the space $z > 0$ is zero.

To prove this, it is easy to see that (4.21) is a potential function whose differential coefficient with respect to z vanishes when $z=0$.

4.3. To find the field due to a point charge situated at (z', r', ϕ') between two planes $z = \pm c$, the upper of which is charged at the point (R, Φ) to potential $F(R, \Phi)$ and the lower to potential $F(R, \Phi)$, we add to (3.11) the expression

$$\left. \begin{aligned} V &= 2 \int_0^\infty \frac{\sinh u(c-z) \sinh u(c+z')}{\sinh 2uc} \\ &\quad \times J_0[u \sqrt{r^2 + r'^2 - 2rr' \cos(\phi - \phi')}] du \\ &\quad \text{when } z' \leq z \leq c, \\ V &= 2 \int_0^\infty \frac{\sinh u(c-z') \sinh u(c+z)}{\sinh 2uc} \\ &\quad \times J_0[u \sqrt{r^2 + r'^2 - 2rr' \cos(\phi - \phi')}] du \\ &\quad \text{when } -c \leq z \leq z'. \end{aligned} \right\} \quad (4.31)$$

To prove this, we must show that the above expressions for V , which are evidently potential functions, vanish when $z = \pm c$, which is obvious, are continuous as z passes through z' , which is also obvious, since both integrals converge and are equal when $z = z'$; and finally we must also show that $\frac{\partial V}{\partial z}$ is continuous as z passes through z' .

The formulæ of (4.31) are given by Gray, Mathews, and MacRobert* in their treatise, but they omit to prove that $\frac{\partial V}{\partial z}$ is continuous. As this is not at all obvious, I take the opportunity of proving it here. If we differentiate either of the integrals of (4.31) under the integral sign with respect to z , we find that the resultant integrals converge uniformly only if $z \neq z'$, and, in fact, when $z = z'$ they diverge. This shows, I think, that the continuity of $\frac{\partial V}{\partial z}$ at $z = z'$ cannot be taken for granted. The proof proceeds as follows. Using the usual exponential formulæ for the hyperbolic sine and cosine, it is easy to show that

$$\begin{aligned} & \frac{2 \sinh u(c-z) \sinh u(c+z')}{\sinh 2uc} \\ &= e^{-u(z-z')} + \frac{e^{-2uc} \cosh u(z-z') - \cosh u(z+z')}{\sinh 2uc}. \end{aligned}$$

With the help of (2.16) it then follows that the upper formula for V in (4.31) is equivalent to

$$\begin{aligned} V &= \{(z-z')^2 + r^2 + r'^2 - 2rr' \cos(\phi - \phi')\}^{-\frac{1}{2}} \\ &+ \int_0^\infty \frac{e^{-2uc} \cosh u(z-z') - \cosh u(z+z')}{\sinh 2uc} \\ &\quad \times J_0[u \sqrt{r^2 + r'^2 - 2rr' \cos(\phi - \phi')}] du, \quad (4.32) \end{aligned}$$

whilst the lower formula for V in (4.31) is equivalent to (4.32) with z and z' interchanged. On differentiating with respect to z under the integral sign in (4.32), we find that the resulting integral is uniformly convergent with respect to z and z' for all values of z and z' lying between $\pm c$, including $z = z'$. Hence, from the upper formula of (4.31), if $r \neq r'$ and $\phi \neq \phi'$, then

$$\begin{aligned} \left(\frac{\partial V}{\partial z}\right)_{z=z'} &= - \int_0^\infty \frac{\sinh 2uz'}{\sinh 2uc} u \\ &\quad \times J_0[u \sqrt{r^2 + r'^2 - 2rr' \cos(\phi - \phi')}] du. \end{aligned}$$

We find the same value of $\left(\frac{\partial V}{\partial z}\right)_{z=z'}$ by this method from the lower formula of (4.31). This shows that $\frac{\partial V}{\partial z}$ is con-

* 'Bessel Functions,' p. 193 (20).

tinuous as z passes through z' and completes the proof of the statement at the beginning of § 4.3.

4.4. To find the field due to a point charge situated at (z', r', ϕ') between two planes $z = \pm c$, the upper of which is charged at the point (R, Φ) to an intensity $F(R, \Phi)$ per unit area on its lower surface and the lower of which is charged to an intensity $f(R, \Phi)$ on its upper surface, we add to (3.21) the expression

$$\left. \begin{aligned} V &= 2 \int_0^\infty \frac{\cosh u(c-z) \cosh u(c+z')}{\sinh 2uc} \times J_0[u \sqrt{r^2 + r'^2 - 2rr' \cos(\phi - \phi')}] du \\ &\quad \text{when } z' \leq z \leq c, \\ V &= 2 \int_0^\infty \frac{\cosh u(c-z') \cosh u(c+z)}{\sinh 2uc} \times J_0[u \sqrt{r^2 + r'^2 - 2rr' \cos(\phi - \phi')}] du \\ &\quad \text{when } -c \leq z \leq z'. \end{aligned} \right\} \quad (4.41)$$

To prove this, we write

$$\begin{aligned} &\frac{2 \cosh u(c-z) \cosh u(c+z')}{\sinh 2uc} \\ &= e^{-u(z-z')} + \frac{e^{-2uc} \cosh u(z-z') + \cosh u(z+z')}{\sinh 2uc} \end{aligned}$$

in the upper formula of (4.41), and, proceeding as in § 4.3, we can show that this formula is equivalent to

$$\begin{aligned} V &= \{(z-z')^2 + r^2 + r'^2 - 2rr' \cos(\phi - \phi')\}^{-\frac{1}{2}} \\ &+ \int_0^\infty \frac{e^{-2uc} \cosh u(z+z') + \cosh u(z-z')}{\sinh 2uc} \\ &\quad \times J_0[u \sqrt{r^2 + r'^2 - 2rr' \cos(\phi - \phi')}] du, \quad (4.42) \end{aligned}$$

whilst the lower formula of (4.41) is equivalent to (4.42) with z and z' interchanged. We may differentiate the integral of (4.42) with respect to z underneath the integral sign, and we obtain

$$\begin{aligned} \left(\frac{\partial V}{\partial z}\right)_{z=z'} &= \int_0^\infty \frac{\sinh 2uz'}{\sinh 2uc} u \\ &\quad \times J_0[u \sqrt{r^2 + r'^2 - 2rr' \cos(\phi - \phi')}] du, \end{aligned}$$

whilst the same value for $\left(\frac{\partial V}{\partial z}\right)_{z=z'}$ is obtained if we start

with the lower formula for V in (4.41). Hence we see that V is a potential function having an infinity at $z=z'$, $r=r'$, $\phi=\phi'$ due to a unit point charge, is continuous at all other points of the plane $z=z'$, and that $\frac{\partial V}{\partial z}$ is also continuous as z passes through z' .

Again, if $z \neq z'$, we may differentiate the integrals of (4.41) with respect to z underneath the integral sign, from which it easily follows that

$$\left(\frac{\partial V}{\partial z}\right)_{z=\pm c} = 0.$$

Hence this system gives rise to no charge on either of the planes $z = \pm c$.

This completes the proof of the statement at the beginning of § 4.4.

C. *The Intensity Distribution of the General and Characteristic X-Radiation from Molybdenum.* By L. R. G. TRELOAR, B.Sc., Wantage Scholar, University of Reading*.

Introduction.

THE experiments described in this paper were made with the object of determining more precisely the nature of the complete radiation emitted under working conditions from a Shearer tube fitted with a molybdenum target. The experiments were intended primarily to be of practical rather than of theoretical interest.

The chief measurements were as follows:—

1. The intensity distribution of the general radiation at various voltages.
2. The corresponding intensities of the $K\alpha$ - and $K\beta$ -line radiation.
3. The ratio of the homogeneous to the general radiation.

Apparatus.

Two methods of excitation of the tube were employed. Most of the experiments were carried out with an induction coil and mercury interrupter, but for purposes of comparison

* Communicated by Prof. J. A. Crowther, Sc.D.

some later experiments were made with a 2-kilowatt oil-immersed transformer. During operations the tube was continuously exhausted by a two-stage diffusion pump, backed by a rotary oil-pump, and was controlled by means of an air-leak. It was run at voltages ranging from 19.75 kv. to 48.4 kv., the current being maintained constant at 3 milliamps. in all readings. The molybdenum target was about 1 mm. thick, and was brazed on to the water-cooled end of the tube at an inclination of 45° to the axis of the tube, and the beam emerged from the tube through an aluminium window .056 mm. thick.

The spectrometer was of the standard Bragg pattern, employing a calcite crystal whose surface was ground. The ionization chamber, which had a length of 15.8 cm. and was closed by an aluminium window .056 mm. thick, was filled with methyl iodide. It was saturated by a potential of 300 volts, supplied by a storage battery, and the ionization was measured by means of a Wilson tilted electroscope. The incident beam of X-rays was limited by two slits, and the reflected beam by a third slit, placed immediately in front of the chamber window.

Method of taking Readings.

Preliminary tests were carried out, sometimes with the help of the photographic method, to see that the crystal was accurately centred, and that it focussed the radiation sharply and accurately into the ionization chamber.

Owing to a slow change in the intensity of the radiation emitted from the tube, due, presumably, to spreading of the cathode stream etc., all the readings for a particular voltage were taken on the same day, with a continuous running of the tube. The voltage was found afterwards from the high-frequency limit of the spectrum. It would have been desirable to have had a more accurate control of the voltage during the course of readings, but this was not found possible. A spark gap between spheres of 5 cm. diameter, for example, was found not to increase the accuracy of the experiments. By the method employed, readings taken during a day's running were consistent to 3 per cent.

In taking readings the integrated reflexion method, which has been fully discussed by Bragg, James, and Bosanquet*, was used throughout. The crystal table was rotated by hand by means of a tangent screw fitted with radial spokes. To take a reading the chamber was set at the desired angle, and

* Bragg, James, and Bosanquet, *Phil. Mag.* xli. p. 309 (1921).
Phil. Mag. S. 7. Vol. 6. No. 39. Nov. 1928.

the crystal table was turned through an angle of $3\frac{3}{4}$ minutes at intervals of $2\frac{1}{2}$ seconds. The total angle swept through by the crystal in each reading was $2\frac{1}{4}^\circ$, the corresponding time taken being 90 seconds.

The electroscope was operated at a comparatively low sensitivity of about 75 scale divisions per volt, and it was adjusted so that its sensitivity was at a maximum (*i. e.*, the sensitivity was reduced either by increasing or diminishing the tilt). In this position the leaf was found to be particularly stable, and, in addition, the deflexion was proportional to its potential. The leaf was connected to a potentiometer for calibration purposes, and its sensitivity was checked at frequent intervals between readings. The charge collected on the leaf could thus be converted directly into volts, after allowance had been made for any leakage of charge or drift of the leaf due to other causes.

Deflexions were made of convenient magnitude by adjusting the widths of the slits limiting the beam, and also, in the case of the lines, by the addition of a small condenser to the electroscope system. A knowledge of the slit-widths and of the condenser factor enabled these various readings to be compared.

In the measurement of the intensity of the general radiation, readings were taken at successive $\frac{1}{2}^\circ$, or (where this was sufficient) 1° intervals of the ionization chamber, except in the neighbourhood of the lines. It was possible, however, to obtain a point on the curve lying between the α - and β -lines. In the measurement of the line intensities the chamber slit was opened sufficiently wide to include all the components of the line, and readings were taken as the chamber was moved through the line by successive $7\frac{1}{2}$ -minute steps. In this way the line was shown as a flat-topped curve on a flat background of general radiation, and the line intensity was obtained by subtracting this background intensity from the maximum intensity. In all measurements, both of the general and of the homogeneous radiation, the mean of the intensities on the left- and right-hand sides of the spectrometer was taken as the true intensity.

At the higher voltages a discontinuity occurred in the general radiation curves at the frequency of the K-absorption limit of iodine. This discontinuity was always near the short wave-length end of the spectrum, and for wave-lengths shorter than this critical wave-length no quantitative significance was attached to the readings obtained, but they were nevertheless necessary for the determination of the limit of the spectrum.

The following data were obtained :—

(a) *With coil and interrupter.*

1. Curves at voltages of 48·4 kv., 38·9 kv., and 26·0 kv., giving the intensity distribution of the general radiation for wave-lengths as far as 1·34 Å.U.
2. The intensities of the α -line at these voltages.
3. The ratio of the α - and β -lines.
4. The relative intensities of the α -line in the 1st, 2nd, and 3rd orders respectively.

(b) *With transformer.*

1. Curves of general radiation at voltages of 34·9 kv. and 19·75 kv.
2. The intensity of the α -line at 34·9 kv. (In the other case no K-lines were present.)

In the comparison of the α - and β -lines, the tube was run at about 38 kv., and by the insertion of the condenser (which reduced the sensitivity of the apparatus to about one-fifth), when measuring the α -line, the deflexions were made of the same order of magnitude, with a consequent gain in accuracy. From a large number of readings taken without this improvement, however, the ratio of the lines was found to be independent of the excitation voltage, and of the method of excitation. Consequently, only the α -line was measured in the final experiments, the β -line intensity being found from the known ratio.

Calculations and Corrections.

(1) Correction for presence of 2nd- and 3rd-order reflexion in the general radiation.

The relative intensities of the α -line in the first three orders respectively were as follows :—

1st order	100
2nd order.....	7·6
3rd order	4·05

The percentages of the 1st-order intensity which appear in the 2nd and 3rd orders respectively are therefore 7·6/2 and 4·05/3, since the dispersion of the general radiation is proportional to the order in which it appears. To apply the order correction, these fractions of the 1st-order intensity, as obtained from the curve, were subtracted from the

intensities at wave-lengths corresponding to the 1st- and 2nd-order reflexions respectively.

(2) Correction for partial absorption in the methyl iodide in the ionization chamber.

The fraction of the shorter wave-lengths absorbed by the vapour was only about one-tenth, whereas the longer wave-lengths were completely absorbed; hence it was necessary to determine with considerable accuracy the quantity of gas actually present in the chamber at any time. The chamber was filled by evaporation of the liquid methyl iodide into a vacuum, to a pressure of about 240 mm. of mercury; but a measurement of the absorption of the α -line in passing through the chamber showed that the vapour-pressure was not a true indication of the quantity of methyl iodide present. This was due, no doubt, to the presence of volatile impurities in the liquid employed, and to the absorption of the gas by the walls of the chamber subsequent to measuring its pressure. It was not found possible, however, to carry out this absorption measurement with the accuracy required by the experiment, so the following method of determining the iodine content of the chamber was devised.

The chamber, connected to a manometer, was filled to a convenient pressure with the vapour, and set to receive a narrow beam of the general radiation of mean wave-length $\cdot 894 \text{ \AA.U.}$ The integrated reflexion was found. The pressure was then successively reduced, and the operation repeated at each pressure, so that a curve could be plotted to show the relation between pressure and ionization. The chamber was then refilled and sealed, and the ionization again measured. It was then ready for use.

Let I_0 , I be the intensities of the beam of radiation at the beginning and end of its path through the vapour respectively, and let p be the corresponding pressure of vapour. Then $I = I_0 e^{-\mu p}$, where μ is a constant. Assuming that the ionization is proportional to the energy absorbed, and denoting by q the ionization produced in the vapour at pressure p , and by q_0 the ionization which would be produced by complete absorption, we have $q = k(I_0 - I)$, hence combining these two equations,

$$\log (q_0 - q) = -\mu p + \text{const.}$$

The curve obtained experimentally, relating q and p , was of logarithmic form, and it was always found possible to assign a value to q_0 such that the curve relating $\log (q_0 - q)$ and p was a straight line. This value was therefore the ionization

which would have been produced if the rays had been completely absorbed, and the fractional absorption of the selected wave-length after refilling of the chamber was q_1/q_0 , where q_1 was the corresponding ionization. Knowing the absorption for that particular wave-length, the absorption of the other wave-lengths was calculated from values of the absorption coefficients for iodine obtained from tables given by Compton*.

The measurements described above were made before and after sets of readings covering a period of four or five days, with the result that the absorption on any day was accurately known. It is estimated that the errors arising from the application of this large and rather difficult correction are certainly within 3 per cent.

(3) Correction for absorption by the aluminium windows of the tube and ionization chamber.

The thickness of aluminium in each of these windows was 0.056 mm., and the requisite corrections for absorption of the various wave-lengths were calculated from tables of absorption coefficients†. This correction amounted to over 100 per cent. for the longer wave-lengths.

(4) Correction for absorption in air.

The total length of air-path traversed by the rays from the window of the tube to the window of the chamber was 28.5 cm. The amounts of absorption were again found from tables of absorption coefficients of the constituent elements‡.

(5) Effects of slit-widths and dispersion.

The quantity measured in the experiments on the general radiation is $I_\lambda \Delta\lambda$, where I_λ is the intensity at the wave-length λ and $\Delta\lambda$ is the range of wave-lengths entering the ionization chamber. The beam, on emerging from the tube, passed through slits distant 12 cm. and 3 cm. respectively from the centre of the crystal, and, after reflexion, through a third slit also at a distance of 12 cm. from the centre of the crystal. In the following discussion these three slits will be denoted by A, B, and C respectively, and the corresponding slit-widths by a , b , and c . Since A and C are

* A. H. Compton, 'X-rays and Electrons.'

† A. H. Compton, *loc. cit.*

‡ A. H. Compton, *loc. cit.*

equidistant from the centre of the crystal, then, by a well-known geometrical property of this arrangement*, all the rays of a given wave-length emerging from a single point of the slit A will be focussed to a point in the plane of C. Let D be the distance of either A or C from the centre of the crystal, then the rays from a point in A which, after reflexion, enter C are all included within an angle equal to c/D . Similarly, the angular range of rays of a given wave-length emerging from the slit A, which, after reflexion, pass through a single point of the slit C, is a/D . Adding these two effects, it follows that all rays of wave-length λ emerging from A, and reflected through C, are deflected through angles lying between 2θ and $2(\theta + \Delta\theta)$, where θ is the angle of reflexion for that wave-length, and $2\Delta\theta = (a+c)/D$. If d is the grating space of calcite, and $\Delta\lambda$ the wave-length range included by the slits, then $\lambda = 2d \cdot \sin \theta$, and

$$\Delta\lambda = 2d \cdot \cos \theta \cdot \Delta\theta = 2d \cdot \cos \theta \cdot \frac{a+c}{2D}.$$

The quantity required for plotting is the intensity at wave-length λ , *i. e.* I_λ , and may be found by dividing the observed quantity $I_\lambda \Delta\lambda$ by the wave-length range $\Delta\lambda$. Thus

$$I = I_\lambda \Delta\lambda \cdot \frac{D \cdot \sec \theta}{(a+c)d}.$$

The total energy emitted is then represented by the area of the curve, *i. e.* $\int I_\lambda d\lambda$. The effect of dispersion is thus completely accounted for. There is, however, another quite distinct question which has to be considered in connexion with the widths of the slits, namely the relative amounts of energy incident upon the crystal for slits of different widths. For this purpose it was assumed that the energy of the beam was proportional to the product ab .

(6) It was assumed that the crystal reflected all wave-lengths equally. The available data do not fully justify this assumption, but the results of Davis and Terrill†, and Wagner and Kulenkampff‡, show that it is, at any rate, approximately true.

* Bragg, 'X-Rays and Crystal Structure,' p. 31.

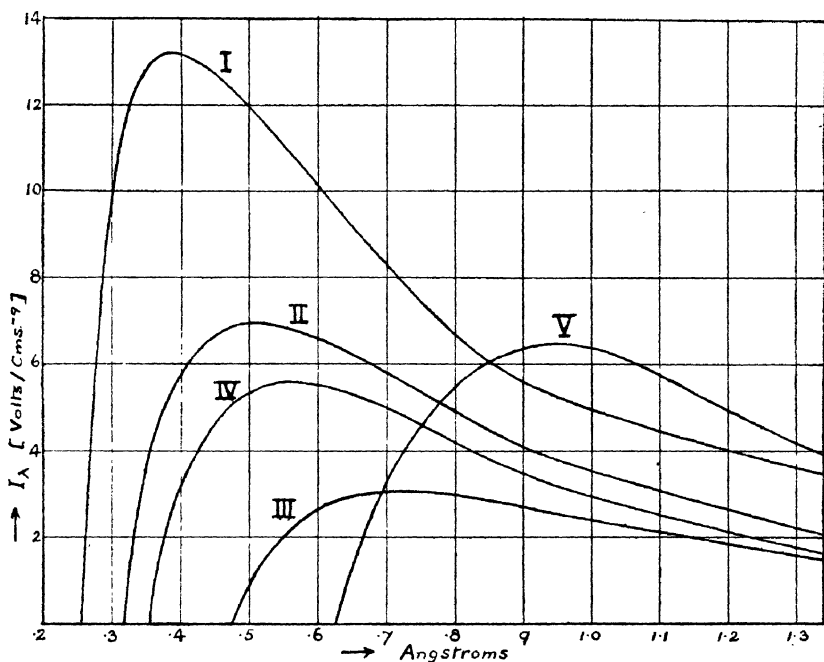
† Davis & Terrill, *Phil. Mag.* xlv. p. 463 (1923).

‡ Wagner & Kulenkampff, *Ann. der Phys.* lxxviii. p. 369 (1922).

Results.(a) *With coil and interrupter.*

1. Curves I., II., and III. (fig. 1) show the relative proportions of general radiation at voltages of 48.4 kv., 38.9 kv., and 26.0 kv. respectively. The areas of these curves, *i. e.* the total energies in the spectrum, as far as a wave-

Fig. 1.



length of 1.34 \AA.U. , together with the measured α -line intensities, are shown in the following table:—

	Kv.	Area (volts).	α -line (volts).
I.	48.4	82.88	38.0
II.	38.9	47.44	16.5
III.	26.0	20.76	3.24

2. The value obtained for the ratio of the intensity of the α -line to that of the β -line (including the γ -line) was $\alpha/\beta = 4.0$.

3. The ratios, obtained from these figures, of the energies of the α - and β -lines to the energy in the general radiation, and the fractions of the total emitted radiation which appear

as homogeneous K-radiation, are given below as percentages :—

	Kv.	α /General.	β /General.	$(\alpha + \beta)$ /Total.
		%.	!%.	%.
I.	48.4	45.8	11.5	36.4
II.	38.9	34.8	8.7	30.3
III.	26.0	15.6	3.9	16.3

Discussion of Accuracy and Sources of Error.

(1) Errors due to gradual changes in the running of the tube.

There was a noticeable falling-off in intensity after several days' running of the tube, presumably due to changes in the cathode beam and in the position and size of the focal spot. In order to avoid, as far as possible, errors arising from these causes, the above readings were all taken within a period of three days, and all readings for a particular voltage were taken at a single running of the tube. Readings taken during the course of a day were consistent to 3 per cent. The effects become more important in connexion with the relative intensities at different voltages, and it is thought that these relative intensities can only be considered significant to an accuracy of about 10 per cent. These difficulties are inherent in the gas-tube.

(2) Errors due to inaccuracy in the estimation of the iodine content of the chamber.

The correction for partial absorption in the chamber was very carefully investigated, and has already been fully discussed. Errors arising from the application of this correction are probably nowhere greater than 2 per cent.

(3) Errors in the correction for absorption in the aluminium windows and air-path.

There is an element of doubt in the values of the absorption coefficients for aluminium, and the inaccuracy introduced on this account may be as great as 5 per cent. in the case of the longest wave-lengths employed (1.34 Å.U.). For this reason the curves are not considered reliable beyond about 1.0 Å.U., but below this wave-length the error due to the above corrections is estimated at less than 2 per cent., and for the shorter wave-lengths (*i. e.* below .5 Å.U.) it is quite negligible.

(4) Error in the measurement of voltage.

The difficulty of this measurement is increased by the proximity of the K-absorption limit of iodine to the limit of the spectrum in many cases. There is also the possibility of a slight variation of voltage during the course of readings, but the latter is included under heading (1). The voltage could be measured to an accuracy of 2 per cent.

(5) In general, taking account of the above considerations, the maximum error in the determination of the ratios of the characteristic radiations to the general radiation, and in the curves for a particular voltage, is estimated at 6 per cent. The ratio of the lines was more accurately determinable, the probable error here being 3 per cent. It was not the object of the work to determine the variation of absolute intensity with voltage, and the relative intensities of curves and lines of different voltages can only be considered as approximate, the error being of the order of 10 per cent.

The intensity of the general radiation is seen to vary approximately as the square of the excitation voltage, according to the following table:—

	V.	A.	A/V ² .
I.	48.4 kv.	82.88	351
II.	38.9 „	47.44	312
III.	26.0 „	20.76	306

The value of A/V^2 would be expected to diminish with decrease in voltage, since at the higher voltages a greater fraction of the total energy emitted occurs at wave-lengths below 1.34 \AA.U.

Many observers have shown that the intensity of the lines is, in general, proportional to $(V - V_0)^n$, where V is the excitation voltage and V_0 is the critical excitation potential. The value of n is usually between 1.5 and 2.0. The results obtained for the α -line at these three voltages agree, to the accuracy obtainable, with this law if a value of about 1.6 is assigned to n .

The variation of the ratio of the energy in the α -line to that in the general radiation, with applied voltage, is shown graphically in fig. 2.

(b) *With transformer.*

(1) Curves IV. and V. give the intensity distribution of the general radiation at 34.9 and 19.75 kv. respectively (fig. 1). The absolute intensities are not significant, the

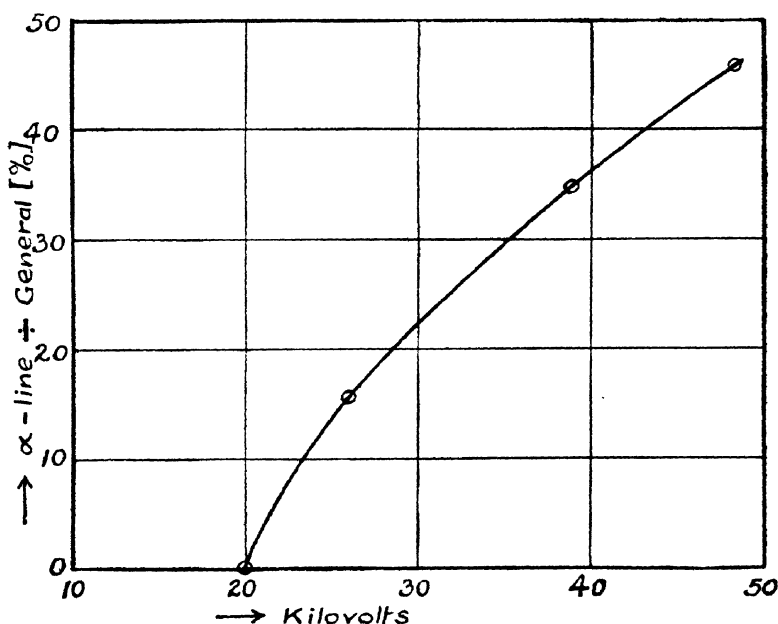
1018 *X-ray Intensity Distribution from Molybdenum.*

curves merely being drawn of convenient magnitude for illustration and comparison. Curve V. is interesting, since at this voltage there are no K-lines present. The following are the figures obtained for the energy in the general radiation and in the α -line, respectively, for curve IV.

	Kv.	Area (volts).	α -line (volts).
IV.	34.9	36.0	12.55

(2) The α -line and β -line were approximately in the same ratio as before.

Fig. 2.



The corresponding figures for the relative proportions of characteristic and general radiation are as follows :—

	Kv.	α /General.	β /General.	$(\alpha + \beta)$ /Total.
		%.	%.	%.
IV.	34.9	34.8	8.7	30.4

Comparison of Results for both Methods of Excitation.

The corresponding value obtained for the ratio $(\alpha + \beta)$ /Total in the case of the coil and interrupter is (by interpolation) 27.0 per cent., and differs from the above figure for the transformer by about 12 per cent. In view of the experimental

error of 6 per cent., it can only be said that these ratios are only slightly different, if at all.

The curves are all of the same form, and the method of excitation appears to have no marked effect on the intensity distribution. In particular, the wave-length of maximum energy is found to bear a constant ratio to the minimum wave-length, as shown below :—

	Kv.	λ_{\max} .	λ_0 .	λ_{\max}/λ_0 .
I.	48.4	.385	.255	1.51
II.	38.9	.505	.317	1.59
III.	26.0	.73	.474	1.59
IV.	34.9	.56	.354	1.58
V.	19.75	.955	.626	1.53

The mean value of the ratio is 1.55.

In conclusion, I should like to express my great indebtedness to Professor J. A. Crowther for his valuable advice and for the energetic interest he has shown in the progress of this work.

Department of Physics,
The University,
Reading.

CI. *The Amount of Uniformly-diffused Light that will go in Series through Two Apertures Forming Opposite Faces of a Cube.* By LEWIS F. RICHARDSON, D.Sc., F.R.S. *

FOR example, the radiation might come out of a blackened enclosure at a uniform temperature through one aperture and thence across the cube and through the other aperture into a calorimeter; the problem being to find Stefan's constant.

We have to evaluate the integral †

$$\iiint \frac{\cos \zeta_1 \cdot dA_1 \cdot \cos \zeta_2 \cdot dA_2}{r^2}, \quad \dots \quad (1)$$

in which dA_1 , dA_2 are elements of area of the apertures, r is the distance between the centres of dA_1 , dA_2 , and ζ_1 , ζ_2

* Communicated by the Author.

† Planck 'Vorlesungen ueber die Theorie der Wärmestralung' (Barth, 1913), p. 19.

are the angles which the normals to dA_1, dA_2 make with the line joining the centre of dA_1 to that of dA_2 .

Let the edge of the cube be of length l . Take two systems of rectangular coordinates x_1, y_1 and x_2, y_2 , one in the plane of each aperture, the origins being at the centres of the apertures and the two x -axes parallel to one another and to edges of the cube.

Then

$$\left. \begin{aligned} dA_1 &= dx_1 dy_1; \quad dA_2 = dx_2 dy_2, \\ r^2 &= l^2 + (x_1 - x_2)^2 + (y_1 - y_2)^2, \\ \cos \zeta_1 &= \cos \zeta_2 = l/r, \end{aligned} \right\} \quad . \quad . \quad . \quad (2)$$

so that (1) becomes

$$l^2 \iiint \frac{dx_1 dy_1 dx_2 dy_2}{r^4} = ql^2, \text{ say,} \quad . \quad . \quad . \quad (3)$$

each integration ranging from $-l/2$ to $+l/2$.

In order to make the calculation, consider instead of (3) a problem in finite differences. Regard each aperture as a window cut into n^2 panes, each pane being square. Take each pane in the first window in turn with each pane in the second, forming n^4 pairs of panes. Then $dx_1 dy_1 dx_2 dy_2$ is analogous to (area of first pane) (area of second pane), and is the same for all pairs being l^4/n^4 . So instead of (3) we calculate

$$\frac{l^6}{n^4} \sum^{n^4 \text{ pairs}} \frac{1}{(\text{separation of mid-points of panes})^4} = Q_n l^2, \text{ say.} \quad (4)$$

Ql^2 varies as l^2 because the distance of mid-points is proportional to l . Let us therefore make the calculation for $l = 1$.

First approximation. One pane in each window :

$$Q_1 = 1.$$

Second approximation, $n = 2$. Four panes in each window :

$$\begin{aligned} Q_2 &= \frac{1}{16} \left\{ \frac{4}{1} + \frac{8}{(1+\frac{1}{4})^2} + \frac{4}{(1+\frac{1}{4}+\frac{1}{4})^2} \right\} \\ &= 0.681, 111, 1. \end{aligned}$$

Third approximation, $n = 3$. Nine panes in each window:

$$Q_3 = \frac{1}{81} \left\{ \frac{9}{1} + \frac{12 \times 2}{(1 + 1/9)^2} + \frac{6 \times 2}{(1 + 4/9)^2} + \frac{8 \times 2}{(1 + 1/9 + 1/9)^2} \right. \\ \left. + \frac{4}{(1 + 4/9 + 4/9)^2} + \frac{16}{(1 + 4/9 + 1/9)^2} \right\} \\ = 0.649, 821, 9.$$

Fourth approximation, $n = 4$. Sixteen panes to each window. To keep account of 256 pairs would be perplexing were it not that we can arrange them in a simple pattern.

Fig. 1.

						1 34
					4 24	2 29
				9 18	6 21	3 26
			16 16	12 17	8 20	4 25

The blank squares can be filled in because the distribution of numbers is symmetrical both about the diagonals of the large square and also about the lines joining the mid-points of its sides.

In fig. 1 let the central square represent *any* pane in one window. All possible relative positions of the panes in the other window are represented by the squares in fig. 1. In each square the upper number is the number of pairs of panes so situated, the lower number is the square of their distance apart multiplied by n^2 . To form Q_4 we have to divide each upper number by the *square* of the lower number, and to sum the quotients. Presumably there is a

corresponding transformation from a fourfold to a double integral. However that may be, the result is

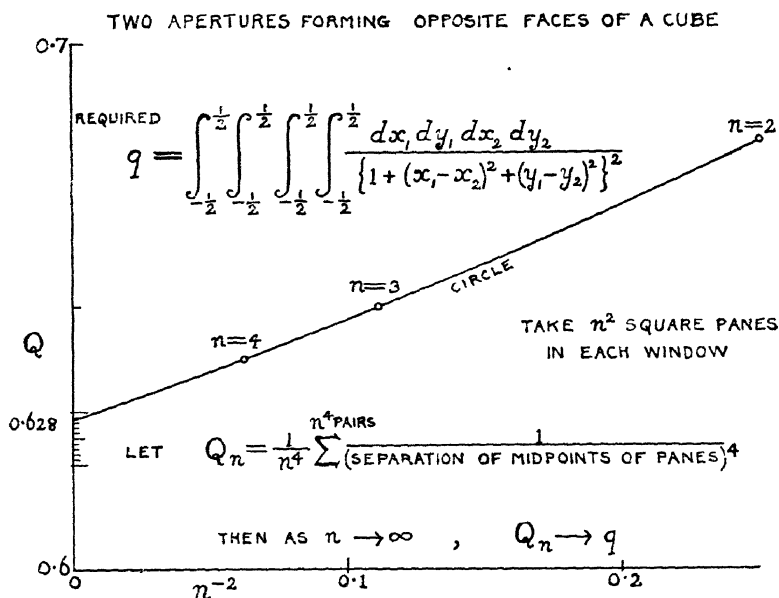
$$Q_4 = 0.639, 910, 5.$$

To continue in this way until the accuracy of experiment were surpassed would be insufferably tedious. Instead, to make the "deferred approach to the limit*", it is assumed that, as there are neither discontinuities nor frills†, in (3)

$$Q_n = q + Bn^{-2} + Cn^{-4} + Dn^{-6}, \dots \quad (5)$$

($n = 1, 2, 3, 4$).

Fig. 2.



On eliminating B, C, D, from this set of four equations it is found that

$$2520 q = 8192 Q_4 - 6561 Q_3 + 896 Q_2 - 7 Q_1, \dots \quad (6)$$

the coefficients in which are useful in other problems.

Whence $q = 0.627, 75.$

This may be called an h^6 -extrapolation. As a rough check Q_2, Q_3, Q_4 are plotted against n^{-2} in fig. 2†, and a circle drawn through the points is found to cut the axis, $n^{-2} = 0$, at

* Phil. Trans. Roy. Soc. A. vol. ccxxvi. pp. 300, 311.

† Loc. cit. p. 315.

‡ Fig. 2 was shown at the British Association, Glasgow, 1928.

$Q=0.628$. To judge how many digits are reliable, we can neglect various parts of the four equations (5), retaining just enough of B, C, D to give a unique solution, B being retained first, then C, then D. Thus we form two sequences of extrapolations both leading to that already obtained :—

Q_4	0.639, 91		Q_1	1.000, 00
from Q_4, Q_3	0.627, 17		from Q_1, Q_2	0.574, 81
from Q_4, Q_3, Q_2 ...	0.627, 95		from Q_1, Q_2, Q_3 ...	0.631, 04
from Q_1, Q_2, Q_3, Q_4 ...			0.627, 75.	

From these numbers it seems safe to conclude that 0.6278 is right to within ± 0.001 . That accuracy is, however, barely enough. An estimate of the error could be obtained by the use of general formulæ expressing the difference between the integral and the sum as a series involving derivatives of the integrand. But it seems more profitable to compute Q_6 by the aid of a diagram like fig. 1. The law of these diagrams is found to be expressed by

$$Q_n = \sum_{s=1-n}^{s=n-1} \sum_{t=1-n}^{t=n-1} \frac{(n-|s|)(n-|t|)}{(n^2 + s^2 + t^2)^2}.$$

It is thus found that $Q_6 = 0.633, 086, 28$.

Extrapolating, as above, from Q_4 and Q_6 gives 0.627, 63.

Extrapolating from Q_2, Q_4, Q_6 gives 0.627, 81.

Conclusion.—The amount of light, uniformly diffused with brightness I, that will go in series through two apertures forming opposite faces of a cube of edge l is

$$(0.6278 \pm 0.0001) l^2 I.$$

The physical meaning of the above result may be understood by comparison with the statement of Stefan's constant. Instead of two squares we have one square of side l , drawn on a flat radiating solid of uniform brightness I. The second square is replaced by a hemisphere-at-infinity, drawn with its centre in the first square and its basal plane containing the radiating surface. The amount of light that will go through the square and hemisphere is known to be $\pi l^2 I$, a result deducible from (1).

The method will obviously extend to parallel rectangular apertures.

The calculations were performed on a machine lent by the Government Grant Committee of the Royal Society.

CII. *Luminous Carborundum Detector and Detection Effect and Oscillations with Crystals.* By O. V. LOSSEV*.

[Plates XVII.-XX.]

ABSTRACT.

IN this paper are described further observations on the phenomenon of the luminescence produced at the contact of a carborundum detector in connexion with a view on luminescence as a consequence of the process in the contact which is very similar to cold electronic discharge.

Early observations were given by the author in the Russian language in 'Wireless Telegraphy and Telephony' (*Telegrafia i Telefonija bez provodov*, "T. i T. b. p." no. 18, p. 61, 1923, and no. 26, p. 403, 1924 †).

Two types of luminescence are suggested—"I." and "II."

The luminescence II. depends upon the fluorescence of the crystal under the effect of electronic process at the contact.

The luminescence II. is more comparable than I. with cathodo-luminescence of carborundum in a discharge tube. The colour of luminescence II. changes considerably on altering the potential difference between the detector terminals, as may likewise be changed the colour of cathodo-luminescence. The spectrum of detector luminescence appears to be nearly identical with the spectrum of cathodo-luminescence.

The luminescence of a carborundum detector is closely connected with its rectifying action, which cannot be explained by a thermoelectric effect.

Increased conductivity of the contact at luminescence II., and the possibility of obtaining on the same carborundum crystal points with different direction of unilateral conductivity, are explained by the imposition of increased conductivity effect of the fluorescent layer upon the effect of electronic discharge properties at the contact.

A luminous detector may be used as a light relay, owing to the very small inertia of both the commencement and cessation of luminescence.

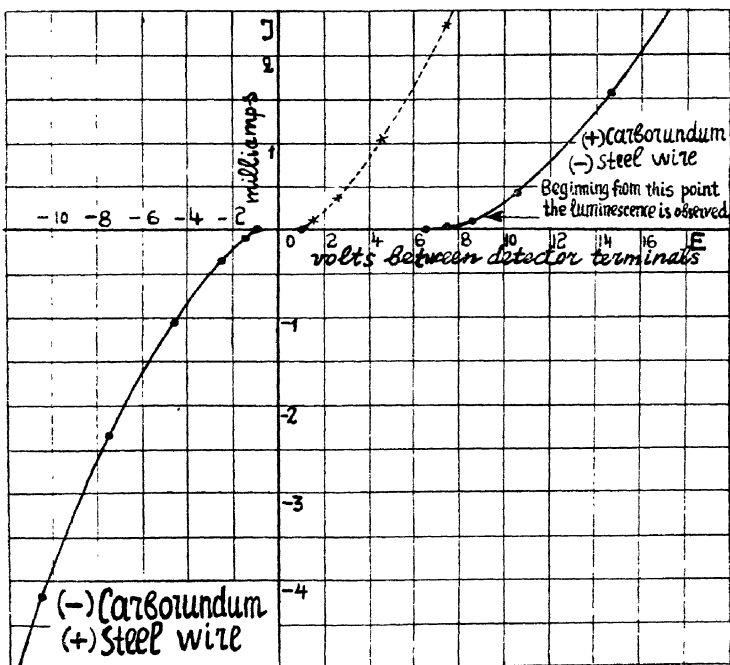
* Communicated by the Author.

† Also Lossev, 'Wireless World and Radio Review,' no. 271, p. 93 (1924); and *Zeit. f. Fernmeldetechnik*, no. 7, p. 97 (1926).

There are also several observations on the behaviour of oscillating crystals (zincite).

EXCEPT for some cases, at the contact of carborundum (SiC)* and metallic wire detector, more intense luminescence takes place when the metallic wire has a negative potential. In the case of current in the opposite direction (at the given luminous point), sometimes the luminescence is not observed at all (see figs. 2 and 3).

Fig. 2.



By the dotted line (in the first quadrant) is shown the branch of third quadrant. Luminescence I.

§1. Two Types of Carborundum-Contact Luminescence.

The Change of Luminescence II. Colour.

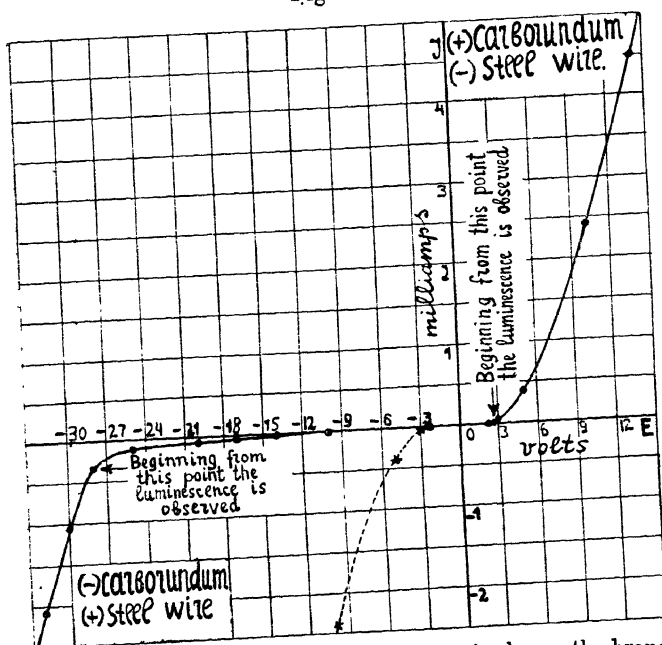
From many observations it was found that two types of luminescence at carborundum contact may be distinguished.

* Silicon carbide.

"*Luminescence I.*"—Luminescence I. has a greenish-bluish colour. It is a bright little point (sometimes several little points) which is surrounded by diffuse luminescence with small brightness. The diffuse luminescence is due to reflected light from the nearest facets of the crystal (see Pl. XVII. fig. 1). The colour of luminescence I. does not perceptibly change with change of the potential difference between detector terminals.

On passing a current in the direction which produces the more intense luminescence I., the detector shows a lower

Fig. 3.



By the dotted line (in the third quadrant) is shown the branch of first quadrant. Luminescence II.

conductivity (see the static characteristic curve on fig. 2). The rectification of high-frequency current occurs in a corresponding direction (unless a continuous displacing of the potential difference is impressed: "polarizing voltage").

In early observations (*T. i T. b. p.*) only the luminescence I. was described*.

"*Luminescence II.*"—When a current is passing in a direction such that the luminescence II. is less intense, the

* Also 'Wireless World and Radio Review,' no. 271, p. 93 (1924); and *Zeit. für Fernmeldetechnik*, no. 7, p. 97 (1926).

contact shows less conductivity (fig. 3); *i. e.*, unilateral conductivity is in the opposite direction to that of luminescence I. (*cf.* figs. 2 and 3).

With luminescence II. strong fluorescence takes place upon a large surface of the crystal. Sometimes that fluorescent surface spreads beyond the limit of touch of the point of the contact wire (see Pl. XVII. fig. 4).

The colour of luminescence II. changes with change of the potential difference between detector terminals from orange to violet, as, for example, is shown in the following table:—

Orange	6 volts (between detector terminals).
Yellow	10 " " "
Light yellow	20 " " "
Greenish	26 " " "
Violet	28 " " "

The change of the colour is somewhat different for different points, even on the same crystal. These results were obtained with a current in the direction which gives the more intense luminescence, *i. e.* (+) carborundum and (–) contact wire.

It must be mentioned that a direct cause for the change of colour is probably to be found in the temperature of the fluorescent surface of the crystal* depending upon the Joule effect at the contact. This suggestion is strengthened by the fact that external heating produced by a special heater changed considerably the colour of luminescence II. at the luminous detector.

All carborundum crystals used for observations were of four kinds. With the first and second kinds can be obtained only luminescence I. With the third and fourth kinds can be obtained (on the same crystal) both luminescences I. and II. The crystals were mounted by stannous in metallic cups. As a contact wire, a steel wire, tantalum, nickelin, and silver were used. The properties of these metals as a contact wire were nearly identical.

Under the microscope it may be seen that both luminescences I. and II. appeared if the contact wire was touched to the sharp edge of the crystal, or when a sharp point of contact wire was touched to the crystal surface.

Sometimes might be observed the cases of imposition of both luminescences I. and II. one upon the other.

* *Cf.* the cases of change of luminescence colour depending on the temperature which are known in photo-luminescence (H. Becquerel, *C. R.* cxlvi. p. 440, 1908; *cli.* p. 981, 1910).

Some typical features of both luminescences will be described later on.

§ 2. *Supposed Cold Electronic Discharge at the Contact of Carborundum Detector.*

(1) The character and intensity of the luminescence depends to a great degree on the direction of the current (even if the same current (abs. value) is taken in both directions with characteristic of type fig. 3, or same tension with characteristic of type fig. 2; see § 1).

(2) Unilateral conductivity of carborundum contact is closely connected with its luminescence (see § 1 & § 3 and *cf.* also § 4).

(3) As may be clearly seen under the microscope, the luminous surface is not incandescent. For example, a drop of benzene put on the luminous surface is not vaporized for a long time. Of course, when a strong current (of order more than 20 milliamps) is flowing through the detector, the part of the crystal near to the contact, in addition to showing the cold luminescence, will be slowly brought to a red heat (see § 5; *cf.* also item 2, § 4).

(4) The substance of carborundum does not produce thermo-luminescence. Hence the cause of luminescence is not due to a Joule effect at the contact (see § 1 and § 5—only the colour of fluorescence at luminescence II. depends on the temperature at the contact).

(5) The inertia of both the commencement and cessation of luminescence, even with possible strong currents through the contact (till the destruction of the contact), is very small (see § 5 and *cf.* also item 1, § 4).

It may be supposed, therefore, that the luminescence at a carborundum contact is a consequence of the process which is very similar to cold electronic discharge (*cf.* § 4).

The suggestion that unilateral conductivity of the contact with crystals can be explained by electronic process (electronic emission at the contact) has already been proposed by F. Braun *, G. Hoffmann †, and Pierce ‡.

Fig. 5 (Pl. XVII.) shows luminescence I., where the stratification of light is near the contact electrodes §. At

* F. Braun, *Pogg. Ann.* cliii. p. 556 (1874); *Wied. Ann.* i. p. 95 (1877), iv. p. 476 (1878), xix. p. 340 (1883). See also H. Lüke, *Phys. Zeit.* xxviii. p. 213 (1927).

† G. Hoffmann, *Phys. Zeit.* xxii. p. 422 (1921).

‡ *Cit.* A. C. James, *Phil. Mag.* xlix. p. 681 (1925).

§ See *T. i T. b. p.* no. 26; 'Wireless World and Radio Review,' no. 271.

the top is the point of contact wire (—) and at the bottom the crystal surface (+). Magnified 505 times; current through the contact = 18 milliamps. If the value of cross-section of the luminescence is counted as a diameter, from fig. 5 it is a simple matter to calculate "the area of luminescence," which is 700 sq. microns. The size of that order in comparison with the size of the fluorescent surface at luminescence II. is very small, and it is typical for luminescence I.

The question of whether the electronic process occurs in the layer of adsorbing gas or in the crystal lattice of the surface-layer of the crystal requires further investigation *. At any rate, the presence of apparent fluorescence of the crystal at luminescence II. (see § 1) shows that some process takes place also in the surface-layer of the crystal †.

Comparison of Detector Luminescence with Cathodo-Luminescence.

Luminescence II. is more comparable than I. with fluorescence of carborundum in a discharge-tube (see Pl. XVIII. fig. 6) under the cathode rays effect. It was found that the colour of carborundum cathodo-luminescence in an evacuated tube may be changed in a similar manner to the luminescence II. at the detector. With softening of the tube (*i. e.* with increase of pressure in it) the colour of cathodo-luminescence changes slowly from orange to violet.

First and third kinds of carborundum (SiC), two kinds of zincite (ZnO), and two kinds of iron glance (Fe_2O_3) were mounted in the tube as shown in fig. 6 (Pl. XVIII.). Strong cathodo-luminescence takes place only with carborundum (both kinds). With both the zincite and iron glance the cathodo-luminescence is very feeble.

The Spectrum of Detector Luminescence and Cathodo-Luminescence.

The spectrum obtained from carborundum contact luminescence (I. and II.) is continuous with a feebly-marked red portion. With increase of the potential difference between detector terminals, with luminescence II., the relative

* Cf. A. F. Joffe, Reports of V. Congress Russ. Phys. p. 11, 1926. It has been stated by A. F. Joffe that in the substance of *dielectric* crystals a process may occur similar to the production of ions at discharge in the gas. Cf. also A. C. James, Phil. Mag. xlix. p. 681 (1925).

† For the present consideration, it is of no importance whether the substance SiC fluoresce or some other admixture in the crystal.

brightness of the spectrum in the region of shorter wavelength is increased (cf. § 1).

The spectrum of carborundum cathodo-luminescence in a discharge-tube appears to be nearly identical with the spectrum of contact luminescence II.

In order to obtain some indications with respect to the essentials of the process at the contact, the luminescence of a carborundum detector was also observed in a magnetic field.

Sometimes the luminescence changed considerably as the luminous detector was transferred from air to another medium; for example, to benzene. The description of these observations is outside the scope of this paper.

§ 3. *Luminous Detector and Unilateral Conductivity of the Contact with Crystals. The Effect of Increased Conductivity of the Fluorescent Layer.*

The points of the crystal which were found at high frequency (without impressed "polarizing voltage") to give the rectified action were always non-equal as regards luminosity with direct current at a different direction of *d. c.* (and in meaning of item 1, § 2).

In order to explain the inverse directions of unilateral conductivity shown by characteristics of figs. 2 and 3* (§ 1), it may be easily supposed that at luminescence II. occurs the increase of conductivity of the fluorescent layer (a very large surface of which is typical for luminescence II.; see fig. 4) under the effect of electronic process at the contact,—analogically to the known fact of increasing conductivity of cathodo-luminescent bodies in discharge-tubes†. (This suggestion was also made by Prof. B. A. Ostroumoff.)

The influence of increased conductivity effect of a layer near to the contact may be partly applied to the actions of some other (and non-luminous) contact detectors and impressed on the effect of properties of hypothetic electronic discharge itself.

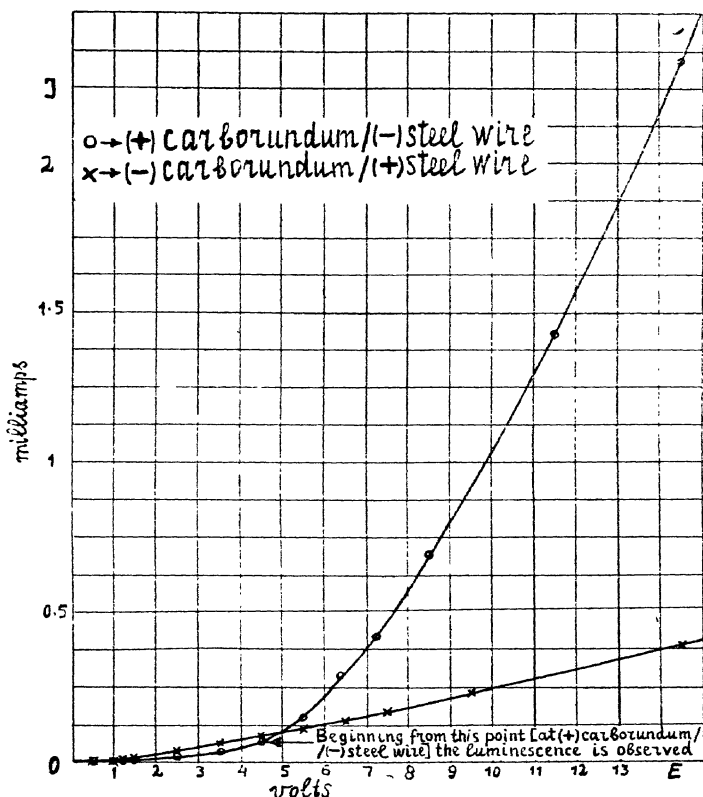
In addition to the characteristics on figs. 2 and 3 (§ 1), on fig. 7 is shown the curve both positive and negative branches of which are crossed (when they are in the same quadrant). The presence of that cross can be explained by the imposition of these two effects. By examination of detector contact under the microscope, when the curve of fig. 7 was plotted, the case of imposition of both luminescences (I. and II.) can

* Cf. A. Schleede and H. Buggish, *Phys. Zeit.* xxviii. p. 174 (1927).

† E. Rupp, *Ann. d. Phys.* lxxiii. p. 127 (1924).

be observed. (The point of the crystal from which the curve of fig. 7 was taken was also tested for rectifying of high frequency (without impressed "polarizing voltage"). It was found that at low tension of H.F. the rectification occurred in one direction, but with increased tension of H.F. the direction was reversed).

Fig. 7.



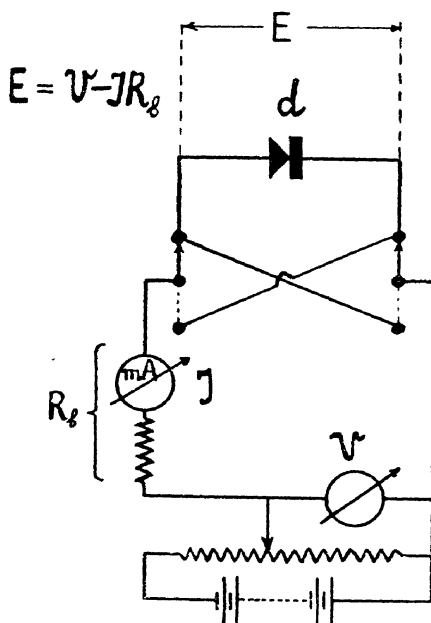
Both positive and negative branches of characteristic are shown in the same quadrant.

Unilateral conductivity of the carborundum detector cannot be explained by thermoelectric effect. In connexion with this an investigation was made*, the description of which is outside the scope of this paper. It was found that

neither the value of the thermo-E.M.F. nor its direction agreed with the continuous component value of the E.M.F. of the rectified current, which at corresponding conditions can be easily obtained from the same detection point of the carborundum crystal*.

All characteristic curves given in this paper were plotted by means of the scheme shown in fig. 8 ($E = V - IR_b$).

Fig. 8.



§ 4. Luminous Detector and Oscillations with Crystals.

The oscillation with crystal detector (galena) was discovered by W. Eccles in 1910†. He formulated an interesting thermal theory of this phenomenon based on the

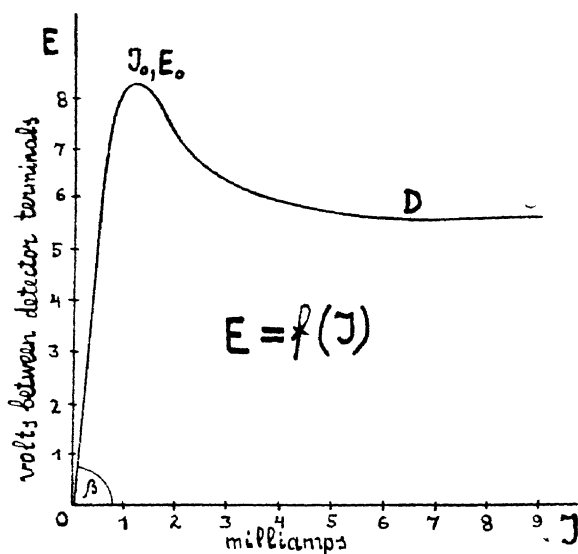
* Cf. F. Trey, *Phys. Zeit.* xxvi. p. 849 (1925). H. Lüke, *Phys. Zeit.* xxviii. p. 213 (1927).

† In May 1910 a communication was made by W. H. Eccles to the London Physical Society ('The Electrician,' p. 385, 1910); see G. W. Pickard, 'Radio News,' vi. p. 1166 (1925); H. J. Round and N. M. Rust, 'Wireless World and Radio Review,' xvii. p. 217 (1925); H. S. Pocock, 'Wireless World and Radio Review,' xiv. p. 299 (1924). See also G. Million, Jr., 'Radio News,' v. p. 714 (1923); R. Pennec, 'Radio Revue,' no. 28, p. 139 (1924).

fact that many detector minerals, having metallic conductivity, have a negative temperature resistance coefficient*.

A carborundum detector seldom gives the characteristics with negative slope ($\frac{dE}{dI} < 0$), even on little space (cf. on fig. 9a the characteristic of oscillating point of zincite detector; on space $I_0 D \frac{dE}{dI} < 0$). Sometimes in a zincite generating detector (zincite and steel' wire) the luminescence can be

Fig. 9a.



obtained, but it is very feeble (cf. § 2. The cathodoluminescence of zincite is also very feeble in comparison with that of carborundum).

(1) The possibility of producing very steadily (continued for some hours), with a generating zincite detector, short waves to 24.3 metres (1.23×10^7 cycles per second) † shows

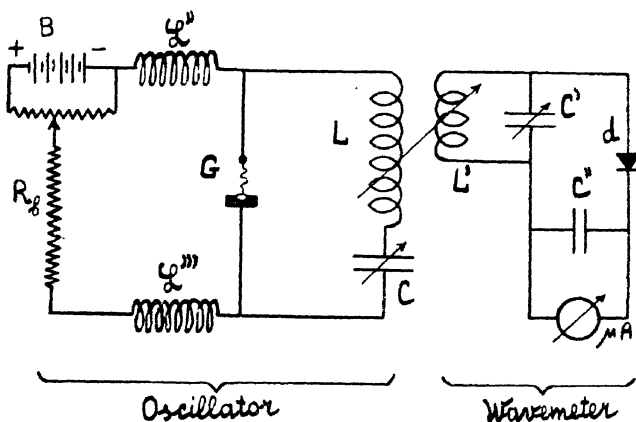
* W. H. Eccles, *Phil. Mag.* xix. p. 869 (1910). (Cited by A. Petrowsky, *Morskoy Sbornik*, no. 10, 1911). For example, for specimens of zincite (ZnO), carborundum (SiC), and iron glance (Fe_2O_3) within 22° to 97° C. temperature resistance coefficients were correspondent to (1) -0.007; (2) -0.0027; (3) -0.0065 (*T. i. T. b. p.* no. 26, p. 403, 1924).

† Cf. R. Ettenreich, *Phys. Zeit.* xxi. p. 208 (1920). "It has been stated by R. Ettenreich that the time of reaction in crystal rectifiers is less than 10^{-6} second" (cit. A. C. James, *Phil. Mag.* xlix. p. 681, 1925).

that the inertia of the corresponding processes at the contact is very small (cf. § 5).

Fig. 10 represents the scheme used for receiving short waves*. The galvanometer μA was used as indicator; d =galena detector; G =zincite generating detector; L =seven turns in the diameter 11 cm.; wire in the diam. 2 mm.; L' =one turn in the same diameter; wire in the diam. 2.2 mm.; R_b =ballast resistance 2300Ω ; L'' and L''' =choke-coils—single-layer coils (without iron core); wire in the diam. 0.1 mm.; C'' =blocking condenser 370 cm.; B =battery 12 volt. (Besides the fundamental frequency 1.23×10^7 the second harmonic was also found.)

Fig. 10.



The scheme as used for short-wave reception; the circuit $L'C'$ has been calibrated by the method of stationary waves on Lecher wires; the coupling between L' and L was loose.

(2) An investigation of temperature influence on generating contact showed that the value (abs.) of the negative resistance produced by the contact was strongly decreased by even comparatively small equable external heating (for example, on 60°C. ; see fig. 11—both positive and negative branches of the characteristic curve are shown in the same quadrant). If the detector is generating the oscillations are stopped by heating. Decrease of the temperature gives the contrary effect†. Thus the contact of a generating detector,

* *T. i T. b. p.* no. 21, p. 349 (1923). Ref. by H. Pocock, 'Wireless World and Radio Review,' xiv. p. 299 (1924); M. Gausner et T. Quinet, *Radio Revue*, no. 30, p. 189 (1924); and by J. Podliasky, *Radioélectricité*, v. p. 196 (1924).

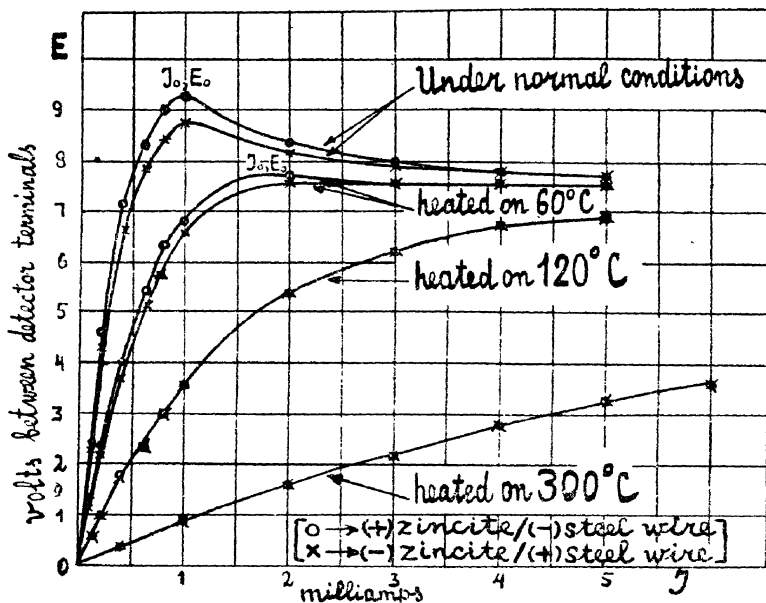
† *T. i T. b. p.* n. 18, p. 45 (1923). Ref. by C. N. Vinogradov, *L'Onde Electrique*, n. 33, p. 441 (1924).

under normal conditions, when working is very feebly heated.

The action of the contact of a zincite generating detector may be regarded as the result of a cold electronic process, but having certain properties of the voltaic arc * (*cf.* § 2). This is in accordance with the observations described above.

For the purpose of the present consideration we may introduce the conception of ohmic resistance (of touch at the contact†) R_s , which is in parallel to the hypothetical

Fig. 11.



The curves $E = f(I)$ under varying conditions of temperature of zincite steel wire detector. The curve at the top and that third from top are plotted with the positive of applied current to the zincite, while the second and fourth were with negative to the zincite. Both the fifth and sixth curves indicate each two branches of characteristics which are considered. All curves were plotted from same oscillating point.

After cessation of heating (approach to normal conditions) initial properties of detector are restored.

(The oscillation circuit was disconnected during the time of plotting.)

* Partly similar to thermionic emission, but under a great deal lower temperature (see fig. 11). Due to the temperature, E_0 changes considerably (which may be somewhat analogous to break-down voltage of ordinary discharge in the gas). See *T. i. T. b. p.* no. 18; C. Vinogradov, *loc. cit.*

† See G. Hoffman, *loc. cit.*

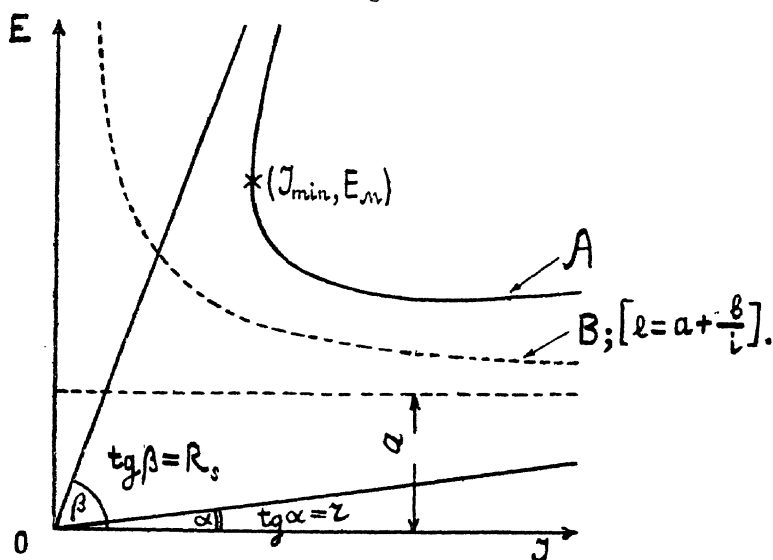
discharge and also takes into account the fact that the electronic discharge at I from 0 to $I < I_0$ is very small, and the current passes chiefly across R_s (i. e. $\tan \beta \doteq R_s$; see fig. 9 a).

For a space of characteristic $I > I_0$ an expression

$$E = \frac{1}{2}(IR_s + a \mp \sqrt{(a - IR_s)^2 - 4R_sb}) + Ir, \quad (I.)$$

is obtained if it be supposed that cold electronic discharge at generating contact at $I > I_0$ is subject to the law $e = a + b/i^*$. Here e and i are tension and current of electronic discharge; a and b = constants; r = resistance of crystal thickness;

Fig. 12.



I = current across the whole detector; E = tension on detector terminals† (cf. § 2). On fig. 12 is shown the curve which corresponds to expression (I.) (curve A). To each value of I correspond two values for E , but only one of them will be stable ($E < E_M$), since at $E > E_M - \frac{de}{di} > R_s$ (see fig. 12).

In most cases formula (I.) is near to experimental results. With regard to the order of magnitude of the constants in

* See Mrs. Ayrton, 'The Electric Arc,' London. V. Mitkevich, Journ. Russian Phys.-Chem. Society, p. 678, 1903, and p. 65, 1904.

† *T. i. T. b. p.* no. 18, p. 45 (1923). C. N. Vinogradov, *loc. cit.* Cf. Gautherot, *Radio Revue*, no. 33, p. 278 (1925).

formula (I.) the following table may give some indications. The calculations are based on characteristics which are plotted from the oscillating points of the zincite.

Contact.	r_{Ω} .	R_{Ω} .	a .	$b \times 10^3$ *.
Zincite N1—steel wire ...	98	20,000	5	1.7
" " "	80	28,000	7.5	3.5
" " "	76	10,000	3.3	0.9
" " "	80	30,000	4.5	1.5
" " "	50	25,000	3.5	1.5
" " "	49	6,000	3.5	0.8
" N2—steel wire ...	150	32,000	9	1.5
" " "	170	40,000	10.5	3

" R_s " can be calculated approximately as

$$R_s = \frac{2E_0 - a}{I_0}, \quad \dots \quad (II.)$$

where E_0 and I_0 are coordinates of the plotted characteristic curve which corresponds to the commencement of the stronger discharge (see fig. 9 a).

When I_0 and E_0 of the curve taken are nearest to the values $I_{\min.}$, E_M respectively (of the corresponding theoretical curve; see fig. 12 [A]), the calculations may be done with close approximation (I_0 neglected).

For one of such cases, on fig. 13 are shown the results of comparison of the slope value of straight line of calculated R_s (expression II.) for given characteristic (dotted line, $\tan \beta = R_s$ †) with the value of slope at its initial part (OA on fig. 13). In this case (see fig. 13) it is clear that they are near together, which is in accordance with the present consideration.

All negative resistances given by conductors with characteristics with negative slope, for the following consideration, may be divided, as was done by G. Ostroumoff ‡, into two different groups: (1) "a negative series-resistance" and (2) "a negative leak-resistance."

* " a " has a dimension of the potential; " b " has a dimension of power.

† For this case $R_s = 18,500_{\Omega}$.

‡ G. Ostroumoff, *T. i. T. b. p.* no. 38, p. 465 (1926). One or another group of negative resistance is determined by characteristic rotation in regard to coordinates (which are displaced by constant components of both a direct current and tension; see fig. 9 b). By this the stability is determined in one circuit or another (G. Ostroumoff considers both the arc and the vacuum-tube). (Cf. H. Barkhausen, *Zeit. für Hochfrequenztechnik*, xxvii. p. 150 (1926). Also Kiebitz, *ibid.* p. 136 (1926) *T. i. T. b. p.* no. 14, p. 384 (1922) and no. 38, p. 436 (1926)).

From the form of static characteristic of the generating detector (see figs. 9 *a*, 11, 13 ; *cf.* also fig. 9 *b*) it can be seen that a generating detector may give "a negative leak-resistance." Thus a steady periodical process may be excited by a generating detector only, either :

(1) In a "capacity circuit" RC (fig. 14—the circuit consists of the capacity *C* and resistance *R*, where self-inductance is very small) with the period of impulses proportional to *RC* analogically to a multivibrator, Abraham and Bloch * ; or

(2) In an ordinary (Thomson) oscillating circuit (LC) connected *in series* to the detector *G* (see fig. 10) †. This was found to be so in all our experiments ‡.

In the following table are shown the observations of frequencies of "capacity oscillations" which are produced by a generating detector in circuit RC § (fig. 14).

$R(\Omega.)$	$C(\mu F.)$	Observed frequencies. $f(\text{cyc./sec.})$	Value of coefficient k in expression $f=1/kRC$ corresponding to observed f .
60	2.9	2200	2.61
40	4.9	1800	2.84
170	0.9	2100	3.12
170	2	850	3.46
170	2.9	620	3.28
170	4	460	3.19
240	2.9	560	2.56
240	2	790	2.62
220	0.9	2300	2.19
40	4.9	1550	3.29

* H. Abraham and E. Bloch, *C. R.* clxviii. p. 1105 (1919). 'Radio Review,' i. no. 2, p. 91 (1919). *Cf.* H. Barkhausen, *E. T. Z.* p. 1338 (1924); E. Friedländer, *Arch. für Electrotech.* xvii. pp. 1 and 103; B. Van der Pol, Jr., *Phil. Mag.* lii. p. 978 (1926). The latter author termed these oscillations "relaxation oscillations." In this paper they are termed "capacity oscillations" to distinguish them from another type of relaxation oscillations,—"self-induction oscillations,"—of which the period is proportional to L/R . "Self-induction oscillations" appear to be steady only in the presence of "negative leak-resistance" (see fig. 9 *b*) in the circuit containing self-induction and resistance, where capacity is very small.

† In the "Thomson circuit in parallel" it is possible to obtain stable oscillations only with "negative leak-resistance," for example, with vacuum-tube (see fig. 9 *b*).

‡ From a generating detector may also be obtained oscillations of which the period is regulated mechanically (quartz, camerton, and so on).

§ *T. i. T. b.* p. no. 38, p. 446 (1926).

Fig. 13.

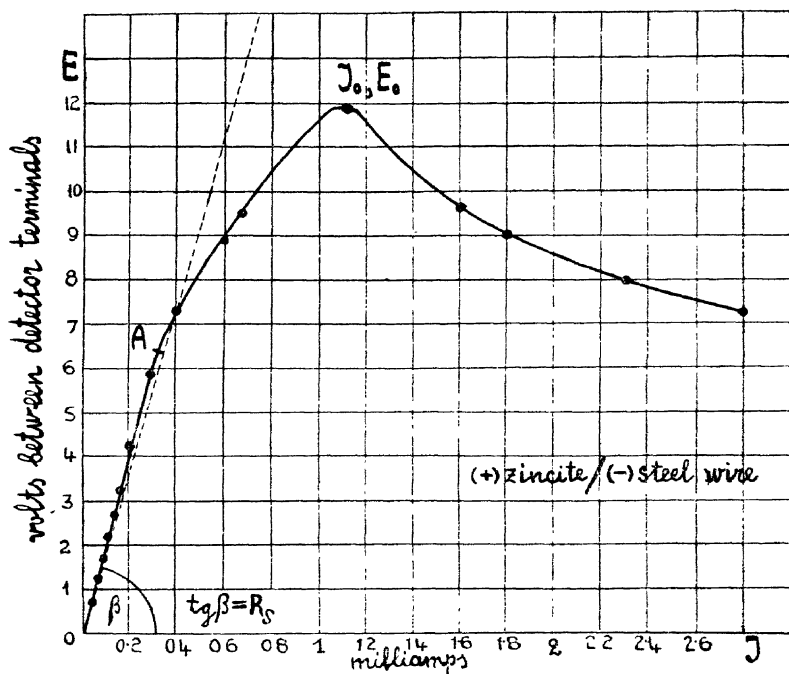
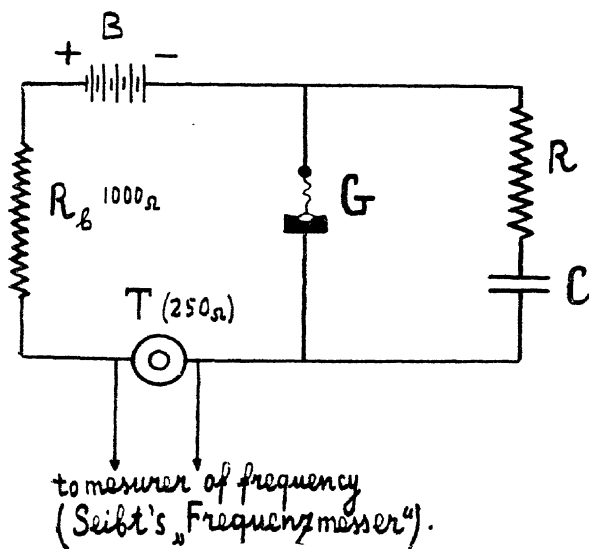


Fig. 14.



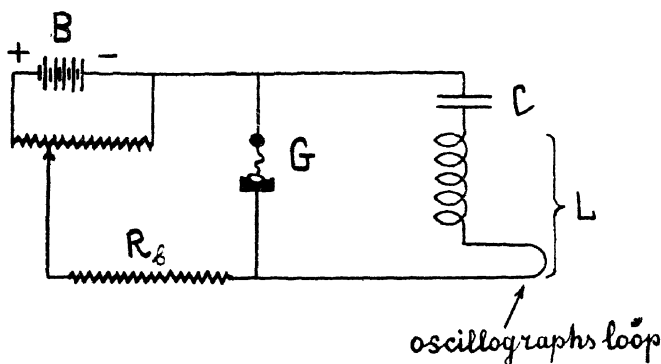
$R = 1000_{\Omega}$; ohmic resistance of the telephone $= 250_{\Omega}$; $B = 12$ volts $= \text{const.}$

In a "Thomson oscillating circuit in series" (LC) the generating detector G (as well as Duddel arc) produces, generally speaking, the oscillations of the "second type" * (see Pl. XIX. fig. 15).

Fig. 15 (Pl. XIX.) represents the oscillograms of oscillating current of low frequency. The oscillograph loop was directly connected to oscillating circuit LC. $C = 2 \mu \text{F.}$; $L = 0.1 \text{ H.}$; ohmic resistance in the circuit $= 11_{\Omega}$; $R_b = 1000_{\Omega}$; $B = 12$ volts (see fig. 16).

The period of these non-sinusoidal oscillations will increase the more in respect to $2\pi \sqrt{L/C}$ (1) the greater C/L , (2) the smaller the resistance of the circuit, (3) the steeper the

Fig. 16.



negative slope on a given space of detector characteristic. For example, with strong increase of direct current I (see fig. 9 a) the period may be decreased approximately to $2\pi \sqrt{L/C}$. Compare the curve "a" on fig. 15 (Pl. XIX.), which is plotted at small I ("a" at $I = 2.5$ milliamps.; E , on detector terminals, $= 7.1$ volts) with "b" plotted at large I ("b" at $I = 4.9$ milliamps.; $E = 6.2$ volts) across the generating detector.

But it may be mentioned that the production of "second type" oscillations cannot be taken as a factor to confirm either the thermal theory or the point of view on the

* *T. i. T. b. p.* no. 14, p. 375 (1922); 'Wireless World and Radio Review,' no. 271, p. 93 (1924). "By Second type" here is meant a large deflexion of the oscillating current in the circuit from a sinusoidal form. The oscillograms were kindly taken by Mr. A. M. Coogucheff.

electronic discharge. It is a consequence of the characteristic form (even if counted as "non-inert") of generating detector (see fig. 9a), and also of its regimen and the properties of the connected oscillating circuit.

There are interesting thermal theories with respect to the actions of generating contact formulated by W. Eccles*, A. Petrowsky†, and G. Ostroumoff‡, and as regards the sounding of detector by K. Lichtenecker§.

F. Seidl discovered an interesting phenomenon of the sounding of crystals, and investigated in connexion with this phenomenon different effects|| under the condition of larger currents than in the case of ordinary oscillation with crystal, and came to view the effect of sounding as a consequence of electronic discharge.

As it is with other sources of negative resistance, in the schemes with a generating detector the regimen of regeneration may be obtained. For practical purposes the detector is easy to connect directly to the aerial of the receiver¶ (figs. 17a & 17b).

More than eighty different natural minerals have been investigated with regard to the oscillations, and it has been found that (besides zincite) tinstone (SnO_2) generated rather well.

The author desires to take this opportunity of expressing his gratitude to Mr. N. A. Smolianinoff for his kind presentation of many specimens of minerals.

For practical purposes the most satisfactory type was found to be a zincite crystal which was prepared by fusing with MnO_2 in an electrical arc furnace**.

Fusion of the crystals increases their conductivity. Fused crystals produce stable oscillations (which may be maintained for more than three days). With fused crystals, tension of d.c. source must not be too great—about 12 volts are enough

* W. Eccles, *loc. cit.* (cit. by A. Petrowsky).

† A. A. Petrowsky, *Morskoy Sbornik*, no. 10 (1911).

‡ G. Ostroumoff, *T. i. T. b. p.* no. 24, p. 204 (1924).

§ K. Lichtenecker, *Zeit. für Tech. Phys.* viii. p. 161 (1927).

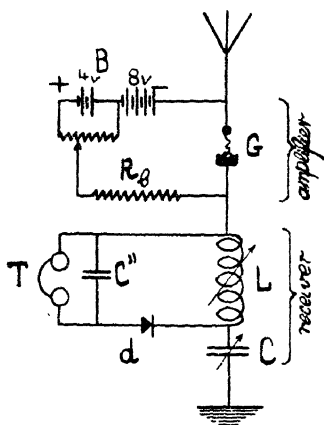
|| F. Seidl, *Vien. Ber. (II. a)* cxxxv. H. 9 (1926); *Phys. Zeit.* xxvii. pp. 64 and 816 (1926). The effect of sounding of crystals has also been discovered by the radio amateur, A. Karpovsky, Nov. 1925 (*T. i. T. b. p.* no. 43, pp. 449–451, 1927).

¶ Lossev, *Technika Sviazi*, ii. nos. 3–4, p. 390 (1924). Ref. by V. Gabel, 'Wireless World and Radio Review,' vol. xv. no. 269, p. 50 (1924). Cf. Britch. pat. J. Smith and S. Pearce, No. 259005 (1925) (*Exp. Wir. & Wir. Eng.* iii. no. 39, p. 776 (1926)).

** *T. i. T. b. p.* no. 21, p. 349 (1923). Also *Zeitschr. für Fernmelde-technik*, no. 9, p. 132 (1925).

on the average. Signs of poles are important. Except for some cases, the branch of characteristic at (+) zincite and (-) steel wire has steeper negative slope (see, for example, fig. 11). Of course, stability occurs only when the resistance R_b (see figs. 8, 10, 14, 16, 17 *a* & 17 *b*) is not less than the absolute value of the negative resistance produced by the detector (at given I and E).

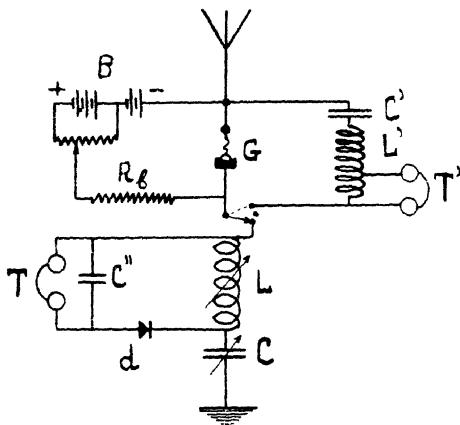
In conclusion, it may be mentioned that a considerable change of zincite detector characteristic may also depend on the Joule effect (*cf.* fig. 11). For example, when the oscillating point giving the characteristic curve is traced by the steady current, of order more than 10 milliams., the

Fig. 17 *a*.

$B=12$ volts (4+8).

During the work of the scheme the current I across the detector G was usually taken of order 4 milliams.

$R_b=1000\Omega$.

Fig. 17 *b* *.

$L'C'$ is "an auxiliary circuit" of low audio-frequency, used to find the oscillating points on the crystal.

$L'=0.035$ H.; $C'=0.25 \mu$ F.

To obtain the oscillations in the circuit LC after switching from $L'C'$ to LC , the conditions

$C/L \geq C'/L'$ and $R < R'$

must be taken.

R and R' are resistances in the circuits.

"hysteretic loop" depending on the Joule effect was observed (*cf.* fig. 11).

Setting the generating zincite detector in benzene, ether (generally in non-conductive intensively evaporating liquids) makes E_0/a greater, and enables the production of negative

* Russian Pats. 996, 75317 (1922); 472, 77717 (1923).

resistance to be greater in absolute value*. (See the influence of the temperature in fig. 11; cf. also § 2.)

§ 5. Luminous Detector as a Light Relay.

The luminescence of a carborundum detector may be observed, beginning with a current through the contact of order 10^{-4} amp. (see the characteristics on figs. 2, 3, & 7).

With strong current of order 10^{-1} amp. bright luminescence may be obtained, and it still remains on a red-hot (by the Joule effect) crystal. Fig. 18 (Pl. XIX.) (orthochromatic plate) shows the piece of carborundum placed between two metallic rods; the current = 0.2 amp.; the potential difference between rods = 29 volts. At the negative electrode a violet spot (fig. 18, on the right) of luminescence II. is marked on the red-hot crystal.

During observations of both luminescences (I. and II.) in a rotating mirror, if an alternating current passes through the contact separate flashes may be clearly seen at frequencies up to 78,500 cyc. per second (current = 0.23 amp. R.M.S.). The limit of discernment of these flashes (frequency 78,500 cyc. per second) depends on the resolving power of the installation of the rotating mirror, but it was independent of "luminescence inertia." Even at frequency 78,500 cyc. per second the lengths of the black intervals were more than the lengths of the flashes, which indicated that the luminescence appeared and disappeared very quickly †.

The brightness of the luminescence may be made sufficiently great to render it possible to record on a moving photographic plate an alternating current of frequency order 10^2 cyc. per second. Fig. 19 a (Pl. XX.) shows the record of a current 500 cyc. per second (with luminescence II.; current through the detector = 0.24 amp., R.M.S.; objective F: 3.5; $F=7$ cm.); see also fig. 19 b (Pl. XX.).

Fig. 20 (Pl. XX.) represents the action of luminescence II. on a photographic plate for different times of exposure (objective "Collinear Voigtländer" F: 18; $F=18$ cm.;

* *T. i. T. b. p.* no. 18.

† With regard to small inertia, compare the very small (and typical for fluorescence) duration of after-luminescence in photo-luminescence; (of order 10^{-8} sec.; less than 10^{-6} sec.). See S. J. Wavilow and W. L. Lewshin, Journ. Russian Phys.-Chem. Society, lviii. p. 555 (1926); *Zeit. für Phys.* xxxv. p. 920 (1926). In the investigation of the photo-luminescence phenomenon it has been stated by the above-named authors that there are no intervening stages between fluorescence and phosphorescence.

the luminescence is projected in natural size; current through the detector = 0.23 amp.; tension on terminals 28 volts). For comparison, in fig. 21 (Pl. XX.) are shown some results for "glimmering" neon lamp (also non-inertia source of light) Osram 125-139 volts, to which was applied d. c. 177 volts with value 15.1 milliamps. From this it is clear that the luminous detector acted more effectually than the lamp (*cf.* figs. 20 & 21, Pl. XX.).

It may be mentioned that with strong currents sometimes, in addition to the contact luminescence, luminescence at the place of contact of single little crystals occurred, in one place or in another, in the middle of the carborundum piece (*cf.* fig. 18). The intensity of these luminescences also depends on current direction, in meaning of item 1, § 2.

In conclusion, the author wishes to thank Professor W. K. Lebedinsky, M.Sc., for his valuable advice in connexion with the work on oscillating crystals.

Nijny-Novgorod, Radio Laboratory.

CIII. *On Jaeger's Method as Applied to the Determination of the Surface Tension of Mercury.* By R. C. BROWN, B.Sc.*

TWO years ago research was commenced with a view to determining, by a small variety of methods, the surface tensions of certain molten metals. As in the literature of the subject the maximum bubble pressure method, sometimes called Jaeger's method, is quoted as having been used extensively for high temperature work, it was decided to make use, in the first place, of this method. A few preliminary experiments were carried out using mercury, for obvious reasons, and difficulties began immediately to appear. Many of these have apparently been encountered also by Bircumshaw (*Phil. Mag.*, Sept. 1928). Throughout the past two years the vagaries of the method have been studied by the present writer, not so much for their own sakes as with a view to their elimination. The observations described in the present paper in many cases fall in with those of Bircumshaw and also break a certain amount of new ground.

* Communicated by Prof. A. W. Porter, F.R.S.

Apparatus and General Manipulation.

The apparatus was of the usual type. The gas to be used for blowing the bubbles was contained in a glass reservoir the volume of which could be controlled by allowing mercury to run in or out of it. On leaving the reservoir the gas passed through rubber tubing, which could be restricted to any required degree by means of a screw-clip, and then to the jet and one arm of a water manometer, which consisted of a tube of 0.5 cm. bore, the other arm being a Woolf's bottle of 10 cm. diameter. Thus pressure changes read on the narrow arm were multiplied by 1.0025 in order to obtain the true pressure change in centimetres of water. During the preliminary experiments the jet was clamped and the mercury under experiment was raised or lowered beneath it on a levelling table fitted with a graduated vertical action. Thus the jet remained stationary and the mercury was set with its surface coinciding with the plane of the jet by visual observation; it was then raised through a known distance. Later the jet was provided with a graduated screw for vertical motion and the mercury container, which was of silica, was fixed. The disposition of this part of the apparatus was such that the whole could be enclosed in a vertical electric furnace, the temperature of the mercury being measured with a calibrated Pt, Pt-Rh thermocouple. A drying tube of wide bore containing calcium-chloride lumps was incorporated between the manometer and the jet. The jets, in the first place, were made of glass, and it was found that these could be drawn and fractured satisfactorily after some practice, and there appeared no necessity to grind them. Later, jets of amalgamated copper, platinum, and monel metal were used. When possible, the setting of the plane of the tip of the jet in the mercury surface, preparatory to lowering it through a known distance, was done visually; but, when the furnace was in use, this became no longer possible and the following technique was adopted. The pressure inside the gas reservoir was reduced and the screw-clip adjusted so as to cause a slow current of air to flow up the jet. The latter was then slowly lowered until the manometer began to rise, showing that the jet orifice had been closed by the mercury surface. The settings of the screw-head thus obtained were found to be in better agreement with those obtained visually than were those obtained by the more generally used method of allowing gas to flow out of the jet, probably because in this last case the outflowing gas forms a depression in the mercury surface and the

movements of the manometer are correspondingly less definite. In the later and more accurate experiments the mercury for each day's readings was collected in the silica vessel direct from a single-stage vacuum still.

The equation used in the calculations was

$$T = \frac{rg}{2} \left[H\sigma - \left(h + \frac{2}{3}r \right) \rho \right],$$

where

T is the surface tension of the liquid in dynes per cm.

r the radius of the jet in cm.

g the acceleration due to gravity.

H the maximum corrected reading of the manometer in cm.

σ the density of the manometric liquid.

h the depth of the tip below the free surface of the mercury in cm.

ρ the density of mercury at the temperature observed.

Results.

During the first experiments the bubbles were blown with air, and it was immediately noticed that the detachment of the bubble from the tip of a glass jet in mercury corresponded, in general, to no definite pressure for any given jet. The first indication of reproducibility was given by a glass jet of internal and external radii 0.026 and 0.045 cm. respectively. Readings of maximum bubble pressure taken immediately after setting the tip 0.391 cm. below the free surface of the mercury always rose consistently, not from a consistent initial reading, but always reaching a definite maximum. A typical series of readings was 38 cm., 42.0 cm., and a maximum of 42.52 cm. of water, the maximum being consistent. If the jet was withdrawn and reset in the liquid a similar series was obtained with the same maximum. When corrected for the rise of water in the wide arm of the manometer 42.52 cm. becomes 42.63 cm. of water with a density of 0.999 gm./cc. Using the internal radius of the jet in the calculations the value for the surface tension of mercury comes out to be 478 dynes/cm., and using the external radius the value is 819 dynes/cm. Of course the bubble is quite invisible during the whole of its life, so that the evidence as to which edge of the jet it is clinging to when the pressure inside it reaches a maximum is derived from the values given when each of the radii is used in turn

in the calculations. Thus in the above case it would appear that the internal radius is the correct one to use, as 478 is a much more probable value for the surface tension of mercury at room-temperature than is 819.

A set of readings covering several days, during which the jet was not removed from the mercury, was taken with this jet. After the first day the readings remained consistently at the maximum, rising slightly with time. Thus on the first day the result was 470 dynes/cm. and on the fifth it was 477, using the internal radius (the external radius, if used in the calculations, will, of course, give 817 for the fifth day). Points to be noticed are :—

1. On the fifth day the maximum pressures were constant to 0.05 cm. of water in 42 cm., and in most cases no variation was noticeable at all on a scale graduated in mm.

2. On withdrawing the jet and re-immersing it on the fifth day the pressure assumed its maximum value after about two bubbles had been released.

3. The pressure at which the bubble became unstable depended not on the time elapsed since setting the jet in the mercury but on the number of bubbles blown since then.

4. The mercury was not protected from atmospheric contamination to any great extent, so that the accuracy of the method would appear to be singularly independent of the state of the free surface of the mercury when once the jet has been immersed below it.

Next a jet was made with thinner walls but larger radii [internal 0.0847 cm., external 0.0970 cm., thickness 0.012 cm.]. The jet was soaked overnight in chromic and sulphuric acids, washed in tap-water and distilled water and dried. The following set of uncorrected pressures, p. 1048 (cm. water) was obtained. A horizontal line separating two consecutive readings indicates that between these two readings the jet was withdrawn and reset in the mercury.

Thus with this jet it would appear that after two or three bubbles had been released, the bubble began to form on the outer edge of the jet, giving a pressure of 16.14 cm. of water (when corrected for the rise of the wide arm), since this pressure gives, when the external radius is used in the calculation, a value of 473 dynes/cm., which is very near to values obtained with other jets, and also those published by other observers. The low value of the pressure obtained with the initial bubbles of the series might be explained by

assuming the presence of an air-film adhering to the jet upon first lowering the latter into the mercury, and the subsequent partial or complete destruction of the film by movements of the mercury following upon the release of the first bubbles.

Uncorrected Pressures.

<u>15.7</u>	} with external radius gives 450 dynes/cm. ; with internal radius gives 399 dynes/cm.	
<u>15.7</u>		
<u>15.7</u>		
16.0		
16.10	} with external radius gives 473 dynes/cm ; with internal radius gives 419 dynes/cm.	
16.10		
16.10		
16.11		
16.60		
16.10		
16.14		
16.45		
16.3		
16.4		
16.5		
16.55		
16.64		
16.63		
16.78		
16.63		
16.83		
16.91		
16.88		
16.95		
17.01		
16.93		
17.09		
17.14 (the highest reading)	} with external radius gives 523 dynes/cm. with internal radius gives 462 dynes/cm.	
17.03		
17.10		
17.08		
16.4		
16.4		
<u>16.9</u>		
<u>15.7</u>		
15.7		

The presence of an air-film on the horizontal face of the tip might also explain the tendency of the pressures to rise above the value of 16.14 cm., since the film would lessen the adhesion of the mercury to the underneath face of the jet,

and so cause the bubble to spread to the outer edge. During its destruction, however, the adhesive forces would be increased, and the mercury-glass circle of contact might find itself nearer to the inner edge of the jet when the maximum bubble-pressure was reached. The maximum reading recorded (17.18 when corrected) gives 462 dynes/cm. with the internal radius, which would indicate that during this series the bubble never actually remained on the inner edge of the jet. An actual change in the value of the surface tension does not seem to be indicated, since the series could be repeated over again by merely withdrawing the jet and re-setting it in the liquid, and also it must be remembered that a fresh surface is formed for each bubble, so that a change in the surface tension could only be brought about by a change in the bulk composition of the mercury. Another possible cause of the phenomena might be the creation—instead of, or in addition to, the destruction of an air-film—of a layer, on the underside of the jet, of some combination of the glass mercury and oxygen molecules which might cause an increase in the adhesion of mercury for glass. It is significant that, as will be seen later, there appeared no tendency for the bubble to be released from any but the outer edge when nitrogen was used instead of air for blowing the bubbles. With other glass jets which were made (and when air was used) it was usually noticed that pressures corresponding to the outer edges were registered on beginning a series of readings, but in some cases these could not be repeated until the jet was cleaned again and fresh mercury was used.

A copper jet (internal radius 0.042 cm., external 0.064 cm.) was then constructed and the tip of it amalgamated with mercury. The object in view was not so much the obtaining of an accurate value of the surface tension as the seeing whether the same large variations in the readings would occur when using a jet which was "wetted" by the mercury. The largest variation noticed was 0.6 cm. in 25 cm. of water which is far less than most of those experienced with glass jets. Taking an average reading and using the internal radius in the calculation we get 397 dynes/cm., and using the external radius 615 dynes/cm. The actual values mean very little since probably the mercury forming the bubble had a considerable amount of copper dissolved in it; but the comparative consistency of the readings was striking when compared with readings taken with glass jets.

Experiments were next carried out using nitrogen instead of air and little or no tendency was shown for the readings

to rise continuously as successive bubbles were blown. Moreover, different jets gave consistent values of the surface tension only when the external radius was used in the calculation. The following is a typical set of readings obtained with a glass jet of radii 0.0450 and 0.0695 cm. :—

Cm. of water
(uncorrected).

19.76

19.78

19.77

19.78 ... Mean 19.78, which, when corrected, becomes 19.83 cm.

19.80 This, with the external radius, gives 469 dynes/cm.
 at 19° C.

19.76

19.80

19.79

19.80

The readings remained constant for periods as long as 24 hours when the jet was kept below the surface of the mercury for that period. After such long periods of immersion, however, it was sometimes noticed that the gas flowed out of the jet in a constant stream and passed continuously up the outside walls of the jet to the free surface of the mercury without forming bubbles in the usual way. When this happened, the manometer registered a pressure less than that caused by bubbles and the surface of the mercury was covered with a pattern of standing ripples. This failure to form the usual bubbles was possibly caused by a weakening of the adhesion of the mercury for the glass of the jet by the formation of a film of gas on the glass, since it could usually be remedied by lowering the tip of the jet to 0.600 instead of 0.400 cm. (which was the usual distance employed) below the free surface of the mercury, thus increasing the hydrostatic pressure on such a film. Sauerwald and Drath (*Z. Anorg. Chem.* cliv. p. 79 (1926)) have noticed that consistent readings of bubble pressure cannot be obtained in general unless the jet is immersed to a depth greater than 0.3 cm. A platinum jet of very small thickness (radii 0.0325 and 0.0352 cm.) behaved very similarly. On changing the dimensions of the jet by turning it in a lathe it was readily seen that the external radius must be used in the calculations in order to give consistent results for the two sizes of jet. A few readings taken with a jet of monel metal of dimensions similar to those of the platinum jets were also satisfactory. The values obtained for the surface tension of mercury at an average temperature

of 18° C. with glass and platinum jets (using nitrogen) are here summarized :—

Jet.	Radii, cm.		T, dynes/cm.
	Int.	Ext.	
Glass 1	0·0415	0·0500	471
„ 2	0·0450	0·0695	469
			472
„ 3	0·043	0·061	475
Platinum 1	0·0325	0·0352	477
			477
			478
„ 2	0·0315	0·0379	476
			476

Mean values :—

Glass jets 472 dynes/cm.

Platinum jets 477 „

Further interesting results were obtained when higher temperatures than that of the air were used. For this the furnace and other arrangements previously referred to were brought into use. The furnace was kept at the temperature required for several hours so as to avoid any temperature lag. At first the second glass jet referred to in the table above was used. The readings were extremely consistent, variations in pressure rarely reaching 0·05 cm. in any determination. The values obtained indicated that the external radius was to be used in the calculations. Unfortunately the jet was chipped and the readings became indefinite after determinations at three different temperatures had been made. Glass jet number 3 was then used, and it was found that, in order to bring the results into line with those already obtained (which agreed well with those of other observers), it was necessary to use the internal radius at the temperatures which were used. The actual pressures were again as consistent as before and there appeared no tendency for the bubble to form on the outer circumference. On the whole, however, the actual results for the surface tension given by this jet were unsatisfactory. Number 1 glass jet was found to be very satisfactory and good values were obtained with this, the bubble appearing to come from the inner edge of the jet except for air temperature. These remarks also apply to a fourth gas jet which was made.

Summary of values obtained for the surface tension of mercury at temperatures up to its boiling point :—

Jet.	Radii, cm.		Radius used in calculation.	Temp., ° C.	T, dynes/cm.
	Int.	Ext.			
Glass 1	0.0415	0.0500	Internal	178	436
			„	218	427
			„	272	411
			„	326	396
Glass 2	0.0450	0.0695	External	78	460
			„	162	443
			„	333	397
Glass 4	0.0350	0.0496	Internal	87	458
			„	118	450
Mean of several glass jets.			External	18	472

Fig. 1.

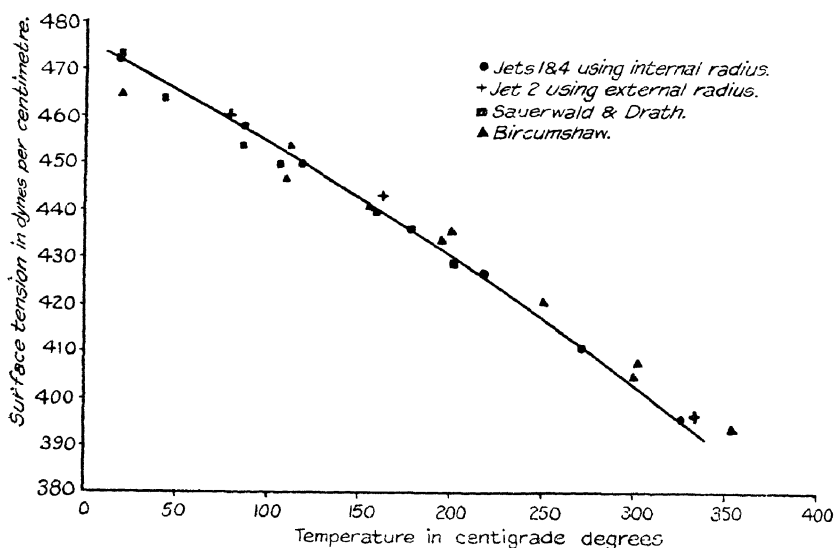


Fig. 1 shows these results graphically. The continuous line is drawn through the points obtained with jets 1 and 4. Results published by Sauerwald and Drath (*loc. cit.*) and by Bircumshaw (*Phil. Mag.* vii. 8, pp. 341 (1926)) are also shown.

Collection of Results and Discussion.

When glass tips were used with air in the determination of the surface tension of mercury by the maximum bubble

pressure method, consistent readings were, as a rule, found only immediately after setting the jet in the liquid. After this the readings rose, but the initial reading could again be obtained by withdrawing the jet and setting it again in the mercury. By using tips of different radii it was found that these initial readings must be used with the external radius of the tip in order to give consistent values for the surface tension. On some occasions maximum pressures were reached which when used with the internal radius also gave fairly good results; but this was not general at air temperatures. Bircumshaw has recently noticed that there is difficulty in obtaining a definite bubble pressure when oxygen is used with glass jets; but that consistent results can be obtained with hydrogen and nitrogen. This (in the case of the nitrogen) was the experience of the present writer. When nitrogen was used, pressures given by any one glass jet were very constant except for one or two low ones usually to be found immediately after immersing the jet, a possible explanation of which is an air layer adhering to the walls of the jet. Thus there seemed little or no tendency for the bubble to detach itself from any but the external circumference of the jet when nitrogen was used. For reasons given earlier in this paper, there seems more possibility of a change in the radii of successive bubbles than of an actual change in surface tension. Platinum and monel metal jets gave similar results to those with glass jets.

When the mercury was heated certain glass jets always formed the bubble on the internal circumference even for temperatures less than 100°C. , although one was discovered which formed the bubble on its outer edge right up to 330°C. This latter had a large wall thickness (0.025 cm. as compared with 0.009 cm. and 0.012 cm. of those in the former category). The deciding factor in the question as to which radius to use in the calculations was, for these high temperature measurements, the agreement of results with those of other observers. As a rule the radii were so different as to leave no doubt as to which radius should be chosen—the smallest difference between the two alternative results being about 30 dynes/cm. Certain it is that with several jets the actual bubble pressure was greater at high temperatures than at air temperature, which can only be interpreted in the above way, especially as the readings were so consistent.

The mechanism of the formation of the bubble on either of the two edges or at any line between them would appear to be obscure. It can only be said that when the adhesion

of mercury for glass is small, the bubble will certainly be formed on the outer edge, and when the adhesion is large it will not spread to the outer edge but will reach its maximum pressure and unstable state while still on the inner edge. These two cases correspond roughly to perfectly non-wetting and perfectly wetting liquids, *i. e.*, with liquids of angles of contact of 180° and 0° . Cantor (*Ann. der Phys.* xlvii. p. 399 (1892)) deals with the subject and expresses the opinion that for non-wetting liquids the radius of the bubble will depend on the angle of contact. Thus for this case he recommends jets of no thickness at their tip so that the internal and external radii coincide. It is found difficult to make such jets in practice, however.

Sauerwald and Drath consider that with liquid metals the bubble forms always on the external edge. Results described in the present paper seem to show that the bubble forms on the outer edge in the case of glass jets in mercury unless, either by the continuous blowing of bubbles with air or by heating the mercury, the adhesion between the two becomes large enough to prevent the bubble spreading to the outer edge. W. C. Baker (*Science*, lxvii. p. 74 (1928)) has shown that mercury at ordinary temperatures will adhere to a glass surface (in his case a spherical lens surface) which is withdrawn from it, and it was often noticed during the course of the present research that the mercury adhered to the jet when the latter was raised out of the free surface. Baker also mentions that, on raising his spherical lens surface, the line of contact did not move in a continuous way over the glass surface, but sometimes stuck and remained adhering at the same place for considerable up and down movements of the lens. This may correspond to the sticking which must take place when the bubble surface, having left the inner edge (it is on this edge during some period of its life since the mercury meniscus is first of all in the bore of the jet), does not spread completely to the outer edge but detaches itself while registering a pressure corresponding to a circumference lying between the two. When used at ordinary temperatures and with nitrogen, the bubble always comes from the outer edge, and in these circumstances the method is most satisfactory, especially in view of the facts that a fresh surface is blown for each bubble and that readings are constant for 24 hours or more even though the free surface of the mercury is exposed to contamination. The results obtained were 472 and 477 dynes/cm. for glass and platinum jets respectively at 18° C. These agree with the 473 at 19° C. of Sauerwald and Drath obtained with a silica

jet and CO_2 , but not so well with Bircumshaw's most recent values, which cluster round 500 dynes/cm. The temperature curve in fig. 1 follows the results of Bircumshaw and Sauerwald and Drath.

I sincerely thank Dr. A. Ferguson and Prof. A. W. Porter for the assistance and encouragement which they have lent during the course of the work.

Carey Foster Laboratory,
University College, London.

CIV. *The Crystal Structure of Mercury, Copper, and Copper Amalgam.* By HENRY TERREY and CYRIL MAYNARD WRIGHT*.

1. CRYSTAL STRUCTURE OF MERCURY.

IN connexion with some work on the crystal structure of amalgams it was necessary to know the crystal structure of mercury.

Two investigations have already been carried out: (1) by Alsen and Aminoff (Gool. For. Fört xlv. 1922), who found that mercury at the temperature of solid carbon dioxide has a hexagonal lattice with $a_0 = 3.84 \text{ \AA.U.}$ and $c = 1.88$; and (2) by McKeehan and Cioffi (Phys. Rev. i. p. 444, 1922), who found that at a temperature of -115°C. mercury has a rhombohedral structure.

In the present investigation the work was carried out at a temperature of approximately -150°C. , and the rhombohedral structure assigned by McKeehan and Cioffi fully confirmed.

Apparatus.

For the production of X-rays the Shearer type of tube was used, fitted with a copper anticathode and operated at 35,000–40,000 volts, the current being from 2–4 M.A.

The camera was constructed on somewhat similar lines to that used by McLennan and Wilhelm for their work on the crystal structure of solid carbon dioxide and solid oxygen (Trans. Roy. Soc. of Canada, May 1925, and Phil. Mag., Feb. 1922). The construction is shown in the sketches (figs. 1 to 5).

* Communicated by the Authors.

The main chamber of the camera was of heavy brass tube about 6 cm. in diameter, a cover being provided by a central,

Fig. 1.

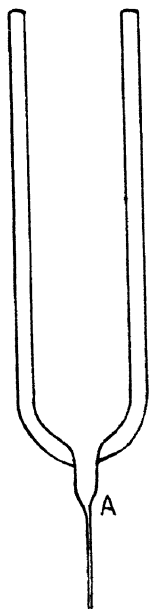
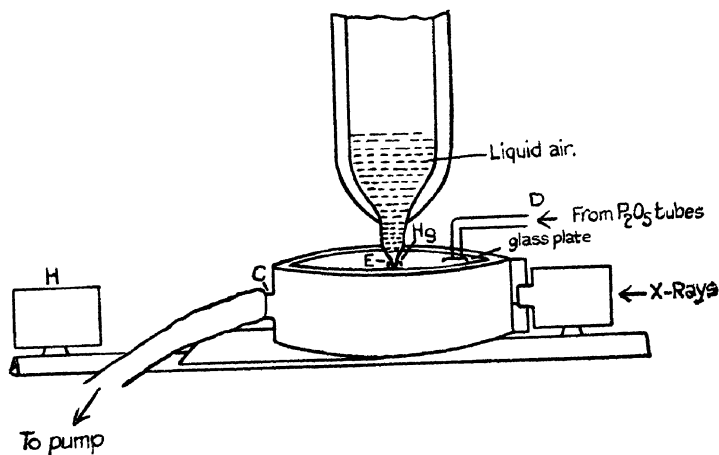


Fig. 2.



well-ground matrix, into which a double-walled vacuum flask fitted.

Fig. 3.

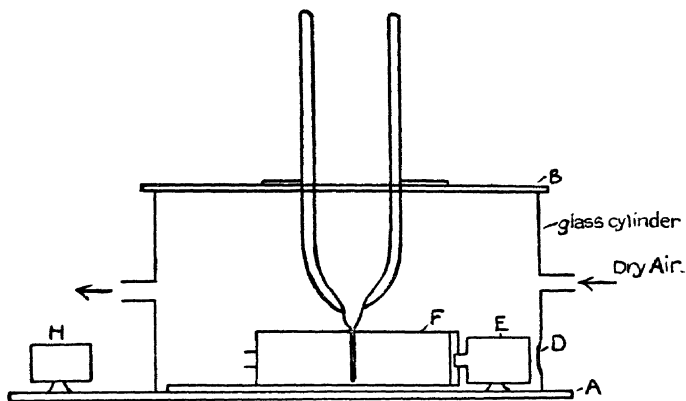
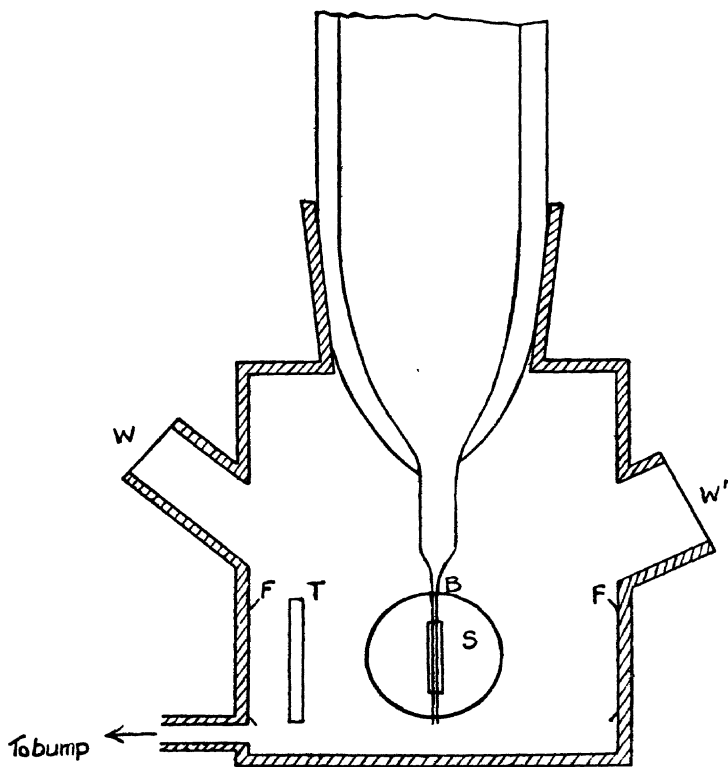
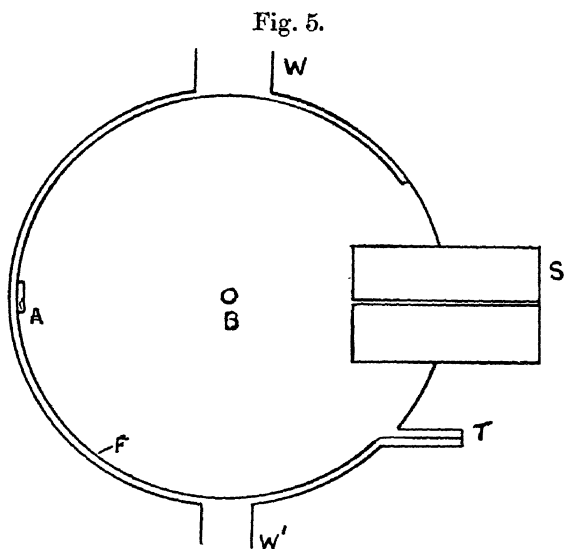


Fig. 4.



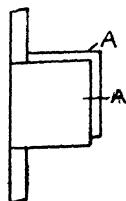
The slit, .5 mm. wide, .8 mm. high, and 3 cm. long, was cut from a brass cylinder 3 cm. long and 2 cm. in diameter, and was sealed into the wall of the camera.

A metal film-holder F, faced with nickel foil, .03 mm. thick, was soldered on the inside of the brass tube, and the



film was introduced at T, where the end of the film protruded through the brass tube. This joint was also soldered, so that the camera could be evacuated while the film remained at normal pressure. The films could thus be protected from mercury vapour in the camera.

Fig. 6.



The holder consisted of a soft metal tube 12-13 cm. long, flattened out in the form of a narrow rectangular tube to allow the passage of the film. The holder was bent into an arc of a circle with the nickel on the inside, before introduction into the brass tube.

A strip of lead of the shape indicated in fig. 6, was fixed

at A to protect the film from the direct beam of rays, and the scattered rays were stopped by the "wings" AA. When the film had been introduced, the end of the holder at T was covered with plasticene to protect the film from the light.

The Dewar vessel of the pattern indicated was made, the tube A (of lead-free glass) being drawn out to a thin-walled fine capillary tube about .8 mm. in diameter, the capillary being sealed at the lower end.

Experimental Method.

The capillary tube was lined up with the slit by rotating the Dewar vessel in the matrix. The position of the Dewar with respect to the camera was marked, so that this alignment need not be repeated with the same capillary tube. A piece of thin aluminium foil was waxed over the outside of the slit. The position of the camera was adjusted so that the X-rays passed through the slit, by viewing the fluorescence on a barium platino-cyanide screen placed in the centre of the camera (the Dewar being removed during this operation).

A little mercury was then placed in a small cavity in the bottom of the camera. The Dewar vessel was then replaced and the camera was evacuated with a Hyvac pump, a McLeod gauge being used to test the vacuum obtained. Liquid air was poured into the Dewar flask, and the base of the camera was very gently warmed. A film of mercury .25-.5 mm. thick soon formed on the capillary tube, and the photograph was then started, an exposure of six hours being given. The lines on the film were quite distinct, but rather broad.

Before the values of d_{hkl} for the planes giving these lines could be calculated, an accurate measure of R, the distance from the film to the mercury surface, had to be obtained. This was found by filling the capillary tube with powdered sodium chloride, and with the Dewar vessel in the same position relative to the camera as for the mercury photograph another photograph was taken. Assuming the value of d_{hkl} for the sodium-chloride lines (Davey, Phys. Rev. xxi. 1923), the value of R was calculated. This did not give an absolutely accurate value for R for the mercury photographs, as the sodium chloride was in the capillary tube, while the mercury was on the outside, but the glass wall was as thin as possible, and it was the most accurate means of determining R.

Results.

Several photographs of mercury were taken, and the complete results from one measurement are included here (Table I.).

TABLE I.
Photograph of Solid Mercury.

Distance between lines.	Intensity.	R (from NaCl lines).	θ .	d_{hkl} .
cm.		cm.		
3.250	Strong.	2.877	$16^{\circ} 10\frac{3}{4}'$	2.760
4.050	"	2.879	$20^{\circ} 10'$	2.230
5.300	Weak.	2.875	$26^{\circ} 24'$	1.730
6.364	Strong.	2.866	$31^{\circ} 48'$	1.460
6.856	"	2.863	$34^{\circ} 17'$	1.365
7.789	Weak.	2.859	$39^{\circ} 1\frac{1}{2}'$	1.221
8.724	Medium.	2.859	$43^{\circ} 43'$	1.113
10.063	"	2.854	$50^{\circ} 31'$.996
11.014	"	2.852	$55^{\circ} 19'$.936
11.560	"	2.852	$58^{\circ} 4'$.906

TABLE II.
Photograph of NaCl.

These values of R are used for the above determinations of d_{hkl} .

Distance between lines.	d_{hkl} (assumed).	R.
cm.		cm.
3.185	2.814	2.877
4.572	1.990	2.880
5.639	1.625	2.872
7.508	1.259	2.858
8.390	1.149	2.860
10.961	.938	2.852

By the use of Hull's plots (Phys. Rev. 1921, p. 17) it was seen that the diffraction given by mercury corresponded to a rhombohedral lattice with axial ratio 1.94. This structure confirmed the work of McKeehan and Cioffi.

Assuming the agreement between the spacings of the planes (111) and (110) to be exact, from the equation

$$d_{hkl} = \frac{(hx_1 + ky_1 + ly_1 - 1) \sqrt{1 + 2 \cos^3 \lambda - 3 \cos^2 \lambda}}{\sqrt{(h^2 + k^2 + l^2) \sin^2 \lambda + 2(hk + kl + hl)(\cos^2 \lambda - \cos \lambda)}},$$

referring the rhombohedron to three trigonal axes, where $\lambda = \mu$, it followed that

$$\begin{aligned} \cos \lambda &= 1/3, \\ i. e. \quad \lambda &= 70^\circ 32'; \end{aligned}$$

knowing λ from the above equation, assuming $d_{111} = 2.233$, it followed that

$$a_0 = 2.996 \text{ \AA.U.}$$

Summary of Results.

A summary of results (Table III.) is given with the theoretical spacings, calculated from the above equation.

TABLE III.

Indices (hexagonal form).	Indices (trigonal form).	d_{hkl} (theoretical).	d_{hkl} (observed).			Intensity.
			1.	2.	3.	
10.1	100	2.735	2.766	2.760	2.760	s.
00.1	111	2.233	2.230	2.238	2.230	s.
10.2	110					
11.0	101	1.730	1.727	1.735	1.730	w.
{ 20.1	111	1.462	1.445	1.466	1.460	s.
{ 10.4	211					
{ 11.3	210	1.367	1.363	1.368	1.365	s.
{ 10.1 (2)	100 (2)					
10.5	221	1.223	...	1.227	1.221	w.
{ 21.1	201					
{ 00.0 (2)	111 (2)	1.116	1.106	1.115	1.113	m.
{ 10.2 (2)	110 (2)					
12.2	211	1.073	1.063	m. w.
{ 10.0	211					
{ 20.5	311	.998	.988	.996	.996	m.
{ 11.6	321					
{ 12.4	301	.938	.928	.935	.936	m.
{ 10.1 (3)	100 (3)					
10.7	322	.911	.901	.906	.906	m.

Rhombohedral system $a_0 = 2.996 \times 10^{-8}$ cm.
 Hexagonal system $a_0 = 3.460 \times 10^{-8}$ cm.
 $c = 1.94$.

The results given in Table III. show very good agreement with the assumed structure. The calculated density, if one atom is associated with each cell (simple rhombohedral lattice), is 14.26 gm./cm.^3 . The value here determined is in agreement with the values for its density, 14.193 gm./cm.^3 at its melting-point (Mallet, Roy. Soc. London Proc. xxiii. p. 71, 1877), and 14.362 gm./cm.^3 at the temperatures of liquid air (Dewar, Chem. News, lxxxv. p. 277, 1902).

2. COPPER.

Considerable divergence exists in the literature with regard to the precise values for the plane spacings of copper, values between 3.597 \AA.U. and 3.634 \AA.U. being given (*cf.* Holgersson, *Ann. d. Physik*, iv. pp. 79, 35, 1926). Our value, 3.603 , is slightly greater than the precision value of Davy (*Phys. Rev.* xxv. 1925), viz. 3.597 .

Lattice Constant for Copper.

For the production of X-rays the Shearer type of tube was employed, photographs being taken with a Müller X-ray spectrograph, a slit of 0.2 mm. being used. The powdered substance mounted in the centre of the camera could be oscillated uniformly through an angle of 12° during exposure, which varied between 2–4 hours. The films were measured on a measuring machine graduated to $1/100$ of a millimetre.

Experimental.

The copper was prepared by deposition from an aqueous solution of pure copper sulphate to which pure zinc and a little sulphuric acid had been added. The deposited copper was washed with water and alcohol, and kept under absolute alcohol to prevent oxidation.

In order to eliminate any uncertainty in the value of R , the distance from powder surface to photographic film, sodium chloride was used as a comparative standard.

The powders were prepared by grinding the halide or copper in an agate mortar and then rubbing through a 200-mesh silk handkerchief. The powdered samples were mounted in thin celluloid tubes, 6.6 to 7 mm. in diameter. Two methods of packing the powders were tried—one where the sodium chloride and copper powder were intimately mixed before introduction into the tube, and the other where one half of the tube was filled with sodium chloride and the other half with copper. The first of these two

methods was found to give better photographs, and was used throughout this investigation.

Results.

The diffraction patterns of sodium chloride and copper were obtained on the films. Assuming the values of d_{hkl} for the various sodium chloride lines (from W. P. Davey, *Phys. Rev.* xxi. 1923), the values of θ were calculated from the equation

$$n\lambda = 2d_{hkl} \sin \theta,$$

where θ is the angle of diffraction, d_{hkl} is the spacing of the reflecting plane whose indices are hkl , λ is the wave-length of the X-rays. Knowing θ , R can be determined, and these values of R for the sodium-chloride lines were plotted against the distance of the line from the mid-point of the film, so that the values of R for the lines of the substance under investigation could be read off from the graph.

The value of a_0 , the side of the unit copper cube, was calculated from the expression

$$d_{hkl} = \frac{a_0}{\sqrt{h^2 + k^2 + l^2}}.$$

Several photographs were taken, using different samples of copper mixed with sodium chloride. The full results from one of these photographs are given in Table IV.

3. COPPER AMALGAMS.

The first paper of note relating to copper amalgams was due to Becquerel (*Comptes Rendus*, lvi. p. 237, 1863, and lxxv. p. 1729, 1872), who prepared the amalgam electrolytically and examined its structure microscopically. He stated that the amalgam crystallized in rhombohedral prisms with pyramidal ends.

Guntz and Greift (*Comptes Rendus*, cliv. p. 357, 1912) carried out an extensive research on the preparation of this amalgam, and came to the conclusion that the final product depended on the mode of preparation and on the conditions of the experiment. This has certainly been confirmed in the present investigation, as it has been found that the metals readily unite in all proportions.

Regarding the chemical nature of this amalgam, there has been much difference of opinion. Joule (*Jahr.* 1863, p. 281) and others considered the amalgam, prepared by

electrolysis and by dissolving copper in mercury, as a simple compound, CuHg , but the evidence for the individuality of this product is meagre.

Puschin (*Z. Anorg. Chem.* xxxvi. p. 241, 1903),¹ considerations of the E.M.F. of the cell $\begin{array}{c} \text{Cu} \\ \text{Hg} \end{array} | \text{N. CuSO}_4 | \text{Cu}$, concluded that no compound was formed.

TABLE IV.

Distance between corresponding lines.	R for NaCl lines.	R for Cu lines.	$\sin \theta$.	d_{hkl} .	Plane.	a_0 .
cm.	cm.	cm.				
* 15·537	3·0015					
14·795	...	3·005	·3338	2·081	111	3·603
14·336	...	3·006	·3697	2·0795	111	3·601
* 14·124	3·007					
13·599	...	3·008	·4269	1·801	100	3·602
* 12·969	3·008					
* 11·964	3·012					
11·110	...	3·009	·6034	1·274	110	3·602
* 10·997	3·0085					
10·574	...	3·011	·6391	1·087	311	3·604
* 10·098	3·013					
9·468	...	3·012	·7067	1·088	311	3·607
8·919	...	3·012	·7383	1·041	111 (2)	3·605

* NaCl lines.

Mean value..... 3·6035 Å.U.

λ_α for copper = 1·5374 Å.U.

λ_β „ „ = 1·3889 Å.U.

A final mean value for a_0 was determined from eight different films, giving the following result:—

$$= 3·603 \pm 0·002 \text{ Å.U.}$$

More recently two papers have been published by Tammann and Mansuri (*Z. Anorg. Chem.* pp. 132–33, 1923–24)* on the properties of various amalgams, including copper amalgam. From a study of the cooling curves, E.M.F., change of volume on solidification, and the microstructure of copper amalgams (1–90 per cent. Cu), it is concluded in

* Cf. also Tammann and Stassfurth, *Z. Anorg. Chemie*, p. 143 (1925).

the latter paper that two series of amalgams exist. On continued heating of an amalgam (5–78 per cent. Cu) at 100° C. a crystallite X is slowly formed. On cooling, a crystallite CuHg separates. At 20° C. neither of these forms is present, but another crystallite X' appears. The two latter differ from the first in that, when heated, drops of mercury exude from them. It cannot be said that the evidence for the existence of these "crystallites" is very conclusive, but it certainly seems probable that copper amalgam can exist in more than one form, since the amalgams when first prepared are quite soft, but on standing set to a hard mass.

The purpose of this investigation was therefore twofold: firstly to determine the structure of copper amalgam, and secondly to see if there was any change in structure when the amalgam was first prepared and after it had hardened.

Preparation of Copper Amalgam.

An amalgam containing any desired amount of mercury could be obtained by rubbing together, in a mortar under very dilute sulphuric acid, the requisite quantities of the two metals. The copper was prepared as in the previous investigation, and pure re-distilled mercury was used.

These amalgams, which are quite soft and pasty when the mercury content exceeds 50 per cent., become much harder on standing. Even an amalgam containing as much as 75 per cent. of mercury will set to a fairly hard mass within 12 hours of its preparation. When the mercury content is less than 50 per cent. the amalgams harden within 3–4 hours of their preparation.

The amalgams—powdered by the same process as was used for copper—were mixed with from 1–2 times their weight of finely-powdered sodium chloride and mounted in thin-walled celluloid tubes. This method of filling the tubes could not be followed in all cases, as the amalgams of high mercury content, when freshly made, were too soft to mix with the sodium chloride, and for these the amalgam was packed in one half of the tube and sodium chloride in the other half.

Experimental.

The apparatus was exactly the same as was used in the previous investigation.

A series of amalgams was prepared from 90 to 20 per cent. copper, and at least two photographs were taken of each, one immediately after its preparation and another a few days later, when the amalgam had hardened. For

these second photographs, fresh samples of the amalgam and sodium chloride were made. The composition of each amalgam was accurately determined by estimating the copper present volumetrically with potassium iodide and standard thiosulphate.

Results.

The results obtained for the series of amalgams containing from 90 to 20 per cent. of copper can be briefly summarized in Table V.

TABLE V.

Percentage of copper.	Freshly prepared.		Hardened amalgam.	
	Copper lattice.	Amalgam lattice.	Copper lattice.	Amalgam lattice.
89.....	Strong.	...	Strong.	Weak.
79.....	"	...	"	"
70.....	Fairly strong.	...	Fairly strong.	"
57.....	Medium.	...	Medium.	"
49.....	"	Weak.	Weak.	Medium weak.
40.....	"	"	...	Medium.
27.....	"	"
18.....	"	Medium weak.

This table shows that :—

1. The amalgams, when first prepared, are merely mechanical mixtures of the two metals, as in every case the diffraction pattern of copper was obtained on the film, and the intensity of the lines decreased with increasing mercury content. The appearance of a weak amalgam pattern in the freshly-prepared amalgams containing 40 and 49 per cent. of copper is probably due to the fact that these amalgams hardened in 3–4 hours, and the time of exposure was also of this order.

2. In the hardened amalgams a definite compound is found containing from 27–40 per cent. of copper. This pattern is masked in the amalgams of high copper content by the copper pattern.

However, in the above photographs there were never more than three or four lines measurable in the amalgam pattern,

although in the 40- and 27-per-cent. copper amalgams there were a number of lines faintly discernible on the films.

Several photographs were taken of the hardened amalgams of mercury content 50-70 per cent. to obtain a more distinct diffraction pattern of the amalgam. It was found that if the amalgam was prepared with a mercury content of

TABLE VI.

Amalgam. 32 per cent. Copper ; 68 per cent. Mercury.

Distance between lines.	Intensity.	d_{hkl} .
cm.		
15.957	v.w.	3.301
15.642	w.	2.977
*15.459	m.	
15.052	w.	2.512
14.953	w.	2.212
14.520	s.	2.212
14.249	v.w.	2.085
14.065	m.	2.006
*14.023	m.	
*12.846	w.	
12.603	w.	1.567
12.426	w.	1.526
11.870	w.	1.279
11.740	w.	1.393
11.546	w.	1.359
11.375	w.	1.334
11.019	m.s.	1.279
*10.879	m.	
10.375	w.	1.193
10.023	m.w.	1.153
*9.984	m.	
8.442	w.	1.012
8.139	w.	.991

* NaCl lines.

more than 70 per cent., and, after drying, it was compressed with the hand through fine-mesh cloth to remove the excess of mercury, an amalgam of composition ranging between 30 and 35 per cent. of copper was obtained. When photographs were taken of these powdered hardened amalgams, a large number of lines were visible and measurable on the films.

The results from two of these amalgams are given in Tables VI. and VII.

A photograph was taken of the pure hardened amalgam, and then of a mixture of the amalgam and sodium chloride, the object of this being to check the amalgam lines on the film of the amalgam-sodium chloride mixture.

The sodium-chloride lines were used, as before, to give an accurate measure of R , which was then employed in the determinations of d_{phl} for the amalgam lines.

TABLE VIII.

Amalgam. 34 per cent. Copper ; 66 per cent. Mercury.

Distance between lines.	Intensity.	d_{hkl} .
15.153	w.	2.522
14.953	w.	2.203
14.530	s.	2.207
14.269	v.w.	2.082
14.073	m.w.	2.001
*14.049	m.w.	
12.597	w.	1.559
12.443	w.	1.524
11.890	w.	1.279
11.744	w.	1.390
11.551	w.	1.356
11.370	w.	1.329
11.033	m.s.	1.279
*10.894	m.	
10.383	w.	1.193
10.050	m.w.	1.153
*10.012	m.	
8.453	w.	1.011

* NaCl lines.

The diffraction pattern given by this amalgam did not fit exactly any of Hull's plots (Phys. Rev. 1921, p. 17) for the simpler crystallographic systems, viz. the cubic tetragonal and hexagonal (including close-packed and rhombohedral).

The best fit that can be obtained is for a simple tetragonal lattice with axial ratio .64. The first five lines fit exactly, and almost all the others except the "2.006" line.

However, many more lines ought to be present which are not visible on the films, so that the most that can be done is to suggest this as a possible structure.

Conclusion.

It is evident that a change in structure occurs when the amalgam hardens; until this takes place the amalgams appear to be merely mechanical mixtures of the two metals. When the amalgam hardens, a definite compound is formed of composition 30–35 per cent. copper, and this compound is present all through the series of amalgams examined. Its structure cannot, however, at present be accurately determined, and it is only suggested that the amalgam possesses a simple tetragonal lattice with axial ratio '64, and possibly of composition Cu_3Hg_4 .

The Sir William Ramsay Laboratory
of Physical and Inorganic Chemistry,
University College,
London.

CV. *Proceedings of Learned Societies.*

GEOLOGICAL SOCIETY.

[Continued from p. 944.]

April 18th, 1928.—Prof. J. W. Gregory, D.Sc., F.R.S.,
President, in the Chair.

THE following communications were read :—

1. 'The Succession and Structure of the Borrowdale Volcanic Series in Troutbeck, Kentmere, and the Western Part of Long Sleddale (Westmorland).' By George Hoole Mitchell, Ph.D., M.Sc., F.G.S.

The area described lies in the eastern part of the Lake District south of the High Street range. It is drained by the Rivers Sprint, Kent, and Trout Beck, all of which flow in a southward direction.

The rocks described belong to the Borrowdale Volcanic Series. The estimated thickness of such members of the series as are exposed is approximately 3700 feet, but nowhere is the base seen. They are overlaid unconformably by the Coniston Limestone Series. Nine subdivisions are recognized :—

- (i) Upper Rhyolites.
- (h) Upper Andesites.
- (g) Coarse tuffs.
- (f) Wrengill Andesites.
- (e) Kentmere Pike Rhyolites.
- (d) Bedded tuffs, with andesite-flows.
- (c) Harter Fell Andesites.
- (b) Froswick Tuffs, with rhyolite-flow.
- (a) Nan Bield Andesites.

There are also minor intrusions of rhyolite, quartz-porphyry, andesite, and lamprophyre.

The lava-flows range in composition from rhyolites to augite-andesites. In most cases flow-brecciation is evident and marked, while many of the andesites are intensely vesicular.

The tuffs, composed in the main of andesitic material, show in many deposits rhyolitic fragments in abundance, and range from very fine-grained and well-bedded examples to ill-assorted agglomerates.

The rocks have been subjected to severe earth-movements. Two systems of folding are recognized, an earlier one of pre-Bala age and a later one of Devonian age. The former system, of simple character, shows axes trending in a north-north-easterly and south-south-westerly direction. In the latter the folding was intense, with an east-north-easterly and west-south-westerly strike, while the pitch of the folds was determined by the folds of pre-Bala date. The rocks are steeply folded in the south-east of the area, and the folds are even overturned to the north. Northwards the folding is less severe, and is marked by the presence of a broad anticlinal fold.

No faulting of earlier date has been recognized, but several faults are referred to the Devonian system of earth-movements, while it is suggested that several north-and-south faults are of late-Carboniferous age.

The rocks are strongly cleaved, the strike of the cleavage coinciding with that of the Devonian folding.

2. 'The Geology of the Marquesas Islands (Central Pacific). By Lawrence John Chubb, M.Sc.

The Marquesas Islands are situated in about 10° lat. S. and 140° long. W. With one doubtful exception all are of volcanic origin. The southernmost, Fatu Hiva, consists of a caldera composed chiefly of lava-flows, within which an ash-cone has been built up. The western half of the whole structure has disappeared, apparently owing to submergence by faulting. Motane is a small ash island. Tahuata is larger, and it also is composed chiefly of ashes in its northern part; its south-eastern side has been faulted down. In Hiva Oa there are three great craters in the western part, some of the coasts are faulted, and there is an elevated plateau at a height of 1300 to 1500 feet above sea-level. Nuka Hiva has a structure similar to that of Fatu Hiva, and it bears a plateau at an elevation of 2600 feet.

A consideration of the directions of elongation of the islands, of the manner in which they are arranged, of the trends of the faulted coasts, and of the strikes of the dykes, leads to the conclusion that the group is situated, not on a crustal fold, but on a system of intersecting fissures.

The uplifted plateaux prove that elevation has occurred, but the embayment of the mouths of the streams that deeply dissect them

Geological Features of the New Mersey Tunnel. 1071

affords evidence of a later subsidence. All the islands are surrounded by a shore-shelf, now standing, owing to a recent fall in sea-level, 3 or 4 feet above high-water mark.

It is suggested that the poor development of coral-reefs in the group is due chiefly to periodic chilling of the water by extensions of the cold Peruvian Current, connected with cyclic climatic changes.

May 23rd, 1928.—Prof. J. W. Gregory, LL.D., D.Sc., F.R.S.,
President, in the Chair.

Prof. P. G. H. BOSWELL, D.Sc., F.G.S., delivered a lecture on the Geological Features of the New Mersey Tunnel. He said that the recent 'holing-through' of the highway-tunnel under the River Mersey, by which connexion was established between Liverpool and Birkenhead, makes the present time appropriate for giving an account of the features of geological interest which were revealed. The tunnel will be the greatest subaqueous tunnel in existence. The predictions of T. Mellard Reade regarding the existence of a buried channel beneath the River Mersey, and of G. H. Morton of a sub-Mersey fault, were verified in the driving of the Mersey Railway-Tunnel some fifty years ago. Subsequent records by local geologists have enabled greater precision to be given to the inferences, and the geological observations made during the operations now proceeding are, in the main, in accord with expectation.

The subaqueous portion of the tunnel (44 feet in diameter) and the two Birkenhead approach-tunnels lie in the Middle Bunter Sandstone ('Pebble-Beds'), which dips eastwards at about 3° to 5° . A fault-system, apparently of small aggregate throw, was met with at about 1828 to 1870 feet from the Liverpool shaft. The hade was eastwards, whereas in the case of the sub-river fault in the Mersey Railway-Tunnel it was westwards. On the Liverpool side, the presence of the 'Castle Street Fault', which throws down the Upper (Soft) Bunter Sandstone on the east, was confirmed. At the Old Haymarket entrance another north-north-west and south-south-east fault throws eastwards, and brings Lower Keuper Sandstone into contact with Upper Bunter.

From observations in the area of the docks and the environs of Liverpool, and the numerous exploratory borings carried out in connexion with the tunnel-works, it has been possible to construct exceptionally accurate profiles of the system of buried channels. They appear to be of subglacial origin, and do not deepen seawards; they are filled with gravel and sand, overlaid by boulder-clay. In place of the single channel found in the Mersey Railway excavations, two (or more) feeding-channels occur farther north.

Interesting, and at present unexplained, features have been observed in the levels of underground water. As would be expected, the fresh-water table rides on the back of the salt-water table in the neighbourhood of the Mersey estuary.

June 13th, 1928.—Prof. J. W. Gregory, LL.D., D.Sc., F.R.S.,
President, in the Chair.

The following communications were read:—

1. 'A Re-Excavated Cretaceous Valley on the Mongolian Border.' By Prof. George Brown Barbour, M.A., Ph.D., F.R.S.E., F.G.S.

The paper traces the history of successive infillings and renewed erosion of a buried Cretaceous valley 600 feet deep, discovered by the author in the course of a survey of the Kalgan district, on the Chinese-Mongolian border. The valley, originally cut in pre-Cretaceous lavas, was completely filled by the Nantienmen Beds, levelled off by erosion, and entirely covered by a heavy capping of plateau-basalts.

During late Pliocene times a stream followed part of this old Mesozoic valley-axis before striking off at an angle. The valley-bottom was again filled up by wind-blown loess in mid-Pleistocene times, again partly excavated in late Pleistocene, and once more filled with very late Pleistocene or early recent gravels. At present, the course is being opened for the fourth time. The Cretaceous-valley deposit (Nantienmen Beds) has been left clinging to the side-walls in many places, so that it has been possible to trace the old landscape and to compare this with the present topography.

2. 'The Volcanic Complex of Calton Hill (Derbyshire).' By Sergei Ivanovich Tomkeieff, F.G.S.

The volcanic complex of Calton Hill shows two phases of vulcanicity:—

(i) Effusive phase—represented by, besides the agglomerate and tuff of the old volcanic cone, a highly decomposed lava. Petrologically and chemically it is comparable with the other contemporaneous Lower Carboniferous lavas of the district. The vesicles are filled up with a chlorite of delessite type.

(ii) Intrusive phase—represented by a fresh analcite-basalt, which has intruded into the old volcanic chimney and spread amœba-like in the volcanic cone, detaching large masses of vesicular lava. Besides abundant analcite, mostly in the form of spheroids, the basalt contains numerous inclusions of peridotite. These inclusions, apparently represent shattered fragments of a pre-existing rock, and contain, besides the normal pyroxene, a definite hydrous augite.

[*The Editors do not hold themselves responsible for the views expressed by their correspondents.*]

THE
LONDON EDINBURGH. AND DUBLIN
PHILOSOPHICAL MAGAZINE
AND
JOURNAL OF SCIENCE.

[SEVENTH SERIES.]

DECEMBER 1928.

CVI. *On the Capture of Electrons by Molecules.* By V. A. BAILEY, M.A., D.Phil.(Oxon), Associate Professor of Physics, University of Sydney, and J. D. MCGEE, M.Sc., Demonstrator in Physics, University of Sydney*.

1. **T**HE method of investigating the attachment of electrons to gas molecules which was described in a previous communication† has now been applied to the gases air‡, hydrogen chloride‡ and ammonia‡.

The seemingly anomalous behaviour of electrons in the last gas and the consequent desirability of using an alternative method of study, provided an inducement for designing and constructing an instrument in which the length c of each of the two diffusion chambers can be varied without affecting the pressure and purity of the gas contained in the instrument.

As will be seen, this elaboration of the original instrument in which c was fixed, enables a notably simpler procedure to be followed in deducing the circumstances of the electrons' behaviour from the observations.

2. *Description of the Instrument.*

Most of the important features of the new instrument are represented in fig. 1, but for the sake of clearness in the

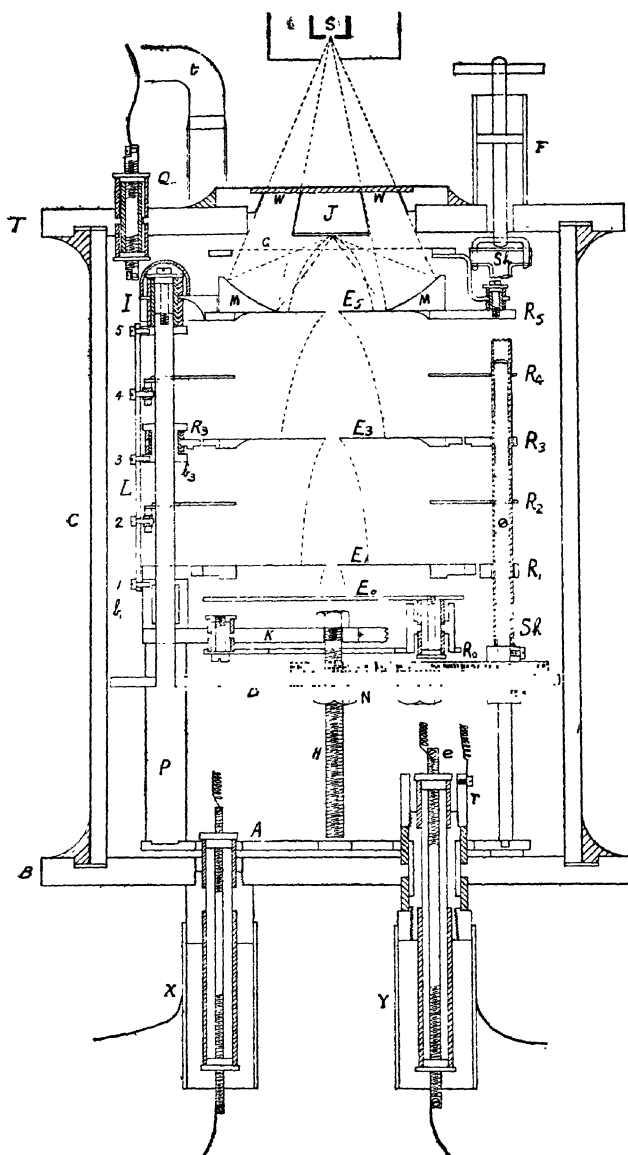
* Communicated by Prof. J. S. Townsend, F.R.S.

† V. A. Bailey, *Phil. Mag.*, Oct. 1925, p. 825.

‡ V. A. Bailey & A. J. Higgs, communicated to *Phil. Mag.* in July 1928.

diagram they are not all shown in their exact relative positions; the conducting parts are of either brass or phosphor-bronze, and the insulators of quartz or glass.

Fig. 1.



The plate B supports a glass cylinder C, insulated current leads like X and Y, and a disk A. Three parallel and

equidistant pillars, such as P, are fixed to the disks A and D, and to the ring R_5 by means of insulating systems like I.

Each pillar is fitted with brass bushes b_1 and b_3 , which enable the attached rings R_1 and R_3 to be moved vertically and not otherwise, R_3 being insulated from b_3 . A "lazy-tongs" system L is attached to each pillar by means of the pins 1, 3, and 5, which screw into b_1 , b_3 , and I respectively, these tongs carrying the rings R_2 and R_4 through pins 2 and 4 and tubular glass insulators. The bushes b_1 are also soldered to a plate K, shaped like an equiangular letter Y, which can be moved vertically by means of the rotation of a nut N acting on the rod H. This nut is turned by means of the shaft Sh through the gear-wheels shown, the shaft being engaged with a rod passing through the air-tight bearing F.

In this way the variable distances between the rings R_1 , R_2 , R_3 , R_4 , and R_5 are kept accurately equal.

Each of the electrodes E_1 and E_3 is supported and insulated from its ring R by three small quartz tubes, and each is connected to a rod e by a spiral spring of phosphor-bronze, its ring being connected to the corresponding guard-ring r .

The electrode E_0 is supported through insulators of tubular quartz by the ring R_0 , which in turn is insulated and supported from K.

A plate T rests upon C and carries four insulated leads Q, the quartz window W, the gas inlet-tube t , and the bearing F.

By suitably connecting the rings R and the gauze G to a battery of cells, a uniform electric field may be set up throughout the space between G and E_0 . The potential of T is adjusted so that an adequate stream of electrons passes through G towards the diffusion chambers, when ultra-violet light falls on the lower surface of the gold plate fixed to J. This light comes from a spark S through the window W, and is reflected on to J by the gold-plated annular spherical mirror M.

To reduce disturbance of the uniformity of the electric field by contact potentials, all the essential electrodes are gold-plated and polished.

The slits in E_5 , E_3 , and E_1 are respectively 1.5, 6.2, and 7.2 cm. long, and 4, 4.2, and 4.2 mm. wide. They were designed all to be 4 mm. wide, but the above errors in construction did not cause difficulty in the use of the instrument on account of the procedure followed with the experiments.

3. *Theory of the New Method.*

For the sake of convenience the relations established previously* are summarized here with the following notation :—

c = distance between successive slits, in cm.

p = pressure of gas, in mm. of mercury.

Z = electric intensity, in volts/cm.

S_1 = fraction of the stream approaching E_2 which passes through its slit.

S_2 = corresponding fraction for E_1 (S may be termed the distribution-ratio for its diffusion chamber).

R = the distribution-ratio with negative ions for either diffusion chamber.

k = mean energy of agitation of an electron in terms of the mean energy of agitation of a molecule at 15°C .

α = probability of attachment, of an electron to a molecule, per unit length of its motion in the direction of the field.

With the quantities c , p , and Z adjusted to known values, the ratios S_1 and S_2 are determined by measuring the mutual ratios of the currents i_0 , i_1 , and i_2 which arrive on E_0 , E_1 , and E_2 respectively. The normal distribution-ratio R can be determined as a known function of Z/c , either by calculation† or by experiments with pure hydrogen in the instrument; this function is represented by the curve in fig. 2.

S_1 and S_2 depend on three unknown quantities: k , α , and the electronic composition of the stream passing through the first slit; but the derived quantity

$$\alpha = S_1 \left(\frac{R - S_2}{R - S_1} \right)$$

is independent of the last factor, and can be expressed as a known function of k and α , namely:

$$\alpha = R(Z/kc)e^{-\alpha c} \dots \dots \dots (1)$$

To obtain another relation between k and α , the quantities

* *Loc. cit.*

$$\dagger R = \operatorname{erf}(v) - (1 - e^{-v^2}) / v\sqrt{\pi},$$

where $v = 1.34 \sqrt{Z/kc}$, and $k = 1$ for ions,

c , p , and Z are altered by the same factor n to the values nc , np , and nZ respectively, and the quantity a_n is determined experimentally as before. This gives

$$a_n = R(nZ/k.nc)e^{-na.nc},$$

since k and α/p depend only on the ratio Z/p ,

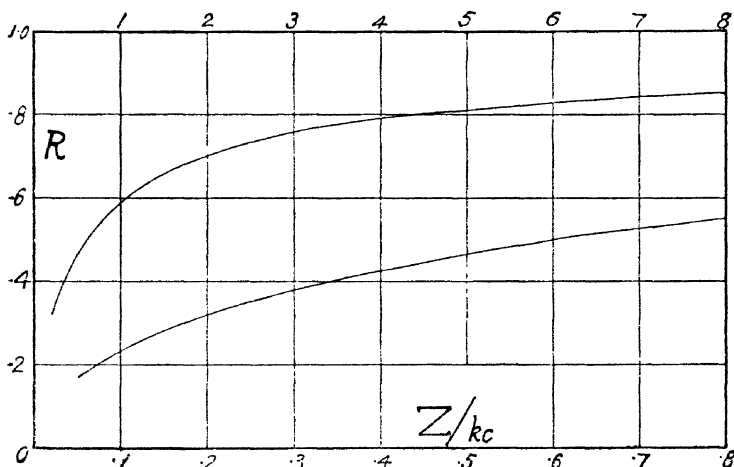
$$\therefore a_n = R(Z/kc)e^{-n^2\alpha c}. \quad . \quad . \quad . \quad (2)$$

From the simultaneous equations (1) and (2) we obtain

$$(n^2 - 1)\alpha c = \log_e(a/a_n),$$

$$R(Z/kc) = a^{\frac{n^2}{n^2-1}} / a_n^{\frac{1}{n^2-1}}.$$

Fig. 2.



The first of these gives the value of α , and the second, in combination with the curve in fig. 2, enables k to be determined.

But the following graphical method is to be preferred, for it supplies both a test of the theory and more accurate values of k and α .

Equation (2) may be expressed in the form :

$$y = -(\alpha c/2.3)x + (1 + \log_{10} R(Z/kc)),$$

where

$$x = n^2 \quad \text{and} \quad y = 1 + \log_{10} a_n.$$

So, if the values of y are determined experimentally for three or more values of x , and the points (x, y) are plotted,

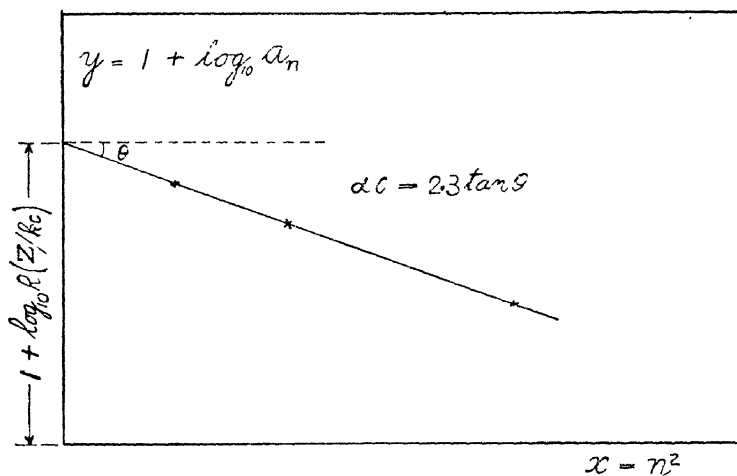
these should lie on a straight line whose slope gives $\alpha c/2.3$ and whose intercept on the y -axis gives $1 + \log_{10} R(Z/kc)$, as illustrated in fig. 3.

When many determinations are to be made, it is convenient to evaluate k by the help of a curve derived from fig. 2, whose abscissæ represent Z/kc and ordinates $1 + \log_{10} R(Z/kc)$.

4. Experiments with H_2 .

As a test of the instrument, pure H_2 gas was introduced up to various pressures, and with different intensities the ratios S_1 and S_2 were obtained; these ratios correspond to

Fig. 3.



known values of Z/kc since k is now well established* for H_2 , so a comparison with the theoretical values of R obtained from fig. 2 is made in the last three columns of Table I.

In general there is good agreement between the values of S_1 , S_2 , and R for the same value of Z/kc , the small differences being due partly to errors in construction of the instrument and to the fact that in the calculation of R it is difficult to determine the effect of diffusion to the edges of the slits, which may be appreciable with widely-spreading streams.

S_1 is consistently from 2 to 3 per cent. less than S_2 , so the simple theory of the last section requires to be modified as follows:—To each diffusion chamber corresponds a different

* J. S. Townsend and V. A. Bailey, Phil. Mag. xlii. (Dec. 1921).

normal distribution-ratio— R' for the upper, and R'' for the lower one. The quantity a is then given by

$$a = S_1 \left(\frac{R'' - S_2}{R' - S_1} \right),$$

and, in equations (1) and (2), R is replaced by R'' .

The numbers in the last three columns of Table I. show that for values of Z/kc greater than 0.75 the best values to adopt for R' are those given in the column under R , and for R'' the values of 1.02 R .

TABLE I.

<i>c.</i>	<i>p.</i>	<i>Z.</i>	<i>Z/p.</i>	<i>Z/kc.</i>	<i>S₁.</i>	<i>S₂.</i>	<i>R.</i>
cm.	mm.	volts/cm.					
4	2	10	5	.096	.197	.201	.228
4	4	10	2.5	.146	.252	.258	.277
4	8	10	1.25	.225	.319	.330	.336
4	8	20	2.5	.292	.359	.367	.377
4	16	20	1.25	.45	.434	.447	.448
4	32	20	.625	.75	.540	.548	.541
4	64	40	.625	1.537	.666	.689	.665
4	128	40	.312	2.8	.758	.780	.750
2	4	10	2.5	.292	.345	.353	.377
2	8	20	2.5	.585	.477	.486	.495
2	16	20	1.25	.90	.567	.571	.574
2	32	20	.625	1.50	.662	.672	.660

6. Experiments with NH_3 .

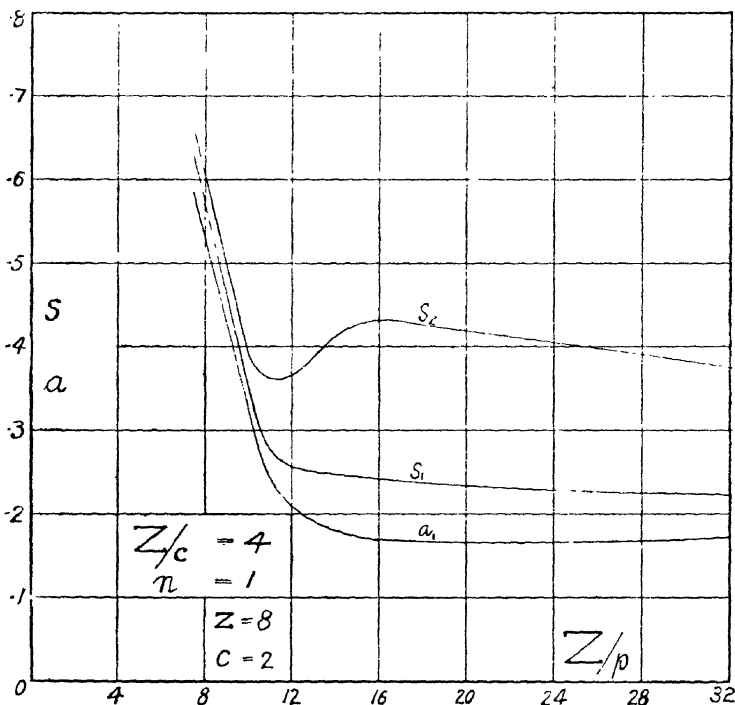
The gas was generated by heating a mixture of pure NH_4Cl and CaO in an evacuated flask to a temperature not exceeding $200^\circ C.$, and, after passing through a long tube packed with caustic potash, it was admitted to a freezing-trap, which was cooled to about $-78^\circ C.$ by a mixture of carbon dioxide snow and ether.

When about 4 litres had been so condensed, the freezing mixture was removed and part of the gas allowed to evaporate into a second trap, where it was similarly condensed. Without removing the freezing mixture the gas was then transferred by means of a mercury column pump to two flasks,

each of which contained a small quantity of anhydrous P_2O_5 , as supplied by Merck and Kahlbaum respectively.

A little later some liquid air was obtained, and this made possible a more effective fractional distillation of the remaining gas at lower temperatures. With this latter the pressure in the above two flasks was raised from 300 to 700 mm., and a third completely empty flask filled up to 700 mm. In order to obtain some information about the effect of the P_2O_5 on the gas in the first two, no drying agent was placed in the last flask.

Fig. 4 a.



During the first day there was a notable absorption of gas by the P_2O_5 , but the rate soon became small, and sufficient gas was left at the end of seven days to make all the observations required.

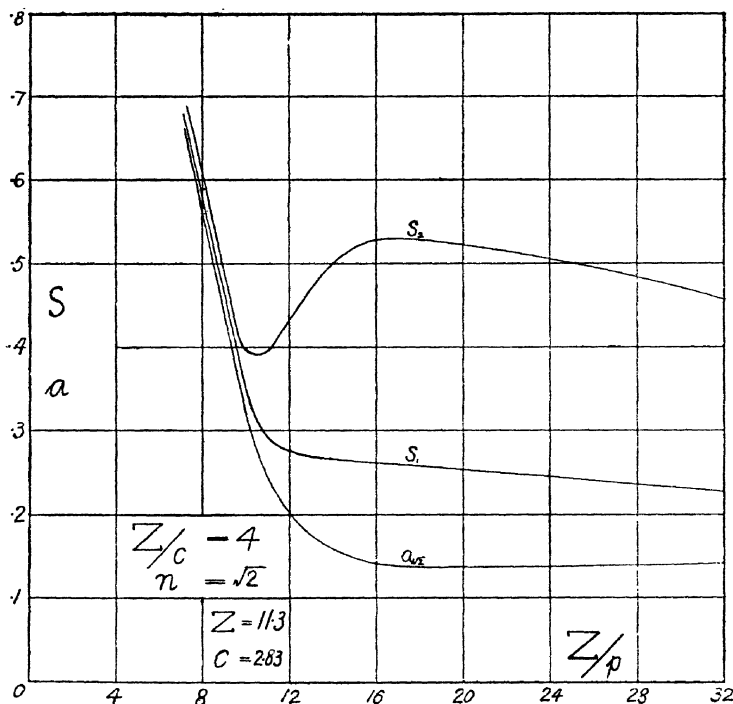
When the dry gas was admitted to the mercury gauges and diffusion instrument, it was found that the former were chiefly responsible for the loss of gas by adsorption, so the tap between the gauges and the instrument was turned off immediately after adjusting the gas-pressure, and after the observations the loss of gas in the gauges was restored

before this tap was turned again to verify that the gas in the instrument had not appreciably changed in pressure.

The first observations were made on a sample of gas from the flask which contained no drying agent, and as these were in substantial agreement with the results obtained for samples of NH_3 from the two flasks which contained P_2O_5 , the bulk of the work was carried out with the latter.

In general the electric intensity Z_g between the gauze G and the source of electrons J was kept approximately equal to the intensity Z of the uniform field extending between G

Fig. 4 b.



and E_0 , but at the higher pressures it required to be increased in order to maintain currents of magnitude sufficient for accurate measurements to be made. The possibility of this practice causing an error was examined by making observations with values of Z_g varying over a range so wide that the currents to the electrodes increased by a factor of about ten; c , p , and Z being kept unaltered.

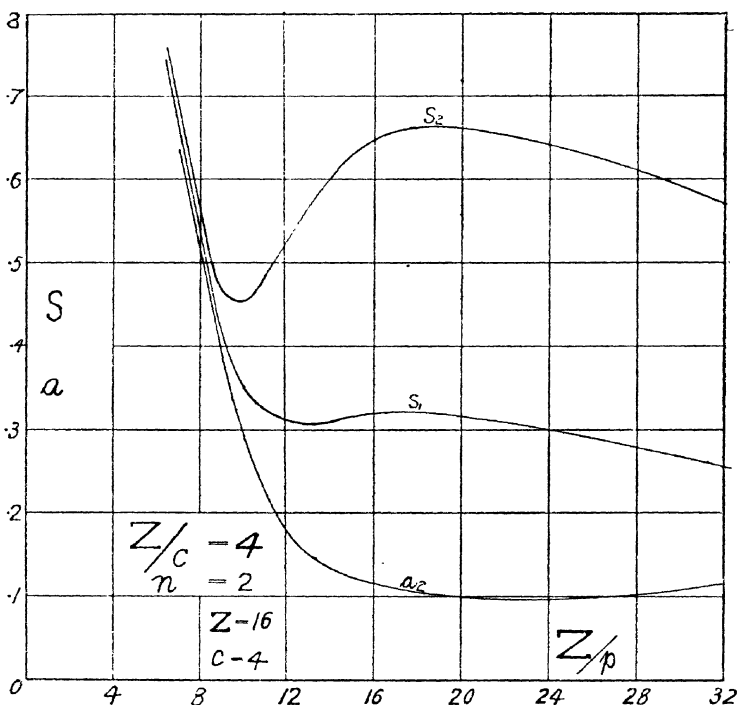
The ratios S_1 and S_2 varied with Z_g , but the quantity a calculated from their values remained constant within the limits of experimental error, which result is in agreement

with the theory, and also renders valid the method of securing convenient currents by variation of Z_0 .

With the three variables c , p , and Z there are several ways of carrying out the work so as to apply the method described in Section 3, but the following plan was found to be the most convenient in practice :—

With the electric intensity Z and the chamber length c kept constant the pressure p was varied, and at the values 8, 10, 11.3, 14.1, 16, and 32 of the ratio Z/p the values of S_1 and S_2 were determined and plotted against Z/p , as shown.

Fig. 4c.



in fig. 4a, which corresponds to $Z=8$ and $c=2$. Similar curves are obtained with Z and c both increased by a factor n , as shown in figs. 4b and 4c, which correspond respectively to the factors $\sqrt{2}$ and 2.

Since Z/c for all the observations has the same value 4, to which correspond $R' = .790$ and $R'' = .810$ (from fig. 2), the values of a_n are given by

$$a_n = S_1 \left(\frac{.810 - S_2}{.790 - S_1} \right).$$

The numbers calculated in this way are represented by the lowest curve in figs. 4 *a*, 4 *b*, and 4 *c*.

It is evident from the curves for *S* that in the neighbourhood of the value 8 of *Z/p* there are very few ions present, and also that *k* must be increasing rapidly between the values 8 and 10. On the other hand, the striking increase of *S*₂, and the large separation of the *S*-curves between the

Fig. 5.

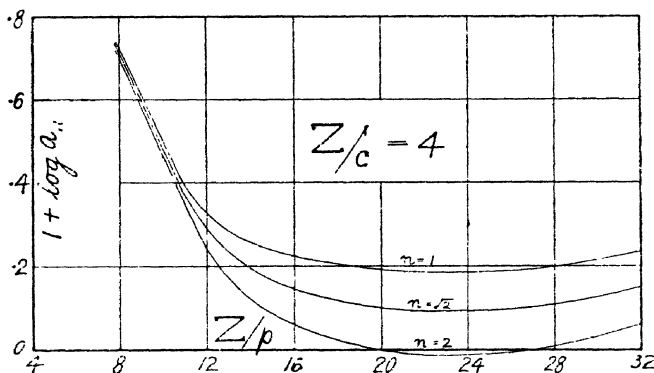
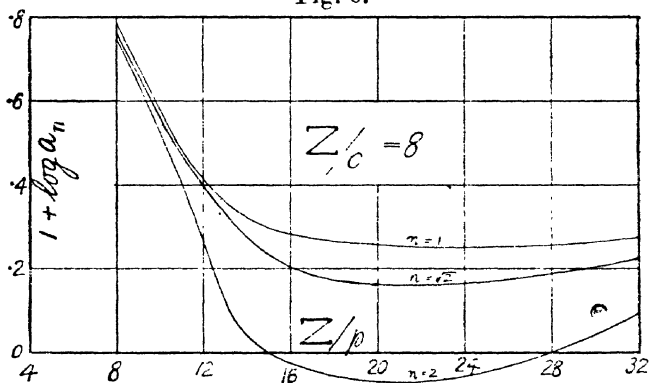


Fig. 6.



values 10 and 16 of *Z/p* indicate a rapidly increasing proportion of ions in the currents. For any given value of *Z/p* greater than 10 the curves for *S*₂, *S*₁, and *a* become further separated as *n* varies from 1 to 2, which is in accord with the conclusion that *α* increases with *p* if *Z/p* remains constant.

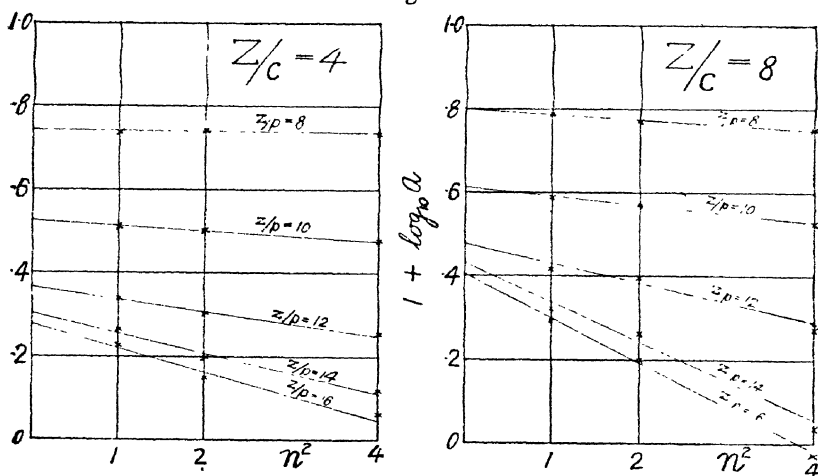
These inferences by inspection are completely confirmed by the quantitative determinations of *k* and *α* given below.

The values $1 + \log_{10} a_n$, obtained from the curves for *a_n*, are represented by curves in fig. 5, which thus correspond to $Z/c=4$.

In order to provide a further test of the reliability of these methods, another complete series of observations was obtained corresponding to $Z/c=8$; that is, curves were obtained similar to those shown in figs. 4 *a*, 4 *b*, and 4 *c*, but with the values of Z fixed at 16, 22.6, and 32, and with pressures of the gas which were twice as large. To save space these are not given, but the corresponding curves for $1 + \log_{10} a_n$ are shown in fig. 6.

With the help of the curves in fig. 5 (or fig. 6) the graphical method given in section 3, and illustrated by fig. 3, was now applied to the determination of the values of k and α corresponding to sets of experiments, the process being shown in fig. 7.

Fig. 7.



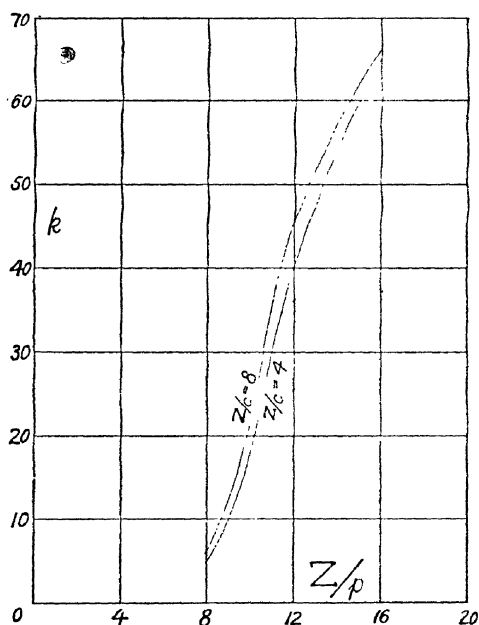
As an actual example we may consider the determinations for $Z/p=12$ with $Z/c=4$. From fig. 5, corresponding to $Z/p=12$, the values of $1 + \log_{10} a_n$ are 3.40, 3.08, and 2.55 for $n=1$, $\sqrt{2}$, and 2 respectively. As shown in fig. 7, points are plotted with these for ordinates, and $n^2=1$, 2, and 4 respectively for abscissæ, and the straight line marked " $Z/p=12$ " is then drawn to lie evenly between the plotted points.

Since the slope of the line is .0282, and c has the value 2, α must be given by $2.3 \times .0282/2$; that is, α is equal to .0324; the value of p being $2 \times 4/12$, therefore $\alpha/p = .0486$.

The line cuts the vertical axis at .367, which must then be the value of $1 + \log_{10} R(Z/kc)$. This gives .233 for $R(Z/kc)$, and thus with the assistance of fig. 2, k is found to be 40.

The values of k and α/p so determined are represented by curves in figs. 8 and 9. In each diagram there is good agreement between the curves obtained under the different conditions represented by the ratios Z/c , despite the facts which are now disclosed : that k and α/p change very rapidly with Z/p in the region under examination. This agreement, and the collinearity displayed in fig. 7 between the three points in each set, may be regarded as experimental confirmation of the theory in section 3, which is now seen to be applicable to NH_3 up to $Z/p=16$.

Fig. 8.



The effect of calculating the values of k by means of the distribution-ratios obtained with H_2 (section 4), instead of calculating by the curve in fig. 2, was to lessen the concordance between the upper parts of the two curves for k , but the results are not substantially different from those shown in fig. 8. The values of α , however, depend only on the upper parts of the distribution curves ($Z/kc > .75$), which agree well with the ratios obtained with H_2 .

For $Z/p=32$ there is some discordance between the results determined with the two different values of Z/c . The present theory may commence to become inapplicable to NH_3 in this region on account of the effects of ionization by collision of

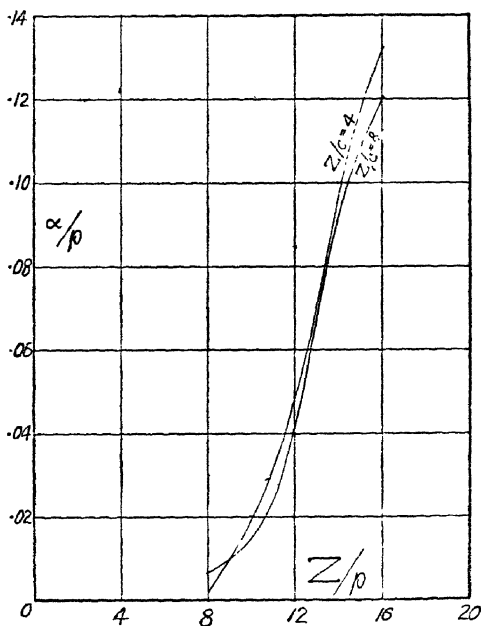
electrons with molecules, which are known to become appreciable in some gases under similar conditions; for example, in H_2O the current would increase by about 5 per cent. between successive slits with this value of Z/p and a pressure of 1 mm. So no deductions are made from the observations with $Z/p=32$.

5. Conclusions.

The probability h of attachment at a collision may be estimated by means of the formula *

$$h = 11 L^2 (\alpha/p) (Z/p) / k$$

Fig. 9.



if the mean free path L , of an electron at 1 mm. pressure of gas, be deduced from measurements of the viscosity of NH_3 . Accordingly, from Roth and Scheel's 'Konstanten der Atomphysik,' $L = 2 \times 10^{-2}$ cm.; and since from figs. 8 and 9 with $Z/p=12$, $k=43$, and $\alpha/p=.045$,

$$\therefore h = 5 \times 10^{-5} \quad \text{when} \quad k=43.$$

This method, however, is not a reliable one by which to examine the dependence of h on the energy k of the electron,

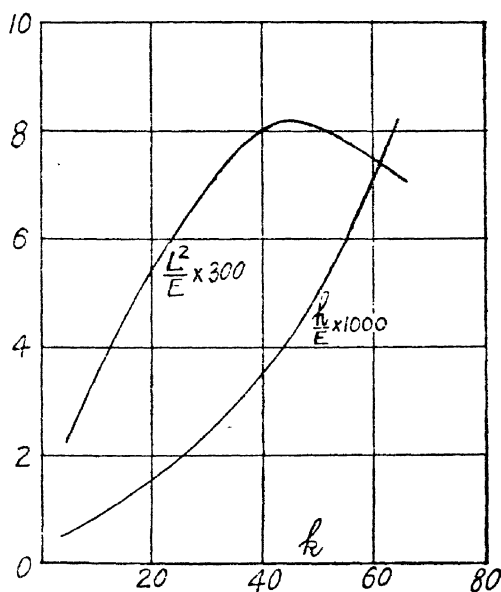
* Deduced from the relations $\alpha = hu/1W$ and $W = .815 \text{ ZeI}/mu$.

as it is known that L itself may vary considerably with k ; so the following argument is to be preferred :—

If E denote the energy (in volts) lost by an electron at a collision with a molecule, then for a given gas E is a function of k alone. The number ν of collisions made by an electron which travels 1 centimetre along the direction of the electric field, in the steady state of motion, is such that the work Z (volts) done by the field is equal to the energy lost in these collisions.

$$\therefore \nu E = Z.$$

Fig. 10.



The probability of attachment in this distance is represented by α and also by νh .

$$\therefore \nu h = \alpha;$$

$$\therefore h/E = \alpha/Z = (\alpha/p)/(Z/p).$$

The values of h/E for different values of k may then be determined from the curves in figs. 8 and 9, and represented by a curve as in fig. 10.

— This shows that as k increases from 5.5 to 64 the ratio h/E also steadily increases from 6×10^{-3} to 8.1×10^{-3} , i. e. by a factor of about 14.

It is easy to show that *

$$E = 7 \times 10^{-16} W^2 \text{ volts}$$

where W is the velocity of the stream of electrons in the direction of Z ; and as none of the many experiments made to date in different gases † has revealed an instance where W decreases as k increases, it may be concluded generally that E never diminishes as k increases ‡. It then follows that in NH_3 h increases by a factor not smaller than 14 when k varies from 5.5 to 64.

Some information concerning the variation of the mean free path L may be obtained in a similar way from a curve whose ordinates represent L^2/E , since it is easy to deduce from the above expressions for h and h/E that

$$L^2/E = k/11(Z/p)^2,$$

and so to determine this curve (fig. 10) by means of fig. 8.

This curve indicates that, as k increases from 5.5 to 45, the ratio L^2/E increases from 2.34 to 8.2, and as E is not diminishing, it follows that L^2 increases in this range by a factor of at least 3.5.

The conclusion that h may vary considerably with k in NH_3 and in air § makes it certain that the method used by L. B. Loeb || and H. B. Wahlin is liable in general to give erroneous results, for it depends on the assumption that h is a constant characteristic of the gas alone. There are other weaknesses in this method, some of which have already been pointed out ¶, so in referring to the table on p. 513 of his book, in which are given the values of $n(=1/h)$ obtained with this method, he states: "It is questionable whether the values are accurate in more than order of magnitude. They do differ, however, so widely in order of magnitude that even these crude early results give a good idea of n ." Further on he adds: "While these results are not of more than qualitative value. . . ."

We are inclined to doubt whether they even "give a good idea of n " on comparing Wahlin's value 10^{-8} for h in NH_3 with our lowest value, which is about 2×10^{-5} ; these are by

* J. S. Townsend and V. A. Bailey, *Phil. Mag.*, Nov. 1922, p. 1045.

† H_2 , O_2 , N_2 , He , A , Ne , CO , CO_2 , NO , N_2O , C_2H_4 , C_6H_{12} .

‡ The experiments of Townsend and Glasson, which might indicate the contrary, correspond to very different conditions, where the energies cause intense ionization by collisions.

§ V. A. Bailey, *loc. cit.*

|| L. B. Loeb, 'Kinetic Theory of Gases,' p. 510.

¶ V. A. Bailey, *Phil. Mag.*, July 1923.

no means of the same order of magnitude. To explain this discrepancy by assuming that our gas contained more of potent impurities than his, requires that ours should have contained a proportion of these at least 1000 times greater than did Wahlin's; there is, however, no reason to suppose that our samples of NH_3 were less pure than his. On the other hand, if it be argued that the disagreement is attributable to the difference in the energies of the electrons, then it has to be admitted that when the mean velocity of the electrons changes from 1.1×10^7 to about 2.6×10^7 cm./sec., the probability of attachment h increases by a factor of at least 1000; a change of such magnitude cannot be ignored, even if only "qualitative" results are sought. Since Loeb admits (p. 513) the greater reliability of the methods we have used, it would appear that the results obtained with his method, and set out in his table, may be quite misleading.

E. M. Wellish* has expressed the view that "an electron cannot effect a permanent union with an uncharged molecule to form a negative ion unless the relative velocity at collision exceed a critical value characteristic of the molecule concerned.... It is probable that the circumstances of an encounter as well as the relative velocity will determine the effectiveness of a collision so that only a fraction of these impacts will result in the formation of ions."

We are unable to see the necessity for his assumption of a minimum critical velocity, for the experimental facts he adduced in support of it can be understood from our point of view without requiring any additional hypothesis.

The NH_4Cl and CaO used was very kindly prepared for us by Mr. G. J. Burrows, of the Department of Chemistry.

We are also much indebted to the Colonial Sugar Refining Co., Ltd., for the supply of carbon-dioxide snow, and to the Commonwealth Oxygen & Accessories Co., Ltd., for the supply of liquid air, both without cost to the University.

It is to be hoped that their example will find imitators in Australia, where the policy adopted with striking success by the industries of other countries, of assisting research in pure and applied science, is still somewhat disregarded.

In conclusion we desire to record our appreciation of the skill and resource shown by Messrs. G. C. Barnes and H. Taylor in the construction of the apparatus used in this work.

* E. M. Wellish, *Am. Journ. Sci.* xliv. p. 26 (July 1917).

CVII. *Spark Ignition.* By E. TAYLOR JONES, D.Sc.,
*Professor of Natural Philosophy in the University of
 Glasgow*.*

[Plates XXI. & XXII.]

THE substance of the following communication was contained in a lecture to Section A of the British Association at Glasgow on September 10th, 1928. The chief topics discussed are the nature of the action of an electric spark in producing ignition of an inflammable gaseous mixture, and the conditions which determine whether a spark will or will not ignite a given mixture.

One of the earliest experimental results published on this subject was the observation by Thornton † that the heat dissipated in a spark just sufficient to cause ignition is less if the spark is produced by the discharge of a condenser than if it is produced (as in "low tension" or "inductance" sparks) by separating the electrodes from contact so as to interrupt a current in an inductive circuit. An explanation of this result, based on the view that spark ignition depends upon the volume of the gas which the spark can by its own heat raise to the ignition temperature ‡, was suggested by Taylor Jones, Morgan, and Wheeler §. A condenser spark of very short length between metal points being regarded as an instantaneous point source of heat in a uniform medium, the temperature θ in its neighbourhood is represented by Fourier's expression

$$\theta = \frac{Qe^{-r^2/4kt}}{8c(\pi kt)^{3/2}}, \quad \dots \dots \dots (1)$$

* Communicated by the Author.

† Phil. Mag., November 1914.

‡ See Wheeler, Trans. Chem. Soc. cxvii. p. 903 (1920); also the 'Third Report of the Explosions in Mines Committee of the Home Office,' 1913. The argument for this view may be stated as follows:—If we suppose that a small spherical volume of the gas is heated by the spark to the ignition temperature, the gas within this volume is burnt, and its temperature is raised further by the heat resulting from the chemical action. At the surface of the sphere there will, therefore, be a large temperature gradient and rapid loss of heat by conduction. The rate of cooling of the sphere due to this cause is proportional to the ratio of its surface to its volume, and is very great if the sphere is very small. Consequently the small flame started in the sphere will soon become extinguished by the conduction from its surface, and will therefore fail to spread throughout the gas, unless the volume of the sphere exceeds a certain minimum value.

§ Phil. Mag., February 1922.

in which Q is the quantity of heat dissipated in the spark, k is the thermometric conductivity, and c the thermal capacity per unit volume of the gas (supposed uniform), r is the distance from the source, and t is the time after the moment at which the heat is communicated. If an inductance spark be regarded as a source in which the heat is supplied to the gas at a uniform rate over an interval of time T , the temperature distribution may be deduced from (1) by integration. In the paper cited the results of numerical calculations based upon (1) were given, which showed that in the case considered the volume of the spherical portion of the gas, the boundary of which was just raised to a certain temperature, was greater in the case of the instantaneous source than in that of a source in which the heat supply was continued at a uniform rate for a finite interval of time, the total heat supplied being the same in both cases*.

The general proof that this result holds also for a point source in which the heat Q is supplied over a finite interval of time, whether uniformly or not, may be arrived at in the following manner:—In fig. 1 let curve A † represent the form of the temperature wave (θ, t) at any distance r from an instantaneous point source. The temperature at this distance rises rapidly to a maximum and falls more slowly from it. The maximum temperature is attained at the time $t=r^2/6k$, and is higher the shorter the distance r from the source, being, in fact, inversely proportional to the cube of the distance from the source, as may be seen by substituting this value for t in (1).

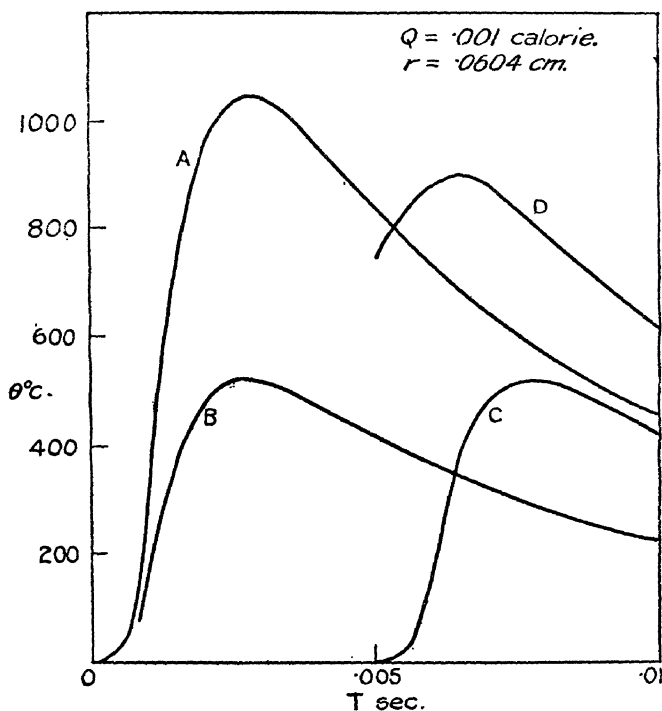
If we now suppose that the heat Q is communicated in two equal parts at an interval of time T (represented in fig. 1 by 0.005 sec.), the temperature at the same distance is given by the sum of the ordinates of the two curves B and C, each of which has one-half the amplitude of A. The maximum in the resultant curve occurs at a time shortly before the maximum of the second component, and it is evident that the resultant maximum is smaller than the sum of the maxima of the two components, and therefore than the maximum of

* Coward and Meiter have recently (Journ. Amer. Chem. Soc. xlix. p. 396, 1927) determined experimentally the least volume which must be heated, by a condenser spark in a methane-air mixture, to the ignition temperature in order to ensure general inflammation, and found that the volume is of the same order of magnitude as that calculated from the expression (1).

† Curve A in fig. 1 is calculated from the expression (1) with $Q=0.001$ calorie, $r=0.0604$ cm., $k=0.2188$, $c=0.00032$. The maximum temperature is 1044° C. at $t=0.002779$ second.

the original curve A. The resultant maximum also evidently diminishes as the interval of time between the two components increases. We may conclude that the result of dividing the heat supplied into two equal instalments separated by any finite interval of time is to lower the maximum temperature at any given point in the neighbourhood. Similar considerations show that the same result holds if the two instalments are unequal, also if the heat is divided into three or more instalments, equal or unequal,

Fig. 1.



supplied at equal or unequal intervals of time. The limiting case of a continued source, *i.e.*, a very large number of infinitesimal instalments following one another at infinitely short intervals of time, is also included. Curve D in fig. 1 shows a portion of the temperature wave at the same distance from a point source of the same total heat, but in which the heat supply is continued uniformly for 0.005 second.

The general result may be stated as follows:—If a given quantity of heat is supplied at a point of a uniform conducting medium in any manner during a finite interval of

time, the maximum temperature at any neighbouring point is lower than it would have been if the heat had been supplied all at the same instant.

By considering the distance from the source at which the temperature just rises to a given value, instead of the maximum temperature at a given distance, we arrive at the following corollary to the above theorem:—If a given quantity of heat is supplied at a point of a uniform conducting medium in any manner during a finite interval of time, the volume of the medium, the boundary of which is just raised to any given temperature, is smaller than it would have been if the heat had been supplied all at the same instant. This follows from the theorem and the result, previously stated, that for instantaneous sources the maximum temperature diminishes with increasing distance from the source.

The introduction of “volume” instead of “distance” in the corollary follows from the assumed uniformity of flow of heat in all directions. Since, however, the proof of the theorem does not depend upon the precise form of curve A in fig. 1, the theorem and its corollary are applicable to the case of a point source in a conducting medium between two plane parallel non-conducting walls at a short distance apart, or to that of a point source in a thin column of conducting material bounded laterally by non-conductors. If in these cases the bounding walls were made conducting some of the heat would enter the walls and would thus be lost to the medium between them, but since there seems to be no reason for supposing that the medium would lose more heat in this way with the instantaneous source than with the divided or continuous source, we may assume the theorem and its corollary to hold also in this case.

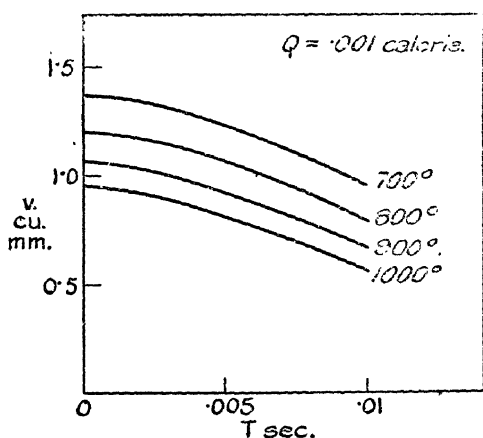
The magnitude of the effect of the duration of the heat supply is illustrated by the curves in fig. 2, in which the ordinate represents the volume of gas, the boundary of which is just raised to a definite temperature by a point source of heat continued at a uniform rate for a time T represented by the abscissa. The volumes are calculated, from the integral of the expression (1)*, for four temperatures (within the range of the ignition temperatures of methane-air mixtures), the values assumed for the constants being those given in the second footnote on p. 1091. It will be seen that the volume is greatest for an instantaneous source ($T=0$), and that it diminishes steadily as the duration of the heat supply is

* See Phil. Mag. p. 364, February 1922.

increased. The same holds when the heat supply, instead of being continued uniformly for time T , is divided into a given number of equal instalments supplied at equal intervals over this time. It is the increase in the total duration of the heat supply, rather than an increase in the number of instalments, which causes the reduction in the volume raised to the given temperature. An increase in the number of instalments (supposed equal and equally spaced in time), without increase in the total duration, has the opposite effect.

According to the hypothesis that ignition depends upon the volume of the gas which is raised to the ignition temperature, it follows from the corollary stated above that an instantaneous point source of heat is more effective in ignition than

Fig. 2.



a point source in which the heat is supplied in any manner (continuous or discontinuous) over a finite interval of time.

Experimentally it is easy to produce sources of approximately the same total heat, but having different time distributions, by connecting a condenser of variable capacity to the electrodes of a spark-gap connected with the secondary of an induction coil fed with a primary current which has a constant value at the moment of break. With a large value of the secondary capacity a single spark is obtained, and as the capacity is diminished the discharge produced by each interruption of the primary current divides into two, three, or more sparks. When the secondary condenser is disconnected we have the ordinary induction coil discharge consisting of a preliminary spark followed by a continuous but pulsating and decaying arc.

In fig. 3 (Pl. XXI.) are shown six induction coil spark discharges produced in this way, between the ends of two wires at a very short distant apart, and photographed with the aid of a rotating mirror. That the energy dissipated in the six discharges was approximately the same is a consequence of the fact that the primary current at break, and therefore the energy supplied to the system, was the same in all. Calorimeter measurements of the heat of the sparks in such experiments also show that it is practically independent of the secondary capacity*.

An experiment described by Morgan† shows that the effectiveness of a magneto spark in ignition increases with the capacity of a condenser connected with the spark-gap electrodes. This result is in agreement with the theoretical views described above, since the total duration of the discharge in general diminishes as the secondary capacity is increased (see fig. 3, Pl. XXI.).

A simple form of explosion vessel which the present writer has found suitable for illustrative experiments on spark ignition consists of a strong glass tube of uniform bore, about 16 inches long and $1\frac{1}{4}$ inches internal diameter, slightly constricted at the upper end in order to hold firmly a plug of insulating material which closes the tube at this end and carries a gas inlet-tube and the electrodes of an adjustable spark-gap. A piston of felt, movable easily in the glass cylinder, is fitted to the end of a long brass tube of $\frac{1}{4}$ in. diameter which acts as air inlet. The glass cylinder is fixed firmly in a vertical position, the brass tube passing through a guide about 2 inches below the lower end of the cylinder. The upper surface of the guide also acts as a buffer from which the piston rebounds after the explosion. A scale of inches runs along the length of the cylinder, to measure the air introduced, the uppermost inch being divided into tenths for the measurement of the volume of gas admitted‡. A magneto (or an induction coil) and a condenser connected with the spark electrodes complete the apparatus. The piston is first set at a suitable mark near the top of the cylinder, gas is admitted for a short time and is then cut off

* A form of calorimeter suitable for comparative measurements of the heat of sparks consists of a gas thermometer the bulb of which contains the spark-gap. The deflexion of the liquid column produced by a series of sparks, and measured from the zero observed after sparking has ceased, gives a measure of the heat produced in the sparks.

+ 'Electric Spark Ignition,' pp. 31, 32 (1920); 'Engineering,' Nov. 3, 1916.

‡ Explosion tubes of this form were used for illustrating the lecture in Glasgow.

by a stopcock in the gas inlet-tube. The piston is drawn down to a suitable distance (depending upon the strength of mixture required) and a stopcock near the lower end of the air inlet-tube is then closed. A half turn of the magneto armature (giving one break of the primary circuit) produces the spark, and if the mixture is such that an explosion of sufficient violence results, the piston is blown out of the cylinder and after the rebound re-enters the cylinder to a certain distance. A scale of tenths of an inch may be marked on the cylinder at the lower end to indicate this distance, which gives a measure of the impulse of the explosion*.

By means of this apparatus the igniting action of sparks of different kinds between electrodes of different forms can be conveniently studied, and the superiority of a condenser spark over the ordinary magneto spark (*e. g.*, with pointed electrodes of steel or tungsten), indicated by the above theory, can easily be demonstrated.

Ignition by Short Sparks between Spherical Electrodes.

When ignition experiments are tried with short sparks between spherical electrodes of metal †, a number of results are found which appear, at first sight, to be contrary to the thermal theory. In the first place ignition is difficult and very erratic unless the metal surfaces are clean. It is scarcely to be expected, however, that the loss of heat which undoubtedly takes place by conduction from the gas to the electrodes would be less when these are clean than when they are covered with a layer of oxide or other substance of smaller conductivity than the metal. The result, therefore, seems to point to some action other than thermal as the cause of ignition. Further, when different metals are used as electrodes the igniting effect does not seem to depend appreciably upon their thermal conductivity. In making this comparison care should be taken to use electrodes of the same curvature (since the igniting power of the spark increases with their curvature), and they should be well cleaned before the experiment. In this way curved surfaces of copper, steel, and zinc were found to be equally effective in ignition, *i. e.*, to be just capable of igniting a given

* The pressure developed in an explosion is usually independent of the nature and intensity of the spark, so long as the spark is sufficient to produce an explosion at all (see Morgan, 'Electric Spark Ignition,' p. 15).

† Short cylinders of about 8 mm. diameter, having spherical ends of about 1 cm. radius of curvature, and placed so as to form a gap 0.15 mm. wide at its narrowest part, were used in most of the experiments described in this section.

mixture when the sparks were of the same kind and length, and were produced by the interruption of the same primary current. Of the metals examined (copper, steel, zinc, platinum, lead) lead was found to be the most suitable for ignition experiments; the surface of this metal is less easily spoilt by the tarnishing due to the sparks or to the flame. Carbon electrodes, though not so effective in ignition as those of clean lead, are also suitable because they do not require to be cleaned as do metallic surfaces.

Another result which appears to be contrary to the thermal theory is found when the effect of connecting a condenser to the spherical electrodes is examined. With electrodes and gap of the dimensions stated above, the effect of the condenser is exactly opposite to that observed when pointed electrodes are used. The condenser produces a decided diminution in the igniting power of the spark, and the inferiority of the condenser spark with the spherical electrodes is quite as marked as its superiority when the electrodes are metal points. In one experiment, with spherical carbon electrodes, ignition without the condenser occurred at a primary current of 0.7 ampere; with the condenser ignition failed at 10 amperes, *i. e.*, with a spark of nearly 200 times as much energy.

This result is directly contrary to that derived from the theory of thermal conduction from point sources, and we must conclude either that the thermal theory is wrong, or that some other action takes place, when spherical electrodes are employed, which is of such greater influence in ignition than thermal conduction as to mask its effect.

For the further investigation of this matter some photographs of the sparks between spherical electrodes were taken, six specimens of which are shown in fig. 4 (Pl. XXI.). These sparks were produced, by a magneto, between lead cylinders 8 mm. in diameter, the spherical ends of which were set at 0.15 mm. apart. The camera used in photographing them had a quartz lens of 15.6 cm. focal length, the linear magnification being 1.5 cm. The sparks shown in fig. 4 (Pl. XXI.) are "ordinary" magneto sparks, no condenser being connected with the electrodes.

An examination of fig. 4 (Pl. XXI.) shows that the ordinary spark between spherical electrodes differs in one important particular from the usual short spark which we have regarded as a point source. The discharge begins at the centre (*i. e.*, the narrowest part) of the gap, but some portion of it spreads towards the sides, and in spreading it lengthens so that it can no longer be regarded as even approximately a

point source*. The spreading of the discharge over the surfaces of the electrodes does not occur when a condenser of considerable capacity is connected with them. In fig. 5 (Pl. XXI.) are shown seven induction-coil sparks between the lead cylinders, the gap in each case being placed centrally just above a Meker burner†. The first five passed while a condenser was connected with the terminals; they show no spreading and they failed to produce ignition‡. The sixth and seventh sparks were produced after the condenser was disconnected; of these the sixth shows spreading and produced ignition, the seventh shows no spreading and failed to ignite. The primary current interrupted was the same in all seven.

In fig. 6 (Pl. XXII.) are shown seven magneto sparks between spherical electrodes of platinum. Of the seven only the second and the fifth show evidence of spreading, and only these two produced ignition.

The conclusions to be drawn from an examination of these photographs, and a number of others of a similar kind which were taken, are that, in the case of short sparks between spherical electrodes of metal or of carbon:

- (1) the ordinary high-tension discharge (without secondary condenser) tends to spread from the centre towards the sides of the gap when the electrodes are of carbon or of clean metal;
- (2) the tendency to spread increases with the primary current;
- (3) the spreading does not occur, or occurs much less readily, over metal surfaces which are not clean;
- (4) ignition does not occur, or occurs only with great difficulty, unless the discharge spreads;
- (5) ignition does not always occur if there is spreading.
- (6) spreading does not occur if a condenser of considerable capacity§ is connected with the electrodes.

* That the spreading is not an effect caused by gaseous combustion is shown by the fact that the discharges in fig. 4 (Pl. XXI.) took place in ordinary air free from inflammable gas.

† Ignition experiments with a burner may be made either while the gas is flowing or in the still gas which remains above the burner for a short time after the gas is turned off. A large Meker burner is the most suitable for the purpose.

‡ Owing to the much greater brightness of the condenser sparks the aperture of the lens was reduced to its minimum for the first five sparks. Their images are, however, still rather enlarged by halation.

§ The capacity must be sufficiently large to prevent the formation of an arc instead of a single or multiple spark (see the author's 'Theory of the Induction Coil,' p. 151).

With these facts in mind it is easy to understand why the ordinary spark is a better igniter than the condenser spark when spherical electrodes are used. The ordinary discharge, in spreading to the outer and wider parts of the gap, is able to warm the requisite volume of gas to the ignition temperature, not by thermal conduction but by its own expansion. The condenser spark, on the other hand, being confined to the narrowest part of the gap, can warm the surrounding gas only by conduction*. It is true that in the case of the ordinary spark between spherical electrodes, only a fraction of the heat is actually utilized in producing ignition, viz., the heat of that portion of the discharge which is near the edge of the gap. It is quite in accordance with the thermal theory, however, that an enlarged source may be a better igniter than a point source of greater heat. For the distribution of temperature round an instantaneous point source at any time after the heat is communicated is such that the temperature is highest in the position of the source, and falls off in all directions from this point. If the boundary of a certain volume of the gas is at the ignition temperature, the inner portions of this volume must be at a temperature above this, and therefore at an unnecessarily high temperature for the production of ignition. It is clear that, in regard to the volume raised to the ignition temperature, a better distribution would be one in which the heat is more evenly distributed, so that the temperature throughout this volume is uniform. An instantaneous point source, though superior to a continued point source, is inferior to an enlarged source of the same or even less total heat.

It appears, therefore, that the results, both with pointed and with spherical electrodes, are consistent with the view that the most effective spark in ignition is that which heats the greatest volume of the gas to the ignition temperature. With pointed electrodes the heating is effected by thermal conduction from the source, with spherical electrodes by expansion of the source itself.

Some further points now remain to be considered in regard to the discharge between spherical electrodes. The horizontal striations which appear in the photograph of the spreading discharge in fig. 5 (Pl. XXI.), and less clearly in

* It might be expected that the condenser spark, being in the position in which it can give heat most readily to the electrodes, would communicate less heat to the gas than would the ordinary spark. Calorimeter experiments, however, with small spherical electrodes of carbon, indicated that the gas receives slightly more heat from condenser sparks than from ordinary sparks produced with the same primary current.

figs. 4 and 6 (Pls. XXI. & XXII.), suggest that the apparent spreading is a radial movement, or wandering, of the arc portion of the discharge, the striations corresponding to the oscillations of the induction coil or magneto system*. That this is the case is confirmed by photographs of the discharge taken with the help of a rotating concave mirror, some of which are reproduced in fig. 7 (Pl. XXII.). They show a number of spark discharges, produced by an induction coil without secondary condenser, between spherical electrodes of carbon. Nearly all the images show the wandering of the arc, the movement being upwards, or downwards, or along other radii. Frequently the arc wanders to the edge of the gap and breaks off there, the discharge then beginning again at the centre, sometimes afterwards wandering along a different radius, as in the fourth, fifth, and sixth images. This is the explanation of the fact that in several of the camera photographs (*e. g.*, the first in fig. 4, Pl. XXI.) the "spreading" appears to take place both upwards and downwards in the same discharge. None of the lines in fig. 7 (Pl. XXII.) show any bifurcation, the discharge passing at only one part of the gap at a time. The curvature of the lines during wandering shows that the speed of the lateral movement of the discharge is greatest at the centre of the gap, which is to be expected since the radial variation of the width of the gap is here smallest †.

With regard to the influence of the wandering on ignition, it is probable that the most effective discharges in this respect are those in which the arc wanders to the edge of the gap and remains there for an appreciable time, as in the sixth and thirteenth images in fig. 7 (Pl. XXII.). On several occasions it was observed that a discharge which broke off just after reaching the edge, to recommence at the centre, was incapable of producing ignition. In such cases it must be concluded that though the wandering is accompanied by a sufficient enlargement of the source, the time for which the enlargement endures is too short to result in ignition ‡.

The wandering of the arc takes place less readily when the width of the gap is increased. Consequently it might be expected that within certain limits a narrow gap between

* See 'The Theory of the Induction Coil,' fig. 61, p. 147, and fig. 93, p. 201.

† The photographs in fig. 7 (Pl. XXII.) suggest that the wandering is accompanied by an increase of width, as well as an increase of length, of the arc.

‡ The whole time of duration of each of the discharges shown in fig. 7 (Pl. XXII.) was about 1/100 second.

spherical electrodes would be more effective in ignition than a wider one. This was found to be the case with the carbon spherical electrodes used in the present experiments. The igniting effect of the spark was distinctly better when they were 0.15 mm. than when they were 0.3 apart, the heat of the spark being practically the same on both occasions. The greater ease of wandering in the narrower gap was more effective than the greater length of the initial spark in the wider one*.

The wandering also depends upon the curvature of the electrodes, and in the case of sharply-pointed electrodes it must be greatly restricted by the fact that here any lateral movement of the arc would be accompanied by excessive increase of length. The possibility suggested itself, however, that some slight effect of wandering might be observable with pointed electrodes if these were of the most suitable material. When ignition was tried with a very short spark between carbon points it was found that the addition of a secondary condenser now produced no improvement. Ignition was effected with equal success whether the condenser was connected or not. The same was found with pointed electrodes of clean lead. In these circumstances the slight wandering over the sides of the electrodes in the case of the ordinary spark apparently produces as much effect in ignition as the superior temperature distribution due to thermal condition in that of the condenser spark.

As to the cause of the wandering of the arc, this cannot be traced to the action of thermal convection arising from the heating of the gas by the initial spark. The photographs in figs. 4 and 7 (Pls. XXI. & XXII.) show that the movement of the arc is as often downwards as upwards. Nor can the wandering be attributed to thermionic action, since the movement is from the centre towards the outer portions of the gap where the surfaces of the electrodes are cooler. The wandering must be attributed to some property of the surfaces which is independent of thermal action. Now it is an observed fact that the wandering takes place much less readily if the electrode surfaces are not clean or are tarnished, and this fact suggests that photoelectric action plays a part in determining the position of the arc. We may suppose that the electrode surfaces at the centre are to some extent "spoilt" by the initial spark, so that the arc

* The condenser spark between spherical electrodes, in which there is no wandering, conforms to the general rule that the igniting power increases with the width of the gap

which follows it passes more readily across a neighbouring part of the gap where the surfaces are cleaner. The wandering of the arc thus represents the tendency of the arc to pass across parts of the gap where the surfaces have not been spoilt by the previous portions of the discharge. According to this view of the matter the direction of the wandering, which is apparently quite capricious, is that along which the surfaces at the time are cleanest, and where the easiest path is prepared for the discharge by photo-electric action.

That the wandering does not occur with condenser sparks is accounted for by the fact that it is a comparatively slow movement, and that it requires a much longer time to develop than that occupied by a single condenser spark. In fig. 8 (Pl. XXII.) are shown rotating-mirror photographs of four multiple spark discharges produced between the carbon spherical electrodes by an induction coil with secondary condenser. The capacity of the condenser was considerably less than the maximum which allowed sparks to pass, so that each discharge consisted of a large number of separate sparks. Each spark appears at the centre of the gap, and no part of the discharge shows any tendency to wander towards the side.

In connexion with the question of the condition requisite for ignition there is another point to which reference should be made here. Observers whose experiments on ignition by electric sparks or other forms of electric discharge have led them to conclude that ignition is not due to any thermal action of the current, have sometimes suggested that the current itself (or the ionization) in the gas is the determining factor in ignition. It is not difficult to show, however, that in the present experiments with spherical electrodes the maximum current crossing the spark gap is much greater in the case of the condenser spark than in that of the ordinary spark, though the latter is, as we have seen, much the better igniter. Let us suppose that a condenser of capacity C is connected with the electrodes, so that the discharge takes the form of a single spark in which the current oscillates with high frequency n , determined by the capacity C , and the self-inductance of the short wires by which it is connected to the electrodes. Then if the sparking potential is V_0 , the maximum value of the current in these oscillations is (if we neglect damping) $2\pi nCV_0$. In the present experiments V_0 was about 1000 volts, C about 0.004 microfarad, and n was not less than

10⁶ per second. Consequently the maximum current in the condenser spark was, at a low estimate, 25 amperes.

When the condenser is replaced by one of very small capacity, the discharge changes into a spark of the ordinary kind, consisting of an initial capacity portion followed by a pulsating and decaying arc. The maximum current in the capacity portion is given by the same expression with the appropriate values of n and C , and since n is inversely proportioned to \sqrt{C} , the maximum current is now considerably less than before, being directly proportional to the square root of the capacity.

As to the maximum current in the arc portion of the ordinary discharge (in which the the current wave consists of one oscillatory and one aperiodic component), an upper limit to its value may be obtained by calculation from the constants of the magneto circuits and the primary current at the moment of "break"*. By such calculations it can be verified that in no case does the maximum current in the inductance portion of the spark given by a high tension magneto of the usual type exceed a few hundred milliamperes†. It is therefore quite certain that when a condenser of considerable capacity is connected with the spark electrodes, the maximum current in the discharge is much greater than that in the discharge which occurs when the condenser is replaced by one of very small capacity, or when the condenser is absent. The great superiority of the igniting action of the ordinary discharge over that of the condenser spark between spherical electrodes cannot therefore be traced to any direct electrical action determined by the value of the current.

In the opinion of the present writer the thermal theory is the only theory which is capable of accounting for the known facts of spark ignition, and it is hoped that the evidence produced in the present communication will tend to renew confidence in it.

Glasgow.
October, 1928.

* The equations required in the calculation are given in the author's 'Theory of the Induction Coil,' Appendix II. pp. 209, 210.

† See also Morgan, 'Electric Spark Ignition,' p. 21, where it is shown that the current in the arc portion is smaller than that in the capacity portion of a magneto spark.

CVIII. *The Phosphorescence of Fused Quartz.*
By A. C. BAILEY and J. W. WOODROW.*

[Plate XXIII.]

DRUMMOND and Webster⁽¹⁾ have shown that a photographic plate will be fogged if kept in contact with certain pieces of quartz which have been previously exposed to ultra-violet light, and they concluded that this effect was most probably due to a phosphorescence of the particular fused quartz which they used. They found that this material would continue to emit a radiation of sufficient intensity to affect a photographic plate for at least three weeks after irradiation with the ultra-violet light. They also found that the effect was enhanced if the quartz plate was kept warm while it was in contact with the photographic plate.

When the above report appeared we were making similar tests, the results of which have confirmed the conclusions of Drummond and Webster and which have also given further information on this type of phosphorescence. Many experiments were carried out upon pieces of fused quartz broken from a large piece which had been obtained from the Thermal Syndicate Co., Ltd., under the trade name of "Vitreosil." It was found that an irradiation of an hour at a distance of 10 cm. from a Cooper-Hewitt quartz mercury arc was sufficient to activate the quartz to such an extent that it would produce a distinct image on a photographic plate in twenty-four hours. The plates were placed in carefully-tested light-proof boxes so as to avoid all possibility of extraneous light-effects. In some of the experiments, the photographic plate was slightly sensitized by a short exposure to a red light before being placed in contact with the quartz.

In one instance a piece of the quartz which had been irradiated for six hours was taken to the dark room, where several people examined it closely in complete darkness. Each observer, however, reported a complete inability to detect the slightest indication of any radiation of visible light, provided the sample was not heated. But this same piece emitted a radiation of sufficient intensity to produce a strong image on the photographic plate even after transmission through a thin piece of glass; and furthermore the ordinary refraction phenomena at the edges of the glass plate were clearly shown in the developed image. This refraction phenomenon and the high transmission of glass obviously

* Communicated by Professor E. C. C. Baly, F.R.S.

indicated a radiation in or near to the visible region of the spectrum.

It has long been known that heating causes a marked increase in the intensity of emission from an excited phosphorescent body and that with continued heating the phosphore soon releases all the energy which has been stored up during the activating process. The irradiated fused quartz was found to possess this property of an activated phosphore, for its power to affect a photographic plate was destroyed by heating for a few minutes in a bunsen flame; however, it could be activated again by a further exposure to ultra-violet radiation. This procedure could be repeated many times, which is in accordance with the results obtained by E. Becquerel⁽²⁾ with fluorspar and by Lenard and Klatt⁽³⁾ with the phosphores which they investigated.

In Pl. XXIII. (figs. 1 and 2) are shown two typical photographs obtained with two different pieces of fused quartz. It is seen that the effects are very prominent at the edges of the broken quartz and that they are not uniform over the surface. Bright spots somewhat circular in shape were produced by the sample shown in fig. 1, while those due to the piece shown in fig. 2 were distinctly rectangular. Many photographs were made both before and after treatment with heat and various acids, but these same spots always appeared in exactly the same places after the quartz had been activated by ultra-violet light. In other samples only one emission-centre was evident, while in still others none at all were present. This was probably due to the manner in which the plate was built up from smaller pieces. These same pieces of quartz were examined carefully under the microscope and photographs were made by allowing diffused light to pass directly through the quartz while in contact with the photographic plate, but nothing irregular could be observed in the region of the spots.

Prof. E. C. C. Baly⁽⁴⁾ has found that fused quartz which had been exposed for a long time to ultra-violet light developed an amethystine colour and became quite opaque to the short-wave ultra-violet. When it was then heated in a powerful blast flame, it emitted a brilliant green phosphorescence which gradually faded away. The pieces of quartz which we had shown to be capable of producing a developable image were also found to emit a green phosphorescence upon heating. The samples were irradiated by exposure to a quartz mercury arc and then taken to a dark room and heated on an electric plate. As soon as they became hot they began to glow very brightly and continued

to do so for more than thirty minutes. A broken quartz flask which had not been used for six months and which had been kept behind glass doors in the laboratory during that time, upon heating gave the characteristic green glow, which was easily observed in the dark room, although it was quite weak.

Tests with natural quartz crystals showed that they did not emit any radiation which would affect the photographic plate or which was visible to the eye upon heating. One of these natural crystals was heated in an electric furnace to a temperature of $575^{\circ}\text{C}.$, at which temperature a change takes place in the form of the quartz, but no phosphorescence was observed. Another crystal was heated to $1200^{\circ}\text{C}.$, but upon being tested exhibited no phosphorescent activity. A third piece from the same crystal was heated very slowly to $1600^{\circ}\text{C}.$, and after cooling was irradiated in the usual manner. Upon heating, this piece gave the same characteristic green glow as was found with the fused quartz plates.

Several other substances were tested for this phosphorescence. Irradiated pyrex glass emitted a radiation upon heating which was visible in a dark room and which was quite similar to that obtained with fused quartz. It would also produce a developable image on a photographic plate without heating. No trace of any phosphorescent activity could be obtained with gypsum. Calcite glowed very brightly for some time when heated; but after it had ceased to glow it could not be reactivated even by an exposure of several hours to the full radiation from a quartz mercury arc.

Fluorite was found to be extremely active and a very short irradiation was sufficient to cause it to emit a bright bluish-violet light upon heating. The fluorite was so sensitive that all pieces tested gave this characteristic glow with a small amount of heating even though it had not received any previous radiation in the laboratory. E. Becquerel⁽²⁾ has found that fluorspar which has been activated by a long exposure to sunlight emits a bright luminescence of visible light when heated to about 90° . After this effect disappears and the crystal has been allowed to cool, it will again emit a visible radiation when the temperature is raised to 90° . Lenard and Klatt have explained this phenomenon by assuming that the fluorspar emits an ultra-violet radiation, which continues after the visible luminescence ceases, and that this in turn activates the cooled fluorspar so that it will again emit a visible radiation when heated a second time. This probably explains why all the pieces of fluorite which we tested gave the characteristic glow when heated even though we had not exposed them to ultra-violet light.

Summary.

In the experiments described here the following facts have been ascertained :—

1. Many samples of fused quartz possess the properties of a phosphorescent body ; that is, they can be excited by ultra-violet light, they will then emit a visible phosphorescent light of considerable strength upon the application of heat, and they can be completely deactivated by bringing to a red heat in a flame.

2. This phosphorescent activity of fused quartz is not uniform, but there is a wide variation between samples and even within the area of a single small piece.

3. Natural quartz crystals do not possess this property of emitting a phosphorescent radiation, but they can be brought into this condition by heating slowly in an electric furnace to a temperature of 1600° C.

4. Pyrex glass, calcite, and fluorite exhibit a prominent phosphorescent activity, but gypsum does not.

References.

- (1) Drummond and Webster, 'Nature,' cxv. p. 837 (1925).
- (2) E. Becquerel, *Compt. Rend.* cxii. p. 557.
- (3) P. Lenard and V. Klatt, *Ann. der Phys.* xv. pp. 225, 425, 633 (1904).
- (4) E. C. C. Baly, 'Spectroscopy,' ii. p. 101 (1927).

Laboratory of Physics,
Iowa State College,
Ames, Iowa.

CIX. *The Motion of Electrons in Pentane.* By J. D. MCGEE, *M.Sc., St. John's College, Demonstrator in Physics, University of Sydney*, and J. C. JAEGER, *B.Sc., Deas-Thompson Research Scholar, University of Sydney**.

IN the *Phil. Mag.* (vol 1. p. 825, Oct. 1925) Professor V. A. Bailey has given a detailed account of a method for investigating the motion of electrons in gases, which is particularly applicable to those gases in which ions are formed by attachment of electrons to molecules as a stream of electrons moves through the gas.

The same apparatus and method have since then been used to investigate the motion of electrons in pentane (C_5H_{12}). This gas was chosen firstly because we had at our disposal,

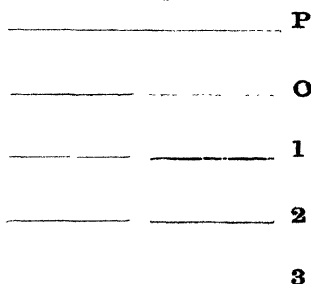
* Communicated by Prof. J. S. Townsend, F.R.S.

through the kindness of Mr. J. G. Burrows of the Chemistry Department, a very pure sample of the liquid, and secondly because Professor E. M. Wellish, in his work on ionic mobilities *, had noticed an "ageing" effect when the gas was allowed to remain in the apparatus for any considerable time. It was therefore of interest to investigate whether these effects still occurred in the more refined apparatus at our disposal, in which the rate of contamination of the gas is very small.

Only a brief account of the theory and experimental procedure is given here; for full details the original paper should be consulted.

2. An electron moving through a gas at a pressure p mm., under the action of an electric force Z volts per cm., will

Fig. 1.



have a drift velocity W in the direction of the electric force, and an agitation velocity U , while the ratio of its kinetic energy to that of a gas molecule is k . Then, if the mean free path of an electron be l , and h be the probability of its attachment to a molecule in collision, the number of electrons remaining free at a plane $z=c$ out of N_0 starting at the plane $z=0$, the axis of z being the direction of the electric force, will be $N_0 e^{-\alpha c}$, where α is the "coefficient of attachment" which a simple calculation makes $\frac{hU}{lW}$.

The apparatus may be represented diagrammatically as in fig. 1. $P, O, 1, 2, 3$ are parallel circular plates maintained at such potentials as to produce a uniform field throughout. Electrons are produced by the photoelectric effect of ultra-violet light on a target at P . A narrow stream of electrons and ions passes through the slit in O and diverges, the electrons more than the ions, so that the stream passing

* Phil. Trans. A, ccix. p. 249 (1909).

through the slit in 1 will be richer in ions relative to that passing through the slit in O. This effect is intensified by the continual formation of ions by attachment in the body of the gas. A similar effect occurs at the slit in plate 2, the stream being ultimately collected on plate 3.

Suitable electrical arrangements permit the measurement of the ratios of the current i_1, i_2, i_3 to electrodes 1, 2, and 3. The actual experiment consists in the determination of

$\xi = \frac{i_2}{i_1}$, and $\eta = \frac{i_3}{i_2}$. From these the distribution ratios S_1

and S_2 , of the current passing through the slit to the current arriving at the plane of the slit, can be determined for slits in plates 1 and 2.

Thus

$$S_1 = \frac{\xi(1+\eta)}{1+\xi(1+\eta)}, \quad S_2 = \frac{\eta}{1+\eta}.$$

If, now, n_0 electrons pass the slit in O, $n_0 \epsilon^{-ac}$ will arrive at electrode 1, where c is the interelectrode distance, and

$n_1 = n_0 \epsilon^{-ac} R\left(\frac{Z}{k}\right) = a n_0$ will pass through the slit in 1,

where $R\left(\frac{Z}{k}\right)$ is the distribution ratio at the slit, calculable

from the dimensions of the instrument for given values of Z/k . Similarly, the number of electrons passing through the slit in 2 will be $n_2 = a^2 n_0$. If, in addition, N_0 ions pass through the slit in O, the number passing the slit in 1 will be

$$N_1 = N_0 R(Z) + n_0(1 - \epsilon^{-ac})r = R N_0 + b n_0,$$

where r is the unknown distribution ratio of the ions formed by attachment. Similarly, the number passing through slit 2 is $N_2 = R^2 N_0 + (Rb + ba)n_0$.

But

$$S_1 = \frac{n_1 + N_1}{n_0 + N_0} \quad \text{and} \quad S_2 = \frac{n_2 + N_2}{n_1 + N_1}.$$

Substituting in these and eliminating b , we have

$$a = \frac{S_1(R - S_2)}{R - S_1}.$$

Since R is a known function of Z , a can be derived from the experiments, and we have the relation $R(Z/k) \epsilon^{-ac} = a_1$.

If the force Z and the pressure p be changed to Z/n and p/n respectively, we obtain the additional relation $R(Z/kn) \epsilon^{-ac/n} = a_n$.

From these two equations we obtain

$$\log_{10} a_1 - n \log_{10} a_n = \log_{10} R(Z/k) - n \log_{10} R(Z/kn) \quad (1)$$

and

$$\alpha = \frac{2.3}{c} \{ \log_{10} R(Z/k) - \log_{10} a_1 \} \quad (2)$$

Equation (1) gives k and equation (2) gives α .

3. In practice slight errors are to be expected for the following reasons:—

- (a) Non-uniform distribution of electrons over the upper slit; maximum value computable and negligible.
- (b) Diffusion of the electrons to the sides of the slits.
- (c) Possible asymmetry of the slits.

So calibration is made with hydrogen in which electrons are known always to remain free, and the values of k are well established over a large range of Z/p *. It is found that, while S_2 plotted against (Z/k) agrees substantially with the theoretical curve, S_1 is consistently lower. This may be ascribed to errors of construction of the apparatus. An

appropriate modification of the theory gives $\alpha = \frac{S_1(R'' - S_2)}{R' - S_1}$,

where R'' and R' are the distribution-ratios for ions obtained from the upper and lower of these curves respectively. The calibration curves used were obtained by Prof. V. A. Bailey and Mr. A. J. Higgs, B.Sc., and were checked before commencing these experiments.

4. The pentane gas was obtained by vaporizing the pure liquid, all precautions being taken to prevent the admixture of foreign gases. After a preliminary drying in preparation, it was dried for twelve months over phosphorus pentoxide at about 250 mm. pressure. The gas was admitted to the apparatus either directly or after a preliminary liquefaction in a small side-tube by liquid air, in which case only the middle third of the liquid was used, the remainder being pumped off. There was no perceptible difference in the results obtained with samples admitted by the different methods.

Samples of gas were tested over several days to examine the possibility of an effect of the ultra-violet light on the gas or an "ageing" effect. Neither was observed, the results remaining constant to within experimental error.

* Townsend and Bailey, *Phil. Mag.* xlii. (Dec. 1921).

Variations from Boyle's Law were observed with this gas at pressures between 20 and 40 cm., the maximum variation amounting to 4 per cent. Corrections were made for this source of error when reading the pressures in a McLeod gauge.

5. Observations were made at pressures of 8.32, 4.16, 2, and 1 mm., and at forces of 40, 20, 10, and 5 volts per cm., the pressures being originally read as 8, 4, 2, and 1 mm. on the assumption that Boyle's Law held for the gas. But as results were required at values of Z and p increasing in geometrical progression, the determined values of a for given

TABLE I.

Z/p .	p .	Z .	a .	$-\log_{10} a_n$.	Z/k .	y .	k .	a .	$a/p \times 10^3$.
1.25	8.0	10	.476	.322	3.6	.322	2.8	.033	4.1
	4.0	5	.387	.412		.412		.017	
2.5	8.0	20	.520	.234	3.64	.236	5.5	.013	1.6
	4.0	10	.403	.396		.392		.006	
	2.0	5	.303	.519		.524		.003	
5.0	8.0	40	.585	.233	4.70	.237	8.5	.006	0.8
	4.0	20	.452	.345		.342		.003	
	2.0	10	.332	.479		.466		.002	
	1.0	5	.250	.602		.618		.001	
10.0	4.0	40	.438	.358	2.18	.358	18.4	.006	0.8
	2.0	20	.327	.485		.485		.003	
	1.0	10	.234	.631		.633		.001	
20.0	2.0	40	.296	.529	.97	.529	41.2	.014	1.7
	1.0	20	.212	.674		.674		.006	
40.0	1.0	40					77.0		

values of Z were plotted against p , and the values of a at $p = 8.0$ and 4.0 mm. were read off from the curves. The changes in each case were very small. Table I. gives the results of the observations, each number being the mean of several determinations. The values of a at 8.0 and 4.0 mm. are those corrected as above.

To obtain the value of Z/k from equation (1) a series of curves were drawn with

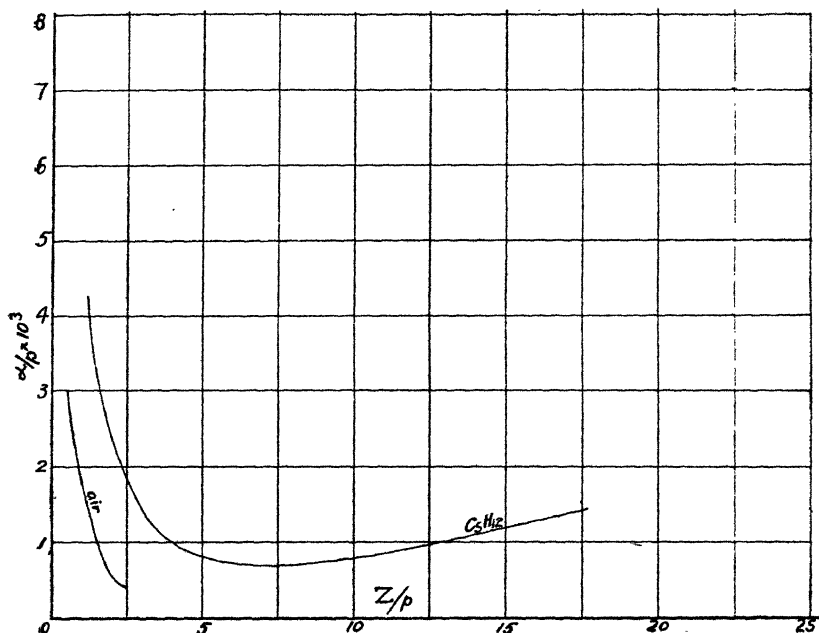
$$x = Z/k \quad \text{and} \quad y = \log_{10} R(Z/k) - n \log_{10} R(Z/kn)$$

for $n = 1, 2, 4$, and 8 , similar to those in fig. 6 in Professor Bailey's paper *. The values of $-n \log_{10} a_n$ were then set

* Phil. Mag. 1. p. 825 (Oct. 1925).

off to the same scale on the edge of a strip of squared paper, and the strip moved parallel to the y -axis till the marked points fell as nearly as possible on the curves. The abscissa then is Z/k , and the values of k so determined are shown in Table I. The actual ordinates of the points of intersection of the curves with the strip are given, divided by n , in the column under y in Table I. These should agree with $-\log_{10} a_n$, and the disagreement will show the magnitude of the experimental error. These values of y are used as smoothed values of $-\log_{10} a_n$ for the calculation of α from

Fig. 2.



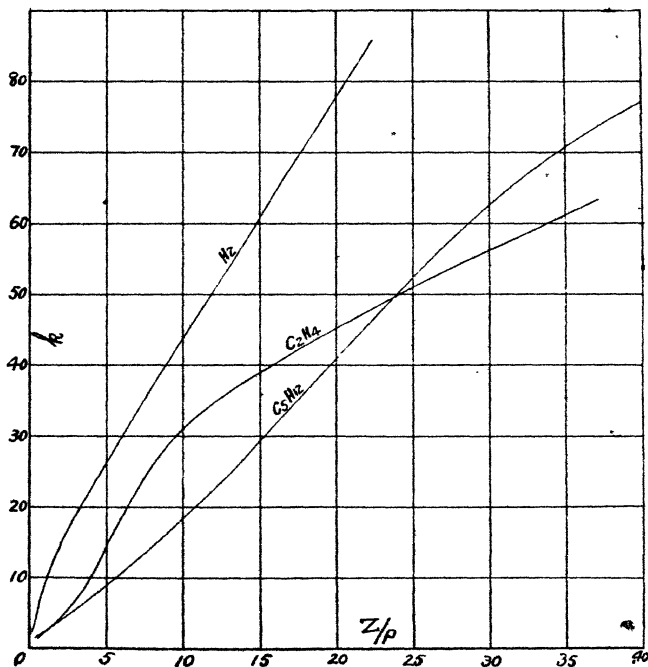
equation (2). The value of k at $Z/p = 40$ is determined directly from the calibration curve, since S_1 and S_2 fall exactly on the theoretical curves at $Z/k = 1$.

6. For the greater part of the range α is very small, being little greater than experimental error, which may be as large as .004. Further at those values of Z/p where α does increase, the results are least reliable, depending on observations at only two pressures. There are definitely very few ions formed, so it is possible that α/p is nearly zero in the perfectly pure gas, the few ions being due to traces of impurity.

The curve showing the variation of α/p with Z/p is given in fig. 2. The curve obtained for air by Professor Bailey is shown also for comparison. They both show the same decrease for increasing Z/p , the values for pentane being consistently higher than those for air.

The curve for k against Z/p is given in fig. 3 with those of ethylene and hydrogen for comparison. The pentane curve is lower than most of the curves, but is not remarkable save for its approximate linearity.

Fig. 3.



7. The values of W were determined in a Townsend diffusion apparatus set up for a research on ethylene by Mr. J. Bannon, B.Sc. We are indebted to him for the value of the eccentricity of the slit, and the constants of the coils producing the magnetic field. The values of W obtained are slightly inaccurate through the presence of a few ions, but the good agreement obtained between experiments at different pressures and forces with the same value of Z/p shows the error to be small. Values of k determined in this instrument agreed well with those obtained in the 3-slit apparatus.

Table II. gives the values of W obtained, each being the mean of several sets of observations at $Z = 40, 20, 10$, and 5 , and $p = 8.32, 4.16, 2.0$, and 1.0 mm.

TABLE II.

Z/p .	p .	Z .	$W \times 10^{-6}$.
60	8.32	5	1.25
1.2	8.32	10	2.39
	4.16	5	2.42
2.4	8.32	20	3.62
	4.16	10	3.68
2.5	2.0	5	3.77
4.8	8.32	40	4.60
	4.16	20	4.62
5.0	2.0	10	4.65
	1.0	5	4.88
9.6	4.16	40	5.10
10.0	2.0	20	5.09
	1.0	10	5.24
20.0	2.0	40	5.50
	1.0	20	5.47
40	1.0	40	6.43

The values of α , and h , of L the mean free path at 1 mm. pressure, and of λ , the fraction of energy lost in a collision, are shown in Table III. These quantities are calculated from the formulæ :

$$U = 1.15 \times 10^7 \sqrt{k}, \quad L = 7 \frac{(WU)}{Z} \times 10^{-16},$$

$$\lambda = 2.46 \frac{W^2}{U^2}, \quad h = 7 \frac{(\alpha W^2)}{Z} \times 10^{-16}.$$

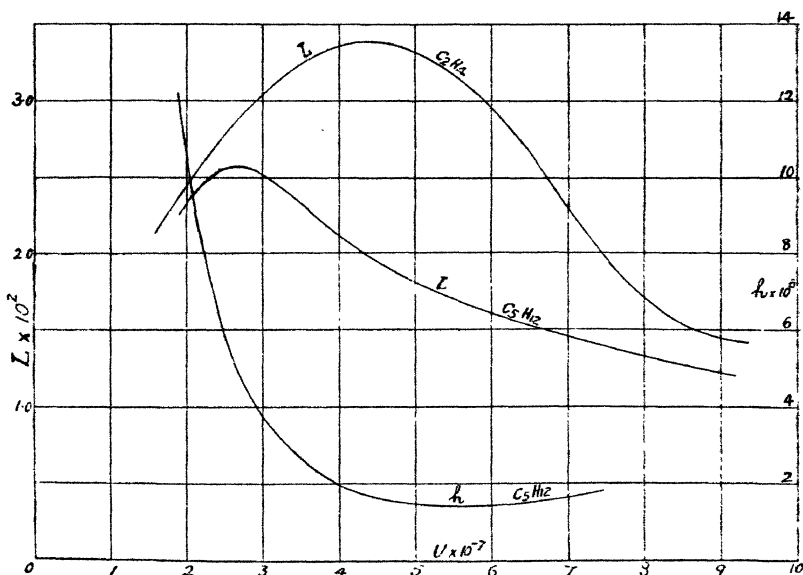
TABLE III.

Z/p .	$W \times 10^{-6}$ cm./sec.	k .	$U \times 10^7$ cm./sec.	$L \times 10^2$ cm.	$\lambda \times 10^2$.	$h \times 10^6$.
625	1.25	1.7	1.5	2.1	1.7	—
1.25	2.42	2.8	1.93	2.26	3.9	13.5
2.5	3.70	4.5	2.46	2.55	5.6	6.1
5.0	4.70	8.8	3.51	2.32	4.4	2.5
10.0	5.10	18.4	4.95	1.77	2.6	1.5
20.0	5.45	41.4	7.4	1.42	1.3	1.8
40.0	6.38	77	10.1	1.13	1.0	—

Fig. 4 gives the curves for L against U for C_5H_{12} and C_2H_4 , and of h against U for C_5H_{12} ; the latter shows a very marked increase of h with decrease of U , beginning in the region of $U = 3 \times 10^7$ cm./sec. The $L-U$ curve for pentane shows a maximum in the early portion of the curve, but there is no minimum in the range used such as occurs with C_2H_4 .

The curve of W against Z/p for pentane is given in fig. 5, with those of C_2H_4 , CO_2 , and H_2 for comparison. It is marked by a very rapid initial rise, the values in the early part of the range being as high as any yet measured,

Fig. 4.



terminated by an almost horizontal portion at the higher values of Z/p .

The curve of λ against U is given in fig. 6, with those of C_2H_4 , CO_2 , and N_2 for comparison. It is noteworthy that the maxima in the L and λ curves occur for the same value of U , indicating that the electrons which penetrate most deeply into the molecules lose the greatest fraction of their energy on collision.

A considerable similarity will be noticed in all the curves between the two hydrocarbons, pentane and ethylene. The curves of $\lambda-U$ show that the gases C_5H_{12} , C_2H_4 , and CO_2 are exceptional in possessing a rapid initial rise and maximum

Fig. 5.

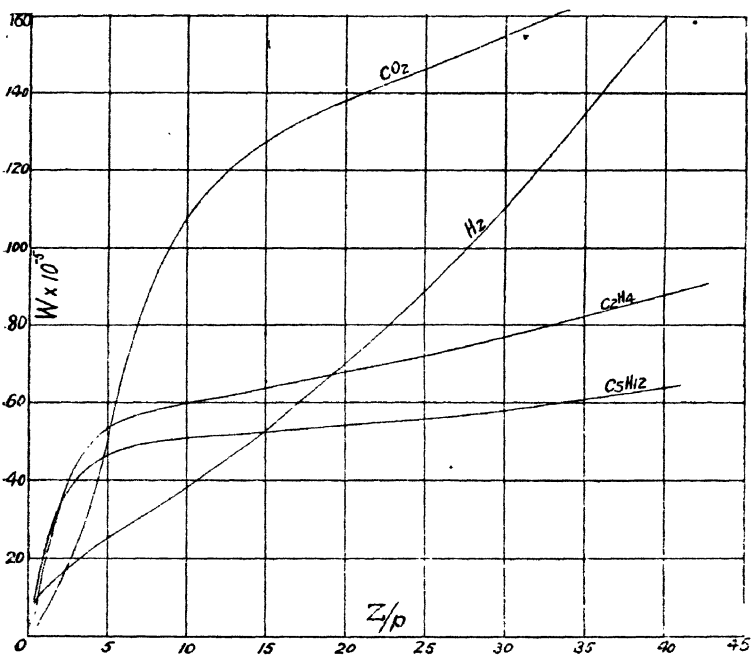
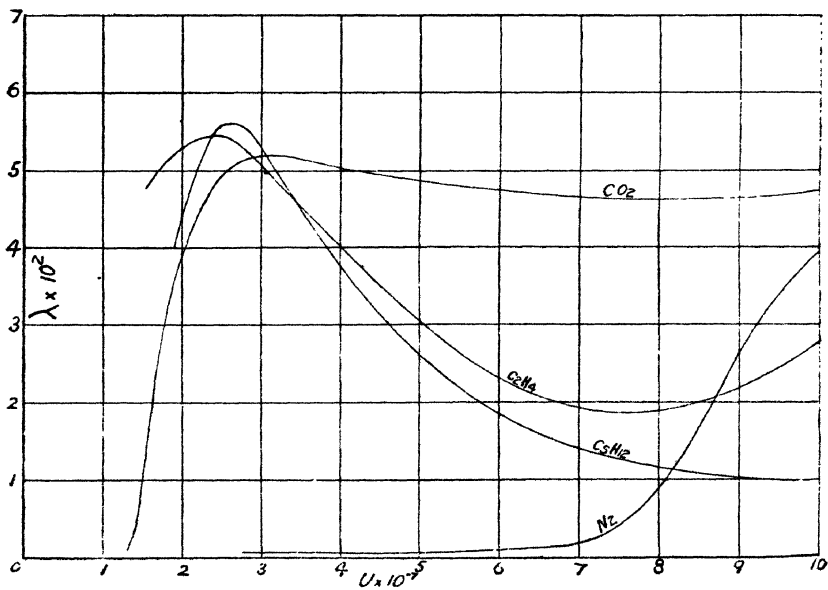


Fig. 6.



in these curves ; all other gases give either consistently low values of λ or a behaviour similar to that of N_2 shown. The large initial values of λ are due to the low initial values of k and high initial values of W . It may be noted that for pentane the maximum in the $\lambda - U$ curve coincides with the rapid rise of the $h - U$ curve, suggesting that this peculiarity may be in some way connected with the formation of ions.

Finally, we wish to thank Professor Bailey, who directed this research, for his advice and assistance during the progress of the work.

CX. *On Spheroidal Harmonics as Hypergeometric Functions.*
By D. M. WRINCH, M.A., D.Sc.*

IN the course of a discussion of harmonics, symmetric about an axis, applicable to surfaces of revolution of some generality, an alternative method was found of constructing harmonics applicable to spheroids, both prolate and oblate.

In the transformation

$$z + i\rho = W(w) = a(e^{iv} + \lambda e^{-iv}) \quad \lambda^2 < 1, \quad (1)$$

where $w = u + iv$, and z and ρ are the usual cylindrical polar coordinates :

$$\left. \begin{aligned} z &= a \cos u (1 + \lambda e^{2v}) e^{-v}, \\ \rho &= a \sin u (1 - \lambda e^{2v}) e^{-v}; \end{aligned} \right\} \quad (2)$$

so that the zero v -level represents the spheroid

$$z, \rho = a[\cos u(1 + \lambda), \sin u(1 - \lambda)],$$

oblate when λ is negative, and prolate when λ is positive, with semi-axes $a(1 + \lambda)$, $a(1 - \lambda)$, $a(1 - \lambda)$, and the level $v = -\infty$ the sphere at infinity.

If the usual form of Laplace's equation for harmonics symmetric about the axis of z be used, namely

$$\left[\rho \frac{\partial}{\partial u} \rho \frac{\partial}{\partial u} V + \rho \frac{\partial}{\partial v} \rho \frac{\partial}{\partial v} \right] V = 0,$$

and if $\cos u = \mu$, and $e^v = \zeta$, the equation for V may be written in the form

$$DV = \lambda D_1 V, \quad (3)$$

* Communicated by the Author.

where, if

$$\mathfrak{S}_\zeta \equiv \zeta \frac{d}{d\zeta},$$

$$D = \frac{d}{d\mu}(1-\mu^2) \frac{d}{d\mu} + \mathfrak{S}_\zeta(\mathfrak{S}_\zeta - 1), \quad . \quad . \quad . \quad (4)$$

$$D_1 = \zeta^2 \left\{ \frac{d}{d\mu}(1-\mu^2) \frac{d}{d\mu} + \mathfrak{S}_\zeta(\mathfrak{S}_\zeta + 1) \right\} . \quad . \quad . \quad (5)$$

Under the proviso that $\lambda^2 < 1$, a solution for V may be taken in the form

$$V = f_0 + \lambda f_1 \dots + \lambda^n f_n, \quad . \quad . \quad . \quad (6)$$

where

$$\left. \begin{aligned} Df_0 &= 0, \\ Df_{n+1} &= D_1 f_n. \end{aligned} \right\} . \quad . \quad . \quad . \quad (7)$$

In the case of the sphere when $\lambda=0$, V reduces to f_0 alone, and satisfies the equation $DV=0$. The Legendre function $P_k(\mu)$ satisfies the equation

$$\left[\frac{d}{d\mu}(1-\mu^2) \frac{d}{d\mu} + mk(m+1) \right] P_m(\mu) = 0, \quad . \quad . \quad (8)$$

and ζ^σ the equation

$$[\mathfrak{S}_\zeta(\mathfrak{S}_\zeta - 1) - \sigma(\sigma - 1)] \zeta^\sigma = 0; \quad . \quad . \quad . \quad (9)$$

and therefore, in the usual manner, a harmonic evanescent on the sphere at infinity is given by

$$V = P_k(\mu) \zeta^{k+1} \quad k=0, 1, 2 \dots n, \quad . \quad . \quad (10)$$

which yields the usual form

$$V = P_k(\mu) \left(\frac{a}{r} \right)^{k+1},$$

since $r=a/\zeta$.

If the spherical harmonics be used as a basis, a simple form of harmonic applicable to spheroids can at once be constructed in the form (6).

Thus with

$$f_0 = P_k(\mu) \zeta^{k+1},$$

the equation for f_1 becomes

$$\begin{aligned} Df_1 &= D_1 P_k(\mu) \zeta^{k+1} \\ &= 2(k+1) P_k(\mu) \zeta^{k+3}. \end{aligned}$$

The complementary function for f_1 and, indeed, for f_n is

$$\sum_p d_p P_p(\mu) \zeta^{p+1},$$

To find a particular integral for f_1 , we remark the fact that

$$\begin{aligned} D\zeta^\sigma P_m(\mu) &= \zeta^\sigma P_m(\mu)[-m(m+1) + \sigma(\sigma-1)] \\ &= (\sigma+m)(\sigma-m-1)\zeta^\sigma P_m(\mu). \end{aligned}$$

Thus a particular integral is available in the form

$$f_1 = \frac{2(k+1)}{2(2h+3)} \zeta^{k+3} P_k(\mu).$$

Indeed, suppose that f_n is of the form

$$\Sigma \alpha_{\sigma, m} \zeta^\sigma P_m(\mu),$$

then

$$\begin{aligned} D_1 f_n &= \zeta^2 \left[\frac{d}{d\mu} (1-\mu^2) \frac{d}{d\mu} + \mathfrak{S}_\zeta (\mathfrak{S}_\zeta + 1) \right] \Sigma \alpha_{\sigma, m} \zeta^\sigma P_m(\mu) \\ &= \Sigma \alpha_{\sigma, m} (\sigma-m)(\sigma+m+1) \zeta^{\sigma+2} P_m(\mu), \end{aligned}$$

and therefore a particular integral is available for f_{n+1} in the form

$$f_{n+1} = \Sigma \alpha_{\sigma, m} \frac{(\sigma-m)(\sigma+m+1)}{(\sigma-m+1)(\sigma+m+2)} \zeta^{\sigma+2} P_m(\mu).$$

The structure of the solutions of the equation is now clear. Suppose we take

$$\begin{aligned} f_0 &= P_k(\mu) \zeta^{k+1}, \\ f_1 &= \frac{1(2k+2)}{2(2k+3)} P_k(\mu) \zeta^{k+3}, \\ f_2 &= \frac{3(2k+4)}{4(2h+5)} \cdot \frac{1(2h+2)}{2(2h+3)} P_k(\mu) \zeta^{k+5}, \end{aligned}$$

and in general

$$\begin{aligned} f_n &= \frac{1 \cdot 3 \dots (2n-1)}{2 \cdot 4 \dots 2n} \cdot \frac{(2k+2)(2h+4) \dots (2k+2n)}{(2h+3)(2h+5) \dots (2h+2n+1)} \\ &\quad \times P_k(\mu) \zeta^{k+2n+1}; \end{aligned}$$

and therefore a solution of the equation is given by

$$\begin{aligned} V &= \zeta^{k+1} P_k(\mu) \left[1 + \frac{1(k+1)}{1!(2h+3)} \lambda \zeta^2 \right. \\ &\quad \left. + \frac{1 \cdot 3(k+1)(k+2)}{2!(2k+3)(2h+5)} \lambda^2 \zeta^4 \dots \right] \\ &= \zeta^{k+1} P_k(\mu) F(k+1, \tfrac{1}{2}; k+\tfrac{3}{2}; \lambda \zeta^2), \end{aligned}$$

where $F(p, q; r; x)$ is the hypergeometric function defined by

$$F(p, q; r; x) = 1 + \frac{pq}{r \cdot 1!}x + \frac{p(p+1)q(q+1)}{r(r+1)2!}x^2 + \dots$$

This solution is available, as we require, for ζ between unity and zero, since the hypergeometric function $F(a, b; c; x)$ is convergent for $x^2 < 1$.

Thus a typical solution for the sphere

$$V = \zeta^{k+1} P_k(\mu)$$

is corrected for the present case into

$$V = \phi_k(\zeta) P_k(\mu),$$

where

$$\phi_k(\zeta) = \zeta^{k+1} F(k+1, \frac{1}{2}; k+\frac{3}{2}; \lambda\zeta^2),$$

and a solution involving N_0 arbitrary constants

$$V = \Sigma A_k \zeta^{k+1} P_k(\mu)$$

is now developed into

$$V = \Sigma A_k \phi_k(\zeta) P_k(\mu). \dots \dots (11)$$

It is interesting to have the solutions in this form, for it is evidently a simple matter when dealing with applications to write down as many terms as the degree of approximation required makes necessary. The results are therefore readily accessible for practical purposes.

Now the case at present under consideration when

$$\left. \begin{aligned} z &= a \cos u (1 + \lambda\zeta^2)/\zeta = \frac{1}{2}c \cos u (1/\zeta\lambda^{1/2} + \zeta\lambda^{1/2}), \\ \rho &= a \sin u (1 - \lambda\zeta^2)/\zeta = \frac{1}{2}c \sin u (1/\zeta\lambda^{1/2} - \zeta\lambda^{1/2}), \end{aligned} \right\} (12)$$

with $c = 2a\lambda^{1/2}$,

is, for λ positive, the well-known and much-discussed case of the prolate spheroid already mentioned, for which, putting

$$z = c \cos u \cosh \xi, \quad \rho = c \sin u \sinh \xi, \dots (13)$$

the form of solution is given by

$$V = \Sigma B_k Q_k(\cosh \xi) P_k(\cos u). \dots (14)$$

This suggests at once that our hypergeometric function $\phi_k(\zeta)$ is a multiple, simply, of the function $Q_k(\cosh \xi)$, where, in view of (12, 13),

$$e^{-\zeta} = \zeta\lambda^{1/2},$$

and we easily find that there is an interesting relation between hypergeometrics whose arguments x and y are connected by the relation

$$y = 4x/(1+x)^2,$$

namely

$$\begin{aligned} & e^{-\frac{k+1}{2}} F(k+1, \tfrac{1}{2}; k+\tfrac{3}{2}; x) \\ &= (y/4)^{\frac{k+1}{2}} F(\tfrac{1}{2}k+\tfrac{1}{2}, \tfrac{1}{2}k+1; k+\tfrac{3}{2}; y). \end{aligned} \quad (15)$$

If we write

$$x = \lambda \xi^2,$$

and therefore

$$y = 1/\cosh^2 \xi,$$

this becomes, in terms of ξ ,

$$\begin{aligned} & e^{-(k+1)\xi} F(k+1, \tfrac{1}{2}; k+\tfrac{3}{2}; e^{-2\xi}) \\ &= (2 \cosh \xi)^{-(k+1)} F(\tfrac{1}{2}k+\tfrac{1}{2}, \tfrac{1}{2}k+1; k+\tfrac{3}{2}; 1/\cosh^2 \xi), \end{aligned}$$

which, since

$$\begin{aligned} Q_k(z) &= \frac{\Gamma(\tfrac{1}{2}) \Gamma(k+1)}{\Gamma(k+\tfrac{3}{2})} \cdot (2z)^{-k-1} \\ & F(\tfrac{1}{2}k+\tfrac{1}{2}, \tfrac{1}{2}k+1; k+\tfrac{3}{2}; 1/z^2) \quad (z^2 > 1), \end{aligned}$$

yields the result :

$$(\xi \sqrt{\lambda})^{k+1} F(k+1, \tfrac{1}{2}; k+\tfrac{3}{2}; \lambda \xi^2) = \frac{\Gamma(k+\tfrac{3}{2})}{\Gamma(\tfrac{1}{2}) \Gamma(k+1)} Q_k(\cosh \xi),$$

so that our harmonics (11) are, of course, equivalent to the harmonics (14) conventionally taken. Thus our procedure for building up solutions of Laplace's equation in this case yields, in fact, functions which are multiples of the Q_k functions: they have the advantage over the Q_k functions, however, that they more readily lend themselves to practical applications.

In the same manner, if λ be negative, we have

$$\left. \begin{aligned} z &= a \cos u (1 + \lambda \xi^2) / \xi = \tfrac{1}{2} d \cos u (1/\xi \sqrt{-\lambda} - \xi \sqrt{-\lambda}), \\ \rho &= a \sin u (1 - \lambda \xi^2) / \xi = \tfrac{1}{2} d \sin u (1/\xi \sqrt{-\lambda} + \xi \sqrt{-\lambda}), \end{aligned} \right\}$$

with $d = 2a \sqrt{-\lambda}$,

$$\dots (16)$$

and the unit ξ -level is the oblate spheroid usually taken as $\xi=1$ in the transformation

$$z = d \cos u \sinh \xi, \quad \rho = d \sin u \cosh \xi;$$

1122 *Spheroidal Harmonics as Hypergeometric Functions.*

so that the relation between ξ and ζ is simply

$$e^{-\zeta} = \zeta \sqrt{-\lambda}.$$

Thus, if in (15) we write

$$x = \lambda \zeta^2 = -e^{-2\zeta},$$

then

$$y = -1/\sinh^2 \xi,$$

and from (15) we deduce that

$$\begin{aligned} V &= \sum \alpha_k \phi_k(\zeta) P_k(\cos u) \\ &= \sum \beta_k P_k(\cos u) (2 \sinh \xi)^{k+1} \\ &\quad \times F\left(\frac{1}{2}k + \frac{1}{2}, \frac{1}{2}k + 1; k + \frac{3}{2}; -1/\sinh^2 \xi\right) \\ &= \sum B_k P_k(\cos u) q_k(\sinh \xi), \end{aligned}$$

which is the usual solution. But we may again point out that our new hypergeometric form of solution (11) allows very simple approximations to be arrived at in all the usual applications concerning oblate spheroids.

It is, in fact, a serious demerit of the treatment of problems relating to spheroids by means of Q_k and q_k functions that these functions do not lend themselves to approximation and computation.

We may also point out that the treatment by hypergeometric functions covers both the cases of prolate and oblate spheroids without the necessity for the separate discussion of the two cases which is called for when the Q_k and q_k functions are used.

Finally, we may direct attention to the fact that the two types of coordinates introduced in (13, 16), as conventionally used in spheroidal problems, are not convenient coordinates to use if a comprehensive view of the problems is taken. We then aim at solving Laplace's equation in the form in which it is applicable to the surface of revolution given by

$$\left. \begin{aligned} z &= a \cos u(1 + \lambda) + \lambda_2 \cos 2u \dots + \lambda_n \cos nu \dots, \\ \rho &= a \sin u(1 - \lambda) - \lambda_2 \sin 2u \dots - \lambda_n \sin nu \dots, \end{aligned} \right\}. \quad (17)$$

and, by developing the treatment which we have just elaborated, we are able, by a simple procedure, to construct harmonics suitable for any more general case. Indeed it appears that there is no essential difference between developing or correcting spherical harmonics so that they may apply to the spheroids, and developing them in a more general manner so that they may apply to any of the surfaces given by the equation (17).

CXI. *The Deterioration of Quartz Mercury Vapour Lamps and the Luminescence of Transparent Fused Quartz.* By A. E. GILLAM and R. A. MORTON*.

[Plate XXIV.]

IN many photochemical reactions in which mercury vapour lamps and fused quartz vessels are used, the efficiency of the processes appears to fall off with time. This may be due to the setting up of chemical equilibria, to a decrease in the output of light from the lamp, or to the development of some degree of opacity in the quartz vessels. There can be no doubt of the fact that most, if not all, makes of quartz mercury lamps deteriorate rather seriously after running for a relatively small number of hours. It is equally certain that fused quartz commonly undergoes a change under the action of light, and that this change is accompanied by some loss in transmission. Little trustworthy information is available as to the extent of these phenomena and as to the connexion which may or may not subsist between them. It is conceivable that the deterioration of the lamps is due to a change in the properties of fused quartz. The purpose of the present investigation is to study the two phenomena a little more closely.

As a result of extended photochemical researches in Prof. Baly's laboratories, a large number of old lamps of the U type have accumulated, and inspection of these shows that the following are the visible signs of ageing:—

(1) The interior surface becomes coated with a brownish black deposit, which is especially noticeable at the thick constriction. In many old lamps the discoloration is distributed over the whole U tube, and the deposit cannot fail materially to reduce the intensity of the transmitted light.

(2) In some lamps the thick quartz at the constriction appears to have been fractured internally, and globules of mercury are seen to be embedded at least a millimetre below the surface. In one case a white mass was seen to be embedded in the quartz.

A number of worn out lamps were broken up and the mercury removed as completely as possible. The black deposit proved to be strongly adherent and resisted the action of strong acids. Boiling aqua regia exerted no

* Communicated by Prof. E. C. C. Baly, C.B.E., F.R.S.

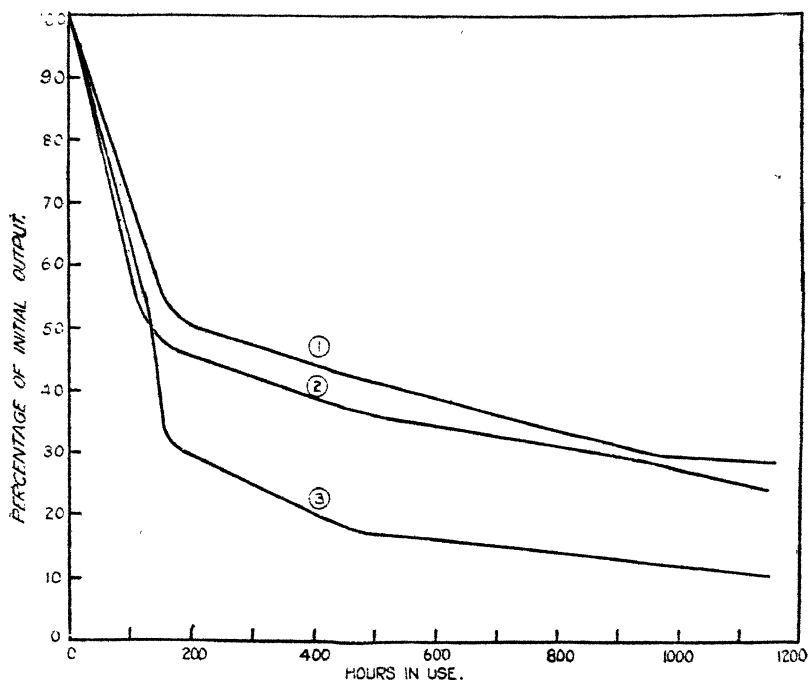
effect, and even after the quartz had been left in contact with aqua regia for some months the stain appeared to be unaffected. If, however, a badly discoloured fragment of quartz was strongly heated in a blow-pipe flame, the black stain was gradually replaced by a white deposit, which again resisted the action of reagents.

No emission of light was seen (*vide infra*) during the heating process. From this it would appear that the deposit is unlikely to consist of mercury or mercury compounds, but may possibly consist of elementary silicon. It has been suggested (Drane, Brit. J. Actinotherapy, June, 1926) that in certain evacuated lamps having a tungsten or molybdenum anode, thin layers of compounds of these metals become deposited on the inner surface of the arc tubes and act as selective filters. Drane also states that "a decrease in intensity is observed as the lamp is used, due essentially to partial devitrification of the silica glass of the arc tube." Prolonged heating causes the "amorphous fused silica to change over to tridymite and cristobalite in varying amounts, depending upon the conditions of heating and the presence of catalysts, if any. In this respect the hot mercury vapour is not without influence upon the devitrification which occurs upon the inner surface of the arc tube." Drane's remarks occur in a paper on "The operation of quartz mercury vapour lamps," and are only incidental to his main theme. The detailed evidence for these views and particularly for the part played by devitrification in the deterioration process does not appear to have been published as yet.

It may be of interest briefly to summarize the evidence for deterioration. The formation of ozone in the surrounding air is much more noticeable with a new lamp than with an old lamp. From this it can be inferred (*cf.* Lenard, *Ann. Physik*, 1900, i. p. 486) that the emission of very short wave ultra-violet rays decreases with time. Spectrum photographs taken with Schumannized plates show not only that the emission from an old lamp is materially less than that from a new lamp for all wave-lengths, but that the spectrum does not extend quite so far into the ultra violet. Actinometric records of the output at different stages in the history of a lamp exhibit the deterioration very clearly, and it is interesting to note that although a gradual decrease in emission is shown over the whole ultra-violet spectrum, a selective decrease is manifest in the very short wave ultra violet. The falling off is most noticeable on the short wave side of $250\text{ }\mu\mu$.

In the figure the life-history of an atmospheric burner as given by three different chemical methods of gauging ultra-violet intensity is shown (for details of these methods see Gillam and Morton, Journ. Soc. Chem. Ind. 1927, xlvii, p. 417). It will be seen that the very high initial output is maintained only for a small fraction of the effective life of the lamp, but that the decrease in intensity tends afterwards to occur much more slowly. The nitrate actinometer (*ibid.* p. 415) registers the greatest drop in output, a fact of some

Fig. 1.



Decrease in output of a 230-volt atmospheric mercury vapour lamp with time. The curves represent the output as measured by:

1. Anderson and Robinson's method.
2. The acetone-methylene-blue gauge.
3. The nitrate method.

significance, since the chemical change which is measured occurs almost exclusively with rays shorter than $270\mu\mu$. The spectroscopic and actinometric data we have obtained are perhaps a little unexpected. There are clearly two factors in the deterioration process, a shortening of the spectrum in the extreme ultra-violet and a gradual loss in

transmission of a less selective type. The relative importance of these two factors changes considerably during the life of the lamp. In the early stages the quartz remains relatively free from dark stains or deposits, but the output decreases very rapidly and the deterioration is largely confined to the extreme ultra-violet. As the period of operation lengthens the short wave limit of transmission ceases to move in the direction of longer wave-lengths. The output does not, however, remain steady, but decreases uniformly over the spectrum, just as if an increasingly dense "grey" screen were being interposed between the incandescent vapour and the arrangement for measuring the light intensity.

In order to test whether the drop in output was due to the formation of a metastable variety of quartz less transparent than the ordinary variety, the atmospheric burner was emptied and the mercury removed as completely as possible. The lamp had been in use for nearly 200 hours. The whole of the lamp was carefully cleaned with nitric acid, washed thoroughly, and heated to redness. The mercury was then replaced and the output of the lamp again measured. No appreciable improvement occurred as a result of such treatment, showing that the deterioration is independent of the luminescence phenomena which will be discussed later.

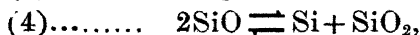
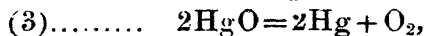
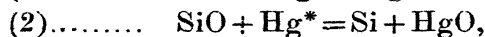
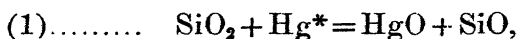
Several hypotheses may be formulated to account for these results. It is possible that light emission from the mercury permanently affects the quartz in some way. Baly ('Spectroscopy,' vol. ii, p. 332) writes as follows :

"It is well known that fused silica in layers about 2 mm. thick is markedly transparent to ultra-violet light to as far as wave-length 1900 Å. If this material is exposed to the radiation from a quartz mercury lamp for some days, then, providing it is kept cool, the silica develops an amethyst colour exactly similar to that of natural amethyst quartz. Not only has the silica now developed a visible colour, but it has also become opaque to ultra-violet light of short wave-length. This new condition of the silica is metastable, and if it is heated to about 500° C., or if it is crushed, it emits a brilliant green phosphorescence, and returns to its normal colourless state which is transparent to short wave ultra-violet light."

Our observations confirm the above quotation, but we are satisfied that the phenomenon has little or no connexion with the problem of the deterioration as observed with the 230-volt lamps available to us. The running temperature is so

high that the new state would, as we shall show, prove quite unstable. A closer investigation of the effect of light on fused quartz has shown that when a piece of the amethystine material is heated a thermo-luminescence occurs, and the quartz tends to revert to its original condition. Even more significant is the fact that the absorption spectra of irradiated and unirradiated fused quartz differ but little, and that in any case the difference could only account for a very small fraction of the observed deterioration.

A second hypothesis may be formulated as follows: In the luminous mercury vapour a large number of excited atoms must exist, and collisions with the walls of the lamp may sometimes be inelastic and the reactions



might all occur.

If this view were correct one might expect to find in an old lamp, silicon, silicon monoxide, and possibly silica formed in the cycle of changes and deposited on the vitreous quartz surface.

Silicon monoxide (see Meilior's 'Comprehensive Treatise on Inorganic Chemistry,' vol. vi. p. 235) is a dark amorphous solid prepared by the interaction of silica and carbon in the electric furnace. It burns in oxygen, decomposes water with evolution of hydrogen, and is soluble in warm alkaline solutions. It may now be asked whether the dark stain found on the inside of old mercury vapour lamps does in fact consist of silicon monoxide. It will be seen that the properties of the deposit (see above) are different from those of the monoxide, but are in agreement with those of silicon. Whilst there is therefore no evidence of the accumulation of solid silicon monoxide, it is scarcely possible to account for the observations without assuming its existence in the vapour state while the lamp is in operation.

Bonhoeffer (*Z. Physikal. Chem.*, 1928, cxxxi. p. 363) has studied the absorption spectrum of silicon monoxide vapour, and has recorded bands at 241·4, 234·4, 234·2, 229·9, 225·6, and 221·5 $\mu\mu$. These observations are of great interest because they provide an explanation of the marked decrease in the output of ultra-violet rays in the short wave region of the spectrum. If the ideas we have suggested are true,

the dominating factor in the early stages of the deterioration will be the absorption of rays up to $242\ \mu\mu$ by silicon monoxide vapour. On switching off the current some dissociation may occur, and the only possibilities are the deposition on the inside walls of a fresh layer of silica, of silicon, or of silicon monoxide in the solid state. Every time the lamp is used some silicon monoxide vapour must again be formed by the interaction of silica and activated mercury, and it is reasonable to expect that the solid deposit, whatever it may be, will gradually grow more dense. Minute specks of a fresh layer of silica or silicon will hinder the transmission of the vitreous quartz, and no doubt the concentration of silicon monoxide vapour in the discharge will approach constancy.

The two factors in the deterioration thus appear successively, and the actinometric data are in complete agreement with this mechanism.

An acceptable hypothesis should account for the fact that the brown deposit first appears at the constriction on the negative arm of the lamp tube. Since activated mercury atoms have a very short life period of the order 10^{-8} sec., the probability of collisions between activated atoms and silica is much greater in a more restricted space. Indeed, it may be stated that the deposit does in fact tend to occur preferentially wherever the shape of the tube causes the bombardment to be unusually severe. It will thus be seen that the observed facts are again consistent with the mechanism of deterioration which has been put forward.

Unfortunately no very ready means of overcoming the ageing effect emerges from the discussion.

Although the phosphorescence of fused quartz now appears to have little connexion with the behaviour of mercury lamps, it is well worthy of study on its own account. Our experiments had been in progress for some time before we became aware of those of Bailey and Woodrow detailed in the preceding communication. On account of the very similar trend of the results obtained in Prof. Woodrow's laboratory and in the present work, it was thought advisable to publish simultaneously.

A *résumé* of our experiments may now be given. In the first place it was found that the effect of ultra-violet rays on fused silica varied with different specimens. Some turned out to be excellent "phosphors," whilst others were apparently quite ineffective. One sample gave a faint but unmistakable green phosphorescence immediately after the lamp was turned out, and in a dark room this light could

be seen for several minutes. Emission of light persists for a very long time, since images can be recorded on a photographic plate (exposure 12–48 hours, see Pl. XXIV.) at least a fortnight after activation. No difference is detectable between the images obtained with the quartz in contact with the emulsion, and the quartz separated from the photographic plate by a slip of glass. The emission which affects the plate must therefore consist largely of rays longer than $325\text{ }\mu\mu$. Samples which had ceased to phosphoresce visibly became luminous again on heating. This thermo-luminescence has been observed to occur in two stages. Gentle heat produces light of a yellow-green colour, whilst with stronger heating the emission is bright blue-green. When a piece of activated quartz is heated with a fine blowpipe the yellow emission is seen to travel outwards from the point at which the flame impinges on the solid, and as the quartz becomes hotter a second zone of bluish light is seen to follow. The two phenomena are quite distinct, and the zones may be a couple of centimetres apart.

The light emission appears to correspond with (a) a highly unstable state, the return to the normal being accompanied by spontaneous emission of visible light; (b) a less stable state, the reversion from which to the normal is accompanied by a slow spontaneous emission, which may not terminate for months, and is detected photographically; (c) a metastable state, in which the absorbed energy can be retained practically indefinitely provided the quartz be not heated much above room temperature. The three stages are thus, a phosphorescence of short duration, another of longer persistence, and a third thermo-luminescence effect.

It is possible that (b) is merely a continuation at a low light intensity of the process which occurs in (a). The fact that two separate zones were observed in the "thermo-luminescence" may mean that the entire sequence of luminescence can be obtained with freshly activated quartz on application of heat, the yellow light being due to the first fall in energy level (which normally occurs spontaneously) and the bluish light being due to the reversion to the normal state from the metastable state associated with the pink colour. These doubtful points might be cleared up if a spectrographic record of the wavelengths emitted could be obtained. Unfortunately the intensity is too low for this purpose. In studying the relation between thermo-luminescence and temperature we have noticed no well defined discontinuity. A sample non-luminous at room temperature became feebly luminous

when dropped into water at as low a temperature as $55^{\circ}\text{C}.$, but in order to effect complete deactivation it is necessary to heat at least as high as $400^{\circ}\text{C}.$

It is interesting to record that specimens of fused quartz from test tubes sent from the United States to Professor E. C. C. Baly by Mr. W. T. Anderson, Jun., showed no sign whatever of phosphorescence or of thermo-luminescence. Natural rock quartz also appears to be completely unaffected by ultra-violet rays. There is no detectable difference in density between the specimens of fused quartz which show the phenomena and those which do not. Neither can we detect any change in density after irradiation.

A small piece of optically true fused quartz (thickness 0.1 in.) was obtained, and after prolonged irradiation under cold water was found to be activated in the sense that light was emitted freely on heating. Investigation of the absorption spectrum of this sample (which was very faintly amethystine), showed that no loss in transparency was detectable for ultra-violet rays longer than 220μ . Considerable difficulty was experienced in determining whether activation resulted in the development of opacity in the region $200\text{--}220\mu$. Some experiments showed a distinct difference between the transmissions of the active and deactivated materials in this region, but the effect was on so small a scale that absolute certainty of its reality is still to be sought. In order to settle this point it seems necessary either to enhance the whole activation phenomenon or to increase the delicacy of the spectroscopic test. We find that fused quartz test tubes do not develop sufficient opacity to affect appreciably the reading with any of the well known chemical methods of measuring ultra-violet intensity. The activation of the quartz has, however, been found by Baly to result in a reduction of yield in photosyntheses requiring rays shorter than 220μ .

If the activation process is concerned with metastable varieties of silica one might expect to find some evidence of incipient devitrification. Microscopic examination and experiments on polarization disclosed not the slightest trace of such an effect. This agrees with the density determinations since the values for various samples of fused quartz fell within the limits 2.210 and 2.228, whilst those of the rock quartz were 2.667 and 2.676. Since, however, the density of cristobalite is 2.21, the measurements of density do not exclude devitrification.

The above results seem to indicate that the phosphorescence and thermo-luminescence of fused silica is due to

the presence of a minute trace of impurity. Such an explanation is perfectly in accord with general notions on luminescence and is indeed supported by the uneven structure of the images illustrated.

Preliminary attempts to prepare silica phosphors using oxides of heavy metals in small amounts, with sodium fluoride as a flux, have not so far proved successful. Such phosphors possess considerable interest because the transparency of the fused quartz medium or diluent should, in favourable cases, allow the absorption spectra of the phosphors to be photographed.

The observations of Chapman and Davies ('Nature,' 1924, cxiii. 309) and Ludlam and West (*ibid.* 389) and also of Curtis (*ibid.* 495) show that quartz discharge tubes exhibit an intense phosphorescence after the current has been switched off. In all cases, it would now seem as if the mechanism of activation is the absorption of radiant energy of very short wave-lengths (90–220 $\mu\mu$). The phosphorescence obtained by using the light from a quartz mercury lamp as the source of activating rays is very much feebler than that obtained with discharge tubes in which ultra-violet rays in the Lyman region are freely generated. Nevertheless, the slow activation which we have studied seems to be essentially the same process, especially since the thermo-luminescence always appears, irrespective of the mode of activation. Ludlam and West favoured the view that the phosphorescence of transparent fused silica was due to minute traces of impurity, a conclusion strongly supported by our own observations.

Summary.

1. There are two factors operating in the deterioration of quartz mercury lamps, (a) a shortening of the spectrum confined to the extreme ultra violet, and (b) a non-selective loss in transmission.

2. The first factor preponderates for the first 150–200 hours and shows itself as a rapid fall in output. After this period the effect becomes fairly constant. During the subsequent history of the lamp the second factor plays an increasingly important part, but manifests itself much more slowly.

3. It is suggested that the first effect may possibly be due to the formation of silicon monoxide vapour inside the lamp, and the second effect may arise from the gradual deposition of a film of opaque elementary silicon.

4. The luminescent properties of fused quartz after treatment with ultra-violet rays have been studied. Little or no connexion subsists between these properties and the deterioration of quartz mercury lamps.

5. Three types of luminescence phenomena have been observed with transparent fused quartz :

- (a) a brief visible phosphorescence ;
- (b) a phosphorescence of long duration ;
- (c) a thermo-luminescence.

6. The balance of evidence points to the view that traces of impurity must be present in those samples of fused silica which exhibit luminescence.

Chemical Department,
The University,
Liverpool.

CXII. *The Electrification of Air by Friction.* By AGNES W. McDIARMID, M.A., *George A. Clark Scholar of the University of Glasgow* *.

ALTHOUGH a number of investigations have recently been described in which the charge of electricity produced by the friction of solid bodies on one another was measured, it appears to be doubtful whether electricity can be produced by the friction of gases on solids. Lenard † stated that when a drop of water splashes against a metal plate a positive charge goes to the water and a negative charge to the surrounding air, and Kelvin ‡ that air bubbled through water is negatively electrified. More recently experiments have been made with the direct object of testing the question whether electricity is produced between solids and gases. E. Perucca § found that mercury vapour flowing along a solid body produced electrification, while M. A. Schirmann || stated that mercury vapour, when flowing at great velocity in a glass tube, produced sparks at the places of greatest friction. It is, however, not quite certain that the electricity developed in these experiments was not due to

* Communicated by Prof. E. Taylor Jones.

† *Wied. Ann.* xlvi. p. 584 (1892).

‡ *Proc. Roy. Soc.* xlvii. p. 335 (1894).

§ *Zeits. f. Physik*, xxxiv. 2-3, pp. 120-130 (1925).

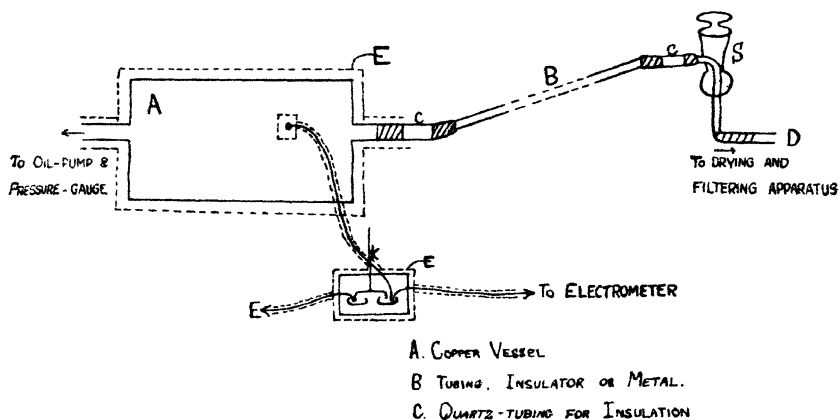
|| *Zeits. f. Physik*, xlvi. 3-4, pp. 209-236 (1927).

minute drops of liquid or to particles of dust contained in the air.

There seems to be definite evidence that dust clouds become electrified when in motion, in which case the electricity is probably due to the impact of solid particles on one another. Also, it has been shown that the number of volts developed by blowing a given mass of dust into a cloud increases very rapidly as the size of the dust particles decreases *.

It seems, therefore, not unlikely that a similar effect might, in suitable conditions, be produced by the impact of gas particles on a solid surface. The experiments described below were undertaken with the object of discovering

Fig. 1.



whether or not electrification can result from the friction of dry, dust-free air with solid surfaces. It was thought that such an investigation might lead to the discovery of facts which would be of use in the formation of a theory concerning the nature of frictional electricity in general.

Apparatus.

The simplest method of bringing about friction between air and solid bodies appeared to be to make a current of air pass quickly through tubes of the various solids. Fig. 1 is a diagram of the apparatus used. It consists essentially of a narrow tube B, and a copper vessel A. The whole

* G. B. Deodhar, Proc. Phys. Soc. xxxix. part 3 (1927); and W. A. Douglas Rudge, M.A., Proc. Roy. Soc. (1914).

apparatus could be rendered air-tight by shutting stop-cock S, and evacuated by means of an oil-pump, a pressure-gauge registering the pressure to which it was evacuated. Tube B was insulated from A and from the stop-cock S by means of short but adequate lengths of quartz tubing. The copper vessel, of volume about 5000 c.c., was connected by thin copper wire to one pair of quadrants of a Dolezalek electrometer. The other quadrants were permanently earthed. The vessel stood on a slab of paraffin-wax and was protected from external influences by means of an earthed metal shield surrounding it. The wire from vessel A led to a mercury key, K, insulated in paraffin-wax, through which connexion could be made either with the earth or with the electrometer. The mercury key and the connecting wire to the electrometer were surrounded by earthed metal shields, the key being worked by a long insulated handle protruding through the shield.

It was necessary that the air used to produce the friction should be dry and perfectly free from dust. With this in view, in the first form of the experiment S was joined to an earthed metal tube 12 in. \times 1½ in., containing tightly-packed glass-wool, which in turn was joined to a U-tube containing calcium chloride. Several readings were taken with this form of drying and filtering apparatus, but it was felt that there was no proof that the smaller dust particles were being removed. Aitken*, in his paper "On the Number of Dust Particles in the Atmosphere," describes experiments in which he investigated the filtering powers of different lengths of tightly-packed cotton-wool. By means of cloud experiments he concluded that filtration is perfect with 4 in. of tightly-packed wool, provided that the air is allowed to pass through very slowly. In the final form of the present experiment the air to be used for producing friction with the tubes was first passed very slowly through concentrated sulphuric acid and then through a glass tube 1½ in. in diameter, containing 8 in. of very tightly-packed glass-wool that had been soaked in concentrated sulphuric acid. From this the air passed through a stop-cock S' into a very large carboy, air-tight and connected to D, in fig. 1, then through an earthed metal tube, 1 in. in diameter, containing less tightly packed glass-wool.

Stop-cock S' was shut and the whole apparatus, *i. e.*, carboy and copper vessel, evacuated to a few millimetres pressure by means of an oil-pump. S' was then opened in

* *Trans. Roy. Soc. Edin.* vol. xxxv. p. 1 (1890).

such a way that air entered extremely slowly into the apparatus, after having passed through the sulphuric acid and the glass-wool. This procedure was repeated several times. Stop-cocks S and S' were then shut. This method of storing dried, filtered air was adopted so as to allow the passage of air very quickly through tube B. It could only be passed through quickly if filtered beforehand.

The essential difference from the earlier type of drying and filtering apparatus lies in the extremely slow passage of the air through the concentrated sulphuric acid and the tightly-packed glass-wool.

The readings obtained with both types of apparatus were of the same order of magnitude. Various suspensions were tried for the electrometer needle, that finally used being a silk fibre coated with platinum, and this proved extremely sensitive. With 12 volts on the needle the deflexion of a spot of light thrown on a scale 90 cm. distant was 600 mm./volt. The scale was calibrated by the difference of potential due to a known current passing through a known resistance. The only drawback to this suspension was that, after a large deflexion, the needle took a few minutes to return to the original zero-point. The electrometer was used throughout at sensitivity varying from 300 to 600 mm./volt. The insulation of the apparatus was tested frequently.

The friction tubes (B) used were of various materials, the insulators being glass, quartz, ebonite, and the metals iron, aluminium, copper, brass, lead. They were of various lengths and diameters and were dried before insertion.

The apparatus, up to stop-cock S, was rendered air-tight by shutting S, and was then exhausted to any required pressure by means of the oil-pump. During this procedure the vessel A was earthed. The position of the spot of light on the scale was noted. The vessel and one pair of quadrants of the electrometer were then insulated by lifting out key K. S was opened quickly, S' being kept shut, and dried, filtered air from the carboy rushed through B into vessel A. The deflexion of the spot on the scale and the time of inrush of the air were noted.

In another form of the experiment the vessel A was kept earthed, and tube B, if of metal (or a tinfoil covering wound tightly round B, if B was of insulating material), was connected with the insulated quadrants, the tube B being in every case surrounded by an earthed shield. The tube B was earthed while the apparatus was being exhausted, then B was insulated, air allowed to run through, and the deflexion noted.

The main idea of the experiment was thus to allow dry, dust-free air to pass rapidly through tubes of various materials, and hence into a metal vessel, either the vessel or the tube being connected to one pair of quadrants of the electrometer. The insulation of the apparatus was very satisfactory, and when the vessel was unearthed by raising key K, no deflexion of the needle was observed until air rushed through tube B. The capacity of the apparatus was determined approximately, and from the capacity and the potential corresponding to any deflexion of the needle the charge on the vessel A or the tube B could be obtained.

Results.

At first no attempt was made to obtain quantitative results, the primary objective being to discover whether the air and the tubes did actually become charged by the friction between them, owing to the air running through the tubes.

In every case, both with metals and insulators, a measurable deflexion of the electrometer needle was noted, showing that the passage of air into vessel A through tube B changed the potential of vessel A.

The potential to which vessel A was raised was of the order of magnitude of 1 volt, the charge given to it being of the order of $\frac{2}{3}$ e.s.u.

It was also found invariably that the deflexion obtained when vessel A was connected to the electrometer was opposite in sign to that obtained when tube B was connected to the electrometer. That is, the charge on vessel A, after the inrush of air, was opposite in sign to that on tube B.

Insulators

In each case, when a tube of insulating material was used, it was found that a second rubbing produced only a small deflexion, but that if the tubes were allowed to rest for a day or so, or in the case of glass or quartz were heated strongly, sometimes while still inserted in the apparatus, and then allowed time to cool between rubs, the deflexion of the electrometer needle was approximately the same as at the first rub. This was the case both when the vessel was connected and when the tube was connected to the electrometer. Thus, for example, a quartz tube 1 cm. \times 61 cm. gave on one occasion, on successive rubbings, deflexions +90, +15, +12, +10, whereas, after heating the tube strongly and rubbing it one hour later, the deflexion was +102. Again, a glass tube, 7 mm. \times 79 cm., gave on successive rubbings -600, -55, -20 mm. deflexion. Another glass tube 6 mm. \times 79 cm.

gave, when the rate of inrush of the air was very small, a deflexion —30 mm. At the second rubbing the speed was greatly increased and the deflexion was —75 mm. A third rubbing at this increased speed gave —10 mm.

These facts seem to point to the existence of a maximum charge for each tube, independent of the amount of air that passes through it.

Various experiments also pointed to the fact that the charge developed depends directly on the length of tube B, other things being equal. Thus, a tube 7 mm. \times 79 cm. gave on one occasion a deflexion —246 mm. This tube was allowed to rest and 46.5 cm. of it were cut off and rubbed under the same conditions as before. This time the deflexion was —154 mm., so that the charge developed on the air was directly proportional to the length of the tube. Many experiments confirmed this.

Occasionally reversals in the sign of electrification were noted. The general conclusion was, however, that the charge on the glass and ebonite used was positive, and on the quartz negative. The vessel A, and hence the air, was charged oppositely to the tube in each case.

A very large number of experiments were made, especially with glass tubes of various bores and lengths, and with various velocities of flow of the air. The difficulty of obtaining exact quantitative results, *e. g.*, as to effect of varying velocity of flow, of difference of bore, of varying length of tube, lies mainly in that of keeping the state of the surface rubbed exactly the same in different experiments. The changes in the state of the surfaces due to exposure to the atmosphere, and also to the friction, make exact results on such points difficult to obtain. These changes in the state of the surfaces may also account for the occasional reversals in the sign of electrification. Owing to the difficulty of keeping the surfaces in a definite state the quantitative results varied considerably on different occasions, but provided the rubbing tubes were examined after given treatment the results were always of the same order of magnitude.

A series of experiments with glass tubes, all of length 78 cm. and of bore varying from $\frac{1}{2}$ mm. to 1.5 cm., seemed to point to the fact that the electrification increases with the speed of flow. Some of the results are given in the following table:—

Bore in mm.	0.5	2	4	5	7	10
Time of flow in secs. ...	300	28	8	7	6	5 $\frac{1}{4}$
Deflexion in mm.	5	90	150	505	845	950

Phil. Mag. S. 7. Vol. 6. No. 40. Dec. 1928. 4 E

The above series would seem to point to a limiting case in which no tube is present and the air rushes directly into vessel A without previous passage through any narrow tube. To investigate this a cylindrical brass vessel, A, was used in the same position as A in fig. 1. The same precautions about insulation, etc., were taken. A hole 2 cm. in diameter was cut in one end of the vessel, and this was filled up with a plug of paraffin-wax, as thin as possible, but able to stand the strain when A was exhausted to a pressure of a few millimetres. A length of steel rod, 25 cm., was sharply pointed, and to its blunt end was attached a length of ebonite tubing with a cross-piece of ebonite to act as an insulating handle. The metal part was earthed, and precautions were taken to prevent charging of A by induction when a hand holding the sharp rod was brought near A. The procedure was to exhaust A, keeping it earthed, and then to push the steel point into and through the plug of wax. This held the vacuum. A was then unearthed and insulated. The spot of light on the scale remained steady, showing that the insulation was satisfactory. The steel rod was then pulled out and air rushed through the orifice thus made into the vessel. The spot of light remained steady, showing that no charge was produced by the inrush of air through the orifice. The size of the opening was varied so that the time of inrush of the air varied from 7 seconds to 14 seconds. In no case was any deflexion of the electrometer needle produced. It seems, then, that the presence of a tube was necessary to produce the electrification, and that the fact that wider tubes gave a bigger charge was due to the fact that they also permitted a greater velocity of flow.

This point was then tested directly with several tubes. For a glass tube 7 mm. \times 79 cm., when the time of flow of air was 7 secs., the deflexion was -246 , while when the time of flow was 45 secs. the deflexion was -10 , and when it was 9 secs. it was -130 . These results are typical and point to the fact that electrification of the air increases with its velocity of flow through the tubes.

Metals.

The metals used were iron, copper, brass, and aluminium, and were of the ordinary commercial grade of purity. With these, reversals in the sign of electrification were more frequent than with the insulators. The general conclusion was, however, that the charge on the brass and copper was positive, and on the iron and aluminium negative, the air being oppositely charged in each case. The results obtained

as to the effect of varying the speed of flow and the length of the tube were the same as in the case of insulators.

General Conclusions.

The results detailed above established at least the fact that the passage of a rapid current of air through a tube causes the current to carry with it charged particles of air and leaves the tube oppositely charged. According to the kinetic theory of gases the collision frequency of particles of the gas with one another and with the walls of the tube is increased by a negligible amount by the flow of the gas. It would thus appear probable that the quick flow of the current of air through the tube into the metal vessel is not primarily the source of the charged particles of air but serves mainly to remove from the vessel particles of air that have been charged by impact, due to their molecular motion, with the walls of the tube.

In May of this year J. Tagger* published a paper describing experiments wherein he measured the potential to which a horizontal helix of chrome-nickel wire, from which the surface layer of gas had been removed, was raised, whilst near its melting-point, by the impact of the molecules in the mass of air surrounding it. With high temperatures, *i. e.*, temperatures near the melting-point, a potential of 30 volts was reached.

There remains to explain the fact that the charge increased with increase in velocity of the air through the tubes. Three possibilities suggest themselves:—

- (1) The inrush of the air through the tube gives to the molecules a slightly larger velocity component in the direction of the flow. As the impacts of the molecules with the tube are in all directions, the charges produced in air at rest may balance one another. The additional velocity component in a fixed direction, though small, caused by the motion of the air through the tube, may call into being charges which will not be balanced by any other charges.
- (2) Quick motion of the air through the tube may be necessary to prevent the charges on the air and on the tube from re-combining and so masking the effect.

* *Phys. Zeits.* xxix. pp. 304-308, May 15 (1928).

- (3) Slow motion of the air through the tube may enable the tube to adsorb a layer of air so that only a very small part of the air passing through the tube is in actual contact with the material of the tube, or at least with a material different from itself. Only the air which passes through first will be in such contact, the remainder coming into contact only with a film of air.

Tagger's experiments, in which no restraint whatever was put on the direction of impact of the particles of air and the wire, seem to nullify the first alternative, although the two experiments differ so much as to make comparison difficult.

In conclusion, the writer wishes to express her thanks to Professor Taylor Jones for his continued advice and encouragement and for many helpful suggestions. The experimental work was performed in the Research Laboratories of the Natural Philosophy Department of the University of Glasgow.

October 1928.

CXIII. Development of Formulæ for the Constants of the Equivalent Electrical Circuit of a Quartz Resonator in Terms of the Elastic and Piezo-Electric Constants. By P. VIGOUREUX, M.Sc., of the National Physical Laboratory.*

CONSIDER a parallelepiped of alpha or low temperature quartz cut with its edges parallel respectively to the optic axis o , the electric axis e , and that axis which is perpendicular to o and to e , and which we shall call the third axis, t , and let o , e , and t denote the lengths of the edges of the parallelepiped.

If the potential difference between the two faces perpendicular to e be V , and the stress along e be $\frac{F}{ot}$, in the direction tending to produce extension, the extension y of the axis e , and the charge Q liberated at either of the $o.t$ faces, are given by the formulæ :

$$y = K_0 F - HV, \dots \dots \dots (1)$$

$$Q = K_1 V + HF, \dots \dots \dots (2)$$

* Communicated, by permission of the Radio Research Board, by Sir J. E. Petavel, K.B.E., F.R.S.

where o, t, e, y are in centimetres, Q and V in electrostatic c.g.s. units, and F in dynes; H is the piezo-electric constant, of value approximately 6.4×10^{-8} ; K_1 is the capacity between the two $o.t$ faces, namely,

$$K_1 = \frac{t \cdot o}{4\pi e} \cdot P, \quad . \quad . \quad . \quad . \quad . \quad (3)$$

where P , the permittivity, is approximately 4.55; the value of K_0 is readily calculated from the equation

$$\text{stress} = E \cdot \text{strain},$$

and found to be

$$K_0 = \frac{e}{t \cdot o} \frac{1}{E} \cdot . \quad . \quad . \quad . \quad . \quad (4)$$

The dimensions of H in electrostatic units are $L_3 M^{-1} T P^{\frac{1}{2}}$. The coefficient K_0 is not a capacity; formula (1) shows that its dimensions are $M^{-1} T^2$.

The modulus of elasticity E is generally taken as 7.85×10^{11} dynes per cm.^2 along e and t ; it has a higher value along the axis o .

The signs of the terms HV and HF in equations (1) and (2) depend upon the direction of the applied electric field and the orientation of the parallelepiped with respect to certain angles and edges of the complete quartz crystal out of which it is cut, but in any pair of equations such as (1) and (2) the signs are always opposite.

If there be, as before, a difference of potential V between the two $o.t$ faces, and if the stress along the third axis t be $\frac{F}{oe}$, the extension y_t of the axis t , and the charge Q liberated at either $o.t$ face, are given by the formulæ:

$$y_t = K_0 F + \frac{t}{e} H V, \quad . \quad . \quad . \quad . \quad (5)$$

$$Q = K_1 V - \frac{t}{e} H F; \quad . \quad . \quad . \quad . \quad (6)$$

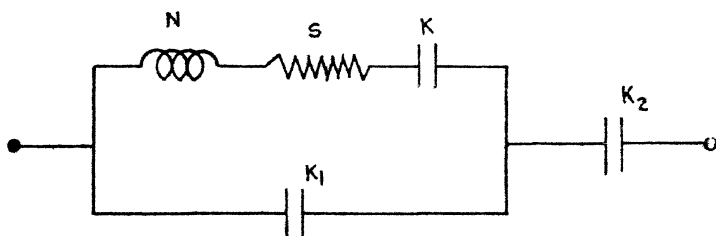
the value of K_1 is, of course, the same as before, but the value of K_0 is now

$$K_0 = \frac{t}{oe} \frac{1}{E} \cdot . \quad . \quad . \quad . \quad . \quad (7)$$

If no stress be exerted by mechanical means, and if the potential difference applied between the $o.t$ faces be alternating, the forced extension produced will also alternate, but will be so small that it could only be detected by using a

very high voltage between the two *o. t* faces ; if, however, the frequency of the applied difference of potential happens to coincide with one of the natural frequencies of the parallelepiped, the amplitude of vibration is greatly increased, because of resonance, and can be detected in several ways. In particular, the difference of potential may be applied by means of two metal plates of dimensions *o. t* placed close to the *o. t* faces of the piece of quartz and connected to the terminals of the condenser of an oscillatory circuit tuned approximately to one of the natural frequencies of the quartz, the coil of the oscillatory circuit being loosely coupled to the output coil of a valve generator. As the frequency of the generator passes through the natural frequency of the quartz, the quartz vibrates strongly and reacts on the oscillatory circuit, causing a diminution of current in the coil. This reaction was first observed by

Fig. 1.



Cady⁽⁴⁾, and was later studied in considerable detail by D. W. Dye⁽¹⁾, who showed experimentally that the behaviour of the vibrating quartz was nearly identical with that of a circuit shown in fig. 1 ; the capacity marked K_2 in the figure is that of the air-gap between the electrodes and the quartz, and is independent of the properties of the quartz. It is the object of the present paper to show how the effective inductance N and the effective capacity K can be estimated from the dimensions of the quartz, its modulus of elasticity, and its piezo-electric constant.

This problem is intimately connected with that of longitudinal vibrations. It is convenient first to calculate the simpler case by working out expressions for a thin bar ; it will be assumed that the variations which take place in its cross-section during the vibrations are negligible. This condition is not strictly satisfied, but the influence of the effect on the final results is very small indeed.

A bar of length e , supported at its middle point, is

subjected to a periodic stress $\frac{F}{to} = \frac{F_0}{to} \cos wt$, assumed uniformly applied throughout its length. We write here $w = 2\pi n$, where n is the frequency of the applied stress; it is required to calculate the displacement z of any point x at any time t . It is obvious that, since we are concerned with vibrations at or near resonance, the damping is of prime importance in determining the amplitude of the resonant vibrations; if it were neglected the equation of motion would lead to an infinitely large value for z at resonance.

Taking the origin of coordinates at the middle point of the bar, and writing E for the modulus of elasticity, s for the specific gravity, and Q for the damping coefficient, the equation of motion is

$$\frac{\partial^2 z}{\partial t^2} = \frac{E}{s} \frac{\partial^2 z}{\partial x^2} + Q \frac{\partial^3 z}{\partial x^2 \partial t}, \quad (8)$$

which is the form given by H. Lamb⁽²⁾ and applied recently by Cady⁽³⁾ to the particular problem of quartz resonators.

The coefficient Q includes not only the viscosity, which is small, but also the air-damping and the resistance to motion due to the mode of support of the bar and to other causes. The term representing air-damping is usually written as

$-P \frac{\partial Z}{\partial t}$, but the particular integral of the above equation being identical with the particular integral of the equation

$$\frac{\partial^2 z}{\partial t^2} + \frac{\pi^2}{e^2} Q \frac{\partial z}{\partial t} = \frac{E}{s} \frac{\partial^2 z}{\partial x^2}, \quad (9)$$

it is permissible to represent the whole of the resistance due to motion by the single term $Q \frac{\partial^3 z}{\partial x^2 \partial t}$. The value of Q is

in all cases very small compared with $\sqrt{\frac{E}{s}} e$, where e is the length of the bar. Writing a^2 for $\frac{E}{s}$, we have

$$\frac{\partial^2 z}{\partial t^2} = a^2 \frac{\partial^2 z}{\partial x^2} + Q \frac{\partial^3 z}{\partial x^2 \partial t}. \quad (10)$$

Two sets of conditions are required for the complete solution, namely the initial conditions which serve to determine the complementary function, and the boundary conditions which are used in the calculation of the particular integral.

The initial conditions give the state of the bar just before the periodic stress is applied ; they are, say,

$$z = f_1(x), \quad \text{and} \quad \frac{\partial z}{\partial t} = f_2(x), \quad . \quad . \quad . \quad (11)$$

where f_1 and f_2 are functions of x . They might even both be zero in our case, but will be considered arbitrary for more generality.

The boundary conditions supply data relating to the state of the bar at one or more particular values of x at any time t . In the present case they are that

$$\text{when} \quad x = 0 \quad z = 0, \quad . \quad . \quad . \quad (12)$$

$$\text{when} \quad x = \frac{1}{2}e \quad \frac{\partial z}{\partial t} = \frac{F_0}{otE} \cos wt, \quad . \quad . \quad . \quad (13)$$

for since the ends of the bar are free, the stress there cannot be influenced by the motion of the bar, but is equal to the applied stress.

Since the force impressed on the bar is of frequency n , part of the motion must take place at this frequency ; the particular integral will be

$$F(x) \cos wt + F_1(x) \sin wt,$$

where the functions $F(x)$ and $F_1(x)$ are determined by the boundary conditions.

The solution satisfying the equation (10) and the boundary conditions (12) and (13) is

$$\begin{aligned} z = & \sum_0^{\infty} A_k \epsilon^{-\frac{1}{2}Q \frac{\pi^2}{e^2} (2k+1)^2 t} \sin \frac{\pi}{e} (2k+1)x \\ & \cos \frac{\pi}{e} (2k+1) \sqrt{a^2 - \frac{Q^2 \pi^2 (2k+1)^2}{4e^2}} t \\ & + \sum_0^{\infty} B_k \epsilon^{-\frac{1}{2}Q \frac{\pi^2}{e^2} (2k+1)^2 t} \sin \frac{\pi}{e} (2k+1)x \\ & \sin \frac{\pi}{e} (2k+1) \sqrt{a^2 - \frac{Q^2 \pi^2 (2k+1)^2}{4e^2}} t \\ & + F(x) \cos wt + F_1(x) \sin wt, \quad . \quad . \quad . \quad (14) \end{aligned}$$

with the conditions that

$$\left. \begin{aligned} F(0) &= F_1(0) = 0, \\ F(\frac{1}{2}e) &= \frac{F_0}{otE}, \\ F_1(\frac{1}{2}e) &= 0, \end{aligned} \right\} \quad . \quad . \quad . \quad (15)$$

where the symbol "¹" represents differentiation with regard to x before substitution of $\frac{1}{2}e$ for x .

The first part of the solution decreases rapidly with time, and after a very short interval the particular integral alone is of importance; moreover, the degree of damping is greater for the overtones than it is for the fundamental, since it is

$$e^{-\frac{1}{2}Q \frac{\pi^2}{e^2} (2k+1)^2 t},$$

and the transient free motion therefore becomes more and more nearly sinusoidal before vanishing.

Once $F(x)$ and $F_1(x)$ have been determined, the coefficients A_k and B_k can, if desired, be calculated by the method usually employed for the Fourier series.

Making use of (11) and putting $t=0$ in (14), we have

$$f_1(x) = \sum_0^{\infty} A_k \sin \frac{\pi}{e} (2k+1)x + F(x);$$

therefore

$$\begin{aligned} \int_0^{\frac{1}{2}e} f_1(x) \sin \frac{\pi}{e} (2k+1)x dx \\ = \frac{1}{4}e A_k + \int_0^{\frac{1}{2}e} F(x) \sin \frac{\pi}{e} (2k+1)x dx, \end{aligned} \quad (16)$$

from which A_k is calculated.

In the same way, when $t=0$,

$$\begin{aligned} f_2(x) = \frac{\partial \tilde{z}}{\partial t} = \sum_0^{\infty} -\frac{1}{2}Q \frac{\pi^2}{e^2} (2k+1)^2 A_k \sin \frac{\pi}{e} (2k+1)x \\ + \sum_0^{\infty} \frac{\pi}{e} (2k+1) \sqrt{\alpha^2 - \frac{Q^2 \pi^2 (2k+1)^2}{4e^2}} B_k \sin \frac{\pi}{e} (2k+1)x \\ + w F_1(x), \end{aligned}$$

and proceeding as before, we find

$$\begin{aligned} \int_0^{\frac{1}{2}e} f_2(x) \sin \frac{\pi}{e} (2k+1)x dx \\ = -\frac{1}{4}e A_k \frac{1}{2}Q \frac{\pi^2}{e^2} (2k+1)^2 \\ + \frac{1}{4}e B_k \frac{\pi}{e} (2k+1) \sqrt{\alpha^2 - \frac{Q^2 \pi^2 (2k+1)^2}{4e^2}} \\ + w \int_0^{\frac{1}{2}e} F_1(x) \sin \frac{\pi}{e} (2k+1)x dx. \quad \dots \quad (17) \end{aligned}$$

The values of A_k and B_k are thus given by equations (16) and (17), and can be evaluated when the functions f_1, f_2, F , and F_1 are known.

In the present case we are not concerned with the values of A_k and B_k , but only with the steady motion, and need only find F and F_1 .

The particular integral is

$$z = F(x) \cos wt + F_1(x) \sin wt, \quad . \quad . \quad (18)$$

where $F(x)$ and $F_1(x)$ must satisfy the general equation and the conditions (15), namely

$$F(0) = F_1(0) = 0,$$

$$F'(\tfrac{1}{2}e) = \frac{F_0}{otE},$$

$$F_1'(\tfrac{1}{2}e) = 0.$$

The procedure is to substitute for z and its derivatives in equation (10), and to equate the sine and cosine terms, thus obtaining two simultaneous differential equations in F and F_1 from which F and F_1 are determined by a linear differential equation of the fourth order. This equation is

$$[(A^4 + w^2 Q^2)D^4 + 2a^2 w^2 D^2 + w^4]F = 0, \quad . \quad . \quad (19)$$

and the same for F_1 .

The expression for F , deduced from the above equation, thus contains four arbitrary constants, as also does the expression for F_1 , but the eight constants are related by four equations, which are easily obtained by substituting the values of F and F_1 in either of the original simultaneous differential equations in F and F_1 .

It therefore remains to determine only four constants from the four boundary conditions (15), when the following final result is obtained :

$$\left. \begin{aligned} F &= 2A \cos vx \sinh ux + 2B \sin vx \cosh ux, \\ F_1 &= 2B \cos vx \sinh ux - 2A \sin vx \cosh ux, \end{aligned} \right\} \quad . \quad (20)$$

where

$$\left. \begin{aligned} 2A &= \frac{F_0}{otE} \frac{u \cos \tfrac{1}{2}ev \cosh \tfrac{1}{2}eu - v \sin \tfrac{1}{2}ev \sinh \tfrac{1}{2}eu}{(u^2 + v^2) (\cos^2 \tfrac{1}{2}ev \cosh^2 \tfrac{1}{2}eu + \sin^2 \tfrac{1}{2}ev \sinh^2 \tfrac{1}{2}eu)} \\ \text{and} \\ 2B &= \frac{F_0}{otE} \frac{u \sin \tfrac{1}{2}ev \sinh \tfrac{1}{2}eu + v \cos \tfrac{1}{2}ev \cosh \tfrac{1}{2}eu}{(u^2 + v^2) (\cos^2 \tfrac{1}{2}ev \cosh^2 \tfrac{1}{2}eu + \sin^2 \tfrac{1}{2}ev \sinh^2 \tfrac{1}{2}eu)}, \end{aligned} \right\} \quad (21)$$

with

$$\left. \begin{aligned} u^2 &= \frac{1}{2} \frac{w^2(\sqrt{a^4 + w^2 Q^2} - a^2)}{a^4 + w^2 Q^2} \\ \text{and} \quad v^2 &= \frac{1}{2} \frac{w^2(\sqrt{a^4 + w^2 Q^2} + a^2)}{a^4 + w^2 Q^2} \end{aligned} \right\} \dots \dots (22)$$

To find the total extension of the rod at any instant we must double z and write $\frac{1}{2}e$ for x . We then obtain, after a very simple reduction,

$$y = 2 \frac{F_0}{otE} \frac{1}{u^2 + v^2} \frac{u \sinh eu + v \sin ev}{\cos ev + \cosh eu} \cos wt \\ + 2 \frac{F_0}{otE} \frac{1}{u^2 + v^2} \frac{v \sinh eu - u \sin ev}{\cos ev + \cosh eu}. \quad (23)$$

In the present case the stress $\frac{F_0}{ot}$ is produced by the difference of potential between the $o.t$ faces, according to equations (1) and (2). From equation (1) we see that a difference of potential V_0 tends to produce an extension $-HV_0$ which is equivalent to a force $-\frac{H}{K_0}V_0$.

Equation (1) shows that the restoring force for an extension y is

$$\frac{y + HV}{K_0}.$$

This, being a restoring force, is in the negative direction according to the convention adopted; when it is substituted for F in equation (2), we obtain

$$Q = K_1 V - H \frac{y + HV}{K_0} \\ = \left(K_1 - \frac{H^2}{K_0}\right)V - \frac{H}{K_0}y, \quad \dots \dots (24)$$

an expression for the total quantity of electricity through the resonator at any time.

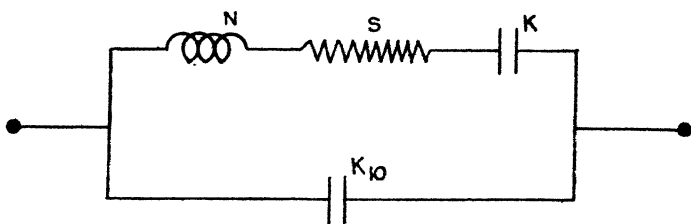
Writing

$$V = V_0 \cos wt \quad \text{and} \quad F_0 = -\frac{H}{K_0}V_0,$$

and substituting the value of y from equation (23), we obtain for the quantity of electricity

$$\begin{aligned}
 Q = & \left(K_1 - \frac{H^2}{K_0} \right) V_0 \cos wt \\
 & + 2 \frac{H^2}{K_0^2} \frac{V_0}{\partial t E} \frac{1}{u^2 + v^2} \frac{u \sinh eu + v \sin ev}{\cos ev + \cosh eu} \cos wt \\
 & + 2 \frac{H^2}{K_0^2} \frac{V_0}{\partial t E} \frac{1}{u^2 + v^2} \frac{v \sinh eu - u \sin ev}{\cos ev + \cosh eu} \sin wt. \quad (25)
 \end{aligned}$$

Fig. 2.



This expression is comparable with that for the quantity of electricity through a circuit represented in fig. 2, where we easily find

$$\begin{aligned}
 Q = & K_{10} V_0 \cos wt \\
 & - \frac{w^2 N - \frac{1}{K}}{\left(w^2 N - \frac{1}{K} \right)^2 + w^2 S^2} V_0 \cos wt \\
 & + \frac{wS}{\left(w^2 N - \frac{1}{K} \right)^2 + w^2 S^2} V_0 \sin wt. \quad \dots \quad (26)
 \end{aligned}$$

In order that the two expressions may be identical, we require

$$K_{10} = K_1 - \frac{H^2}{K_0}, \quad \dots \quad (27)$$

$$\frac{U}{U^2 + W^2} = -2 \frac{H^2}{K_0^2} \frac{1}{\partial t E} \frac{1}{u^2 + v^2} \frac{u \sinh eu + v \sin ev}{\cos ev + \cosh eu},$$

$$\frac{W}{U^2 + W^2} = 2 \frac{H^2}{K_0^2} \frac{V_0}{\partial t E} \frac{1}{u^2 + v^2} \frac{v \sinh eu - u \sin ev}{\cos ev + \cosh eu},$$

in which we have written for brevity

$$w^2N - \frac{1}{K} = U,$$

$$wS = W.$$

It is easily found from the above that

$$U = -\frac{1}{2} \frac{K_0^2}{H^2} \cot E \frac{u \sinh eu + v \sin ev}{\cosh eu - \cos ev}, \quad . \quad . \quad (28)$$

$$W = \frac{1}{2} \frac{K_0^2}{H^2} \cot E \frac{v \sinh eu - u \sin ev}{\cosh eu - \cos ev}. \quad . \quad . \quad . \quad (29)$$

For all the resonant frequencies of the parallelepiped w^2Q^2 is small compared with a^4 , and we have from equations (22) the approximate relations :

$$v = \frac{w}{a},$$

$$u = \frac{1}{2} \frac{w^2Q}{a^3},$$

$$\sinh eu = eu = \frac{1}{2} e \frac{w^2Q}{a^3},$$

$$\cosh eu = 1 + \frac{1}{2} e^2 u^2 = 1 + \frac{1}{2} e^2 \frac{1}{4} \frac{w^4Q^2}{a^6},$$

$$\sin ev = \sin \frac{ew}{a},$$

$$\cos ev = \cos \frac{ew}{a}.$$

Therefore

$$\begin{aligned} -Nw^2 + \frac{1}{K} &= -U = \frac{1}{2} \frac{K_0^2}{H^2} \cot E \frac{\frac{w}{a} \sin \frac{ew}{a}}{1 - \cos \frac{ew}{a}} \\ &= \frac{1}{2} \frac{K_0^2}{H^2} \cot E \frac{w}{a} \cot \frac{1}{2} \frac{ew}{a} \\ &= \frac{1}{2} \frac{K_0^2}{H^2} \cot E \frac{w}{a} \tan \left\{ \left(k + \frac{1}{2} \right) \pi - \frac{1}{2} \frac{ew}{a} \right\} \end{aligned}$$

But the condition for the resonance of the circuit of fig. 2 is that U should be approximately zero, so that

$$(k + \frac{1}{2})\pi - \frac{1}{2} \frac{ew}{a} \doteq 0$$

or

$$n \doteq (2k + 1) \frac{a}{2e}, \quad . \quad . \quad . \quad . \quad . \quad (30)$$

where n denotes the frequency.

For the fundamental mode of vibration

$$n \doteq \frac{a}{2e}.$$

We have

$$U = Nw^2 - \frac{1}{K} = -\frac{1}{2} \frac{K_0^2}{H^2} otE \frac{w}{a} \cot \frac{1}{2} e \frac{w}{a}.$$

To obtain the separation of N and K , differentiate this expression thus :

$$\begin{aligned} \frac{dU}{dw} = 2Nw = & -\frac{1}{2} \frac{K_0^2}{H^2} otE \frac{1}{a} \cot \frac{1}{2} e \frac{w}{a} \\ & + \frac{1}{2} \frac{K^2}{H^2} otE \frac{w}{a} \frac{1}{2} \frac{e}{a} \operatorname{cosec}^2 \frac{1}{2} e \frac{w}{a}; \end{aligned}$$

and since near resonance

$$\cot \frac{1}{2} e \frac{w}{a} \doteq 0 \quad \text{and} \quad \operatorname{cosec} \frac{1}{2} e \frac{w}{a} \doteq 1,$$

we have

$$\begin{aligned} N \doteq & \frac{1}{4} \frac{K_0^2}{H^2} otE \frac{1}{2} \frac{e}{a^2} \\ \doteq & \frac{K_0^2}{H^2} \frac{ote}{8} s \\ \doteq & \frac{K_0^2 M}{H^2} \frac{1}{8}, \quad . \quad . \quad . \quad . \quad . \quad (31) \end{aligned}$$

where s is the density and M the mass of the bar.

Near resonance the value of U is approximately zero, so that

$$NKw^2 \doteq 1.$$

Substituting in this the values of n and N as found by equations (30) and (31), we obtain

$$K = \frac{H^2}{K_0^2} \frac{8}{ote} \frac{4e^2}{4\pi^2(2k+1)^2a^2}$$

$$= \frac{H^2}{K_0^2} \frac{8}{\pi^2} K_0 \frac{1}{(2k+1)^2} \quad \dots \quad (32)$$

by making use of the expression for K_0 , formula (4).

The expression for S can be obtained in the same manner from equation (29) by calculating the value of w , from which it is found that

$$S = \frac{M}{8} \frac{K_0^2}{H^2} \frac{(2k+1)^2}{e^2} \pi^2 Q. \quad \dots \quad (33)$$

This expression for S is of no direct use, because Q represents several types of resistance to motion, the chief of which are viscosity, air-damping, and the effect of the support of the bar. The resistance S also includes the effect of dielectric loss in the quartz, due to the electric fields produced by the alternating stress. The value of S is determined directly from the reaction of the resonator on an electric circuit by methods developed by W. G. Cady⁽⁴⁾ and D. W. Dye⁽¹⁾. The above analysis therefore leads to the conclusion that the piezo-electric quartz bar, in the neighbourhood of one of its resonant frequencies, has the same impedance as an electrical circuit made up of a resistance S , an inductance N , and a capacity K in series, shunted by a condenser K_{10} , as in fig. 2, where the values of N , S , K , K_{10} are given by formulæ (31), (33), (32), and (27).

The auxiliary quantities M , K , and K_0 are

$$M = ote \cdot s,$$

$$K_1 = P \frac{ot}{4\pi e}, \quad \dots \quad (3)$$

$$K_0 = \frac{e}{to} \frac{1}{E}. \quad \dots \quad (4)$$

In the case of a disk cut perpendicular to the electric axis and vibrating along the electric axis, the product ot , wherever it occurs in the formulæ, should be replaced by $\pi o^2 = \pi t^2$, the sectional area.

Similar formulæ hold for vibrations along the third axis t , if instead of H we write $\frac{t}{e} \bar{H}$, and if we use for K the value

given by formulæ (7), namely $\frac{t}{oe} \frac{1}{\bar{E}}$. The values of K and

K_{10} are therefore the same as before, and N is altered in the

ratio of t^2 to e^2 so that the resonant frequency is altered in the ratio of e to t .

The above values hold only in the neighbourhood of resonance; by this we mean that they hold good for all values of $\frac{ew}{a}$ for which one can write without great error

$$\left| \cot \frac{1}{2} \frac{we}{a} \right| = \left| \left(k + \frac{1}{2} \right) - \frac{1}{2} \frac{ew}{a} \right|.$$

Thus, whenever the value of w is such that

$$\left\{ (2k+1) - \frac{ew}{a} \right\}^2$$

is small compared with unity, the electrical circuit gives a good representation of the quartz resonator.

Since the decrement of quartz is very small, and therefore the range of frequency over which it reacts on an electrical system only a small fraction of the fundamental frequency—at most one in a thousand, and generally not more than one in five thousand,—the above condition is always satisfied for the range of frequency with which we are concerned.

The equivalence between mechanical vibrating systems and electrical oscillatory circuits is, of course, well known, and S. Butterworth⁽⁵⁾ pointed out several years ago that many problems could be simplified by making use of the analogy. W. G. Cady⁽³⁾ subsequently mentioned the equivalence in the particular case of quartz rods, and K. S. Van Dyke⁽⁶⁾ gave expressions similar to the above for N , K , and K_{10} .

The equivalent capacity K can be measured experimentally, for example by D. W. Dye's⁽¹⁾ methods, and the average piezo-electric constant H can be calculated from formula (32). This requires that the quartz should be free from electrical twinning as well as from optical twinning, a condition very rarely met with even in the best specimens. An important figure, which is in some ways a measure of the suitability of the quartz for resonators and oscillators, is the ratio of K_1 to K . From equations (3) and (32) this is found to be for the fundamental:

$$\frac{K_1}{K} = \frac{\pi}{32} \frac{H^2}{E} P,$$

which, with the values of H , E , and P , given at the beginning of this paper, is 140. Most pieces of quartz give a value well above this figure, but the nearer the value is to 140 the better is the quartz, provided its damping S is low.

It is necessary to point out that the overtone frequencies are not given exactly by the formula (30):

$$n = (2k + 1) \frac{a}{2e}, \quad (30)$$

where k is an integer, because the formula was developed without taking into account the lateral motion of the vibrating bar. For a long thin rod the variations are small, although irregular, as shown by Giebe and Scheibe⁽⁸⁾.

An important result can be deduced from the above analysis, concerning the strain at any point of the vibrating rod. Since in all cases u is small, approximate expressions for 2A and 2B of formula (21), in the neighbourhood of resonance, are

$$2A = \text{constant} \cdot u,$$

$$2B = \text{same constant} \cdot \frac{w}{a}.$$

In an approximate expression we can neglect A in comparison with B, and we obtain

$$Z = F \cos wt + F_1 \sin wt,$$

substituting for F and F_1 by (20) gives

$$Z = \text{constant} (\sin vx \cosh ux \cos wt + \cos vx \sinh ux \sin wt),$$

and since x is never greater than $\frac{1}{2}e$, $\sinh ux$ can be neglected in comparison with unity, and the simple expression for Z is

$$Z = \text{constant} \cdot \sin vx \cdot \cos wt.$$

The displacement is therefore sinusoidal, being zero at the centre and a maximum at the ends, where $x = \pm \frac{1}{2}e$, and the strain is a maximum at the centre and decreases to zero at the ends. This was illustrated in a beautiful manner by Giebe and Scheibe⁽⁸⁾ with their luminous resonators.

This work has been carried out under the auspices of the Radio Research Board, to whom thanks are due for permission to publish.

List of References.

- (1) D. W. Dye, Proc. Phys. Soc. xxxviii. (5) pp. 399-458.
- (2) H. Lamb, 'Dynamical Theory of Sound.'
- (3) W. G. Cady, Phys. Rev. xix. p. 1 (1922).
- (4) W. G. Cady, Proc. Inst. Radio Eng. x. p. 83 (1922).
- (5) S. Butterworth, Proc. Phys. Soc. xxvii. p. 410 (1915).
- (6) K. S. Van Dyke, Abstract 52, Phys. Rev., June 1925.
- (7) And more recently Proc. Inst. Radio Engrs., June 1928.
- (8) Giebe and Scheibe, *Elektrotechnische Zeitschrift*, pp. 380-385 (1926)
Phil. Mag. S. 7. Vol. 6. No. 40. Dec. 1928. 4 F

CXIV. *The Power Relation of the Intensities of the Lines in the Optical Excitation of Mercury.*—Theory I. By E. GAVIOLA, Ph.D., Fellow of the International Education Board*.

IN a former paper by Wood and Gaviola † we have seen that the prediction of Wood ‡, that the intensity of some of the mercury lines appearing in the fluorescence of the optically-excited vapour (3650 for example) should be proportional to the cube of the exciting intensity, while others, such as 3654, 4358, etc., are proportional to the square, and others (2537) to the primary intensity itself, has been proved experimentally in a large range of variation. It has been found, for instance, that a 10·5-fold increase of the intensity of the exciting light was able to increase the intensity of the fluorescence line 3654 about 120 times, and of the line 3650 no less than 1200 times. The optically-excited vapour represents then a light-source which radiated energy, regarded in the light of the line 3650, apparently increases with the third power of the absorbed energy, or at least with the third power of the exciting intensity. This seems to be in contradiction with the principle of conservation of energy, and one must ask oneself, if it were possible to increase a hundred-fold the intensity of the mercury arc, would 3650 increase a million times in its brightness? And if so, where would the energy come from? To answer those questions it is necessary to make a quantitative study of the relations between the intensities of the primary exciting lines of the arc and of the secondary fluorescence lines in the vapour. We shall see that this theory will enable us at the same time to explain many of the results of Wood's experimental observations that could not be understood otherwise, for instance, the differences in the falling off of the intensity of the diverse lines along the cross-section of the tube when viewed "end on," and the changes in the intensity curves if gases are admitted to it.

The Intensity of 3650.

If we consider the diagram of energy levels of fig. 1 we see that the line 3650 is emitted by the 3^3D_3 level. Its intensity is then proportional to the number of atoms that

* Communicated by Prof. R. W. Wood.

† Phil. Mag., Aug. 1928, p. 352.

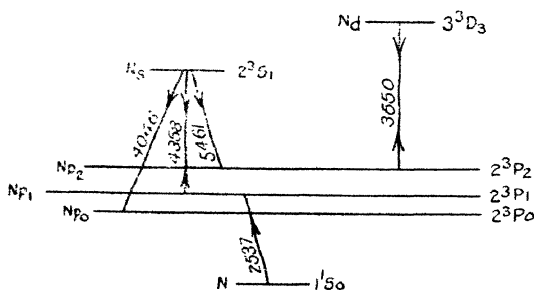
‡ R. W. Wood, Phil. Mag., Sept. 1927, p. 471.

happen to be excited in that level. This level is reached in our case of mercury vapour at room temperature, where the time between two collisions is large in regard to the life-time of an excited atom, so that collisions of the first or second kind do not play a significant role, only by the absorption of the line 3650 of the arc by the atoms on the level 2^3P_2 . We will call N_d , N_s , N_{p_1} , N , etc., the number of atoms in the different levels, as illustrated by fig. 1. N_d , the number of atoms in the level 3^3D_3 , is then proportional to N_{p_2} , and to the intensity of the line 3650 of the arc, that we will call I_{3650} or simply I_3 . It is then

$$N_d = c \cdot I_{3650} N_{p_2} \dots \dots \dots (1)$$

where c is a constant factor that does not interest us for the moment.

Fig. 1.



The level 2^3P_2 is supplied with electrons chiefly by the emission of the line 5461 by atoms with electrons on the level 2^3S_1 . The emission of 3341, 3663, 3654, and 3023 by the fluorescent vapour also brings electrons to that level (fig. 2), but the sum of the intensities of these lines in fluorescence is about 0.08 of the intensity of the green line 5461, so that one can neglect them in a first approximation. This is the reason why Wood found that only electrons coming down from 2^3S_1 seemed to be effective in producing the absorption and re-emission of 3650. The absorption of 4358 in the exciting light by means of a filter placed between arc and tube made 3650 practically disappear, in spite of the fact that 3131 and 3650 were not reduced by the filter*. The number of atoms on the level of 2^3P_2 is then proportional to the intensity of the green line in fluorescence that we will call J_{5461} . In general we will denote

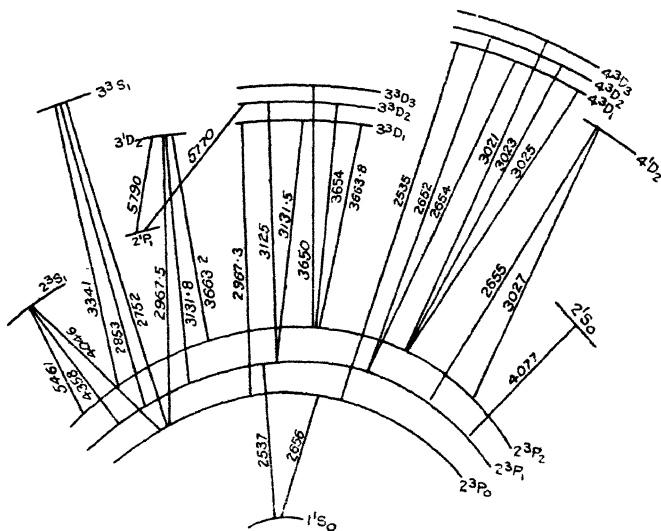
the intensities of the arc or exciting lines by I_{ss} , and the fluorescence or re-emission lines by J_{ss} . J_{5461} is on its side proportional to N_s , the number of atoms in the level 2^3S_1 . The level 2^3S_1 is reached, as we shall see later, mainly by absorption of the arc-line 4358 by the atoms in 2^3P_1 , so that

$$N_s \sim I_{4358} \cdot N_{p_1} \cdot \cdot \cdot \cdot \cdot (2)$$

Finally, the 2^3P_1 level is fed by the absorption of the resonance line 2537 by the normal atoms N,

$$N_{p_1} \sim I_{2537} N. \quad . \quad . \quad . \quad . \quad . \quad (3)$$

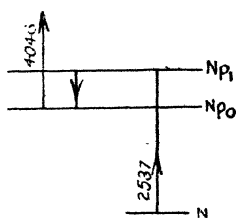
Fig. 2.



This last expression needs a justification: 2^3P_1 is not only supplied with electrons by the absorption of the resonance line, but by the emission of 4358, 3131, 3125, 4077, etc., by the fluorescent vapour, which brings atoms down to that level. But the sum of the intensities of all these lines is small in comparison with the absorbed intensity of 2537, which shows that the number of atoms that reach that level from below is large in proportion to the number of atoms that fall from above. Furthermore, the intensity of 2537, emitted as resonance radiation, is many times (about 1000 times) stronger than the added intensities of all the fluorescence lines footing on 2^3P_1 , which shows that most of the electrons raised to that level by the absorption of the

arc-line 2537 fall back to the normal level again, emitting that same line in resonance, and that only a small number of them are raised to higher levels owing to the absorption of 4358, 3131, 3125. Thus the total number of excited atoms in levels higher than 2^3P_1 is small in comparison with the number in this level. We can then calculate its density, neglecting the contributions from above. On the other hand, the number of normal atoms N is in all practical cases large in comparison with the sum of all the excited atoms, so that we can consider it as constant and independent of the intensity of the exciting light. One might think that this would be no longer true if we were able to increase the intensity of the arc sufficiently, especially considering the existence of metastable levels in which excited atoms might accumulate in such quantity as to diminish sensibly the amount of normal atoms. The following simple considera-

Fig. 3.



tions show that this cannot be the case; in fact, let us calculate the maximum amount of metastable atoms that can be obtained under ideal conditions.

If we assume that every atom excited by the absorption of 2537 becomes in one way or another, sooner or later, a metastable atom, the number of atoms falling to the level 2^3P_0 will be in the unit time $N\gamma I_{2537}$, where γ is the absorption coefficient of 2537. Let us also assume that atoms leave the level 2^3P_0 only because of the absorption of the line 4046; $\pi I_{4046} N_{p_0}$ is then the number of atoms leaving 2^3P_0 in the unit time, if π is the absorption coefficient of 4046. Under stationary conditions those two quantities must be equal, thus

$$N_{p_0} = N \frac{\gamma I_{2537}}{\pi I_{4046}}.$$

Now $\frac{I_{2537}}{I_{4046}} = 4$ in the arc, so that the ratio N/N_{p_0} is mainly determined by the ratio of the absorption coefficients of 4046

and 2537. This last ratio is not known, but one may safely assume that it is at least equal to 10. The ideal maximum number of metastable atoms can be then no more than $\frac{4}{10}$ of the amount of normal atoms,

$$\frac{N}{N_{p_0}} > 2.5.$$

In the practical case collisions of the second kind with impurities (H_2), and especially with the walls of the tube, and emission of the "forbidden line" 2656, will reduce the amount of metastable atoms, and thus increase considerably the ratio given above. N is then practically constant and the expression (3) is justified.

Summing up, we can write

$$N_d \sim I_3 \cdot N_{p_2} \sim I_3 \cdot N_s \sim I_3 \cdot I_2 \cdot N_{p_1} \sim I_3 \cdot I_2 \cdot I_1 \cdot N, \quad (4)$$

where I_1 , I_2 , I_3 are the intensities of the arc lines 2537, 4358, and 3650 respectively, and N , as said before, the number of normal atoms.

The intensity of the re-emission line 3650 will be

$$J_{3650} \sim N_d \sim I_1 I_2 I_3. \quad . \quad . \quad . \quad . \quad . \quad (5)$$

We must, however, consider the reduction of the intensity of the light of the arc by the vapour absorption as the rays traverse the tube. Owing to this, the intensity of the fluorescence may fall off appreciably along the diameter of the tube. Let us consider a volume element, v , in the interior of the vapour. Let its position be characterized by the coordinate x , measured from the entrance-point of the rays. The intensity of the lines 2537, 4358, and 3650 of the arc in the volume element v will be a function of x . The same is true for the fluorescence line 3650. We ought then to write

$$J_{3650}^{(x)} = A I_1^{(x)} I_2^{(x)} I_3^{(x)}, \quad . \quad . \quad . \quad . \quad . \quad (6)$$

where the exponents (x) will denote that those quantities are functions of x .

We can now answer the question set at the beginning of the paper. The intensity of the fluorescence line 3650 emitted by the volume element v will increase with the cube of the arc intensity as far as the intensities of the three arc lines concerned in its emission, *measured in the volume element v* , do really increase proportional to the intensity of the arc. We shall see that this is not always the case. To know how the primary intensities change with the position of the element v , we have to study the absorption laws for the different lines of the arc in the excited mercury vapour.

The Absorption of 2537 and of 4358.

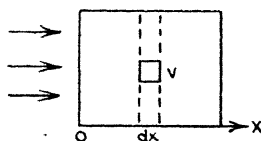
To simplify the calculations we will assume that our resonance tube is of square section, and that the exciting light is parallel. The position of a volume element v will be then characterized by its distance x from the entrance wall of the exciting light, and all of our quantities will be functions of that single variable.

The absorption law of 2537 is well known and reads

$$I_{2537} = I_{2537}^0 e^{-\gamma x}, \quad . \quad . \quad . \quad . \quad . \quad (7)$$

where I^0 is the intensity at the entrance wall of the tube, e is the basis of the natural logarithms, and γ is the absorption coefficient of the line which depends only on the density N of normal atoms in the vapour. At a given temperature of the saturated vapour that number will not depend on the intensity of the exciting light, as we saw above, and γ is then a constant.

Fig. 4.



To calculate the absorption of 4358 we need to know the number of atoms in the level 2^3P_1 as a function of x . The number of atoms raised to that level in the layer dx during the time t at the distance x of the entrance wall will be equal to

$$dI_1 = \gamma I_1 dx, \quad . \quad . \quad . \quad . \quad . \quad (8)$$

where $\gamma = cN$.

To that number we must add the number of atoms that fall from higher levels, but we have already seen that this number is small in comparison with the quantity raised by absorption of 2537, and we can, therefore, neglect them.

In the stationary state an equal number of atoms will abandon the level 2^3P_1 owing to spontaneous emission of the resonance line 2537, to absorption of lines like 4358 originating in that level, and to collisions of the first and second kind. If we call A , B , C , and D the probabilities of those four processes, the number of atoms leaving the level 2^3P_1 in the layer dx , and during the time unit, will be given by

$$N_{p_1}(A + B + C + D)dx. \quad . \quad . \quad . \quad . \quad (9)$$

The mean life-time of an excited atom in that level will be then

$$\tau_{p_1} = \frac{1}{A+B+C+D} \quad \dots \quad (10)$$

We have already seen that collisions of the first or second kind do not come into consideration because of the low temperature and of the low pressure of the vapour (the mean time between two collisions is of the order of 10^{-4} sec.), and that experimental results show that the number of atoms raised by absorption to higher levels is small in comparison with the number of atoms falling back to the normal state by re-emission of the resonance line, which means that B, C, and D are small in regard to the probability A of spontaneous emission, and we can neglect them safely. We have, then, practically

$$\tau_{p_1} = 1/A \quad \dots \quad (11)$$

Equating (8) and (9), and considering (10) and (11), we have

$$N_{p_1} = \gamma \tau_{p_1} I_1 = \gamma \tau_{p_1} I^0 e^{-\gamma x} \quad \dots \quad (12)$$

If we consider the excited atoms as forming a different gas, we can say that we have a gas the density of which falls exponentially as we retreat from the entrance wall of the light. We could say that the partial pressure of the gas falls exponentially, but it is not safe to speak of a partial pressure in this case. In fact, pressure is a thing that is given only by collisions, and since the mean life of an atom in the level 2^3P_1 (10^{-7} sec.) is much shorter than the time between two collisions of the excited atom in a gas of a pressure of 0.001 mm. (about $2 \cdot 10^{-4}$ sec.), the definition of pressure loses here its meaning in this case. We can speak of the density of the excited atoms, but not of a partial pressure. For the same reason, in spite of the fact that we have a gradient of the density, no diffusion will take place from the regions of higher to the regions of lower density. The path that an excited atom traverses during its mean life is only of the order of 10^{-8} cm. We shall see later that in the case of the metastable levels diffusion must be taken into account.

Now that the density distribution in the level 2^3P_1 is known, one can go a step farther and reckon the absorption of 4358. The absorption coefficient for this line will be proportional to the number of excited atoms, in the same way as the absorption coefficient of 2537 was proportional to the number of normal atoms. The difference is that in

the former case the coefficient was constant, while here it is a function of x . We can then write

$$dI_{4358} = -\delta I_{4358} dx, \quad . \quad . \quad . \quad (13)$$

where $\delta = aN_{p1} = a\gamma\tau_{p1}I_1^0 e^{-\gamma x}$.

We set

$$\alpha = a \cdot \gamma \cdot \tau_{p1}, \quad . \quad . \quad . \quad (14)$$

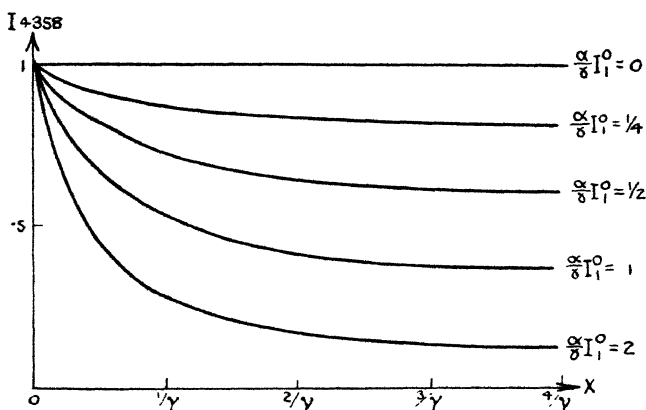
and (13) becomes

$$dI_2 = -\alpha I_1^0 \cdot e^{-\gamma x} \cdot I_2 \cdot dx. \quad . \quad . \quad (15)$$

The integral of this expression is

$$I_{4358} = I_2 = p \cdot e^{-\alpha \cdot I_1^0 \cdot \int_0^x e^{-\gamma x} \cdot dx} = p \cdot e^{\frac{\alpha}{\gamma} \cdot I_1^0 \cdot e^{-\gamma x}}.$$

Fig. 5.



The constant p is given by the condition that for $x=0$, $I_2 = I_2^0$ to

$$p = I_2^0 e^{-\frac{\alpha}{\gamma} I_1^0 (1 - e^{-\gamma x})}.$$

We have then

$$I_{4358} = I_2^0 \cdot e^{-\frac{\alpha}{\gamma} I_1^0 (1 - e^{-\gamma x})} \quad . \quad . \quad . \quad (16)$$

This expression can be abbreviated to

$$I_2 = I_2^0 \cdot e^{-\frac{\alpha}{\gamma} (I_1^0 - I_1)} \quad . \quad . \quad . \quad (17)$$

This is the absorption law for 4358. The same law will govern the absorption of 2894, 3131, 3125, 2652, 2654, 2655, and 4077.

Fig. 5 illustrates formula (17) for different values of $\frac{\alpha}{\gamma} I_1^0$. I_2^0 is set = 1.

The constant α plays in regard to 4358 a similar rôle as γ in regard to 2537. In that sense α could be called the absorption coefficient of 4358. The numerical value of α can be obtained by measuring the absorption of 4358 for a given value of x . Actually the absorption of 4358 is very small, and the line appears without a trace of reversal if examined with the large Lummer-Gehrke plate after traversing a 10 cm. layer of strongly excited vapour. That

means that $\frac{\alpha}{\gamma} I_1^0$ is small, and that I_2 is practically constant and equal to I_2^0 all along the cross-section of the tube. This would no longer be the case if we were able to increase sufficiently the intensity of 2537 (I_1^0).

The Number of Atoms on the Level 2^3S_1 .

Now that we know the absorption law of 4358 we can calculate the density distribution on the level 2^3S_1 , which will enable us to reckon the intensity of the fluorescence line 5461 in order to calculate the absorption of 3650. The absorption of 4358 in the layer dx at the distance x during unit time will bring a number

$$dI_2 = \alpha \cdot I_2 \cdot I_1 \cdot dx = \frac{1}{a} \cdot I_2 \cdot N_{p_1} \cdot dx \quad . \quad . \quad (18)$$

of atoms to the level 2^3S_1 . By emission of the triplet 4046, 4358, and 5461 these atoms will leave 2^3S_1 and distribute themselves among the three 2^3P levels. Now the upper and the lower of these levels are metastable, and the mean life of atoms on them, as measured by Dorgelo*, is of the order 10^{-3} sec. at least. We shall see later that we can confirm this result. Due to this long life, atoms will accumulate in the metastable levels, and if they do it in sufficient numbers they will absorb on their part the lines 4046 and 5461 of the arc, and thus bring a new contingent of atoms to the level 2^3S_1 . We cannot know *a priori* in which way most of the atoms reach that level, but we can make the following consideration:—If most of the atoms that reach 2^3S_1 are due to the absorption of 4358, the intensity of the re-emission lines 4046, 4358, and 5461 must be proportional to the square of the intensity of the exciting light, because two successive absorptions would be needed. On the other hand, if most of the atoms on that level were due to the absorption of 4046 or 5461 by the metastable

* *Physika*, vol. v. p. 435 (1925).

atoms, we would need three successive absorptions (absorption of 2537, absorption of 4358, emission of 4046 and 5461, and absorption of 4046 and 5461), to reach that level, thus the intensity of the re-emission lines ought to be proportional to the cube of the arc intensity. It has been found experimentally that the lines in question change with the square of the primary intensity, which shows that only the absorption of 4358 is of importance for the supply of electrons to the level 2^3S_1 .

We do not need then to consider the re-absorption by the metastable atoms.

The number of atoms that leave the level 2^3S_1 in the layer dx and during the time unit will be

$$N_s \frac{1}{\tau_s} dx, \quad . \quad . \quad . \quad . \quad . \quad (19)$$

if τ_s is the mean life-time of that level. In the stationary state the quantities (18) and (19) must be equal, and we have

$$N_s = \alpha \cdot \tau_s \cdot I_1 \cdot I_2. \quad . \quad . \quad . \quad . \quad . \quad (20)$$

This gives us the density distribution on the level 2^3S_1 . The intensities of the lines emitted by that level will be given by the same expression multiplied with the numerical factor corresponding to the transition probability of each of the three lines. It is then

$$J_{5461} = \epsilon_2 N_s, \quad J_{4358} = \epsilon_1 N_s, \quad J_{4046} = \epsilon_0 N_s, \quad . \quad . \quad (21)$$

where
$$\epsilon_0 + \epsilon_1 + \epsilon_2 = \frac{1}{\tau_s}.$$

Let us consider more closely one of these expressions, for instance, J_{5461} . Its intensity is by formulæ (20) and (21) proportional to the product of the intensities of two lines of the arc, 2537 and 4358. I_{2537} is an exponentially falling curve (formula 7), and its intensity will increase everywhere in the same ratio if we increase the light of the arc. I_{4358} is practically constant along the cross-section of the tube because the absorption of that line is weak, as we saw above. The product of both curves will give again, then, an exponentially falling curve with an extinction coefficient equal to the absorption coefficient of 2537. We should, therefore, expect that the intensity distribution of the fluorescence line 5461 along the cross-section of the tube will be given by an exponential function with an exponent coefficient γ . This can be tested experimentally. If we form an image of the cross-section of the tube upon the slit

of the spectrograph (see fig. 13 in the following paper) by means of a long-focus quartz achromatic lens, as described by Wood in one of his former papers, the intensity at the top of the slit will correspond to the light emitted by the layers at the entrance wall of the tube, while the intensity at the bottom of the slit will originate in the layers near the exit wall of the tube. Wood (*l. c.*) has already published a photograph of the lines 3654, 3663, and 3650 taken in that way, which shows that the experiment confirms our theory. A quantitative agreement cannot be expected, because in the experimental case the exciting light is not parallel, as assumed in our calculations, but divergent. The divergence of the intensity is probably proportional to the distance or less, and not to the square of the distance, because the light-source is long (10 cm.) and has a thickness of about 1 cm.

Expressions similar to (20) will give the density distribution of excited atoms in all the levels that are reached after two successive absorptions, like 2^1S_0 , 3^3S_1 , 3^1D_2 , 3^3D_1 , 3^3D_2 , and so forth, and expressions similar to (21) the intensity of the lines emitted by them.

The Number of Atoms in the Level 2^3P_2 .

The last expression for the intensity of the green line 5461 in fluorescence, or better, the differential of that expression, gives us the number of atoms that in the layer dx and unit time fall to the level 2^3P_2 . As we saw at the beginning, the emission of other lines like 3654, 3663, etc., brings also atoms to that level, but their quantity is negligible in comparison with the quantity brought down by the green line.

Because of the long life of the metastable level we should expect that the atoms falling to it (the density of which, as a function of x , is practically given by an exponential curve) would diffuse in the tube, so that they would distribute themselves homogeneously all over the cross-section of it. If that should take place, the absorption of 3650 would be constant along the section of the tube (3650 of the arc is absorbed very little in 2 cm. vapour, so that I_{3650} is practically constant), and the re-emission line 3650 should be also of constant intensity along the cross-section of the tube. Experiments show that this is not the case. The intensity distribution of 3650 along the slit of the spectrograph is the same as that of 4358 or 3654. That seems to show that diffusion does not take place in the level 2^3P_2 , under our

conditions, which signifies that the life of that level cannot be longer than 10^{-5} sec. The reasons for the shortening of the life of the metastable atoms on that level are probably to be sought in the absorption of the green line of the arc. If we remember formula (10) we see that the mean life of an excited level is inversely proportional to the sum of emission, absorption, and collision probabilities. Here the spontaneous emission probability is nearly equal to zero, and the collision probabilities are small, but the absorption probability for the lines originating on our level seems to be sufficiently large to shorten the life of the metastable level by the amount necessary to avoid diffusion*. We can thus go on in our calculation without considering it.

The number of atoms that reach 2^3P_2 in the layer dx is

$$J_{5461} dx. \quad . \quad . \quad . \quad . \quad . \quad . \quad (22)$$

The number of atoms that leave it is

$$N_{p_2} \frac{1}{\tau_{p_2}} dx. \quad . \quad . \quad . \quad . \quad . \quad . \quad (23)$$

Therefore

$$N_{p_2} = \tau_{p_2} \cdot J_{5461}. \quad . \quad . \quad . \quad . \quad . \quad . \quad (24)$$

This gives the density distribution in 2^3P_2 and enables us to calculate the absorption of 3650.

The Absorption Law of 3650.

The absorption coefficient of 3650 is given now by

$$\frac{dI_3}{I_3} = b \cdot N_{p_2} \cdot dx = \omega \cdot \alpha \cdot I_1 \cdot I_2 \cdot dx, \quad . \quad . \quad (25)$$

where

$$\omega = b \epsilon_2 \tau_{p_2} \tau_s.$$

The integration of this expression gives as a result

$$I_{3650} = I_3 = I_3^0 e^{-\omega I_2^0 \left[1 - e^{-\frac{\alpha}{\gamma} I_1^0 (1 - e^{-\gamma x})} \right]} = I_3^0 e^{-\omega (I_2^0 - I_2)}. \quad (26)$$

This is the absorption law for 3650. This equation looks very complicated, but in the experimental case ω is small; thus I_3 is practically constant and equal to I_3^0 .

The density distribution in the level 3^3D_3 will be then given by

$$Nd = \omega \alpha \tau_d I_1 I_2 I_3, \quad . \quad . \quad . \quad . \quad . \quad . \quad (27)$$

* Meissner and Graffunder (*Ann. d. Phys.* lxxxiv. p. 1009 (1927)) have found that side radiation is able to shorten the life of the metastable levels of Neon and Argon from 2 to 5 times.

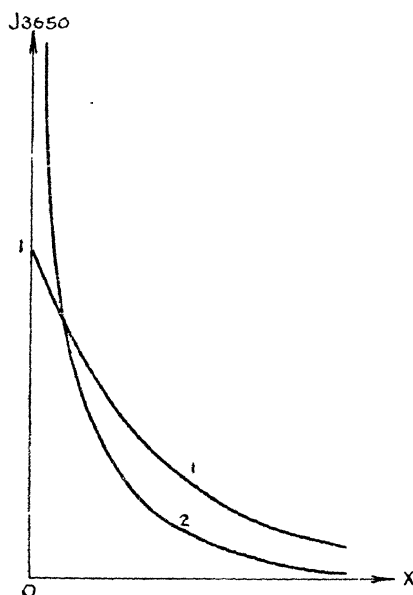
and the intensity of the fluorescence line 3650 by

$$J_{3650} = \frac{N_d}{\tau_d} = \omega \alpha I_1 I_2 I_3 = \omega \alpha I_1^{\circ} \cdot I_2^{\circ} \cdot I_3^{\circ} e^{-\gamma x} \cdot e^{-\frac{\alpha}{\gamma}(I_1^{\circ} - I_1)} \cdot e^{-\omega(I_2^{\circ} - I_2)} \quad (28)$$

Discussion of the Intensity Question.

We are now able to state what will happen in each volume element of the resonance tube if we increase constantly the intensity of the exciting light. We have already seen that in the actual case the two last factors of

Fig. 6



formula (28) are practically equal to one, thus the intensity distribution of 3650 as a function of x will be determined by $e^{-\gamma x}$, and its intensity will increase in every part of the tube proportional to the product of $I_1^{\circ} \cdot I_2^{\circ} \cdot I_3^{\circ}$, or, if we assume that the ratio $I_1^{\circ} : I_2^{\circ} : I_3^{\circ}$ is constant in the arc, proportional to the cube of the intensity of the arc. Fig. 6, curve 1, represents J_{3650} for this case. If we are able to increase the arc intensity sufficiently, the last two factors of the formula (28) would no longer be equal to one, but they would be more and more rapidly falling curves. J_{3650} would then be equal to the product of three falling curves, and could be represented by the curve 2 of fig. 6. We see that

the intensity of 3650 would still increase proportional to the cube of the arc intensity only in the first layer by $x=0$, but would eventually *decrease* for larger values of x . This means physically that the volume fluorescence of 3650 would concentrate more and more at the entrance wall of the tube, and we should have a thing similar to surface fluorescence. We cannot realize experimentally this case for the Hg fluorescence *in vacuo*, because we are not able to increase sufficiently the intensity of the arc, but we can do it by admitting gases into the tube, as we shall see in the following paper. The admission of 2 mm. water vapour, for instance, increases 4358 about 20 times for small x , but actually decreases it for larger values of x . (See Theory II.)

Summary.

The intensity of the different lines of mercury vapour at room temperature when excited optically by a water-cooled mercury arc has been calculated as a function of the primary intensities, and of the position of the emitting volume element in the tube, and the results allow us to understand the special behaviour of some lines like 3650.

The absorption laws for lines like 4358 and 3650 in excited mercury vapour have been calculated.

It is a pleasure for the author to acknowledge his indebtedness to Professor R. W. Wood for his many advices and assistance during the present work, and to Professor K. F. Herzfeld, who was so kind as to read this paper in manuscript and to suggest several improvements.

The Johns Hopkins University,
Baltimore, Md.
June 30, 1928.

CXV. *The Influence of Foreign Gases on the Optical Excitation of Mercury.*—Theory II. By E. GAVIOLA, Ph.D., Fellow of the International Education Board*.

[Plates XXV. & XXVI.]

IN the course of his extensive investigation of the fluorescence of mercury vapour, excited by the light of a water-cooled, magnetically deflected, mercury arc, Wood † has

* Communicated by Prof. R. W. Wood.

† Wood, Phil. Mag., Oct. 1925, Sept. 1927.

found that the admission of other gases to the tube containing the fluorescing mercury vapour at a pressure of 0.001 mm. (saturated vapour at room temperature) produced various effects upon the different remission lines, depending on the nature of the particular gas and on the partial pressure of it in the tube. It was found, for instance, that nitrogen at pressures of from 0.05 to 0.4 mm. decreased several times the intensity of the line 3650, while higher pressures up to 6 or more mm. increased it considerably. At 3 mm. it decreased the lines 3654, 3125, 4077, 2537, 3021, and at the same time enhanced many others like 5461, 4358, 4046, 3131, 3341, 2654, 2535. Carbon monoxide at low pressures decreased 3650, 3654, 3125, 3021, etc., and increased 3341, 3131, 2653, 2534, etc. Argon and helium behave similarly. Wood has also found that many of these changes can be explained if we assume that the collisions with molecules of the foreign gases bring a large number of atoms to the metastable level 2^3P_0 , where they accumulate due to the stability of that level, and become capable of absorbing strongly the line 4046 of the arc, practically not absorbed without the foreign gas; and he showed the existence of this absorption by photographing the 4046 line of the arc, after traversing a layer of excited vapour, with the large quartz Lummer-Gehrke plate, with the result that it appeared strongly reversed when nitrogen was present, but not in its absence. During the present work the action of different gases upon the absorption of 4046 has been studied in detail. This study has brought new and interesting facts to light in regard to the diffusion and lifetime of the metastable atoms and to the efficiency of their collisions with different gases—facts that enable us to calculate and predict the behaviour of the lines, especially the intensity distribution along the cross-section of the tube and its change when gases are admitted.

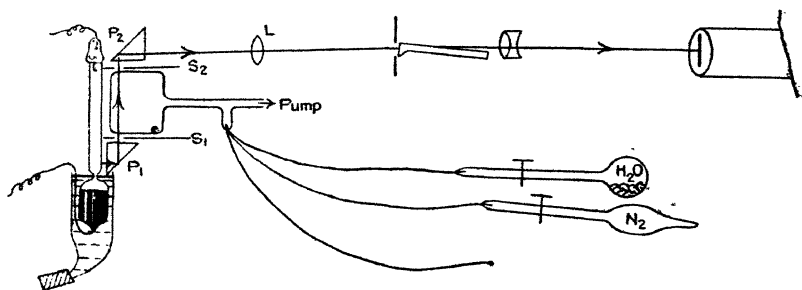
The Absorption of the Line 4046.

The arrangement used was similar to that used by Wood (*l. c.*), and is shown schematically by fig. 8.

A very clear and large quartz tube, 10 cm. long and 10 cm. in diameter, with plane end-surfaces was illuminated by the magnetically-deflected light of the water-cooled mercury arc, a part of which light was received by the quartz prism P_1 and sent parallel to the illuminated wall of the tube through the excited mercury vapour. A second quartz prism P_2 sent the light to the lens L of fused quartz, which made it parallel or slightly convergent to allow it to enter the large quartz

Lummer-Gehrke plate after traversing a polarizer. A quartz-fluorite achromat of 42.5 cm. focal distance threw an image of the interference system upon the wide open slit of the spectrograph. Two screens S_1 and S_2 limited the light-beam, and could be displaced so as to make the beam traverse the vapour at different distances from the entrance wall of the exciting light. The tube was in connexion with the pump and with bulbs containing the desired gases. A very fine capillary was occasionally used for admitting air or oxygen. Series of photographs of the line 4046 were taken with different pressures of CO, water vapour, and nitrogen in the tube. Fig. 1 (Pl. XXV.) shows the results. The first horizontal series corresponds to CO at partial pressures 0, .015, .1, .35, and 4 mm., the second to water vapour at pressures 0, .005, .03, .1, 1.5 mm., and the third to nitrogen at 0, .13, .55 mm. All the photographs had the same time

Fig. 8.



of exposure, 4 minutes. We can see that the presence of 0.015 mm. CO is sufficient to show a clear reversal of the main component (indicated by an arrow) of the line. If we increase the pressure, the reversal increases up to 0.1 to 0.2 mm. CO, and decreases again at higher pressures. At 4 mm. the reversal has disappeared completely, and no traces of absorption are left. Water vapour shows a trace of reversal at 0.005 mm., which increases rapidly by increasing water-vapour density until at 1 to 2 mm. the whole line is practically absorbed. At low pressures the behaviour of CO and H_2O is practically the same. Above 0.2 mm., on the contrary, the absorption of 4046 diminishes with CO, while it still increases with H_2O . We shall see later on that the theory is able to explain this fact on the assumption that the collisions of the second kind of metastable atoms with CO are more efficient than with H_2O . On the other hand, N_2 shows no clear reversal until a pressure of about 0.5 mm. is

reached; but a diffuse absorption of the line takes place from 0.1 mm. up, showing that in the presence of nitrogen not only the core of the line is absorbed, but the whole line, which seems to mean that nitrogen is capable of broadening the absorption line 4046. At higher pressures N_2 behaves similarly to H_2O , but water seems to be still more efficient than N_2 in accumulating atoms in the lower metastable level.

It was of importance to determine if a diffusion of the metastable atoms takes place. Metastable atoms are mostly generated at the entrance wall of the exciting light, because of the strong absorption of the resonance line in the mercury vapour at room temperature. A layer of 5 mm. reduces 2537 to $\frac{1}{2}$ of its original value; thus at 2 cm. distance of the entrance wall its intensity is only $\frac{1}{16}$. Now, the number of metastable atoms generated in each volume element of the tube, as we shall see later, is proportional to the intensity of the line 2357 of the arc at that volume element. If diffusion of the metastable atoms does not take place, the absorption of the line 4046 should decrease 16 times if the light-beam traverses the tube at a distance of 2 cm. from the illuminated wall of the tube; which amounts to saying that the absorption should practically disappear. On the other hand, if the metastable atoms live so long as to diffuse all along the cross-section of the tube, the absorption of 4046 should be the same everywhere. To test this point the screens S_1 and S_2 (see fig. 8) were so placed as to make the beam of light traverse the tube parallel to the illuminated wall at distances of 2 and 5 cm. from it. Fig. 2 (Pl. XXV.) shows the result of a series of photographs taken with different pressures of water vapour in the tube, and with the beam traversing it at 2 cm. distance from the illuminated wall. We see that *in vacuo* no reversal takes place, as is to be expected, but a clear reversal of the main component of the line (indicated with arrows) appears with 0.2 to 0.5 mm. water in the tube, to disappear again if the pressure attains 2 mm. If the beam traverses the tube at 5 cm. distance from the wall, no reversal is to be detected under any water pressure. These facts show that diffusion of the metastable atoms does actually take place at low water pressure, and that the mean life of the excited atoms is long enough to allow them to diffuse 2 cm., but not long enough to allow them to diffuse 5 cm. With these values we shall make, in a following paragraph, an approximate calculation of the mean lifetime of a metastable atom on the level 2^3P_0 .

The reason why the diffusion disappears if the water pressure is increased to 2 mm. is probably two-fold: the

higher pressure shortens the mean life of the metastable atoms, and, on the other hand, the diffusion velocity diminishes with the pressure, so that in the case in which the mean life is not decreased, the path travelled during that life would diminish in proportion to the pressure.

The same experiments were repeated with N_3 , with the result that no reversal of 4046 could be found at 2 cm. distance with any nitrogen pressure. This result is to be expected because we have already seen that, with N_2 , when the beam traverses the tube close to the illuminated wall, the reversal begins at the pressure of 0.5 mm., which is already too high to allow them to diffuse. No diffusion experiments have been made with CO so far, but I should expect it to behave at low pressures like water vapour.

The Metastable Level 2^3P_2 .

These experiments show that large quantities of atoms accumulate on the metastable level 2^3P_0 . Now, mercury has another metastable level, the level 2^3P_2 . It was of importance to ascertain if atoms accumulate in this level also. To examine this question, the lines 5461 and 3650 of the arc were photographed as before, to see if they reverse when gases are introduced. The result was that no reversal or absorption of 5461 could be detected under any conditions. This proves that the upper metastable level must be many times less densely occupied than the lower one in the presence of gases. On the other hand, Wood has observed that the arc line 3650 appears slightly reversed if it traverses a 10 cm. long layer of excited mercury vapour in the absence of any gases. I can confirm this result. Now, if we introduce gases into the tube, the reversal at first disappears (gases at low pressure), to come up again if we attain a water or nitrogen pressure of 1 or 2 millimetres, which shows that the number of atoms in 2^3P_2 decreases at first to increase afterwards. The change of the intensity of the fluorescence line 3650 is in accordance with this result. Its intensity can be given by the formula

$$J_{3650} = a \cdot I_{3650} \cdot N_{P_2},$$

where I_{3650} is the intensity of the arc line 3650, and N_{P_2} is the density of atoms on the level 2^3P_2 (see preceding publication: Theory I., formula (1)). Now, the introduction of gases at low pressure does not change I_{3650} of the arc, so that the changes in the intensity of the remission line 3650 are, so to speak, a measure for the changes in the density of

atoms on the level 2^3P_2 . In fact, at foreign gas pressures below 1 mm. the time between two collisions of an excited Hg atom is larger than 10^{-7} sec., so that collisions of the second kind play a rôle only in regard to the 2^3P levels, the mean life of which is longer than this time. All the other levels will be practically undisturbed by collisions. Wood has already measured the changes in the intensity of the fluorescence lines with different pressures of nitrogen. The following is an abstract of his measurements :—

Nitrogen pressure .	1.25	0.43	0.2	0.1	0.05	0.00 mm.
5461	12	6	4	2	1.5	1
3650	1	1	$\frac{1}{2}$	$\frac{1}{4}$	$\frac{1}{5}$	$\frac{1}{1}$
5461 3650	12	6	8	8	$7\frac{1}{2}$	1

We see in the second line that the intensity of 3650 decreases at first and increases slowly afterwards with growing pressures of nitrogen, while 5461 increases steadily (the initial intensities are arbitrarily set equal). Now, we have seen that the level 2^3P_2 is supplied with electrons practically exclusively by the emission of 5461 (Theory I.). The increase of that line means an increase in the number of atoms that reach that level. In spite of this fact the number of atoms in the level diminishes as shown by the intensity of 3650. The density of atoms on 2^3P_2 can diminish only as a result of collisions with the nitrogen molecules. The ratio of the increase of 5461 to the increase of 3650 will give the number of times that the density in the level 2^3P_2 decreases due to the collisions. That ratio is given above. We should expect the ratio to grow with the pressure. It grows with it, but in an irregular way. But we must remember that Wood considered the given values as provisional. In that light the result can be regarded as satisfactory. The level 2^3P_2 seems, then, to be very sensitive to collisions with nitrogen molecules. The fact that 0.1 mm. of nitrogen is able to diminish 8 times the number of atoms in 2^3P_2 is very remarkable if we remember that the same gas pressure would quench the re-emission line 2537 only to about 97 per cent. of its original value (see the known quenching curves of Stuart), which means that the number of atoms on the level 2^3P_1 is only very slightly decreased. We have here the interesting case in which a "metastable level" becomes much less stable against collisions than an "unstable level." This may be correlated with the fact that Lord Rayleigh has observed the "forbidden" line 2270, which is emitted by the level 2^3P_2 in both emission and absorption.

The extremely great sensibility of the excited atoms in the level 2^3P_2 to collisions is not only shown in regard to nitrogen, but to all the other gases that have been tried.

We can make a rough calculation of the mean life of the atoms in the metastable level 2^3P_2 on the base of the facts outlined above. The number of atoms in the level 2^3P_2 is given by formula (24) of Theory I. :

$$N_{P_2} = \tau_{P_2} \cdot J_{5461}.$$

This relation is true for every gas pressure. We can plot now J_{5461} and N_{P_2} as function of the pressure if we admit J_{3650} as a measure for N_{P_2} . The division of both curves gives us the mean life τ_{P_2} as a function of the pressure. The

Fig. 9.

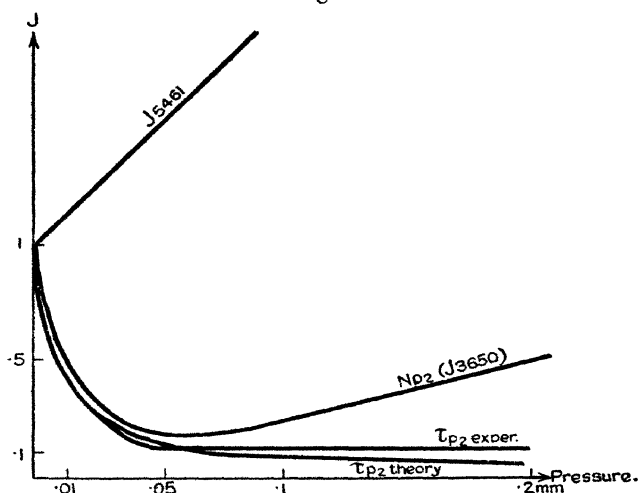


diagram (fig. 9) shows that τ_{P_2} decreases with the pressure, which is to be expected. At 0.01 mm. nitrogen τ_{P_2} decreases to $\frac{1}{2}$ of its original value. The time between two collisions of an excited atom at that pressure of nitrogen is about 10^{-5} sec.

Now

$$\tau_{P_2} = \frac{1}{B_2 + D_2}$$

if B_2 is the absorption and D_2 the collision probability, and if we neglect the emission probability. On its side $D_2 = Z \cdot E_2$ if Z is the number of collisions and E_2 the efficiency of them ; hence

$$\tau_{P_2} = \frac{1}{B_2 + ZE_2} \quad \dots \dots \dots (29)$$

This value will decrease to $\frac{1}{2}$ when the pressure is such that $B_2 = ZE_2$. Experimentally it does so at 0.01 mm. pressure, at which $Z = 10^5$ collisions per sec. That means $B_2 = 10^5 \cdot E_2$, and for $Z = 0$:

$$\tau_{P_2} = \frac{1}{B_2} = 10^{-5} \cdot E_2 \text{ sec.}$$

If every collision is effective ($E_2 = 1$), 10^{-5} sec. is the mean life of the metastable level 2^3P_2 for the case of vacuo; that is, when no foreign gas is present. If gases are admitted, τ_{P_2} decreases according to formula (29). In fact, if we plot (29) according to the value given above, we obtain the lower curve of fig. 9, which is in surprisingly good agreement with the empiric curve for τ_{P_2} .

Summing up, we can say that the primary and principal action of gases consists in bringing excited atoms from the levels 2^3P_2 and 2^3P_1 to the metastable level 2^3P_0 . If the gas pressure is sufficiently low, diffusion of the metastable atoms takes place; otherwise not. We will now see that the theory enables us to explain all the other changes due to gases, especially the changes in the distribution of the intensity along the cross-section of the tube, without making further assumptions.

The Levels 2^3P_1 and 2^3P_0 .

We have seen in the first part of this investigation (Theory I., formula (12)) that the density distribution of atoms on the level 2^3P_1 in the case of vacuo, that is, in the case when only Hg vapour at room temperature is in the tube, was given by the formula

$$N_{P_1} = \gamma \tau_{P_1} I_1^0 e^{-\gamma x}, \quad \dots \quad (12)$$

where γ is the coefficient of absorption of the resonance line 2537 of the arc, τ_{P_1} the mean life of an excited atom on the level 2^3P_1 , and x the distance of the volume element considered from the illuminated wall of the tube. This formula holds also for the case of gases with the sole difference that τ_{P_1} was determined *in vacuo* practically exclusively by the emission probability A_1 of the line 2537 (see formula (11), Theory I.), and it was $\tau_{P_1} = 1/A_1$, while now the mean life is shortened by the collisions with the gas molecules that bring atoms to the lower level 2^3P_0 . It is now

$$\tau_{P_1} = \frac{1}{A_1 + D_1}, \quad \dots \quad (29')$$

where D_1 is the probability that a collision of the second kind will take place, which is given by the number of collisions in the time unit multiplied with the efficiency E_1 of those collisions in producing transitions without radiation :

$$D_1 = z \cdot E_1 \dots \dots \dots (30)$$

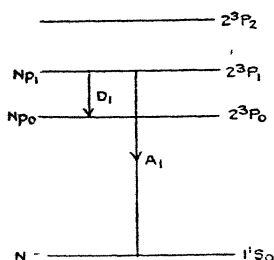
z is proportional to the gas pressure.

The number of atoms in the layer dx , which during unit time will reach the metastable level 2^3P_0 because of collisions, will be

$$D_1 N_{P_1} dx.$$

Another contingent of atoms will reach the level 2^3P_0 because of the emission by the fluorescent vapour of lines like 4046, 2967, etc. (see fig. 2, Theory I., p. 1156); this contingent is

Fig. 10.



but negligible compared with the amount of metastable atoms produced by collisions. If no diffusion takes place, the number of atoms that in unit time leave that level in the layer dx will be

$$N_{P_0} \cdot \frac{1}{\tau_{P_0}} \cdot dx,$$

where τ_{P_0} is the mean life duration of the metastable atoms. Equating these expressions, we have

$$N_{P_0} = \tau_{P_0} \cdot N_{P_1} \cdot D_1 = \pi \gamma I_1 = \pi \gamma I_1^0 e^{-\gamma x} \dots \dots (31)$$

if we set

$$\pi = D_1 \cdot \tau_{P_1} \cdot \tau_{P_0}, \dots \dots \dots (31')$$

and put for N_{P_1} its value given above. The mean life τ_{P_0} of the metastable level was determined in the case of vacuo mainly by the absorption of lines terminating on that level, and by the collisions with the walls of the tube. In our

case, the collisions of the second kind with gas molecules will play an important rôle. We can write

$$\tau_{P_0} = \frac{1}{A_0 + B_0 + D_0},$$

where A_0 is the emission probability of the forbidden line 2656, which is emitted by the metastable atoms, B_0 the absorption, and D_0 the collision probability. Now, the emission probability of the forbidden line is extremely low; thus we can practically put

$$\tau_{P_0} = \frac{1}{B_0 + D_0} \quad \dots \quad (32)$$

D_0 will be given by the number of collisions of the metastable atoms multiplied with the efficiency of those collisions:

$$D_0 = z \cdot E_0.$$

The numerical values of E_0 are not as well known as for the case of the level 2^3P_1 . According to results of Donat* Dorgelo†, Loria‡, Franck and Cario§, and ourselves, E_0 is very large for H_2 , O_2 , small for CO , N_2 , He , and smaller still for Ar and H_2O . Quantitative determinations have not yet been made so far as I know.

Diffusion of Metastable Atoms.

Formula (31) was calculated under the assumption that no diffusion takes place, which, as we have seen, is not the case for gases at low pressure. The diffusion will not affect the total number of metastable atoms in first approximation, since it does not alter D_1 nor τ_{P_0} . It influences only the density distribution in the section of the tube. If we assume that in the case of diffusion the density becomes constant, which is not completely true in the experimental case, as we saw before, but very nearly realized, the average density will be

$$\bar{N}_{P_0} = \int_0^1 N_{P_0} dx$$

if l is the length of the cross-section of the tube. The integration gives as result

$$\bar{N}_{P_0} = \pi I_1^0 (1 - e^{-\gamma}) = \phi \cdot I_1^0, \quad \dots \quad (33)$$

where

$$\phi = \pi (1 - e^{-\gamma}).$$

* Donat, *Zeits. f. Phys.* xxix. p. 345 (1924).

† Dorgelo, *Physika*, v. p. 435 (1925).

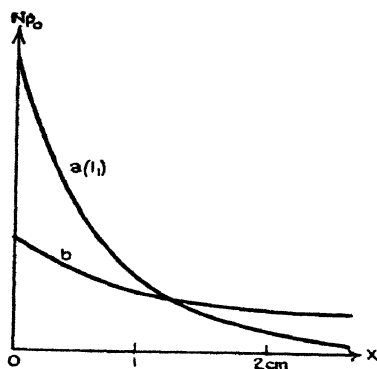
‡ Loria, *Phys. Rev.* xxvi. p. 573 (1925).

§ Franck & Cario, *Zeit. f. Phys.* xvii. pp. 202, 223 (1923).

The average density will thus be simply proportional to the total absorption of the line 2537 of the arc.

We can test formulas (31) and (33) by means of the "forbidden" line 2656. This line is emitted by the metastable atoms, and its intensity distribution along the cross-section of the tube will show directly the density distribution of the metastable atoms. Fig. 3 (Pl. XXVI.) gives a $6\times$ enlargement of two photographs of the forbidden line 2656 (on the long wave-length side of the pseudo-triplet 2652, 2654, 2655) taken while an image of the cross-section of the tube was thrown upon the slit of the spectrograph so that the light at the top of the slit corresponds to the emission near the entrance wall of the resonance tube ($x = 0$), and at the bottom to light near the exit wall ($x = 1$). a was taken

Fig. 11.



while 2 mm., b while 0.2 mm. water vapour were in the tube. We see that, in the first case, the intensity of 2656 decreases along the slit, while in the second it remains practically constant, as is to be expected after formulæ (31) and (33). The behaviour of the other lines will be explained later. The verification of our formulæ shows again that diffusion of the metastable atoms takes place with 0.2, but not with 2 mm. water vapour in the tube.

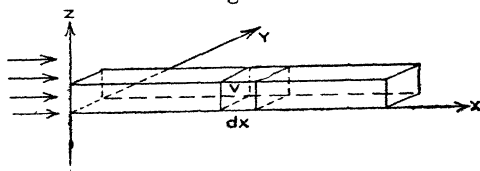
The Mean Life of the Metastable Atoms in the Level 2^3P_0 .

We saw in a former paragraph that when 2 mm. of water vapour are present in the tube, diffusion of the metastable atoms does not take place. The density distribution along the cross-section of the tube is given by the absorption law of the resonance line 2537, as shown by formula (31) and by fig. 11 (curve a). If we diminish the pressure, diffusion does

take place, and the density of the N_{P_0} atoms will be represented by a curve like b . The form of the curve b will depend on the mean lifetime of the metastable atoms, and on the diffusion-coefficient, which at a given temperature is inversely proportional to the pressure, and can be calculated with the help of the kinetic gas theory. Curve b will depend, then, at a given pressure, only on the mean life τ_{P_0} of the metastable atoms; for growing τ_{P_0} it will approximate to a horizontal line, and for small τ_{P_0} it will coincide with curve a . Now, curve b can be experimentally determined by measuring the absorption of 4046, or the intensity of the "forbidden" line 2656, for different x -values, and that will allow us to calculate the mean lifetime τ_{P_0} .

Let us consider a parallelepipedon of section $dy dz$ along the x -axis, which is perpendicular to the light entrance-wall of the tube (fig. 12), and a volume element $v = dx dy dz$ at the distance x of that wall, in which N metastable atoms are present. The number of metastable atoms that enter this

Fig. 12.



volume element in the time unit will be equal to the number of atoms diffusing from the left through the section x , that is,

$-D dy dz \frac{dN}{dx}$, where D is the diffusion-coefficient, plus the

amount produced in the volume v by the absorption of 2537 and successive collisions of the second kind, which, as we have seen (formula (31)), is proportional to the intensity of I_{2537} in the volume v , and it is $= v \cdot G e^{-\gamma x}$, where G is a factor which is constant for a given pressure.

$-D dy dz \left(\frac{dN}{dx} + \frac{d^2N}{dx^2} \cdot dx \right)$ atoms will leave v diffusing through the section at $x+dx$, and a fraction $v \cdot N/\tau$ of the metastable atoms N in the volume v will die because of collisions of the second kind.

In the stationary state

$$\begin{aligned} & -D dy dz \frac{dN}{dx} + v G e^{-\gamma x} \\ & = -D dy dz \left(\frac{dN}{dx} + \frac{d^2N}{dx^2} \cdot dx \right) + \frac{N}{\tau} dx dy dz \end{aligned}$$

or

$$(a) \quad D \frac{d^2 N}{dx^2} - \frac{N}{\tau} + G e^{-\gamma x} = 0.$$

This is the differential equation of our curve *b*.

It is non-homogeneous and linear. The general solution of the homogeneous equation is

$$N = A e^{-x \sqrt{\frac{1}{\tau D}}} + B e^{x \sqrt{\frac{1}{\tau D}}},$$

and a special solution of the non-homogeneous one is

$$N = H e^{-\gamma x} \quad \text{if} \quad H = \frac{G \tau}{1 - \tau D \gamma^2}.$$

The sum of both expressions gives us our general solution

$$N = A e^{-x \sqrt{\frac{1}{\tau D}}} + B e^{x \sqrt{\frac{1}{\tau D}}} + H e^{-\gamma x}.$$

The boundary conditions are $N = N^0$ for $x = 0$, and $N = 0$ for $x = \infty$, which makes $B = 0$ and $A = N^0 - H$, and we obtain finally

$$(b) \quad N = (N^0 - H) e^{-x \sqrt{\frac{1}{\tau D}}} + H e^{-\gamma x}.$$

This is the density distribution of the metastable atoms as a function of x for given values of τ and D (curve *b* of fig. 11). N is equal to the sum of two exponential falling curves with different coefficients of extinction. The last term, which is originated by the absorption of 2537, decreases very rapidly, and will fall already to $\frac{1}{8}$ of its original value for $x = 1.5$ cm. (2537 is reduced to $\frac{1}{2}$ in 5 mm. Hg vapour); and if we consider the curve beyond that value, it will be a simple exponential curve with the coefficient of extinction $\sqrt{\frac{1}{\tau D}}$.

If we measure, then, two values of N for two x -values in that region, we can calculate this coefficient. Now, judging from the absorption of 4046 for different distances x (see figs. 1 and 2, Pl. XXV.) and from the intensity distribution of the forbidden line 2356 along the slit (see fig. 3, Pl. XXVI.), we may make the rough estimate that N decreases to $\frac{1}{2}$ of its value from $x = 1.5$ to $x = 2.5$ cm.* when water vapour at 0.2 mm. pressure is in the tube. We therefore have

$$\sqrt{\frac{1}{\tau D}} = \ln 2 = 0.7 \quad \text{and} \quad \tau = \frac{2}{D}.$$

* An exact measurement has not yet been attempted, but could be easily done; the present is only a provisional calculation.

Now, the diffusion coefficient of excited Hg in H₂O is given by the kinetic theory as $D = \frac{118}{p}$, where p is the pressure in mm.

At a pressure $P = 0.2$ mm. we have

$$D = \frac{118}{0.2} = 590 \quad \text{and} \quad \tau_{P_0} = \frac{2}{590} = \frac{1}{295} \text{ sec.}$$

under our conditions. This value of the mean life of the metastable atoms is in good agreement with the results of Dorgelo (*l. c.*). The number of collisions of a $3P_0$ atom with water molecules at 0.2 mm. pressure is of the order of magnitude of $2 \cdot 10^6$ per sec., which means that a metastable atom can survive 10^4 collisions with a water molecule before giving up its energy in a collision of the second kind. Orthmann and Pringsheim* found a similar value for collisions with neutral mercury atoms at atmospheric pressure in presence of 0.01 mm. of thallium vapour.

Discussion.

Several authors have attempted to measure or calculate the long lifetime of the metastable atoms postulated by Franck and Reiche† in order to describe the absorption of certain He lines observed by Paschen. M. Marshall‡, applying the method of the low-voltage arc with alternate current, used by Kamenstine§ for helium, which apparently gives a very direct method of measuring the life of the metastable atoms to the case of mercury, found rather surprising results. He finds that the higher metastable level 2^3P_2 has a longer life ($\frac{1}{24}$ sec.) than the lower one 2^3P_0 ($\frac{1}{170}$ sec.), and that the admission of gases like CO, CO₂, N₂, H₂O, and H₂ had no influence upon the life of 2^3P_2 , but shortened the life of the lower level 2^3P_0 and all the gases by the same amount. These results are in open contradiction with all subsequent experience. There is no doubt now that the life of the higher metastable level is shorter than that of the lower one, and that the first is very sensitive against collisions with any of the named gases, while the second can endure thousands of collisions with N₂, CO, or H₂O. C. Eckart|| showed that the results

* Orthmann & Pringsheim, *Zeit. f. Phys.* xxxv. p. 626 (1926).

† Franck & Reiche, *Zeits. f. Phys.* i. pp. 154, 320 (1920).

‡ Marshall, *Astrophys. Journ.* lx. p. 243 (1924).

§ Kamenstine, *Astrophys. Journ.* xlix. p. 135 (1924).

|| Eckart, *Phys. Rev.* xxvi. p. 454 (1925).

of Kamenstine and Marshall were probably due to the survival of ions rather than metastable atoms. Dorgelo* made a direct measurement of the life of the metastable atoms in neon and Hg, observing the absorption of the lines footing on the metastable levels a certain time after the electrical excitation of the vapour had ceased. He found that the life of the higher level (2^3P_2) was about $\frac{1}{200}$ sec. in pure mercury vapour at room temperature, and the life of the lower one (2^3P_0) still longer than this value, and that both were very sensitive to impurities, especially to the presence of hydrogen†.

The time calculated by us for the level 2^3P_2 (10^{-5} sec.) is considerably shorter than the result of Dorgelo, but we must remember that the experimental conditions are completely different. In the case of Dorgelo, the life of the metastable atoms is only shortened by collisions with impurities or with the walls of the tube, while in our case of very intense side illumination, the absorption of lines like 5461, 3650, and 4046, 2967 by the metastable atoms must shorten the lives of them in a sensible degree. Meissner and Graffunder‡ have recently found that in the case of neon the life is considerably reduced by side illumination.

In the case of 2^3P_0 , the lower level, the effect of side illumination is less noticeable because the total amount of metastable atoms in this level is enormously larger than in the case of the higher level.

On the whole, we can say that the life of the metastable atoms, when undisturbed by exterior agencies, is probably limited only by the emission probability of the "forbidden lines" 2270 and 2656, which for the last one has been measured by the author to be about 10^8 times smaller than for 2537 §. Since the life of the resonance level is 10^{-7} sec., the life of 2^3P_0 would be $10^8 \cdot 10^{-7} = 10$ sec. under best conditions. These conditions may exist in some stars.

The Amount of Metastable Atoms.

Formulas (31) and (33) show that the density of metastable atoms will be governed by the constant π . Because in many physio-chemical investigations it is desired to have

* Dorgelo, *Physica*, v. p. 429 (1925).

† G. Ramsauer (*Naturwissenschaften*, xvi. p. 576 (1928); and T. Asada, R. Ladenburg, and W. Tietze, *Phys. Zs.* xxix. pp. 549, 708 (1928) have recently published new measurements of τ_{P_0} obtaining a value of 10^{-3} sec. in agreement with my result.

‡ Meissner & Graffunder, *Ann. der Phys.* lxxxiv. p. 1041 (1927).

§ Details of the calculation will appear shortly.

a large concentration of metastable atoms, we may discuss it more in detail. At the same time, we can try to explain the fact that CO is very efficient at low pressures in producing metastable atoms, but not at pressures above 0.2 mm. Considering (29'), (30), and (32), we can write π in the following form:—

$$\pi = \frac{zE_1}{z^2E_1E_0 + z(E_1B_0 + E_0A_1) + A_1B_0} \quad (34)$$

If the efficiency of collisions of the second kind with the metastable atoms for the gas in consideration is very small ($E_0=0$), π will reduce to

$$\pi = \frac{zE_1}{B_0(zE_1 + A_1)}; \quad (34')$$

that means π will increase steadily with the pressure at a rate depending on the value of E_1 . For smaller E_1 (efficiency of collisions quenching 2^3P_1) we shall require a larger z (pressure) to obtain the same amount of metastable atoms, as in the formula only the product zE_1 appears, and not z or E_1 separated. The maximum of π will be $\pi_{\max.} = \frac{1}{B_0}$, and will be obtained for $z=\infty$. The number of metastable atoms would then be given (see formula (33), where $e^{-\gamma}$ is small and can be neglected) by

$$N_{P_0 \max.} = \frac{I_1^0}{B_0},$$

and could be still increased, diminishing the absorption probability of lines like 4046 ($B_0 = bI_{4046} + b'I_{2967} + \dots$ if b are the absorption coefficients), which can be done by absorbing them out of the arc light without absorbing 2537. One-half of the maximum value would be obtained already when $zE_1 = A_1$; that is, when the number of efficient collisions is equal to the probability of emission of 2537, which is the inverse of the mean lifetime of the level 2^3P_1 . Now, this life is known to be 10^{-7} sec., and Wood's measurements show that the line 5461 in fluorescence, which can be used as a measure for the number of metastable atoms N_{P_0} , as 3650 was used for N_{P_2} , increases to one-half of its maximum intensity at a nitrogen pressure of 0.65 mm. At this pressure the number of collisions z per sec. of excited atoms (diameter 1.62 times normal) with nitrogen molecules is $7 \cdot 10^7$ per sec., which allows us to calculate E_1 , the efficiency of the quenching collisions of nitrogen, as

$$E_1 = \frac{A_1}{z} = \frac{10^7}{7 \cdot 10^7} = 1.4.$$

This value is in contradiction with the value 0.013 calculated by Stuart. If we suppose with Foote * that $E_1=1$, that is, that every collision is effective with the 2^3P_1 level, we shall obtain a mean life $\tau_{P_1}=1.4 \cdot 10^{-7}$, which is something larger than the known value. We will consider this point and the quenching of resonance radiation by gases in detail in a subsequent paper.

In our practical case the collisions of the second kind will play always a certain rôle so that E_0 will never be completely $=0$; but it seems that gases like water vapour (avoiding free H_2 or O_2), argon, and, more or less, nitrogen behave very nearly ideally.

If E_0 cannot be neglected, but is still small, the number of metastable atoms will at first increase with the pressure and proportional to the efficiency E_1 of collisions with the level 2^3P_1 , as in the ideal case, but afterwards the term in z^2 (formula 34) will predominate and π will decrease again. The maximum will be obtained for

$$z = \left(\frac{A_1 B_0}{E_1^2 E_0} \right)^{\frac{1}{2}},$$

and will occur at lower pressures the larger the product $E_1^2 E_0$ is. This product seems to be larger in the case of CO than in the case of N_2 . The maximum concentration of metastable atoms is reached with CO at about 0.2 mm., and with nitrogen at from 5 mm. to 70 mm., depending on its purity. This explains the special behaviour of CO with increasing pressure, as shown by fig. 1 (Pl. XXV.).

The Absorption of 4046, and the Density of 2^3S_1 for Low Pressure.

The absorption of the line 4046 of the arc will be different for the case of low pressure when diffusion takes place, and for the case of higher pressures when it does not. In the first case the absorption law will be simply

$$I_{4046} = I_{4046}^0 e^{-\lambda x}, \quad . \quad . \quad . \quad . \quad (35)$$

where λ is proportional to \bar{N}_{P_0} : $\lambda = f \cdot \bar{N}_{P_0} = g \cdot I_1^0$. That absorption law is similar to the law for the resonance line 2537. The only difference lies in the numerical values of the absorption-coefficients. For low gas pressures the absorption of 4046 is considerably smaller than the absorption of 2537, due to which I_{4046} will be very nearly constant

* P. D. Foote, Phys. Rev. xxx. p. 288 (1927).

along the cross-section of the tube. Similar laws will govern the absorption of the lines 2967, 2753, 2534.

To calculate the number of atoms in 2^3S_1 we need only consider the absorption of 4046 and can neglect the atoms brought up by 4358, because when gases are present (large concentration of metastable atoms) the absorption of 4358 is many times smaller than the absorption of 4046.

The number of atoms that reach the level 2^3S_1 in the time unit will be then

$$-d(I_{4046}) \cdot dx = \lambda I_{4046} dx = \mathfrak{S} \cdot I_1^0 \cdot I_{4046} \cdot dx;$$

the number of atoms that leave it

$$N_s \frac{1}{\tau_s} dx,$$

where τ_s is not only determined by the emission probabilities of the lines originating in the level, as in the case of vacuo (see formula (21)), but also by the collisions of the second kind :

$$\frac{1}{\tau_s} = \epsilon_0 + \epsilon_1 + \epsilon_2 + D_s.$$

Therefore

$$N_s = \lambda \tau_s I_{4046} = \mathfrak{S} \cdot \tau_s \cdot I_1^0 \cdot I_{4046} \cdot e^{-\lambda x}, \quad . \quad . \quad (36)$$

gives the density distribution of the excited atoms on the level 2^3S_1 . The intensity of the lines emitted by the excited atoms in that level will be

$$J_{4358} = \epsilon_1 \cdot N_s, \quad J_{4046} = \epsilon_0 N_s, \quad J_{5461} = \epsilon_2 N_s, \quad . \quad (37)$$

where the ϵ_1 , as in the case of vacuo, are the transition probabilities for each of the lines. We see that the intensity distribution along the cross-section of the tube is governed by the absorption of the line 4046, and must therefore be nearly constant. We shall see presently that this is confirmed by the experiment. The intensity curves of all the lines emitted by levels supplied with electrons mainly by absorption of the metastable atoms will be similar to those above. Such is the case for the levels 3^3S_1 , 3^3D_1 , and 4^3D_1 .

Case of Higher Pressure.

For the case of higher pressures of foreign gas, where diffusion does not occur, the absorption law of the line 4046 will be similar to the absorption law of the line 4358 in the case of vacuo (see formulas (16) and (17)), since the density

distribution of the metastable atoms in our case (formula (31)) is similar to the distribution in the level 2^3P_1 (see formula (12)) in the case of vacuo. It is then

$$I_{4046} = I_{4046}^0 e^{-\frac{\phi}{\gamma} I_1 (1 - e^{-\gamma x})} = I_{4046}^0 \cdot e^{-\frac{\phi}{\gamma} (I_1^0 - I_1)}. \quad (38)$$

The difference in the case of vacuo is that the constant ϕ is considerably larger than the constant α of 4358, due to the large number of atoms in the level 2^3P_0 . In the former case the exponential function was practically equal 1, while it is here a markedly falling curve, which is shown by the fact that the line 4046 of the arc is reduced to less than $\frac{1}{2}$ by the absorption in the cross-section of the tube (25 mm.), while the absorption of 4358 is not noticeable.

The level 2^3S_1 will be supplied, as before, practically only by the absorption of 4046. Its density distribution is then expressed by

$$N_s = \phi \cdot \tau_s \cdot I_1 \cdot I_{4046}. \quad (39)$$

The re-emission lines will be

$$J_{4046} = \epsilon_0 N_s, \quad \therefore J_{4358} = \epsilon_1 N_s, \quad \therefore J_{5461} = \epsilon_2 N_s;$$

or, if we write one of them in full, for instance, 4358,

$$J_{4358} = \epsilon_1 \cdot \phi \cdot \tau_s \cdot I_{2537}^0 \cdot I_{4046}^0 \cdot e^{-\gamma x} \cdot e^{-\frac{\phi}{\gamma} (I_{2537}^0 - I_{2537})}. \quad (40)$$

The Intensity Distribution of the Lines.

Now, let us compare this last expression with the corresponding ones for the cases of vacuo and at low pressures. In vacuo it was (see formulas (21), (20), (17), and (7), Theory I.):

$$(\text{vacuo}) \quad J_{4358} = \epsilon_1 \cdot \alpha \cdot \tau_s \cdot I_{2537}^0 \cdot I_{4358}^0 \cdot e^{-\gamma x} \cdot e^{-\frac{\alpha}{\gamma} (I_{2537}^0 - I_{2537})}^*, \quad (41)$$

and in gases at low pressure ((37) and (36)):

$$(\text{low pressure}) \quad J_{4358} = \epsilon_1 \cdot \beta \cdot \tau_s \cdot I_{2537}^0 \cdot I_{4046}^0 e^{-\lambda x}. \quad (42)$$

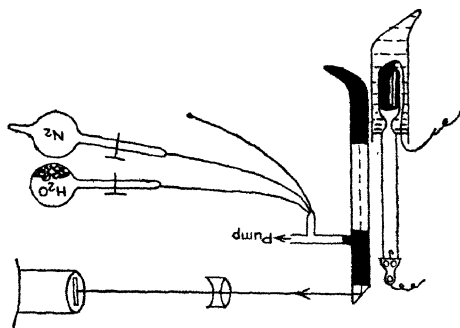
* A comparison of the two formulæ (40) and (41) allows us to calculate the ratio N_{P_0}/N_{P_1} of the amount of metastable atoms in the case of gases in regard to the amount of excited atoms in the level 2^3P_1 in the case of vacuo. We consider a volume element at the entrance-wall of the tube ($x=0$), and divide the two mentioned formulæ:

$$\frac{J_{4358}^0 (\text{gas})}{J_{4358}^0 (\text{vacuo})} = \frac{\phi I_{4046}^0}{\alpha I_{4358}^0}.$$

Now, this ratio has been found experimentally to be about 25 (enhancement of the lines by foreign gases). On the other hand, α is proportional

In the last case, as we have seen before, λ is very small, so that we should expect that the intensity distribution along the slit of the spectrograph, if we form an image of the cross-section of the tube upon it (see fig. 13), will be practically constant, or at least fall slowly. The central image of fig. 4 (Pl. XXVI.) shows this case. In the case of vacuo, the last factor is practically equal 1, as we have seen in the former paper, because of the faint absorption of 4358; thus the intensity distribution will be given by the absorption curve of 2537; that is, we should expect the intensity to fall exponentially along the slit with the extinction constant γ . The left-hand image of fig. 4 (Pl. XXVI.) gives 4358 for this case. Finally, in the case of gases at higher pressure, the last factor of formula (40) is no longer equal to

Fig. 13.



to the transition probability of 4358 and the density N_{P_1} (see formulæ (14) and (12)):

$$\alpha = \frac{A_{4358}}{I_1} N_{P_1}$$

and similarly

$$\phi = \frac{A_{4046}}{I_1} N_{P_0}.$$

Therefore

$$25 = \frac{A_{4046}}{A_{4358}} \cdot \frac{I_{4046}^0}{I_{4358}^0} \cdot \frac{N_{P_0}}{N_{P_1}}.$$

In the arc

$$\frac{I_{4358}}{I_{4046}} = 2,$$

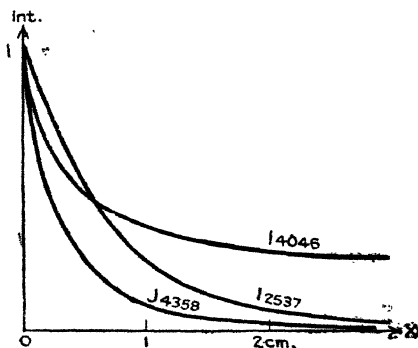
and therefore A_{4358}/A_{4046} is also $= 2$ (both lines are emitted by the same level, so that their intensity ratio gives at the same time the ratio of the transition probabilities), and we have that

$$N_{P_0}/N_{P_1} = 100.$$

This allows us to calculate the transition probability of the forbidden line 2656, as we shall see in a subsequent paper.

unity, but a falling function, and the intensity distribution of the line will be given by the product of two falling curves, the absorption curves of 2537 and 4046 of the arc. Fig. 14 illustrates this case. The lower curve is the product of the two upper ones, and represents the distribution of the intensity of 4358 we should expect in this case. The right-hand image of fig. 4 (Pl. XXVI.) gives 4358 while 2 mm. water vapour were present in the tube. We see that the results are completely in agreement with the theory. The slow falling of the intensity in the case of low pressure confirms once more the fact of the diffusion of the metastable atoms. The same changes are to be expected for all the lines emitted by levels supplied with electrons mainly from the level 2^3P_1 in *vacuo*, and from the level 2^3P_0 in presence

Fig. 14.



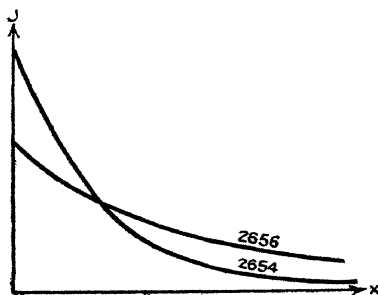
of gases (see fig. 2, Theory I., p. 1156), like 3^3S_1 , 3^3D_1 , 4^3D_1 . The line 2654 of fig. 3 (Pl. XXVI.) is included in this case. It is interesting to observe in fig. 3, *a* (Pl. XXVI.) that the forbidden line 2656 is stronger than the strongest line of the pseudo-triplet (2654) at the bottom of the slit*, but that the contrary happens at the top of it. Fig. 15 illustrates this case. This "crossing" of the intensities of the lines is due to the fact that the line 2656 requires only one absorption for its appearance, while 2654 requires two, and therefore behaves like 4358. We shall see in the following paper that the "crossing" of the lines is very useful in determining the origin of the band spectra that appear in the optically-excited mercury vapour under certain conditions. Special allowance must be made for the fluorescence lines 4046,

* See also R. W. Wood and E. Gaviola, *Phil. Mag.* vi. p. 271 (1928).

2967, 2753, and 2535, because they are partly re-absorbed in the tube before reaching the quartz prism at the top of it, due to the large concentration of metastable atoms. Fig. 6 (Pl. XXVI.) illustrates this case. We see that 4046, instead of increasing when water vapour is admitted into the tube, actually diminishes. This means that the absorption of it, proportional to the number of metastable atoms, increases faster than its intensity. This may be due to collisions of the second kind of atoms in the level 2^3S_1 .

Fig. 4 (Pl. XXVI.) shows, further, that 4358 increases about twenty times at the top of the slit if we introduce 2 mm. of water vapour in the tube, but does not change, or rather, decreases, at the bottom of it. This is specially plainly shown by fig. 5 of the same Plate. If we measure changes in the intensity of a line due to gases, the value obtained

Fig. 15.



will then greatly depend on the part of the image thrown upon the slit we allow to enter the spectrograph: then, it is usual to restrict the length of the slit in order to get more images into the plate. We can measure a *decrease* of 4358 due to H_2O or N_2 if we use the bottom of the line, while we obtain a 20 times increase using the top of it. Wood had already observed* that the increments due to 2 mm. nitrogen were in general larger for the region where the exciting beam enters than for the region of exit. That for 4046 he found the contrary is to be explained by re-absorption.

The Density Distribution in the Levels 2^3P_2 and 2^3P_1 .

We have already seen that the effect of gases is to decrease the number of atoms on the level 2^3P_2 , as a result of collisions:

* Phil. Mag., Sept. 1927, p. 486.

of the second kind, and to increase it again if the pressure grows, because of the enormous enhancement of the green line which supplies that level with electrons. Because no diffusion of the atoms in 2^3P_2 takes place, the density curve along the cross-section of the tube will be determined by the density distribution of the green line 5461 in each case; that is, it will fall exponentially in the case of vacuo, it will be practically constant in the case of gases at low pressure, and it will fall sharply in the case of higher pressures. The same will also be true for the upper levels communicating only with 2^3P_2 , like 3^3D_3 and 4^3D_3 ; thus the lines 3650 and 3021 will present the same changes of relative intensity along the slit, under different conditions, as the line 4358; their absolute intensity will decrease at first and increase afterwards, while the intensity of 4358 increases steadily with the gas pressure. These predictions have all been confirmed experimentally. The distribution in the level 2^3P_1 will not be changed by the gases; only its mean life will diminish, due to collisions of the second kind, and with it the number of atoms on that level. The density distribution of the level 2^1S_0 (see fig. 2, Theory I., p. 1156) will be then always given by the absorption curve of the resonance line 2537. The intensity of the line 4077 emitted by that level will then decrease with gases without changing its intensity distribution. That has been found also experimentally to be the case.

The levels like 3^3D_2 , 4^3D_2 , 4^1D_2 , etc., which are supplied with electrons more or less from both levels 2^3P_2 and 2^3P_1 at the same time and in comparable quantities, will take a position more or less midway between the behaviour of 3650 and 4077. The lines emitted by those levels will, in general, decrease if gases are present. That is really the case for the lines 3125, 3654, 3024, 2652, 2655, 5770. Fig. 7 (Pl. XXVI.) shows the clear decrease of 3125 if gases are admitted; also that the decrease is stronger at the bottom than at the top of the line, as would be expected. The level 3^1D_2 occupies a special position in that it communicates already with the level 2^3P_0 by means of the line 2967.5, but this line is extremely weak; thus the density of the level decreases with gases, but less rapidly than the level 3^3D_2 . This explains the different behaviour of the yellow lines. The intensity of both lines decreases if gases are admitted, but 5770 about twice faster than 5790. The line 3131 takes a position midway between the behaviour of 4358 and 3125, due to the fact of its being a double line. The same is true of 3663 and 2967.

The special behaviour of the levels 3^3S_1 , and 3^1S_0 in the case when the tube is illuminated through a combined chlorine-bromine filter and gases are admitted (see R. W. Wood, *Phil. Mag.*, Sept. 1927, p. 480), has been satisfactorily explained by Beutler and Josephy * to be due to the fact that those levels have an energy very nearly equal to double the energy of a metastable atom; and it seems that, by collisions of two metastable atoms, there is a large probability for one of the atoms to take over the whole energy, provided the rest of the energy that has to be transformed in kinetic energy is small.

We see, then, that the behaviour of all the lines appearing in the mercury fluorescence can be readily explained by means of our theory.

Summary.

(a) The increases and decreases of the intensities of the mercury lines in the optical excitation of mercury vapour when foreign gases are admitted into the fluorescence tube are readily explained, using the results of our theory on the optical excitation of mercury vapour (Theory I.).

(b) The influence of diverse gases upon the absorption of the line 4046 by the metastable mercury atoms has been studied experimentally in order to determine the amount of metastable atoms produced by each of the gases at different pressures.

(c) Diffusion of metastable atoms has been directly demonstrated, showing their long lifetime.

(d) The higher metastable level 2^3P_2 is very sensitive to collisions with gas molecules, and its lifetime when no foreign gas is present has been calculated to be of the order 10^{-5} sec.

(e) The mean life of the lower metastable level 2^3P_0 has been calculated to be of the order of $\frac{1}{300}$ of a second under our conditions, and a further calculation shows that it can increase to about 10 seconds under ideal conditions (in stars, for instance).

(f) The efficiency of quenching collisions of nitrogen with excited atoms in the resonance level is found to be of the order of magnitude 1, as assumed by Foote, and not 0.13, as calculated by Stuart.

(g) The number of metastable atoms produced by the presence of a few millimetres of nitrogen or water vapour

* Beutler & Josephy, *Phil. Mag.* v. p. 222 (1928).

is estimated to be about one hundred times larger than the number of excited atoms in the resonance level.

(h) The different changes of the intensities of the lines along the slit of the spectrograph when gases are admitted and an image of the cross-section of the tube is formed upon it, are explained for every one of the lines appearing in fluorescence.

Professors R. W. Wood and K. F. Herzfeld had the kindness to read this work in manuscript, and to suggest many improvements, for which I wish to express my indebtedness to them.

The Johns Hopkins University,
Baltimore, Md.
June 30, 1928.

CXVI. *Photosensitized Band Fluorescence of OH, HgH, NH, H₂O, and NH₃ Molecules.* By E. GAVIOLA, *Ph.D.*, *Fellow of the Int. Educ. Board*, and R. W. WOOD, *LL.D.*, *For. Memb.R.S.**

[Plates XXVII. & XXVIII.]

Introduction.

THE appearance of several band spectra as a result of photosensitized fluorescence was observed by Wood ⁽¹⁾ in his early work on the optical excitation of mercury vapour, and a summary description (page 781), and a few photographs of the bands have been already published. The OH band ("water-band") at 3064 was especially conspicuous, and appeared when nitrogen was present in the tube ⁽²⁾. During the work of the authors on the best conditions for the appearance of the "forbidden line" 2656 of mercury ⁽³⁾, it was observed that the OH band was present in the fluorescence also when water vapour is introduced into the tube, if care was taken that too much free hydrogen did not accumulate in the tube as a result of the decomposition of the water molecules into H and OH, which can be easily avoided by admitting a suitable quantity of oxygen, which takes care of the excess of free hydrogen by combining with it to form H₂O, H₂O₂, and H₂O. It was also observed that in general the conditions under which the forbidden line 2656 was brightest were the same for which the OH band appeared

* Communicated by the Authors.

with the maximum intensity, which is due to the fact that both are directly or indirectly originated by the presence of a large amount of metastable atoms with electrons on the level 2^3P_0 .

A more detailed study of the bands was taken up in the present work in order to identify the rest of the bands and to find out the conditions under which each of them appears, together with the possible chemical reactions that give rise to the molecules responsible for the emission of the bands. As an additional result very interesting data on the dissociation energy of water and nitrogen have been found.

Apparatus.

The apparatus was the same as described in the earlier papers (see fig. 13, Theory II., p. 1186). A drop of mercury was always at the bottom of the resonance tube. The desired gases could be admitted through capillaries connected with the different bulbs or the air of the room, and a palladium tube served for the admission of hydrogen, while the resonance tube was disconnected from the pump by a barometric mercury seal. The fluorescence tube was always saturated with mercury vapour and at room temperature.

Conditions for the Appearance of the Bands.

OH and HgH.—If the tube is evacuated and the mercury diffusion pump kept running no bands appear, with the exception of a faint one beginning at 2537 and fading rapidly towards the red side of the spectrum, in spite of fairly long exposures. If, now, 2 to 10 mm. of nitrogen are admitted, and if this nitrogen has not been specially freed from humidity, the OH band at 3064 and 2811 appears fairly bright, and further to the red a set of bands with clearly separated lines and with heads at 4222, 4012, 3724, 3509, etc., which can be obtained on the plate with a few minutes' exposure. The spectrum 1 of fig. 1 (Pl. XXVII.) shows this case, and was taken while 5 mm. of moist nitrogen were in the tube. A rough measurement of the set of bands at the red side of the OH band 3064 showed that they are identical with the mercury hydride bands, which were formerly erroneously classified as the "mercury band spectrum."

If we introduce a very small amount of oxygen (.001 mm.) into the tube containing the moist nitrogen, the mercury-hydride bands disappear as shown by spectrum 3 (fig. 1), leaving the OH bands stronger than before (not shown stronger in the photograph because 3 has a shorter exposure

than 1), and a diffuse band with maxima at 3360–70 Å. (indicated by an arrow in spectrum 3) which was rather faint in spectrum 1 increases considerably in its relative intensity.

NH.—This band has been found to be the so-called “ammonia” band, due probably to a NH molecule, which will be discussed more fully presently. If we admit more oxygen to the tube, the NH band at 3360–70 Å. disappears also, leaving the OH bands alone, as shown in spectrum 4. All these changes are perfectly reproducible, and, with a little practice, it is easy to obtain any of the desired band combinations

H₂O and HgH.—If we pump out the nitrogen and introduce 2 mm. of water vapour from a bulb containing CuSO₄ crystals, we obtain spectrum 2 of fig. 1 (Pl. XXVII.), which shows the OH and the HgH bands as in the case of nitrogen, but in which a new continuous spectrum appears extending from 2537 to 3200 Å. with a maximum around 2800 Å. very clearly visible in spectrum 2, forming a background for the OH band at 2811. The NH band of the former case is now absent, as was to be expected.

It is interesting to compare the HgH bands obtained with nitrogen and water vapour. We see in spectra 1 and 2 of fig. 1, or better in its enlargement in fig. 2 (Pl. XXVIII.), that in the case of water vapour the band-heads are much brighter than the higher rotational terms, while the contrary happens in the case of nitrogen. The very distinct band-head at 3722–28 Å. (fig. 2) in the case of water appears lost among the tail lines of the band 4012–17 in the case of nitrogen. This curious disparity might be due to the fact that water vapour quenches the higher rotational levels, throwing the excited HgH molecules to lower levels, an effect which would not be exerted by nitrogen.

If we introduce oxygen (few thousands of mm.) to the tube containing about 2 mm. water vapour, we obtain spectrum 5 of fig. 1. The HgH bands have disappeared, leaving the OH and the continuous band at 2800 Å. alone. The intensity of the continuous band at 2800 is proportional to the amount of water vapour, provided the little free hydrogen that develops is continually neutralized with oxygen.

NH₃.—We would confirm the results of Dickinson and Mitchell ^{(14), (15)} that the introduction of NH₃ in the tube produces the 3360–70 band, and in addition to it a continuous band extending from 2900 to 4000 Å. with a maximum at about 3450 Å. Spectrum 6 of fig. 1 was taken while about 5 mm. of N₂ and a few tenths of a millimetre of NH₃ were in the tube, and shows well the continuous band and the

3360-70 band at the long wave-length side of the line 3341 of mercury. It is interesting to observe that the OH band at 3064 has disappeared for the first time, or is at least greatly reduced from its customary intensity, which is probably due to the formation of some $\text{NH}_3\text{-OH}$ or similar molecules, which take care of the OH formed, before it has a chance of being excited by an excited mercury atom.

Spectrum 7 shows the effect of a mixture of nitrogen, water vapour, ammonia, and some air for neutralizing the excess of hydrogen; all of the bands described so far appear together, demonstrating the possibility of the coexistence of N_2 , H_2O , OH, NH, NH_3 , and HgH molecules.

The Intensity Relations.

In a previous paper the authors have described ⁽⁴⁾ how the intensity of the different mercury lines in fluorescence is proportional to the first, second, or third power of the intensity of the exciting light, according to the number of successive absorptions necessary for the emission of each line, and how this could be easily tested by reducing the primary intensity a known number of times, using a wire gauze interposed between the arc and fluorescence tube and measuring the consequent reduction in the intensity of each of the secondary lines. If the primary light is reduced 5 times, the resonance line 2537 and the "forbidden line" 2656 are decreased 5 times, nearly all of the others 25 times (or 5^2), and 3650 and 3021 125 times ($=5^3$). Knowing this we can tell, independent of any level diagram, that 3650 requires three successive absorptions for its emission, while 2656 requires only one. The theoretical foundation of this rule has been given in a paper by one of us (Theory I.). Now, we can apply the same test to the bands, and that will help us to guess the chemical gas-reactions which go on in the tube and give rise to the bands. All of the bands are produced by collisions with excited mercury atoms, and not by direct absorption of light of the mercury arc, which is plainly proved by the fact that, as soon as the line 2537 of the arc reverses owing to overheating of the arc or to absence of the deflecting magnetic field, the bands disappear without exception, together with the mercury fluorescence. The power-relation of the intensity of a band in regard to the primary intensity tells us then how many excited mercury atoms are used in the production of an excited molecule responsible for the emission of the band.

As a result of careful measurements it has been found that the intensity of the two continuous bands due to the presence

of water vapour and ammonia are directly proportional to the primary intensity; the emission of them requires, then, a single collision with an excited mercury atom while the HgH band grows with the second power, which indicates that the emission of each light-quantum of the band requires the co-operation of two excited Hg atoms. The NH and OH bands appear to be proportional to a power intermediate between 1 and 2, the reason for which is to be sought in the greater stability of those molecules, some of which can survive, under given conditions, more than one excitation, a case which will be more fully discussed presently.

Fig. 4 (Pl. XXVIII.) gives an illustration of the wire-gauze method: spectrum *a* was taken while nitrogen, ammonia, and some water and air were in the tube, and shows the 3064 OH, the continuous ammonia band, the 3360-70 NH, and the 4012 HgH band; spectrum *b* was taken with exactly the same mixture while a wire gauze reducing the primary intensity about 4 times was interposed between arc and tube and the time of exposure increased about six-fold: bands proportional to the first power should be enhanced 1.5 times, while those proportional to the second should diminish about ten-fold in image *b*. We see that the continuous NH₃ band has become enhanced, while the HgH band-head at 4012 has practically disappeared and the NH and OH bands are greatly reduced in intensity. Removing the gauze and giving a short exposure again, we obtained an image equal to *a*, showing that the gas mixture had not changed practically during the experiment. It is curious and interesting that the intensities of different bands appearing as photosensitized fluorescence can be changed relative to each other simply by modifying the intensity of the exciting light.

There is another very elegant and simple method of determining the power relation of the intensities: the falling off of the brightness of the bands along the cross-section of the tube. If we form an image of the cross-section of the tube upon the slit of the spectrograph, we obtain a spectrum like the one in fig. 3 (Pl. XXVIII.), which shows that the bands decrease in their intensity along the slit with different rates of speed. This rate will depend on the way the bands are excited by the excited mercury atoms

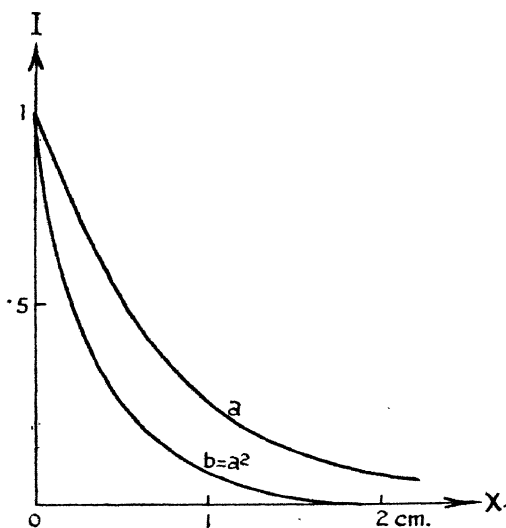
The only excited atoms which come into consideration for the excitation of the bands are the atoms in the resonance level 2^3P_1 and the metastable ones in the lower level 2^3P_0 . All other excited atoms are so few in number and of such short life that they have little or no chance of hitting any

molecules if the gas pressure is kept below a few millimetres, as has always been the case in the present work. Now the density distribution of the relevant atoms along the cross-section of the tube is given by the absorption law of the line 2537 of the arc

$$I = I^0 e^{-\gamma x},$$

which represents an exponential falling curve (see E. Gaviola, *Theory II.*, p. 1187) like curve *a* in fig. 5. The intensity distribution of the bands, whose intensity is directly proportional to the primary intensity, that is, to the number of excited atoms, will be given also by curve *a*, while the bands propor-

Fig. 5.



tional to the second power will decrease along the slit with the square of curve *a*, which is represented by curve *b* in fig. 5. (A similar condition occurred in the case of the "forbidden line" 2656 (first power) as compared with 2654 (second power), and was illustrated by fig. 3, *a*, of Pl. XXVI. in *Theory II.*) We come now to fig. 3 (Pl. XXVIII.), which was obtained while 2 mm. of water vapour were present in the tube, and shows how the HgH bands decrease very rapidly in their intensity along the slit (quadratic relation), while the OH band does it less suddenly and the continuous H₂O band at 2800 less still (first power). That the OH band falls more rapidly than the continuous water band can be seen plainly by comparing this last with the 2811 branch

of the first, which is superposed on the continuous water band: the lines of the OH band appear bright upon the continuous background at the top of the slit, while they become lost in it at the bottom of the slit. Image 3 of fig. 1, which was taken in the same way, shows that the NH band at 3360-70 decreases along the slit parallel with the OH band. All of this confirms the results obtained with the wire gauge, that the intensity of both continuous bands is proportional to the first power, the HgH to the second, and the NH and OH bands to a power between the first and second.

Interpretation of Results.

Now that we know the conditions under which each of the bands appears and the number of excited Hg atoms which each molecule requires for its production and excitation, we can try to interpret the processes which take place in the tube in the different cases.

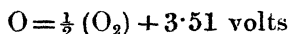
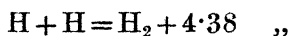
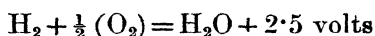
The Action of Water Vapour.

Let us consider first what happens when we introduce a few millimetres of water vapour into the tube containing excited mercury vapour; Wood⁽¹⁾ and, later, Senftleben & Rehren⁽¹⁷⁾ and Bates⁽¹⁸⁾ have observed that the H₂O molecule is dissociated in this case, and they were able to detect the presence of free hydrogen after the illumination. The appearance of the HgH and OH bands in our case confirms that dissociation takes place, and the fact that a little oxygen is able to bring the radiation back to full intensity when it begins to decrease by continued operation of the tube, shows the presence of free hydrogen which quenches the fluorescence. So far our results are in full agreement with those of the previous authors. Senftleben and Rehren concluded that the dissociation energy of H₂O into H and OH had to be smaller than 4.9 volts, the excitation energy of the mercury atoms. They showed also that only the reaction

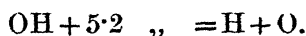
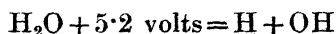


comes into consideration. Now, on the other hand, it has been found by us that water vapour is most efficient in producing metastable Hg atoms, which shows that by collisions of an H₂O molecule with an excited Hg atom in the 2³P₁ level in most cases no dissociation takes place, but that the atoms are thrown down to the metastable level 2³P₀,

as happens with N_2 . Furthermore, we have seen in our calculation of the lifetime of metastable atoms (Theory II.) that these atoms can survive at least 10^4 collisions with water molecules without giving up their energy. These facts speak in favour of the assumption that 4.9 volts are probably not quite sufficient for the dissociation of H_2O into H and OH, and that dissociation takes place only in the very few cases when the difference of energy can be taken out of the kinetic energy of fast-moving molecules. This is corroborated by the fact that Senftleben could never obtain more than 10^{-4} mm. of H_2 out of 4.6 mm. of water vapour after one illumination, and that Bates found for the reaction a very low efficiency compared with other processes. The dissociation energy of H_2O into $H + H + O$ is 10.4 volts; therefore



If we assume with Senftleben and Rehren that the dissociation into H and OH requires less than 4.9 volts, we shall have to admit that OH requires more than $10.4 - 4.9 = 5.5$ volts to dissociate. There is no good reason why the separation of the first H atom from $H-O-H$ should require at least 0.6 volt less energy than the separation of the second one. We have seen that our results make it probable that the dissociation energy of H_2O into H and OH is slightly more than 4.9 volts. If we assume that the separation of each of the H atoms from H_2O requires about the same energy, we obtain 5.2 volts as the linkage energy of $H-OH$ and of $O-H$:—



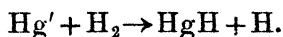
These two values need not, of course, be absolutely equal. All that our results say is that the value for the first reaction is slightly larger than 4.9 volts. The value 5.2 volts is quite plausible if we consider that at room temperature about $\frac{1}{2} 10^{-5}$ of the molecules have a kinetic energy sufficient to make up the difference between the 4.9 volts of the excited mercury and the required 5.2 volts. This proportion represents about the number of collisions effective in dissociating H_2O . Water vapour is practically inoperative in destroying

the metastable atoms in the level 2^3P_0 , because in this case the difference between the 5.2 volts required and the 4.68 volts of the mentioned atoms is too large to be taken out of the heat energy of the vapour.

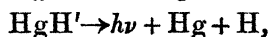
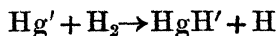
Resuming, we can say that the action of water vapour consists mainly in the bringing of excited atoms, which were in the level 2^3P_1 , down to the metastable level 2^3P_0 as a result of collisions, very few of which may lead to dissociation of H_2O into H and OH, and that collisions with metastable atoms are completely ineffective.

The HgH Bands.

The mercury-hydride bands have been carefully measured by Liese⁽⁵⁾, and afterwards by Hulthén⁽⁶⁾, who attributed them to a HgN molecule. Kratzer⁽⁷⁾ objected that the momentum of inertia of HgN would be too large for the bands and suggested that they may be due to mercury hydride instead—a suggestion that was accepted by Hulthén⁽⁸⁾ and supported by Mulliken⁽⁹⁾. Compton and Turner⁽¹⁰⁾ found that the bands appear in electrical discharge-tubes only when mixtures of mercury and hydrogen are present, and assumed that the reaction involved was



They tried to excite the HgH bands optically with a mercury arc, but without success, which was probably due to the fact that they had too much free H_2 in the tube which destroyed the excited mercury atoms, so that, also supposing that HgH were formed according to the reaction given above, the HgH molecules would have no chance of being excited by collisions with further excited Hg atoms, which is necessary for the emission of the bands. We shall see later that the reaction involved is probably $Hg' + H_2 \rightarrow Hg + 2H$, and not the one given above. In a further analysis of the bands, Hulthén⁽¹¹⁾,⁽¹²⁾ calculated the dissociation energy of the normal HgH molecule to be 0.37 volt, and assumed that the reaction involved⁽¹²⁾ was

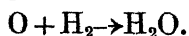
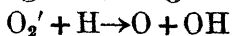
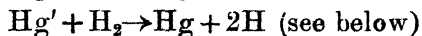
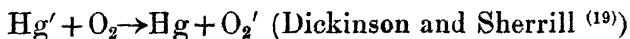


where the excited Hg atom was supposed to be in one of the 2^3P levels. This reaction is not possible because the energy of the excited Hg in the levels 2^3P is not nearly sufficient to dissociate the hydrogen molecule (4.4 volts) and at the same time excite the HgH molecule, for which at least

4 volts are necessary. The second assumption that the excited mercury-hydride molecule dissociates after emission is in agreement with our results, as we shall see later.

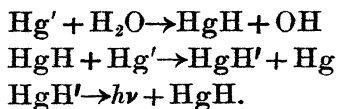
We have seen above that the HgH bands appear when water vapour, or also when moist nitrogen, is present in the tube. Both gases are very effective in producing a large concentration of metastable atoms, and in both cases a small amount of free hydrogen is developed in the tube. These are the two necessary conditions for the appearance of the HgH band. In fact, if we introduce pure dry nitrogen, metastable atoms are generated, but the band does not appear. Introducing, now, a small amount of hydrogen (0.001 mm.) through the palladium tube, the band shines out immediately. On the other hand, a small amount of hydrogen alone is not able to produce the HgH band, in spite of the presence of excited mercury vapour, showing that the presence of a large concentration of metastable atoms (generated by the nitrogen) is necessary. This discards the assumption of Hulthén⁽¹²⁾ that collision of an excited mercury atom with hydrogen would produce an *excited* HgH' molecule and a H atom, for in this case the band should appear with hydrogen alone, but we have seen already that this reaction is also impossible from the energy point of view. If the amount of hydrogen introduced through the palladium tube is increased, the HgH band fades away together with the whole fluorescence, owing to the quenching action of hydrogen.

We have also seen above that the admission of a little oxygen (or air) produces the disappearance of the HgH band and at the same time enhances the OH band. Obviously, the oxygen neutralizes the little free hydrogen forming more OH, and at the same time the concentration of metastable atoms increases, due to the disappearance of the quenching free hydrogen. The reaction involved is probably

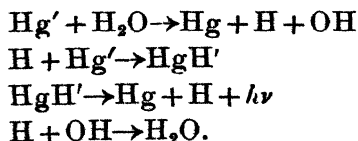


When about 2 mm. of nitrogen are present in the tube, the disappearance of the HgH band is then due to the full neutralization by the oxygen of the little free hydrogen present, giving OH and H₂O as a result, and since no free hydrogen is left, no HgH can be formed. When 2 mm. of

water vapour are present in the tube, the disappearance of the HgH band produced by a little oxygen is not so easy to explain: Hulthén^{(11), (12)} has calculated that the linkage energy of normal HgH is 0·37 volt. This being so, the reaction $\text{Hg}' + \text{H}_2\text{O} \rightarrow \text{HgH} + \text{OH}$ is energetically quite possible if we admit for the dissociation energy of $\text{H}-\text{OH}$ about 5·2 volt, as we have done before. Now, if this reaction should occur to any considerable extent, water vapour would quench the resonance radiation without producing metastable atoms, and the energy would thus be used for the dissociation of H_2O into H and OH , and water would behave like hydrogen; but we know that this is not the case, and that by collisions with water the 2^3P_1 atoms fall down to the 2^3P_0 level, which shows that the above reaction occurs rarely, if at all. This fact could be interpreted either by assuming that the dissociation energy of $\text{H}-\text{OH}$ is more than $4\cdot9 + 0\cdot37 = 5\cdot27$ volts, or that HgH is not able to exist in the normal state, but only when it is excited. It is known⁽¹²⁾ that the excited molecule is more stable than the unexcited, and that excited ones probably dissociate after the emission of light. Furthermore, if normal HgH molecules were formed directly by collisions with water, and persisted for at least 10^{-3} sec., such molecules would have a good chance of meeting excited (metastable) mercury atoms, becoming excited by them, and emitting the HgH bands. The reaction would be

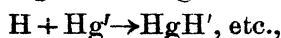
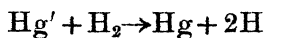


If this were the case, the emission of the HgH band in the case of water vapour should not depend on the presence of free H_2 ; on the contrary, it should be strongest when no quenching H_2 is present. We have seen that this is not the case: the HgH band disappears together with the free H_2 . Normal HgH is then not formed, or, if formed, it lives less than 10^{-3} sec. (time necessary to meet an excited atom) and dissociates. To describe the appearance of the HgH bands with an intensity proportional to the square of the arc-intensity, we propose the following reaction:—

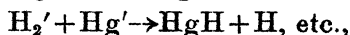
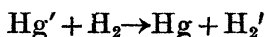


The concentration of H-atoms will be (in first approximation) in this case proportional to the exciting light-intensity; the concentration of Hg' atoms is also proportional to it. Thus the concentration of HgH' molecules and the intensity of the band emitted by them, which is proportional to the product of the two factors, should be proportional to the square of the primary light-intensity; and this is really the case, as we saw before*.

The appearance of the HgH band when N_2 and little H_2 are present in the tube can be described in the following way:—



or also



where H_2 in the second case would have to be brought up to some metastable state, in order to await the next collision with an excited mercury atom. This last reaction has already been suggested by Dickinson⁽²⁰⁾ and Mitchell⁽¹⁹⁾, in order to describe the photochemic formation of water out of H_2 and O_2 in the presence of mercury vapour. In both cases the quadratic intensity relation is satisfied.

The OH Bands.

The OH bands were discovered by Huggins and Liveing & Dewar⁽²¹⁾ in 1880, and studied and analysed afterwards by Watson⁽²²⁾, Tanaka⁽²³⁾, and Jack⁽²⁴⁾, among others. They often appear in discharge-tubes as an impurity.

In our case, as said before, the relation of the intensity of the band in regard to the primary intensity lies between the first and the second power, and we will try to interpret this behaviour. Let us consider the case when water vapour is in the tube. OH will be formed by following reaction:



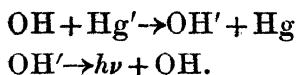
and the rate of formation, which we know is very small, would be proportional to the arc intensity (number of Hg'

* Another possible description of the facts is



where water would be brought up to some metastable level in order to await the next collision with Hg' .

atoms). The OH is a rather stable molecule, and by collision with another excited mercury atom will itself become excited and emit as a result of it the OH band :



If the lifetime of the OH molecule is such that it does not survive in general more than one excitation, the intensity of the band should be proportional to the second power of the arc intensity because each band-quantum would require two excited mercury atoms for its emission : one for the formation of OH out of H_2O and one for its excitation according to the reactions outlined above ; on the other hand, if the lifetime of OH is so long that it survives several successive excitations, the concentration of OH in the tube will be practically constant, and the chance of meeting an excited mercury atom will be simply proportional to the number of them ; that is, to the first power of the primary intensity. The experimental fact that the power relation lies between 1 and 2 shows that OH survives more than one excitation, but less than, say, three. The mean life of the OH molecule is then of the order of magnitude of the time-interval between two collisions with excited mercury atoms, which can be roughly calculated using the results obtained by one of us in Theory II. It was found there that we have in our own case about 100 times more metastable than $^3\text{P}_1$ atoms. Now, our resonance tube absorbs roughly 10^{18} 2537 light-quanta per sec. in a volume of 20 cm.³, and since the life of $^3\text{P}_1$ is 10^{-7} sec.,

$$N_{\text{P}_1} = 10^{18} \cdot 10^{-7} = 10^{11} \quad \text{and} \quad N_{\text{P}_0} = 100 \cdot 10^{11} = 10^{13},$$

which is about one hundredth of the number of normal atoms.

The number of collisions of a OH molecule with this number of metastable atoms is about 100 per sec., and the time between two consecutive collisions $\frac{1}{100}$ sec., which is then the order of magnitude of the lifetime of the OH molecule. Since the lifetime of OH is limited, it must be destroyed in some way.

Senftleben and Rehren ⁽¹⁷⁾ assume that the reaction



might account for it, although they could not detect the formation of hydrogen peroxide. Marshall and, later, Bates & Taylor ⁽¹⁸⁾ and Bonhoeffer & Loch ⁽²⁵⁾ have detected and measured it. If we assume that this is the way in which

OH is destroyed, the probability of meeting another OH molecule must be of the same order of magnitude as the probability of meeting another excited mercury atom, which amounts to saying that the concentration of OH must be about equal to the concentration of excited mercury atoms. We know this last concentration to be

$$N_{P_0} = 10^{13} \text{ atoms.}$$

Now, knowing the concentration N and the mean lifetime τ , we can calculate the rate F of formation of OH since

$$F = N/\tau.$$

There are, then, $F = 100 \cdot 10^{13} = 10^{15}$ OH molecules produced per second.

The number of collisions of one 2^3P_1 atom with water molecules (water pressure 2 mm.) is of the order of magnitude of $2 \cdot 10^7$. The total number of such collisions is then $2 \cdot 10^7 \cdot 10^{11} = 2 \cdot 10^{18}$ per sec.; and since the number F of water molecules dissociated is 10^{15} , only one in $2 \cdot 10^3$ collisions leads to dissociation. This number is larger than the number found before for the ratio of molecules having a kinetic energy of 0.3 volt (difference between the 4.9 of Hg' and the assumed dissociation energy of 5.2 volts for the H_2O molecule). The agreement would be complete if we assumed 5.1 volts for the said dissociation energy, but we do not lay stress upon this calculation because the number of light-quanta emitted by the arc is not known with sufficient accuracy.

The NH Band.

The NH band at 3360–70 Å. was first photographed by Eder in 1892, who called it the "ultra-violet ammonia band," and obtained it by burning an ammonia oxygen flame. Deslandres calls it the third positive group of nitrogen, and Kaiser (v. p. 836) says that it doubtless belongs, not to NH_3 , but probably to NO. Later, Lewis⁽²⁶⁾ found that it appears in a discharge-tube with all mixtures of N_2 and H_2 , but not with N_2 or H_2 alone, and concluded that it "might reasonably be attributed to ammonia." Fowler and Gregory⁽²⁷⁾ published beautiful photographs of it. Bair⁽²⁸⁾ thought that the 3360–70 Å. band was very probably due to ammonia, and that "it may be due to a compound of nitrogen and hydrogen, which is more stable than ammonia." Barrat⁽²⁹⁾ was the first to suggest NH as the origin of the band, in spite of which Kwei⁽³⁰⁾ still believed it to belong to NH_3 . Finally,

Hulthén and Nakamura ⁽³¹⁾ analysed the spectrum and decided that it belonged to NH, which is in complete agreement with our results.

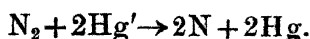
As we saw at the beginning, the NH band, together with the HgH and the OH band, appears if moist nitrogen is introduced into the tube. Apparently, the necessary factors for its production are, besides excited mercury atoms, nitrogen and very little free hydrogen; then, after a certain time of illumination, the 3360-70 band decreases in favour of the mercury hydride band, due probably to the fact that too much free hydrogen is developed from the moisture in the tube, which is confirmed by the fact that the introduction of a little oxygen restores the NH, diminishing at the same time the HgH band. The interesting fact that of the two hydride bands, NH and HgH, the nitrogen one reaches its maximum intensity in our case with a smaller hydrogen quantity than the mercury one, is confirmed by the following direct experiment: we admit to the tube only fully-dried nitrogen at a pressure of about 4 mm., and no bands appear; we warm the palladium tube with the reducing zone of a small gas flame in order to let hydrogen in at a very low rate, and we observe that the NH band appears first alone, reaches its maximum intensity and begins to decrease slowly when the HgH band first appears, increasing until it reaches a maximum, when the NH band has already weakened considerably. This curious difference in the behaviour of the two hydrides may be due to the greater stability of the NH molecule when very little hydrogen is present: in fact, if very little hydrogen is in the tube, it will be probably completely dissociated by collisions with excited mercury atoms, so that only hydrogen atoms will be present, which, if they meet a nitrogen atom, will be bound by it to form NH, and they remain bound to it for a long time, due to the great stability of this molecule. On the other hand, if they meet excited mercury atoms, they will form HgH, which will dissociate after emission of one quantum of radiation, leaving the H-atoms free for combination with nitrogen atoms, the result of which will be that in a short time all the hydrogen will be used up in the formation of NH, and that only this band, excited by collisions with metastable mercury atoms, will be present. If more hydrogen is admitted, H-atoms will be available for the formation of HgH and the emission of its band, which explains its enhancement, while, on the other hand, some of the NH will be destroyed by H₂ forming ammonia ($\text{NH} + \text{H}_2 \rightarrow \text{NH}_3$) or also by H forming NH₂, and at the same time the amount of metastable atoms will begin to

be quenched by the molecular hydrogen, which explains the decrease of the NH band. The destruction of NH to form NH_3 is supported by the fact that Noyes⁽³²⁾ found ammonia formed photochemically out of nitrogen and hydrogen under conditions similar to ours.

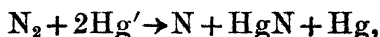
If the given explanation is correct, the intensity of the NH band in the case of very little hydrogen (NH appears alone) should be very nearly proportional to the first power of the arc intensity, for in this case the amount of NH present would be constant (great stability), and, excited again and again by collisions, the intensity of the band should be simply proportional to the number of collisions with excited mercury atoms; that is, proportional to the number of excited Hg atoms, or, what is the same, to the primary intensity. In the case of more hydrogen, which would put a limit to the life of the NH molecules, the concentration of the latter would depend on the arc intensity, and we should expect a higher power relation than the first. Now, this is precisely what happens: with very little hydrogen the intensity relation approximates to the first power, while with more hydrogen it approaches the second power. We have now to find an explanation for the appearance of the band with that intensity relation of the last case. NH is probably formed by the combination of atomic nitrogen and atomic hydrogen



giving an excited hydride molecule due to the heat of combination of about 4 volts (see Bates and Andrews⁽³³⁾). The number of excited molecules formed in this way is proportional to the product of concentrations of N and H, and since the concentration of atomic hydrogen is probably constant (due to the fact that all H_2 present is dissociated), the concentration of atomic nitrogen as a function of the primary intensity will determine the power relation of the intensities, which, as we know, lies between 1st and 2nd. Now, if we make an allowance for the NH molecules which are excited more than once during their lifetime, as was done in the case of OH, which lowers the power relation, we can assume that the concentration of atomic nitrogen is proportional to the square of the number of excited mercury atoms, which means that the production of a nitrogen atom requires two excited mercury atoms. This would be the case if we assume that N_2 is dissociated by a three-body collision with two excited mercury atoms



The only excited atoms which come into consideration are the 2^3P_1 with 4.9 and the metastable with 4.68 volts energy. The maximum energy available in the most favourable case for the dissociation of N_2 would be then 9.8 volts; two metastable atoms would give only 9.36 volts, which is 1.5 to 2 volts less than the value of 11.4 volts calculated by Sponer and Birge. We could secure more energy for the dissociation of N_2 if we suppose that mercury nitride is formed by the reaction



in which case the combination energy of HgN could be added; but we should then expect an explosive black deposit of mercury nitride which has never been observed in the tube in spite of operating it uninterruptedly for several days. Mercury nitride is not formed, and we have only 9.8 volts for the dissociation of N_2 . This would indicate that the dissociation energy of nitrogen is less than or about 9.8 volts, the value which recent results of several authors seem to show. To avoid the assumption of the low dissociation energy for N_2 we should be compelled to make hypotheses less plausible than this one*.

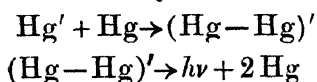
The Continuous Spectra.

Two continuous spectra have been observed to appear as a result of photosensitized fluorescence as described above: the first one (when water vapour at pressures from 0.5 to 10 mm. is in the tube), at 2800 Å. (see spectra 2 and 5, figs. 1 & 3, Pls. XXVII. & XXVIII.), seems to have been first observed and photographed by Wood⁽¹⁾; the second one (when ammonia is in the tube), at 3400 Å., has been observed by Mitchell⁽¹⁵⁾ and perhaps before by Dickinson and Mitchell⁽¹⁴⁾, although it is not clearly stated in their paper: they speak of a "diffuse band with a maximum around 3370," which may also be the NH band at 3360–70 Å. The continuous band with a maximum at about 3400 Å. looks very similar to the ultra-violet band of mercury obtained by illuminating pure mercury vapour at 300° with a cadmium or aluminum spark, studied by Wood and Van der Lingen⁽³⁴⁾, Lord Rayleigh⁽³⁵⁾, Houtermans⁽³⁶⁾, Niewodniczanski⁽³⁷⁾, Pringsheim and Terenin⁽³⁸⁾, and others; and Mitchell

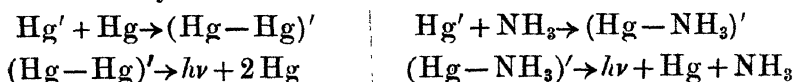
* The results of this investigation, specially in regard to the low dissociation energy of nitrogen, were already reported at the Washington meeting of the Am. Phys. Soc. in April 20–21, 1928. A part of them appeared in 'Nature,' Sept. 1st, 1928.

suggested that the band observed with mercury at 300° might be due to NH_3 contained as impurity, which is improbable since this band has been observed by all of the mentioned authors with equal intensity, and they very probably used mercury of different degrees of purity. The coincidence is probably more or less a chance due to the similar type of emission of both bands: the emission of the pure mercury band at 3400 is due, according to Houtermans and Niewodniczanski, to the dissociation of a quasi-stable molecule formed by collision of a metastable mercury atom in the level 2^3P_0 with a normal one, during which dissociation part of the energy of the excited atom is emitted and the rest transformed into kinetic energy of the separating atoms; on the other hand, the emission of the continuous NH_3 band is probably due to the dissociation of a quasi-stable mercury-ammonia molecule formed by collision of a metastable atom with a normal NH_3 molecule, dissociation occurring in the same way as in the former case.

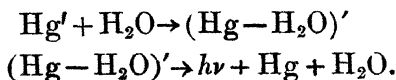
Mercury Band.



Ammonia Band.



The emission of the continuous water band at 2800 may be accounted for in the same way, only in this case the excited mercury atom which forms the quasi-stable molecule is surely a 2^3P_1 atom, since the band extends beyond 2656, as can be seen in spectrum 2, fig. 1 (Pl. XXVII.), which means that its emission requires more energy than that of a metastable atom. The reaction would be



The reactions outlined above are in agreement with the fact that the intensity of both the continuous bands is proportional to the first power of the primary light.

Summary.

(a) The photosensitized fluorescence of HgH , OH , NH , $\text{Hg}-\text{H}_2\text{O}$, and $\text{Hg}-\text{HN}_3$ molecules has been observed, the conditions for the appearance of each of the bands determined, and the most probable chemical processes which give rise to them suggested.

(b) The dissociation energy of a water molecule into H and OH is probably about 5.2 volts, and not less than 4.9 as assumed by Senftleben and Rehren.

(c) The concentration of OH and of NH in the fluorescence tube is, under the best conditions, of the order of magnitude of the concentration of excited mercury atoms (10^{-5} mm. pressure).

(d) The dissociation energy of the nitrogen molecule seems to be less, or about, 9.8 volts, and not 11.4 as calculated by Sponer and Birge.

(e) Collisions of excited mercury atoms in the resonance level 2^3P_1 with normal water-vapour molecules may lead to several different processes: in most of the cases the excited mercury atom is thrown down to the metastable 2^3P_0 level, in a few cases (about 1 in 10,000 collisions) the water molecule is dissociated into H and OH, and finally in some cases (less than 1 in 1000) a complex quasi-molecule $Hg-H_2O$ is formed which dissociates, emitting the continuous band at 2800 \AA .

(f) Collisions of excited mercury atoms in the resonance level with nitrogen molecules bring the first ones down to the metastable level; three-body collisions of two excited atoms with a nitrogen molecule may lead to dissociation of the nitrogen molecule.

Literature.

- (1) R. W. Wood, *Phil. Mag.* (Oct. 1925).
- (2) R. W. Wood, *Phil. Mag.* (Sept. 1927).
- (3) R. W. Wood & E. Gaviola, *Phil. Mag.* vi. p. 271 (1928).
- (4) R. W. Wood & E. Gaviola, *Phil. Mag.* vi. p. 352 (1928); E. Gaviola, Theory I. and Theory II. (appearing together with this paper).
- (5) Liese, *Zs. Wiss. Phot.* xi. p. 349 (1912).
- (6) Hulthén, *Z. Physik*, xi. p. 284 (1922).
- (7) Kratzer, *Ann. d. Phys.* lxxi. p. 72 (1923).
- (8) Hulthén, *C. R.* clxxix. p. 528 (1924).
- (9) Mulliken, 'Nature,' cxiii. p. 489 (1924).
- (10) Compton & Turner, *Phil. Mag.* xlviii. p. 360 (1924).
- (11) Hulthén, *Z. Physik*, xxxii. p. 32 (1925).
- (12) Hulthén, 'Nature,' cxvi. p. 642 (1925).
- (13) Ludloff, *Z. Physik*, xxxiv. p. 485 (1925).
- (14) Dickinson & Mitchell, *Proc. Nac. Ac. Sc.* xii. p. 692 (1926).
- (15) Mitchell, *J. Am. Chem. Soc.* xlix. p. 2699 (1927).
- (16) K. Gleu, *Z. Physik*, xxxviii. p. 176 (1926).
- (17) Sentfleben & Rehren, *Z. Physik*, xxxvii. p. 529 (1926).
- (18) Bates & Taylor, *J. Am. Chem. Soc.* xlix. p. 2438 (1927).
- (19) Mitchell, *Proc. Nac. Ac. Sc.* xi. p. 458 (1925).
- (20) Dickinson, *Proc. Nac. Ac. Sc.* x. p. 409 (1924).
- (21) Huggins, *Proc. Roy. Soc.* xxx. p. 576 (1880); Liveing & Dewar, *id.* xxx. p. 494 (1880).
- (22) Watson, *Astrophys. J.* lx. p. 145 (1924).
- (23) Tanaka, *Proc. Roy. Soc.* cviii. p. 592 (1925).
- (24) Jack, *Proc. Roy. Soc.* cxv. p. 373 (1927); cxviii. p. 645 (1928).
- (25) Bonhoeffer & Loch, *Z. Phys. Chem.* cxix. p. 474 (1926).
- (26) Lewis, *Astrophys. J.* xl. p. 154 (1914).

- (27) Fowler & Gregory, *Phil. Trans. Roy. Soc.* ccxviii. p. 351 (1919).
- (28) Bair, *Astrophys. J.* lii. p. 301 (1920).
- (29) Barrat, *Proc. Roy. Soc.* xcvi. p. 40 (1920).
- (30) Kwei, *Phys. Rev.* xxvi. p. 537 (1925).
- (31) Hulthén & Nakamura, '*Nature*,' cxix. p. 235 (1927).
- (32) Noyes, *J. Am. Chem. Soc.* lxxiv. p. 1003 (1925).
- (33) Bates & Andrews, *Proc. Nat. Ac. Sc.* xiv. p. 124 (1928).
- (34) Van der Lingen & Wood, *Astrophys. J.* liv. p. 149 (1921); Wood & Voss, *Proc. Roy. Soc.* cxix. p. 698 (1928).
- (35) Lord Rayleigh, *Proc. Roy. Soc.* cxiv. p. 633 (1927); June (1928).
- (36) Houtermans, *Z. Physik*, xli. p. 140 (1927).
- (37) Nievođniczanski, *Z. Physik*, xlix. p. 59 (1928).
- (38) P. Pringsheim & Terenin, *Z. Physik*, xlvii. p. 330 (1928).

Johns Hopkins University.

July 28, 1928.

Addition by the correction.—It has been suggested by several authors that the activation of foreign gas molecules takes place mainly at the walls of the tube. We have not found any signs of it. The formation and excitation of all the bands observed by us is a gas reaction and the walls do not act as a catalyser.

CXVII. *Reversals in the Arc-Spectrum of Nickel.* By A. C. MENZIES, M.A., *Head of the Physics Department, University College, Leicester* *.

Low Terms in the Ni I Spectrum.

ACCORDING to Hund † the low terms in the spectrum of Ni I should be as in the following table, where the first two columns give the electron-grouping in the outer levels and the term-types of Ni II, the third and fourth columns give the resulting groupings and term-types for Ni I, and the last column the terms found in the spectrum by Bechert and Sommer ‡, with their values for the lowest component of each multiplet.

From this it will be seen that the lowest term so far observed is the 3F_4 term, which Bechert and Sommer have accordingly made the zero of their term-scheme.

Other atoms which might be expected to have a similar structure in their spectra are Pd I, Pt I, Cu II, Ag II, and

* Communicated by the Author.

† '*Linienpektren*,' p. 165 (Julius Springer, Berlin, 1927).

‡ *Ann. d. Physik*, lxxvii. p. 351 (1925).

Au II. The first, third, and fourth of these have been shown to have 1S_0 as the ground-term, while Pt I has 3D_3 , and Au II has not been analysed (according to the author's unfinished analysis it seems likely that it will not be 1S_0 , but probably a 3D term). It is accordingly not possible to conclude from similarity what the ground-term should be. The atomic-ray experiments of Gerlach would, however, suggest that the ground-term should be 1S_0 . This could be the 1S_0 term belonging to d^{10} predicted by Hund, and the \bar{S}_0^1 term of Bechert and Sommer would then have to be attributed to s^2d^8 .

TABLE I.

Ni I.

Ni II.

Electron-grouping.	Term-type.	Electron-grouping.	Term-type.	Terms observed.
$s d^8$	4F	s^2d^8	3F	$f_4^1 = 0$
		$s d^9$	3D	$\bar{d}_3^1 = 204.82$
	4P	s^2d^8	3P	$p_2^1 = 15609.81$
	2F	$s d^9$	1D	$\bar{D}_2^1 = 3409.95$
s^2d^7	2F	s^2d^7	1G	—
			1D	$\bar{D}_2^2 = 13521.29$
d^9	2D	d^{10}	1S	$\bar{S}_0^1 = 14728.92$

Under these circumstances it seemed worth while to explore the spectrum of nickel as far as possible towards the short waves, in an endeavour to find lines belonging to a hypothetical 1S_0 term. It would show its presence by very strong lines, easily reversible, with successive wave-number differences equal to the differences between the middle terms of Bechert and Sommer having $j = 1$. The region between 3858 and 2253 Å.U. has been covered by Majumdar* working with the oven and the under-water spark in the search for low terms, so in this work attention has been directed to wave-lengths below these.

* *Zeits. f. Physik*, xxxix. p. 562 (1926).

Method.

The author has recently developed a method * of obtaining spectra with very short exposures by the fusing of wires, and has applied it to the Schumann region as well as to the ultra-violet and visible regions. Among the properties characteristic of this source is a tendency for lines involving low-terms (and particularly ground-terms) to be reversed in the fuse in air, and consequently this procedure was adopted in searching for the 1S_0 lines in the ultra-violet.

When the fuse is made horizontally in the vacuum grating spectrograph, there is a tendency to form long and short lines, the long lines being lines involving low-level terms. This property was used in seeking the 1S_0 lines in this region.

Since an account of the method and of the apparatus has been published before, it will not be repeated here.

Results.

(a) *Schumann Region*.—No long lines appeared in this region which did not belong to the spark spectrum. The long lines involved the ground-terms 2D_3 and 2D_2 of Ni II, which were found in this way †. It is conceivably possible that very low-level arc lines might under the conditions of the fuse *in vacuo* be completely absorbed, but this has so far not been observed in any other case. The spectrum was photographed as far as 1150 Å.U. Air-absorption prevented the examination going any further, owing to the poorness of the pumping system. (There was as compensation, however, the knowledge that all the lines in the region measured must be first-order lines.) An improved pumping system is being erected, and it is hoped to be able to go very much further.

(b) *Ultra-violet Region*.—In the fuse-spectrum in air there were many reversals, especially near 2300 and 2000 Å.U. These were measured in the spectrum of the arc between rods of pure nickel (supplied by Adam Hilger Ltd.) of 5 mm. diameter; the current was $4\frac{1}{2}$ amperes, and was maintained by an accumulator battery of 110 volts. The spectrograph was a small Hilger quartz instrument, giving a dispersion of about 12 Å.U. per mm. As standards for the calculation of Hartmann formulæ, the nickel spark lines measured by Shenstone ‡ were used. The fuse spectrograms were used

* Proc. Roy. Soc. A, cxvii. p. 88 (1927), and cxix. p. 249 (1928).

† Proc. Roy. Soc. (In process of publication.)

‡ Phys. Rev. xxx. p. 255 (1927).

merely to pick out the reversed lines in the arc spectrograms. The error is less than 0.1 Å.U. in the lines measured by the author. These lines are set out in Table II.

In the first column is the wave-length (above 2100 Å.U. the values of Hamm * have been adopted, and are indicated by H, while the other wave-lengths are the measurements made by the author). The second column gives the strength of the reversal (weak w, strong s), in the third the initials of previous observers of the reversal, in the fourth the wave-number, and in the last column the term-combination, using Bechert and Sommer's nomenclature. For the most part the initial terms in the transitions are terms not found before ; these are indicated by giving their values in place of a letter, thus making the newly-found terms more obvious.

TABLE II.
Reversals in the Fuse-spectrum.

Wave-length.	Strength of reversal.	Previous observers.	Wave-number.	Terms.
2346.635 H	w	AJ, MLC	42601.2	$f_3^1-u^1$
2345.545 H	s	AJ, MLC, Ma	42621.0	$f_4^1-e^1$
2337.488 H	s	AJ, MLC	42767.8	$f_4^1-l^1$
2329.974 H	w		42905.8	$f_2^1-45122.4$
2325.799 H	s	AJ, MLC	42982.8	$f_3^1-r^1$
2324.653 H	w		43004.0	$d_3^1-43208.8$
2322.688 H	w		43040.3	$d_1^1-44753.4$
2321.387 H	s	MLC, MLML	43064.5	$f_2^1-v^1$
2320.034 H	s	AJ, MLC, Ma	43089.5	$f_4^1-n_5^1$
2317.158 H	w	AJ, MLC	43143.1	$f_3^1-t_2^1$
2313.982 H	s	AJ, MLC	43202.3	$f_2^1-f_2^3$
2313.656 H	s		43208.3	$f_4^1-43208.3$
2312.338 H	w	AJ, MLC, Ma	43233.0	$f_3^1-f_3^3$
2310.955 H	s	AJ, MLC, Ma	43258.8	$f_4^1-f_4^3$
2306.420 H	w		43343.9	
2302.973 H	w		43408.8	$d_1^1-45121.9$
2300.773 H	w	MLC	43450.3	$d_3^1-o_3^1$
2293.114 H	w		43595.4	$d_2^1-t_2^1$
2289.979 H	s	Ma	43655.0	$f_4^1-o_3^1$
2288.388 H	w		43685.3	$d_2^1-f_3^3$
2279.553 H	w		43856.7	

* Z. wiss. Photogr. xiii. p. 105 (1913).

TABLE II. (*continued*).

Reversals in Fuse-spectrum.

Wave-length.	Strength of reversal.	Previous observers.	Wave-number.	Terms.
2273·85	w		43966·6	
2270·206 H	w		44035·2	$a^4\bar{F}_4 - a^4\bar{G}_5$ spk.
2244·246 H	w		44544·5	$\bar{d}_3^1 - 44749·3$
2216·459 H	w		45102·9	$a^4\bar{F}_5 - a^4\bar{G}_6$ spk.
2201·529 H	w		45408·7	$\bar{d}_1^1 - 47121·8$
2183·334 H	w		45787·2	$f_3^1 - 47119·4$
2095·57	w		47704·5	
2094·94	w		47718·8	$\bar{D}_2^1 - 51128·8$
2088·90	w		47856·8	$\bar{d}_2^1 - 48736·6$
2082·94	w		47993·6	$f_3^1 - 49325·8$
2069·54	w		48304·4	$\bar{d}_1^1 - 50017·5$
2068·89	s		48319·6	
2064·30	w		48427·0	$\bar{d}_1^1 - 50140·1$
2063·58	s		48443·9	$\bar{d}_2^1 - 49323·7$
2059·97	s		48528·8	$\bar{d}_3^1 - 48733·6$
2055·44	s		48635·8	$f_2^1 - 50852·4$
2052·19	s		48712·7	
2050·91	w		48743·2	$f_4^1 - 48743·2$
2047·35	s		48828·0	
2041·17	w		48975·8	$\bar{d}_1^1 - 50688·9$
2035·15	s		49120·6	$\bar{d}_3^1 - 49325·4$
2034·51	s		49136·0	$\bar{d}_1^1 - 50849·1$
				$\bar{d}_2^1 - 50015·8$
2026·66	s		49326·3	$f_4^1 - 49326·3$
2025·91	s		49344·6	
2025·41	w		49356·7	$f_3^1 - 50688·9$
2014·12	s		49633·4	$\bar{d}_1^1 - 51346·5$
2007·74	w		49791·0	$f_3^1 - 51123·2$
2007·05	w		49808·1	$\bar{d}_2^1 - 50687·9$
				$\bar{d}_3^1 - 50012·9$
2001·77	s		49939·5	$\bar{d}_3^1 - 50144·3$
2000·46	s		49972·2	$\bar{d}_2^1 - 50852·0$
(vac.)				
1994·40	w		50140·4	$f_4^1 - 50140·4$
1990·18	s		50246·7	$\bar{d}_2^1 - 51126·3$
1889·28	w	MLC	50269·4	
1881·48	w		50467·1	$\bar{d}_2^1 - 51346·9$

TABLE II. (*continued*).
Reversals in Fuse-spectrum.

Wave-length.	Strength of reversal.	Previous observers.	Wave-number.	Terms.
1976·87	s	MLC	50585·0	$\bar{d}_3^1-50789\cdot8$
1974·53	w		50644·7	$\bar{d}_3^1-50849\cdot5$
1968·92	w		50789·3	$f_4^1-50789\cdot3$
1963·89	w		50919·4	$\bar{d}_3^1-51124\cdot2$
1882·7	w		53115	
1873·1	vs		53386	
1852·8	s		53971	
1840·4	s		54337	

H, Hamm; AJ, Angerer and Joos*; MLC, McLennan and Cooley†; Ma, Majumdar; MLML, McLennan and McLay‡.

The last four lines were difficult to measure exactly, owing to their broadness as well as to their position at the end of the spectrum. Confirmation of three of the new terms suggested above was obtained from Hamm's list, in which the following lines appear (with the exception of the fourth, measured by the author):—

Wave-length (air).	Wave-number (vac.).	Terms.
2259·550	44242·9	$\bar{d}_2^1-45122\cdot7$
2396·637	41712·3	$\bar{D}_2^1-45122\cdot3$
2278·759	43870·0	$\bar{d}_2^1-44749\cdot8$
2302·48 M	43418·0	$f_3^1-44750\cdot2$
2350·472	42531·7	$f_2^1-44748\cdot3$
2226·296	44903·6	$f_2^1-47120\cdot2$
2287·086	43710·2	$\bar{D}_2^1-47120\cdot2$

Some of the terms are a bit doubtful, particularly 48734, 50013, and 50140.

Conclusion.

It will be seen that it has been possible to account for the majority of the reversed lines. It is not possible to fit in a 1S_0 ground-term in the region of the spectrum investigated, and so the term 3F_4 must still be regarded as the lowest found in the spectrum of Ni I.

* *Ann. der Phys.* lxxiv. p. 743 (1924).

† *Trans. Roy. Soc. Can., Sect. III.* p. 349 (1926).

‡ *Trans. Roy. Soc. Can., Sect. III.* p. 89 (1925).

Summary.

The ground-term of Ni I empirically is a term 3F_4 . Doubt exists that this is the ground-term to be expected theoretically; it might be a 1S_0 term.

Fuse-spectra in air in the ultra-violet and *in vacuo* in the Schumann region have been examined. Many reversed lines in the former region have been found, but most of them can be accounted for as transitions to low levels already known, from middle terms already known and from new middle terms. In the Schumann region no long lines occur which could be attributed to the arc; they all appear to belong to the ground-terms 2D_3 and 2D_2 of Ni II.

It is concluded that the hypothetical term 1S_0 must give rise to lines below the region examined, if the term exists at all.

Physics Department,
University College, Leicester.
7th October, 1928.

CXVIII. General Solution of $\nabla^2\psi=\omega$.

To the Editors of the Philosophical Magazine.

GENTLEMEN,—

IN my paper "General Solution of $\nabla^2\psi=\omega$," which appeared on pp. 241 *et seq.* of the August 1928 issue of this Magazine, I regret to notice the occurrence of some errors, chiefly my own. May I beg space to point out the corrections?

On p. 245, bottom line, read " $d\theta_{n-1}$," not " $d\theta_n$."

„ „ footnote, „ " r_n ," not " v_n ."

„ p. 246, end of l. 2 fr. bottom, supply " θ_n ."

„ p. 248, in equation (12), " $d\theta_s$ " comes *after* bracket.

„ p. 249, l. 7, read " $dV_{n-1}^2 = J_s J_s \{d\theta_{n-1}\}^2$."

„ p. 250, l. 6, „ " $R=\infty$," not " $n=\infty$."

„ „ end of l. 2 fr. bottom, read " du_4 ."

„ p. 251, beginning of l. 2 fr. bottom, read " $\frac{\dot{v}}{c^2}$ " not " $\frac{v}{c^2}$."

„ p. 252, end of l. 1, "along the normal to the two-."

On p. 253, l. 1, read " $4c \int \Sigma R dv$," not " $4c \int \frac{\Sigma R}{r} dv$ ".

„ „ l. 8, „ " $\phi\omega$," not " ω ."

„ „ l. 20, „ " $\left(\frac{1}{r}\right) F(ct_1 + r)$,"

not " $\left(\frac{1}{r}\right) F\left(t_1 + \frac{r}{c}\right)$."

„ „ l. 22, „ " $\left(\frac{1}{2r}\right) f(ct + r)$,"

not " $\left(\frac{1}{2rc}\right) f\left(t_1 + \frac{r}{c}\right)$."

„ p. 254, l. 3, „ " $\xi(z) f(z)$," not " $f(z)$."

„ p. 255, l. 16, „ " $U_1 \frac{\partial y}{\partial u_1}$," not " $U_1 \frac{\partial y}{\partial u_2}$."

„ „ l. 5 fr. bottom, read " $\int_0^{2\pi} \frac{1}{y} \frac{\partial x}{\partial \theta} . d\theta$."

„ p. 257, l. 9, read " $2\pi\psi_A$," not " ψ_A ."

I am sorry to give you all this trouble, mainly through negligence on my part, but to any who care to read the paper these corrections must seem necessary.

Thanking you for publishing this note,

Yours faithfully,

97 Thornbury Road,
Osterley Park,
Middlesex.

ARTHUR J. CARR.

CXIX. *On the Buckling of a Thin Circular Plate by Heat.*
By F. E. RELTON, B.A., B.Sc., Imperial College*.

Summary.

THE circular plate is assumed to be thin and at uniform temperature. The analysis is limited by the fact that the temperature must not generate stresses that exceed the

* Communicated by Prof. S. Chapman, F.R.S.

elastic limit, and that the relative dimensions are bounded in order that buckling may occur before the elastic limit is reached. This latter justifies the ignorance of the most awkward term in the equations of equilibrium, of which three are deduced from first principles. As two of these are sufficient, the two most suitable are chosen. Their exact solution is impracticable, and recourse is had to power series. By substitution and a comparison of coefficients, there results a number of equations which are two in defect of the number of coefficients involved at any stage of the work. The deficiency is made up by the boundary conditions, including the peripheral strain due to heat. All the unknowns are expressible in terms of two quantities which are connected with the relative dimensions of the disk and its central curvature. By giving values to the one the other can be determined; hence all the coefficients can be found and the problem completely solved. The method is inverse inasmuch as the appropriate temperature is deduced from the configuration of the disk. Full discussion of the clamped plate necessitates computing rather many terms to a high degree of accuracy; the method is much more efficacious when applied to the unclamped plate.

(1) **W**E consider a thin, plane, circular disk whose temperature and thickness are uniform and whose periphery is prohibited from radial movement. If the temperature of the disk be raised, it is a contingency that the disk will buckle; the present paper is an attempt to determine the deflexions and stresses engendered when buckling occurs.

(2) At the outset we are called upon to examine two possibilities which may limit the validity of the analysis. In the first place, the peripheral transverse strain (*i. e.* perpendicular to the radius in the plane of the disk) in $\alpha\theta$, determined by the rise in temperature θ and the coefficient α of expansion of the material. So long as the disk does not buckle, the radial strain is this same quantity $\alpha\theta$, being somewhat less when buckling occurs. Thus, before buckling, we have a uniform state of plane stress of magnitude $E\alpha\theta/(1-\sigma)$, and the analysis becomes the less reliable the more closely this quantity approaches the elastic limit f . We have a provisional upper limit for the temperature θ in the relation $\theta = f(1-\sigma)/E\alpha$.

(3) Coming to figures *, we have in c.g.s. units :

	$10^{-8} . f.$	$10^{-11} . E.$	$\sigma.$	$10^6 . a.$	$\theta^{\circ} . C.$
Steel.....	30	22	0.25	10	100
Copper	0.5	10	0.34	16	2
Aluminium ...	5	7	0.34	23	20

the computed approximate value of θ in degrees centigrade being given in the last column. It appears that the range of validity varies considerably from one metal to another.

(4) The second limitation arises from the necessity of the elastic limit not being reached before the buckling load becomes critical, a criterion which furnishes a bound to the relative dimensions of the disk. Taking a clamped disk of radius c and thickness $2h$, the "buckling" thrust T per unit length of periphery is given † by

$$T = 2Eh^3\gamma^2/3c^2(1-\sigma^2),$$

where γ is the least root of $J_1(\gamma)=0$, to be taken as 3.832. The condition that T is less than $2hf$ gives

$$(c/h)^2 > E\gamma^2/3f(1-\sigma^2).$$

Using the previous figures, this provides a lower limit to c/h of approximately 60, 330, 90 for steel, copper, and aluminium respectively.

(5) For an unclamped plate the $\gamma=3.832$ is replaced by the smallest root of $\gamma J_0(\gamma)=(1-\sigma)J_1(\gamma)$, which may be taken ‡ as 2.017 when σ is a quarter. The corresponding minimum values of c/h will accordingly be about half those given above.

(6) Coming now to the analysis, we see that the solution will be symmetrical, there being only one independent variable r , the distance from the centre; we shall accordingly use primes to denote differentiations with respect to r . The stress zz perpendicular to the faces of the disk vanishes at both faces, and since the disk is thin will be ignored throughout.

(7) We conceive a point on the middle surface whose coordinates are $r, \phi, 0$ to be moved to $r+u, \phi, w$, so that

* "Recueil de Constantes Physiques," Soc. Fran. de Phys.

† G. H. Bryan, Proc. Lond. Math. Soc. xxii. (1890).

‡ Precott 'Applied Elasticity,' p. 488.

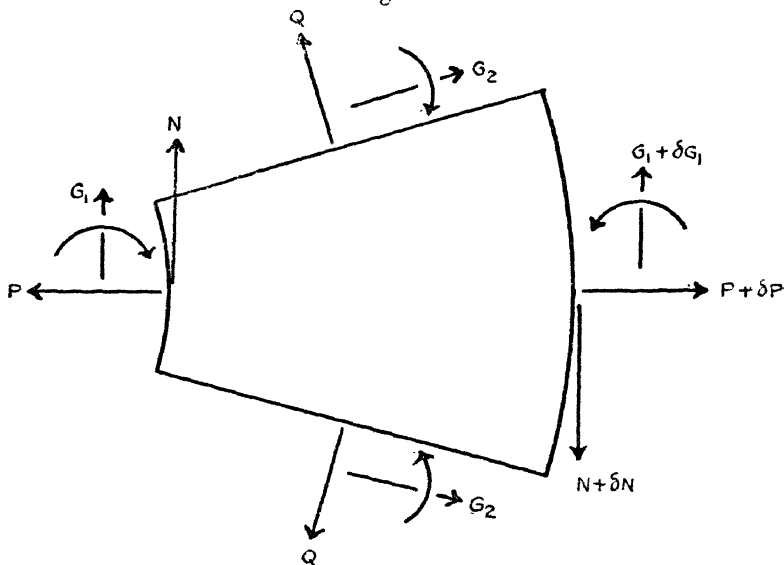
w is the deflexion. In the principal direction $\phi = \text{constant}$ we have the length element δr becoming $\{(\delta r + \delta u)^2 + \delta w^2\}^{1/2}$, so that the strain $e_{rr} \doteq u' + \frac{1}{2}w'^2$. In the other principal direction $r = \text{constant}$ we have the length element $r \cdot \delta \phi$ becoming $(r + u) \cdot \delta \phi$, so that the strain $e_{\phi\phi} = u/r$. These lead to

$$\left. \begin{aligned} P_1 - \sigma Q_1 &= E(u' + \tfrac{1}{2}w'^2), \\ Q_1 - \sigma P_1 &= Eu/r, \end{aligned} \right\} \dots \dots (1)$$

where P_1, Q_1 are the tensile stresses in the middle surface. For the principal curvatures we have

$$\left. \begin{aligned} 1/\rho_1 &= w''(1 + w'^2)^{-3/2} \doteq w'', \\ 1/\rho_2 &= w'/r(1 + w'^2)^{1/2} \doteq w'/r \end{aligned} \right\} \dots \dots (2)$$

Fig. 1.



along and perpendicular to the meridian respectively. The assumption is made that w' is everywhere small, though w is not necessarily small compared with the thickness $2h$. We shall further assume that the tensile stresses have a straight-line distribution through the thickness; this is tantamount to ignoring powers of h above the second in comparison with h . We then have $P = 2hP_1$, $Q = 2hQ_1$, where P, Q denote the force per unit length of edge, acting radially and transversely respectively.

(8) In the diagram (fig. 1) showing the arrangement of forces and couples we conceive the disk to be concave

upwards, whilst w is measured upwards above the level of the centre. Hence *

$$G_1 = \frac{2}{3} \cdot \frac{Eh^3}{1-\sigma^2} \left(\frac{1}{\rho_1} + \frac{\sigma}{\rho_2} \right), \quad G_2 = \frac{2}{3} \cdot \frac{Eh^3}{1-\sigma^2} \cdot \left(\frac{1}{\rho_2} + \frac{\sigma}{\rho_1} \right). \quad (3)$$

For the equations of equilibrium we have, by normal resolution,

$$\frac{d}{dr} (Nr \cdot d\theta) dr = Pr \cdot d\theta \cdot \frac{dr}{\rho_1} + Q \cdot dr \cdot \frac{r \cdot d\theta}{\rho_2}$$

or

$$P/\rho_1 + Q/\rho_2 = d(Nr)/r \cdot dr. \quad (4)$$

Along the meridian tangent

$$\frac{d}{dr} (Pr \cdot d\theta) dr + (Nr \cdot d\theta) \cdot \frac{dr}{\rho_1} = (Q \cdot dr) d\theta$$

or

$$Nr/\rho_1 = Q - d(Pr)/dr. \quad (5)$$

The binormal naturally leads to nothing owing to the symmetry, but moments about the inner curved edge give

$$\frac{d}{dr} (G_1 r \cdot d\theta) dr = (G_2 \cdot dr) d\theta + (Nr \cdot d\theta) dr$$

or

$$Nr = d(G_1 r)/dr - G_2. \quad (6)$$

Denoting by E_1 the quantity $2Eh^3/3(1-\sigma^2)$, equations (2) and (3) give

$$\left. \begin{aligned} G_1 &= E_1(w'' + \sigma w'/r), \\ G_2 &= E_1(w'/r + \sigma w''), \end{aligned} \right\} \quad (7)$$

whence equation (6) becomes

$$N = E_1 d(\nabla^2 w)/dr. \quad (8)$$

(9) It will be observed that, if in equation (4) we put $P=Q=\text{constant}$, the equation becomes the well-known equation for the critical buckling load †:

$$P \nabla^2 w = E_1 \nabla^4 w.$$

Further, if we can ignore the left side of equation (5), it becomes possible to express P , Q in terms of a single function U so that $P=U'/r$, $Q=U''$, in which case the elimination of u from equations (1) gives

$$r \nabla^4 U + 2hEw'w'' = 0;$$

* Love, 'Elasticity,' 4th ed. p. 464.

† *Vide* Bryant, *l. c.*

whilst equation (4), in the presence of a pressure p normal to one face of the disk, becomes *

$$d(U'w')/r \cdot dr = E_1 \nabla^4 w + p.$$

The exact solution of these two well-known simultaneous, non-linear differential equations may be ruled out as impracticable †, and matters are not made easier by the absence of p with the retention of the left side of equation (5).

(10) The equations (1) can be replaced by

$$\left. \begin{aligned} P(1-\sigma^2) &= 2hE(u' + \sigma u/r + \tfrac{1}{2}w'^2), \\ Q(1-\sigma^2) &= 2hE(u/r + \sigma u' + \tfrac{1}{2}\sigma w'^2). \end{aligned} \right\} \quad \cdot \quad \cdot \quad (9)$$

Using these and equation (8), the equilibrium equations (4) and (5) respectively become

$$(u' + \tfrac{1}{2}w'^2)(w'' + \sigma w'/r) + (\sigma w'' + w'/r)u/r = h^2 \nabla^4 w/3, \quad (10)$$

$$u/r - u' - ru'' = \tfrac{1}{2}(1-\sigma)w'^2 + rw'w'' + \tfrac{1}{3}h^2 w'' rd(\nabla^2 w)/dr, \quad \cdot \quad \cdot \quad \cdot \quad (11)$$

and the problem before us now is to solve these two equations.

(11) The most hopeful procedure lies in the adaptation of the method employed by Hencky ‡ in a similar connexion. From the symmetry of the meridian curve we propose to express w as an even function in ascending powers of r , vanishing at the origin. Using s to denote the ratio r/c , where c is the radius of the disk, we accordingly take

$$\left. \begin{aligned} w' &= a_1 s + a_3 s^3 + a_5 s^5 + \dots, \\ cw'' &= a_1 + 3a_3 s^2 + 5a_5 s^4 + \dots, \\ c^2 w''' &= 3 \cdot 2a_3 s + 5 \cdot 4a_5 s^3 + \dots, \end{aligned} \right\} \quad \cdot \quad \cdot \quad \cdot \quad (12)$$

where the a 's are dimensionless constants. Equation (11) then shows that u is an odd function of r ; we accordingly take

$$\left. \begin{aligned} u/r &= b_0 + b_2 s^2 + b_4 s^4 + \dots, \\ u' &= b_0 + 3b_2 s^2 + 5b_4 s^4 + \dots, \\ ru'' &= 3 \cdot 2b_2 s^2 + 5 \cdot 4b_4 s^4 + \dots, \end{aligned} \right\} \quad \cdot \quad \cdot \quad \cdot \quad (13)$$

* Cf. Föppl, *Vorl. ü. tech. mech.* Bd. v. § 24.

† Cf. Th. v. Kármán, *Ency. d. Math. Wiss.* iv. 4, c. art. 27.

‡ *Zeitsch. für Math. u. Phys.* lxxiii. p. 311 (1914).

where the b 's are dimensionless. The method consists in substituting for the various differentials of u and w in equations (10) and (11). A comparison of the coefficients of corresponding powers of s then supplies two sets of relations between the a 's and b 's. We thus obtain two expressions for any particular b in terms of the a 's, and the equivalence of these two expressions furnishes a relation connecting the a 's alone.

(12) It is evident *à priori* that the number of such relations available at any stage of the work must be in defect of the number of a 's present; otherwise the a 's, and hence the b 's, would be determinable, leaving no latitude for the fulfilment of boundary and other conditions. In practice it eventuates that the defect is two, and these are supplied from our knowledge: first, that the transverse strain $u/r = \alpha\theta$ at the boundary $r=c$; second, the condition which varies according as the periphery is clamped or not. The number of available relations is then theoretically sufficient to solve the problem to any required degree of approximation.

(13) In actual fact, the degree of approximation obtainable in general terms is severely limited; for since the differential equations to be solved are non-linear, the resulting algebraical equations which determine the a 's are also non-linear. From this it follows that, even if u and w are presumed to be given with sufficient accuracy by quite a small number of terms in their equivalent expansions, the eliminant that determines any particular a soon transcends the fourth degree. The coefficients in this eliminant are not wholly arithmetical, being, in fact, dependent on σ and the ratio h/c , so that very soon the a 's are no longer determinable.

(14) If the relative dimensions and the values of the physical constants for the disk are known, the above-mentioned eliminants have purely arithmetical coefficients and the a 's can be determined as accurately as desired. But a further difficulty here arises. Each a will be susceptible of several values, and the resulting expressions for u and w are not unique. This, of course, is to be expected, since the equilibrium configuration of the disk is, theoretically at least, not unique. There would remain, in such a case, the task of determining the conditions appropriate to each particular solution.

(15) Reverting now to the analysis, a slight modification is desirable before we carry our proposal into effect. We see from equations (4) and (5) that we can eliminate Q and derive a relation between P and N ; but this relation is more readily found from statical considerations. If we consider the equilibrium of a concentric circular portion of the disk and resolve in the axial direction, we get quite simply

$$N = Pw' \dots \dots \dots (14)$$

There are certain advantages in using equation (14) in preference to equation (10), and this we shall do in conjunction with equation (11).

(16) Since the quantity $(h/c)^2$ is of frequent occurrence, we shall denote its value by n , a number whose magnitude is 10^{-3} or less. The relations furnished by equation (14) may then be succinctly written

$$(\mu^2 - 1)a_\mu n/3 = \Sigma a_p b_q (q + 1 + \sigma) + \frac{1}{2} B(\overline{\mu - 2} : 3), \dots (15)$$

where $p + q = \mu - 2$ and $B(\overline{\mu - 2} : 3)$ denotes the aggregate of coefficients of order 3 and weight $\overline{\mu - 2}$ in w'^3 or $(\Sigma a)^3$, the weight of any letter being its suffix.

(17) Equation (11) furnishes no information concerning b_0 , but it provides relations which may be summarized as

$$(1 - \overline{\nu + 1}^2)b_\nu = \frac{1}{2}(\nu + 1 - \sigma)A(\nu : 2) + nc(\overline{\nu + 2} : 2)/3, \dots (16)$$

where $A(\nu : 2)$ is the aggregate of coefficients of order 2 and weight ν in w'^2 or $(\Sigma a)^2$, and $c(\overline{\nu + 2} : 2)$ is the aggregate of coefficients of order 2 and weight $(\nu + 2)$ in $w''d(\nabla^2 w)/dr$.

(18) We know that, at the periphery where $r = c$ and s is unity, the magnitude of the transverse strain u/r is $\alpha\theta$; hence from equation (13) we have

$$-\alpha\theta = b_0 + b_2 + b_4 + \dots = \Sigma b, \dots \dots (1)$$

the negative sign on the left being necessary for compression.

The Clamped Plate.

(19) When the plate is clamped round the periphery, we have w' zero when s is unity, so that from equation (12) we have

$$0 = a_1 + a_3 + a_5 + \dots = \Sigma a. \dots \dots (18)$$

A possible solution is evidently to have all the a 's zero

together with all the b 's except b_0 , whose value is then $-\alpha\theta$. In this case w is everywhere zero and

$$P=Q=-2hE\alpha\theta/(1-\sigma),$$

which is simply the particular case where the heat-stresses are not great enough to cause buckling.

(20) For the general case where buckling occurs we are provided with an infinite number of non-linear equations for the determination of an infinite number of unknowns, so that we necessarily adopt some method of approximation. At the outset it appears from equation (16) that it would be safe to omit the last term on the right in comparison with the others in virtue of the smallness of n . This is equivalent to omitting the last term on the right in equation (11), or ignoring the left side of equation (5). Further, if we use k to denote the ratio a_3/a_1 , it becomes possible to express all the unknowns in terms of a_1 and k . Thus, using equations (15) and (16) alternately, we deduce as the first few values

$$\begin{aligned} b_0 &= 8nk/3(1+\sigma), & b_4 &= -(5-\sigma)a_1^2k/24, \\ b_2 &= -(3-\sigma)a_1^2/16, & a_7 &= a_1k^3/18 - a_1^3k(1-\sigma^2)/128n, \\ a_5 &= a_1k^2/3 - (1-\sigma^2)a_1^3/128n, \\ b_6 &= -\frac{7-\sigma}{96}\left(\frac{5}{3}a_1^2k^2 - \frac{1-\sigma^2}{64n}a_1^4\right), \end{aligned}$$

whence b_8 , a_9 , and so on can be determined in succession.

(21) The quantity a_1 has a physical meaning; we see from equation (12) that it is the common value, at the centre, of the ratio (radius of plate)/(radius of curvature). This ratio is necessarily small in practice, and closer inspection of the above and succeeding values of the first few a 's and b 's shows that there are considerable advantages in equating a_1 to $\beta\sqrt{n}$. It eventuates that a_{2t+1}/a_1 becomes homogeneous of degree t in k and β , as also does $b_{2(t-1)}/n$. For a known value of σ the condition (18) is then expressible in terms of k and β with purely arithmetical coefficients, so that by giving values to the one the other can be determined. In this manner the a 's can be expressed as multiples of \sqrt{n} , and the b 's as multiples of n . The success of the method depends on the degree of reliability with which the modified condition (11) can be solved.

(22) For a plate of known size the deflexion can be computed from the integrated form of equation (12), while

the corresponding value of $\alpha\theta$ is given by equation (17). The method will, of course, not immediately give the deflexion corresponding to a specific value of $\alpha\theta$; this would have to be deduced by interpolation from computed values.

(23) Making the substitution mentioned in § 21, and using δ as a convenient abbreviation for the quantity $\beta^2(1-\sigma^2)/128$, we derive from equations (15) and (16) the following values :—

$$\left. \begin{aligned} a_1/\beta \sqrt{n} &= 1, & a_3/\beta \sqrt{n} &= k, & a_5/\beta \sqrt{n} &= k^2/3 - \delta, \\ a_7/\beta \sqrt{n} &= k^3/3.6 - k\delta, \\ a_9/\beta \sqrt{n} &= k^4/3.6.10 - 29k^2\delta/60 + 2\delta^2/5, \\ a_{11}/\beta \sqrt{n} &= k^5/3.6.10.15 - 143k^3\delta/900 + 38k\delta^2/75, \\ a_{13}/\beta \sqrt{n} &= k^6/3.6.10.15.21 - 38k^4\delta/945 \\ &\quad + 47k^2\delta^2/140 - 64\delta^3/525, \\ a_{15}/\beta \sqrt{n} &= k^7/3.6.10.15.21.28 - 29k^5\delta/28.126 \\ &\quad + 1702k^3\delta^2/75.147 - 158k\delta^3/525, \end{aligned} \right\} \quad (19)$$

and so on, together with

$$\left. \begin{aligned} b_0/n &= 8k/3(1+\sigma), & b_2/n &= -\beta^2(3-\sigma)/16, \\ b_4/n &= -k\beta^2(5-\sigma)/24, \\ b_6/n &= -\frac{(7-\sigma)}{96} \beta^2 \left(\frac{5}{3} k^2 - 2\delta \right), \\ b_8/n &= -\frac{(9-\sigma)}{80} k\beta^2 \left(\frac{7}{11} k^2 - 2\delta \right), \\ b_{10}/n &= -\frac{(11-\sigma)}{240} \beta^2 \left(\frac{7}{30} k^4 - \frac{109}{30} k^2\delta + \frac{9}{5} \delta^2 \right), \\ b_{12}/n &= -\frac{(13-\sigma)}{168} k\beta^2 \left(\frac{11}{450} k^4 - \frac{232}{225} k^2\delta + \frac{143}{75} \delta^2 \right). \end{aligned} \right\} \quad (20)$$

There is no intrinsic difficulty in extending either of these series; the main deterrent is the tedium, which is the inevitable concomitant of lengthy computations.

(24) The above values show that the condition (18) is always satisfied by a zero value of β , which corresponds to the physical fact that the undeflected state is always a

possible equilibrium position. Apart from this value the condition can be written in the expressive form:

$$1+k+\frac{k^2}{3}+\frac{k^3}{3.6}+\dots$$

$$= \delta \left(1+k+\frac{29}{60}k^2+\dots\right) - \delta^2 \left(\frac{2}{5}+\frac{38}{75}k+\dots\right)$$

$$+ \delta^3 \left(\frac{64}{525}+\frac{158}{525}k+\dots\right) - \dots, \quad (21)$$

where the left side is independent of whatever value of σ may be adopted. By making β infinitesimal we have the corresponding deflexion, from the integrated form of equation (12), expressible as

$$w = ca_1 \left(\frac{s^2}{2} + \frac{s^4}{4}k + \frac{s^6}{6} \cdot \frac{k^3}{3} + \frac{s^8}{8} \cdot \frac{k^3}{3.6} + \dots \right)$$

$$= ca_1 \{ J_0(s\sqrt{-8k}) - 1 \} / 4k. \quad \dots \quad (22)$$

This succinct form of the result is by no means fortuitous, but is a necessary consequence of its mode of derivation; such a choice of β makes all the α 's infinitesimal and likewise the deflexion. The analysis accordingly reverts to that for determining the critical buckling load, whence the result stated above. It appears that the quantity $\sqrt{-8k}$ is what we have previously called γ , to be taken as 3.832; the appropriate value of k is accordingly -1.835 , whilst the left side of equation (21) is always $J_1(2\sqrt{-2k})/\sqrt{-2k}$, which is convenient for computation.

(25) In illustration of the remarks in § 21, let us take σ to be $1/3$, so that δ becomes $(\beta/12)^2$, which we may denote by η . Equation (21) then becomes

$$\frac{J_1(2\sqrt{-2k})}{\sqrt{-2k}} = \eta \left(1+k+\frac{29}{60}k^2+\dots\right) - \eta^2 \left(\frac{2}{5}+\frac{38}{75}k+\dots\right)$$

$$+ \eta^3 \left(\frac{64}{525}+\dots\right) - \dots$$

If we assume that the deflexion of the plate is given with sufficient accuracy by a series terminating at the sixteenth power of the radius inclusive, then, with $k = -1.805$, we have

$$\sqrt{-2k} = 1.9 \quad \text{and} \quad J_1(2\sqrt{-2k})/\sqrt{-2k} = 0.006748.$$

The above equation then becomes

$$0.006748 = 0.10461 \eta + 0.32850 \eta^2 - 0.42128 \eta^3,$$

whence η is 0.0555 and β is 2.827. From equations (19) we have for the values of the a 's, taken in order: +1, -1.8050, +1.0303, -0.2272, -0.0273, +0.0419, -0.0197, +0.0060, each multiplied by $\beta\sqrt{n}$. According to equation (18), the value of Σa should be zero; with the present approximation the sum totals -0.0010.

(26) From equations (20) we have the following values of the b 's, taken in order, each being multiplied by n : -3.61, -1.3320, +2.8046, -2.9514, +1.8061, -0.6482, +0.0858. To these may be added +0.0514, -0.0421, as the values of b_{14} , b_{16} respectively, computed from equation (16). The condition (17) gives $\alpha\theta = 3.836 n$; for a plate whose diameter is a hundred thicknesses we have $n = 10^{-4}$, so that the present instance would cover the case of an aluminium plate heated about 16.7°C .

(27) By integration of equation (12) we have

$$\frac{w}{c} = \frac{s^2}{2} a_1 + \frac{s^4}{4} a_3 + \frac{s^6}{6} a_5 + \dots,$$

so that the central deflexion, obtained by putting s equal to unity, is given by

$$w = ca_1 \left(\frac{1}{2} + \frac{a_3}{a_1} \cdot \frac{1}{4} + \frac{a_5}{a_1} \cdot \frac{1}{6} + \dots \right).$$

As a_1 is $\beta\sqrt{n}$, and h is $c\sqrt{n}$, we can replace ca_1 by βh . For the figures given above, the central deflexion evaluates to $0.542 h$, or little more than a quarter of the thickness, which is, perhaps, surprisingly small in view of the fact that the material is not far removed from its elastic limit.

(28) It must be regarded as unfortunate that the a -series and b -series are not more rapidly convergent; it greatly impedes the discussion of associated phenomena. For example, the clamped disk is necessarily inflected, and if we seek to inquire how the greater deflexion affects the position of this inflexion, we do so by equating w'' to zero. With the present figures we solve the resulting equation of the fourteenth degree in s (actually the seventh degree in s^2), and we obtain $s^2 = 0.232(3)$, so that s is 0.482. The corresponding value for the critical buckling load when the deflexion is infinitesimal is derived from $J_1(x) = xJ_0(x)$, where x is $3.8317 s$. This gives x as 1.8412 and s as 0.4805,

whence it appears that the effect of the greater deflexion is to move the inflexion further from the centre. But the labour in obtaining the result is considerable and the verdict not very emphatic.

(29) Of the two series, the b -series is the less satisfactory. If we seek to compare the principal stresses at the periphery, we can do so by using equations (1) and (13). Since w' is zero we have

$$\frac{P - \sigma Q}{Q - \sigma P} = \frac{b_0 + 3b_2 + 5b_4 + \dots}{b_0 + b_2 + b_4 + \dots}.$$

With the values in § 26 this becomes

$$\frac{P - Q/3}{Q - P/3} = \frac{3.9474}{3.8356}.$$

According to this, $P \propto 5.8066$ and $Q \propto 5.7238$ whereas, had the plate remained undeflected at this temperature, we should have had $P = Q \propto 5.7534$, which would make it appear that one effect of buckling was slightly to increase the radial force and diminish the transverse force. Such an improbable conclusion would be warranted only by proceeding to a much higher degree of approximation.

(30) It may be noted, finally, that equation (11) provides a severe check on the computed values of the b 's. For since the last term on the right has been ignored and w' is zero at the periphery, we have from equation (13), after removing 8 as a factor,

$$b_2 + 3b_4 + 6b_6 + 10b_8 + 15b_{10} + \dots \equiv 0.$$

The last of our computed values is $b_{16} = -0.0421$, and with its appropriate factor, $36b_{16} = -1.5156$. The difficulty of getting a close fit with a series subject to such violent oscillations is evident. As an indication of the convergence of this series to zero, we may treat it as "summable (C1)" by Cesàro's method*. The values of S_r for $r=1, 4, 6, 8$, are $-1.3320 + 0.6394, -0.0363, +0.0214$ respectively.

The Unclamped Plate.

(31) For the unclamped plate the condition (18) is replaced by the fact that G_1 is zero at the periphery, so that from equations (7) and (12) we have

$$\Sigma a_r(\tau + \sigma) = 0, \quad . \quad . \quad . \quad . \quad . \quad (23)$$

* *Vide* Whittaker & Watson, 'Modern Analysis,' 2nd ed. 8.43.

where τ is odd. Let us suppose for a moment that we are concerned with an infinitesimal deflexion, so that the values of the a 's indicated in equations (19) are replaced by their leading terms. The above condition then becomes

$$\left(1 + 3k + \frac{5}{3}k^2 + \frac{7}{18}k^3 + \dots\right) + \sigma \left(1 + k + \frac{1}{3}k^2 + \frac{1}{18}k^3 + \dots\right) = 0. \quad (24)$$

Using ζ to denote $2\sqrt{-2k}$, the value of the second bracket, as pointed out in § 24, is $2J_1(\zeta)/\zeta$. The value of the first bracket is readily shown to be $2\{J_0(\zeta) - J_1(\zeta)/\zeta\}$, so that equation (24) is equivalent to

$$2\{\zeta J_0(\zeta) - (1 - \sigma)J_1(\zeta)\}/\zeta = 0,$$

which accords with § 5. In analogy with equation (21) we can now write equation (23) as

$$\begin{aligned} \frac{2}{\zeta} \left\{ \zeta J_0(\zeta) - (1 - \sigma)J_1(\zeta) \right\} \\ = \delta \left\{ (5 + \sigma) + k(7 + \sigma) + \frac{29}{60}k^2(9 + \sigma) + \dots \right\} \\ - \delta^2 \left\{ \frac{2}{5}(9 + \sigma) + \frac{38}{75}k(11 + \sigma) + \dots \right\} + \dots \end{aligned} \quad (25)$$

by using the values given in § 23.

(32) For an infinitesimal deflexion with $\sigma = 1/3$, the appropriate value of k is determined from $\zeta J_0(\zeta) = 2J_1(\zeta)/3$, so that $\zeta = 2.069$. As an illustration of the method for finite deflexion we may take ζ to be 2, so that k is -0.5 . The equation (25) then becomes

$$0.063298 = 2.59893\eta - 1.68539\eta^2 - 0.68190\eta^3,$$

from which η is 0.02476 and β is 1.888. The relations (19) then furnish the values of the a 's, in order up to a_{13} , as the the following multiples of $\beta\sqrt{n}$: $+1$, -0.5 , -0.05857 , $+0.00544$, -0.00240 , $+0.00033$, -0.00001 . These values satisfy the relation (23) with an error of 0.0003, and give the peripheral value of w' as $0.5619\beta\sqrt{n}$.

(33) The relations (20) give the values of the b 's in order as the following multiples of n : -1 , -0.59424 , $+0.34664$, -0.09091 , $+0.00921$, $+0.00108$, -0.00050 . The condition (18) yields $\alpha\theta = 1.329n$, which corresponds to about 5.8°C . for the aluminium plate previously mentioned. The

central deflexion, computed as in § 27, is $0.727h$, or slightly more than a third of the thickness. As in § 29, we can compare the principal stresses at the periphery; we have

$$(P - Q/3)/(Q - P/3) = 1.0346/1.3287,$$

so that $P \propto 1.6622$ and $Q \propto 1.8828$; whereas, had the plate remained undeflected at this temperature, we should have had $P = Q \propto 1.9931$. It appears that even this slight deflexion appreciably relieves the principal stresses, and the radial more than the transverse. In conclusion, it will be noted that the method is much more effective when applied to the unclamped plate than to the clamped plate.

CXX. *The Electrical Conductivity of Dilute Liquid Amalgams of Gold and Copper at Various Temperatures.* By T. C. WILLIAMS, M.Sc., and E. J. EVANS, D.Sc., *Physics Department, University College, Swansea* *.

INTRODUCTION.

THE present work is a continuation of the investigations commenced by Johns and Evans † on the electrical conductivities of the amalgams of the metals in group I. (b) of the periodic table. It deals with the conductivities of gold and copper amalgams of various concentrations at temperatures between room temperature and 300°C ., whilst the work of Johns and Evans was concerned with the amalgams of silver and copper.

The results in each case were examined in relation to Skaupy's theory of conduction in metallic solutions ‡. According to this theory, if L and η represent the electrical conductivity and viscosity respectively of pure mercury; and ΔL the increase of conductivity produced when the concentration of the metal expressed in gram. atoms dissolved in 100 gram. atoms of mercury is C , and $\Delta\eta$ the increase in viscosity for the same concentration of dissolved metal, the value of $H = \frac{1}{C} \cdot \frac{\Delta L}{L} + \frac{1}{C} \cdot \frac{\Delta\eta}{\eta}$

at infinite dilution is of the same order of magnitude for all metals dissolved in mercury. If for convenience we write

* Communicated by Prof. E. J. Evans.

† Phil. Mag., Feb. 1928, p. 271.

‡ Skaupy, *Zeit für Physik. Chemie*, lxxviii. p. 560 (1907); *Verhd. Deut. Phys. Ges.* xvi. p. 156 (1914); *ibid.* xviii. p. 252 (1916); *Phys. Zeit.* xxi. p. 597 (1920).

$\frac{1}{C} \cdot \frac{\Delta L}{L} = l$, and $\frac{1}{C} \frac{\Delta \eta}{\eta} = r$, it follows then that $H_{\infty} = l_{\infty} + r_{\infty}$. If the change of viscosity on dissolving the metal in mercury be small, it is found that $\left(\frac{1}{C} \cdot \frac{\Delta L}{L}\right)_{\infty}$ or l_{∞} has approximately the same value for all such metals.

The solution of most metals in mercury increases the conductivity, and the only exceptions to the rule are the alkali metals. According to Skaupy* these exceptions can be explained by the experimental work of Feningert†, who found that the internal friction of mercury is very much increased by solution of the alkali metals in it. Therefore, when comparing all metals, it is necessary to consider the values of $(l_{\infty} + r_{\infty})$, and not l_{∞} alone.

Skaupy further showed that $\frac{H_{\infty} - H}{C}$ is constant, and therefore if the variation of viscosity can be neglected the value of $\frac{l_{\infty} - l}{C}$ should be constant.

In the present work the values of l were determined for copper and gold amalgams of various concentrations at temperatures between 0° and 300° C., and the values of l_{∞} and $\frac{l_{\infty} - l}{C}$ evaluated in each case.

The full expressions could not be calculated owing to the lack of data concerning the viscosities of the amalgams used in the present investigations.

In order to calculate the values of l it was necessary to determine the resistance of a mercury column of the same dimensions as the amalgam column, and under exactly the same conditions. The values of the electrical conductivities of pure mercury at various temperatures between 0° and 300° C., deduced from these experiments, agreed within the limits of experimental error with those obtained by Williams‡ and Edwards§.

EXPERIMENTAL ARRANGEMENT.

The resistivities and conductivities of pure mercury and of the various amalgams at various temperatures were determined by measuring the electrical resistance of a fine

* *Loc. cit.*

† H. Feningert, 'Die Electriche Leitfähigkeit und innere Reibung Verunnter Amalgame,' Freiburg, 1914.

‡ E. J. Williams, *Phil. Mag.*, Sept. 1925, p. 589.

§ T. I. Edwards, *Phil. Mag.*, July 1926, p. 1.

cylindrical column of the conductors enclosed in a quartz capillary tube.

It is only necessary to give a brief account of the method, as it does not differ appreciably from that previously described by Williams * and Edwards †.

The instrument employed to measure the resistance of the column was a Callendar-Griffiths bridge, which was used in conjunction with a sensitive moving coil galvanometer capable of detecting a current of 10^{-9} ampere. The resistance could be measured accurately to $\cdot 00005$ ohm, which at high temperatures corresponded approximately to a change of $0\cdot 1^{\circ}$ C. in the temperature of the mercury or amalgam column, and to a change of $0\cdot 17^{\circ}$ C. at low temperatures. In the first place, the Callendar-Griffiths bridge was calibrated in the usual way, and the relative values of the bridge resistances in terms of the largest one determined. A knowledge of the correct absolute values of these bridge resistances is not necessary for the determination of either the temperature coefficient of resistivity, or even the absolute values of the resistivities of mercury and the amalgams. The standard value of the resistivity of mercury at 0° C. is taken to be 94074×10^{-9} , and this corresponds to a known value of the resistance of the given mercury column determined at the same temperature. It is then possible to calculate the resistivity at any temperature from the temperature coefficient. The method employed in calculating the resistivities of the various amalgams will be described later. The current entered the mercury or amalgam contained in the quartz tube by means of specially constructed leads which have been previously described ‡, and the resistance of the column was determined by subtracting the resistance of the leads, which was determined separately, from the total resistance measured. In the case of gold and copper amalgams, which oxidize only to small extent in air, the vertical limbs of the quartz tube carrying the leads were open to the atmosphere.

Method of Heating, and of Measuring Temperature.

The resistances of the mercury and amalgams were measured at several temperatures between 0° C. and 300° C. For measurements at 0° C., and at room temperatures, the quartz tube was immersed in a bath of ice and of water respectively. For observations at higher temperatures the tube was immersed in an iron bath, which contained

* *Loc. cit.*

† *Loc. cit.*

‡ Edwards, *loc. cit.*

substances boiling at different temperatures, and which was heated by a row of gas-jets placed underneath. In the present experiments, water, diethylaniline, eugenol, and diphenylamine boiling at approximately 100°C ., 215°C ., 256°C ., and 300°C . respectively were used in the heating-bath. By heating these substances to their boiling-points a steady temperature was reached, and accurate readings of the resistances could be taken, even at temperatures in the neighbourhood of 300°C . It was found that the temperatures of the boiling liquids generally increased slowly with long-continued heating; but this did not affect the accuracy with which measurements could be taken, as the change of temperature was negligible during the time required for a particular set of readings. Observations at each of these practically constant temperatures were continued over a long period, so that a large number of values of the resistance at a known temperature was obtained.

The temperature of the boiling liquid was measured by means of a platinum resistance thermometer previously calibrated, and a suitable mercury thermometer placed in the bath near the quartz capillary tube. The mercury thermometers were calibrated at the Reichsanstalt, and the high temperature and low temperature ones were divided into fifths and tenths of a degree centigrade respectively. The degree of accuracy attained in the measurement of the bath temperature is shown by the agreement between the temperatures indicated by the mercury and platinum thermometers in the neighbourhood of 300°C . The difference between them was never greater than 0.1°C . when the liquid was at its boiling-point.

EXPERIMENTAL DIFFICULTIES AND POSSIBLE ERRORS.

The chief difficulties encountered in the present investigation were: (i.) Thermoelectric currents; (ii.) formation of air-bubbles in the capillary, especially at high temperatures; and (iii.) variable contact resistance between the platinum wires fused through the glass leads and the amalgam contained in the quartz tube. Special precautions were taken to eliminate as far as possible errors due to the above causes.

The difficulty caused by thermoelectric currents was overcome by keeping the galvanometer circuit closed and adjusting the bridge resistance until there was no change in the continuous deflexion of the galvanometer on completing the battery circuit. Under these conditions, the value of the bridge resistance is equal to the resistance

to be measured in virtue of the properties of conjugate conductors.

The presence of air-bubbles could be detected quite easily during the experiments, as their effect was to increase the resistance of the amalgams, whereas the addition to the mercury of the metals employed in the preparation of the amalgams produced a decrease in the resistance. This difficulty was overcome by heating the quartz tube in a furnace to a temperature of about $315^{\circ}\text{C}.$ and running all the amalgam into one of the vertical limbs of the tube, which was then closed by a stopper. Keeping the tube and contents still in the furnace, the amalgam was then allowed to run slowly through the capillary, and the rate of flow was regulated by the amount of air allowed to enter the limb through the stopper. By this means the bubbles were removed fairly quickly, but if, on examination with a lens, the presence of bubbles was still detected the process was repeated. Determinations of the resistance were then made, both at room and at high temperatures. After every high temperature reading, the presence of air-bubbles was again tested, both by means of a lens and also by re-determining the resistance of the column at room temperature. If this value was found to be the same as before, as was generally the case, it was assumed that no bubbles had been produced during the heating.

The possible errors introduced by variable contacts were found to be negligible in the case of mercury, but were appreciable in the case of the amalgams, especially those of the higher concentrations. The surface of the amalgam in each limb was generally covered with a thin film, probably caused by slight oxidation. Unless these films were cleanly pierced by the platinum points when the leads were introduced, the best contact was not obtained, and the resistance of the amalgam plus the leads was thus not correctly determined. This effect would not be serious if in the determination of the leads resistance the platinum points were similarly affected. Experience, however, showed that this was not the case, but the difficulty was largely overcome by removing as much of the film as possible, and by cleaning the platinum points with concentrated nitric acid before every determination.

It is estimated that the possible average error in the determination of $\frac{1}{C} \cdot \frac{\Delta L}{L}$ is not more than 10 per cent. for the lowest concentrations, and not more than 4 per cent.

for the highest concentrations. This corresponds to an average error in the resistance measurement of $\cdot 0001_{25}$ ohm

METHOD OF CALCULATING THE RESISTIVITY AND CONDUCTIVITY OF THE AMALGAMS.

From the values obtained for the resistances of the column of mercury, and of amalgam, at a given temperature $t^{\circ}\text{C.}$, and the value of the resistivity of the former at the same temperature, the resistivity and conductivity of the amalgam at temperature $t^{\circ}\text{C.}$ were calculated as follows:—

Let R and R_{Am} be the resistances of the column of mercury and of amalgam respectively at temperature $t^{\circ}\text{C.}$; also let ρ and L be the values of the resistivity and conductivity respectively of mercury at temperature $t^{\circ}\text{C.}$, and ρ_{Am} and L_{Am} the corresponding values for the amalgam at the same temperature. If l and A denote the length and cross-section respectively of the column at the above temperature, then

$$\rho = R \left(\frac{A}{l} \right) \text{ and } \rho_{Am} = R_{Am} \left(\frac{A}{l} \right)$$

From these equations we obtain

$$\rho_{Am} = R_{Am} \left(\frac{\rho}{R} \right) (1)$$

From (1), and the relation

$$L_{Am} = \frac{1}{\rho_{Am}} (2)$$

the resistivity and conductivity of the amalgam at temperature $t^{\circ}\text{C.}$ can then be calculated in terms of the resistances of mercury and amalgam, and the resistivity of mercury at the same temperature.

If ΔL be the difference between L_{Am} and L at temperature $t^{\circ}\text{C.}$, and C the concentration of the amalgam expressed in gram atoms of metal dissolved in 100 gram atoms of mercury, then the value of $l \left(= \frac{1}{C} \cdot \frac{\Delta L}{L} \right)$ at temperature $t^{\circ}\text{C.}$ can be calculated. For this calculation the actual value of ΔL need not be obtained, for the value of $\frac{\Delta L}{L}$ can be found directly from the resistances thus:

$$\begin{aligned} \frac{\Delta L}{L} &= \frac{L_{Am} - L}{L} \\ &= \left(\frac{\rho}{\rho_{Am}} - 1 \right). \end{aligned}$$

Applying equation (1) we get

$$\frac{\Delta L}{L} = \left(\frac{R}{R_{Am}} - 1 \right). \quad . \quad . \quad . \quad (3)$$

Then

$$l = \frac{1}{C} \frac{\Delta L}{L}$$

$$= \frac{1}{C} \cdot \left(\frac{R - R_{Am}}{R_{Am}} \right). \quad . \quad . \quad . \quad (4)$$

This was the method actually employed in the present investigation for evaluating l .

EXPERIMENTAL RESULTS.

The Electrical Resistivity of Pure Mercury.

As previously explained, the method used in calculating the resistivity of an amalgam of known concentration involves measurements of the resistances of the mercury and the amalgam column under identical conditions. Such measurements in the case of mercury were carried out in the quartz tube, and the results are collected in Table I. Assuming the resistivity of mercury at 0° C. to

TABLE I.—Mercury.

Temperature, t° C.	Resistance in ohms, R_t .	Average temperature coefficient of resistance from 0° C. to t° C. (un- corrected for expansion of Quartz), $\times 10^4$.	Correction for expansion of Quartz, $= + \frac{R_t}{R_0} \cdot g,$ $\times 10^4$.	Corrected average temperature coefficient of resistance (and resistivity) from 0° C. to t° C., $\times 10^4$.	Resistivity of Mercury at t° C. $\times 10^8$.	Con- ductivity of Mercury at t° C.
0.0	3333 ₄	—	—	—	9407 ₄	10629 ₉
11.5	3367 ₈	8.974	.005	8.979	9504 ₇	10521 ₁
100.0	3362 ₃	9.867	.005	9.872	10336 ₁	9674 ₈
217.3	4136 ₂	11.083	.006	11.089	11674 ₂	8565 ₈
257.5	4321 ₇	11.514	.006	11.520	12197 ₅	8198 ₄
300.0	4530 ₄	11.970	.007	11.977	12787 ₆	7820 ₁

be 94074×10^{-9} , and correcting for the expansion of the quartz envelope, the resistivities of mercury at various temperatures can be calculated. The results obtained agree within the limits of experimental error with values obtained by Edwards *, who found that,

$$\rho_t = 94074 \times 10^{-9} [1 + 0.8877t + 0.9777t^2 + 0.19t^3].$$

The Electrical Conductivity of dilute Gold Amalgams.

So far as the author is aware, no previous determinations of the conductivity of dilute gold amalgams have been made. Determinations, however, have been made of the conductivity of gold amalgams whose concentrations were much greater than those employed in this investigation. Matthiesen and Vogt † measured the conductivity of amalgams containing between 80 per cent. and 90 per cent. of gold, whilst Parravano and Jovanovich ‡ made observations with amalgams containing about 60 per cent. of gold. In both cases the conductivity was found to increase with increase in the concentration of gold dissolved in mercury. However, owing to the great difference in the concentrations, the results for the above amalgams are not comparable with those obtained in the present experiments.

The gold employed in the present investigation was very pure, and was obtained in the form of thin foil from Johnson, Matthey & Co., London. The amalgams were prepared by the direct addition of the gold to the mercury. It was found that the gold goes into solution only very slowly at ordinary room temperatures, but much more rapidly if the mercury is heated beforehand.

Determinations of resistivity were made for nine different amalgams having concentrations varying between .04 per cent. and .32 per cent. by weight of gold in mercury. According to Gouy §, the solubility of gold in mercury at room temperatures is .13 per cent. by weight. In the present work, however, it was found possible to prepare, and also to make determinations with amalgams containing even .32 per cent. of gold at room temperatures. This also represents the limit of solubility, for, any further addition of gold produced no change in the resistance of the amalgam column, and the excess of gold remained out of solution.

* *Loc. cit.*

† Matthiesen and Vogt, *Pogg. Ann.* cxvi. p. 376 (1862).

‡ Parravano and Jovanovich, *Gazz. Chim. Ital.* xlix. (i.), p. 1 (1919).

§ A. Gouy, *Journ. Phys.* (3) iv. p. 320 (1895).

The amalgams were contained in the same quartz tube as that used for the mercury determinations, and the resistance determined at the following temperatures :—11·5° C., 100° C., and 300° C. For two amalgams of concentration ·12 per cent. and ·24 per cent., the resistance was further determined at 217·3° C. and 257·5° C.; thus enabling the average temperature coefficient of resistivity of the amalgam to be calculated at various stages of temperature between 11·5° C. and 300° C.

TABLE II.—Gold Amalgams.

Percentage weight of Gold in Mercury.	Concentration "C."	Resistance in ohms of column at temperature t° C.				
		$R_{11\cdot5^{\circ}}$	$R_{100^{\circ}}$	$R_{217\cdot3^{\circ}}$	$R_{257\cdot5^{\circ}}$	$R_{300^{\circ}}$
0 (Mercury).		·3367 ₈	·3662 ₃	·4136 ₂	·4321 ₇	·4530 ₄
·04004	·0407	·3362 ₄	·3654 ₀	—	—	·4514 ₈
·06006	·0611	·3359 ₄	·3649 ₈	—	—	·4507 ₀
·08001	·0814	·3357 ₀	·3645 ₀	—	—	·4500 ₅
·12000	·1221	·3350 ₄	·3636 ₈	·4101 ₇	4282 ₇	·4487 ₂
·16015	·1629	·3344 ₇	·3629 ₃	—	—	·4475 ₉
·20020	·2036 ₅	·3340 ₁	·3620 ₃	—	—	·4464 ₅
·24001	·2441	·3333 ₁	·3613 ₁	·4072 ₇	·4254 ₁	·4456 ₈
·28002	·2848	·3328 ₅	·3606 ₈	—	—	·4448 ₇
·32000	·3255	·3324 ₀	·3601 ₀	—	—	·4442 ₃

The resistances obtained for the column of amalgams of various concentrations are given in Table II., and their relative values are shown in Graph I. Table III. gives the corresponding values obtained for the resistivities and conductivities of the amalgams. The average temperature coefficient of resistivity of an amalgam of percentage weight ·12 (or "C"=·1221) for various temperature intervals between 11·5° C. and 300° C. as determined from the observed resistances, is given in Table IV., and the values of this coefficient between 11·5° C. and 100° C., for amalgams of various concentrations are collected in Table V.

TABLE III.—Gold Amalgam.

Temperature, t° C.	Percentage weight of Gold in Mercury.	Concen- tration "C."	Resistivity of Pure Mercury at t° C., $\times 10^6$.	Conduc- tivity of Pure Mercury at t° C.	Resistivity of Amalgam: at t° C., $\times 10^3$.	Conduc- tivity of Amalgam at t° C.
11.5	.04004	.0407	9505	10521	9490	10538
	.06006	.0611	"	"	9481	10547
	.08001	.0814	"	"	9475	10555
	.12000	.1221	"	"	9456	10576
	.16015	.1629	"	"	9440	10594
	.20020	.2036 ₅	"	"	9427	10608
	.24001	.2441	"	"	9407	10631
	.28002	.2848	"	"	9394	10645
	.32000	.3255	"	"	9381	10660
100	.04004	.0407	10336	9675	10313	9697
	.06006	.0611	"	"	10301	9708
	.08001	.0814	"	"	10287	9721
	.12000	.1221	"	"	10264	9743
	.16015	.1629	"	"	10243	9763
	.20020	.2036 ₅	"	"	10217	9787
	.24001	.2441	"	"	10197	9807
	.28002	.2848	"	"	10179	9824
	.32000	.3255	"	"	10163	9840
217.3	.12000	.1221	11674	8566	11577	8638
	.24001	.2441	"	"	11495	8700
257.5	.12000	.1221	12197.5	8198	12087	8273
	.24001	.2441	"	"	12007	8329
300	.04004	.0407	12788	7820	12743	7847
	.06006	.0611	"	"	12722	7860
	.08001	.0814	"	"	12704	7872
	.12000	.1221	"	"	12666	7895
	.16015	.1629	"	"	12634	7915
	.20020	.2036 ₅	"	"	12602	7935
	.24001	.2441	"	"	12580	7949
	.28002	.2848	"	"	12557	7963.5
	.32000	.3255	"	"	12539	7975

Conductivity of Amalgams of Gold and Copper. 1241

The variation of this coefficient with the concentration can be seen from Graph II. For purposes of comparison, the

TABLE IV.—Gold Amalgams.

Amalgam of Concentration "C" = .1221.

Temperature, $t^{\circ}\text{C.}$	Resistivity of Mercury at $t^{\circ}\text{C.}$, $\times 10^3$.	Resistivity of Amalgam at $t^{\circ}\text{C.}$, $\times 10^4$.	Average temperature coefficient of resistivity of Mercury from 11.5°C. to $t^{\circ}\text{C.}$, $\times 10^4$.	Average temperature coefficient of resistivity of Amalgam from 11.5°C. to $t^{\circ}\text{C.}$, $\times 10^4$.	$\frac{\Delta L}{L} \times 10^2$.
11.5	9505	9416	—	—	.519
100.0	10336	10264	9.886	9.664	.701
217.3	11674	11577	11.093	10.902	.841
257.5	12197.5	12087	11.520	11.318	.911
300.0	12788	12666	11.973	11.768	.963

TABLE V.—Gold Amalgams.

Concentration "C."	Average tem- perature coefficient of resistivity of Amalgams from 11.5°C. to 100°C. , $\times 10^4$.	Concentration "C."	Average tem- perature coefficient of resistivity of Amalgams from 11.5°C. to 100°C. , $\times 10^4$.
0 (Mercury).	9.886	.1629	9.610
.0407	9.804	.2036 ₅	9.484
.0611	9.773	.2441	9.497
.0814	9.699	.2848	9.452
.1221	9.664	.3255	9.421

values of $\frac{\Delta L}{L}$, $\frac{1}{C} \frac{\Delta L}{L} (=l)$, l_{∞} , and $(l_{\infty} - l)$ are included together with the corresponding values for copper amalgams

in Table IX. and the variations of $\frac{\Delta L}{L}$, l , and $(l_{\infty} - l)$, with changes in concentration can be seen from Graphs III., IV., and V. respectively.

The Electrical Conductivity of dilute Copper Amalgams.

As in the case of the gold amalgams, very little work has been done on the conductivities of dilute amalgams of copper, and the only investigation dealing with concentrations comparable with those used in the present experiments is that due to Johns and Evans *. The conductivities of very concentrated amalgams, however, were determined by Batelli†, Schleicher‡, and Michaelis§; but, on account of the large difference in the respective ranges of concentrations, their results cannot be compared with those obtained in the present work. The results of Johns and Evans ||, on the other hand, were obtained for amalgams containing respectively .01 per cent., .015 per cent., and .02 per cent., by weight of copper, and their determinations were all made at 300° C. Their observations, covering only a small range of concentrations, were, however, rather irregular.

In the present investigation, determinations of the conductivities were made at 11.5° C., 100° C., as well as at 300° C., and the measurements were carried out over a greater range of concentrations than those studied by Johns and Evans. In fact, at each temperature, determinations were made for increasing concentrations up to the limit of solubility of copper in mercury. Different values are given by different workers for the solubility of copper in mercury. This is undoubtedly due to the difficulty in getting the copper into solution, and depends to a great extent on the method by which the amalgam is prepared. In the present work the amalgam was prepared by direct addition of the finest electrolytic copper to mercury. The copper had previously been cleaned with dilute sulphuric acid, washed with distilled water, dried, and then reduced to very fine filings. Even when the mercury was heated to about 300° C., the copper was found to be only sparingly soluble in it.

* *Loc. cit.*

† *Loc. cit.*

‡ Schleicher, *Zeit. Electrochem.*, xviii. p. 998 (1912).

§ Michaelis, *Dissert.* Berlin (1883).

|| *Loc. cit.*

The conductivities of seven different amalgams, of concentrations ranging between .010 per cent. and .044 per cent. by weight, were determined at 300° C. It was found impossible to prepare amalgams containing more than .01 per cent. of copper at room temperatures, and more than .015 per cent. of copper at 100° C., for any further addition of copper was found to produce no change in the resistance, and the excess of copper remained out of solution.

The observed values of the resistances of the amalgam column of various concentrations are given in Table VI. and

TABLE VI.—Copper Amalgams.

Percentage weight of Copper in Mercury.	Concentration "C."	Resistance in ohms of column at temperature $t^{\circ}\text{C.}$		
		$R_{115^{\circ}}$	$R_{100^{\circ}}$	$R_{300^{\circ}}$
0 (Mercury).		.3367 ₈	.3362 ₃	.4530 ₄
.01020	.0322	.3363 ₅	.3655 ₈	.4517 ₉
.01531	.0483	—	.3652 ₃	.4512 ₀
.02042	.0643	—	—	.4506 ₅
.02540	.0802	—	—	.4501 ₉
.03137	.0990	—	—	.4495 ₉
.03516	.1110	—	—	.4492 ₃
.04437	.1406	—	—	.4485 ₃

the corresponding values of the resistivities and conductivities in Table VII. Table VIII. gives the comparison between the values of the temperature coefficient of resistivity, and the resistivity of mercury with the corresponding values obtained for an amalgam containing .01 per cent. by weight

("C" = .0322) of copper. The values obtained for $\frac{\Delta L}{L}$, l ,

l_{∞} , and $(l_{\infty} - l)$ are shown in Table IX., and the variations of these values, with concentration, are shown in Graphs III., IV., and V.

TABLE VII.—Copper Amalgams.

Temperature, $t^{\circ}\text{C.}$	Per- centage weight of Copper in Mercury.	Con- centration “C.”	Resistivity of Pure Mercury at $t^{\circ}\text{C.}$, $\times 10^8$.	Con- ductivity of Pure Mercury at $t^{\circ}\text{C.}$	Resistivity of Amalgam at $t^{\circ}\text{C.}$, $\times 10^8$.	Con- ductivity of Amalgam at $t^{\circ}\text{C.}$
11.5	.01020	.0322	9505	10521	9493	10534
100.0	.01020	.0322	10336	9675	10318	9692
	.01531	.0483	„	„	10308	9701
300.0	.01020	.0322	12788	7820	12753	7841
	.01531	.0483	„	„	12736	7852
	.02042	.0643	„	„	12721	7861
	.02540	.0802	„	„	12708	7869
	.03137	.0990	„	„	12691	7880
	.03516	.1110	„	„	12680	7886
	.04437	.1406	„	„	12661	7898

TABLE VIII.—Copper Amalgam.

Amalgam of Concentration “C” = .0322.

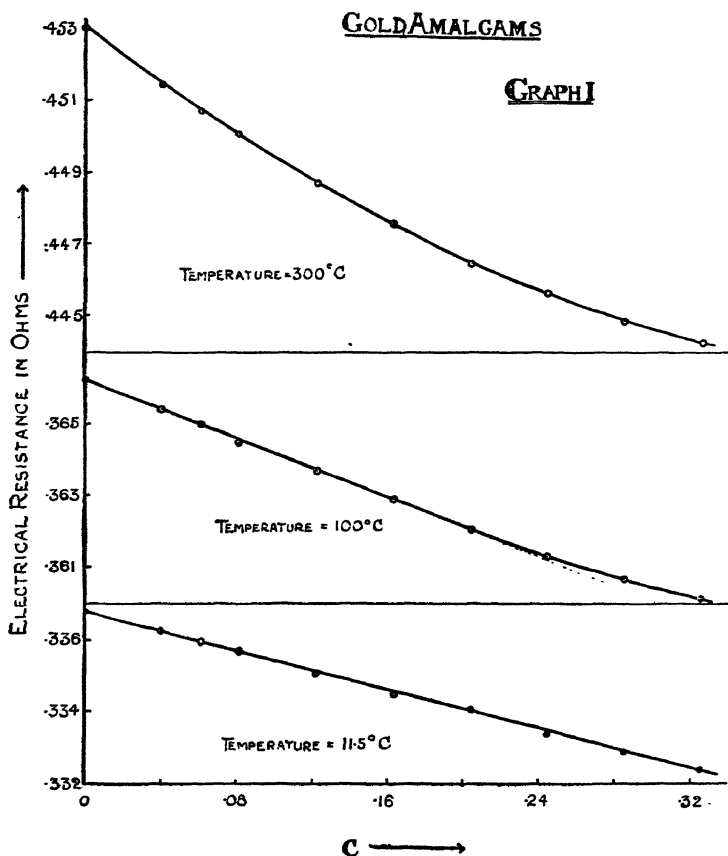
Tem- perature, $t^{\circ}\text{C.}$	Resistivity of Pure Mercury at $t^{\circ}\text{C.}$, $\times 10^8$.	Resistivity of Amalgam at $t^{\circ}\text{C.}$, $\times 10^8$.	Average temperature coefficient of resistivity of Mercury from 11.5°C. to $t^{\circ}\text{C.}$, $\times 10^4$.	Average temperature coefficient of resistivity of Amalgam from 11.5°C. to $t^{\circ}\text{C.}$, $\times 10^4$.	$\frac{\Delta L}{L} \times 10^2$.
11.5	9505	9493	—	—	.128
100.0	10336	10318	9.886	9.828	.178
300.0	12788	12753	11.973	11.903	.277

TABLE IX.

Nature of Amalgam.	Temperature $t^{\circ}\text{C.}$	Concentration "C."	$\frac{\Delta L}{L} \times 10^2.$	$\frac{1}{C} \cdot \frac{\Delta L}{L} (=l) \times 10^2.$	$l_{\infty} \times 10^2.$	$(l_{\infty} - l) \times 10^2.$
Gold.	11.5	.0407	.161	3.95	4.1	
	"	.0611	.250	4.09		
	"	.0814	.322	3.95		
	"	.1221	.519	4.25		
	"	.1629	.691	4.24		
	"	.2036 ₅	.829	4.07		
	"	.2441	1.041	4.27		
	"	.2848	1.181	4.15		
	"	.3255	1.318	4.05		
Gold.	100.0	.0407	.228	5.60	5.6	
	"	.0611	.343	5.61		
	"	.0814	.475	5.83		
	"	.1221	.701	5.74		
	"	.1629	.909	5.58		
	"	.2036 ₆	1.160	5.70		
	"	.2441	1.362	5.58		
	"	.2848	1.539	5.40		
	"	.3255	1.702	5.23		
Gold.	300.0	.0407	.350	8.60	9.0	.40
	"	.0611	.519	8.50		.50
	"	.0814	.664	8.16		.84
	"	.1221	.963	7.88		1.12
	"	.1629	1.218	7.48		1.52
	"	.2036 ₆	1.476	7.25		1.75
	"	.2441	1.651	6.76		2.24
	"	.2848	1.836	6.45		2.55
	"	.3255	1.983	6.09		2.91
Copper.	11.5	.0322	.128	3.97	4.0	
Copper.	100.0	.0322	.178	5.52	5.6	
	"	.0483	.274	5.67		
Copper.	300.0	.0322	.277	8.59	9.0	.41
	"	.0483	.408	8.44		.56
	"	.0643	.530	8.25		.75
	"	.0802	.633	7.89		1.11
	"	.0990	.768	7.75		1.25
	"	.1110	.848	7.64		1.36
	"	.1406	1.006	7.15		1.85

DISCUSSION OF RESULTS.

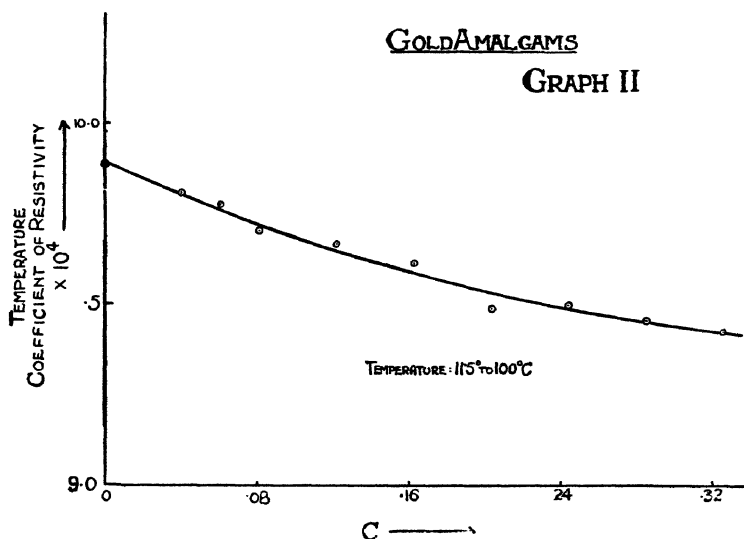
It can be seen from Tables II. and VI. that the resistance of mercury is decreased by the addition of gold or copper, and that this change becomes greater with increase in temperature. From Graph I. for gold amalgams, it is observed that at 11.5°C . the resistance of the amalgams is a linear function of the concentration; whereas at 100°C .



and 300°C . there is a deviation from the linear law, and this deviation is seen to be more rapid at the higher temperature. This is also the case with the copper amalgams.

Correspondingly, as shown in Tables III. and VII., there is an increase in the conductivity of the amalgam with concentration, and this change of conductivity as compared with mercury increases with increase in temperature, when the concentration of the amalgam is small.

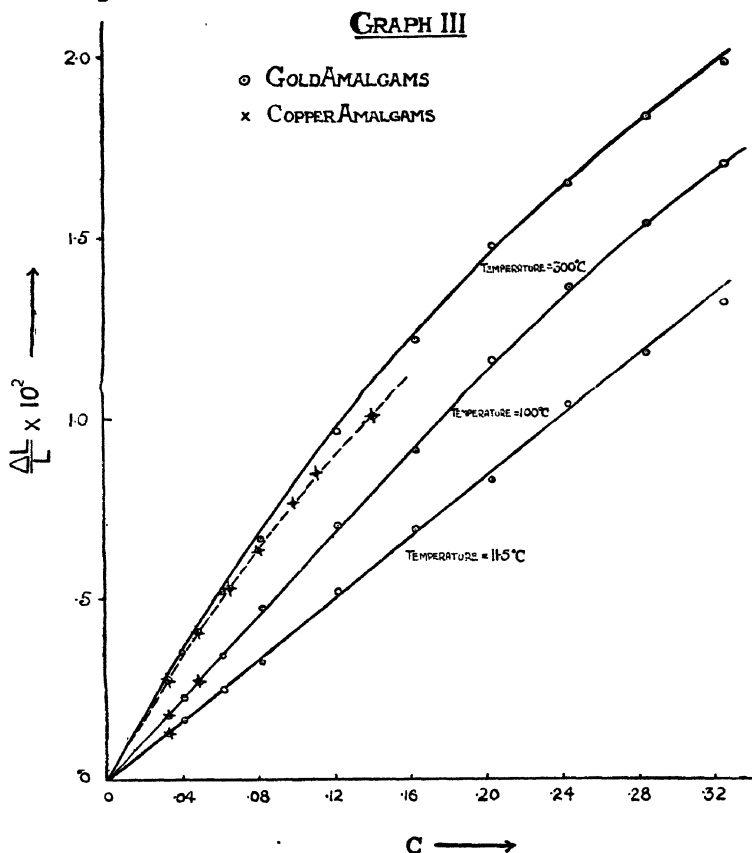
From Tables IV. and VIII. it can be seen that both for a gold amalgam of concentration " C " = .1221, and for a copper amalgam of concentration " C " = .0322, the average temperature coefficient of resistivity of the amalgam between 11.5°C . and the various higher temperatures increases with increase in temperature-difference. However, the values in each case are seen to be less than the corresponding values obtained for mercury. In addition, it is clearly shown in Table V. and Graph II., that for the gold amalgams, the difference between the average temperature-coefficient of resistivity of the amalgam and that of mercury between 11.5° and 100°C . becomes greater as the concentration of the amalgam is increased.



The values obtained for the quantities necessary to discuss the results for copper and gold amalgams in relation to Skaupy's theory*, have been collected in Table IX. The concentration " C " is expressed in gram atoms of metal per 100 gram atoms of mercury; and $\frac{\Delta L}{L}$ is the increase in conductivity relative to that of mercury at the same temperature. The sixth column gives the value of l for infinite dilution, i.e., the value of the ratio of the increase of conductivity relative to mercury at the same temperature, to the concentration, when the latter is very small.

* *Loc. cit.*

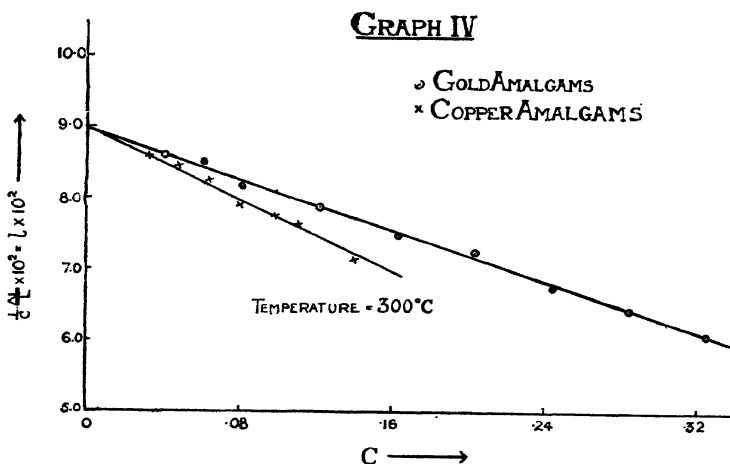
It can be seen from column 4, Table IX., and also from Graph III., that the value of $\frac{\Delta L}{L}$ increases both with increase in concentration and with increase in temperature for gold and copper amalgams. At room temperatures the relation between $\frac{\Delta L}{L}$ and "C" is linear, but at high temperatures



the relation deviates from the linear law. The values obtained for copper amalgams have been plotted in Graph III. for comparison with those obtained for the gold amalgams. However, owing to the impossibility of preparing more concentrated amalgams at 11.5° C. and 100° C., an extended set of curves for copper amalgams analogous to those obtained for gold amalgams cannot be obtained, and a complete comparison of the respective values of $\frac{\Delta L}{L}$ at the lower

temperatures cannot be made. At the lower concentrations the corresponding values of $\frac{\Delta L}{L}$ are practically the same for both amalgams, but at higher concentrations at a temperature of 300° C. there is a marked difference between them, the copper amalgams having the smaller values. This shows that the effect of copper and gold on the conductivity of mercury is practically the same for small concentrations; but, with increase in concentration, the effect of copper is less than that of gold, especially at high temperatures.

The values of $l \left(= \frac{1}{C} \frac{\Delta L}{L} \right)$ are given in column 5, Table IX.,



and its variation with concentration "C" at 300° C. is shown in Graph IV. The relation in both cases (copper and gold) is a linear one, sloping downwards towards the axis of concentration. The value of l_{∞} is the value of l at the point where the straight line graph meets the axis of l . This value was found to be 9.0×10^{-2} both for copper and for gold amalgams. It is not in agreement with the value obtained by Johns and Evans * for copper amalgams. In their experiments, however, they only considered three low concentrations, and the values they obtained for l varied irregularly with concentration. They took l_{∞} to be the mean of these three values of l , and in this way found its value to

* *Loc. cit.*

be 6.5×10^{-2} . The disagreement between these two values of l_{∞} for copper amalgams is probably due to the experimental difficulties met with in dealing with this amalgam, namely, the low concentrations possible, the liability of its surface to oxidize, and the slowness with which the copper goes into solution. Any consequent errors would have a serious effect on the value of l for low concentrations, such as those considered by Johns and Evans. By increasing the concentration, however, the effect of errors of observation on the value of l would be greatly diminished. This was done in the present experiments, and the results obtained for copper amalgams of different concentrations are in better agreement amongst themselves than those obtained by Johns and Evans*, and clearly indicate that their values were too low. The lower values of l obtained by them may possibly be due to their having taken insufficient precautions to ensure that the copper was completely dissolved.

At 11.5° C. and 100° C. for gold amalgams the values of l were found to be practically constant for all concentrations, and l_{∞} was taken to be the mean value. In this way it was found that l_{∞} was 4.1×10^{-2} at 11.5° C., and 5.6×10^{-2} at 100° C. For copper amalgams only one value of l was obtained at 11.5° C., and this was taken to be the value of l_{∞} . Even at 100° C. only two values of l were obtained, and in this case l_{∞} was taken to be the mean of both. In this way it was found that l_{∞} for copper amalgams was 4.0×10^{-2} at 11.5° C., and 5.6×10^{-2} at 100° C.

It can therefore be taken that the corresponding values of l_{∞} are the same within experimental error for both the copper and the gold amalgams.

Johns and Evans* in their work also made a thorough investigation of the change produced in the conductivity of mercury by the addition of silver; and it is interesting to note that the values they obtained for l_{∞} for silver amalgams agree, within experimental error, with those obtained in the present work for copper and gold amalgams. The comparison can be made from the values collected in Table X.

According to Skaupy's theory†, which has been referred to previously, the value of $(l_{\infty} + r_{\infty})$ should be of the same order of magnitude for different metals dissolved in mercury. Unfortunately, the values of r_{∞} at 11.5° , 100° , and 300° C. are not known for amalgams of concentrations equal to those employed in the present experiments, and, therefore, one is

* *Loc. cit.*

† *Loc. cit.*

obliged to consider the values of l_{∞} alone in relation to the different amalgams. As we have already seen from the values obtained by the present authors for copper and gold amalgams, and those obtained by Johns and Evans for silver amalgams (as seen in Table X.), it can be concluded that the value of l_{∞} , at the same temperature, is the same, within experimental error, for amalgams of all the metals in Group 1 (b) in the Periodic Table. This means that, atom for atom, the effect of copper, silver, and gold on the conductivity of mercury is the same, provided the concentration is small.

A further point in Skaupy's* theory is that, neglecting the variation of viscosity with concentration, the value of $\left(\frac{l_{\infty}-l}{C}\right)$ should be constant. At 11.5° C. and 100° C. there

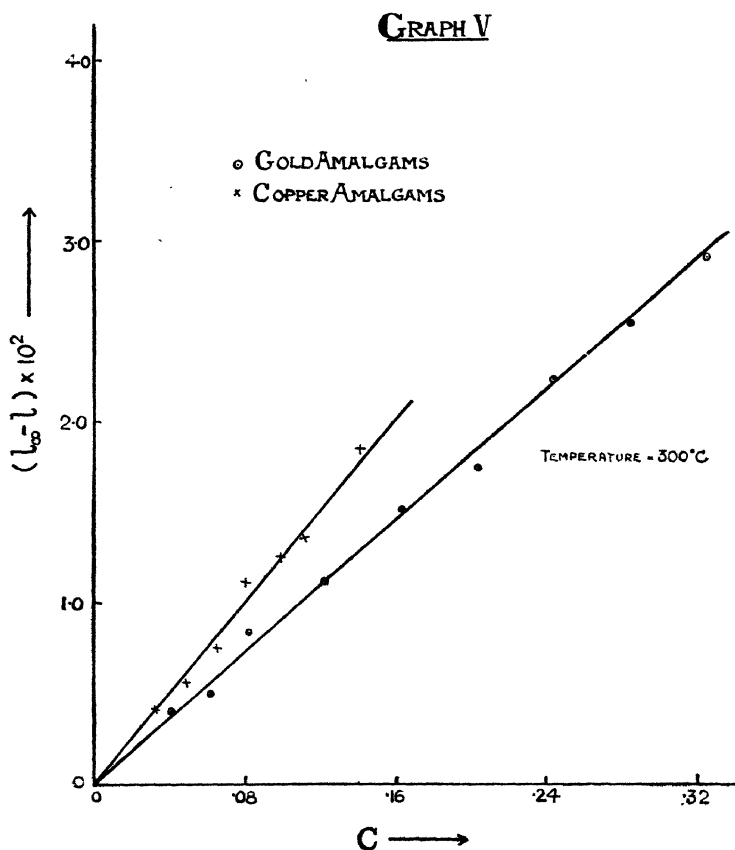
TABLE X.

Temperature ° C.	$l_{\infty} \times 10^2$ for Copper.	$l_{\infty} \times 10^2$ for Silver.	$l_{\infty} \times 10^2$ for Gold.
11.5	4.0	4.0 (at 15° C.)	4.1
100.0	5.6	5.3	5.6
300.0	9.0	9.0	9.0

was very little change in the value of l with concentration, and, consequently, the values of $\left(\frac{l_{\infty}-l}{C}\right)$ at those temperatures are not discussed. However, at 300° C., as seen in Table IX., the value of $(l_{\infty}-l)$ increased with concentration in the case of both copper and gold amalgams. The variation of $(l_{\infty}-l)$ with "C" is shown in Graph V., and the relation between the two quantities is approximately a linear one, thus showing that $\left(\frac{l_{\infty}-l}{C}\right)$ is approximately constant. It is important to point out here that an accurate experimental determination of l is very difficult for low concentrations and that any error in its value involves a much greater percentage error in the value of $(l_{\infty}-l)$.

* *Loc. cit.*

A possible explanation of the increase in the value of $l \left(= \frac{1}{C} \frac{\Delta L}{L} \right)$ with temperature is that the electron concentration in the amalgam as compared with mercury is increased with increase of temperature; but the question of whether viscosity enters into the problem in any form



must be left until experiments have been carried out on alkali amalgams.

SUMMARY.

1. The conductivities of dilute amalgams of copper and gold have been determined at 11.5°, 100°, and 300° C. In the case of gold amalgams, at each temperature the conductivity was determined over a range of concentrations equal

to the maximum range possible at $11.5^{\circ}\text{C}.$; whilst for copper amalgams, at each temperature the determinations were made for increasing concentrations up to the limit of solubility of copper in mercury at that temperature. For gold amalgams of concentrations " C " = $\cdot 1221$ and " C " = $\cdot 2441$, the conductivity was also measured at 217.3° and $257.5^{\circ}\text{C}.$

2. The average temperature coefficients of resistivity between 11.5° and $t^{\circ}\text{C}.$ of gold amalgam of concentration " C " = $\cdot 1221$, and of copper amalgam of concentration " C " = $\cdot 0322$, were measured, and in both cases were found to increase as the temperature difference increased. However, the values were less than the corresponding ones in the case of pure mercury.

3. The values of the average temperature coefficients of resistivity of gold amalgams of various concentrations, between 11.5° and $100^{\circ}\text{C}.$, showed a diminution as the concentration increased.

4. In the case of gold amalgams, at 11.5° and $100^{\circ}\text{C}.$ the increase of conductivity relative to the conductivity of mercury at the same temperature was practically proportional to the concentration, but at $300^{\circ}\text{C}.$, in the case of both copper and gold amalgams, this was found not to be the case.

5. For copper and gold amalgams, the value of $\frac{1}{C} \cdot \frac{\Delta L}{L}$ (*i.e.*, the ratio of the increase of conductivity relative to mercury to the concentration) was determined at each temperature and for each concentration, and the values compared with the corresponding ones obtained by Johns and Evans* for silver amalgams. It was found that the value of $\frac{1}{C} \cdot \frac{\Delta L}{L}$ at infinite dilution (*i.e.*, for extremely small concentrations) was practically the same at the same temperature for amalgams of copper, silver, and gold. This means that, atom for atom, the effect on the conductivity of mercury of the different metals in Group I. (b) in the Periodic Table is the same.

October 1st, 1928.

* *Loc. cit.*

CXXI. *Electronic Waves and the Electron.* By Sir J. J. THOMSON, O.M., F.R.S., Master of Trinity College, Cambridge*.

SUMMARY.

RECENT experiments have shown that a moving electron is accompanied by a train of waves. No such waves would be produced by the motion of an electron if, as hitherto assumed, it consisted solely of a point charge of electricity. The electric and magnetic forces round a moving electron of this type can be calculated from Maxwell's equations and have long been known, and there is nothing in the distribution of these forces approaching that in a train of waves. In this paper it is shown that if the structure of the electron were such that this point charge or something analogous to it formed a nucleus which was surrounded by a system such as we shall proceed to describe, then the motion of the electron would from the ordinary laws of electro-dynamics give rise to a train of waves, and, moreover, that the relation between the wave-length of this train and the velocity of the electron is exactly that indicated by the experiments of G. P. Thomson. The electronic waves on this view are electrical waves, but they do not travel through the normal ether, but through an ether modified by the system which envelops the nucleus of the electron. These waves would be produced if the system enveloping the nucleus, and which we shall call the "sphere" of the electron, were made up of parts which can be set in motion by electric forces, and when in motion produce the effects of electric currents. Such a structure might consist either of a distribution of discrete lines of force, or of a number of positively- and negatively-electrified particles distributed through the sphere of the electron. These would behave like free particles, even though the opposite charges were bound together in doublets, if the frequency of the forces acting upon them were large compared with the natural frequencies of the doublets. The properties of a structure of this kind are discussed, and it is shown that the sphere of the electron would have a definite period of vibration, the frequency of the vibration being proportional to the square root of the number of electrified systems per unit volume. These vibrations are of a peculiarly interesting kind, inasmuch as though they are electrical vibrations they are not accompanied by any radiation of energy, so that when once started

* Communicated by the Author.

they are maintained for an indefinite time. The vibrations consist of an oscillating electric field which is not accompanied by a magnetic one, the Poynting vector vanishes, and there is no transmission of energy. The sphere of the electron can thus vibrate, and so also can the nucleus, the time of vibration for the nucleus being proportional to the time light takes to travel round its circumference. Thus the two parts of the electron, the nucleus and the sphere, are each capable of vibration, and when the electron is in a steady state the vibrations of the two parts will be in resonance. The electron has thus, in addition to the steady electric field due to the negative charge on the nucleus, an alternating field in which the energy remains constant since there is no radiation. The oscillating field is the seat of energy, and thus the total energy of the electron is that due to the charge on the nucleus plus that due to the oscillating field. This is important in connexion with the calculation of the size of the electron. The usual estimate 1.4×10^{-13} cm. for the radius, a , is deduced on the assumption that the energy due to the charge on the nucleus $e^2/2a$ accounts for the whole of the energy of the electron; if $e^2/2a$ represents but a part, and it may be a small part, of the total energy, the corresponding value of a would be much larger.

Stationary Electron.

When the nucleus is not in motion it is shown that the components of the oscillating electric and magnetic forces are represented by equations of the form

$$\cos p_0 t \cdot f(x, y, z), \quad . \quad . \quad . \quad . \quad (I.)$$

where p_0 is the period of vibration of the electron and f a function such that

$$\frac{d^2 f}{dx^2} + \frac{d^2 f}{dy^2} + \frac{d^2 f}{dz^2} = 0.$$

An interesting special case representing a symmetrical electron is when

$$X=A \cos p_0 t \cdot \frac{d}{dx} \frac{1}{r}, \quad Y=A \cos p_0 t \cdot \frac{d}{dy} \frac{1}{r}, \quad Z=A \cos p_0 t \cdot \frac{d}{dz} \frac{1}{r};$$

$$\alpha = \beta = \gamma = 0.$$

(X, Y, Z) (α, β, γ) are the components of the electric and magnetic forces respectively and r the distance from the centre of the nucleus. Here the oscillating electric force is radial and always proportional to the steady force due to the

charge on the nucleus. The energy per unit volume due to the oscillating field and that due to the steady field bear a constant ratio to each other. It should be noticed that the total energy due to the oscillations remains constant, although the electric forces vanish periodically, for this energy is made up of two parts—one due to the electric field itself, the other to the kinetic energy of the moving electrified particles in the sphere; the sum of these two parts is constant. Since in each unit of volume the energy due to the oscillating field bears a constant ratio to that due to the field of the nucleus, the total energy of this field in the electronic sphere will be proportional to that of the nucleus, *i. e.* to $e^2/2a$, the total energy of the electron which is the sum of these parts will also be proportional to $1/a$. The time of vibration of the electron is proportional to the time light takes to travel round the circumference of the nucleus, and thus the frequency is proportional to $1/a$. The ratio of the energy of the electron to the frequency of its vibrations is thus independent of the size of the nucleus—this ratio is Planck's constant for the electron. Reasons are given for thinking that when an electron of this type emits *light* the energy in the quantum of the light it emits will bear to the frequency of the light the same ratio as the energy of the electron bears to the frequency of its vibrations. Thus Planck's law would be a consequence of the structure of the electron.

The Electron in Motion.

By using Maxwell's equations we find that when an electron of this type moves parallel to the axis of x with uniform velocity u , the field is given by the equations

$$Y = A' \cos p \left(t - \frac{ux}{c^2} \right) \cdot \frac{d}{dy} \frac{1}{R}, \quad Z = A' \cos p \left(t - \frac{ux}{c^2} \right) \cdot \frac{d}{dz} \frac{1}{R},$$

$$\alpha = 0, \quad \beta = -uA' \cos p \left(t - \frac{ux}{c^2} \right) \cdot \frac{d}{dz} \frac{1}{R},$$

$$\gamma = uA' \cos p \left(t - \frac{ux}{c^2} \right) \cdot \frac{d}{dy} \frac{1}{R},$$

where

$$R^2 = k^2(x - ut)^2 + y^2 + z^2, \quad p = p_0 k,$$

$$k^2 = \frac{1}{1 - \frac{u^2}{c^2}}.$$

Thus the field consists of plane waves of electric and magnetic force of diminishing amplitude travelling along the direction of motion of the electron. The wave-length λ of the waves is given by the equation

$$\lambda = 2\pi c^2 \sqrt{1 - \frac{u^2}{c^2}} / p_0 u; \dots \dots (II.)$$

thus λu is proportional to $\sqrt{1 - \frac{u^2}{c^2}}$. This is precisely the relation found by G. P. Thomson in his experiments on the diffraction of electrons. This expression for the wave-length is not confined to any particular distribution of the alternating field in the electron at rest. In the most general case, where one of the components of electric force in the electron at rest is given by an expression of the form $\cos p_0 t \cdot f(x, y, z)$, it can be shown that for the moving electron the solution is $\cos p \left(t - \frac{ux}{c^2} \right) f(k(x - ut), y, z)$, giving waves of the same length as the special solution we considered. Thus it follows from the principles of classical electrodynamics that a moving electron of the type we are discussing will be accompanied by a train of waves; the electronic waves on this view are waves of electric and magnetic force differing from plane waves passing through the normal ether in that the magnetic force in the electronic waves is, relatively to the electric force, smaller than in the normal electric waves.

The electronic waves and the electron must always move in the same direction. Hence, if the direction of the electronic waves is deflected, as in the experiments on diffraction, the path of the electron will be bent; conversely, if the path of the nucleus is changed by the action of applied forces on its charge, the path of the waves will be changed also.

The periods and properties of the electronic waves afford some evidence as to the sizes both of the nucleus and the sphere which surrounds it. The wave-length of waves associated with electrons moving with known speed have been determined by G. P. Thomson. From these values we find from equation (II.) that p_0 is about 1.1×10^{20} . Since the vibrations of the sphere and the nucleus are in resonance, this will also be the frequency of the vibrations of the nucleus. The time of these vibrations will be comparable with the time light takes to travel over the circumference of the nucleus, so that the frequency will be of the order $c/2\pi a$;

comparing this with the value 1.1×10^{20} , we find that a must be of the order 5×10^{-11} , which is very much larger than the value 1.4×10^{-13} deduced from the hypothesis that the electron consists of the nucleus alone.

Size of the "Sphere" round the Electron.

The electronic waves must be in a super-dispersive medium, *i. e.* in the sphere, hence the length of the train of these waves will be a guide to the diameter of the sphere. G. P. Thomson, from his experiments on diffraction, estimates the length of the train as at least 5×10^{-8} cm., which indicates that the size of the sphere is large compared with an atom. It is possible, however, that though there must be a super-dispersive medium of at least this length, the whole of that medium need not consist of the sphere of the moving electron. For if the sphere of an electron is even as large as an atom, then in a solid the spheres of the electrons in the closely-packed molecules will overlap, so that an electron travelling through it would be surrounded by a super-dispersive medium as large as the solid itself. The moving electron will excite in this medium waves whose length is the same as that of the electronic waves given by equation (II.); hence the length of the train will be fixed by the dimensions of the solid, and not by that of the sphere of a single electron. This would not apply unless the size of this sphere were comparable with the size of an atom, and therefore large compared with the nucleus, even if we adopt the new instead of the old estimate of the size of the latter.

Field Equations inside an Atom.

If the sphere of the electrons is comparable in size with the atom, the region inside an atom containing several electrons will be a super-dispersive region, and the field equations for the components of the electric and magnetic forces will be of the type

$$c^2 \left(\frac{d^2 \psi}{dx^2} + \frac{d^2 \psi}{dy^2} + \frac{d^2 \psi}{dz^2} \right) = \frac{d^2 \psi}{dt^2} + p_0^2 \psi. \quad (\text{III.})$$

It must be remembered that the sphere of the electron only comes into evidence when it is exposed to exceedingly rapid vibrations; when the frequency of the vibration is small compared with p_0 , the sphere behaves like the normal ether.

In a solid where the molecules are tightly packed the spheres of their electrons might overlap and fill the solid with a super-dispersive medium in which the field equations

would be of the type (III.). If an electrical wave, of frequency p , whether accompanied by an electron or not passed through the solid, the refractive index would be $\sqrt{p^2 - p_0^2}/p$; hence if p were greater than p_0 but comparable with it, the properties of the wave would vary rapidly with the value of p , and there would also be great differences between the properties of waves whose frequency was considerably less than p_0 and those whose frequencies were greater, though not infinitely greater. Now, among the γ -rays from radium C there are some whose frequencies are greater than p_0 (1.1×10^{20}), others whose frequencies are much smaller, so that if we could isolate these rays the point under discussion could be subject to a very direct test. It is very difficult, however, to get anything like a monochromatic beam of γ -rays. I tried an experiment of another kind, testing whether or not the harder γ -rays were, like electrons, deflected by an electric force. Since the nucleus of the electron and the electronic waves always travel in the same direction, the deflexion of the electron by electric force might be due to either to the deflexion of the waves or the deflexion of the nucleus. The waves would be deflected if the electric force produced a gradient in the refractive index of the medium through which they travel, the bending being analogous to that in a mirage; if this were the cause of the deflexion, γ -rays of the same frequency as the electronic waves would also be deflected by the electric force. If, however, the deflexion of the electron were due to the action of the electric field on the negative charge on the nucleus, and not to the effect on the sphere surrounding it, the γ -rays would not be deflected by the electric field. The experiments are in favour of this view rather than the former.

THE discovery by G. P. Thomson and Davisson & Germer of electronic waves implies that the electron must be something much more complex than the point charge of negative electricity which had previously been regarded as its adequate representation. In 'Beyond the Electron' and in a paper (Phil. Mag. xxxiii. p. 191) I have suggested a constitution for the electron which would cause a moving electron to be accompanied by a train of waves. I propose in this paper to develop the consequences of this hypothesis, and to describe some experiments I have made in connexion with it.

On this view the electron consists

(I.) of a nucleus which, like the old conception of the electron, is a charge e of negative electricity concentrated in

a small sphere. If a is the radius of this sphere, the energy due to the nucleus alone would be equal to qe^2/a , where q is a numerical constant if e is measured in electrostatic units. Its value will depend upon the way the electric charge is distributed throughout the region occupied by the sphere whose radius is a . It would, for example, be least if all the charge were on the surface of the sphere, it would be greater if the charge were uniformly distributed through the sphere, and greater still if the density increased towards the centre. This nucleus will have definite periods of vibration, for when it is in equilibrium the lines of force starting from it will be symmetrically distributed around it; if this symmetry is disturbed, the new arrangement will not be in equilibrium, but will oscillate about the old one. The time of the vibration will be proportional to the time light takes to travel round the nucleus, *i.e.* to $2\pi a/c$, where c is the velocity of light. Let the time of vibration be $k2\pi a/c$, where k is a numerical constant; the frequency ν is therefore $c/2\pi ak$, and since E the energy is equal to qe^2/a , we have the relation

$$E = 2\pi qke^2 \frac{\nu}{c}.$$

This is a relation of the form $E = h\nu$; $2\pi qke^2/c$ corresponding to Planck's constant h .

(II.) The nucleus does not constitute the whole of the electron; surrounding it there is a structure of much larger dimensions which we shall call the sphere of the electron, made up of parts which under electric forces of very high frequency are set in motion and produce effects of the same type as are produced by convective currents of electricity. We shall suppose that these parts can be represented by a number of negative charges each with a mass μ and an electric charge $-\epsilon$, and an equal number of positive charges each with a mass μ' and a charge $+\epsilon$.

Field Equations for a Stationary Electron.

Let (X, Y, Z) (α, β, γ) be respectively the components of electric and magnetic forces, N the number of either positive or negative charges per unit volume, and x_r, y_r, z_r coordinates fixing the position of one of the charges. Then by Maxwell's equations we have

$$\frac{1}{c^2} \frac{dX}{dt} + 4\pi \Sigma \epsilon \frac{dx_r}{dt} = \frac{d\gamma}{dy} - \frac{d\beta}{dz}, \quad . \quad . \quad (1)$$

with similar equations for Y and Z .

Again

$$\frac{d\mathbf{X}}{dy} - \frac{d\mathbf{Y}}{dx} = \frac{d\boldsymbol{\gamma}}{dt} \cdot \cdot \cdot \cdot \cdot \cdot \quad (2)$$

When the frequency of the vibrations is large compared with that of the individual system formed by a doublet of $+\epsilon$ and $-\epsilon$,

$$\mu \frac{d^2 x}{dt^2} = X\epsilon. \quad . \quad . \quad . \quad . \quad . \quad . \quad (3)$$

From (1), (2), and (3) we get three equations of the type

$$\begin{aligned} & \frac{d^2 \mathbf{X}}{dt^2} + p_0^2 \mathbf{X} \\ &= c^2 \left\{ \frac{d^2 \mathbf{X}}{dx^2} + \frac{d^2 \mathbf{X}}{dy^2} + \frac{d^2 \mathbf{X}}{dz^2} - \frac{d}{dx} \left(\frac{d\mathbf{X}}{dx} + \frac{d\mathbf{Y}}{dy} + \frac{d\mathbf{Z}}{dz} \right) \right\}, \end{aligned} \quad (4)$$

where

$$p_0^2 = 4\pi c^2 \left(\frac{N\epsilon^2}{\mu} + \frac{N\epsilon_1^2}{\mu'} \right), \quad . \quad . \quad . \quad (5)$$

and three of the type

$$\frac{d^2\alpha}{dt^2} + p_0^2\alpha = c^2\left(\frac{d^2\alpha}{dx^2} + \frac{d^2\alpha}{dy^2} + \frac{d^2\alpha}{dz^2}\right). \quad (6)$$

From equations (4) we get

$$\frac{d^2}{dt^2} \left(\frac{dX}{dx} + \frac{dY}{dy} + \frac{dZ}{dz} \right) + p_0^2 \left(\frac{dX}{dx} + \frac{dY}{dy} + \frac{dZ}{dz} \right) = 0. \quad (7)$$

This equation is of the type

$$\frac{d^2\psi}{dt^2} + p_0^2\psi = 0,$$

and represents a vibration whose frequency is p_0 . Thus the region round the nucleus of the electron—"the sphere"—has a natural frequency p_0 .

Vibrations of Ionized Gas.

The fact that a mixture of positive and negative charges vibrates with a definite frequency has applications to many problems besides the one under discussion. An ionized gas which contains free electrons and positive ions is a system quite analogous to the one we are considering. When an electric current passes through a discharge-tube containing gas at a low pressure, the negative glow, the positive column, the striations, etc. are all places where there are free

electrons and positive ions, and which therefore have definite times of vibration. For the ionized gas $\epsilon = e$ the charge on the electron and μ is equal to its mass; in this case the mass of the positive charge is so great compared with the electron that we may neglect the term in μ' in equation (5), and substituting the numerical values of e and m in that equation, we find that the number of vibrations per second in the ionized gas is $2.8\sqrt{N \times 10^7}$; if f is the fraction of the molecules ionized, p the pressure in millimetres of mercury,

$$N = f \cdot \frac{p}{760} \times 2.75 \times 10^{19},$$

so that the number of vibrations per second is

$$1.6 \times 10^{12} \sqrt{pf}.$$

When the system vibrates with the frequency p_0 it is easy to show that

$$\frac{1}{c} \frac{dX}{dt} + 4\pi \Sigma N \epsilon \cdot \frac{dx}{dt} = 0.$$

thus the convection currents balance the displacement ones so that there is no effective current. There are no currents to produce magnetic force so that the magnetic force will vanish, and with it the Poynting vector. Thus there is no transference of energy, and therefore no radiation. We have here the very interesting case of electrical vibrations without radiation. The oscillations in the ionized gas in the discharge-tube would be accompanied by oscillating electrical forces of the same period. These would not be detected by the ordinary methods of measuring the distribution of electric force along the tube. Thus, for example, such measurements show that the steady electric force in the negative glow is exceedingly small. It is possible, however, that owing to these electrical oscillations there may be forces of considerable magnitude but high frequency acting throughout the negative glow, and that these may have some influence in producing its luminosity. We can produce by the aid of hot-wire valves electrical forces of very high frequency. If these were applied to any ionized gas, pronounced effects might be expected when the frequency of the forces coincided with that of the free vibrations of the gas.

We have seen that when a system of the type we have assumed for the sphere of the electron is vibrating in its natural period the magnetic forces vanish, and hence the

electric forces must be derivable from a potential, so that we may write

$$X = \frac{d\phi}{dx}, \quad Y = \frac{d\phi}{dy}, \quad Z = \frac{d\phi}{dz}.$$

*Velocity of Phase Propagation and Group Velocity
in the Super-dispersive Medium.*

If a plane wave whose frequency is p is travelling through the medium parallel to the axis of z , we may put

$$X = \cos p \left(t - \frac{z}{V} \right), \quad Y = 0, \quad Z = 0,$$

where V is the phase velocity. Substituting these values in equation (4), we find

$$V^2 = c^2 \cdot \frac{p^2}{p^2 - p_0^2}, \quad . \quad . \quad . \quad . \quad . \quad (8)$$

or in terms of the wave-length $\lambda = 2\pi \cdot V/p$,

$$V^2 = c^2 + \frac{p_0^2 \lambda^2}{4\pi^2} \cdot . \quad . \quad . \quad . \quad . \quad (9)$$

If μ is the refractive index c/V , then from (8)

$$\mu^2 = 1 - \frac{p_0^2}{p^2} \cdot . \quad . \quad . \quad . \quad . \quad (10)$$

We see from (8) that waves whose frequency is less than p_0 cannot be propagated through the "sphere" of the electron. This need not apply if p is very much smaller than p_0 , for equation (3) is only true where the frequency of the vibrations is large compared with that of the free vibrations of the units forming the sphere of the electron. When this is not the case the field equations reduce to the ordinary equations of wave-motion.

The group velocity, which is also the velocity with which energy travels along the wave, is equal to

$$1/\frac{d}{dp}(p/V) = c \frac{\sqrt{p^2 - p_0^2}}{p} = c^2/V. \quad . \quad (11)$$

*Distribution of Energy when the "Sphere" is vibrating
in its Free Period.*

Let the components of the electric force be represented by

$$X = A \cos p_c t, \quad Y = B \cos p_0 t, \quad Z = C \cos p_0 t,$$

where A, B, C may vary from place to place. The energy per unit volume due to the electric force is

$$(X^2 + Y^2 + Z^2) / 8\pi c^2,$$

and is thus equal to

$$\frac{1}{8\pi c^2} (A^2 + B^2 + C^2) \cos^2 p_0 t.$$

The kinetic energy per unit volume of the moving electrified parts is

$$\begin{aligned} \frac{1}{2} N \mu \left(\left(\frac{dx_r}{dt} \right)^2 + \left(\frac{dy_r}{dt} \right)^2 + \left(\frac{dz_r}{dt} \right)^2 \right) \\ + \mu' \left(\left(\frac{dx_r'}{dt} \right)^2 + \left(\frac{dy_r'}{dt} \right)^2 + \left(\frac{dz_r'}{dt} \right)^2 \right). \end{aligned}$$

From the equations

$$\mu \frac{d^2 x_r}{dt^2} = X\epsilon,$$

$$\mu' \frac{d^2 x_r'}{dt^2} = X\epsilon,$$

we find that the kinetic energy is equal to

$$\frac{1}{2} \cdot \frac{\left(\frac{N\epsilon^2}{\mu} + \frac{N\epsilon^2}{\mu'} \right)}{p_0^2} (A^2 + B^2 + C^2) \sin^2 p_0 t.$$

But by equation (5) this equals

$$\frac{1}{8\pi c^2} (A^2 + B^2 + C^2) \sin^2 p_0 t.$$

Thus the sum of the energy of the electric field and the kinetic energy of the moving parts is, per unit volume,

$$\frac{1}{8\pi c^2} (A^2 + B^2 + C^2), \quad . \quad . \quad . \quad . \quad (12)$$

and thus does not alter with the time, so that the energy in the "sphere" of the electron will be constant.

If the oscillations have the frequency p instead of p_0 , the kinetic energy per unit volume of the moving electrified parts is equal to

$$\frac{1}{8\pi c^2} \cdot \frac{p_0^2}{p^2} (A^2 + B^2 + C^2) \sin^2 pt. \quad . \quad . \quad . \quad (13)$$

As p is always greater than p_0 , the average kinetic energy

is less than the average energy due to the electrostatic field. The nucleus and the sphere of the electron form a connected system, and energy can flow from the one into the other; when a steady distribution of energy is reached the nucleus of the electron will be in resonance with the sphere. The frequency of vibrations of the sphere, p_0 , depends upon the *density* of the electrified units of which it is composed, and not upon the total number in the sphere; thus by expansion or contraction it may adjust its period so as to be in resonance with the nucleus. On this view p_0 will have a definite value, which will be the same whether the electron is free or whether it forms a part of an atom or molecule containing many other electrons. There is evidence, as we shall see, that the sphere of the electron is, on a low estimate, comparable in size with the dimension of an atom or molecule; so that in a molecule containing many electrons their spheres would overlap and form practically a continuous medium in which p_0 would be constant and equal to the frequency of the vibrations of the nucleus of the electron. When such molecules unite to form a solid, the whole solid, from the point of view of the transmission of waves of very high frequency, may be regarded as an enormously large electronic sphere. We shall return to this point later.

The Electron in Motion.

Let us now consider what will happen to an electron of this type if it is in motion instead of at rest; we shall suppose that it is moving uniformly parallel to the axis of x with the velocity u . The motion of the lines of electric forces will produce magnetic forces whose direction at any point is at right angles to the lines of electric force at that point and to the direction of their motion; the magnetic forces will thus be at right angles to the axis of x . These magnetic forces, like the electric forces whose motion produces them, are alternating with great rapidity, and, as an alternating magnetic force produces electric forces which cannot be derived from a potential, the electric forces will not be given by the same expressions as for the electron at rest, but will be modified in a way we proceed to determine.

The displacement current parallel to z in the moving electron will not be dZ/dt if d/dt denotes a partial differential coefficient, but $\left(\frac{d}{dt} - u \frac{d}{dx}\right)Z$. Similarly, the rate of increase

of the magnetic force will not be $d\beta/dt$, but $\left(\frac{d}{dt} - u \frac{d}{dx}\right)\beta$.

Again, as the electric charges in the sphere of the electron are moving, the form parallel to z on one of these units is not $Z\epsilon$ but $(Z-u\beta)\epsilon$.

Hence the equations of the field become

$$\frac{1}{c^2} \left(\frac{dZ}{dt} - u \frac{dZ}{dx} \right) + 4\pi \Sigma \epsilon \frac{dz}{dt} = \frac{d\beta}{dx} - \frac{d\alpha}{dy},$$

$$\frac{1}{c^2} \left(\frac{dY}{dt} - u \frac{dY}{dx} \right) + 4\pi \Sigma e \frac{dy}{dt} = \frac{d\alpha}{dz} - \frac{d\gamma}{dx},$$

$$\frac{d\gamma}{dt} - u \frac{d\gamma}{dx} = \frac{dX}{dy} - \frac{dY}{dx},$$

$$\frac{d\beta}{dt} - u \frac{d\beta}{dx} = \frac{dZ}{dx} - \frac{dX}{dz},$$

$$\mu \frac{d^2 z}{dt^2} = -\epsilon(Z-u\beta).$$

We can find by inspection a solution when u/c is exceedingly small; it is evidently

$$\alpha = 0, \quad \beta = -\frac{u}{c^2} Z, \quad \gamma = \frac{u}{c^2} Y,$$

$$\frac{u}{c^2} \frac{dY}{dt} = -\frac{dY}{dx},$$

$$\frac{u}{c^2} \frac{dZ}{dt} = -\frac{dZ}{dx}.$$

Hence, if

$$Y = \cos p_0 t \cdot \frac{d}{dy} f(x, y, z); \quad Z = \cos p_0 t \cdot \frac{d}{dz} f(x, y, z)$$

is the solution when the electron is at rest, then, retaining only the lowest powers of u/c , the solution for the moving electron is

$$Y = \cos p_0 \left(t - \frac{ux}{c^2} \right) \frac{d}{dy} f((x-ut), y, z),$$

$$Z = \cos p_0 \left(t - \frac{ux}{c^2} \right) \frac{d}{dz} f((x-ut), y, z),$$

$$\alpha = 0, \quad \beta = -\frac{u}{c^2} \cos p_0 \left(t - \frac{ux}{c^2} \right) \frac{d}{dz} f((x-ut), y, z),$$

$$\gamma = \frac{u}{c^2} \cos p_0 \left(t - \frac{ux}{c^2} \right) \frac{d}{dy} f((x-ut), y, z).$$

By using the Lorentzian transformation we can find a solution which is not limited to the case when u/c is exceedingly small; it is

$$\left. \begin{aligned} Y &= k \cos p \left(t - \frac{ux}{c^2} \right) \frac{d}{dy} f(k(x-ut), y, z), \\ Z &= k \cos p \left(t - \frac{ux}{c^2} \right) \frac{d}{dz} f(k(x-ut), y, z), \\ \alpha &= 0, \quad \beta = -\frac{u}{c^2} Z, \quad \gamma = \frac{u}{c^2} Y, \end{aligned} \right\} \quad (14)$$

where

$$k = \frac{1}{\sqrt{1 - \frac{u^2}{c^2}}} \quad \text{and} \quad p = p_0 k.$$

Thus the frequency of the moving electron is greater than that of the stationary. We see that the expressions for the electric and magnetic force round the moving electron contain the factor $\cos p \left(t - \frac{ux}{c^2} \right)$; this factor represents plane waves travelling in the direction of motion of the electron. The phase velocity is equal to c^2/u , and thus depends only on the velocity of the electron, and not upon the density of the electric charges in its sphere. The wave-length λ of the waves is given by the equation

$$\lambda = \frac{2\pi c^2}{pu}, \quad \text{or} \quad \lambda u = \frac{2\pi c^2}{p_0} \sqrt{\frac{1-u^2}{c^2}}.$$

This is exactly the relation established by G. P. Thomson's experiments on the diffraction of electrons. We saw, equation (11), that if V is the phase velocity and U the velocity with which the energy travels through the medium,

$$U = \frac{c^2}{V}.$$

We have just seen that $V = c^2/u$; hence $U = u$, so that the energy travels along with the electron. This investigation shows that if the electron is of the type we are considering, then it follows from the laws of classical electrodynamics that when it is in motion it will be accompanied by a train of waves, and that the relation between the wave-length and the velocity is exactly that indicated by G. P. Thomson's experiments. The electronic waves on this view are waves

of electric and magnetic forces ; they differ from electric waves through the normal ether, not only in the phase velocity, but also in that in the electronic waves the magnetic force is smaller relatively to the electric than in normal electric waves.

We proceed to illustrate these principles by considering the waves that would accompany electrons of special types.

Take first the case when in the stationary electron the alternating electric force is parallel to the axis of z , so that the electron is polarized. The equations for the stationary electron are

$$Z = A \cos p_0 t, \quad Y = 0, \quad X = 0, \\ \alpha = \beta = \gamma = 0.$$

The energy per unit volume : the sum of the energy due to the electrostatic field and the kinetic energy of the moving charges is, by equation (12), equal per unit volume to $A^2/8\pi$. If the nucleus moves with uniform velocity u parallel to the axis of x , the electric and magnetic forces are by (14) given by

$$Z = Ak \cos p \left(t - \frac{ux}{c^2} \right), \quad Y = 0, \quad X = 0 ; \\ \beta = -\frac{uk}{c^2} A \cos p \left(t - \frac{ux}{c^2} \right), \quad \alpha = 0, \quad \gamma = 0,$$

where

$$k = 1/\sqrt{1 - \frac{u^2}{c^2}}, \quad p = kp_0.$$

Thus the electric and magnetic forces are represented by trains of waves of constant amplitude. As in electric waves through the normal ether, the magnetic force is at right angles to the electric and proportional to it ; but in the electronic waves the ratio of the magnetic to the electric force is only u/c of the same ratio for normal electrical waves.

The energy per unit volume due to the electrostatic field is

$$\frac{1}{8\pi} A^2 k^2 \cos^2 p \left(t - \frac{ux}{c^2} \right).$$

From equation (13) the energy due to the moving electrified systems is

$$\frac{1}{8\pi} \frac{p_0^2}{p^2} A^2 k^2 \sin^2 p \left(t - \frac{ux}{c^2} \right).$$

The energy due to the magnetic field is

$$\frac{1}{8\pi} \frac{u^2}{c^2} k^2 \cos^2 p \left(t - \frac{ux}{c^2} \right).$$

Since $p_0^2/p^2 = 1 - \frac{u^2}{c^2}$, we see that the mean energy due to the electrostatic field is equal to the mean of the sums of the kinetic and magnetic energies.

Symmetrical Electron.

Another very interesting case is when the field round the stationary electron is defined by the equations

$$X = A \cos p_0 t \cdot \frac{d}{dx} \frac{1}{r}, \quad Y = A \cos p_0 t \cdot \frac{d}{dy} \frac{1}{r}, \quad Z = A \cos p_0 t \cdot \frac{d}{dz} \frac{1}{r},$$

. . . (15)

and consequently

$$\alpha = \beta = \gamma = 0.$$

Here r is the distance from the centre of the nucleus. These equations represent an electric field where the distribution of the alternating electric force is the same as that of the steady electric field due to the charge on the nucleus. Thus on this view there is in the electron a steady radial electric force equal to e^2/r^2 , and superposed on this an alternating electric force also radial and also proportional to $1/r^2$.

The sum of the energy per unit volume due to the electric field and to the kinetic energy of the electric charges in the sphere is, by equation (12), equal to

$$\begin{aligned} \frac{1}{8\pi} A^2 \left\{ \left(\frac{d}{dx} \frac{1}{r} \right)^2 + \left(\frac{d}{dy} \frac{1}{r} \right)^2 + \left(\frac{d}{dz} \frac{1}{r} \right)^2 \right\} \\ = \frac{A^2}{8\pi} \frac{1}{r^4}. \end{aligned}$$

The energy per unit volume due to the charge on the nucleus is equal to $e^2/8\pi r^4$.

Thus the energy due to the charge on the nucleus and that due to the alternating field have a constant ratio to each other, and the total energy of the electron is

$$\frac{1}{2} \frac{e^3}{a} + \frac{1}{2} \frac{A^2}{a},$$

where a is the radius of the nucleus.

The energy outside a sphere whose centre is at the nucleus and radius b is $(e^2 + A^2)/2b$.

The Size of the Nucleus of the Electron.

The usual way of calculating the size of the electron is from the equation

$$\text{Energy of the electron} = mc^2,$$

where m is the mass of the electron. If a is the radius of the nucleus, the energy of the electric field due to it is $e^2/2a$, so that if the electron consisted of nothing but the nucleus, we should have

$$\frac{e^2}{2a} = m_0c^2 \quad \text{or} \quad 2a = e^2/m_0c^2,$$

where m_0 is the mass of a stationary electron; this equation leads to the value 1.4×10^{-13} cm. for a .

When, as in the type of electron we are considering, the nucleus is surrounded by a sphere, the energy is not $e^2/2a$ but $(e^2 + A^2)/2a$, so that $2a = (e^2 + A^2)/m_0c^2$. Thus for an electron of this kind the radius of the nucleus is greater than the conventional value, and if A is large compared with e it may be very much greater.

Planck's Constant.

The energy of the electron is $(e^2 + A^2)/2a$ and the time of vibration that of the nucleus; this will be proportional to the time light takes to travel round $2\pi a$, the circumference of the nucleus. Let it equal $2\pi qa/c$, where q is a constant. Thus the frequency $p_0 = c/2\pi qa$, while E the energy is equal to $(e^2 + A^2)/2a$; hence

$$E = \frac{P_0}{c} \cdot \pi q(e^2 + A^2),$$

so that Planck's constant is $(e^2 + A^2)\pi q/c$. This expression leads to the conclusion that A must be large compared with e , i. e. that the greater part of the energy must be in the sphere. For if A were zero the value of Planck's constant would be $\pi q e^2/c$, i. e. $2.4q \times 10^{-29}$; the actual value is 6.65×10^{-27} . Hence we conclude that A is probably at least 100 times e^2 , or that only some 1 per cent. of the energy is due to the electric field of the nucleus.

We arrive at the same conclusion from the fact that p_0 , the frequency of vibration of the nucleus, is from G. P. Thomson's experiments 1.1×10^{20} ; so that in the time of one

vibration light will travel over 3×10^{-10} cm. This distance will be comparable with the circumference of the nucleus ; so that a can hardly be less than 10^{-11} , which is about one hundred times the radius calculated on the assumption that all the energy is in the nucleus. The "sphere" of the electron is a system with a much larger number of degrees of freedom than the nucleus ; so that if there is anything corresponding to equi-partition of energy, we should expect the sphere to contain the bulk of the energy.

Planck's Constant for Light.

It follows as a result of G. P. Thomson's experiments that p_0 , the frequency of vibration of the electron, bears to the energy of the electron the same, or nearly the same, ratio as the frequency of a quantum of light bears to the energy in the quantum. With an electron of the type we are considering we can see some reason why this should be the case. For suppose that the energy E' required for a quantum of light is abstracted by some process from an electron. It seems not unreasonable to suppose that when the electron loses energy the loss begins at the outside and goes on until enough has been obtained in this way to supply the energy E' required for the quantum. We may thus imagine that the energy comes from an outer sheath of the electron and absorbs all the energy in the sheath. Let b be the internal radius of the sheaths ; the energy in the quantum will be that in the electron between the region $r=b$ and $r=\infty$, i. e. $(e^2 + A^2)/2b$. The sheath when detached will have a hole inside it whose radius is b , and the time of its vibration will be proportional to the time light takes to branch over the circumference of this cavity ; thus p the frequency will be given by the equation $p=c/2\pi bq_1$. Hence

$$E' = p(e^2 + A^2)q\pi/c.$$

Thus, on this view, the relation between the energy in the quantum and its frequency will be the same as for the electron. Though the energy in the quantum is the same as that in the sheath of the electron from which it is derived, the disposition of the lines of electric force in the quantum when it has settled down into a steady state will be very different, the lines of electric force will no longer be radial, but will form closed curves, the frequency of the vibrations will be too small for the medium to show its super-dispersive properties, and the energy which was previously in the sheath in the form of the kinetic energy of the moving

particles will become the energy due to the magnetic forces in the light-quantum.

The Moving Electron.

If an electron where the electric and magnetic forces when it is stationary are represented by the equations (15) is moving uniformly parallel to the axis with the velocity u , the periodic electric and magnetic forces will, by equations (14), p. 1267, be given by the equations

$$Y = kA \cos p \left(t - \frac{ux}{c^2} \right) \frac{y}{R^3},$$

$$Z = kA \cos p \left(t - \frac{ux}{c^2} \right) \frac{z}{R^3},$$

$$\alpha = 0, \quad \beta = -\frac{u}{c^2} Z, \quad \gamma = \frac{\mu}{c^2} Y,$$

where

$$k = 1 / \sqrt{1 - \frac{u^2}{c^2}}, \quad p = kp_0,$$

and

$$R^2 = k^2(x - ut)^2 + y^2 + z^2.$$

Thus again we have a plane wave travelling in the direction of x , with the same relation between the wave-length and velocity as before; the amplitude of the waves diminishes as the distance from the nucleus increases.

The non-periodic forces in the electron due to the charge on the nucleus are given by

$$X = ke \frac{(x - ut)}{R^3}, \quad Y = ke \frac{y}{R^3}, \quad Z = ke \frac{z}{R^3},$$

$$\alpha = 0, \quad \beta = -\frac{u}{c^2} Z, \quad \gamma = \frac{u}{c^2} Y.$$

Size of the Sphere of the Electron.

If when the electron is passing through a thin film as in the experiment on the diffraction of electrons, the film behaves like a non-dispersive ether, then the consideration of the separation of spectra of different orders in the diffraction pattern will lead to an inferior limit to the size of the sphere of the electron. To separate these spectra will require a train of waves containing not less than a certain number of wave-lengths. G. P. Thomson calculates from the separation he obtained in his experiments that the train of waves must have extended over at least 5×10^{-8} cm.

If the medium in the film through which the electron is passing is the normal ether, then this train of waves must be in the sphere of the electron, as this is the only super-dispersive medium. Thus the diameter of the sphere of the electron must be at least 5×10^{-8} cm., and thus large compared with the diameter of a molecule. But if this is so, the assumption that the ether in the film is not dispersive, is not tenable. The molecules in the film contain many electrons, and if the spheres of these were large compared with the dimensions of a molecule, they would overlap; thus the film would be filled not with the normal ether, but with the super-dispersive medium of electronic spheres. When the moving electron enters this medium it will excite waves in it of frequency p , where $p = kp_0$ is the frequency of the moving electron. The field equation in the whole of the film is of the form

$$\frac{d^2\phi}{dt^2} + p_0^2\phi = c^2\nabla^2\phi,$$

and we see that a vibration of frequency p will excite in this medium waves whose length λ is given by

$$\lambda = \frac{2\pi c}{\sqrt{p^2 - p_0^2}} = \frac{2\pi c^2}{u\mu_0 k},$$

which is the same as the wave-length of the waves accompanying the moving electron. Since the whole of the metallic film is filled with the super-dispersive medium, there is room for a train of waves equal in length to the thickness of the film; the length of the train is no longer determined by the size of the sphere round a single electron.

It must be remembered, too, that the problem of determining the length of the train of waves necessary to separate two diffraction rings produced by light is not, on the Classical Theory of Light, identical with that required to produce the separation for electronic waves. The rings observed with electronic waves mark the paths of the nuclei of the electrons: an electron has to remain intact, and a single electron cannot spread out over the whole of the region where diffraction theory indicates the presence of waves. If the chance of an electron going in any direction were directly proportional to the intensity of the waves travelling in that direction, then the conditions for separation would be the same for electronic as for light-waves. But it may be, since the two parts of the electron, the nucleus and the sphere through which the waves travel, have to remain

together, that the electron will have a special tendency to move in a direction in which the intensity of the waves is symmetrical on either side of the direction in which the electron is moving; this direction is one along which the intensity of the waves is a maximum; this would make the intensity of a ring change more rapidly in the neighbourhood of the maximum than for the corresponding light-waves, and would increase the resolution. It would follow from this that the size of the sphere need not be quite so large as would be indicated by purely optical considerations; it must, however, I think, from the result of experiments, be at least comparable with atomic dimensions. If this is so, then the ether inside an atom must be in the super-dispersive state; and when as in a solid we have a closely-packed aggregation of molecules, the ether throughout the solid will also be in this state for vibrations of frequency comparable with p_0 . The field equations for the electric and magnetic force will be of the type

$$\frac{d^2\phi}{dt^2} + p_0^2\phi = c^2\nabla^2\phi,$$

and determine the propagation of all such vibrations through the medium.

The form of the field equations, when there is an external electric field, depends upon whether the force exerted on an electron by an electric field is due to the direct action of the force on the negative charge of the nucleus, or whether it is due to the bending of the electronic waves by refraction, owing to the gradient in the refractive index produced by the electric field.

On the first view the super-dispersive properties of the medium are not affected by the presence of an electric field. So that the field equations are of the form

$$c^2\left(\frac{d^2\phi}{dx^2} + \frac{d^2\phi}{dy^2} + \frac{d^2\phi}{dz^2}\right) = \frac{d^2\phi}{dt^2} + p_0^2\phi.$$

Thus, to take a special case, that of an electron moving under the attraction of a proton, when the velocity of the electron is u , the frequency of the vibrations it emits is

$$p_0\sqrt{1 - \frac{u^2}{c^2}};$$

hence

$$\frac{d^2\phi}{dt^2} = -\frac{p_0^2}{1 - \frac{u^2}{c^2}},$$

and the equation becomes

$$c^2 \nabla^2 \phi + \frac{p_0^2 \frac{u^2}{c^2}}{\left(1 - \frac{u^2}{c^2}\right)} \phi = 0.$$

If m is the mass of the electron, R its distance from the proton, E_0 a constant,

$$\frac{1}{2} m u^2 = E_0 + \frac{e^2}{R},$$

so that the field equation becomes

$$c^2 \nabla^2 \phi + \frac{\frac{2p_0^2}{mc^2} \left(E_0 + \frac{e^2}{R}\right)}{1 - \frac{2\left(E_0 + \frac{e^2}{R}\right)}{mc^2}} \phi = 0,$$

or approximately

$$c^2 \nabla^2 \phi + \frac{2p_0^2}{mc^2} \left(E_0 + \frac{e^2}{R}\right) \phi = 0.$$

When the deflexion of the electron is due to the refraction of the wave μ , the refractive index of the dispersive medium at the point x, y, z is given by the equation

$$\mu^2 = \mu_0^2 + 2V/mc^2,$$

where

$$\frac{dV}{dx}, \quad \frac{dV}{dy}, \quad \frac{dV}{dz}$$

are the components of the force which would act on an electron if it were at the point x, y, z .

The field equations when the frequency is p can be written in the form

$$c^2 \nabla^2 \phi + 4\pi^2 \mu^2 p^2 \phi = 0,$$

or, substituting the value of μ^2 ,

$$c^2 \Delta^2 \phi + 4\pi^2 p^2 (\mu_0^2 + 2V/mc^2) \phi = 0.$$

When the electric field is that due to a proton, $V = -e^2/r$, where $r^2 = x^2 + y^2 + z^2$, and the equation becomes

$$c^2 \nabla^2 \phi + 4\pi^2 p^2 \left(\mu_0^2 + \frac{2e^2}{r}/mc^2\right) \phi = 0.$$

The frequency p_0 is equal to 1.1×10^{20} , the quantum of light for this frequency is about 500,000 volts; hence light

whose quantum is greater than this would, when it passed through a solid, behave as if it were travelling through a super-dispersive medium, *i. e.* its phase velocity would be greater than that of light; on the other hand, light whose quantum is considerably less than this would behave as if it were travelling through the normal ether. Now, among the γ -rays given out by radium C there are some whose quantum is less than the critical value, others whose quantum is greater. We should expect these two types to behave differently when passing through a solid, *e. g.* that the scattering of the harder rays would not follow the same laws as that of the softer, a point which could be settled if we could measure the scattering of rays of different types. It is, however, difficult to get anything like a monochromatic spectrum of γ -rays, so that tests of this kind would involve very difficult experiments. There is, however, another test which can be applied much more easily; the interpretation of the results of this test is, however, more ambiguous than that for the scattering test; the test we refer to is the effect of electric force on the γ -rays. We know that when an electric force acts upon an electron the electron is deflected. Is this deflexion due primarily to the deflexion of the electronic waves, or is it, as on the usual theory, due to the action of the electric force on the negative charge on the nucleus? The electronic waves must always travel in the direction in which the nucleus is moving, so that if the path of the waves is altered, as in the experiments on diffraction, the path of the nucleus will be altered too, so that anything which deflected the waves would deflect the path of the nucleus and produce effects of the same type as would be produced by forces acting directly on the nucleus. The direction of the waves could be altered by refraction as well as by diffraction, and if the electric force produced a gradient in the refractive index of the medium, the path of the electronic waves would be curved like the rays in a mirage. If the application of an electric force X made the refractive index, μ , of the medium through which the electron is moving vary according to the law,

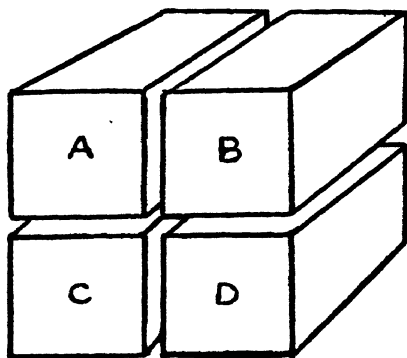
$$\mu \frac{d\mu}{dx} = \frac{Xe}{mc^2},$$

then the path of the electron would, in consequence of the refraction of the waves, be the same as if the electron were acted on by an electric force equal to X .

On this view the electric force deflects the electron by producing a gradient in the refractive index of the

super-dispersive medium which surrounds it ; this bends the electronic waves, and they carry the nucleus along with them. If this view is true, the gradient in the refractive index would bend to the same extent as it does the electron any waves of the same period as the electronic waves, whether they were accompanied by an electron or not. The alternative view is that, as in ordinary electrostatic theory, the electric force acts on the negative charge on the nucleus and the nucleus drags the waves along with it, since the two must travel in the same direction. On this view, the charge on the electron is essential for the deflexion, so that waves of the same period as the electronic waves, but not accompanied by an electron, would not be deflected by an electric field. Thus, on the first view, γ -rays of the same period as

Fig. 1.

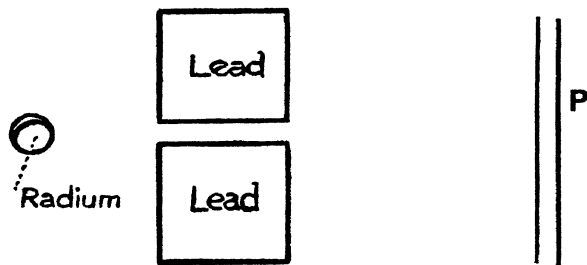


electronic waves would be deflected by an electric force ; on the second they would not. Now, among the γ -rays from radium C there are some which, since their quantum of energy is greater than 500,000 volts, have the same frequency as the electronic waves which accompany an electron moving at a suitable speed. It is thus interesting to determine whether such γ -rays would, like the electron with its waves, be deflected by electric force. We may hope to detect such a deflexion if it exists among some of the constituents of a mixed group of γ -rays, even though we are not able to isolate the various types of rays. The γ -rays with quanta less than 500,000 volts would not be deflected on either view. I have made some experiments to test the effect of electric force on the path of γ -rays, using the following arrangement :—

A, B, C, D (fig. 1), are four lead rectangular parallelepipeds 4 cm. by 2 cm. by 2 cm. The surfaces of the parallelepipeds

which face each other were carefully worked so as to be smooth planes; the inside faces of A and C were in the same vertical plane, as were also those of B and D. A was carefully insulated from B, C, D, and B from A, C, D; C and D were connected with the earth so as to be at the same potential; A and C were connected with the terminals of a dynamo giving constant potential differences up to 5500 volts; the interval between the blocks AC and BD was filled by thin flat plates of a dielectric; mica, sulphur, paraffin, glass, and quartz were tried; the faces of the lead blocks were pressed against the plate of dielectric. As some of the mica plates were only $\cdot 3$ mm. thick, electric forces up to 183,000 volts per centimetre could be obtained. The narrow space between the faces of AC and BD formed a slit through which could pass the γ -rays from radium emanation contained in a small glass vessel whose centre was on the

Fig. 2.

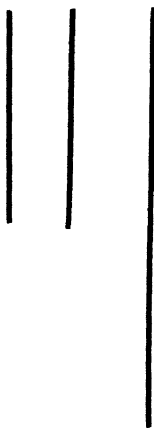


line of intersection of the planes of the horizontal slit between the blocks AB and CD and of the vertical slit between AC and BD. The rays after passing through the slit fell on a photographic plate, at some distance from the lead blocks and set so as to be at right angles to both the vertical and horizontal slits between the blocks. A plate of lead 1.5 mm. thick was placed parallel to the photographic plate P (fig. 2), and about a centimetre away from it, to prevent β -rays reaching the plate. The rays passing through the upper part of the slit between the blocks A and B (fig. 1) are subject to a very intense electric force from which those passing through the lower half are free. If the harder γ -rays are deflected by electric force, we might expect that there would be a difference between the upper and lower halves of the image of the slit formed on the photographic plate by the γ -rays. If there were some bending, but not enough to drive the rays against the sides of the slit, we should expect to find

on the upper part of the plate, but not on the lower, lines parallel to the image of the slit, formed by rays which had been deflected by the electric force, as in fig. 3, while if the deflexion were great enough to drive the rays against the side of the slit, the upper half of the image of the slit would be fainter than the lower.

If the bending of the path of the electron by electric force is due to the bending of the electronic waves, owing to the refractive index of the medium varying from point to point in an electric field, the connexion between the

Fig. 3.



refractive index μ and the applied electric force X is (see 'Beyond the Electron') given by the equation

$$\frac{d\mu^2}{dx} = \frac{Xe}{mc^2/2} \quad \dots \quad (16)$$

The radius of curvature ρ of a ray travelling through such a medium at right angles to the direction of x is given by

$$\frac{1}{\rho} = \frac{1}{\mu} \frac{d\mu}{dx}$$

or

$$\frac{1}{\rho} = \frac{Xe}{\mu^2 mc^2}.$$

If p is the frequency of the waves and h Planck's constant,

$$hp = mc^2, \quad \mu^2 = 1 - \frac{p_0^2}{p^2},$$

where p_0 is the critical frequency ; hence, when $p > p_0$,

$$\frac{1}{\rho} = \frac{Xe}{hp \left(1 - \frac{p_0^2}{p^2}\right)}.$$

If the energy of the quantum of the γ -ray is represented by V volts, $hp = Ve$, so that

$$X\rho = V \left(1 - \frac{p_0^2}{p^2}\right). \quad . \quad . \quad . \quad . \quad . \quad (17)$$

The value of V for the critical frequency p_0 is about 500,000 volts. The value of ρ given by (17) is the curvature of the γ -ray in the super-dispersive medium. If the dielectric through which the ray is passing is not super-dispersive through the whole of the region, but only so in patches, the average value of ρ would be greater than this by an amount depending on the fraction of the volume occupied by the super-dispersive portion.

In some of the experiments the thickness of mica between the blocks was $\cdot 3$ mm. and the potential difference between the blocks A and B 5500 volts ; thus X would be 183,000 volts per cm. ; for the strong γ -ray for which $V = 610,000$ ρ would be 1 cm., and with this curvature a ray would be bent through $\cdot 3$ mm. and thus driven against the plate after passing through about 2.4 mm. As the length of the path in the dielectric was 40 mm., these γ -rays would be unable to pass through the upper part of the slit if even a small fraction of the dielectric were super-dispersive.

The first experiment I tried was one where the γ -rays passed through a plate of mica 1 mm. thick exposed to a potential difference of 5500 volts. With an exposure of 12 hours I obtained a photograph of the type of fig. 3. There was the direct image of the slit with the upper and lower portions in the same straight line, and in the upper half of the photograph where the rays had been exposed to the electric field there were two lines parallel to the slit, the deflexion from the direct image being in the direction in which electrons going through the slit would be deflected. There were no such lines in the lower part of the photograph where the rays had not been exposed to electric force. This seemed very convincing proof that the electric force did produce a gradient in the refractive index, and that the deflexion of electrons by electric force was due to the bending of the electronic waves, and not to the direct action of the electric force on the nucleus.

However, as the result of further experiments, I have come to the conclusion that the results obtained in the first photograph could not have been due to the cause we are considering; for, on trying the experiment with sulphur for the dielectric instead of mica, I got nothing but the direct image of the slit. There were no parallel bands in either the upper or lower portions of the photograph. Again, I got no evidence of such bands with paraffin-paper, with glass, or with quartz, varying the strength of the electric field from 5000 to 1200 volts. Nor on trying mica again could I get the effects I had observed with the mica plate I had used at first. Being unable to get the bands, I tried if I could get any evidence of any difference in intensity between the parts of the direct image of the slit formed by rays which had passed through the electric field and those which had not, using a plate of mica .3 mm. thick and a potential difference of 5500 volts. This, as the calculation given above shows, would drive all the harder of the γ -rays against the sides of the slit and thus prevent them from getting through. I got with an exposure of 12 hours a very clear and well-defined image of the slit, but I could not detect any difference between the upper part formed by γ -rays exposed to electric force and the lower part formed by rays which had not been exposed.

Thus the majority of the experiments favour the view that the electric force acts directly on the nucleus, and not by deflecting the waves*.

I am much indebted to Dr. Chadwick and Dr. Ellis for advice and information on radioactive experiments, to Mr. Crowe for the preparation of the radium emanation, and to my assistant, Mr. Everett, for help in the experiments.

* Since the above was in type I have seen a paper by A. Joffé (*Ann. der Phys.* lxxii. p. 461 (1923)) in which he describes some experiments which may modify this conclusion. He shows that when a plate of dielectric between electrodes is exposed to steady electric forces the drop in potential in many cases, though not in all, occurs quite close to the electrodes, and that the electric force may be very small, except in layers of almost molecular thickness next the electrodes. In my experiments it is possible that it was only in my first experiment that there was any considerable electric force between the plates, and that in the others it was confined to the immediate neighbourhood of the electrodes. I hope to make further experiments on this point.

CXXII. *Note on Raman Lines under High Dispersion.*
*By Prof. R. W. WOOD *.*

[Plate XXIX.]

SINCE the publication of my first paper on the Raman effect (Phil. Mag., Oct. 1928), I have photographed the spectra scattered by benzol and carbon tetrachloride with a 6-inch plane grating combined with a lens of 3-metres focus. Small portions of the spectra are reproduced on Plate XXIX. Fig. 2 shows the Raman line 4554·87 of benzene (wave-length determined from this photograph), together with the comparison spectrum of iron. The width of the line scattered by the liquid benzene excited by Hg 4358 is not much over half an Ångström unit in this case. Most of the other lines are wider (1 to 2·5 Å.). The one at 4618, excited by the mercury line 4046, which in my earlier photographs resembled a narrow band sharp and strong on the red side, turns out to be a strong line about 1 Å. wide, with a fainter line, 2·5 Å. wide, close to it on the violet side. The wave-lengths of the strongest lines determined from the grating photograph are as follows :—

4686·74	4554·87
4682·11	4525·0
4659·30	4476·0
4618·36	

Fig. 1 of Plate XXIX. shows a portion of the spectrum scattered by carbon tetrachloride, the three broad lines marked R being the strong triplet on the red side of Hg 4358 shown in the photograph accompanying the earlier paper. The scale of enlargement of this photograph is only about one half of that of the lower photograph, the width of the lines being about 2 Ångström units. One of the "ghosts" of the 4358 mercury line appears at the left of the photograph.

I feel disposed to think that such high resolving powers are quite unnecessary, owing to the considerable width of most of the lines. That some of them are as narrow as they are is very surprising. The range of frequencies comprised within the 4554·87 line (0·5 Å.U. wide) when translated into the frequency range of the corresponding

* Communicated by the Author.

infra-red absorption band gives a band enormously narrower than the band observed by Coblentz near $10\ \mu$.

Attention should be drawn to an error in the placing of the figures in my earlier paper. The mercury arc of fig. 2 was originally drawn just above and close to the water-cooled tube of fig. 1.

Johns Hopkins University,
Baltimore.

CXXIII. *The Hall Effect in Galena and Molybdenite.* By
C. W. HEAPS, Ph.D., Professor of Physics, The Rice
Institute, Houston, Texas*.

THE Hall coefficient in plates cast from molten lead sulphide has been found by van Aubel † to be negative and small compared with the coefficient for bismuth. A. W. Smith ‡, on the other hand, has found in a natural crystal of lead sulphide a value of -251 for this coefficient. L. L. Campbell § intimates that the discrepancy between the two results may be due to differences of crystalline structure.

The writer has performed some experiments on this substance and on molybdenite, and has come to the conclusion that impurities probably exert a big influence on the phenomenon in lead sulphide.

The apparatus was of the usual type, the Hall e.m.f. being balanced by a potentiometer. A Weiss electromagnet with pole-pieces 10 cm. in diameter and 1.315 cm. apart was used for producing the magnetic field. The field-strength was measured with a fluxmeter calibrated in the usual way by means of a standard of mutual inductance.

In determining the Hall coefficient observations of the e.m.f. were made for both directions of magnetic field and the mean taken as the correct result. Disturbing thermomagnetic effects were considered negligible for the following reason:—A magnetic field of about 10,000 gauss was allowed to act constantly on a specimen, the galvanometer circuit

* Communicated by the Author.

† E. van Aubel, *Phys. Zeits.* iv. p. 551 (1903).

‡ A. W. Smith, *Phys. Rev.* i. p. 339 (1913).

§ L. L. Campbell, 'Galvanomagnetic and Thermomagnetic Effects,' p. 63.

being left open, and the primary current allowed to flow for about a minute. The primary current was then broken and immediately the galvanometer circuit closed. The resulting deflexion, which must have been due to residual thermoelectromotive forces, was, in the case of all the specimens examined, too small to affect materially the value of the Hall coefficient.

Lead Sulphide.—Four different specimens have been investigated. The first specimen was cut from a group of large cubic crystals of galena obtained from Joplin, Missouri. Cleavage planes were well developed in this specimen, but grinding and polishing revealed the presence of imperfections and irregularities due to tilting of small plane areas. The dimensions of the plate were $1.5 \times 0.8 \times 0.229$ cm., and its sides and edges were parallel to the respective natural cleavage planes of the crystal.

Electrical connexions were made by copper-plating and soldering with Wood's metal. The specific resistance of this specimen was found to be approximately 0.037 ohm-cm. The Hall e.m.f. was proportional to the magnetic field up to field-strengths of 12,000 gauss, and the average value of the Hall coefficient was found to be -108.3 .

The second specimen was cut from the same crystal group as the first. Its dimensions were $1.0 \times 0.407 \times 0.28$ cm., and the plate was cut so that its plane was approximately perpendicular to the trigonal axis of the crystal. The value of the Hall coefficient for this specimen was found to be the same, within experimental error, as for the first specimen. Thus the conclusion may be drawn that the Hall coefficient in galena is independent of the orientation of the crystal axis. A similar conclusion has been reached by Wold* for the cubic crystals of iron.

The third specimen was a crystal conglomerate made by fusing a mixture of lead and sulphur till chemical combination occurred. The specific resistance was 0.0012 and its Hall coefficient less than 0.008. It appears probable that some uncombined lead was present in the crystalline mass, otherwise the above results are difficult to explain.

The fourth specimen was from a very perfect crystal of unknown origin. Cleavage planes were mirror-like. Some slight difficulty was encountered in securing a flat plate because of the readiness of the crystal to split along any of three mutually perpendicular directions. The dimensions

* P. I. Wold, *Phys. Rev.* xxxi. p. 1116 (1928).

of the plate used were $0.197 \times 0.305 \times 0.831$ cm., and its specific resistance was 1.76 ohm-cm.

The Hall coefficient of this specimen was independent of field-strength up to 12,000 gauss, was positive in sign, and had the exceptionally large value +4802.

The remarkable difference in the Hall coefficients of the two crystals of galena examined is probably due to impurities. This mineral is known to have various impurities, such as silver, zinc, selenium, cadmium, bismuth, antimony, etc., and the proportions present appear to vary with the locality from which the crystals are secured. The specific gravity of specimen No. 1 was 7.2, that of No. 4 was 7.4. The first specimen was slightly pitted, and this fact may explain the difference of observed specific gravities. The resistivity of specimen No. 4 was much greater than that of No. 1. In view of Kapitza's work * on bismuth crystals we may expect a high resistance to be associated with transverse cleavage planes, such planes apparently having a tendency to produce incipient cracks. Under the blow-pipe each of the above crystals fused in similar fashion, yielding sulphurous fumes and a globule of metallic lead.

Molybdenite.—A thin plate, of dimensions $1.0 \times 2.0 \times 0.035$ cm., was cut from a foliated sheet of the mineral. Side arms 0.6 cm. long were left on the plate for the attachment of the Hall terminals. The resistance of the plate was 418 ohms. Using a primary current of 5 milliamperes the Hall e.m.f. was found to be proportional to the field up to 12,000 gauss, and the average of the Hall coefficient was -1907.

Adiabatic and Isothermal Coefficients.—Gottstein † has observed for the adiabatic Hall coefficient in molybdenite a value, $R_a = -3030$, from which he calculates by the formula of Gans ‡ the isothermal coefficient of $R_t = -1520$. As the result of a number of experiments on molybdenite the writer has come to the conclusion that there is not much difference between the values of the two coefficients. The adiabatic coefficient is supposed to be obtained when the transverse temperature gradient, which results from interaction of magnetic field and electric current, is allowed to develop. This phenomenon, the Ettingshausen effect, is, according to

* Kapitza, Proc. Roy. Soc. cxix. p. 358 (1928).

† G. Gottstein, *Ann. d. Phys.* xliii. p. 1079 (1914).

‡ R. Gans, *Ann. d. Phys.* xx. p. 293 (1906).

Gottstein, quite large in molybdenite. In the present experiments, therefore, a transverse temperature gradient should be set up by the magnetic field. An appreciable time must be required for this gradient to reach its maximum value, so that if R_a is much larger than R_i then the apparent Hall effect should increase with the time after excitation of the magnet. In other words, the initial Hall effect is isothermal, and the adiabatic is approximated only after an appreciable time interval. If Gottstein's values for R_a and R_i are correct the apparent Hall effect should increase, while the temperature gradient is being set up, to about double its initial value. No such large increase could be observed in the present experiments with molybdenite, though it was specially sought for in the following way:—The adiabatic Hall e.m.f. was balanced carefully by adjusting the potentiometer. Switches in both the Hall circuit and the primary circuit were then opened and the specimen allowed to remain several minutes in the magnetic field without carrying any current. A uniform temperature was thus secured. The switch in the primary circuit was then closed and immediately afterwards (within a small fraction of a second) the switch in the Hall circuit. A small deflexion of the galvanometer resulted, and in about 15 seconds this deflexion became practically zero. From the value of the initial small deflexion it was calculated that the isothermal Hall coefficient was about 6 per cent. smaller than the adiabatic. Gottstein calculated it to be almost half as large.

The same type of experiment with galena showed the adiabatic and isothermal coefficients not to differ by more than 2 per cent. in this mineral.

Summary.—The chief points of interest which have been brought out are (1) galena and molybdenite crystals exhibit a very large Hall effect; (2) the magnitude of the Hall coefficient in the cubic crystal of galena does not appear to depend on the orientation of crystal axes; (3) impurities probably exert a very great influence on the Hall effect in lead sulphide, apparently even changing the coefficient from a large negative to a large positive value; (4) the difference between the adiabatic and the isothermal Hall effects appears to be small in these minerals. It is appreciable in molybdenite but by no means as great as Gottstein has calculated.

CXXIV. *Notice respecting New Book.*

A Comprehensive Treatise on Inorganic and Theoretical Chemistry.
By J. W. MELLOR, D.Sc., F.R.S. Vol. VIII. [Pp. x+1110,
with 156 diagrams.] (London: Longmans, Green & Co., 1928.
Price 63s. net.)

THE eighth of the thirteen volumes of which Dr. Mellor's 'Comprehensive Treatise' will consist is devoted to nitrogen and phosphorus. The treatment is along lines similar to that in the earlier volumes, which have received notice in these pages, and a detailed review is therefore unnecessary. It may be stated, however, that the latest volume to be issued fully maintains the high standard of its predecessors, in its completeness, in the care which has been devoted to the smallest detail, in the numerous diagrams and tabulation of data, and in the valuable lists of references to original publications. About one-eighth part of the whole volume is occupied by these references, and the fact that many bear the date 1927 is an indication that the author has included the results of the most recent original work. A detailed index, extending to 30 pages, increases the value of the volume for reference purposes. Dr. Mellor's 'Treatise' will undoubtedly become the standard work of reference on all matters pertaining to inorganic or theoretical chemistry.

EDITORIAL NOTE.

ACOUSTICS OF STRINGS STRUCK BY A HARD HAMMEL.

IN reference to Messrs. Das and Datta's note on this subject in our September number (p. 479), Messrs. K. C. Kar and S. C. Laha have written stating that they do not consider that slipping at the bridge is the cause of the irregular and wide discrepancies between the observed and the calculated values of the amplitudes; and further, that their own observed value of the displacement at the centre agrees quite well with the value calculated from Kaufmann's theory. In regard to a paper by Prof. Raman and Dr. Banerji which is cited against them, they call attention to a paper by one of them in the Phil. Mag. for August 1928, where the results arrived at in that paper are shown to be incorrect. They also refer to their previous paper for their objections to the limits which Datta takes in his pressure integral. The unit of momentum in their own paper should have appeared as a "gramme-weight second."

[The Editors do not hold themselves responsible for the views expressed by their correspondents.]

INDEX to VOL. VI.

- ABSOLUTE** zero of temperature, on a method of determining the, 318.
- Acoustics** of strings struck by a hard hammer, on the, 479, 1287.
- Adsorption**, onselective, from gaseous mixtures by a mercury surface, 422.
- Aggregates** of active deposit atoms in gases containing radon, on the existence of, 685.
- Air**, on the velocity of sound in, 920; on the electrification of, by friction, 1132.
- Alkali metals**, on the photoelectric properties of thin films of the, 633; on the adsorption of the, on a mercury-vacuum interface, 775.
- Allen** (Prof. F.) on the graphical representation of the stimulation of the retina by colours, 337.
- Alternating currents** in cylindrical wires, on Heaviside's formulæ for, 842.
- Aluminium**, on the atomic scattering power of X-rays from, for Cu K α radiation, 178; on the X-ray analysis of alloys of, and silver, 280; on the crystal structure of δ copper-, 878.
- crystal, on the reflexion of electrons from an, 712.
- Ammonia**, on the photosensitized band fluorescence of, 1191.
- Antimony**, on the electrical conductivity of, at low temperatures, 666.
- Arc**, on the electric, in gases at low pressures, 811.
- Arc-spectrum** of nickel, on reversals in the, 1210.
- Arsenic**, on a ferromagnetic compound of manganese and, 593; on the electrical conductivity of, at low temperatures, 666.
- Auroral green line**, on the Zeeman resolution of the, 558.
- Bailey** (A. C.) on the phosphorescence of fused quartz, 1104.
- Bailey** (Prof. V. A.) on the capture of electrons by molecules, 1073.
- Bannon** (J.) on the motions of electrons in ethylene, 817.
- Barber** (D. R.) on a quartz fibre electrometer, 458.
- Barbour** (Prof. G. B.) on a re-excavated cretaceous valley on the Mongolian border, 1072.
- Bates** (Dr. L. F.) on a ferromagnetic compound of manganese and arsenic, 593.
- Bhatnagar** (Prof. S. S.) on the magnetic susceptibility of electronic isomers, 217.
- Biggs** (H. F.) on covalency, the paramagnetism of oxygen and stereochemistry, 659.
- Bircumshaw** (L. L.) on the surface tension of mercury, 510.
- Black** (Dr. D. H.) on the direct current conductivity of insulating oils, 369.
- Bond** (Dr. W. N.) on the thermal measurement of X-ray energy, 401.
- Books**, new:—Darrow's Introduction to Contemporary Physics, 239; Lorentz's Lectures on Theoretical Physics, 239; The Collected Papers of Spinivasa Ramanujan, 240; Findlay's The Phase Rule and its Applications, 240; Jellinek's Lehrbuch der Physikalischen Chemie, 363; Everest's The Higher Coal-Tar Hydrocarbons, 364; Baly's Spectroscopy, 364; Whittaker's Treatise on the Analytical Dynamics of Particles and Rigid Bodies, 365; Hess's The Electrical Conductivity of the Atmosphere and its Causes, 365; Pullin & Wiltshire's X-Rays: Past and Present, 366; Hobson's The Theory of Functions of a Real Variable and the Theory of Fourier's Series, 366; Hudleston's Chemical Affinity, 367; Jeffreys's Operational Methods in

- Mathematical Physics, 368; Veblen's Invariants of Quadratic Differential Forms, 368; Hudson's Cremona Transformations, 598; Crandall's Theory of Vibrating Systems and Sound, 598; Davis & Kaye's The Acoustics of Buildings, 599; Forder's Foundations of Euclidean Geometry, 599; Bedford's Practical Physics, 600; Güntherschulze's Electric Rectifiers and Valves, 600; Handbuch der Radiologie, 942; Burnside's The Theory of Probability, 943; Mellor's Comprehensive Treatise on Inorganic and Theoretical Chemistry, 1287.
- Boswell (Prof. P. G. H.) on the geological features of the new Mersey tunnel, 1071.
- Bradley (Dr. A. J.) on the X-ray analysis of silver aluminium alloys, 280; on the crystal structure of Cu_3Al , 878.
- Bradley (R. S.) on the adsorption of the alkali metals on a mercury-vacuum interface, 775.
- Brentano (Dr. J.) on the atomic scattering power for X-rays from powders of gold, silver, and aluminium, for Cu K α radiation, 178.
- Bromwich (Dr. T. J. P.) on a method of calculation suitable in certain physical problems, 98; on Heaviside's formulæ for alternating currents in cylindrical wires, 842; on an example of operational methods, 992.
- Brose (Dr. H. L.) on the motions of electrons in ethylene, 817.
- Brown (R. C.) on Jaeger's method as applied to the determination of the surface tension of mercury, 1044.
- Buckley (H.) on the radiation from the inside of a circular cylinder, 447.
- Buckling of a thin circular plate by heat, on the, 1217.
- Butterworth (Miss J.) on the photoelectric emission from potassium, 1, 352.
- Cadmium, on the effect of, on the conductivity of lead, 678.
- Cæsium, on the resistance of, at low temperatures, 672.
- Calcite, on the polarization of infra-red radiation by, 88.
- Calcium, on the crystal structure of, 665.
- Calculation, on a method of, suitable in certain physical problems, 98.
- Callendar radio balance, on the, 828.
- Campbell (Dr. N. R.) on the photoelectric properties of thin films of the alkali metals, 633.
- Carbon atom, on the anisotropy of the, 433.
- Carborundum detector, on the, 1024.
- Carr (A. J.) on Hamilton-Jacobi's differential equation in dynamics, 229; on the general solution of the equation $\nabla^2\psi = \omega$ in n -dimensional Euclidean space, 241, 1216.
- Ceric hydroxide, on the action of X-rays on colloidal, 385.
- Chalmers (J. A.) on ionization measurements of gamma rays, 745.
- Chemical interactions, on, 195, 648.
- Chivers (E. W.) on the steady flow of heat in a rectangular parallelepiped, 305.
- Chromium, on the magnetic properties of salts of, 481; on the resistance of, at low temperatures, 672.
- Chubb (J. L.) on the geology of the Marquesas Islands, 1070.
- Clarkson (Dr. W.) on the measuring of lags in discharge, 312.
- Cobalt, on the magnetic properties of salts of, 481; on the resistance of, at low temperatures, 672.
- Coe (R. T.) on problems in electrical machine design involving elliptic functions, 100.
- Cohesion, on molecular, 695.
- Colour vision, on, 337.
- Conductivity, on the direct current, of insulating oils, 369.
- Copper and copper amalgam, on the crystal structure of, 1055; on the electrical conductivity of, 1231.
- Copper-aluminium, on the crystal structure of δ , 878.
- K α radiation, on the atomic scattering power of X-rays for, 178.

- Correction factors for harmonic coefficients, on the best, 824.
- Cotter (J. R.) on a method of determining the absolute zero of temperature, 318.
- Covalency, on, 659.
- Crowther (Prof. J. A.) on the thermal measurement of X-ray energy, 401.
- Crystal detector, on the analogy between the, and a vacuum tube, 175.
- structure, on the, of δ copper-aluminium, 878; on the, of copper and copper amalgam, 1055.
- Crystals, on detection effect and oscillations with, 1024.
- Cube, on the amount of uniformly diffused light passing through a, 1019.
- Currents, on the magnetic energy of linear, 192.
- Cylinder, on the radiation from the inside of a circular, 447; on the variation of velocity amplitude at the surface of a, moving through a viscous liquid, 970.
- Das (P.) on the acoustics of strings struck by a hard hammer, 479.
- Datta (S. K.) on acoustics of strings struck by a hard hammer, 479.
- Deodhar (Dr. D. B.) on new bands in the secondary spectrum of hydrogen, 466.
- Determinantal equation, on a type of, 839.
- Dynamics of an electron, on the, 977.
- Eagle (A.) on the best correction factors for harmonic coefficients, 824.
- Electric arc, on the, in gases at low pressures, 811.
- discharge, on the measuring of lags in, 312.
- field, on the penetration of an, through wire-gauze, 795.
- wave-filters, on the theory of, 146.
- Electrical currents, on Heaviside's formulæ for alternating, in cylindrical wires, 842.
- conductivity of metals, on the, 965.
- machine design, on some problems of, involving elliptic functions, 100.
- Electrical properties of neon, on the, 857.
- resistance of arsenic and antimony, on the, 666; of cæsium, cobalt, and chromium, on the, 672.
- Electrification of air by friction, on the, 1132.
- Electrolytes, on the molecular structure of strong and weak, 50.
- Electrolytic ions, on the influence of the solvent on the mobility of, 258.
- Electrometer, on a quartz fibre, 458.
- Electron, on electronic waves and the, 1254.
- diffraction, on the effect of refraction on, 939.
- Electronic isomers, on the magnetic susceptibilities of, 217.
- theory of valency, on the, 50.
- Electrons, on a new method of determining the mobility of, in gases, 210; on the reflexion of, from an aluminium crystal, 712; on the motions of, in ethylene, 817; on the energy losses of, in hydrogen, 889; on the dynamics of, 977; on the capture of, by molecules, 1073; on the motion of, in pentane, 1107.
- Elliptic functions, on some problems in electrical machine design involving, 100.
- Equation $\nabla^2\psi = \omega$, general solution of the, in n -dimensional Euclidean space, 241, 1216.
- of state of a perfect gas, on the, 743.
- , on a type of determinantal, 839.
- Ethylene, on the motions of electrons in, 817.
- Evans (Prof. E. J.) on the electrical conductivity of liquid amalgams of gold and copper, 1231.
- Fairbrother (J. A. V.) on the action of X-rays on colloidal cerichydroxide, 385.
- Ferromagnetic compound of manganese and arsenic, on a, 593.
- Films, on the photoelectric properties of thin, of the alkali metals, 633.
- Fleming (A. J.) on the graphical representation of the stimulation of the retina by colours, 337.

- Fluorescent liquids, on anti-Stokes radiation of, 310.
- Forbidden line 2656 in the optical excitation of mercury, on the, 271.
- Fox (Dr. C.) on the potential function due to certain plane boundary distributions, 994.
- Galena, on the Hall effect in, 1283.
- Gamma rays, on ionization measurements of, 745.
- Gaseous mixtures, on selective adsorption from, by mercury, 422.
- Gases, on a new method of determining the mobility of ions or electrons in, 210; on the equation of state of perfect, 743; on the existence of aggregates of active deposit atoms in, containing radon, 685; on the electric arc in, 811.
- Gaviola (Dr. E.) on the factors governing the appearance of the forbidden line 2656 in the optical excitation of mercury, 271; on the power relation of the intensities of the lines in the optical excitation of mercury, 352, 1154; on the influence of foreign gases on the optical excitation of mercury, 1167; on the photosensitized band fluorescence of OH, HgH, NH, H₂O, and NH₃ molecules, 1191.
- Geological Society, proceedings of the, 943, 1069.
- Gillam (A. E.) on the deterioration of quartz mercury vapour lamps and the luminescence of fused quartz, 1123.
- Gold, on the atomic scattering power for X-rays from, for Cu K α radiation, 178; on the electrical conductivity of amalgams of, 1231.
- Green's lemma, on, 241.
- Hall effect in galena and molybdenite, on the, 1283.
- Hamilton-Jacobi's differential equation in dynamics, on, 229, 320.
- Harkins (Prof. W. D.) on the separation of isotopes and the separation of mercury by evaporative-diffusion, 601.
- Harmonic coefficients, on the best correction factors for, 824.
- Harmonics, on spheroidal, as hypergeometric functions, 1117.
- Harrington (Prof. E. L.) on the existence of aggregates of active deposit atoms in gases containing radon, 685.
- Heaps (Prof. C. W.) on the Hall effect in galena and molybdenite, 1283.
- Heartbeat considered as a relaxation oscillation, on the, 763.
- Heat, on the steady flow of, in a rectangular parallelepiped, 305; on the flow of, through an insulating wall, 567; on the escape of, from an harmonically oscillating hot wire, 945; on the buckling of a thin circular plate by, 1217.
- radiation from the inside of a circular cylinder, on the, 447.
- Heaviside's formulæ for alternating currents in cylindrical wires, on, 842.
- Hoare (F. E.) on the Stefan-Boltzmann radiation constant, 828.
- Howland (R. C. J.) on a type of determinantal equation, 839.
- Hydrogen, on new bands in the secondary spectrum of, 466; on the continuous spectrum of, 807; on the energy losses of electrons in, 889.
- Hypergeometric functions, on spheroidal harmonics as, 1117.
- Ignition, on spark, 1090.
- Impedances, on screened, 788.
- Ince (Dr. E. L.) on Mathieu functions of stable type, 547.
- Infra-red radiation, on the polarization of, by calcite, 88.
- Insulating oils, on the direct current conductivity of, 369.
- Iodine bands, on optically excited, with alternate missing lines, 231.
- Ionization, on reversible, of electrolytes, 50; on multiple, and the absorption of X-rays, 64.
- measurements of gamma rays, on, 745.
- Ions, on a new method of determining the mobility of, in gases, 210; on the influence of the solvent on the mobility of electrolytic, 258.
- Iron, on the K X-ray absorption edge of, 910; on the magnetic properties of salts of, 481.
- Isomers, on the magnetic susceptibilities of electronic, 217.

- Isotopes, on the separation of, 601.
- Jaeger (J. C.) on the motion of electrons in pentane, 1107.
- Jaeger's method as applied to determine the surface tension of mercury, on, 1044.
- Jones (Prof. E. T.) on spark ignition, 1090.
- Jones (H.) on the energy losses of electrons in hydrogen, 889.
- K X-ray absorption edge of iron, on the, 910.
- Kar (Dr. K. C.) on the theory of the pianoforte string, 276.
- Kenrick (Dr. G. W.) on radio transmission formulæ, 289.
- Kinematic pairs and links in a mechanism, on, 631.
- Kleeman (Dr. R. D.) on chemical interactions, 195, 648; on the equation of state of a perfect gas, 743.
- Lags in discharge, on the measuring of, 312.
- Lattey (R. T.) on the influence of the solvent on the mobility of electrolytic ions, 258.
- Lead, on the effect of cadmium on the conductivity of, 678.
- sulphide, on the Hall effect in, 1283.
- Light, on the scattering of, in liquids, 204; on the amount of uniformly diffused, passing through a cube, 1019.
- Lindsay (G. A.) on the K X-ray absorption edge of iron, 910.
- Links, on kinematic pairs and, 631.
- Liquids, on light-scattering in, 204; on anti-Stokes radiation of fluorescent, 310.
- Lonsdale (Dr. K.) on the anisotropy of the carbon atom, 433.
- Loomis (Prof. F. W.) on optically excited iodine bands with alternate missing lines, 231.
- Lossev (O. V.) on the luminous carborundum detector, 1024.
- Lowry (H. V.) on the magnetic energy of permanent magnets and of linear currents, 192.
- Lowry (Prof. T. M.) on the electronic theory of valency, 50.
- MacCallum (S. P.) on the electrical properties of neon, 857.
- McDiarmid (Miss A. W.) on the electrification of air by friction, 1132.
- McGee (Dr. J. D.) on the capture of electrons by molecules, 1073; on the motion of electrons in pentane, 1107.
- Machine design, on electrical, involving elliptic functions, 100.
- McLennan (Prof. J. C.) on the Zeeman resolution of the oxygen spectral line at λ 5577 Å., 558; on the electrical conductivity of arsenic and antimony at low temperatures, 666; on the resistance of cesium, cobalt, and chromium at low temperatures, 672; on the effect of cadmium as an impurity on the conductivity of lead, 678.
- McLeod (J. H.) on the Zeeman resolution of the oxygen spectral line at λ 5577 Å., 558.
- Magnetic field, on the, of a rectilinear circuit, 205.
- studies on salts, 481.
- susceptibilities, on the, of electronic isomers, 217.
- Magnets, on the magnetic energy of permanent, 192.
- Mahajani (G. S.) on Hamilton-Jacobi's differential equation in dynamics, 320.
- Manganese and arsenic, on a ferromagnetic compound of, 593.
- van der Mark (J.) on the heartbeat considered as a relaxation oscillation, 763.
- Martyn (D. F.) on frequency variations of the triode oscillator, 223.
- Mass action, on the constant of, 195, 648.
- Mathieu functions of stable type, on, 547.
- Mathur (R. N.) on the magnetic susceptibilities of electronic isomers, 217.
- Maxwell (R. S.) on the escape of heat from an harmonically oscillating hot wire, 945.
- Mechanism, on kinematic pairs and links in a, 631.
- Meksyn (D.) on the dynamics of an electron, 977.
- Menzies (Prof. A. C.) on reversals in the arc-spectrum of nickel, 1210.

- mercury, on the forbidden line 2656 in the optical excitation of, 271; on the power relation of the intensities of the lines in the optical excitation of, 352, 1154; on selective adsorption from gaseous mixtures by, 422; on the surface tension of, 510, 1044; on the separation of, by evaporative-diffusion, 601; on the crystal structure of, 1055; on the influence of foreign gases on the optical excitation of, 1167.
- hydride, on the photosensitized band fluorescence of, 1191.
- vacuum interface, on the adsorption of the alkali metals on a, 775.
- vapour lamps, on the deterioration of, 1123.
- Metals, on the surface tension of liquid, 510; on the photoelectric properties of thin films of the alkali, 633; on the adsorption of the alkali, on a mercury-vacuum interface, 775; on the electrical conductivity of, 965.
- Microscopic resolution, on a method for extending, 356.
- Mitchell (Dr. G. H.) on the Borrowdale volcanic series in Westmorland, 1069.
- Molecular cohesion, on, 695.
- Molecules, on the capture of electrons by, 1073.
- Molybdenite, on the Hall effect in, 1283.
- Molybdenum, on the intensity distribution of the X-radiation from, 1008.
- Mortimer (Dr. B.) on the separation of isotopes and the separation of mercury by evaporative diffusion, 601.
- Morton (R. A.) on the deterioration of quartz vapour lamps and the luminescence of fused quartz, 1123.
- Morton (Prof. W. B.) on the penetration of an electric field through wire-gauze, 795.
- Murnaghan (Prof. F. D.) on the theory of wave filters containing a finite number of sections, 146; on the application of tensor analysis to physical problems, 779.
- Neon, on the electrical properties of, 857.
- Newman (Prof. F. H.) on the continuous spectrum of hydrogen, 807; on the electric arc in gases at low pressures, 811.
- Nickel, on reversals in the arc-spectrum of, 1210.
- Nitrogen, on active, 335; on the velocity of sound in, 920.
- hydride, on the photosensitized band fluorescence of, 1911.
- Niven (C. D.) on the crystal structure of calcium, 665; on the electrical conductivity of arsenic and antimony at low temperatures, 666; on the resistance of caesium, cobalt, and chromium at low temperatures, 672; on the effect of cadmium as an impurity on the conductivity of lead, 678.
- Observations, on quantum theory and the analysis of, 801.
- Ogawa (W.) on the analogy between the crystal detector and a vacuum tube, 175.
- Oils, on the direct current conductivity of insulating, 369.
- Oliphant (M. L.) on selective adsorption from gaseous mixtures by a mercury surface, 422.
- Operational methods, on an example of, 992.
- Oxygen, on the paramagnetism of, 659; on the velocity of sound in, 920.
- hydride, on the photosensitized band fluorescence of, 1191.
- spectral line at $\lambda 5577 \text{ \AA.}$, on the Zeeman resolution of the, 558.
- Parallelepiped, on the steady flow of heat in a, 305.
- Partington (Prof. J. R.) on the velocity of sound in air, nitrogen, and oxygen, 920.
- Pentane, on the motion of electrons in, 1107.
- Phosphorescence of fused quartz, on the, 1104.
- Photoelectric effects, on the application of a valve amplifier to the measurement of, 324.
- emission from potassium, on the complete, 1.
- Photosensitized band fluorescence of OH, HgH, NH, H₂O, and NH₃ molecules, on the, 1191.

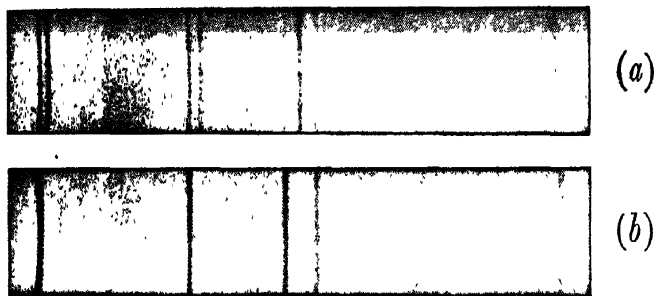
- Physical problems, on a method of calculation suitable in certain, 98; on the application of tensor analysis to, 779.
- Pianoforte string, on the theory of the, 276.
- Piercy (Dr. N. A. V.) on the variation of velocity amplitude near the surface of a cylinder in a viscous fluid, 970.
- Plate, on the buckling of a thin circular, by heat, 1217.
- Point discharges, on the ultra-violet radiations emitted by, 526.
- van der Pol (Dr. B.) on the heart-beat considered as a relaxation oscillation, 763.
- Potassium, on the complete photoelectric emission from, 1; on the photoelectric thresholds of, 352.
- Potential function due to certain plane boundary distributions, on the, 994.
- Predischarges, on the investigation of, 854.
- Press (Prof. A.) on the quantum theory and Schrödinger's equation, 33.
- Quantum theory on the classical reasonableness of the, 33; on the, and the analysis of observations, 801.
- Quartz, on the phosphorescence of fused, 1104; on the luminescence of fused, 1123.
- fibre electrometer, on a, 458.
- resonator, on formulæ for the constants of the electrical circuit of a, 1140.
- Radiation from the inside of a circular cylinder, on the, 447; on the Raman spectra of scattered, 729, 1282.
- constant, on the determination of the Stefan-Boltzmann, 828.
- Radio balance, on the Callendar, 828.
- transmission formulæ, on, 289.
- Radon, on the determination of the volume of 1 curie of, 17; on the existence of aggregates of active deposit atoms in gases containing, 685.
- Raman spectra of scattered radiation, on the, 729, 1282.
- Rectilinear circuit, on the magnetic field of a, 205.
- Refraction, on the effect of, on electron diffraction, 939.
- Relaxation oscillation, on the heart-beat considered as a, 763.
- Relton (F. E.) on the buckling of a thin circular plate by heat, 1217.
- Resonator, on formulæ for the constants of the electrical circuit of a, 1140.
- Retina, on the graphical representation of the stimulation of the, by colours, 337.
- Richardson (Dr. E. G.) on the variation of velocity amplitude near the surface of a cylinder in a viscous fluid, 970.
- Richardson (Dr. L. F.) on the amount of light that will pass through two apertures in a cube, 1019.
- Richtmyer (Prof. F. K.) on multiple ionization and the absorption of X-rays, 64.
- Rocard (Dr. Y.) on the theory of light-scattering in liquids, 204.
- Rose (Dr. D. C.) on the reflexion of electrons from an aluminium crystal, 712.
- Ruark (Dr. A. E.) on active nitrogen, 335.
- Ruedy (Dr. R.) on the Zeeman resolution of the oxygen spectral line at λ 5577 Å., 558.
- Salts, magnetic studies on, 481.
- Schofield (F. H.) on the heat-flow through an insulating wall, 567.
- Schrödinger's equation, on simple operative solutions of, 33.
- Screened impedances, on, 788.
- Selby (F. J.) on the quantum theory and the analysis of observations, 801.
- Shilling (Dr. W. G.) on the velocity of sound in air, nitrogen, and oxygen, 920.
- Silver, on the atomic scattering power of X-rays from, for Cu K α radiation, 178; on the X-ray analysis of alloys of, and aluminium, 280.
- Solvent, on the influence of the, on the mobility of electrolytic ions, 258.

- Sound, on the velocity of, in air, nitrogen, and oxygen, 920.
- Spark ignition, on, 1090.
- Spectra, on the Raman, of scattered radiation, 729, 1282.
- Spectrum, on new bands in the secondary, of hydrogen, 466; on the continuous, of hydrogen, 807; on reversals in the arc-, of nickel, 1210.
- Spheroidal harmonics as hypergeometric functions, on, 1117.
- Stefan - Boltzmann radiation constant, on the determination of the, 828.
- Stereochemistry, on, 659.
- Strings, on the acoustics of, struck by a hard hammer, 479, 1287.
- Surface tension, on the, of mercury, 510; on Jaeger's method as applied to the determination of, 1044.
- Synge (E. H.) on a method for extending microscopic resolution, 356.
- Taylor (Dr. A. M.) on the polarization of infra-red radiation by calcite, 88.
- Taylor (H. W.) on problems in electrical machine design involving elliptic functions, 100.
- Temperature, on a method of determining the absolute zero of, 318.
- Tensor analysis, on the application of, to physical problems, 779.
- Terrey (H.) on the crystal structure of mercury, copper, and copper amalgam, 1055.
- Thomson (Prof. G. P.) on the effect of refraction on electron diffraction, 939.
- Thomson (J.) on the ultra-violet radiations emitted by point discharges, 526.
- Thomson (Sir J. J.) on electronic waves and the electron, 1254.
- Tomkeieff (S. I.) on the volcanic complex of Calton Hill, 1072.
- Tomkins (J. A.) on the magnetic field of a rectilinear circuit and the attraction of a straight wire, 205.
- Tomlinson (G. A.) on molecular cohesion, 695.
- Townsend (Prof. J. S.) on the electrical properties of neon, 857.
- Treloar (L. R. G.) on the intensity distribution of the X-radiation from molybdenum, 1008.
- Trey (Dr. F.) on the investigation of predischarges, 854.
- Triode oscillator, on the frequency variations of the, 223.
- Tyrrell (Dr. G. W.) on the analcitesyenites of Ayrshire, 943.
- Ultra-microscopic region, on a method for extending microscopic resolution into the, 356.
- Ultra-violet radiations emitted by point discharges, on the, 525.
- Valency, on the electronic theory of, 50.
- Valve amplifier, on the application of a, to the measurement of X-ray and photoelectric effects, 324.
- Van der Graaff (R. J.) on a method of determining the mobility of ions or electrons in gases, 210.
- Velocity amplitude, on the variation of, in a viscous fluid, 970.
- Vigoureux (P.) on formulæ for the constants of the electrical circuit of a quartz resonator, 1140.
- Viscous fluid, on the variation of velocity amplitude in a, 970.
- Voorhees (H. R.) on the K X-ray absorption edge of iron, 910.
- Walker (Prof. W. J.) on the relation between kinematic pairs and links in a mechanism, 631.
- Wall, on the heat-flow through an insulating, 567.
- Water, on the photosensitized band fluorescence of, 1191.
- Waterman (Prof. A. T.) on the electrical conductivity of metals as a function of pressure, 965.
- Wave filters containing a finite number of sections, on the theory of, 146.
- Welo (L. A.) magnetic studies on salts, 481.
- Wertenstein (Prof. L.) on a method of determination of the volume of 1 curie radon, 17.
- Westgren (Prof. A. F.) on the X-ray analysis of silver aluminium alloys, 280.
- Wheeler (H. A.) on the theory of wave filters containing a finite number of sections, 146.

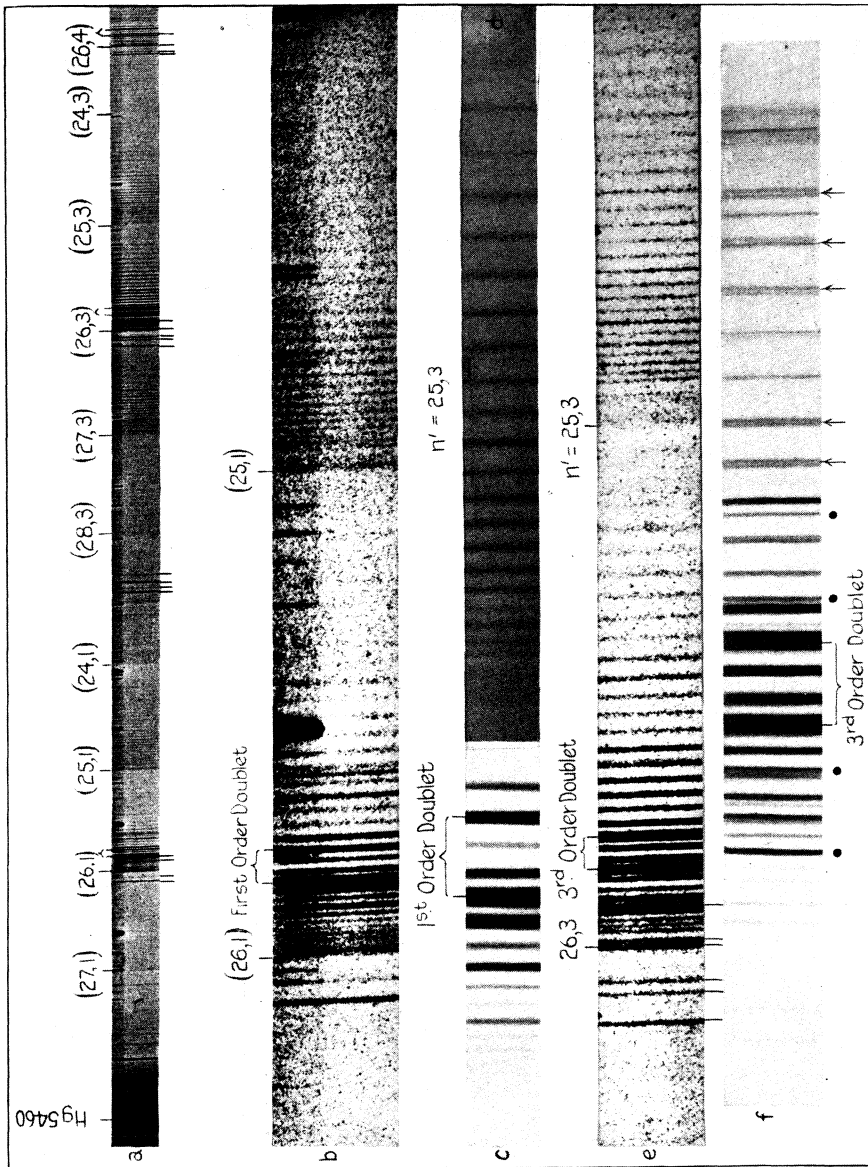
- Whiddington (Prof. R.) on the energy losses of electrons in hydrogen, 889.
- Wilhelm (J. O.) on the electrical conductivity of arsenic and antimony at low temperatures, 666; on the resistance of cesium, cobalt, and chromium at low temperatures, 672; on the effect of cadmium as an impurity on the conductivity of lead, 678.
- Williams (T. C.) on the electrical conductivity of liquid amalgams of gold and copper, 1231.
- Wilmotte (R. M.) on screened impedances, 788.
- Wire gauze, on the penetration of an electrical field through, 795.
- Wires, on the attraction of straight, 205; on Heaviside's formulæ for alternating currents in cylindrical, 842; on the escape of heat from harmonically oscillating hot, 945.
- Wood (Prof. R. W.) on optically excited iodine bands with alternate missing lines, 231; on the factors governing the appearance of the forbidden line 2656 in the optical excitation of mercury, 271; on anti-Stokes radiation of fluorescent liquids, 310; on the power relation of the intensities of the lines in the optical excitation of mercury, 352; on the Raman spectra of scattered radiation, 729, 1282; on the photosensitized band fluorescence of OH, HgH, NH, H₂O, and NH₃ molecules, 1191.
- Woodrow (D. J. W.) on the phosphorescence of fused quartz, 1104.
- Wright (C. M.) on the crystal structure of mercury, copper, and copper amalgam, 1055.
- Wrinch (Dr. D. M.) on spheroidal harmonics as hypergeometric functions, 1117.
- Wynn-Williams (C. E.) on the application of a valve amplifier to the measurement of X-ray and photoelectric effects, 324.
- X-ray absorption spectrum of iron, on the, 910.
- analysis of silver aluminium alloys, on the, 280.
- effects, on the application of a valve amplifier to the measurement of, 324.
- energy, on the thermal measurement of, 401.
- X-radiation from molybdenum, on the intensity distribution of the, 1008.
- X-rays, on the absorption of, 64; on the atomic scattering power for, from powders of gold, silver, and aluminium for Cu K α radiation, 178; on the action of, on colloidal ceric hydroxide, 385.
- Yardley (Miss K.) *see* Lonsdale (Mrs. K.).
- Zeeman resolution of the auroral green line, on the, 558.

END OF THE SIXTH VOLUME.

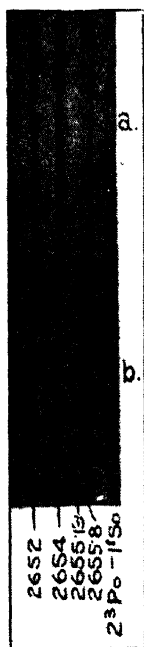
FIG. 1.

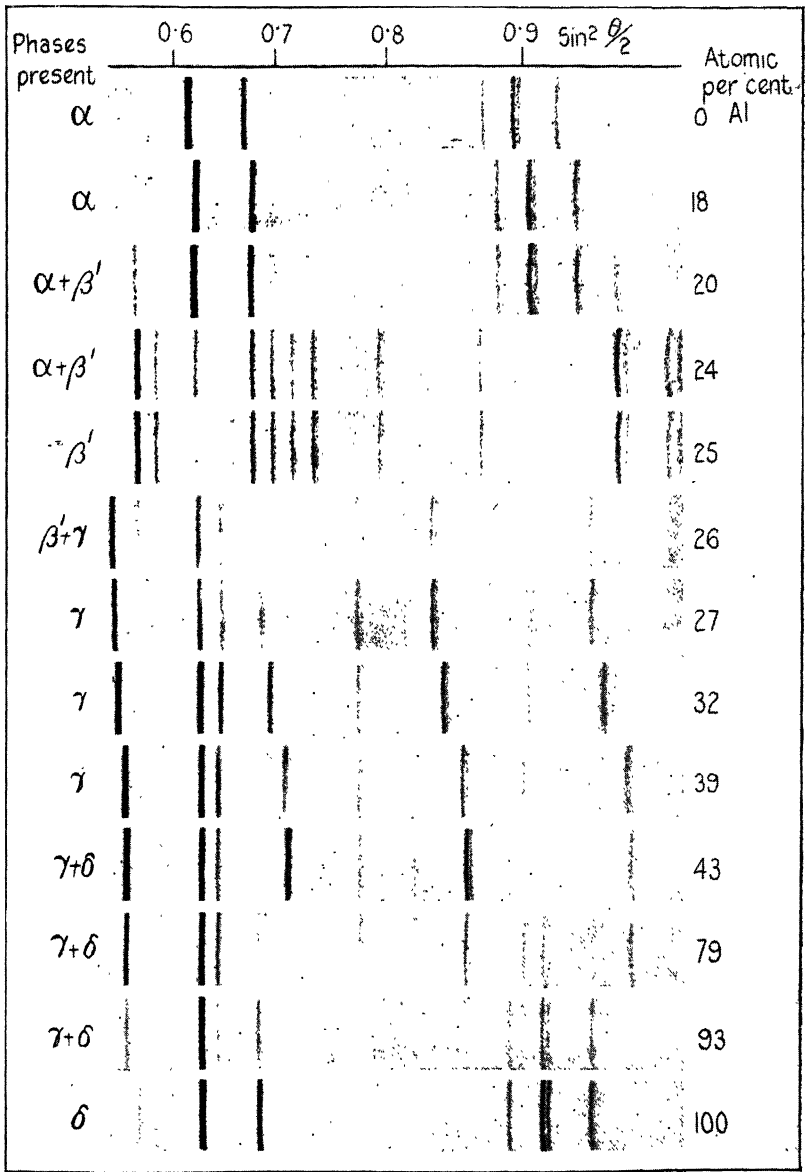


Photographs from composite layers containing equal
parts of nickel-oxide and gold.

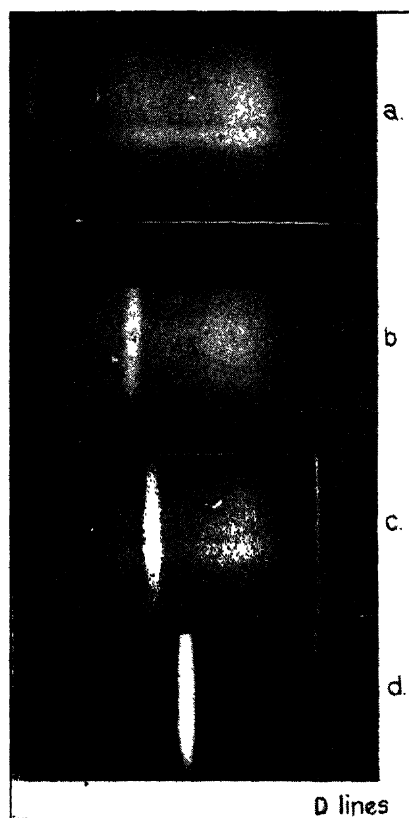


Fundamental doublets are indicated above the spectra, non-fundamental doublets below.





Powder Photograms of Silver-Aluminium Alloys. Fe-K-Radiation.



Anti-Stokes Radiation.

FIG. 1.

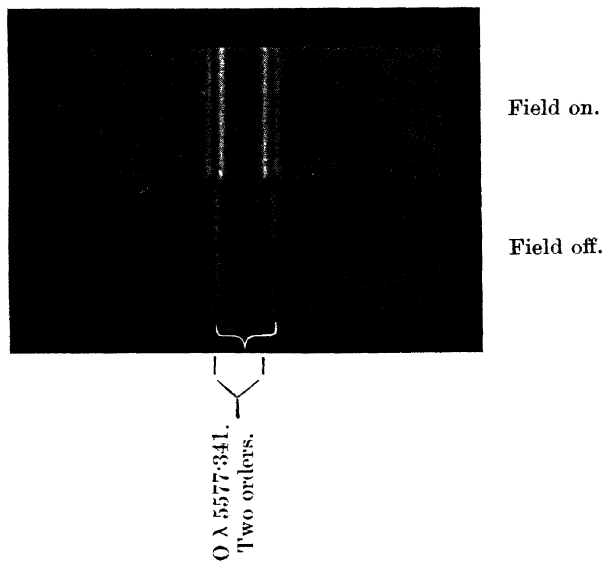
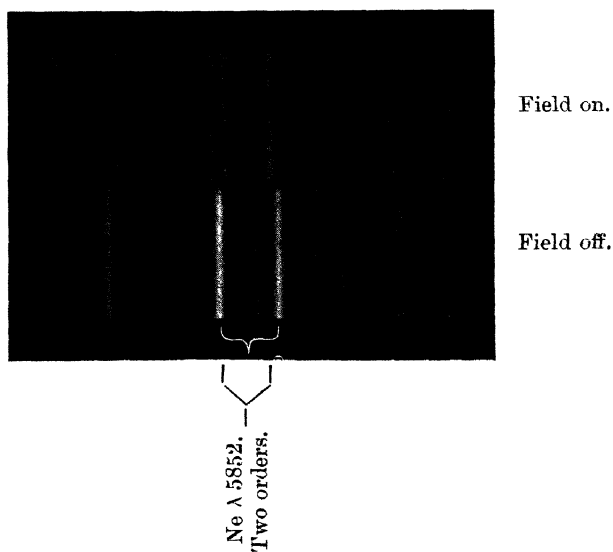


FIG. 2.



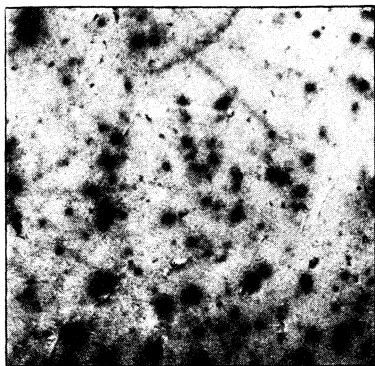


FIG. 4.

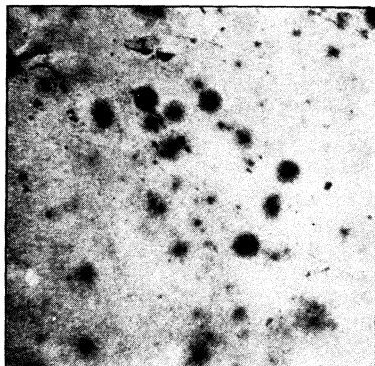


FIG. 5.

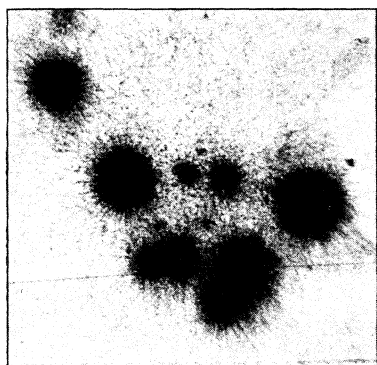


FIG. 6.

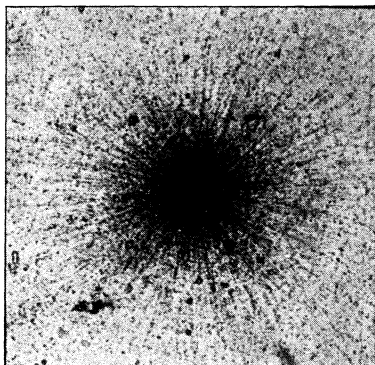


FIG. 7.

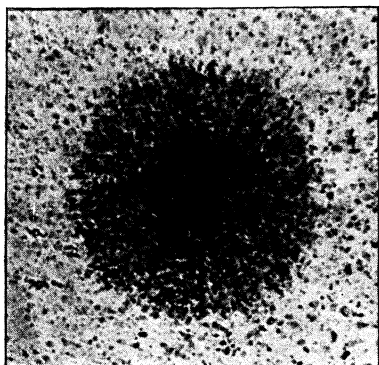


FIG. 8.

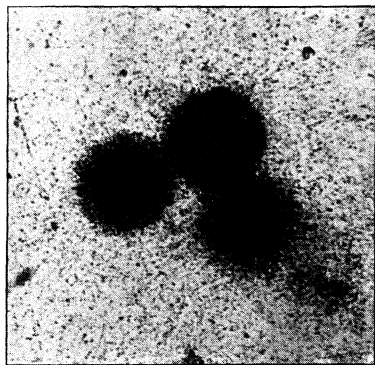
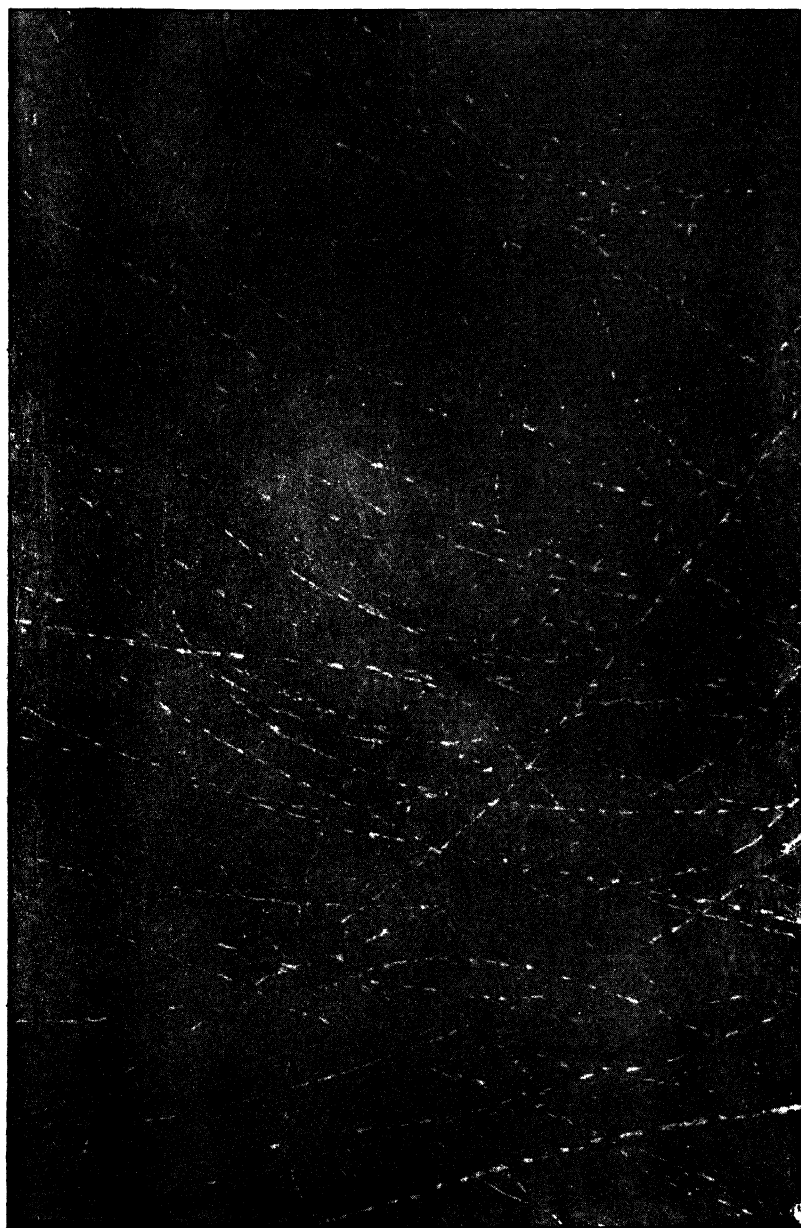


FIG. 9.

FIG. 3.



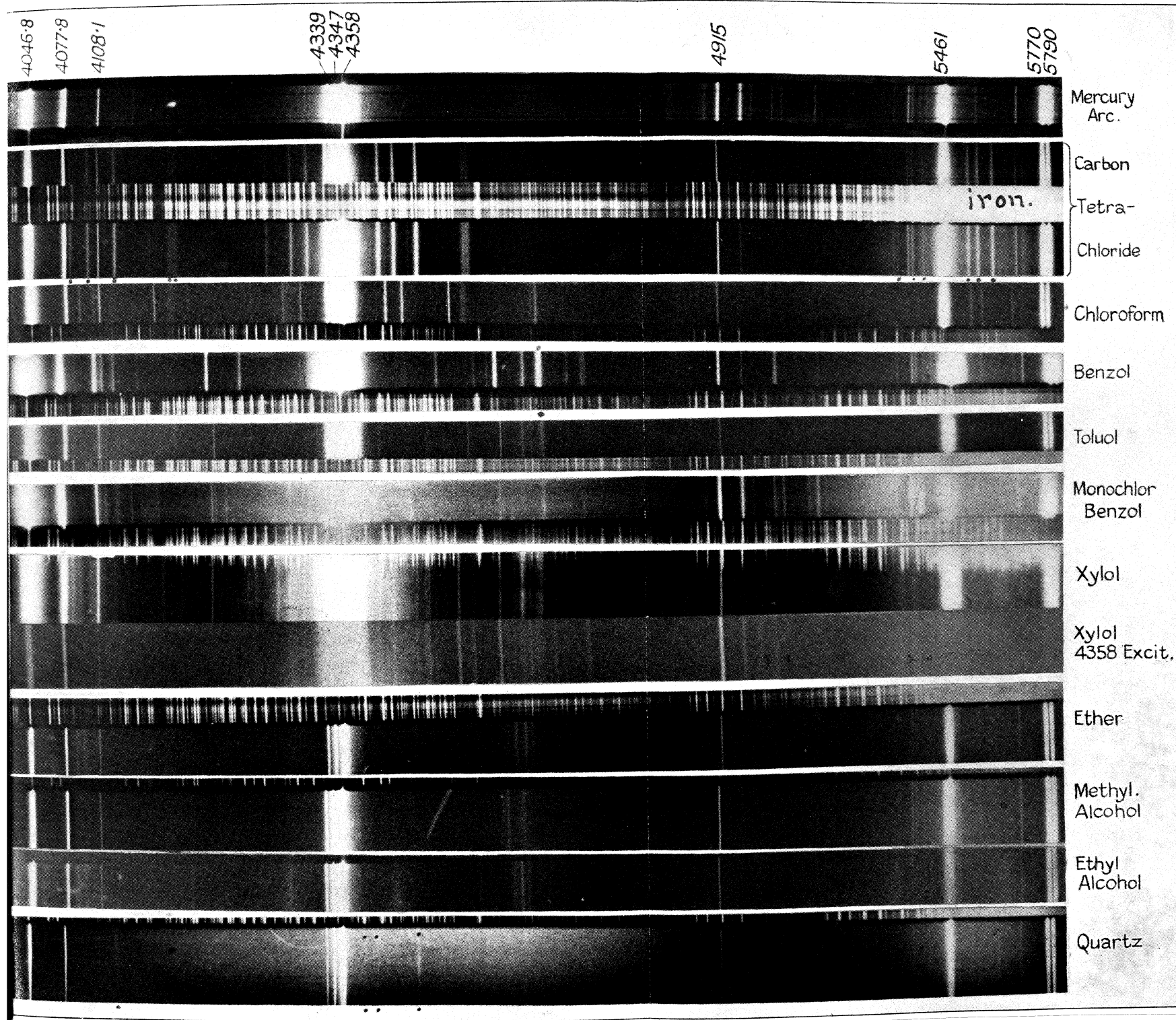
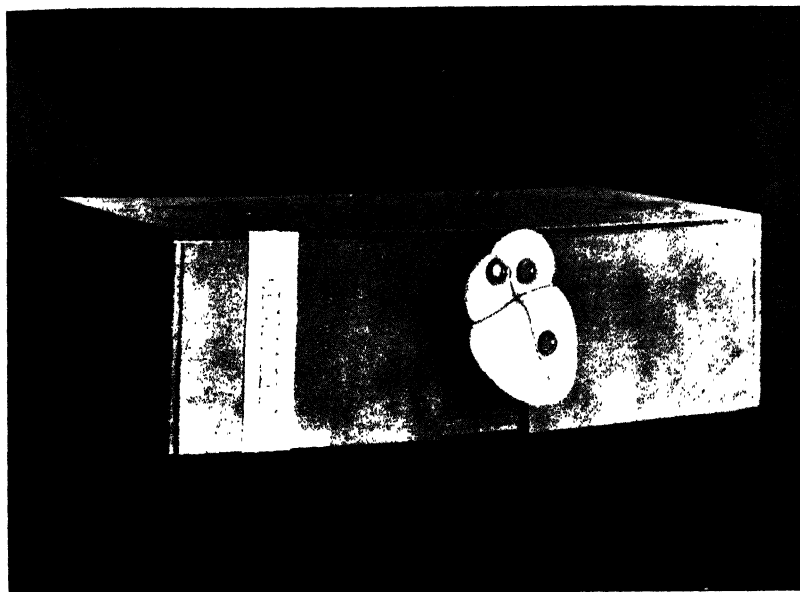
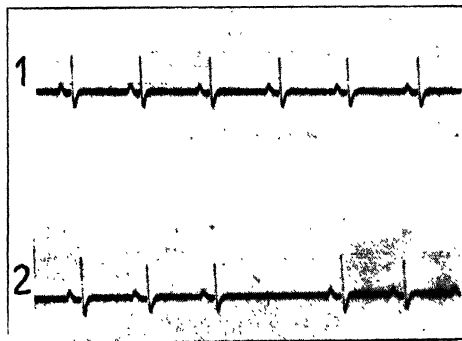


FIG. 4.



Outside view of model.

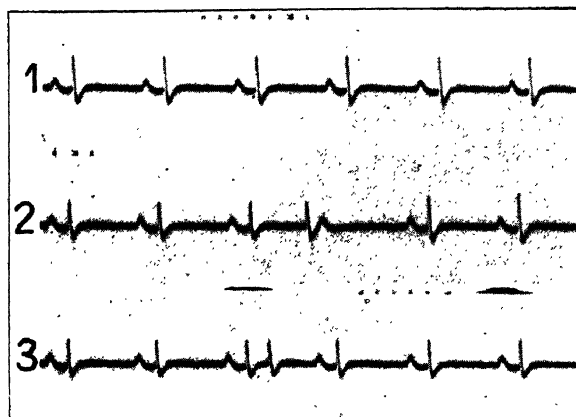
FIG. 7.



1. Normal heart beat.
2. Sino-auricular block.

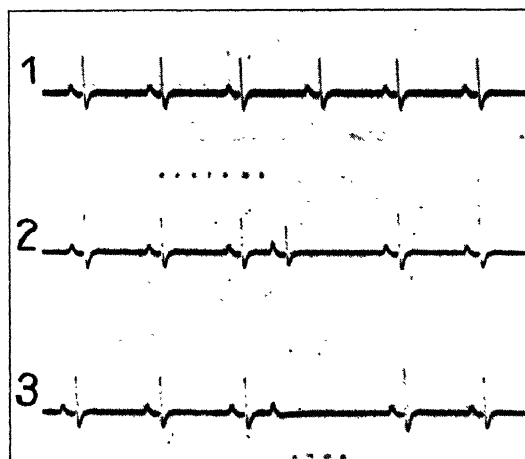
VAN DER POL & VAN DER MARK.

FIG. 8.



Ventricular extrasystole:—1. normal heart beat: 2. late ventricular extrasystole resulting in the ventricle being in the refractory state when the next following normal stimulus arrives from the auricle: 3. early ventricular extrasystole: here the ventricle is *not* any more in the refractory period when the next following normal stimulus arrives from the auricle and thus an *interpolated ventricular systole* is obtained.

FIG. 9.

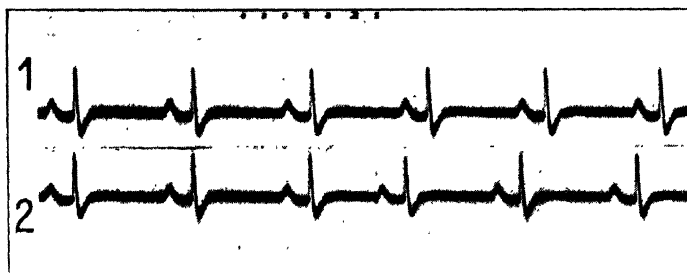


1. Normal heart beat.
2. Auricular extrasystole (with the ventricle responding).
3. Auricular extrasystole (ventricle still in refractory period).

Note the increased amplitude of the following normal ventricular systole.

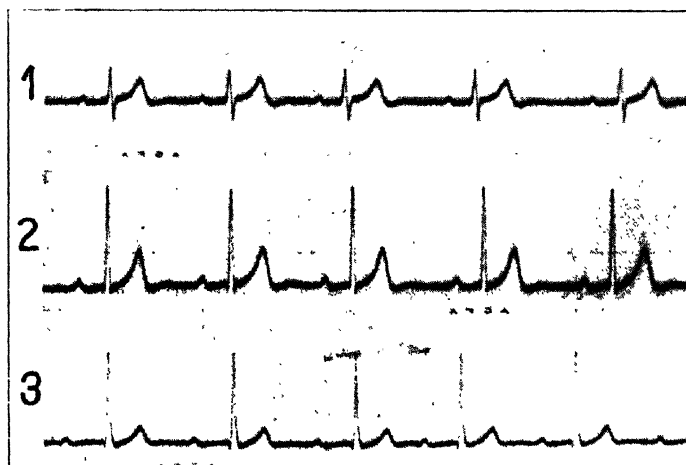
VAN DER POL & VAN DER MARK.

FIG. 10.

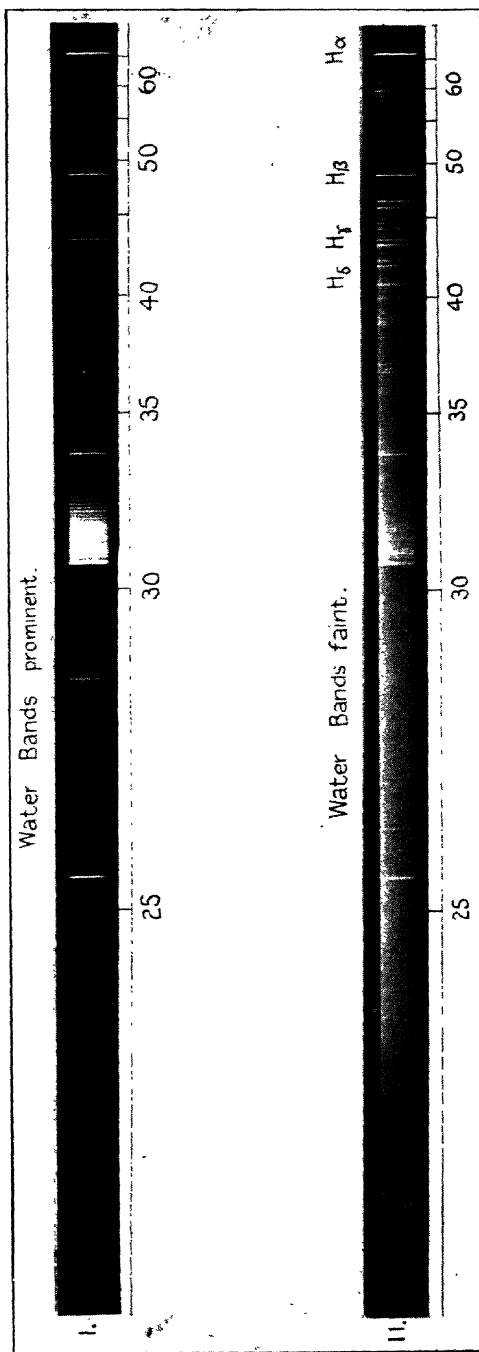


1. Normal heart beat.
2. Sinus extrasystole disturbing the whole heart rhythm.

FIG. 11.



Electrocardiogram of the real heart taken in the standard positions 1, 2. and 3 with the aid of a special very low frequency amplifier and a Cambridge oscillograph.



THE CONTINUOUS SPECTRUM OF HYDROGEN.

FIG. 1.



FIG. 2.

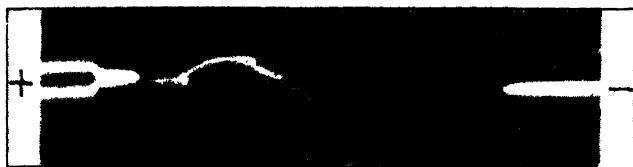
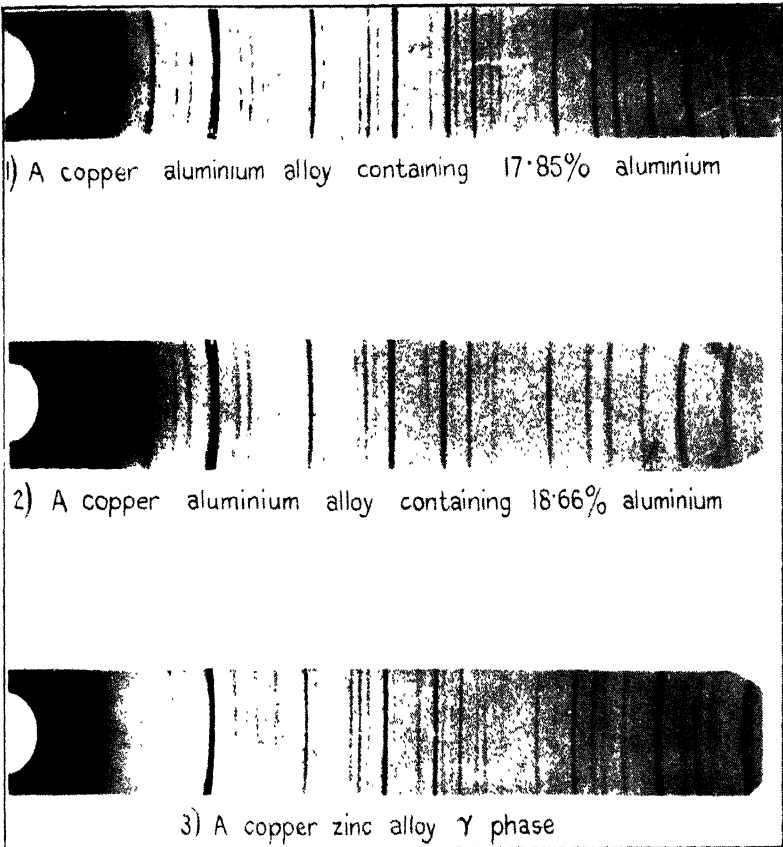


FIG. 3.





POWDER PHOTOGRAMS OF δ Cu-Al ALLOYS COMPARED
WITH γ Cu-Zn.

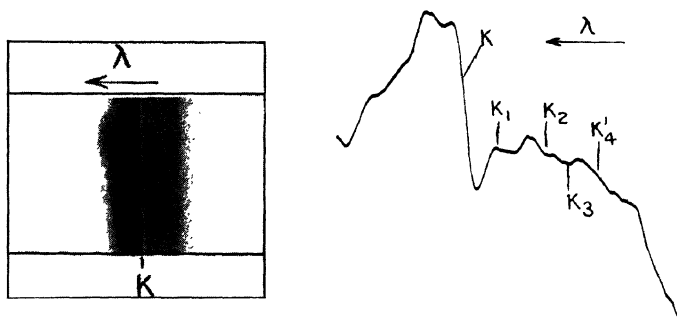
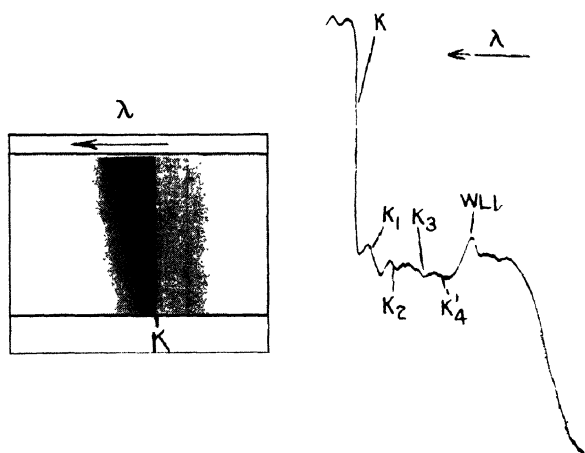
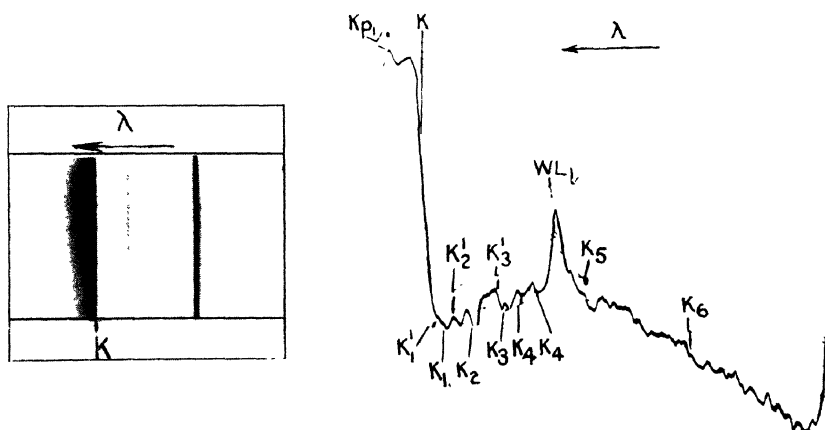
FIG. 1. - K Absorption of Fe in FeS_2 crystal.FIG. 2. - K Absorption of Fe in screen of Fe_3O_4 .

FIG. 3. - K Absorption of Fe in screen of metallic iron.

FIG. 1.

The point (end
of contact wire; -).



The crystal (+).

Luminescence I.

FIG. 4.

The point (end
of contact wire; -).

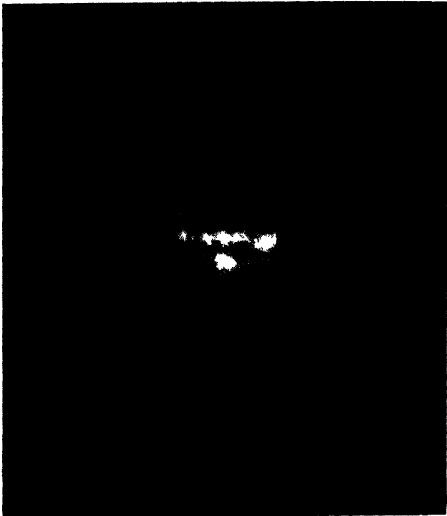


The crystal (+).

Luminescence II.

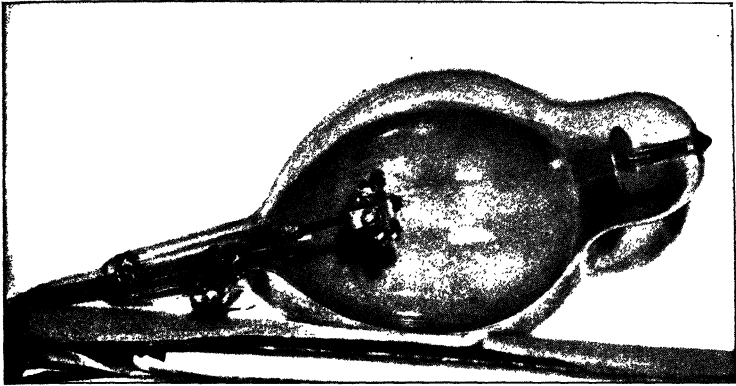
Magnified 30 times.

FIG. 5



Luminescence I. $\times 505$.

FIG. 6.

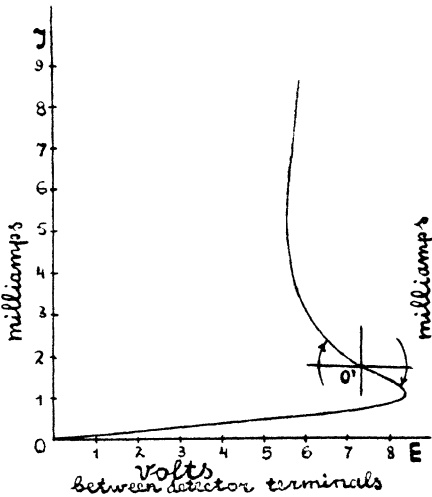


Discharge-tube, used for observations of cathodo luminescences.

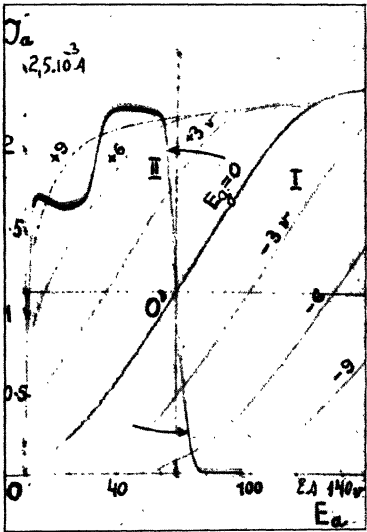
FIG. 9b.

Vacuum-tube.

Oscillating detector (zincite).



O' = displaced beginning of coordinates. The arrows indicate the rotation direction of characteristic with respect to coordinates in the neighbourhood of O', which is typical for "a negative series-resistance."



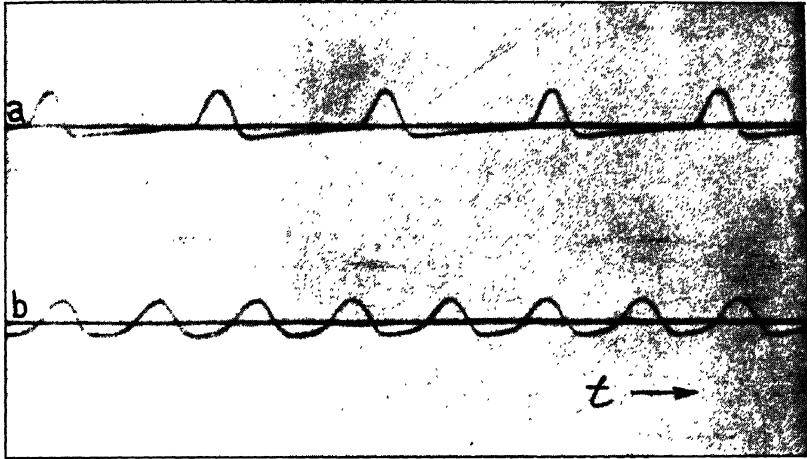
$$I \quad J_a = f(E_a)$$

$$II \quad J_a = f(E_a, E_g)$$

II. = the "regeneration-characteristic" of vacuum-tube (with negative slope). The arrows indicate the rotation direction of characteristic with respect to coordinates in the neighbourhood of O', which is typical for "a negative leak-resistance."

The characteristics of vacuum-tube were plotted by means of B. A. Ostroumoff's "characterograph" (Zeit. f. Techn. Phys. no. 4, p. 163, 1927).

FIG. 15.

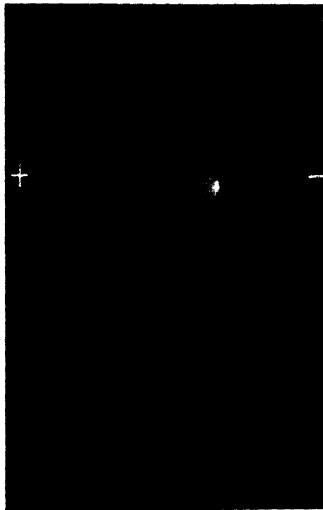


"a" at $I=2.5$ milliamps.; $E=7.1$ volts.

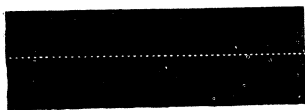
"b" at $I=4.9$ milliamps.; $E=6.2$ volts.

Both curves (*a* and *b*) were plotted from same oscillating point.

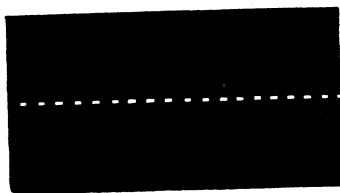
FIG. 18.



Glimm spot of luminescence II. on a red-hot crystal: the crystal is placed between two vertical metallic rods. $1\frac{1}{2}$ natural size.

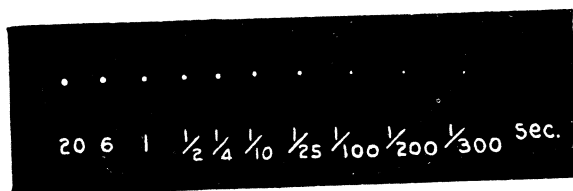
FIG. 19 *a*.

Record of current 500 cyc. per sec. on a moving photographic plate (with luminescence II.; value R.M.S. of current $I = 0.24$ amp.; objective F:3.5).

FIG. 19 *b*.

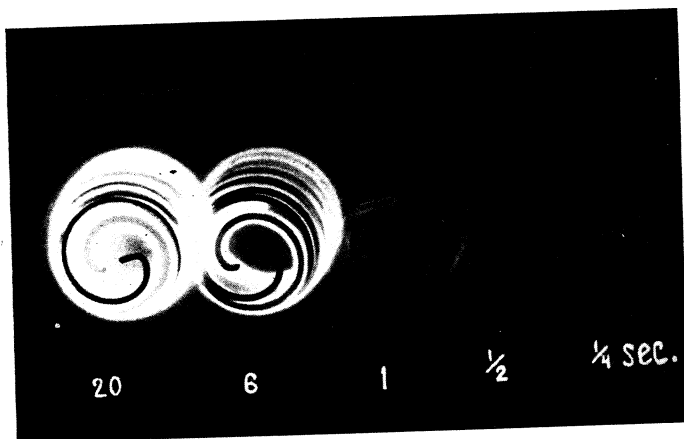
Record of fig. 19 *a*. Magnified from the original 3 times.

FIG. 20.



Detector luminescence (luminescence II.); $I = 0.23$ amp.; $E = 28$ v.; (6.44 w.); F:18. Natural size.

FIG. 21.



Neon lamp, at same optical conditions (cliché diminished 1.25 times): $I = 15.1$ milliamps.; $E = 177$ v. (2.67 w.); or 132.8 v. — without potential difference the ballast resistance $\approx 2.93 \Omega$, placed in the cap of lamp (2.0 w.).

FIG. 3.

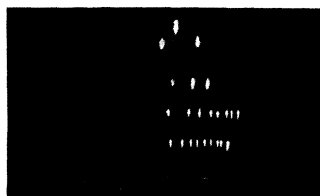


FIG. 4



FIG. 5.

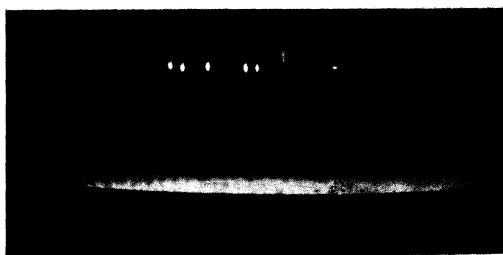
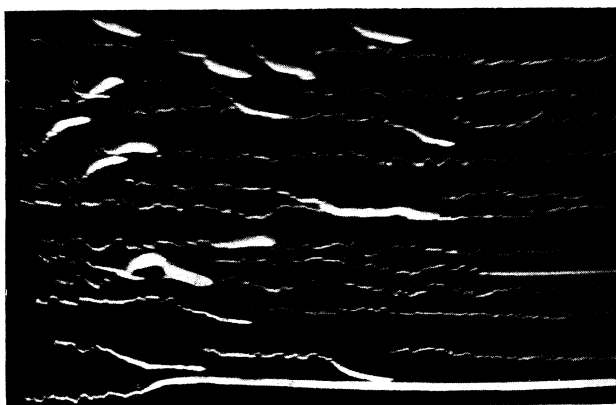


FIG. 6.



FIG. 7.



[FIG. 8.

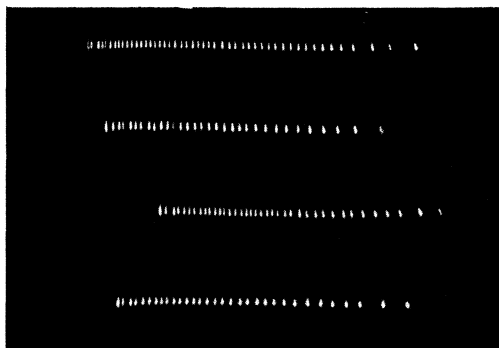


FIG. 1.

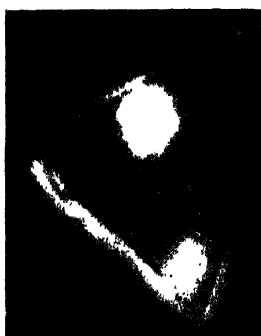
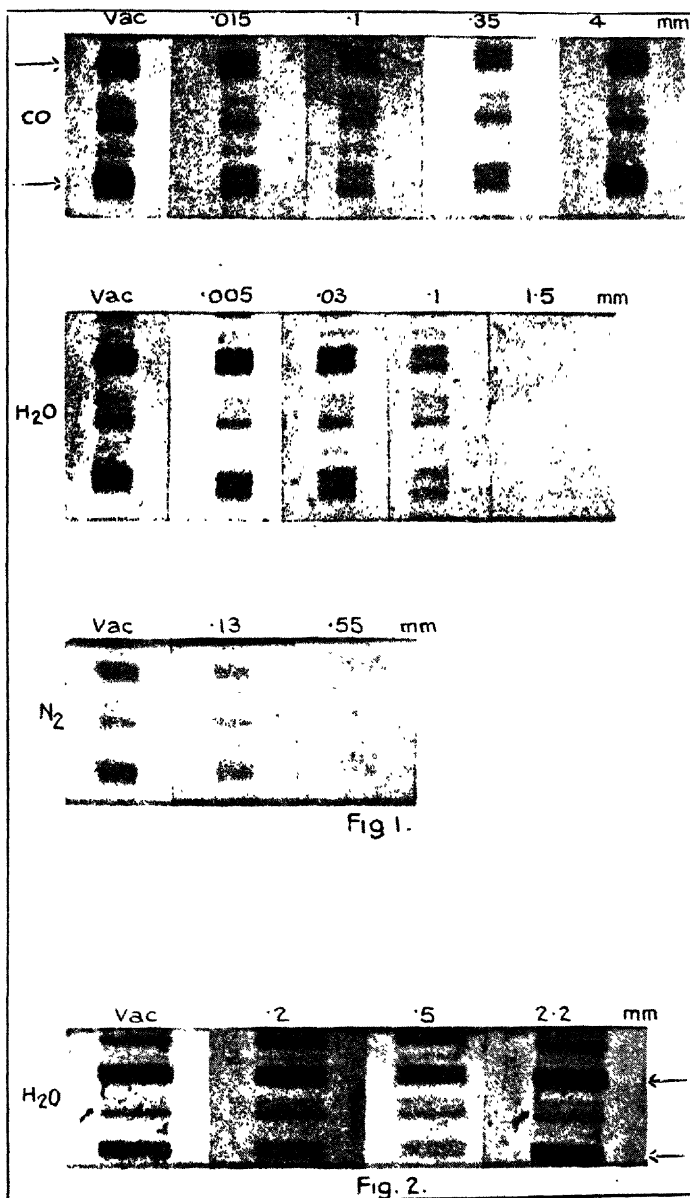


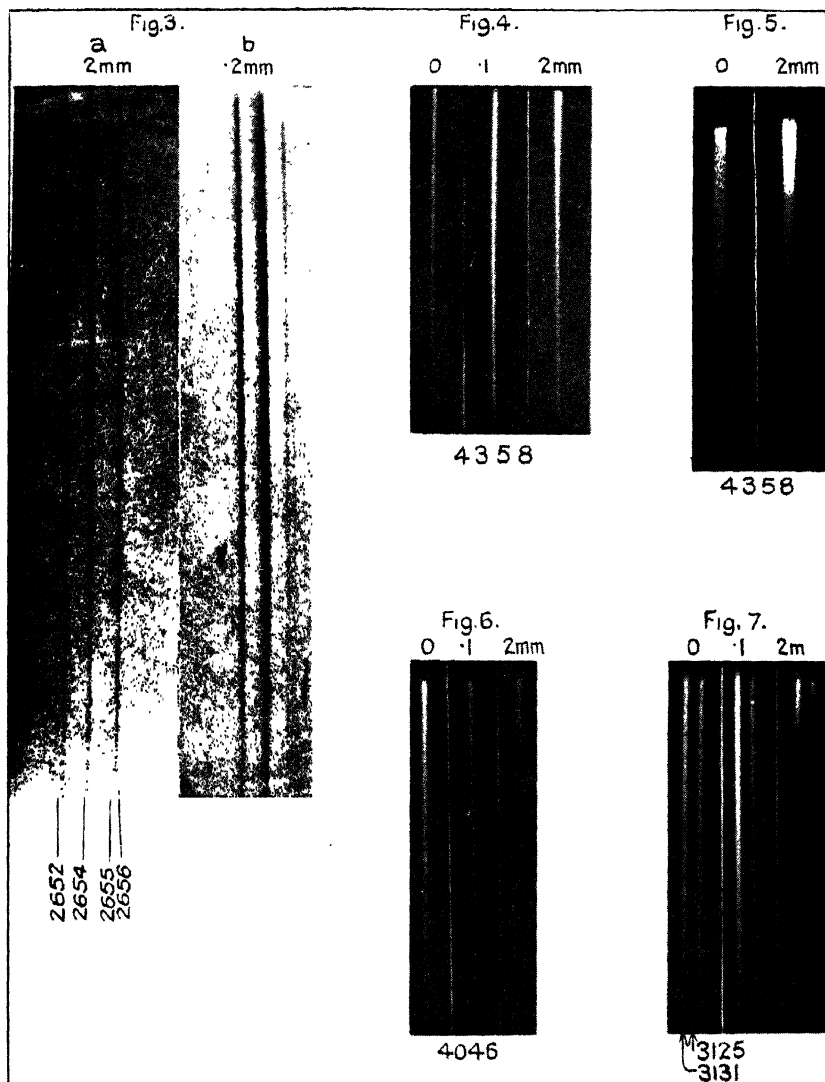
FIG. 2.

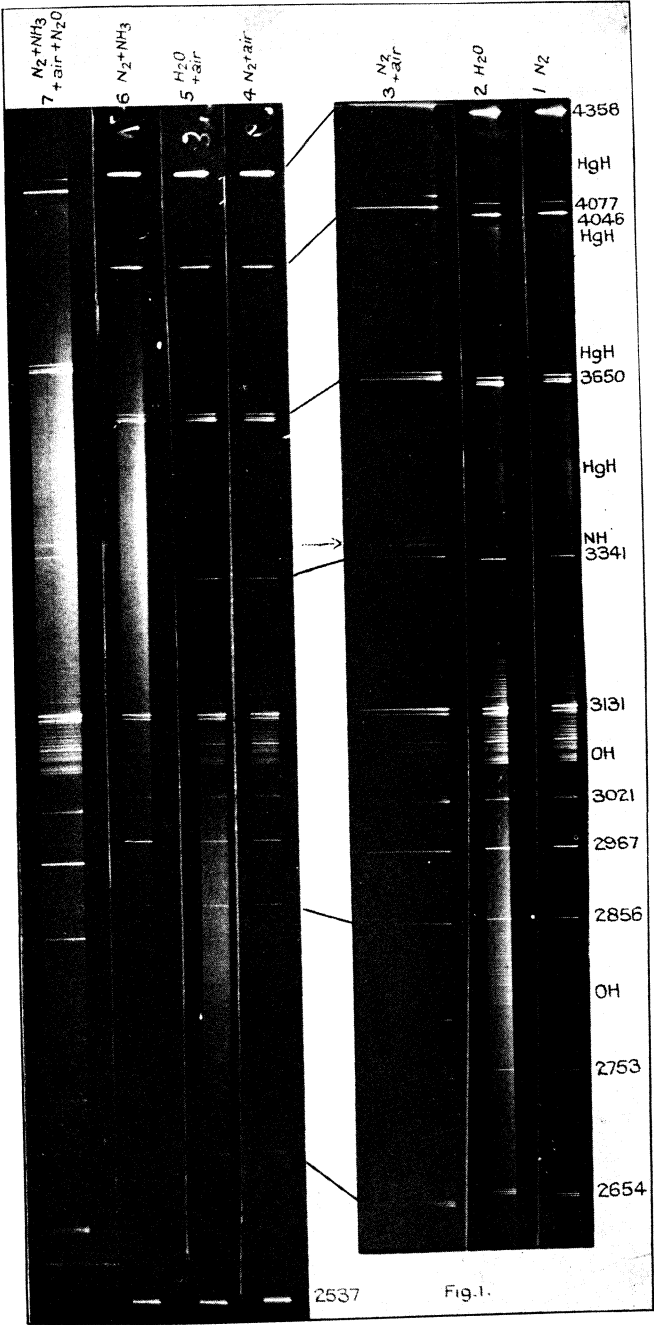




Prints of images obtained by placing certain pieces of fused quartz, activated by ultra-violet rays, upon a photographic plate for 12 hours.







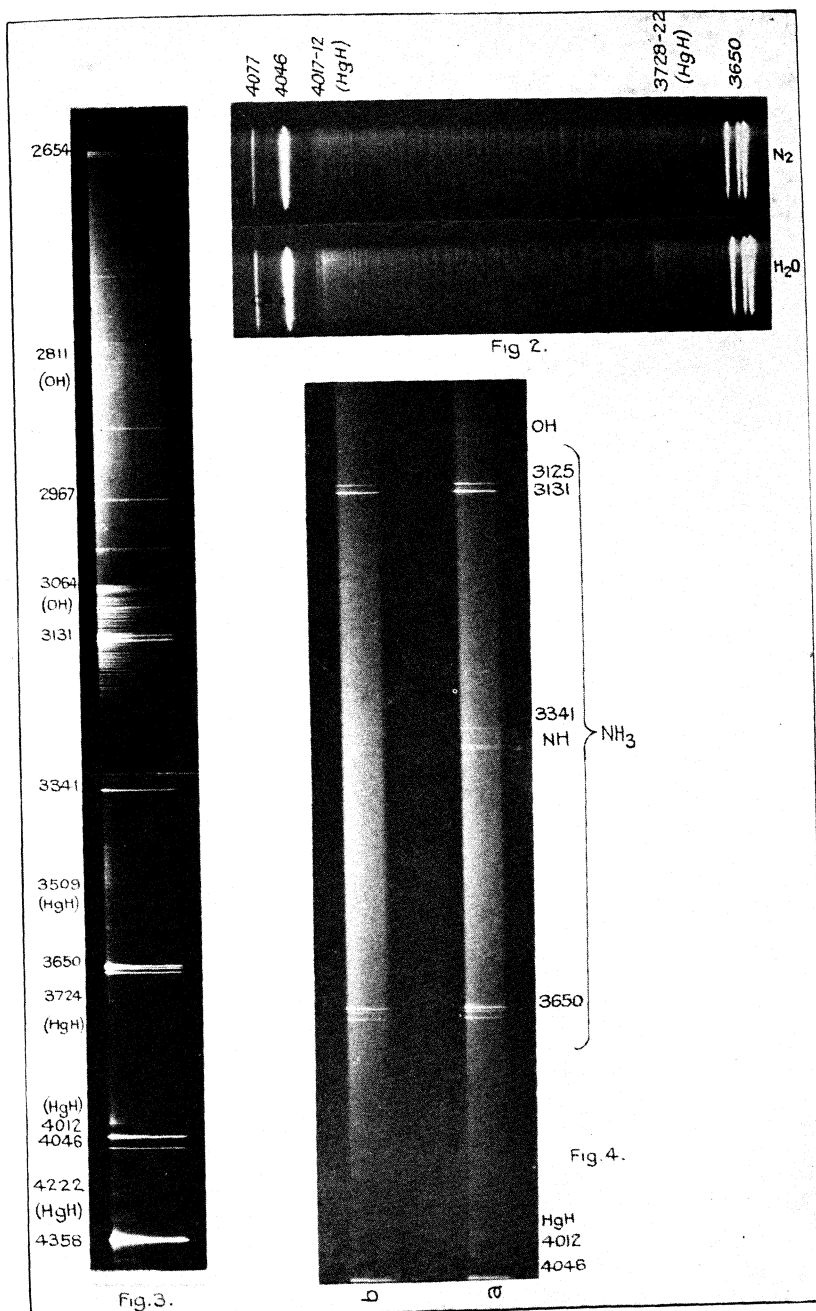
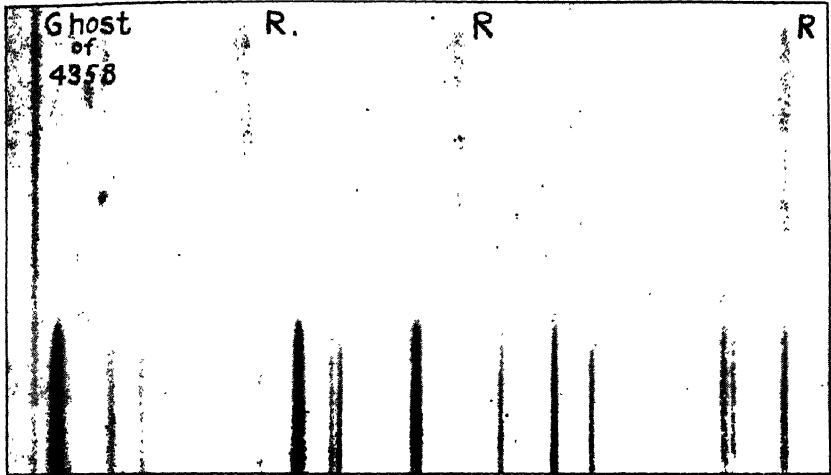
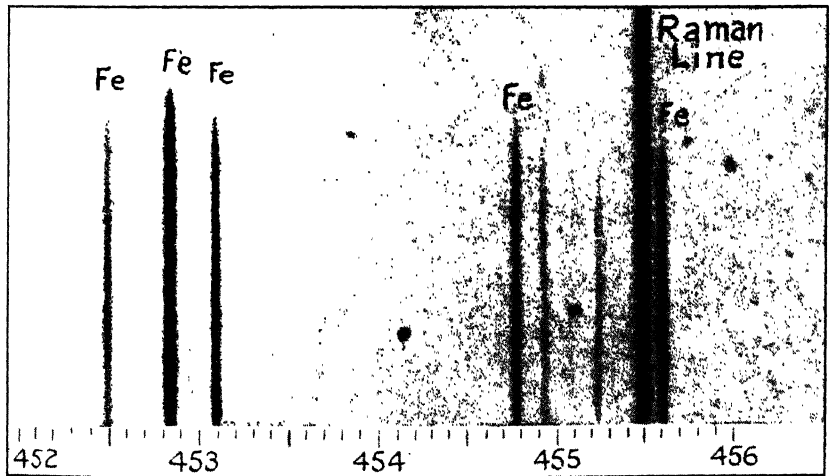


FIG. 1.



Carbon tetrachloride.

FIG. 2.



Benzene.

IMPERIAL JAPANESE RESEARCH
INSTITUTE LIBRARY
NEW DELHI.

[illegible]